NOVEL THERAPEUTIC TARGET AND DRUG DISCOVERY FOR NEUROLOGICAL DISEASES

EDITED BY: Rui Liu, Liu Qing-Shan, Yong Cheng, George Barreto and Asma Perveen

PUBLISHED IN: Frontiers in Pharmacology and Frontiers in Neuroscience

frontiers Research Topics

ISSN 1664-8714
ISBN 978-2-83250-563-2
DOI 10.3389/978-2-83250-563-2

About Frontiers

Frontiers is more than just an open-access publisher of scholarly articles: it is a pioneering approach to the world of academia, radically improving the way scholarly research is managed. The grand vision of Frontiers is a world where all people have an equal opportunity to seek, share and generate knowledge. Frontiers provides immediate and permanent online open access to all its publications, but this alone is not enough to realize our grand goals.

Frontiers Journal Series

The Frontiers Journal Series is a multi-tier and interdisciplinary set of open-access, online journals, promising a paradigm shift from the current review, selection and dissemination processes in academic publishing. All Frontiers journals are driven by researchers for researchers; therefore, they constitute a service to the scholarly community. At the same time, the Frontiers Journal Series operates on a revolutionary invention, the tiered publishing system, initially addressing specific communities of scholars, and gradually climbing up to broader public understanding, thus serving the interests of the lay society, too.

Dedication to Quality

Each Frontiers article is a landmark of the highest quality, thanks to genuinely collaborative interactions between authors and review editors, who include some of the world's best academicians. Research must be certified by peers before entering a stream of knowledge that may eventually reach the public - and shape society; therefore, Frontiers only applies the most rigorous and unbiased reviews.
Frontiers revolutionizes research publishing by freely delivering the most outstanding research, evaluated with no bias from both the academic and social point of view. By applying the most advanced information technologies, Frontiers is catapulting scholarly publishing into a new generation.

What are Frontiers Research Topics?

Frontiers Research Topics are very popular trademarks of the Frontiers Journals Series: they are collections of at least ten articles, all centered on a particular subject. With their unique mix of varied contributions from Original Research to Review Articles, Frontiers Research Topics unify the most influential researchers, the latest key findings and historical advances in a hot research area! Find out more on how to host your own Frontiers Research Topic or contribute to one as an author by contacting the Frontiers Editorial Office: frontiersin.org/about/contact

NOVEL THERAPEUTIC TARGET AND DRUG DISCOVERY FOR NEUROLOGICAL DISEASES

Topic Editors:
Rui Liu, Institute of Medicinal Biotechnology, Chinese Academy of Medical Sciences, China
Liu Qing-Shan, Minzu University of China, China
Yong Cheng, Minzu University of China, China
George Barreto, University of Limerick, Ireland
Asma Perveen, Glocal University, India

Citation: Liu, R., Qing-Shan, L., Cheng, Y., Barreto, G., Perveen, A., eds. (2022). Novel Therapeutic Target and Drug Discovery for Neurological Diseases. Lausanne: Frontiers Media SA. doi: 10.3389/978-2-83250-563-2

Table of Contents

05 ***Editorial: Novel Therapeutic Target and Drug Discovery for Neurological Diseases***
Kaiyue Zhao, Zhuorong Li, Qingshan Liu, Yong Cheng, George E. Barreto and Rui Liu

08 ***Extracellular Vesicles: Emerging Roles in Developing Therapeutic Approach and Delivery Tool of Chinese Herbal Medicine for the Treatment of Depressive Disorder***
Qian Wu, Wen-Zhen Duan, Jian-Bei Chen, Xiao-Peng Zhao, Xiao-Juan Li, Yue-Yun Liu, Qing-Yu Ma, Zhe Xue and Jia-Xu Chen

25 ***Agathisflavone as a Single Therapy or in Association With Mesenchymal Stem Cells Improves Tissue Repair in a Spinal Cord Injury Model in Rats***
Ravena P. do Nascimento, Lívia B. de Jesus, Markley S. Oliveira-Junior, Aurea M. Almeida, Eduardo L. T. Moreira, Bruno D. Paredes, Jorge M. David, Bruno S. F. Souza, Maria de Fátima D. Costa, Arthur M. Butt, Victor Diogenes A. Silva and Silvia L. Costa

39 ***Edaravone Dexborneol Treatment Attenuates Neuronal Apoptosis and Improves Neurological Function by Suppressing 4-HNE-Associated Oxidative Stress After Subarachnoid Hemorrhage***
Qian Chen, Yichen Cai, Xiaoyu Zhu, Jing Wang, Feng Gao, Mingfeng Yang, Leilei Mao, Zongyong Zhang and Baoliang Sun

51 **Coeloglossum viride *Var.* Bracteatum *Extract Attenuates MPTP-Induced Neurotoxicity* in vivo *by Restoring BDNF-TrkB and FGF2-Akt Signaling Axis and Inhibiting RIP1-Driven Inflammation***
Xiu-Yuan Lang, Yang Hu, Jin-Peng Bai, Jun Wang, Xiao-Yan Qin and Rongfeng Lan

62 ***DAPT Attenuates Cadmium-Induced Toxicity in Mice by Inhibiting Inflammation and the Notch/HES-1 Signaling Axis***
Jia-Ying Yang, Dan-Yang Shen, Jun Wang, Jing-Feng Dai, Xiao-Yan Qin, Yang Hu and Rongfeng Lan

72 ***Activation of Wnt/Beta-Catenin Signaling Pathway as a Promising Therapeutic Candidate for Cerebral Ischemia/Reperfusion Injury***
Zhizhun Mo, Zhongyi Zeng, Yuxiang Liu, Linsheng Zeng, Jiansong Fang and Yinzhong Ma

81 ***Comparative Metabolomics Analysis Reveals Key Metabolic Mechanisms and Protein Biomarkers in Alzheimer's Disease***
Zhao Dai, Tian Hu, Shijie Su, Jinman Liu, Yinzhong Ma, Yue Zhuo, Shuhuan Fang, Qi Wang, Zhizhun Mo, Huafeng Pan and Jiansong Fang

94 ***Mangiferin Alleviates Postpartum Depression–Like Behaviors by Inhibiting MAPK Signaling in Microglia***
Meichen Yan, Xuena Bo, Xinchao Zhang, Jingdan Zhang, Yajin Liao, Haiyan Zhang, Yong Cheng, Junxia Guo and Jinbo Cheng

104 ***Sigma-1 Receptors in Depression: Mechanism and Therapeutic Development***
Peng Ren, Jingya Wang, Nanxi Li, Guangxiang Li, Hui Ma, Yongqi Zhao and Yunfeng Li

115 ***Mechanism of Neural Regeneration Induced by Natural Product LY01 in the 5×FAD Mouse Model of Alzheimer's Disease***
Xiao-Wan Li, Yang-Yang Lu, Shu-Yao Zhang, Ning-Ning Sai, Yu-Yan Fan, Yong Cheng and Qing-Shan Liu

130 ***Xiaoyaosan Ameliorates Chronic Restraint Stress-Induced Depression-Like Phenotype by Suppressing A2AR Signaling in the Rat Striatum***
Xiaoxu Zhu, Qingyu Ma, Furong Yang, Xiaojuan Li, Yueyun Liu, Jianbei Chen, Lan Li, Man Chen, Xiaojuan Zou, Li Yan and Jiaxu Chen

143 ***NEU1—A Unique Therapeutic Target for Alzheimer's Disease***
Aiza Khan and Consolato M. Sergi

155 ***Shumian Capsule Improves the Sleep Disorder and Mental Symptoms Through Melatonin Receptors in Sleep-Deprived Mice***
Wenhua Li, Yinlong Cheng, Yi Zhang, Yazhi Qian, Mo Wu, Wei Huang, Nan Yang and Yanyong Liu

167 ***Scorpion Venom Heat–Resistant Synthesized Peptide Increases Stress Resistance and Extends the Lifespan of* Caenorhabditis elegans via *the Insulin/IGF-1-Like Signal Pathway***
Ying-Zi Wang, Song-Yu Guo, Rui-Li Kong, Ao-Ran Sui, Zhen-Hua Wang, Rong-Xiao Guan, Kundu Supratik, Jie Zhao and Shao Li

180 ***Microglia Pyroptosis: A Candidate Target for Neurological Diseases Treatment***
Xian Wu, Teng Wan, Xiaoyu Gao, Mingyuan Fu, Yunfeng Duan, Xiangru Shen and Weiming Guo

194 ***The Efficacy and Safety of Ischemic Stroke Therapies: An Umbrella Review***
Yongbiao Li, Ruyi Cui, Fangcheng Fan, Yangyang Lu, Yangwen Ai, Hua Liu, Shaobao Liu, Yang Du, Zhiping Qin, Wenjing Sun, Qianqian Yu, Qingshan Liu and Yong Cheng

208 ***Research Progress on Classical Traditional Chinese Medicine Formula Xiaoyaosan in The Treatment of Depression***
Jianbei Chen, Chaofang Lei, Xiaojuan Li, Qian Wu, Chenyue Liu, Qingyu Ma and Jiaxu Chen

227 ***Cryo-EM Structure and Activator Screening of Human Tryptophan Hydroxylase 2***
Kongfu Zhu, Chao Liu, Yuanzhu Gao, Jianping Lu, Daping Wang and Huawei Zhang

240 ***Exposure of Metal Toxicity in Alzheimer's Disease: An Extensive Review***
Fahadul Islam, Sheikh Shohag, Shomaya Akhter, Md. Rezaul Islam, Sharifa Sultana, Saikat Mitra, Deepak Chandran, Mayeen Uddin Khandaker, Ghulam Md Ashraf, Abubakr M. Idris, Talha Bin Emran and Simona Cavalu

260 ***RNA Sequencing-Based Identification of The Regulatory Mechanism of microRNAs, Transcription Factors, and Corresponding Target Genes Involved in Vascular Dementia***
Kaiyue Zhao, Li Zeng, Zhongdi Cai, Mimin Liu, Ting Sun, Zhuorong Li and Rui Liu

frontiers | Frontiers in Pharmacology

TYPE Editorial
PUBLISHED 07 October 2022
DOI 10.3389/fphar.2022.1042266

OPEN ACCESS

EDITED AND REVIEWED BY
Nicholas M. Barnes,
University of Birmingham,
United Kingdom

*CORRESPONDENCE
Rui Liu,
liurui@imb.pumc.edu.cn

SPECIALTY SECTION
This article was submitted to Neuropharmacology, a section of the journal Frontiers in Pharmacology

RECEIVED 12 September 2022
ACCEPTED 21 September 2022
PUBLISHED 07 October 2022

CITATION
Zhao K, Li Z, Liu Q, Cheng Y, Barreto GE and Liu R (2022), Editorial: Novel therapeutic target and drug discovery for neurological diseases. *Front. Pharmacol.* 13:1042266. doi: 10.3389/fphar.2022.1042266

Editorial: Novel therapeutic target and drug discovery for neurological diseases

Kaiyue Zhao[1], Zhuorong Li[1], Qingshan Liu[2], Yong Cheng[3], George E. Barreto[4] and Rui Liu[1]*

[1]Institute of Medicinal Biotechnology, Chinese Academy of Medical Sciences and Peking Union Medical College, Beijing, China, [2]College of Pharmacy, Minzu University of China, Beijing, China, [3]College of Life and Environmental Sciences, Minzu University of China, Beijing, China, [4]Department of Biological Sciences, University of Limerick, Limerick, Ireland

KEYWORDS

Alzheimer's disease, dementia, depression, drug target, natural products, neurological disorders, neurotrophic factor, stroke

Editorial on the Research Topic
Novel therapeutic target and drug discovery for neurological diseases

The Research Topic "*Novel Therapeutic Target and Drug Discovery for Neurological Diseases*" consists of 20 articles, including 12 original research papers, seven reviews, and one systematic review, with contributions from more than 140 authors. This work aims to compile a collection of articles focused on recent advances in promising therapeutic targets and biomarkers, new pathological mechanisms, and novel therapeutic agents in order to provide valuable clues for developing new therapeutic strategies for neurological diseases.

One group of included articles discusses targets with potential applications for drug discovery and therapeutic strategies. One such target is the Sigma-1 receptor, a mitochondrion-associated endoplasmic reticulum membrane protein active in the central nervous system, whose antagonists showed attractive potential in treating neuropathic pain and psychostimulant abuse (Hayashi and Su, 2007; Yano et al., 2018). Ren et al. provide a systematic overview of the role of the Sigma-1 receptor in regulating neurotransmission, including regulation of excitatory and inhibitory (E/I) balance *via* glutamatergic, serotonergic, and GABAergic neurotransmitters, suggesting that Sigma-1 receptor agonists may be a potent therapeutic target for depression, particularly in the development of fast-acting antidepressants. Neuraminidase 1 (NEU1) is a subtype of the sialidase family responsible for removing sialic acid residues from protein-bound oligosaccharides. Notably, mutation of NEU1 results in sialidosis, a rare genetic metabolic disease (Miyagi and Yamaguchi, 2012). Khan et al. discuss the associations of NEU1 with neurological disorders and underscore its role in amyloid precursor protein (APP) and amyloid beta-peptide (Aβ) accumulation and Toll-like receptor (TLR) activation-dominated microglial activation in Alzheimer's disease (AD). The researchers conclude that NEU1 is an emerging therapeutic target for AD.

Genomic analysis and transcriptome profiling have recently been used as a hypothesis-free approach to identify novel drug targets for neurological diseases (Zeng et al., 2021; Jiang et al., 2022; Sun et al., 2022). Using RNA sequencing analyses and experimental verification, Zhao et al. identify differentially expressed genes, microRNAs (miRNAs), and transcription factors (TFs), constructed miRNA-TF-gene regulatory networks, and propose several new molecules, such as miR-145-5p and cysteine and serine-rich nuclear protein 1 (*Csrnp1*), as potential therapeutic targets for vascular dementia.

Another group of articles advances our understanding of the pathological mechanisms of neurological diseases. AD is the primary factor leading to dementia with unclear pathogenesis. Islam et al. reveal the specific roles of environmental metals in aberrant protein misfolding and neuroinflammation in the brains of multiple AD animal models, implicating cerebral metabolic disorder as an essential feature of AD. Dai et al. compare the metabolic properties of AD animal models and patients based on 78 metabolomic profiles from the public available data. They propose two proteins, namely Erb-B2 receptor tyrosine kinase 2 (HER2) and neurogenic differentiation factor 2 (NDF2), as promising biomarkers of AD along with 16 metabolic pathways common to AD in mice and patients, implying close associations with the etiology of AD. Cerebrovascular events are also important causes of neurological disorders and often lead to secondary tissue injury; however, there are currently few effective therapeutic treatments (Rost et al., 2022). Mo et al. highlight the roles of the Wnt/catenin signaling pathway in diverse cell types of neurovascular units, including maintaining blood-brain barrier integrity, reducing neuroinflammation and synapse damage, and promoting remyelination, and suggest this pathway as a potential therapeutic target for ischemic stroke. Due to the critical role of microglia in maintaining immune-inflammatory homeostasis, neuroinflammation is closely associated with neurological disorders (Schwartz and Deczkowska, 2016; Colonna and Butovsky, 2017). Wu et al. address the pathological process driven by microglial pyrosis in neurological diseases and present advances in immunological strategies for treating neuroinflammation by targeting the nod-like receptor family pyrin domain containing 3 (NLRP3), caspase-1, and gasdermins (GSDMs).

Several articles cover drug discovery for nervous system diseases. Research related to small molecule entities with specific targets has long attracted attention for AD. Yang et al. report that the N-[N-(3, 5-difluorophenylacetyl)-l-propanoyl]-s-phenylglycine butyl ester (DAPT), an inhibitor of γ-secretase, attenuates cadmium-induced multi-organic damage and cognitive impairment in mice. Furthermore, they report that the neuroprotective effect of DAPT against cadmium toxicity might be associated with inhibition of the Notch/HES-1 signaling axis. Natural products are significant sources of leading compounds in drug research and development. Li et al. report that LY-01, which is derived from the Chinese herbal medicine *Sophora alosecuroides*, alleviates early cognitive decline in 5×familial AD (5×FAD) mice (10 or 13 weeks old) by promoting endogenous neural regeneration. They demonstrate that LY-01 exerts neuroprotective functions by increasing the number of new cells, neuronal precursor cells, and length of neurites in the dentate gyrus of 5×FAD mice, and has similar effects on promoting proliferation of primary neurons, astrocytes, and primary NSCs *in vitro*. Lang et al. report the therapeutic effects of *Coeloglossum viride* var. *bracteatum* extract (CE) on the 1-methyl-4-phenyl-1,2,3,6-tetrahydropyridine (MPTP)-induced mouse model of Parkinson's disease (PD). CE, which was extracted from tubers of *Coeloglossum viride* var. *bracteatum* (a traditional Tibetan medicine), shows beneficial effects on behavioral disability in mice with MPTP injury. Further investigation of the substantia nigra and striatum of CE-treated mice revealed inhibition of astrocyte activation and neuroinflammation as well as increased neuronal survival *via* recovery of the BDNF-TrkB and FGF2-Akt signaling pathways. Edaravone dexborneol is a novel drug approved in China for the treatment of acute ischemic stroke. Chen et al. report the neuroprotective effect and underlying mechanism of edaravone dexborneol in a rat model of subarachnoid hemorrhage (SAH). They demonstrate that edaravone dexborneol contributes to sensorimotor functions in rats after SAH, inhibits neuronal apoptosis in the affected hippocampus and basal cortex, alleviates oxidative stress, and specifically reduces toxic lipid peroxide-4-hydroxynonenal (4-HNE) levels in neurons and astrocytes. Agathisflavone, a flavonoid with anti-neuroinflammatory and myelinogenic properties, is demonstrated by do Nascimento et al. to protect injured spinal cord tissue by increasing the expression of neurotrophins and modulating the inflammatory response. Mangiferin, which exerts a wide range of pharmacological activities, is shown by Yan et al. to potentially alleviate postpartum depression-like behaviors in mice by inhibiting microglial activation and neuroinflammation *via* mitogen-activated protein kinase (MAPK) signaling pathways. Other studies demonstrate how a structure-based drug discovery strategy contributes to innovative drug development for neurological diseases. For example, by analyzing the low-temperature electromagnetic structure of human tryptophan hydroxylase 2 (TPH2) in the tetrameric state of 3.0 Å using cryoelectron microscopy and testing small molecule activators by molecular docking and molecular dynamics simulation, Zhu et al. suggest that CMPD1 is a potentially promising TPH2-targeted compound for mental disorders.

In summary, the current Research Topic includes original studies, reviews, and a systematic review regarding novel therapeutic targets, molecular mechanisms, and potential drug candidates for the treatment of neurological diseases. The use of advanced technologies such as transcriptomics, network pharmacology, and structural biology technology can help shed light on the complex etiology of central nervous system diseases, identify new targets, and develop novel active substances. Furthermore, natural products with ideal

neuropharmacological activity are expected to be developed from substances in fundamental research to translational medicine. Lastly, we extend our sincere gratitude to the Editorial Office of Frontiers in Pharmacology, all of the authors, and all of the reviewers for their valuable contributions to this Research Topic.

Author contributions

RL contributed to the conception and design of the Research Topic and the Editorial. KZ and ZL contributed to the writing of the Editorial. QL, YC, and GB contributed to the revision of the submitted version. All authors read and agreed with this Editorial.

Conflict of interest

The authors declare that the research was conducted in the absence of any commercial or financial relationships that could be construed as a potential conflict of interest.

Publisher's note

References

Colonna, M., and Butovsky, O. (2017). Microglia function in the central nervous system during health and neurodegeneration. *Annu. Rev. Immunol.* 35, 441–468. doi:10.1146/annurev-immunol-051116-052358

Hayashi, T., and Su, T. P. (2007). Sigma-1 receptor chaperones at the ER-mitochondrion interface regulate Ca(2+) signaling and cell survival. *Cell* 131, 596–610. doi:10.1016/j.cell.2007.08.036

Jiang, H., Liu, J., Guo, S., Zeng, L., Cai, Z., Zhang, J., et al. (2022). miR-23b- 3p rescues cognition in Alzheimer's disease by reducing tau phosphorylation and apoptosis via GSK-3β signaling pathways. *Mol. Ther. Nucl. Acids.* 28, 539–557. doi:10.1016/j.omtn.2022.04.008

Miyagi, T., and Yamaguchi, K. (2012). Mammalian sialidases: Physiological and pathological roles in cellular functions. *Glycobiology* 22, 880–896. doi:10.1093/glycob/cws057

Rost, N. S., Brodtmann, A., Pase, M. P., van Veluw, S. J., Biffi, A., Duering, M., et al. (2022). Post-stroke cognitive impairment and dementia. *Circ. Res.* 130, 1252–1271. doi:10.1161/CIRCRESAHA.122.319951

Schwartz, M., and Deczkowska, A. (2016). Neurological disease as a failure of brain-immune crosstalk: The multiple faces of neuroinflammation. *Trends Immunoi* 37, 668–679. doi:10.1016/j.it.2016.08.001

Sun, T., Zhao, K., Liu, M., Cai, Z., Zeng, L., Zhang, J., et al. (2022). miR- 2078 30a-5p induces Aβ production via inhibiting the nonamyloidogenic pathway 2079 in Alzheimer's disease. *Pharmacol. Res.* 178, 106153. doi:10.1016/j.phrs.2022.10.2080.6153

Yano, H., Bonifazi, A., Xu, M., Guthrie, D. A., Schneck, S. N., Abramyan, A. M., et al. (2018). Pharmacological profiling of sigma 1 receptor ligands by novel receptor homomer assays. *Neuropharmacology* 133, 264–275. doi:10.1016/j.neuropharm.2018.01.042

Zeng, L., Jiang, H., Ashraf, G. M., Liu, J., Wang, L., Zhao, K., et al. (2021). Implications of miR-148a-3p/p35/PTEN signaling in tau hyperphosphorylation and autoregulatory feedforward of Akt/CREB in Alzheimer's disease. *Mol. Ther. Nucl. Acids.* 27, 256–275. doi:10.1016/j.omtn.2021.11.019

frontiers in Pharmacology

REVIEW
published: 24 March 2022
doi: 10.3389/fphar.2022.843412

Extracellular Vesicles: Emerging Roles in Developing Therapeutic Approach and Delivery Tool of Chinese Herbal Medicine for the Treatment of Depressive Disorder

Qian Wu[1,2], Wen-Zhen Duan[2,3,4], Jian-Bei Chen[1], Xiao-Peng Zhao[1], Xiao-Juan Li[5], Yue-Yun Liu[1], Qing-Yu Ma[5], Zhe Xue[1]* and Jia-Xu Chen[1,5]**

[1]School of Traditional Chinese Medicine, Beijing University of Chinese Medicine, Beijing, China, [2]Division of Neurobiology, Department of Psychiatry and Behavioral Sciences, Johns Hopkins University School of Medicine, Baltimore, MD, United States, [3]The Solomon H Snyder Department of Neuroscience, Johns Hopkins University School of Medicine, Baltimore, MD, United States, [4]Program in Cellular and Molecular Medicine, Johns Hopkins University School of Medicine, Baltimore, MD, United States, [5]Guangzhou Key Laboratory of Formula-Pattern of Traditional Chinese Medicine, School of Traditional Chinese Medicine, Jinan University, Guangzhou, China

OPEN ACCESS

Edited by:
Liu Qing-Shan,
Minzu University of China, China

Reviewed by:
Yong Cheng,
Minzu University of China, China
Yan Jouroukhin,
Johns Hopkins Medicine, United States
Guangxin Yue,
China Academy of Chinese Medical Science, China

***Correspondence:**
Qing-Yu Ma
tmaqingyu@jnu.edu.cn
Zhe Xue
xuezhesanctity@163.com
Jia-Xu Chen
chenjiaxu@hotmail.com

Specialty section:
This article was submitted to Neuropharmacology, a section of the journal Frontiers in Pharmacology

Received: 25 December 2021
Accepted: 28 February 2022
Published: 24 March 2022

Citation:
Wu Q, Duan W-Z, Chen J-B, Zhao X-P, Li X-J, Liu Y-Y, Ma Q-Y, Xue Z and Chen J-X (2022) Extracellular Vesicles: Emerging Roles in Developing Therapeutic Approach and Delivery Tool of Chinese Herbal Medicine for the Treatment of Depressive Disorder. Front. Pharmacol. 13:843412. doi: 10.3389/fphar.2022.843412

Extracellular vesicles (EVs) are lipid bilayer-delimited particles released by cells, which play an essential role in intercellular communication by delivering cellular components including DNA, RNA, lipids, metabolites, cytoplasm, and cell surface proteins into recipient cells. EVs play a vital role in the pathogenesis of depression by transporting miRNA and effector molecules such as BDNF, IL34. Considering that some herbal therapies exhibit antidepressant effects, EVs might be a practical delivery approach for herbal medicine. Since EVs can cross the blood-brain barrier (BBB), one of the advantages of EV-mediated herbal drug delivery for treating depression with Chinese herbal medicine (CHM) is that EVs can transfer herbal medicine into the brain cells. This review focuses on discussing the roles of EVs in the pathophysiology of depression and outlines the emerging application of EVs in delivering CHM for the treatment of depression.

Keywords: phytochemials, herbal therapies, extracellular vehicles, exosomes, ectosomes, microvescicles, depressive disorder

1 INTRODUCTION

1.1 The Potential Application of Extracellular Vesicles for Promoting Herbal Medicine in Treating Depressive Disorder

Characterized by severe and persistent emotional symptoms, cognitive symptoms, and somatic symptoms (Bhatt et al., 2020), depression is negatively impacting more than 264 million people as one of the most prevalent psychiatric disorders (James et al., 2018). The coronavirus disease 2019 (COVID-19) pandemic has also exacerbated the prevalence of depression (Salari et al., 2020). "Depression" can refer to any of several depressive disorders (DD). Thus, we comprehensively included depression-related works of literature by searching Mesh term "depressive disorder" and all entry terms in PubMed. DD requires long-term treatment, placing a heavy burden on public healthcare systems worldwide. While western medicines, such as tricyclic antidepressants (TCAs), are often prescribed for DD, efficacy can vary among individuals, in addition to detrimental impact

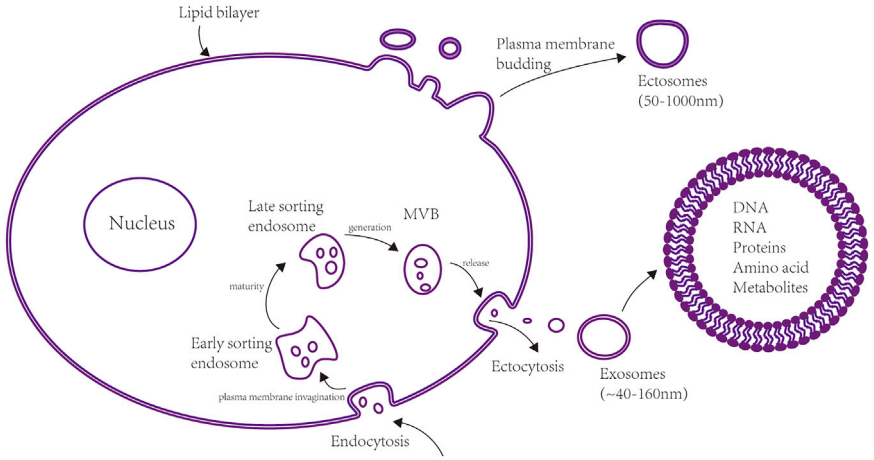

FIGURE 1 | Formation mechanisms of two types of extracellular vesicles (EVs). Ectosomes and exosomes are two significant classifications of EVs. Ectosomes are formed by plasma membrane budding, and their diameter range from ~50 to 1,000 nm. Exosomes range from ~40 to 160 nm and originate in the endosomal pathway via the formation of early-sorting endosomes (ESEs), late-sorting endosomes (LSEs), and ultimately multivesicular bodies (MVBs). Exosomes are formed when MVBs are released by ectocytosis. The exosome population in cells can be highly heterogeneous. Exosomes exhibit different abilities to produce complicated biological responses in recipient cells depending on their cellular origins and specific content (e.g., amino acids, proteins, lipids, metabolites, cytoplasm).

due to their anticholinergic properties (McClintock et al., 2010) (Prado et al., 2018). Thus, complementary and alternative therapies with fewer adverse effects in treating DD are urgently needed. Traditional Chinese medicine (TCM) treatment includes Chinese herbal medicine (CHM), acupuncture, moxibustion, and naprapathy. The complementary and alternative approach to treating depression is widely applied in China with fewer severe side effects. Many preclinical and clinical studies have demonstrated the antidepressant effects of different Chinese herbal medicine (Wang et al., 2017; Milajerdi et al., 2018; Ruan et al., 2019; Ghasemzadeh Rahbardar and Hosseinzadeh 2020). This paper mainly discusses the potential of herbal therapeutics in TCM for treating DD.

Extracellular vesicles (EVs) are lipid bilayer membrane structures that can carry various nucleic acids, lipids, proteins, and other small metabolisms. All cells, including both prokaryotes and eukaryotes, can release EVs as intercellular communication molecules. EVs play vital roles in interrelated physiological and pathophysiological processes, including intercellular communication in the brain. The classification of different EV types is continuously evolving with advances in relevant research (Théry et al., 2018). For example, a study by E. Cocucci suggested that EVs should be broadly categorized as ectosomes or exosomes based on their size and mechanism of formation (Théry et al., 2018) (see **Figure 1**). Ectosomes are vesicles shed from the superficies of the plasma membrane by budding outside. These structures can vary in diameter from ~50 to 1,000 nm and thus include microparticles, microvesicles and large vesicles (Zhang H. et al., 2018). Exosomes originate from endosomes recycled by exocytosis or endocytosis and range from ~40 to 160 nm in diameter. The formation of exosomes goes through four stages. Firstly, the cup-shaped early-sorting endosome (ESE) consists of soluble proteins related to the extracellular environment and cell surface proteins are formed by endocytosis. Secondly, late-sorting endosomes (LSEs) are matured from ESE. Thirdly, intracellular multivesicular bodies (MVBs) are formed by inward invagination of ESE's membrane. Finally, MVBs are released by ectocytosis eventually generate exosomes (Kalluri and LeBleu 2020). One hypothesis about the function of EVs proposes that exosomes may take off excessive components in cells to preserve cellular homeostasis (Kalluri and LeBleu 2020). Although the physiological purpose of exosome production remains largely unknown, the studies reviewed in this article indicate that the function, targeting, and particular constituent in exosomes suggest that they could play a significant part by adjusting cell-to-cell communication.

In this article, we deliberate about the application potential of EVs in herbal therapies for DD by summarizing the body of work available in PubMed published over the last 10 years. Hence, this review provides a reference for further research of EVs, particularly in developing CHM for treating DD.

2 THE PATHOGENIC ROLE OF EXTRACELLULAR VESICLES IN DEPRESSION

Depending on the cellular sources, different subcellular components containing DNA, RNA, proteins, lipids, metabolites et al. are delivered into recipient cells by EVs, which can effectively alter the biological response to diseases. The pathogenesis of depression mainly involves synaptic plasticity, oxidative stress, intestinal flora, dysregulation of the hypothalamic pituitary adrenal (HPA) axis, and altered neurotransmitter metabolism and neuroinflammation (Bhatt et al., 2021; Zhang et al., 2021). Signal transmission from one nerve cell to another is essential for synaptic plasticity (Chivet

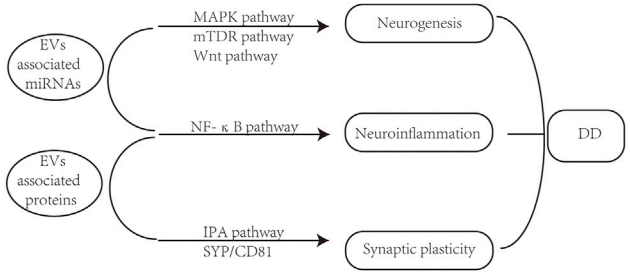

FIGURE 2 | EVs associated pathogenic changes in DD. EV associated microRNAs and proteins can regulate neurogenesis, neuroinflammation, and synaptic plasticity in the development of DD.

et al., 2012). Given their prominent role in regulating intercellular communication, more and more researches have explored the potential parts of circulating EVs in the etiopathogenesis of depression via the regulation of neurotransmitters. It has been reported that exosomes are associated with cell-to-cell communication, neuroinflammation, neurogenesis and synaptic plasticity in the brain (Saeedi et al., 2019). These pathophysiological changes in the central nervous system (CNS) reflect EVs' functional potential and emerging significance in developing DD (see **Figure 2**). In particular, most preclinical studies have focused on the roles of microRNA (miRNA, see **Table 1**) or protein (**Table 2**) contents of EVs in DD.

2.1 Extracellular Vesicle-Associated microRNAs in Depressive Disorders

MiRNAs are small noncoding RNAs(~22 nucleotides) that perform as post-transcriptional gene regulators through uniting with target messenger RNAs, typically leading to their degradation and subsequent silencing of the target gene (Ramshani et al., 2019). Small (~30–150 nm), secreted EVs transport miRNAs between cells (Valadi et al., 2007; Mathivanan et al., 2010; Théry et al., 2018), enabling these miRNA cargoes to target genes that directly or indirectly contribute to pathological processes (such as accelerating neuroplasticity and brain development) related to depression. For example, one study showed that exosomes isolated from DD patients could cause depressive-like behaviors in normal mice, while exosomes isolated from healthy volunteers and exosomal miR-139-5p apparently alleviated these behavioral changes (Wei ZX. et al., 2020). In addition, exosomal miR-207 was found to alleviate depressive symptoms of stressed mice through targeting Tril, resulting in inhibition of NF-κB signaling in astrocytes (Li et al., 2020). These findings thus supported a relationship between miRNA-bearing exosomes and depression-like behaviors (Li et al., 2020). Collectively, these findings suggest that miRNA-bearing exosomes can attenuate or exacerbate the pathogenesis of depression, although clinical studies are needed to explore these possibilities in humans (see **table 1**).

TABLE 1 | EV-associated miRNAs and their expression in DD.

miRNA	Sample source	Application model/disease	Applied species	Expression	References
miR-139-5p	Blood	MDD	human	↑	(Wei et al., 2020b; Liang et al., 2020)
miR-207	NK cells	CMS	mice	↑	Li et al. (2020)
miR-17-5p	Blood	Subthreshold depression	human	↑	Mizohata et al. (2021)
miR-29c	Whole-brain lysates and hippocampal	Flinders Sensitive Line depression model	rats	↑	Choi et al. (2017)
miR-149	Whole-brain lysates	Flinders Sensitive Line depression model	rats	↑	Choi et al. (2017)

TABLE 2 | EV-associated proteins and their potential targets in DD.

Proteins	Molecular weight	Model/disease/intervention	Species	Sample source	Expression	References
Aldolase C	~39 kDa	Restraint	rat	serum	↑	Gómez-Molina et al. (2019)
Aldolase C	~39 kDa	Immobilization	rat	serum	↓	Gómez-Molina et al. (2019)
astrocytic GFAP	~51 kDa	Restraint	rat	serum	↑	Gómez-Molina et al. (2019)
astrocytic GFAP	~51 kDa	Immobilization	rat	serum	↓	Gómez-Molina et al. (2019)
synaptophysin	38 kDa	Restraint	rat	serum	↓	Gómez-Molina et al. (2019)
synaptophysin	38 kDa	Immobilization	rat	serum	↓	Gómez-Molina et al. (2019)
reelin	~388 kDa	Restraint	rat	serum	↓	Gómez-Molina et al. (2019)
reelin	~388 kDa	Immobilization	rat	serum	↓	Gómez-Molina et al. (2019)
BDNF	~13 kDa	Ketamine	rat	astrocytes	↓	Stenovec et al. (2016)
IL34	39 kDa	MDD	human	blood	↑	Kuwano et al. (2018)
L1CAM	200–220 kDa	MDD	human	plasma	↑	Nasca et al. (2020)
IRS-1	180 kDa	MDD	human	plasma	↑	Nasca et al. (2020)
Sig-1R	25 kDa	MDD	human	plasma	↑	Wang et al. (2021b)
CD40 ligand	33 kDa	MDD	human	plasma	↑	Wallensten et al. (2021)

2.2 Extracellular Vesicle-Associated Proteins in Depressive Disorders

Clinical and preclinical proteomics studies have indicated that proteins carried by EVs could potentially serve as biomarkers for depression (Kuwano et al., 2018; Gómez-Molina et al., 2019; Nasca et al., 2020). A study by comparing the proteins in small EVs in two animal models of stress response with depressive-like behaviors has revealed aldolase C, astrocytic GFAP (glial fibrillary acidic protein), synaptophysin (SYP, a synaptic protein), and reelin among the different treatment groups significantly changed (Gómez-Molina et al., 2019; Li et al., 2020). In addition, a study established that SYP, tumor necrosis factor receptor 1 (TNFR1), and interleukin 34 (IL-34) in DD patients' neuron derived exosomes (NDE) were all positively correlated with the exosomes surface marker cluster of differentiation 81 (CD81) (Kuwano et al., 2018). Another clinical study reported more insulin receptor substrate 1 (IRS-1) in L1 Cell Adhesion Molecule + (L1CAM) exosomes from DD patients. The increased IRS levels in the L1CAM + exosomes were associated with suicidality and anhedonia (Nasca et al., 2020). In addition to screening for EV-associated protein biomarkers of DD, other studies have explored mechanistic connections between MDD and EV protein cargoes. One such study reported that ketamine could suppress the secretion of BDNF and ATP-triggered EV fusion through decreasing astrocytic Ca^{2+} excitability and elevating the possibility of oping narrow fusion pore (Stenovec et al., 2016). Furthermore, Stenovec et al. found that ketamine can diminish the cytoplasmic mobility of EVs to alter the astroglial ability to regulate extracellular K+ (Stenovec et al., 2020). These cumulative findings suggest that protein-bearing EVs contribute to the development of DD (possibly related to the EV fusion process) and could be potential clinical biomarkers for DD (see **Table 2**).

3 HERBAL THERAPIES FOR DEPRESSIVE DISORDERS

Herbal therapies are an integral component of traditional Chinese medicines (TCM). Currently, herbal therapies are widely used in China as essential alternative medicine and have been reported to ameliorate clinical symptoms of COVID-19 (Hu et al., 2021). Herbal remedies can be taken in many forms in TCM, and studies into their mechanisms of action and therapeutic efficacy are typically categorized by whether they are administered as herbal formulas (multiple herbs prescriptions), individual herbs, or specific phytochemicals (bioactive herbal constituents) (Hirshler and Doron 2017; Lin et al., 2019). Below, we discuss the antidepressant effects of these three types of herbal therapies.

3.1 Herbal Formulas for Treating Depressive Disorders

Numerous preclinical and clinical studies of herbal formulas have described the antidepressant effects of herbs such as Yueju (Ren and Chen 2017), Chai Hu Shu Gan San (Sun et al., 2018), or lily bulb and Rehmannia Decoction (Chi et al., 2019). The antidepressant mechanisms differ among these herbal formulas. For example, Bangpungtongsung-San was shown to reduce levels of nitric oxide (NO), inducible nitric oxide synthase (iNOS), cyclooxygenase (COX)-2, tumor necrosis factor-α (TNF-α), interleukin-1β (IL-1β), and interleukin-6 (IL-6) in a dose-dependent manner via decreased expression of nuclear factor (NF)-κB p65, which suggested that its antidepressant effects were likely related to the suppression of neuroinflammation (Park et al., 2020). By contrast, the antidepressant mechanisms of Jiaweisinisan appeared to be associated with regulating immune-mediated inflammation, cell apoptosis and synaptic transmission (Chen et al., 2020). In addition, Xiaoyaosan exhibited synergistic antidepression effects by adjusting Caspase-3 and Nitric oxide synthase-3 (Liu et al., 2021). These studies provide mechanistic evidence that at least partially explains the therapeutic effects of these herbal formulas, although further analytical chemistry is needed to narrow down the contributions of each herbal component.

3.2 Individual Herbs for Treating Depressive Disorders

While herbal formulas comprised of multiple herbal components are commonly prescribed for DD, several herbal therapies reported to provide antidepressant effects use individual herbs, such as Cistanche (Wang et al., 2017), rosemary (Ghasemzadeh Rahbardar and Hosseinzadeh 2020), Angelicae Sinensis Radix (Gong et al., 2019). Senegenin (Li H. et al., 2017), Panax ginseng (Wang W. et al., 2018), *Lonicera japonica* Thunb (Liu et al., 2019), Polygonum aviculare L. (Park et al., 2018), Hemerocallis citrina (Li CF. et al., 2017), Ginkgo (Zhao et al., 2015) and Armillaria mellea (Vahl) P. Kumm. (Lin et al., 2021). exert the antidepression effect through inhibiting neuroinflammation. Lycium barbarum deploys a protective effect on depression by promoting neurogenesis (Po et al., 2017). Baicalin exerts an antidepressant effect through enhancing neuronal differentiation (Zhang R. et al., 2019). Perilla frutescens (Ji et al., 2014a), Tribulus terrestris (Wang Z. et al., 2013), and Rehmannia glutinosa Libosch (Wang JM. et al., 2018) alleviate depression by regulating neuroendocrine. Angelicae Sinensis Radix manifests an antidepression effect by modulating the hematological anomalies (Gong et al., 2019). Agarwood exhibits the antidepressive effect by suppressing the HPA axis (Wang S. et al., 2018). Here we listed herbs that were reported to be effective in treating depression published in the past 10 years (see **Table 3**).

3.3 Phytochemicals for Treating Depressive Disorders

Although many herbs can exhibit various biological responses, the specific molecular mechanisms of these activities are still mainly uncharacterized. Because of the complexity of multiple chemicals and their efficacies, few herbal pharmacokinetic parameters have been applied successfully for therapeutic monitoring. From the herbal formulas to the individual

TABLE 3 | Antidepressant mechanism of herbs.

Herbs	Model	Species	Antidepressant mechanism	References
Senegenin	CUMS	mice	↑ BDNF and NT-3. ↓NF-κB, NLRP3	Li et al. (2017c)
Lycium barbarum	DXM	rats	↑hippocampal neurogenesis induced by DXM.	Po et al. (2017)
Panax ginseng	LPS	mice	↓IL-6 and TNF-α in serum; IκB-α, NF-κB.↑BDNF, TrkB, Sirt 1 in the hippocampus; SOD.	Wang et al. (2018d)
Lonicera japonica Thunb	CUMS	mice	↑NLRP3, IL-1β, caspase-1 in the hippocampus	Liu et al. (2019)
Perilla frutescens	CUMS	mice	↑5-HT and 5-HIAA in the hippocampus. ↓IL-6, IL-1β, TNF-α	Ji et al. (2014a)
Polygonum aviculare L	RS	mice	↓CORT, 5-HT, adrenaline, noradrenaline in the brain and serum; CD68, Ibal-1, TNF-α, IL-6, and IL-1β in the brain	Park et al. (2018)
Hemerocallis citrina	LPS	mice	↓NF-κB, iNOS, COX-2 in the prefrontal cortex	Li et al. (2017a)
Ginkgo	LPS	mice	↓TNF-α, IL-1β, IL-6, IL-17A.↑BDNF, IL-10 in hippocampus	Zhao et al. (2015)
Tribulus terrestris	CMS	rats	↓CRH and CORT in serum	Wang et al. (2013b)
Rehmannia glutinosa Libosch	CUMS	rats	↓CORT in serum.↑protein and mRNA of BDNF, mRNA of TrkB in the hippocampus	Wang et al. (2018b)
Agarwood	RS	mice	↓IL-1α, IL-1β, IL-6 in serum; nNOS mRNA in the cerebral cortex and hippocampus; nNOS protein in the hippocampus	Wang et al. (2018c)
Armillaria mellea (Vahl) P. Kumm	FST, UCMS	rats	↓IL-1β, TNF-α in the serum and cerebrum; IBA1	Lin et al. (2021)
Angelicae Sinensis Radix	CUMS	rats	↓PDK-1, LDHA	Gong et al. (2019)
Baicalin	CUMS	mice	↑p-Akt, FOXG1, and FGF2	Zhang et al. (2019b)

phytochemicals, the object of study becomes more precise. Because the structure of phytochemicals is explicit, it is gained more and more attention recently. As chemical compounds produced by herbs, phytochemicals can be used as the basic unit of herbal research. **Table 4** presents antidepressant mechanisms of reported phytochemicals in recently 10 years (see **Table 4**).

4 EXTRACELLULAR VESICLES AND HERBAL THERAPIES

Herbal formulas are composed of various herbs, and the individual herb is composed of a variety of phytochemicals. Due to the complex composition of herbal formulae and individual herbs, it is challenging to use EVs to deliver herbal formulas. There are studies using EVs to deliver phytochemicals. A study reported that EVs packaged with curcumin preserve mice from septic shock provoked by lipopolysaccharide (LPS), and it also shown EVs can increase their bioavailability stability and solubility when served as vehicles of curcumin (Sun et al., 2010). Another study reported daily intranasal delivery of curcumin-loaded EVs diminished experimental autoimmune encephalomyelitis, whose mechanism may resulted from increasing induction of apoptosis in microglial cells (Zhuang et al., 2011). These studies demonstrate the potential of EVs for delivering phytochemicals.

In addition, the EVs secreted from cells treated with herb and herb-derived EVs exhibit a therapeutic effect. Ruan et al. found Suxiao Jiuxin pill promotes cardiac mesenchymal stem cells (CMSC) secret exosome through a GTPase-dependent pathway (Ruan et al., 2018a). Exosomes extracted from Suxiao Jiuxin pill-treated CMSC can also decline the expression of H3K27 demethylase UTX, furthermore, enhance cardiomyocyte proliferation (Ruan et al., 2018b). Besides EVs secreted by cells treated with herbal formulas, the EVs isolated from plant samples also had therapeutic functions (Kim et al., 2021). Vesicles derived from plants are structural units composed of various primary and secondary metabolites, which play a synergistic role in biological transport and pharmacodynamics (Cao et al., 2019b). Zhang et al. reported that plant cell secrets, EVs, and plant-derived EVs could be a new therapeutic method against diseases (Zhang et al., 2016c). For example, EVs-liked ginseng-derived nanoparticles (GDNPs) can be recognized and internalized with macrophages and induce M1-type polarization of macrophages to inhibit melanoma growth in mice (Cao et al., 2019c). Exosomes derived from ginseng can promote the neural differentiation of bone marrow derived mesenchymal stem cells (Xu et al., 2021). In addition, the targeting specificity of plant-derived EVs can also be improved by modifying their surface. For example, folate-conjugated arrowtail pRNA-3WJ were reported to facilitate the binding and uptake of ginger-derived exosome-like nanovesicles to NK cells (Li et al., 2018).

Moreover, EVs are used as biomarkers in herbal research. For example, Platelet-derived microvesicles (PMVs) were the indicator of platelets activation in a study that explores Tanshinone IIA's function in a cluster of differentiation 36 (CD36) and mitogen-activated protein kinase kinase 4/c-Jun NH 2 terminal kinase (MKK4/JNK2) signaling pathway (Wang H. et al., 2020). Tanshinone IIA also elicited its impacts by the eicosanoid metabolism pathway and provoking endothelial microparticles production (Liu et al., 2011). Macropinocytosis is known to be a form of actin-dependent endocytosis, which is an endocytic procedure that typifies the engulfment of macropinosomes. Macropinosomes are large vesicles that consist of extracellular fluid. Tubeimoside-1 (TBM1), a low toxic triterpenoid saponin isolated from

TABLE 4 | Antidepressant mechanism of phytochemicals.

Phytochemicals	Molecular weight	Original medical herbs	Model	Species	Antidepressant mechanism	References
Trans-cinnamaldehyde	132.16 g/mol	Ramulus Cinnamomi	FST	mice	↑5-HT, Glu/GABA; ↓COX-2, TRPV1, CB1	Lin et al. (2019)
Trans-cinnamaldehyde	132.16 g/mol	Cinnamomum cassia	CUMS	rats	↓ TLR4, NF-κB-1, p-p65, TNF-α, NLRP3, ASC, caspase-1, IL-1β, and IL-18 in the prefrontal cortex and hippocampus	Wang et al. (2020b)
Perillaldehyde	150.22 g/mol	Perilla frutescens	LPS	mice	↓ the levels of TNF-α and IL-6 in both the serum and the prefrontal cortex; ↑ 5-HT and NE in the prefrontal cortex	Ji et al. (2014b)
Perillaldehyde	150.22 g/mol	Perilla frutescens	CUMS	rats	↓ TXNIP, NLRP3, Cleaved caspase-1 and p-NF-κB p65 in the hippocampus	Song et al. (2018)
Ferulic acid	194.18 g/mol	Radix Glycyrrhizae	CUMS	mice	↓IL-1β, IL-6,TNF-α, NF-κB, NLRP3 in the prefrontal cortex	Liu et al. (2017b)
Resveratrol	228.24 g/mol	Veratrum album	Ouabain	mice	↓ IL-1β, IL-17A, IL-8, TNF-α in plasma	Wang et al. (2018a)
Resveratrol	228.24 g/mol	Veratrum album	CUMS	rats	↓ CORT in plasma and CRH mRNA in the hypothalamus; ↑IL-6, CRP, TNF-α in plasma	Yang et al. (2017)
Honokiol	266.3 g/mol	Magnolia officinalis	LPS	mice	↓ TNF-α, IL-1β, IDO, IFN-γ, free calcium in brain tissue; ↑quinolinic acid	Zhang et al. (2019a)
Baicalein	270.24 g/mol	Scutellaria baicalensis	EAP	mice	↓mRNA of TNF-α, IL-1β, IL-6, IL-8	Du et al. (2019)
Helicid	284.2 g/mol	Helicia nilagirica	CUMS	rats	↑cAMP, PKA C-α, and p-CREB the proliferation of neurons; ↓SERTs	Li et al. (2019)
Gastrodin	286.28 g/mol	gastrodia elata	CUS	rats	↑NSCs proliferation in the hippocampus; ↓p-iκB, NF-κB, IL-1β	Wang et al. (2014b)
Salidroside	300.3 g/mol	Rhodiola rosea	Olfactory bulbectomized	rats	↓IL-1β, IL-6; ↓NF-κB	Zhang et al. (2016d)
Salidroside	300.3 g/mol	Rhodiola rosea	Olfactory bulbectomized	rats	↑GR, BDNF in the hippocampus; ↓CRH in hypothalamus	Yang et al. (2014)
Z-guggulsterone	312.4 g/mol	Commiphora mukul	CUS	mice	↑ERK1/2, CREB, pAkt, BDNF in the hippocampus, hippocampal neurogenesis	Liu et al. (2017a)
3-(3,4-methylenedioxy-5-trifluoromethyl phenyl)-2E-propenoic acid isobutyl amide	315.29 g/mol	Piper laetispicum C. DC	LH and SDS	mice	↑TSPO, VADC1, Park, Beclin 1, KIFC2, Snap25	Wei et al. (2020a)
Sinomenine	329.4 g/mol	Sinomenium acutum	CUMS	mice	↑NE and 5-HT in the hippocampus, NLRP3; ↓IL-1β, IL-6, and TNF-α in the hippocampus	Liu et al. (2018)
Andrographolide	350.4 g/mol	Andrographis paniculata	CUMS	mice	↓NO, COX-2, iNOS, IL-1β, IL-6, TNF-α, p-p65, p-IκBα, NLRP3, ASC, caspase-1 in the prefrontal cortex	Geng et al. (2019)
Curcumin	368.4 g/mol	Rhizoma Curcumae longae	CUMS	rats	↓ IL-1β, IL-6, TNF-α and NF-κB	Fan et al. (2018)
Curcumin	368.4 g/mol	Rhizoma Curcumae longae	CUMS	rats	↓ mRNA of IL-1β, IL-6, TNF-α, NF-κB	Zhang et al. (2019c)
2,3,5,4′-Tetrahydroxystilbene-2-O-beta-D-glucoside	406.4 g/mol	Polygonum multiflorum	CRS	mice	↓TNF-α, IL-1β, IL-6 in hippocampal and prefrontal cortex	Jiang et al. (2018)
2,3,5,4′-Tetrahydroxystilbene-3-O-beta-D-glucoside	406.4 g/mol	Polygonum multiflorum	LPS	mice	↓ IL-1β, IL-6, TNF-α, and oxido-nitrosative stress hippocampus and prefrontal cortex	Chen et al. (2017)
Puerarin	416.4 g/mol	Radix Bupleuri	CUS	rats	↑ progesterone, allopregnanolone, 5-HT, and 5-HIAA in the prefrontal cortex and hippocampus	Qiu et al. (2017)
Baicalin	446.4 g/mol	Scutellaria baicalensis Georgi	CUMS	mice	↑ neurogenesis, p-Akt, FOXG1, FGF2	Zhang et al. (2019b)
Baicalin	446.4 g/mol	Scutellaria baicalensis Georgi	CUMS	mice	↓IL-1β, IL-6, TNF-α in the hippocampus, and TLR4; ↑PI3K, AKT, and FoxO1	Guo et al. (2019)
Baicalin	446.4 g/mol	Scutellaria baicalensis Georgi	CUMS	rats	↑DCX, NSE, BDNF in the hippocampus, SOD; ↓caspase-1, IL-1β in the hippocampus, MDA.	Zhang et al. (2018b)
Baicalin	446.4 g/mol	Scutellaria baicalensis Georgi	Corticosterone	mice	↑ the protein of 11β-HSD2 in the hippocampus, mRNA, and protein of GR	Li et al. (2015)

(Continued on following page)

TABLE 4 | (*Continued*) Antidepressant mechanism of phytochemicals.

Phytochemicals	Molecular weight	Original medical herbs	Model	Species	Antidepressant mechanism	References
					and BDNF; ↓SGK1 in the hippocampus and serum	
Iridoids	456.4 g/mol	Gardeniae fructus	SRS	mice	↑GluA1, p-Akt/Akt, p-mTOR/mTOR, p-P70S6K, PSD-95, Synapsin-1	Xia et al. (2021)
Paeoniflorin	480.5 g/mol	Radix Paeoniae Alba	Interferon-alpha	mice	↓ IL-6, IL-10,TNF-α in the medial prefrontal cortex	Li et al. (2017d)
Senegenin	537.1 g/mol	Polygala tenuifolia Willd	CUMS	mice	↑BDNF, NT-3; ↓ IL-1β	Li et al. (2017c)
Icariin	676.7 g/mol	Epimedium herb	Ovary remove and CUS	rats	↑AKT, p-AKT, PI3K (110 kDa, 85 kDa), Bcl-2 in the ovaries; ↓Bax	Cao et al. (2019a)
Icariin	676.7 g/mol	Herba Epimedii	CMS	rats	↓ TNF-α, IL-1β, NF-κB, NLRP3, mRNA of iNOS.	Liu et al. (2015)
Salvianolic acid B	718.6 g/mol	Salvia militiorrhiza Bunge	CMS	rats	↓NLRP3, MDA; ↑CAT, SOD, GPx	Huang et al. (2019)
Salvianolic acid B	718.6 g/mol	Salvia militiorrhiza Bunge	CMS	mice	↓ IL-1β, TNF-α, apoptosis, and microglia activation in the hippocampus and cortex; ↑IL-10, TGF-β in the hippocampus and cortex	Zhang et al. (2016a)
Saikosaponin A	781 g/mol	Bupleurum chinense	MCAO with CUMS and isolation	rats	↓Bax, Caspase-3, hippocampal neuronal apoptosis; ↑BDNF, p-CREB and Bcl-2	Wang et al. (2021a)
Saikosaponin-D	781 g/mol	Bupleurum chinense	LPS	mice	↓ HMGB1 translocation from nuclear to extracellular, TLR4, p-IκB-α, NF-κBp65	Su et al. (2020)
Saikosaponin-D	781 g/mol	Bupleurum chinense	CUMS	rats	↑ DCX, p-CREB, BDNF.	Li et al. (2017b)
Ginsenoside Rg3	785 g/mol	Panax ginseng	LPS	mice	↓ mRNA of pro-inflammatory cytokines, IDO; ↓ IL-6, TNF-α in plasma	Kang et al. (2017)
Ginsenoside Rg3	785 g/mol	Panax ginseng	CUS	rats	↑ progesterone, allopregnanolone, 5-HT in the prefrontal cortex and hippocampus; ↓ CRH, CORT, ACTH.	Xu et al. (2018)
Ginsenoside-Rg1	801 g/mol	Panax ginseng	CUMS	rats	↑SOD, GSH-Px; ↓MDA, NO, ROS, 4-HNE, 8-OHdG	Cao et al. (2019b)
Ginsenoside-Rg1	801 g/mol	Panax ginseng	CUMS	rats	↓CORT in serum; ↑testosterone in serum, GR protein in the PFC and hippocampus	Mou et al. (2017)
Ginsenoside-Rg1	801 g/mol	Panax ginseng	CSDS	mice	↓iNOS, COX2, caspase-9, caspase-3, Iba1 in the hippocampus, IL-6, TNF-α, IL-1β	Jiang et al. (2020)
Chiisanoside	955.1 g/mol	Acanthopanax sessiliflorus	LPS	mice	↓IL-6, TNF-α in serum, BDNF, TrkB, NF-κB in hippocampal; ↑SOD and MDA.	Bian et al. (2018)
Crocin	977 g/mol	Gardenia jasminoides and Crocus sativus	LPS	mice	↓ CD16/32 (M1), iNOS, NF-κB p65, NLRP3, cleavage caspase-1; ↑CD206 (M2) in the hippocampus	Zhang et al. (2018d)

Bolbostemma paniculatum (Maxim.), efficiently lead to *in vitro* and *in vivo* micropinocytosis, which is able to traffic small molecules into colorectal cancer (CRC) cells (Gong et al., 2018). Another study demonstrated that matrine could induce macropinocytosis and the regulation of adenosine triphosphate (ATP) metabolism (Zhang B. et al., 2018). In Fructus Meliae Toosendan -induced liver injury mice, serum exosomal miR-222 and miR-370-3p were reported as significantly downregulated miRNAs (Zheng et al., 2018; Yu et al., 2020). By suppressing TGF1 exosomes transferring from Glomerular mesangial cells to glomerular endothelial cells, Tongxinluo can impede renal fibrosis in diabetic nephropathy (Wu et al., 2017). Buyang Huanwu Decoction can enhance angiogenic by elevating miRNA-126 levels in mesenchymal stem cell secreted exosomes (Yang et al., 2015).

5 FUTURE PERSPECTIVES

5.1 Extracellular Vesicles: A New Delivery Approach for Treatments of Depression?

Blood-brain barrier (BBB) restricts the substances passing between the CNS and the vascular circulation system, thereby protecting the CNS from exposure to overactive immune responses or toxic substances (Obermeier et al., 2013; Andreone et al., 2015). Since the substrates from the blood to the CNS is controlled by the BBB (Kadry et al., 2020), effective drug transfer to the brain poses a challenge for treating CNS disorders, including neurodegenerative diseases, stroke, autoimmune diseases, or neuropsychiatric diseases like DD (Abbott et al., 2006; Upadhyay 2014). Almost all large molecule biologics and about 98% of small molecule

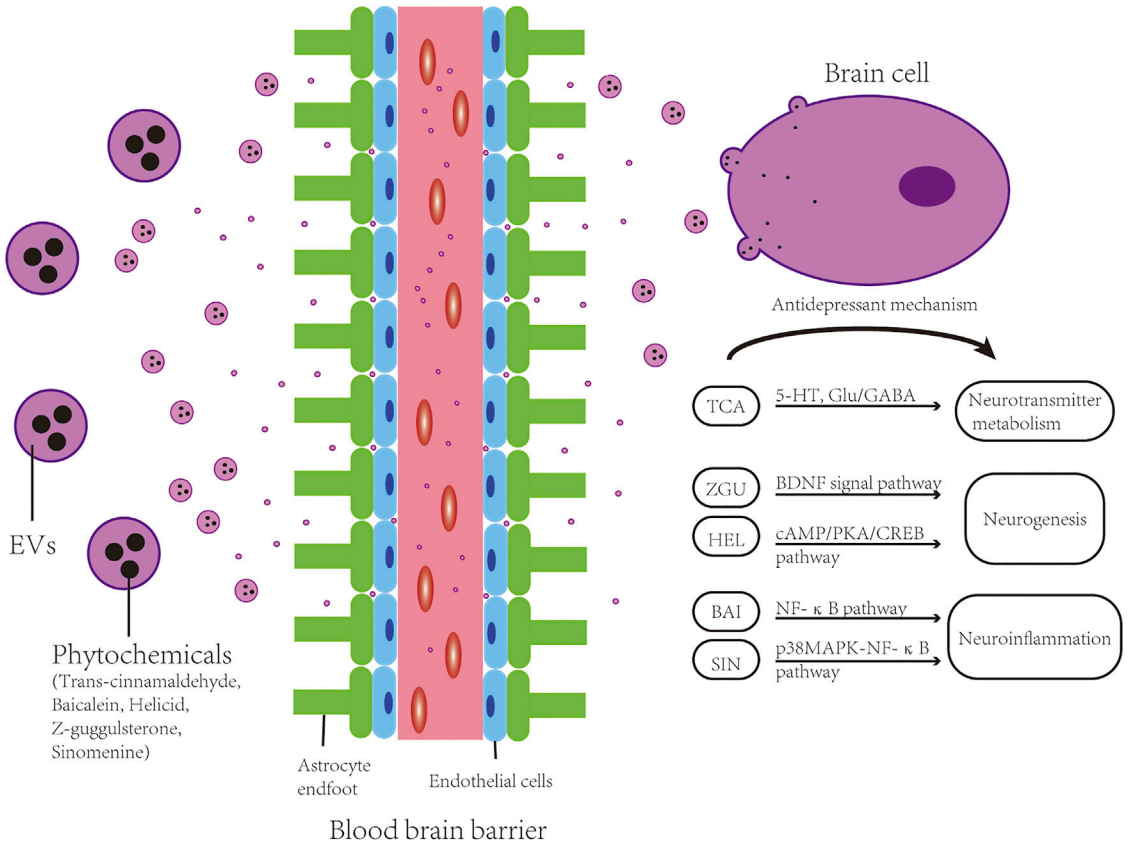

FIGURE 3 | EVs for DD treatment by drug delivery. Phytochemicals such as Trans-cinnamaldehyde (TCA), Baicalein (BAI), Helicid (HEL), Z-guggulsterone (ZGU) and Sinomenine (SIN) can be packaged into extracellular vesicles and conveyed through the BBB to the brain cells (neurons and neuroglial cells), and exert antidepressant effect by regulating neuroinflammation, neurogenesis and neurotransmitter metabolism through a variety of pathways.

drugs cannot traverse the BBB (Pardridge 2012). Nevertheless, the BBB permits transmembrane diffusion of lipid soluble (lipophilic) molecules smaller than 400 Da and can selectively transport some compounds into and out of the brain (Sanchez-Covarrubias et al., 2014). In this context, EVs could have advantages as drug vehicles, such as their small size, low immunogenicity, and ability to cross the BBB carrying cellular components or pharmacological agents (see **Figure 3**). Since EVs have the regenerative ability, they can also be exploited to potentially inhibit ongoing neurodegenerative processes associated with DD (Bhatt et al., 2021). Previous researches have established the successful transmission of exosomes to the brain in mice via intranasal injection or intravenous administration (Zhuang et al., 2011; Yuan et al., 2017). Another study also showed that exosomes could pass over the BBB and communicate bi-directionally between the brain and the rest of body (Bhatt et al., 2021). Despite the expected benefits of EVs for the treatment of DD, precise mechanisms of action and routes of delivery still require careful and rigorous investigation (Bhatt et al., 2021).

Herbal compounds are derived from diverse natural products. Since Chinese herbal concoctions are complex and undefined mixtures, it is challenging to demonstrate which component of the herbal therapy is responsible for a given effect (Corson and Crews 2007; Xu 2011). In particular, small phytochemicals could serve as viable cargoes for EV delivery (Liu et al., 2021) (Li et al., 2021). Indeed, studies exploring the application of EVs as vehicles for drug delivery have already begun. For example, curcumin-loaded EVs were found to protect mice from lipopolysaccharide (LPS)- induced septic shock (Sun et al., 2010). However, very few studies have examined DD treatment with phytochemical-loaded EVs, suggesting great potential for this line of research. For further references of phytochemical-loaded EVs research of DD, we screened potential phytochemicals from **Table 4** by Lipinski's rule of five, the rule of thumb to evaluate if a chemical compound has chemical properties and physical properties would make it an orally active drug in humans (see **Table 5**).

Besides serving as cargoes for EV delivery, herbs can also be applied to be the vehicle of EV. Distinct from artificially fabricated liposomes, plant-derived nanovector was reported to transport chemotherapeutic agents through mammalian hindrances such as BBB, and refrain from inflammatory response or necrosis (Wang Q. et al., 2013). Moreover, the lipid bilayer structure of plant-derived nanovector can protect

TABLE 5 | Potential phytochemicals screened by Lipinski's rule.

Phytochemicals	Molecular weight	Hdon	Hacc	AlogP	RBN	Lipinski's rule	OB (%)	BBB
Honokiol	266.3 g/mol	2	2	4.83	5	Yes	60.67	0.92
Z-guggulsterone	312.4 g/mol	0	2	3.75	0	Yes	42.45	0.33
Ferulic acid	194.18 g/mol	2	3	2	3	Yes	40.43	0.56
Perillaldehyde	150.22 g/mol	0	1	2.67	2	Yes	39	1.57
Baicalein	270.24 g/mol	3	5	2.33	1	Yes	33.52	–0.05
Trans-cinnamaldehyde	132.16 g/mol	0	1	1.95	2	Yes	31.99	1.48
Sinomenine	329.4 g/mol	1	5	1.32	2	Yes	30.98	0.43
Resveratrol	228.24 g/mol	3	3	3.01	2	Yes	19.07	–0.01
Gastrodin	286.28 g/mol	5	7	-0.95	4	Yes	8.19	–2.29
Salidroside	300.3 g/mol	5	7	-0.47	5	Yes	7.01	–1.41
Curcumin	368.4 g/mol	3	6	3.36	7	Yes	5.15	–0.76

Hdon and Hacc are possible number hydrogen-bond donors and acceptors, respectively; RBN, means the number of the bonds allowing free rotation around themselves; AlogP value is the partition coefficient between octanol and water, which is crucial for measuring hydrophobicity of molecule; OB: oral bioavailability; BBB: blood-brain barrier, BBB $<$ *-0.3 were considered as non-penetrating (BBB-), from -0.3 to +0.3 moderate penetrating (BBB±), and* $>$ *0.3 strong penetrating (BBB+).*

the cargo from the enzymatic decomposition of proteinases and nucleases (Wang et al., 2015). Since plants do not retain zoonotic or human pathogens, plant-derived EVs take advantage of non-immunogenic and innocuous compared with mammalian cell-derived EVs(Schuh et al., 2019; Dad et al., 2021). On the other side, plant-derived EVs do not have cell targeting specificity because they have no ligands in comparison to mammalian cell-derived EVs. Previous studies reported that plant-derived EVs arrive at the liver and intestines through their natural biodistribution properties (Wang B. et al., 2014; Zhuang et al., 2015; Zhang et al., 2016b). Fortunately, plant-derived EVs can obtain specific cellular targeting by modification (Wang Q. et al., 2013).

5.2 Herb-Derived Extracellular Vesicles: Emerging Therapeutics for Depression?

As mentioned before, plant-derived EVs are beneficial to be the vehicle of phytochemicals since they are innocuous, low immunogenicity, and editable for target specificity. They can also promote cellular uptake and have higher stability in the GI tract (GIT) (Fujita et al., 2018), and the versatile therapeutic potential of plant-derived EVs rooted in their active source plants (Mu et al., 2014). Moreover, EVs extracted from the plant have been reported to be introduced via oral (Wang B. et al., 2014; Zhang et al., 2017), intravenous (Li et al., 2018), intramuscular, and intranasal administration (Wang Q. et al., 2013; Ju et al., 2013). This is another advantage of herb-derived EVs compared with Chinese herb decoction because the component complexity is always troubling applying effective Chinese herb to intramuscular, intravenous, and intranasal administration. These characteristics above make herb-derived EVs attractive to be an emerging therapeutic. Although many research have explained the anti-depressant mechanism of Chinese herbs (see **table 3**), few studies explored the effect of Chinese herb-derived EVs in treating depression, which is an exciting direction required to be followed.

5.3 Extracellular Vesicles: Potential Biomarkers for Diagnostic Depression

The unique property of EVs that can easily traverse BBB makes EVs a potential early diagnostic marker of CNS disorders like depression (Chen et al., 2016; Yao et al., 2018; Cufaro et al., 2019). Candidate protein biomarkers and potential diagnostic miRNAs for DD have been suggested (Al Shweiki et al., 2017; Tavakolizadeh et al., 2018; Saeedi et al., 2019). Besides miRNAs and proteins, exosomes as nanocarriers own the potential to be diagnostic biomarkers in various CNS disorders including DD (Perets et al., 2018; Wallensten et al., 2021).

The reasons why exosomes have the potential to be clinical diagnostics and biomarker are as follow (Kanninen et al., 2016): Firstly, exosomal contents can be changed along with disease conditions, which can reflect the dynamic state of disease in real-time; Secondly, exosomes can be easily extracted non-invasively from biological fluids (Bhatt et al., 2021), which is particular important because non-invasive availability is beneficial to early diagnosis of DD; Thirdly, exosomal contents are protected by the membranous structure, which keeps off the degradation of potential biomarkers (Kanninen et al., 2016); Fourthly, exosomes are very stable and can be preserved for prolonged periods (Grapp et al., 2013), making their clinical application feasible; Fifthly, exosomes can express their original cellular surface markers, so that they can be traced to their origin; Last but not least, since exosomes are able to pass over the BBB, which provide information of CNS cells that is hard to obtain without invasive techniques (Boukouris and Mathivanan 2015; Kawikova and Askenase 2015; Lin et al., 2015; Aryani and Denecke 2016). Because exosomes are distributed in all biological fluids and all cells can secret them, their biogenesis enables the arresting of the complex extracellular and intracellular molecular cargo (Kalluri and LeBleu 2020), rendering exosome-based liquid biopsy attractive in diagnosing the prognosis of DD. Liquid biopsies can allow us to understand the pathophysiology change of DD and diagnose the progressive disorders in the early stages (Topuzoğlu and Ilgın 2020). Moreover, studies relating the biomarkers associated with EVs in the context of

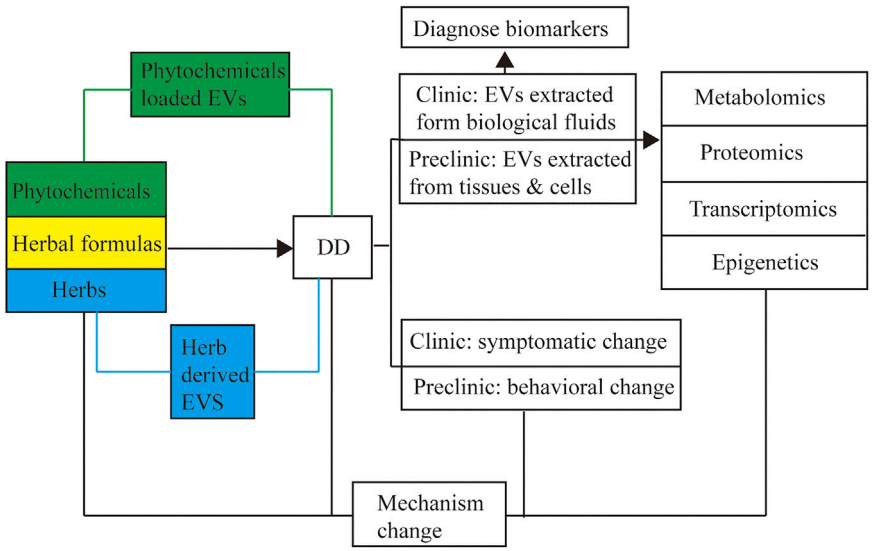

FIGURE 4 | EVs application for CHM. Combined with metabolomics, proteomics, transcriptomics, and epigenetics, extracellular vesicles can be applied to explore the mechanism when treating DD with herbal formulas and act as the potential diagnose biomarkers in the clinic and preclinic studies.

DD still need more exploration. However, with the utility of liquid biopsy in diagnosing the prognosis of DD, the multicomponent analysis of EVs in the future may determine the disease progression and response to treatment.

5.4 Extracellular Vesicles: A Connection Bridge Between Herbal Therapies for Depression and Metabolomics, Proteomics, Transcriptomics and Epigenetics Studies

Metabolomics is a discipline to obtain all information of metabolites in a biological sample and would give mechanistic insights into the etiology of DD (Nedic Erjavec et al., 2018; Du et al., 2022). For example, nine potential biomarkers involved the depression pathogenesis were identified based on metabolomics analysis by comparing the rats' serum metabolites of CUMS(chronic unpredictable mild stress) model group and Xiao-Chai-Hu-Tang group (Xiong et al., 2016). Proteomics includes all levels of protein composition, structure, and activity exploration of proteomes. Shweiki et al. summarized 42 differentially regulated proteins in DD and discussed the diagnostic potential of the biomarker candidates and their association with the suggested pathologies (Al Shweiki et al., 2017). Transcriptomics is the study associated with the process of all RNA transcripts during the biological process of transcription, and many transcriptomics studies provide insight into DD (Belzeaux et al., 2018; Cho et al., 2019; Rainville et al., 2021). By transferring key miRNAs, exosomes from the neuron, astrocyte, and neural progenitor cell exhibited significant efficiency in promoting neurogenesis (Takeda and Xu 2015; You et al., 2020; Yuan et al., 2021). Xu et al. systematically identified the miRNAs of exosomes from the juice of ginseng by transcriptomic technology, and found 44 kinds of miRNAs perfectly match to the ginseng genome database (Xu et al., 2021). Epigenetics covers heritable phenotype changes that are not involved in alterations of the DNA sequence, which is associated with DD reported by numerous studies (Yeshurun and Hannan 2019; Wheater et al., 2020; Xu et al., 2020). As discussed above, EVs are ideal herbal drug carriers due to their remarkable biocompatibility. Moreover, since DNA, RNA, lipids, proteins, cytoplasm, and metabolites are delivered by EVs, it can be taken as the critical point connecting herbal therapies to metabolomics, proteomics, transcriptomics and epigenetics in DD (see **Figure 4**).

6 CONCLUSION

Although CHM has been applied in China for thousands of years to help people fight many diseases, and some of Chines herbal original phytochemicals such as artemisinin have already been proved effective, composition complexity still remains a strenuous challenge for the mechanistic studies of CHM. Opportunely, the cargos and ligands of EVs can be determined by metabolomics, proteomics, and transcriptomics technologies, which means that the composition of herb-derived EVs can be specified for further mechanism study. Once the composition is precise, it can also be applied to different delivery routes such as intravenous or intranasal administration, which used to be limited to explore by the composition complexity of CHM. In addition, non-immunogenic, innocuous, and target-specific features make herb-derived EVs attractive to be therapeutic agents.

EVs can serve as drug vehicles for phytochemicals and biomarkers in developing the treatment for DD. Trials in intranasal administration of EVs indicate their significance in CNS diseases and show high promise to be a new medical way to transfer phytochemicals across the BBB. Since there are no

specific biomarkers available for DD, the diagnosis has to depend on the combination of psychiatric evaluation, physical exam and lab tests. However, combined with metabolomics, proteomics, transcriptomics, and epigenetics technologies, the specifically altered contents in EVs from DD patients can be measured.

Even though EVs own promising advantages for delivering CHM, especially effective phytochemicals for treating DD, the components complexity of herbs and herbal formulas makes it challenging to be delivered by EVs. Moreover, there are few studies on pharmacological functions and *in vivo* transport pathways of CHM-derived EVs, which need more exploration before clinical practice. Therefore, the CHM study of EVs is still in the initial stage. More in-depth study in different CHM-derived EVs will be helpful to explain the complicated pharmacology of CHM and develop a new administration mode.

This review has summarized the reported effective CHM for treating DD and the advantages of EVs in facilitating CHM for DD treatment. Currently, few studies have been focused on herb-derived EVs in treating DD, which is exciting but remains to be explored in this area.

AUTHOR CONTRIBUTIONS

QW completed the literature review and wrote the review, W-ZD thoroughly reviewed and edited the review, J-BC extracted helpful information from included studies, X-PZ helped with the abstract, X-JL classified the pieces of literature, Y-YL helped check the writing of the essay, ZX helped with the tables and the revision of the whole manuscript, Q-YM and J-XC, as primary reviewers screened titles and abstracts for eligibility. All authors read and approved the final manuscript.

FUNDING

This research work and publication were financially supported by Key Program of National Natural Science Foundation of China (No. 81630104), National Natural Science Foundation of China (No. 81973748, No. 82174278), Youth Science Fundation Project of National Natural Science Foundation of China (No. 81803972).

REFERENCES

Abbott, N. J., Rönnbäck, L., and Hansson, E. (2006). Astrocyte-endothelial Interactions at the Blood-Brain Barrier. *Nat. Rev. Neurosci.* 7, 41–53. doi:10.1038/nrn1824

Al Shweiki, M. R., Oeckl, P., Steinacker, P., Hengerer, B., Schönfeldt-Lecuona, C., and Otto, M. (2017). Major Depressive Disorder: Insight into Candidate Cerebrospinal Fluid Protein Biomarkers from Proteomics Studies. *Expert Rev. Proteomics* 14, 499–514. doi:10.1080/14789450.2017.1336435

Andreone, B. J., Lacoste, B., and Gu, C. (2015). Neuronal and Vascular Interactions. *Annu. Rev. Neurosci.* 38, 25–46. doi:10.1146/annurev-neuro-071714-033835

Aryani, A., and Denecke, B. (2016). Exosomes as a Nanodelivery System: a Key to the Future of Neuromedicine? *Mol. Neurobiol.* 53, 818–834. doi:10.1007/s12035-014-9054-5

Belzeaux, R., Lin, R., Ju, C., Chay, M. A., Fiori, L. M., Lutz, P. E., et al. (2018). Transcriptomic and Epigenomic Biomarkers of Antidepressant Response. *J. Affect. Disord.* 233, 36–44. doi:10.1016/j.jad.2017.08.087

Bhatt, S., Kanoujia, J., Dhar, A. K., Arumugam, S., Silva, A. K. A., and Mishra, N. (2021). Exosomes: A Novel Therapeutic Paradigm for the Treatment of Depression. *Curr. Drug Targets* 22, 183–191. doi:10.2174/1389450121999201006193005

Bhatt, S., Nagappa, A. N., and Patil, C. R. (2020). Role of Oxidative Stress in Depression. *Drug Discov. Today* 25, 1270–1276. doi:10.1016/j.drudis.2020.05.001

Bian, X., Liu, X., Liu, J., Zhao, Y., Li, H., Cai, E., et al. (2018). Study on Antidepressant Activity of Chiisanoside in Mice. *Int. Immunopharmacol.* 57, 33–42. doi:10.1016/j.intimp.2018.02.007

Boukouris, S., and Mathivanan, S. (2015). Exosomes in Bodily Fluids Are a Highly Stable Resource of Disease Biomarkers. *Proteomics Clin. Applclin. Appl.* 9, 358–367. doi:10.1002/prca.201400114

Cao, L. H., Qiao, J. Y., Huang, H. Y., Fang, X. Y., Zhang, R., Miao, M. S., et al. (2019a). PI3K-AKT Signaling Activation and Icariin: The Potential Effects on the Perimenopausal Depression-like Rat Model. *Molecules* 24. doi:10.3390/molecules24203700

Cao, M., Yan, H., Han, X., Weng, L., Wei, Q., Sun, X., et al. (2019c). Ginseng-derived Nanoparticles Alter Macrophage Polarization to Inhibit Melanoma Growth. *J. Immunother. Cancer* 7, 326. doi:10.1186/s40425-019-0817-4

Cao, M., Yan, H. H., Han, X., Weng, L., Wei, Q., Sun, X., et al. (2019b). Astrocytes at the Hub of the Stress Response: Potential Modulation of Neurogenesis by miRNAs in Astrocyte-Derived Exosomes. *J. Ethnopharmacol.* 7, 144–158. 10.1016/j.jad.2020.05.017. doi:10.1186/s40425-019-0817-4

Chen, C. C., Liu, L., Ma, F., Wong, C. W., Guo, X. E., Chacko, J. V., et al. (2016). Elucidation of Exosome Migration across the Blood-Brain Barrier Model *In Vitro*. *Cell. Mol. Bioeng.* 9, 509–529. doi:10.1007/s12195-016-0458-3

Chen, J., Huang, Y., Li, L., Niu, J., Ye, W., Wang, Y., et al. (2020). Antidepressant Pathways of the Chinese Herb Jiaweisinisan through Genetic Ontology Analysis. *J. Integr. Neurosci.* 19, 385–395. doi:10.31083/j.jin.2020.02.1246

Chen, Z., Huang, C., He, H., and Ding, W. (2017). 2, 3, 5, 4'-Tetrahydroxystilbene-2-O-β-D-Glucoside Prevention of Lipopolysaccharide-Induced Depressive-like Behaviors in Mice Involves Neuroinflammation and Oxido-Nitrosative Stress Inhibition. *Behav. Pharmacol.* 28, 365–374. doi:10.1097/FBP.0000000000000307

Chi, X., Wang, S., Baloch, Z., Zhang, H., Li, X., Zhang, Z., et al. (2019). Research Progress on Classical Traditional Chinese Medicine Formula Lily Bulb and Rehmannia Decoction in the Treatment of Depression. *Biomed. Pharmacother.* 112, 108616. doi:10.1016/j.biopha.2019.108616

Chivet, M., Hemming, F., Pernet-Gallay, K., Fraboulet, S., and Sadoul, R. (2012). Emerging Role of Neuronal Exosomes in the central Nervous System. *Front. Physiol.* 3, 145. doi:10.3389/fphys.2012.00145

Cho, J. H., Irwin, M. R., Eisenberger, N. I., Lamkin, D. M., and Cole, S. W. (2019). Transcriptomic Predictors of Inflammation-Induced Depressed Mood. *Neuropsychopharmacology* 44, 923–929. doi:10.1038/s41386-019-0316-9

Choi, J. L., Kao, P. F., Itriago, E., Zhan, Y., Kozubek, J. A., Hoss, A. G., et al. (2017). miR-149 and miR-29c as Candidates for Bipolar Disorder Biomarkers. *Am. J. Med. Genet. B Neuropsychiatr. Genet.* 174, 315–323. doi:10.1002/ajmg.b.32518

Corson, T. W., and Crews, C. M. (2007). Molecular Understanding and Modern Application of Traditional Medicines: Triumphs and Trials. *Cell* 130, 769–774. doi:10.1016/j.cell.2007.08.021

Cufaro, M. C., Pieragostino, D., Lanuti, P., Rossi, C., Cicalini, I., Federici, L., et al. (2019). Extracellular Vesicles and Their Potential Use in Monitoring Cancer Progression and Therapy: The Contribution of Proteomics. *J. Oncol.* 2019, 1639854. doi:10.1155/2019/1639854

Dad, H. A., Gu, T. W., Zhu, A. Q., Huang, L. Q., and Peng, L. H. (2021). Plant Exosome-like Nanovesicles: Emerging Therapeutics and Drug Delivery Nanoplatforms. *Mol. Ther.* 29, 13–31. doi:10.1016/j.ymthe.2020.11.030

Du, H. X., Chen, X. G., Zhang, L., Liu, Y., Zhan, C. S., Chen, J., et al. (2019). Microglial Activation and Neurobiological Alterations in Experimental Autoimmune Prostatitis-Induced Depressive-like Behavior in Mice. *Neuropsychiatr. Dis. Treat.* 15, 2231–2245. doi:10.2147/NDT.S211288

Du, Y., Dong, J. H., Chen, L., Liu, H., Zheng, G. E., Chen, G. Y., et al. (2022). Metabolomic Identification of Serum Exosome-Derived Biomarkers for Bipolar Disorder. *Oxid. Med. Cell. Longev.* 2022, 5717445. doi:10.1155/2022/5717445

Fan, C., Song, Q., Wang, P., Li, Y., Yang, M., Liu, B., et al. (2018). Curcumin Protects against Chronic Stress-Induced Dysregulation of Neuroplasticity and Depression-like Behaviors via Suppressing IL-1β Pathway in Rats. *Neuroscience* 392, 92–106. doi:10.1016/j.neuroscience.2018.09.028

Fujita, D., Arai, T., Komori, H., Shirasaki, Y., Wakayama, T., Nakanishi, T., et al. (2018). Apple-Derived Nanoparticles Modulate Expression of Organic-Anion-Transporting Polypeptide (OATP) 2B1 in Caco-2 Cells. *Mol. Pharm.* 15, 5772–5780. doi:10.1021/acs.molpharmaceut.8b00921

Geng, J., Liu, J., Yuan, X., Liu, W., and Guo, W. (2019). Andrographolide Triggers Autophagy-Mediated Inflammation Inhibition and Attenuates Chronic Unpredictable Mild Stress (CUMS)-induced Depressive-like Behavior in Mice. *Toxicol. Appl. Pharmacol.* 379, 114688. doi:10.1016/j.taap.2019.114688

Ghasemzadeh Rahbardar, M., and Hosseinzadeh, H. (2020). Therapeutic Effects of Rosemary (Rosmarinus Officinalis L.) and its Active Constituents on Nervous System Disorders. *Iran. J. Basic Med. Sci.* 23, 1100–1112. doi:10.22038/ijbms.2020.45269.10541

Gómez-Molina, C., Sandoval, M., Henzi, R., Ramírez, J. P., Varas-Godoy, M., Luarte, A., et al. (2019). Small Extracellular Vesicles in Rat Serum Contain Astrocyte-Derived Protein Biomarkers of Repetitive Stress. *Int. J. Neuropsychopharmacol.* 22, 232–246. doi:10.1093/ijnp/pyy098

Gong, W., Zhu, S., Chen, C., Yin, Q., Li, X., Du, G., et al. (2019). The Anti-depression Effect of Angelicae Sinensis Radix Is Related to the Pharmacological Activity of Modulating the Hematological Anomalies. *Front. Pharmacol.* 10, 192. doi:10.3389/fphar.2019.00192

Gong, X., Sun, R., Gao, Z., Han, W., Liu, Y., Zhao, L., et al. (2018). Tubeimoside 1 Acts as a Chemotherapeutic Synergist via Stimulating Macropinocytosis. *Front. Pharmacol.* 9, 1–10. doi:10.3389/fphar.2018.01044

Grapp, M., Wrede, A., Schweizer, M., Hüwel, S., Galla, H. J., Snaidero, N., et al. (2013). Choroid Plexus Transcytosis and Exosome Shuttling Deliver Folate into Brain Parenchyma. *Nat. Commun.* 4, 2123. doi:10.1038/ncomms3123

Guo, L. T., Wang, S. Q., Su, J., Xu, L. X., Ji, Z. Y., Zhang, R. Y., et al. (2019). Baicalin Ameliorates Neuroinflammation-Induced Depressive-like Behavior through Inhibition of Toll-like Receptor 4 Expression via the PI3K/AKT/FoxO1 Pathway. *J. Neuroinflammation* 16, 95. doi:10.1186/s12974-019-1474-8

Hirshler, Y., and Doron, R. (2017). Neuroplasticity-related Mechanisms Underlying the Antidepressant-like Effects of Traditional Herbal Medicines. *Eur. Neuropsychopharmacol.* 27, 945–958. doi:10.1016/j.euroneuro.2017.07.008

Hu, K., Guan, W. J., Bi, Y., Zhang, W., Li, L., Zhang, B., et al. (2021). Efficacy and Safety of Lianhuaqingwen Capsules, a Repurposed Chinese Herb, in Patients with Coronavirus Disease 2019: A Multicenter, Prospective, Randomized Controlled Trial. *Phytomedicine* 85, 153242. doi:10.1016/j.phymed.2020.153242

Huang, Q., Ye, X., Wang, L., and Pan, J. (2019). Salvianolic Acid B Abolished Chronic Mild Stress-Induced Depression through Suppressing Oxidative Stress and Neuro-Inflammation via Regulating NLRP3 Inflammasome Activation. *J. Food Biochem.* 43, e12742. doi:10.1111/jfbc.12742

James, S. L., Abate, D., Abate, K. H., Abay, S. M., Abbafati, C., Abbasi, N., et al. (2018). Global, Regional, and National Incidence, Prevalence, and Years Lived with Disability for 354 Diseases and Injuries for 195 Countries and Territories, 1990-2017: A Systematic Analysis for the Global Burden of Disease Study 2017. *Lancet* 392, 1789–1858. doi:10.1016/S0140-6736(18)32279-7

Ji, W. W., Li, R. P., Li, M., Wang, S. Y., Zhang, X., Niu, X. X., et al. (2014a). Antidepressant-like Effect of Essential Oil of Perilla Frutescens in a Chronic, Unpredictable, Mild Stress-Induced Depression Model Mice. *Chin. J. Nat. Med.* 12, 753–759. doi:10.1016/S1875-5364(14)60115-1

Ji, W. W., Wang, S. Y., Ma, Z. Q., Li, R. P., Li, S. S., Xue, J. S., et al. (2014b). Effects of Perillaldehyde on Alternations in Serum Cytokines and Depressive-like Behavior in Mice after Lipopolysaccharide Administration. *Pharmacol. Biochem. Behav.* 116, 1–8. doi:10.1016/j.pbb.2013.10.026

Jiang, C. Y., Qin, X. Y., Yuan, M. M., Lu, G. J., and Cheng, Y. (2018). 2,3,5,4'-Tetrahydroxystilbene-2-O-beta-D-glucoside Reverses Stress-Induced Depression via Inflammatory and Oxidative Stress Pathways. *Oxid. Med. Cell. Longev.* 2018, 9501427. doi:10.1155/2018/9501427

Jiang, N., Lv, J., Wang, H., Huang, H., Wang, Q., Lu, C., et al. (2020). Ginsenoside Rg1 Ameliorates Chronic Social Defeat Stress-Induced Depressive-like Behaviors and Hippocampal Neuroinflammation. *Life Sci.* 252, 117669. doi:10.1016/j.lfs.2020.117669

Ju, S., Mu, J., Dokland, T., Zhuang, X., Wang, Q., Jiang, H., et al. (2013). Grape Exosome-like Nanoparticles Induce Intestinal Stem Cells and Protect Mice from DSS-Induced Colitis. *Mol. Ther.* 21, 1345–1357. doi:10.1038/mt.2013.64

Kadry, H., Noorani, B., and Cucullo, L. (2020). A Blood-Brain Barrier Overview on Structure, Function, Impairment, and Biomarkers of Integrity. *Fluids Barr. CNS* 17, 69. doi:10.1186/s12987-020-00230-3

Kalluri, R., and LeBleu, V. S. (2020). The Biology, Function, and Biomedical Applications of Exosomes. *Science* 367, eaau6977. doi:10.1126/science.aau6977

Kang, A., Xie, T., Zhu, D., Shan, J., Di, L., and Zheng, X. (2017). Suppressive Effect of Ginsenoside Rg3 against Lipopolysaccharide-Induced Depression-like Behavior and Neuroinflammation in Mice. *J. Agric. Food Chem.* 65, 6861–6869. doi:10.1021/acs.jafc.7b02386

Kanninen, K. M., Bister, N., Koistinaho, J., and Malm, T. (2016). Exosomes as New Diagnostic Tools in CNS Diseases. *Biochim. Biophys. Acta* 1862, 403–410. doi:10.1016/j.bbadis.2015.09.020

Kawikova, I., and Askenase, P. W. (2015). Diagnostic and Therapeutic Potentials of Exosomes in CNS Diseases. *Brain Res.* 1617, 63–71. doi:10.1016/j.brainres.2014.09.070

Kim, J., Li, S., Zhang, S., and Wang, J. (2022). Plant-derived Exosome-like Nanoparticles and Their Therapeutic Activities. *Asian J. Pharm. Sci.* 17, 53–69. doi:10.1016/j.ajps.2021.05.006

Kuwano, N., Kato, T. A., Mitsuhashi, M., Sato-Kasai, M., Shimokawa, N., Hayakawa, K., et al. (2018). Neuron-related Blood Inflammatory Markers as an Objective Evaluation Tool for Major Depressive Disorder: An Exploratory Pilot Case-Control Study. *J. Affect. Disord.* 240, 88–98. doi:10.1016/j.jad.2018.07.040

Li, C. F., Chen, X. Q., Chen, S. M., Chen, X. M., Geng, D., Liu, Q., et al. (2017a). Evaluation of the Toxicological Properties and Anti-inflammatory Mechanism of Hemerocallis Citrina in LPS-Induced Depressive-like Mice. *Biomed. Pharmacother.* 91, 167–173. doi:10.1016/j.biopha.2017.04.089

Li, D., Wang, Y., Jin, X., Hu, D., Xia, C., Xu, H., et al. (2020). NK Cell-Derived Exosomes Carry miR-207 and Alleviate Depression-like Symptoms in Mice. *J. Neuroinflammation* 17, 126. doi:10.1186/s12974-020-01787-4

Li, H., Lin, S., Qin, T., Li, H., Ma, Z., and Ma, S. (2017c). Senegenin Exerts Anti-depression Effect in Mice Induced by Chronic Un-predictable Mild Stress via Inhibition of NF-Kb Regulating NLRP3 Signal Pathway. *Int. Immunopharmacol.* 53, 24–32. doi:10.1016/j.intimp.2017.10.001

Li, H. Y., Zhao, Y. H., Zeng, M. J., Fang, F., Li, M., Qin, T. T., et al. (2017b). Saikosaponin D Relieves Unpredictable Chronic Mild Stress Induced Depressive-like Behavior in Rats: Involvement of HPA axis and Hippocampal Neurogenesis. *Psychopharmacology (Berl)* 234, 3385–3394. doi:10.1007/s00213-017-4720-8

Li, J., Huang, S., Huang, W., Wang, W., Wen, G., Gao, L., et al. (2017d). Paeoniflorin Ameliorates Interferon-Alpha-Induced Neuroinflammation and Depressive-like Behaviors in Mice. *Oncotarget* 8, 8264–8282. doi:10.18632/oncotarget.14160

Li, X., Qin, X. M., Tian, J. S., Gao, X. X., Du, G. H., and Zhou, Y. Z. (2021). Integrated Network Pharmacology and Metabolomics to Dissect the Combination Mechanisms of Bupleurum Chinense DC-Paeonia Lactiflora Pall Herb Pair for Treating Depression. *J. Ethnopharmacol.* 264, 113281. doi:10.1016/j.jep.2020.113281

Li, X. Y., Qi, W. W., Zhang, Y. X., Jiang, S. Y., Yang, B., Xiong, L., et al. (2019). Helicid Ameliorates Learning and Cognitive Ability and Activities cAMP/PKA/CREB Signaling in Chronic Unpredictable Mild Stress Rats. *Biol. Pharm. Bull.* 42, 1146–1154. doi:10.1248/bpb.b19-00012

Li, Y. C., Wang, L. L., Pei, Y. Y., Shen, J. D., Li, H. B., Wang, B. Y., et al. (2015). Baicalin Decreases SGK1 Expression in the hippocampus and Reverses Depressive-like Behaviors Induced by Corticosterone. *Neuroscience* 311, 130–137. doi:10.1016/j.neuroscience.2015.10.023

Li, Z., Wang, H., Yin, H., Bennett, C., Zhang, H. G., and Guo, P. (2018). Arrowtail RNA for Ligand Display on Ginger Exosome-like Nanovesicles to Systemic Deliver siRNA for Cancer Suppression. *Sci. Rep.* 8, 14644. doi:10.1038/s41598-018-32953-7

Liang, J. Q., Liao, H. R., Xu, C. X., Li, X. L., Wei, Z. X., Xie, G. J., et al. (2020). Serum Exosome-Derived miR-139-5p as a Potential Biomarker for Major Depressive Disorder. *Neuropsychiatr. Dis. Treat.* 16, 2689–2693. doi:10.2147/NDT.S277392

Lin, J., Li, J., Huang, B., Liu, J., Chen, X., Chen, X. M., et al. (2015). Exosomes: Novel Biomarkers for Clinical Diagnosis. *ScientificWorldJournal* 2015, 657086. doi:10.1155/2015/657086

Lin, J., Song, Z., Chen, X., Zhao, R., Chen, J., Chen, H., et al. (2019). Trans-cinnamaldehyde Shows Anti-depression Effect in the Forced Swimming Test and Possible Involvement of the Endocannabinoid System. *Biochem. Biophys. Res. Commun.* 518, 351–356. doi:10.1016/j.bbrc.2019.08.061

Lin, Y. E., Wang, H. L., Lu, K. H., Huang, Y. J., Panyod, S., Liu, W. T., et al. (2021). Water Extract of Armillaria Mellea (Vahl) P. Kumm. Alleviates the Depression-like Behaviors in Acute- and Chronic Mild Stress-Induced Rodent Models via Anti-inflammatory Action. *J. Ethnopharmacol.* 265, 113395. doi:10.1016/j.jep.2020.113395

Liu, B., Xu, C., Wu, X., Liu, F., Du, Y., Sun, J., et al. (2015). Icariin Exerts an Antidepressant Effect in an Unpredictable Chronic Mild Stress Model of Depression in Rats and Is Associated with the Regulation of Hippocampal Neuroinflammation. *Neuroscience* 294, 193–205. doi:10.1016/j.neuroscience.2015.02.053

Liu, F. G., Hu, W. F., Wang, J. L., Wang, P., Gong, Y., Tong, L. J., et al. (2017a). Z-guggulsterone Produces Antidepressant-like Effects in Mice through Activation of the BDNF Signaling Pathway. *Int. J. Neuropsychopharmacol.* 20, 485–497. doi:10.1093/ijnp/pyx009

Liu, J. Q., Lee, T. F., Miedzyblocki, M., Chan, G. C., Bigam, D. L., and Cheung, P. Y. (2011). Effects of Tanshinone IIA, a Major Component of Salvia Miltiorrhiza, on Platelet Aggregation in Healthy Newborn Piglets. *J. Ethnopharmacol.* 137, 44–49. doi:10.1016/j.jep.2011.03.047

Liu, P., Bai, X., Zhang, T., Zhou, L., Li, J., and Zhang, L. (2019). The Protective Effect of *Lonicera japonica* Polysaccharide on Mice with Depression by Inhibiting NLRP3 Inflammasome. *Ann. Transl. Med.* 7, 811. doi:10.21037/atm.2019.12.64

Liu, S., Xu, S., Wang, Z., Guo, Y., Pan, W., and Shen, Z. (2018). Anti-Depressant-Like Effect of Sinomenine on Chronic Unpredictable Mild Stress-Induced Depression in a Mouse Model. *Med. Sci. Monit.* 24, 7646–7653. doi:10.12659/MSM.908422

Liu, X. J., Wang, Y. Z., Wei, F. X., Lv, M., Qu, P., Chen, S. J., et al. (2021). The Synergistic Anti-depression Effects of Different Efficacy Groups of Xiaoyaosan as Demonstrated by the Integration of Network Pharmacology and Serum Metabolomics. *J. Pharm. Biomed. Anal.* 197, 113949. doi:10.1016/j.jpba.2021.113949

Liu, Y. M., Shen, J. D., Xu, L. P., Li, H. B., Li, Y. C., and Yi, L. T. (2017b). Ferulic Acid Inhibits Neuro-Inflammation in Mice Exposed to Chronic Unpredictable Mild Stress. *Int. Immunopharmacol.* 45, 128–134. doi:10.1016/j.intimp.2017.02.007

Mathivanan, S., Ji, H., and Simpson, R. J. (2010). Exosomes: Extracellular Organelles Important in Intercellular Communication. *J. Proteomics* 73, 1907–1920. doi:10.1016/j.jprot.2010.06.006

McClintock, S. M., Husain, M. M., Greer, T. L., and Cullum, C. M. (2010). Association between Depression Severity and Neurocognitive Function in Major Depressive Disorder: a Review and Synthesis. *Neuropsychology* 24, 9–34. doi:10.1037/a0017336

Milajerdi, A., Jazayeri, S., Shirzadi, E., Hashemzadeh, N., Azizgol, A., Djazayery, A., et al. (2018). The Effects of Alcoholic Extract of Saffron (Crocus Satious L.) on Mild to Moderate Comorbid Depression-Anxiety, Sleep Quality, and Life Satisfaction in Type 2 Diabetes Mellitus: A Double-Blind, Randomized and Placebo-Controlled Clinical Trial. *Complement. Ther. Med.* 41, 196–202. doi:10.1016/j.ctim.2018.09.023

Mizohata, Y., Toda, H., Koga, M., Saito, T., Fujita, M., Kobayashi, T., et al. (2021). Neural Extracellular Vesicle-Derived miR-17 in Blood as a Potential Biomarker of Subthreshold Depression. *Hum. Cell* 34, 1087–1092. doi:10.1007/s13577-021-00553-9

Mou, Z., Huang, Q., Chu, S. F., Zhang, M. J., Hu, J. F., Chen, N. H., et al. (2017). Antidepressive Effects of Ginsenoside Rg1 via Regulation of HPA and HPG axis. *Biomed. Pharmacother.* 92, 962–971. doi:10.1016/j.biopha.2017.05.119

Mu, J., Zhuang, X., Wang, Q., Jiang, H., Deng, Z. B., Wang, B., et al. (2014). Interspecies Communication between Plant and Mouse Gut Host Cells through Edible Plant Derived Exosome-like Nanoparticles. *Mol. Nutr. Food Res.* 58, 1561–1573. doi:10.1002/mnfr.201300729

Nasca, C., Dobbin, J., Bigio, B., Watson, K., de Angelis, P., Kautz, M., et al. (2020). Insulin Receptor Substrate in Brain-Enriched Exosomes in Subjects with Major Depression: on the Path of Creation of Biosignatures of central Insulin Resistance. *Mol. Psychiatry* 26, 5140–5149. doi:10.1038/s41380-020-0804-7

Nedic Erjavec, G., Konjevod, M., Nikolac Perkovic, M., Svob Strac, D., Tudor, L., Barbas, C., et al. (2018). Short Overview on Metabolomic Approach and Redox Changes in Psychiatric Disorders. *Redox Biol.* 14, 178–186. doi:10.1016/j.redox.2017.09.002

Obermeier, B., Daneman, R., and Ransohoff, R. M. (2013). Development, Maintenance and Disruption of the Blood-Brain Barrier. *Nat. Med.* 19, 1584–1596. doi:10.1038/nm.3407

Pardridge, W. M. (2012). Drug Transport across the Blood-Brain Barrier. *J. Cereb. Blood Flow Metab.* 32, 1959–1972. doi:10.1038/jcbfm.2012.126

Park, B. K., Kim, N. S., Kim, Y. R., Yang, C., Jung, I. C., Jang, I. S., et al. (2020). Antidepressant and Anti-neuroinflammatory Effects of Bangpungtongsung-San. *Front. Pharmacol.* 11, 958. doi:10.3389/fphar.2020.00958

Park, S. H., Jang, S., Son, E., Lee, S. W., Park, S. D., Sung, Y. Y., et al. (2018). Polygonum Aviculare L. Extract Reduces Fatigue by Inhibiting Neuroinflammation in Restraint-Stressed Mice. *Phytomedicine* 42, 180–189. doi:10.1016/j.phymed.2018.03.042

Perets, N., Hertz, S., London, M., and Offen, D. (2018). Intranasal Administration of Exosomes Derived from Mesenchymal Stem Cells Ameliorates Autistic-like Behaviors of BTBR Mice. *Mol. Autism* 9, 57. doi:10.1186/s13229-018-0240-6

Po, K. K., Leung, J. W., Chan, J. N., Fung, T. K., Sánchez-Vidaña, D. I., Sin, E. L., et al. (2017). Protective Effect of Lycium Barbarum Polysaccharides on Dextromethorphan-Induced Mood Impairment and Neurogenesis Suppression. *Brain Res. Bull.* 134, 10–17. doi:10.1016/j.brainresbull.2017.06.014

Prado, C. E., Watt, S., and Crowe, S. F. (2018). A Meta-Analysis of the Effects of Antidepressants on Cognitive Functioning in Depressed and Non-depressed Samples. *Neuropsychol. Rev.* 28, 32–72. doi:10.1007/s11065-018-9369-5

Qiu, Z. K., Zhang, G. H., Zhong, D. S., He, J. L., Liu, X., Chen, J. S., et al. (2017). Puerarin Ameliorated the Behavioral Deficits Induced by Chronic Stress in Rats. *Sci. Rep.* 7, 6266. doi:10.1038/s41598-017-06552-x

Rainville, J. R., Lipuma, T., and Hodes, G. E. (2022). Translating the Transcriptome: Sex Differences in the Mechanisms of Depression and Stress, Revisited. *Biol. Psychiatry* 91, 25–35. doi:10.1016/j.biopsych.2021.02.003

Ramshani, Z., Zhang, C., Richards, K., Chen, L., Xu, G., Stiles, B. L., et al. (2019). Extracellular Vesicle microRNA Quantification from Plasma Using an Integrated Microfluidic Device. *Commun. Biol.* 2, 189–9. doi:10.1038/s42003-019-0435-1

Ren, L., and Chen, G. (2017). Rapid Antidepressant Effects of Yueju: A New Look at the Function and Mechanism of an Old Herbal Medicine. *J. Ethnopharmacol.* 203, 226–232. doi:10.1016/j.jep.2017.03.042

Ruan, J., Liu, L., Shan, X., Xia, B., and Fu, Q. (2019). Anti-depressant Effects of Oil from Fructus Gardeniae via PKA-CREB-BDNF Signaling. *Biosci. Rep.* 39. doi:10.1042/BSR20190141

Ruan, X. F., Ju, C. W., Shen, Y., Liu, Y. T., Kim, I. M., Yu, H., et al. (2018a). Suxiao Jiuxin Pill Promotes Exosome Secretion from Mouse Cardiac Mesenchymal Stem Cells *In Vitro*. *Acta Pharmacol. Sin.* 39, 569–578. doi:10.1038/aps.2018.19

Ruan, X. F., Li, Y. J., Ju, C. W., Shen, Y., Lei, W., Chen, C., et al. (2018b). Exosomes from Suxiao Jiuxin Pill-Treated Cardiac Mesenchymal Stem Cells Decrease H3K27 Demethylase UTX Expression in Mouse Cardiomyocytes *In Vitro*. *Acta Pharmacol. Sin.* 39, 579–586. doi:10.1038/aps.2018.18

Saeedi, S., Israel, S., Nagy, C., and Turecki, G. (2019). The Emerging Role of Exosomes in Mental Disorders. *Transl PsychiatryPsychiatry* 9, 122. doi:10.1038/s41398-019-0459-9

Salari, N., Hosseinian-Far, A., Jalali, R., Vaisi-Raygani, A., Rasoulpoor, S., Mohammadi, M., et al. (2020). Prevalence of Stress, Anxiety, Depression Among the General Population during the COVID-19 Pandemic: a Systematic Review and Meta-Analysis. *Glob. Health* 16, 57. doi:10.1186/s12992-020-00589-w

Sanchez-Covarrubias, L., Slosky, L. M., Thompson, B. J., Davis, T. P., and Ronaldson, P. T. (2014). Transporters at CNS Barrier Sites: Obstacles or Opportunities for Drug Delivery? *Curr. Pharm. Des.* 20, 1422–1449. doi:10.2174/13816128113199990463

Schuh, C. M. A. P., Cuenca, J., Alcayaga-Miranda, F., and Khoury, M. (2019). Exosomes on the Border of Species and Kingdom Intercommunication. *Transl. Res.* 210, 80–98. doi:10.1016/j.trsl.2019.03.008

Song, Y., Sun, R., Ji, Z., Li, X., Fu, Q., and Ma, S. (2018). Perilla Aldehyde Attenuates CUMS-Induced Depressive-like Behaviors via Regulating TXNIP/TRX/NLRP3 Pathway in Rats. *Life Sci.* 206, 117–124. doi:10.1016/j.lfs.2018.05.038

Stenovec, M., Lasič, E., Božić, M., Bobnar, S. T., Stout, R. F., Grubišić, V., et al. (2016). Ketamine Inhibits ATP-Evoked Exocytotic Release of Brain-Derived Neurotrophic Factor from Vesicles in Cultured Rat Astrocytes. *Mol. Neurobiol.* 53, 6882–6896. doi:10.1007/s12035-015-9562-y

Stenovec, M., Li, B., Verkhratsky, A., and Zorec, R. (2020). Astrocytes in Rapid Ketamine Antidepressant Action. *Neuropharmacology* 173, 108158. doi:10.1016/j.neuropharm.2020.108158

Su, J., Pan, Y. W., Wang, S. Q., Li, X. Z., Huang, F., and Ma, S. P. (2020). Saikosaponin-d Attenuated Lipopolysaccharide-Induced Depressive-like Behaviors via Inhibiting Microglia Activation and Neuroinflammation. *Int. Immunopharmacol.* 80, 106181. doi:10.1016/j.intimp.2019.106181

Sun, D., Zhuang, X., Xiang, X., Liu, Y., Zhang, S., Liu, C., et al. (2010). A Novel Nanoparticle Drug Delivery System: The Anti-inflammatory Activity of Curcumin Is Enhanced when Encapsulated in Exosomes. *Mol. Ther.* 18, 1606–1614. doi:10.1038/mt.2010.105

Sun, Y., Xu, X., Zhang, J., and Chen, Y. (2018). Treatment of Depression with Chai Hu Shu Gan San: a Systematic Review and Meta-Analysis of 42 Randomized Controlled Trials. *BMC Complement. Altern. Med.* 18, 66. doi:10.1186/s12906-018-2130-z

Takeda, Y. S., and Xu, Q. (2015). Neuronal Differentiation of Human Mesenchymal Stem Cells Using Exosomes Derived from Differentiating Neuronal Cells. *PLoS One* 10, e0135111. doi:10.1371/journal.pone.0135111

Tavakolizadeh, J., Roshanaei, K., Salmaninejad, A., Yari, R., Nahand, J. S., Sarkarizi, H. K., et al. (2018). MicroRNAs and Exosomes in Depression: Potential Diagnostic Biomarkers. *J. Cell. Biochem.* 119, 3783–3797. doi:10.1002/jcb.26599

Théry, C., Witwer, K. W., Aikawa, E., Alcaraz, M. J., Anderson, J. D., Andriantsitohaina, R., et al. (2018). Minimal Information for Studies of Extracellular Vesicles 2018 (MISEV2018): a Position Statement of the International Society for Extracellular Vesicles and Update of the MISEV2014 Guidelines. *J. Extracell. Vesicles* 7, 1535750. doi:10.1080/20013078.2018.1535750

Topuzoğlu, A., and Ilgın, C. (2020). Mentalexo Approach for Diagnosis of Psychiatric Disorders. *Med. Hypotheses* 143, 109823. doi:10.1016/j.mehy.2020.109823

Upadhyay, R. K. (2014). Drug Delivery Systems, CNS protection, and the Blood Brain Barrier. *Biomed. Res. Int.* 2014, 869269. doi:10.1155/2014/869269

Valadi, H., Ekström, K., Bossios, A., Sjöstrand, M., Lee, J. J., and Lötvall, J. O. (2007). Exosome-mediated Transfer of mRNAs and microRNAs Is a Novel Mechanism of Genetic Exchange between Cells. *Nat. Cell Biol.* 9, 654–659. doi:10.1038/ncb1596

Wallensten, J., Nager, A., Åsberg, M., Borg, K., Beser, A., Wilczek, A., et al. (2021). Leakage of Astrocyte-Derived Extracellular Vesicles in Stress-Induced Exhaustion Disorder: a Cross-Sectional Study. *Sci. Rep.* 11, 2009. doi:10.1038/s41598-021-81453-8

Wang, A. R., Mi, L. F., Zhang, Z. L., Hu, M. Z., Zhao, Z. Y., Liu, B., et al. (2021a). Saikosaponin A Improved Depression-like Behavior and Inhibited Hippocampal Neuronal Apoptosis after Cerebral Ischemia through P-Creb/bdnf Pathway. *Behav. Brain Res.* 403, 113138. doi:10.1016/j.bbr.2021.113138

Wang, B., Zhuang, X., Deng, Z. B., Jiang, H., Mu, J., Wang, Q., et al. (2014a). Targeted Drug Delivery to Intestinal Macrophages by Bioactive Nanovesicles Released from Grapefruit. *Mol. Ther.* 22, 522–534. doi:10.1038/mt.2013.190

Wang, D., Wang, H., and Gu, L. (2017). The Antidepressant and Cognitive Improvement Activities of the Traditional Chinese Herb Cistanche. *Evid. Based. Complement. Alternat. Med.* 2017, 3925903. doi:10.1155/2017/3925903

Wang, F., Wang, J., An, J., Yuan, G., Hao, X., and Zhang, Y. (2018a). Resveratrol Ameliorates Depressive Disorder through the NETRIN1-Mediated Extracellular Signal-Regulated kinase/cAMP Signal Transduction Pathway. *Mol. Med. Rep.* 17, 4611–4618. doi:10.3892/mmr.2018.8379

Wang, H., Zhang, R., Qiao, Y., Xue, F., Nie, H., Zhang, Z., et al. (2014b). Gastrodin Ameliorates Depression-like Behaviors and Up-Regulates Proliferation of Hippocampal-Derived Neural Stem Cells in Rats: Involvement of its Anti-inflammatory Action. *Behav. Brain Res.* 266, 153–160. doi:10.1016/j.bbr.2014.02.046

Wang, H., Zhong, L., Mi, S., Song, N., Zhang, W., and Zhong, M. (2020a). Tanshinone IIA Prevents Platelet Activation and Down-Regulates CD36 and MKK4/JNK2 Signaling Pathway. *BMC Cardiovasc. Disord.* 20, 81–87. doi:10.1186/s12872-019-01289-z

Wang, J. M., Pei, L. X., Zhang, Y. Y., Cheng, Y. X., Niu, C. L., Cui, Y., et al. (2018b). Ethanol Extract of Rehmannia Glutinosa Exerts Antidepressant-like Effects on a Rat Chronic Unpredictable Mild Stress Model by Involving Monoamines and BDNF. *Metab. Brain Dis.* 33, 885–892. doi:10.1007/s11011-018-0202-x

Wang, M., Yan, S., Zhou, Y., and Xie, P. (2020b). trans-Cinnamaldehyde Reverses Depressive-like Behaviors in Chronic Unpredictable Mild Stress Rats by Inhibiting NF-Kb/nlrp3 Inflammasome Pathway. *Evid. Based. Complement. Alternat. Med.* 2020, 4572185. doi:10.1155/2020/4572185

Wang, Q., Ren, Y., Mu, J., Egilmez, N. K., Zhuang, X., Deng, Z., et al. (2015). Grapefruit-Derived Nanovectors Use an Activated Leukocyte Trafficking Pathway to Deliver Therapeutic Agents to Inflammatory Tumor Sites. *Cancer Res.* 75, 2520–2529. doi:10.1158/0008-5472.CAN-14-3095

Wang, Q., Zhuang, X., Mu, J., Deng, Z. B., Jiang, H., Zhang, L., et al. (2013a). Delivery of Therapeutic Agents by Nanoparticles Made of Grapefruit-Derived Lipids. *Nat. Commun.* 4, 1867. doi:10.1038/ncomms2886

Wang, S., Wang, C., Yu, Z., Wu, C., Peng, D., Liu, X., et al. (2018c). Agarwood Essential Oil Ameliorates Restrain Stress-Induced Anxiety and Depression by Inhibiting HPA Axis Hyperactivity. *Int. J. Mol. Sci.* 19, 3468. doi:10.3390/ijms19113468

Wang, W., Liu, X., Liu, J., Cai, E., Zhao, Y., Li, H., et al. (2018d). Sesquiterpenoids from the Root of Panax Ginseng Attenuates Lipopolysaccharide-Induced Depressive-like Behavior through the Brain-Derived Neurotrophic Factor/Tropomyosin-Related Kinase B and Sirtuin Type 1/Nuclear Factor-Kb Signaling Pathways. *J. Agric. Food Chem.* 66, 265–271. doi:10.1021/acs.jafc.7b04835

Wang, Y., Gao, C., Gao, T., Zhao, L., Zhu, S., and Guo, L. (2021b). Plasma Exosomes from Depression Ameliorate Inflammation-Induced Depressive-like Behaviors via Sigma-1 Receptor Delivery. *Brain Behav. Immun.* 94, 225–234. doi:10.1016/j.bbi.2021.02.004

Wang, Z., Zhang, D., Hui, S., Zhang, Y., and Hu, S. (2013b). Effect of Tribulus Terrestris Saponins on Behavior and Neuroendocrine in Chronic Mild Stress Depression Rats. *J. Tradit Chin. Med.* 33, 228–232. doi:10.1016/s0254-6272(13)60130-2

Wei, Q., Zhou, W., Zheng, J., Li, D., Wang, M., Feng, L., et al. (2020a). Antidepressant Effects of 3-(3,4-Methylenedioxy-5-Trifluoromethyl Phenyl)-2e-Propenoic Acid Isobutyl Amide Involve TSPO-Mediated Mitophagy Signalling Pathway. *Basic Clin. Pharmacol. Toxicol.* 127, 380–388. doi:10.1111/bcpt.13452

Wei, Z. X., Xie, G. J., Mao, X., Zou, X. P., Liao, Y. J., Liu, Q. S., et al. (2020b). Exosomes from Patients with Major Depression Cause Depressive-like Behaviors in Mice with Involvement of miR-139-5p-Regulated Neurogenesis. *Neuropsychopharmacology* 45, 1050–1058. doi:10.1038/s41386-020-0622-2

Wheater, E. N. W., Stoye, D. Q., Cox, S. R., Wardlaw, J. M., Drake, A. J., Bastin, M. E., et al. (2020). DNA Methylation and Brain Structure and Function across the Life Course: A Systematic Review. *Neurosci. Biobehav. Rev.* 113, 133–156. doi:10.1016/j.neubiorev.2020.03.007

Wu, X. M., Gao, Y. B., Xu, L. P., Zou, D. W., Zhu, Z. Y., Wang, X. L., et al. (2017). Tongxinluo Inhibits Renal Fibrosis in Diabetic Nephropathy: Involvement of the Suppression of Intercellular Transfer of TGF-[Formula: See Text]1-Containing Exosomes from GECs to GMCs. *Am. J. Chin. Med.* 45, 1075–1092. doi:10.1142/S0192415X17500586

Xia, B., Huang, X., Sun, G., and Tao, W. (2021). Iridoids from Gardeniae Fructus Ameliorates Depression by Enhancing Synaptic Plasticity via AMPA Receptor-mTOR Signaling. *J. Ethnopharmacol.* 268, 113665. doi:10.1016/j.jep.2020.113665

Xiong, Z., Yang, J., Huang, Y., Zhang, K., Bo, Y., Lu, X., et al. (2016). Serum Metabonomics Study of Anti-depressive Effect of Xiao-Chai-Hu-Tang on Rat Model of Chronic Unpredictable Mild Stress. *J. Chromatogr. B Analyt Technol. Biomed. Life Sci.* 1029-1030, 28–35. doi:10.1016/j.jchromb.2016.06.044

Xu, J. N., Chen, L. F., Su, J., Liu, Z. L., Chen, J., Lin, Q. F., et al. (2018). The Anxiolytic-like Effects of Ginsenoside Rg3 on Chronic Unpredictable Stress in Rats. *Sci. Rep.* 8, 7741. doi:10.1038/s41598-018-26146-5

Xu, Q., Jiang, M., Gu, S., Wang, F., and Yuan, B. (2020). Early Life Stress Induced DNA Methylation of Monoamine Oxidases Leads to Depressive-like Behavior. *Front. Cell Dev. Biol.* 8, 582247. doi:10.3389/fcell.2020.582247

Xu, X. H., Yuan, T. J., Dad, H. A., Shi, M. Y., Huang, Y. Y., Jiang, Z. H., et al. (2021). Plant Exosomes as Novel Nanoplatforms for MicroRNA Transfer Stimulate Neural Differentiation of Stem Cells *In Vitro* and *In Vivo*. *Nano Lett.* 21, 8151–8159. doi:10.1021/acs.nanolett.1c02530

Xu, Z. (2011). Modernization: One Step at a Time. *Nature* 480, S90–S92. doi:10.1038/480S90a

Yang, J., Gao, F., Zhang, Y., Liu, Y., and Zhang, D. (2015). Buyang Huanwu Decoction (BYHWD) Enhances Angiogenic Effect of Mesenchymal Stem Cell by Upregulating VEGF Expression after Focal Cerebral Ischemia. *J. Mol. Neurosci.* 56, 898–906. doi:10.1007/s12031-015-0539-0

Yang, S. J., Yu, H. Y., Kang, D. Y., Ma, Z. Q., Qu, R., Fu, Q., et al. (2014). Antidepressant-like Effects of Salidroside on Olfactory Bulbectomy-Induced Pro-inflammatory Cytokine Production and Hyperactivity of HPA axis in Rats. *Pharmacol. Biochem. Behav.* 124, 451–457. doi:10.1016/j.pbb.2014.07.015

Yang, X. H., Song, S. Q., and Xu, Y. (2017). Resveratrol Ameliorates Chronic Unpredictable Mild Stress-Induced Depression-like Behavior: Involvement of the HPA axis, Inflammatory Markers, BDNF, and Wnt/β-Catenin Pathway in Rats. *Neuropsychiatr. Dis. Treat.* 13, 2727–2736. doi:10.2147/NDT.S150028

Yao, Z. Y., Chen, W. B., Shao, S. S., Ma, S. Z., Yang, C. B., Li, M. Z., et al. (2018). Role of Exosome-Associated microRNA in Diagnostic and Therapeutic Applications to Metabolic Disorders. *J. Zhejiang Univ. Sci. B* 19, 183–198. doi:10.1631/jzus.B1600490

Yeshurun, S., and Hannan, A. J. (2019). Transgenerational Epigenetic Influences of Paternal Environmental Exposures on Brain Function and Predisposition to Psychiatric Disorders. *Mol. Psychiatry* 24, 536–548. doi:10.1038/s41380-018-0039-z

You, Y., Borgmann, K., Edara, V. V., Stacy, S., Ghorpade, A., and Ikezu, T. (2020). Activated Human Astrocyte-Derived Extracellular Vesicles Modulate Neuronal Uptake, Differentiation and Firing. *J. Extracell. Vesicles* 9, 1706801. doi:10.1080/20013078.2019.1706801

Yu, L., Zheng, J., Li, J., Wang, Y., Lu, X., and Fan, X. (2020). Integrating Serum Exosomal microRNA and Liver microRNA Profiles Disclose the Function Role of Autophagy and Mechanisms of Fructus Meliae Toosendan-Induced Hepatotoxicity in Mice. *Biomed. Pharmacother.* 123, 109709. doi:10.1016/j.biopha.2019.109709

Yuan, D., Zhao, Y., Banks, W. A., Bullock, K. M., Haney, M., Batrakova, E., et al. (2017). Macrophage Exosomes as Natural Nanocarriers for Protein Delivery to Inflamed Brain. *Biomaterials* 142, 1–12. doi:10.1016/j.biomaterials.2017.07.011

Yuan, P., Ding, L., Chen, H., Wang, Y., Li, C., Zhao, S., et al. (2021). Neural Stem Cell-Derived Exosomes Regulate Neural Stem Cell Differentiation through miR-9-Hes1 Axis. *Front. Cell Dev. Biol.* 9, 601600. doi:10.3389/fcell.2021.601600

Zhang, B., Wang, P. P., Hu, K. L., Li, L. N., Yu, X., Lu, Y., et al. (2019a). Antidepressant-Like Effect and Mechanism of Action of Honokiol on the Mouse Lipopolysaccharide (LPS) Depression Model. *Molecules* 24, 2035. doi:10.3390/molecules24112035

Zhang, B., Wang, X., Li, Y., Wu, M., Wang, S.-Y., and Li, S. (2018a). Matrine Is Identified as a Novel Macropinocytosis Inducer by a Network Target Approach. *Front. Pharmacol.* 9, 1–11. doi:10.3389/fphar.2018.00010

Zhang, C. Y., Zeng, M. J., Zhou, L. P., Li, Y. Q., Zhao, F., Shang, Z. Y., et al. (2018b). Baicalin Exerts Neuroprotective Effects via Inhibiting Activation of GSK3β/NF-Kb/nlrp3 Signal Pathway in a Rat Model of Depression. *Int. Immunopharmacol.* 64, 175–182. doi:10.1016/j.intimp.2018.09.001

Zhang, H., Freitas, D., Kim, H. S., Fabijanic, K., Li, Z., Chen, H., et al. (2018c). Identification of Distinct Nanoparticles and Subsets of Extracellular Vesicles by Asymmetric Flow Field-Flow Fractionation. *Nat. Cell Biol.* 20, 332–343. doi:10.1038/s41556-018-0040-4

Zhang, J. Q., Wu, X. H., Feng, Y., Xie, X. F., Fan, Y. H., Yan, S., et al. (2016a). Salvianolic Acid B Ameliorates Depressive-like Behaviors in Chronic Mild Stress-Treated Mice: Involvement of the Neuroinflammatory Pathway. *Acta Pharmacol. Sin.* 37, 1141–1153. doi:10.1038/aps.2016.63

Zhang, L., Previn, R., Lu, L., Liao, R. F., Jin, Y., and Wang, R. K. (2018d). Crocin, a Natural Product Attenuates Lipopolysaccharide-Induced Anxiety and Depressive-like Behaviors through Suppressing NF-kB and NLRP3 Signaling Pathway. *Brain Res. Bull.* 142, 352–359. doi:10.1016/j.brainresbull.2018.08.021

Zhang, M., Viennois, E., Prasad, M., Zhang, Y., Wang, L., Zhang, Z., et al. (2016b). Edible Ginger-Derived Nanoparticles: A Novel Therapeutic Approach for the Prevention and Treatment of Inflammatory Bowel Disease and Colitis-Associated Cancer. *Biomaterials* 101, 321–340. doi:10.1016/j.biomaterials.2016.06.018

Zhang, M., Viennois, E., Xu, C., and Merlin, D. (2016c). Plant Derived Edible Nanoparticles as a New Therapeutic Approach against Diseases. *Tissue barriers* 4, e1134415. doi:10.1080/21688370.2015.1134415

Zhang, M., Wang, X., Han, M. K., Collins, J. F., and Merlin, D. (2017). Oral Administration of Ginger-Derived Nanolipids Loaded with siRNA as a Novel Approach for Efficient siRNA Drug Delivery to Treat Ulcerative Colitis. *Nanomedicine (Lond)* 12, 1927–1943. doi:10.2217/nnm-2017-0196

Zhang, R., Ma, Z., Liu, K., Li, Y., Liu, D., Xu, L., et al. (2019b). Baicalin Exerts Antidepressant Effects through Akt/FOXG1 Pathway Promoting Neuronal Differentiation and Survival. *Life Sci.* 221, 241–248. doi:10.1016/j.lfs.2019.02.033

Zhang, W. Y., Guo, Y. J., Han, W. X., Yang, M. Q., Wen, L. P., Wang, K. Y., et al. (2019c). Curcumin Relieves Depressive-like Behaviors via Inhibition of the NLRP3 Inflammasome and Kynurenine Pathway in Rats Suffering from Chronic Unpredictable Mild Stress. *Int. Immunopharmacol.* 67, 138–144. doi:10.1016/j.intimp.2018.12.012

Zhang, X., Du, Q., Liu, C., Yang, Y., Wang, J., Duan, S., et al. (2016d). Rhodioloside Ameliorates Depressive Behavior via Up-Regulation of Monoaminergic System Activity and Anti-inflammatory Effect in Olfactory Bulbectomized Rats. *Int. Immunopharmacol.* 36, 300–304. doi:10.1016/j.intimp.2016.05.008

Zhang, Y., Long, Y., Yu, S., Li, D., Yang, M., Guan, Y., et al. (2021). Natural Volatile Oils Derived from Herbal Medicines: A Promising Therapy Way for Treating Depressive Disorder. *Pharmacol. Res.* 164, 105376. doi:10.1016/j.phrs.2020.105376

Zhao, Y., Zhang, Y., and Pan, F. (2015). The Effects of EGb761 on Lipopolysaccharide-Induced Depressive-like Behaviour in C57BL/6J Mice. *Cent. Eur. J. Immunol.* 40, 11–17. doi:10.5114/ceji.2015.49427

Zheng, J., Yu, L., Chen, W., Lu, X., and Fan, X. (2018). Circulating Exosomal microRNAs Reveal the Mechanism of Fructus Meliae Toosendan-Induced Liver Injury in Mice. *Sci. Rep.* 8, 2832. doi:10.1038/s41598-018-21113-6

Zhuang, X., Deng, Z. B., Mu, J., Zhang, L., Yan, J., Miller, D., et al. (2015). Ginger-derived Nanoparticles Protect against Alcohol-Induced Liver Damage. *J. Extracell. Vesicles* 4, 28713. doi:10.3402/jev.v4.28713

Zhuang, X., Xiang, X., Grizzle, W., Sun, D., Zhang, S., Axtell, R. C., et al. (2011). Treatment of Brain Inflammatory Diseases by Delivering Exosome Encapsulated Anti-inflammatory Drugs from the Nasal Region to the Brain. *Mol. Ther.* 19, 1769–1779. doi:10.1038/mt.2011.164

Conflict of Interest: The authors declare that the research was conducted in the absence of any commercial or financial relationships that could be construed as a potential conflict of interest.

The reviewer YJ declared a shared affiliation with the author(s) QW and WD to the handling editor at the time of review.

Publisher's Note: All claims expressed in this article are solely those of the authors and do not necessarily represent those of their affiliated organizations, or those of the publisher, the editors, and the reviewers. Any product that may be evaluated in this article, or claim that may be made by its manufacturer, is not guaranteed or endorsed by the publisher.

GLOSSARY

4-HNE 4-hydroxynonenal
5-HIAA 5-hydroxyindoleacetic acid
5-HT 5-hydroxytryptamine
8-OHdG 8-hydroxy-2′-deoxyguanosine
11β-HSD2 11β-hydroxysteroid dehydrogenase-2
ACTH adrenocorticotropic hormone
AKT protein kinase B
ASC Anti-TMS1
ATP adenosine triphosphate
Bax Bcl-2-associated X protein
BBB blood brain barrier
Bcl-2 B-cell lymphoma 2
BDNF brain-derived neurotrophic factor
CA1 the first region in the hippocampal circuit
CAT Catalase
CD36 cluster of differentiation 36
CD81 cluster of differentiation 81
CHM Chinese herbal medicine
CMS chronic mild stress
CMSC cardiac mesenchymal stem cells
CNS central nervous system
CORT CORT
COVID-19 coronavirus disease 2019
COX Cyclooxygenase
CRC colorectal cancer
CRH corticotropin-releasing hormone
CRP C-reactive protein
CRS chronic restraint stress
CSDS Chronic social defeat stress
CUMS chronic unpredictable mild stress
CUS chronic unpredictable stress
DCX doublecortin
DG dentate gyrus
DXM dextromethorphan
EAP experimental autoimmune prostatitis
EVs extracellular vesicles
FGF2 Fibroblast growth factor
FOXG1 Forkhead box transcription factor
FoxO1 forkhead box protein O 1
FST forced swimming test
GDNPs ginseng-derived nanoparticles
GFAP glial fibrillary acidic protein
GluA1 Glutamate Receptor 1
GPx Glutathione peroxidase
GR glucocorticoid receptor
GSH-pX glutathione peroxidase
HPA hypothalamic pituitary adrenal
Iba1 Ionized calcium binding adaptor molecule 1
IBA1 Ionized calcium binding adaptor molecule 1
IDO indoleamine 2,3-dioxygenase
IFN-γ interferon *γ*
IL-18 interleukin-18
IL-1β interleukin-1β
IL-34 interleukin 34
IL-6 interleukin-6
iNOS inducible nitric oxide synthase
IRS-1 insulin receptor substrate 1
IκB-α inhibitor of κB-α
JNK2 c-Jun NH 2 terminal kinase
KIFC2 Kinesin Family Member C2
Kir4.1 inward rectifying potassium channel
L1CAM L1 Cell Adhesion Molecule
LDHA lactate dehydrogenase A
LH learned helplessness
LPS lipopolysaccharide
Maxim. Bolbostemma paniculatum
MCAO middle cerebral artery occlusion
MDA malondialdehyde
MDD major depressive disorder
miRNAs microRNAs
MKK4 mitogen-activated protein kinase kinase 4
NF-κB nuclear factor kappa-light-chain-enhancer of activated B cells
NLRP3 oligomerization domain-like receptor family pyrin domain-containing 3
nNOS neural nitric oxide synthase
NO nitric oxide
NSCs neural stem cells
NSE Neuron-specific enolase
NT-3 Neurotrophin-3
p-AKT phosphorylation-akt
p-CREB phospho-cAMP response element-binding protein
PDK-1 pyruvate dehydrogenase lipoamide kinase isozyme 1
PI3K phosphoinositide 3-kinase
p-iκB phospho-inhibitor of kappa B
PMVs platelet-derived microvesicles
p-p65 anti-p-NF-κB p65

p-P70S6K Phospho-p70 S6 kinase
PSD-95 Postsynaptic density protein 95
ROS reactive oxide species
RS restraint stress
SDS social defeat stress
SERTs serotonin transporters
SGK1 glucocorticoid-regulated kinase 1
Sig-1R sigma-1 receptor
Sirt 1 sirtuin type 1
SOD superoxide dismutase
SRS spatial restraint stress
TBM1 tubeimoside-1
TCAs tricyclic antidepressants
TLR4 Toll Like Receptor 4
TNFR1 tumor necrosis factor receptor 1
TNF-α TNF-α
TrkB tropomyosin-related kinase B
TSPO translocator protein

frontiers | Frontiers in Pharmacology

ORIGINAL RESEARCH
published: 05 April 2022
doi: 10.3389/fphar.2022.858190

Agathisflavone as a Single Therapy or in Association With Mesenchymal Stem Cells Improves Tissue Repair in a Spinal Cord Injury Model in Rats

*Ravena P. do Nascimento[1], Lívia B. de Jesus[1], Markley S. Oliveira-Junior[1], Aurea M. Almeida[1], Eduardo L. T. Moreira[2], Bruno D. Paredes[3], Jorge M. David[4], Bruno S. F. Souza[3,5], Maria de Fátima D. Costa[1,6], Arthur M. Butt[7], Victor Diogenes A. Silva[1,8] and Silvia L. Costa[1,5,8]**

[1]Laboratory of Neurochemistry of Cellular Biology, Department of Biochemistry and Biophysics, Institute of Health Sciences, Federal University of Bahia, Salvador, Brazil, [2]Department of Anatomy, Pathology and Veterinary Clinics, Hospital of Veterinary Medicine, Federal University of Bahia, Salvador, Brazil, [3]Center for Biotechnology and Cell Therapy, São Rafael Hospital, D'Or Institute for Research and Education, Salvador, Brazil, [4]Department of General and Inorganic Chemistry, Institute of Chemistry, Federal University of Bahia, Salvador, Brazil, [5]Gonçalo Moniz Institute, FIOCRUZ-BA, Salvador, Brazil, [6]INCT–Translational Neuroscience (INCT-TN, BR), Salvador, Brazil, [7]School of Pharmacy and Biomedical Sciences, University of Portsmouth, Portsmouth, United Kingdom, [8]INCT for Excitotoxicity and Neuroprotection (INCT-EN, BR), Salvador, Brazil

OPEN ACCESS

Edited by:
Rui Liu,
Chinese Academy of Medical Sciences, China

Reviewed by:
Masahito Nakazaki,
Yale Medicine, United States
Liu Qing-Shan,
Minzu University of China, China

***Correspondence:**
Silvia L. Costa
costasl@ufba.br

Specialty section:
This article was submitted to Neuropharmacology, a section of the journal Frontiers in Pharmacology

Received: *19 January 2022*
Accepted: *28 February 2022*
Published: *05 April 2022*

Citation:
do Nascimento RP, de Jesus LB, Oliveira-Junior MS, Almeida AM, Moreira ELT, Paredes BD, David JM, Souza BSF, de Fátima D. Costa M, Butt AM, Silva VDA and Costa SL (2022) Agathisflavone as a Single Therapy or in Association With Mesenchymal Stem Cells Improves Tissue Repair in a Spinal Cord Injury Model in Rats. Front. Pharmacol. 13:858190. doi: 10.3389/fphar.2022.858190

Agathisflavone is a flavonoid with anti-neuroinflammatory and myelinogenic properties, being also capable to induce neurogenesis. This study evaluated the therapeutic effects of agathisflavone—both as a pharmacological therapy administered *in vivo* and as an *in vitro* pre-treatment aiming to enhance rat mesenchymal stem cells (r)MSCs properties–in a rat model of acute spinal cord injury (SCI). Adult male Wistar rats (n = 6/group) underwent acute SCI with an F-2 Fogarty catheter and after 4 h were treated daily with agathisflavone (10 mg/kg ip, for 7 days), or administered with a single i.v. dose of 1×10^6 rMSCs either unstimulated cells (control) or pretreated with agathisflavone (1 μM, every 2 days, for 21 days *in vitro*). Control rats (n = 6/group) were treated with a single dose methylprednisolone (MP, 60 mg/kg ip). BBB scale was used to evaluate the motor functions of the animals; after 7 days of treatment, the SCI area was analyzed after H&E staining, and RT-qPCR was performed to analyze the expression of neurotrophins and arginase. Treatment with agathisflavone alone or with of 21-day agathisflavone–treated rMSCs was able to protect the injured spinal cord tissue, being associated with increased expression of NGF, GDNF and arginase, and reduced macrophage infiltrate. In addition, treatment of animals with agathisflavone alone was able to protect injured spinal cord tissue and to increase expression of neurotrophins, modulating the inflammatory response. These results support a pro-regenerative effect of agathisflavone that holds developmental potential for clinical applications in the future.

Keywords: MSCs, mesenchymal stem cells, agathisflavone, acute spinal cord injury, neurotrophins, regeneration

INTRODUCTION

Spinal cord injury (SCI) is a devastating neurological condition, with a global incidence of 10.4–83 cases/million/year (Karsy and Hawryluk, 2019). Treatment of SCI requires multidisciplinary action in the acute phase and also for secondary complications associated with long-term injury (Liu et al., 2017). Currently, routine therapy employed in the early stages of SCI mainly involves surgical procedures combined with high doses of methylprednisolone (MP) for the inhibition of lipid peroxidation and maintenance of the blood barrier of the spinal cord, although this treatment is controversial (Cabrera-Aldana et al., 2017; Liu et al., 2018). Mesenchymal stem cells/stromal cells (MSCs) have arisen as a treatment for SCI in animal models and in patients, either alone or in association with drugs (Mendonça et al., 2014; Assinck et al., 2017; Larocca et al., 2017; Allahdadi et al., 2019; Jin et al., 2019). Recent studies have shown that MSCs release exosomes that attenuate apoptosis and inflammation; they also suppress glial scarring, attenuate lesion size and promote axonal regeneration culminating in better behavioral recovery (Yin et al., 2019; Yuan et al., 2019). However, direct transplantation of MSCs to target tissues remains challenging, as low cell survival rates, cell dedifferentiation, immune rejection and tumor formation can all compromise the efficacy of this therapy (Caplan et al., 2019).

Flavonoids stand out as an important class of natural antioxidants with demonstrated neuroprotective effects in animal models of SCI, including curcumin (Akar et al., 2017), huangqin (Zhang et al., 2018) and baicalin (Kang et al., 2018). In addition, the flavonoid apigenin has been reported to significantly reduce side effects in an animal model of SCI (Zhang and Liao, 2014). Agathisflavone, a biflavonoid composed of two apigenins, exhibits anti-inflammatory (dos Santos Souza et al., 2018), neurogenic and neurodifferentiating activities *in vitro*, as well as a neurogenic effect on embryonic stem cells and multipotent stem cells (Paulsen et al., 2011). We therefore postulated that agathisflavone may be a useful adjuvant to MSC therapy in SCI. Our results show that the infusion of rat (r)MSC treated with agathisflavone increased the production of neurotrophic and anti-inflammatory factors in a rat model of SCI.

MATERIALS AND METHODS

A summary of the experimental design is presented in **Figure 1**.

Animals

Thirty-six 30-day-old male Wistar rats were obtained from the animal facility of the Center for Biotechnology and Cell Therapy, São Raphael Hospital and kept in the vivarium of the Institute of Health Sciences of the Federal University of Bahia, Salvador, Brazil. They were maintained in a controlled environment (12 h light/dark cycle, 22 ± 1°C, with access to food and water *ad libitum*). Rats were used experimentally after reaching 3 months of age and weight ranging from 250 to 280 g. All animal procedures were performed according to the National Institute of Health (NIH) Guide to the Care and Use of Laboratory Animals and approved by the Animal Use Ethics Committee of the Institute of Health Sciences of the Federal University of Bahia (process number 117/2017).

Purification and Culture of rMSC

Rat mesenchymal stem cells were isolated using the method originally described by Friedenstein et al. (1974), which is based on their ability to adhere to plastic. Briefly, bone marrow aspirate was made from isolated femur bones of male adult rats and then processed using the hydrophilic polysaccharide Ficoll® as the centrifugation gradient. For this, bone femur epiphysis was minimally cut and then a needle was attached to a syringe containing DMEM medium and inserted into the epiphysis to wash the bone cavity. This bone marrow was then collected, resuspended in DMEM medium in a 2-ml volume added to a 10 ml tube falcon and centrifuged for 10 min at 1,750 centrifugal g force (Hettiche® Universal 320R Centrifuge). Then, the pellet was resuspended in a volume of 2 ml of DMEM medium and transferred to a 10-ml tube falcon. 1 ml of the Ficoll® density gradient was added and then centrifugation was performed for 15 min at 4,820 centrifugal g force (Hettiche® Universal 320R Centrifuge). After that, the ring of cells at the Ficoll®/DMEM interface was collected and resuspended in DMEM medium in volume 1: 5 ml cells: medium. Cells were collected and plated in Dulbecco's Modified Eagle Medium (DMEM), enriched with fetal bovine serum (FBS) and antibiotics (100 IU/Ml penicillin G, 100 μg ml^{-1} streptomycin, Gibco). After 24 h, the culture medium was changed to remove non-adherent cells. The remaining cells were grown in a humid incubator (37°C, 5% CO_2) and the culture medium was changed every 2–3 days until cells reached a confluence of about 80%, which occurred around 10 days *in vitro* (DIV). Cells were then trypsinized and expanded by subsequent passages. In this work, all the tests were run with passage 3 rMSCs and in triplicates (**Figure 1**).

Characterization of rMSC

Rat mesenchymal stem cells (rMSC) were characterized according to the criteria of the International Society for Cellular Therapy (Horwitz et al., 2005; Caplan 2009), namely expression of specific markers (CD29, CD73, CD90, CD11b, CD34 and MHC-II), measured by flow cytometry (Complementary Material I), and their adipogenic and osteogenic potential in culture (Complementary Material II). In brief, 1×10^6 rMSC were cultured for 10 DIV in 10-mm diameter plates (TPP®) in DMEM with 10% FBS, antibiotics (100IU/Ml penicillin G, 100 μg/ml^{-1} streptomycin, Gibco®), 10 M dexamethasone (Sigma®). For adipogenic differentiation, the medium was supplemented with insulin (2.5 μg/ml), indomethacin (100 μM) and 3-isobutyl methylxanthine (0.5 mM); as for osteogenic differentiation, the medium was supplemented with ascorbic acid (50 μg/ml) and β-glycerolphosphate (3.15 mg/ml). After 11 days, cells were fixed with 4% paraformaldehyde for 30 min and stained for 5 min at room temperature with Oil Red O for adipocytes, or alizarin red for osteoblasts (Muniswami et al., 2018). The cultures were then washed with PBS and examined under bright field microscopy (**Figure 1**).

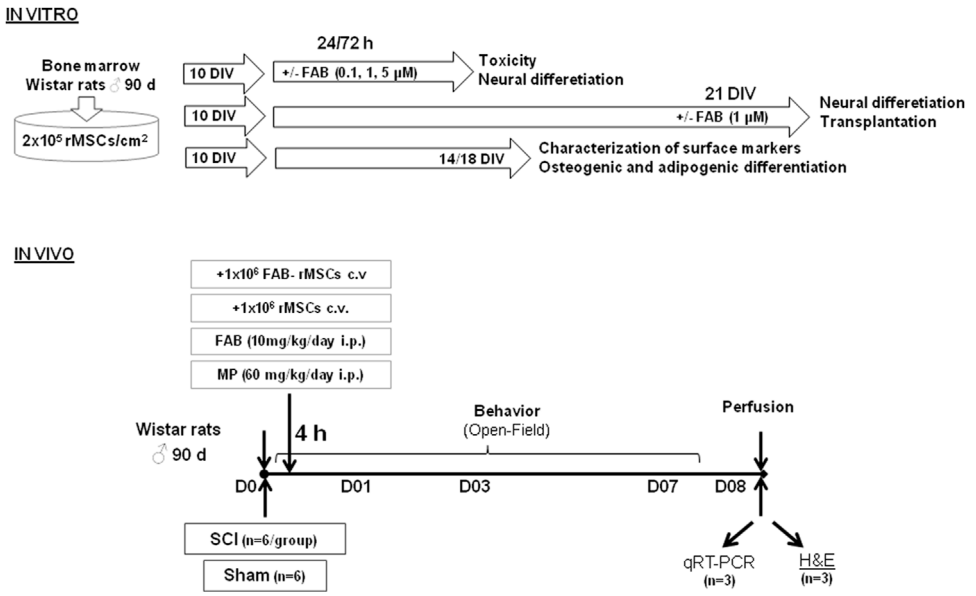

FIGURE 1 | Experimental design showing model adopted to investigate effects of rat bone marrow mesenchymal stem cells (rMSCs) and agathisflavone (FAB) treatments in a model of spinal cord injury (SCI). Days *in vitro* (DIV).

Flavonoid Treatment of rMSC

Agathisflavone was extracted from the aqueous extract of the leaves of *P. pyramidalis* Tull as previously described (Mendes et al., 2000; Bahia et al., 2005; Bahia et al., 2010). Agathisflavone was dissolved in dimethyl sulfoxide (DMSO; Sigma®) to yield a 100-mM stock solution that was stored and protected from light at −4°C. As described above, rMSC were cultured to passage (P)3 and plated at a density of 2×10^5 cells/cm^2 and cultured for 24 h, prior to treatment with agathisflavone diluted directly into the culture medium to achieve the final concentration (see below). Multiple analyses were performed after 1–21 days in culture (see below).

Analysis of rMSC Viability

Viability of rMSC was assessed using the MTT assay (3-(4,5-dimethylthiazol-2-yl)-2,5-diphenyltetrazolium bromide test; Sigma®, St. Louis, MO), which is based on the conversion of the yellow MTT by the dehydrogenases of living cells to purple-colored formazan (Hansen et al., 1989). The experiment was performed in 96-well plates (Kasvi®, Brazil) of cultured rMSC. Cells were incubated in 0.01% DMSO (control) or with agathisflavone (0.1, 1.0 or 5 µM). 24 h or 72 h after treatment, cells were incubated with MTT (1 mg/ml) for 2 h. Subsequently, cells were lysed with 20% (vw^{-1}) with sodium dodecyl sulfate (SDS) and 50% (vv^{-1}) dimethylformamide (DMF) (pH 4.7). The plates were incubated overnight at 37°C to dissolve the formazan crystals and the optical density of each sample was measured at 590 nm using a spectrophotometer (Thermo Plate-Reader®). At least three independent experiments were performed with eight replicate wells for each analysis. MTT results are expressed as percentages of cells converting MTT compared to control cultures (considered as 100%).

Characterization of rMSC Morphology

Based on the results of the MTT test, morphological analysis was performed in cultures treated with agathisflavone at 0.1 and 1 µM for 72 h, compared to DMSO controls. 72 h after treatment, cultures were washed three times with phosphate buffered saline (PBS), fixed and permeabilized with cold methanol at −20°C for 20 min and analyzed by Rosenfeld staining, by adding ed to the plates previously fixed with cold methanol at −20°C in enough volume to completely cover the cells. After 3 min, 20 drops of distilled water were added to the dye solution and the stain was allowed to act for a further 20 min at room temperature. The plates were then washed with distilled water, dried and analyzed by means of light microscopy.

Characterization of Neural and Glial Markers in rMSC

In order to investigate whether the flavonoid agathisflavone induces phenotypic changes in rMSC associated with neural and glial differentiation, immunocytochemistry was performed 72 h after treatment with 1 µM agathisflavone, compared to DMSO-treated controls. Immunocytochemistry was performed as described by dos Santos Souza et al., 2018. Briefly, cells were fixed with 4% paraformaldehyde (PFA) and 4% sucrose for 20 min and permeabilized with 0.2% 4- (1,1,3,3-tetramethylbutyl) phenyl polyethylene glycol (Triton X-100, Merck®) for 5 min at room temperature. After permeabilization, cells were blocked with 5% bovine serum albumin (BSA; Invitrogen®) in PBS (blocking solution) for 1 h and incubated overnight at room temperature with primary antibodies diluted in blocking solution: mouse anti-β-III-tubulin antibody, 1:1,000 (Promega®, Madison, WI); anti-

TABLE 1 | Characterization of mesenchymal stem cells by flow cytometry.

	% Positive cells	% Negative cells
CD11b+	0.8	99.2
CD34	3.33	96.67
MHC II	3.48	96.52
CD29	99.7	0.3
CD73	67.6	32.4
CD90	68.9	31.1

rabbit glial fibrillary acidic protein (GFAP) antibody, 1:200 (Dako Corporation, Glostrup®, Denmark). After incubation with primary antibodies, cells were washed extensively with PBS and incubated with secondary antibodies for 1 h at room temperature. Secondary antibodies were purchased from Molecular Probes® (Eugene, OR): Alexa fluor 488 conjugated goat anti-mouse IgG (1: 400), Alexa fluor 546 conjugated goat anti-rabbit IgG (1: 1,000). Negative controls were performed by omitting the primary antibody during immunostaining and, in all cases, no reactivity was observed when the primary antibody was absent. Cell preparations were mounted directly on 3,4,5-trihydroxy benzoate (N-propyl gallate, Sigma-Aldrich®) and visualized using a Leica® EBQ 100 fluorescence light microscope.

SCI Experimental Design

Male Wistar rats were divided into six groups (n = 6 animals/group): sham; spinal cord injury (SCI); treated with a single application (via caudal vein) of 1×10^6 21 DIV control rMSCs; treated with a single application (via caudal vein) of 1×10^6 21 DIV agathisflavone-treated rMSC; treated with one single dose of methylprednisolone (MP, 60 mg/kg i. p.); or treated daily with agathisflavone (10 mg/kg i.p.) once a day, at the same time for 7 days. Caudal vein administration was performed based on studies with other flavonoids in an SCI model (Zhang et al., 2014; Akar et al., 2017).

On the day of surgery, the animals were individually weighed to obtain the volume of the anesthetic mixture. The combination used was ketamine chloridate (ketalar®) 75 mg/kg IP and xylazine chloridate (rompum®) 10 mg/kg IP. Spinal cord injury was induced as previously described (Vanický et al., 2001). We performed trichotomy and asepsis of the skin in the thoracic region with Betadine®. Then, a midline incision of 20 mm was made in the thoracic region, and the spine was exposed. Laminectomy was performed at vertebral level T-10, exposing the dorsal cord. A Fogarty F-2® catheter was inserted into the dorsal epidural space through a small hole in the T10 spinal arch, cranially advanced at the level of the T8-9 spine and inflated for 5 min with the aid of a Hamilton® syringe and 15 µl of saline solution (**Figure 1**). After surgery, animals were submitted post-operative care: they were kept in individualized cages heated to a constant temperature of 27°C to avoid hypothermia, received saline solution subcutaneously (3 ml) and were monitored at least 4 times a day to assess the presence of pain in the post-procedure and for the emptying of the urinary bladder. Until normalization of excretory functions, bladder massage was performed 4 times a day to assist urinary bladder emptying. All animals received topical application of rifocina® to combat topical infections (Rifamycin sodium salt, 10 mg/ml, spray). During the experimental period, the animals were monitored for feeding, water intake and excretory function (urine and feces). They all received water and food *ad libitum*.

Motor and Weight Variation Analysis of Animals Submitted to Acute Spinal Cord Injury

Animals were examined and weighed do determine their general health on days 0, 1 and 7, where day 0 refers to the day of surgery. Motor assessment was performed using the Basso, Beattie, Bresnahan scale (BBB) (Basso et al., 1995), by observing the movements of the hip, knee, ankle joint, trunk position, tail and hind legs. From these observations, points were assigned from zero to 21, with zero corresponding to the total absence of movements and 21 to the presence of normal movements (Barros Filho and Molina, 2008). The animals were placed in an open field, observed and filmed for 10 min. Motor assessment was performed on days 0, 1 and 7 post-surgery.

Histopathological Analysis of the Spinal Cord by Hematoxylin and Eosin

For morphological analysis, rats were intracardially perfused with saline solution and fixed with 4% PFA for 10 min under terminal anesthesia. A ketamine/xylazine mixture (up to 75 mg/kg body weight ketamine and 10 mg/kg xylazine body weight) was administered by intraperitoneal injection (27-gauge needle and a cc syringe). Additional anesthetic administration was performed as needed during each operation to maintain an anesthesia surgical plan. Once the animal reached a surgical plan for anesthesia, surgery and perfusion were performed. Spinal cords were removed and fixed in 10% formalin buffer for approximately 7 days at RT. After fixation, the spinal cord tissue was dehydrated and included in paraffin. It was then halved in the posterior median sulcus and embedded in paraffin. Serial longitudinal 4-µm sections were cut on a microtome at the level of the SCI, between 5 mm before the T7 vertebra and 5 mm after the T8 vertebra. Serial sections were dewaxed in ascending xylene stained using hematoxylin and eosin (H&E) and mounted on slides. The slides were evaluated under light microscope by a pathologist blinded to the groups. The histopathological evaluation was evaluated by the semiquantitative classification system, as described by Ustun et al. (2014) **Table 4**. Quantification of macrophages was made in ten randomly assigned photomicrographs (50-µm range) for each experimental group.

Molecular Analyses of Neuroinflammatory Profile in the Site of the SCI

Three spinal cord samples were randomly assigned to each group of animals for ribonucleic acid (RNA) extraction using Trizol® reagent (Invitrogen, Life Technologies™) according to the manufacturer's specifications. cDNA synthesis was performed

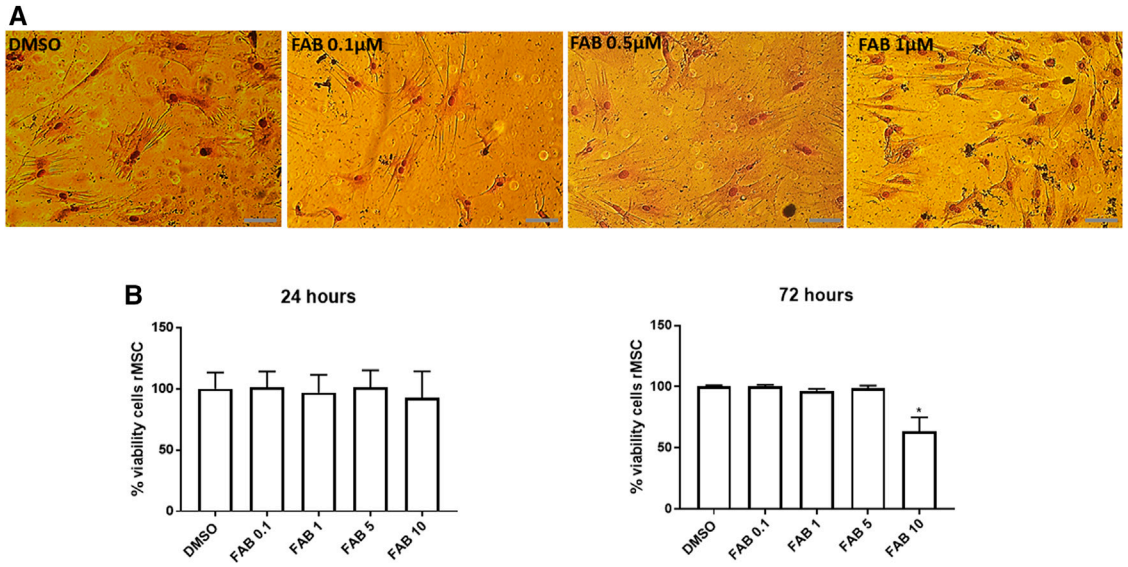

FIGURE 2 | (A) Morphological aspect of 30 days *in vitro* (DIV) of rMSCs of cultures in control conditions (0.01% DMSO) and 72 h after treatment with FAB (0.1, 0.5 and 1 μM); Rosenfeld staining; obj. x40, scale bar 50 μm. After treatment with 0.1 and 0.5 μM FAB, the cells presented a flat polygonal morphology similar to that of the control (DMSO). However, after treatment with 1 μM FAB, the cells presented Y-shaped extensions. **(B)** Analysis of viable rMSCs of cultures in control conditions (0.01% DMSO) and 24 and 72 h after treatment with FAB (0.1, 1, 5 and 10 μM), showing no toxicity in 24 h and toxicity only for FAB 10 μM 72 h after treatment; MTT test; Each graph is representative of three independent experiments and the data are expressed as means ± standard deviation. An ANOVA one-way test followed by Turkey's test for multiple comparisons was performed.

using SuperScript® VILO ™ Master Mix (Invitrogen, Life Technologies ™) following the manufacturer's instructions. Quantitative real-time polymerase chain reaction (RT-qPCR) was performed using Taqman® gene expression assays (Applied Biosystems, CA, United States) containing two primers to amplify the sequence of interest and the Taqman® MGB-specific probe labeled FAM fluorophore with TaqMan® Universal Master Mix II (Invitrogen, Life Technologies ™). Assay identifications for the genes quantified in this study were: Arginase 1 (RN00681090_m1), nerve growth factor/NGF (RN01533872_m1) and glia-derived neurotrophic factor/GDNF (RN00569519_m1), both distributed by Thermo Fisher (TaqMan® Gene Expression assay). RT-qPCR was performed using the QuantStudio ™ 7 Flex Real-Time PCR System instrument (Applied Biosystems, CA, United States). Thermocycling conditions were performed according to the manufacturer's specifications. B-actin (Mm00607939_S1) and HPRT1 (Mm01545399_m1) were used as reference genes (endogenous controls) for normalization of gene expression data. The analysis of real-time polymerase chain reaction data was based on Schmittgen and Livak (2008), using the 2-ΔΔCt method. All tests were performed in triplicate.

Statistical Analysis

Statistical analyses were performed with the GraphPad Prism software version 5.00 for Windows. Data were shown as means with standard deviation or means with range according to their distribution, analyzed with the Shapiro–Wilk normality test and Skewness (normal: < 1 or > −1) and Kurtosis (normal: < 2 or > −2) calculation. In addition, according to the distribution, parametric or nonparametric statistic tests were chosen. The most appropriate test for each experiment was used, and this information is given in the respective result. All analyses were carried out with triplicates.

RESULTS

Characterization of Rat Mesenchymal Stem Cells (rMSC)

First, we characterized rMSCs isolated from adult rat femur bone marrow on the third passage (P3), by their differentiation and surface expression of key markers measured by flow cytometry (**Supplementary Figures S1, S2**). rMSCs adhered to plastic and presented a fibroblast-like morphology 7–10 days after being seeded onto culture flasks (**Supplementary Figure S1A**). rMSC submitted to adipogenic differentiation displayed lipid droplet formation after 9 days, and this was remained up to 15 days, as determined by Oil red O staining (**Supplementary Figure 1SB**). rMSC submitted to osteogenic differentiation displayed calcium deposition during the first 10 days after induction and remained for 21 days, characterizing matrix mineralization as determined by alizarine red staining (**Supplementary Figure S1C**). As controls for both differentiation protocols, cultures were cultivated with expansion medium during the entire protocol and, as expected, showed no formation of lipid vacuoles or calcium deposits; the doubling time of these cells was approximately 60 h and linear between P3 and P5. In addition, flow cytometry demonstrated that 68.5, 67.6 and 99.7% of the

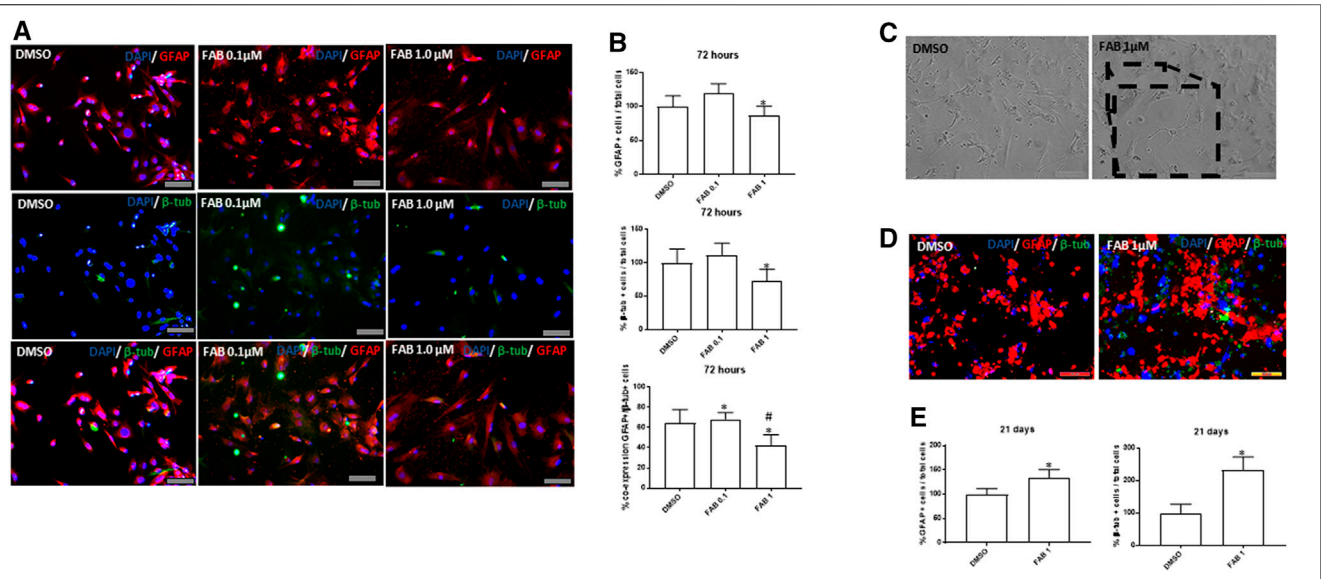

FIGURE 3 | Analysis of the expression of neural markers GFAP (red) and β-tubulin III (β-tub, green) in rat bone marrow-derived mesenchymal stem cells (rMSCs). **(A)** Photomicrographies of cultures in control conditions (0.01% DMSO) and 72 h after treatment with agathisflavone (0.1, 1 µM FAB); immunocytochemistry; scale bar 100 µm. Note that there is an discret increase compare to control in the proportion of GFAP + cells distributed in the cell body of flat polygonal cells in cultures exposed to 0.1 µM FAB, with some polygonal cells co-expressing β-tub, typical of neural progenitor cells. Such effect was not observed at the extension in cultures exposed to 1 µM FAB. **(B)** Quantification of the proportion of GFAP + cells and β-tub + cells related to the total of cell nuclei counted by DAPI-stained nucleus (blue); the results are expressed as the percentage of means ± SD related to control, considered as 100%, in three independent experiments and were analyzed by Kruskal–Wallis ANOVA, followed by Turkey's test for multiple comparisons (*) representing $p \leq 0.05$ compared to control; **(C)** Morphological analysis of rMSCs maintained 21 days in control conditions (0.01% DMSO) or treated with a single dose of 1 µM FAB; obj. x20, scale bar 100 µm. In the inserts of image at obj. 40x, one can see some cells with neuronal morphology, presenting cellular process similar to neurites and interacting with other cells. **(D)** Photomicrographies of cultures in control conditions (0.01% DMSO) and 72 h after treatment with agathisflavone (1 µM FAB); immunocytochemistry, obj. x20, scale bar 100 µm. Note that there is an increase in the proportion of cells co-expressing GFAP and β-tub compared to control cultures, which is confirmed in **(E)** by quantifying the proportion of GFAP+/β-tub + cells, related to the total of cell nuclei; the results are expressed as the means of percentage in three independent experiments and analyzed by Kruskal–Wallis ANOVA followed by Turkey's test for multiple comparisons (*) representing $p \leq 0.05$ compared to control.

rMSC cell population were respectively positive for CD90 (VLA-β integrin), CD73 and CD29, and the vast majority (>95%) were negative for typical hematopoietic and endothelial cell markers CD11b (immune cell marker–integrin Mac-1) and CD34, with negligible expression of MHC-II, respectively (**Supplementary Figure S2** and **Table 1**). Together, these findings demonstrate our protocols provided cultures of characteristic MSC in corroboration with other studies (Caplan, 2009; Dariolli et al., 2013).

Effects of Agathisflavone on Morphology and Viability of rMSC

The next step was to evaluate the potential toxicity of agathisflavone on P3 rMSC. Culture of rMSC with 0.1–5 µM agathisflavone had no effect on cell viability after 24 h. A reduction on cell viability was observed only in 72 h for a treatment with agathisflavone 10 µM, as determined by the MTT assay, compared to control cultures treated with 0.01% DMSO vehicle (**Figure 2B**). The effects of agathisflavone on rMSC morphology was evaluated by Rosenfeld's staining (**Figure 2A**). In control cultures treated with 0.01% DMSO vehicle, rMSC was presented as large cells with a flat polygonal morphology, with very short processes or without processes, and a clearly visible nucleus, typical of mature cells with the classification of "smaller stem potential" (Sekiya et al., 2002; Neuhuber et al., 2008). Cells treated with 0.1 or 0.5 µM agathisflavone for 72 h presented the same pavement morphology as control cultures, whereas following treatment with 1 µM agathisflavone a subpopulation of rMSC displayed a very clear cell body, refringent nucleus and long and thin Y-shaped extensions. It was also observed that some cells presented an astrocyte-like polyhedral morphology, with processes extending from their cell body. The cells retain their characteristic morphology, but at 1 µM agathisflavone evidently altered rMSC morphology, which may be indicative of inducing cellular pluripotency.

The MTT results demonstrate that agathisflavone is non-toxic for rMSC at any of the concentration used (0.1, 1 or 0.5 µM agathisflavone) after 24 h.

Effects of Agathisflavone on rMSC Differentiation

In order to determine whether the morphogenic effects of agathisflavone on rMSCs were associated with induction of differentiation, we performed immunocytochemistry for the astrocyte marker GFAP and the neuronal marker β-TubIII,

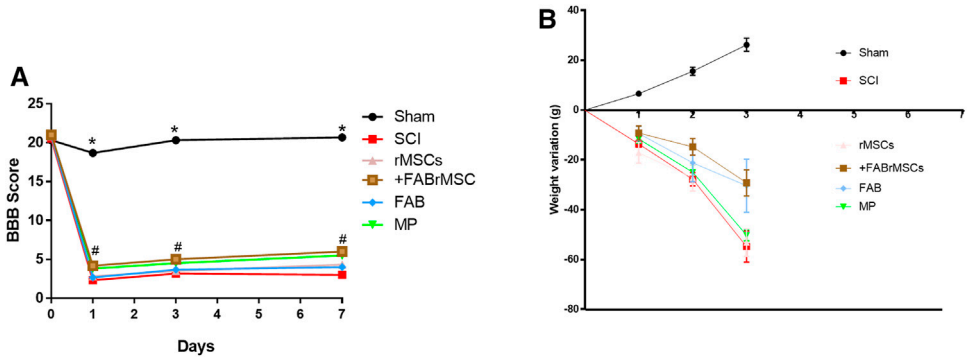

FIGURE 4 | Behavioral outcomes in animals subjected to spinal cord injury (SCI). **(A)** Motor function assessment based on the Basso, Beattie, Bresnahan scale (BBB) on day zero (before SCI), day 1, day 3 and day 7 after SCI. Adult male Wistar rats (n = 6/group) underwent acute SCI and after 4 h were treated with a single application of 1 × 10^6 control rMSCs or 1 × 10^6 rMSCs pretreated with agathisflavone (+FABrMSCs), treated with one single dose of methylprednisolone (60 mg/kg i.p., MP), or treated daily with agathisflavone (10 mg/kg i. p., FAB) (#) $p \leq 0.05$ vs. SCI rats. Data are the means ± SD **(B)** Weight variations of animals with SCI and different treatments.

TABLE 2 | Comparison between BBB scores. Data are expressed as means ± SD.

Day	Sham	SCI	rMSCs	rMSCs	+FABrMSCs	MP
1	20	2.7	2.8	4	4.8	4.6
3	20	2.9	3	4.5	5.0	4.8
7	21	3.4	3.3	4.8	5.3	5
Mean ± SD	20,33 ± 05,773	3 ± 1.3	3 ± 1.3	4.43 ± 1.0	5.03 ± 1.0	4.8 ± 0.8

SD, standard deviation.
Probability obtained from Student's t-test.
Mean of the samples (α = 0.05).

72 h after treatment with 0.1 or 1 μM agathisflavone or 0.01% DMSO vehicle in controls (**Figure 3**). In control cultures, the majority of rMSC were GFAP immunopositive, but labeling was restricted to the perinuclear region, whereas very few cells showed low β-TubIII expression (**Figure 3A**). In contrast, there was an evident increase in the intensity of GFAP and β-TubIII immunolabeling in rMSC cultures treated with 0.1 μM, but not observed with 1 μM agathisflavone treatment. The same analysis was performed in cultures 21 days after treatment with agathisflavone and it was determined that the majority of rMSC treated with 1 μM agathisflavone were immunopositive for GFAP and β-TubIII (**Figures 3C–E**). The results indicate that agathisflavone promotes neural differentiation of rMSC.

Effects of Agathisflavone and rMSCs Treatment on Spinal Cord Injury (SCI)

Functional Motor Recovery

Following the evaluation of the effects of agathisflavone on cultured rMSC, we examined the effects of its administration on the outcome of SCI, besides treatment of animals with the flavonoid. There were six experimental groups (n = 6 rats/group): 1) sham; 2) spinal cord injury (SCI); 3) SCI treated daily with agathisflavone (10 mg/kg i.p.); 4) SCI treated with control rMSCs; 5) SCI treated with agathisflavone treated rMSC (FABrMSCs); 6) SCI treated with methylprednisolone (MP, 60 mg/kg i.p.). Locomotor skills were assessed by the open-field test prior to SCI (day 0) and one, three and 7 days after SCI using the BBB score (**Figure 4A**; **Table 2**). Rats submitted only to laminectomy (Sham) recovered a score of 21 within 7 days after injury, which reflects no neurological impairments. Following SCI, rats achieved a mean BBB score of 3.0 ± 0.29 without treatment and that was not sigificantly altered by a single treatment with rMSC, which attained a mean BBB score of 3.0 ± 0.20 7 days after injury (DPI); both these experimental groups remained generally more apathetic than did sham controls. In contrast, the BBB score was significantly improved in the SCI + FABrMSC treatment group, attaining 5.36 ± 0.49 at 7 DPI; in addition, some of the animals had a trend towards improved motor function, compared to the other groups, with slight hind limb reflexes and rapid movement over the open field, as well as presenting grooming behavior. The motor behavior was very heterogeneous in the group of animals with SCI and treated with one single dose of methylprednisolone (60 mg/kg i.p.,MP). One animal presented being apathetic in the first 3 days after injury, the other animals, although injured, moved when stimulated in the open field reaching a BBB score of 4.8 ± 0.16. The animals with SCI and treated daily with agathisflavone (10 mg/kg i.p., FAB) presented similar behavior to the animals treated with MP, with the mean

TABLE 3 | Comparison of weight variation between SCI groups. Average daily weight loss/gain over 7 days.

Day	Sham	SCI	rMSCs	FAB	+FABrMSCs	MP
1	5.3 g	−8.51 g	−5.8 g	−5.5 g	−4.6 g	−4.3 g
3	12.9 g	−25.6 g	−13.l g	−13.7 g	−13.3 g	−12.8 g
7	29.8 g	59.71 g	−30.6 g	−30.l g	−29.8 g	−30.2 g
Mean	4.257 g	−8.53 g	−4.371 g	−4.3 g	−4.257 g	−4.314 g

BBB score of 4.4 ± 0.32; they moved only when stimulated and an animal was shown to lean on its right side.

Body Weight Change

After SCI, the animals were placed in cages with water and food *ad libitum*, and their weight gain or loss was monitored as a measure of general health, on the days on which the animals underwent motor evaluation (**Figure 4B**; **Table 3**). Control (Sham) animals gained approximately 30 g over the 7 days, with an average daily gain of 4.3 g. Animals with SCI presented an average daily loss of 8.53 g (**Table 3**). The groups of animals treated with rMSCs pretreated with agathisflavone (+FABrMSCs), or with MP or with FAB, presented an average daily loss of approximately 4.3 g. There are no statistical differences between these groups.

Histological Changes

All animals were sacrificed 8 days after treatments for H&E histological analysis of the spinal cord (**Figure 5A**). The degree of lesion was determined according to the semi quantitative classification system, described by Ustun et al. (2014) (**Table 4**). Control (sham) animals did not present any tissue disruption of the spinal cord; both white matter and gray matter were intact, with no necrosis, inflammatory infiltrate or hemorrhage, classified with grade 0 of injury when comparing Ustun's H&E histological analysis classification in **Tables 4**, **5**. Animals with SCI presented an extensive area of liquefactive necrosis with the presence of severe hemorrhage, and numerous spongy macrophages at the lesion site, which was classified as Grade 3 of injury. Similar lesions were observed in the spinal cord of animals that received an implant of control rMSC, which had a mean score of 2.66 ± 0.47 (**Table 5**). In contrast, the group of animals treated daily with FAB presented injuries classified in Grade 2 and 3 depending on the tissue of animal analyzed. Animals treated with MP presented diffuse and mild vacuolization due to white matter demyelination in the spinal cord and the lesions were also classified as of Grade 2. However, animals that received a single application of +FABrMSCs presented spinal cords with walerian degeneration and isolated vacuolization by white matter demyelination vacuolations, and

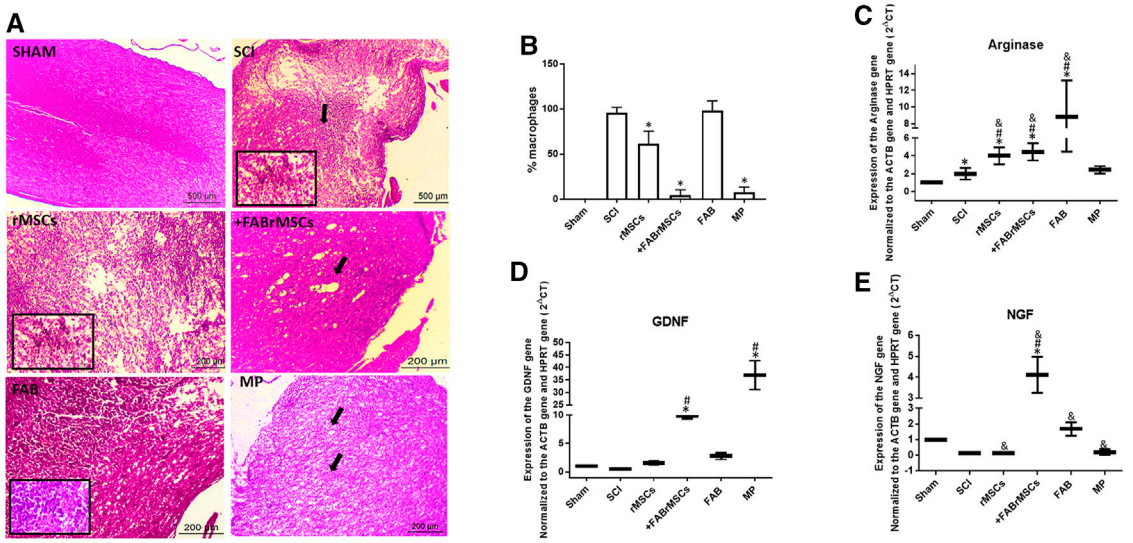

FIGURE 5 | General histopathology of the spinal cord of animals 8 days after being subjected to spinal cord injury (SCI) and different treatments. **(A)** Representative longitudinal section of a normal spinal cord (sham animals), and from animals treated with a single application of 1 × 10^6 control rMSCs or 1 × 10^6 rMSCs pretreated with agathisflavone (+FABrMSCs), treated with one single dose of methylprednisolone (60 mg/kg i.p., MP), or treated daily with agathisflavone (10 mg/kg i.p., FAB); hematoxylin and eosin (H&E), x40; details x100. Abundant foamy macrophages and extensive area of liquefactive necrosis with strong macrophage reaction are observed in the spinal cord of animals with SCI (spotlight), also observed in the spinal cord of animals that received implant of control rMSC (spotlight), and in less expansion of animals treated daily with FAB. However, in the spinal cord of animals that received implant of +FABrMSCs, isolated vacuolization by demyelization and walerian degeneration (arrow) are observed. In the spinal cord of animals treated with MP, diffuse and mild vacuolization by demyelination of white matter is observed. **(B)** Quantification of foamy macrophages in injured spinal cord tissue. The results are expressed as the media of percentage in three independent experiments and were analyzed by Kruskal–Wallis ANOVA followed by Dunn's post-test (*) $p \leq 0.05$ compared to SCI group. **(C–E)**: Expression of neurotrophic factors and arginase in the spinal cord of animals 8 days after being subjected to spinal cord injury (SCI) and different treatments. Expression of mRNA for neurotrophic factors NGF and GFDN, and for enzyme arginase, was analyzed with RT-qPCR; Sham = Non-lesioned; SCI and other groups = Lesioned; values expressed as mean ± standard deviation; significant differences are expressed as *$p \leq 0.05$ when compared to the control NL; #$p \leq 0.05$ when compared to FAB 0.1 µM NL treatment; and $p \leq 0.05$ when compared to the control L; and &$p \leq 0.05$ when compared to FAB 0.1 µM treatment. Kruskal–Wallis and one-way ANOVA followed by Dunn's post-hoc were used.

TABLE 4 | A semi-quantitative grading system according to Ustun et al. (2014). Spinal cord segment was examined for hemorrhage, spongiosis and liquefactive necrosis semi-quantatively for histopathological changes.

	Grade
No abnormal cells and change	0
Mild hemorrhage, spongiosis	1
Moderate hemorrhage and spongiosis with liquefactive necrosis	2
Some hemorrhage and spongiosis with glial cell proliferation and liquefactive necrosis	3

According Ustun et al. (2014).

TABLE 5 | Histopathological evaluation by semi-quantitative Ustun classification system.

Rat	Sham	SCI	FAB	rMSCs	+FABrMSCs	MP
1	0	3	3	3	2	2
2	0	3	2	2	1	2
3	u	3	I	3	I	I
Mean ± SD	—	3 ± 0.0	2.33 ± 0.47	2.66 ± 0.47	1.66 ± 0.47	2.0 ± 0.0
p	—	—	0.198	0.0153	0.0377	—

SD: standard deviation.
*Mean of the samples. * significance level α = 0.05.*

lesions classified in the majority as of Grade 2, demonstrating that agathisflavone-treated rMSC had potential to repair spinal cord injury. Moreover, quantification of foamy macrophages showed a significant reduction in the proportion of macrophages in the lesioned area in animals treated with rMSCs, and mainly in animals treated with +FABrMSCs and the anti-inflammatory MP.

Gene Expression Changes

In order to better characterize the inflammatory profile in the site of lesion, RT-qPCR was performed with samples of the site of SCI to analyze expression of neurotrophins and arginase, an enzyme directly related to the M2 anti-inflammatory profile of macrophages (**Figures 5B–E**). A significant increase in nerve growth factor (NGF) mRNA expression was observed in the spinal cord tissue of animals with SCI treated with +FABrMSCs (about 10 times) or FAB (about 2 times) compared with animals with the lesion. Moreover, a significant increase in mRNA expression for glial-derived growth factor (GDNF) was also observed in the spinal cord tissue of animals with SCI treated with rMSCs (about 2 times), +FABrMSCs (about 10 times) or FAB (about 3 times) compared with animals with the lesion. Aghathisflavone (FAB) treatment also induced a significant increase (about 8 times) in mRNA expression for the enzyme arginase, a tendency also observed in the spinal cord tissue of animals with SCI treated with rMSCs (about 3.7 times), +FABrMSCs (about 4.2 times). Treatment of animals with MP induced a decrease in NGF and an increase in GDNF compared with the tissue of control animals without lesion (Sham).

DISCUSSION

Research with MSCs has shown that these cells can differentiate in specific conditions into neural lineages and could be used in clinical situations such as SCI (Foudah et al., 2014; Assinck et al., 2017; Jin et al., 2019). In addition, the phytoestrogen agathisflavone has prominent neuroprotective effects and is capable of inducing neurogenesis in embryonic and pluripotent stem cells (Paulsen et al., 2011; Andrade et al., 2018). Studies in the literature show the neuroprotective activity of flavonoids, including the ability of these compounds to cross the blood-brain barrier. Rutin and quercetin (Ferri et al., 2015), hesperetin and naringenin (Youdim et al., 2003), and polyphenols in general (Figueira et al., 2017), which suggests the ability of agathisflavone to also act directly enter the cerebrospinal fluid for direct efficacy alone or combinated with other molecules. Here, we show that the treatment of rMSCs cells with agathisflavone promotes a neural phenotype differentiation *in vitro* in a small population, reinforcing the heterogeneity of MSC subpopulations.

According to Neuhuber et al. (2008), rMSCs naturally present heterogeneous morphology. However, this heterogeneity is related to the "stemness" of these cells. According to these authors, rMSCs cells that have a fusiform or fibroblastic morphology have multipotent characteristics and, therefore, this morphology is characterized as immature (Sekiya et al., 2002). Large cells with a flat polygonal morphology and a clearly visible nucleus without processes, or with very short processes, were classified as "smaller stem potential" or mature cells (Colter et al., 2001; Prockop et al., 2001; Sekiya et al., 2002; Neuhuber et al., 2008).

Depending on the agathisflavone concentration and DIV, rMSCs retained the two characteristic morphological profiles typical of immature multipotency. Treating with the flavonoid at the concentration of 1 μM, the proportion of cells with long and thin process was increased, and that may be indicative of flavonoid modulation in these cells to a more mature neuronal profile, as we described previously in embryonic stem cell cultures (Paulsen et al., 2011).

Spinal cord injury is characterized by primary events and secondary events. Primary events refer to loss of spinal cord integrity due to mechanical factors. Late secondary damage refers to a complex set of pathophysiological processes including ischemia, edema, inflammation, excitotoxicity, oxidative cell damage and digestive system complications with changes in nutrient absorption and intestinal motility (Zhang and Liao, 2014; Hakim et al., 2019). Consequently, there is glial scar formation and neurological dysfunction (Byrnes et al., 2007; Bradbury and Burnside, 2019).

Secondary injury begins within minutes of the initial primary injury and continues for weeks or months causing progressive damage to the spinal cord around the injury site. The secondary lesion may be temporarily divided into acute, subacute and chronic phases. The acute phase begins immediately after SC and includes vascular damage, ionic imbalance, neurotransmitter accumulation (excitotoxicity), free radical formation, inflammation, edema and necrotic cell death (Oyinbo, 2011; von Leden et al., 2016; Alizadeh et al., 2019). Demyelination of white matter, liquefactory necrosis and the presence of spongy macrophages also reflect secondary SCI (Oyinbo, 2011).

Corticosteroids, especially methylprednisolone (MP), have the potential to stabilize cell membrane structure by maintaining an intact blood-brain barrier, reducing vasogenic edema, decreasing medullary blood flow, altering electrolyte concentrations at the site of injury, inhibiting endorphin release, decreasing free radical damage and limiting post-traumatic inflammatory response (Wang et al., 2019). However, their use has little success on motor and functional recovery and numerous efforts have been made by the scientific community regarding cell therapy for motor and functional recovery and the use of new drugs to reduce inflammation and tissue destruction in the spinal cord injury environment as an alternative to MP. Hence, as an alternative, the implant of MSCs has been largely used, both *in situ* and administered via the tail vein in view to evaluate tissue recovery and inflammatory response at the injury site (Leypold et al., 2007; Hakim et al., 2019). Moreover, there are growing evidences that the product of secretion of MSCs is the major responsible for restoring tissue in models of SCI. In this context, in the present study, we adopted two strategies in male Wistar rats subject to acute SCI: a single application (via caudal vein) of control rMSCs and with a differentiated profile induced by the agathisflavone treatment *in vitro* before implant. Treatment of animals with 21-day agathisflavone-treated rMSCs was able to protect the injured spinal cord tissue and improve motor functions (with the highest BBB score), effects that are associated with the increase in expression of NGF, GDNF and arginase, and reduction on the macrophage infiltrate. Treatment of animals with agathisflavone alone (10 mg/kg) was also able to protect injured spinal cord tissue, increase the expression of neurotrophins and modulate the inflammatory response.

Zhang et al. (2014) demonstrated that the agathisflavone monomer apigenin (10 mg/kg) in a SCI model improved neurological recovery after injury, obtaining results like treatment with MP, neuroprotective effect that was at least partially associated with its antioxidant and anti-inflammatory effects. In the present study, treatment with MP presented results like those described by Zhang et al. (2014) and by Leypold et al. (2007), who demonstrate that MP, when administered in the initial period of spinal cord injury, may decrease the extent of spinal cord hemorrhage, reducing secondary damage caused by injury protecting motor functions. In a study developed by Shi et al. (2016), the flavonoid narigenin, repeatedly administered at higher concentrations (100 mg/kg), protected animals from SCI damages. That happened possibly due to the inhibition of inflammation via miR 233, a known microRna associated with inflammatory response that is a product of secretion that could be investigated, besides othe miRNAs, in rMSCs treated with agathisflavone and in the area of the damage. The ensemble of the results showed that rMSC had the potential to repair the injured cord. It is possible, however, that due to the fact that the observation window of the study is short, only 7 days, it was not possible to verify this tissue recovery and motor improvement in animals treated with rMSCs.

Nevertheless, the group of animas that receive agathisflavone pre-treated rMSCs presented lower tissue injury and motor improvement, when compared to the other groups, effects also associated with the increase in expression of NGF and GDNF, besides the attenuation of the inflammatory infiltrate. This increase in neurotrophins expression is very interesting, since NGF has demonstrated neuroprotective role in the recovery of SCIs, and is related to the inhibition of stress-induced cell death of reactive oxygen species by activating signals in the regulation of inflammatory process (Zhang and Liao, 2014); also, Keefe et al. (2017) showed that NGF expression in the spinal cord induced the growth of nociceptive axons and hyperalgesia in animals with SCI. On the other hand, GDNF is also known to be an important neurotrophic factor for CNS development because it promotes neuronal survival and axonal regeneration, reduces secondary damage, decreases lesion size and improves functional recovery (Ortmann and Hellenbrand, 2018); GDNF, when expressed in traumatic injuries, favors nerve fiber growth and improves motor effects of injured animals (Pöyhönen et al., 2019). Together, these findings corroborate the results of the present study, which showed improvement in motor function and preservation of the spinal cord tissue associated with GDNF and NGF.

Finally, another important finding in the present study was the increase in the expression of the enzyme arginase in the injured tissue of animals that received treatment with the flavonoid agathisflavona alone or flavonoid treated-MSCs; also, the last case was associated with a drastic reduction on the macrophage infiltrate in the injured tissue, compared with animals without treatments. Arginase expression is related to the activation of M2 antiiflamatory profile of macrophages. Macrophages could promote repair of injured tissue by regulating transitions through different phases of the healing response and facilitating transitions through inflammatory, proliferative and repair remodeling phases

(Ahn et al., 2012; Gensel and Zhang, 2015). In this sense, treatment with agathisflavone-treated rMSCs presented advantages when compared to the other groups, because it protects the injured spinal cord tissue, evidenced by the histopathological findings, as well as by the modulation expression of neurotrophins and neuroinflammation, which appears to be related to the modulation of releasing factors in the flavonoid-treated mesenchymal stem.

CONCLUSION

All these findings together demonstrated that the flavonoid agathisflavone was not toxic to rMSCs, and induced these cells to a neural differentiated profile, with increased expression of neural markers GFAP and β-tubulin III. Moreover, in the SCI model, agathisflavone alone at the doses tested was unable to protect completely the injured spinal cord tissue, but increased the expression of neurotrophins that are related to nerve growth and increased arginase expression suggesting activation of the anti-inflammatory M2 macrophage profile. In addition, the administration of agathisflavone-treated rMSCs showed anti-inflammatory properties, protecting injured spinal cord tissue, also increasing NGF and GDNF expression, reflecting improved motor function, ensemble of results that may be considered in further studies for clinical application.

DATA AVAILABILITY STATEMENT

The original contributions presented in the study are included in the article/**Supplementary Material**, further inquiries can be directed to the corresponding author.

ETHICS STATEMENT

The animal study was reviewed and approved by Animal Use Ethics Committee of the Institute of Health Sciences of the Federal University of Bahia (process number 117/2017).

AUTHOR CONTRIBUTIONS

Conceptualization, SC and VS; writing original draft preparation, RdN, LdJ, MO-J, AA, EM, BP, JD, and SC; writing review and editing, SC, RdN, BS, AB and VS; visualization, BS, MC, and AB; supervision, SC and VS; project administration, SC; funding acquisition, SC and MC. All authors have read and agreed to the published version of the manuscript.

FUNDING

This work was supported by the Foundation for Research Support of the State of Bahia (FAPESB, process RED0016/2013 and process N° INT 0016/2016) the Coordination of Personnel Improvement of Higher Level (CAPES, process PGCI N° 88881.117666/2016-01) and by the National Council for Scientific and Technological Development (CNPq, EU Edital MCTI/CNPq/Universal Process EU N° 443723/2014-1; INCT for Excitotoxicity and Neuroprotection; INCT–Translational Neuroscience). We thank the support of the Post-Graduation Program in Biotechnology–State University of Feira de Santana, and we thank CAPES (Process N° 0001) and CNPq (process DSE N°205792/2017-0) for PhD fellowship to RN and Researcher felowship to SC (process PQ N° 307539/2018-0). This study was financed in part by the Coordenação de Aperfeiçoamento de Pessoal de Nível Superior–Brazil (CAPES)–Finance Code 001.

SUPPLEMENTARY MATERIAL

The Supplementary Material for this article can be found online at: https://www.frontiersin.org/articles/10.3389/fphar.2022.858190/full#supplementary-material

Supplementary Figure S1 | Characterization of rat mesenchymal stem cells (rMSCs). **(A)** Morphological aspect of 15 days *in vitro* (DIV). **(B)** rMSC differentiation characterization in adipocytes by Oil red O staining. **(C)** differentiation characterization in osteocytes by alizarine red staining.

Supplementary Figure S2 | Supplementary Figure S2 | Characterization of rat mesenchymal stem cells (rMSCs) by flow cytometry surface markers for the *Ratus novergicus*.

REFERENCES

Ahn, M., Yang, W., Kim, H., Jin, J. K., Moon, C., and Shin, T. (2012). Immunohistochemical Study of Arginase-1 in the Spinal Cords of Lewis Rats with Experimental Autoimmune Encephalomyelitis. *Brain Res.* 1453, 77–86. doi:10.1016/j.brainres.2012.03.023

Akar, İ., İnce, İ., Arici, A., Benli, İ., Aslan, C., Şenol, S., et al. (2017). The Protective Effect of Curcumin on a Spinal Cord Ischemia-Reperfusion Injury Model. *Ann. Vasc. Surg.* 42, 285–292. doi:10.1016/j.avsg.2016.12.016

Alizadeh, A., Dyck, S. M., and Karimi-Abdolrezaee, S. (2019). Traumatic Spinal Cord Injury: An Overview of Pathophysiology, Models and Acute Injury Mechanisms. *Front. Neurol.* 10, 282. doi:10.3389/fneur.2019.00282

Allahdadi, K. J., de Santana, T. A., Santos, G. C., Azevedo, C. M., Mota, R. A., Nonaka, C. K., et al. (2019). IGF-1 Overexpression Improves Mesenchymal Stem Cell Survival and Promotes Neurological Recovery after Spinal Cord Injury. *Stem Cel Res Ther* 10 (1), 146. doi:10.1186/s13287-019-1223-z

Andrade, A. W. L., Machado, K. D. C., Machado, K. D. C., Figueiredo, D. D. R., David, J. M., Islam, M. T., et al. (2018). *In Vitro* antioxidant Properties of the Biflavonoid Agathisflavone. *Chem. Cent. J.* 12 (1), 75–79. doi:10.1186/s13065-018-0443-0

Assinck, P., Duncan, G. J., Hilton, B. J., Plemel, J. R., and Tetzlaff, W. (2017). Cell Transplantation Therapy for Spinal Cord Injury. *Nat. Neurosci.* 20 (5), 637–647. doi:10.1038/nn.4541

Bahia, M. V., Santos, J. B. D., David, J. P., and David, J. M. (2005). Biflavonoids and Other Phenolics From Caesalpinia Pyramidalis (Fabaceae). *J. Braz. Chem. Soc.* 16, 1402–1405. doi:10.1590/S0103-50532005000800017

Bahia, M. V., David, J. P., and David, J. M. (2010). Occurrence of Biflavones in Leaves of Caesalpinia Pyramidalis Specimens. *Química Nova.* 33 (6), 1297–1300.

Barros Filho, T. E., and Molina, A. E. (2008). Analysis of the Sensitivity and RReproducibility of the Basso, Beattie, Bresnahan (BBB) Scale in Wistar Rats. *Clinics (Sao Paulo)* 63 (1), 103–108. doi:10.1590/s1807-59322008000100018

Basso, D. M., Beattie, M. S., and Bresnahan, J. C. (1995). A Sensitive and Reliable Locomotor Rating Scale for Open Field Testing in Rats. *J. Neurotrauma.* 12, 1–21. doi:10.1089/neu.1995.12.1

Bradbury, E. J., and Burnside, E. R. (2019). Moving beyond the Glial Scar for Spinal Cord Repair. *Nat. Commun.* 10 (1), 3879. doi:10.1038/s41467-019-11707-7

Byrnes, K. R., Stoica, B. A., Fricke, S., Di Giovanni, S., and Faden, A. I. (2007). Cell Cycle Activation Contributes to post-mitotic Cell Death and Secondary Damage after Spinal Cord Injury. *Brain* 130 (11), 2977–2992. doi:10.1093/brain/awm179

Cabrera-Aldana, E. E., Ruelas, F., Aranda, C., Rincon-Heredia, R., Martínez-Cruz, A., Reyes-Sánchez, A., et al. (2017). Methylprednisolone Administration Following Spinal Cord Injury Reduces Aquaporin 4 Expression and Exacerbates Edema. *Mediators Inflamm.* 2017, 4792932. doi:10.1155/2017/4792932

Caplan, A. I. (2009). Why Are MSCs Therapeutic? New Data: New Insight. *J. Pathol.* 217 (2), 318–324. doi:10.1002/path.2469

Caplan, H., Olson, S. D., Kumar, A., George, M., Prabhakara, K. S., Wenzel, P., et al. (2019). Mesenchymal Stromal Cell Therapeutic Delivery: Translational Challenges to Clinical Application. *Front. Immunol.* 10, 1645. doi:10.3389/fimmu.2019.01645

Colter, D. C., Sekiya, I., and Prockop, D. J. (2001). Identification of a Subpopulation of Rapidly Self-Renewing and Multipotential Adult Stem Cells in Colonies of Human Marrow Stromal Cells. *Proc. Natl. Acad. Sci. U. S. A.* 98, 7841–7845. doi:10.1073/pnas.141221698

Dariolli, R., Bassaneze, V., Nakamuta, J. S., Omae, S. V., Campos, L. C., and Krieger, J. E. (2013). Porcine Adipose Tissue-Derived Mesenchymal Stem Cells Retain Their Proliferative Characteristics, Senescence, Karyotype and Plasticity after Long-Term Cryopreservation. *PLoS One* 8 (7), e67939. doi:10.1371/journal.pone.0067939

dos Santos Souza, C., Grangeiro, M. S., Lima Pereira, E. P., dos Santos, C. C., da Silva, A. B., Sampaio, G. P., et al. (2018). Agathisflavone, a Flavonoid Derived from Poincianella Pyramidalis (Tul.), Enhances Neuronal Population and Protects against Glutamate Excitotoxicity. *Neurotoxicology* 65, 85–97. doi:10.1016/j.neuro.2018.02.001

Ferri, P., Angelino, D., Gennari, L., Benedetti, S., Ambrogini, P., Del Grande, P., et al. (2015). Enhancement of Flavonoid Ability to Cross the Blood-Brain Barrier of Rats by Co-administration with α-tocopherol. *Food Funct.* 6 (2), 394–400. doi:10.1039/c4fo00817k

Figueira, I., Garcia, G., Pimpão, R. C., Terrasso, A. P., Costa, I., Almeida, A. F., et al. (2017). Polyphenols Journey through Blood-Brain Barrier towards Neuronal protection. *Sci. Rep.* 7 (1), 11456. doi:10.1038/s41598-017-11512-6

Foudah, D., Monfrini, M., Donzelli, E., Niada, S., Brini, A. T., Orciani, M., et al. (2014). Expression of Neural Markers by Undifferentiated Mesenchymal-like Stem Cells from Different Sources. *J. Immunol. Res.* 2014, 987678. doi:10.1155/2014/987678

Friedenstein, A. J., Chailakhyan, R. K., Latsinik, N. V., Panasyuk, A. F., and Keiliss-Borok, I. V. (1974). Stromal Cells Responsible for Transferring the Microenvironment of the Hemopoietic Tissues. Cloning *In Vitro* and Retransplantation *In Vivo*. *Transplantation* 17 (4), 331–340. doi:10.1097/00007890-197404000-00001

Gensel, J. C., and Zhang, B. (2015). Macrophage Activation and its Role in Repair and Pathology after Spinal Cord Injury. *Brain Res.* 1619, 1–11. doi:10.1016/j.brainres.2014.12.045

Hakim, R., Covacu, R., Zachariadis, V., Frostell, A., Sankavaram, S. R., Brundin, L., et al. (2019). Mesenchymal Stem Cells Transplanted into Spinal Cord Injury Adopt Immune Cell-like Characteristics. *Stem Cel Res. Ther.* 10 (1), 115. doi:10.1186/s13287-019-1218-9

Hansen, M. B., Nielsen, S. E., and Berg, K. (1989). Re-examination and Further Development of a Precise and Rapid Dye Method for Measuring Cell Growth/cell Kill. *J. Immunol. Methods* 119 (2), 203–210. doi:10.1016/0022-1759(89)90397-9

Horwitz, E. M., Le Blanc, K., Dominici, M., Mueller, I., Slaper-Cortenbach, I., Marini, F. C., et al. (2005). Clarification of the Nomenclature for MSC: The International Society for Cellular Therapy Position Statement. *Cytotherapy* 7 (5), 393–395. doi:10.1080/14653240500319234

Jin, M. C., Medress, Z. A., Azad, T. D., Doulames, V. M., and Veeravagu, A. (2019). Stem Cell Therapies for Acute Spinal Cord Injury in Humans: A Review. *Neurosurg. Focus.* 46 (3), E10. doi:10.3171/2018.12.FOCUS18602

Kang, S., Liu, S., Li, H., Wang, D., and Qi, X. (2018). Baicalin Effects on Rats with Spinal Cord Injury by Anti-inflammatory and Regulating the Serum Metabolic Disorder. *J. Cel. Biochem.* 119 (9), 7767–7779. doi:10.1002/jcb.27136

Karsy, M., and Hawryluk, G. (2019). Modern Medical Management of Spinal Cord Injury. *Curr. Neurol. Neurosci. Rep.* 19 (9), 65. doi:10.1007/s11910-019-0984-1

Keefe, K. M., Sheikh, I. S., and Smith, G. M. (2017). Targeting Neurotrophins to Specific Populations of Neurons: NGF, BDNF, and NT-3 and Their Relevance for Treatment of Spinal Cord Injury. *Int. J. Mol. Sci.* 18 (3), 548. doi:10.3390/ijms18030548

Larocca, T. F., Macêdo, C. T., Souza, B. S. F., Andrade-Souza, Y. M., Villarreal, C. F., Matos, A. C., et al. (2017). Image-guided Percutaneous Intralesional Administration of Mesenchymal Stromal Cells in Subjects with Chronic Complete Spinal Cord Injury: a Pilot Study. *Cytotherapy* 19 (10), 1189–1196. doi:10.1016/j.jcyt.2017.06.006

Leypold, B. G., Flanders, A. E., Schwartz, E. D., and Burns, A. S. (2007). The Impact of Methylprednisolone on Lesion Severity Following Spinal Cord Injury. *Spine (Phila Pa 1976)* 32 (3), 373–381. doi:10.1097/01.brs.0000253964.10701.00

Liu, J. J., Huang, Y. J., Xiang, L., Zhao, F., and Huang, S. L. (2017). A Novel Method of Organotypic Spinal Cord Slice Culture in Rats. *Neuroreport* 28 (16), 1097–1102. doi:10.1097/WNR.0000000000000892

Liu, X., Zhang, Y., Yang, Y., Lin, J., Huo, X., Du, X., et al. (2018). Therapeutic Effect of Curcumin and Methylprednisolone in the Rat Spinal Cord Injury. *Anat. Rec. (Hoboken)* 301 (4), 686–696. doi:10.1002/ar.23729

Mendes, C. C., Bahia, M. V., David, J. M., and David, J. P. (2000). Constituents of Caesalpinia Pyramidalis. *Fitoterapia* 71 (2), 205–207. doi:10.1016/s0367-326x(99)00145-8

Mendonça, M. V., Larocca, T. F., de Freitas Souza, B. S., Villarreal, C. F., Silva, L. F., Matos, A. C., et al. (2014). Safety and Neurological Assessments after Autologous Transplantation of Bone Marrow Mesenchymal Stem Cells in Subjects with Chronic Spinal Cord Injury. *Stem Cel Res Ther* 5 (6), 126. doi:10.1186/scrt516

Muniswami, D. M., Kanthakumar, P., Kanakasabapathy, I., and Tharion, G. (2018). Motor Recovery after Transplantation of Bone Marrow Mesenchymal Stem Cells in Rat Models of Spinal Cord Injury. *Ann. Neurosci.* 25 (3), 126–140. doi:10.1159/000487069

Neuhuber, B., Swanger, S. A., Howard, L., Mackay, A., and Fischer, I. (2008). Effects of Plating Density and Culture Time on Bone Marrow Stromal Cell Characteristics. *Exp. Hematol.* 36 (9), 1176–1185. doi:10.1016/j.exphem.2008.03.019

Ortmann, S. D., and Hellenbrand, D. J. (2018). Glial Cell Line-Derived Neurotrophic Factor as a Treatment after Spinal Cord Injury. *Neural Regen. Res.* 13 (10), 1733–1734. doi:10.4103/1673-5374.238610

Oyinbo, C. A. (2011). Secondary Injury Mechanisms in Traumatic Spinal Cord Injury: A Nugget of This Multiply cascade. *Acta Neurobiol. Exp. (Wars)* 71 (2), 281–299.

Paulsen, B. S., Souza, C. S., Chicaybam, L., Bonamino, M. H., Bahia, M., Costa, S. L., et al. (2011). Agathisflavone Enhances Retinoic Acid-Induced Neurogenesis and its Receptors α and β in Pluripotent Stem Cells. *Stem Cell Dev* 20 (10), 1711–1721. doi:10.1089/scd.2010.0446

Pöyhönen, S., Er, S., Domanskyi, A., and Airavaara, M. (2019). Effects of Neurotrophic Factors in Glial Cells in the central Nervous System: Expression and Properties in Neurodegeneration and Injury. *Front. Physiol.* 10, 486. doi:10.3389/fphys.2019.00486

Prockop, D. J., Sekiya, I., and Colter, D. C. (2001). Isolation and Characterization of Rapidly Self-Renewing Stem Cells from Cultures of Human Marrow Stromal Cells. *Cytotherapy* 3 (5), 393–396. doi:10.1080/146532401753277229

Schmittgen, T. D., and Livak, K. J. (2008). Analyzing Real-time PCR Data by the Comparative C(T) Method. *Nat Protoc.* 3 (6), 1101–1108. doi:10.1038/nprot.2008.73

Sekiya, I., Larson, B. L., Smith, J. R., Pochampally, R., Cui, J. G., and Prockop, D. J. (2002). Expansion of Human Adult Stem Cells from Bone Marrow Stroma: Conditions that Maximize the Yields of Early Progenitors and Evaluate Their Quality. *Stem Cells* 20 (6), 530–541. doi:10.1634/stemcells.20-6-530

Shi, L. B., Tang, P. F., Zhang, W., Zhao, Y. P., Zhang, L. C., and Zhang, H. (2016). Naringenin Inhibits Spinal Cord Injury-Induced Activation of Neutrophils through miR-223. *Gene* 592 (1), 128–133. doi:10.1016/j.gene.2016.07.037

Üstün, N., Aras, M., Ozgur, T., Bayraktar, H. S., Sefil, F., Ozden, R., et al. (2014). Thymoquinone Attenuates Trauma Induced Spinal Cord Damage in an Animal Model. *Ulus Travma Acil Cerrahi Derg* 20 (5), 328–332. doi:10.5505/tjtes.2014.05021

Vanický, I., Urdzíková, L., Saganová, K., Cízková, D., and Gálik, J. (2001). A Simple and Reproducible Model of Spinal Cord Injury Induced by Epidural Balloon Inflation in the Rat. *J. Neurotrauma.* 18 (12), 1399–1407. doi:10.1089/08977150152725687

von Leden, R. E., Selwyn, R. G., Jaiswal, S., Wilson, C. M., Khayrullina, G., and Byrnes, K. R. (2016). (18)F-FDG-PET Imaging of Rat Spinal Cord Demonstrates Altered Glucose Uptake Acutely after Contusion Injury. *Neurosci. Lett.* 621, 126–132. doi:10.1016/j.neulet.2016.04.027

Wang, W., Zuo, B., Liu, H., and Cui, L. (2019). Intermittent Injection of Methylprednisolone Sodium Succinate in the Treatment of Cervical Spinal Cord Injury Complicated with Incomplete Paraplegia. *Pak J. Med. Sci.* 35 (1), 141–145. doi:10.12669/pjms.35.1.211

Yin, K., Wang, S., and Zhao, R. C. (2019). Exosomes from Mesenchymal Stem/stromal Cells: a New Therapeutic Paradigm. *Biomark Res.* 7 (1), 8. doi:10.1186/s40364-019-0159-x

Youdim, K. A., Dobbie, M. S., Kuhnle, G., Proteggente, A. R., Abbott, N. J., and Rice-Evans, C. (2003). Interaction between Flavonoids and the Blood-Brain Barrier: *In Vitro* Studies. *J. Neurochem.* 85 (1), 180–192. doi:10.1046/j.1471-4159.2003.01652.x

Yuan, L., Liu, Y., Qu, Y., Liu, L., and Li, H. (2019). Exosomes Derived from Microrna-148b-3p-Overexpressing Human Umbilical Cord Mesenchymal Stem Cells Restrain Breast Cancer Progression. *Front. Oncol.* 9, 1076. doi:10.3389/fonc.2019.01076

Zhang, F., Li, F., and Chen, G. (2014). Neuroprotective Effect of Apigenin in Rats after Contusive Spinal Cord Injury. *Neurol. Sci.* 35 (4), 583–588. doi:10.1007/s10072-013-1566-7

Zhang, Q., Zhang, L. X., An, J., Yan, L., Liu, C. C., Zhao, J. J., et al. (2018). Huangqin Flavonoid Extraction for Spinal Cord Injury in a Rat Model. *Neural Regen. Res.* 13 (12), 2200–2208. doi:10.4103/1673-5374.241472

Zhang, Z., and Liao, L. (2014). Risk Factors Predicting Upper Urinary Tract Deterioration in Patients with Spinal Cord Injury: A Prospective Study. *Spinal Cord* 52 (6), 468–471. doi:10.1038/sc.2014.63

Conflict of Interest: The authors declare that the research was conducted in the absence of any commercial or financial relationships that could be construed as a potential conflict of interest.

Publisher's Note: All claims expressed in this article are solely those of the authors and do not necessarily represent those of their affiliated organizations, or those of the publisher, the editors and the reviewers. Any product that may be evaluated in this article, or claim that may be made by its manufacturer, is not guaranteed or endorsed by the publisher.

GLOSSARY

BBB Basso, Beattie, Bresnahan scale

BSA bovine serum albumin

CD11b integrin alpha M

CD29 integrin beta 1

CD34 transmembrane phosphoglycoprotein protein cluster

CD73 ecto-5′-nucleotidase

CD90 VLA-β integrin

cDNA complementary Deoxyribonucleic acid

DMEM Dulbecco's Modified Eagle Medium

DMSO dimethyl sulfoxide

FAB agathisflavone

FBS fetal bovine serum

GDNF glia-derived neurotrophic factor

GFAP glial fibrillary acidic protein

H&E hematoxylin and eosin

HPRT1 hypoxanthine phosphoribosyltransferase 1

IP intra peritoneal

MHC-II histocompatibility complex class II

miR microRNA

MP methylprednisolone

MSCs mesenchymal stem cells

MTT assay 3-(4,5-dimethylthiazol-2-yl)-2,5-diphenyltetrazolium bromide test

NGF nerve growth factor

PBS Phosphate-buffered saline

PFA paraformaldehyde

rMSC rat mesenchymal stem cells

RNA ribonucleic acid

RT room temperature

RT-qPCR quantitative real-time polymerase chain reaction

SCI spinal cord injury

Triton X-100 4- (1,1,3,3-tetramethylbutyl) phenyl polyethylene glycol

frontiers | Frontiers in Pharmacology

ORIGINAL RESEARCH
published: 21 April 2022
doi: 10.3389/fphar.2022.848529

Edaravone Dexborneol Treatment Attenuates Neuronal Apoptosis and Improves Neurological Function by Suppressing 4-HNE-Associated Oxidative Stress After Subarachnoid Hemorrhage

Qian Chen, Yichen Cai, Xiaoyu Zhu, Jing Wang, Feng Gao, Mingfeng Yang, Leilei Mao, Zongyong Zhang* and Baoliang Sun**

The Second Affiliated Hospital, Brain Science Institute, School of Basic Medical Sciences of Shandong First Medical University and Shandong Academy of Medical Sciences, Taian, China

OPEN ACCESS

Edited by:
Liu Qing-Shan,
Minzu University of China, China

Reviewed by:
Jia Liu,
Capital Medical University, China
Xingshun Xu,
The First Affiliated Hospital of Soochow University, China
Peiying Li,
Shanghai Jiao Tong University School of Medicine, China

***Correspondence:**
Leilei Mao
leilei-0318@163.com
Zongyong Zhang
zyzhang@sdfmu.edu.cn
Baoliang Sun
blsun88@163.com

Specialty section:
This article was submitted to Neuropharmacology, a section of the journal Frontiers in Pharmacology

Received: *04 January 2022*
Accepted: *11 March 2022*
Published: *21 April 2022*

Citation:
Chen Q, Cai Y, Zhu X, Wang J, Gao F, Yang M, Mao L, Zhang Z and Sun B (2022) Edaravone Dexborneol Treatment Attenuates Neuronal Apoptosis and Improves Neurological Function by Suppressing 4-HNE-Associated Oxidative Stress After Subarachnoid Hemorrhage. Front. Pharmacol. 13:848529. doi: 10.3389/fphar.2022.848529

Edaravone dexborneol is a novel neuroprotective drug that comprises edaravone and (+)-borneol in a 4:1 ratio. Phase II and III studies have demonstrated that Chinese patients treated with edaravone dexborneol within 48 h of AIS onset have better functional outcomes than those treated with edaravone alone. However, the effect of edaravone dexborneol on subarachnoid hemorrhage (SAH) has not yet been elucidated. This study aimed to investigate the therapeutic effects of edaravone dexborneol on SAH-induced brain injury and long-term behavioral deficits and to explore the possible mechanisms. The experimental rat SAH model was induced by an intraluminal puncture of the left middle cerebral artery (MCA). Edaravone dexborneol or edaravone at a clinical dose was infused into the tail vein for 3 days post-SAH surgery. Behavioral outcomes were assessed by a modified Garcia scoring system and rotarod, foot-fault, and corner tests. Immunofluorescence, Western blot, and ELISA methods were used to evaluate neuronal damage and oxidative stress. Our results showed that a post-SAH therapeutic regimen with edaravone dexborneol helped improve neurological function up to 21 days after SAH surgery and demonstrated a greater beneficial effect than edaravone alone, accompanied by an obvious inhibition of neuronal apoptosis in the CA1 hippocampus and basal cortex regions. Mechanistically, edaravone dexborneol not only suppressed the lipid peroxidation product malondialdehyde (MDA) but also improved the total antioxidant capability (TAC) 3 days after SAH. Notably, edaravone dexborneol treatment significantly inhibited the expression of another lipid peroxidation product, 4-hydroxynonenal (4-HNE), in the CA1 hippocampus and basal cortex, which are vital participants in the process of neuronal oxidative damage and death after SAH because of their acute cytotoxicity. Together, our results demonstrate that edaravone dexborneol confers neuroprotection and stabilizes long-term behavioral ability after SAH injury, possibly by suppressing 4-HNE-associated oxidative stress. These results may help develop new clinical strategies for SAH treatment.

Keywords: oxidative stress, subarachnoid hemorrhage, edaravone dexborneol, 4-HNE, edaravone

INTRODUCTION

Subarachnoid hemorrhage (SAH) is considered an uncommon and severe subtype of stroke, which accounts for only 5% of strokes, but occurs at a fairly young age (van Gijn et al., 2007; Macdonald and Schweizer, 2017). Moreover, the high disability and fatality rates of patients after SAH result in huge spiritual and financial burdens for the patients and their families (Macdonald and Schweizer, 2017). As one of the significant pathological mechanisms of SAH-induced brain injury, oxidative stress has been shown to induce neuronal apoptosis and tissue necrosis by producing excessive reactive oxygen species (ROS), MDA, 4-HNE, and so on (Yang et al., 2017; Liu et al., 2020; Wu et al., 2021). When oxidative stress occurs, 4-HNE is a vital participant in the process of DNA damage (Liu et al., 2020). Meanwhile, MDA is regarded as a key marker of oxidation in the cell membrane (Tsikas, 2017).

As a potent free radical scavenger, edaravone has been shown to protect ischemic neurons after stroke via its antioxidant property, including suppression of lipid peroxidation and oxidant-induced DNA damage (Kikuchi et al., 2013; Wu et al., 2014a). In addition, edaravone can efficiently diminish apoptosis of neurons and thus prevent the neurologic impairment after SAH (Munakata et al., 2011). At present, edaravone is widely used in the clinic as a neuroprotective agent. Notably, a novel neuroprotective agent called edaravone dexborneol, which comprises (+)-borneol and edaravone in a ratio of 1:4, has been recently synthetized in China (Xu et al., 2019). A phase III clinical trial demonstrated that Chinese patients treated with edaravone dexborneol showed better functional outcomes within 48 h of AIS onset than those treated with edaravone alone (Xu et al., 2021). Edaravone dexborneol is presumed to protect against AIS by multifunctional cytoprotective pathways, including oxidative, inflammatory, excitotoxic, and apoptotic insults (Wu et al., 2014b). We speculated that edaravone dexborneol treatment might attenuate SAH-induced brain injury by suppressing oxidative stress. Nevertheless, the therapeutic effects of edaravone dexborneol on SAH injury have not been evaluated.

In this study, we evaluated the protective effect of edaravone dexborneol on a rat model of SAH and explored the potential underlying mechanism. Our results indicated that compared with edaravone, edaravone dexborneol treatment conferred better protection against neurological deficits after SAH and that this effect was accompanied by the inhibition of neuronal apoptosis in the CA1 hippocampus and basal cortex. Furthermore, edaravone dexborneol treatment not only suppressed the lipid peroxidation product malondialdehyde (MDA) but also improved the total antioxidant capability (TAC method) 3 days after SAH. Notably, another lipid peroxidation product, 4-HNE, was also obviously inhibited by edaravone dexborneol in the CA1 hippocampus and basal cortex, which are vital participants in the process of neuronal oxidative damage and death after SAH because of their acute cytotoxicity. Our findings suggest that edaravone dexborneol treatment is a novel and clinically feasible therapy to protect the brain against SAH injury.

MATERIALS AND METHODS

Animals and Experimental Design

Male Sprague–Dawley (SD) rats (14 weeks old, 280–300 g) were purchased from the Pengyue Laboratory Animal Center (Jinan, China). All animal experiments were approved by the Institutional Animal Care and Use Committee of Shandong First Medical University (Approval No: W202103030172) and conducted in accordance with the National Institutes of Health (NIH) Guide for the Care and Use of Laboratory Animals. All animals were housed in a temperature- and humidity-controlled 12-h light/dark cycle with *ad libitum* access to food and water.

All experiments were performed following the experimental design (**Figure 1A**). Rats were randomly assigned to experimental groups. Edaravone dexborneol, edaravone, or the same volume PBS was administered by tail vein injection for 3 days post-SAH surgery, and the specified dosage (edaravone dexborneol: 3.75 mg/kg, edaravone: 3 mg/kg, twice a day) was the determined reference to the clinical dose (Xu et al., 2021). All experiments were performed by an investigator blinded to experimental group assignments.

Rat Subarachnoid Hemorrhage Model

The experimental SAH model was induced by intraluminal puncture of the left middle cerebral artery (MCA) as previously (Sugawara et al., 2008; Dong et al., 2021). In brief, rats were deeply anesthetized with 6% isoflurane and maintained with 2.5% isoflurane in a 30% O2/70% N2O mixture via a facemask by a rodent ventilator (RWD, China). In brief, an incision in midline neck skin was made, and then the left common, external, and internal carotid arteries were isolated. A blunted nylon (4-0) suture was inserted into the left internal carotid artery via the left external carotid artery and then moved toward the puncture of the left middle cerebral artery. The incoming length of the nylon suture was approximately 18–20 mm. Subsequently, the suture was withdrawn to enable reperfusion. Sham-operated animals underwent the same anesthesia and surgical procedures but were not subjected to intracranial endovascular perforation.

The success of the SAH models was evaluated by the SAH grade scoring system (Sugawara et al., 2008). The SAH grade score system includes two approaches: the bleed grade score system and the modified Garcia scoring system. The bleed grade score system (score <8 was excluded from the study) was used for animals that were killed 24 h or 3 d after SAH, and the modified Garcia scoring system (score >14 on day 1 after SAH was excluded from the study) was used 1 day after surgery for animals that needed to survive for a long time. The mortality rate for the SAH animals was approximately 5.4% (six of 113 total rats died after SAH surgery), and the success rate was approximately 91.6% (9 excluded of 107 rats).

Behavioral Tests

Behavioral tests were performed in a blinded manner to evaluate the sensorimotor function of the rats. The modified Garcia scoring system was performed as described previously (2) and used to evaluate the comprehensive neurological function after SAH. In brief, the modified Garcia scoring system includes six items (3 points/item): body sensations, spontaneous activity of the extremities, motor ability, climbing ability, movement and strength of the forelimbs, and responses to stimulating whiskers.

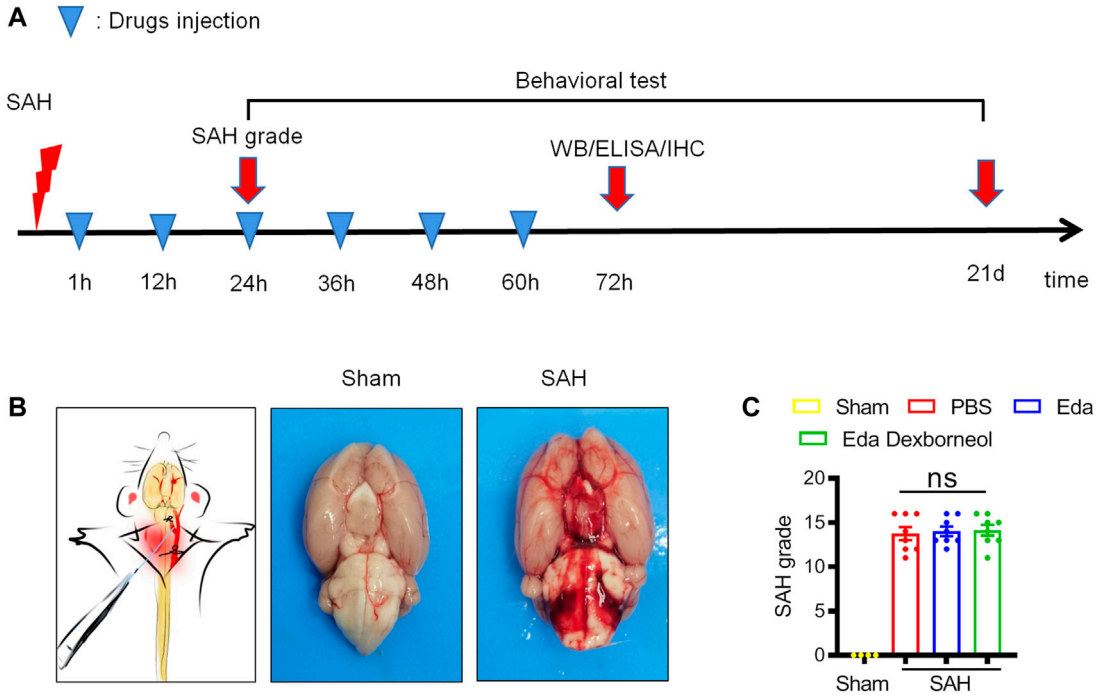

FIGURE 1 | Establishment of a stable SAH rat model. **(A)** Diagramshowing the time points for drug injection and outcome evaluation. **(B)** Schematic representation of the SAH model (left) and representative images of rat brains in the sham/SAH group. **(C)** SAH grading scores of the four groups were assessed after 24 h. $n = 4$/group. Data are given as mean ± SE. ns: no significant difference; Eda: edaravone; Eda dexborneol: edaravone dexborneol.

The rotarod test was performed to evaluate the balance and sensorimotor coordination (Mao et al., 2020). After the animals were placed on the rods, the rods began to accelerate to 40 r/min within 30 s, and this speed was maintained until 300 s. The duration on the rods was recorded. The foot-fault test was related to deficits in motor control. The rats were placed on a stainless steel grid floor and allowed to move on it for 1 min during each trial. A foot fault was recorded when a paw slipped. The percentages of foot faults were calculated by errors versus total steps made by the contralateral limbs. The corner test was used to assess asymmetric behavior after SAH (Lei et al., 2020; Mao et al., 2020). The rats were placed between two boards angled at 30°. Normal rats randomly turned back without a preference for direction, but rats with focalized sensorimotor dysfunction showed a preference to turn toward the non-impaired side. We repeated the corner test ten times and recorded the number of right or left turns.

Immunofluorescence Staining

Three days after SAH, the animals were euthanized and perfused with cold saline, followed by PBS containing 4% paraformaldehyde. Their brains were removed and fixed in 4% paraformaldehyde for 24 h, followed by 20% sucrose/paraformaldehyde buffer and 30% sucrose/PBS buffer for 72 h. Serial sections (20 μm thickness) were prepared by a freezing microtome. The slices at specific levels were selected for immunohistochemical staining. First, the selected slices were incubated with primary antibodies at 4°C overnight. The primary antibodies included goat anti-4-HNE (Millipore), rabbit anti-GFAP (ProteinTech), cleaved caspase 3 (Cell Signaling Technology), and rabbit anti-NeuN (Millipore). Second, after three washes in 0.3% PBST, slices were incubated with a secondary antibody labeled with a fluorescent dye (Jackson ImmunoResearch Laboratories) for 1 h at room temperature. The slices were then washed and mounted with DAPI Fluoromount-G (Southern Biotech). Finally, images were acquired under a confocal microscope (Nikon), and immunopositive cell quantification in the cortex or hippocampus was performed by ImageJ software.

Western Blot

The basal cortex and hippocampus of the ipsilateral hemisphere were harvested 72 h after SAH, frozen in dry ice, and stored at -80°C until use. The samples were homogenized and centrifuged for 10 min (12,000 r/min). Equal amounts of protein samples were loaded and probed with antibodies recognizing cleaved caspase 3, 4-HNE (Millipore), cleaved caspase 3 (Cell Signaling Technology), or β-actin (Sigma, United States). After incubating with secondary antibodies for 1 h, the membranes were detected by a chemiluminescence substrate and visualized by using a ChemiDoc MP Imaging System (Bio–Rad). The optical density of the bands was measured by ImageJ and normalized to the corresponding β-actin band.

MDA and Total Antioxidant Capability (TAC)

The basal cortex and hippocampus of the ipsilateral hemisphere were homogenized in cold PBS (W/V = 20 mg/100 μL) and then subjected to centrifugal separation. The supernatant was collected for MDA (Beyotime, China) or TAC (Beyotime, China) detection. The detailed testing procedures were carried out according to the manufacturer's instructions.

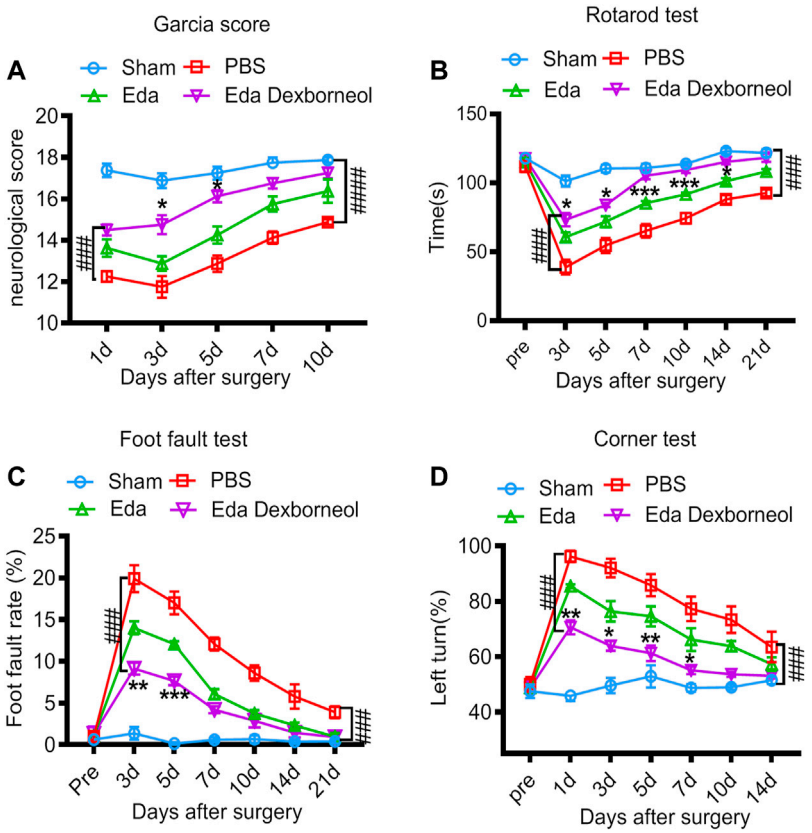

FIGURE 2 | Edaravone dexborneol treatment improves sensorimotor functions after SAH. **(A)** Neurological scores were determined 1–10 days after SAH with the modified Garcia scoring system. **(B–D)** Acute sensorimotor dysfunction at 1–21 days after SAH was assessed by **(A)** Garcia score, **(B)** rotarod test, **(C)** foot-fault test, and **(D)** corner test. N = 8/group. Data are given as mean ± SE. $^{*}p < 0.05$, $^{**}p < 0.01$, $^{***}p < 0.001$ vs. Eda. $^{\#\#\#}p < 0.001$, $^{\#\#\#\#}p < 0.0001$ vs. PBS. Eda: edaravone; Eda dexborneol: edaravone dexborneol.

Statistical Analysis

All results are presented as means ± SEM (standard error of the mean). Differences among the four groups were analyzed using one-way or two-way ANOVA using Bonferroni's multiple comparisons test in GraphPad Prism software 7.0. In all results, a p value <0.05 was considered statistically significant.

RESULTS

Edaravone dexborneol treatment confers long-term protection against neurological dysfunction after SAH.

Male SD rats were randomly assigned to experimental groups and then subjected to SAH or sham surgery. Edaravone dexborneol, edaravone, or the same volume of PBS was administered by tail vein injection twice a day from 1 h to 3 d post-SAH surgery (**Figure 1A**). The experimental SAH model was induced by an intraluminal puncture of the left middle cerebral artery (MCA). Subarachnoid blood clots were observed on the circle of Willis (**Figure 1B**). There were no significant differences between the PBS, edaravone, and edaravone dexborneol groups, suggesting that variation in SAH size did not confound the results (**Figure 1C**).

To assess the therapeutic effects of edaravone dexborneol or edaravone on SAH-induced neurological dysfunction, we employed the Garcia scoring system, rotarod test, foot-fault test, and corner test to examine neurobehavioral capacity before and up to 21 days after SAH. The neurological score results suggested that edaravone dexborneol treatment significantly improved neurobehavioral deficits within 10 days after SAH surgery, and the efficacy was much better than that of edaravone alone at 3 and 5 d post-SAH (**Figure 2A**). Similarly, sensorimotor deficits were significantly reduced in edaravone dexborneol-treated SAH rats compared to SAH rats treated with edaravone alone, as demonstrated by the performance on the rotarod test for sensorimotor coordination, the foot-fault test for balance function, and the corner test for turning asymmetry (**Figures 2B–D**). Taken together, these results suggest a better beneficial role of edaravone dexborneol than edaravone alone in improving long-term neurobehavioral functions following SAH.

Edaravone Dexborneol Treatment Attenuates Neuronal Apoptosis After Subarachnoid Hemorrhage in Rats

Since neuronal apoptosis has been considered a significant structural basis of neurobehavioral deficits after SAH, we

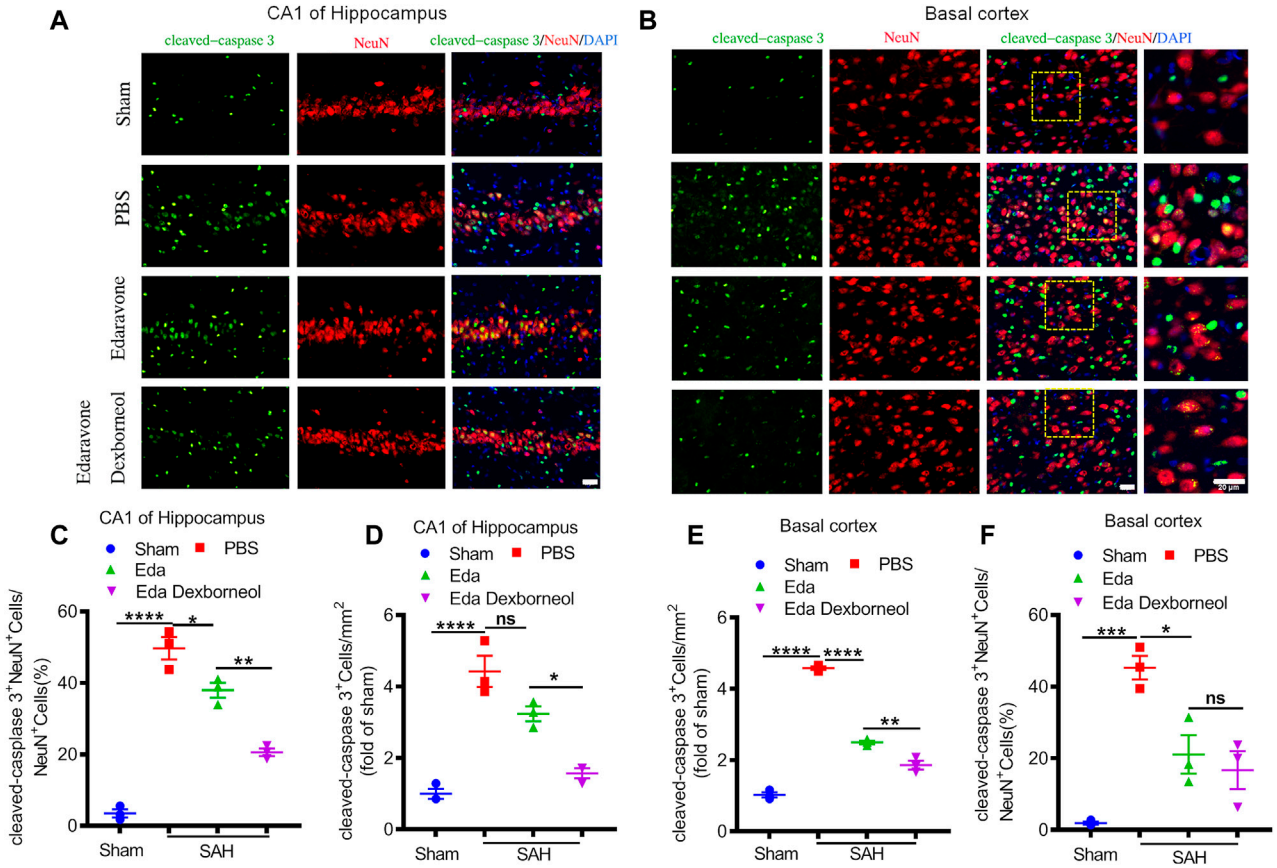

FIGURE 3 | Immunofluorescent staining showing that edaravone dexborneol treatment profoundly decreased the levels of cleaved caspase 3 in the brain after SAH injury. **(A,B)** Representative immunofluorescence images of cleaved caspase 3 (green)/NeuN (red)-stained neurons in CA1 of the hippocampus **(A)** and basal cortex **(B)** at 3 d after SAH. Scale bar: 20 μm. **(C–F)** Quantitative analysis of caspase 3^+NeuN$^+$ neurons and cleaved caspase 3^+ cells in each group. Data are normalized to sham. n = 3/group. Data are given as mean ± SE. $^*p < 0.05$, $^{**}p < 0.01$, $^{***}p < 0.001$, $^{****}p < 0.0001$. Eda: edaravone; Eda dexborneol: edaravone dexborneol.

killed the rats 3 days after surgery and detected the expression of cleaved caspase 3 in the CA1 hippocampus and basal cortex by immunofluorescent staining, where cleaved caspase 3 is a key factor leading to apoptosis. As shown in **Figures 3A, B**, significant increases in cleaved caspase 3 staining were observed in neurons of the CA1 hippocampus and basal cortex regions in PBS-treated rats, resulting in an increased cleaved caspase 3^+ neuron ratio and cleaved caspase 3^+ cell number (**Figures 3C–F**). Both treatments of edaravone dexborneol and edaravone alone significantly decreased the cleaved caspase 3-positive neuron ratio compared to PBS treatment in both brain regions, and treatment with edaravone dexborneol showed greater effects than treatment with edaravone in the CA1 hippocampal region (**Figures 3C, E**). In addition, edaravone dexborneol treatment was more efficient in decreasing the number of cleaved caspase 3-positive cells in both brain regions (**Figures 3D, F**).

Furthermore, to determine the neuroprotective effect of edaravone dexborneol on cerebral cell resistance, we detected the expression of cleaved caspase 3 in the brain basal cortex and CA1 hippocampal regions by Western blot analysis. Western blots validated the immunostaining data (**Figures 4A, B**). The levels of cleaved caspase 3 increased in both regions 3 days after SAH, while both edaravone dexborneol and edaravone treatments evidently inhibited the expression of cleaved caspase 3. Moreover, edaravone dexborneol showed a better inhibitory effect on cleaved caspase 3. Collectively, these data indicated that compared to edaravone, edaravone dexborneol treatment conferred greater neuroprotection against SAH-induced cell apoptosis, which may underlie the improved long-term neurobehavioral functions.

Edaravone Dexborneol Treatment Inhibits Oxidative Stress After SAH

We next investigated the neuroprotective mechanism of edaravone dexborneol treatment. Oxidative stress is widely considered to be an important mechanism of SAH-induced cell apoptosis, and edaravone has been reported to be a powerful antioxidant. Therefore, we focused on the antioxidant roles of edaravone dexborneol and edaravone treatment, measured by total antioxidant capability (TAC) and lipid peroxidation MDA assays 3 days after SAH. As shown in

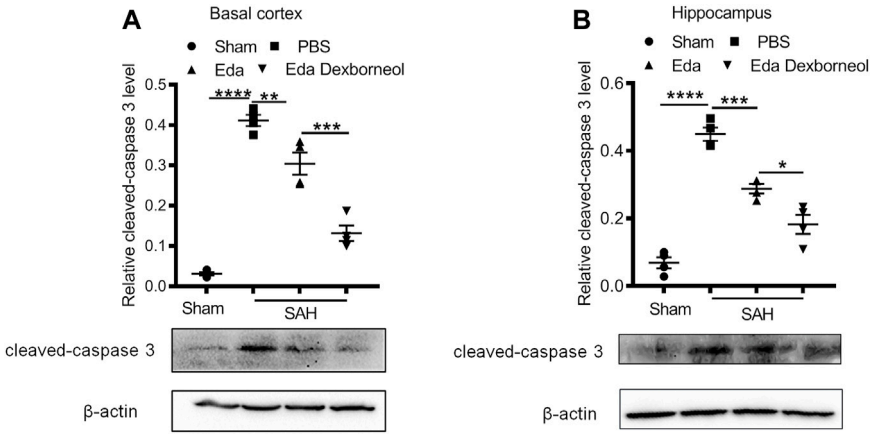

FIGURE 4 | Western blot showing that edaravone dexborneol treatment profoundly decreased the levels of cleaved caspase 3 in the brain after SAH injury. **(A,B)** Representative Western blot images and semiquantitative data show the expression of cleaved caspase 3 in the basal cortex **(A)** and CA1 hippocampus **(B)** at 3 d after SAH. Data are normalized to sham. n = 4/group. *p < 0.05, **p < 0.01, ***p < 0.001, ****p < 0.0001. Eda: edaravone; Eda dexborneol: edaravone dexborneol.

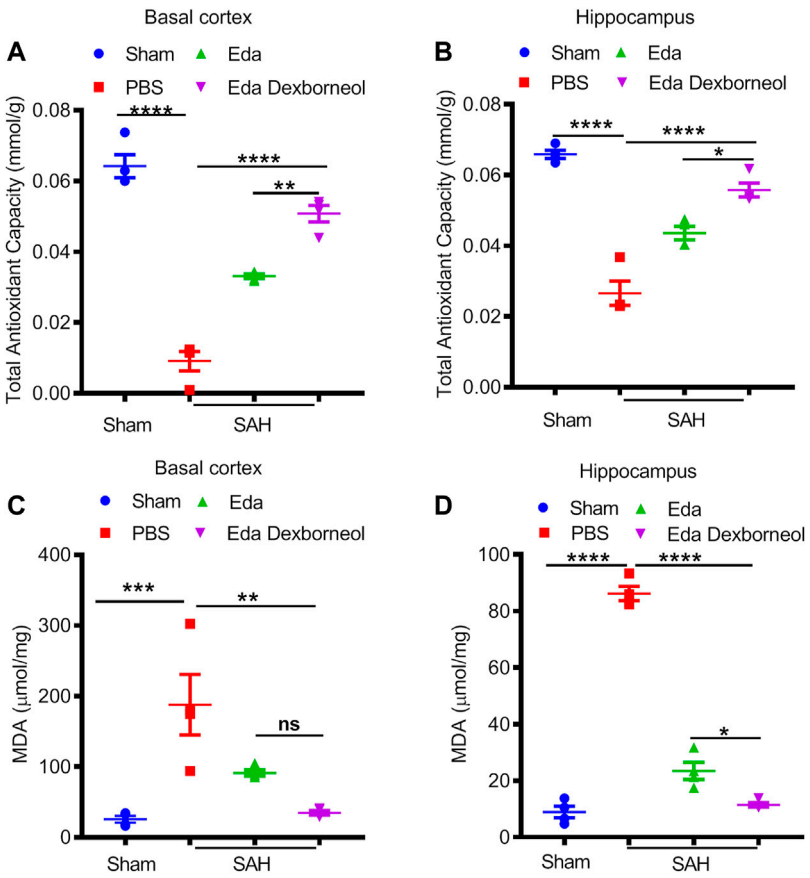

FIGURE 5 | Edaravone dexborneol treatment significantly suppressed oxidative stress after SAH. ABTS assay was used to detect the total antioxidant capability of cortical **(A)** and hippocampal tissues **(B)** after SAH. An MDA assay was used to evaluate SAH-induced lipid peroxidation in the cortex **(C)** and hippocampus **(D)**. Data are given as mean ± SEM. *p < 0.05, **p < 0.01, ***p < 0.001, ****p < 0.0001. Eda: edaravone; Eda dexborneol: edaravone dexborneol.

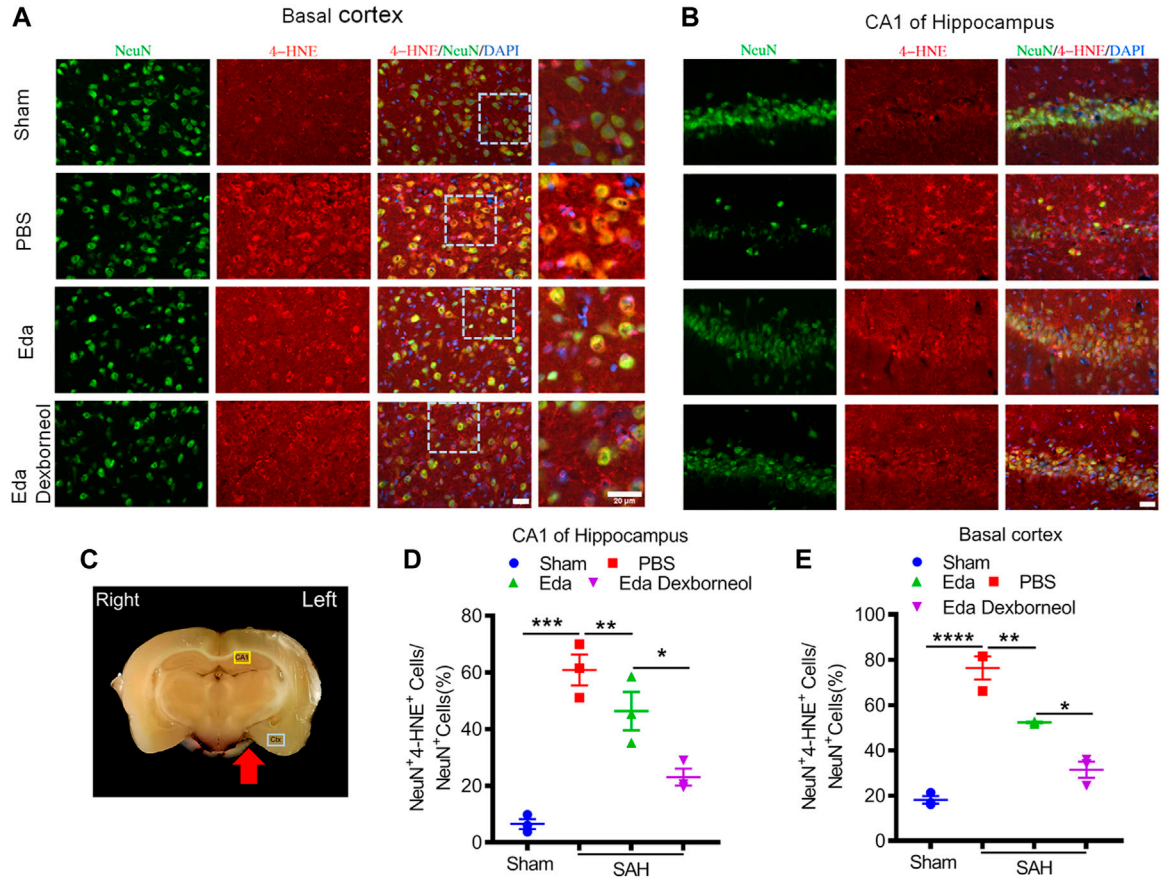

FIGURE 6 | Edaravone dexborneol treatment decreases the levels of 4-HNE in neurons after SAH injury. **(A,B)** Representative immunofluorescence images of 4-HNE (red)/NeuN (green)-stained neurons in the basal cortex **(A)** and CA1 of the hippocampus **(B)** at 3 d after SAH. Scale bar: 20 μm. **(C)** The schema illustrates the regions of interest related to fluorescence staining in the brain cortex or hippocampus. **(D,E)** Quantitative analysis of 4-HNE + neurons in the basal cortex **(D)** and CA1 of the hippocampus **(E)** at 3 d after SAH. *n* = 3/group. Data are given as mean ± SE. $^{*}p < 0.05$, $^{**}p < 0.01$, $^{***}p < 0.001$, $^{****}p < 0.0001$. Eda: edaravone; Eda dexborneol: edaravone dexborneol.

Figures 5A, B, both edaravone dexborneol and edaravone treatment displayed significant antioxidant functions, and the antioxidant ability of edaravone dexborneol was much stronger than that of edaravone alone. The expression of lipid peroxidation MDA was significantly increased both in the CA1 hippocampus and basal cortex regions 3 d after SAH surgery, which could be inhibited by edaravone dexborneol or edaravone treatment alone (**Figures 5C, D**). Significantly, compared to edaravone, edaravone dexborneol treatment showed a stronger ability to suppress MDA production in the CA1 hippocampus (**Figure 5D**). Taken together, these data suggest that edaravone dexborneol treatment confers antioxidant capability against SAH-induced cerebral injury.

Edaravone dexborneol treatment decreases the levels of 4-HNE in the brain after SAH.

As an important product of lipid peroxidation, MDA appears to be the most mutagenic product, whereas 4-HNE is the most toxic (Ayala et al., 2014), causing neuronal oxidative damage and death. Next, we investigated the inhibitory effects of edaravone dexborneol on 4-HNE in the brain after SAH. As shown in **Figure 6**, the 4-HNE level in the neurons were significantly increased both in the basal cortex and CA1 hippocampal regions 3 d after SAH surgery compared with the sham-operated group, whereas edaravone dexborneol or edaravone treatment effectively inhibited the SAH-elevated level of 4-HNE in the neurons, and edaravone dexborneol showed a stronger inhibitory effect. Meanwhile, we detected the level of 4-HNE in astrocytes after SAH using double immunofluorescence staining for 4-HNE and GFAP (**Figure 7**). Similarly, the results indicated that the 4-HNE level in astrocytes was also significantly increased both in the basal cortex and CA1 hippocampal regions 3 d after SAH surgery. Compared with edaravone treatment, edaravone dexborneol treatment provided a stronger inhibitory effect on 4-HNE levels in astrocytes after SAH.

Finally, we collected fresh basal cortex and hippocampal tissues 3 d after surgery for Western blotting (**Figure 8**). The expression of 4-HNE was significantly increased in both the

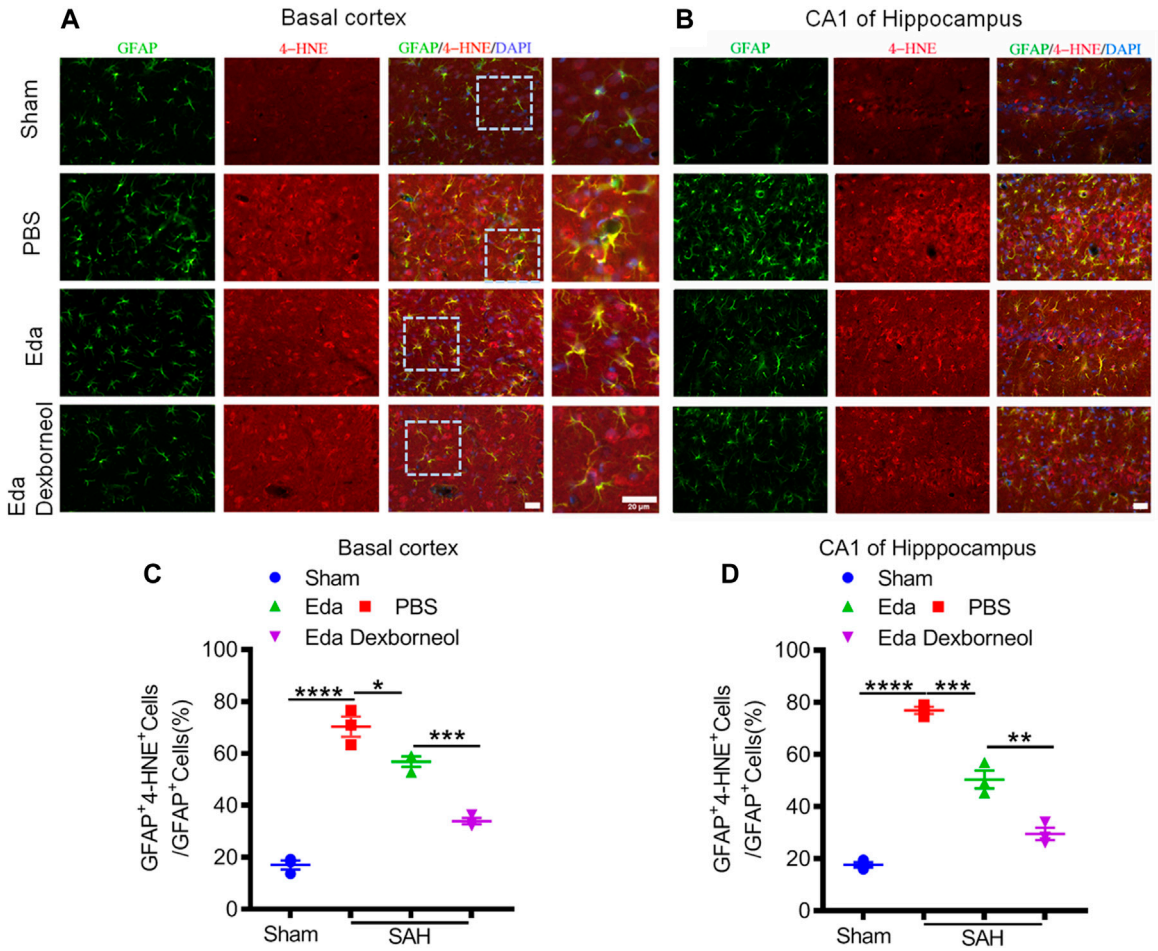

FIGURE 7 | Edaravone dexborneol treatment decreases the levels of 4-HNE in astrocytes after SAH injury. **(A,B)** Representative immunofluorescence images of 4-HNE (red)/GFAP (green)-stained astrocytes in the basal cortex **(A)** and CA1 of the hippocampus **(B)** at 3 d after SAH. Scale bar: 20 μm. **(C,D)** Quantitative analysis of 4-HNE + astrocytes in the basal cortex **(C)** and CA1 of the hippocampus **(D)** at 3 d after SAH. $n = 3$/group. Data are given as mean ± SE. $^{*}p < 0.05$, $^{**}p < 0.01$, $^{***}p < 0.001$, $^{****}p < 0.0001$. Eda: edaravone; Eda dexborneol: edaravone dexborneol.

cortex and hippocampus after SAH and could be inhibited by edaravone dexborneol or edaravone treatment. Moreover, Western blot results validated the immunofluorescent staining data showing that the inhibitory effect of edaravone dexborneol on 4-HNE was greater than that of edaravone. In summary, compared with edaravone, edaravone dexborneol treatment was able to provide greater antioxidant ability against SAH-induced brain injury by inhibiting 4-HNE expression.

DISCUSSION

In this study, we demonstrated that edaravone dexborneol treatment significantly attenuated neuronal apoptosis and improved long-term neurological outcomes up to 21 days after SAH injury. Moreover, we further illustrated that edaravone dexborneol treatment provided a protective effect against SAH injury by, at least partially, inhibiting the 4-HNE-related oxidative stress response.

Edaravone dexborneol is a novel neuroprotective drug that comprises edaravone and (+)-borneol in a 4:1 ratio (Wu et al., 2014b). Phase II and III studies have demonstrated that Chinese patients treated with edaravone dexborneol within 48 h of acute ischemic stroke onset have better functional outcomes than those treated with edaravone alone. Moreover, edaravone dexborneol has been found to be safe and well tolerated at different doses compared with edaravone alone (Xu et al., 2019; Xu et al., 2021). Edaravone dexborneol has been cleared by the National Medical Products Administration (NMPA) of China for clinical use in AIS patients since July 2020 and has obtained good outcomes. The neuroprotective mechanisms of edaravone dexborneol against AIS are thought to involve a multifunctional cytoprotective pathway, including oxidative, excitotoxic, inflammatory, and apoptotic insults. However, the effects of edaravone dexborneol in the treatment of SAH have not been studied.

As a free radical scavenger, edaravone (3-methyl-1-phenyl-2-pyrazolin-5-one) has been widely used to improve

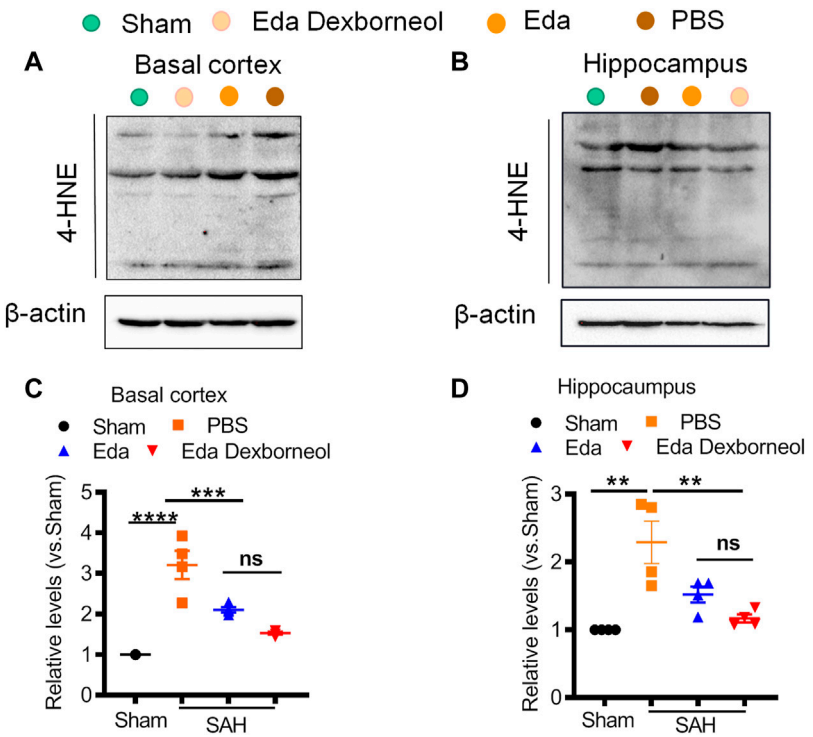

FIGURE 8 | Western blot showing that edaravone dexborneol treatment profoundly decreased the levels of 4-HNE in the brain after SAH injury. **(A,B)** Representative Western blot images show the expression of 4-HNE in the basal cortex **(A)** and CA1 hippocampus **(B)** tissue at 3 d after SAH. **(C,D)** Semiquantitative data of Western blot bands for 4-HNE in each group. Data are normalized to sham. $n = 4$/group. $^{*}p < 0.05$, $^{***}p < 0.001$, $^{****}p < 0.0001$. Eda: edaravone; Eda dexborneol: edaravone dexborneol.

functional outcomes in AIS patients in recent years. Furthermore, previous reports showed that edaravone is a useful agent for the treatment of SAH, manifested by a lower incidence of delayed ischemic neurological deficits and a lower incidence of poor outcome in SAH patients (Munakata et al., 2009; Munakata et al., 2011). In order to investigate the advantage of edaravone dexborneol on SAH injury, we chose edaravone as the positive control drug. (+)-Borneol is a bicyclic terpene compound that can prevent nerve injury in ischemic stroke. The related mechanisms of neuroprotection include resistance to reactive oxygen species injury, improvement of cerebral blood flow, blocking of Ca^{2+} overload, and inhibition of neuronal excitotoxicity (Li et al., 2021). Edaravone dexborneol, comprising edaravone and (+)-borneol, is regarded to confer neuroprotection upon stroke injury, which may be more effective than edaravone alone against stroke (Wu et al., 2014b; Xu et al., 2019; Xu et al., 2021). This study is aimed to ascertain the effects of edaravone dexborneol on SAH injury and explore the therapeutic differences between the two drugs. We found that compared to edaravone alone, post-SAH edaravone dexborneol treatment conferred a stronger long-term protection against neurological dysfunction.

Oxidative stress has been identified as an important mechanism by which acute brain damage causes neurological dysfunction after SAH (Jarocka-Karpowicz et al., 2020; Wei et al., 2020). In addition, neuronal apoptosis has been shown to occur in the brain cortex and hippocampus which are associated with oxidative stress injury following SAH (Ayer and Zhang, 2008). Furthermore, the basal cortex and CA1 hippocampus are the most concerned regions that show more severe damage (Sehba et al., 2012; Mo et al., 2019; Zhang et al., 2020). Interestingly, our study showed that compared to edaravone, edaravone dexborneol treatment conferred greater neuroprotection against SAH-induced cell apoptosis in the basal cortex and CA1 hippocampal regions. Under physiological conditions, redox homeostasis is the result of a balance between the expression of oxidative stress products and the antioxidant capacity. Oxidative stress injury occurs when the production of free radical moieties and lipid peroxides exceeds the antioxidant capacity of the related brain regions (Fumoto et al., 2019; Jarocka-Karpowicz et al., 2020). Oxidative stress plays an important role in the course of various pathological changes in early brain injury after SAH, whereas pharmacological or genetic suppression of oxidative stress has been regarded to alleviate early brain injury which is involved in the development of cerebral ischemia and poor outcome (Fumoto et al., 2019). Our study shows that both edaravone dexborneol and edaravone treatment display powerful antioxidant functions according to a total antioxidant

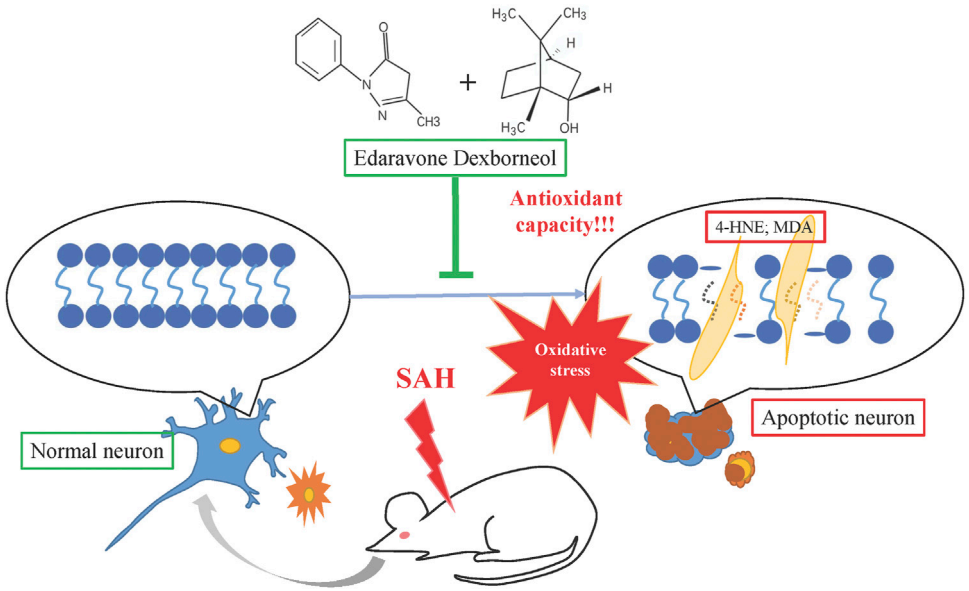

FIGURE 9 | Schematic illustration of the mechanisms by which edaravone dexborneol afforded neuroprotection against SAH-induced brain injury. SAH could cause neuronal apoptosis by inducing oxidative stress injury. Edaravone dexborneol treatment attenuates neuronal apoptosis by affording powerful antioxidant capacity after SAH, accompanied by the inhibition of lipid peroxidation products such as 4-HNE and MDA.

capability assay with a rapid ABTS method, and the antioxidant ability of edaravone dexborneol is much stronger than that of edaravone alone. In addition, compared to edaravone, edaravone dexborneol treatment shows a stronger ability to suppress the production of MDA, which may be related to DNA damage after SAH as an important product of lipid peroxide (Zhuang et al., 2019; Jarocka-Karpowicz et al., 2020).

4-HNE is considered as another important lipid peroxidation product not only as a biomarker of oxidative stress but also as one of the most formidable reactive aldehydes (Breitzig et al., 2016; Deng et al., 2020). 4-HNE has been implicated in neuronal oxidative damage and death after SAH because of its toxicity (Siuta et al., 2013). Additionally, recent studies have reported that the cytotoxicity of 4-HNE involves several mechanisms, specifically 1) 4-HNE has been shown to play a role in altering signal transduction by altering protein structure, such as to upregulating proapoptotic factors or accelerating protein degradation (Moldogazieva et al., 2019), and 2) 4-HNE has been reported to promote inflammation by stimulating MCP-1, TNF-α, TGF-β, or other pro-inflammatory cytokines (Vistoli et al., 2013; Zhang et al., 2016). Furthermore, studies report that 4-HNE could induce deactivation of proteins, such as ALDH2, by modes of inhibition or structural change (Jinsmaa et al., 2009). Our data showed that the expression of 4-HNE significantly increased in the brain cortex and hippocampal regions on day 3 after SAH, and edaravone dexborneol treatment significantly suppressed the increase in 4-HNE expression. Thus, the antioxidant ability of edaravone dexborneol is well confirmed. Nevertheless, to verify the key role of 4-HNE in the neuroprotective mechanisms of edaravone dexborneol, we will explore whether supplementation with 4-HNE in the brain could deplete the neuroprotection of edaravone dexborneol in the protection against SAH-induced brain injury. Moreover, future studies are warranted to elucidate the precise signaling mechanism by which edaravone dexborneol inhibits 4-HNE expression after SAH.

Our current study first investigated the therapeutic effects of edaravone dexborneol on an experimental SAH model. Similar to edaravone dexborneol studies on AIS (Wu et al., 2014b), our study further confirmed its antioxidant and anti-apoptosis ability against brain injury. These findings are also consistent with accumulating evidence showing the neuroprotective mechanism of edaravone involving its antioxidant ability (Wu et al., 2014a; Fumoto et al., 2019; Nakanishi et al., 2019). Meanwhile, this was the first study to discuss the inhibitory effect of edaravone dexborneol on MDA and 4-HNE. Similarly, edaravone-alone treatment also showed the inhibition of 4-HNE against traumatic brain injury (Itoh et al., 2010) or AIS (Lukic-Panin et al., 2010)-induced oxidative stress. Furthermore, the effects of edaravone dexborneol on some other mechanisms of SAH-induced brain injury such as neuroinflammation, excitotoxicity, or vessel spasm warrant further investigation. Accompanied by the wide clinical application of edaravone dexborneol on AIS, we look forward to clinical trials on SAH patients.

In summary, this study is the first to demonstrate that edaravone dexborneol confers neuroprotection and stabilizes long-term behavioral ability after SAH injury, possibly by improving antioxidant capacity and suppressing lipid peroxidation products such as MDA and 4-HNE, as shown in **Figure 9**. Our results reveal a novel neuroprotective agent against SAH injury. These results may help develop new clinical strategies for SAH treatment.

DATA AVAILABILITY STATEMENT

The original contributions presented in the study are included in the article/**Supplementary Material**, further inquiries can be directed to the corresponding authors.

ETHICS STATEMENT

The animal study was reviewed and approved by the Institutional Animal Care and Use Committee of Shandong First Medical University and conducted in accordance with the National Institutes of Health (NIH) Guide for the Care and Use of Laboratory Animals.

AUTHOR CONTRIBUTIONS

LM, ZZ, and BS designed the study and wrote the manuscript. BS revised the manuscript. QC performed the experiments and processed the data. YC, XY, JW, and FG helped to perform experiments. MY prepared the experimental protocols.

FUNDING

This work was supported by grants the Natural Science Foundation of China (Nos. 81871855 to MY, 81870938 to BS, and 82071303 to ZZ) and by the Fund of Taishan Scholar Project and Fund of Academic Promotion Program of Shandong First Medical University and Shandong Academy of Medical Sciences (Nos. 2019QL016 and 2019PT007).

SUPPLEMENTARY MATERIAL

The Supplementary Material for this article can be found online at: https://www.frontiersin.org/articles/10.3389/fphar.2022.848529/full#supplementary-material

REFERENCES

Ayala, A., Muñoz, M. F., and Argüelles, S. (2014). Lipid Peroxidation: Production, Metabolism, and Signaling Mechanisms of Malondialdehyde and 4-Hydroxy-2-Nonenal. *Oxid Med. Cel Longev* 2014, 360438. doi:10.1155/2014/360438

Ayer, R. E., and Zhang, J. H. (2008). Oxidative Stress in Subarachnoid Haemorrhage: Significance in Acute Brain Injury and Vasospasm. *Acta Neurochir Suppl.* 104, 33–41. doi:10.1007/978-3-211-75718-5_7

Breitzig, M., Bhimineni, C., Lockey, R., and Kolliputi, N. (2016). 4-Hydroxy-2-nonenal: a Critical Target in Oxidative Stress? *Am. J. Physiol. Cel Physiol* 311 (4), C537–C43. doi:10.1152/ajpcell.00101

Deng, H. F., Yue, L. X., Wang, N. N., Zhou, Y. Q., Zhou, W., Liu, X., et al. (2020). Mitochondrial Iron Overload-Mediated Inhibition of Nrf2-HO-1/gpx4 Assisted ALI-Induced Nephrotoxicity. *Front. Pharmacol.* 11, 624529. doi:10.3389/fphar.2020.624529

Dong, G., Li, C., Hu, Q., Wang, Y., Sun, J., Gao, F., et al. (2021). Low-Dose IL-2 Treatment Affords Protection against Subarachnoid Hemorrhage Injury by Expanding Peripheral Regulatory T Cells. *ACS Chem. Neurosci.* 12 (3), 430–440. doi:10.1021/acschemneuro.0c00611

Fumoto, T., Naraoka, M., Katagai, T., Li, Y., Shimamura, N., and Ohkuma, H. (2019). The Role of Oxidative Stress in Microvascular Disturbances after Experimental Subarachnoid Hemorrhage. *Transl Stroke Res.* 10 (6), 684–694. doi:10.1007/s12975-018-0685-0

Itoh, T., Satou, T., Nishida, S., Tsubaki, M., Imano, M., Hashimoto, S., et al. (2010). Edaravone Protects against Apoptotic Neuronal Cell Death and Improves Cerebral Function after Traumatic Brain Injury in Rats. *Neurochem. Res.* 35 (2), 348–355. doi:10.1007/s11064-009-0061-2

Jarocka-Karpowicz, I., Syta-Krzyżanowska, A., Kochanowicz, J., and Mariak, Z. D. (2020). Clinical Prognosis for SAH Consistent with Redox Imbalance and Lipid Peroxidation. *Molecules* 25 (8). doi:10.3390/molecules25081921

Jinsmaa, Y., Florang, V. R., Rees, J. N., Anderson, D. G., Strack, S., and Doorn, J. A. (2009). Products of Oxidative Stress Inhibit Aldehyde Oxidation and Reduction Pathways in Dopamine Catabolism Yielding Elevated Levels of a Reactive Intermediate. *Chem. Res. Toxicol.* 22 (5), 835–841. doi:10.1021/tx800405v

Kikuchi, K., Tancharoen, S., Takeshige, N., Yoshitomi, M., Morioka, M., Murai, Y., et al. (2013). The Efficacy of Edaravone (Radicut), a Free Radical Scavenger, for Cardiovascular Disease. *Int. J. Mol. Sci.* 14 (7), 13909–13930. doi:10.3390/ijms140713909

Lei, X., Li, H., Li, M., Dong, Q., Zhao, H., Zhang, Z., et al. (2020). The Novel Nrf2 Activator CDDO-EA Attenuates Cerebral Ischemic Injury by Promoting Microglia/macrophage Polarization toward M2 Phenotype in Mice. *CNS Neurosci. Ther.* 27, 82–91. doi:10.1111/cns.13496

Li, Y., Ren, M., Wang, J., Ma, R., Chen, H., Xie, Q., et al. (2021). Progress in Borneol Intervention for Ischemic Stroke: A Systematic Review. *Front. Pharmacol.* 12, 606682. doi:10.3389/fphar.2021.606682

Liu, H., Guo, W., Guo, H., Zhao, L., Yue, L., Li, X., et al. (2020). Bakuchiol Attenuates Oxidative Stress and Neuron Damage by Regulating Trx1/TXNIP and the Phosphorylation of AMPK after Subarachnoid Hemorrhage in Mice. *Front. Pharmacol.* 11, 712. doi:10.3389/fphar.2020.00712

Lukic-Panin, V., Deguchi, K., Yamashita, T., Shang, J., Zhang, X., Tian, F., et al. (2010). Free Radical Scavenger Edaravone Administration Protects against Tissue Plasminogen Activator Induced Oxidative Stress and Blood Brain Barrier Damage. *Curr. Neurovasc Res.* 7 (4), 319–329. doi:10.2174/156720210793180747

Macdonald, R. L., and Schweizer, T. A. (2017). Spontaneous Subarachnoid Haemorrhage. *Lancet* 389 (10069), 655–666. doi:10.1016/S0140-6736(16)30668-7

Mao, L., Sun, L., Sun, J., Sun, B., Gao, Y., and Shi, H. (2020). Ethyl Pyruvate Improves white Matter Remodeling in Rats after Traumatic Brain Injury. *CNS Neurosci. Ther.* 27, 113–122. doi:10.1111/cns.13534

Mo, J., Enkhjargal, B., Travis, Z. D., Zhou, K., Wu, P., Zhang, G., et al. (2019). AVE 0991 Attenuates Oxidative Stress and Neuronal Apoptosis via Mas/PKA/CREB/UCP-2 Pathway after Subarachnoid Hemorrhage in Rats. *Redox Biol.* 20, 75–86. doi:10.1016/j.redox.2018.09.022

Moldogazieva, N. T., Mokhosoev, I. M., Mel'nikova, T. I., Porozov, Y. B., and Terentiev, A. A. (2019). Oxidative Stress and Advanced Lipoxidation and Glycation End Products (ALEs and AGEs) in Aging and Age-Related Diseases. *Oxid Med. Cel Longev* 2019, 3085756. doi:10.1155/2019/3085756

Munakata, A., Ohkuma, H., Nakano, T., Shimamura, N., Asano, K., and Naraoka, M. (2009). Effect of a Free Radical Scavenger, Edaravone, in the Treatment of Patients with Aneurysmal Subarachnoid Hemorrhage. *Neurosurgery* 64 (3), 423–429. doi:10.1227/01.NEU.0000338067.83059.EB

Munakata, A., Ohkuma, H., and Shimamura, N. (2011). Effect of a Free Radical Scavenger, Edaravone, on Free Radical Reactions: Related Signal Transduction and Cerebral Vasospasm in the Rabbit Subarachnoid Hemorrhage Model. *Acta Neurochir Suppl.* 110 (Pt 2), 17–22. doi:10.1007/978-3-7091-0356-2_4

Nakanishi, T., Tsujii, M., Asano, T., Iino, T., and Sudo, A. (2019). Protective Effect of Edaravone against Oxidative Stress in C2C12 Myoblast and Impairment of Skeletal Muscle Regeneration Exposed to Ischemic Injury in Ob/ob Mice. *Front. Physiol.* 10, 1596. doi:10.3389/fphys.2019.01596

Sehba, F. A., Hou, J., Pluta, R. M., and Zhang, J. H. (2012). The Importance of Early Brain Injury after Subarachnoid Hemorrhage. *Prog. Neurobiol.* 97 (1), 14–37. doi:10.1016/j.pneurobio.2012.02.003

Siuta, M., Zuckerman, S. L., and Mocco, J. (2013). Nitric Oxide in Cerebral Vasospasm: Theories, Measurement, and Treatment. *Neurol. Res. Int.* 2013, 972417. doi:10.1155/2013/972417

Sugawara, T., Ayer, R., Jadhav, V., and Zhang, J. H. (2008). A New Grading System Evaluating Bleeding Scale in Filament Perforation Subarachnoid Hemorrhage Rat Model. *J. Neurosci. Methods* 167 (2), 327–334. doi:10.1016/j.jneumeth.2007.08.004

Tsikas, D. (2017). Assessment of Lipid Peroxidation by Measuring Malondialdehyde (MDA) and Relatives in Biological Samples: Analytical and Biological Challenges. *Anal. Biochem.* 524, 13–30. doi:10.1016/j.ab.2016.10.021

van Gijn, J., Kerr, R. S., and Rinkel, G. J. (2007). Subarachnoid Haemorrhage. *Lancet* 369 (9558), 306–318. doi:10.1016/S0140-6736(07)60153-6

Vistoli, G., De Maddis, D., Cipak, A., Zarkovic, N., Carini, M., and Aldini, G. (2013). Advanced Glycoxidation and Lipoxidation End Products (AGEs and ALEs): an Overview of Their Mechanisms of Formation. *Free Radic. Res.* 47 (1), 3–27. doi:10.3109/10715762.2013.815348

Wei, C., Guo, S., Liu, W., Jin, F., Wei, B., Fan, H., et al. (2020). Resolvin D1 Ameliorates Inflammation-Mediated Blood-Brain Barrier Disruption after Subarachnoid Hemorrhage in Rats by Modulating A20 and NLRP3 Inflammasome. *Front. Pharmacol.* 11, 610734. doi:10.3389/fphar.2020.610734

Wu, F., Liu, Z., Li, G., Zhou, L., Huang, K., Wu, Z., et al. (2021). Inflammation and Oxidative Stress: Potential Targets for Improving Prognosis after Subarachnoid Hemorrhage. *Front Cel Neurosci* 15, 739506. doi:10.3389/fncel.2021.739506

Wu, H. Y., Tang, Y., Gao, L. Y., Sun, W. X., Hua, Y., Yang, S. B., et al. (2014). The Synergetic Effect of Edaravone and Borneol in the Rat Model of Ischemic Stroke. *Eur. J. Pharmacol.* 740, 522–531. doi:10.1016/j.ejphar.2014.06.035

Wu, S., Sena, E., Egan, K., Macleod, M., and Mead, G. (2014). Edaravone Improves Functional and Structural Outcomes in Animal Models of Focal Cerebral Ischemia: a Systematic Review. *Int. J. Stroke* 9 (1), 101–106. doi:10.1111/ijs.12163

Xu, J., Wang, A., Meng, X., Yalkun, G., Xu, A., Gao, Z., et al. (2021). Edaravone Dexborneol versus Edaravone Alone for the Treatment of Acute Ischemic Stroke: A Phase III, Randomized, Double-Blind, Comparative Trial. *Stroke* 52 (3), 772–780. doi:10.1161/STROKEAHA.120.031197

Xu, J., Wang, Y., Wang, A., Gao, Z., Gao, X., Chen, H., et al. (2019). Safety and Efficacy of Edaravone Dexborneol versus Edaravone for Patients with Acute Ischaemic Stroke: a Phase II, Multicentre, Randomised, Double-Blind, Multiple-Dose, Active-Controlled Clinical Trial. *Stroke Vasc. Neurol.* 4 (3), 109–114. doi:10.1136/svn-2018-000221

Yang, Y., Chen, S., and Zhang, J. M. (2017). The Updated Role of Oxidative Stress in Subarachnoid Hemorrhage. *Curr. Drug Deliv.* 14 (6), 832–842. doi:10.2174/1567201813666161025115531

Zhang, C., Jiang, M., Wang, W. Q., Zhao, S. J., Yin, Y. X., Mi, Q. J., et al. (2020). Selective mGluR1 Negative Allosteric Modulator Reduces Blood-Brain Barrier Permeability and Cerebral Edema after Experimental Subarachnoid Hemorrhage. *Transl Stroke Res.* 11 (4), 799–811. doi:10.1007/s12975-019-00758-z

Zhang, X. M., Guo, L., Huang, X., Li, Q. M., and Chi, M. H. (2016). 4-Hydroxynonenal Regulates TNF-α Gene Transcription Indirectly via ETS1 and microRNA-29b in Human Adipocytes Induced from Adipose Tissue-Derived Stromal Cells. *Anat. Rec. (Hoboken)* 299 (8), 1145–1152. doi:10.1002/ar.23371

Zhuang, K., Zuo, Y. C., Sherchan, P., Wang, J. K., Yan, X. X., and Liu, F. (2019). Hydrogen Inhalation Attenuates Oxidative Stress Related Endothelial Cells Injury after Subarachnoid Hemorrhage in Rats. *Front. Neurosci.* 13, 1441. doi:10.3389/fnins.2019.01441

Conflict of Interest: The authors declare that the research was conducted in the absence of any commercial or financial relationships that could be construed as a potential conflict of interest.

Publisher's Note: All claims expressed in this article are solely those of the authors and do not necessarily represent those of their affiliated organizations, or those of the publisher, the editors, and the reviewers. Any product that may be evaluated in this article, or claim that may be made by its manufacturer, is not guaranteed or endorsed by the publisher.

frontiers | Frontiers in Pharmacology

ORIGINAL RESEARCH
published: 28 April 2022
doi: 10.3389/fphar.2022.903235

Coeloglossum viride Var. *Bracteatum* Extract Attenuates MPTP-Induced Neurotoxicity *in vivo* by Restoring BDNF-TrkB and FGF2-Akt Signaling Axis and Inhibiting RIP1-Driven Inflammation

Xiu-Yuan Lang[1†], *Yang Hu*[1†], *Jin-Peng Bai*[1], *Jun Wang*[1], *Xiao-Yan Qin*[1*] *and Rongfeng Lan*[2*]

[1]*Key Laboratory of Ecology and Environment in Minority Areas National Ethnic Affairs Commission, Center on Translational Neuroscience, College of Life and Environmental Sciences, Minzu University of China, Beijing, China,* [2]*Department of Cell Biology and Medical Genetics, School of Basic Medical Sciences, Shenzhen University Health Science Center, Shenzhen, China*

OPEN ACCESS

Edited by:
Rui Liu,
Chinese Academy of Medical Sciences, China

Reviewed by:
Hongguang Li,
Wuyi University, China
Jiang Lijun,
Central China Normal University, China

***Correspondence:**
Xiao-Yan Qin
bjqinxiaoyan@muc.edu.cn
Rongfeng Lan
lan@szu.edu.cn

[†]*These authors have contributed equally to this work*

Specialty section:
This article was submitted to Neuropharmacology, a section of the journal Frontiers in Pharmacology

Received: *24 March 2022*
Accepted: *13 April 2022*
Published: *28 April 2022*

Citation:
Lang X-Y, Hu Y, Bai J-P, Wang J, Qin X-Y and Lan R (2022) Coeloglossum viride Var. Bracteatum Extract Attenuates MPTP-Induced Neurotoxicity in vivo by Restoring BDNF-TrkB and FGF2-Akt Signaling Axis and Inhibiting RIP1-Driven Inflammation. Front. Pharmacol. 13:903235. doi: 10.3389/fphar.2022.903235

The tuber of *Coeloglossum viride* var. *bracteatum* is a Tibetan medicine that has been used for generations as a tonic for Yang and Qi, tranquilizing, to enhance intelligence and to promote longevity. We have previously characterized the constituents of *Coeloglossum viride* var. *bracteatum* extract (CE) and investigated its anti-Alzheimer's disease (AD) effect in mice models. However, the exact role of CE in Parkinson's disease (PD), especially the neurotrophic and inflammatory pathways regulated by CE, remains unknown. In this study, we investigated the anti-PD effects of CE in an MPTP-induced acute mouse model and its underlying mechanisms, focusing on BDNF, FGF2 and their mediated signaling pathways and RIP1-driven inflammatory signaling axis. Pole test and traction test were performed for behavioral analysis. RT-PCR, IHC and Western blotting were performed to assay the mRNA, tissues, and protein, respectively. We found that CE improved dyskinesia in MPTP-intoxicated mice, which was confirmed by the pole test and traction test. Also, oxidative stress and astrocyte activation and inflammation were alleviated. MPTP-intoxication disrupted the levels of BDNF, FGF2 and their mediated signaling pathways, triggered elevation of pro-inflammatory factors such as TNF-α, IL-1β, and IL-6, and activated RIP1-driven inflammatory axis. However, CE restored the levels of BDNF, FGF2 and TrkB/Akt signaling pathways while inhibiting the RIP1-driven inflammatory signaling axis, thereby inhibiting apoptosis, preventing loss of nigrostriatal neurons, and maintaining cellular homeostasis. Thus, CE is a promising agent for the treatment of PD.

Keywords: BDNF, LC-3, Parkinson's disease, RIP1, TBK1

Abbreviations: BDNF, brain-derived neurotrophic factor; CE, Coeloglossum viride var. bracteatum extract; FGF2, fibroblast growth factor 2; IL-6, interleukin-6; IL-1β, interleukin-1β; MDA, malondialdehyde; MLKL, Mixed lineage kinase domain-like protein; MPTP, 1-methyl-4-phenyl-1, 2, 3, 6-tetrahydropyridine; PD, Parkinson's disease; RIP1, receptor-interacting serine/threonine-protein kinase 1; RIP3, receptor-interacting serine/threonine-protein kinase 3; SOD, superoxide dismutase; T-AOC, total antioxidant capacity; TBK1, TANK-binding kinase 1; TH, tyrosine hydroxylase; TNF-α, tumor necrosis factor alpha.

INTRODUCTION

The tuber of *Coeloglossum viride* var. *bracteatum* is a traditional Tibetan medicine used to strengthen the Yang and Qi, to treat impotence and bronchial asthma (Shang et al., 2017). It has long been used as a tonic for cough, kidney asthenia and dyspnea in Asian countries such as China and Nepal, and is documented in the classical Tibetan medical classics "Si Bu Yi Dian" and "Jing Zhu Ben Cao" (Udo-Gendaan-Gompo, 1983; Dilma-Tenzin-Phuntsok, 2012). The preparations using *Coeloglossum viride* var. *bracteatum* extract (CE) as the main ingredient, such as "Shi Wei Shou Shen San", "Fu Fang Shou Shen Wan", have been approved by the State Medical Products Administration of China (https://www.nmpa.gov.cn) and are listed in the Chinese Pharmacopeia. We have previously identified the composition of CE and demonstrated its neuroprotective effects in $AlCl_3$/Gal-induced cognitive impairment or 5xFAD Alzheimer's disease mouse models (Zhong et al., 2019; Cai et al., 2021; Li et al., 2021). CE exerts a large number of antioxidant, anti-aging and anti-inflammatory properties and has no auto-toxicity, thus a potential drug for the treatment of neurodegenerative diseases (Shang et al., 2017). CE is mainly composed of a large number of glycosides, such as Militarine, Dactylorhin A, Dactylorhin B, Loroglossin, and Coelovirin A and so on. Increasing evidence suggests that the mechanism of CE activity depends on attenuating oxidative stress and inflammation and enhancing the activity of neurotrophic factors, including BDNF, FGF2, etc. and their regulated downstream signaling pathways, such as PI3K-Akt/Bcl-2, and Erk1/2 (Shang et al., 2017; Li et al., 2022). In contrast, glial cell activation and the typical inflammatory process they mediate and the subsequent release of pro-inflammatory factors such as TNF-α, IL-1β, and IL-6 are inhibited by CE. As a result, neuronal apoptosis is inhibited and the cellular homeostasis of the central nervous system (CNS) is maintained. Indeed, we have previously investigated the anti-PD and antidepressant effects of 2,3,5,4′-tetrahydoxystilbene-2-O-β-D-glucoside (THSG) in cultured cells and MPTP-induced PD mouse models as well as in mice with chronic stress-induced depression (Yu et al., 2019; Li et al., 2020). THSG is a potent agent that increases activity of FGF2 and BDNF levels and their downstream signaling pathways in the CNS. THSG inhibits apoptosis and promotes cell survival, thereby improving dyskenesia in PD mouse models.

MPTP (1-methyl-4-phenyl-1, 2, 3, 6-tetrahydropyridine) is non-toxic and permeable and accumulates in the CNS after crossing the blood-brain barrier, especially in astrocytes, where it is metabolized to toxic 1-methyl-4-phenylpyridinium (MPP+). MPP + then destroys dopaminergic neurons in the substantia nigra and striatum, leading to permanent PD-like symptoms (Dauer and Przedborski, 2003). Indeed, the loss of mesencephalic dopaminergic neurons is the most remarkable feature of PD pathogenesis and of the MPTP-induced murine models. Tyrosine hydroxylase (TH), the rate-limiting enzyme of catecholamine biosynthesis (Dauer and Przedborski, 2003; Battaglia et al., 2006), directly regulates levodopa biosynthesis, especially in dopaminergic neurons, and thus it can be used as a marker to monitor nigrostriatal damage. BDNF is a neurtrophic factor of dopaminergic neurons that increases its survival (Hyman et al., 1991). Indeed, one hypothesis proposes that deficiencies of neurotrophins and other regulatory factors lead to neuronal atrophy and apoptosis, and that restoring the expression of these factors and their downstream signaling axes improves neuronal integrity and plasticity (Martinowich et al., 2007; Chen et al., 2016; Zhong et al., 2019). PI3K/Akt-Bcl-2 is the most prevalent signaling axis that maintains cell survival and is actually required for neuronal survival (Long et al., 2021). BDNF acts as an upstream trigger to activate Akt signaling and initiate signaling cascades by binding to the neurotrophic tyrosine kinase receptor TrkB. Thus, BDNF and its mediated signaling is a promising target for neurodegenerative diseases and drug development.

In this study, we investigate the anti-PD effects of CE in an MPTP-induced mouse model. The levels of BDNF, FGF2 and their associated signaling pathways, oxidative stress and glial cell activation-mediated inflammation and RIP1-driven inflammatory pathways were detected to verify the activity of CE as well as the underlying mechanisms.

MATERIALS AND METHODS

Animals

C57BL/6 mice (8–10 weeks, 20 g) were provided by Beijing Vital River Laboratory Animal Technology Co. Ltd. under license No. SCXK-2016-2002. Mice were provided with food and water ad libitum and maintained on a 12-h light/dark cycle. All procedures were performed in accordance with the National Institutes of Health Laboratory Animal Care and Use Guidelines (NIH Publication No. 80-23) and approved by Animal Care and Use Committee of Minzu University of China.

A total of 60 mice were randomly divided into six groups (n = 10) of Control, MPTP, MPTP +125 mg/kg Madopar, MPTP +5 mg/kg CE, MPTP +10 mg/kg CE, and MPTP +20 mg/kg CE. The acute mouse PD model was established as described (Jackson-Lewis and Przedborski, 2007). Briefly, MPTP (20 mg/kg) was administrated subcutaneously to the animals four times in 1 day (day 8). From day 1 to day 21, mice in the MPTP + CE and MPTP + Madopar groups received daily oral CE or Madopar, while mice in the control group received equal amounts of saline. Behavioral procedures were performed on days 7, 9 and 21. Finally, mice were anesthetized with 5% chloral hydrate (0.1 ml/g), perfused and dissected in the substantia nigra and striatum for further experiments.

CE and Chemicals

Coeloglossum viride var. *bracteatum* was identified, collected, and processed as previously described (Huang et al., 2004; Shang et al., 2017; Li et al., 2022). In this work, CE was prepared and its chemical composition was characterized according to previous methods (Cai et al., 2021; Li et al., 2021). In brief, the dried tubers of *Coeloglossum viride* var. *bracteatum* was extracted with 70% ethanol at reflux, then suspended in water and partitioned successively with petroleum ether, ethyl acetate, and n-butanol. The n-butanol extract was furthered purified by passing through a

HP-20 macroporous resin. The final product used in this study was characterized by a hydrosphere C18 column for the main components of CE, including Dactylorhin A, Dactylorhin B, Loroglossin, and Militarine (Cai et al., 2021). Madopar is a clinical anti-PD drug containing two active ingredients, levodopa (#S2176, Selleck) and benserazide (#S2453, Selleck) in a ratio of 4:1. MPTP was purchased from Sigma-Aldrich (#M0896).

Behavior Procedures

The Pole test was used to examine the locomotion and motor coordination in PD mice (Matsuura et al., 1997). A 25-mm diameter cork ball was secured to the top of a wooden pole (height 50 cm and diameter 1 cm) with gauze to prevent slippage. Mice were placed face up on top of the cork ball and tested for the time required to descend from the cork ball to the middle of the wooden pole and the time to descend from the middle to the ground. Trials completed within 3 s were scored three points; 3–6 s, two points; > 6 s, one point. Three trails were performed for each animal to obtain an average.

The traction test was used to measure muscle strength and equilibrium (Cryan et al., 2005). Mice are suspended by their front paws from a horizontal rope approximately 40–50 cm above the table to provide sufficient time and space for the animal to land. Duration time was recorded and scored according to the following criteria: 0–4 s, 0 point; 5–9 s, one point; 10–14 s, two points; 15–19 s, three points; 20–24 s, four points; 25–29 s, five points; and >30 s, six points.

Real-Time PCR

Total RNA was purified from substantia nigra using TRIzol reagent (#15596018, Ambion). First strand cDNAs were yielded from 2.0 μg RNA using EasyQuick RT MasterMix Kit (#CW 2019M, Cowin Bio.) and then diluted 1:10 in nuclease-free water for a 20 μl reaction. Quantitative PCR were performed in a Light Cycler 96 Real-Time PCR System (Roche) using 2x RealStar Green Fast Mixture (#A301-05, GenStar) containing primers for TNF-α, IL-1β, IL-6 and IL-10, respectively, for 20 μl reactions. Three replicates of each dilution were performed and five samples were examined.

Oxidative Stress Assay

The substantia nigra was isolated and resolved (~0.3 g) into 1.5 ml of distilled water at 4°C, and homogenates in a grinder (#SCENTZ-48, Ningbo Scientz Biotechnology Co., Ltd.) for 2 min, followed by centrifugation at 3,000 rpm for 10 min collection of the supernatant. Protein concentrations were determined by BCA assay (#P0011, Beyotime Biotechnology).

Total antioxidant capacity (T-AOC) (#A015-1-2), enzymatic activity of superoxide dismutase (T-SOD) (#A001-3-2), and the contents of malondialdehyde (MDA) (#A003-1-2) in substantia nigra were determined by spectrophotometer, and the kits were purchased from Nanjing Jiancheng Biological Engineering Research Institute, according to the manufacturer's instructions.

Immunohistochemistry

Mouse brains were fixed with 4% formaldehyde overnight at 4°C, rinsed with PBS, successively dehydrated with 10%, 20%, 30% sucrose solutions, embedded in optimized cryo-sectioning medium, sectioned, and placed onto poly-L-lysine coated slides. Sections were then incubated in 3% H_2O_2 for 15 min to inhibit endogenous peroxidases, washed 3 times with PBS, and incubated in blocking buffer (0.3% Triton-X-100, 5% serum in PBS) for 1 h. Sections were incubated with anti-tyrosine hydroxylase (1:200, #P40101) or GFAP (1:1,000, #16825-1-AP, Proteintech) antibodies overnight at 4°C. Subsequently, sections were incubated with HRP-labeled secondary antibody and signaled with 3, 3′-diaminobenzidine (DAB) as a substrate. After mounting on glass slides, sections were successively dehydrated in ethanol (50%, 75%, 85%, 95% and 100%), washed with xylene and coated with resinene. Microscopic imaging of TH or GFAP-positive cells was performed and the number of cells per image was manually counted by marking points in the software Image-Pro Plus 6.0 (Media Cybernetics, Inc.) (Battaglia et al., 2006). The number of cells was divided by the area of the image to obtain the number of cells per square millimeters.

Western Blotting

Proteins were extracted from the substantia nigra and corpus striatum using RIPA lysis buffer (#P0013B, Beyotime Biotechnology). After measuring protein concentrations using the BCA assay (#P0011, Beyotime Biotechnology), equal amounts of protein from each sample were separated by SDS-PAGE gels and transferred to a nitrocellulose membranes. After blocking with 5% skim milk for 1 h at room temperature, the membranes were incubated separately with primary antibodies. Primary antibodies specific for Akt (#AF0045), phospho-Akt (Ser473) (#AF1546), Erk1/2 (#AF1051), phosphor-Erk1 (Thr202/Tyr204)/Erk2 (Thr185/Tyr187) (#AF 1891), Bcl-2 (#AF0060), β-actin (#AF0003), phosphor-TrkB (Tyr817) (#AF 1963) and RIP3 (#AF7893) were provided by Beyotime Biotechnology. Anti BDNF (#47808), TrkB (#4603), cleaved-Caspase-3 (#9664), TBK1 (#3504), phosphor-TBK1 (#5483), RIP1 (#3493), phospho-RIP1 (Ser166) (#31122) antibodies were provided by Cell Signaling Technology, Inc. Anti LC-3 (#bs-8878R), Beclin1 (#bs-1353R) and tyrosine hydroxylase (TH) (#bs-0016R) antibodies were provided by Beijing Biosynthesis Biotechnology. Anti GFAP (#16825-1-AP), MAP2 (#17490-1-AP) and MLKL (#21066-1-AP) were purchased from Proteintech Group, Inc. Anti FGF2 antibody (#sc-136255) was purchased from Santa Cruz Biotechnology and anti phospho-MLKL (#MABC1158) was purchased from Sigma-Aldrich. WB images were captured by an Odyssey CLx infrared fluorescence imaging system (LI-COR Biosciences). The optical density of the protein band was quantified by ImageJ software and normalized to β-actin.

Statistical Analysis

Data were showed as mean ± s.e.m and plotted in GraphPad Prism 8.0 software. One-way ANOVA (analysis of variance) was used to determine statistical significance between groups, followed by Dunnett's multiple comparisons test. For non-parametric tests, the Mann-Whitney test was applied. *, **, and *** denote $p < 0.05$, $p < 0.01$, or $p < 0.001$, respectively.

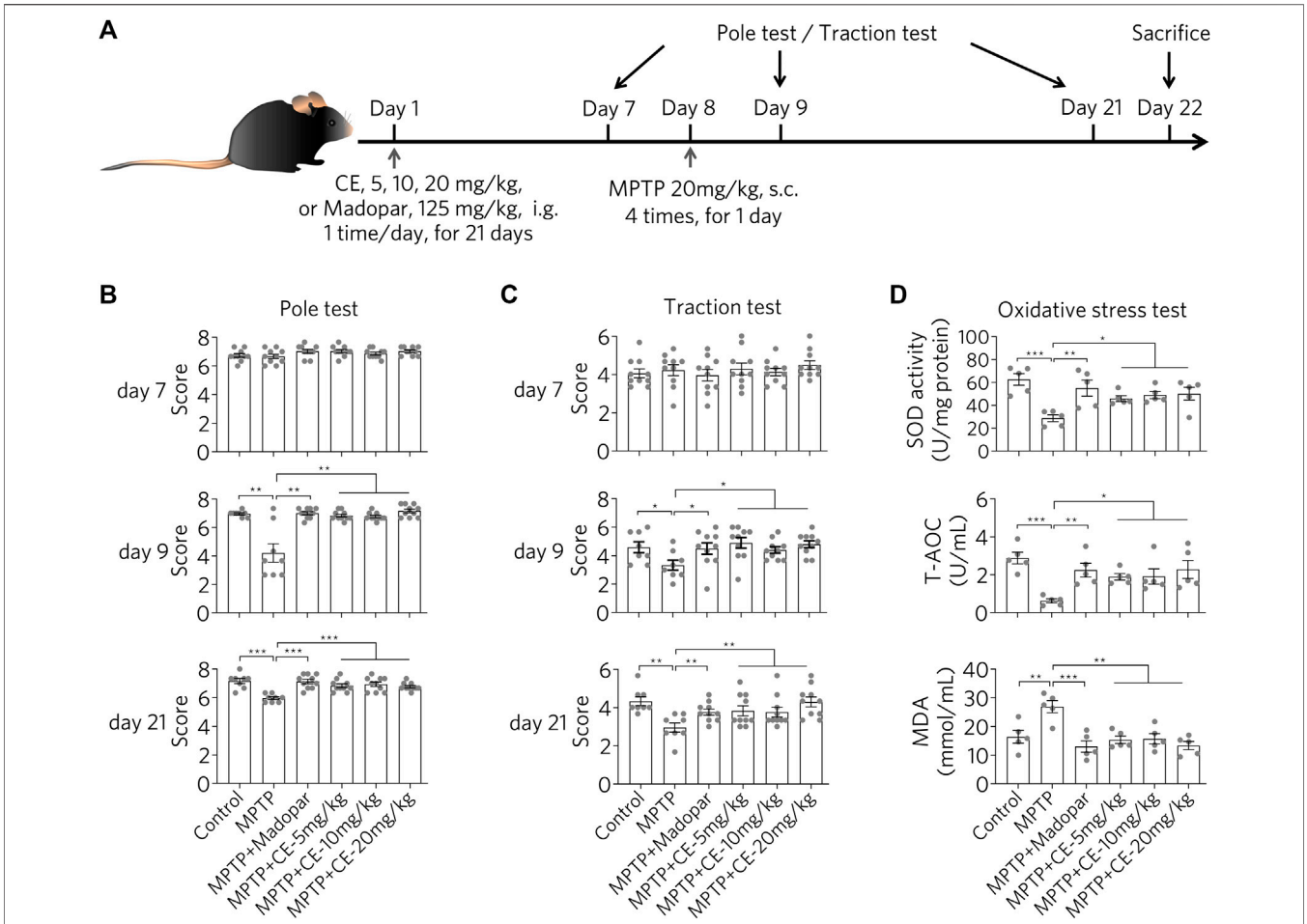

FIGURE 1 | CE attenuates MPTP-induced neurotoxicity in mice. **(A)** Experimental flow of the MPTP-induced PD mouse model. **(B,C)** Behavioral analyses were performed at days 7, 9 and 21, including the pole test and traction test. Non-parametric analyses were determined by Mann-Whitney test, $n = 10$. **(D)** CE attenuates oxidative stress and promotes MDA clearance in substantia nigra. One-way ANOVA with post hoc Dunnett's test, $n = 5$.

RESULTS

CE Attenuates MPTP-Induced Neurotoxicity and Improves Dyskinesia in Mice

After injection of parkinsonian toxin MPTP (20 mg/kg, 4 times in 1 day), C57BL/6 mice exhibited motor deficits as determined by the pole test and traction test (**Figure 1A**), as MPTP-intoxicated mice received significantly fewer scores in behavioral analysis (**Figures 1B,C**, MPTP). In contrast, mice in the control and CE- or Madopar-treated groups showed resistance to MPTP-induced toxicity, as they scored similarly in the test (**Figures 1B,C**, MPTP + CE or MPTP + Madopar). Thus, CE was able to protect mice from the toxicity of MPTP. In addition, MPTP induced oxidative stress in the brain as total antioxidant capacity (T-AOC) and SOD decreased significantly, corresponding to the increase in the peroxidation product MDA (**Figure 1D**, MPTP). However, the decrease in T-AOC and SOD was alleviated by CE or Madopar treatment and facilitated the clearance of MDA (**Figure 1D**), so that the redox state returned to normal compared to the control. Taken together, CE attenuates MPTP-induced toxicity as well as oxidative effects and maintains its physiological function.

CE Prevents the Loss of Dopaminergic Neurons in MPTP-Induced PD Mouse Model

Loss of dopaminergic neurons in the substantia nigra and striatum is the most characteristic feature of PD. IHC staining was performed using an antibody specific for TH to identify dopaminergic neurons in nigrostriatal sections (**Figure 2**). In MPTP-induced PD mice, the signal of dopaminergic neurons was remarkably reduced (**Figure 2A**, MPTP), while dopaminergic neurons were normally aligned in a dovetail shape, which was observed in both control and CE or Madopar treatment groups (**Figure 2A**, MPTP + CE or MPTP + Madopar). Likewise, the counts of dopaminergic neuron numbers on IHC sections confirmed the MPTP-induced reduction and CE- or Madopar-mediated recovery (**Figure 2B**). Furthermore, protein levels of TH were determined by Western blotting. As shown in

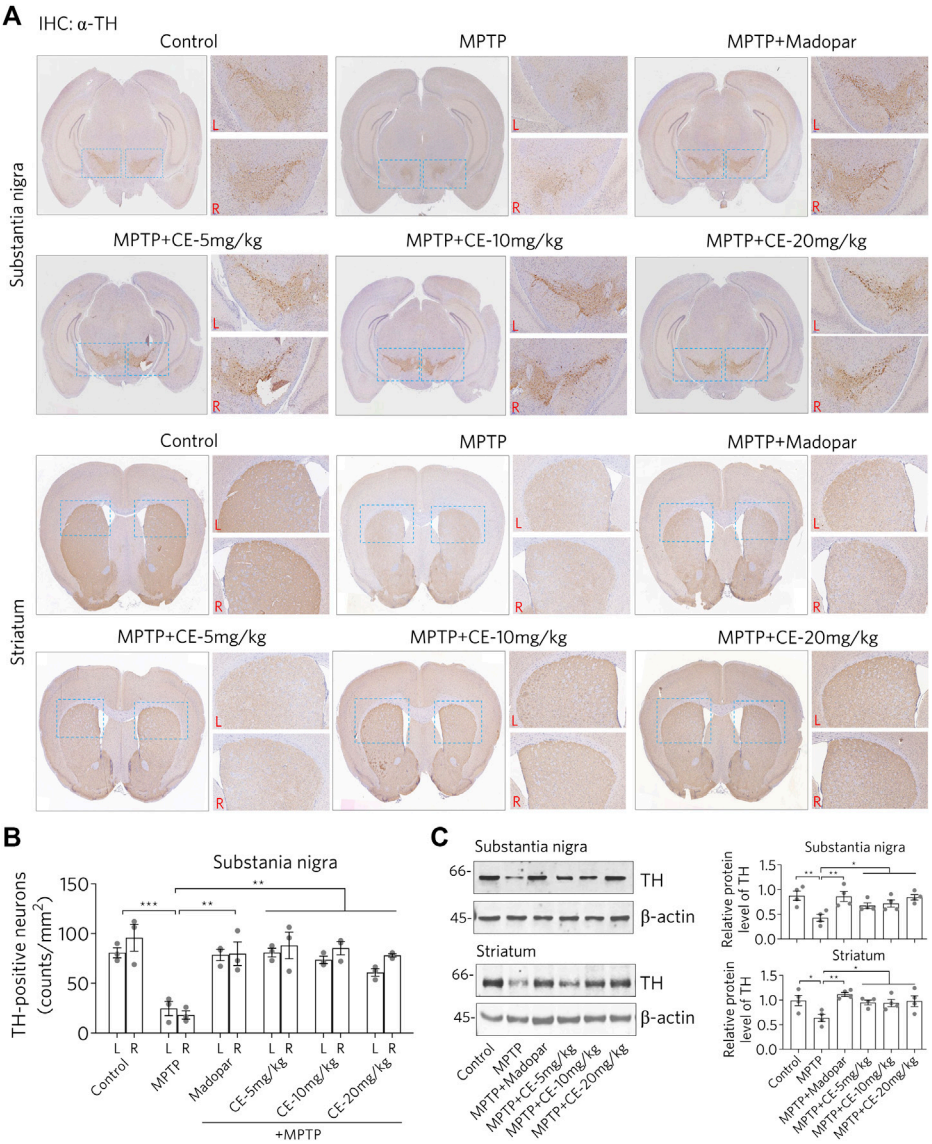

FIGURE 2 | CE attenuates MPTP-induced loss of dopaminergic neurons in substantia nigra and striatum. **(A)** IHC analysis of nigrostriatal TH-positive cells. Scale bar, 1 mm. L, left; R, right. Statistical differences between groups were calculated by one-way ANOVA and post hoc Dunnett's test, $n = 3$. **(B)** Counts of TH-positive cells. **(C)** Western blotting of TH protein. Relative protein levels were measured based on the density of blotted bands and normalized to β-actin. One-way ANOVA and post hoc Dunnett's test were performed to verify the significance of differences between groups, $n = 4$.

Figure 2C, TH was significantly reduced by MPTP treatment, but was rescued by CE- or Madopar-treatments. Therefore, CE was able to inhibit the loss of dopaminergic neurons induced by MPTP. In other words, the anti-PD effect of CE was similar to that of Madopar, a drug used clinically.

CE Attenuates MPTP-Induced Astrocyte Activation and Inflammation to Protect Neurons

As shown in **Figure 2**, MPTP leads to the loss of dopaminergic neurons, probably through apoptosis. Glial cells are activated when the damaged cells are processed. It was after injection of MPTP that we observed activation of astrocytes in the substantia nigra and striatum, as evidenced by IHC staining using an antibody specific for GFAP, a marker protein for astrocytes (**Figure 3A**, MPTP). However, the activation of astrocytes was attenuated under CE or Madopar treatment (**Figure 3A**, MPTP + CE or MPTP + Madopar). Changes in the number of GFAP-positive cells in the substantia nigra and striatum also confirmed the results of IHC staining, as CE or Madopar treatment attenuated the MPTP-induced increase in GFAP-positive cells (**Figure 3B**). In addition, the changes in GFAP-positive cells were replicated by Western blotting to detect GFAP protein (**Figure 3C**). In detail, the

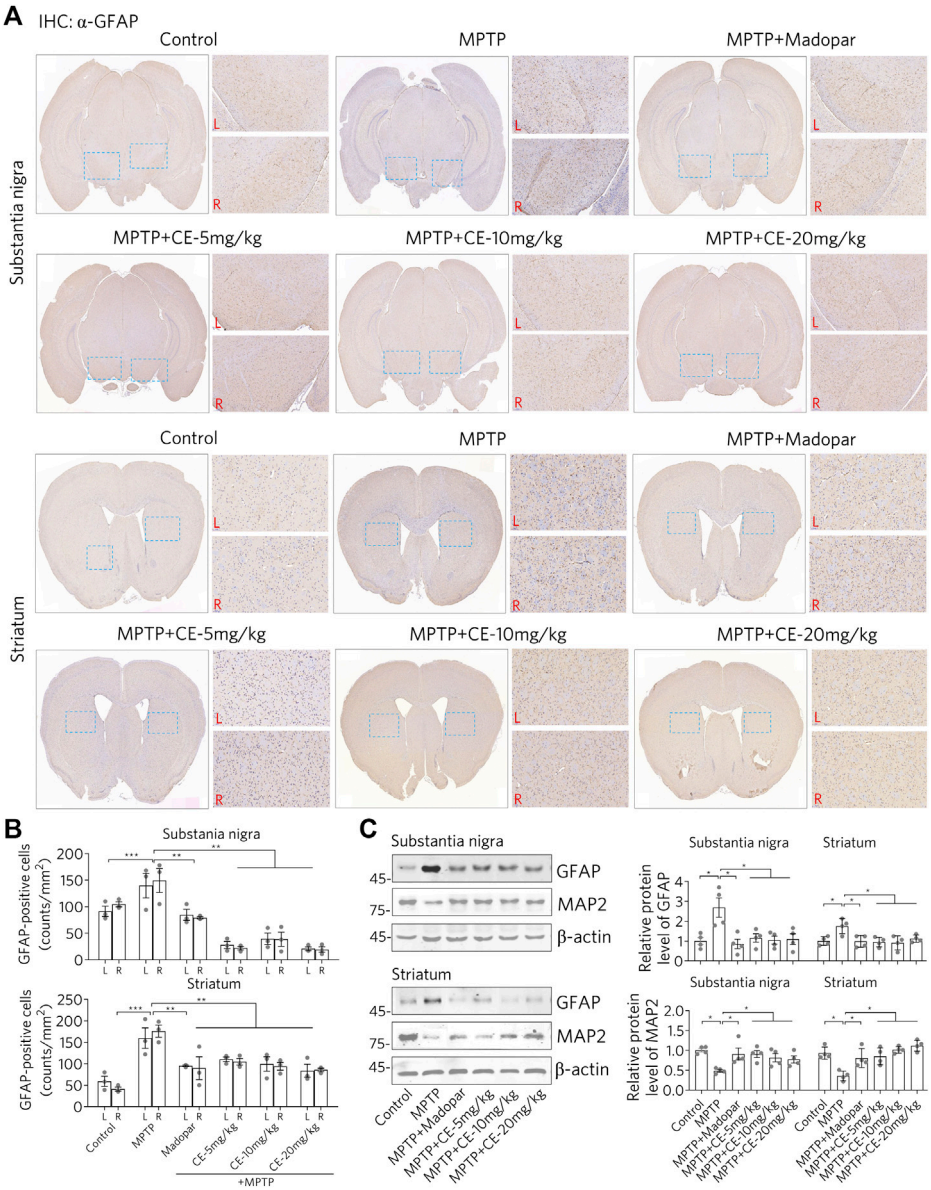

FIGURE 3 | CE attenuates astrocyte activation and protects neurons from MPTP-induced toxicity. **(A)** IHC staining of GFAP-positive cells in substantia nigra and striatum. **(B)** Counts of TH-positive cells, $n = 3$. **(C)** Western blotting of GFAP and MAP2 proteins. Relative protein levels were examined according to the density of blotted bands and normalized to β-actin, $n = 4$. One-way ANOVA, post hoc Dunnett's test was performed to verify the significance of differences between groups.

levels of GFAP protein in the substantia nigra and striatum were significantly increased after MTTP intoxication (**Figure 3C**, MPTP). The increase in GFAP protein levels was mitigated after treatment with CE or Madopar. In addition, the protein marker MAP2 in neurons showed antagonistic changes compared to GFAP, but consistent with changes in dopaminergic neurons. That is, the MPTP-induced decrease in MAP2 protein corresponded to the loss of dopaminergic neurons, whereas the recovery of MAP2 corresponded to the maintenance of dopaminergic neurons (**Figure 3C**, MAP2). Thus, CE prevents MPTP-induced nigrostriatal atrophy and maintains cellular homeostasis in the brain.

Consistent with the changes in astrocytes status, there was a corresponding response to typical pro-inflammatory factors (**Figure 4**). After MPTP-treatment, we observed increased mRNA and protein levels of TNF-α, IL-1β and IL-6 (**Figure 4**, MPTP). Interestingly, IL-10, an anti-inflammatory factor, was down regulated (**Figure 4**, MPTP column for IL-10). These results suggest that MPTP intoxication in the CNS triggers a pro-inflammatory response. However, under CE or Madopar treatment, increases in pro-inflammatory factors including TNF-α, IL-1β, and IL-6 were suppressed, while IL-10 was recovered (**Figure 4**, MPTP + CE or MPTP + Madopar). Thus, we conclude that CE attenuates MPTP-induced inflammation in the substantia nigra and striatum.

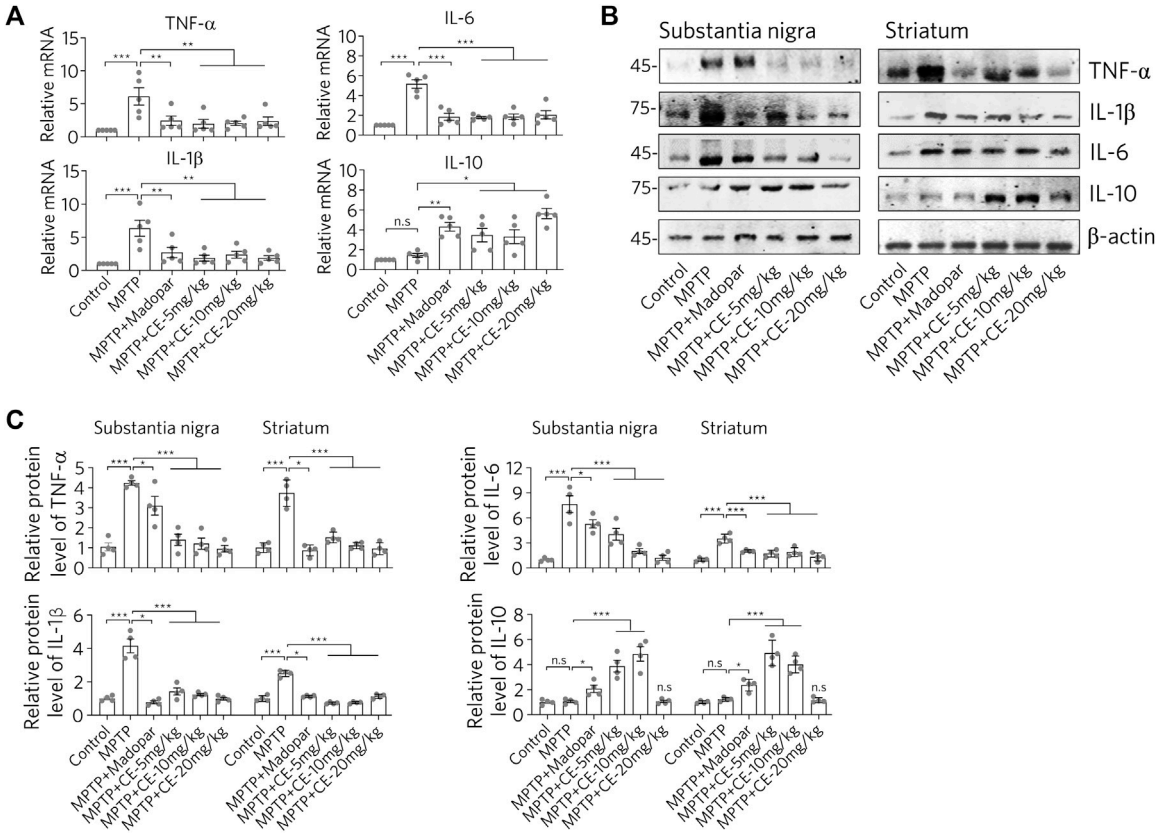

FIGURE 4 | CE restores elevated levels of pro-inflammatory factors. **(A)** RT-PCR determination of mRNA levels of pro-inflammatory factors in substantia nigra, n = 5. **(B)** Western blotting analysis of pro-inflammatory factors and anti-inflammatory factor IL-10. **(C)** Relative protein levels normalized to β-actin, n = 4. In A and C, one-way ANOVA followed by Dunnett's test were performed.

CE maintains the activity of the BDNF-TrkB and FGF2-Akt signaling pathways and inhibits apoptosis and autophagy, thereby attenuating MPTP-induced neurotoxicity.

We have previously shown that the FGF2-PI3K/Akt and BDNF-TrkB signaling pathways are required for neural survival and activity (Zhong et al., 2019). Therefore, we wanted to ask whether BDNF, FGF2 and their downstream signaling regulators are involved in CE-mediated anti-PD activity. In MPTP-intoxicated mice, we found significantly decreased protein levels of BDNF and FGF2 in the substantia nigra and striatum (**Figure 5A**, MPTP). Accordingly, the TrkB/Akt-Bcl-2 signaling pathway regulated by BDNF and FGF2 was inhibited. In detail, the active forms of TrkB and Akt indicating by their phosphorylation were reduced. Similar change was observed for Erk1/2, another kinase that regulates cell proliferation and apoptosis. In addition, the anti-apoptosis protein Bcl-2 was down regulated (**Figure 5A**, Bcl-2). In contrast, the active form of the apoptotic enzyme Caspase-3 (cleaved Casp-3) was increased (**Figure 5A**, cleaved-Casp-3). However, the BDNF-TrkB/Akt-Bcl-2 and Erk1/2 signaling pathways were restored under CE or Madopar treatment, as the aforementioned proteins were restored. In particular, the antagonistic change of Bcl-2/cleaved-Casp-3 clearly implied the inhibition of apoptosis (**Figure 5A**). The above changes were also confirmed by the relative protein levels calculated from the optical densities of the blotted bands (**Figure 5B**). In addition, we examined LC-3 and Beclin1, two proteins that are indicators of autophagy. We found that both LC-3 and Beclin1 increased after MPTP-intoxication (**Figure 5**, LC-3 and Beclin1). In other words, MPTP-induced atrophy of nigrostriatal neurons and induced the activity of autophagy, which may be required for the removal of damaged cells and substances. In contrast, CE or Madopar attenuated the increase in LC-3 and Beclin1, suggesting a restoration of cellular homeostasis. From these results, we found that CE was able to restore the levels of BDNF and FGF2, reactivate their downstream signaling axes, and inhibit apoptosis and autophagy. Also, BDNF-TrkB and FGF2-Akt signaling pathways are essential for CE-mediated anti-PD function.

CE Alleviates the RIP1-Driven Inflammatory Pathway in the MPTP-Induced PD Mice Model

Consistent with the typical inflammation mediated by glial cell activation and release of pro-inflammatory factors (**Figures 3**, **4**), we found that the RIP1-driven inflammatory pathway was also activated after MPTP-intoxication (**Figure 6A**, MPTP). In detail,

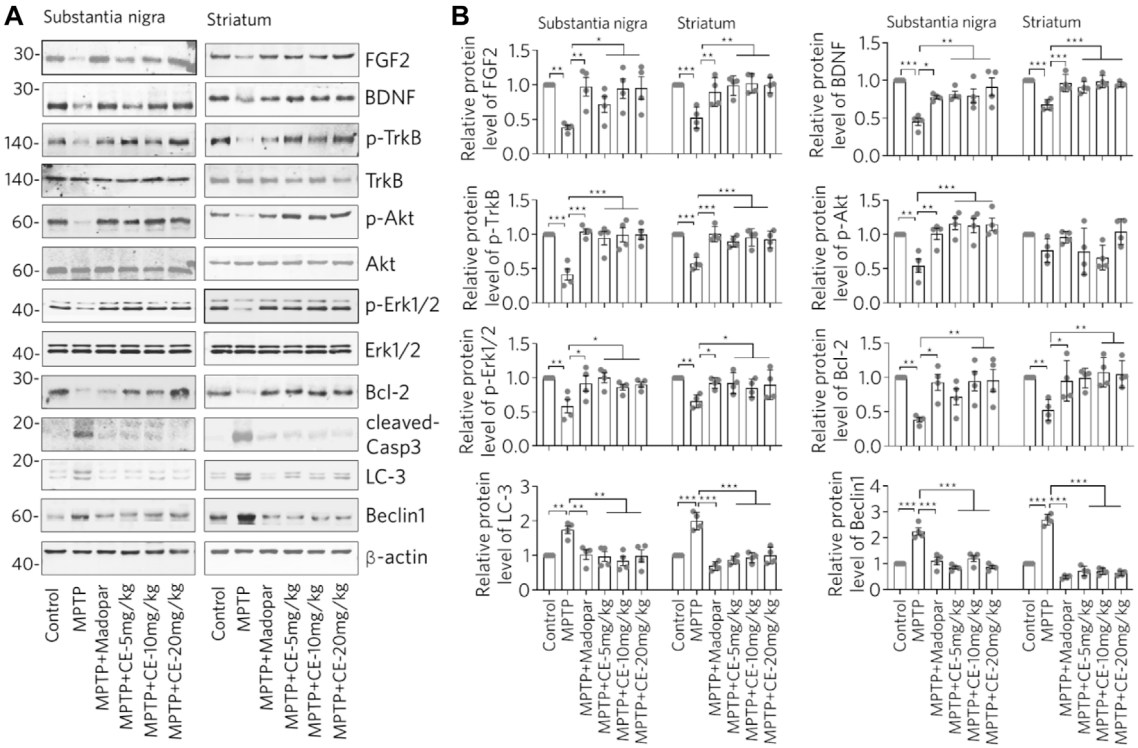

FIGURE 5 | CE maintains the BDNF-TrkB and FGF2-Akt signaling pathways and inhibits apoptosis and autophagy to attenuate MPTP-induced toxicity. **(A)** Western blotting analysis of BDNF, FGF2 and their mediated signaling pathways, as well as marker proteins for apoptosis and autophagy. **(B)** Relative protein levels were calculated from the density of blotted bands and normalized to β-actin. One-way ANOVA with post hoc Dunnett's test, $n = 4$.

RIP1, RIP3 and MLKL along with their phosphorylated forms, were increased with MPTP treatment, indicating activation. Correspondingly, TBK1, an endogenous inhibitor of RIP1 was reduced. Similar to the changes in the BDNF-TrkB/Akt signaling axis, TBK1 was recovered with the inhibition of RIP1/RIP3/MLKL by CE or Madopar treatment, and all three proteins were down regulated (**Figure 6A**, MPTP + CE or MPTP + Madopar). Computational and statistical analysis of protein band density confirmed the observed changes (**Figure 6B**). Thus, CE is able to inhibit RIP1-driven inflammatory pathway.

In summary, we explored the anti-PD effects of CE in an MPTP-induced mouse model (**Figure 6C**). The BDNF-TrkB and FGF2-Akt signaling axes are involved in inhibiting apoptosis and maintaining neuronal survival. After MPTP intoxication, BDNF and FGF2 were inhibited, while the TrkB/Akt signaling pathway is inactive, accompanied by apoptosis and RIP1-driven inflammation. In contrast, under CE treatment, the levels of BDNF and FGF2 and their regulated signaling pathways were restored, leading to inhibition of apoptosis and attenuation of inflammation.

DISCUSSION

Genetically or environmentally induced loss of nigrostriatal neurons in the brain is a major feature of PD pathology and has been confirmed in studies of MPTP-intoxicated mice (**Figures 2**, **3**). Maintenance of cellular homeostasis or rescue of neuronal loss should contribute to the treatment of PD. Currently, the treatment of PD is focused on controlling symptoms, delaying the progression of the disease and improving the quality of life of patients. Levodopa (L-3,4-dihydroxyphenylalanine, called levodopa), dopamine agonists, monoamine oxidase B inhibitors, and anticholinergic agents are commonly used to treat PD. Otherwise, cell transplantation is another approach to treat PD, where cells are injected into the substantia nigra in the hope of replacing the dopamine-producing neurons that have been lost (Chao et al., 2016). However, obtaining suitable transplanted cells and avoiding side effects are major obstacles that need further research. Moreover, natural products, especially medicinal plants used in ethnomedicine, have been accumulated and practiced for thousands of years, providing a rich resource for drug development, especially for drugs with good neuromodulatory activity that have been clinically and ethnically validated. In fact, we have previously demonstrated the antioxidant, anti-inflammatory, anti-aging and anti-AD effects of CE in cell-based *in vitro* and *in vivo* mouse models (Pan et al., 2017; Zhong et al., 2019; Li et al., 2021; Li et al., 2022). Thus, it is very useful to investigate the anti-PD effects of CE in this work. With reference to the establishment of experimental PD models, MPTP is a widely used and reused agent that induces the loss of dopaminergic neurons through its toxic metabolite MPP+ in the brain (Dauer and Przedborski, 2003). Therefore, we used the MPTP-induced PD model in mice to assess the anti-PD activity of CE. To investigate the protective effects of CE on nigrostriatal neurons, we focused on signaling pathways related to cell survival

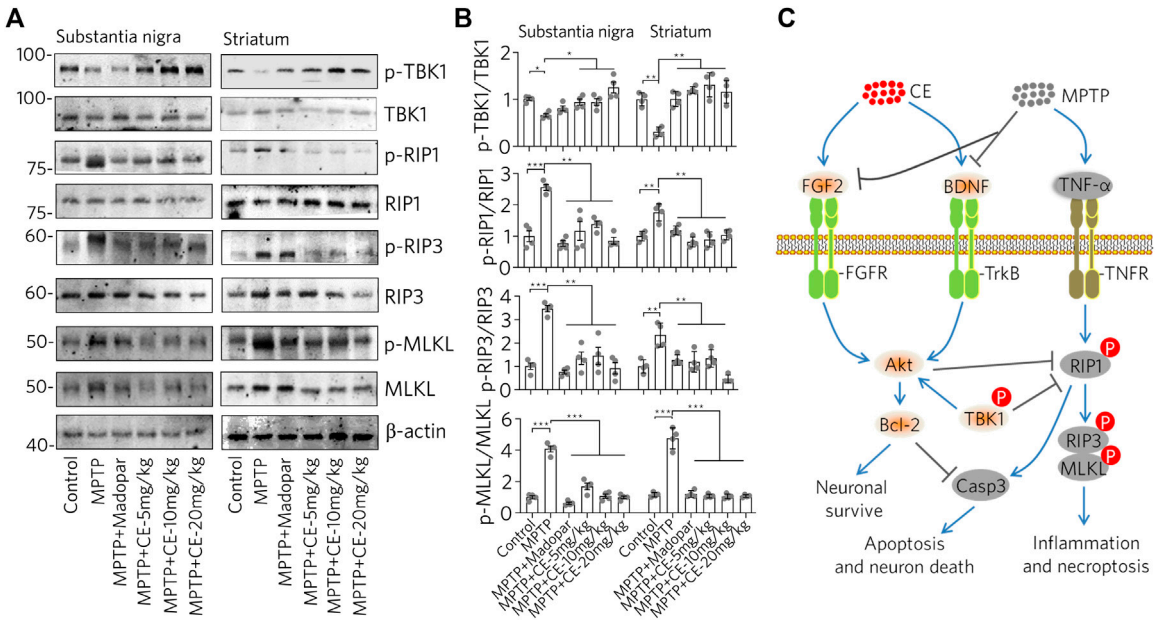

FIGURE 6 | CE inhibits the RIP1-driven inflammatory pathway triggered by MPTP-induced neurotoxicity. **(A)** Western blot of RIP1-driven inflammatory pathways in substantia nigra and striatum. **(B)** Statistical analysis of protein levels based on the blots in **(A)** and normalized to β-actin. One-way ANOVA wihtc Dunnett's test, $n = 4$. **(C)** Schematic representation of the anti-PD effects mediated by CE in a mouse model of MPTP-induced PD. In the brain, MPTP impaired the levels of BDNF, FGF2 and its regulated signaling pathways, as well as the RIP1-driven inflammatory pathway, leading to apoptosis of dopaminergic neurons. However, CE attenuated MPTP-induced toxicity and abnormalities in the above-mentioned signaling pathways to protect neurons.

and apoptosis, such as PI3K/Akt and Bcl-2/Caspase-3. Prevailing evidence supports the role of BDNF, FGF2 and its regulated TrkB/Akt, MAPK and PLC signaling axes in regulating neuronal survival and maintaining cellular homeostasis (Yoshii and Constantine-Paton, 2007; Franke, 2008). Consistently, insufficient expression of BDNF and impairment of the BDNF-TrkB signaling axis are frequently observed in AD, PD and even chronic stress-induced depression (Martinowich et al., 2007; Lu et al., 2013; Zhong et al., 2019). At the mechanistic level, the positive feedback loop of BDNF-TrkB signaling depends on CREB and C/EBPβ mediated-transcription, which is crucial for neuronal survival and synaptic plasticity (Bambah-Mukku et al., 2014; Kowianski et al., 2018). Indeed, we found in this work that MPTP-intoxication induced a significant reduction in BDNF, FGF2 and their related signaling axis, corresponding to the activation of apoptosis-related enzyme such as cleaved-Casp-3 and the reduction of anti-apoptotic protein Bcl-2 (**Figure 5**). In light of this, improving the pathological state of BDNF and the signaling pathways it regulates is a promise strategy for the pharmacological treatment of CNS diseases.

In addition, the inflammatory pathway is also in focus because it is a common phenomenon and pathology of the CNS. Glial cells including microglia and astrocytes are the most abundant cells in the CNS that respond to insults from intracellular or exogenous sources and remove damaged cells, plaques and toxic substances, thereby maintaining cellular homeostasis (Salter and Stevens, 2017). On the other hand, widespread activation of glial cells adversely affects neurons by releasing pro-inflammatory factors and free radicals, and even evokes inflammatory storms that lead to neuronal damage and cell death. Moreover, the RIP1-driven inflammatory pathway is the master signal that regulates the decision between promoting survival and cell death in response to a large number of stimuli. RIP1-mediated necroptosis is accomplished through the formation of the RIP1/RIP3/MLKL complex, which is regulated by cascade phosphorylation. RIP1 activation and necroptosis have been genetically and mechanistically linked to human neurodegenerative diseases (Mifflin et al., 2020). Indeed, we found activation of astrocytes and RIP1-driven inflammation after MPTP-intoxication. Conversely, CE or Madopar could alleviate the aforementioned inflammation and normalize the cellular state (**Figures 3**, **4**, **6**). Also, predictably, RIP1 inhibitors may be chemicals of interest for PD treatment by inhibiting RIP1-mediated inflammation, and the presence of inhibitors of RIP1 in CE is an interesting question. However, identifying the direct targets or molecules directly regulated by CE that then exert subsequent anti-PD activity remains a difficulty. This is mainly due to the fact that CE has multiple metabolites in the body and the exact molecule that interacts directly with CE-derived neurons in the CNS remains unidentified. Nevertheless, CE is effective to protect dopaminergic neurons from MPTP-induced toxicity and rescued motor deficits in mice. This also suggests that BDNF, FGF2 and their associated signaling pathways may be effective targets for drug design and PD treatment. Since CE has been used since ancient times and some medical products derived from CE are already available, it is important to validate the anti-PD effects of CE in PD patients in further studies. Thus, pharmacological treatment of CE may protect nigrostriatal neurons from MPTP-mediated toxicity and may pave a new pathway for BDNF, FGF2 and TrkB/Akt signaling axis as targets for the treatment of PD.

DATA AVAILABILITY STATEMENT

The original contributions presented in the study are included in the article/**Supplementary Material**, further inquiries can be directed to the corresponding authors.

ETHICS STATEMENT

The animal study was reviewed and approved by the Animal Care and Use Committee of Minzu University of China.

AUTHOR CONTRIBUTIONS

X-YL performed the experiments. YH analyzed the data and revised the materials and methods. J-PB assisted in making the animal models. JW performed the Western blots assay and analyzed the data. X-YQ designed the study and revised the paper. RL analyzed the data, performed the statistical analysis, made the graphs, and wrote and submitted the manuscript.

FUNDING

This work was supported by the National Natural Science Foundation of China (81873088, 82174085) and Shenzhen University Top-Ranking Project (86000000210).

SUPPLEMENTARY MATERIAL

The Supplementary Material for this article can be found online at: https://www.frontiersin.org/articles/10.3389/fphar.2022.903235/full#supplementary-material

REFERENCES

Bambah-Mukku, D., Travaglia, A., Chen, D. Y., Pollonini, G., and Alberini, C. M. (2014). A Positive Autoregulatory BDNF Feedback Loop via C/EBPβ Mediates Hippocampal Memory Consolidation. *J. Neurosci.* 34, 12547–12559. doi:10.1523/JNEUROSCI.0324-14.2014

Battaglia, G., Busceti, C. L., Molinaro, G., Biagioni, F., Traficante, A., Nicoletti, F., et al. (2006). Pharmacological Activation of mGlu4 Metabotropic Glutamate Receptors Reduces Nigrostriatal Degeneration in Mice Treated with 1-Methyl-4-Phenyl-1,2,3,6-Tetrahydropyridine. *J. Neurosci.* 26, 7222–7229. doi:10.1523/JNEUROSCI.1595-06.2006

Cai, Z. P., Cao, C., Guo, Z., Yu, Y., Zhong, S. J., Pan, R. Y., et al. (2021). Coeloglossum Viride Var. Bracteatum Extract Attenuates Staurosporine Induced Neurotoxicity by Restoring the FGF2-PI3K/Akt Signaling axis and Dnmt3. *Heliyon* 7, e07503. doi:10.1016/j.heliyon.2021.e07503

Chao, C., Jing, D., Aifang, S., Wei, F., Hao, S., Yanming, L., et al. (2016). Transplantation of Human Umbilical Cord Blood-Derived Mononuclear Cells Induces Recovery of Motor Dysfunction in a Rat Model of Parkinson's Disease. *J. Neurorestoratol*, 2016, 23–33. doi:10.2147/JN.S98835

Chen, T., Yang, Y. J., Li, Y. K., Liu, J., Wu, P. F., Wang, F., et al. (2016). Chronic Administration Tetrahydroxystilbene Glucoside Promotes Hippocampal Memory and Synaptic Plasticity and Activates ERKs, CaMKII and SIRT1/miR-134 *In Vivo*. *J. Ethnopharmacol* 190, 74–82. doi:10.1016/j.jep.2016.06.012

Cryan, J. F., Mombereau, C., and Vassout, A. (2005). The Tail Suspension Test as a Model for Assessing Antidepressant Activity: Review of Pharmacological and Genetic Studies in Mice. *Neurosci. Biobehav. Rev.* 29, 571–625. doi:10.1016/j.neubiorev.2005.03.009

Dauer, W., and Przedborski, S. (2003). Parkinson's Disease: Mechanisms and Models. *Neuron* 39, 889–909. doi:10.1016/s0896-6273(03)00568-3

Dilma-Tenzin-Phuntsok (2012). *Jing Zhu Ben Cao*. Shanghai: Shanghai Scientific and Technical Publishers.

Franke, T. F. (2008). PI3K/Akt: Getting it Right Matters. *Oncogene* 27, 6473–6488. doi:10.1038/onc.2008.313

Huang, S. Y., Li, G. Q., Shi, J. G., and Mo, S. Y. (2004). Chemical Constituents of the Rhizomes of Coeloglossum Viride Var. Bracteatum. *J. Asian Nat. Prod. Res.* 6, 49–61. doi:10.1080/1028602031000119826

Hyman, C., Hofer, M., Barde, Y. A., Juhasz, M., Yancopoulos, G. D., Squinto, S. P., et al. (1991). BDNF Is a Neurotrophic Factor for Dopaminergic Neurons of the Substantia Nigra. *Nature* 350, 230–232. doi:10.1038/350230a0

Jackson-Lewis, V., and Przedborski, S. (2007). Protocol for the MPTP Mouse Model of Parkinson's Disease. *Nat. Protoc.* 2, 141–151. doi:10.1038/nprot.2006.342

Kowianski, P., Lietzau, G., Czuba, E., Waskow, M., Steliga, A., and Morys, J. (2018). BDNF: a Key Factor with Multipotent Impact on Brain Signaling and Synaptic Plasticity. *Cell Mol. Neurobiol.* 38, 579–593. doi:10.1007/s10571-017-0510-4

Li, X.-X., Cai, Z.-P., Lang, X.-Y., Pan, R.-Y., Ren, T.-T., Lan, R., et al. (2021). Coeloglossum Viride Var. Bracteatum Extract Improves Cognitive Deficits by Restoring BDNF, FGF2 Levels and Suppressing RIP1/RIP3/MLKL-Mediated Neuroinflammation in a 5xFAD Mouse Model of Alzheimer's Disease. *J. Funct. Foods* 85, 104612. doi:10.1016/j.jff.2021.104612

Li, X. X., Lang, X. Y., Ren, T. T., Wang, J., Lan, R., and Qin, X. Y. (2022). Coeloglossum Viride Var. Bracteatum Extract Attenuates Aβ-Induced Toxicity by Inhibiting RIP1-Driven Inflammation and Necroptosis. *J. Ethnopharmacol.* 282, 114606. doi:10.1016/j.jep.2021.114606

Li, X. X., Yu, Y., Lang, X. Y., Jiang, C. Y., Lan, R., and Qin, X. Y. (2020). 2,3,5,4'-Tetrahydroxystilbene-2-O-β-d-glucoside Restores BDNF-TrkB and FGF2-Akt Signaling Axis to Attenuate Stress-Induced Depression. *Neuroscience* 430, 25–33. doi:10.1016/j.neuroscience.2020.01.025

Long, H. Z., Cheng, Y., Zhou, Z. W., Luo, H. Y., Wen, D. D., and Gao, L. C. (2021). PI3K/AKT Signal Pathway: a Target of Natural Products in the Prevention and Treatment of Alzheimer's Disease and Parkinson's Disease. *Front. Pharmacol.* 12, 648636. doi:10.3389/fphar.2021.648636

Lu, B., Nagappan, G., Guan, X., Nathan, P. J., and Wren, P. (2013). BDNF-based Synaptic Repair as a Disease-Modifying Strategy for Neurodegenerative Diseases. *Nat. Rev. Neurosci.* 14, 401–416. doi:10.1038/nrn3505

Martinowich, K., Manji, H., and Lu, B. (2007). New Insights into BDNF Function in Depression and Anxiety. *Nat. Neurosci.* 10, 1089–1093. doi:10.1038/nn1971

Matsuura, K., Kabuto, H., Makino, H., and Ogawa, N. (1997). Pole Test Is a Useful Method for Evaluating the Mouse Movement Disorder Caused by Striatal Dopamine Depletion. *J. Neurosci. Methods* 73, 45–48. doi:10.1016/s0165-0270(96)02211-x

Mifflin, L., Ofengeim, D., and Yuan, J. (2020). Receptor-interacting Protein Kinase 1 (RIPK1) as a Therapeutic Target. *Nat. Rev. Drug Discov.* 19, 553–571. doi:10.1038/s41573-020-0071-y

Pan, R. Y., Ma, J., Wu, H. T., Liu, Q. S., Qin, X. Y., and Cheng, Y. (2017). Neuroprotective Effects of a Coeloglossum Viride Var. Bracteatum Extract *In Vitro* and *In Vivo*. *Sci. Rep.* 7, 9209. doi:10.1038/s41598-017-08957-0

Salter, M. W., and Stevens, B. (2017). Microglia Emerge as central Players in Brain Disease. *Nat. Med.* 23, 1018–1027. doi:10.1038/nm.4397

Shang, X., Guo, X., Liu, Y., Pan, H., Miao, X., and Zhang, J. (2017). Gymnadenia Conopsea (L.) R. Br.: a Systemic Review of the Ethnobotany, Phytochemistry, and Pharmacology of an Important Asian Folk Medicine. *Front. Pharmacol.* 8, 24. doi:10.3389/fphar.2017.00024

Udo-Gendaan-Gompo (1983). *Si Bu Yi Dian*. Beijing: People's Health Publishing House.

Yoshii, A., and Constantine-Paton, M. (2007). BDNF Induces Transport of PSD-95 to Dendrites through PI3K-AKT Signaling after NMDA Receptor Activation. *Nat. Neurosci.* 10, 702–711. doi:10.1038/nn1903

Yu, Y., Lang, X. Y., Li, X. X., Gu, R. Z., Liu, Q. S., Lan, R., et al. (2019). 2,3,5,4'-Tetrahydroxystilbene-2-O-β-d-glucoside Attenuates MPP+/MPTP-induced Neurotoxicity *In Vitro* and *In Vivo* by Restoring the BDNF-TrkB and FGF2-Akt Signaling axis and Inhibition of Apoptosis. *Food Funct.* 10, 6009–6019. doi:10.1039/c9fo01309a

Zhong, S.-J., Wang, L., Wu, H.-T., Lan, R., and Qin, X.-Y. (2019). Coeloglossum Viride Var. Bracteatum Extract Improves Learning and Memory of Chemically-Induced Aging Mice through Upregulating Neurotrophins BDNF and FGF2 and Sequestering Neuroinflammation. *J. Funct. Foods* 57, 40–47. doi:10.1016/j.jff.2019.03.045

Conflict of Interest: The authors declare that the research was conducted in the absence of any commercial or financial relationships that could be construed as a potential conflict of interest.

Publisher's Note: All claims expressed in this article are solely those of the authors and do not necessarily represent those of their affiliated organizations, or those of the publisher, the editors and the reviewers. Any product that may be evaluated in this article, or claim that may be made by its manufacturer, is not guaranteed or endorsed by the publisher.

frontiers | Frontiers in Pharmacology

ORIGINAL RESEARCH
published: 29 April 2022
doi: 10.3389/fphar.2022.902796

DAPT Attenuates Cadmium-Induced Toxicity in Mice by Inhibiting Inflammation and the Notch/HES-1 Signaling Axis

Jia-Ying Yang[1], Dan-Yang Shen[1], Jun Wang[1], Jing-Feng Dai[1], Xiao-Yan Qin[1], Yang Hu[1] and Rongfeng Lan[2]**

[1]Key Laboratory of Ecology and Environment in Minority Areas National Ethnic Affairs Commission, Center for Translational Neuroscience, College of Life and Environmental Sciences, Minzu University of China, Beijing, China, [2]Department of Cell Biology and Medical Genetics, School of Basic Medical Sciences, Shenzhen University Health Science Center, Shenzhen, China

The small molecule DAPT inhibits the Notch signaling pathway by blocking γ-secretase mediated Notch cleavage. Given the critical role of the Notch signaling axis in inflammation, we asked whether DAPT could block Notch-mediated inflammation and thus exert neuronal protection. We established a mouse model of chronic exposure to cadmium (Cd)-induced toxicity and treated it with DAPT. DAPT was effective in ameliorating Cd-induced multi-organ damage and cognitive impairment in mice, as DAPT restored abnormal performance in the Y-maze, forced swimming and Morris water maze (MWM) tests. DAPT also reversed Cd-induced neuronal loss and glial cell activation to normal as observed by immunofluorescence and immunohistochemistry of brain tissue sections. In addition, Cd-intoxicated mice showed significantly increased levels of the Notch/HES-1 signaling axis and NF-κB, as well as decreased levels of the inflammatory inhibitors C/EBPβ and COP1. However, DAPT down regulated the elevated Notch/HES-1 signaling axis to normal, eliminating inflammation and thus protecting the nervous system. Thus, DAPT effectively eliminated the neurotoxicity of Cd, and blocking γ-secretase as well as Notch signaling axis may be a potential target for the development of neuronal protective drugs.

Keywords: GFAP, γ-secretase, HES-1, IBA1, MAP2

OPEN ACCESS

Edited by:
Rui Liu,
Chinese Academy of Medical Sciences, China

Reviewed by:
Long-Chuan Yu,
Peking University, China
Jianjun Zhang,
Institute of Psychology (CAS), China

****Correspondence:***
Yang Hu
yang.hu@muc.edu.cn
Rongfeng Lan
lan@szu.edu.cn
orcid.org/0000-0003-2124-7232

Specialty section:
This article was submitted to Neuropharmacology, a section of the journal Frontiers in Pharmacology

Received: *23 March 2022*
Accepted: *15 April 2022*
Published: *29 April 2022*

Citation:
Yang J-Y, Shen D-Y, Wang J, Dai J-F, Qin X-Y, Hu Y and Lan R (2022) DAPT Attenuates Cadmium-Induced Toxicity in Mice by Inhibiting Inflammation and the Notch/HES-1 Signaling Axis. Front. Pharmacol. 13:902796. doi: 10.3389/fphar.2022.902796

INTRODUCTION

Gamma-secretase is a highly conserved membrane-embedded protease with activity in cleaving the intracellular structural domains of receptors (Lu et al., 2014). In particular, there is a special interest in γ-secretase because of its key role in the pathogenesis of Alzheimer's disease (AD) and cancer. The amyloid precursor protein (APP) of AD is cleaved by β-secretase to a secreted derivative, sAPP-β, and a 99-residue membrane-bound fragment, CTF-β, which is then cleaved by γ-secretase into CTF-γ and even pathogenic β-amyloid (Aβ) proteins, such as Aβ 40 and Aβ 42 (Kimberly and Wolfe, 2003; Marlow et al., 2003). In addition, Notch is another important target of γ-secretase (Kopan and Ilagan, 2009). γ-secretase exerts proteolytic activity that is required to liberate the intracellular structural domain of Notch and therefore plays a key role in the Notch signaling axis. Aberrant cleavage of APP and Notch has been reported to be highly associate with AD and cancer (Lopez-Nieva et al., 2021; Yang et al., 2021). Thus, it is a potential

drug-target for the treatment of AD or anti-cancer drugs. γ-secretase inhibitors (GSIs) are thought to inhibit their cleavage of APP, thereby reducing the production of toxic Aβ (Dovey et al., 2001). Moreover, GSIs have been experimentally demonstrated to have anti-cancer activity in several types of tumor cells by inhibiting the activity of Notch signaling axis (Han and Shen, 2012; Peng et al., 2020; Liu et al., 2021).

In previous studies, we reported multi-organ damage and cognitive dysfunction in mice chronically exposed to cadmium (Cd) (Fan et al., 2021; Ren et al., 2021). Increased levels of Cd in the brain, as well as loss of neurons and activation of glial cells and the resulting oxidative stress and inflammation were found in Cd-intoxicated mice, (Wang and Du, 2013; Branca et al., 2019; Branca et al., 2020). With this in mind, we subsequently treated mice with Cd to induce cognitive impairment and demonstrated that antioxidants such as Edaravone were able to eliminate the toxicity of Cd, thereby protecting organs and the central nervous system (CNS) from the toxic damages of Cd (Fan et al., 2021). As Cd-induced neurotoxicity triggers significant inflammation in the brain, inflammatory signaling pathways, such as the Notch/HES-1 signaling axis and the RIP1-driven necroptosis pathways were found to be significantly activated (Ofengeim and Yuan, 2013; Ren et al., 2021). In light of this, in the current study, we considered whether inhibition of the Notch/HES-1 signaling axis could inhibit inflammation in the brain and thus attenuate Cd-induced neurotoxicity. Among the known compounds, DAPT (N-[N-(3, 5-difluorophenylacetyl)-l-propanoyl]-s-phenylglycine butyl ester) is an inhibitor of γ-secretase that indirectly inhibits the activity of the Notch signaling pathway (Dovey et al., 2001). Therefore, we tested the neuroprotective effect of DAPT to see if it could scavenge Cd toxicity by inhibiting the Notch/HES-1 signaling axis.

MATERIALS AND METHODS

Animal and Ethical Statement

ICR mice (6-8 weeks) were obtained from Beijing Vital River Laboratory Animal Technology Co., Ltd., under license No. SYXK-2017-0005. Mice were housed under a 12 h/12 h light/dark cycle at a temperature of 22-24°C and 60 ± 10% humidity, with ad libitum access to water and food. The animal study was reviewed and approved by the Animal Care and Use Committee of the Minzu University of China.

Drug Treatment

ICR mice were randomly divided into 4 groups (n = 10) including Control, Cd (5 mg/kg of $CdCl_2$), Cd+DAPT ($CdCl_2$ 5 mg/kg + DAPT 50 mg/kg), and DAPT (50 mg/kg). $CdCl_2$ was injected subcutaneously every other day for 28 days. DAPT was administered intragastrically once daily for 28 days. In addition, for the control group, intragastric administration was also performed with saline. $CdCl_2$ (CAS #10108-64-2) was provided by Macklin Inc. Shanghai, China. DAPT (CAS #208255-80-5) was purchased from Selleck Chemicals LLC, China.

Behavioral Procedures

The cognitive function of mice was tested of by the MWM test, as previously described (Ren et al., 2021). Briefly, in the acquired training, mice were placed in a large circular pool (110 cm in diameter) filled with opaque water (25°C) and allowed to escape to a hidden platform submerged 1 cm below the water surface, the location of which could only be identified by spatial memory. The training lasted for 6 days, during which the escape latency was shortened due to learning memory and the direct swimming routes of the mice. After the end of the training, the platform was removed and the probe trail was performed. In the above experiments, a video-image system and behavioral tracking software (WMT-100S, Chengdu Coman Software Co., Ltd.) was used to record the residence time of the mice in the target quadrant where the platform was initially placed, the number of times the mice crossed the area where the platform was located, and the trajectory of the mice.

The Y-maze spontaneous alternation experiment was used to test the willingness of animals to explore new environments (Kraeuter et al., 2019; Ren et al., 2021). The maze consisted of three equal Y-shaped arms (30 cm long, 6 cm wide and 15 cm high) with an angle of 120° between them. Animals were allowed to explore freely from the top of one arm of the maze. The animal was considered to have entered the maze when all four of its limbs were inside the arms. Correct spontaneous alternation occurred when the entering arm was different from the first two arms. The order in which the animal entered each arm over a 10-min period was recorded. Finally, the total alternation times and the number of spontaneous alternations were calculated. Alternations (%) = (number of spontaneous alternations/number of arm entries-2) × 100.

A forced swimming test (FST) was performed to assess the depression-like phenotype of the animals (Yan et al., 2010). The experiment was performed in a transparent plastic cylindrical water tank (diameter 10 cm, height 38 cm). Water at 25°C was poured into the tank (height 25 cm), the mice were gently placed above the water surface and then released for swimming for a 6-min swim. The first minute was set as an adaption and was not recorded. The next 5 min were recorded by Taimeng FST-100 software. The immobility time of mice within these 5 min was calculated.

Immunofluorescence

Brain sections were fixed in 4% paraformaldehyde for 15 min at room temperature, rinsed three times with PBS, incubated with 0.2% Triton X-100 for 10 min, and then blocked with 10% goat serum in PBS for 1 h and immuno-labeled with antibodies specific for microtubule-associated protein 2 (MAP2) (#17490-1-AP), GFAP (#16825-1-AP) or IBA1 (#10904-1-AP) overnight at 4°C, and then incubated with Alexa Fluor 488- or 596- conjugated goat anti-rabbit IgG (H+L) (#ZF-0511, ZSBG-Bio). Nuclei were stained with DAPI (4′, 6-diamidino-2-phenylindole). Images were taken using a Leica TCS SP8 confocal microscope.

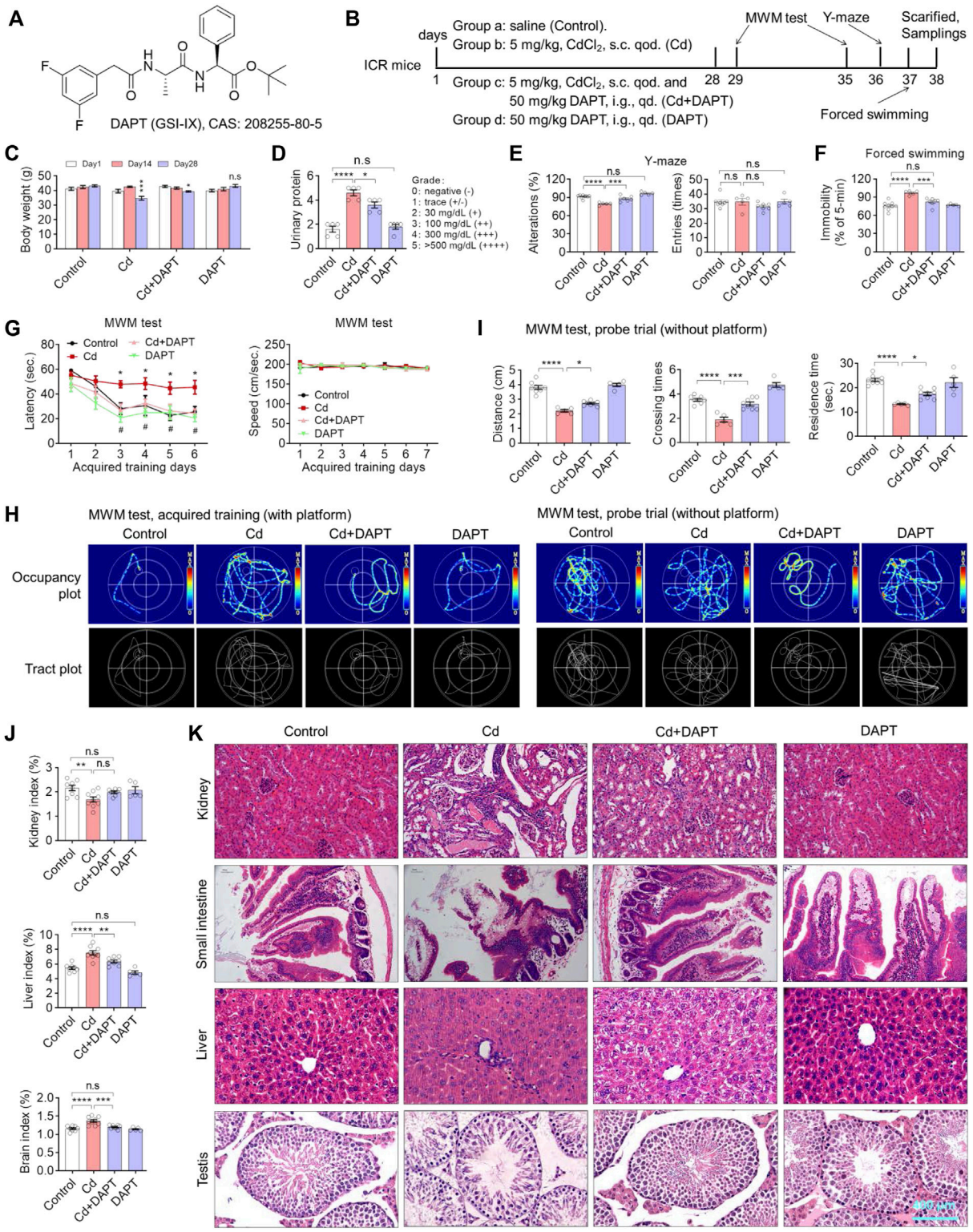

FIGURE 1 | DAPT attenuates Cd-induced multi-organic damage and cognitive impairment in ICR mice. **(A)** Chemical structure of DAPT, a γ-secretase inhibitor IX. **(B)** Schedule of animal experiments. s.c. qod., subcutaneous injection, every other day. i.g. qd., intragastric administration, once daily. **(C)** DAPT prevented the Cd-induced body weight loss in mice. **(D)** DAPT attenuated the Cd-induced elevation of urinary proteins. **(E)** DAPT rescued the decrease of spontaneous alterations induced by Cd as tested in the Y-maze. **(F)** DAPT improved the performance of mice in forced swimming test. **(G)** Escape latency of ICR mice in the acquired training (with platform) in the MWM test. **(H)** Representative occupancy or tract plots of mice in the MWM test. **(I)** Probe trails in the MWM test showing the residence time and distance

(*Continued*)

FIGURE 1 | moved in the target quadrant, as well as the number of crossing times in the area where the platform was originally placed. **(J)** Organ indices of liver, kidney and brain. Cd-induced toxicity caused renal atrophy and hepatic or cerebral edema according to organ/body mass index. **(K)** H & E staining showing that Cd-induced tissue damage was ameliorated by DAPT treatment. Scale bar, 400 μm. In this figure, in C, E, F, G and J, one-way ANOVA, post hoc Tukey's test was performed. In D, the Mann-Whitney *U*-test for non-parametric analysis was performed. In H, two-way RM ANOVA, post hoc Tukey's test was performed. n.s, not significant; $*p < 0.05$; $**p < 0.01$; $***p < 0.001$; $***p < 0.0001$ (Cd vs. Control); $\#p < 0.05$ (Cd + DAPT vs. Cd).

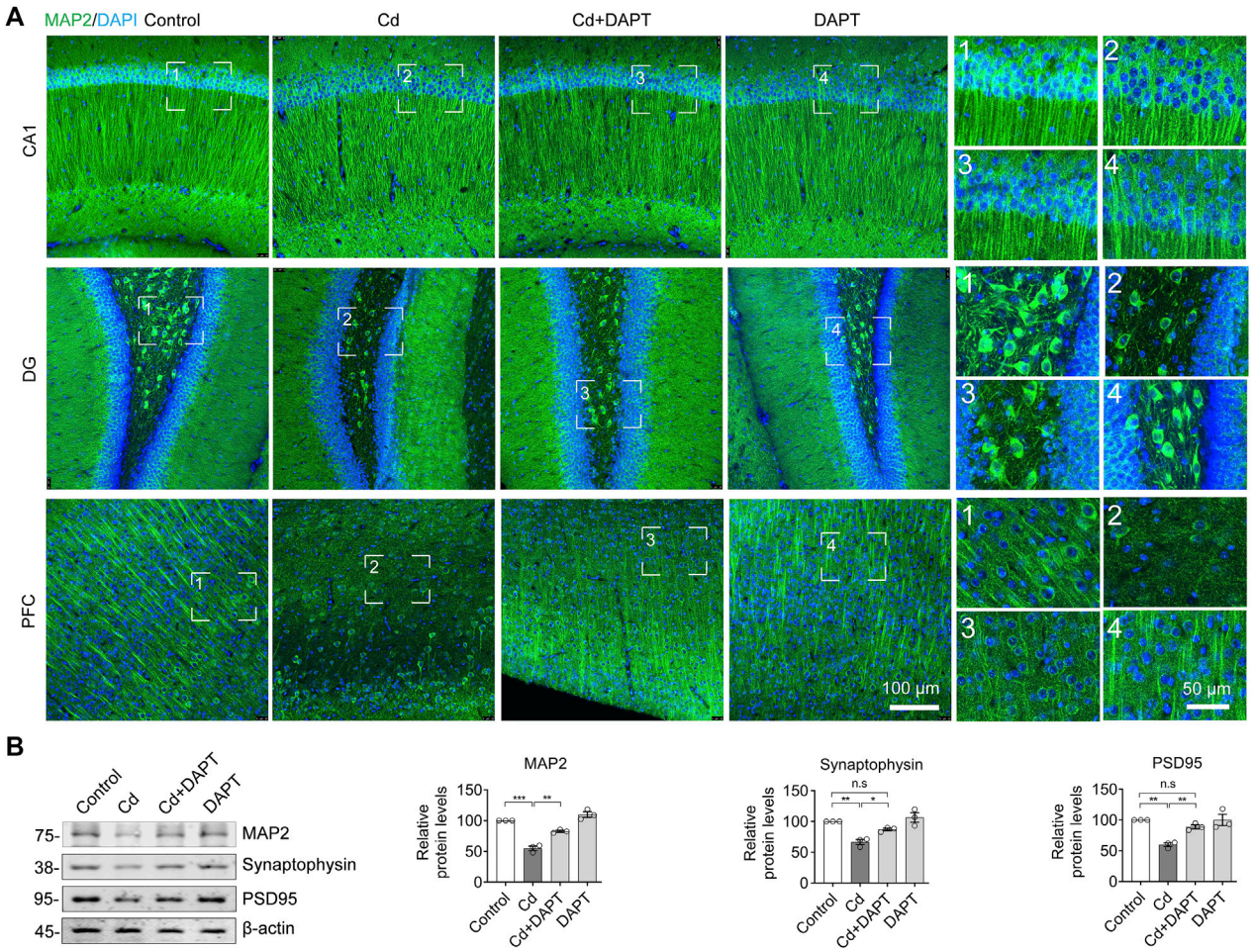

FIGURE 2 | DAPT protects neurons from Cd-induced toxicity. **(A)** IF staining of neurons in the hippocampal regions CA, DG and in the prefrontal cortex (PFC) using an antibody specific for MAP2. **(B)** Western blotting detected the levels of MAP2 and the neuronal synaptic proteins Synaptophysin and PSD95 in the hippocampus. The intensity of the blotted bands was quantified using ImageJ software and normalized to β-actin. One-way ANOVA with post hoc Tukey's test was performed. n.s, not significant; $*p < 0.05$; $**p < 0.01$; $***p < 0.001$.

Western Blotting

Western blotting was performed as previously described (Li et al., 2021). Briefly, 50 μg of proteins extracted from the hippocampus or prefrontal cortex was loaded onto SDS-PAGE and separated, then transferred to a nitrocellulose membrane. After blocking the nonspecific binding sites with skim milk, proteins were detected with the following antibodies. Antibodies specific for RBP-Jκ (#14613-1-AP, dilution 1:1,000) were provided by Proteintech, Inc. NF-κB p65 (#BD-PT5770, dilution 1:1,000) was provided by Biodragon. Notch1 (#AF5249, dilution 1:1,000), phospho-NF-κB p65 (Ser536) (#AF5881, dilution 1:1,000) and HES-1 (#AF2167, dilution 1:1,000) were purchased from Beyotime Biotechnology. COP1 (#bs-13925R, 1:1,000) antibody was purchased from Bioss Antibodies. β-actin antibody (13E5) (#4970S, 1:1,000) was purchased from Cell Signaling Technologies. Western blotting results were scanned by Odyssey CLx infrared fluorescence imaging system (LI-COR Biosciences). The relative expression levels of proteins were normalized according to their optical density and quantified in ImageJ software.

H & E Staining

In brief, after de-paraffinization and rehydration, sections were stained with Harris modified hematoxylin solution for 5 min, followed by 5 immersions in 0.5% acidic ethanol (0.5%

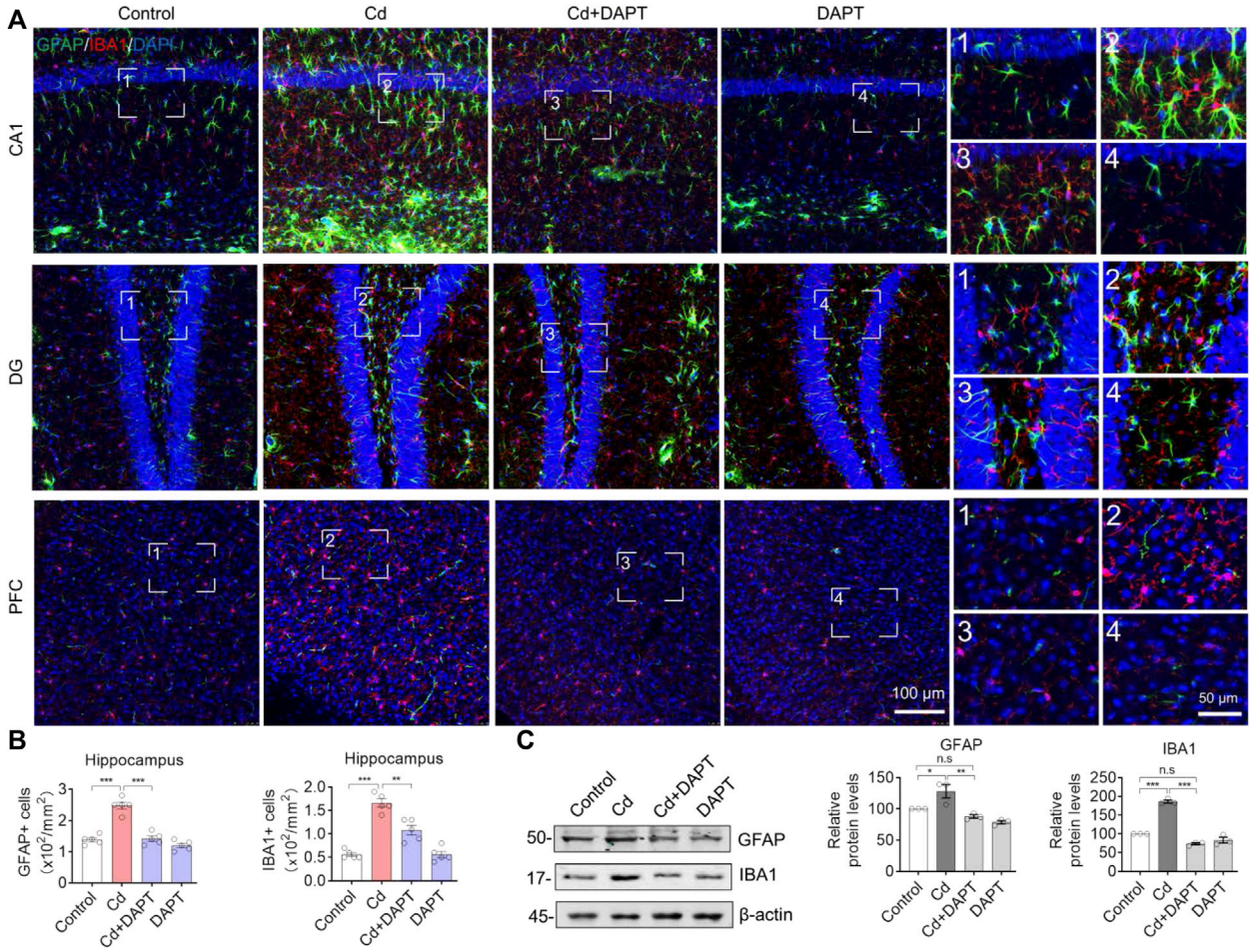

FIGURE 3 | Representative IF images of GFAP and IBA1. **(A)** DAPT antagonized the activation of microglia and astrocytes induced by Cd-toxicity, as shown by IF staining of GFAP and IBA1 using specific antibodies, respectively. **(B)** GFAP+ or IBA1+ cells were manually counted in images of **(A)**. **(C)** Western blots analysis the protein levels of GFAP and IBA1. In B-C, one-way ANOVA and post hoc Tukey's test was performed. n.s, not significant; *, $p < 0.05$; **, $p < 0.01$; ***, $p < 0.001$.

HCl in 70% ethanol), following by rinsing with distilled water, staining with eosin solution for 1 min, and then gradual dehydration in alcohol and in xylene for 30 s. The mounted slides were examined using an upright microscope (BX53, Olympus, Japan).

Immunohistochemical Staining

IHC staining of brain sections was performed for histological analysis by Wuhan Servicebio Technology Co. Ltd. Briefly, brain tissue was dissected from the prefrontal cortex and hippocampus, and paraffin embedded, sectioned, antigens retrieved, and finally immunostained with antibodies. Antibodies specific for GFAP (#16825-1-AP), IBA1 (#10904-1-AP) and TNF-α (#bsm-33207M) were provided by Proteintech Inc. or Bioss, respectively, to indicate neurons, astrocytes, microglia and inflammation. Results were examined and processed with Image Pro Plus 6.0 software (Media Cybernetics, Inc.).

Data and Statistics

All data are expressed as mean ± s.e.m. Analysis of variance (ANOVA) and Tukey's multiple tests were performed by GraphPad Prism software to determine statistical significance between groups and were plotted, as well as illustrated in the figure legends. The Mann Whitney's test was performed for non-parametric analysis.

RESULTS

DAPT Attenuates Cd-Induced Multi-Organ Damage and Cognitive Impairment in Mice

We first established a chronic Cd-exposured ICR mouse model by administering 5 mg/kg of $CdCl_2$ every other day for 4 weeks. Accordingly, a DAPT treatment group (Cd+DAPT) and a separate DAPT group were set up (**Figures 1A,B**). During the experiment, body weight and urine protein were measured to track the damage of Cd on the organs of the mice (**Figures 1C,D**). After drug treatment, behavioral tests were performed on the mice, including the MWM test, Y maze and forced swimming test. The results showed that the body weight of mice changed significantly after 4 weeks of Cd treatment, i.e.

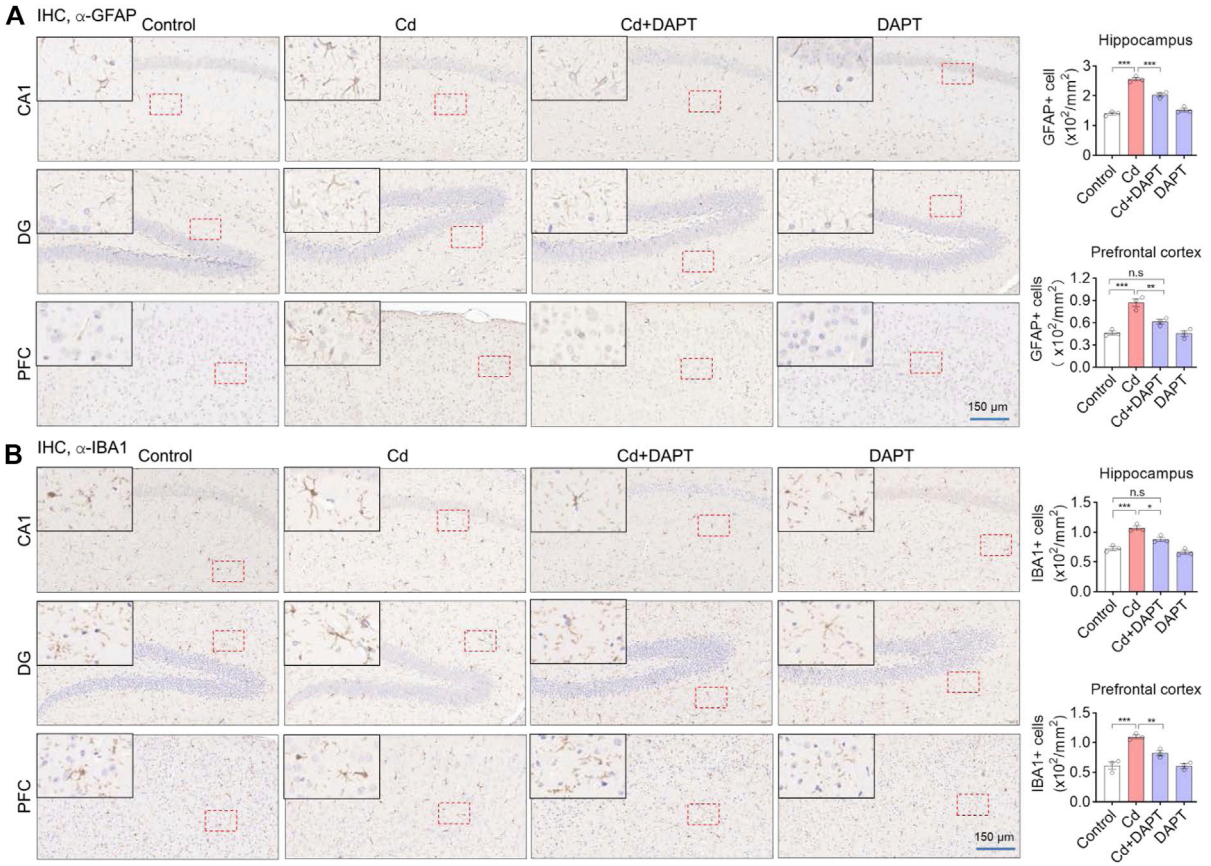

FIGURE 4 | IHC staining of GFAP and IBA1 in the prefrontal cortex (PFC) and hippocampal regions CA1 and DG. **(A,B)** Representative IHC images showing Cd-induced activation of astrocytes and microglia, such as an increase in the number of GFAP+ and IBA1+ cells, but this can be restored by DAPT treatment. GFAP+ and IBA+ cells was manually counted and divided by the corresponding area. One-way ANOVA with post hoc Tukey's test was performed. n.s, not significant; $^{*}p < 0.05$; $^{**}p < 0.01$; $^{***}p < 0.001$.

the body weight of Cd-treated mice was significantly lower on day 28 than on day 1 (**Figure 1C**, Cd, $p < 0.001$), whereas the body weight of control mice increased naturally with the increase in weeks of age. Mice treated with DAPT recovered their body weight compared to the Cd group, and their difference was significantly reduced compared with day 1 (**Figure 1C**, Cd + DAPT, $p < 0.05$). Correspondingly, urinary protein increased in mice treated with Cd, with a significant difference compared to the control group (**Figure 1D**, $p < 0.0001$), while urinary protein decreased in mice treated with DAPT, with a difference compared to the Cd group (**Figure 1D**, $p < 0.05$), while there was no change in mice treated with DAPT alone (**Figure 1D**, n.s).

As confirmed by the Y-maze test, the environmental exploration and memory abilities of Cd-poisoned mice were significantly reduced, whereas the performance of mice in the DAPT-treated group recovered significantly, and their environmental exploration abilities were similar to those of the control group (**Figure 1E**). Correspondingly, in the forced swimming experiment, the resting time was significantly increased in the Cd-intoxicated mice (**Figure 1F**, $p < 0.0001$), while in the DAPT-treated mice, the resting time was shortened and did not differ from the control group (**Figure 1F**, Cd+DAPT, not significant). In the MWM experiment, after 6 days of training, mice took significantly less time to find the platform and showed learning memory (**Figure 1G**, control). Then, Cd-treated mice then took significantly longer to find the platform than the control group, and the improvement was not significant as the number of training days increased (**Figure 1G**, Cd). In contrast, mice in the DAPT-treated group showed a significant improvement in learning and memory, i.e., regained the ability to find the underwater platform similar to control mice (**Figure 1G**, Cd+DAPT). In this experiment, there was no difference in the swimming speed of the mice in the water maze. Corresponding to these results, the swimming path of mice recorded by thermal infrared imaging also reflected changes in their learning and memory ability (**Figure 1H**). On this basis, at day 7 of the experiment, the platform was removed and the mice were allowed to perform a 1-min swimming test (probe trail). We found that mice in the control and DAPT-treated groups had more residence time, more times crossing the platform position and more swimming distance in the area where the

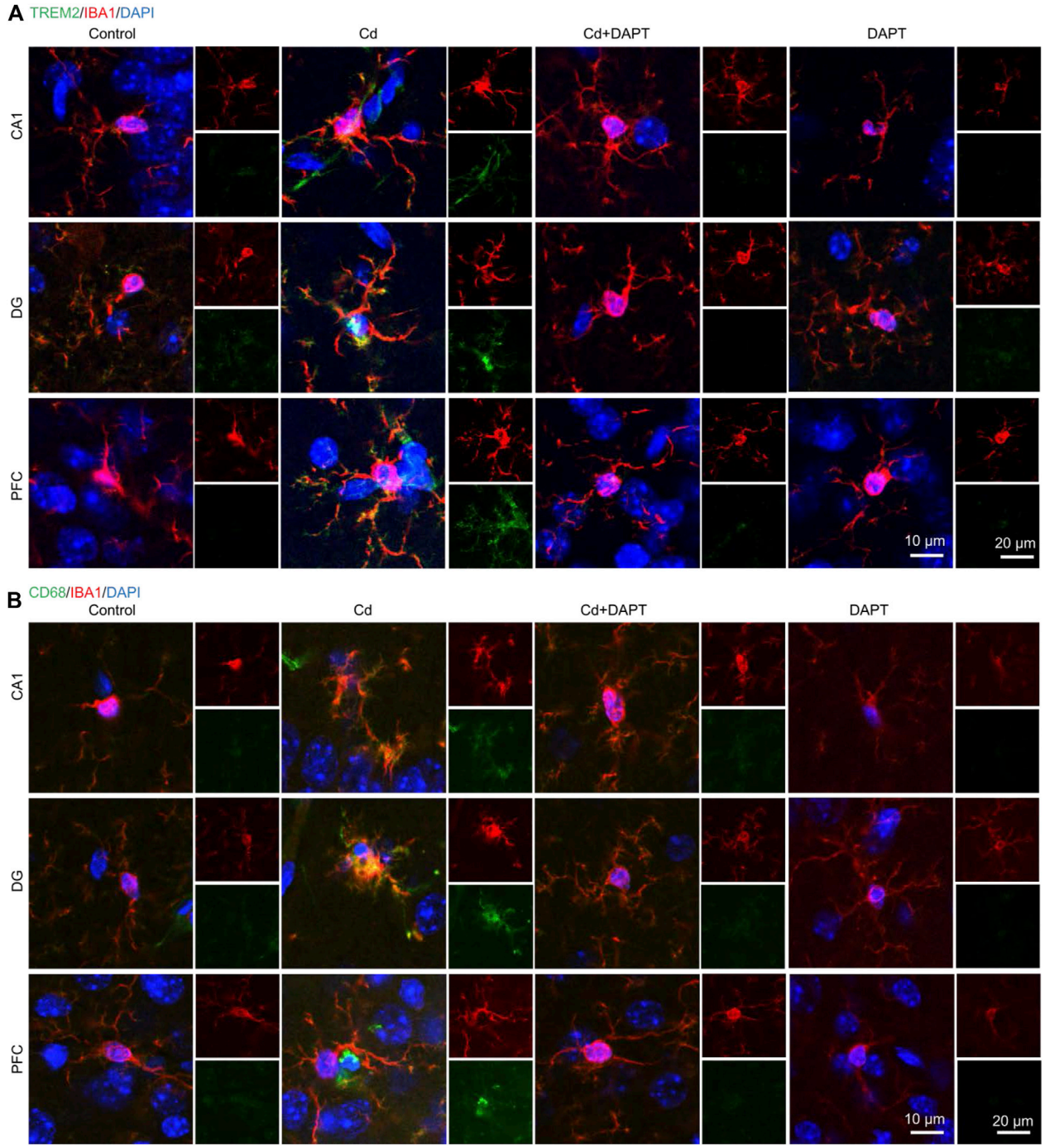

FIGURE 5 | IF co-staining of TREM2 or CD68 with IBA1 in brain tissue sections. **(A)** Cd toxicity activated microglia, as evidenced by increased levels of TREM2 and CD68. DAPT attenuated Cd toxicity and microglia activation, and restored the CD68 upregulation. **(B)** Schematic diagram showing DAPT-mediated attenuation of Cd toxicity and restoration of homeostasis in the neuronal system.

platform was originally placed compared to the Cd-treated group, i.e. the mice showed the ability to remember the location of the underwater platform. In contrast, Cd-intoxicated mice had a significant impaired ability to do so and showed no sense of purpose while swimming (**Figures 1H,I**). Consistently, organic indices (organ/body weight) also showed that damage caused by Cd exposure resulted in kidney atrophy, while the liver and brain showed enlargement or hyperplasia (**Figure 1J**). H&E staining also confirmed that Cd exposure caused significant damage to the kidney, liver,

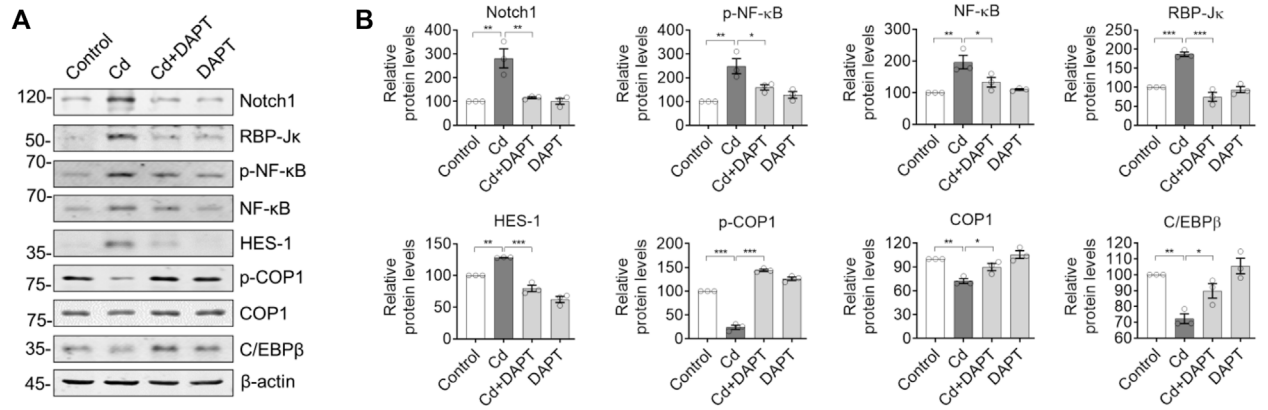

FIGURE 6 | DAPT restores the Notch/HES-1 signaling axis to mitigate Cd-induced toxicity in mice. **(A)** Western blots of proteins in the Notch/HES-1 signaling axis. **(B)** Relative protein levels in **(A)**. One-way ANOVA with post hoc Tukey's test was performed. $^{*}p < 0.05$; $^{**}p < 0.01$ or $^{***}p < 0.001$.

small intestine and testes, while the damage in mice treated with DAPT was effectively repaired (**Figure 1K**).

DAPT Facilitates the Clearance of Cd and Avoids the Loss of Neurons in the Brain

Brain tissue was surgically isolated from mice after animal experiments, sectioned and immunofluorescence stained with MAP2 antibody to identify neurons. The results showed that a significant reduction of neurons in the brains of Cd-intoxicated mice, such as in the CA1 and DG regions of the hippocampus, and in the prefrontal cortex (PFC) region (**Figure 2A**, Cd). After DAPT treatment, the number of neurons in these regions was restored. Correspondingly, MAP2 and synaptic-associated proteins such as Synaptophysin and PSD95 were reduced due to Cd toxicity but were restored after DAPT treatment (**Figure 2B**). Quantitative optical density analysis of the protein bands in the Western blot results also confirmed these changes. These results suggest that the clearance of Cd toxicity and recovery of neurons by DAPT treatment are consistent with the results of behavioral experiments previously observed in mice.

DAPT Inhibits Cd Toxicity-Induced Glial Cell Activation

In the brains of Cd-intoxicated mice, we found increased GFAP+ and IBA1+ cells by staining for the characteristic proteins in microglia and astrocytes (**Figure 3A**, Cd), indicating that the glial cells were activated in the brains of chronically Cd-exposed mice. In contrast, the number of GFAP+ and IBA1+ cells was significantly lower in the brains of mice in the DAPT treated group (Cd+DAPT) and the DAPT alone treated group (**Figure 3A**). Statistically, there was a significant difference in the number of GFAP+ and IBA1+ cells between the above experimental groups (**Figure 3B**). In addition, protein assays of GFAP and IBA1 showed that the expression of GFAP and IBA1 increased in Cd-intoxicated mice, while the levels of these two proteins returned to normal after DAPT treatment (**Figure 3C**, Cd+DAPT).

In addition, brain sections from the hippocampus and prefrontal cortex (PFC) were used for IHC staining to label GFAP+ and IBA1+ cells. Very similar to the results of IF (**Figure 3**), we found that a significant increase in the number of GFAP+ and IBA1+ cells in Cd-intoxicated mice, and DAPT was able to eliminate this change and restore glial cells to a normal state (**Figure 4**). In addition, microglia can be activated by stress and the need to clear damaged cells, as indicated by elevated expression of triggering receptor expressed on myeloid cells 2 (TREM2) and macrosialin (CD68), suggesting their enhanced phagocytic capacity. TREM2 is a receptor for Aβ42 or damaged cells that mediate their uptake and degradation by microglia (Yeh et al., 2016; Zhao et al., 2018), while CD68 is a marker protein indicative of microglia phagocytic activity (Wong et al., 2005; Chistiakov et al., 2017). In view of this, immunofluorescence observations on microglia showed a significant increase in the expression of TREM2 and CD68, which was associated with microglia phagocytosis in response to Cd toxicity, possibly enhance cellular clearance of Cd (**Figure 5**). In contrast, after DAPT treatment, the levels of TREM2 and CD68 were down-regulated and returned to normal (**Figure 5**, Cd+DAPT). The above results consistently suggest that DAPT can effectively inhibit Cd-induced glial cell activation and eliminate neuronal inflammation.

DAPT Inhibits the Notch/HES-1 Signaling Axis to Eliminate the Toxicity of Cd

We examined the expression of Notch/HES-1 signaling pathway and its related proteins such as NF-κB. The results showed that the activity of Notch/HES-1 signaling axis was significantly enhanced in Cd-poisoned mice, i.e. Notch1, RBP-Jk, HES-1 and NF-kB were significantly increased, while its negative regulators such as constitutive photomorphogenesis protein 1 homolog (COP1) and CCAAT/enhancer-binding protein beta (C/EBPβ) were significantly decreased (**Figure 6**). This suggests

that the activity of the Notch/HES-1 signaling axis is significantly enhanced in Cd-intoxicated mice. In contrast, Notch/HES-1 signaling axis activity was significantly down-regulated in the DAPT-treated mice (**Figure 6**, Cd+DAPT), i.e., the levels of Notch1, RBP-Jk, HES-1, NF-kB and other proteins were significantly reduced and returned to normal (compared with controls). At the same time, the protein levels of COP1 and C/EBPβ were restored (**Figure 6**, Cd+DAPT). These results suggest that DAPT, as an inhibitor of γ-secretase, significantly inhibits the activity of the Notch/HES-1 signaling axis, thereby protecting the nervous system.

DISCUSSION

In the present study, we established a mouse model of chronic Cd exposure and confirmed Cd-induced multi-organ toxicity and neurotoxicity. DAPT, an inhibitor of γ-secretase, was successfully used to eliminate Cd toxicity in the mouse model and its effectiveness against Cd toxicity was confirmed in biochemical, histological and animal behavioral experiments. In addition, we found that Cd induced an increase in the number of glial cells and the activation of the Notch/HES-1 signaling axis in the mouse brain. The expression levels of the Notch/HES-1 signaling axis and related factors were also ameliorated. These results indicate that DAPT can effectively alleviate Cd-induced neurotoxicity and exert neuroprotective activity.

Under normal conditions, Cd barely enters the brain and directly harms the CNS due to the presence of blood-brain barrier (BBB) (Wang and Du, 2013). However, Cd can still reach the basement membrane cells of the BBB through the blood circulation (Branca et al., 2020). Chronic exposure to Cd can damage these cells that make up the BBB, thereby disrupting the integrity of the BBB and allowing Cd to enter the CNS (Branca et al., 2019). Death receptor-mediated signaling pathways, such as those driven by RIP1, lead to neuronal death (Xu et al., 2018). Loss of neurons in brain regions associated with functions such as learning and memory will produce significant cognitive deficits, hence the significant cognitive impairment and other functional deficits observed in our previous studies in mice chronically exposed to Cd (Fan et al., 2021). Fortunately, clinically applied antioxidants such as Edaravone, as well as the natural product ginsenoside Rg1 are effective in alleviating these Cd-induced symptoms (Ren et al., 2021). Accordingly, we also observed a restoration of antioxidant capacity in the blood and brain, a reduction in inflammation and neuronal recovery. These results are very similar to the effects of DAPT in the current study, although the direct antioxidant and anti-inflammatory effects of DAPT have not been demonstrated, it did inhibit the Notch/HES-1-mediated inflammatory pathway (**Figure 6**) and we did observe tissue and organ damage, such as in the liver in Cd-intoxicated mouse model. In particular, in the CNS, we observed neuronal recovery and reduced inflammation in mice, resulting in improved cognitive function (**Figures 1**, **2**). The above evidence suggests that we can use DAPT in mouse models in an attempt to counteract the toxicity of Cd or protect the organism from its deletrious effects. Furthermore, the effectiveness of DAPT in eliminating Cd toxicity suggests that suppressing excessive inflammation in the CNS and restoring neuronal activity is an effective neuroprotective strategy.

It is worthwhile to explore in depth how DAPT exerts its role in eliminating Cd toxicity. The first step may be to reduce the uptake of Cd by the CNS. DAPT has been reported to modulate the permeability of the BBB, affecting the movement of substances into and out of the CNS (Zhang et al., 2013), so it is of interest whether DAPT could reduce the influx of Cd into the brain via this pathway (Sun et al., 2019). Furthermore, by inhibiting the Notch/HES-1 signaling pathway, DAPT attenuates the inflammatory response in the CNS, which is important for reducing pathological inflammation-induced neuronal loss and may even modulate microglia functions, such as inhibiting their excessive inflammation and release of inflammatory factors, enhancing their phagocytosis, and facilitating the clearance of Cd and other harmful substances in the CNS. Because microglia have been shown to act as scavengers in the CNS, they are able to act as phagocytes to clear toxins or eliminate damaged cell bodies under the right conditions. However, the above possible mechanism remains a hypothesis to be tested in depth in subsequent experiments. Nevertheless, the neuroprotective effects of DAPT that we demonstrated in this study may have implications for the design and development of novel neuroprotective compounds or for the prevention and treatment of clinical disorders of the CNS.

In conclusion, DAPT attenuates Cd-induced multi-organ damage and cognitive dysfunction in mice and avoided the loss of neurons in the brain. And the above effects of DAPT are likely to be achieved by inhibiting Cd toxicity-induced glial cell activation and Notch/HES-1 signaling axis.

DATA AVAILABILITY STATEMENT

The original contributions presented in the study are included in the article/Supplementary Material, further inquiries can be directed to the corresponding authors.

ETHICS STATEMENT

The animal study was reviewed and approved by the Animal Care and Use Committee of the Minzu University of China.

AUTHOR CONTRIBUTIONS

J-Y Y established the mouse model and performed IF, IHC. D-YS and JW performed the behavioral tests. J-FD helped for the WB. X-YQ performed the cell counting and statistical analysis. YH and RL conceived the project and wrote the manuscript.

ACKNOWLEDGMENTS

We thank the National Natural Science Foundation of China (81873088, 82174085) for financial support.

REFERENCES

Branca, J. J. V., Maresca, M., Morucci, G., Mello, T., Becatti, M., Pazzagli, L., et al. (2019). Effects of Cadmium on ZO-1 Tight Junction Integrity of the Blood Brain Barrier. *Int. J. Mol. Sci.* 20 (23), 6010. doi:10.3390/ijms20236010

Branca, J. J. V., Fiorillo, C., Carrino, D., Paternostro, F., Taddei, N., Gulisano, M., et al. (2020). Cadmium-induced Oxidative Stress: Focus on the Central Nervous System. *Antioxidants (Basel)* 9 (6), 492. doi:10.3390/antiox9060492

Chistiakov, D. A., Killingsworth, M. C., Myasoedova, V. A., Orekhov, A. N., and Bobryshev, Y. V. (2017). CD68/macrosialin: Not Just a Histochemical Marker. *Lab. Invest.* 97 (1), 4–13. doi:10.1038/labinvest.2016.116

Dovey, H. F., John, V., Anderson, J. P., Chen, L. Z., de Saint Andrieu, P., Fang, L. Y., et al. (2001). Functional Gamma-Secretase Inhibitors Reduce Beta-Amyloid Peptide Levels in Brain. *J. Neurochem.* 76 (1), 173–181. doi:10.1046/j.1471-4159.2001.00012.x

Fan, S. R., Ren, T. T., Yun, M. Y., Lan, R., and Qin, X. Y. (2021). Edaravone Attenuates Cadmium-Induced Toxicity by Inhibiting Oxidative Stress and Inflammation in ICR Mice. *Neurotoxicology* 86, 1–9. doi:10.1016/j.neuro.2021.06.003

Han, J., and Shen, Q. (2012). Targeting γ-secretase in Breast Cancer. *Breast Cancer (Dove Med. Press.* 4, 83–90. doi:10.2147/BCTT.S26437

Kimberly, W. T., and Wolfe, M. S. (2003). Identity and Function of Gamma-Secretase. *J. Neurosci. Res.* 74 (3), 353–360. doi:10.1002/jnr.10736

Kopan, R., and Ilagan, M. X. (2009). The Canonical Notch Signaling Pathway: Unfolding the Activation Mechanism. *Cell* 137 (2), 216–233. doi:10.1016/j.cell.2009.03.045

Kraeuter, A. K., Guest, P. C., and Sarnyai, Z. (2019). The Y-Maze for Assessment of Spatial Working and Reference Memory in Mice. *Methods Mol. Biol.* 1916, 105–111. doi:10.1007/978-1-4939-8994-2_10

Li, X.-X., Cai, Z.-P., Lang, X.-Y., Pan, R.-Y., Ren, T.-T., Lan, R., et al. (2021). Coeloglossum Viride Var. Bracteatum Extract Improves Cognitive Deficits by Restoring BDNF, FGF2 Levels and Suppressing RIP1/RIP3/MLKL-Mediated Neuroinflammation in a 5xFAD Mouse Model of Alzheimer's Disease. *J. Funct. Foods* 85, 104612. doi:10.1016/j.jff.2021.104612

Liu, L., Tao, T., Liu, S., Yang, X., Chen, X., Liang, J., et al. (2021). An RFC4/Notch1 Signaling Feedback Loop Promotes NSCLC Metastasis and Stemness. *Nat. Commun.* 12 (1), 2693. doi:10.1038/s41467-021-22971-x

Lopez-Nieva, P., González-Sánchez, L., Cobos-Fernández, M. Á., Córdoba, R., Santos, J., and Fernández-Piqueras, J. (2021). More Insights on the Use of γ-Secretase Inhibitors in Cancer Treatment. *Oncologist* 26 (2), e298–e305. doi:10.1002/onco.13595

Lu, P., Bai, X. C., Ma, D., Xie, T., Yan, C., Sun, L., et al. (2014). Three-dimensional Structure of Human γ-secretase. *Nature* 512 (7513), 166–170. doi:10.1038/nature13567

Marlow, L., Cain, M., Pappolla, M. A., and Sambamurti, K. (2003). Beta-secretase Processing of the Alzheimer's Amyloid Protein Precursor (APP). *J. Mol. Neurosci.* 20, 233–239. doi:10.1385/JMN:20:3:233

Ofengeim, D., and Yuan, J. (2013). Regulation of RIP1 Kinase Signalling at the Crossroads of Inflammation and Cell Death. *Nat. Rev. Mol. Cel Biol.* 14 (11), 727–736. doi:10.1038/nrm3683

Peng, X., Zhou, J., Li, B., Zhang, T., Zuo, Y., and Gu, X. (2020). Notch1 and PI3K/Akt Signaling Blockers DAPT and LY294002 Coordinately Inhibit Metastasis of Gastric Cancer through Mutual Enhancement. *Cancer Chemother. Pharmacol.* 85 (2), 309–320. doi:10.1007/s00280-019-03990-4

Ren, T. T., Yang, J. Y., Wang, J., Fan, S. R., Lan, R., and Qin, X. Y. (2021). Gisenoside Rg1 Attenuates Cadmium-Induced Neurotoxicity *In Vitro* and *In Vivo* by Attenuating Oxidative Stress and Inflammation. *Inflamm. Res.* 70 (10-12), 1151–1164. doi:10.1007/s00011-021-01513-7

Sun, Z., Xie, Q., Pan, J., and Niu, N. (2019). Cadmium Regulates von Willebrand Factor and Occludin Expression in Glomerular Endothelial Cells of Mice in a TNF-α-dependent Manner. *Ren. Fail.* 41 (1), 354–362. doi:10.1080/0886022X.2019.1604383

Wang, B., and Du, Y. (2013). Cadmium and its Neurotoxic Effects. *Oxid. Med. Cel Longev.* 2013, 898034. doi:10.1155/2013/898034

Wong, A. M., Patel, N. V., Patel, N. K., Wei, M., Morgan, T. E., de Beer, M. C., et al. (2005). Macrosialin Increases during Normal Brain Aging are Attenuated by Caloric Restriction. *Neurosci. Lett.* 390 (2), 76–80. doi:10.1016/j.neulet.2005.07.058

Xu, D., Jin, T., Zhu, H., Chen, H., Ofengeim, D., Zou, C., et al. (2018). TBK1 Suppresses RIPK1-Driven Apoptosis and Inflammation during Development and in Aging. *Cell* 174 (6), 1477–e19. doi:10.1016/j.cell.2018.07.041

Yan, H. C., Cao, X., Das, M., Zhu, X. H., and Gao, T. M. (2010). Behavioral Animal Models of Depression. *Neurosci. Bull.* 26 (4), 327–337. doi:10.1007/s12264-010-0323-7

Yang, G., Zhou, R., Guo, X., Yan, C., Lei, J., and Shi, Y. (2021). Structural Basis of γ-secretase Inhibition and Modulation by Small Molecule Drugs. *Cell* 184 (2), 521. doi:10.1016/j.cell.2020.11.049

Yeh, F. L., Wang, Y., Tom, I., Gonzalez, L. C., and Sheng, M. (2016). TREM2 Binds to Apolipoproteins, Including APOE and CLU/APOJ, and Thereby Facilitates Uptake of Amyloid-Beta by Microglia. *Neuron* 91 (2), 328–340. doi:10.1016/j.neuron.2016.06.015

Zhang, G. S., Tian, Y., Huang, J. Y., Tao, R. R., Liao, M. H., Lu, Y. M., et al. (2013). The γ-secretase Blocker DAPT Reduces the Permeability of the Blood-Brain Barrier by Decreasing the Ubiquitination and Degradation of Occludin during Permanent Brain Ischemia. *CNS Neurosci. Ther.* 19 (1), 53–60. doi:10.1111/cns.12032

Zhao, Y., Wu, X., Li, X., Jiang, L. L., Gui, X., Liu, Y., et al. (2018). TREM2 is a Receptor for β-Amyloid that Mediates Microglial Function. *Neuron* 97 (5), 1023. doi:10.1016/j.neuron.2018.01.031

Conflict of Interest: The authors declare that the research was conducted in the absence of any commercial or financial relationships that could be construed as a potential conflict of interest.

frontiers | Frontiers in Pharmacology

REVIEW
published: 20 May 2022
doi: 10.3389/fphar.2022.914537

Activation of Wnt/Beta-Catenin Signaling Pathway as a Promising Therapeutic Candidate for Cerebral Ischemia/Reperfusion Injury

Zhizhun Mo[1], Zhongyi Zeng[1], Yuxiang Liu[1], Linsheng Zeng[1], Jiansong Fang[2] and Yinzhong Ma[3]**

[1]Emergency Department, Shenzhen Traditional Chinese Medicine Hospital, Shenzhen, China, [2]Science and Technology Innovation Center, Guangzhou University of Chinese Medicine, Guangzhou, China, [3]Shenzhen Key Laboratory of Biomimetic Materials and Cellular Immunomodulation, Institute of Biomedicine and Biotechnology, Shenzhen Institute of Advanced Technology, Chinese Academy of Sciences, Shenzhen, China

Stroke is one of the leading causes of mortality, and survivors experience serious neurological and motor behavioral deficiencies. Following a cerebral ischemic event, substantial alterations in both cellular and molecular activities occur because of ischemia/reperfusion injury. Wnt signaling is an evolutionarily conserved signaling pathway that has been manifested to play a key role in embryo development and function maintenance in adults. Overactivation of Wnt signaling has previously been investigated in cancer-based research studies. Recently, abnormal Wnt signaling activity has been observed in ischemic stroke, which is accompanied by massive blood–brain barrier (BBB) disruption, neuronal apoptosis, and neuroinflammation within the central nervous system (CNS). Significant therapeutic effects were observed after reactivating the adynamic signaling activity of canonical Wnt signaling in different cell types. To better understand the therapeutic potential of Wnt as a novel target for stroke, we reviewed the role of Wnt signaling in the pathogenesis of stroke in different cell types, including endothelial cells, neurons, oligodendrocytes, and microglia. A comprehensive understanding of Wnt signaling among different cells may help to evaluate its potential value for the development of novel therapeutic strategies based on Wnt activation that can ameliorate complications and improve functional rehabilitation after ischemic stroke.

Keywords: ischemic stroke, ischemia/reperfusion injury, Wnt signaling, neuroprotection, blood-brain barrier

OPEN ACCESS

Edited by:
Yong Cheng,
Minzu University of China, China

Reviewed by:
Rong Yan,
Shanghai University of Traditional Chinese Medicine, China
Wenbin He,
Shanxi University of Chinese Medicine, China

****Correspondence:***
Jiansong Fang
fangjs@gzucm.edu.cn
Yinzhong Ma
yz.ma@siat.ac.cn

Specialty section:
This article was submitted to Neuropharmacology, a section of the journal Frontiers in Pharmacology

Received: *07 April 2022*
Accepted: *22 April 2022*
Published: *20 May 2022*

Citation:
Mo Z, Zeng Z, Liu Y, Zeng L, Fang J and Ma Y (2022) Activation of Wnt/Beta-Catenin Signaling Pathway as a Promising Therapeutic Candidate for Cerebral Ischemia/Reperfusion Injury. Front. Pharmacol. 13:914537. doi: 10.3389/fphar.2022.914537

INTRODUCTION

Stroke is the leading cause of disability and mortality worldwide and is classified as ischemic or hemorrhagic. Ischemic stroke accounts for 87% of all stroke incidences and is defined as the interruption of blood flow to the brain due to blockage of the cerebral artery, causing severe damage to focal brain tissue (Collaborators, 2019). Patients who survive the initial ischemic attack often suffer from associated complications, such as hemiparesis, cognitive deficits, and dependency in daily activities, the rehabilitation of which has always been a challenging issue (Richards et al., 2015). According to an estimation put forth by the American Heart Association/American Stroke Association, the total economic cost to the society for stroke is likely to rise up to $184.1 billion for the year of 2030 (Collaborators, 2019).

Vascular recanalization remains the primary therapeutic option (Powers et al., 2019). To date, thrombolytic therapy with intravenous recombinant tissue-type plasminogen activator (rtPA) is recommended within the first 3–4.5 h. Thrombolysis beyond the time window has a certain recanalization ability, but the main side effects of intracerebral hemorrhage increase concomitantly (Emberson et al., 2014). As for embolization of larger vessels (anterior circulatory arterial occlusion), which accounts for one-fourth of all ischemic strokes, intravenous thrombolysis has a low recanalization rate of about 13–20% (Ma et al., 2019). Therefore, rtPA thrombolysis paired with mechanical thrombectomy has become the first line therapy for large vessel occlusion. According to the American Heart Association, mechanical thrombectomy is prescribed in cases where indications of middle cerebral artery embolism or internal carotid artery embolism are evident within 6 h of symptom onset (Alawieh et al., 2017). More recently, screening by imaging methods has shown that patients with penumbra can also benefit from mechanical thrombectomy 16–24 h after the onset of symptoms (Albers et al., 2018). Additionally, to achieve recanalization as soon as possible, there are studies on mechanical thrombectomy that skip intravenous thrombolysis (DIRECT-MT, DEVT) and show non-inferiority (Yang et al., 2020). In addition to vascular recanalization therapy, the treatment of acute ischemic stroke includes antiplatelet and anticoagulant therapies, improvement of microcirculation, lipid control, and neuroprotection (Phipps and Cronin, 2020).

The above studies suggest that the ischemic penumbra still has great therapeutic potential for neuroprotection. The Wnt pathway is part of an evolutionarily conserved intracellular signal transduction cascade that regulates multiple processes crucial for cell proliferation, differentiation, migration, and fate decision during development (Schulte and Bryja, 2017; Eubelen et al., 2018). Recently, several studies have reported the mechanism by which Wnt/β-catenin signaling is regulated in the adult brain and serves as an endogenous protective mechanism against the central nervous system (CNS) diseases (Schulte and Bryja, 2017; Menet et al., 2020; Cheng et al., 2022). In this review, we discuss the recent research updates on the regulatory mechanism of the classical Wnt (Wnt/β-catenin) signaling pathway and summarize the biological functions of the cells (endothelial cells, neurons, oligodendrocytes, microglia, and astrocytes) affected by stroke pathology. Furthermore, various therapeutic studies targeting the Wnt/β-catenin signaling pathway have been conducted. This review provides insights into the potential and the value of the Wnt/β-catenin signaling pathway as a therapeutic target for ischemic stroke.

ACUTE PATHOLOGY IN POST-ISCHEMIC STROKE

Several studies suggest that a series of biochemical reactions occur within a few minutes after ischemia/reperfusion, causing strong oxidative stress and excitotoxic damage to the brain tissue (Chamorro et al., 2016). Meanwhile, circulating immune cells (mostly neutrophils) rapidly adhere to the endovascular cortex of the ischemic region and infiltrate the brain parenchyma by releasing proteolytic enzymes and matrix metalloproteinases (MMPs) to affect the integrity of the blood–brain barrier (BBB) (Wang et al., 2021a). The innate immune mechanism of neutrophils can also release large amounts of reactive oxygen species (ROS) through respiratory burst which may damage vascular endothelial cells (Wang et al., 2021a). Days after the primary stroke and transient ischemic attack, more circulating immune cells (monocytes/macrophages and T lymphocytes) enter the brain parenchyma, and along with local microglia, release a large number of inflammatory factors, such as tumor necrosis factor α (TNF-α), interleukin 1-β (IL-1β), and interleukin 6 (IL-6), which cause serious inflammatory damage to the glia and neurons, ultimately leading to neuronal apoptosis and necrosis (Wang et al., 2021b; Qiu et al., 2021). Large amounts of dead cell debris form damage-associated molecular patterns (DAMPs), which further activate the immune response and cause damage to the brain tissue (**Figure 1**).

PROGRESS IN DRUG DEVELOPMENT TOWARD ISCHEMIC STROKE

Owing to the complexity of the physiological and pathological mechanisms of the human brain, drug development to ameliorate ischemic stroke is acknowledged as a very challenging task. Thousands of lead compounds that show promising therapeutic effects in preclinical trials rarely show sufficient efficacy during the trial phases (O'Collins et al., 2006). In 2020, a combination of Edaravone and Dexcamphenol (Xianbixin) showed promising results for the treatment of acute ischemic stroke in clinical trials. Innovation of the therapeutic strategy relies on powerful dual targets against free radicals and inflammation. The only new drug approved for stroke over the past 5 years, Xianbixin, which blocks cascading damage in the brain tissue during ischemia/reperfusion injury, provides new insights into the development of drugs for ischemic stroke. Therefore, signaling pathways that exist in a variety of brain cells and exert their corresponding protective effects will be more suitable as drug targets for treatment of stroke.

THE INTRACELLULAR TRAFFICKING OF WNT SIGNALING

Previous studies in drug development have shown that a single protective mechanism cannot completely block the cascading damage after ischemic stroke; therefore, it is difficult to achieve adequate therapeutic effects (Moskowitz et al., 2010; Zhou et al., 2018). The treatment for stroke requires multiple protective mechanisms. In recent years, the Wnt signaling pathway has been shown to play an important regulatory role in maintaining cerebrovascular and neural cell functions (Menet et al., 2020). The Wnt signaling pathway is widely found in invertebrates and vertebrates and is a highly evolutionarily conserved signaling pathway. It plays a crucial role in the early development of

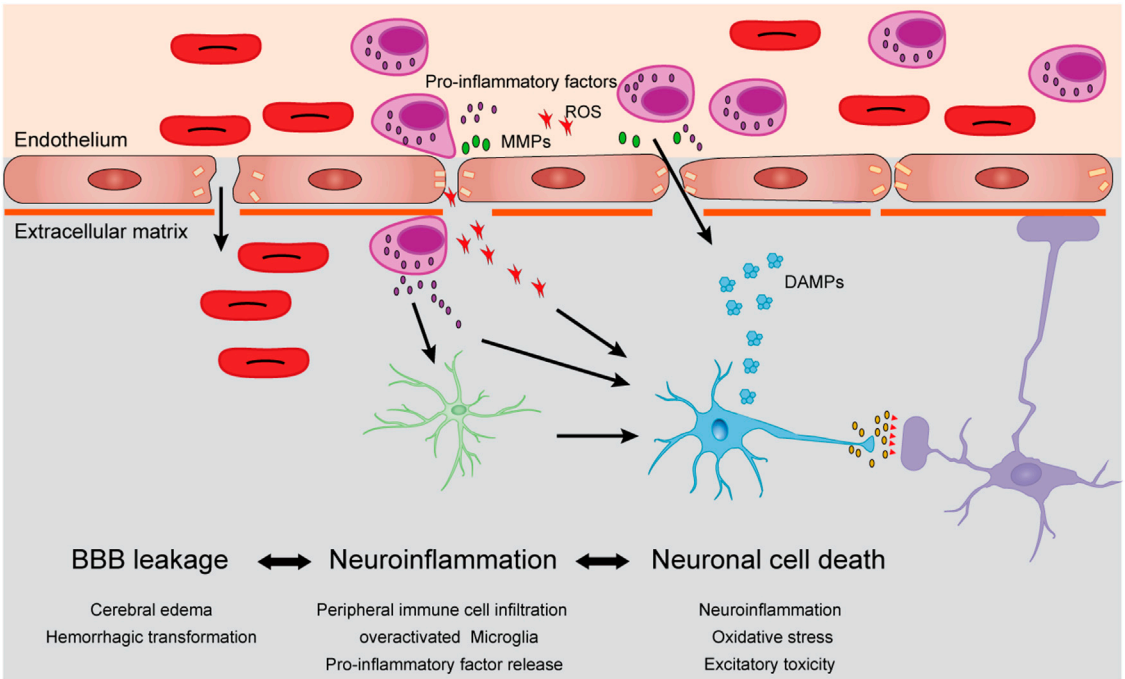

FIGURE 1 | Cellular mechanisms of cerebral ischemia/reperfusion injury. After stroke, dying cells from ischemic brain tissue begin to produce damage-related molecular patterns (DAMPs), which induced circulating neutrophils to infiltrate into ischemic brain parenchyma. Neutrophils released matrix metalloproteinases (MMPs), reactive oxygen species (ROS) and pro-inflammatory factors, accelerate their infiltration and damage the vascular endothelial cells and extracellular basal membrane, which induced brain edema and even hemorrhagic transformation. A large number of inflammatory factors and ROS can also stimulate the overactivation of microglia, which further aggravates neuronal damage caused by neuroinflammation and leads to neuronal death.

embryos, organogenesis, and maintenance of normal physiological functions in adults (Schulte and Bryja, 2017; Jean LeBlanc et al., 2019; Routledge and Scholpp, 2019).

Wnt signaling is a complex regulatory network consisting of two branches: canonical and non-canonical pathways (Eubelen et al., 2018; Routledge and Scholpp, 2019). The canonical Wnt signaling pathway, also known as the Wnt/β-catenin signaling pathway, begins with the binding of the ligand of Wnt protein with the receptors of Frizzled (FZD) and low-density lipoprotein receptor-related proteins 5 and 6 (LRP5/6), which activates a series of complex biochemical reactions and blocks the cytoplasmic β-catenin degradation pathway, thereby enabling β-catenin accumulation in the cytoplasm. After accumulation in the nucleus, β-catenin assembles with T cytokines (TCF/LEF) to form a transcription complex, which ultimately regulates the expression of target genes (Routledge and Scholpp, 2019).

Wnt proteins were discovered 30 years ago, with 19 Wnt proteins clustered into 12 subfamilies and distributed in tissues and organs across the body (Clevers and Nusse, 2012). It is noteworthy that in addition to Wnt proteins, the activity of the Wnt/β-catenin signaling pathway is also regulated by a variety of extracellular signaling molecules, such as Dickkopf proteins (DKK1-4; competitively inhibits Wnt proteins by binding to LRP5/6) and secreted Frizzled-related proteins (sFRPs; inhibits Wnt signaling by directly binding to Wnt protein) (Wang et al., 2000; Zorn, 2001). Seib et al. found that the expression of *Dkk1* gene in mouse neural stem cells in the sub granular zone increased with age and inhibited Wnt signaling activity, while neural stem cell-specific *Dkk1* knockout significantly increased Wnt signaling activity and adult neurogenesis in aged mice (Seib et al., 2013). Similarly, Zhu et al. found that the expression of *Dkk3* in neural stem cells in the subventricular zone was upregulated with age, and neurogenesis and olfactory function were downregulated in aged mice (Zhu et al., 2014). In another study, it was found that sFRP3 is highly expressed in the dentate gyrus and inhibits the proliferation of neural stem cells in the sub granular zone (Jang et al., 2013). Cho et al. showed that the knockdown of sFRP3 in the dentate gyrus significantly improved adult neurogenesis in a mouse model of premature aging induced by the mitotic checkpoint kinase *BubR1* gene mutation (Cho et al., 2019). The extracellular and intracellular Wnt/β-catenin signaling pathways are shown in **Figure 2**.

IMPLICATIONS OF WNT/β-CATENIN SIGNALING PATHWAY WITHIN NEURAL VASCULAR UNIT DURING ISCHEMIC STROKE

The CNS, including the brain and spinal cord, is characterized by a highly active metabolism and high sensitivity to extraneous substances. To maintain normal function and the microenvironment, blood vessels within the CNS have special

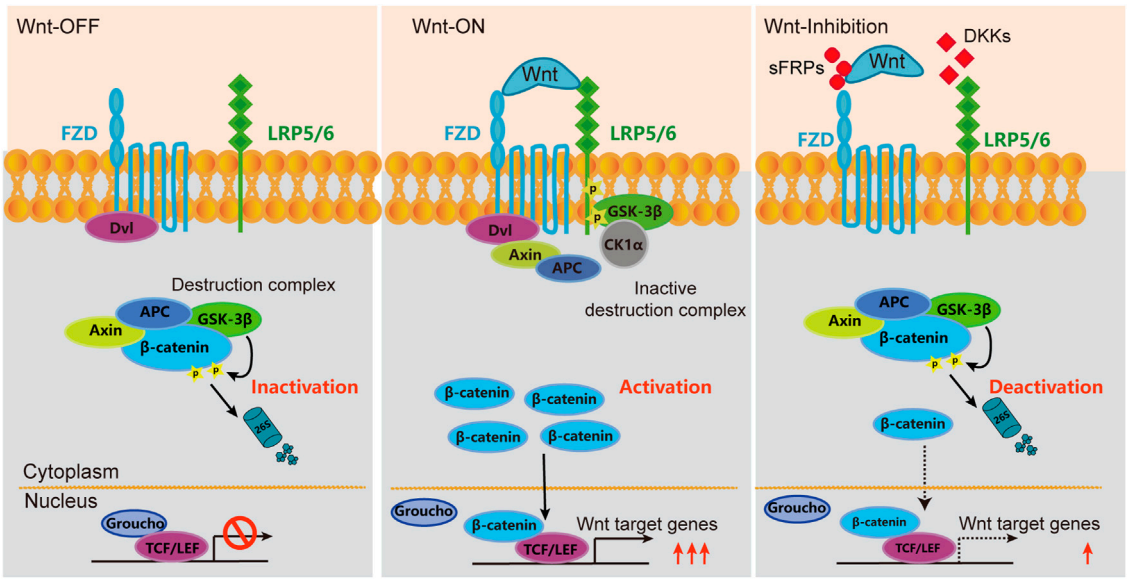

FIGURE 2 | Schematic diagram of Wnt/β-catenin signaling pathway in inactivated, activated and deactivated states. In the quiescent Wnt/β-catenin-dependent pathway (Wnt Off), β-catenin undergoes continuous ubiquitination in the absence of Wnt protein by the destruction complex. In this state, Wnt target genes are suppressed by Groucho and TCF/LEF transcription factors. Upon Wnt binding to FZD receptors and the co-receptor Lrp5/6 and formed a ligand-receptor complex called the "signalosome," which further recruit the intracellular Dvl and components of the destruction complex to the cell membrane (Wnt On). This would prohibit the formation of destruction complex and thus prevents the degradation of β-catenin and allowing its nuclear translocation. β-catenin would subsequently bind with TCF/LEF transcription factors to inhibit their DNA binding. Wnt target genes, such as *Axin2* and *Nkd1*, are disinhibited to transcript. Some extracellular molecules could inhibit the formation of signalosome. For example, DKKs can competitively bind to LRP6, while sFRPs can directly bind to Wnt proteins and reduce the activity of signal transduction.

functions that other tissue vessels do not. A notable function is maintaining the blood–brain barrier (BBB) (Liebner et al., 2008; Jean LeBlanc et al., 2019). The BBB, which mainly exists in small arteries, capillaries, and veins, blocks circulating cells and molecules from the brain parenchyma and discharges metabolites or exotic substances to maintain the low permeability of the cerebrovascular system. Structurally, the BBB mainly refers to the layer of cerebrovascular endothelial cells in direct contact with blood, which in turn closely combines with perivascular cells, extracellular matrix membranes, astrocytes, and a small number of neurons. In the NVU, these cells and noncellular matrix components interact with endothelial cells, which play an important role in supporting and regulating BBB functions (Schaeffer and Iadecola, 2021).

The Wnt/β-catenin signaling pathway plays a critical regulatory role in regulating cerebrovascular development and BBB formation during embryonic development. This is determined by the following three aspects: 1) deficiency of the endothelial Wnt/β-catenin signaling pathway affects the development of cerebrovascular and BBB, but does not affect the development and function of other organs and tissues (Stenman et al., 2008; Daneman et al., 2009); 2) knockout of *Wnt7a/7b* (which shows the highest expression in the brain tissue) or receptor *Fzd4,2,7*, *LRP5/6*, receptor activator *GPR124* in endothelial cells, or *Ctnnb1* (β-catenin) can lead to abnormal cerebrovascular development and BBB function (Cullen et al., 2011; Wang et al., 2012; Zhou et al., 2014); and 3) upregulation of the Wnt signaling activity significantly upregulates the expression of BBB-function-related genes in cultured endothelial cells (Liebner et al., 2008).

In recent years, many studies have shown that the activity of the Wnt/β-catenin signaling pathway in ischemic brain tissue is significantly decreased in animal models of cerebral ischemia-reperfusion. Clinically, some genetic variants of *Lrp6* may be correlated with the risk of ischemic stroke (Calvier et al., 2022). Additionally, the levels of plasma DKK1 have been reported to be higher in patients with acute ischemic stroke than in healthy individuals (He et al., 2016; Zhu et al., 2019; Stavrinou et al., 2021). Systematic investigation of all types of cells in the brain affected by the downregulation of Wnt signaling is still lacking. However, studies have shown that in cerebrovascular endothelial cells, neurons, pericytes, astrocytes, microglia, and oligodendrocytes, Wnt signaling not only regulates their survival and proliferation but also affects their unique biological functions.

Cerebrovascular Endothelial Cells

As the first barrier for peripheral tissue and blood components to enter the brain parenchyma, cerebrovascular endothelial cells are the core components of the BBB and have a series of special structural and molecular characteristics that determine the high selective permeability of the BBB. High expression of intercellular tight junction proteins is one of the main characteristics of cerebrovascular endothelial cells. Claudin-5, occludin, and scaffold protein ZO-1/2 are responsible for anchoring the former two proteins to the cytoskeleton (Zhao et al., 2015). A

study has shown that the liposolator-induced lipoprotein receptor LSR (angulin-1) is specifically overexpressed in the BBB and acts as a tight junction protein between the three cells to enhance BBB function (Sohet et al., 2015).

Appropriately active Wnt signaling is essential for maintaining the BBB, both structurally and functionally. A variety of co-receptors on the surface of endothelial cells can affect signal transduction through interaction with Wnt receptors. For instance, Reck, a GPI-anchored membrane protein, and Gpr124, an orphan G-protein-coupled receptor, have been implicated in Wnt7a/Wnt7b mediated canonical Wnt signaling in the CNS vascular development and functional maintenance. Cho et al. showed that cerebral vascular endothelial cell-specific knockout of *Reck* impairs CNS angiogenesis and BBB integrity (Cho et al., 2017). Another study showed that the disruption of BBB integrity under acute brain ischemia/reperfusion (I/R) was significantly weakened in mice with conditional knockout of endothelial *Gpr124*, a Wnt7-specific coactivator of Wnt/β-catenin signaling, which could be rescued by genetic activation of endothelial β-catenin (Chang et al., 2017). A follow-up study showed that the variants of *Gpr124* and *Wnt7a* are associated with an increased risk of hemorrhagic transformation in patients with acute ischemic stroke after intravenous thrombolysis (Ta et al., 2021). Mechanistically, Reck binds with low micromolar affinity to the intrinsically disordered linker region of Wnt7. This process is manifested as the interaction between Gpr124 and Dishevelled, which aggregated Gpr124 with Reck-Wnt7 into Wnt/Frizzled/Lrp5/6 complex, resulting in increased local availability of Wnt7 for downstream signaling (Eubelen et al., 2018). Most recently, an engineered *Wnt7a* mutant lacking the C-terminal domain and an embedded Frizzled-contact site could retain partial but selective activity on the Gpr124/Reck-containing receptor complexes of endothelial cells. From a therapeutic standpoint, this artificial Wnt protein can specifically target Gpr124/Reck to repair the BBB in rodent ischemic stroke and glioblastoma models (Martin et al., 2022). The above studies define a modality to repair the BBB by reactivating the endothelial Wnt/β-catenin signaling, which, therefore, may have potential therapeutic value in other CNS diseases, such as multiple sclerosis, epilepsy, and Alzheimer's disease.

The endothelial tight junctions and extracellular basal membrane ensure low passive transportation between blood and brain parenchyma. Apart from this, the profoundly low rate of transcytosis is also an important property of BBB. Although Wnt signaling has not been shown to influence transcytosis in BBB, in blood–retinal barrier (BRB), Wnt signaling directly regulate the transcription of an endothelium-specific transcytosis inhibitor called major facilitator superfamily domain-containing protein 2a (MFSD2A), in a Wnt/β-catenin-dependent manner. Mice lacking either the Lrp5 or the Wnt ligand Norrin exhibit increased retinal vascular leakage and enhanced endothelial transcytosis (Wang et al., 2020). Therefore, it can further be suggested that the Wnt/β-catenin signaling pathway possibly influences the CNS endothelium integrity by affecting the transcytosis mechanism as well (Wang et al., 2020; Yemanyi et al., 2021).

Neuron

Wnt signaling pathway has been well-established to play a critical role in neural development, axonal outgrowth, synaptogenesis, fate decision, and survival (Lie et al., 2005; Kuwabara et al., 2009; Alves dos Santos and Smidt, 2011). Dysregulation of Wnt/β-catenin signaling has also been observed in many distinct pathologies, including hepatic fibrosis, tumor growth, and ischemic stroke (Mastroiacovo et al., 2009; Okamoto et al., 2011; Clevers and Nusse, 2012). However, whether Wnt/β-catenin signaling plays a role in the functional maintenance of mature neurons and changes under pathological conditions such as neuronal injury have not been thoroughly examined. It has been reported that sustained overexpression of Wnt by lentivirus ameliorates deficient motor behavior, and increases neuronal survival by promoting axon regeneration and inhibiting astrocytic scar formation in a spinal cord injury model (Suh et al., 2011). As for ischemic stroke, intranasal administration of Wnt-3a protein has been found to reduce cerebral infarction and neuronal apoptosis, which may be mediated through the dephosphorylation of GSK-3β, which in turn increases nuclear β-catenin and relieves overactive caspase-3 through Foxm1 after ischemia/reperfusion injury (Wei et al., 2017; Matei et al., 2018). Interestingly, the dephosphorylation of GSK-3β has been shown to influence the expression of apoptotic/cell death-related and survival/neurotrophic genes, which may contribute to the pro-neuronal survival effects of Wnt/β-catenin signaling (Tang et al., 2010).

Although Wnt3a protein-mediated Wnt/β-catenin signaling activation showed a decent neuronal effect, due to its hydrophobicity, Wnt3a can barely exert any biological function through systematic administration without a cosolvent, such as detergents (e.g., CHAPS) or solubilizers (e.g., MβCD), which makes it almost impossible to conduct clinical studies. Therefore, genetic engineering-based Wnt surrogates may be a promising strategy for the development of BBB protective drugs in the future.

Oligodendrocytes

The white matter consists of axons, oligodendrocytes, and astrocytes, which are the most common injury sites for ischemic stroke (Qian et al., 2016). Neuronal axons are wrapped in myelin sheets, which are critical for the accuracy and speed of nerve signal conduction. Therefore, axonal damage is often accompanied by a reduction in myelin sheaths, known as demyelination, which accounts for the loss of oligodendrocytes.

To achieve remyelination after brain injury, oligodendrocytes must develop from oligodendrocyte precursor cells (OPCs). Wnt/β-catenin appears to play a crucial role in spatiotemporal regulation of oligodendrocyte differentiation (Garcia-Martin et al., 2021). A recent study employed transplantation of OPCs in a transient middle artery occlusion (MCAO) model and found significant functional angiogenesis and increased myelin basic protein expression (Wang et al., 2021c). Furthermore, this process is likely dependent on angiogenesis induced by Wnt7a-mediated activation of the Wnt/β-catenin signaling pathway.

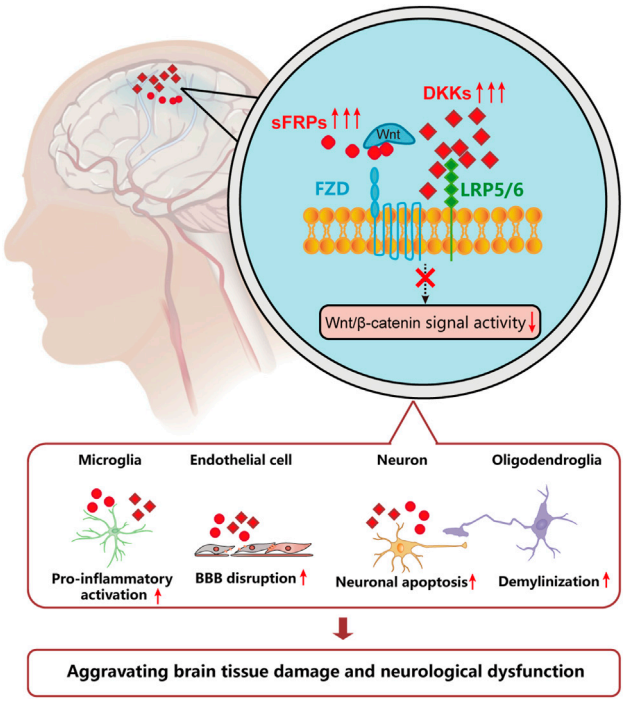

FIGURE 3 | The potential implications of Wnt/β-catenin among cells from ischemic brain. After an ischemia incident, the microenvironment in ischemic brain leads to decreased activity of Wnt/β-catenin signaling pathway. The regulatory mechanisms of which include increased level of Dkks and sFRPs, which leads to increased BBB disruption, neuronal apoptosis, demyelination, and overactivation of microglia.

Microglia

As the dominant immune cells in the CNS, microglia are well-characterized for their secretory and phagocytic properties. More importantly, microglia express various immunological receptors, which endow them with a Janus face to function in both positive and negative manner towards neurons. For instance, triggering receptor expressed in myeloid cells 2 (TREM2) is a pattern recognition receptor expressed in myeloid cells, including microglia. TREM2 was found to prohibit β-catenin degradation, thereby activating the canonical Wnt pathway (Meilandt et al., 2020). Genetically, TREM2 mutations cause abnormalities in Wnt/β-catenin signaling and microglial overactivation, which in turn increases the risk of Alzheimer's disease (Huang et al., 2022).

From the perspective of neurogenesis, microglia were found to selectively engulf synapses based on specific chemokine signals such as CR3/CX3CL1. CX3CL1 interacts with its receptor, fractalkine, specifically expressed on neurons, and thus activates microglia by phagocytosis (Cardona et al., 2006; Paolicelli et al., 2011). This process is important for maintaining an adequate number of synapses and to promote the formation of neuronal circuits. Interestingly, when the Wnt/β-catenin signaling pathway is suppressed in neurons, fractalkine expression decreases substantially, causing synapse degeneration. Therefore, Wnt signaling may play a role in microglial-involved synapse modification.

Furthermore, when the CNS is confronted with pathological conditions such as neurodegenerative diseases or ischemic stroke, the deleterious circumstance can enhance the combination of the complement fragment C1q and synapses, which causes the over-activation of microglial phagocytosis towards synapses and eventually damages the neuronal cells (Mercurio et al., 2022). Dying neurons undergo p53-mediated apoptotic signaling pathway, which leads to the expression of the downstream target gene *Dkk1* and further inactivates the Wnt/β-catenin signaling pathway (Wang et al., 2000). Meanwhile, deleterious substances from the eliminated synapses increase the delivery of inflammatory factors from microglia and further aggravate microglial inflammation and synapse damage.

Astrocytes

As a major component in CNS, astrocytes play an important role in maintaining brain function. Astrocytic abnormality has been observed in many CNS diseases, such as Alzheimer's disease, multiple sclerosis, and hemorrhagic stroke. It has been shown that the receptor of Wnt7b, Frizzled-7 was widely expressed among cells in CNS, including endothelial cells, neurons, and astrocytes. In an experimental intracerebral hemorrhage model in mice, activation of Wnt signaling by Frizzled-7 modified by CRISPR substantially reduced cerebral edema, BBB leakage,

TABLE 1 | Pharmacological agents target Wnt/β-catenin in experimental stroke.

Agents	Models	Proposed Mechanisms	References
lithium chloride	Transient MCAO in mice; Brain hemorrhage in mice	Inhibitor of GSK-3	Ji et al. (2021); Song et al. (2022)
TWS119	Permanent MCAO with hypoxia treatment in mice	Specific inhibitor of GSK-3β	Song et al. (2019)
6-bromoindirubin-3′-oxime	Transient MCAO with rtPA treatment in mice	Inhibitor of GSK-3	Jean LeBlanc et al. (2019)
Gpr124/Reck/Fz1	Transient MCAO in mice	Engineered Wnt7A fusion protein	Martin et al. (2022)
Wnt3a protein	Transient MCAO in mice	Wnt3a protein with cosolvent	Matei et al. (2018)
Wnt1 protein		Activation of Akt1	Chong et al. (2010)
Sulindac	Permanent MCAO in rat	upregulated the expression of Dvl, beta-catenin, and downregulated APC	Xing et al. (2012)
Dkk-1 antisense oligonucleotides	Permanent MCAO in mice		Cappuccio et al. (2005); Mastroiacovo et al. (2009)

and associated behavioral deficiency, while downregulated expression of Frizzled-7 markedly aggravated the above phenomenon. Further, it was found that the activation of Frizzled-7-mediated Wnt/β-catenin signaling mostly takes place in the perihematomal endothelial cells, neurons, and astrocytes (He et al., 2021). The potential implications of Wnt/β-catenin among cells from ischemic brain are depicted in **Figure 3**.

CONCLUSION

The Wnt/β-catenin signaling pathway has been proved to be involved in a variety of physiological and pathological processes. More recently, several preclinical studies have found a decline in Wnt signaling activity after stroke onset, and activators of the Wnt/β-catenin signaling pathway have shown encouraging therapeutic effects. Current mechanisms of action aiming at stimulating the Wnt/β-catenin signaling pathway mainly include inhibitors of GSK-3β phosphorylation, engineered Wnt proteins, antagonists of Wnt inhibitors (DKKs, SFRs), and agonists towards the co-receptor of Wnt receptors (**Table 1**). However, extensive studies are needed to investigate the metabolic characteristics and safety of the protein molecules used. Lithium chloride is extensively used in clinical practice to treat bipolar mood disorders. Recently, lithium has also been used as an inhibitor of GSK-3β, which is a chemical activator of the Wnt/β-catenin signaling pathway. The administration of lithium exhibits a protective effect on BBB function, as observed in an experimental mice for ischemic stroke (Ji et al., 2021; Song et al., 2022). Therefore, future clinical studies are needed to evaluate the systematic effects and safety of targeting the Wnt/β-catenin signaling pathway for the treatment of ischemic stroke. Moreover, because BBB breakdown also occurs in metastatic encephaloma, leukemia, and toxic or metabolic encephalopathy, it is worthwhile to investigate the therapeutic potential of Wnt activators in diseases involving BBB dysfunction.

AUTHOR CONTRIBUTIONS

ZM designed and drafted the manuscript. YM and JF participated in the design and writing of this manuscript. ZZ, YL, and LZ provided constructive advice and edited the manuscript. All authors contributed to the manuscript and approved the submitted version.

FUNDING

This work was supported by Science and Technology Foundation of Shenzhen. (JSGG20220226085800001 to YL, JCYJ20190812164009243 to ZZ),Guangdong Medical Research Foundation (B2020135 to LZ),National Natural Science Foundation of China (881803528 to YM, 82074278 to JF).

ACKNOWLEDGMENTS

The authors acknowledge Editage for English language editing.

REFERENCES

Alawieh, A., Pierce, A. K., Vargas, J., Turk, A. S., Turner, R. D., Chaudry, M. I., et al. (2017). The Golden 35 Min of Stroke Intervention with ADAPT: Effect of Thrombectomy Procedural Time in Acute Ischemic Stroke on Outcome. *J. Neurointerv Surg.* 10 (3), 213–220. doi:10.1136/neurintsurg-2017-013040

Albers, G. W., Marks, M. P., Kemp, S., Christensen, S., Tsai, J. P., Ortega-Gutierrez, S., et al. (2018). Thrombectomy for Stroke at 6 to 16 hours with Selection by Perfusion Imaging. *N Engl J Med.* 378 (3), 708–718. doi:10.1056/NEJMoa1713973

Alves dos Santos, M. T., and Smidt, M. P. (2011). En1 and Wnt Signaling in Midbrain Dopaminergic Neuronal Development. *Neural Dev.* 6, 23. doi:10.1186/1749-8104-6-23

Calvier, L., Herz, J., and Hansmann, G. (2022). Interplay of Low-Density Lipoprotein Receptors, LRPs, and Lipoproteins in Pulmonary Hypertension. *JACC Basic Transl. Sci.* 7 (2), 164–180. doi:10.1016/j.jacbts.2021.09.011

Cappuccio, I., Calderone, A., Busceti, C. L., Biagioni, F., Pontarelli, F., Bruno, V., et al. (2005). Induction of Dickkopf-1, a Negative Modulator of the Wnt Pathway, Is Required for the Development of Ischemic Neuronal Death. *J. Neurosci.* 25 (10), 2647–2657. doi:10.1523/JNEUROSCI.5230-04.2005

Cardona, A. E., Pioro, E. P., Sasse, M. E., Kostenko, V., Cardona, S. M., Dijkstra, I. M., et al. (2006). Control of Microglial Neurotoxicity by the Fractalkine Receptor. *Nat. Neurosci.* 9 (7), 917–924. doi:10.1038/nn1715

Chamorro, Á., Dirnagl, U., Urra, X., and Planas, A. M. (2016). Neuroprotection in Acute Stroke: Targeting Excitotoxicity, Oxidative and Nitrosative Stress, and Inflammation. *Lancet Neurol.* 15 (8), 869–881. doi:10.1016/S1474-4422(16)00114-9

Chang, J., Mancuso, M. R., Maier, C., Liang, X., Yuki, K., Yang, L., et al. (2017). Gpr124 Is Essential for Blood-Brain Barrier Integrity in Central Nervous System Disease. *Nat. Med.* 23 (4), 450–460. doi:10.1038/nm.4309

Cheng, P., Liao, H. Y., and Zhang, H. H. (2022). The Role of Wnt/mTOR Signaling in Spinal Cord Injury. *J. Clin. Orthop. Trauma* 25, 101760. doi:10.1016/j.jcot.2022.101760

Cho, C., Smallwood, P. M., and Nathans, J. (2017). Reck and Gpr124 Are Essential Receptor Cofactors for Wnt7a/Wnt7b-specific Signaling in Mammalian CNS Angiogenesis and Blood-Brain Barrier Regulation. *Neuron* 95 (5), 1221–1225. doi:10.1016/j.neuron.2017.08.032

Cho, C. H., Yoo, K. H., Oliveros, A., Paulson, S., Hussaini, S. M. Q., van Deursen, J. M., et al. (2019). sFRP3 Inhibition Improves Age-Related Cellular Changes in BubR1 Progeroid Mice. *Aging Cell* 18 (2), e12899. doi:10.1111/acel.12899

Chong, Z. Z., Shang, Y. C., Hou, J., and Maiese, K. (2010). Wnt1 Neuroprotection Translates into Improved Neurological Function during Oxidant Stress and Cerebral Ischemia through AKT1 and Mitochondrial Apoptotic Pathways. *Oxid. Med. Cell Longev.* 3 (2), 153–165. doi:10.4161/oxim.3.2.11758

Clevers, H., and Nusse, R. (2012). Wnt/β-catenin Signaling and Disease. *Cell* 149 (6), 1192–1205. doi:10.1016/j.cell.2012.05.012

Collaborators, G. B. D. S. (2019). Global, Regional, and National Burden of Stroke, 1990-2016: a Systematic Analysis for the Global Burden of Disease Study 2016. *Lancet Neurol.* 18 (5), 439–458. doi:10.1016/S1474-4422(19)30034-1

Cullen, M., Elzarrad, M. K., Seaman, S., Zudaire, E., Stevens, J., Yang, M. Y., et al. (2011). GPR124, an Orphan G Protein-Coupled Receptor, Is Required for CNS-specific Vascularization and Establishment of the Blood-Brain Barrier. *Proc. Natl. Acad. Sci. U. S. A.* 108 (14), 5759–5764. doi:10.1073/pnas.1017192108

Daneman, R., Agalliu, D., Zhou, L., Kuhnert, F., Kuo, C. J., and Barres, B. A. (2009). Wnt/beta-catenin Signaling Is Required for CNS, but Not Non-CNS,

Angiogenesis. *Proc. Natl. Acad. Sci. U. S. A.* 106 (2), 641–646. doi:10.1073/pnas.0805165106

Emberson, J., Lees, K. R., Lyden, P., Blackwell, L., Albers, G., Bluhmki, E., et al. (2014). Effect of Treatment Delay, Age, and Stroke Severity on the Effects of Intravenous Thrombolysis with Alteplase for Acute Ischaemic Stroke: a Meta-Analysis of Individual Patient Data from Randomised Trials. *Lancet* 384 (9958), 1929–1935. doi:10.1016/S0140-6736(14)60584-5

Eubelen, M., Bostaille, N., Cabochette, P., Gauquier, A., Tebabi, P., Dumitru, A. C., et al. (2018). A Molecular Mechanism for Wnt Ligand-specific Signaling. *Science* 361 (6403), eaat1178. doi:10.1126/science.aat1178

Garcia-Martin, G., Alcover-Sanchez, B., and Wandosell, F. (2021). Pathways Involved in Remyelination after Cerebral Ischemia. *Curr. Neuropharmacol.* 20 (4), 751–765. doi:10.2174/1570159X19666210610093658

He, W., Lu, Q., Sherchan, P., Huang, L., Hu, X., Zhang, J. H., et al. (2021). Activation of Frizzled-7 Attenuates Blood-Brain Barrier Disruption through Dvl/β-catenin/WISP1 Signaling Pathway after Intracerebral Hemorrhage in Mice. *Fluids Barriers CNS* 18 (1), 44. doi:10.1186/s12987-021-00278-9

He, X. W., Wang, E., Bao, Y. Y., Wang, F., Zhu, M., Hu, X. F., et al. (2016). High Serum Levels of Sclerostin and Dickkopf-1 Are Associated with Acute Ischaemic Stroke. *Atherosclerosis* 253, 22–28. doi:10.1016/j.atherosclerosis.2016.08.003

Huang, S., Liao, X., Wu, J., Zhang, X., Li, Y., Xiang, D., et al. (2022). The Microglial Membrane Receptor TREM2 Mediates Exosome Secretion to Promote Phagocytosis of Amyloid-β by Microglia. *FEBS Lett.* 596 (8), 1059–1071. doi:10.1002/1873-3468.14336

Jang, M. H., Bonaguidi, M. A., Kitabatake, Y., Sun, J., Song, J., Kang, E., et al. (2013). Secreted Frizzled-Related Protein 3 Regulates Activity-dependent Adult Hippocampal Neurogenesis. *Cell Stem Cell* 12 (2), 215–223. doi:10.1016/j.stem.2012.11.021

Jean LeBlanc, N., Menet, R., Picard, K., and Parent, G. (2019). Canonical Wnt Pathway Maintains Blood-Brain Barrier Integrity upon Ischemic Stroke and its Activation Ameliorates Tissue Plasminogen Activator Therapy. *Mol. Neurobiol.* 56 (9), 6521–6538. doi:10.1007/s12035-019-1539-9

Ji, Y. B., Gao, Q., Tan, X. X., Huang, X. W., Ma, Y. Z., Fang, C., et al. (2021). Lithium Alleviates Blood-Brain Barrier Breakdown after Cerebral Ischemia and Reperfusion by Upregulating Endothelial Wnt/β-Catenin Signaling in Mice. *Neuropharmacology* 186, 108474. doi:10.1016/j.neuropharm.2021.108474

Kuwabara, T., Hsieh, J., Muotri, A., Yeo, G., Warashina, M., Lie, D. C., et al. (2009). Wnt-mediated Activation of NeuroD1 and Retro-Elements during Adult Neurogenesis. *Nat. Neurosci.* 12 (9), 1097–1105. doi:10.1038/nn.2360

Lie, D. C., Colamarino, S. A., Song, H. J., Désiré, L., Mira, H., Consiglio, A., et al. (2005). Wnt Signalling Regulates Adult Hippocampal Neurogenesis. *Nature* 437 (7063), 1370–1375. doi:10.1038/nature04108

Liebner, S., Corada, M., Bangsow, T., Babbage, J., Taddei, A., Czupalla, C. J., et al. (2008). Wnt/beta-catenin Signaling Controls Development of the Blood-Brain Barrier. *J. Cell Biol.* 183 (3), 409–417. doi:10.1083/jcb.200806024

Ma, H., Campbell, B. C. V., Parsons, M. W., Churilov, L., Levi, C. R., Hsu, C., et al. (2019). Thrombolysis Guided by Perfusion Imaging up to 9 hours after Onset of Stroke. *N. Engl. J. Med.* 380 (19), 1795–1803. doi:10.1056/NEJMoa1813046

Martin, M., Vermeiren, S., Bostaille, N., Eubelen, M., Spitzer, D., Vermeersch, M., et al. (2022). Engineered Wnt Ligands Enable Blood-Brain Barrier Repair in Neurological Disorders. *Science* 375 (6582), eabm4459. doi:10.1126/science.abm4459

Mastroiacovo, F., Busceti, C. L., Biagioni, F., Moyanova, S. G., Meisler, M. H., Battaglia, G., et al. (2009). Induction of the Wnt Antagonist, Dickkopf-1, Contributes to the Development of Neuronal Death in Models of Brain Focal Ischemia. *J. Cereb. Blood Flow. Metab.* 29 (2), 264–276. doi:10.1038/jcbfm.2008.111

Matei, N., Camara, J., McBride, D., Camara, R., Xu, N., Tang, J., et al. (2018). Intranasal Wnt3a Attenuates Neuronal Apoptosis through Frz1/PIWIL1a/FOXM1 Pathway in MCAO Rats. *J. Neurosci.* 38 (30), 6787–6801. doi:10.1523/JNEUROSCI.2352-17.2018

Meilandt, W. J., Ngu, H., Gogineni, A., Lalehzadeh, G., Lee, S. H., Srinivasan, K., et al. (2020). Trem2 Deletion Reduces Late-Stage Amyloid Plaque Accumulation, Elevates the Aβ42:Aβ40 Ratio, and Exacerbates Axonal Dystrophy and Dendritic Spine Loss in the PS2APP Alzheimer's Mouse Model. *J. Neurosci.* 40 (9), 1956–1974. doi:10.1523/JNEUROSCI.1871-19.2019

Menet, R., Lecordier, S., and ElAli, A. (2020). Wnt Pathway: An Emerging Player in Vascular and Traumatic Mediated Brain Injuries. *Front. Physiol.* 11, 565667. doi:10.3389/fphys.2020.565667

Mercurio, D., Fumagalli, S., Schafer, M. K., Pedragosa, J., Ngassam, L. D. C., Wilhelmi, V., et al. (2022). Protein Expression of the Microglial Marker Tmem119 Decreases in Association with Morphological Changes and Location in a Mouse Model of Traumatic Brain Injury. *Front. Cell Neurosci.* 16, 820127. doi:10.3389/fncel.2022.820127

Moskowitz, M. A., Lo, E. H., and Iadecola, C. (2010). The Science of Stroke: Mechanisms in Search of Treatments. *Neuron* 67 (2), 181–198. doi:10.1016/j.neuron.2010.07.002

O'Collins, V. E., Macleod, M. R., Donnan, G. A., Horky, L. L., van der Worp, B. H., and Howells, D. W. (2006). 1,026 Experimental Treatments in Acute Stroke. *Ann. Neurol.* 59 (3), 467–477. doi:10.1002/ana.20741

Okamoto, M., Inoue, K., Iwamura, H., Terashima, K., Soya, H., Asashima, M., et al. (2011). Reduction in Paracrine Wnt3 Factors during Aging Causes Impaired Adult Neurogenesis. *FASEB J.* 25 (10), 3570–3582. doi:10.1096/fj.11-184697

Paolicelli, R. C., Bolasco, G., Pagani, F., Maggi, L., Scianni, M., Panzanelli, P., et al. (2011). Synaptic Pruning by Microglia Is Necessary for Normal Brain Development. *Science* 333 (6048), 1456–1458. doi:10.1126/science.1202529

Phipps, M. S., and Cronin, C. A. (2020). Management of Acute Ischemic Stroke. *BMJ* 368, l6983. doi:10.1136/bmj.l6983

Powers, W. J., Rabinstein, A. A., Ackerson, T., Adeoye, O. M., Bambakidis, N. C., Becker, K., et al. (2019). Guidelines for the Early Management of Patients with Acute Ischemic Stroke: 2019 Update to the 2018 Guidelines for the Early Management of Acute Ischemic Stroke: A Guideline for Healthcare Professionals from the American Heart Association/American Stroke Association. *Stroke* 50 (12), e344–e418. doi:10.1161/STR.0000000000000211

Qian, C., Li, P. C., Jiao, Y., Yao, H. H., Chen, Y. C., Yang, J., et al. (2016). Precise Characterization of the Penumbra Revealed by MRI: A Modified Photothrombotic Stroke Model Study. *PLoS One* 11 (4), e0153756. doi:10.1371/journal.pone.0153756

Qiu, Y. M., Zhang, C. L., Chen, A. Q., Wang, H. L., Zhou, Y. F., Li, Y. N., et al. (2021). Immune Cells in the BBB Disruption after Acute Ischemic Stroke: Targets for Immune Therapy? *Front. Immunol.* 12, 678744. doi:10.3389/fimmu.2021.678744

Richards, C. L., Malouin, F., and Nadeau, S. (2015). Stroke Rehabilitation: Clinical Picture, Assessment, and Therapeutic Challenge. *Prog. Brain Res.* 218, 253–280. doi:10.1016/bs.pbr.2015.01.003

Routledge, D., and Scholpp, S. (2019). Mechanisms of Intercellular Wnt Transport. *Development* 146 (10), dev176073. doi:10.1242/dev.176073

Schaeffer, S., and Iadecola, C. (2021). Revisiting the Neurovascular Unit. *Nat Neurosci*.24, 1198. doi:10.1038/s41593-021-00904-7

Schulte, G., and Bryja, V. (2017). WNT Signalling: Mechanisms and Therapeutic Opportunities. *Br. J. Pharmacol.* 174 (24), 4543–4546. doi:10.1111/bph.14065

Seib, D. R., Corsini, N. S., Ellwanger, K., Plaas, C., Mateos, A., Pitzer, C., et al. (2013). Loss of Dickkopf-1 Restores Neurogenesis in Old Age and Counteracts Cognitive Decline. *Cell Stem Cell* 12 (2), 204–214. doi:10.1016/j.stem.2012.11.010

Sohet, F., Lin, C., Munji, R. N., Lee, S. Y., Ruderisch, N., Soung, A., et al. (2015). LSR/angulin-1 Is a Tricellular Tight Junction Protein Involved in Blood-Brain Barrier Formation. *J. Cell Biol.* 208 (6), 703–711. doi:10.1083/jcb.201410131

Song, D., Zhang, X., Chen, J., Liu, X., Xue, J., Zhang, L., et al. (2019). Wnt Canonical Pathway Activator TWS119 Drives Microglial Anti-inflammatory Activation and Facilitates Neurological Recovery Following Experimental Stroke. *J. Neuroinflammation* 16 (1), 256. doi:10.1186/s12974-019-1660-8

Song, D., Ji, Y. B., Huang, X. W., and Ma, YZ (2022). Lithium Attenuates Blood-Brain Barrier Damage and Brain Edema Following Intracerebral Hemorrhage via an Endothelial Wnt/beta-Catenin Signaling-dependent Mechanism in Mice. *CNS Neurosci Ther*.28. doi:10.1111/cns.13832

Stavrinou, E., Sarafidis, P. A., Loutradis, C., Memmos, E., Faitatzidou, D., Giamalis, P., et al. (2021). Associations of Serum Sclerostin and Dickkopf-Related Protein-1 Proteins with Future Cardiovascular Events and Mortality in Haemodialysis Patients: a Prospective Cohort Study. *Clin. Kidney J.* 14 (4), 1165–1172. doi:10.1093/ckj/sfaa069

Stenman, J. M., Rajagopal, J., Carroll, T. J., Ishibashi, M., McMahon, J., and McMahon, A. P. (2008). Canonical Wnt Signaling Regulates Organ-specific

Assembly and Differentiation of CNS Vasculature. *Science* 322 (5905), 1247–1250. doi:10.1126/science.1164594

Suh, H. I., Min, J., Choi, K. H., Kim, S. W., Kim, K. S., and Jeon, S. R. (2011). Axonal Regeneration Effects of Wnt3a-Secreting Fibroblast Transplantation in Spinal Cord-Injured Rats. *Acta Neurochir. (Wien)* 153 (5), 1003–1010. doi:10.1007/s00701-011-0945-1

Ta, S., Rong, X., Guo, Z. N., Jin, H., Zhang, P., Li, F., et al. (2021). Variants of WNT7A and GPR124 Are Associated with Hemorrhagic Transformation Following Intravenous Thrombolysis in Ischemic Stroke. *CNS Neurosci. Ther.* 27 (1), 71–81. doi:10.1111/cns.13457

Tang, Z., Arjunan, P., Lee, C., Li, Y., Kumar, A., Hou, X., et al. (2010). Survival Effect of PDGF-CC Rescues Neurons from Apoptosis in Both Brain and Retina by Regulating GSK3beta Phosphorylation. *J. Exp. Med.* 207 (4), 867–880. doi:10.1084/jem.20091704

Wang, H. Y., Ye, J. R., Cui, L. Y., and Chu, S. F. (2021). Regulatory T Cells in Ischemic Stroke. *Acta Pharmacol. Sin.* 43 (1), 1–9. doi:10.1038/s41401-021-00641-4

Wang, J., Shou, J., and Chen, X. (2000). Dickkopf-1, an Inhibitor of the Wnt Signaling Pathway, Is Induced by P53. *Oncogene* 19 (14), 1843–1848. doi:10.1038/sj.onc.1203503

Wang, L. P., Geng, J., Qu, M., and Yuan, F (2021). Oligodendrocyte Precursor Cell Transplantation Promotes Angiogenesis and Remyelination via Wnt/beta-Catenin Pathway in a Mouse Model of Middle Cerebral Artery Occlusion. *J. Cereb. Blood Flow. Metab.* 11 (1), 9. doi:10.1038/s41419-019-2206-9

Wang, R., Zhu, Y., Liu, Z., Chang, L., Bai, X., Kang, L., et al. (2021). Neutrophil Extracellular Traps Promote tPA-Induced Brain Hemorrhage via cGAS in Mice with Stroke. *Blood*. 138 (6), 91–103. doi:10.1182/blood.2020008913

Wang, Y., Rattner, A., Zhou, Y., Williams, J., Smallwood, P. M., and Nathans, J. (2012). Norrin/Frizzled4 Signaling in Retinal Vascular Development and Blood Brain Barrier Plasticity. *Cell* 151 (6), 1332–1344. doi:10.1016/j.cell.2012.10.042

Wang, Z., Liu, C. H., Huang, S., Fu, Z., Tomita, Y., Britton, W. R., et al. (2020). Wnt Signaling Activates MFSD2A to Suppress Vascular Endothelial Transcytosis and Maintain Blood-Retinal Barrier. *Sci. Adv.* 6 (35), eaba7457. doi:10.1126/sciadv.aba7457

Wei, Z. Z., Zhang, J. Y., Taylor, T. M., Gu, X., Zhao, Y., and Wei, L. (2017). Neuroprotective and Regenerative Roles of Intranasal Wnt-3a Administration after Focal Ischemic Stroke in Mice. *J. Cereb. Blood Flow. Metab.* 38 (3), 404–421. doi:10.1177/0271678x17702669

Xing, Y., Zhang, X., Zhao, K., Cui, L., Wang, L., Dong, L., et al. (2012). Beneficial Effects of Sulindac in Focal Cerebral Ischemia: a Positive Role in Wnt/β-Catenin Pathway. *Brain Res.* 1482, 71–80. doi:10.1016/j.brainres.2012.08.057

Yang, P., Zhang, Y., Zhang, L., Zhang, Y., Treurniet, K. M., Chen, W., et al. (2020). Endovascular Thrombectomy with or without Intravenous Alteplase in Acute Stroke. *N. Engl. J. Med.* 382 (21), 1981–1993. doi:10.1056/NEJMoa2001123

Yemanyi, F., Bora, K., Blomfield, A. K., Wang, Z., and Chen, J. (2021). Wnt Signaling in Inner Blood-Retinal Barrier Maintenance. *Int. J. Mol. Sci.* 22 (21). doi:10.3390/ijms222111877

Zhao, Z., Nelson, A. R., Betsholtz, C., and Zlokovic, B. V. (2015). Establishment and Dysfunction of the Blood-Brain Barrier. *Cell* 163 (5), 1064–1078. doi:10.1016/j.cell.2015.10.067

Zhou, Y., Wang, Y., Tischfield, M., Williams, J., Smallwood, P. M., Rattner, A., et al. (2014). Canonical WNT Signaling Components in Vascular Development and Barrier Formation. *J. Clin. Invest.* 124 (9), 3825–3846. doi:10.1172/JCI76431

Zhou, Z., Lu, J., Liu, W. W., Manaenko, A., Hou, X., Mei, Q., et al. (2018). Advances in Stroke Pharmacology. *Pharmacol Ther*. 191 (7), 23–42. doi:10.1016/j.pharmthera.2018.05.012

Zhu, Y., Demidov, O. N., Goh, A. M., Virshup, D. M., Lane, D. P., and Bulavin, D. V. (2014). Phosphatase WIP1 Regulates Adult Neurogenesis and WNT Signaling during Aging. *J. Clin. Invest.* 124 (7), 3263–3273. doi:10.1172/JCI73015

Zhu, Z., Guo, D., Zhong, C., Wang, A., Xie, X., Xu, T., et al. (2019). Serum Dkk-1 (Dickkopf-1) Is a Potential Biomarker in the Prediction of Clinical Outcomes Among Patients with Acute Ischemic Stroke. *Arterioscler. Thromb. Vasc. Biol.* 39 (2), 285–293. doi:10.1161/ATVBAHA.118.311960

Zorn, A. M. (2001). Wnt Signalling: Antagonistic Dickkopfs. *Curr. Biol.* 11 (15), R592–R595. doi:10.1016/s0960-9822(01)00360-8

Conflict of Interest: The authors declare that the research was conducted in the absence of any commercial or financial relationships that could be construed as a potential conflict of interest.

Publisher's Note: All claims expressed in this article are solely those of the authors and do not necessarily represent those of their affiliated organizations, or those of the publisher, the editors and the reviewers. Any product that may be evaluated in this article, or claim that may be made by its manufacturer, is not guaranteed or endorsed by the publisher.

frontiers | Frontiers in Pharmacology

ORIGINAL RESEARCH
published: 25 May 2022
doi: 10.3389/fphar.2022.904857

Comparative Metabolomics Analysis Reveals Key Metabolic Mechanisms and Protein Biomarkers in Alzheimer's Disease

Zhao Dai[1,2], Tian Hu[1], Shijie Su[1], Jinman Liu[1], Yinzhong Ma[3], Yue Zhuo[3], Shuhuan Fang[1], Qi Wang[1], Zhizhun Mo[4], Huafeng Pan[1]* and Jiansong Fang[1]**

[1]Science and Technology Innovation Center, Guangzhou University of Chinese Medicine, Guangzhou, China, [2]Department of Rheumatology, First Affiliated Hospital of Guangzhou University of Chinese Medicine, Guangzhou, China, [3]Institute of Biomedicine and Biotechnology, Shenzhen Institute of Advanced Technology, Chinese Academy of Sciences, Shenzhen, China, [4]Emergency Department, Shenzhen Traditional Chinese Medicine Hospital, Shenzhen, China

OPEN ACCESS

Edited by:
Liu Qing-Shan,
Minzu University of China, China

Reviewed by:
Yi Yan,
LMU Munich University Hospital, Germany
Yin Huang,
China Pharmaceutical University, China

***Correspondence:**
Zhizhun Mo
mozhizhun@126.com
Huafeng Pan
gzphf@gzucm.edu.cn
Jiansong Fang
fangjs@gzucm.edu.cn

Specialty section:
This article was submitted to Neuropharmacology, a section of the journal Frontiers in Pharmacology

Received: 26 March 2022
Accepted: 19 April 2022
Published: 25 May 2022

Citation:
Dai Z, Hu T, Su S, Liu J, Ma Y, Zhuo Y, Fang S, Wang Q, Mo Z, Pan H and Fang J (2022) Comparative Metabolomics Analysis Reveals Key Metabolic Mechanisms and Protein Biomarkers in Alzheimer's Disease. Front. Pharmacol. 13:904857. doi: 10.3389/fphar.2022.904857

Alzheimer's disease (AD) is one of the most common progressive neurodegenerative diseases, accompanied by global alterations in metabolic profiles. In the past 10 years, over hundreds of metabolomics studies have been conducted to unravel metabolic changes in AD, which provides insight into the identification of potential biomarkers for diagnosis, treatment, and prognostic assessment. However, since different species may lead to systemic abnormalities in metabolomic profiles, it is urgently needed to perform a comparative metabolomics analysis between AD animal models and human patients. In this study, we integrated 78 metabolic profiles from public literatures, including 11 metabolomics studies in different AD mouse models and 67 metabolomics studies from AD patients. Metabolites and enrichment analysis were further conducted to reveal key metabolic pathways and metabolites in AD. We totally identified 14 key metabolites and 16 pathways that are both differentially significant in AD mouse models and patients. Moreover, we built a metabolite-target network to predict potential protein markers in AD. Finally, we validated HER2 and NDF2 as key protein markers in APP/PS1 mice. Overall, this study provides a comprehensive strategy for AD metabolomics research, contributing to understanding the pathological mechanism of AD.

Keywords: Alzheimer's disease, metabolome, biomarker, HER2, NDF2

1 INTRODUCTION

The prevalence of neurodegenerative disorder dementia is projected to increase from 50 million individuals worldwide in 2010 to 113 million individuals by 2050 (Knopman et al., 2021). Alzheimer's disease (AD) is the most common cause of dementia leading to cognitive impairment. The core pathological hallmarks of AD is characterized by accumulation of extracellular β-amyloid (Aβ) plaques and intracellular neurofibrillary tangles (NFTs) composed of hyperphosphorylated tau protein (Long and Holtzman, 2019). However, no anti-amyloid or anti-tau small molecule approved by the United States Food and Drug Administration (FDA) currently exist, with many clinical trials for such AD treatments having failed in the past decade (Cummings et al., 2020; Fang et al., 2020). Accumulating evidence have suggested both pathologies of Aβ and tau have synergistic effects but not act independently (Busche and Hyman, 2020). Recently our group have demonstrated that dually targeting the molecular

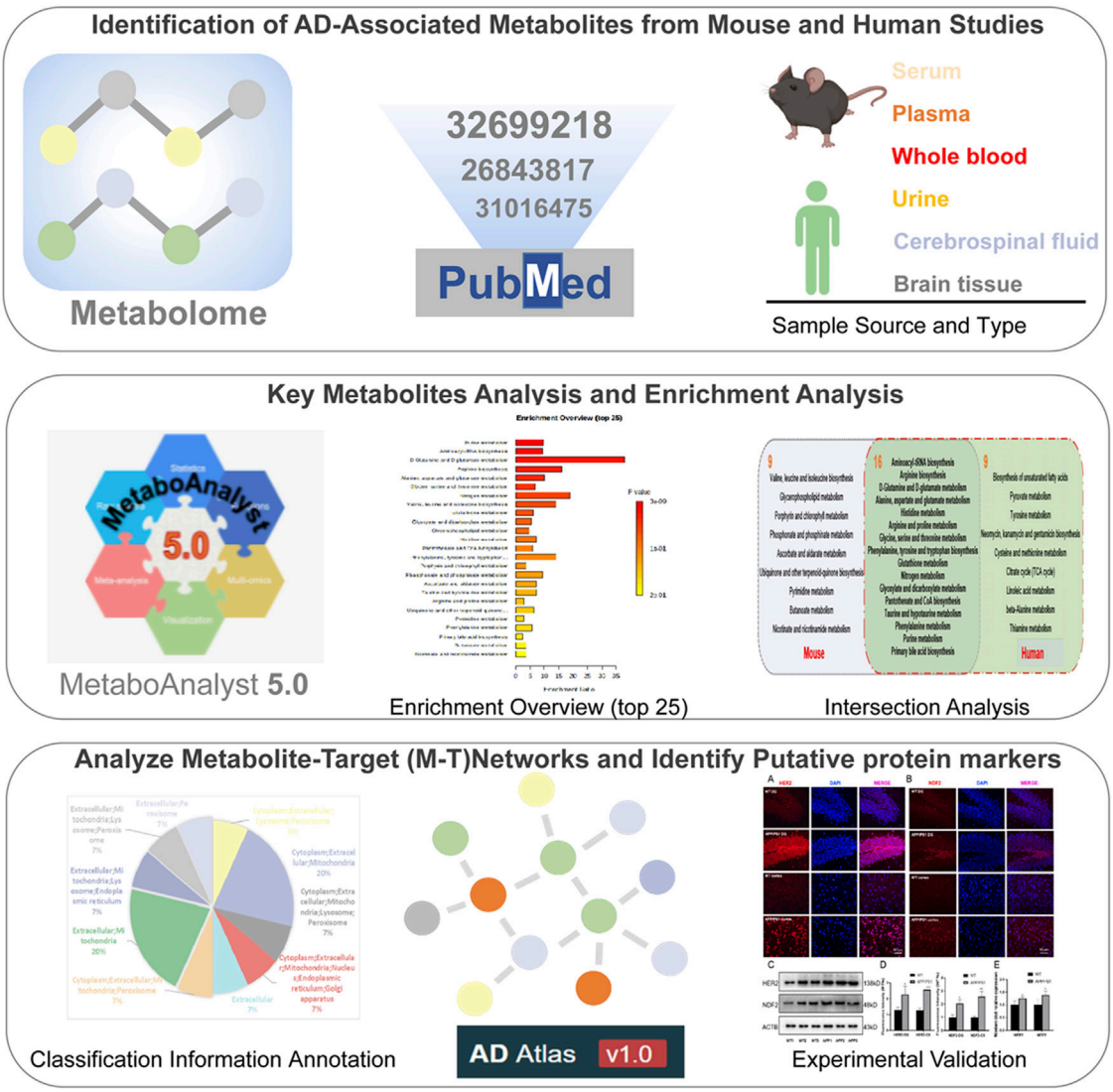

FIGURE 1 | Workflow of the experimental scheme.

network intersection of amyloid and tau endophenotypes provide the greatest potential in AD drug discovery (Fang et al., 2021).

Despite significant progress in our understanding of the underlying pathological mechanisms involved in AD, the relationships between systemic abnormalities in metabolism and the pathogenesis of AD are poorly understood. Metabolites are located in downstream of genes and proteins and are most relevant to phenotypic outcomes (Nicholson et al., 2002), allowing more sensitive detection of subtle fluctuations in disease system processes (Bundy et al., 2002). At the same time, it is distinct from the genome and proteome involving different isoforms and is structurally conserved across species. Metabolite detection is an effective means to discover new AD biomarkers (Bundy et al., 2002). Metabolome profiling and positron emission tomography (PET) neuroimaging techniques demonstrate that brain hypoglycemia in AD patients precedes cognitive impairment (Petersen et al., 2000). Proton Magnetic Resonance Spectroscopy (^{1}H-MRS) in animal experiments indicates that metabolic changes exist before overt cognitive impairment in early AD (Chen et al., 2012). Large-scale AD multimodal biomarker discovery study suggests that plasma metabolites primary fatty acid amides (PFAMs) have been found increased and associated with Aβ burden in cerebrospinal fluid (CSF) and clinical measures (Min et al., 2019). Integrative metabolomics-genomics approach reveals that increase of circulating adiponectin and metabolite-dependent ABCA1 mRNA expression could be a compensatory effect against Alzheimer's disease (Horgusluoglu et al., 2021). The analysis of metabolomics has far-reaching significance for in-depth understanding of the pathogenesis of AD and the search for more accurate disease targets. However, based on the complexity of the metabolites, different tissue distributions, different detection

TABLE 1 | The summary information of metabolomics studies in AD mouse models.

ID	PMID	Year	Metabolome technique	Animal model	Gender	Age (month)	Sample	Targeted or untargeted	Statistics	Filter criteria
1	32699218	2020	UPLC-QTQF, LC-MS, MRM HILIC–LC–MS/MS, HILIC–LC–QTOF, GC–MS	APP/PS1	Male	6, 12, 24	Brain, spleen	Both	t test	$p < 0.05$
2	33197957	2020	UHPLC-MRM-MS	3xTg	Male	2, 6	Hippocampus	Targeted	Student's t test	$p < 0.05$
3	26843817	2015	UPLC/MS	APP/PS1	Male	7	Brains	Unknown	Student's t test	$p < 0.05$, VIP < 1.5
4	31016475	2019	GC-TOF-MS	APP/PS1	Both	4.5	Brain (cortex, hippocampus, midbrain, cerebellum), plasma	Unknown	Two-tailed independent t test	$p < 0.05$
5	26827653	2015	Quantitative mass spectrometry	APP/PS1	Male	6, 8, 10, 12, 18	Brain, Plasma	Targeted	Nonparametric 1-way analysis of variance analysis (Kruskal-Wallis)	$p < 0.05$
6	32033569	2020	LC-MS	5xFAD	Male	6, 8, 12	Hippocampal	Untargeted	Independent t test	FDR adjusted p-value (q-value) < 0.05
7	29107091	2017	^{1}H NMR spectroscopy	APP/PS1	Male	1, 5, 10	Brain	Unknown	Student's t test with Bonferroni adjustment	Bonferroni adjusted p value < 0.05
8	28411106	2017	MALDI-MSI	3xTg	Male	unknown	Brain	Untargeted	t test	$p < 0.01$
9	24145382	2014	^{1}H NMR spectroscopy	Tg2576	Male	1, 3, 6, 11	Brain (frontal cortex, rhinal cortex, hippocampus, midbrain, cerebellum)	Unknown	CV-ANOVA	Q2 > 0.5, p-value < 0.05, response permutation test, p-values of t-tests <0.05
10	25281826	2014	GC–MS UPLC–MS	APP/PS1	Both	6	Brain (cortex and cerebellum)	Unknown	t-test with Bonferroni correction	VIP < 1.5, $p < 0.05$
11	25459942	2014	QTOF-MS	APP/PS1	Both	6	Brain (hippocampus, cortex, cerebellum, olfactory bulbs)	Untargeted	t-test with Bonferroni correction	VIP < 1.5, $p < 0.05$

techniques, different populations and species can systemic abnormalities in metabolomic profiles. In this study, to compare AD-specific metabolomics alterations between AD animal models and human patients, we integrate multiple metabolic profiles from AD patients (Xie et al., 2021) and mouse models. Significant metabolic pathways and metabolites are identified in AD. Then we further speculate potential targets through constructing and analyzing metabolite-target (M-T) networks, and verify potential protein markers *via* molecular biology experiments (**Figure 1**).

2 MATERIALS AND METHODS

2.1 Identification of Alzheimer's Disease-Associated Metabolites From Mouse and Human Studies

AD-related mouse brain tissue metabolites were derived from 11 literatures, including four transgenic mouse, which are APPswe/PS1dE9 (APP/PS1), Triple transgenic (3xTg), AβPPswe Tg2576 and 5 familial AD mutations (5xFAD). Detailed animal model information is presented in **Supplementary Material**. The age of mice covers from 1 to 24 months, and the gender includes male and female. The detection methods involve GC-TOF-MS, ^{1}H NMR spectroscopy, MALDI-MSI, etc. All the metabolites collected are significant in data preprocessing with p value < 0.05 or adjusted p value < 0.05. The detailed information are provided in **Table 1**.

AD-related human metabolites were collected from one recent systematic review (Xie et al., 2021), which summarized 67 AD or mild cognitive impairment (MCI) patient metabolic profiling studies. Among the 67 studies, the number of AD cases ranged from 7 to 1,356, the number of MCI cases ranged from 10 to 356, and the number of healthy controls ranged from 7 to 23,882. The biosample sources included serum, plasma, brain tissue, cerebrospinal fluid, saliva, and urine. We then analyzed the frequency of differential metabolites in these studies. The detailed information is presented in **Supplementary Table S1**.

2.2 Pathway Enrichment Analysis

We used the online analysis platform MetaboAnalyst 5.0 (https://www.metaboanalyst.ca) to analyze 27 differential metabolites in AD mice and 60 human differential metabolites pathway enrichment based on extraction from the original study. The website contains statistical analysis, enrichment analysis, pathway analysis, functional analysis, etc. Pathway enrichment is classified and compared according to different biological samples (mouse or human). Brain tissue specificity data for each gene comes from AlzGPS (https://alzgps.lerner.ccf.org). Subcellular localization sourced from COMPARTMENTS (https://compartments.jensenlab.org/).

2.3 Construction of Metabolite-Centric Subnetworks Using Alzheimer's Disease Atlas

Metabolite related genes information comes from AD atlas (https://www.adatlas.org/). The AD Atlas is a dataset resource for studying AD-related biomarkers and AD-related endophenotypes based on a multi-omics background. It provides an interactive network of phenotypes, genes, proteins or metabolites. In this work, 14 common metabolites between AD mouse and human studies were input into AD Atlas to generate a metabolite-centric subnetwork. We used genome-wide as significance threshold, brain cortex to filter coregulation links. Five interaction types were covered in network, including coexpression, coregulation, genetic association, metabolic association, and partial correlation. Furthermore, the topology analysis in cytoHubba plug was used to measure important nodes in the network graph.

2.4 Experimental Validation

2.4.1 APPswe/PS1dE9 Animal Models

APP/PS1 male mouse and wild type (WT) mouse were purchased from Guangzhou Dean Gene Technology Co., Ltd. 8.5 and 17 month-old APP/PS1 mice (n = 10), and matched WT mice (n = 10) were selected for experiments respectively. All experimental procedures follow the requirements of the Ethical Review Regulations for Laboratory Animals of Guangzhou University of Chinese Medicine. Mice were housed in single cages in an air-conditioned room with a relative humidity of 40%–70% and a temperature of 20–26°C with a light-dark cycle for 12 h. Mice have free access to food and water.

2.4.2 Western Blot Analysis

We selected mouse brain cortex for western blot analysis. Add 10 μl of RIPA lysate containing phosphatase inhibitor and PMSF to each 1 mg of tissue. After treatment with a cell sonicator or tissue homogenizer, centrifuge to take the supernatant, add 1/4 of the total volume of loading buffer, and boil at 100°C for 5 min to completely denature the protein. The protein lysates were separated in equal volume on 10% Precast Protein Gels and transferred to an 0.22 μm Immobilon-PSQ polyvinylidene difluoride membrane (PVDF, Millipore, cat. #ISEQ00010). The following antibodies were used: Neuronal differentiation 2 (NDF2) Antibody (1:1000, Affnity Biosciences, cat. #AF0635); Human EGF Receptor (HER2/ErbB2) Antibody (1:1000, Affnity Biosciences, cat. #AF7681); beta Actin Antibody (1:3000, Affnity Biosciences, cat. #AF7018). At the end of the immunoreaction, Immobilon Western Chemilum HRP Substrate (Millipore, cat. #WBKLS0100) was prepared in a 1:1 ratio, and the western blot was recorded by a versatile gel imager ChemiDocXRS + (Bio-RAD, United States).

2.4.3 Immunofluorescence

The 3 μm coronal brain slices were blocked in 5% BSA at 37°C for 1 h, then incubated with primary antibodies at 4°C overnight. The next day, the slices were washed three times in PBS for 5 min each and incubated with corresponding secondary antibodies at 37°C for 2 h. The slices were stained with DAPI nuclear staining (Cell Signaling Technology, cat. #4083) for 1 min. Use the same antibody as for western blot.

2.5 Network Visualization and Statistical Analysis

Statistical analysis of this study was done by SPSS, GraphPad Prism 8 (v8.0.2, https://www.graphpad.com/). The mean ± standard deviation was used for statistical description, and the independent sample T test was used to compare with the control group, $^{*}p < 0.05$, $^{**}p < 0.01$, $^{***}p < 0.001$. The network was constructed using Cytoscape (v3.2.1, http://www.cytoscape.org/), GraphPad Prism 8, and Microsoft Office 2019.

3. RESULTS

3.1 Collection of Differential Metabolites in Mouse and Human Metabolomics

AD-related differential metabolites were collected from 11 previous metabolomics studies using AD mouse brain tissue. Seven of them are APP/PS1 transgenic mouse models, two are 3xTg transgenic mouse models, and the remaining two are Tg2576 and 5xFAD transgenic mouse model, respectively. A total of 408 differential metabolites were identified in the 11 literatures. After analysis and sorting, 27 key metabolites in mouse brain tissue were obtained by taking the frequency of three or more reports (**Figure 2**). Among the 11 studies, the study (González-Domínguez et al., 2014) has the highest overlap (n = 17) compared with the 27 differential metabolites. In addition, we observe that both of two metabolites (glycine, adenosine monophosphate) were detected in six studies. *In vitro* studies show that glycine increases viability and counteracts deleterious responses to LPS/IFN-γ-induced apoptosis in BV-2 microglia (Egger et al., 2020). *In vivo* studies have demonstrated that glycine exerts neuroprotective effects by mediating inactivation of the JNK signaling pathway, and it can reverse D-galactose-induced oxidative stress, neuroinflammation, synaptic dysfunction, and memory impairment (Rahat et al., 2020). Likewise, cyclic adenosine monophosphate (cAMP) as an endogenous modulator of the amyloid-beta precursor protein metabolism (Canepa et al., 2013). cAMP controls amyloid precursor protein (APP) translation and Aβ levels, regulates long-term potentiation (LTP) and ameliorates memory in healthy and diseased brain (Ricciarelli et al., 2014). These findings confirm the veracity and accuracy of our research.

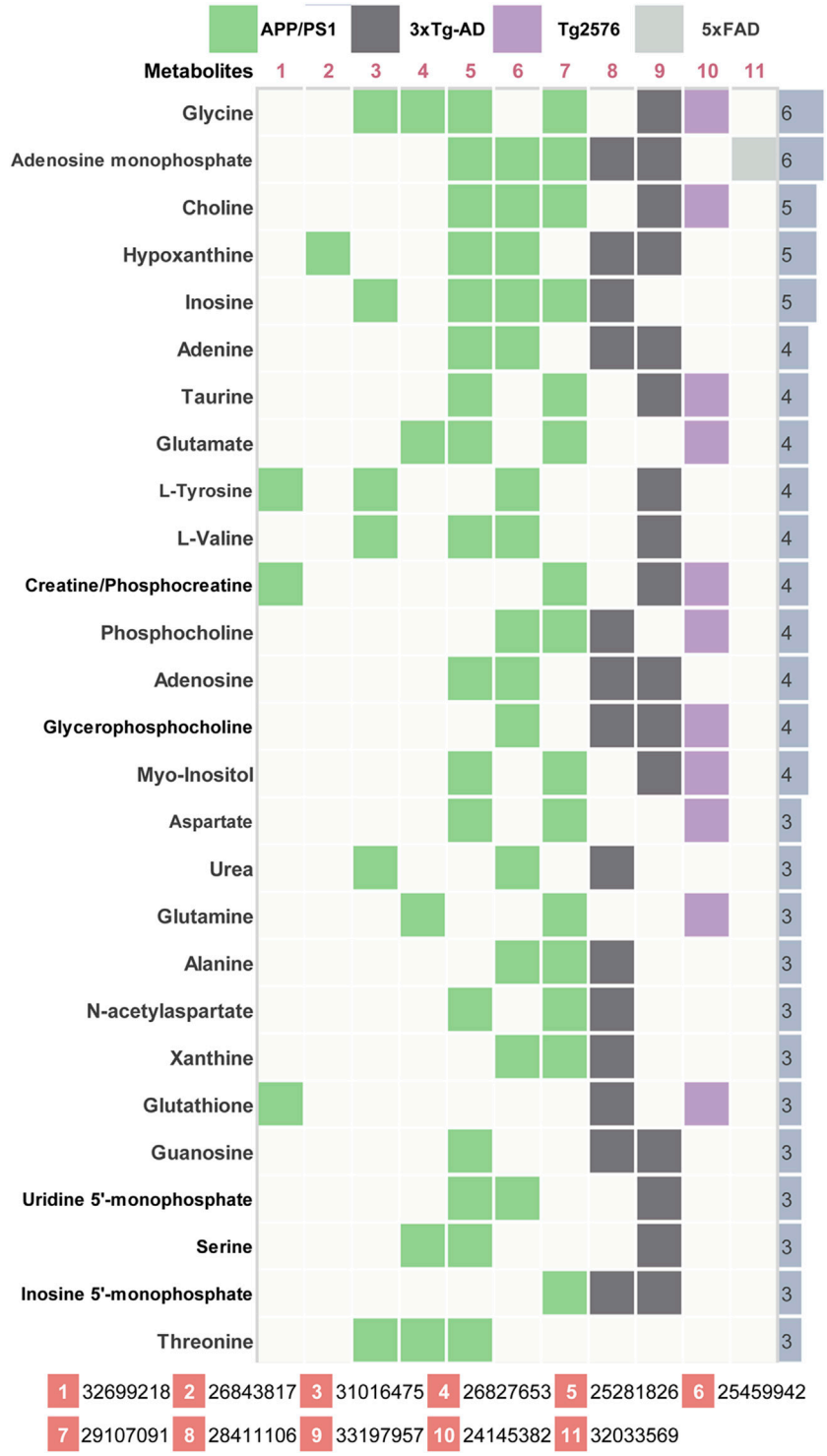

FIGURE 2 | Key differential metabolites in AD model mice. 11 previous metabolomics studies (PMID number) using AD mouse brain tissue were included. The key metabolites were listed together with their significant frequency in these studies.

Among 67 human metabolomics studies, there were 830 altered metabolites in AD patients compared to healthy individuals, of which 60 metabolites were reported three or more times (**Figure 3**). These 60 metabolites cover 37 literatures. Four metabolites (L-tryptophan, L-phenylalanine, palmitic acid, L-arginine) were detected significant in 7

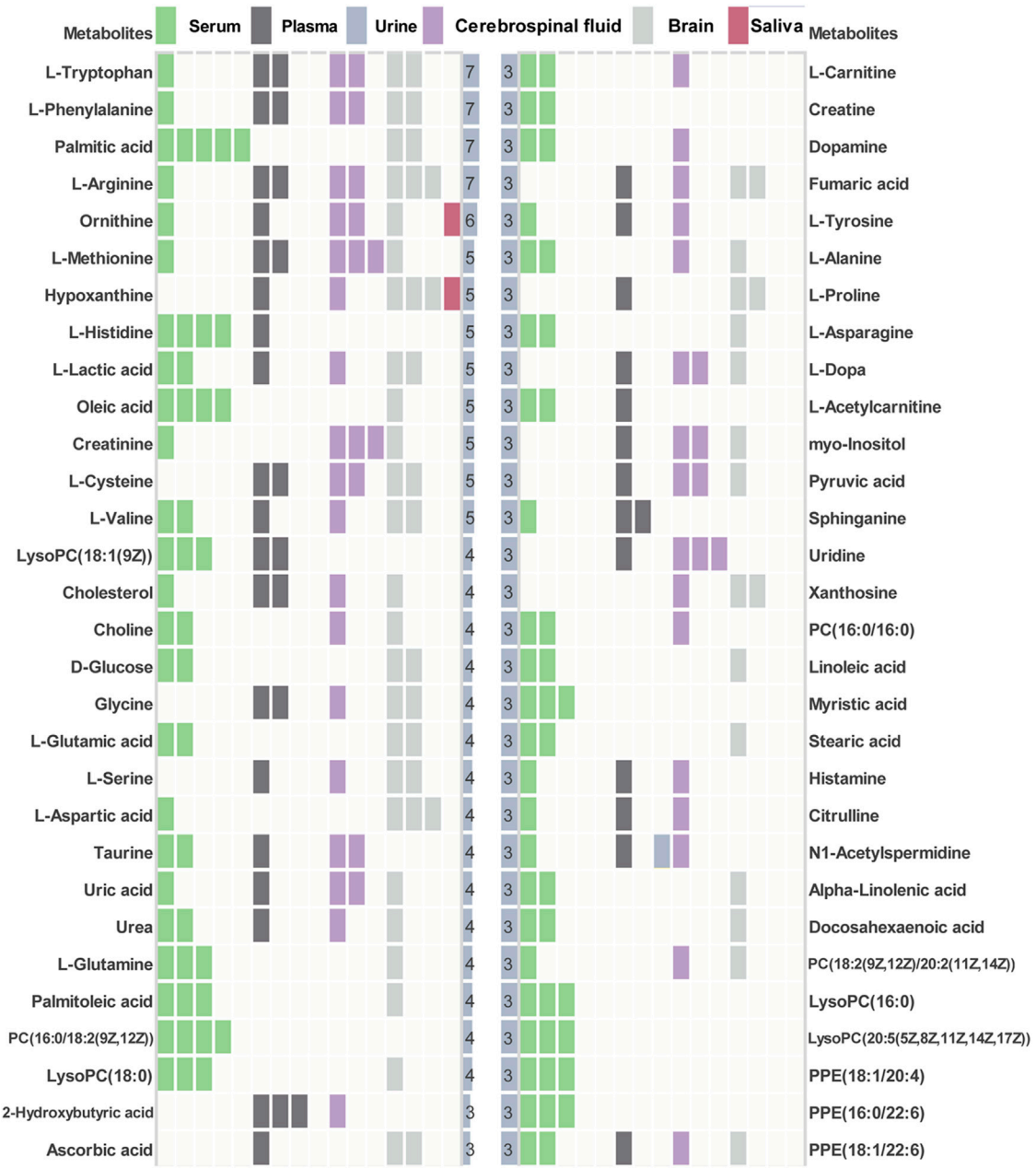

FIGURE 3 | Key differential metabolites in AD patients. Key metabolites with significant frequencies greater than three are listed and colored to distinguish different tissue types.

studies. *In vitro* studies demonstrated that extra-cellular palmitic acid coupled with G protein-coupled receptor 40 (GPR40) induces the expression of APP and BACE1 to facilitate Aβ production *via* the Akt-mTOR-HIF-1α and Akt-NF-κB pathways in SK-N-MC cells (Kim et al., 2017). In addition, studies have shown that palmitic acid abolished the migration and phagocytic activity of microglia in response to interferon-γ, thereby aggravating cellular inflammatory damage (Yanguas-Casas et al., 2018). A mouse model of CVN-AD, in which immune-mediated nitric oxide is reduced to mimic human levels, found areas of hippocampal neuronal death associated with the presence of immunosuppressive CD11c (+) microglia and extracellular arginase, resulting in decreased arginine catabolism and total levels of brain arginine (Kan et al., 2015). Moreover, a study of male APPswe/PS1ΔE9 transgenic (Tg) showed significantly altered plasma arginine metabolism profiles in 7-month Tg mice prior to major behavioral impairment (Bergin et al., 2018). These studies provide cogent evidence on the importance of high repetition rate metabolites in AD.

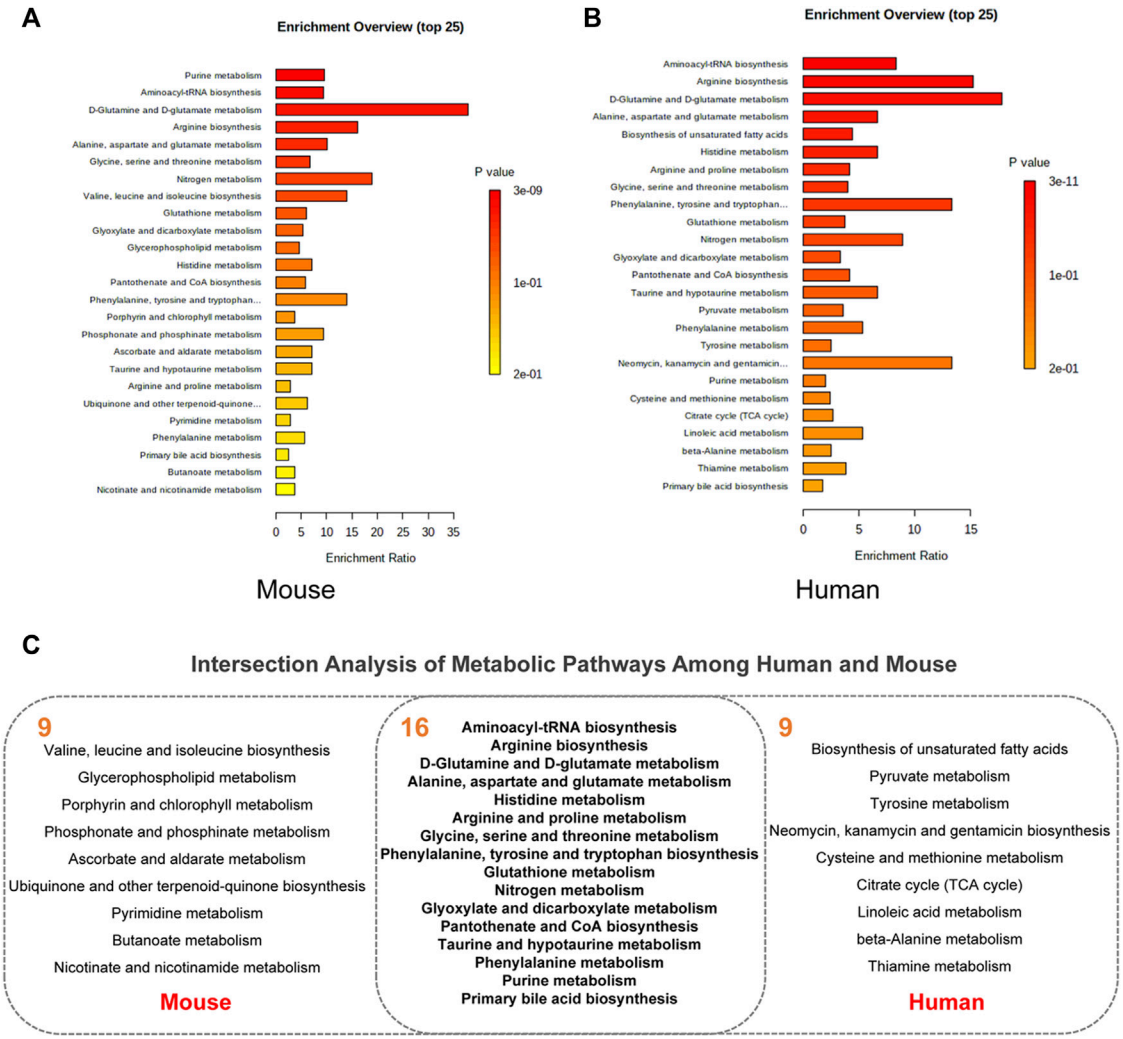

FIGURE 4 | Pathway enrichment analysis. **(A)** The top 25 pathway in AD animal models. **(B)** The top 25 pathway in AD patients. **(C)** Intersection analysis of metabolic pathways among human and mouse.

3.2 Key Metabolites Analysis and Enrichment Analysis

Pathway enrichment analysis was performed for key differential metabolites and top 25 significant pathways were kept for both types of metabolites. As shown in **Figure 4A**, analysis of 27 differential metabolites in AD mice revealed that 33 pathways exhibited alterations in the AD-related mouse brain tissue. The top 25 pathways were mainly related to D-glutamine and D-glutamate metabolism (Enrichment Ratio = 37.74, $p < 0.001$), nitrogen metabolism (Enrichment Ratio = 18.87, $p < 0.01$), arginine biosynthesis (Enrichment Ratio = 16.13 $p < 0.001$) and valine, leucine, and isoleucine biosynthesis (Enrichment Ratio = 14.08, $p < 0.01$). As for 60 key differential metabolites in AD patients (**Figure 4B**), there are 50 pathways that exhibited alterations in the AD patients. The top 25 pathways were mainly related to D-glutamine and D-glutamate metabolism (Enrichment Ratio = 17.78, $p < 0.001$), arginine biosynthesis (Enrichment Ratio = 15.27, $p < 0.001$), phenylalanine, tyrosine and tryptophan biosynthesis (Enrichment Ratio = 13.33, $p < 0.01$), and aminoacyl-tRNA biosynthesis (Enrichment Ratio = 8.33, $p < 0.001$). Enrichment Ratio is computed by hits/expected, where hits = observed hits; expected = expected hits. Details of pathway enrichment are presented in **Supplementary Tables S2, S3**.

3.3 Intersection Analysis of Metabolic Pathways Between Human and Alzheimer's Disease Mouse

We further aimed to examine the common regulated metabolic pathways between AD patients and AD mice. **Figure 4C** presents 16 overlapping pathways between them. Most of these pathways have high enrichment ratio and low p values,

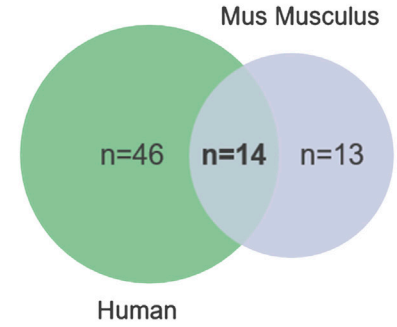

B

Metabolite Information

Metabolites names	HMDB	PubChem	KEGG
Choline	HMDB0000097	305	C00114
Hypoxanthine	HMDB0000157	790	C00262
Glycine	HMDB0000123	750	C00037
Taurine	HMDB0000251	1123	C00245
L-Tyrosine	HMDB0000158	6057	C00082
L-Valine	HMDB0000883	6287	C00183
Creatine	HMDB0000064	586	C00300
myo-Inositol	HMDB0000211	892	C00137
Urea	HMDB0000294	2447	C00086
L-Glutamine	HMDB0000641	5961	C00064
L-Alanine	HMDB0000161	5950	C00041
Serine	HMDB0062263	5951	C00716
L-Glutamic acid	HMDB0000148	33032	C00025
L-Aspartic acid	HMDB0000191	5960	C00049

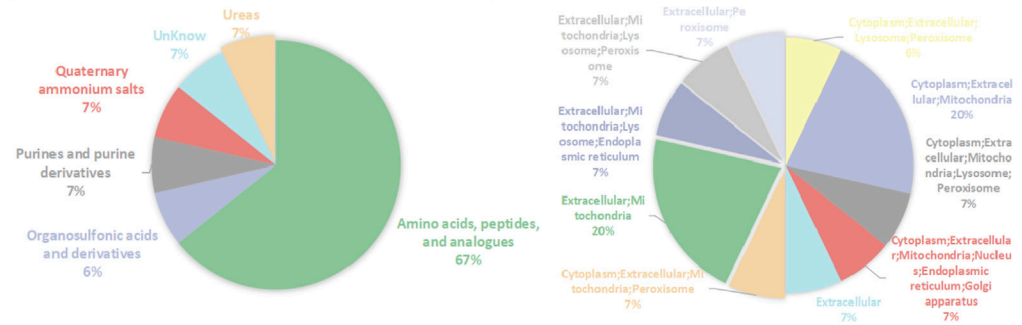

FIGURE 5 | Analysis of key metabolites. **(A)** Venn diagrams of animal and human metabolites. **(B)** The 14 key metabolites information. **(C)** Annotation and statistics of chemical classification information of metabolites. **(D)** Subcellular localization analysis of metabolites.

such as D-glutamine and D-glutamate metabolism, arginine biosynthesis, alanine, aspartate, and glutamate metabolism. Glutamate is the most common excitatory transmitter in the mammalian central nervous system and plays an important role in normal brain function and brain development. Low synaptic clearance and excitotoxicity of glutamate resulting from altered glutamatergic neurotransmission are thought to play critical roles in AD progression (Acosta et al., 2017; Nuzzo et al., 2021). A recent study has demonstrated that subjects with MCI show paradoxical elevations in glutamatergic presynaptic bolton density, which are then depleted and decreased as the disease progresses (Bell et al., 2007). Recently, substantial evidence implicates that altered L-arginine metabolism is involved in AD pathogenesis (Griffin and Bradshaw, 2017; Meloni et al., 2020). Arginase converts L-arginine to L-ornithine, which is further metabolized by ornithine decarboxylase (ODC) to the polyamine putrescine (Wu and Morris, 1998). Polyamines promote the aggregation of Aβ oligomers and reduce their toxicity by reducing the hydrophobic surface and increasing the size of the oligomers (Luo et al., 2013) and are essential for the maintenance of normal cellular function. In a study on APP/PS1 mice, the content of L-arginine continued to increase with age. Amyloid plaques were distributed widely across the brain at 17 months of age, the content of L-arginine in this time was significantly higher than that of the normal group (Vemula et al., 2020). Collectively, accumulating evidence has supported that these metabolic pathways play important roles in both AD patients and animal models.

3.4 Analyze Metabolite-Target Networks and Identify Putative Protein Markers in Alzheimer's Disease

In addition to 16 overlapping enriched pathways, we also found 14 key metabolites overlap between AD mouse models and patients (**Figure 5A**). Their detailed information is presented in **Figure 5B**. Annotation and statistics were performed on the chemical classification and attribution information of metabolites (**Figure 5C**). Metabolites in different categories were displayed in different color blocks. Nine metabolites belong to amino acids, peptides, and analogues (creatine, glycine, alanine, aspartate, glutamate, glutamine, serine, valine, tyrosine), metabolite taurine belongs to organ sulfonic acids and derivatives, metabolite hypoxanthine belongs to purines and purine derivatives, metabolite choline belongs to quaternary ammonium salts, metabolite urea belongs to ureas and myo-Inositol unclear attribution. Subcellular localization analysis of metabolites was performed based on the information included in

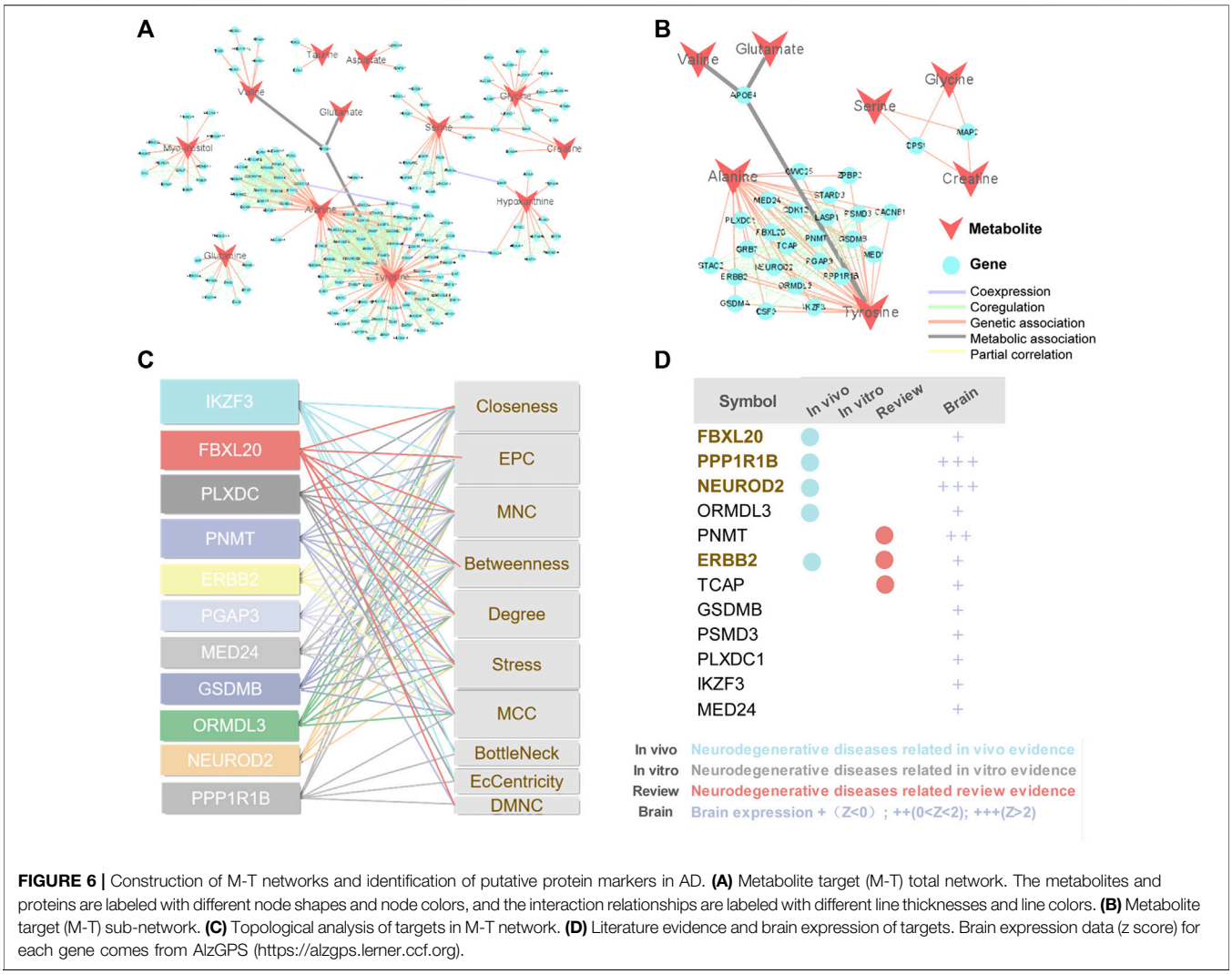

FIGURE 6 | Construction of M-T networks and identification of putative protein markers in AD. **(A)** Metabolite target (M-T) total network. The metabolites and proteins are labeled with different node shapes and node colors, and the interaction relationships are labeled with different line thicknesses and line colors. **(B)** Metabolite target (M-T) sub-network. **(C)** Topological analysis of targets in M-T network. **(D)** Literature evidence and brain expression of targets. Brain expression data (z score) for each gene comes from AlzGPS (https://alzgps.lerner.ccf.org).

the Human Metabolome Database (HMDB) (**Figure 5D**). All metabolites are distributed extracellularly (n = 14) and most metabolites are distributed in mitochondria (n = 11), in contrast, only choline is distributed in the nucleus and golgi apparatus, which is the most widely subcellularly localized metabolite (cytoplasm, extracellular, mitochondria, nucleus, endoplasmic reticulum, golgi apparatus). Choline, a B vitamin nutrient found in common foods, is important for various cellular functions. Experiments demonstrate that lifelong choline supplementation significantly reduces amyloid-beta plaque burden and improves spatial memory in APP/PS1 mice (Velazquez et al., 2019).

Metabolites are downstream of the genome, transcriptome, and proteome, whereas proteins are the ultimate carriers of functions in an organism. In biological systems, metabolite-protein interactions control a variety of cellular processes, therefore, we used AD Atlas to construct M-T network, in order to find potential AD markers associated with metabolites (**Figure 6A**). The M-T networks include 12 metabolites except choline and urea. We retained proteins with linkages to at least two metabolites, resulting in a sub-network diagram (**Figure 6B**). Ten topology analysis methods, including Closeness, EPC, MNC, Betweenness Degree, Stress, MCC, BottleNeck, EcCentricity and DMNC are used to measure the true efficiency of nodes in the sub-network to evaluate their importance (**Figure 6C**). Topological analysis has sorted out the 11 most important proteins in the network diagram. Combined with the expression levels in the brain (Zhou et al., 2021) and the supporting literature evidence related to neurodegenerative diseases *in vivo* and *in vitro*, we screened out FBXL20, PPP1R1B, NEUROD2 (NDF2), and ERBB2 (HER2) for follow-up molecular biology experiments (**Figure 6D**).

3.5 Experimental Validation of Human EGF Receptor and Neuronal Differentiation 2 as Putative Protein Markers in APP/PS1 Models

We selected APP/PS1 mice in two different months of age to verify the four proteins selected in the above analysis, of which

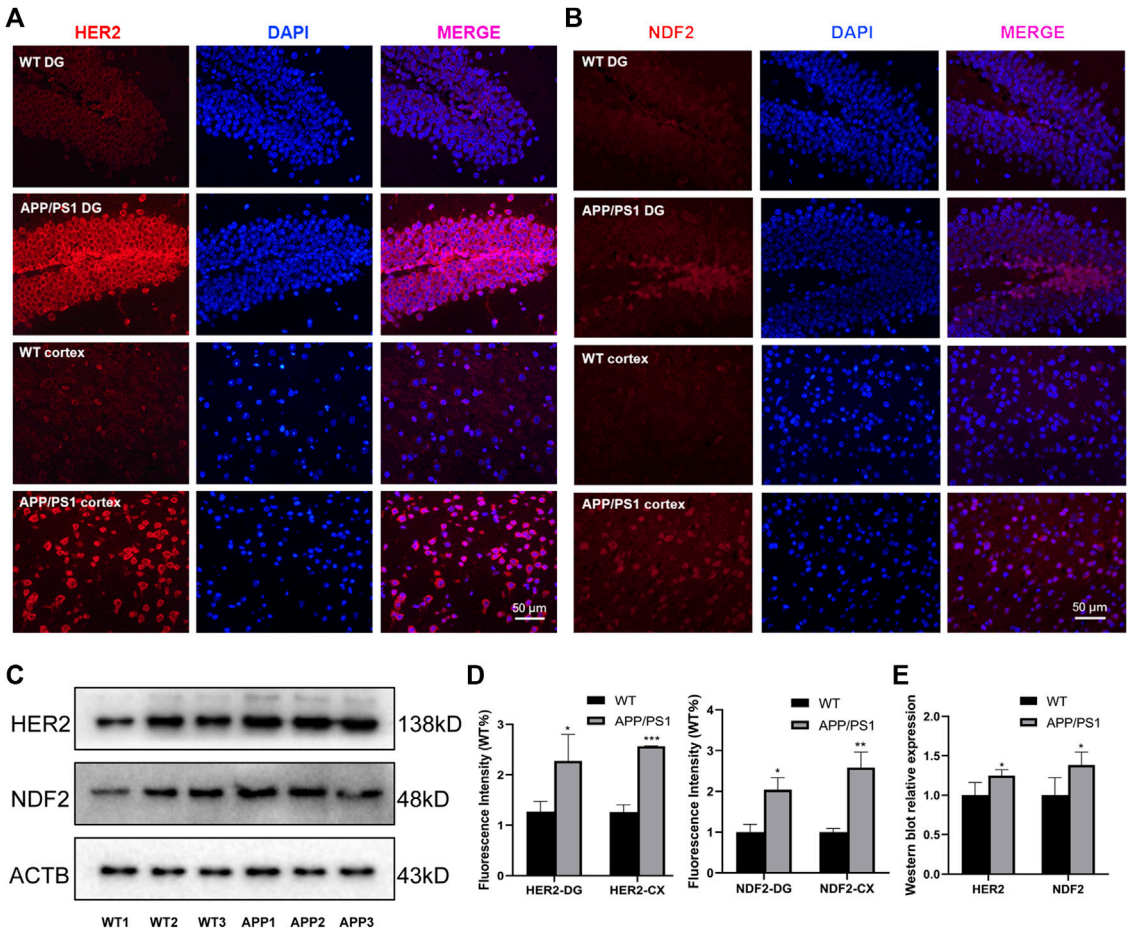

FIGURE 7 | Experimental validation of HER2 and NDF2. **(A)** Immunofluorescence expression of HER2 (8.5 months). **(B)** Immunofluorescence expression of NDF2 (8.5 months). **(C)** Western blot results of NDF2 and HER2 (17 months). **(D,E)** Statistical analysis of immunofluorescence and western blot. $^{*}p < 0.05$, $^{**}p < 0.01$, $^{***}p < 0.001$.

FBXL20 and PPP1R1B had no significant difference between WT and APP/PS1 mice. 8.5-month-old APP/PS1 mice exhibited abundant Aβ accumulation in the hippocampus and cortex (Jankowsky et al., 2004), while 17-month-old APP/PS1 mice exhibited learning impairment (Savonenko et al., 2005). **Figure 7A** shows the immunofluorescence expression of the protein HER2 of 8.5-month-old APP/PS1 mice, the results show that the expression in the hippocampal dentate gyrus area and cortical area of APP/PS1 is significantly higher than that in WT ($p < 0.05$, $p < 0.001$). **Figure 7B** shows the immunofluorescence expression of the protein NDF2, and the results show that the expression in the hippocampal dentate gyrus area and cortical area of APP/PS1 is significantly higher than that in WT ($p < 0.05$, $p < 0.01$). Moreover, **Figure 7C** shows the western blot expression of the proteins NDF2 and HER2 of 17-month-old APP/PS1 mice. The results showed that the expressions of NDF2 in APP/PS1 mice is significantly higher than that in WT ($p < 0.05$) and HER2 in the brain tissue of APP/PS1 mice is significantly higher than that in WT ($p < 0.05$).

4 DISCUSSION AND CONCLUSION

Metabolites drive cells to perform basic functions including signal transduction, energy production and storage. As the biochemical products of the cellular process, metabolites reflect alterations in biochemical pathways related to the pathogenesis of AD. Thus, studying metabolites has profound implications in the identification of potential biomarkers for diagnosis, treatment, and prognostic assessment.

In this work, we perform a comparative metabolomics analysis to offer a global view of metabolic changes between AD animal models and AD patients. We integrate multiple metabolic profiles from public data source, and conduct metabolites and metabolic pathway overlap analysis. The key metabolites and enriched pathways are identified, which are both differentially significant in AD mouse models and patients. Through construction of M-T network, we finally predicted and experimentally validated HER2 and NDF2 as key protein markers in APP/PS1 mice.

HER2, commonly known as Erb-B2 Receptor Tyrosine het Kinase 2 (ErbB2), is a member of the epidermal growth factor

receptor (EGFR) family, including four members EGFR (ErbB1, HER1), ErbB2 (HER2), ErbB3 (HER3) and ErbB4 (HER4). In peripheral nerve regeneration after trauma, HER2 regulates Schwann cell proliferation, yet its high expression drives cancer development and progression in certain tissue types. The important reason of HER2 receptor leading to carcinogenesis is ligand-independent activation, which activates downstream signals. Neuregulin-1 (Nrg1) is a member of the active epithelial growth factor (EGF) family (Patricia et al., 2005), which binds to ErbB receptors, NRG1 is a ligand of ErbB3 or ErbB4, and is more likely to heterodimerizes with ErbB2 after binding to ErbB3 or ErbB4 aggregates. Nrg1 mediated intercellular and intracellular communication regulates multiple biological processes involved in nervous system development by binding to ErbB receptors, and they play key roles in regulating nervous system development and regeneration. NRG1 signaling in microglia stimulates microglial proliferation, chemotaxis, and survival through the ErbB2 receptor, as well as interleukin-1β release *in vitro* (Calvo et al., 2010). Changes in ErbB expression appear to play an important role in nerve injury and subsequent nerve regeneration (Calvo et al., 2010; Kanzaki et al., 2013; Ronchi et al., 2013). NRG accelerates Schwann cell migration through ErbB2/3-dependent FAK pathway, thereby promoting nerve regeneration (Hung-Ming et al., 2013). NRG1 activates heteromeric ErbB2 and ErbB3 receptors on Schwann cells and plays an important role in Schwann cell development and myelination (Garratt et al., 2000; Lemke, 2006). Plasma soluble neuregulin-1 levels were significantly elevated in mild AD patients and moderate AD patients compared with healthy controls (Shin et al., 2016). cDNA microarray technology was used to study the changes of gene expression profiles in the cerebral cortex of Balb/c mice injected with Aβ fragment 25–35 into the ventricle, and it was found that ErbB2 gene expression was upregulated (Kong et al., 2010).

NDF2, commonly referred to as Neurod2, is a neurogenesis marker in the hippocampal dentate gyrus and is thought to play a role in the determination and maintenance of neuronal cell fate. The findings suggest that alterations in Neurod2 can lead to neurodevelopmental disorders, including intellectual disability and autism spectrum disorder (Runge et al., 2021). Higher levels of RE1-silencing transcription factor (REST) were detected in the hippocampus of Neurod2 knockout mice. REST inhibits neuronal differentiation, and the neuronal differentiation program must be activated for progenitor cells to become neurons (Ravanpay et al., 2010). In the APP/PS1 mouse model, targeted expression of Neurod1 in hippocampal progenitor cells significantly reduced the defect in dendritic spine density in new hippocampal neurons, and the highly connected new neurons were able to restore spatial memory in these diseased mice (Kevin et al., 2014). Reduced neurogenesis and synaptic plasticity, thought to be associated with age-related cognitive decline (Bettio et al., 2017). Memory deficits, a typical feature of AD, develop decades before they are detected as mild cognitive impairment. New neurons and glial cells in the adult hippocampus are added to the granular cell layer of the dentate gyrus committed to learning and memory. Conversely, defects in neurogenesis with aging, neuroinflammation, oxidative damage, mitochondrial dysfunction, etc., may impair hippocampal function and gradually lead to memory loss. The enhanced neurogenesis in our experiments may be a compensatory response, representing an endogenous brain repair mechanism.

There are two novel findings in our study. First, our comparative metabolomics analysis integrating multiple data sources revealed the metabolite similarities and differences between AD patients and animal models, confirming that the existing AD animal models have good commonality with AD patients at the metabolite level. Secondly, two potential protein markers (HER2 and NDF2) were predicted and verified in APP/PS1 mouse model, which provided some new directions and explorations for AD research. However, several limitations of the presented study should be recognized. First, our data was derived from the differential metabolites listed in the literature and lack a standardized analytical workflow for sample acquisition, processing and preparation, instrumental analysis, and data analysis. Second, the included data was mostly cross-sectional studies, while the early diagnostic and prognostic potential of metabolite biomarkers should be further assessed in high-quality, large-scale longitudinal cohort studies. Third, due to insufficient data on patient brain tissue, 67 metabolomics studies from AD patients included multiple tissue sources, compared with only brain tissue source in AD mouse models. This might have some impact on the results.

Generally, metabolomics is an exciting and growing field of research, and its study has illuminated its ability to expand from biomarker discovery to understanding the mechanisms behind phenotypes. Our study may bring some directions and implications for AD metabolomics research, providing a comprehensive understanding of HER2 and NDF2.

DATA AVAILABILITY STATEMENT

The original contributions presented in the study are included in the article/**Supplementary Material**, further inquiries can be directed to the corresponding authors.

ETHICS STATEMENT

The animal study was reviewed and approved by the Ethics committee member of Guangzhou University of Chinese Medicine.

AUTHOR CONTRIBUTIONS

JF: conceptualization. ZD: writing—original draft preparation. ZD, TH, SS, and JL: performing the experiments and analyzing the data. YM, YZ, SF, and QW: providing constructive advice and editing the manuscript. JF, ZM, and HP: supervision. All authors contributed to the manuscript and approved the submitted version.

FUNDING

The work was supported by the National Natural Science Foundation of China (No.82074278), Key Laboratory (Pi Wei diseases and Pi-deficiency syndrome) of State Administration of

Traditional Chinese Medicine (No. 202110071448237400), Special Foundation of Guandong Educational Committe (No. 2021ZDZX 2001), and Guangdong Province Science and Technology Plan International Cooperation Project (No. 2020A0505100052).

REFERENCES

Acosta, C., Anderson, H. D., and Anderson, C. M. (2017). Astrocyte Dysfunction in Alzheimer Disease. *J. Neurosci. Res.* 95, 2430–2447. doi:10.1002/jnr.24075

Bell, K. F., Bennett, D. A., and Cuello, A. C. (2007). Paradoxical Upregulation of Glutamatergic Presynaptic Boutons during Mild Cognitive Impairment. *J. Neurosci.* 27, 10810–10817. doi:10.1523/JNEUROSCI.3269-07.2007

Bergin, D. H., Jing, Y., Mockett, B. G., Zhang, H., Abraham, W. C., and Liu, P. (2018). Altered Plasma Arginine Metabolome Precedes Behavioural and Brain Arginine Metabolomic Profile Changes in the APPswe/PS1ΔE9 Mouse Model of Alzheimer's Disease. *Transl Psychiatry* 8, 108. doi:10.1038/s41398-018-0149-z

Bettio, L. E. B., Rajendran, L., and Gil-Mohapel, J. (2017). The Effects of Aging in the hippocampus and Cognitive Decline. *Neurosci. Biobehav Rev.* 79, 66–86. doi:10.1016/j.neubiorev.2017.04.030

Bundy, J. G., Spurgeon, D. J., Svendsen, C., Hankard, P. K., Osborn, D., Lindon, J. C., et al. (2002). Earthworm Species of the Genus Eisenia Can Be Phenotypically Differentiated by Metabolic Profiling. *FEBS Lett.* 521, 115–120. doi:10.1016/s0014-5793(02)02854-5

Busche, M. A., and Hyman, B. T. (2020). Synergy between Amyloid-β and Tau in Alzheimer's Disease. *Nat. Neurosci.* 23, 1183–1193. doi:10.1038/s41593-020-0687-6

Calvo, M., Zhu, N., Tsantoulas, C., Ma, Z., Grist, J., Loeb, J. A., et al. (2010). Neuregulin-ErbB Signaling Promotes Microglial Proliferation and Chemotaxis Contributing to Microgliosis and Pain after Peripheral Nerve Injury. *J. Neurosci.* 30, 5437–5450. doi:10.1523/JNEUROSCI.5169-09.2010

Canepa, E., Domenicotti, C., Marengo, B., Passalacqua, M., Marinari, U. M., Pronzato, M. A., et al. (2013). Cyclic Adenosine Monophosphate as an Endogenous Modulator of the Amyloid-β Precursor Protein Metabolism. *Iubmb Life* 65, 127–133. doi:10.1002/iub.1109

Chang, H. M., Shyu, M. K., Tseng, G. F., Liu, C. H., Chang, H. S., Lan, C. T., et al. (2013). Neuregulin Facilitates Nerve Regeneration by Speeding Schwann Cell Migration *via* ErbB2/3-dependent FAK Pathway. *PLoS ONE* 8, e53444. doi:10.1371/journal.pone.0053444

Chang, K. A., Shin, K. Y., Nam, E., Lee, Y. B., Moon, C., and Lee, Y. H. S. H. (2016). Plasma Soluble Neuregulin-1 as a Diagnostic Biomarker for Alzheimer's Disease. *Neurochem. Int.* 97, 1–7. doi:10.1016/j.neuint.2016.04.012

Chen, S. Q., Cai, Q., Shen, Y. Y., Wang, P. J., Teng, G. J., Zhang, W., et al. (2012). Age-related Changes in Brain Metabolites and Cognitive Function in APP/PS1 Transgenic Mice. *Behav. Brain Res.* 235, 1–6. doi:10.1016/j.bbr.2012.07.016

Cummings, J., Lee, G., Ritter, A., Sabbagh, M., and Zhong, K. (2020). Alzheimer's Disease Drug Development Pipeline: 2020. *Alzheimers Dement (N Y)* 6, e12050. doi:10.1002/trc2.12050

Egger, F., Jakab, M., Oberascher, J. K., Brachtl, G., Ritter, M., Kerschbaum, H. H., et al. (2020). Effect of Glycine on BV-2 Microglial Cells Treated with Interferon-γ and Lipopolysaccharide. *Int. J. Mol. Sci.* 21, 804. doi:10.3390/ijms21030804

Fang, J., Pieper, A. A., Nussinov, R., Lee, G., Bekris, L., Leverenz, J. B., et al. (2020). Harnessing Endophenotypes and Network Medicine for Alzheimer's Drug Repurposing. *Med. Res. Rev.* 40, 2386–2426. doi:10.1002/med.21709

Fang, J., Zhang, P., Zhou, Y., Chiang, C.-W., Tan, J., Hou, Y., et al. (2021). Endophenotype-based In Silico Network Medicine Discovery Combined with Insurance Record Data Mining Identifies Sildenafil as a Candidate Drug for Alzheimer's Disease. *Nat. Aging* 1, 1175–1188. doi:10.1038/s43587-021-00138-z

Garratt, A. N., Britsch, S., and Birchmeier, C. (2000). Neuregulin, a Factor with many Functions in the Life of a Schwann Cell. *Bioessays* 22, 987–996. doi:10.1002/1521-1878(200011)22:11<987::AID-BIES5>3.0.CO;2-5

González-Domínguez, R., García-Barrera, T., Vitorica, J., and Gómez-Ariza, J. L. (2014). Region-specific Metabolic Alterations in the Brain of the APP/PS1 Transgenic Mice of Alzheimer's Disease. *Biochim. Biophys. Acta (BBA) - Mol. Basis Dis.* 1842, 2395–2402. doi:10.1016/j.bbadis.2014.09.014

Griffin, J. W., and Bradshaw, P. C. (2017). Amino Acid Catabolism in Alzheimer's Disease Brain: Friend or Foe? *Oxid Med. Cel Longev* 2017, 5472792. doi:10.1155/2017/5472792

Horgusluoglu, E., Neff, R., Song, W. M., Wang, M., Wang, Q., Arnold, M., et al. (2021). Integrative Metabolomics-genomics Approach Reveals Key Metabolic Pathways and Regulators of Alzheimer's Disease. *Alzheimer's Demen.* 2021. doi:10.1002/alz.12468

Jankowsky, J. L., Fadale, D. J., Anderson, J., Xu, G. M., Gonzales, V., Jenkins, N. A., et al. (2004). Mutant Presenilins Specifically Elevate the Levels of the 42 Residue β-amyloid Peptide *In Vivo*: Evidence for Augmentation of a 42-specific γ Secretase. *Hum. Mol. Genet.* 13, 159–170. doi:10.1093/hmg/ddh019

Kan, M. J., Lee, J. E., Wilson, J. G., Everhart, A. L., Brown, C. M., Hoofnagle, A. N., et al. (2015). Arginine Deprivation and Immune Suppression in a Mouse Model of Alzheimer's Disease. *J. Neurosci.* 35, 5969–5982. doi:10.1523/JNEUROSCI.4668-14.2015

Kim, J. Y., Lee, H. J., Lee, S. J., Jung, Y. H., Yoo, D. Y., Hwang, I. K., et al. (2017). Palmitic Acid-BSA Enhances Amyloid-β Production through GPR40-Mediated Dual Pathways in Neuronal Cells: Involvement of the Akt/mTOR/HIF-1α and Akt/NF-κB Pathways. *Sci. Rep.* 7, 4335. doi:10.1038/s41598-017-04175-w

Kim, M., Snowden, S., Suvitaival, T., Ali, A., Merkler, D. J., Ahmad, T., et al. (2019). Primary Fatty Amides in Plasma Associated with Brain Amyloid burden, Hippocampal Volume, and Memory in the European Medical Information Framework for Alzheimer's Disease Biomarker Discovery Cohort. *Alzheimer's & Demen.* 15, 817–827. doi:10.1016/j.jalz.2019.03.004

Knopman, D. S., Amieva, H., Petersen, R. C., Chételat, G., Holtzman, D. M., Hyman, B. T., et al. (2021). Alzheimer Disease. *Nat. Rev. Dis. Primers* 7, 33. doi:10.1038/s41572-021-00269-y

Kong, L. N., Zuo, P. P., Mu, L., Liu, Y. Y., and Yang, N. (2010). Gene Expression Profile of Amyloid Beta Protein-Injected Mouse Model for Alzheimer Disease. *Acta Pharmacol. Sin* 26, 666–672. doi:10.1111/j.1745-7254.2005.00129.x

Lemke, G. (2006). Neuregulin-1 and Myelination. *Sci. STKE* 2006, pe11. doi:10.1126/stke.3252006pe11

Long, J. M., and Holtzman, D. M. (2019). Alzheimer Disease: An Update on Pathobiology and Treatment Strategies. *Cell* 179, 312–339. doi:10.1016/j.cell.2019.09.001

Luo, J., Yu, C.-H., Yu, H., Borstnar, R., Kamerlin, S. C. L., GräSlund, A., et al. (2013). Cellular Polyamines Promote Amyloid-Beta (Aβ) Peptide Fibrillation and Modulate the Aggregation Pathways. *ACS Chem. Neurosci.* 4, 454–462. doi:10.1021/cn300170x

Meloni, B. P., Mastaglia, F. L., and Knuckey, N. W. (2020). Cationic Arginine-Rich Peptides (CARPs): A Novel Class of Neuroprotective Agents with a Multimodal Mechanism of Action. *Front. Neurol.* 11, 108. doi:10.3389/fneur.2020.00108

Mizobuchi, S., Kanzaki, H., Omiya, H., Obata, N., Kaku, R., Nakajima, H., et al. (2013). Spinal Nerve Injury Causes Upregulation of ErbB2 and ErbB3 Receptors in Rat Dorsal Root Ganglia. *J. Pain Res.* 6, 87–94. doi:10.2147/JPR.S40967

Nicholson, J. K., Connelly, J., Lindon, J. C., and Holmes, E. (2002). Metabonomics: a Platform for Studying Drug Toxicity and Gene Function. *Nat. Rev. Drug Discov.* 1, 153–161. doi:10.1038/nrd728

Nuzzo, T., Mancini, A., Miroballo, M., Casamassa, A., Di Maio, A., Donati, G., et al. (2021). High Performance Liquid Chromatography Determination of L-Glutamate, L-Glutamine and glycine Content in Brain, Cerebrospinal Fluid and Blood Serum of Patients Affected by Alzheimer's Disease. *Amino acids* 53, 435–449. doi:10.1007/s00726-021-02943-7

Petersen, R. C., Jack, C. R., Xu, Y. C., Waring, S. C., O'Brien, P. C., Smith, G. E., et al. (2000). Memory and MRI-Based Hippocampal Volumes in Aging and AD. *Neurology* 54, 581–587. doi:10.1212/wnl.54.3.581

SUPPLEMENTARY MATERIAL

The Supplementary Material for this article can be found online at: https://www.frontiersin.org/articles/10.3389/fphar.2022.904857/full#supplementary-material

Ravanpay, A. C., Hansen, S. J., and Olson, J. M. (2010). Transcriptional Inhibition of REST by NeuroD2 during Neuronal Differentiation. *Mol. Cel Neurosci* 44, 178–189. doi:10.1016/j.mcn.2010.03.006

Ricciarelli, R., Puzzo, D., Bruno, O., Canepa, E., Gardella, E., Rivera, D., et al. (2014). A Novel Mechanism for Cyclic Adenosine Monophosphate-Mediated Memory Formation: Role of Amyloid Beta. *Ann. Neurol.* 75, 602–607. doi:10.1002/ana.24130

Richetin, K., Leclerc, C., Toni, N., Gallopin, T., Pech, S., Roybon, L., et al. (2014). Genetic Manipulation of Adult-Born Hippocampal Neurons Rescues Memory in a Mouse Model of Alzheimer's Disease. *Brain* 138, 440–455. doi:10.1093/brain/awu354

Ritch, P. S., CarrollSteven, S. L., and Sontheimer, H. (2005). Neuregulin-1 Enhances Survival of Human Astrocytic Glioma Cells. *Glia* 51, 217–228. doi:10.1002/glia.20197

Ronchi, G., Gambarotta, G., Di Scipio, F., Salamone, P., Sprio, A. E., Cavallo, F., et al. (2013). ErbB2 Receptor Over-expression Improves Post-Traumatic Peripheral Nerve Regeneration in Adult Mice. *Plos One* 8, e56282. doi:10.1371/journal.pone.0056282

Runge, K., Mathieu, R., Bugeon, S., Lafi, S., Beurrier, C., Sahu, S., et al. (2021). Disruption of NEUROD2 Causes a Neurodevelopmental Syndrome with Autistic Features *via* Cell-Autonomous Defects in Forebrain Glutamatergic Neurons. *Mol. Psychiatry* 26, 6125–6148. doi:10.1038/s41380-021-01179-x

Savonenko, A., Xu, G. M., Melnikova, T., Morton, J. L., Gonzales, V., Wong, M. P., et al. (2005). Episodic-like Memory Deficits in the APPswe/PS1dE9 Mouse Model of Alzheimer's Disease: Relationships to Beta-Amyloid Deposition and Neurotransmitter Abnormalities. *Neurobiol. Dis.* 18, 602–617. doi:10.1016/j.nbd.2004.10.022

Ullah, R., Jo, M. H., Riaz, M., Alam, S. I., Saeed, K., Ali, W., et al. (2020). Glycine, the Smallest Amino Acid, Confers Neuroprotection against D-Galactose-Induced Neurodegeneration and Memory Impairment by Regulating C-Jun N-Terminal Kinase in the Mouse Brain. *J. Neuroinflammation* 17, 303. doi:10.1186/s12974-020-01989-w

Velazquez, R., Ferreira, E., Knowles, S., Fux, C., Rodin, A., Winslow, W., et al. (2019). Lifelong Choline Supplementation Ameliorates Alzheimer's Disease Pathology and Associated Cognitive Deficits by Attenuating Microglia Activation. *Aging Cell* 18, e13037. doi:10.1111/acel.13037

Vemula, P. K., Jing, Y., Cicolini, J., Zhang, H., Mockett, B. G., Abraham, W. C., et al. (2020). Altered Brain Arginine Metabolism with Age in the APPswe/PSEN1dE9 Mouse Model of Alzheimer's Disease. *Neurochem. Int.* 140, 104798. doi:10.1016/j.neuint.2020.104798

Wu, G., and Morris, S. M. (1998). Arginine Metabolism: Nitric Oxide and beyond. *Biochem. J.* 336, 1–17. doi:10.1042/bj3360001

Xie, K., Qin, Q., Long, Z., Yang, Y., Peng, C., Xi, C., et al. (2021). High-Throughput Metabolomics for Discovering Potential Biomarkers and Identifying Metabolic Mechanisms in Aging and Alzheimer's Disease. *Front Cel Dev Biol* 9, 602887. doi:10.3389/fcell.2021.602887

Yanguas-Casás, N., Crespo-Castrillo, A., De Ceballos, M. L., Chowen, J. A., Azcoitia, I., Arevalo, M. A., et al. (2018). Sex Differences in the Phagocytic and Migratory Activity of Microglia and Their Impairment by Palmitic Acid. *Glia* 66, 522–537. doi:10.1002/glia.23263

Zhou, Y., Fang, J., Bekris, L. M., Kim, Y. H., Pieper, A. A., Leverenz, J. B., et al. (2021). AlzGPS: a Genome-wide Positioning Systems Platform to Catalyze Multi-Omics for Alzheimer's Drug Discovery. *Alz Res. Ther.* 13, 24. doi:10.1186/s13195-020-00760-w

Conflict of Interest: The authors declare that the research was conducted in the absence of any commercial or financial relationships that could be construed as a potential conflict of interest.

Publisher's Note: All claims expressed in this article are solely those of the authors and do not necessarily represent those of their affiliated organizations, or those of the publisher, the editors and the reviewers. Any product that may be evaluated in this article, or claim that may be made by its manufacturer, is not guaranteed or endorsed by the publisher.

frontiers | Frontiers in Pharmacology

ORIGINAL RESEARCH
published: 03 June 2022
doi: 10.3389/fphar.2022.840567

Mangiferin Alleviates Postpartum Depression–Like Behaviors by Inhibiting MAPK Signaling in Microglia

Meichen Yan[1], Xuena Bo[1], Xinchao Zhang[1], Jingdan Zhang[1], Yajin Liao[1], Haiyan Zhang[2], Yong Cheng[1], Junxia Guo[3] and Jinbo Cheng[1,4]**

[1]Center on Translational Neuroscience, College of Life and Environmental Science, Minzu University of China, Beijing, China, [2]Key Laboratory of Modern Preparation of TCM, Ministry of Education, Jiangxi University of Traditional Chinese Medicine, Nanchang, China, [3]Beijing Key Laboratory of Bioactive Substances and Functional Foods, Beijing Union University, Beijing, China, [4]The Brain Science Center, Beijing Institute of Basic Medical Sciences, Beijing, China

Postpartum depression (PPD), a severe mental health disorder, is closely associated with decreased gonadal hormone levels during the postpartum period. Mangiferin (MGF) possesses a wide range of pharmacological activities, including anti-inflammation. Growing evidence has suggested that neuroinflammation is involved in the development of depression. However, the role of MGF in the development of PPD is largely unknown. In the present study, by establishing a hormone-simulated pregnancy PPD mouse model, we found that the administration of MGF significantly alleviated PPD-like behaviors. Mechanistically, MGF treatment inhibited microglial activation and neuroinflammation. Moreover, we found that MGF treatment inhibited mitogen-activated protein kinase (MAPK) signaling *in vivo* and *in vitro*. Together, these results highlight an important role of MGF in microglial activation and thus give insights into the potential therapeutic strategy for PPD treatment.

Keywords: postpartum depression, mangiferin, microglia, neuroinflammation, MAPK signaling

OPEN ACCESS

Edited by:
Karl Tsim,
Hong Kong University of Science and Technology, Hong Kong SAR, China

Reviewed by:
Xiang Cao,
Nanjing Drum Tower Hospital, China
Wenting Wang,
Fourth Military Medical University, China

****Correspondence:***
Jinbo Cheng
cheng_jinbo@126.com
Junxia Guo
junxia@buu.edu.cn

Specialty section:
This article was submitted to Neuropharmacology, a section of the journal Frontiers in Pharmacology

Received: *21 December 2021*
Accepted: *03 May 2022*
Published: *03 June 2022*

Citation:
Yan M, Bo X, Zhang X, Zhang J, Liao Y, Zhang H, Cheng Y, Guo J and Cheng J (2022) Mangiferin Alleviates Postpartum Depression–Like Behaviors by Inhibiting MAPK Signaling in Microglia. Front. Pharmacol. 13:840567. doi: 10.3389/fphar.2022.840567

INTRODUCTION

Postpartum depression (PPD) is a mental health disorder that frequently occurs in women during the postpartum period. The disorder is characterized by emotional changes, including melancholic and languid mood, low self-evaluation, lack of confidence, and even suicidal tendencies. Self-harm behaviors have been reported to be common in PPD patients, ranging from 5 to 14% (Lindahl et al., 2005). The average prevalence rate of PPD was previously reported to be approximately 13% (Weissman et al., 2004); however, recent studies have shown that the global prevalence rate of PPD was higher than the earlier estimate varying across countries (Hahn-Holbrook et al., 2017). Currently, drugs for the treatment of PPD in clinics are mainly monoamine oxidase inhibitors (MAOIs), tricyclic antidepressants, and selective 5-HT reuptake inhibitors (SSRIs). However, owing to the associated side effects, such as anorexia, nausea, diarrhea, headache, nervousness, anxiety, and insomnia (Gjerdingen, 2003), the development of new anti-PPD drugs with higher efficacy and fewer side effects is urgently needed.

The levels of progesterone and estrogen increase steadily during pregnancy but decrease rapidly and remain at lower levels for a long time after childbirth (Hendrick et al., 1998). Dramatic changes in postpartum gonadal hormone levels are thought to be an important reason for the occurrence of PPD in the clinic. Based on this theory, multiple studies have established a PPD animal model by injecting progesterone and estrogen to mimic postpartum gonadal hormone changes (Zhang S et al.,

2017; Zhu and Tang, 2020; Zhang et al., 2021). However, to date, the potential etiology of PPD has remained unclear, and the regulatory mechanisms are largely unknown. Growing evidence has suggested that neuroinflammation is involved in the development of depression. Increased levels of inflammatory cytokines, such as interleukin-1 beta (IL-1β), IL-8, and tumor necrosis factor-α (TNF-α), have been found in depressed patients in the clinic (Bauer et al., 2014; Walker et al., 2014). Microglia are one of the major types of immunological cells in the central nervous system and are involved in multiple neurological diseases, including Alzheimer's (Heneka et al., 2013; Pan et al., 2019; Cheng et al., 2021), Parkinson's (Gao et al., 2002; Lee et al., 2018; Cheng et al., 2020), and stroke (Zhao et al., 2016; Liao et al., 2020). For mental health disorders, it has been documented that microglial activation and NLRP3 inflammasome contribute to the development of post-traumatic stress disorder (Dong et al., 2020; Li S et al., 2021). In addition, it has been reported that the knockout of Dlg1 in microglia alleviated LPS-induced depression in mice by inhibiting microglial activation and neuroinflammation (Peng et al., 2021). Recently, too, neuroinflammation was reported to be involved in PPD pathology (Kendall-Tackett, 2007; Maes et al., 2000; Anderson and Maes, 2013; O'Mahony et al., 2006; Zhang X. L et al., 2017).

Mangiferin (MGF) is a type of tetrahydroxy pyrone carbonate, which can be extracted from several plants, such as *Mangifera indica L* and *Amygdalus communis L*. MGF possesses a wide range of pharmacological properties, including antitussive, anti-asthmatic, antiviral, immunoregulatory, antitumor, and anti-inflammatory activities (Saleh et al., 2014; Sellamuthu et al., 2014; Benard and Chi, 2015; Jang et al., 2016; Shi et al., 2016; Fan et al., 2017). In this study, we established a hormone-simulated pregnancy PPD mouse model and found that MGF alleviated PPD-like behaviors in mice. Mechanistically, MGF inhibited mitogen-activated protein kinase (MAPK) signaling *in vivo* and *in vitro*, thus inhibiting microglial activation and neuroinflammation.

RESULTS

MGF Treatment Alleviates Depression-Like Behavior

To study the effects of MGF on PPD, we established a hormone-simulated pregnancy (HSP) mouse model combined with ovariectomy (OVX). As shown in **Figure 1**, behavioral tests began 10 days after progesterone (P4) withdrawal. Two doses of MGF (20 and 60 mg/kg) were orally administered once per day. Moreover, the novelty-suppressed feeding (NSF) test was used to evaluate exploration and anhedonia behaviors, while the forced swim test (FST) and tail-suspension test (TST) were utilized to assess depression-like behaviors. We found that mice in the PPD model group showed increased immobility time in the NSF test, FST, and TST (**Figures 2A–F**), indicating impaired emotional functions. Interestingly, administration of MGF significantly decreased the immobility time in the NSF test in a dose-dependent manner compared with the PPD group ($p < 0.001$) (**Figures 2A,B**). Consistently, administration of MGF significantly decreased the immobility time in the FST and TST, suggesting alleviated depression-like behaviors (**Figures 2C–F**). Furthermore, we compared the PPD/MGF groups with the control groups through behavioral tests and found that PPD/MGF groups reduced the immobility time of PPD mice in NSF, which was still higher than that in the control groups. However, there was no difference in immobility time between high doses of the MGF and the control group in TST and FST, indicating a protective effect of MGF. Collectively, these results suggest that the administration of MGF could alleviate HSP-induced depression-like behavior in mice.

MGF Treatment Decreases Inflammatory Cytokine Levels in the Mouse Brain

To further study the mechanism underlying the protective effect of MGF, we examined the expression of synaptic plasticity–related protein 95 (PSD95) and brain-derived neurotrophic factor (BDNF) in the hippocampus. However, no significant differences were observed between the MGF-treated groups and the PPD model groups (**Figures 3A–C**). Multiple studies have suggested that neuroinflammation is involved in the development of depression (Engler et al., 2017; Moisan et al., 2021). To determine whether neuroinflammation is involved in this process, we first examined the protein levels of IBA1 and GFAP in the mouse brain. We found that the expression level of IBA1 was increased in the PPD group compared to that in the control group. MGF treatment inhibited this increase in a dose-dependent manner. There were no significant changes in the protein levels of GFAP among the four groups (**Figures 3D–F**).

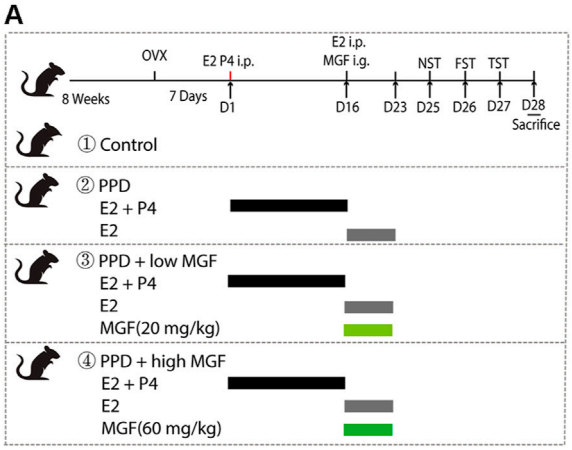

FIGURE 1 | Timeline of experimental design, including the schedule of the hormone-stimulated pregnancy (HSP)-induced postpartum depression (PPD) mice model and drug administration and behavior tests. Female BALA/c mice were ovariectomized bilaterally for 7 days. The ovariectomized mice were injected intraperitoneally with β-estradiol (E2, 0.5 μg/day) and progesterone (P4, 0.8 mg/day) for 16 consecutive days. Progesterone was then withdrawn, and a high dose of β-estradiol (10 μg/day) was administrated alone. At the same time, two-dose concentrations of mangiferin (MGF) were administrated to the treatment group mice.

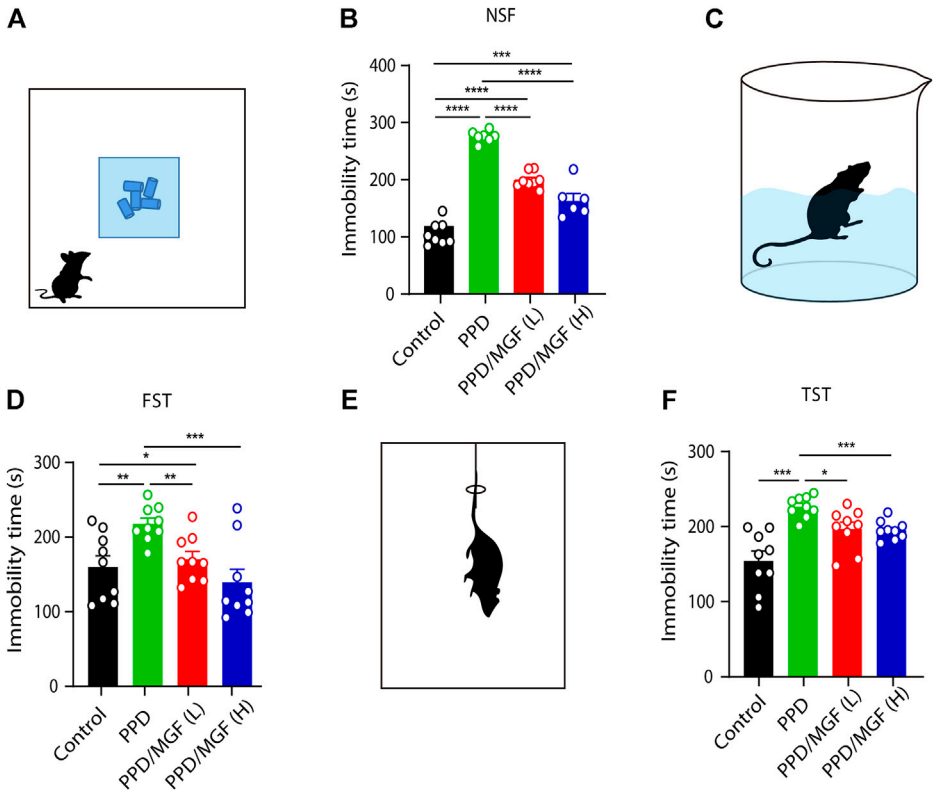

FIGURE 2 | MGF-alleviated HSP-induced depression-like behavior in mice. **(A)** Schematic representation of the novelty suppressed feeding test (NST). **(B)** Analysis of immobility time in the NST [control, n = 8, PPD, n = 7, PPD/MGF (L), n = 8, and PPD/MGF (H), n = 6]. **(C)** Schematic representation of the forced swim test (FST). **(D)** Analysis of immobility time in the FST, n = 9 in each group. **(E)** Schematic representation of the tail-suspension test (TST). **(F)** Analysis of immobility time in the TST, n = 9 in each group; Error bars are mean ± S.E.M. $^{*}p < 0.05$, $^{**}p < 0.01$, and $^{***}p < 0.001$.

Moreover, we found that the levels of inflammatory cytokines TNF-α, IL-6, and IL-1β were significantly increased in the PPD group mice. Interestingly, treatment with MGF significantly inhibited the increase in the levels of these cytokines (**Figures 3G–I**). Together, these results show that MGF treatment inhibited inflammatory cytokine levels in the PPD mouse brain.

MGF Treatment Inhibits Microglia Numbers in the Mouse Brain

Next, we investigated whether microglial activation is involved in this process. To address this, we performed an IBA1 immunofluorescence staining assay, which showed that a higher number of microglia existed in the hippocampus of PDD mice (**Figures 4A,B**). Using Image-Pro Plus software, we analyzed the number of microglia in the CA1 and DG areas of the hippocampus in these four groups of mice. The number of microglia was significantly increased in the CA1 and DG areas of the hippocampus in the PPD group mice ($p < 0.001$ and $p < 0.01$, respectively), while treatment with a high concentration of MGF significantly inhibited this increase, with a decreasing trend seen in the low concentration of MGF treatment groups (**Figures 4C,D**). Thus, these results suggest that microglia were activated in the PPD model mouse brain and that MGF treatment could significantly inhibit microglial activation.

MGF Inhibits Microglial Activation by Targeting MAPK Signaling

To find the potential molecular targets of MGF, bioinformatic analysis of 3D similarity searching, ranking, and superposition was performed using ChemMapper (http://www.lilab-ecust.cn/chemmapper/index.html). Among the predicted targets (MAP kinase–activated protein kinase 2, amine oxidase [flavin-containing] A, sialidase, fatty acid synthase, and transcription factor p65), MAP kinase–activated protein kinase 2 (MAPK) was ranked first, with a 3D similarity score of 1.0 (**Figures 5A,B**). Next, to study changes in MAPK signaling in the hippocampus of the mouse brain, the levels of p-JNK, p-p38, and p-ERK were investigated. As shown in **Figure 5C**, increased levels of these three markers were observed in the PPD group compared to the control group. Notably, administration of MGF inhibited the increase in p-JNK, p-p38, and p-ERK levels, suggesting downregulation of MAPK signaling in the mouse brain. To further confirm the effects of MGF on microglia, we cultured microglial BV2 cells and studied the effect of MGF on

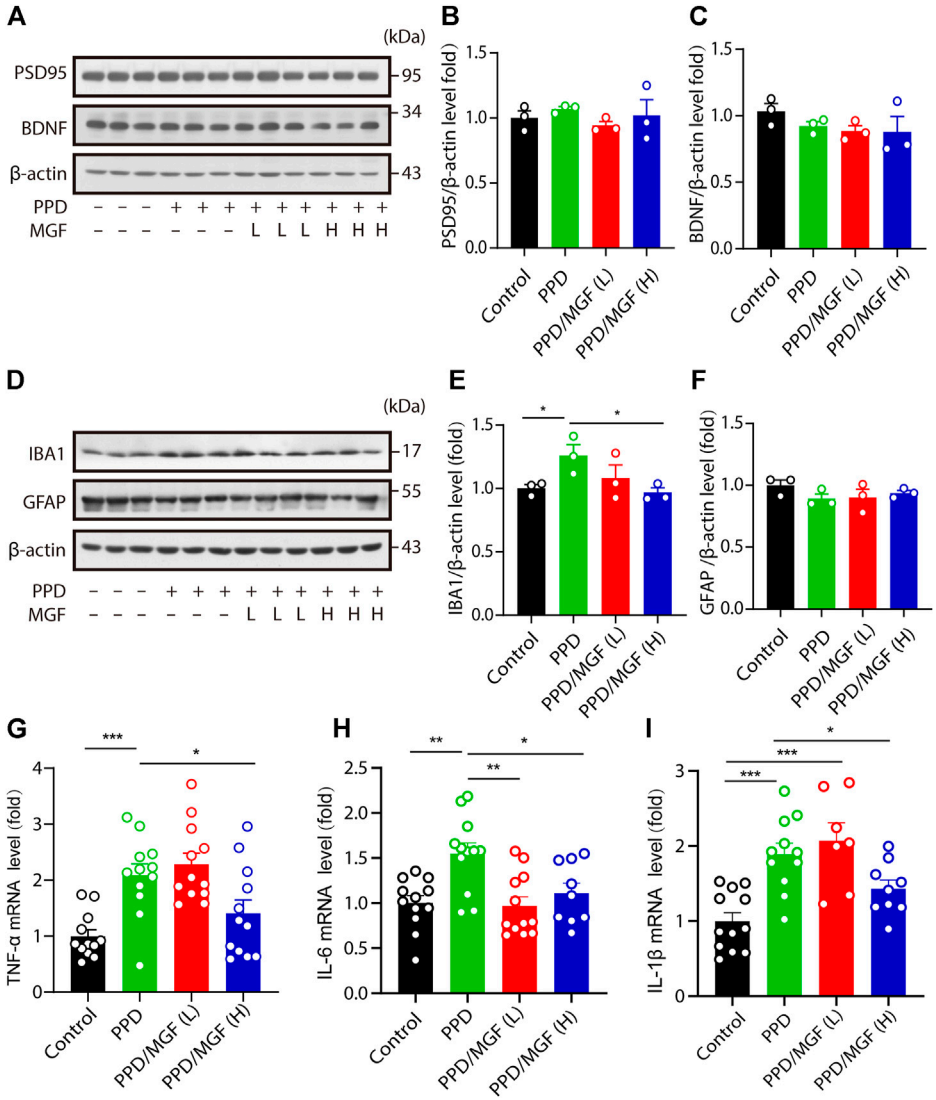

FIGURE 3 | MGF decreased inflammatory cytokine levels in the mouse brain. **(A–C)** Immunoblotting and quantitative analysis of plasticity-related protein 95 (PSD95) and brain-derived neurotrophic factor (BDNF) levels in the hippocampus of mice. **(D–F)** Immunoblotting and quantitative analysis of IBA1 and GFAP protein levels in the cortex of the indicated-group mice. **(G–I)** RT-PCR analysis of TNF-α, IL-6, and IL-1β mRNA levels in the hippocampus of mice. Error bars are mean ± SEM. $^{*}p < 0.05$, $^{**}p < 0.01$, and $^{***}p < 0.001$.

LPS-induced MAPK signaling activation *in vitro* (**Figure 5D**). As shown in **Figure 5E**, LPS treatment increased the protein levels of iNOS, p-JNK, and p-p38, whereas pretreatment with MGF largely inhibited increased levels. Consistently, the levels of the downstream inflammatory cytokines TNF-α, IL-6, and IL-1β were significantly inhibited in the MGF treatment group (**Figures 5F–H**). Collectively, these results show that MGF inhibits microglia-mediated inflammation by targeting MAPK signaling.

In summary, our results show that treatment with MGF significantly alleviated PPD-like behaviors in mice. Mechanistically, we found that MGF inhibited microglial activation by targeting MAPK signaling *in vivo* and *in vitro* (**Figure 6**), providing a potential therapeutic strategy for PPD treatment.

DISCUSSION

As a common but severe mental health disorder, PPD poses a serious global burden worldwide. Multiple animal models of PPD have been established to explore its pathogenesis, including stress-induced (Boccia et al., 2007; Haim et al., 2016), HSP-induced (Stoffel and Craft, 2004; Schiller et al., 2013), and transgenic animal models (Tillmann et al., 2019; McDonnell et al., 2020). Among these, the HSP-induced model is commonly used due to its advantages such as good reproducibility and easier procedure. In this study, increased immobility times were found in the NSF test, FST, and TST in the PPD model group mice, indicating impaired emotional functions. Based on this mouse model, we found that MGF significantly

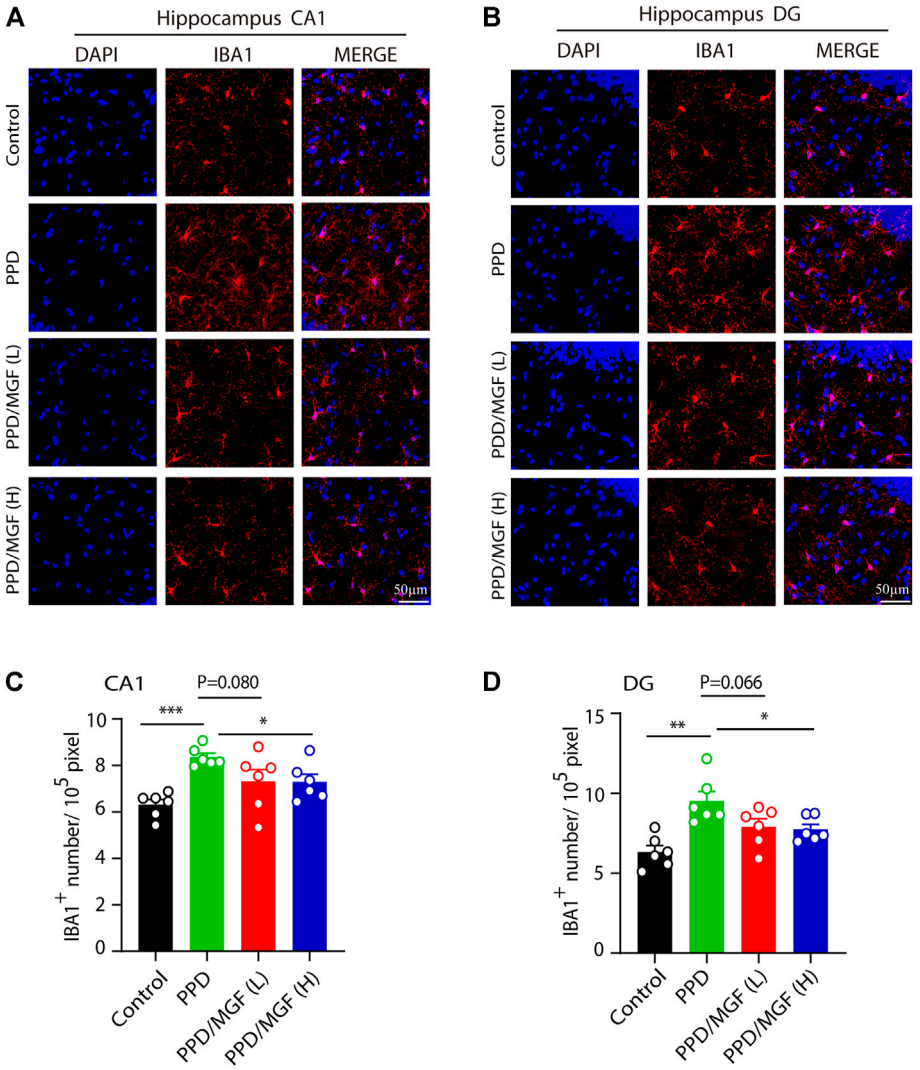

FIGURE 4 | MGF inhibited microglial numbers *in vivo*. **(A–B)** Immunofluorescent staining of IBA1 in CA1 and DG areas of the hippocampus. The scale bar represents 50 μm. **(C–D)** Quantitative analysis of IBA1 cell numbers. Error bars are mean ± SEM. $^{*}p < 0.05$, $^{**}p < 0.01$, and $^{***}p < 0.001$.

alleviated PPD-like behaviors. Mechanistically, we found that MGF modulated MAPK signaling in microglia, thus inhibiting microglial activation and neuroinflammation.

Multiple studies have shown that reproductive hormone levels rapidly decline after delivery and are considered the main contributor to the occurrence of PPD (Bloch et al., 2000; Galea et al., 2001; Studd, 2015). Neuroinflammation, GABAergic inhibition, and hippocampal neurogenesis impairment are associated with the development of PPD (Zhang et al., 2016; Yang et al., 2017; Zhu and Tang, 2020). In this study, we found no significant changes in the levels of synaptic plasticity–related proteins PSD95 and BDNF in the hippocampus of PPD group mice. However, the IBA1 levels, a microglial marker, were significantly increased, and higher levels of the inflammatory cytokines TNF-α, IL-6, and IL-1β were also noted, suggesting involvement of neuroinflammation. IL-6 and IL-1β levels have been reported to be positively correlated with depression scores in postpartum women (Cassidy-Bushrow et al., 2012). Herein, the dose of MGF was determined based on previous *in vivo* experiments. Administration of 20 mg/kg of MGF possesses several beneficial biological activities, including inhibition of mastitis induced by LPS (Qu et al., 2017), ameliorating learning deficits (Jung et al., 2009), and antidepressant effects in a chronic mild stress mouse model (Cao et al., 2017). Moreover, concentrations of 30, 40, and 60 mg/kg were used in previous studies (Jangra et al., 2014; Song et al., 2020). Therefore, concentrations of 20 and 60 mg/kg MGF were chosen for this study. Notably, we found that treatment with MGF effectively suppressed the increase in inflammatory levels and alleviated HSP-induced depression-like behavior in mice, suggesting that the beneficial role of MGF in PPD may be due to its anti-inflammatory effects.

As resident immune cells of the central nervous system, microglia play a critical role in neuroinflammation. Microglial

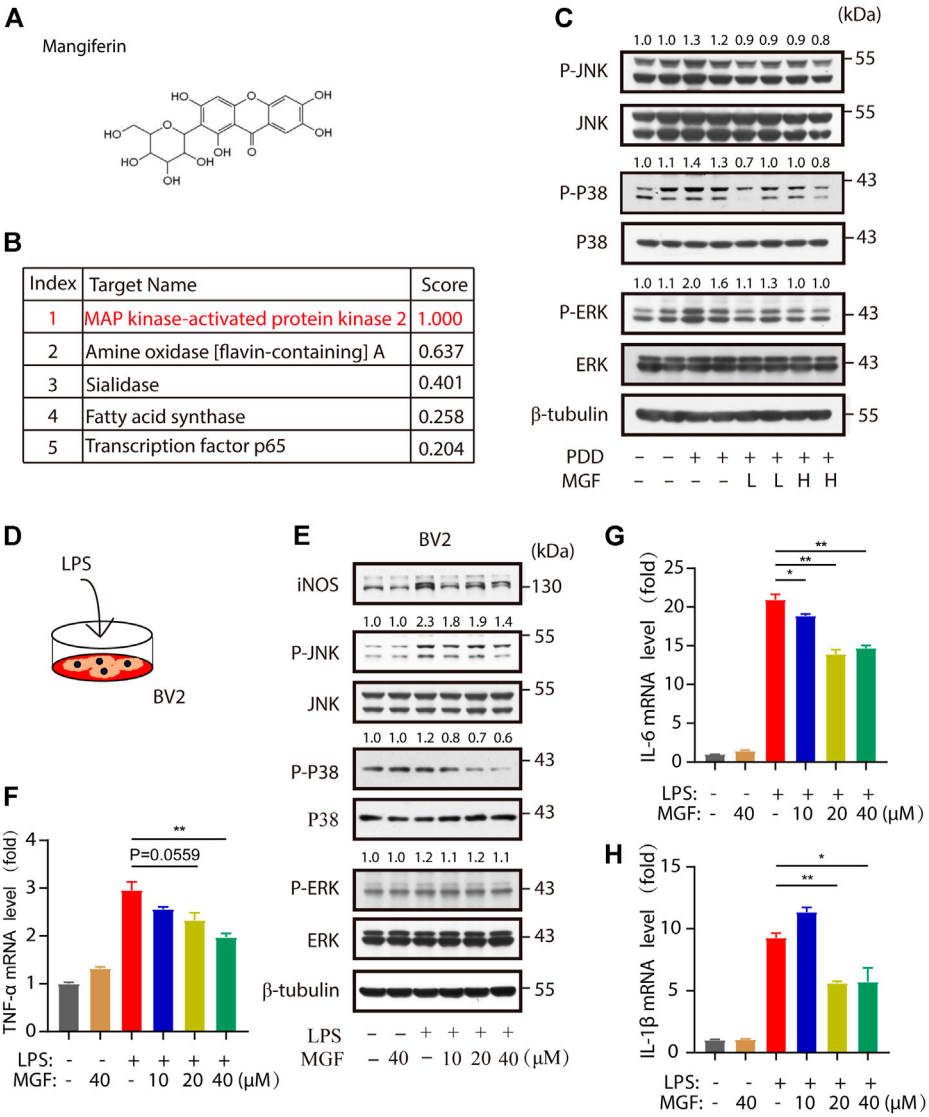

FIGURE 5 | MGF-regulated mitogen-activated protein kinase (MAPK) signaling *in vivo* and *in vitro*. **(A)** MGF structure. **(B)** Potential protein targets of MGF ranked by the standard score of the probabilities. **(C)** Immunoblotting analysis of p-JNK, JNK, p-p38, p38, p-ERK, ERK, and β-tubulin protein levels in the hippocampus of mice. The number represents the normalized quantitative value of the protein. **(D)** The schematic representation of LPS stimulation in BV2 cells. **(E)** Immunoblotting analysis of iNOS, p-JNK, JNK, p-p38, p38, p-ERK, ERK, and β-tubulin protein levels from BV2 cells after being treated with MGF for 0.5 h and then stimulated LPS (1 μg/ml) for 6 h. The number represents the normalized quantitative value of the protein. **(F–H)** RT-PCR analysis of TNF-α, IL-6, and IL-1β mRNA levels in BV2 cells after being treated with MGF for 0.5 h and then stimulated LPS (1 μg/ml) for 6 h. Error bars are mean ± SEM. $^{*}p < 0.05$, $^{**}p < 0.01$, and $^{***}p < 0.001$.

activation is closely associated with neurodegenerative diseases, strokes, and psychiatry disorders (Dong et al., 2020; Liao et al., 2020; Li S et al., 2021; Cheng et al., 2021). Here, we found that the number of microglia significantly increased in the hippocampus of the PPD group mouse brain, suggesting that microglial activation might be involved in the development of PPD. Moreover, treatment with MGF significantly inhibited the increase in microglial number in the hippocampus, suggesting that the neuroprotective role of MGF might be associated with its inhibitory effect on microglial activation. To further elucidate the potential targets of MGF, we performed bioinformatics analysis and found that MGF targets MAPK signaling, which regulates cell proliferation, stress response, inflammation, cell differentiation, and apoptosis (Li Z et al., 2021; Qin et al., 2021; Wang et al., 2021; Yang et al., 2021). More importantly, the MAPK signal pathway has been linked to several diseases, including depression (Duman et al., 2007; Wang and Mao, 2019; Humo et al., 2020). In this study, we confirmed the inhibitory effect of MGF on MAPK signaling *in vivo* and *in vitro*. Nevertheless, further regulatory mechanisms must be clarified in the future.

Our results demonstrate that treatment with MGF attenuated HSP-induced PPD-like behaviors in mice. Mechanistically, we found that MGF suppressed microglial activation by targeting and inhibiting MAPK signaling activation, thus inhibiting

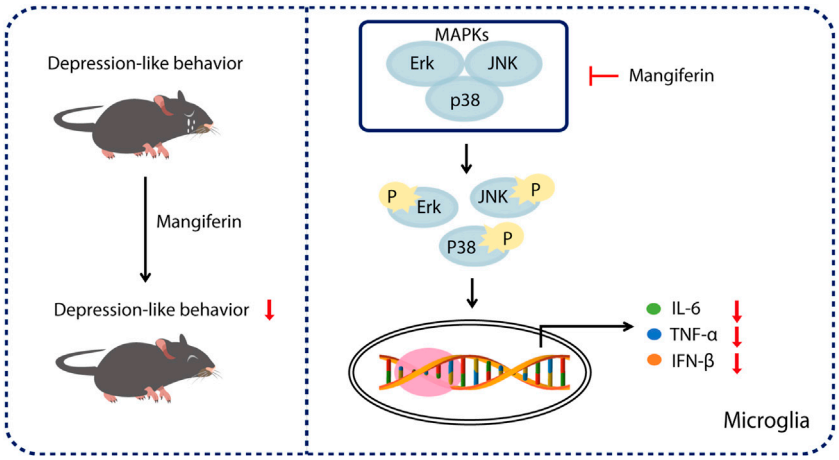

FIGURE 6 | Schematic representation of the mechanism of MGF in treatment of PDD in mice. Treatment of MGF could significantly alleviate the HSP-induced PPD-like behaviors in mice. Mechanistically, MGF inhibited microglial activation by targeting MAPK signaling *in vivo* and *in vitro*.

downstream inflammatory cytokine levels, suggesting a potential therapeutic target for the clinical treatment of PPD.

MATERIAL AND METHODS

Reagents and Antibodies

MGF (purity ≥98%) was purchased from Chengdu Desite Biotechnology (Chengdu, China). β-estradiol (E8875), dimethyl sulfoxide (DMSO), and LPS were purchased from Sigma-Aldrich (St. Louis, MO, United States). Progesterone was obtained from VETEC (V900699). The antibodies used for western blotting were as follows: Iba1/AIF-1 (E4O4W) (#17198), GFAP (E4L7M) (#80788), PSD95 (D27E11) (#3450), BDNF (#47808), iNOS (D6B6S) (#13120), anti-p-ERK1/2 (Thr202/Tyr204) (#9101), anti-ERK1/2 (#9102), anti-p-p38 MAPK (Thr180/Tyr182) (#4511), anti-p38 MAPK (#9212), and anti-p-JNK (Thr183/Tyr185) (#9251) were purchased from Cell Signaling Technology (Beverly, MA, United States). β-tubulin (#CW0098A) and β-actin (#CW0096M) were procured from CWBiotech (Beijing, China).

Mice

Female BALA/c mice (8 weeks old, 20–25 g) were housed in the animal care facility of our institute. All animal experimental procedures were approved by the Biological and Medical Ethics Committee of Minzu University of China. All mice were maintained under conditions of a 12-h light/dark cycle at 23°C and were provided with food and water.

Cell Culture and Treatment

BV-2 microglial cell lines were maintained in Dulbecco's Modified Eagle's Medium (DMEM, #11965-092, Life Technologies, Waltham, MA, United States) supplemented with 10% heat-inactivated fetal bovine serum (FBS, #04-001-1A, Biological Industries, Israel) and 1% penicillin-streptomycin solution (#03-031-1B, Biological Industries) at 37°C in a humidified atmosphere with 5% CO_2.

PPD Model

Two-month-old female mice were chosen, and hormone-induced pseudopregnancy (HSP)-induced PPD models were established as previously described (Li et al., 2018; Zhang et al., 2021). Mice were randomly divided into four groups (control, PPD, PPD/low MGF, and PPD/high MGF). OVX was performed under isoflurane anesthesia. After 7 days of recovery from OVX operation, mice in the PPD and PPD with MGF treatment groups were intraperitoneally injected with β-estradiol (E2, 0.5 g/day) and progesterone (P4, 0.8 mg/day) dissolved in 0.1 ml sesame oil daily for 16 days, resulting in a gradual increase in the concentration of E2 and P4 in mice to mimic the increases in hormone levels. Subsequently, mice were intraperitoneally injected with E2 (10 μg/day) alone for seven consecutive days to mimic high levels of E2 during pregnancy. Meanwhile, MGF was administered intragastrically at two different doses (20 and 60 mg/kg), as indicated in **Figure 1**.

NST

The NST was performed as previously described, with minor modifications (Barbieri et al., 2021). Briefly, before the test, the mice were deprived of food but had free access to water for 24 h. Each mouse was positioned into the device with food placed on white paper in the same direction and allowed to freely explore for 5 min. The immobility time of each mouse was recorded.

FST

One day before the test, mice were allowed to swim in water for 5 min. During the test, the mice were placed in a beaker (volume, 3 L) filled with water at 23–25°C. The total test time was 6 min, and the immobility time of the mice in the last 4 min was recorded.

TST

Mice were placed in the test room 2 h before the test and hung on the instrument with a clip. Similar to the FST, the total experimental time was 6 min, and the immobility time of the mice in the last 4 min was recorded.

Real-Time Quantitative and Reverse Transcription-PCR

Total RNA was isolated from the hippocampus of mice in each group using a TRIzol reagent (Invitrogen, cat#15596018), and 1 μg of RNA was used to synthesize cDNA using a one-step first-strand cDNA synthesis kit (Transgen Biotech, cat#AT341). Quantitative real-time PCR was performed using a 2 × SYBR Green PCR master mix (Transgen Biotech, cat#AQ131) and an Agilent Mx3005P RT-PCR system. The expression levels of the tested genes were normalized to those of β-actin. The primers for mouse IL-1β, TNF-α, IL-6, and β-actin were as follows:

Mouse IL-1β: Forward: 5′-TGTAATGAAAGACGGCAC ACC-3′; Reverse: 5′-TCTTCTTTGGGTATTGCTTGG-3′.

Mouse TNF-α: Forward: 5′-CAGGCGGTGCCTATGTCTC-3’; Reverse: 5′-CGATCACCCCGAAGTTCAGTA G-3′.

Mouse IL-6: Forward: 5′-CTACCAAACTGGATATAATCA GGA-3′; Reverse: 5′-CCAGGTAGCTATGGTACTCCAGAA-3′.

Mouse β-actin: Forward: 5′-GGCTGTATTCCC CTCCATCG-3′; Reverse: 5′-CCAGTTGGTAACAATGCCATG T-3′.

Western Blotting Analysis

The concentration of the extracted protein was determined using the BCA assay. Equal amounts of protein were separated by polyacrylamide gel electrophoresis (SDS-PAGE) and incubated with the primary antibody overnight at 4°C, followed by incubation with a secondary antibody (1:5,000) for 1 h at room temperature. An ECL luminescent solution was used for detection.

Immunofluorescent Staining

After anesthesia, the mice were perfused with normal saline, and then the whole brain was isolated and fixed with 4% paraformaldehyde for 24 h and dehydrated overnight in 30% sucrose solution. Whole brain tissue was embedded in OCT and sectioned using a freezing microtome (Leica CM3050S). Tissue sections were incubated with anti–goat IBA1 antibody (1:500, WAKO, Japan) overnight at 4°C with shaking. On the following day, tissue sections were incubated with secondary antibodies for 1 h at room temperature. Finally, images were captured using a laser scanning confocal microscope (Nikon, Tokyo, Japan).

Statistical Analysis

All data are presented as mean ± SEM. The significance of the differences was determined by the *t*-test and one-way ANOVA using GraphPad Prism (GraphPad Software, San Diego, CA, United States). $^{*}p < 0.05$, $^{**}p < 0.01$, and $^{***}p < 0.001$ were considered as significant.

DATA AVAILABILITY STATEMENT

The original contributions presented in the study are included in the article/**Supplementary Material**; further inquiries can be directed to the corresponding authors.

ETHICS STATEMENT

The animal study was reviewed and approved by the Biological and Medical Ethics Committee, Minzu University of China.

AUTHOR CONTRIBUTIONS

MY designed and performed the experiments and analyzed the data. XB, XZ, and JZ contributed to the parts of the experiments. HZ, YL, YC, and JG analyzed data and provided suggestions. JC supervised the research.

FUNDING

This work was supported by grants from the National Nature Science Foundation of China (Grant No. 81870839 and No. 82071218) and the open fund of the Key Laboratory of Modern Preparation of TCM, Ministry of Education, Jiangxi University of Traditional Chinese Medicine (TCM-201915).

SUPPLEMENTARY MATERIAL

The Supplementary Material for this article can be found online at: https://www.frontiersin.org/articles/10.3389/fphar.2022.840567/full#supplementary-material

REFERENCES

Anderson, G., and Maes, M. (2013). Postpartum Depression: Psychoneuroimmunological Underpinnings and Treatment. *Neuropsychiatr. Dis. Treat.* 9, 277–287. doi:10.2147/NDT.S25320

Barbieri, S. S., Sandrini, L., Musazzi, L., Popoli, M., and Ieraci, A. (2021). Apocynin Prevents Anxiety-like Behavior and Histone Deacetylases Overexpression Induced by Sub-chronic Stress in Mice. *Biomolecules* 11, 885. doi:10.3390/biom11060885

Bauer, I. E., Pascoe, M. C., Wollenhaupt-Aguiar, B., Kapczinski, F., and Soares, J. C. (2014). Inflammatory Mediators of Cognitive Impairment in Bipolar Disorder. *J. Psychiatr. Res.* 56, 18–27. doi:10.1016/j.jpsychires.2014.04.017

Benard, O., and Chi, Y. (2015). Medicinal Properties of Mangiferin, Structural Features, Derivative Synthesis, Pharmacokinetics and Biological Activities. *Mini Rev. Med. Chem.* 15, 582–594. doi:10.2174/1389557515666150401111410

Bloch, M., Schmidt, P. J., Danaceau, M., Murphy, J., Nieman, L., and Rubinow, D. R. (2000). Effects of Gonadal Steroids in Women with a History of Postpartum Depression. *Am. J. Psychiatry* 157, 924–930. doi:10.1176/appi.ajp.157.6.924

Boccia, M. L., Razzoli, M., Vadlamudi, S. P., Trumbull, W., Caleffie, C., and Pedersen, C. A. (2007). Repeated Long Separations from Pups Produce Depression-like Behavior in Rat Mothers. *Psychoneuroendocrinology* 32, 65–71. doi:10.1016/j.psyneuen.2006.10.004

Cao, C., Su, M., and Zhou, F. (2017). Mangiferin Inhibits Hippocampal NLRP3 Inflammasome and Exerts Antidepressant Effects in a Chronic Mild Stress Mice Model. *Behav. Pharmacol.* 28, 356–364. doi:10.1097/FBP.0000000000000305

Cassidy-Bushrow, A. E., Peters, R. M., Johnson, D. A., and Templin, T. N. (2012). Association of Depressive Symptoms with Inflammatory Biomarkers Among Pregnant African-American Women. *J. Reprod. Immunol.* 94, 202–209. doi:10.1016/j.jri.2012.01.007

Cheng, J., Dong, Y., Ma, J., Pan, R., Liao, Y., Kong, X., et al. (2021). Microglial Calhm2 Regulates Neuroinflammation and Contributes to Alzheimer's Disease Pathology. *Sci. Adv.* 7, eabe3600. doi:10.1126/sciadv.abe3600

Cheng, J., Liao, Y., Dong, Y., Hu, H., Yang, N., Kong, X., et al. (2020). Microglial Autophagy Defect Causes Parkinson Disease-like Symptoms by Accelerating Inflammasome Activation in Mice. *Autophagy* 16, 1–13. doi:10.1080/15548627.2020.1719723

Dong, Y., Li, S., Lu, Y., Li, X., Liao, Y., Peng, Z., et al. (2020). Stress-induced NLRP3 Inflammasome Activation Negatively Regulates Fear Memory in Mice. *J. Neuroinflammation* 17, 205. doi:10.1186/s12974-020-01842-0

Duman, C. H., Schlesinger, L., Kodama, M., Russell, D. S., and Duman, R. S. (2007). A Role for MAP Kinase Signaling in Behavioral Models of Depression and Antidepressant Treatment. *Biol. Psychiatry* 61, 661–670. doi:10.1016/j.biopsych.2006.05.047

Engler, H., Brendt, P., Wischermann, J., Wegner, A., Röhling, R., Schoemberg, T., et al. (2017). Selective Increase of Cerebrospinal Fluid IL-6 during Experimental Systemic Inflammation in Humans: Association with Depressive Symptoms. *Mol. Psychiatry* 22, 1448–1454. doi:10.1038/mp.2016.264

Fan, K., Ma, J., Xiao, W., Chen, J., Wu, J., Ren, J., et al. (2017). Mangiferin Attenuates Blast-Induced Traumatic Brain Injury via Inhibiting NLRP3 Inflammasome. *Chem. Biol. Interact.* 271, 15–23. doi:10.1016/j.cbi.2017.04.021

Galea, L. A., Wide, J. K., and Barr, A. M. (2001). Estradiol Alleviates Depressive-like Symptoms in a Novel Animal Model of Post-partum Depression. *Behav. Brain Res.* 122, 1–9. doi:10.1016/s0166-4328(01)00170-x

Gao, H. M., Jiang, J., Wilson, B., Zhang, W., Hong, J. S., and Liu, B. (2002). Microglial Activation-Mediated Delayed and Progressive Degeneration of Rat Nigral Dopaminergic Neurons: Relevance to Parkinson's Disease. *J. Neurochem.* 81, 1285–1297. doi:10.1046/j.1471-4159.2002.00928.x

Gjerdingen, D. (2003). The Effectiveness of Various Postpartum Depression Treatments and the Impact of Antidepressant Drugs on Nursing Infants. *J. Am. Board Fam. Pract.* 16, 372–382. doi:10.3122/jabfm.16.5.372

Hahn-Holbrook, J., Cornwell-Hinrichs, T., and Anaya, I. (2017). Economic and Health Predictors of National Postpartum Depression Prevalence: A Systematic Review, Meta-Analysis, and Meta-Regression of 291 Studies from 56 Countries. *Front. Psychiatry* 8, 248. doi:10.3389/fpsyt.2017.00248

Haim, A., Albin-Brooks, C., Sherer, M., Mills, E., and Leuner, B. (2016). The Effects of Gestational Stress and Selective Serotonin Reuptake Inhibitor Antidepressant Treatment on Structural Plasticity in the Postpartum Brain--A Translational Model for Postpartum Depression. *Horm. Behav.* 77, 124–131. doi:10.1016/j.yhbeh.2015.05.005

Hendrick, V., Altshuler, L. L., and Suri, R. (1998). Hormonal Changes in the Postpartum and Implications for Postpartum Depression. *Psychosomatics* 39, 93–101. doi:10.1016/S0033-3182(98)71355-6

Heneka, M. T., Kummer, M. P., Stutz, A., Delekate, A., Schwartz, S., Vieira-Saecker, A., et al. (2013). NLRP3 Is Activated in Alzheimer's Disease and Contributes to Pathology in APP/PS1 Mice. *Nature* 493, 674–678. doi:10.1038/nature11729

Humo, M., Ayazgök, B., Becker, L. J., Waltisperger, E., Rantamäki, T., and Yalcin, I. (2020). Ketamine Induces Rapid and Sustained Antidepressant-like Effects in Chronic Pain Induced Depression: Role of MAPK Signaling Pathway. *Prog. Neuropsychopharmacol. Biol. Psychiatry* 100, 109898. doi:10.1016/j.pnpbp.2020.109898

Jang, J. H., Lee, K. H., Jung, H. K., Sim, M. O., Kim, T. M., Woo, K. W., et al. (2016). Anti-inflammatory Effects of 6'-O-Acetyl Mangiferin from Iris Rossii Baker via NF-Kappab Signal Blocking in Lipopolysaccharide-Stimulated RAW 264.7 Cells. *Chem. Biol. Interact.* 257, 54–60. doi:10.1016/j.cbi.2016.07.029

Jangra, A., Lukhi, M. M., Sulakhiya, K., Baruah, C. C., and Lahkar, M. (2014). Protective Effect of Mangiferin against Lipopolysaccharide-Induced Depressive and Anxiety-like Behaviour in Mice. *Eur. J. Pharmacol.* 740, 337–345. doi:10.1016/j.ejphar.2014.07.031

Jung, K., Lee, B., Han, S. J., Ryu, J. H., and Kim, D. H. (2009). Mangiferin Ameliorates Scopolamine-Induced Learning Deficits in Mice. *Biol. Pharm. Bull.* 32, 242–246. doi:10.1248/bpb.32.242

Kendall-Tackett, K. (2007). A New Paradigm for Depression in New Mothers: the Central Role of Inflammation and How Breastfeeding and Anti-inflammatory Treatments Protect Maternal Mental Health. *Int. Breastfeed. J.* 2, 6. doi:10.1186/1746-4358-2-6

Lee, E., Hwang, I., Park, S., Hong, S., Hwang, B., Cho, Y., et al. (2018). MPTP-driven NLRP3 Inflammasome Activation in Microglia Plays a Central Role in Dopaminergic Neurodegeneration. *Cell Death Differ* 26 (2), 213–228. doi:10.1038/s41418-018-0124-5

Li, S., Liao, Y., Dong, Y., Li, X., Li, J., Cheng, Y., et al. (2021). Microglial Deletion and Inhibition Alleviate Behavior of Post-traumatic Stress Disorder in Mice. *J. Neuroinflammation* 18, 7. doi:10.1186/s12974-020-02069-9

Li, X. B., Liu, A., Yang, L., Zhang, K., Wu, Y. M., Zhao, M. G., et al. (2018). Antidepressant-like Effects of Translocator Protein (18 kDa) Ligand ZBD-2 in Mouse Models of Postpartum Depression. *Mol. Brain* 11, 12. doi:10.1186/s13041-018-0355-x

Li, Z., Wang, X., Hong, T. P., Wang, H. J., Gao, Z. Y., and Wan, M. (2021). Advanced Glycosylation End Products Inhibit the Proliferation of Bone-Marrow Stromal Cells through Activating MAPK Pathway. *Eur. J. Med. Res.* 26, 94. doi:10.1186/s40001-021-00559-x

Liao, Y., Cheng, J., Kong, X., Li, S., Li, X., Zhang, M., et al. (2020). HDAC3 Inhibition Ameliorates Ischemia/reperfusion-Induced Brain Injury by Regulating the Microglial cGAS-STING Pathway. *Theranostics* 10, 9644–9662. doi:10.7150/thno.47651

Lindahl, V., Pearson, J. L., and Colpe, L. (2005). Prevalence of Suicidality during Pregnancy and the Postpartum. *Arch. Womens Ment. Health* 8, 77–87. doi:10.1007/s00737-005-0080-1

Maes, M., Lin, A. H., Ombelet, W., Stevens, K., Kenis, G., De Jongh, R., et al. (2000). Immune Activation in the Early Puerperium Is Related to Postpartum Anxiety and Depressive Symptoms. *Psychoneuroendocrinology* 25, 121–137. doi:10.1016/s0306-4530(99)00043-8

McDonnell, C. W., Dunphy-Doherty, F., Rouine, J., Bianchi, M., Upton, N., Sokolowska, E., et al. (2020). The Antidepressant-like Effects of a Clinically Relevant Dose of Ketamine Are Accompanied by Biphasic Alterations in Working Memory in the Wistar Kyoto Rat Model of Depression. *Front. Psychiatry* 11, 599588. doi:10.3389/fpsyt.2020.599588

Moisan, M. P., Foury, A., Dexpert, S., Cole, S. W., Beau, C., Forestier, D., et al. (2021). Transcriptomic Signaling Pathways Involved in a Naturalistic Model of Inflammation-Related Depression and its Remission. *Transl. Psychiatry* 11, 203. doi:10.1038/s41398-021-01323-9

O'Mahony, S. M., Myint, A. M., van den Hove, D., Desbonnet, L., Steinbusch, H., and Leonard, B. E. (2006). Gestational Stress Leads to Depressive-like Behavioural and Immunological Changes in the Rat. *Neuroimmunomodulation* 13, 82–88. doi:10.1159/000096090

Pan, R. Y., Ma, J., Kong, X. X., Wang, X. F., Li, S. S., Qi, X. L., et al. (2019). Sodium Rutin Ameliorates Alzheimer's Disease-like Pathology by Enhancing Microglial Amyloid-β Clearance. *Sci. Adv.* 5, eaau6328. doi:10.1126/sciadv.aau6328

Peng, Z., Li, X., Li, J., Dong, Y., Gao, Y., Liao, Y., et al. (2021). Dlg1 Knockout Inhibits Microglial Activation and Alleviates Lipopolysaccharide-Induced Depression-like Behavior in Mice. *Neurosci. Bull.* 37, 1671. doi:10.1007/s12264-021-00765-x

Qin, Z., Hua, S., Chen, H., Wang, Z., Wang, H., Xu, J., et al. (2021). Parathyroid Hormone Promotes the Osteogenesis of Lipopolysaccharide-Induced Human Bone Marrow Mesenchymal Stem Cells through the JNK MAPK Pathway. *Biosci. Rep.* 41, BSR20210420. doi:10.1042/BSR20210420

Qu, S., Wang, W., Li, D., Li, S., Zhang, L., Fu, Y., et al. (2017). Mangiferin Inhibits Mastitis Induced by LPS via Suppressing NF-κb and NLRP3 Signaling Pathways. *Int. Immunopharmacol.* 43, 85–90. doi:10.1016/j.intimp.2016.11.036

Saleh, S., El-Maraghy, N., Reda, E., and Barakat, W. (2014). Modulation of Diabetes and Dyslipidemia in Diabetic Insulin-Resistant Rats by Mangiferin: Role of Adiponectin and TNF-Alpha. *Acad Bras Cienc* 86, 1935–1948. doi:10.1590/0001-3765201420140212

Schiller, C. E., O'Hara, M. W., Rubinow, D. R., and Johnson, A. K. (2013). Estradiol Modulates Anhedonia and Behavioral Despair in Rats and Negative Affect in a

Subgroup of Women at High Risk for Postpartum Depression. *Physiol. Behav.* 119, 137–144. doi:10.1016/j.physbeh.2013.06.009

Sellamuthu, P. S., Arulselvan, P., Fakurazi, S., and Kandasamy, M. (2014). Beneficial Effects of Mangiferin Isolated from Salacia Chinensis on Biochemical and Hematological Parameters in Rats with Streptozotocin-Induced Diabetes. *Pak J. Pharm. Sci.* 27, 161–167. doi:10.1016/S2221-1691(12)60457-2

Shi, W., Deng, J., Tong, R., Yang, Y., He, X., Lv, J., et al. (2016). Molecular Mechanisms Underlying Mangiferin-Induced Apoptosis and Cell Cycle Arrest in A549 Human Lung Carcinoma Cells. *Mol. Med. Rep.* 13, 3423–3432. doi:10.3892/mmr.2016.4947

Song, Y., Liu, W., Tang, K., Zang, J., Li, D., and Gao, H. (2020). Mangiferin Alleviates Renal Interstitial Fibrosis in Streptozotocin-Induced Diabetic Mice through Regulating the PTEN/PI3K/Akt Signaling Pathway. *J. Diabetes Res.* 2020, 9481720. doi:10.1155/2020/9481720

Stoffel, E. C., and Craft, R. M. (2004). Ovarian Hormone Withdrawal-Induced "depression" in Female Rats. *Physiol. Behav.* 83, 505–513. doi:10.1016/j.physbeh.2004.08.033

Studd, J. (2015). Personal View: Hormones and Depression in Women. *Climacteric* 18, 3–5. doi:10.3109/13697137.2014.918595

Tillmann, S., Happ, D. F., Mikkelsen, P. F., Geisel, J., Wegener, G., and Obeid, R. (2019). Behavioral and Metabolic Effects of S-Adenosylmethionine and Imipramine in the Flinders Sensitive Line Rat Model of Depression. *Behav. Brain Res.* 364, 274–280. doi:10.1016/j.bbr.2019.02.011

Walker, A. K., Kavelaars, A., Heijnen, C. J., and Dantzer, R. (2014). Neuroinflammation and Comorbidity of Pain and Depression. *Pharmacol. Rev.* 66, 80–101. doi:10.1124/pr.113.008144

Wang, J. Q., and Mao, L. (2019). The ERK Pathway: Molecular Mechanisms and Treatment of Depression. *Mol. Neurobiol.* 56, 6197–6205. doi:10.1007/s12035-019-1524-3

Wang, S., Guo, Y., Yang, C., Huang, R., Wen, Y., Zhang, C., et al. (2021). Swainsonine Triggers Paraptosis via ER Stress and MAPK Signaling Pathway in Rat Primary Renal Tubular Epithelial Cells. *Front. Pharmacol.* 12, 715285. doi:10.3389/fphar.2021.715285

Weissman, A. M., Levy, B. T., Hartz, A. J., Bentler, S., Donohue, M., Ellingrod, V. L., et al. (2004). Pooled Analysis of Antidepressant Levels in Lactating Mothers, Breast Milk, and Nursing Infants. *Am. J. Psychiatry* 161, 1066–1078. doi:10.1176/appi.ajp.161.6.1066

Yang, R., Zhang, B., Chen, T., Zhang, S., and Chen, L. (2017). Postpartum Estrogen Withdrawal Impairs GABAergic Inhibition and LTD Induction in Basolateral Amygdala Complex via Down-Regulation of GPR30. *Eur. Neuropsychopharmacol.* 27, 759–772. doi:10.1016/j.euroneuro.2017.05.010

Yang, X., Zhou, Y., Chen, Z., Chen, C., Han, C., Li, X., et al. (2021). Curcumenol Mitigates Chondrocyte Inflammation by Inhibiting the NF-κB and MAPK Pathways, and Ameliorates DMM-induced OA in Mice. *Int. J. Mol. Med.* 48, 192. doi:10.3892/ijmm.2021.5025

Zhang, Q., Huang, Q., Yao, L., Liu, W., Ruan, J., Nong, Y., et al. (2021). Gestational Folic Acid Administration Alleviated Maternal Postpartum Emotional and Cognitive Dysfunction in Mice. *Front. Pharmacol.* 12, 701009. doi:10.3389/fphar.2021.701009

Zhang, S., Hong, J., Zhang, T., Wu, J., and Chen, L. (2017). Activation of Sigma-1 Receptor Alleviates Postpartum Estrogen Withdrawal-Induced "Depression" through Restoring Hippocampal nNOS-NO-CREB Activities in Mice. *Mol. Neurobiol.* 54, 3017–3030. doi:10.1007/s12035-016-9872-8

Zhang, X. L., Wang, L., Xiong, L., Huang, F. H., and Xue, H. (2017). Timosaponin B-III Exhibits Antidepressive Activity in a Mouse Model of Postpartum Depression by the Regulation of Inflammatory Cytokines, BNDF Signaling and Synaptic Plasticity. *Exp. Ther. Med.* 14, 3856–3861. doi:10.3892/etm.2017.4930

Zhang, Z., Hong, J., Zhang, S., Zhang, T., Sha, S., Yang, R., et al. (2016). Postpartum Estrogen Withdrawal Impairs Hippocampal Neurogenesis and Causes Depression- and Anxiety-like Behaviors in Mice. *Psychoneuroendocrinology* 66, 138–149. doi:10.1016/j.psyneuen.2016.01.013

Zhao, S., Yin, J., Zhou, L., Yan, F., He, Q., Huang, L., et al. (2016). Hippo/MST1 Signaling Mediates Microglial Activation Following Acute Cerebral Ischemia-Reperfusion Injury. *Brain Behav. Immun.* 55, 236–248. doi:10.1016/j.bbi.2015.12.016

Zhu, J., and Tang, J. (2020). LncRNA Gm14205 Induces Astrocytic NLRP3 Inflammasome Activation via Inhibiting Oxytocin Receptor in Postpartum Depression. *Biosci. Rep.* 40, BSR20200672. doi:10.1042/BSR20200672

Conflict of Interest: The authors declare that the research was conducted in the absence of any commercial or financial relationships that could be construed as a potential conflict of interest.

Publisher's Note: All claims expressed in this article are solely those of the authors and do not necessarily represent those of their affiliated organizations, or those of the publisher, the editors, and the reviewers. Any product that may be evaluated in this article, or claim that may be made by its manufacturer, is not guaranteed or endorsed by the publisher.

frontiers | Frontiers in Pharmacology

REVIEW
published: 16 June 2022
doi: 10.3389/fphar.2022.925879

Sigma-1 Receptors in Depression: Mechanism and Therapeutic Development

Peng Ren[1†], Jingya Wang[1†], Nanxi Li[2], Guangxiang Li[1], Hui Ma[1], Yongqi Zhao[1]* and Yunfeng Li[1,3]**

[1]Beijing Institute of Basic Medical Sciences, Beijing, China, [2]Department of Pharmaceutical Sciences, Beijing Institute of Radiation Medicine, Beijing, China, [3]State Key Laboratory of Toxicology and Medical Countermeasures, Beijing Key Laboratory of Neuropsychopharmacology, Beijing Institute of Pharmacology and Toxicology, Beijing, China

Depression is the most common type of neuropsychiatric illness and has increasingly become a major cause of disability. Unfortunately, the recent global pandemic of COVID-19 has dramatically increased the incidence of depression and has significantly increased the burden of mental health care worldwide. Since full remission of the clinical symptoms of depression has not been achieved with current treatments, there is a constant need to discover new compounds that meet the major clinical needs. Recently, the roles of sigma receptors, especially the sigma-1 receptor subtype, have attracted increasing attention as potential new targets and target-specific drugs due to their translocation property that produces a broad spectrum of biological functions. Even clinical first-line antidepressants with or without affinity for sigma-1 receptors have different pharmacological profiles. Thus, the regulatory role of sigma-1 receptors might be useful in treating these central nervous system (CNS) diseases. In addition, long-term mental stress disrupts the homeostasis in the CNS. In this review, we discuss the topical literature concerning sigma-1 receptor antidepressant mechanism of action in the regulation of intracellular proteostasis, calcium homeostasis and especially the dynamic Excitatory/Inhibitory (E/I) balance in the brain. Furthermore, based on these discoveries, we discuss sigma-1 receptor ligands with respect to their promise as targets for fast-onset action drugs in treating depression.

Keywords: sigma-1 receptors, depression, E/I balance, proteostasis, calcium

OPEN ACCESS

Edited by:
Liu Qing-Shan,
Minzu University of China, China

Reviewed by:
Manuel Narvaez Peláez,
University of Malaga, Spain
Ying Xu,
University at Buffalo, United States

****Correspondence:***
Hui Ma
mahui_bjmu@163.com
Yongqi Zhao
yqzhaoprc@sina.com
Yunfeng Li
lyf619@aliyun.com

†These authors have contributed equally to this work

Specialty section:
This article was submitted to Neuropharmacology, a section of the journal Frontiers in Pharmacology

Received: *22 April 2022*
Accepted: *26 May 2022*
Published: *16 June 2022*

Citation:
Ren P, Wang J, Li N, Li G, Ma H, Zhao Y and Li Y (2022) Sigma-1 Receptors in Depression: Mechanism and Therapeutic Development. Front. Pharmacol. 13:925879. doi: 10.3389/fphar.2022.925879

INTRODUCTION

Mood disorders are the most common types of neuropsychiatric illness and are increasingly becoming a major cause of disability (Zhao et al., 2022). Among them, depression is a mainly persistent mood disorder that negatively impacts the social, vocational and educational aspects of people's life (Chen et al., 2021). Furthermore, people suffering from long-term mental stress can develop mood disorders and they are especially vulnerable to cognitive impairment thus leading to a poor quality of life. Depression is a commonly occurring and recurrent mood disorder worldwide that is becoming a matter of global health (He et al., 2022). Unfortunately, the pandemic of COVID-19 in recent years has only aggravated those conditions (Zhang et al., 2020; Hampshire et al., 2021). Antidepressants are widely prescribed and act by increasing brain monoamine levels but they have a disappointingly low response rate (around 50%) and a significant lag period (4–6 weeks) in their

activities when compared to placebos in clinical trials (de Vries et al., 2018). Thus, it is urgent to perform further research and develop new and effective antidepressants.

Sigma receptors are divided into two subtypes (sigma-1 and sigma-2 receptors) and recently, the sigma-1 receptor, a type of chaperonin (28 kD), has attracted increasing attention for its broad spectrum of biological functions and as a potential target for drugs treating many medical conditions. Extensive research has revealed that sigma receptors play pivotal roles in the etiology of CNS diseases, including Alzheimer's disease (Maurice et al., 1998), Parkinson's disease (Francardo et al., 2014), schizophrenia (Hashimoto, 2009a; Takizawa et al., 2009), Huntington's disease (Bol'Shakova et al., 2017; Vetel et al., 2021), ischemic stroke (Urfer et al., 2014), drug addiction (Meunier et al., 2006), analgesia (Davis, 2015; Shin et al., 2020), depression (Kulkarni and Dhir, 2009; Salaciak and Pytka, 2022), anxiety (Kulkarni and Dhir, 2009; Wang et al., 2019; Salaciak and Pytka, 2022) and cognitive disorders (Salaciak and Pytka, 2022). Among them, mental disorders and cognitive deficits are currently the most widely studied areas. Agonist-associated ligands targeting the sigma receptor system have entered clinical trials (Ye et al., 2020) and have already been shown to be beneficial for patients suffering from these types of psychiatric disorders. Herein, based on preclinical studies, we discuss the functions and roles of sigma-1 receptors, mainly in depression, and we highlight the potential mechanism of action involved and therapeutic development as well as discussing future directions in this field.

Sigma-1 Receptor Localization and Biologic Effects

The sigma-1 receptor is encoded by the sigma-1 gene and was initially classified as an opioid receptor subtype (Ye et al., 2020), but subsequent research has illuminated a vast and unique array of structural phenotypes and a unique amino acid sequence distinct from other mammalian transmembrane proteins (Kruse, 2017; Ossa et al., 2017). More information about the discovery history of sigma-1 receptors has been published (Ye et al., 2020). Sigma-1 receptors are resident proteins of the endoplasmic reticulum (ER) and are predominantly localized in the cholesterol-rich region of ER mitochondria-associated membranes (MAM) (Schmidt and Kruse, 2019; Voronin et al., 2020). This protein is identical in peripheral tissues and in the brain, and probably is similar in other tissues as well (Rousseaux and Greene, 2016; Schmidt and Kruse, 2019). In the brain, sigma-1 receptors are distributed most abundantly in the hippocampus and hypothalamus, followed by the cerebellar area, the dorsal raphe nucleus (DRN) and the locus coeruleus (LC) (Voronin et al., 2020; Salaciak and Pytka, 2022), and are mainly expressed in neurons and glial cells in the brain (Nguyen et al., 2015). These various sites are related to cognition and motor, emotion and endocrine functions, and are also further involved in the pathophysiology of psychiatric disturbances of depression (Voronin et al., 2020). In normal conditions, sigma-1 receptors are able to form Ca^{2+}-sensitive complexes with the main ER chaperone binding immunoglobulin protein (Bip) (Weng et al., 2017; Schmidt and Kruse, 2019). However, specific activation of sigma-1 receptors, upon ligand-directed activation, leads to their separation from Bip, after which they can translocate to multiple cellular destinations, including mitochondrial membranes, nuclear membranes and plasma membranes to elicit their biological functions such as stabilizing IP3R, maintaining Ca^{2+} flow from the ER to mitochondria and producing ATP (Rousseaux and Greene, 2016; Kruse, 2017; Ossa et al., 2017; Weng et al., 2017; Schmidt and Kruse, 2019; Voronin et al., 2020; Ye et al., 2020).

Sigma-1 Receptors Are Involved in Proteostasis and Calcium Homeostasis

Many aspects of proteostasis have been shown to be critical to normal cellular biological functions and disturbances in this homeostasis can lead to abnormal cellular functions, shorter cellular lifespans and can provide a pathological basis for disease development (Suhm et al., 2018). Proteostasis has been found to be closely involved in the pathogenesis of diseases such as depression, Huntington's chorea, Parkinson's disease, Alzheimer's disease (Fornai and Puglisi-Allegra, 2021) and most cancers (Arpalahti et al., 2020). The abnormal aggregation of damaged proteins usually occurs in neurodegenerative diseases and other age-related disorders (Kurtishi et al., 2019; López-Otín and Kroemer, 2021). Therefore, maintaining the protein homeostasis of cells is essential to ensure normal brain conditions. Calcium ions are essential in maintaining normal cell biology, regulating cell membrane excitability by rapid depolarization, acting as secondary messengers and regulating protein activity and gene expression (Nicholls, 1986). In depression, calcium has been reported to be involved in neuroplasticity within neuronal circuits (Deutschenbaur et al., 2016), a significant role that was confirmed in a clinical trial (Bertone-Johnson et al., 2012). Available studies have revealed that sigma-1 receptors play an important role in the regulation of both types of homeostasis conditions. Herein we focused on the regulation of both types of homeostasis by sigma-1 receptors in depression.

The Unfolded Protein Response (UPR)

Impaired cellular proteostasis contributes to the pathogenesis of depressive disorders (Ii and Dwivedi, 2019; Mao et al., 2019). Long term chronic emotional stress eventually leads to cellular stress, which is partly reflected in ER stress (Hayashi, 2015; Seo et al., 2017). The universal cellular response to ER stress is the activation of adaptation processes aimed at maintaining proteostasis (Hetz, 2012). Sigma-1 receptors have been shown to modulate the ER stress response and the subsequent UPR, which can influence protein stability and localization (Ho et al., 2018), through binding and modulating the ER stress response via the ER stress sensor inositol-requiring enzyme 1 (IRE1) (Rosen et al., 2019; Delprat et al., 2020). In fact, a large number of proteins that are included in the UPR are considered promising targets for pharmacological regulation in various deleterious conditions (Almanza et al., 2019).

In a series of animal behavioral experiments, increases in the expression of genes associated with the UPR and inflammation account for the pronounced depressive-like behaviors (Timberlake et al., 2019). In primary cultures of mouse hippocampal neurons, glutamate-dependent induction of the IRE1-XBP1 signaling pathway in distal dendrites facilitated the expression of brain-derived neurotrophic factor (BDNF) in the bodies of neurons. It has also been suggested that BDNF drives its own expression via activation of the PKA-IRE1-XBP1 cascade in dendrites thus regulating neurite development (Saito et al., 2018). Mori et al. (Mori et al., 2013), revealed that a sigma-1 receptor agonist stabilized IRE1 in the MAM region and activated the transcription factor X-box-binding protein 1 (XBP1), which may modulate BDNF expression and further regulate the antidepressive effect. In regard to the UPR involvement in inflammation, sigma-1 receptors regulate IRE1 activity *in vivo*, in LPS-treated sigma-1 receptor knockout mice, and enhance IRE1 activation and the inflammatory response observed (Rosen et al., 2019).

Together, these data demonstrate the substantial contribution of UPR processes to the pathogenesis of depression. The agonistic effect on sigma-1 receptors ensures the regulation of ER stress sensors, the activation of transcription factors, the increased expression of the BDNF gene, anti-inflammation proteins and chaperones. The combination of these processes probably contributes to the survival of neurons in target areas of the brain and the development of antidepressant action.

Sigma-1 Receptors Directly Modulate the Biophysical Properties of Ca^{2+} Ion Channels

Sigma-1 receptors have been shown to associate with and directly regulate voltage-gated ion channels (VGICs) that belong to all superfamilies (Na^+, K^+ and Ca^{2+}) and ionotropic glutamate receptors (NMDARs) (Aishwarya et al., 2021). These considerations make Sigma-1 receptors powerful and pluripotent regulators of neuronal activity, from synaptic transmission to intrinsic excitability. Thus, sigma-1 receptors may have great significance in the regulation of Ca^{2+}-dependent mechanisms of antidepressant action.

It is well known that Ca^{2+} controls neuronal activity and plays an important role in many use-dependent forms of neuroplasticity induced by BDNF and glutamatergic mechanisms (Catterall, 2010; Baydyuk et al., 2015). Sigma-1 receptors were reported to modulate the intracellular Ca^{2+} concentration through both the regulation of membrane voltage-gated Ca^{2+} channels and Ca^{2+} mobilization from endoplasmic stores (Monnet, 2005; Su et al., 2010). Tchedre et al. (Tchedre et al., 2008) showed that sigma-1 receptor activation with (C)-SKF-10047 inhibits Ca^{2+} currents, while that effect was reversed by a sigma-1 receptor antagonist BD-1047, which appears to be mediated directly through sigma-1 receptor binding to L-type voltage-gated Ca^{2+} channels. Consistent with these findings, sigma-1 receptors also inhibit store-operated Ca^{2+} entry by diminishing the coupling of stromal interaction molecule 1 (STIM1) to calcium release-activated calcium channel protein 1 (Orai1) (Srivats et al., 2016). Besides voltage-gated Ca^{2+} channels, sigma-1 receptors also regulate non-voltage-gated Ca^{2+}-permeable channels via direct protein-protein interactions (PPI), including IP3 receptors at the ER level and plasma membrane acid-sensing ion channels 1a (ASIC1a) (Mari et al., 2015).

In an animal behavior model, Ca^{2+}-dependent mechanisms have been proven to be involved in the mechanism of the antidepressant effect. Urani et al. (Urani et al., 2002) reported that EGTA, a Ca^{2+} chelator, when administered to Swiss mice 10 min before a forced swim test (FST), had no effect on their immobilization time, but abolished the antidepressant-like action of igmesine (a selective sigma-1 receptor agonist) in a dose-dependent manner. Similarly, verapamil, a Ca^{2+} channel blocker, had a comparable effect (Urani et al., 2002). In fact, intracellular Ca^{2+} modulators also play an important role in the action of igmesine; more information is summarized in (Guo et al., 2020).

When it comes to the Ca^{2+} signal pathway, Calmodulin-dependent protein kinases (CaMKs) are inevitably involved. Among them, CaMKIV and CaMKII have been intensively studied and are involved in the transcription factor CREB-mediated BDNF signal pathway (Voronin et al., 2020). CaMKIV/II is an intracellular Ca^{2+}-sensitive sensor. High concentrations of Ca^{2+} activate CaMK IV/II, and then eventually activate (phosphorylate) intermediates in the ERK1/2 and mTOR pathways (Cabanu et al., 2022), thus inducing a rapid synthesis of PSD95 as well as facilitating the phosphorylation of CREB, thus boosting the expression of BDNF involved in neuroplasticity (Fukunaga and Moriguchi, 2017) (**Figure 1**). Moriguchi et al. (Moriguchi et al., 2015) used a CaMK deficiency strategy *in vivo* to reveal that the mechanism of antidepressant action of sigma-1 receptors may be due to regulation of the intracellular Ca^{2+} level and activation of an alternative CaMKII-dependent mechanism for controlling the expression of BDNF. Moreover, chronic administration of fluoxetine and paroxetine to $CaMKIV^{-/-}$ mice did not cause a pronounced antidepressant-like effect or the induction of neurogenesis in the hippocampal dentate gyrus (Moriguchi et al., 2015). In contrast, administration of the selective agonist SA4503 or fluvoxamine (with a high affinity for Sigma-1 receptor) for 2 weeks caused a decrease in the immobilization time of $CaMKIV^{-/-}$ mice in the FST and the tail suspension test (TST), while those effects were abolished by preliminary treatment with the sigma-1 receptor antagonist NE-100 (Moriguchi et al., 2015). The abovementioned evidence indicates that a significant role of sigma-1 receptors in regulating Ca^{2+}-dependent mechanisms of antidepressant action may not only be related to extracellular Ca^{2+} influx but also to intracellular Ca^{2+} homeostasis (Urani et al., 2002; Choi et al., 2022).

SIGMA-1 RECEPTORS REGULATE EXCITATORY AND INHIBITORY BALANCE

The classic "monoamine hypothesis" underlies the development of most clinical antidepressants that primarily exert their effects by enhancing the function of monoamine transmitters (Li, 2020). The translocation property of sigma-1 receptors allows them to

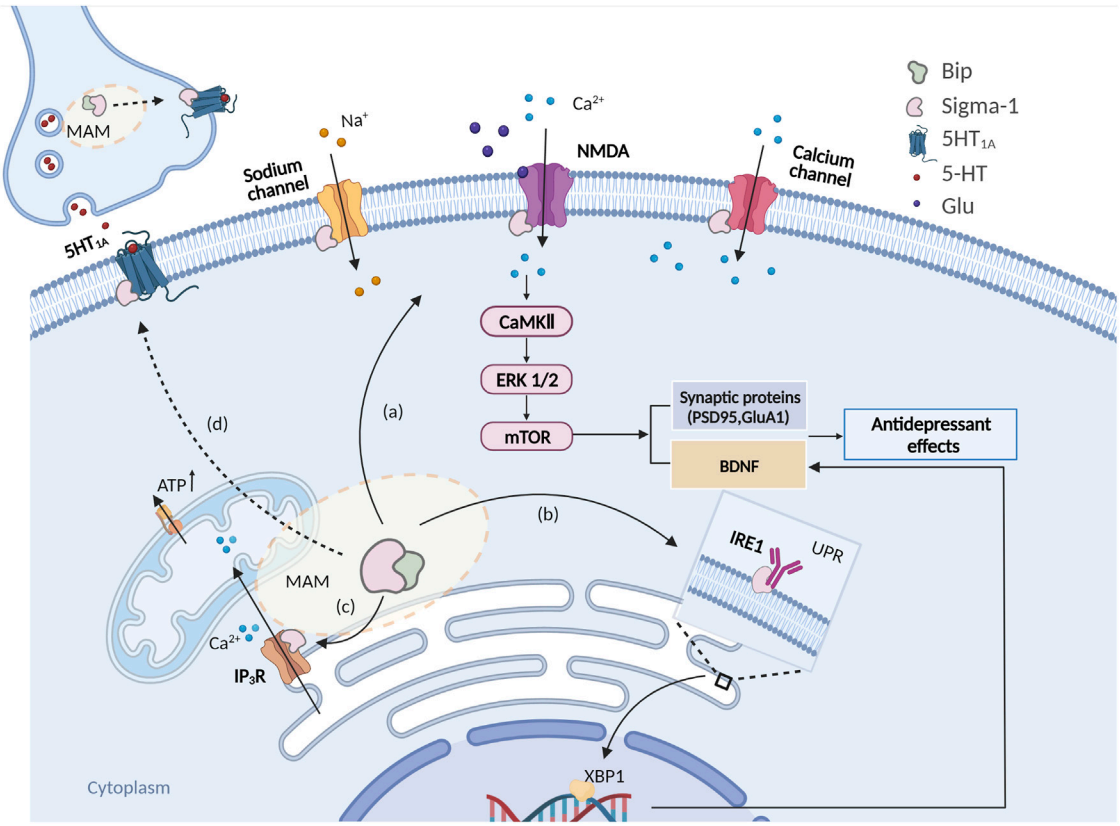

FIGURE 1 | Schema of intracellular signaling pathways involved in the antidepressant-like effects of sigma-1 receptors. **(A)** Sigma-1 receptors are activated and translocated to the plasma membrane to interact with the NMDAR of pyramidal cells, which would result in a rapid intracellular activation of CaMKII that would eventually activate (phosphorylate) intermediates in the ERK1/2 and mTOR pathways, thus inducing a rapid synthesis of PSD95, BDNF etc; **(B)** Sigma-1 receptors are activated and then disassociate from Bip thus stabilizing IP3R, maintaining the Ca^{2+} flow from the ER to mitochondria and ATP production; **(C)** Sigma-1 receptor activates and thus binds and modulates the ER stress response via ER stress sensors IRE1 and facilitates BDNF expression via the IRE1-XBP1 signaling pathway. **(D)** Sigma-1 receptors may also modulate 5HT1A function through sigma-1 receptor-5HT1A interaction.

modulate proteins directly not only at the ER-mitochondrion interface but also at the membrane where many ion channels, receptors and kinases are found, rendering sigma-1 receptors a unique inter-organelle signaling modulator in living tissues, including the CNS that we focused on (Su et al., 2010). In recent years, an increasing body of evidence suggests that sigma-1 receptors directly interact with proteins at neuronal cell membranes (more information is reviewed in (Ryskamp et al., 2019)) and enhance neurotransmission (Bermack and Debonnel, 2001; Bermack and Debonnel, 2005; Sambo et al., 2017; Sambo et al., 2018). The active roles of sigma-1 receptors in the regulation of neurotransmission, including the glutamatergic, GABAergic, serotonergic, dopaminergic (Sambo et al., 2018) and noradrenergic systems (Dhir A. and Kulkarni SK., 2008), is well documented. Those neurotransmission systems may form the basis for the dynamic balance of E/I neural networks in the brain. Especially, sigma-1 receptors have been reported to regulate presynaptic glutamate release and modulate NMDA receptor activity via direct PPI associations (Kourrich, 2017). Furthermore, sigma-1 receptor activation can also lead to alterations in NMDA receptors that upregulate and traffic to the plasma membrane thus further modulating neuronal intrinsic excitability (Pabba et al., 2014). In addition, Mtchedlishvil et al. found that pregnenolone and a selective sigma-1 receptor agonist (SKF-10047) inhibit the GABA-dependent inhibitory postsynaptic currents in rat hippocampal cell cultures (Mtchedlishvili and Kapur, 2003). We therefore suggest that sigma-1 receptors may regulate the E/I balance in direct or indirect manners. Importantly, there is abundant evidence that the medial prefrontal cortex (mPFC) or the hippocampus rely on the dynamic balance between E/I neurotransmitters for various advanced functions, such as emotion regulation and expression, as well as cognitive functions. Those two neurotransmitters achieve a dynamic balance to maintain normal physiological function under normal circumstances (Ferguson and Gao, 2018). Preclinical studies have shown that chronic stress can lead to decreased E/I neurotransmitter transmission in the mPFC (Fee et al., 2017). Consistent with this, a recent study found that chronic stress can lead to decreased glutamate and GABA neurotransmitter transmission in rat mPFC (Fee et al., 2017; Duman et al., 2019). In this context, GABAergic and glutamatergic neurotransmission may be almost rebalanced

but the synapses remain impaired, thus the E/I rebalance may be at a low level. However, we recently found in our laboratory that regulation of the E/I rebalance in the mPFC may be an important mechanism and rate-limiting step in the efficacy of antidepressant effects (Yin et al., 2021).

The glutamatergic and GABAergic as well as serotonergic systems are heavily implicated in antidepressant actions. In this section, we mainly focused on the possible mechanisms by which sigma-1 receptors exert their antidepressant effects through the regulation of E/I balance by theseneurotransmitter systems.

Sigma-1 Receptors and Glutamatergic Neurotransmission

Cortical excitability reflects a balance between E/I. Glutamate is the main excitatory neurotransmitter in the mammalian cortex (Petroff, 2002). Glutamate receptors have been pharmacologically classified as ionotropic and metabotropic receptors. Ionotropic glutamate receptors include the N-methyl-D-aspartic acid (NMDA) receptor (GluNs/NMDAr, GluAs), α-amino-3-hydroxy-5-methylisoxazole-4-propionic acid (AMPA) and kinase families of receptors. In this review, we will focus on NMDA and AMPA receptors due to their close link to depression and/or antidepressant action (Bermack and Debonnel, 2005). It appears that glutamatergic neurotransmission is altered during depressive episodes (Sanacora et al., 2003; Bermack and Debonnel, 2005; Duman et al., 2019). In addition, a clinical study revealed that glutamate metabolism differed significantly between depressed patients and controls (Paul and Skolnick, 2003), while those differences can be resolved with chronic antidepressant treatments (Mauri et al., 1998).

Similarly, numerous studies have shown interactions between sigma receptor and NMDA-receptor mediated responses in neurotransmission. The regulation of sigma-1 receptors with GluN1 can be explained by the PPI (Balasuriya et al., 2013) and an increase in its phosphorylation by protein kinases A and C (PK A/C) under sigma-1 receptor ligand activation of the chaperone protein (Kim et al., 2008). Moreover, Pabba et al. (Pabba et al., 2014) reported that a robust upregulation of GluN2A and GluN2B subunit expression was observed after treatment with the sigma-1 receptor agonist pentazocine (PTZ) or SKF-10074 injection and chronic administration of BD1047 prevented that effect. Conversely, a decreased protein level of GluN1 in the prefrontal cortex, hippocampus and amygdala was observed in a depression rat model while a two-week administration of SA4503 caused an anti-depressive-like effect, accompanied by a restoration of the GluN1 level (Wang et al., 2007).

Furthermore, in a sigma-1 receptor function deficient mouse model, sigma-1 receptor knockout (KO) mice are characterized by an inhibition of neurite outgrowth and impaired GluN2b function in the hippocampal dentate gyrus (Sha et al., 2013). Conversely, a study by Snyder et al. (Snyder et al., 2016), reported that compared to wild-type (WT) mice, AMPA receptor and NMDA receptors were unaffected in sigma-1 receptor KO mice. However, in regard to NMDA receptor-dependent long-term potentiation (LTP) and neuronal plasticity, sigma-1 receptor KO mice showed a mild deficiency (Snyder et al., 2016; Zhang et al., 2017). Interestingly, sigma-1 receptor agonists increased the expression of GluN2A and GluN2B subunits and postsynaptic density protein 95 (PSD-95), which is required for synaptic plasticity associated with NMDA receptor signaling (Pabba et al., 2014). Thus, sigma-1 receptors may play an important role in NMDA-receptor mediated functions, e.g., depression and cognitive disorder. On the other hand, sigma-1 receptors involved in a "long feedback loop" participated in the NMDA-receptor mediated antidepressant effect. Sustained treatments with sigma-1 ligands lead to a potentiation of NMDA-receptor-mediated responses in the mPFC and/or other brain regions, which in turn could lead to the modulation of serotonergic neurotransmission in the DRN (Peyron et al., 1998; Bermack and Debonnel, 2005). Overall, sigma-1 receptors have been indicated to be involved in the mechanism of action of antidepressants via the regulation of glutamatergic neurotransmission.

Sigma-1 Receptors and GABAergic Neurotransmission

Chronic stress induced emotional disorders such as anxiety and depression involve imbalances between the excitatory glutamatergic system and the inhibitory GABAergic system in the PFC, GABA being the main inhibitory neurotransmitter in the mature mammalian CNS (Page and Coutellier, 2019) (**Figure 2**). Moreover, the majority of data on GABAergic deficiencies in depression have been gathered and demonstrated by means of indirect/direct methods, such as assessments of GABA levels in cerebrospinal fluid (CSF), brain specimens obtained post-mortem, by brain imaging, or by other pharmacological studies (Della et al., 2021). There is currently little compelling evidence that any sigma receptor(s) interacts with GABA receptors directly *in vivo*. Recent evidence has revealed that sigma-1 receptors modulate GABA uptake, transport-mediated release and exocytosis. Interestingly, a sigma-1 receptor antagonist decreased glutamate release but induced a biphasic response for GABA, while low doses of NE-100 increased GABA uptake, and with increasing doses, the uptake rate decreased (Pozdnyakova et al., 2020). Neurosteroids are a class of endogenous steroids that have potent effects on GABA receptors. In a circulating neurosteroid deficient rat model, Ago et al. (Ago et al., 2016) suggested that interactions between brain 5-HT1A and sigma-1 receptors may contribute to the treatment of $GABA_A$ receptor deficit-related psychiatric disorders. On the other hand, a sigma-1 receptor deficiency reduces GABAergic inhibition in the basolateral amygdala leading to long term depression (LTD) impairment and depressive-like behaviors (Zhang et al., 2017).

Importantly, sigma-1 receptors may be involved in the "long feedback loop" that projects from the dorsal DRN to the mPFC and back to the DRN (Bermack and Debonnel, 2005). Hypidone hydrochloride (YL-0919) is a new antidepressant with a novel chemical structure that was

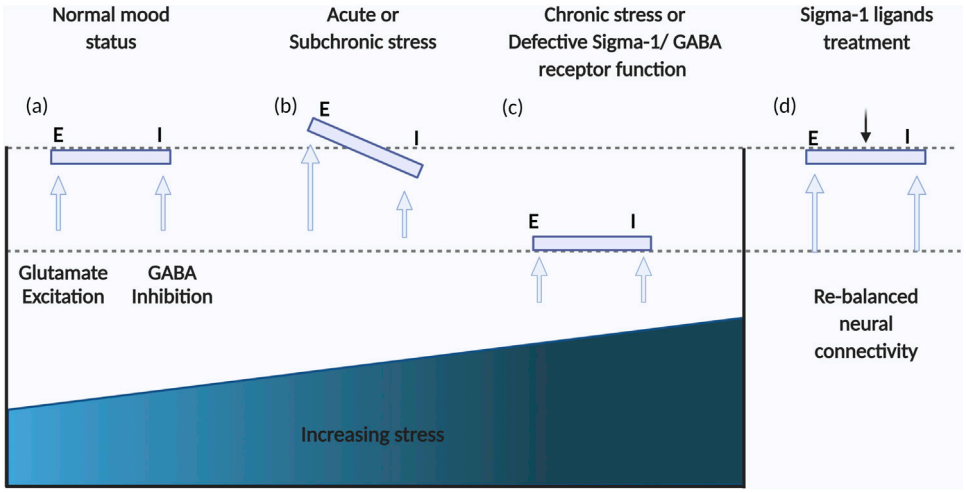

FIGURE 2 | Schema of the dynamic balance of GABAergic and glutamatergic neurotransmission. **(A)** In a normal mood status, GABAergic and glutamatergic neurotransmission are balanced; **(B)** Acute stress can result in imbalances between GABAergic and glutamatergic neurotransmission; **(C)** Further adaptation to chronic stress may result in a new balance of GABAergic and glutamatergic neurotransmission but at lower levels, contributing to depression; **(D)** Regulating 5-HT-Glu/GABA long neural circuit through treatment with sigma-1 receptor ligands has the potential to rapidly restore the primary balance and level.

developed by our laboratory, which has been found to have a high affinity for sigma-1 receptors (unpublished data). A recent study suggested that YL-0919 preferentially inhibits GABAergic neurons and reduces inhibitory input to pyramidal neurons, and that 5-HT1A receptor participates in the inhibition of GABA neurons thus regulating the E/I balance related to depression (Zhang et al., 2021). In general, inhibition of the spontaneous release of GABA may facilitate the release of other neurotransmitters throughout the CNS, thus altering the functions of other neurotransmitter systems. However, further study is essential to investigate whether sigma receptors are involved in this regulation in a direct and/or indirect manner.

Effect of Sigma-1 Receptors on Serotonergic Neurotransmission

When it comes to antidepressant effects, the 5-HT system is necessarily involved. It is well known that 5-HT plays a key role in depression and/or the mechanism of action of antidepressants (Liu et al., 2017; Miquel-Rio et al., 2022). Both animal behavioral experiments and electro-physiological studies revealed that sigma-1 receptors increase 5-HT neurotransmission exerting antidepressant effects through various mechanisms. In a behavioral model, progesterone and BD-1047 (a sigma-1 receptor antagonist) counteracted the antidepressant-like effect induced by co-administration of pramipexole and sertraline (Rogoz and Skuza, 2006). In addition, in cell assays, classical antidepressants (fluvoxamine, etc.) significantly potentiated the NGF-induced neurite outgrowth, and the effects of all these drugs were antagonized by NE-100. Furthermore, the similar effects of mirtazapine were abolished by the 5-HT1A receptor antagonist WAY-100635 (Ishima et al., 2014). In another behavioral study, the sigma receptor ligand EMD- 57445 did not affect several 5-HT related parameters such as 8-OH-DPAT-induced behavioral syndrome or L-5-hydroxytryptophan-induced head twitches (Skuza et al., 1997). Thus, the effects of sigma-1 receptors on the 5-HT system seem to be controversial and fortunately electrophysiological experiments on 5-HT neurons have given us more direct evidence that sigma-1 receptors enhance serotonergic neurotransmission in a rapid manner (Robichaud and Debonnel, 2004; Lucas et al., 2008).

Previous studies have shown that acute and short-term treatments with SSRIs lead to a decreased firing activity of 5-HT DRN neurons, while long-term treatments lead to the restoration of 5-HT firing activity and this phenomenon explains the delayed onset of the action of SSRIs (Le Poul et al., 2000). Based on this model, Bermack and Debonnel assessed the effects of sigma-1 receptor ligands on the firing activity of 5-HT neurons in the DRN using an electrophysiological model with *in vivo* extracellular recording. Their study provided direct evidence that sigma-1 receptors are involved in serotonergic neurotransmission (Bermack and Debonnel, 2001). In that study, an increase in firing rates of 5-HT neurons of the DRN was observed after short term (2-days) or long-term (21-days) treatments with (+)-pentazocine, while those effects were completely abolished by co-administration of NE-100 (10 mg/kg/day) (Bermack and Debonnel, 2001). Similar evidence was found in another study (Lucas et al., 2008), where a 2-days continuous treatment with SA-4503 (1–40 mg/kg/day) increased the 5-HT neuron firing rate in a dose-dependent manner. Moreover, the firing rate of pyramidal neurons was recorded in the CA3 subfield of the hippocampus in further studies, the results

suggesting that WAY100635 had a clear excitatory action in rats receiving chronic treatment of SA- 4,503 (10 mg/kg/day) for 2 days (Lucas et al., 2008; Maurice, 2021). Thus, facilitation of the 5-HT neuron firing rate induced by 2-days treatment with SA-4503 translated into the appearance of a 5-HT1A-mediated tonic inhibitory effect on CA3 pyramidal neurons, which may be involved in a 5-HT-Glu/GABA long neural circuit. In this way, sigma-1 receptors may be involved in modulating 5-HT neuronal activity and the E/I balance by 5-HT transporter combined with some receptors such as 5-HT1A (Li, 2020).

Importantly, these experiments show that sigma-1 receptor ligands have the potential to work as antidepressants with a rapid onset of action, due to an increase in 5-HT neuron firing activity after drug administration in just 2 days, a more rapid and robust anti-depressive effect than the majority of known antidepressant medications (Bermack and Debonnel, 2001).

Sigma-1 Receptors and Other Neurotransmission System

In addition to the three neurotransmitter systems mentioned above, sigma-1 receptors also act on other neurotransmitter systems in the brain, including dopamine (DA) neurotransmission, noradrenaline (NE) neurotransmission and acetyl choline (Ach) neurotransmission (Katz et al., 2016). Among them, sigma-1 receptors modulate depression by acting on dopamine neurotransmitters is widely reported. For instance, PTZ enhances the antidepressant activity of the dopamine reuptake inhibitor bupropion while sigma-1 receptor antagonist reversed the effects (Dhir A. and Kulkarni S., 2008). Likewise, ropinirole (a D2/3 dopamine receptor agonist), elicited a significant anti-immobility effect in FST or FST, and the reduced immobility time exhibited by ropinirole attenuated by a sigma-1 receptor antagonist (Dhir and Kulkarni, 2007). These results reflect the regulatory role of sigma-1 receptor on the dopaminergic system in the brain. However, researchers have not intensively explored the potential mechanism of this unexpected results. Fortunately, the results of studies in recent years on sigma-1 receptors and DA neurotransmission in other disease models may help us to solve this confusion. Borroto-Escuela et al. (Borroto-Escuela et al., 2017) reported that cocaine self-administration induced a selective and significant increase in the density of D2R-sigma-1receptor positive clusters in the nucleus accumbens shell. Furthermore, the formation of the D2R-sigma-1 receptor heterodimer enhanced the ability of acute cocaine to increase the function of the D2R protomer and significantly reduced its internalization (Borroto-Escuela et al., 2019). In fact, receptor-receptor interactions in heterogeneous receptor complexes are widely present in CNS and are involved in the regulation of a variety of neuropsychiatric dysfunctions (Borroto-Escuela et al., 2020). Especially, the translocator property of the sigma-1 receptors gives it the opportunity to form heteroreceptor complexes with a variety of receptors to enhance the function of the original receptors, and this partly explains why sigma-1 receptor antagonists can block many of the unexpected effects aforementioned. The sigma-1 receptor complexs appear to hold the highest promise, it not only provides a new vision for our future research, but also a new strategy for the treatment of depression.

SIGMA RECEPTOR LIGAND DEVELOPMENT FOR TREATING CLINICAL DEPRESSION

Sigma-1 receptors are recently explored targets for treating depression and anxiety. Many antidepressants that are currently marketed are known to act through the sigma-1 receptor pathway (Hashimoto, 2009b). Furthermore, some novel compounds based on the sigma-1 receptor confirmation are being synthesized and tested in depressive animal models, more information reviewed in (Salaciak and Pytka, 2022). Although the exact therapeutic contribution of sigma-1 receptor binding remains to be unraveled, available data suggests that the anti-depressive efficacy is partly ascribed to sigma-1 receptor modulation. Some of the ongoing or completed clinical studies of sigma receptors are listed in **Table 1**. Herein, we focus on clinical advances in the treatment of depression with sigma-1 receptor ligands.

Igmesine (JO-1784), one of the first discovered sigma-1 receptor ligands, was investigated in a clinical study of major depression in 1999 (Pande et al., 1999). Igmesine (25 mg/day) showed a statistically significant superiority over the placebo in the outpatient group, however, the compound ultimately failed to be effective in phase III clinical trials (Pande et al., 1999). SA-4503 (Cutamesine) is an orally available, potent and highly selective sigma-1 receptor agonist. Cutamesine not only decreased the immobility time in the FST but also played an anti-depressive-like behavior in an olfactory bulbectomized rat model of depression. In 2007, a phase II clinical study of SA4503 was performed, where SA4503 was given once daily for 8 weeks and then tested to determine safety and efficacy in 150 subjects with major depression. However, the trial data and outcome summaries have yet to be released (NCT00551109).

The sum of these results suggests that sigma-1 receptors affect the release of various neurotransmitter systems that have been shown to be involved in the pathophysiology of depression. We conclude that sigma-1 receptor agonists may have an antidepressant activity and are expected to be effective drugs for treating depression in the future. However, inconclusive results from different clinical trials have led to setbacks in the further development of these molecules for the treatment of depression.

DISCUSSION AND CONCLUSION

Depression is a common mental disorder that affects approximately 300 million people worldwide (Zhao et al., 2022). Even worse, according to a scientific brief that was recently released by the World Health Organization (WHO), the COVID-19 pandemic triggered a 25% increase in the prevalence of anxiety and depression globally, which poses a significant challenge to mental health care (Who, 2022). Classical "monoamine strategy" drugs mostly target a series of defects in clinical applications. Therefore,

TABLE 1 | Sigma-1 receptor agonists in clinical studies.

Sigma-1 Agonist	Conditions	Clinic phase	ClinicalTrials.gov identifier
SA-4503	Major depressive disorder	Phase 2 unreleased	NCT00551109 (2007)
	Acute ischemic stroke	Completed	NCT00639249 (2008)
Pridopidine	Huntington disease	Phase 3 recruiting	NCT04556656 (2020)
	levodopa-induced dyskinesia	Phase 2 recruiting	NCT03922711 (2019)
	Huntington's disease	Completed	NCT00724048 (2008)
	Huntington's disease	Completed	NCT00665223 (2008)
ANAVEX2-73	Alzheimer's disease	Phase 2b/3 recruiting	NCT04314934 (2020) NCT03790709 (2018)
	Rett syndrome	Phase 2 recruiting	NCT04304482 (2020) NCT03941444 (2019)
	Parkinson's disease with dementia	Phase 2 recruiting	NCT03774459 (2018)
	Mild to moderate Alzheimer's disease	Phase 2 active	NCT02756858 (2016)
	Alzheimer's disease	Completed	NCT02244541 (2014)
T-817MA (Edonerpic Maleate)	Mild to moderate Alzheimer's disease	Phase 2 completed	NCT02079909 (2014) NCT00663936 (2008)
	Mild cognitive impairment	Phase 2 recruiting	NCT04191486 (2019)
Igmesine	Major depression	Completed	https://doi.org/10.1016/S0924-977X(99)80011-X (1999)

there is an increasing interest in investigating modern monoamine (optimized multi-targets) strategies with faster-acting and fewer side-effects. In this way, sigma-1 receptors have entered the limelight, with their translocation property allowing them to modulate proteins directly.

To date, at least 49 proteins with highly divergent sequences and structures have been reported to interact with sigma-1 receptors. Due to the complicated nature of their effects on the downstream signaling pathways, it is not surprising that sigma-1 receptors play a role in maintaining the balance of glutamatergic, GABAergic, serotonergic, noradrenergic, and dopaminergic systems in the brain (Katz et al., 2016). As mentioned earlier, *in vivo* electrophysiological recordings revealed that sigma-1 receptor agonists, such as (+)-pentazocine or SA-4503, markedly increased 5-HT neuron firing after 2 or 21 days of treatment while a selective sigma-1 receptor antagonist, NE-100, blocked those effects. In addition, SA-4503 at 10 mg/kg/day induced the appearance of a 5-HT1A-mediated inhibitory tonus on hippocampal pyramidal neurons, as revealed by intravenous injections of the selective 5-HT1A antagonist WAY100635. In fact, recent findings from our laboratory revealed a similar phenomenon, where YL-0919 (mentioned above as a potential sigma-1 receptor ligand) significantly inhibited the excitability of GABAergic neurons in GAD67-GFP transgenic mice. Moreover, the inhibition of GABAergic neurons by YL-0919 was abolished by pretreatment with WAY100635 (Zhang et al., 2021). Although we need to further investigate the specific regulatory mechanisms of this discovery, it further strengthens the idea that the 5-HT system plays a central role in the "antidepressant-like" properties of sigma-1 receptors. This antidepressant mechanism may be involved in the "monoamine(5-HT)-Glu/GABA long neural circuit" (more information is reviewed by Prof. Li (Li, 2020)), and E/I rebalancing should be the critical rate-limiting step for the onset of action. It is important to note that available studies on sigma-1 receptors in relation to the 5-HT system are limited, and still lack direct evidence that sigma-1 receptors regulate 5-HT release in the brain. Moreover, some clues have suggested that sigma-1 receptors play a positive role in regulating the 5-HT system, and many antidepressants are known to act via the sigma-1 receptor pathway, even classical SSRIs with or without affinity for sigma-1 receptors have different pharmacological profiles. In the future, whether sigma-1 receptors can interact directly with the serotonin transporter (SERT), 5HT1A, etc. needs further confirmation (**Figure 1**). Besides, if sigma-1 receptors are activated by pre-administered sigma-1 receptor agonists, is it possible that there will be a higher affinity with 5HT1A? These considerations may be a breakthrough for clarifying the roles of sigma-1 receptors in the regulatory mechanisms of depression.

The pharmacological antidepressant-like effects of sigma-1 receptor ligands tested in animal models and in human clinical trials showed somewhat useful effects, and sigma-1 receptor ligands seem to be potential psychotherapeutic agents. However, there are no drugs that selectively target sigma-1 receptors on the market at this time, which does not mean that the development of drugs targeting sigma-1 receptors is not promising. In contrast, to clearly define the molecular mechanisms of sigma-1 receptors in depression requires more direct evidence and another major concern is regarding the safety profiles of these potential drugs. In the circumstances of the global COVID-19 pandemic, the "magic molecule" sigma-1 receptor may provide new hope. Sigma-1 receptors play an important role in the replication of SARS-CoV-2 in cells and thus serve as a promising therapeutic target for COVID-19 infections (Hashimoto et al., 2022). In this way, the development of antidepressants based on sigma-1 receptor targets appear to be "game changers" for people with COVID-19, such as the widely available fluvoxamine etc.

AUTHOR CONTRIBUTIONS

Conceptualization: YL, YZ, and HM. Writing original draft preparation: PR and JW. Writing-review and editing: YL and PR. Figure presentation: NL and PR. Revising: PR, JW, GL, and HM. All authors have read and approved the final manuscript.

ACKNOWLEDGMENTS

We appreciate Prof. Ujjal K Bhawal from Nihon University, Japan provided helpful advice in preparing the original draft.

REFERENCES

Ago, Y., Hasebe, S., Hiramatsu, N., Mori, K., Watabe, Y., Onaka, Y., et al. (2016). Involvement of GABAA Receptors in 5-HT1A and σ1 Receptor Synergism on Prefrontal Dopaminergic Transmission under Circulating Neurosteroid Deficiency. *Psychopharmacol. Berl.* 233 (17), 3125–3134. doi:10.1007/s00213-016-4353-3

Aishwarya, R., Abdullah, C. S., Morshed, M., Remex, N. S., and Bhuiyan, M. S. (2021). Sigmar1's Molecular, Cellular, and Biological Functions in Regulating Cellular Pathophysiology. *Front. Physiol.* 12, 705575. doi:10.3389/fphys.2021.705575

Almanza, A., Carlesso, A., Chintha, C., Creedican, S., Doultsinos, D., Leuzzi, B., et al. (2019). Endoplasmic Reticulum Stress Signalling - from Basic Mechanisms to Clinical Applications. *FEBS J.* 286 (2), 241–278. doi:10.1111/febs.14608

Arpalahti, L., Haglund, C., and Holmberg, C. I. (2020). Proteostasis Dysregulation in Pancreatic Cancer. *Adv. Exp. Med. Biol.* 1233, 101–115. doi:10.1007/978-3-030-38266-7_4

Balasuriya, D., Stewart, A. P., and Edwardson, J. M. (2013). The σ-1 Receptor Interacts Directly with GluN1 but Not GluN2A in the GluN1/GluN2A NMDA Receptor. *J. Neurosci.* 33 (46), 18219–18224. doi:10.1523/JNEUROSCI.3360-13.2013

Baydyuk, M., Wu, X. S., He, L., and Wu, L. G. (2015). Brain-derived Neurotrophic Factor Inhibits Calcium Channel Activation, Exocytosis, and Endocytosis at a Central Nerve Terminal. *J. Neurosci.* 35 (11), 4676–4682. doi:10.1523/JNEUROSCI.2695-14.2015

Bermack, J. E., and Debonnel, G. (2001). Modulation of Serotonergic Neurotransmission by Short- and Long-Term Treatments with Sigma Ligands. *Br. J. Pharmacol.* 134 (3), 691–699. doi:10.1038/sj.bjp.0704294

Bermack, J. E., and Debonnel, G. (2005). The Role of Sigma Receptors in Depression. *J. Pharmacol. Sci.* 97 (3), 317–336. doi:10.1254/jphs.crj04005x

Bertone-Johnson, E. R., Powers, S. I., Spangler, L., Larson, J., Michael, Y. L., Millen, A. E., et al. (2012). Vitamin D Supplementation and Depression in the Women's Health Initiative Calcium and Vitamin D Trial. *Am. J. Epidemiol.* 176 (1), 1–13. doi:10.1093/aje/kwr482

Bol'Shakova, A. V., Kraskovskaya, N. A., Gainullina, A. N., Kukanova, E. O., Vlasova, O. L., and Bezprozvanny, I. B. (2017). Neuroprotective Effect of σ1-Receptors on the Cell Model of Huntington's Disease. *Bull. Exp. Biol. Med.* 164 (2), 252–258. doi:10.1007/s10517-017-3968-7

Borroto-Escuela, D. O., Ferraro, L., Narvaez, M., Tanganelli, S., Beggiato, S., Liu, F., et al. (2020). Multiple Adenosine-Dopamine (A2A-D2 like) Heteroreceptor Complexes in the Brain and Their Role in Schizophrenia. *Cells* 9 (5). doi:10.3390/cells9051077

Borroto-Escuela, D. O., Narváez, M., Romero-Fernández, W., Pinton, L., Wydra, K., Filip, M., et al. (2019). Acute Cocaine Enhances Dopamine D2R Recognition and Signaling and Counteracts D2R Internalization in Sigma1R-D2r Heteroreceptor Complexes. *Mol. Neurobiol.* 56 (10), 7045–7055. doi:10.1007/s12035-019-1580-8

Borroto-Escuela, D. O., Narváez, M., Wydra, K., Pintsuk, J., Pinton, L., Jimenez-Beristain, A., et al. (2017). Cocaine Self-Administration Specifically Increases A2AR-D2R and D2R-sigma1R Heteroreceptor Complexes in the Rat Nucleus Accumbens Shell. Relevance for Cocaine Use Disorder. *Pharmacol. Biochem. Behav.* 155, 24–31. doi:10.1016/j.pbb.2017.03.003

Cabanu, S., Pilar-Cuéllar, F., Zubakina, P., Florensa-Zanuy, E., Senserrich, J., Newman-Tancredi, A., et al. (2022). Molecular Signaling Mechanisms for the Antidepressant Effects of NLX-101, a Selective Cortical 5-HT1A Receptor Biased Agonist. *Pharm. (Basel)* 15 (3). doi:10.3390/ph15030337

Catterall, W. A. (2010). Signaling Complexes of Voltage-Gated Sodium and Calcium Channels. *Neurosci. Lett.* 486 (2), 107–116. doi:10.1016/j.neulet.2010.08.085

Chen, S., Gao, L., Li, X., and Ye, Y. (2021). Allopregnanolone in Mood Disorders: Mechanism and Therapeutic Development. *Pharmacol. Res.* 169, 105682. doi:10.1016/j.phrs.2021.105682

Choi, J. G., Choi, S. R., Kang, D. W., Kim, J., Park, J. B., Lee, J. H., et al. (2022). Sigma-1 Receptor Increases Intracellular Calcium in Cultured Astrocytes and Contributes to Mechanical Allodynia in a Model of Neuropathic Pain. *Brain Res. Bull.* 178, 69–81. doi:10.1016/j.brainresbull.2021.11.010

Davis, M. P. (2015). Sigma-1 Receptors and Animal Studies Centered on Pain and Analgesia. *Expert Opin. Drug Discov.* 10 (8), 885–900. doi:10.1517/17460441.2015.1051961

de Vries, Y. A., Roest, A. M., de Jonge, P., Cuijpers, P., Munafò, M. R., and Bastiaansen, J. A. (2018). The Cumulative Effect of Reporting and Citation Biases on the Apparent Efficacy of Treatments: the Case of Depression. *Psychol. Med.* 48 (15), 2453–2455. doi:10.1017/S0033291718001873

Della Vecchia, A., Arone, A., Piccinni, A., Mucci, F., and Marazziti, D. (2021). GABA System in Depression: Impact on Pathophysiology and Psychopharmacology. *Cmc* 28. doi:10.2174/0929867328666211115124149

Delprat, B., Crouzier, L., Su, T. P., and Maurice, T. (2020). At the Crossing of ER Stress and MAMs: A Key Role of Sigma-1 Receptor? *Adv. Exp. Med. Biol.* 1131, 699–718. doi:10.1007/978-3-030-12457-1_28

Deutschenbaur, L., Beck, J., Kiyhankhadiv, A., Mühlhauser, M., Borgwardt, S., Walter, M., et al. (2016). Role of Calcium, Glutamate and NMDA in Major Depression and Therapeutic Application. *Prog. Neuropsychopharmacol. Biol. Psychiatry* 64, 325–333. doi:10.1016/j.pnpbp.2015.02.015

Dhir, A., and Kulkarni, S. (2008b). Involvement of Sigma (Sigma1) Receptors in Modulating the Anti-depressant Effect of Neurosteroids (Dehydroepiandrosterone or Pregnenolone) in Mouse Tail-Suspension Test. *J. Psychopharmacol.* 22 (6), 691–696. doi:10.1177/0269881107082771

Dhir, A., and Kulkarni, S. K. (2007). Involvement of Dopamine (DA)/serotonin (5-HT)/sigma (Sigma) Receptor Modulation in Mediating the Antidepressant Action of Ropinirole Hydrochloride, a D2/D3 Dopamine Receptor Agonist. *Brain Res. Bull.* 74 (1-3), 58–65. doi:10.1016/j.brainresbull.2007.05.004

Dhir, A., and Kulkarni, S. K. (2008a). Possible Involvement of Sigma-1 Receptors in the Anti-immobility Action of Bupropion, a Dopamine Reuptake Inhibitor. *Fundam. Clin. Pharmacol.* 22 (4), 387–394. doi:10.1111/j.1472-8206.2008.00605.x

Duman, R. S., Sanacora, G., and Krystal, J. H. (2019). Altered Connectivity in Depression: GABA and Glutamate Neurotransmitter Deficits and Reversal by Novel Treatments. *Neuron* 102 (1), 75–90. doi:10.1016/j.neuron.2019.03.013

Fee, C., Banasr, M., and Sibille, E. (2017). Somatostatin-Positive Gamma-Aminobutyric Acid Interneuron Deficits in Depression: Cortical Microcircuit and Therapeutic Perspectives. *Biol. Psychiatry* 82 (8), 549–559. doi:10.1016/j.biopsych.2017.05.024

Ferguson, B. R., and Gao, W. J. (2018). PV Interneurons: Critical Regulators of E/I Balance for Prefrontal Cortex-dependent Behavior and Psychiatric Disorders. *Front. Neural Circuits* 12, 37. doi:10.3389/fncir.2018.00037

Fornai, F., and Puglisi-Allegra, S. (2021). Autophagy Status as a Gateway for Stress-Induced Catecholamine Interplay in Neurodegeneration. *Neurosci. Biobehav Rev.* 123, 238–256. doi:10.1016/j.neubiorev.2021.01.015

Francardo, V., Bez, F., Wieloch, T., Nissbrandt, H., Ruscher, K., and Cenci, M. A. (2014). Pharmacological Stimulation of Sigma-1 Receptors Has Neurorestorative Effects in Experimental Parkinsonism. *Brain* 137 (Pt 7), 1998–2014. doi:10.1093/brain/awu107

Fukunaga, K., and Moriguchi, S. (2017). Stimulation of the Sigma-1 Receptor and the Effects on Neurogenesis and Depressive Behaviors in Mice. *Adv. Exp. Med. Biol.* 964, 201–211. doi:10.1007/978-3-319-50174-1_14

Guo, W., Sun, B., Estillore, J. P., Wang, R., and Chen, S. R. W. (2020). The Central Domain of Cardiac Ryanodine Receptor Governs Channel Activation, Regulation, and Stability. *J. Biol. Chem.* 295 (46), 15622–15635. doi:10.1074/jbc.RA120.013512

Hampshire, A., Trender, W., Chamberlain, S. R., Jolly, A. E., Grant, J. E., Patrick, F., et al. (2021). Cognitive Deficits in People Who Have Recovered from COVID-19. *EClinicalMedicine* 39, 101044. doi:10.1016/j.eclinm.2021.101044

Hashimoto, K. (2009a). Can the Sigma-1 Receptor Agonist Fluvoxamine Prevent Schizophrenia? *CNS Neurol. Disord. Drug Targets* 8 (6), 470–474. doi:10.2174/187152709789824633

Hashimoto, K. (2009b). Sigma-1 Receptors and Selective Serotonin Reuptake Inhibitors: Clinical Implications of Their Relationship. *Cent. Nerv. Syst. Agents Med. Chem.* 9 (3), 197–204. doi:10.2174/1871524910909030197

Hashimoto, Y., Suzuki, T., and Hashimoto, K. (2022). Mechanisms of Action of Fluvoxamine for COVID-19: a Historical Review. *Mol. Psychiatry* 27, 1898–1907. doi:10.1038/s41380-021-01432-3

Hayashi, T. (2015). Conversion of Psychological Stress into Cellular Stress Response: Roles of the Sigma-1 Receptor in the Process. *Psychiatry Clin. Neurosci.* 69 (4), 179–191. doi:10.1111/pcn.12262

He, G., Zhang, X., Yan, T., Wang, J., Li, Q., Liu, T., et al. (2022). The Efficacy of Tai Chi for Depression: A Protocol for Systematic Review and Meta-Analysis. *Med. Baltim.* 101 (5), e28330. doi:10.1097/MD.0000000000028330

Hetz, C. (2012). The Unfolded Protein Response: Controlling Cell Fate Decisions under ER Stress and beyond. *Nat. Rev. Mol. Cell Biol.* 13 (2), 89–102. doi:10.1038/nrm3270

Ho, N., Xu, C., and Thibault, G. (2018). From the Unfolded Protein Response to Metabolic Diseases - Lipids under the Spotlight. *J. Cell Sci.* 131 (3). doi:10.1242/jcs.199307

Ii Timberlake, M., and Dwivedi, Y. (2019). Linking Unfolded Protein Response to Inflammation and Depression: Potential Pathologic and Therapeutic Implications. *Mol. Psychiatry* 24 (7), 987–994. doi:10.1038/s41380-018-0241-z

Ishima, T., Fujita, Y., and Hashimoto, K. (2014). Interaction of New Antidepressants with Sigma-1 Receptor Chaperones and Their Potentiation of Neurite Outgrowth in PC12 Cells. *Eur. J. Pharmacol.* 727, 167–173. doi:10.1016/j.ejphar.2014.01.064

Katz, J. L., Hong, W. C., Hiranita, T., and Su, T. P. (2016). A Role for Sigma Receptors in Stimulant Self-Administration and Addiction. *Behav. Pharmacol.* 27 (2-3 Spec Issue), 100–115. doi:10.1097/FBP.0000000000000209

Kim, H. W., Roh, D. H., Yoon, S. Y., Seo, H. S., Kwon, Y. B., Han, H. J., et al. (2008). Activation of the Spinal Sigma-1 Receptor Enhances NMDA-Induced Pain via PKC- and PKA-dependent Phosphorylation of the NR1 Subunit in Mice. *Br. J. Pharmacol.* 154 (5), 1125–1134. doi:10.1038/bjp.2008.159

Kourrich, S. (2017). Sigma-1 Receptor and Neuronal Excitability. *Handb. Exp. Pharmacol.* 244, 109–130. doi:10.1007/164_2017_8

Kruse, A. (2017). Structural Insights into Sigma1 Function. *Handb. Exp. Pharmacol.* 244, 13–25. doi:10.1007/164_2016_95

Kulkarni, S. K., and Dhir, A. (2009). sigma-1 Receptors in Major Depression and Anxiety. *Expert Rev. Neurother.* 9 (7), 1021–1034. doi:10.1586/ern.09.40

Kurtishi, A., Rosen, B., Patil, K. S., Alves, G. W., and Møller, S. G. (2019). Cellular Proteostasis in Neurodegeneration. *Mol. Neurobiol.* 56 (5), 3676–3689. doi:10.1007/s12035-018-1334-z

Le Poul, E., Boni, C., Hanoun, N., Laporte, A. M., Laaris, N., Chauveau, J., et al. (2000). Differential Adaptation of Brain 5-HT1A and 5-HT1B Receptors and 5-HT Transporter in Rats Treated Chronically with Fluoxetine. *Neuropharmacology* 39 (1), 110–122. doi:10.1016/s0028-3908(99)00088-x

Li, Y. F. (2020). A Hypothesis of Monoamine (5-HT) - Glutamate/GABA Long Neural Circuit: Aiming for Fast-Onset Antidepressant Discovery. *Pharmacol. Ther.* 208, 107494. doi:10.1016/j.pharmthera.2020.107494

Liu, B., Liu, J., Wang, M., Zhang, Y., and Li, L. (2017). From Serotonin to Neuroplasticity: Evolvement of Theories for Major Depressive Disorder. *Front. Cell. Neurosci.* 11, 305. doi:10.3389/fncel.2017.00305

López-Otín, C., and Kroemer, G. (2021). Hallmarks of Health. *Cell* 184 (1), 33–63. doi:10.1016/j.cell.2020.11.034

Lucas, G., Rymar, V. V., Sadikot, A. F., and Debonnel, G. (2008). Further Evidence for an Antidepressant Potential of the Selective Sigma1 Agonist SA 4503: Electrophysiological, Morphological and Behavioural Studies. *Int. J. Neuropsychopharmacol.* 11 (4), 485–495. doi:10.1017/S1461145708008547

Mao, J., Hu, Y., Ruan, L., Ji, Y., and Lou, Z. (2019). Role of Endoplasmic Reticulum Stress in Depression (Review). *Mol. Med. Rep.* 20 (6), 4774–4780. doi:10.3892/mmr.2019.10789

Mari, Y., Katnik, C., and Cuevas, J. (2015). σ-1 Receptor Inhibition of ASIC1a Channels Is Dependent on a Pertussis Toxin-Sensitive G-Protein and an AKAP150/Calcineurin Complex. *Neurochem. Res.* 40 (10), 2055–2067. doi:10.1007/s11064-014-1324-0

Mauri, M. C., Ferrara, A., Boscati, L., Bravin, S., Zamberlan, F., Alecci, M., et al. (1998). Plasma and Platelet Amino Acid Concentrations in Patients Affected by Major Depression and under Fluvoxamine Treatment. *Neuropsychobiology* 37 (3), 124–129. doi:10.1159/000026491

Maurice, T. (2021). Bi-phasic Dose Response in the Preclinical and Clinical Developments of Sigma-1 Receptor Ligands for the Treatment of Neurodegenerative Disorders. *Expert Opin. Drug Discov.* 16 (4), 373–389. doi:10.1080/17460441.2021.1838483

Maurice, T., Su, T. P., and Privat, A. (1998). Sigma1 (Sigma 1) Receptor Agonists and Neurosteroids Attenuate B25-35-Amyloid Peptide-Induced Amnesia in Mice through a Common Mechanism. *Neuroscience* 83 (2), 413–428. doi:10.1016/s0306-4522(97)00405-3

Meunier, J., Demeilliers, B., Célérier, A., and Maurice, T. (2006). Compensatory Effect by Sigma1 (Sigma1) Receptor Stimulation during Alcohol Withdrawal in Mice Performing an Object Recognition Task. *Behav. Brain Res.* 166 (1), 166–176. doi:10.1016/j.bbr.2005.07.019

Miquel-Rio, L., Alarcón-Arís, D., Torres-López, M., Cóppola-Segovia, V., Pavia-Collado, R., Paz, V., et al. (2022). Human α-synuclein Overexpression in Mouse Serotonin Neurons Triggers a Depressive-like Phenotype. Rescue by Oligonucleotide Therapy. *Transl. Psychiatry* 12 (1), 79. doi:10.1038/s41398-022-01842-z

Monnet, F. P. (2005). Sigma-1 Receptor as Regulator of Neuronal Intracellular Ca2+: Clinical and Therapeutic Relevance. *Biol. Cell.* 97 (12), 873–883. doi:10.1042/BC20040149

Mori, T., Hayashi, T., Hayashi, E., and Su, T. P. (2013). Sigma-1 Receptor Chaperone at the ER-Mitochondrion Interface Mediates the Mitochondrion-ER-Nucleus Signaling for Cellular Survival. *PLoS One* 8 (10), e76941. doi:10.1371/journal.pone.0076941

Moriguchi, S., Sakagami, H., Yabuki, Y., Sasaki, Y., Izumi, H., Zhang, C., et al. (2015). Stimulation of Sigma-1 Receptor Ameliorates Depressive-like Behaviors in CaMKIV Null Mice. *Mol. Neurobiol.* 52 (3), 1210–1222. doi:10.1007/s12035-014-8923-2

Mtchedlishvili, Z., and Kapur, J. (2003). A Presynaptic Action of the Neurosteroid Pregnenolone Sulfate on GABAergic Synaptic Transmission. *Mol. Pharmacol.* 64 (4), 857–864. doi:10.1124/mol.64.4.857

Nguyen, L., Lucke-Wold, B. P., Mookerjee, S. A., Cavendish, J. Z., Robson, M. J., Scandinaro, A. L., et al. (2015). Role of Sigma-1 Receptors in Neurodegenerative Diseases. *J. Pharmacol. Sci.* 127 (1), 17–29. doi:10.1016/j.jphs.2014.12.005

Nicholls, D. G. (1986). Intracellular Calcium Homeostasis. *Br. Med. Bull.* 42 (4), 353–358. doi:10.1093/oxfordjournals.bmb.a072152

Ossa, F., Schnell, J. R., and Ortega-Roldan, J. L. (2017). A Review of the Human Sigma-1 Receptor Structure. *Adv. Exp. Med. Biol.* 964, 15–29. doi:10.1007/978-3-319-50174-1_3

Pabba, M., Wong, A. Y., Ahlskog, N., Hristova, E., Biscaro, D., Nassrallah, W., et al. (2014). NMDA Receptors Are Upregulated and Trafficked to the Plasma Membrane after Sigma-1 Receptor Activation in the Rat hippocampus. *J. Neurosci.* 34 (34), 11325–11338. doi:10.1523/JNEUROSCI.0458-14.2014

Page, C. E., and Coutellier, L. (2019). Prefrontal Excitatory/inhibitory Balance in Stress and Emotional Disorders: Evidence for Over-inhibition. *Neurosci. Biobehav Rev.* 105, 39–51. doi:10.1016/j.neubiorev.2019.07.024

Pande, A. C., Genève, J., Scherrer, B., Smith, F., Leadbetter, R. A., and de Meynard, C. (1999). A Placebo-Controlled Trial of Igmesine in the Treatment of Major Depression. *Eur. Neuropsychopharmacol.* 9, 138. doi:10.1016/S0924-977X(99)80011-X

Paul, I. A., and Skolnick, P. (2003). Glutamate and Depression: Clinical and Preclinical Studies. *Ann. N. Y. Acad. Sci.* 1003, 250–272. doi:10.1196/annals.1300.016

Petroff, O. A. (2002). GABA and Glutamate in the Human Brain. *Neuroscientist* 8 (6), 562–573. doi:10.1177/1073858402238515

Peyron, C., Petit, J. M., Rampon, C., Jouvet, M., and Luppi, P. H. (1998). Forebrain Afferents to the Rat Dorsal Raphe Nucleus Demonstrated by Retrograde and Anterograde Tracing Methods. *Neuroscience* 82 (2), 443–468. doi:10.1016/s0306-4522(97)00268-6

Pozdnyakova, N., Krisanova, N., Dudarenko, M., Vavers, E., Zvejniece, L., Dambrova, M., et al. (2020). Inhibition of Sigma-1 Receptors Substantially Modulates GABA and Glutamate Transport in Presynaptic Nerve Terminals. *Exp. Neurol.* 333, 113434. doi:10.1016/j.expneurol.2020.113434

Robichaud, M., and Debonnel, G. (2004). Modulation of the Firing Activity of Female Dorsal Raphe Nucleus Serotonergic Neurons by Neuroactive Steroids. *J. Endocrinol.* 182 (1), 11–21. doi:10.1677/joe.0.1820011

Rogóz, Z., and Skuza, G. (2006). Mechanism of Synergistic Action Following Co-treatment with Pramipexole and Fluoxetine or Sertraline in the Forced Swimming Test in Rats. *Pharmacol. Rep.* 58 (4), 493–500.

Rosen, D. A., Seki, S. M., Fernandez-Castaneda, A., Beiter, R. M., Eccles, J. D., Woodfolk, J. A., et al. (2019). Erratum for the Research Article: "Modulation of the Sigma-1 Receptor-IRE1 Pathway Is Beneficial in Preclinical Models of Inflammation and Sepsis" by D. A. Rosen, S. M. Seki, A. Fernández-Castañeda, R. M. Beiter, J. D. Eccles, J. A. Woodfolk, A. Gaultier. *Sci. Transl. Med.* 11 (478). doi:10.1126/scitranslmed.aau526610.1126/scitranslmed.aax3130

Rousseaux, C. G., and Greene, S. F. (2016). Sigma Receptors [σRs]: Biology in Normal and Diseased States. *J. Recept Signal Transduct. Res.* 36 (4), 327–388. doi:10.3109/10799893.2015.1015737

Ryskamp, D. A., Korban, S., Zhemkov, V., Kraskovskaya, N., and Bezprozvanny, I. (2019). Neuronal Sigma-1 Receptors: Signaling Functions and Protective Roles

in Neurodegenerative Diseases. *Front. Neurosci.* 13, 862. doi:10.3389/fnins.2019.00862

Saito, A., Cai, L., Matsuhisa, K., Ohtake, Y., Kaneko, M., Kanemoto, S., et al. (2018). Neuronal Activity-dependent Local Activation of Dendritic Unfolded Protein Response Promotes Expression of Brain-Derived Neurotrophic Factor in Cell Soma. *J. Neurochem.* 144 (1), 35–49. doi:10.1111/jnc.14221

Sałaciak, K., and Pytka, K. (2022). Revisiting the Sigma-1 Receptor as a Biological Target to Treat Affective and Cognitive Disorders. *Neurosci. Biobehav. Rev.* 132, 1114–1136. doi:10.1016/j.neubiorev.2021.10.037

Sambo, D. O., Lebowitz, J. J., and Khoshbouei, H. (2018). The Sigma-1 Receptor as a Regulator of Dopamine Neurotransmission: A Potential Therapeutic Target for Methamphetamine Addiction. *Pharmacol. Ther.* 186, 152–167. doi:10.1016/j.pharmthera.2018.01.009

Sambo, D. O., Lin, M., Owens, A., Lebowitz, J. J., Richardson, B., Jagnarine, D. A., et al. (2017). The Sigma-1 Receptor Modulates Methamphetamine Dysregulation of Dopamine Neurotransmission. *Nat. Commun.* 8 (1), 2228. doi:10.1038/s41467-017-02087-x

Sanacora, G., Rothman, D. L., Mason, G., and Krystal, J. H. (2003). Clinical Studies Implementing Glutamate Neurotransmission in Mood Disorders. *Ann. N. Y. Acad. Sci.* 1003, 292–308. doi:10.1196/annals.1300.018

Schmidt, H. R., and Kruse, A. C. (2019). The Molecular Function of σ Receptors: Past, Present, and Future. *Trends Pharmacol. Sci.* 40 (9), 636–654. doi:10.1016/j.tips.2019.07.006

Seo, J. S., Wei, J., Qin, L., Kim, Y., Yan, Z., and Greengard, P. (2017). Cellular and Molecular Basis for Stress-Induced Depression. *Mol. Psychiatry* 22 (10), 1440–1447. doi:10.1038/mp.2016.118

Sha, S., Qu, W. J., Li, L., Lu, Z. H., Chen, L., Yu, W. F., et al. (2013). Sigma-1 Receptor Knockout Impairs Neurogenesis in Dentate Gyrus of Adult hippocampus via Down-Regulation of NMDA Receptors. *CNS Neurosci. Ther.* 19 (9), 705–713. doi:10.1111/cns.12129

Shin, S. M., Wang, F., Qiu, C., Itson-Zoske, B., Hogan, Q. H., and Yu, H. (2020). Sigma-1 Receptor Activity in Primary Sensory Neurons Is a Critical Driver of Neuropathic Pain. *Gene Ther.* 29, 1–15. doi:10.1038/s41434-020-0157-5

Skuza, G., Rogóz, Z., and Gołembiowska, K. (1997). EMD 57445, the Selective Sigma Receptor Ligand, Has No Effect on the 5-hydroxytryptamine System. *Pol. J. Pharmacol.* 49 (6), 489–493.

Snyder, M. A., Mccann, K., Lalande, M. J., Thivierge, J. P., and Bergeron, R. (2016). Sigma Receptor Type 1 Knockout Mice Show a Mild Deficit in Plasticity but No Significant Change in Synaptic Transmission in the CA1 Region of the hippocampus. *J. Neurochem.* 138 (5), 700–709. doi:10.1111/jnc.13695

Srivats, S., Balasuriya, D., Pasche, M., Vistal, G., Edwardson, J. M., Taylor, C. W., et al. (2016). Sigma1 Receptors Inhibit Store-Operated Ca2+ Entry by Attenuating Coupling of STIM1 to Orai1. *J. Cell Biol.* 213 (1), 65–79. doi:10.1083/jcb.201506022

Su, T. P., Hayashi, T., Maurice, T., Buch, S., and Ruoho, A. E. (2010). The Sigma-1 Receptor Chaperone as an Inter-organelle Signaling Modulator. *Trends Pharmacol. Sci.* 31 (12), 557–566. doi:10.1016/j.tips.2010.08.007

Suhm, T., Kaimal, J. M., Dawitz, H., Peselj, C., Masser, A. E., Hanzén, S., et al. (2018). Mitochondrial Translation Efficiency Controls Cytoplasmic Protein Homeostasis. *Cell Metab.* 27 (6), 1309–e6. e6. doi:10.1016/j.cmet.2018.04.011

Takizawa, R., Hashimoto, K., Tochigi, M., Kawakubo, Y., Marumo, K., Sasaki, T., et al. (2009). Association between Sigma-1 Receptor Gene Polymorphism and Prefrontal Hemodynamic Response Induced by Cognitive Activation in Schizophrenia. *Prog. Neuropsychopharmacol. Biol. Psychiatry* 33 (3), 491–498. doi:10.1016/j.pnpbp.2009.01.014

Tchedre, K. T., Huang, R. Q., Dibas, A., Krishnamoorthy, R. R., Dillon, G. H., and Yorio, T. (2008). Sigma-1 Receptor Regulation of Voltage-Gated Calcium Channels Involves a Direct Interaction. *Invest Ophthalmol. Vis. Sci.* 49 (11), 4993–5002. doi:10.1167/iovs.08-1867

Timberlake Ii, M., Roy, B., and Dwivedi, Y. (2019). A Novel Animal Model for Studying Depression Featuring the Induction of the Unfolded Protein Response in Hippocampus. *Mol. Neurobiol.* 56 (12), 8524–8536. doi:10.1007/s12035-019-01687-6

Urani, A., Romieu, P., Portales-Casamar, E., Roman, F. J., and Maurice, T. (2002). The Antidepressant-like Effect Induced by the Sigma(1) (Sigma(1)) Receptor Agonist Igmesine Involves Modulation of Intracellular Calcium Mobilization. *Psychopharmacol. Berl.* 163 (1), 26–35. doi:10.1007/s00213-002-1150-y

Urfer, R., Moebius, H. J., Skoloudik, D., Santamarina, E., Sato, W., Mita, S., et al. (2014). Phase II Trial of the Sigma-1 Receptor Agonist Cutamesine (SA4503) for Recovery Enhancement after Acute Ischemic Stroke. *Stroke* 45 (11), 3304–3310. doi:10.1161/STROKEAHA.114.005835

Vetel, S., Foucault-Fruchard, L., Tronel, C., Buron, F., Vergote, J., Bodard, S., et al. (2021). Neuroprotective and Anti-inflammatory Effects of a Therapy Combining Agonists of Nicotinic α7 and σ1 Receptors in a Rat Model of Parkinson's Disease. *Neural Regen. Res.* 16 (6), 1099–1104. doi:10.4103/1673-5374.300451

Voronin, M. V., Vakhitova, Y. V., and Seredenin, S. B. (2020). Chaperone Sigma1R and Antidepressant Effect. *Int. J. Mol. Sci.* 21 (19). doi:10.3390/ijms21197088

Wang, D., Noda, Y., Tsunekawa, H., Zhou, Y., Miyazaki, M., Senzaki, K., et al. (2007). Role of N-Methyl-D-Aspartate Receptors in Antidepressant-like Effects of Sigma 1 Receptor Agonist 1-(3,4-Dimethoxyphenethyl)-4-(3-Phenylpropyl) piperazine Dihydrochloride (SA-4503) in Olfactory Bulbectomized Rats. *J. Pharmacol. Exp. Ther.* 322 (3), 1305–1314. doi:10.1124/jpet.107.124685

Wang, L., Zhang, Y., Wang, C., Zhang, X., Wang, Z., Liang, X., et al. (2019). A Natural Product with High Affinity to Sigma and 5-HT7 Receptors as Novel Therapeutic Drug for Negative and Cognitive Symptoms of Schizophrenia. *Neurochem. Res.* 44 (11), 2536–2545. doi:10.1007/s11064-019-02873-7

Weng, T. Y., Tsai, S. A., and Su, T. P. (2017). Roles of Sigma-1 Receptors on Mitochondrial Functions Relevant to Neurodegenerative Diseases. *J. Biomed. Sci.* 24 (1), 74. doi:10.1186/s12929-017-0380-6

Who (2022). COVID-19 Pandemic Triggers 25% Increase in Prevalence of Anxiety and Depression Worldwide. Available at: https://www.who.int/news/item/02-03-2022-covid-19-pandemic-triggers-25-increase-in-prevalence-of-anxiety-and-depression-worldwide.

Ye, N., Qin, W., Tian, S., Xu, Q., Wold, E. A., Zhou, J., et al. (2020). Small Molecules Selectively Targeting Sigma-1 Receptor for the Treatment of Neurological Diseases. *J. Med. Chem.* 63 (24), 15187–15217. doi:10.1021/acs.jmedchem.0c01192

Yin, Y. Y., Wang, Y. H., Liu, W. G., Yao, J. Q., Yuan, J., Li, Z. H., et al. (2021). The Role of the Excitation:inhibition Functional Balance in the mPFC in the Onset of Antidepressants. *Neuropharmacology* 191, 108573. doi:10.1016/j.neuropharm.2021.108573

Zhang, B., Wang, L., Chen, T., Hong, J., Sha, S., Wang, J., et al. (2017). Sigma-1 Receptor Deficiency Reduces GABAergic Inhibition in the Basolateral Amygdala Leading to LTD Impairment and Depressive-like Behaviors. *Neuropharmacology* 116, 387–398. doi:10.1016/j.neuropharm.2017.01.014

Zhang, J., Lu, H., Zeng, H., Zhang, S., Du, Q., Jiang, T., et al. (2020). The Differential Psychological Distress of Populations Affected by the COVID-19 Pandemic. *Brain Behav. Immun.* 87, 49–50. doi:10.1016/j.bbi.2020.04.031

Zhang, Y.-m., Ye, L.-y., Li, T.-y., Guo, F., Guo, F., Li, Y., et al. (2021). New Monoamine Antidepressant, Hypidone Hydrochloride (YL-0919), Enhances the Excitability of Medial Prefrontal Cortex in Mice via a Neural Disinhibition Mechanism. *Acta Pharmacol. Sin.* Online ahead of print. doi:10.1038/s41401-021-00807-0

Zhao, X. P., Li, H., and Dai, R. P. (2022). Neuroimmune Crosstalk through Brain-Derived Neurotrophic Factor and its Precursor Pro-BDNF: New Insights into Mood Disorders. *World J. Psychiatry* 12 (3), 379–392. doi:10.5498/wjp.v12.i3.379

Conflict of Interest: The authors declare that the research was conducted in the absence of any commercial or financial relationships that could be construed as a potential conflict of interest.

Publisher's Note: All claims expressed in this article are solely those of the authors and do not necessarily represent those of their affiliated organizations, or those of the publisher, the editors and the reviewers. Any product that may be evaluated in this article, or claim that may be made by its manufacturer, is not guaranteed or endorsed by the publisher.

frontiers | Frontiers in Pharmacology

ORIGINAL RESEARCH
published: 22 June 2022
doi: 10.3389/fphar.2022.926123

Mechanism of Neural Regeneration Induced by Natural Product LY01 in the 5×FAD Mouse Model of Alzheimer's Disease

Xiao-Wan Li[1,2†], Yang-Yang Lu[1†], Shu-Yao Zhang[1], Ning-Ning Sai[3], Yu-Yan Fan[4], Yong Cheng[1,5] and Qing-Shan Liu[1*]*

[1]Key Laboratory of Ethnomedicine for Ministry of Education, Center on Translational Neuroscience, Minzu University of China, Beijing, China, [2]Center for Life Sciences, School of Life Science and Technology, Harbin Institute of Technology, Harbin, China, [3]University Hospital, Tianjin Normal University, Tianjin, China, [4]Traditional Chinese Medicine Department, Beijing Tiantan Hospital, Capital Medical University, Beijing, China, [5]Institute of National Security, Minzu University of China, Beijing, China

OPEN ACCESS

Edited by:
Yunfeng Li,
Academy of Military Medical Sciences (AMMS), China

Reviewed by:
Paul F. Seke Etet,
Université de Ngaoundéré, Cameroon
Xiaoqin Wu,
Cleveland Clinic, United States

***Correspondence:**
Yong Cheng
yongcheng@muc.edu.cn
Qing-Shan Liu
nlqsh@163.com

[†]These authors have contributed equally to this work

Specialty section:
This article was submitted to Neuropharmacology, a section of the journal Frontiers in Pharmacology

Received: 22 April 2022
Accepted: 31 May 2022
Published: 22 June 2022

Citation:
Li X-W, Lu Y-Y, Zhang S-Y, Sai N-N, Fan Y-Y, Cheng Y and Liu Q-S (2022) Mechanism of Neural Regeneration Induced by Natural Product LY01 in the 5×FAD Mouse Model of Alzheimer's Disease. Front. Pharmacol. 13:926123. doi: 10.3389/fphar.2022.926123

Background: A sharp decline in neural regeneration in patients with Alzheimer's disease (AD) exacerbates the decline of cognition and memory. It is of great significance to screen for innovative drugs that promote endogenous neural regeneration. Cytisine N-methylene-(5,7,4′-trihydroxy)-isoflavone (LY01) is a new compound isolated from the Chinese herbal medicine *Sophora alopecuroides* with both isoflavone and alkaloid characteristic structures. Its pharmacological effects are worth studying.

Objective: This study was designed to determine whether LY01 delays the cognitive and memory decline in the early stage of AD and whether this effect of LY01 is related to promoting neural regeneration.

Methods: Eight-week-old 5×Familial Alzheimer's Disease (5×FAD) mice were used as disease models of early AD. Three doses of LY01 administered in two courses (2 and 5 weeks) of treatment were tested. Cognition, memory, and anxiety-like behaviors in mice were evaluated by the Morris water maze, fear conditioning, and open field experiments. Regeneration of neurons in the mouse hippocampus was observed using immunofluorescence staining. The effect of LY01 on cell regeneration was also demonstrated using a series of tests on primary cultured neurons, astrocytes, and neural stem cells (NSCs). In addition, flow cytometry and transcriptome sequencing were carried out to preliminarily explored the mechanisms.

Results: We found that LY01 reduced the decline of cognition and memory in the early stage of 5×FAD mice. This effect was related to the proliferation of astrocytes, the proliferation and migration of NSCs, and increases in the number of new cells and neural precursor cells in the dentate gyrus area of 5×FAD mice. This phenomenon could be observed both in 2-week-old female and 5-week-old male LY01-treated 5×FAD mice. The neuronal regeneration induced by LY01 was related to the regulation of the extracellular matrix and associated receptors, and effects on the S phase of the cell cycle.

Conclusion: LY01 increases the proliferation of NSCs and astrocytes and the number of neural precursor cells in the hippocampus, resulting in neural regeneration in 5×FAD mice by acting on the extracellular matrix and associated receptors and regulating the S phase of the cell cycle. This provides a new idea for the early intervention and treatment of AD.

Keywords: isoflavone-cytisine, Alzheimer's disease, 5×FAD mice, neural stem cells, neural regeneration

INTRODUCTION

Alzheimer's disease (AD) is a progressive neurodegenerative disease (Berchtold and Cotman, 1998). According to the data published by the Alzheimer's Disease International association in 2015, there are more than 54.4 million patients with dementia worldwide, with an average increase of one case every 3 s (Dos Santos Picanco et al., 2018), and most of them are related to AD (Bradley et al., 2015; Livingston et al., 2017; Alzheimer's Association, 2020). The most recent data indicate that, by 2050, the prevalence of dementia will triple worldwide (Scheltens et al., 2021), and that estimate is three times higher when based on a biological (rather than clinical) definition of AD. The main pathological features (Zilka and Novak, 2006; Cipriani et al., 2011) of AD are extracellular amyloid plaques, intracellular neurofibrillary tangles, and loss of neurons (Blennow et al., 2006).

Neural regeneration, including the proliferation and functional differentiation of NSCs, is a process in which neural networks are established and maintained to function well through continual plastic changes and establishing synaptic connections with other neurons. Adult NSCs have the ability to self-renew and differentiate into neurons and glial cells. In the developed nervous system, NSCs derived from embryonic cells carried on the neural plate can exist in the adult hippocampus and lateral ventricle for a long time. The identity of NSCs between pluripotent state and post differentiation state is regulated by the response of the NSCs transcription program under the influence of external and internal factors. External factors and internal factors act at the same time, endowing the central nervous system (CNS) with different levels of plasticity and necessary complexity (Massirer et al., 2011). Studies using human brain samples taken under strict conditions and advanced tissue processing technology revealed that adult hippocampal nerve regeneration is very rich in healthy subjects, but decreases sharply in patients with AD (Moreno-Jimenez et al., 2019). Other studies have pointed out that the interactions between sleep disorders and inhibition of nerve regeneration exacerbate the cognitive decline associated with AD (Kent and Mistlberger, 2017). Recovery of the number of new stem cells in the brain of AD patients is of great value for the improvement of the disease condition (Wareham et al., 2022). Therefore, the research on NSC therapy for AD has persisted (Hayashi et al., 2020; Aboul-Soud et al., 2021). However, the costs of the operation are high and the compliance of patients with targeted transplantation is poor. Therefore, alternatives, such as active compounds that can promote the proliferation and migration of endogenous NSCs in the CNS, are needed.

Cytisine N-methylene-(5,7,4′-trihydroxy)-isoflavone is a new compound isolated from the Chinese herbal medicine *Sophora alopecuroides*. It is a new type of cytisine with an alkaloid and isoflavone structure (**Figure 1**) (Yin and Liu, 2016). Alkaloids are an important type of secondary metabolites in plants. They usually have significant pharmacological activities and biological functions and have rich chemical structures in nature. Known studies have found that the activities of alkaloids are diverse, including anti-tumor (Manayi et al., 2018), antibacterial (de Oliveira et al., 2019), blood glucose-regulating (Li et al., 2017), and antiviral (Varghese et al., 2016) activities. Other studies have shown that alkaloids can selectively bind to and serve as an agonist of the α4β2 nicotinic acetylcholine receptor, thus inhibiting addiction. It has been used in the study of smoking cessation (Rigotti, 2014), which indicates the potential value of alkaloids in the treatment of nervous system diseases. Flavones have many functions. They are a strong antioxidants whose capacities are more than 10 times that of vitamin E. They effectively remove oxygen free radicals in the body (Popovic et al., 2019), prevent cell degeneration and aging, and prevent cancer (Mazewski et al., 2018; Chen et al., 2020); they also improve blood circulation and lower cholesterol (Singh et al., 2018), inhibit the exudation of inflammatory enzymes, promote wound healing, and relieve pain (Shoaib et al., 2019). Isoflavone is a flavonoid that mainly exists in leguminous plants. It is called phytoestrogen because of its structural similarity to estrogen, which can be used for the prevention and even treatment of Alzheimer's disease (Duan et al., 2021). Phytoestrogens are not pharmaceutical estrogens and have few side effects (Escande et al., 2006), and have a two-way regulation function. When the estrogen in the body is high, they show anti-estrogen activity and reduce the risk of related cancers. As a new compound with both alkaloid and isoflavone active structures, there has been no report on the biological activity of LY01 before. This research on the treatment of AD with the bioactive substance LY01 will provide a new choice for the prevention and treatment of the disease. Likewise, the research on the biological activities of LY01 related to neurons, astrocytes, and NSCs will further enrich the understanding of the mechanism of action of isoflavones.

MATERIALS AND METHODS

Primary Cell Culture and Treatment

Primary astrocytes (Chen et al., 2019), neurons (Pan et al., 2017), and NSCs (Wei et al., 2020) were cultured according to the previous protocols. Primary hippocampal neurons were evenly spread into 96-well plates at the concentration of 5×10^5 cells/mL. On the third to fifth day of culture *in vitro*, LY01 (3, 6, 12, 24, 48 μm) treatment was performed when the morphology and structure of neurons were relatively mature. Cell viability was measured at 48 h after the cells were incubated with LY01.

FIGURE1 | Molecular structure of LY01.

Purified astrocytes were evenly spread into 96-well plates at the concentration of 1×10^5 cells/mL. The media was changed after 12 h of culturing and treated with LY01 (1.5, 3, 6 μm). After 48 h, cell viability was measured. Three replicates were set up and the experiment was repeated three times independently.

The primary NSCs with good proliferation and property were evenly spread into 96 well plate and 6-well plate at the concentration of 1×10^5 cells/mL. LY01 treatment (0.75, 1.5, 3, 6 μm) was carried out 24 h after plating cells. The cell viability, neurospheres number and gene expression level of laminin subunit gamma 2 (Lamc2) were measured 24 h after the treatment. The cells in the 6-well plate were collected for cell cycle detection. In addition, the primary NSCs digested into single cells were evenly plated on coverslips coated with poly-L-lysine at the concentration of 2×10^4 cells/mL. After 12 h, NSC proliferation medium was changed into NSC differentiation medium (Dulbecco's modified Eagle's medium (DMEM)/F12 medium containing 10% fetal bovine serum (FBS)) and cultured for 7 days. LY01 was added to the differentiation medium at the concentration of 1.5 μm and the medium was changed every other day. The differentiated cells was detected by immunofluorescence. Images were randomly captured for quantification.

The experiments were repeated three times independently. LY01 was dissolved in DMSO and basic medium, and the final concentration of DMSO was less than 1‰. The control group was treated with the same amount of vehicle as the experimental group.

Cell Viability Test

Cell viability was detected by water-soluble tetrazolium salt 1 (WST1) kit (Beyotime Biotechnology, C0036) according to the previous protocols (Wei et al., 2020).

Neurospheres Counting

After treatment, NSC neurospheres were counted in the bright field of fluorescence microscope. Three replications were set for each independent experiment, and four images were randomly captured in each replication for neurospheres counting. The image Pro software was used for statistical analysis. The experiment was repeated three times independently.

Transwell Migration Assay

The primary NSCs with good properties were prepared into a single cell suspension of 1×10^6 cells/mL in serum-free DMEM/F12 medium. The volume of cell suspension in the upper chamber of transwell was 100 μL. 600 μL DMEM/F12 medium containing 10% FBS supplemented with or without 1.5 μM LY01 was added into the bottom wells, followed by incubation for 12 h. The medium in the upper chamber was discarded, and 800 μL phosphate buffer (PBS) was used to gently clean the upper membrane twice. After that, 800 μL methanol was uesd to fix the cells on the membrane for 30 min at room temperature. After staining with 0.1% crystal violet solution for 20 min at room temperature, the nonmigrating cells on the upper membrane were gently removed with a cotton swab. Images were randomly captured, and the number of migrating cells were manually quantified. The experiment was repeated three times independently.

Morphological Analysis of Primary NSC Migration

On the fourth day of primary NSC passage, the neurospheres were collected and plated to 24 well plate coated with poly-L-lysine. After 4 h, 1.5 μm LY01 was administered, and then cultured for 19–24 h 10 neurospheres were randomly captured from each group, and The ratio of the diameter of the radiation circle after migration to the diameter of the protoneurospheres was used to reflect the effect of LY01 on cell migration. The experiment was repeated three times.

Cell Cycle Detection

After centrifugation at 800 g for 5 min, neurospheres were collected and digested, and then the cells were washed twice with precooled PBS. Each sample was added with 500–1000 μL precooled 70% ethanol, and the cell suspension concentration was $0.5–2\times10^6$ cells/mL, followed by being fixed overnight at 4°C or long-term storage at −20°C. The cells were collected by centrifugation, washed with 1 ml of precooled PBS once, and then resuspended with 500 μL PBS containing 50 μg/ml propidium iodide (Solarbio, P8080), 100 μg/ml RNase A, 0.2% Triton X-100, and incubated in dark at 4°C for 30 min. The samples were detected by FlowSight multi-dimensional panoramic flow cytometry, and cell cycle was analyzed by IDEAS®. Three replications were set in each group.

RNA Sequencing

NSCs were plated into a 12 well plate at the concentration of 1×10^5 cells/mL. After 24 h, the cells were divided into two groups:

control group treated with vehicle and experimental group treated with 1.5 μm LY01 for 6 h. The cells were resuspended with 1 ml Trizol and then frozen at −80°C for testing. Samples prepared according to the above steps were sent to the Shanghai Majorbio Bio-pharm Technology Co., Ltd. for RNA extraction, illumina transcriptome sequencing and bioinformatics analysis (Ren et al., 2022).

RNA Extraction and Quantitative RT-PCR

RNA was extracted from primary NSCs using Trizol reagent (ThermoFisher, Waltham, MA, United States) and converted to cDNA using TaqManTM MicroRNA Reverse Transcription kit (ThermoFisher) following the manufacturer's protocol. The quantitative reverse transcriptase-polymerase chain reaction (RT-PCR) were performed2×RealStar Fast SYBR qPCR Mix (Genestar, A301-10). The cycling c-onditions were: 2 min denaturation at 95°C and 45 cycles of DNA synthe-sis at 95°C for 15 s and 60°C for 30 s. Primer sequences for Lamc2 forward: 5′-GCATCTACAACACAGCGGGAA-3′, reverse: 5′-ACAGCT GCCATCACTTCGAC-3'; for GADPH forward: 5′-ATCAAC GGGAAACCCATCACC-3′, reverse: 5′-AAGACGCCAGTA GACTCCAC-3'. All quantitative RT-PCR reactions were performed using a LightCycler® 96 Real-Time PCR Detection System (Roche, Basel, Switzerland).

Animals

The 5×FAD mice overexpressing the K670 N/M671 L (Swedish), I716V (Florida), and V717I (London) mutations in human APP, as well as M146 L and L286 V mutations in human PS1, were provided by Z. Q Zhang (Beijing Institute of Basic Medical Sciences, Beijing, China). Genotypes were confirmed by PCR analysis of tail biopsy specimens. Mice were housed four to five per cage with a 12-h light/12-h dark cycle and food and water adlibitum. All experimental animal procedures were approved by the Institutional Animal Care and Use Committees of the Minzu University of China.

Drug Treatment

The experiment was divided into six groups, wild type (WT) group, 5×FAD group, Rg1 group, and LY01-high, middle, low group. Except WT group, other groups were 5×FAD mice. This experiment mainly focused on the effect of LY01 in the early stage of AD, so the drug was administered at the age of 8 weeks when 5×FAD mice exhibit amyloid deposition (Eimer and Vassar, 2013; Gu., 2015) and the rate of hippocampal neural regeneration changed relatively little with age (Harris et al., 2021). The age difference was within 5 days for female mice, and 7 days for male mice. The dosage of Rg1 group was 20 mg/kg/day, while that of LY01 was 0.025, 0.1 and 0.4 mg/kg/day, respectively. The other two groups were intraperitoneally injected with the same amount of normal saline every day. WT mice used in the experiment were siblings of 5×FAD mice. All the mice weighed in the range of 20 ± 2 g (g), and were randomly divided into each group, and there was no significant difference in body weight between groups. Under the advocacy of the 3R (Reduction, RepIacement, Refinement) principle of animal experiment, two different courses of treatment were used for female and male mice to get more information about the efficacy of the new drugs in the course of treatment and gender, rather than their differences, with as few animals as possible. As pathological characteristics of 5×FAD mice were more obvious at the age of 3 months (Jawhar et al., 2012), the AD-like behavioral phenotype should be more significant at this age. In addition, compared with female mice, male mice are less disturbed by the fluctuation of hormone level, and have better physical strength for water maze experiment (Pan et al., 2017). Therefore, a 5-weeks treatment course was set for male mice, the sample size of each group was no less than eight mice, and for female mice, a 2-weeks course (Liu et al., 2021) of treatment was used, the sample size of each group was no less than three mice. The mice were intraperitoneally injected with BrdU solution at a dose of 50 mg/kg/day for three consecutive days starting from the fourth days before sampling (**Figure 2**).

Morris Water Maze

Water maze is a classical experimental method to test the learning and memory ability of experimental animals. The experimental site is divided into four quadrants. In one quadrant, a transparent platform can be set for mice to stand. Once the platform position is set, it cannot be changed during the experiment. At the same time, a graphic mark can be made around the experimental pool for reference. Before the experiment, diluted milk should be added to the pool to make the water turbid. The temperature of water requires constant temperature during the experiment, which is generally 18–22°C. The experiment is divided into two stages, positioning navigation and space exploration. The training days of the positioning navigation experiment were 6 days, and the single training time was 60 s each mouse was put into the water from four quadrants to find the platform in the water. The time used in this process is called the escape latency. If the mice cannot find the platform within the specified time, they will stay for 10 s after arriving at the platform to deepen learning. On the seventh day, the platform was removed, and the movement of mice within 60 s was recorded.

Fear Conditioning

Fear conditioning is a common experimental method to test the conditioned memory ability of animals. A box is used as the isolation environment for behavioral test. There are 2 W incandescent lamps installed in it, and small exhaust fan is used for ventilation. The bottom of the box is stainless steel bar for foot electrical stimulation, and the top is equipped with loudspeaker for sound stimulation. After the test, the training arena was wiped with alcohol to eliminate the interference of odor on the experimental results. On the first day of the experiment, the mice were put into the box. After 60 s of adaptation, 75 dB white noise stimulation lasting for 30 s was given at 110, 160, 210, 260, 310, 360, 410, 460 s respectively, and foot shock (30 mA) lasting for 2 s was given at the last 2 s of each white noise stimulation. The whole experiment lasted 490 s, and the animal's freezing time was observed by camera. On the second day of the experiment, the animals were placed in the experimental box for 120 s without any sound or electrical

FIGURE 2 | Schedule for drug administration and behavioral testing.

stimulation. The animal's freezing time was detected through the camera. On the third day of the experiment, the color of the test box was changed with colored paper. After 30 s of adaptation time, white noise (75 dB) stimulation lasting for 30 s was given at 30, 80, 110, 160, 210 s. The whole experiment lasted 150 s, and the animal's freezing time was recorded.

Open Field Test

The open field test is used to evaluate the state of autonomic movement, aiming to identify agitation, and pathological behavior. The experimental device consists of an trial chamber, an automatic data acquisition and processing system. The open field lighting is all artificial lighting. The laboratory personnel, computers and other equipment are located in another room to reduce the interference to animals. The background noise of the laboratory is controlled below 65 dB. The mouse trial chamber is 25–30 cm high, the bottom edge is 72 cm long, the inner wall is blackened, and the bottom surface (software) is divided into 64 small squares on average. The rearing times, movement speed, central movement time and other information of mice were recorded within 5 min.

Immunofluorescence

Specific proteins in cells and tissues were labeled with fluorescence according to the previous experimental protocols (Wei et al., 2020).

For immunofluorescent staining, the cells plated on the coverslips and brain sections were labeled with primary antibody and fluorescent secondary antibodies as follows: GFAP antibody (Millipore, MAB360, 1:1000), MAP2 antibody (CST, 8707S, 1:1000), Ki67 antibody (Invitrogen, 12H15L5, 1: 500), DCX antibody (CST, 4604S, 1:2000), BrdU antibody (CST, 5292, 1:800), Donkey anti-Mouse IgG (Invitrogen, A-21202, 1: 2000), Donkey anti-Rabbit IgG (Invitrogen, A-21207, 1:2000). For the primary cell experiment, pictures were taken randomly from four areas in each group according to the upper, lower, left and right positions, and take the mean for statistical analysis (Pan et al., 2017; Wei et al., 2020). For animal experiments, continuous slices of the whole hippocampus were made with a thickness of 30 microns. Three slices were selected randomly and evenly, and the positions of brain slices selected in each group were the same. BrdU-positive cells in the dentate gyrus were counted and the mean was taken for statistical analysis (Cheng et al., 2015; Wei et al., 2020).

Statistical Analysis

All statistical analyses were performed using GraphPad Prism version 6.0 software. Outliers were eliminated by the statistical elution method (values that deviate from the mean ± 2 times the standard deviation are excluded) (Nakagawa and Cuthill, 2007). The significance of differences was assessed by unpaired Student's t test or one-way ANOVA analysis. The significant threshold was set at $p < 0.05$. The data before analysis of variance were subject to a normality test (D'Agostino-Pearson omnibus test) and variance homogeneity test (Brown-Forsythe test). If not, a nonparametric test was used. For one-way ANOVA analyses, post hoc comparisons were performed using the Bonferroni post hoc tests test. In this paper, the data of *in vitro* experiment were analyzed by *t*-test, and the data of *in vivo* experiment were analyzed by one-way ANOVA.

RESULTS

Effect of LY01 on Mouse Body Weight

The mice were administered LY01 starting at the age of 8 weeks. During the experiment, body weights of mice was recorded and monitored every week. The results (**Figures 3A,B**) showed that the body weight of female and male mice increased in the first 2 weeks of the experiment, but there was no significant difference in body weight between the groups. Two weeks after the experiment, the overall increase rate of body weight of male mice slowed down, but there was no significant difference in body weight between the groups. The experimental results show that LY01 did not cause side effects sufficient to affect the weight of mice and can assist in excluding the influence of the health status of mice on the experimental results.

LY01 Alleviates Cognitive and Memory Decline in AD Mice

The Morris water maze is a classic behavioral experiment used to test learning and memory in mice. The mice were administrated LY01 intraperitoneally every day starting at the age of 8 weeks and behavior was analyzed after 3 weeks **Figure 4A** shows the curve of the latency to find the target platform during the training of each group of mice. The results show that the escape latency of mice in each group decreased with the increase in training times, indicating that the training of mice was effective. In addition, except for the model 5×FAD group, the latency of the other groups converged to a minimum value. Although there was no significant difference between the groups, the memories of the three groups and the positive drug Rg1 group tended to appear to be enhanced. According to **Figure 4D**, the trajectories of mice in the 5×FAD mice group are disordered, and those in the WT group, Rg1 group, and LY01 high-dose administration group are enriched in the target quadrant. As shown in **Figure 4B**, the space exploration experiment showed that the escape latency of the 5×FAD mice group was much

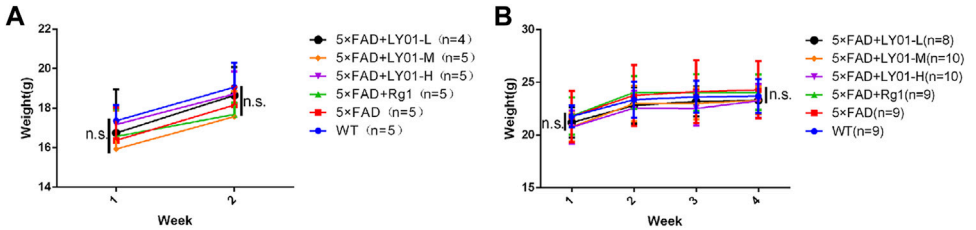

FIGURE 3 | Body weight changes of mice in each group **(A)** Body weight trend of female mice. WT: the control group of wild type mice treated with physiological saline solution for 2 weeks; 5×FAD: the model group of 5×FAD mice treated with physiological saline solution for 2 weeks; 5×FAD + Rg1: the positive control group of 5×FAD mice treated with 20 mg/kg/day ginsenoside Rg1 for 2 weeks; 5×FAD + LY01-H: the experimental group of 5×FAD mice with treated with 0.4 mg/kg/day LY01 for 2 weeks; 5×FAD + LY01-M: the experimental group of 5×FAD mice treated with 0.1 mg/kg/day LY01 for 2 weeks; 5×FAD + LY01-L: the experimental group of 5×FAD mice treated with 0.025 mg/kg/day LY01 for 2 weeks n = 4–5 **(B)** Body weight trend of male mice. WT: the control group of wild type mice treated with physiological saline solution for 5 weeks; 5×FAD: the model group of 5×FAD mice treated with physiological saline solution for 5 weeks; 5×FAD + Rg1: the positive control group of 5×FAD mice treated with 20 mg/kg/day ginsenoside Rg1 for 5 weeks; 5×FAD + LY01-H: the experimental group of 5×FAD mice treated with 0.4 mg/kg/day LY01 for 5 weeks; 5×FAD + LY01-M: the experimental group of 5×FAD mice treated with 0.1 mg/kg/day LY01 for 5 weeks; 5×FAD + LY01-L: the experimental group of 5×FAD mice treated with 0.025 mg/kg/day LY01 for 5 weeks n = 8–10. n. s, no significance. The results are expressed as means ± SD.

longer than that of the WT group ($p < 0.05$), indicating the success of modeling AD. The escape latency of the LY01 high-dose administration group was significantly lower than that of the 5×FAD mice group ($p < 0.05$). For the Rg1 administration group, there was a downward trend in data distribution compared with the model group ($p = 0.1162$). Overall, these results showed that LY01 delayed the decline of spatial memory in the early stage of 5×FAD mice. **Figure 4C** shows the number of mice in each group crossing the platform in the space exploration experiment. There is no significant difference between the WT group and the 5×FAD group, but a trend of difference ($p = 0.0837$), and there is no significant difference in other groups compared with the model group. The evaluation index (the number of platform crossings) does not correspond well to the memory decline at the early stage of 5×FAD mice.

In the fear conditioning experiment, environmental and sound stimulation were used to establish a connection with electric shock. Spatial conditioned memory and sound conditioned memory were evaluated using whole-body freezing caused by fear of electric shock. **Figure 4E** shows the short-term conditioned memory of mice after learning for 24 h, in which there is a significant downward trend in freezing time in 5×FAD groups compared with the WT group ($p < 0.05$), indicating the success of the model. In addition, compared with the model group, the conditioned memory of the high-dose and medium-dose LY01 group increased ($p < 0.05$), indicating that LY01 is beneficial for the improvement of short-term conditioned memory ability in 5×FAD mice. **Figure 4F** shows the conditioned memory ability of mice 48 h after learning. For this test, the difference between the model group and high-dose LY01 group was significant ($p < 0.05$), indicating that a high dose of LY01 can improve the conditioned memory ability of 5×FAD mice. However, the conditioned memory ability 48 h after training does not reflect the early memory decline of 5×FAD mice at the early stage ($p = 0.0629$).

In the open field test, the mice successively entered the experimental field independently. The mice in each group mainly focused their activities in the surrounding area, with many standing times and a little activity time in the central area (**Supplementary Figure S1A**), showing obvious exploratory behavior and excitement. There was no significant difference in movement speed and rearing time between the model group and the LY01-administered group (**Supplementary Figures S1B,C**). The analysis of the open field test results shows that there were no significant differences in exercise ability and anxiety-like behavior at the early stage of 5×FAD mice compared with WT mice, and LY01 did not affect exercise ability and anxiety-like behavior in AD model mice.

LY01 Could Increase the Number of New Cells in Dentate Gyrus Area of 5×FAD Mice

Bromodeoxyuridine (BrdU) is a thymine nucleoside analogue that can replace thymine to infiltrate DNA molecules in the process of cell proliferation, thus marking new cells. According to the results shown in **Figures 5A,B**, the number of new cells in the dentate gyrus area of female 5×FAD mice treated for 2 weeks in the group treated with the high concentration of LY01 increased significantly compared with that in the model group ($p < 0.01$). In male 5×FAD mice treated for 5 weeks, the same phenomenon was observed in the high-dose group (**Figure 5C**, $p < 0.05$). In addition, the number of new cells in 10-week-old female and 13-week-old male 5×FAD mice was significantly lower than that in the WT group ($p < 0.05$).

Doublecortin (DCX) is a marker of neuronal precursor cells. Immunofluorescence staining results of both 10-week-old female and 13-week-old male mice showed that the number of neuronal precursor cells in 5×FAD mice was small and the cell processes were short. Mice administered high-dose LY01 had a higher number of neuronal precursor cells and longer cell neurites than those not treated with LY01 (**Figure 6**).

LY01 Promotes the Proliferation of Primary Astrocytes

Primary hippocampal neurons cultured *in vitro* (**Supplementary Figure S2A**) for 3–5 days were divided into six groups: the control group and five experimental groups (3, 6, 12, 24, and 48 μm LY01). After 8 h of treatment, the viability of neurons in

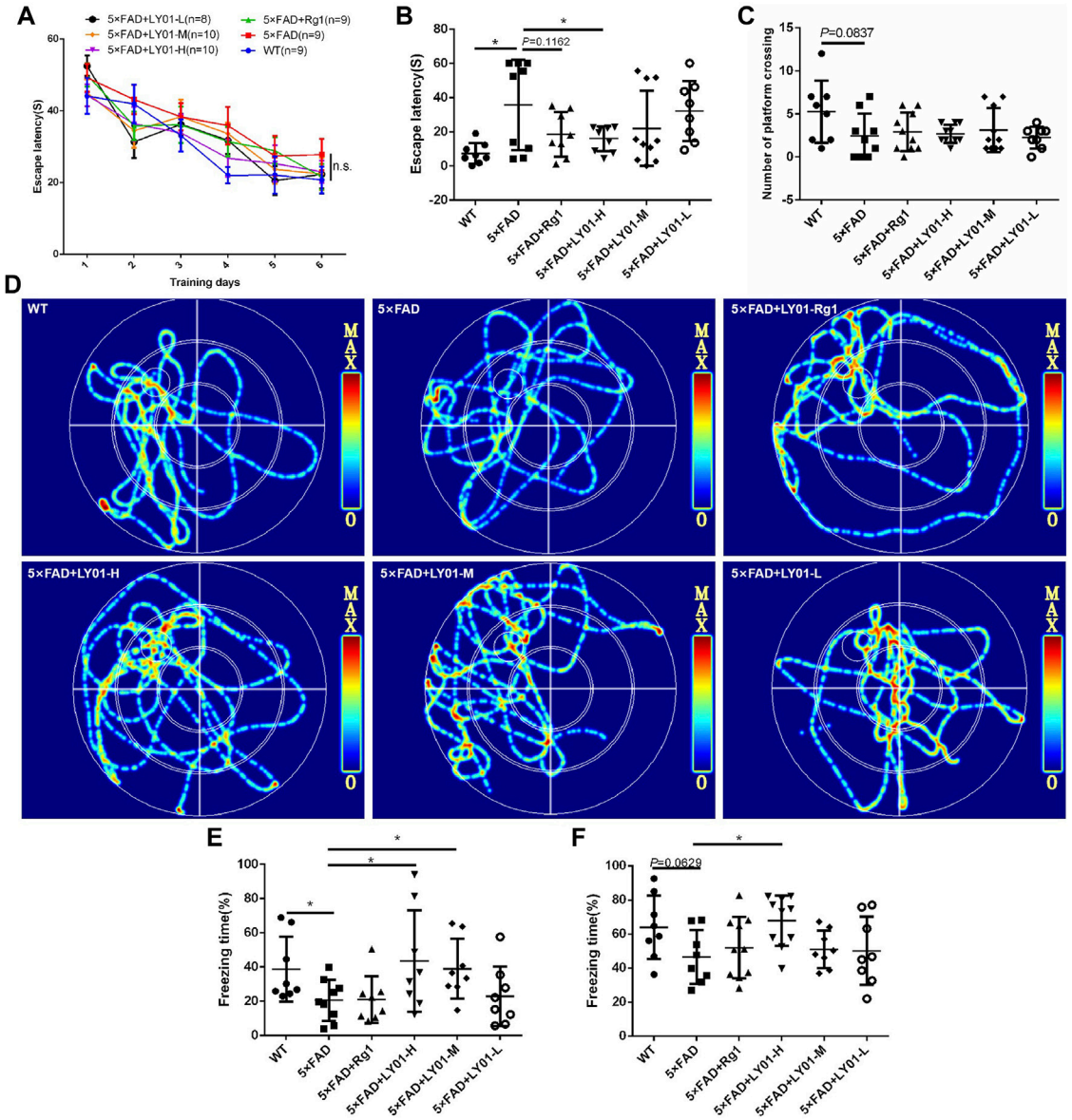

FIGURE 4 | The results of behavioral tests **(A)** Escape latency to the platform during the training trails in the Morris water maze **(B)** Escape latency on the seventh day in the Morris water maze. *$p < 0.05$ vs. 5×FAD, $n = 8–10$ **(C)** Platform crossings on the seventh day in the Morris water maze. $n = 8–10$ **(D)** Representative track images of mice on the seventh day in the Morris water maze **(E)** Spatial conditioned memory of mice 24 h after training in the fear conditioning test **(F)** conditioned memory ability of mice 48 h after training in the fear conditioning test. WT: the control group of wild type mice treated with physiological saline solution for 5 weeks; 5×FAD: the model group of 5×FAD mice treated with physiological saline solution for 5 weeks; 5×FAD + Rg1: the positive control group of 5×FAD mice treated with 20 mg/kg/day ginsenoside Rg1 for 5 weeks; 5×FAD + LY01-H: the experimental group of 5×FAD mice treated with 0.4 mg/kg/day LY01 for 5 weeks; 5×FAD + LY01-M: the experimental group of 5×FAD mice treated with 0.1 mg/kg/day LY01 for 5 weeks; 5×FAD + LY01-L: the experimental group of 5×FAD mice treated with 0.025 mg/kg/day LY01 for 5 weeks. The results are expressed as means ± SD.

the 3, 6, and 12 μm groups had no significant change compared with the control group ($p > 0.05$). The viability of neurons in the 24 and 48 μm groups was lower than that in the control group ($p < 0.05$). Thus, the concentration of LY01 used on neurons in subsequent experiments was less than 24 μm (**Figure 7A**).

As shown in **Figure 7B**, primary astrocytes (**Supplementary Figure S2B**) were treated with 1.5–6 μm LY01 and cell viability was detected 48 h later. It was found that the cell viability was significantly enhanced at concentrations higher than 3 μm ($p < 0.05$). The results of glial fibrillary acidic protein (GFAP) and nuclear protein Ki67 double staining of primary astrocytes treated with 3 μm LY01 showed that LY01 significantly increased the number of new astrocytes and there were approximately double the number of GFAP and Ki67 double-positive cells compared with the control group (**Figures 7C,D**),

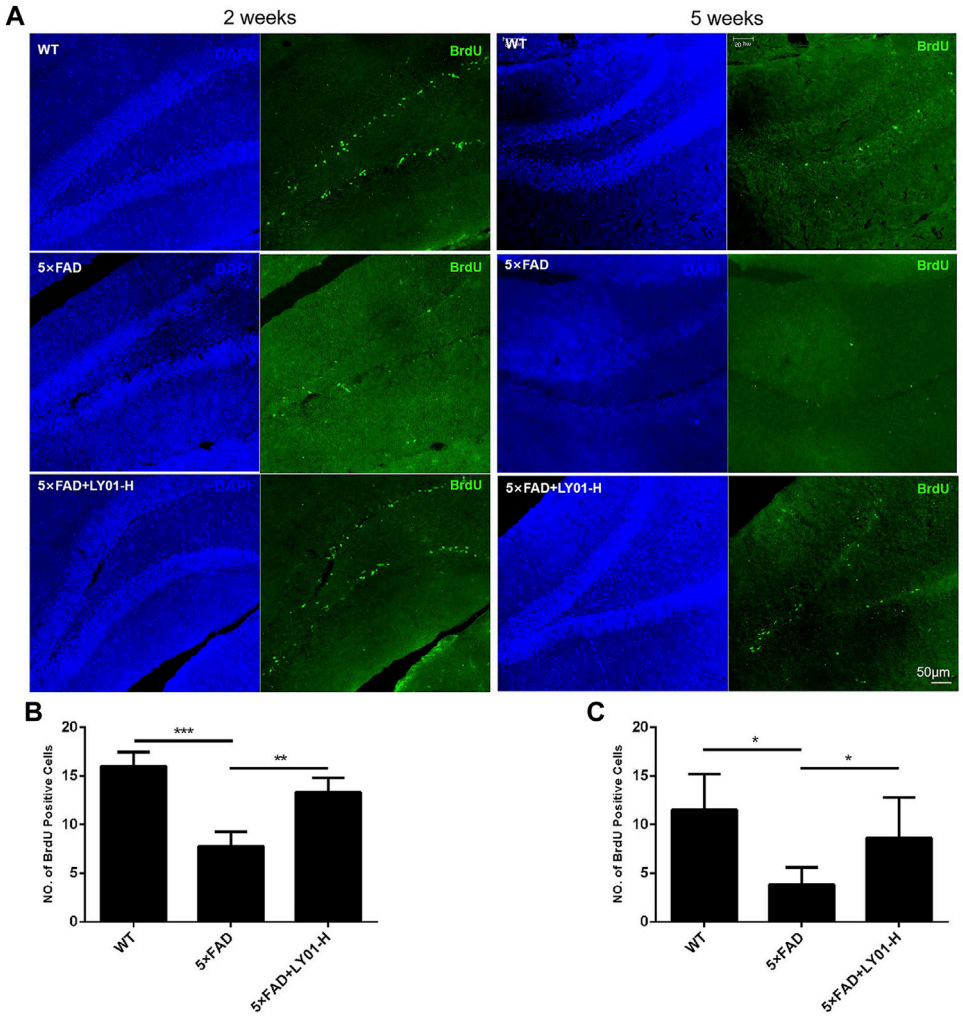

FIGURE 5 | The effect of LY01 on the number of new cells in the dentate gyrus area of 5×FAD mice **(A)** Representative images of new cells in the dentate gyrus of the hippocampus. The images show the result of female mice treated for 2 weeks and male mice treated for 5 weeks. The nuclei are labeled with 4′,6-diamidino-2-phenylindole (DAPI) (blue) and new cells are labeled with BrdU antibody (green) **(B)** The number of new cells in the dentate gyrus of female mice treated for 2 weeks $^{**}p < 0.01$, $^{***}p < 0.001$ vs. 5×FAD; $n = 3$ **(C)** The number of new cells in the dentate gyrus of male mice treated for 5 weeks $^{*}p < 0.05$ vs. 5×FAD; $n = 4$. WT: the control group of wild type mice treated with physiological saline solution; 5×FAD: the model group of 5×FAD mice treated with physiological saline solution; 5×FAD + LY01-H: the experimental group of 5×FAD mice treated with 0.4 mg/kg/day LY01. The results are expressed as means ± SD.

indicating that LY01 promoted the proliferation of astrocytes ($p < 0.05$).

LY01 Promotes Proliferation and Migration of Primary NSCs

The primary NSCs with good proliferation and properties (**Supplementary Figures S2C–F**) were evenly spread into a 96-well plate for WST1 testing; when the concentration of LY01 reached 1.5 μm, the viability of NSCs was increased ($p < 0.05$, **Figure 8A**). At concentrations lower than 1.5 μm, the number of NSCs with a diameter of 25–45 μm and the number of clone balls with a diameter greater than 45 μm were significantly higher than those of the control group ($p < 0.05$), indicating that LY01 promoted the proliferation of NSCs (**Figures 8B,C**).

As shown in **Figure 8D**, poly-L-lysine induced the adherent neurospheres to migrate radially. The ratio of the diameter of the radiation circle after migration to the diameter of the protoneurospheres was used to reflect the migration ability of stem cells. The results show that LY01 promoted the outward migration of NSCs (**Figure 8E**). The Transwell migration assay, as a classic method to detect cell migration and invasion, was used to verify the effect of LY01 on the migration of NSCs. As shown in **Figure 8F**, NSCs in the culture system with 1.5 μm LY01 were twice as large as those in the control group and migrated to the lower layer of the Transwell chamber (**Figure 8G**), indicating that LY01 promoted the migration of NSCs.

As shown in **Supplementary Figure S3A**, NSCs differentiated into astrocytes and neuron-like cells after 7 days of induction in DMEM/F12 medium plus FBS (10%). The proportion of GFAP-

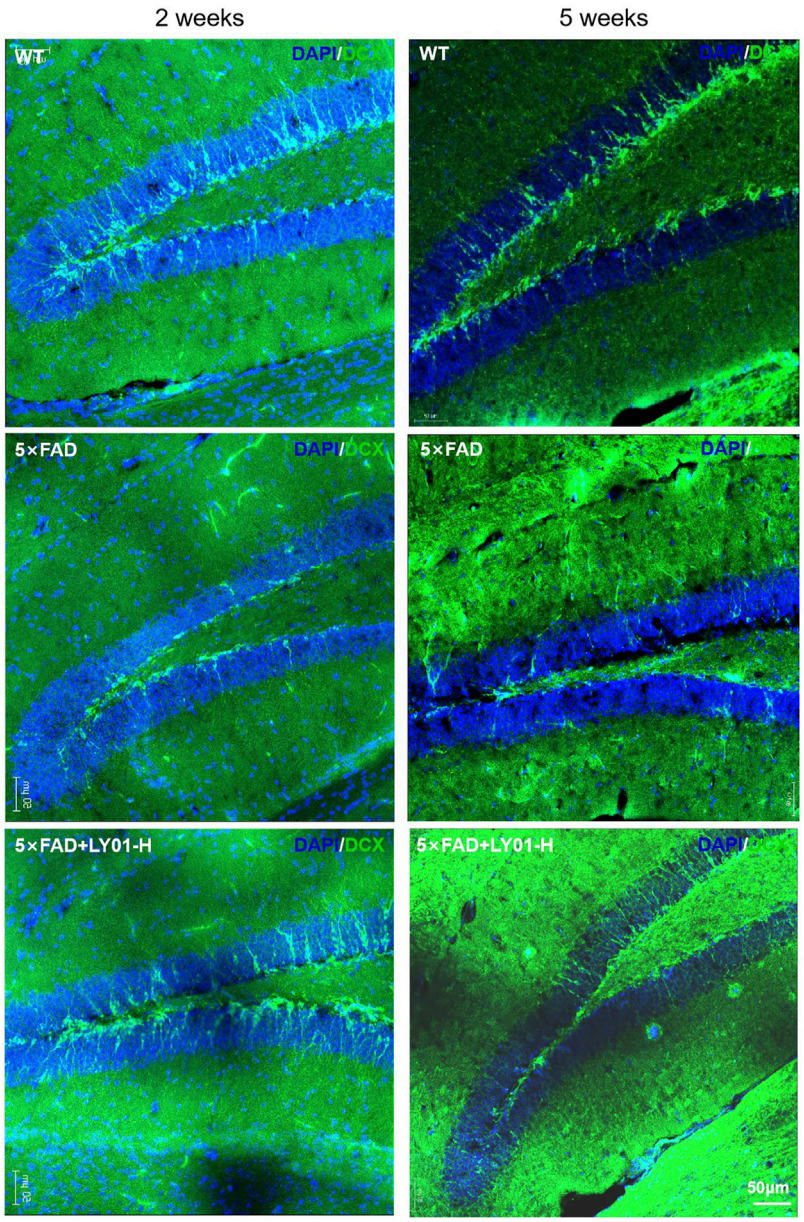

FIGURE 6 | Representative images of neural precursor cells in the dentate gyrus area of 5×FAD mice. The images show the result of female mice treated for 2 weeks and male mice treated for 5 weeks. The nuclei are labeled with DAPI (blue) and neural precursor cells are labeled with doublecortin (DCX) antibody (green).

positive astrocytes and microtubule-associated protein 2 (MAP2)-positive neurons after differentiation indicated that 1.5 μm LY01 had no effect on the selection of cell type during differentiation of NSCs (**Supplementary Figure S3B**).

Effects of LY01 on Cell Cycle and Transcription of Primary NSCs

NSCs treated with and without 1.5 μm LY01 were collected. After propidium iodide staining, the distribution of NSCs in each cell cycle was measured using flow cytometry to identify the stage that LY01 regulates the proliferation of NSCs. As shown in **Figures 9A,B**, μm LY01 treatment induced more cells to enter the G2/M phase through the S phase ($p < 0.01$) but had no effect on the proportion of cells in the G0/G1 phase. These results indicate that LY01 may regulate the S phase of the cell cycle to make more cells enter G2/M, thus promoting NSCs proliferation.

Transcriptome sequencing is an effective method to study the effects of drugs on cells at the transcriptional level. However, combining transcriptome sequencing results with functional enrichment analysis [such as Gene Ontology (GO) and Kyoto Encyclopedia of Genes and Genomes (KEGG) analysis] allows researcher to draw conclusions based on a group of related genes rather than a single gene, which

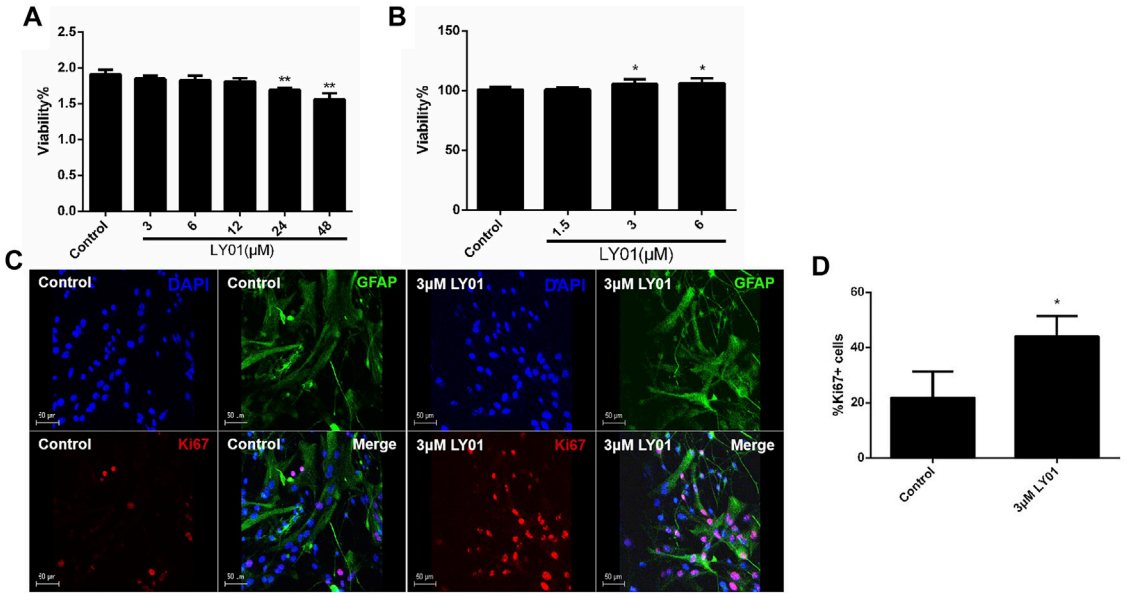

FIGURE 7 | Effects of LY01 on primary hippocampal neurons and primary astrocytes **(A)** Effect of LY01 on the viability of primary hippocampal neurons. Cell viability was detected using water-soluble tetrazolium 1 (WST1); $^{**}p < 0.01$ vs. Control; $n = 3$ **(B)** Effect of LY01 on the viability of primary astrocytes. Cell viability was detected by WST1; $^{*}p < 0.05$ vs. Control; $n = 3$ **(C)** Effect of LY01 on astrocyte proliferation. The nuclei are labeled with DAPI (blue), proliferating cells are labeled with Ki67 antibody (red), and neural stem cells (NSCs) are labeled with nestin antibody (green) **(D)** Proportion of cells labeled with both Ki67 and glial fibrillary acidic protein (GFAP) antibodies compared to total GFAP + cells. $^{**}p < 0.01$ vs. Control; $n = 3$. The results are expressed as means ± SD.

increases the reliability of the study and identifies the biological processes most related to the observed phenomena. GO and KEGG analysis were performed and stored using the online platform of Majorbio Cloud Platform (www.majorbio.com). According to the professional feedback provided by Meggie biological company, the sample quality met the requirements of accurate sequencing and the percentage of the Q30 base was more than 94.66%. A total of 37,464 transcripts were analyzed and detected, including 23,986 known transcripts and 13,478 new transcripts. Among them, 21,456 transcripts were annotated to the GO library, 16,477 transcripts were annotated to the KEGG library, and 237 differentially expressed genes were identified. There were significant differences between the two groups (**Supplementary Figure S4**). The larger the value of $-\log_{10}$ (false discovery rate), the more significant the functional enrichment. Both GO (**Figure 9C**) and KEGG (**Figure 9D**) annotation analysis indicated that the extracellular matrix (ECM) and associated receptors may participate in the mechanism of LY01. Lamc2, as a component of the ECM, had the most significant upregulation between the LY01-administered group and the control group (**Supplementary Figure S5**). In addition, functional enrichment analysis indicated that aging, glutathione metabolism, and other biological processes may also play an important role in the function of LY01. The data for this study have been deposited to the sequence read archive (SRA), and the accession number is PRJNA833033. (https://www.ncbi.nlm.nih.gov/sra/?term=PRJNA833033).

DISCUSSION

The nervous system is composed of many types of cells, among which neurons, astrocytes, and NSCs play important roles. Neurons integrate incoming information and send out information, effects directly related to human emotion, cognition, and memory changes. Astrocytes are the most widely distributed neural cells in mammals, and their functions include nutrition supply, protection, signal transmission, and inflammatory regulation. Neurotrophic factors secreted by astrocytes at injured sites play an important role in neuronal survival and regeneration. Our study showed that LY01 promotes the proliferation of astrocytes and primary NSCs *in vitro* and increased the number of new neurons in the dentate gyrus of the hippocampus *in vivo*. We speculate that LY01 may promote the proliferation, migration, and differentiation into functional neurons of NSCs in the dentate gyrus area of AD mice under the influence of the microenvironment at the lesion site and maintain the stability of the number of neurons in the hippocampus. Likewise, LY01 promotes the proliferation of hippocampal astrocytes (thus the secretion of more neurotrophic factors) and results in the nutrition supply and protection of neurons.

By analyzing the results of male and female mice after administration of LY01, we found that although LY01 has estrogen like structure, intravenous injection of LY01 will not cause obvious side effects on mice of both genders due to excessive estrogen, and both showed obvious effect of promoting neural regeneration. As natural plant products have fewer or no side effects and are easily available, their effect of AD

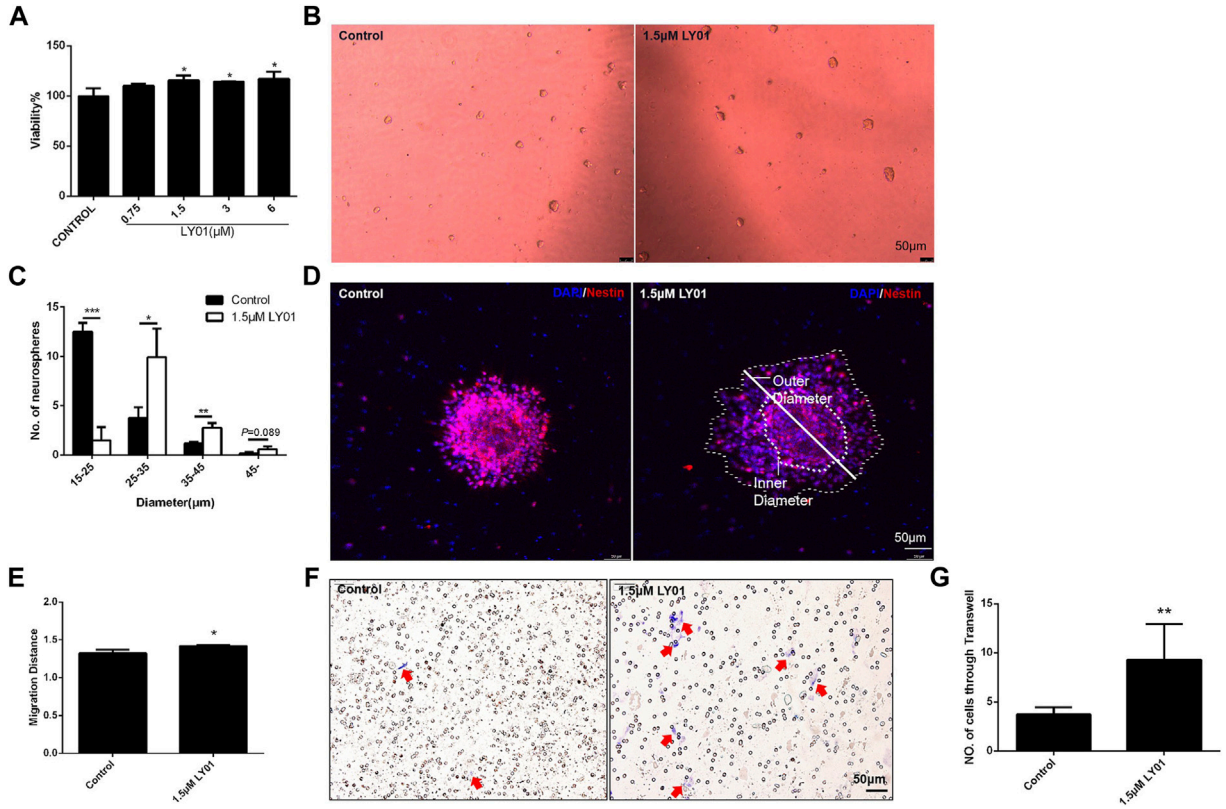

FIGURE 8 | Effects of LY01 on primary NSCs **(A)** Effect of LY01 on the viability of primary NSCs. Cell viability was detected using WST1; *$p < 0.05$ vs. Control; $n = 3$ **(B)** Neurospheres after LY01 treatment **(C)** Quantification of diameter and quantity of neurospheres after LY01 treatment. *$p < 0.05$, **$p < 0.01$, ***$p < 0.001$ vs. Control; $n = 3$ **(D)** Effect of LY01 on the migration of neurospheres. NSCs are labeled with nestin antibody (red) and the nuclei are labeled with DAPI (blue); the outer and inner diameters are indicated in figure **(E)** Quantification of migration distance of neurospheres. The migration distance is equal to the ratio of the outer diameter after migration to the diameter of the neurosphere (inner diameter). *$p < 0.05$ vs. Control **(F)** Representative images of Transwell migration assay experiments. The cells that migrated to the chamber below were stained blue with 0.1% crystal violet **(G)** Quantification of Transwell experimental results. *$p < 0.05$,**$p < 0.01$ vs. Control. The results are expressed as means ± SD.

treatment has been widely studied (Varshney and Siddique, 2021). But most of their mechanisms focus on neuroprotection, antioxidation, acetylcholinesterase inhibition and Aβ deposition reduction (Varshney and Siddique, 2021; Park et al., 2014). This study enriches the mechanism of natural products in the AD prevention or treatment. Meanwhile, most studies on the prevention or treatment of AD by promoting endogenous neural regeneration are about growth factors (Hassouna et al., 2016; Vasic et al., 2019), and a few of these studies have been conducted in AD animal models (Cevik et al., 2017). Among them, there are few studies on natural plant products. Therefore, this study will have great reference value for the exploration of natural products in the treatment of AD through neural regeneration mechanism in 5×FAD mice. In recent years, more researchers began to pay attention to the important role of neuron loss in AD, the results of this study support the hypothesis of prevention or treatment of AD by promoting endogenous hippocampal neural regeneration (Oakley et al., 2006; Eimer and Vassar, 2013). However, many therapies have failed in clinical trials (Cummings et al., 2019) in patients with established AD, suggesting that, once developed, disease-modifying agents may need to be deployed earlier in the course of illness (Hort et al., 2010; Grossberg et al., 2019). According to the results of this study, the strategy of treatment at a early stage of AD is feasible, which supports this assumption. However, there are some deficiencies, such as it is impossible to obtain the difference of drug response between male and female mice under the same administration conditions. But this problem can be a subject of follow-up research.

Transcriptome sequencing revealed that the proliferation and migration of astrocytes and NSCs promoted by LY01 may be related to the regulation of the ECM and associated receptors, such as Lamc2. The ECM includes insoluble structural components, such as collagen and glycoprotein, and proteinases and cytokines related to matrix metabolism (Wilems et al., 2019). Some studies have shown that laminin is the main type of glycoprotein in the ECM and can promote adhesion and regulate cell proliferation and migration to repair brain injury (Qian et al., 2018; Ma et al., 2020), consistent with the functional research results of this study. However, this study lacks direct experimental evidence on how ECM and associated receptors participate in LY01 induced neural regeneration.

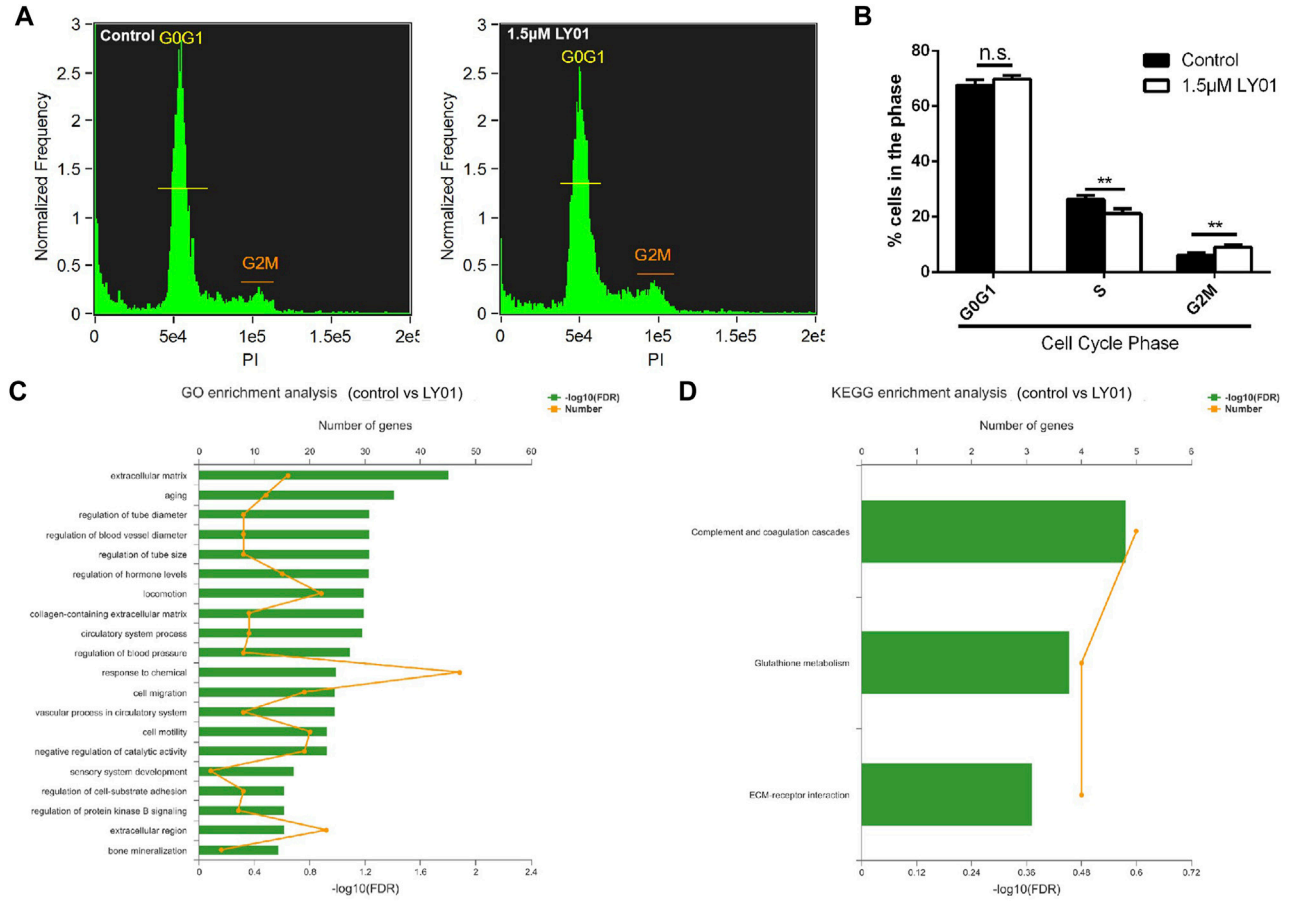

FIGURE 9 | Effects of LY01 on the cell cycle and transcription of primary NSCs **(A)** Cell cycle analysis of primary NSCs after LY01 treatment **(B)** Distribution of NSCs in each cycle. $^{**}p < 0.01$ vs. Control; $n = 3$ **(C)** Gene Ontology (GO) enrichment analysis **(D)** Kyoto Encyclopedia of Genes and Genomes (KEGG) enrichment analysis. Primary NSCs cultured *in vitro* were treated with 1.5 μm LY01 and the control group was treated with vehicle. After 6 h of treatment, Trizol was used to collect cells and the samples were sent for transcriptome sequencing and analysis. Three parallel samples were set in each group. The results are expressed as means ± SD.

And the up regulation of Lamc2 detected in this study has been reported to be related to the occurrence of a variety of cancers (Yamamoto et al., 2009; Zhang et al., 2018; Jing et al., 2020). Thus, whether LY01 has carcinogenicity and other side effects need to be further studied.

Because of the earlier administration of LY01 in this study's experimental design, some of the conventional behavioral indicators of cognitive and memory decline were not significant reflections of the effects of the drug. The behavioral test data collected from 5×FAD mice were highly variable and thus not conducive to reflect sensitively the effects of LY01. The positive control mice in Rg1 group also did not show significant cognitive and memory improvement in the behavioral tests. According to the current researches, the potential mechanisms, by which Rg1 significantly improved cognitive behavioral impairments in most Alzheimer's disease models, included antioxidant and anti-inflammatory effects, amelioration of Alzheimer's disease-related pathology, synapse protection, and up-regulation of nerve cells via multiple signaling pathways (Liang et al., 2021). However, considering Alzheimer's disease is a multi-mechanism disease, we speculate that the main mechanism regulated by Rg1 is not the essential mechanism causing dementia-like behaviors in the early stage of 5×FAD mice in this study. In addition, the results of BrdU and DCX staining indicated that for the 13-week-old 5×FAD mice, the number of new cells and the number and neurite length of neural precursor cells in the dentate gyrus area were significantly lower than those in WT mice, indicating that the abnormal neural regeneration ability and neural cell morphology may be the earlier pathological changes of AD.

The first clinical symptom of AD is the decline of short-term memory; the decline of neural regeneration in patients with AD affects the number and functional maintenance of neurons and subsequently affects the construction of new short-term memory loops in the neural network. Therefore, maintaining the number and vitality of regenerated neural cells in the brains of patients with AD is an important idea in the treatment of AD. There is no clinical drug for AD patients that targets the endogenous neural regeneration process. LY01 has shown to play a significant role in promoting endogenous neural regeneration, and thus is expected to fill this gap.

CONCLUSION

All these findings together demonstrated that LY01 could reduce the decline of cognition and memory in the early stage of 5×FAD mice by regulating the extracellular matrix and improving neuronal regeneration in the hippocampus. It induced the proliferation of astrocytes, the proliferation and migration of NSCs, and increased the number of new cells and neural precursor cells in the dentate gyrus area of 5×FAD mice. This phenomenon could be observed both in female and male 5×FAD mice after LY01 treatment for more than 2 weeks. And after 5-weeks LY01 treatment, the spatial and conditioned memory abilities were significantly improved in 5×FAD mice according to the results of the Morris water maze and fear conditioning test. The neuronal regeneration induced by LY01 was related to the regulation of the extracellular matrix, associated receptors, and the S phase of the cell cycle. LY01 promoted the regeneration of neuronal cells and alleviates the symptoms of AD in the early stage, which provided new ideas and alternative drugs for the AD prevention and treatment.

DATA AVAILABILITY STATEMENT

The datasets presented in this study can be found in online repositories. The names of the repository/repositories and accession number(s) can be found in the article/ **Supplementary Material**.

ETHICS STATEMENT

The animal study was reviewed and approved by the Animal Care and Use Committee of the Minzu University of China.

AUTHOR CONTRIBUTIONS

Conceptualization, Q-SL and YC; writing original draft preparation, X-WL, Y-YL, and S-YZ; writing review and editing, Q-SL, YC, and X-WL; visualization, N-NS, Y-YF; supervision, Q-SL and YC; project administration, Q-SL; funding acquisition, Q-SL and YC. All authors have read and agreed to the published version of the manuscrip.

FUNDING

This work was supported by the National Nature Science Foundation of China (grant no. 82174085, 82071676).

SUPPLEMENTARY MATERIAL

The Supplementary Material for this article can be found online at: https://www.frontiersin.org/articles/10.3389/fphar.2022.926123/full#supplementary-material

REFERENCES

Aboul-Soud, M. A. M., Alzahrani, A. J., and Mahmoud, A. (2021). Induced Pluripotent Stem Cells (iPSCs)-Roles in Regenerative Therapies, Disease Modelling and Drug Screening. *Cells* 10 (9), 2319. doi:10.3390/cells10092319

Alzheimer's Association (2020). 2020 Alzheimer's Disease Facts and Figures. *Alzheimers Dement.* 16, 391–460. doi:10.1002/alz.12068

Berchtold, N. C., and Cotman, C. W. (1998). Evolution in the Conceptualization of Dementia and Alzheimer's Disease: Greco-Roman Period to the 1960s. *Neurobiol. Aging* 19 (3), 173–189. doi:10.1016/s0197-4580(98)00052-9

Blennow, K., de Leon, M. J., and Zetterberg, H. (2006). Alzheimer's Disease. *Lancet* 368 (9533), 387–403. doi:10.1016/S0140-6736(06)69113-7

Bradley, P., Akehurst, R., Ballard, C., Banerjee, S., Blennow, K., Bremner, J., et al. (2015). Taking Stock: A Multistakeholder Perspective on Improving the Delivery of Care and the Development of Treatments for Alzheimer's Disease. *Alzheimers Dement.* 11 (4), 455–461. doi:10.1016/j.jalz.2014.01.007

Cevik, B., Solmaz, V., Yigitturk, G., Cavusoğlu, T., Peker, G., and Erbas, O. (2017). Neuroprotective Effects of Erythropoietin on Alzheimer's Dementia Model in Rats. *Adv. Clin. Exp. Med.* 26 (1), 23–29. doi:10.17219/acem/61044

Chen, F., Yin, X., Wang, Y., Lv, Y., Sheng, S., Ouyang, S., et al. (2020). Pharmacokinetics, Tissue Distribution, and Druggability Prediction of the Natural Anticancer Active Compound Cytisine N-Isoflavones Combined with Computer Simulation. *Biol. Pharm. Bull.* 43 (6), 976–984. doi:10.1248/bpb.b20-00004

Chen, X., Li, Z., Cheng, Y., Kardami, E., and Loh, Y. P. (2019). Low and High Molecular Weight FGF-2 Have Differential Effects on Astrocyte Proliferation, but Are Both Protective against Aβ-Induced Cytotoxicity. *Front. Mol. Neurosci.* 12, 328. doi:10.3389/fnmol.2019.00328

Cheng, Y., Rodriguiz, R. M., Murthy, S. R., Senatorov, V., Thouennon, E., Cawley, N. X., et al. (2015). Neurotrophic Factor-A1 Prevents Stress-Induced Depression through Enhancement of Neurogenesis and Is Activated by Rosiglitazone. *Mol. Psychiatry* 20 (6), 744–754. doi:10.1038/mp.2014.136

Cipriani, G., Dolciotti, C., Picchi, L., and Bonuccelli, U. (2011). Alzheimer and His Disease: a Brief History. *Neurol. Sci.* 32 (2), 275–279. doi:10.1007/s10072-010-0454-7

Cummings, J., Lee, G., Ritter, A., Sabbagh, M., and Zhong, K. (2019). Alzheimer's Disease Drug Development Pipeline: 2019. *Alzheimers Dement. (N Y)* 5, 272–293. doi:10.1016/j.trci.2019.05.008

de Oliveira, C. F., Moura, P. F., Rech, K. S., da Silva Paula de Oliveira, C., Hirota, B. C. K., de Oliveira, M., et al. (2019). Antagonistic Activity of Diplodia Pinea against Phytopathogenic Fungi. *Folia Microbiol. (Praha)* 64 (3), 415–419. doi:10.1007/s12223-018-00667-y

Dos Santos Picanco, L. C., Ozela, P. F., de Fatima de Brito Brito, M., Pinheiro, A. A., Padilha, E. C., Braga, F. S., et al. (2018). Alzheimer's Disease: A Review from the Pathophysiology to Diagnosis, New Perspectives for Pharmacological Treatment. *Curr. Med. Chem.* 25 (26), 3141–3159. doi:10.2174/0929867323666161213101126

Duan, X., Li, Y., Xu, F., and Ding, H. (2021). Study on the Neuroprotective Effects of Genistein on Alzheimer's Disease. *Brain Behav.* 11 (5), e02100. doi:10.1002/brb3.2100

Eimer, W. A., and Vassar, R. (2013). Neuron Loss in the 5XFAD Mouse Model of Alzheimer's Disease Correlates with Intraneuronal Aβ42 Accumulation and Caspase-3 Activation. *Mol. Neurodegener.* 8 (1), 2. doi:10.1186/1750-1326-8-2

Escande, A., Pillon, A., Servant, N., Cravedi, J. P., Larrea, F., Muhn, P., et al. (2006). Evaluation of Ligand Selectivity Using Reporter Cell Lines Stably Expressing Estrogen Receptor Alpha or Beta. *Biochem. Pharmacol.* 71 (10), 1459–1469. doi:10.1016/j.bcp.2006.02.002

Grossberg, G. T., Tong, G., Burke, A. D., and Tariot, P. N. (2019). Present Algorithms and Future Treatments for Alzheimer's Disease. *J. Alzheimers Dis.* 67 (4), 1157–1171. doi:10.3233/JAD-180903

Gu, L. H. (2015). *Age-related Myelin Changes in the 5XFAD Mouse Model*. Nanjing, China: Southeast University.

Harris, L., Rigo, P., Stiehl, T., Gaber, Z. B., Austin, S. H. L., Masdeu, M. D. M., et al. (2021). Coordinated Changes in Cellular Behavior Ensure the Lifelong Maintenance of the Hippocampal Stem Cell Population. *Cell Stem Cell* 28 (5), 863–876.e6. doi:10.1016/j.stem.2021.01.003

Hassouna, I., Ott, C., Wüstefeld, L., Offen, N., Neher, R. A., Mitkovski, M., et al. (2016). Revisiting Adult Neurogenesis and the Role of Erythropoietin for Neuronal and Oligodendroglial Differentiation in the hippocampus. *Mol. Psychiatry* 21 (12), 1752–1767. doi:10.1038/mp.2015.212

Hayashi, Y., Lin, H. T., Lee, C. C., and Tsai, K. J. (2020). Effects of Neural Stem Cell Transplantation in Alzheimer's Disease Models. *J. Biomed. Sci.* 27 (1), 29. doi:10.1186/s12929-020-0622-x

Hort, J., O'Brien, J. T., Gainotti, G., Pirttila, T., Popescu, B. O., Rektorova, I., et al. (2010). Efns Scientist Panel on DementiaEFNS Guidelines for the Diagnosis and Management of Alzheimer's Disease. *Eur. J. Neurol.* 17 (10), 1236–1248. doi:10.1111/j.1468-1331.2010.03040.x

Jawhar, S., Trawicka, A., Jenneckens, C., Bayer, T. A., and Wirths, O. (2012). Motor Deficits, Neuron Loss, and Reduced Anxiety Coinciding with Axonal Degeneration and Intraneuronal Aβ Aggregation in the 5XFAD Mouse Model of Alzheimer's Disease. *Neurobiol. Aging* 33 (1), 196 e29–40. doi:10.1016/j.neurobiolaging.2010.05.027

Jing, F., Ruan, X., Liu, X., Yang, C., Wang, D., Zheng, J., et al. (2020). The PABPC5/HCG15/ZNF331 Feedback Loop Regulates Vasculogenic Mimicry of Glioma via STAU1-Mediated mRNA Decay. *Mol. Ther. Oncolytics* 17, 216–231. doi:10.1016/j.omto.2020.03.017

Kent, B. A., and Mistlberger, R. E. (2017). Sleep and Hippocampal Neurogenesis: Implications for Alzheimer's Disease. *Front. Neuroendocrinol.* 45, 35–52. doi:10.1016/j.yfrne.2017.02.004

Li, C., He, J. Z., Zhou, X. D., and Xu, X. (2017). Berberine Regulates Type 2 Diabetes Mellitus Related with Insulin Resistance. *Zhongguo Zhong Yao Za Zhi* 42 (12), 2254–2260. doi:10.19540/j.cnki.cjcmm.20170307.014

Liang, H. Y., Zhang, P. P., Zhang, X. L., Zheng, Y. Y., Huang, Y. R., Zheng, G. Q., et al. (2021). Preclinical Systematic Review of Ginsenoside Rg1 for Cognitive Impairment in Alzheimer's Disease. *Aging (Albany NY)* 13 (5), 7549–7569. doi:10.18632/aging.202619

Liu, C., Ying, Z., Li, Z., Zhang, L., Li, X., Gong, W., et al. (2021). Danzhi Xiaoyao Powder Promotes Neuronal Regeneration by Downregulating Notch Signaling Pathway in the Treatment of Generalized Anxiety Disorder. *Front. Pharmacol.* 12, 772576. doi:10.3389/fphar.2021.772576

Livingston, G., Sommerlad, A., Orgeta, V., Costafreda, S. G., Huntley, J., Ames, D., et al. (2017). Dementia Prevention, Intervention, and Care. *Lancet* 390 (10113), 2673–2734. doi:10.1016/S0140-6736(17)31363-6

Ma, R., Wang, M., Gao, S., Zhu, L., Yu, L., Hu, D., et al. (2020). miR-29a Promotes the Neurite Outgrowth of Rat Neural Stem Cells by Targeting Extracellular Matrix to Repair Brain Injury. *Stem Cells Dev.* 29 (9), 599–614. doi:10.1089/scd.2019.0174

Manayi, A., Nabavi, S. M., Setzer, W. N., and Jafari, S. (2018). Piperine as a Potential Anti-cancer Agent: A Review on Preclinical Studies. *Curr. Med. Chem.* 25 (37), 4918–4928. doi:10.2174/0929867324666170523120656

Massirer, K. B., Carromeu, C., Griesi-Oliveira, K., and Muotri, A. R. (2011). Maintenance and Differentiation of Neural Stem Cells. *Wiley Interdiscip. Rev. Syst. Biol. Med.* 3 (1), 107–114. doi:10.1002/wsbm.100

Mazewski, C., Liang, K., and Gonzalez de Mejia, E. (2018). Comparison of the Effect of Chemical Composition of Anthocyanin-Rich Plant Extracts on Colon Cancer Cell Proliferation and Their Potential Mechanism of Action Using *In Vitro*, In Silico, and Biochemical Assays. *Food Chem.* 242, 378–388. doi:10.1016/j.foodchem.2017.09.086

Moreno-Jiménez, E. P., Flor-García, M., Terreros-Roncal, J., Rábano, A., Cafini, F., Pallas-Bazarra, N., et al. (2019). Adult Hippocampal Neurogenesis Is Abundant in Neurologically Healthy Subjects and Drops Sharply in Patients with Alzheimer's Disease. *Nat. Med.* 25 (4), 554–560. doi:10.1038/s41591-019-0375-9

Nakagawa, S., and Cuthill, I. C. (2007). Effect Size, Confidence Interval and Statistical Significance: a Practical Guide for Biologists. *Biol. Rev. Camb Philos. Soc.* 82 (4), 591–605. doi:10.1111/j.1469-185X.2007.00027.x

Oakley, H., Cole, S. L., Logan, S., Maus, E., Shao, P., Craft, J., et al. (2006). Intraneuronal Beta-Amyloid Aggregates, Neurodegeneration, and Neuron Loss in Transgenic Mice with Five Familial Alzheimer's Disease Mutations: Potential Factors in Amyloid Plaque Formation. *J. Neurosci.* 26 (40), 10129–10140. doi:10.1523/JNEUROSCI.1202-06.2006

Pan, R. Y., Ma, J., Wu, H. T., Liu, Q. S., Qin, X. Y., and Cheng, Y. (2017). Neuroprotective Effects of a Coeloglossum Viride Var. Bracteatum Extract *In Vitro* and *In Vivo*. *Sci. Rep.* 7 (1), 9209. doi:10.1038/s41598-017-08957-0

Park, H., Yoo, J. S., Kim, J. Y., Hwang, B. Y., Han, J. S., Yeon, S. W., et al. (2014). Anti-amyloidogenic Effects of ID1201, the Ethanolic Extract of the Fruits of Melia Toosendan, through Activation of the Phosphatidylinositol 3-kinase/Akt Pathway. *Environ. Toxicol. Pharmacol.* 37 (2), 513–520. doi:10.1016/j.etap.2014.01.008

Popovic, D., Kocic, G., Katic, V., Zarubica, A., Velickovic, L. J., Nickovic, V. P., et al. (2019). Anthocyanins Protect Hepatocytes against CCl4-Induced Acute Liver Injury in Rats by Inhibiting Pro-inflammatory Mediators, Polyamine Catabolism, Lipocalin-2, and Excessive Proliferation of Kupffer Cells. *Antioxidants (Basel)* 8 (10), 451. doi:10.3390/antiox8100451

Qian, J., Zhao, X., Wang, W., Zhang, S., Hong, Z., Chen, X., et al. (2018). Transcriptomic Study Reveals Recovery of Impaired Astrocytes Contribute to Neuroprotective Effects of Danhong Injection against Cerebral Ischemia/Reperfusion-Induced Injury. *Front. Pharmacol.* 9, 250. doi:10.3389/fphar.2018.00250

Ren, Y., Yu, G., Shi, C. P., Liu, L. M., Guo, Q., Han, C., et al. (2022). Majorbio Cloud: A One-Stop, Comprehensive Bioinformatic Platform for Multiomics Analyses. *IMeta* 1, e12. doi:10.1002/imt2.12

Rigotti, N. A. (2014). Cytisine--a Tobacco Treatment Hiding in Plain Sight. *N. Engl. J. Med.* 371 (25), 2429–2430. doi:10.1056/NEJMe1412313

Scheltens, P., De Strooper, B., Kivipelto, M., Holstege, H., Chételat, G., Teunissen, C. E., et al. (2021). Alzheimer's Disease. *Lancet* 397 (10284), 1577–1590. doi:10.1016/S0140-6736(20)32205-4

Shoaib, M., Shah, S. W. A., Ali, N., Umar, N., Shah, I., Shafiullah, et al. (2019). A Possible Mechanistic Approach of Synthetic Flavonoids in the Management of Pain. *Pak J. Pharm. Sci.* 32 (3), 911–917.

Singh, J. V., Kaur, A., Bhagat, K., Gupta, M. K., Singh, M., Singh, H., et al. (2018). 5,6-Benzoflavones as Cholesterol Esterase Inhibitors: Synthesis, Biological Evaluation and Docking Studies. *Medchemcomm* 9 (3), 490–502. doi:10.1039/c7md00565b

Varghese, F. S., Thaa, B., Amrun, S. N., Simarmata, D., Rausalu, K., Nyman, T. A., et al. (2016). The Antiviral Alkaloid Berberine Reduces Chikungunya Virus-Induced Mitogen-Activated Protein Kinase Signaling. *J. Virol.* 90 (21), 9743–9757. doi:10.1128/JVI.01382-16

Varshney, H., and Siddique, Y. H. (2021). Role of Natural Plant Products against Alzheimer's Disease. *CNS Neurol. Disord. Drug Targets* 20 (10), 904–941. doi:10.2174/1871527320666210420135437

Vasic, V., Barth, K., and Schmidt, M. H. H. (2019). Neurodegeneration and Neuro-Regeneration-Alzheimer's Disease and Stem Cell Therapy. *Int. J. Mol. Sci.* 20 (17), 4272. doi:10.3390/ijms20174272

Wareham, L. K., Liddelow, S. A., Temple, S., Benowitz, L. I., Di Polo, A., Wellington, C., et al. (2022). Solving Neurodegeneration: Common Mechanisms and Strategies for New Treatments. *Mol. Neurodegener.* 17 (1), 23. doi:10.1186/s13024-022-00524-0

Wei, Z. X., Xie, G. J., Mao, X., Zou, X. P., Liao, Y. J., Liu, Q. S., et al. (2020). Exosomes from Patients with Major Depression Cause Depressive-like Behaviors in Mice with Involvement of miR-139-5p-Regulated Neurogenesis. *Neuropsychopharmacology* 45 (6), 1050–1058. doi:10.1038/s41386-020-0622-2

Wilems, T., Vardhan, S., Wu, S., and Sakiyama-Elbert, S. (2019). The Influence of Microenvironment and Extracellular Matrix Molecules in Driving Neural Stem Cell Fate within Biomaterials. *Brain Res. Bull.* 148, 25–33. doi:10.1016/j.brainresbull.2019.03.004

Yamamoto, H., Kitadai, Y., Yamamoto, H., Oue, N., Ohdan, H., Yasui, W., et al. (2009). Laminin Gamma2 Mediates Wnt5a-Induced Invasion of Gastric Cancer Cells. *Gastroenterology* 137 (1), 242–252. 252 e1-6. doi:10.1053/j.gastro.2009.02.003

Yin, X. Y., and Liu, Q. S. (2016). Compound Having Neuron Protection Function as Well as Preparation Method and Application of Compound.

CN106046001A. Available at: http://pss-system.cnipa.gov.cn/sipopublicsearch/patentsearch/showViewList-jumpToView.shtml

Zhang, Y., Zoltan, M., Riquelme, E., Xu, H., Sahin, I., Castro-Pando, S., et al. (2018). Immune Cell Production of Interleukin 17 Induces Stem Cell Features of Pancreatic Intraepithelial Neoplasia Cells. *Gastroenterology* 155 (1), 210–223.e3. doi:10.1053/j.gastro.2018.03.041

Zilka, N., and Novak, M. (2006). The Tangled Story of Alois Alzheimer. *Bratisl. Lek. Listy* 107 (9-10), 343–345.

Conflict of Interest: The authors declare that the research was conducted in the absence of any commercial or financial relationships that could be construed as a potential conflict of interest.

Publisher's Note: All claims expressed in this article are solely those of the authors and do not necessarily represent those of their affiliated organizations, or those of the publisher, the editors and the reviewers. Any product that may be evaluated in this article, or claim that may be made by its manufacturer, is not guaranteed or endorsed by the publisher.

frontiers | Frontiers in Pharmacology

ORIGINAL RESEARCH
published: 23 June 2022
doi: 10.3389/fphar.2022.897436

Xiaoyaosan Ameliorates Chronic Restraint Stress-Induced Depression-Like Phenotype by Suppressing A2AR Signaling in the Rat Striatum

Xiaoxu Zhu[1,2†], Qingyu Ma[1†], Furong Yang[3], Xiaojuan Li[1], Yueyun Liu[4], Jianbei Chen[4], Lan Li[2], Man Chen[2], Xiaojuan Zou[2], Li Yan[1] and Jiaxu Chen[1,4]**

[1]Guangzhou Key Laboratory of Formula-Pattern of Traditional Chinese Medicine, Formula-Pattern Research Center, School of Traditional Chinese Medicine, Jinan University, Guangzhou, China, [2]School of Basic Medical Sciences, Hubei University of Chinese Medicine, Wuhan, China, [3]Medical School, Hubei Minzu University, Enshi, China, [4]School of Traditional Chinese Medicine, Beijing University of Chinese Medicine, Beijing, China

OPEN ACCESS

Edited by:
Yong Cheng,
Minzu University of China, China

Reviewed by:
Xuemei Qin,
Shanxi University, China
Evandro Fei Fang,
University of Oslo, Norway
Rongjuan Guo,
Dongfang Hospital, China

***Correspondence:**
Li Yan
liyan@jnu.edu.cn
Jiaxu Chen
chenjiaxu@hotmail.com

†These authors have contributed equally to this work and share first authorship

Specialty section:
This article was submitted to Neuropharmacology, a section of the journal Frontiers in Pharmacology

Received: 16 March 2022
Accepted: 23 May 2022
Published: 23 June 2022

Citation:
Zhu X, Ma Q, Yang F, Li X, Liu Y, Chen J, Li L, Chen M, Zou X, Yan L and Chen J (2022) Xiaoyaosan Ameliorates Chronic Restraint Stress-Induced Depression-Like Phenotype by Suppressing A2AR Signaling in the Rat Striatum. Front. Pharmacol. 13:897436. doi: 10.3389/fphar.2022.897436

Depression is a common mental disorder characterized by pessimism and world-weariness. In our previous study, we found that Xiaoyaosan (XYS) could have antidepressive effects, however the underlying mechanisms remain unclear. Several studies have shown that adenosine A (2 A) receptor (A2AR) in the brain is a key point in the treatment of depression. Our present study aimed to investigate the effects of XYS on A2AR signaling in the striatum of rats exposed to chronic restraint stress (CRS). Ninety-six male Sprague–Dawley rats were randomly divided into 8 groups (control, model, negative control, XYS, A2AR antagonist, A2AR antagonist + XYS, A2AR agonist, A2AR agonist + XYS). The rats in the model group, XYS group, A2AR antagonist group and A2AR antagonist + XYS group were subjected to CRS for 3 h a day. The XYS decoction [2.224 g/(kg·d)] was intragastrical administered by oral gavage to the rats in the negative control group, XYS group, A2AR antagonist + XYS group, and A2AR agonist + XYS group. The rats in the A2AR antagonist group and A2AR antagonist + XYS group were treated with SCH 58261 [0.05 mg/(kg·d)], and the rats in the A2AR agonist and A2AR agonist + XYS group were treated with CGS 21680 [0.1 mg/(kg·d)]. These procedures were performed for 21 consecutive days. Behavioral studies including the open field test, elevated plus maze test, sucrose preference test and forced swimming test, were performed to examine depression-like phenotypes. Then, the effects of XYS on CRS- or A2AR agonist-induced striatal subcellular damage, microglial activation and A2AR signaling changes in the striatum were examined. Here, we report that XYS ameliorates depression-like phenotypes (such as body weight loss as well as depression- and anxiety-like behaviors) and improves synaptic survival and growth in the stratum of the

Abbreviations: CRS, chronic restraint stress; XYS, Xiaoyaosan; AR, adenosine receptor; A1R, adenosine A1 receptor; A2AR, adenosine A2A receptor; MEK, mitogen-activated protein kinase kinase; ERK, extracellular signal-regulated kinase; NF-κB, nuclear factor-κB; OFT, open field test; EPMT, elevated plus maze test; SPT, sucrose preference test; FST, forced swimming test; ATP, adenosine triphosphate; ATPase, adenosine triphosphatase; Glu, glutamic acid; WB, Western blot; BDNF, brain-derived neurotrophic factor; IBA-1, ionized calcium-binding protein-1; Arg-1, arginase-1; iNOS, inducible nitric oxide synthase; TNF-α, tumor necrosis factor-α; PSD, post-synaptic density.

CRS rats. Moreover, XYS reduces A2AR activity and suppresses hyper-activation of striatal microglia. The tissue and cellular effects of XYS were similar to those of the known A2AR antagonists. In conclusion, XYS alleviates depression in the CRS rats via inhibiting A2AR in the striatum.

Keywords: xiaoyaosan, depression, chronic restraint stress, adenosine receptor, microglia activation

INTRODUCTION

Depression is a common mental disorder characterized by depressed mood, loss of interest or happiness, a sense of guilt or self-negation, pessimism, poor sleep or appetite, fatigue, and inattention (Dubovsky et al., 2021). Approximately 350 million people of various ages suffer from depression worldwide (Summergrad, 2016). Patients with major depressive disorder show symptoms such as hallucinations, delusions and suicide attempts, which seriously limit their psychosocial function and reduce the quality of life of patients and their families (McCarron et al., 2021). Some studies indicated that chronic stress and psychological trauma leaded to nerve injure could induce depression (Williams et al., 2020).

Microglia are the resident immune cells of the brain. It has the function of immune surveillance in the central nervous system and can promote neural network pruning, regulate neural plasticity, and maintain and promote the smooth flow of neural pathways. Currently, microglia are gradually regarded as targets for the treatment of neurological and mental diseases (Biber et al., 2016). When neuromicroenvironmental changes are caused by local nerve injury (during neurodegenerative diseases) or social circumstance stress (stress) in the central nervous system, microglia can convert phenotypes. This process is called "microglia activation" (Dubbelaar et al., 2018). Microglia can be activated as immune-stimulatory (M1) or immunosuppressive (M2) phenotypes. There is ample evidence that microglial activation is involved in some mental disorders including depression (Dheen et al., 2007; Santiago et al., 2017). Therefore, depression can be caused by microglial lesion (Yirmiya et al., 2015).

As a metabolite of adenosine triphosphate (ATP) production, adenosine is an endogenous neuroprotective agent and neuro-regulator (Borroto-Escuela et al., 2018). The function of adenosine is mainly mediated by the adenosine receptor (AR). AR is very important for emotion regulation and is the main candidate target for regulating cognitive processes, enhancing sleep intention, and improving severe depression (Lazarus et al., 2019). AR directly regulates intrasynaptic information transmission and plasticity, which in turn affects various emotions, cognition, motor activity, neuroinflammation and cell death (Ohta and Sitkovsky, 2001). AR primarily includes the A1, A2A, A2B, and A3 receptors (A1R, A2AR, A2BR, and A3R). The main ARs involved in the regulation of neuroinflammation are adenosine A1 receptor (A1R) and adenosine A2A receptor (A2AR) (Peleli et al., 2017). At low concentrations, adenosine mainly activates A1R. Conversely, a high concentration of adenosine activates A2AR. A2AR can block heteromeric A1R through receptor–receptor allosteric trans-inhibition (Martí Navia et al., 2020). Caffeine, an A2AR antagonist, can effectively inhibit the activation of microglia, reduce neuroinflammation and exert an antidepressant effect through the A2AR/mitogen-activated protein kinase kinase (MEK)/extracellular signal-regulated kinase (ERK)/nuclear factor-κB (NF-κB) signaling pathway (Kaster et al., 2015; Mao et al., 2020).

The striatum is the origin of the basal ganglia and is the largest nucleus in it, where numerous A2AR heteroreceptor complexes are present. Some scholars believe that striatal morphology may be a biomarker of neurodegenerative diseases, or it may be the basis of internal phenotypes (Looi and Walterfang, 2013). Clinical studies have found that striatal abnormalities play a role in emotional and cognitive changes associated with severe depression (Furuyashiki and Deguchi, 2012). Experimental studies have found that chronic stress can cause behavioral changes, which is consistent with the morphological changes of the striatum subregion. Depression and other emotions are related to the abnormal activity of striatal neurons (Admon et al., 2017).

Xiaoyaosan (XYS) is one of the classic prescriptions for the treatment of mental disorders in traditional Chinese medicine. The experimental studies found that XYS has a significant antidepressant effect in the aspects of behavior, biochemistry, neurochemistry, intestinal microorganisms, gene expression profile and so on (Li et al., 2019; Ma et al., 2019). There are 121 bioactive compounds in XYS, which are related to 99 depression-related targets and participate in immune and inflammatory responses closely related to depression. UPLC-Q-TOF/MS analysis successfully identified all the key compounds of XYS as paeoniflorin, quercetin, luteolin, farnesin, aloe emodin, glyasperin C, and kaempferol, and the main compounds were flavonoids (Yuan et al., 2020). Our previous studies have found that XYS can improve depression-like behavior induced by chronic restraint stress (CRS) or chronic unpredictable mild stress, and its mechanism may include reducing the neuroinflammatory response (reduce IL-6, IL-1, NF-κB, TNF-α) (Zhu et al., 2021) and decreasing the level of glutamic acid (Glu) in the rat hippocampus (Zhou et al., 2021). In this study, we aimed to further explore whether the antidepressant effects of XYS are associated with A2AR signaling in the striatum.

METHODS AND MATERIALS

Animals and Grouping

Ninety-six 8-week-old male Sprague–Dawley rats, weighing approximately 180–200 g, were purchased from Beijing

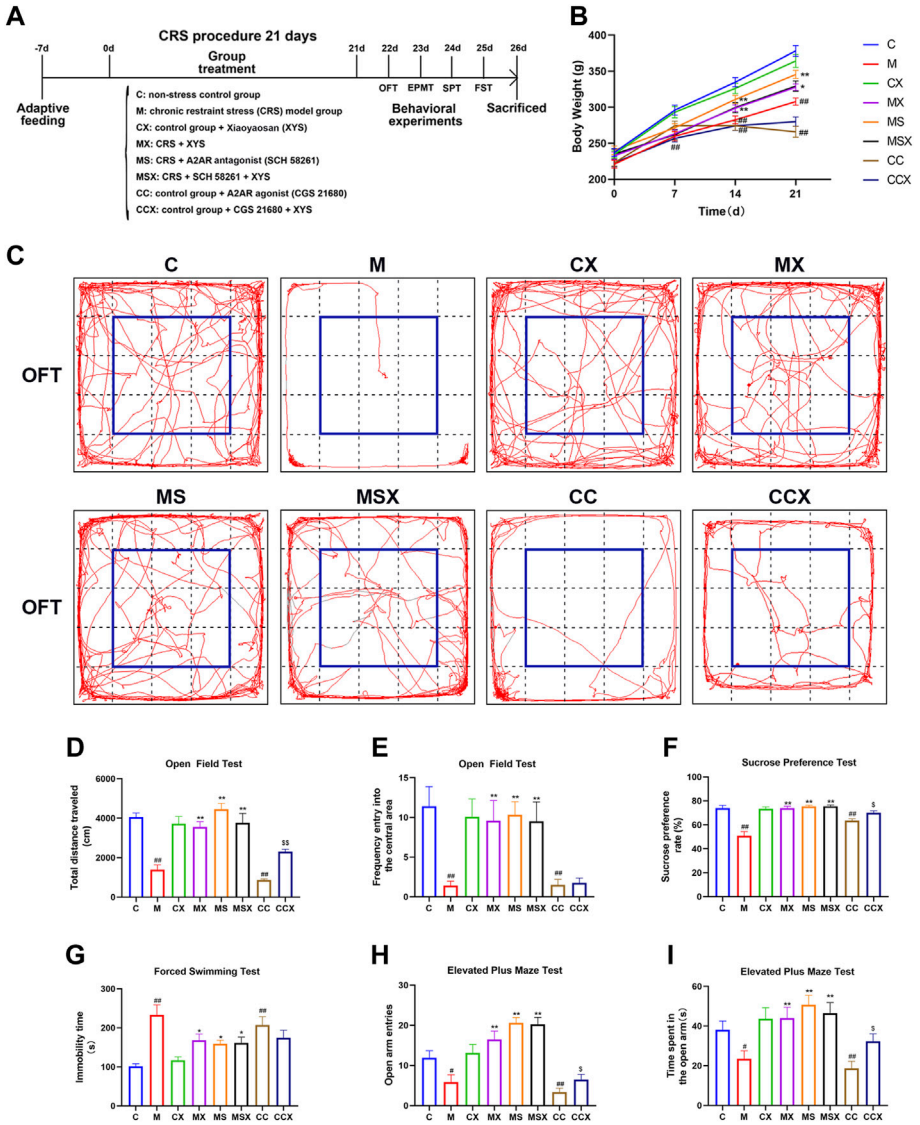

FIGURE 1 | Effects of XYS on depression-like phenotypes. **(A)** Experimental flow chart. During the course of the experiment, the body weight of the rats was weighed and recorded every 7 days, and behavioral tests were performed on the rats in each group at the end of the experiment, including the OFT, EPMT, SPT, and FST. **(B)** Changes in body weight. **(C)** The representative trajectory map of rats in the OFT. **(D)** The total distance traveled in the OFT. **(E)** The frequency of entry into the central area in the OFT. **(F)** The sucrose preference rate in the SPT. **(G)** The immobility time in the FST. **(H)** The open arm entries in the EPMT. **(I)** The time spent in the open arm in the EPMT. Values are presented as the means ± SEM with 12 rats in each group. $^{\#}p < 0.05$ or $^{\#\#}p < 0.01$ versus the C group; $^{*}p < 0.05$ or $^{**}p < 0.01$ versus the M group; $^{\$}p < 0.05$ or $^{\$\$}p < 0.01$ versus the CC group. XYS, Xiaoyaosan; OFT, open field test; EPMT, elevated plus maze test; SPT, sucrose preference test; FST, forced swimming test.

Weitong Lihua Biotechnology Co., Ltd., Beijing. The rats were housed with 4 rats in plastic cages in SPF animal rooms: room temperature (25 ± 1)°C, relative humidity 30–40%, light and dark for 12 h (light 7:00:19:00, dark 19:00), free access to distilled water, and a regular rodent diet.

After 1 week of adaptive feeding, the rats were randomly divided into 8 groups: 1) control group (C, nonstress); 2) model group (M, CRS); 3) negative control group (CX, XYS); 4) XYS group (MX, CRS + XYS); 5) A2AR antagonist group (MS, CRS + SCH 58261); 6) A2AR antagonist + XYS group (MSX, CRS + SCH 58261 + XYS); 7) A2AR agonist group (CC, CGS 21680); and 8) A2AR agonist + XYS group (CCX, CGS 21680 + XYS). See **Figure 1A** for the flow chart of the experiment. In the whole process of the animal experiment, the welfare and ethical guidelines for experimental animals issued by the Animal Experimental Ethics Committee of Jinan University were strictly implemented, and the suffering of experimental animals was minimized.

Chronic Restraint Stress Procedure

The rats were subjected to CRS as previously described (Zhu et al., 2019). The rats in the M group, MX group, MS group and MSX

group were fixed to a special restraint rack for 3 h a day for 21 consecutive days. The rats in the other groups were freely dispersed in their respective feeding boxes, gently handled for 2–4 min, and returned back to the holding room, about 3 h later for 21 consecutive days.

Xiaoyaosan Preparation and Drug Intervention

XYS powder was purchased from Jiuzhitang Group Co., Ltd.; the previously published literature (Hao et al., 2021) investigated the quality control of XYS using UPLC-Q-TOF/MS with the same formulation, batch number: 20190724. According to a previous study (Zhu et al., 2021), the XYS suspension (mixed with distilled water) was intragastrical administered by oral gavage to the rats in the CX group, MX group, MSX group, and CCX group at a dosage of 2.224 g/kg·d at 10 ml/kg body weight. The dosage was calculated according to the average body weight of an adult (60 kg/d). The rats in the other groups received 10 ml/kg distilled water by gavage. This procedure was performed 30 min before daily restraint stress and was performed for 21 consecutive days.

The A2AR antagonist SCH 58261 (M7282-01, Abmole, America) and A2AR agonist CGS 21680 (M2282-02, Abmole, America) were prepared with normal saline (NS, 0.9%) and injected intraperitoneally according to a body weight of 3 ml/kg. After 1 week of adaptation, the rats in the MS group and MSX group were treated with the A2AR antagonist SCH 58261, and the rats in the CC group and CCX group were treated with the A2AR agonist CGS 21680. The dosages were 0.05 mg/kg·d and 0.1 mg/kg·d, respectively (Pan and Chen, 2007; Costenla et al., 2011; Kaster et al., 2015; Huang et al., 2018). The rats in the other groups were given the same amount of 0.9% NS. This procedure was performed 30 min after daily restraint stress for 21 consecutive days.

Behavioral Testing

Behavioral tests, including the open field test (OFT), elevated plus maze test (EPMT), sucrose preference test (SPT) and forced swimming test (FST) were performed. The behavioral tests were recorded by a camera, and the data were analyzed with a small animal behavior trajectory tracking and analysis system (NOLDUS EthoVision XT, Netherlands).

Open Field Test

Rats were introduced to an open-field apparatus (100 × 100 × 40 cm) with a black background. The rats were placed in the middle of the box, and allowed rats to explore for 10 min. Their behavior was monitored by using a camera. The frequency of entry into the central square (60 × 60 cm) and total distance were calculated automatically (Schulz, 2018).

Elevated Plus Maze Test

The EPMT apparatus consists of two open arms and two closed arms. Rats were placed in the central square and introduced into to the western arms to move freely for 5 min. The number of times the rats entered the open arm (two foreclaws must enter the arm) and the total time spent in the open arm within 5 min were calculated automatically by the software (Li et al., 2017).

Sucrose Preference Test

Prior to the test, rats were housed in cages and trained to drink 1% sucrose solution for 24 h. Subsequently, rats were deprived of both food and water for the next 24 h. After that, the rats were tested in a single cage, and each cage was placed with a bottle of sucrose solution and a bottle of regular water. Rats were allowed to drink freely in 1 h, and each bottle was weighed before and after the test. The sucrose preference of the rats was calculated by the equation: sucrose preference (%) = [sucrose solution intake (g)/(sucrose solution intake (g) + regular water intake (g)] × 100% (Li et al., 2020).

Forced Swimming Test

The rats were placed into plastic cylinder (50 cm deep, 20 cm in diameter) filled with water at 23–25°C up to a height of 30 cm from the base, and forced to swim for 6 min. The time of immobility behaviors (rat floating on the surface of the water, immobility of limbs, or slight body wiggling to maintain its balance) was calculated in the last 4 min (Ma et al., 2021).

Detection of the Levels of Adenosine Triphosphate and Glutamic Acid in Striatum

On the 26th day, all rats were anesthetized with an intraperitoneal injection of pentobarbital sodium (100 mg/kg), and the brain tissues were collected. The levels of ATP and Glu in the striatum were determined using commercial ELISA kits (ATP, Solarbio, Beijing, China; Glu, Nanjing Jiancheng Bioengineering Institute, Nanjing, China) according to the manufacturer's instructions.

Immunohistochemical Staining of Striatum

The rat brain specimens were fixed with 4% paraformaldehyde overnight, sectioned into 3-μm-thick paraffin sections. Before staining, the sections underwent dewaxing hydration and antigen retrieval. Soon after, the sections were blocked with 5% BSA for 1 h at room temperature. The primary antibodies (anti-rabbit IBA-1, ab178847, Abcam, United States, 1:8,000; anti-mouse A2AR, ab79714, Abcam, United States, 1:200) were used for incubation of sections overnight at 4°C. The sections were then incubated with secondary antibodies (donkey anti-rabbit IgG H&L, ab150073, Abcam, United States, 1:500; goat anti-mouse IgG H&L, E032410-01, EarthOx Life Sciences, United States, 1:500) for 1 h at room temperature. Finally, anti-fluorescence quenching agent with 4′-6-diamidino-2-phenylindole (DAPI) (#P0131; Beyotime, Shanghai, China) was used for mounting the sections. The stained sections were observed and the images were acquired by Axio Vert.A1 inverted microscope (Zeiss, Jena, Germany). The images were analyzed by measuring the mean optical density of the fluorescence with ImageJ software (NIH, United States) and normalized by the area.

Golgi Staining

Golgi staining was performed by using a Hito Golgi-Cox OptimStainTM kit (Hito Biotec, Beijing, China). The right

brain of rats were dissected out and placed in the impregnate solution, where they were stored in the dark for 24 h and were replaced with the same solution. After being stored for 2 weeks at room temperature in the dark, brains were transferred into solution-3, kept at 4 °C in the dark, replaced with solution-3 after 12 h, and stored at 4°C for 24 h. The coronal section of the brain tissue was cut into 160-μm-thick sections with a Leica vibrating microtome (VT1000S, Germany). The slices were then affixed to gelatin-coated slides, dried in the dark at room temperature for 12 h, stained with Solution-4 and Solution-5 according to the instructions, and sealed with neutral resin. The spine morphology was analyzed by Olympus laser scanning confocal microscope (FV3000, Japan). Spine densities were analyzed by cellSensDimension software. According to the classical classification of protruding morphology, dendritic spines are categorized into thin, mushroom, and stubby spines (Qiao et al., 2016). Spines are thin if the length is greater than the neck diameter and the diameters of the head and neck are similar. Spines are classified as mushrooms if the diameter of the head is greater than the diameter of the neck. Spines are considered stubby if the length and width are equal.

Transmission Electron Microscopy Analysis

The specimens were removed from the striatum of the rat brains, which conformed to stereotaxic coordinates of interaural 10.20 mm and bregma 1.20 mm, fixed with fixative for TEM (G1102, Servicebio, Wuhan, China) and 1% OsO4 (Ted Pella Inc. CA, United States), then sectionalized to 100 nm, and finally dual stained with uranium acetate-lead citrate. Transmission electron microscopy (Hitachi, Tokyo, Japan) was used for observation of sealed sections as described previously (Peter et al., 2020). The observation focused on the sections of the microstructural alterations of the synaptic ultrastructure in the rat striatum. Excitatory asymmetric synapses were selected according to their typical structural organization, including the presynaptic terminal characterized by the presence of numerous synaptic vesicles, the synaptic cleft and a fuzzy electron-dense thickening of the post-synaptic membrane defining the post-synaptic density (PSD). PSD length and width were quantified using the ImageJ software (NIH, United States).

Western Blotting Analysis

The expression of Na-K ATPase, A2AR, brain-derived neurotrophic factor (BDNF), Arg-1, iNOS, ERK and NF-κB p65 in the striatum was detected by WB analysis. Total striatal proteins were extracted using a total protein extraction kit (KTP300, Abbkine, China). Membrane proteins were extracted using a membrane protein extraction kit (P0033, Beyotime, China). Nuclear proteins were extracted using a nuclear protein and cytoplasm protein extraction kit (P0027, Beyotime, China). The total proteins were used for the detection of Na-K ATPase, BDNF, Arg-1, iNOS, and ERK, the membrane proteins were used for the detection of A2AR, while the nuclear proteins were used for the detection of NF-κB p65. The protein concentration was determined by a NanoDrop One (Thermo Scientific, United States). Then, an equal amount of protein (20 μg) from each sample was separated on 8% or 10% SDS–PAGE gels and transferred to polyvinylidene fluoride (PVDF) membranes. After transformation, the blot was placed into 5% defatted milk for 1–2 h at room temperature and then incubated with primary antibodies (anti-rabbit Na-K ATPase, #3010S, CST, United States, 1:1,000; anti-mouse A2AR, ab79714, Abcam, United States, 1:1,000; anti-rabbit BDNF, ab108319, Abcam, United States, 1:1,000; anti-rabbit Arg-1, #93668, CST, United States, 1:1,000; anti-mouse iNOS, SC-7271, Santa Cruz, United States, 1:500; anti-rabbit ERK1+ERK2, ab184699, Abcam, United States, 1:50,000; anti-rabbit phospho-ERK1+ERK2, #4370, CST, United States, 1:2,000; anti-rabbit NF-κB p65, GB11997, Servicebio, Wuhan, China, 1:500; anti-rabbit β-tubulin, #86298, CST, United States, 1:50,000; and anti-rabbit GAPDH, #5174, CST, United States, 1:1,000) overnight at 4°C, with β-tubulin and GAPDH as internal controls. The membrane was then incubated with a suitable secondary antibody for rabbits or mice for 1 h. Finally, the bands were observed with enhanced chemiluminescence reagent (Biorigin, Beijing, China), and the protein signals were analyzed by a ChemiDoc™ Imaging system (Bio–Rad, United States).

Statistical Analysis

All the data in this study are expressed as the mean ± standard error of the mean (SEM). SPSS 25.0 software (Chicago, IL, United States) was used to perform these statistical analyses. The normality and variance uniformity of the experimental data were tested first, then repeated analysis of variance (ANOVA) was performed for the repeated measurement data, and one-way analysis of variance was used for the rest of the data. The least significant difference method was used for comparison. If the data were not normally distributed or the variance was not uniform, a nonparametric test with K independent samples was used. $p < 0.05$ was considered statistically significant. GraphPad Prism 8.0 Software (GraphPad Software Inc., San Diego, CA, United States) was used to perform plotting operations.

RESULTS

Effects of Xiaoyaosan on Depression-Like Phenotype

To evaluate the effects of XYS on the depression-like phenotype, we measured body weight of rats and conducted a series of behavioral tests.

As shown in **Figure 1B**, there was no significant difference in the body weight of the rats among the 8 groups on the 0th day ($p > 0.05$). However, compared with the C group, CRS and A2AR agonist significantly suppressed increases in body weight in the M group (from the 7th day, $p < 0.01$) and CC group (from the 14th day, $p < 0.01$), respectively. Compared with the M group, treatment with XYS and A2AR antagonists resulted in a significant increase in body weight gain in the MX group (from day 14, $p < 0.01$ or $p < 0.05$) and MS group (from day 14, $p < 0.01$). XYS also alleviated the trend of A2AR agonist-induced weight loss in rats, athough there was no significant difference ($p > 0.05$).

To investigate the effects of XYS on depression-like behaviors, the OFT, SPT and FST were performed. As shown in **Figures 1C–G**, compared with the rats in the C group, the rats subjected to CRS or A2AR agonist treatment displayed a lower total distance traveled ($p < 0.01$, $p < 0.01$) and lower frequency of entry into the central area

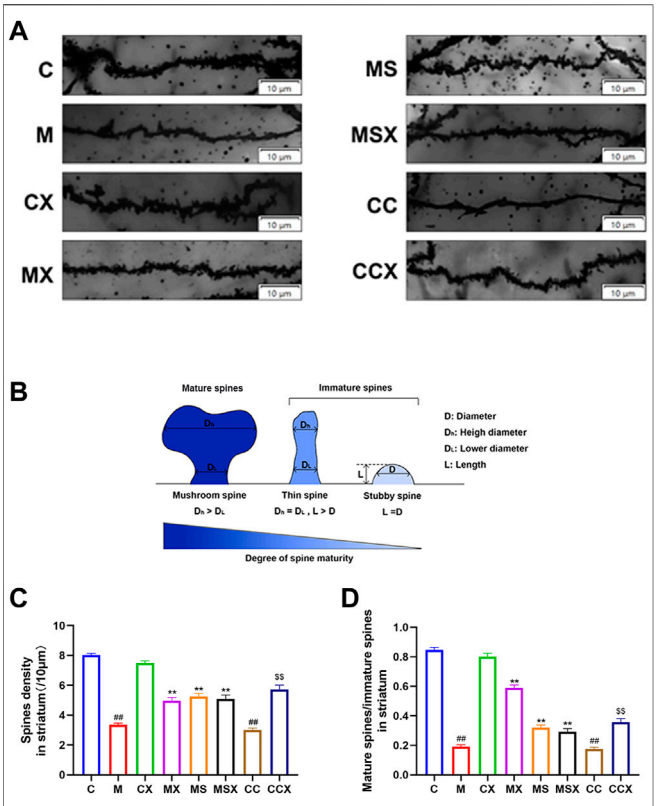

FIGURE 2 | Effects of XYS on the microstructural alterations of dendritic spine morphology and spine density in the rat striatum. **(A)** Representative Golgi-stained dendritic spine image from the striatum region (scale bar = 10 μm). **(B)** Schematic map of mature and immature spines. **(C)** Spine density, 60 axons in each group. **(D)** The ratio of mature spines to immature spines; 60 axons in each group. The value is expressed as the means ± SEM, $n = 3$. $^{\#\#}p < 0.01$ versus the C group; $^{**}p < 0.01$ versus the M group; $^{\$\$}p < 0.01$ versus the CC group.

($p < 0.01$, $p < 0.01$) in the OFT, a lower sucrose preference rate ($p < 0.01$, $p < 0.01$) in the SPT, and a higher immobility time ($p < 0.01$, $p < 0.01$) in the FST. However, treatment with XYS or A2AR antagonist effectively reversed the changes caused by CRS ($p < 0.05$ or $p < 0.01$). XYS could also reverse the decrease in the total distance traveled in the OFT ($p < 0.01$) and sucrose preference rate in the SPT ($p < 0.05$) induced by A2AR agonists; however, there were no statistically significant differences in the frequency of entry into the central area in the OFT ($p > 0.05$) or the immobility time in the FST ($p > 0.05$) after XYS treatment.

To examine the effects of XYS on anxiety-like behaviors, the EPMT was observed. As shown in **Figures 1H,I**, the open arm entries ($p < 0.05$, $p < 0.05$) and time spent in the open arm ($p < 0.01$, $p < 0.01$) were lower in the M group and CC group than in the C group. Treatment with XYS or an A2AR antagonist reversed the changes induced by CRS ($p < 0.01$). XYS reversed the decrease in open arm entries ($p < 0.05$) and time spent in the open arms ($p < 0.05$) caused by A2AR agonists.

Taken together, our results indicate that treatment with XYS may mitigate CRS or the A2AR agonist-induced depression-like phenotype.

Effects of Xiaoyaosan on the Microstructural Alterations of Dendritic Spine Morphology and Spine Density in the rat Striatum

In this study, we observed microstructural alterations in dendritic spine morphology in the striatum of rats.

Figure 2A shows a representative Golgi-stained dendritic spine image from the striatum region. According to the classical classification of protruding morphology, as shown in **Figure 2B**, the spine density and ratio of mature/immature spines in the striatum region of rats was calculated.

The spine densities, as shown in **Figure 2C**, revealed that a significant reduction was present in the M group ($p < 0.01$) and the CC group ($p < 0.01$) compared with that observed in the C group. Spine densities in the MX group ($p < 0.01$), MS group ($p < 0.01$) and the MSX group ($p < 0.01$) were significantly greater than those in the M group. Spine densities in the CCX ($p < 0.01$) group were significantly greater than those in the CC group.

The ratio of mature/immature spines, as shown in **Figure 2D**, revealed a significant reduction in the M group ($p < 0.01$) and the CC group ($p < 0.01$) compared with the C group. XYS or A2AR antagonist increased the low ratio of mature/immature spines caused by CRS ($p < 0.01$, $p < 0.01$). XYS also increased the low ratio of mature/immature spines caused by A2AR agonist ($p < 0.01$).

In summary, XYS ameliorated the microstructural alterations in dendritic spine morphology and spine density in the rat striatum induced by CRS and A2AR agonists.

Effects of Xiaoyaosan on the Synaptic Ultrastructure in rat Striatum

The rat striatum was sectioned and photographed under an electron microscope according to **Figure 3A**. **Figure 3B** is a representative microphotograph of the striatum under a transmission electron microscope.

We performed an ultra-structure analysis of PSD by transmission electron microscopy. As shown in **Figures 3C,D**, compared with the rats in the C group, both PSD length and width in the striatum region of rats in the M group ($p < 0.01$, $p < 0.01$) and CC group ($p < 0.01$, $p < 0.01$) were significantly reduced, whereas treatment with XYS ($p < 0.01$, $p < 0.01$) or A2AR antagonist ($p < 0.01$, $p < 0.01$) effectively reversed the changes caused by CRS. XYS also reversed the reduce in the PSD length in the striatum induced by A2AR agonists ($p < 0.01$). However, there were no statistically significant differences in the PSD width induced by A2AR agonists after XYS treatment ($p > 0.05$).

As shown in **Figure 3E**, compared with the C group, the protein expression level of BDNF in the rat striatum was decreased in the M group ($p < 0.01$). XYS or the A2AR antagonist ameliorated the decrease in synapse-associated proteins caused by CRS ($p < 0.01$). The A2AR agonist decreased the protein expression of BDNF compared with the C group ($p < 0.05$). XYS down-regulated the A2AR agonist-induced reduction in BDNF protein expression, although the difference was not statistically significant ($p > 0.05$).

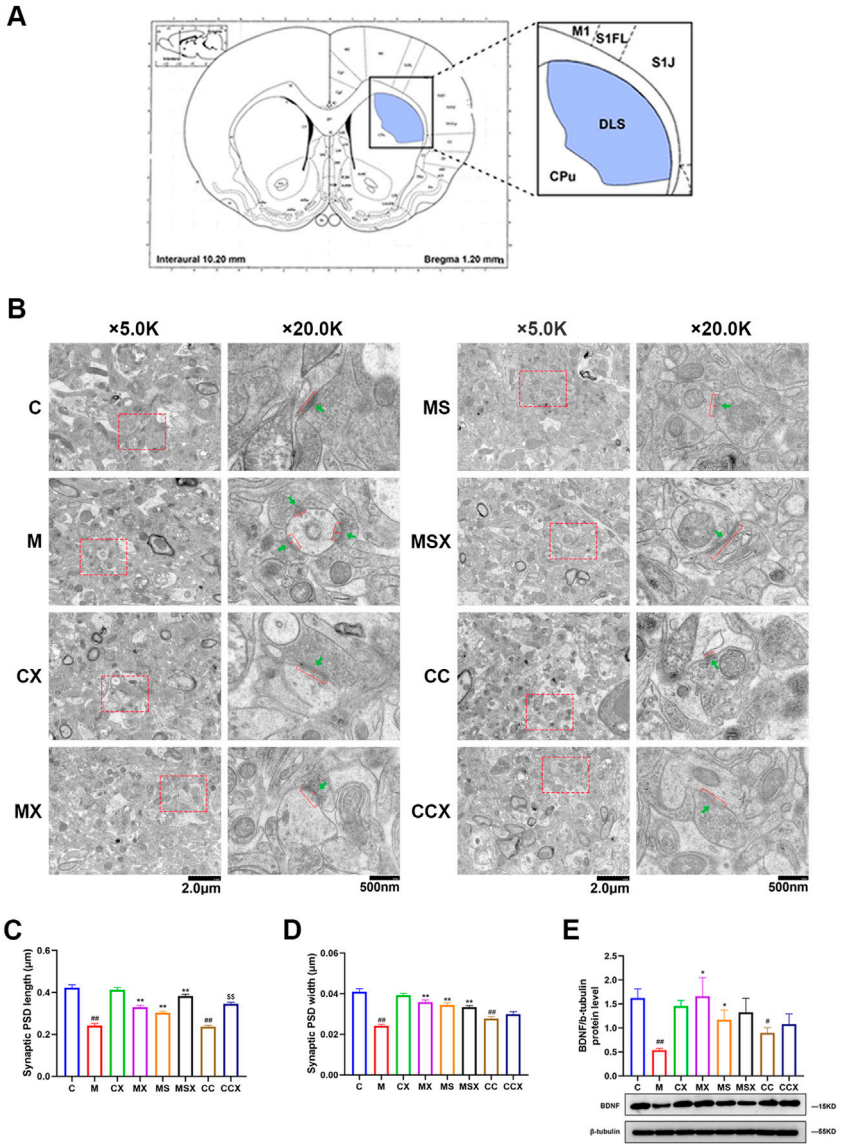

FIGURE 3 | Effects of XYS on the synaptic ultrastructure in the rat striatum. **(A)** Electron microscope section and photographic site diagram of the striatum. Synapses were observed under transmission electron microscopy. **(B)** Representative microphotographs of the rat striatum. The first column of microphotographs was taken at low magnification (scale = 2 μm, 5,000× magnification) under the electron microscope, and the second column of microphotographs was taken at high magnification (scale = 500 nm, 20,000× magnification) under the electron microscope. Red bars and red arrows in lower panels indicate PSD length and PSD width, respectively. Green arrows indicate synaptic vesicles. **(C)** Synaptic PSD length in the rat striatum, 60 synapses in each group. **(D)** Synaptic PSD width in the rat striatum, 60 synapses in each group. **(E)** Expression of BDNF protein in the rat striatum. The value is expressed as the means ± SEM, $n = 3$. $^{\#}p < 0.05$ or $^{\#\#}p < 0.01$ versus the C group; $^{*}p < 0.05$ or $^{**}p < 0.01$ versus the M group; $^{\$\$}p < 0.01$ versus the CC group. PSD, post-synaptic density; BDNF, brain-derived neurotrophic factor.

These results suggest that XYS can reduce the damage to the synaptic ultrastructure in the rat striatum induced by CRS and plays a protective role in the synaptic ultrastructure.

Effects of Xiaoyaosan on the Activation of Microglia in rat Striatum

In this study, immunofluorescence assays and WB were used to detect the activation of microglia in the rat striatum.

As shown in **Figures 4A,B**, the fluorescence intensity of the microglial activation marker IBA-1 was significantly increased in the M group ($p < 0.01$) and CC group ($p < 0.01$) compared with the C group. Treatment with XYS ($p < 0.01$) or an A2AR antagonist ($p < 0.01$) reversed the changes caused by CRS. XYS also reversed the increase in IBA-1 expression and microglial activation caused by the A2AR agonist ($p < 0.05$).

As shown in **Figures 4C,D**, compared to the C group, the protein expression of the M1-associated marker iNOS ($p < 0.01$, $p < 0.05$) was

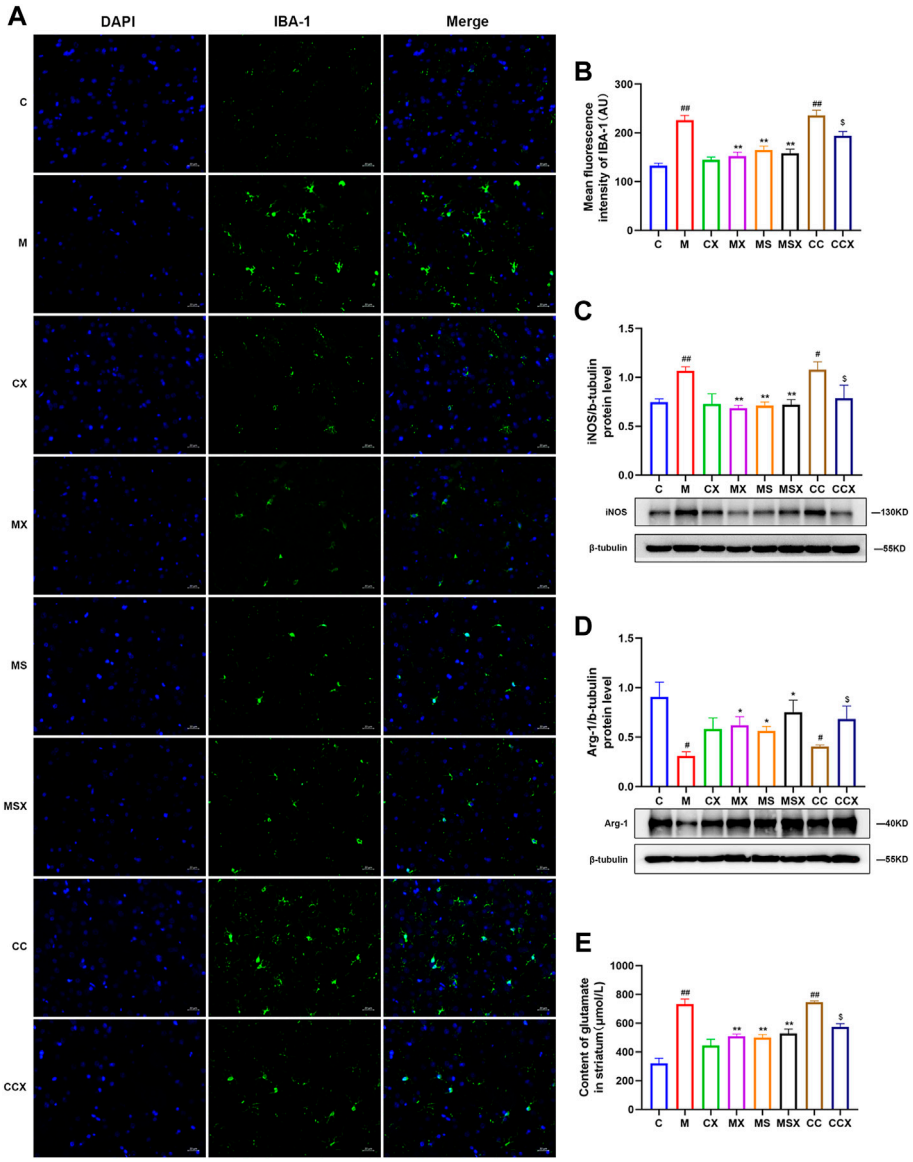

FIGURE 4 | Effects of XYS on microglial activation in the rat striatum. **(A)** Representative micrographs of immunofluorescence staining for the microglial activation marker IBA-1 in the rat striatum (scale = 20 μm, 400× magnification). **(B)** Mean fluorescence density of IBA-1. **(C)** The protein expression of iNOS in the rat striatum. **(D)** Arg-1 protein expression in the rat striatum. **(E)** The content of Glu in the rat striatum. The value is expressed as the mean ± SEM, $n = 3$. $^{\#}p < 0.05$ or $^{\#\#}p < 0.01$ versus the C group; $^{*}p < 0.05$ or $^{**}p < 0.01$ versus the M group; $^{\$}p < 0.05$ versus the CC group. IBA-1, ionized calcium-binding protein-1; iNOS, inducible nitric oxide synthase; Arg-1, arginase-1; Glu, glutamate.

higher and that of the M2-associated marker Arg-1 ($p < 0.05$, $p < 0.05$) was lower in the M group and CC group. XYS or SCH 58261 reversed the changes caused by CRS ($p < 0.05$ or $p < 0.01$). XYS also reversed the changes caused by the A2AR agonist ($p < 0.05$).

As shown in **Figure 4E**, the Glu levels in the striatum of rats were measured, and the results showed that CRS ($p < 0.01$) and the A2AR agonist ($p < 0.01$) increased the secretion of Glu in the striatum compared with the C group. XYS ($p < 0.01$) or SCH 58261 ($p < 0.01$) decreased the Glu levels in the striatum compared with the M group. XYS also decreased the Glu levels compared with those in the CC group ($p < 0.05$).

In summary, the above results confirmed that treatment with XYS may alleviate CRS or A2AR agonist-induced overactivation of microglia in the rat striatum.

Effects of Xiaoyaosan on the Striatal Adenosine A2A Receptor-Extracellular Signal-Regulated Kinase-Nuclear Factor-κB Pathway

The expression of the A2AR-ERK-NF-κB pathway was detected by immunofluorescence assay and WB analysis.

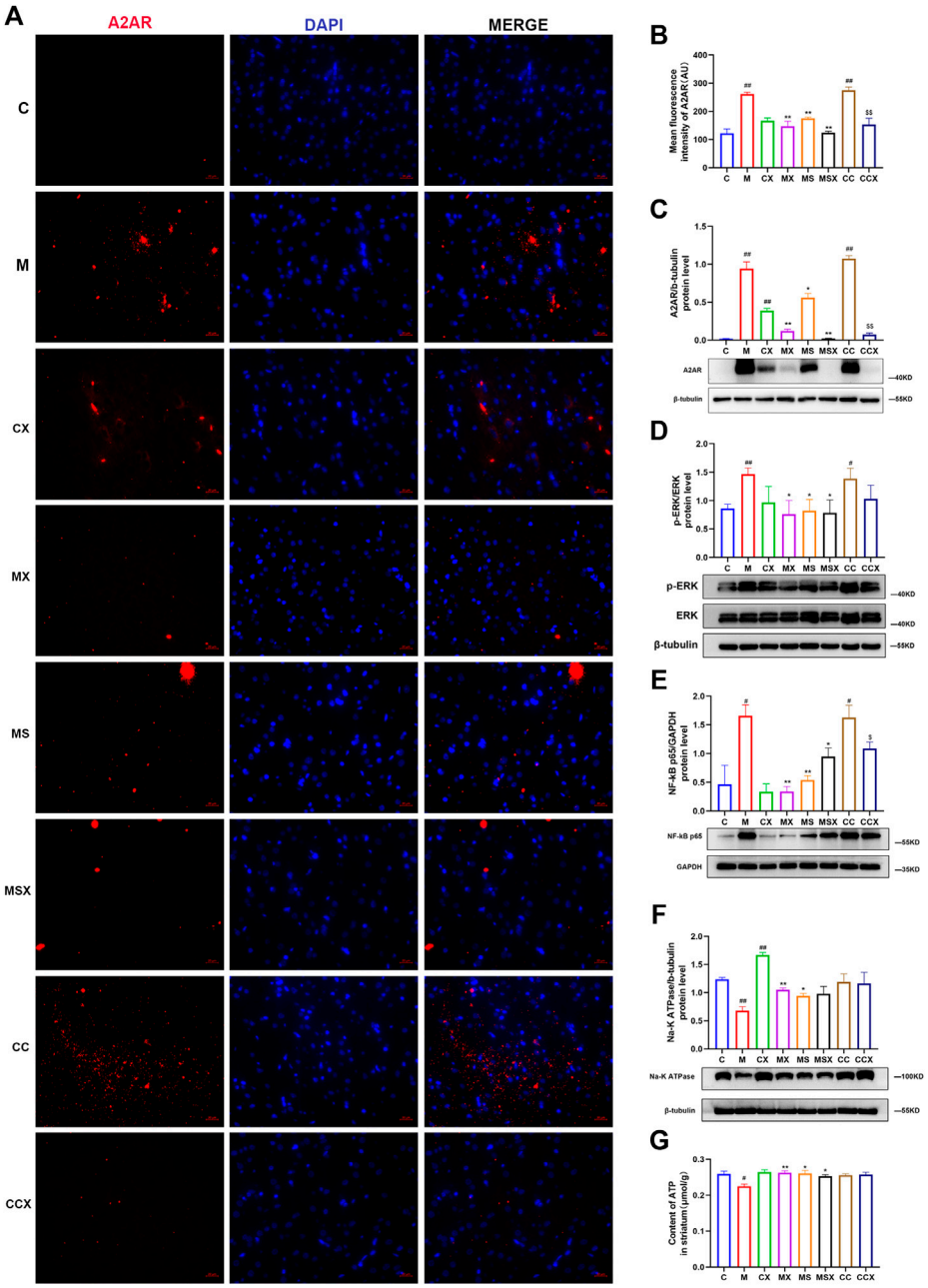

FIGURE 5 | Effects of XYS on the striatal A2AR-ERK-NF-κB pathway. **(A)** Immunofluorescence staining of striatal A2AR (scale= 20 μm, 400× magnification). **(B)** Mean fluorescence density of A2AR. **(C)** The protein expression of A2AR in the rat striatum. **(D)** The protein expression of ERK in the rat striatum. **(E)** The protein expression of NF-κB p65 in the rat striatum. **(F)** The protein expression of NA-K ATPase in the rat striatum. **(G)** The ATP content in the rat striatum. The value is expressed as the mean ±SEM, $n = 3$. $^{\#}p < 0.05$ or $^{\#\#}p < 0.01$ versus the C group; $^{*}p < 0.05$ or $^{**}p < 0.01$ versus the M group; $^{\$}p < 0.05$ or $^{\$\$}p < 0.01$ versus the CC group. A2AR, adenosine A2A receptor; ERK, extracellular signal-regulated kinase; NF-κB, nuclear factor kappa B; ATP, adenosine triphosphate.

As shown in **Figures 5A–E**, compared with those in the C group, the expression levels of A2AR ($p < 0.01$, $p < 0.01$), p-ERK ($p < 0.05$, $p < 0.01$), and NF-κB p65 ($p < 0.05$, $p < 0.05$) in the striatum of rats in the M group and CC group were higher. These increases in the protein expression levels were downregulated by XYS and SCH 58261 treatment ($p < 0.05$ or $p < 0.05$). XYS also decreased the protein expression levels of A2AR ($p < 0.01$), p-ERK ($p < 0.05$), and NF-κB p65 ($p < 0.05$) in the striatum of rats treated with the A2AR agonist.

As shown in **Figures 5F,G**, compared with the C group, the protein expression of NA-K ATPase ($p < 0.01$) and the contents of ATP ($p < 0.05$) in the rat striatum were decreased in the M group. XYS ($p < 0.01$, $p < 0.01$) or SCH 58261 ($p < 0.05$, $p < 0.05$) treatment increased these changes. The A2AR agonist did not change the

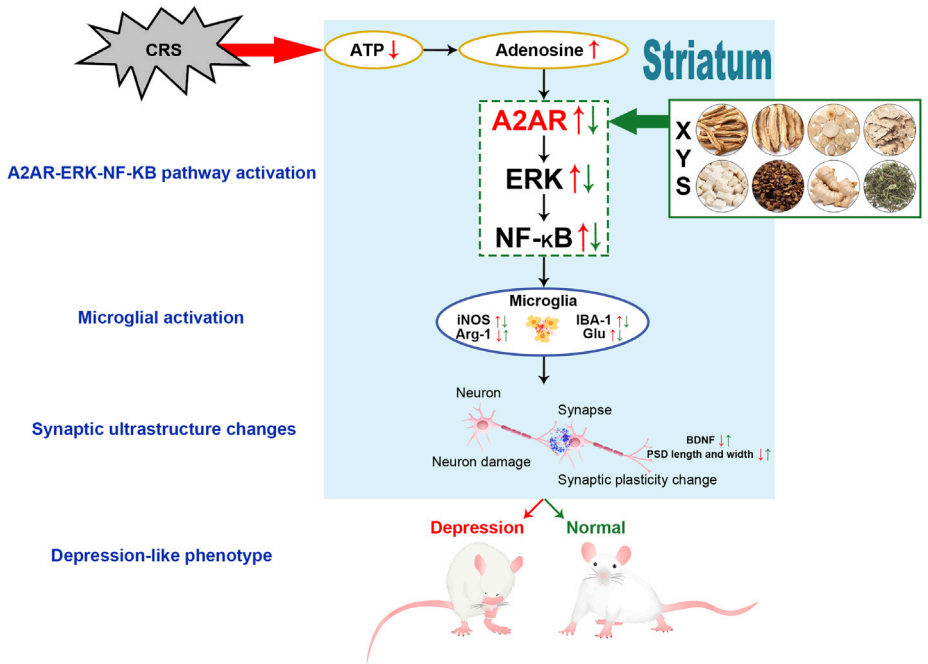

FIGURE 6 | Potential mechanism by which XYS ameliorates the CRS-induced depression-like phenotype.

protein expression of NA-K ATPase or the ATP content in the rat striatum compared with the C group ($p > 0.05$, $p > 0.05$).

Taken together, our results indicated that treatment with XYS could reverse the CRS-induced A2AR-ERK-NF-κB pathway in the rat striatum.

DISCUSSION

The purpose of this study was to investigate the effects of XYS on the depression-like phenotype of rats exposed to CRS, and to explore whether the potential mechanism is associated with A2AR signaling in the striatum. We found that XYS could alleviate the CRS-induced depression-like phenotype (such as body weight loss and depression- and anxiety-like behaviors) and played a protective role in the rat striatal synaptic ultrastructure. Furthermore, exposure to CRS and an A2AR agonist (CGS 21680) induced the activation of microglia and the A2AR-ERK-NF-κB pathway in the striatum, which was reversed by treatment with XYS.

XYS has been used to treat depression in China for thousands of years, and the clinical effect is remarkable. With the increasing attention of complementary alternative medicine, the safety and efficacy of XYS in treating depression have been recognized by many clinical researchers (Ding et al., 2020; Liu et al., 2020). Previous studies have indicated that XYS significantly improves anxiety-like behaviors and hippocampal neuron damage in stressed rats (Li et al., 2017). In this study, the results of behavioral tests indicated that treatment with XYS may mitigate CRS-induced depression-like phenotypes. Moreover, XYS also ameliorated the microstructural alterations in dendritic spine morphology and spine density in the rat striatum induced by CRS. Additionally, XYS is involved in the regulation of adenosine receptors, which are responsible for the beneficial biological effects against depression.

Clinical studies have indicated that morphological changes in the striatum can lead to a decrease in logical memory, recall delays and other psychiatric test scores (Madsen et al., 2010). In this study, microstructural alterations in dendritic spine morphology and spine density in the rat striatum caused by CRS were reversed by XYS. Moreover, XYS reduced the damage to the synaptic ultrastructure in the rat striatum induced by CRS and plays a protective role in the synaptic ultrastructure. In this study, XYS increased the protein expression of BDNF. BDNF is considered an instructive mediator of functional and structural plasticity in the central nervous system (Colucci-D'Amato et al., 2020). A2AR activation modulates several brain processes, ranging from neuronal maturation to synaptic plasticity. Most of these actions occur through the modulation of the actions of the BDNF (Ribeiro et al., 2021). A previous study reported that exercise alleviates depression-like behavior in chronically stressed rats by increasing BDNF in the striatum (Marais et al., 2009).

Microglial activation and neuroinflammation play very important roles in the process of depression (Troubat et al., 2021). Microglia can mediate some biological processes, such as abnormal secretion of toxic and health hazardous substances, removal of damaged cells and dysfunctional synapses through physical contact with biological neurons (Yirmiya et al., 2015). However, overactivation of microglia may result in the elimination and engulfment of functional synapses. This condition is known as "synaptic stripping", and even leads to morphological changes in the brain (Kettenmann et al., 2013). In this study, the rats in the CRS group and A2AR agonist group showed increased Glu secretion and

overactivation of microglia in the striatum, but XYS and A2AR antagonists reduced these changes. The abnormal release of Glu can quickly attract microglia to these brain regions, which then surround the overactive neurons (Eyo et al., 2014). This suggests that XYS may play a protective role in the synaptic ultrastructure by reducing the microglial activation. It is reported that microglia-mediated synaptic pruning can be mitigated by minocycline, an agent that reduces microglial activation (Jawaid et al., 2018).

A2AR is specifically enriched in the striatum and localized in glutamatergic synapses (Rebola et al., 2005) and glial cells (Matos et al., 2012). A2AR expression is usually low under physiological conditions but increases in the brain during stress. In terms of treatment, inhibition of A2AR can prevent neuroinflammation (Martí Navia et al., 2020). Therefore, adenosine A2AR antagonists are very important for the protection of the central nervous system. In this study, we found that XYS treatment downregulated the increases in the protein expression levels of A2AR in the striatum of rats induced by CRS. Studies have found that A2AR mediates phosphorylation and upregulation of the extracellular signal ERK1/2, resulting in increased Glu release (Braga et al., 2019; Köfalvi et al., 2020), causing high NF-κB expression and promoting microglial proliferation and activation (Mohamed et al., 2016). Our data also showed that the expression levels of p-ERK and NF-κB p65 in the striatum of rats in the CRS model group were increased, whereas XYS treatment downregulated these protein levels. The results above support our hypothesis and shows that XYS inhibits the A2AR-ERK-NF-κB pathway in the striatum, and this effect is similar to that of an A2AR antagonist.

We used a group of rats treated with CGS 21680 (an A2AR agonist) to investigate the effects of XYS on A2AR signaling in the striatum. Previous studies have suggested that A2AR serves an important role in the onset of microglial activation and inflammation after exposure to a low glucose/hypoxia in a NF-κB-dependent manner (Huang et al., 2018). We found that intraperitoneal injection of CGS 21680 can also activate the A2AR-ERK-NF-κB pathway in the striatum and induce a depression-like phenotype, which was reversed by treatment with XYS. These results further validated our hypothesis that the antidepressive effects of XYS are associated with A2AR signaling in the striatum.

There were several limitations of the current study. First, only male adult rats were included in the present study. As it has been pointed out in many studies that sex differences may affect the onset of depression, more investigations will be performed in the future. Second, we only used an A2AR antagonist to block the ERK-NF-κB pathway, but according to the A1R-A2AR imbalance theory, enhanced A1R also has an antidepressant effect (Serchov et al., 2015). Whether A1R agonists have similar effects requires further research.

CONCLUSION

In summary, in this study, we found that XYS can ameliorate depression-like phenotypes and plays a protective role in the synaptic ultrastructure of the striatum. The mechanisms of these effects may be related to inhibition of the A2AR-ERK-NF-κB pathway in the striatum (**Figure 6**). Our findings serve as a pharmacological basis for the clinical application of XYS and provide a better understanding of the mechanisms associated with the regulatory effects of XYS on AR signaling.

DATA AVAILABILITY STATEMENT

The original contributions presented in the study are included in the article/**Supplementary Material**, further inquiries can be directed to the corresponding authors.

ETHICS STATEMENT

The animal study was reviewed and approved by the Animal Experimental Ethics Committee of Jinan University Jinan University, Guangzhou, China.

AUTHOR CONTRIBUTIONS

XZ and QM contribute equally to this paper. Conception and design of research: JC, LY, XZ, and QM; Performed experiments: XZ, FY, LL, MC, and JC; Analyzed data: XZ and QM; Interpretation of results of experiments: LY, XZ, QM, and XZ; Prepared figures: XZ, QM, YL, and XL; Drafted manuscript: LY, XZ, and QM. All authors read and approved the final article.

FUNDING

This study was supported by the National Natural Science Foundation of China (No. 81973748, 82174278), the National Science Foundation for Young Scientists of China (No. 81903617), Huang Zhendong Research Fund for Traditional Chinese Medicine of Jinan University (No. 201911), Key-Area Research and Development Program of Guangdong Province (No. 2020B1111100001), Guangzhou Key Laboratory of Formula-Pattern of Traditional Chinese Medicine (No. 202102010014), Guangdong Basic and Applied Basic Research Foundation, China (2022A1515011699), Postdoctoral Science Foundation of China (No. 2021M691259).

SUPPLEMENTARY MATERIAL

The Supplementary Material for this article can be found online at: https://www.frontiersin.org/articles/10.3389/fphar.2022.897436/full#supplementary-material

REFERENCES

Admon, R., Kaiser, R. H., Dillon, D. G., Beltzer, M., Goer, F., Olson, D. P., et al. (2017). Dopaminergic Enhancement of Striatal Response to Reward in Major Depression. *Am. J. Psychiatry* 174 (4), 378–386. doi:10.1176/appi.ajp.2016.16010111

Biber, K., Möller, T., Boddeke, E., and Prinz, M. (2016). Central Nervous System Myeloid Cells as Drug Targets: Current Status and Translational Challenges. *Nat. Rev. Drug Discov.* 15 (2), 110–124. doi:10.1038/nrd.2015.14

Borroto-Escuela, D. O., Hinz, S., Navarro, G., Franco, R., Müller, C. E., and Fuxe, K. (2018). Understanding the Role of Adenosine A2AR Heteroreceptor Complexes in Neurodegeneration and Neuroinflammation. *Front. Neurosci.* 12, 43. doi:10.3389/fnins.2018.00043

Braga, D. V., Wanderley Picanço-Diniz, D. L., Herculano Matos Oliveira, K. R., Luz, W. L., Soares de Moraes, S. A., Fonseca Passos, A. C., et al. (2019). Adenosine A1 Receptors Modulate the Na+-Hypertonicity Induced Glutamate Release in Hypothalamic Glial Cells. *Neurochem. Int.* 126, 64–68. doi:10.1016/j.neuint.2019.02.013

Colucci-D'Amato, L., Speranza, L., and Volpicelli, F. (2020). Neurotrophic Factor BDNF, Physiological Functions and Therapeutic Potential in Depression, Neurodegeneration and Brain Cancer. *Int. J. Mol. Sci.* 21 (20), 7777. doi:10.3390/ijms21207777

Costenla, A. R., Diógenes, M. J., Canas, P. M., Rodrigues, R. J., Nogueira, C., Maroco, J., et al. (2011). Enhanced Role of Adenosine A(2A) Receptors in the Modulation of LTP in the Rat hippocampus upon Ageing. *Eur. J. Neurosci.* 34 (1), 12–21. doi:10.1111/j.1460-9568.2011.07719.x

Dheen, S. T., Kaur, C., and Ling, E. A. (2007). Microglial Activation and its Implications in the Brain Diseases. *Curr. Med. Chem.* 14 (11), 1189–1197. doi:10.2174/092986707780597961

Ding, F., Wu, J., Liu, C., Bian, Q., Qiu, W., Ma, Q., et al. (2020). Effect of Xiaoyaosan on Colon Morphology and Intestinal Permeability in Rats with Chronic Unpredictable Mild Stress. *Front. Pharmacol.* 11, 1069. doi:10.3389/fphar.2020.01069

Dubbelaar, M. L., Kracht, L., Eggen, B. J. L., and Boddeke, E. W. G. M. (2018). The Kaleidoscope of Microglial Phenotypes. *Front. Immunol.* 9, 1753. doi:10.3389/fimmu.2018.01753

Dubovsky, S. L., Ghosh, B. M., Serotte, J. C., and Cranwell, V. (2021). Psychotic Depression: Diagnosis, Differential Diagnosis, and Treatment. *Psychother. Psychosom.* 90 (3), 160–177. doi:10.1159/000511348

Eyo, U. B., Peng, J., Swiatkowski, P., Mukherjee, A., Bispo, A., and Wu, L. J. (2014). Neuronal Hyperactivity Recruits Microglial Processes via Neuronal NMDA Receptors and Microglial P2Y12 Receptors after Status Epilepticus. *J. Neurosci.* 34 (32), 10528–10540. doi:10.1523/JNEUROSCI.0416-14.2014

Furuyashiki, T., and Deguchi, Y. (2012). Roles of Altered Striatal Function in Major Depression. *Brain Nerve* 64 (8), 919–926. doi:10.11477/mf.1416101268

Hao, W., Wu, J., Yuan, N., Gong, L., Huang, J., Ma, Q., et al. (2021). Xiaoyaosan Improves Antibiotic-Induced Depressive-like and Anxiety-like Behavior in Mice through Modulating the Gut Microbiota and Regulating the NLRP3 Inflammasome in the Colon. *Front. Pharmacol.* 12, 619103. doi:10.3389/fphar.2021.619103

Huang, W., Bai, S., Zuo, X., Tang, W., Chen, P., Chen, X., et al. (2018). An Adenosine A1R-A2aR Imbalance Regulates Low Glucose/hypoxia-Induced Microglial Activation, Thereby Contributing to Oligodendrocyte Damage through NF-κB and CREB Phosphorylation. *Int. J. Mol. Med.* 41 (6), 3559–3569. doi:10.3892/ijmm.2018.3546

Jawaid, S., Kidd, G. J., Wang, J., Swetlik, C., Dutta, R., and Trapp, B. D. (2018). Alterations in CA1 Hippocampal Synapses in a Mouse Model of Fragile X Syndrome. *Glia* 66 (4), 789–800. doi:10.1002/glia.23284

Kaster, M. P., Machado, N. J., Silva, H. B., Nunes, A., Ardais, A. P., Santana, M., et al. (2015). Caffeine Acts through Neuronal Adenosine A2A Receptors to Prevent Mood and Memory Dysfunction Triggered by Chronic Stress. *Proc. Natl. Acad. Sci. U. S. A.* 112 (25), 7833–7838. doi:10.1073/pnas.1423088112

Kettenmann, H., Kirchhoff, F., and Verkhratsky, A. (2013). Microglia: New Roles for the Synaptic Stripper. *Neuron* 77 (1), 10–18. doi:10.1016/j.neuron.2012.12.023

Köfalvi, A., Moreno, E., Cordomí, A., Cai, N. S., Fernández-Dueñas, V., Ferreira, S. G., et al. (2020). Control of Glutamate Release by Complexes of Adenosine and Cannabinoid Receptors. *BMC Biol.* 18 (1), 9. doi:10.1186/s12915-020-0739-0

Lazarus, M., Chen, J. F., Huang, Z. L., Urade, Y., and Fredholm, B. B. (2019). Adenosine and Sleep. *Handb. Exp. Pharmacol.* 253, 359–381. doi:10.1007/164_2017_36

Li, X. J., Ma, Q. Y., Jiang, Y. M., Bai, X. H., Yan, Z. Y., Liu, Q., et al. (2017). Xiaoyaosan Exerts Anxiolytic-like Effects by Down-Regulating the TNF-α/JAK2-STAT3 Pathway in the Rat hippocampus. *Sci. Rep.* 7 (1), 353. doi:10.1038/s41598-017-00496-y

Li, X. H., Zhou, X. M., Li, X. J., Liu, Y. Y., Liu, Q., Guo, X. L., et al. (2019). Effects of Xiaoyaosan on the Hippocampal Gene Expression Profile in Rats Subjected to Chronic Immobilization Stress. *Front. Psychiatry* 10, 178. doi:10.3389/fpsyt.2019.00178

Li, X. J., Qiu, W. Q., Da, X. L., Hou, Y. J., Ma, Q. Y., Wang, T. Y., et al. (2020). A Combination of Depression and Liver Qi Stagnation and Spleen Deficiency Syndrome Using a Rat Model. *Anat. Rec. Hob.* 303 (8), 2154–2167. doi:10.1002/ar.24388

Liu, X., Liu, C., Tian, J., Gao, X., Li, K., Du, G., et al. (2020). Plasma Metabolomics of Depressed Patients and Treatment with Xiaoyaosan Based on Mass Spectrometry Technique. *J. Ethnopharmacol.* 246, 112219. doi:10.1016/j.jep.2019.112219

Looi, J. C., and Walterfang, M. (2013). Striatal Morphology as a Biomarker in Neurodegenerative Disease. *Mol. Psychiatry* 18 (4), 417–424. doi:10.1038/mp.2012.54

Ma, Q., Li, X., Yan, Z., Jiao, H., Wang, T., Hou, Y., et al. (2019). Xiaoyaosan Ameliorates Chronic Immobilization Stress-Induced Depression-like Behaviors and Anorexia in Rats: The Role of the Nesfatin-1-Oxytocin-Proopiomelanocortin Neural Pathway in the Hypothalamus. *Front. Psychiatry* 10, 910. doi:10.3389/fpsyt.2019.00910

Ma, J. C., Zhang, H. L., Huang, H. P., Ma, Z. L., Chen, S. F., Qiu, Z. K., et al. (2021). Antidepressant-like Effects of Z-Ligustilide on Chronic Unpredictable Mild Stress-Induced Depression in Rats. *Exp. Ther. Med.* 22 (1), 677. doi:10.3892/etm.2021.10109

Madsen, S. K., Ho, A. J., Hua, X., Saharan, P. S., Toga, A. W., Jack, C. R., et al. (2010). 3D Maps Localize Caudate Nucleus Atrophy in 400 Alzheimer's Disease, Mild Cognitive Impairment, and Healthy Elderly Subjects. *Neurobiol. Aging* 31 (8), 1312–1325. doi:10.1016/j.neurobiolaging.2010.05.002

Mao, Z. F., Ouyang, S. H., Zhang, Q. Y., Wu, Y. P., Wang, G. E., Tu, L. F., et al. (2020). New Insights into the Effects of Caffeine on Adult Hippocampal Neurogenesis in Stressed Mice: Inhibition of CORT-induced Microglia Activation. *FASEB J.* 34, 10998–11014. doi:10.1096/fj.202000146RR

Marais, L., Stein, D. J., and Daniels, W. M. (2009). Exercise Increases BDNF Levels in the Striatum and Decreases Depressive-like Behavior in Chronically Stressed Rats. *Metab. Brain Dis.* 24 (4), 587–597. doi:10.1007/s11011-009-9157-2

Martí Navia, A., Dal Ben, D., Lambertucci, C., Spinaci, A., Volpini, R., Marques-Morgado, I., et al. (2020). Adenosine Receptors as Neuroinflammation Modulators: Role of A_1 Agonists and A_{2A} Antagonists. *Cells* 9 (7), 1739. doi:10.3390/cells9071739

Matos, M., Augusto, E., Santos-Rodrigues, A. D., Schwarzschild, M. A., Chen, J. F., Cunha, R. A., et al. (2012). Adenosine A2A Receptors Modulate Glutamate Uptake in Cultured Astrocytes and Gliosomes. *Glia* 60 (5), 702–716. doi:10.1002/glia.22290

McCarron, R. M., Shapiro, B., Rawles, J., and Luo, J. (2021). Depression. *Ann. Intern Med.* 174 (5), ITC65–ITC80. doi:10.7326/AITC202105180

Mohamed, R. A., Agha, A. M., Abdel-Rahman, A. A., and Nassar, N. N. (2016). Role of Adenosine A2A Receptor in Cerebral Ischemia Reperfusion Injury: Signaling to Phosphorylated Extracellular Signal-Regulated Protein Kinase (pERK1/2). *Neuroscience* 314, 145–159. doi:10.1016/j.neuroscience.2015.11.059

Ohta, A., and Sitkovsky, M. (2001). Role of G-Protein-Coupled Adenosine Receptors in Downregulation of Inflammation and Protection from Tissue Damage. *Nature* 414 (6866), 916–920. doi:10.1038/414916a

Pan, H. Z., and Chen, H. H. (2007). Hyperalgesia, Low-Anxiety, and Impairment of Avoidance Learning in Neonatal Caffeine-Treated Rats. *Psychopharmacol. Berl.* 191 (1), 119–125. doi:10.1007/s00213-006-0613-y

Peleli, M., Fredholm, B. B., Sobrevia, L., and Carlström, M. (2017). Pharmacological Targeting of Adenosine Receptor Signaling. *Mol. Asp. Med.* 55, 4–8. doi:10.1016/j.mam.2016.12.002

Peter, S., Urbanus, B. H. A., Klaassen, R. V., Wu, B., Boele, H. J., Azizi, S., et al. (2020). AMPAR Auxiliary Protein SHISA6 Facilitates Purkinje Cell Synaptic

Excitability and Procedural Memory Formation. *Cell Rep.* 31 (2), 107515. doi:10.1016/j.celrep.2020.03.079

Qiao, H., Li, M. X., Xu, C., Chen, H. B., An, S. C., and Ma, X. M. (2016). Dendritic Spines in Depression: What We Learned from Animal Models. *Neural Plast.* 2016, 8056370. doi:10.1155/2016/8056370

Rebola, N., Rodrigues, R. J., Lopes, L. V., Richardson, P. J., Oliveira, C. R., and Cunha, R. A. (2005). Adenosine A1 and A2A Receptors Are Co-expressed in Pyramidal Neurons and Co-localized in Glutamatergic Nerve Terminals of the Rat hippocampus. *Neuroscience* 133 (1), 79–83. doi:10.1016/j.neuroscience.2005.01.054

Ribeiro, F. F., Ferreira, F., Rodrigues, R. S., Soares, R., Pedro, D. M., Duarte-Samartinho, M., et al. (2021). Regulation of Hippocampal Postnatal and Adult Neurogenesis by Adenosine A2A Receptor: Interaction with Brain-Derived Neurotrophic Factor. *Stem Cells* 39 (10), 1362–1381. doi:10.1002/stem.3421

Santiago, A. R., Bernardino, L., Agudo-Barriuso, M., and Gonçalves, J. (2017). Microglia in Health and Disease: A Double-Edged Sword. *Mediat. Inflamm.* 2017, 7034143. doi:10.1155/2017/7034143

Schulz, D. (2018). Acute Food Deprivation Separates Motor-Activating from Anxiolytic Effects of Caffeine in a Rat Open Field Test Model. *Behav. Pharmacol.* 29 (6), 543–546. doi:10.1097/FBP.0000000000000396

Serchov, T., Clement, H. W., Schwarz, M. K., Iasevoli, F., Tosh, D. K., Idzko, M., et al. (2015). Increased Signaling via Adenosine A1 Receptors, Sleep Deprivation, Imipramine, and Ketamine Inhibit Depressive-like Behavior via Induction of Homer1a. *Neuron* 87 (3), 549–562. doi:10.1016/j.neuron.2015.07.010

Summergrad, P. (2016). Investing in Global Mental Health: the Time for Action Is Now. *Lancet Psychiatry* 3 (5), 390–391. doi:10.1016/S2215-0366(16)30031-1

Troubat, R., Barone, P., Leman, S., Desmidt, T., Cressant, A., Atanasova, B., et al. (2021). Neuroinflammation and Depression: A Review. *Eur. J. Neurosci.* 53 (1), 151–171. doi:10.1111/ejn.14720

Williams, J. R., Cole, V., Girdler, S., and Cromeens, M. G. (2020). Exploring Stress, Cognitive, and Affective Mechanisms of the Relationship between Interpersonal Trauma and Opioid Misuse. *PloS one* 15 (5), e0233185. doi:10.1371/journal.pone.0233185

Yirmiya, R., Rimmerman, N., and Reshef, R. (2015). Depression as a Microglial Disease. *Trends Neurosci.* 38 (10), 637–658. doi:10.1016/j.tins.2015.08.001

Yuan, N., Gong, L., Tang, K., He, L., Hao, W., Li, X., et al. (2020). An Integrated Pharmacology-Based Analysis for Antidepressant Mechanism of Chinese Herbal Formula Xiao-Yao-San. *Front. Pharmacol.* 11, 284. doi:10.3389/fphar.2020.00284

Zhou, X. M., Liu, C. Y., Liu, Y. Y., Ma, Q. Y., Zhao, X., Jiang, Y. M., et al. (2021). Xiaoyaosan Alleviates Hippocampal Glutamate-Induced Toxicity in the CUMS Rats via NR2B and PI3K/Akt Signaling Pathway. *Front. Pharmacol.* 12, 586788. doi:10.3389/fphar.2021.586788

Zhu, H. Z., Liang, Y. D., Ma, Q. Y., Hao, W. Z., Li, X. J., Wu, M. S., et al. (2019). Xiaoyaosan Improves Depressive-like Behavior in Rats with Chronic Immobilization Stress through Modulation of the Gut Microbiota. *Biomed. Pharmacother.* 112, 108621. doi:10.1016/j.biopha.2019.108621

Zhu, H. Z., Liang, Y. D., Hao, W. Z., Ma, Q. Y., Li, X. J., Li, Y. M., et al. (2021). Xiaoyaosan Exerts Therapeutic Effects on the Colon of Chronic Restraint Stress Model Rats via the Regulation of Immunoinflammatory Activation Induced by the TLR4/NLRP3 Inflammasome Signaling Pathway. *Evid. Based Complement. Altern. Med.* 2021, 6673538. doi:10.1155/2021/6673538

Conflict of Interest: The authors declare that the research was conducted in the absence of any commercial or financial relationships that could be construed as a potential conflict of interest.

Publisher's Note: All claims expressed in this article are solely those of the authors and do not necessarily represent those of their affiliated organizations, or those of the publisher, the editors and the reviewers. Any product that may be evaluated in this article, or claim that may be made by its manufacturer, is not guaranteed or endorsed by the publisher.

frontiers | Frontiers in Pharmacology

REVIEW
published: 29 June 2022
doi: 10.3389/fphar.2022.902259

NEU1—A Unique Therapeutic Target for Alzheimer's Disease

Aiza Khan[1] *and Consolato M. Sergi*[1,2]*

[1]Department of Laboratory Medicine and Pathology, University of Alberta, Edmonton, AB, Canada, [2]Division of Anatomic Pathology, Children's Hospital of Eastern Ontario, University of Ottawa, Ottawa, ON, Canada

Neuraminidase 1 (NEU1) is considered to be the most abundant and ubiquitous mammalian enzyme, with a broad tissue distribution. It plays a crucial role in a variety of cellular mechanisms. The deficiency of NEU1 has been implicated in various pathological manifestations of sialidosis and neurodegeneration. Thus, it is a novel therapeutic target for neurodegenerative changes in the Alzheimer's brain. However, to manipulate NEU1 as a therapeutic target, it is imperative to understand that, although NEU1 is commonly known for its lysosomal catabolic function, it is also involved in other pathways. NEU1 is involved in immune response modulation, elastic fiber assembly modulation, insulin signaling, and cell proliferation. In recent years, our knowledge of NEU1 has continued to grow, yet, at the present moment, current data is still limited. In addition, the unique biochemical properties of NEU1 make it challenging to target it as an effective therapeutic option for sialidosis, which is a rare disease but has an enormous patient burden. However, the fact that NEU1 has been linked to the pathology of Alzheimer's disease, which is rapidly growing worldwide, makes it more relevant to be studied and explored. In the present study, the authors have discussed various cellular mechanisms involving NEU1 and how they are relevant to sialidosis and Alzheimer's disease.

Keywords: NEU1, metabolic disease, sialidosis, neurodegeneration, Alzheimer's disease, gene, gene therapy

OPEN ACCESS

Edited by:
Rui Liu,
Chinese Academy of Medical Sciences, China

Reviewed by:
Kohji Itoh,
University of Tokushima, Japan
Myron R. Szewczuk,
Queen's University, Canada

***Correspondence:**
Consolato M. Sergi
csergi@cheo.on.ca

Specialty section:
This article was submitted to Neuropharmacology, a section of the journal Frontiers in Pharmacology

Received: *22 March 2022*
Accepted: *17 May 2022*
Published: *29 June 2022*

Citation:
Khan A and Sergi CM (2022) NEU1—A Unique Therapeutic Target for Alzheimer's Disease. Front. Pharmacol. 13:902259. doi: 10.3389/fphar.2022.902259

1 INTRODUCTION

NEU1 belongs to the family of neuraminidases (sialidases). This enzyme mediates the removal of sialic acid (Sia) residues from glycoconjugates in vertebrates, subsequently regulating numerous physiological and pathological cellular activities (Smutova et al., 2014). Evidence suggests that NEU1 plays a role in various human disorders. These disorders include lysosomal disease, infectious disease, cancer, and neurodegenerative disorders, thus making it a critical therapeutic target (Glanz et al., 2019). The most associated condition with NEU1 is sialidosis, which occurs due to mutation in the neuraminidase gene (*NEU1*), located on 6p21.33 (Pshezhetsky et al., 1997; Uhl et al., 2002). Sialidosis is a lysosomal storage disease. Also, it is autosomal recessive, caused by a gene mutation (*NEU1*). The *NEU1* gene encodes the lysosomal sialidase NEU1 (Sergi et al., 1999). The subsequent deficiency of the enzyme activity causes a compromise in the process of degradation of sialoglycoproteins, consequently causing an accumulation of over-sialylated metabolites (Pshezhetsky et al., 1997). Sialidosis is a heterogeneous disorder with a diversified range of symptoms (Sergi et al., 1999; Sergi et al., 2001; Khan and Sergi, 2018; Sergi, 2020). Based on the onset and severity of clinical manifestations, sialidosis is divided into two types. Type I sialidosis is the less severe form, with a late onset of symptoms (d'Azzo et al., 2015). Typical symptoms of type I sialidosis, also known as cherry-red spot myoclonus syndrome, include progressive visual loss,

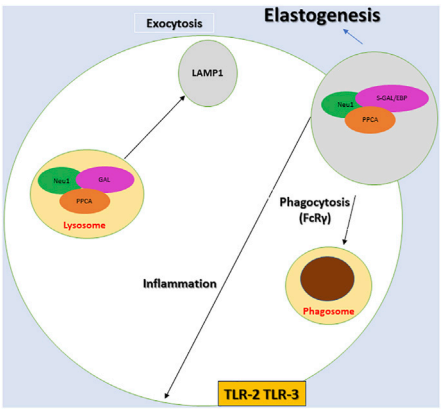

FIGURE 1 | Diagram depicting the components of the multienzyme lysosomal complex, neuraminidase 1 (NEU1), protective protein/cathepsin A (PPCA) and β-galactosidase (Gal), and the associated proposed cellular mechanisms. NEU1 activation depends on PPCA within the NEU1-PPCA-Gal and NEU1-PPCA- S-Gal/EBP complex. The process of desialylation activates the receptors for phagocytosis (FcRγ), inflammation (TLR-2 and TLR3). NEU1 is also crucial for lysosomal exocytosis and elastogenesis. It should be noted that a variant of β-galactosidase S-Gal/EBP, NEU1, and CathA constitutes the elastin receptor that is targeted to the plasma membrane and is crucial in extracellular assembly of elastic fibers.

bilateral cherry-red spots, and myoclonus, and are generally manifested during adolescence (Coppola et al., 2020). Type II sialidosis, in contrast, takes a more severe course and is further subdivided into three subtypes. In congenital type II sialidosis, patients are either stillborn or diagnosed at birth. The critical features include facial dysmorphism, skeletal dysplasia, mental retardation, and hepatomegaly and splenomegaly. The other two types are the infantile and juvenile types, in which sialidosis patients are born relatively healthy. However, soon after birth, these patients develop progressive visceromegaly and dysostosis multiplex. Also, there is moderate to severe mental retardation (Lowden and O'Brien, 1979). The most severe form is congenital sialidosis, which occurs entirely prenatally after the second trimester of pregnancy with non-immunological hydrops fetalis (NIHF) or isolated fetal ascites (Bonten et al., 2013).

Currently, there is a lack of practical therapy for sialidosis due to the rarity of this disease (d'Azzo et al., 2015; Khan and Sergi, 2018). This lack of available therapeutic options has been attributed to the biochemical characteristics of NEU1. These characteristics are its tendency to aggregate, immune reactivity, and instability in the absence of PPCA (d'Azzo et al., 2015). Another critical aspect to consider is that although the catabolic role of NEU1 is profoundly crucial and remains central in the context of sialidosis. Nevertheless, recent studies suggest that NEU1 is involved in diverse cellular regulatory mechanisms. In addition to its role as a negative regulator of exocytosis (Pshezhetsky and Hinek, 2011), NEU1 plays a role in the modulation of the immune response (Pshezhetsky and Hinek, 2011), the generation of extracellular matrix, cell proliferation, and differentiation through desialylation of specific protein targets (Pshezhetsky and Hinek, 2011; **Figure 1**). It is essential to consider the diverse array of roles of NEU1, as it may lead to the use of NEU1 for other relatively common adult diseases. For example, numerous recent studies have demonstrated a therapeutic role of NEU1 in Alzheimer's disease (AD), which is the most common type of neurodegenerative disease causing dementia [1213] (Serrano-Pozo et al., 2011; Chaudhary et al., 2018). Thus, as suggested before, if therapeutic targets such as NEU1 for rare diseases like sialidosis may prove helpful for other common conditions in adults, it may encourage the in-depth research and subsequent availability of therapeutic options for rare diseases and orphan diseases (d'Azzo et al., 2015).

In this study, the authors review the diverse roles of NEU1 in various cellular mechanisms, its potential substrates that have been reported in the literature so far, and its roles in different cellular mechanisms that have been associated with both sialidosis and AD. Also, the authors discuss the progress that has been made in the therapeutic interventions specific to sialidosis.

2 CELLULAR MECHANISM AND NEU1 INVOLVEMENT

The NEU1 enzyme belongs to the family of sialidases. These enzymes remove sialic acid from the oligosaccharide chain (Yamaguchi et al., 2005; Miyagi and Yamaguchi, 2012). These sialidases, or neuraminidases, are widely distributed. They are required for many biological processes, including gangliosides and glycoproteins catabolism, plasma protein clearance, cell adhesion, and immunocyte function. NEU1 is the first and most abundantly found member of the sialidase family (Smutova et al., 2014). Substantially, NEU1 is a lysosomal exo-glycosidase. Functioning as a catalyst, it separates the terminal N-acetylated neuraminic acids (sialic acid) attached to the saccharide chains of glycoproteins, glycolipids, and oligo polysaccharides (Pshezhetsky and Ashmarina, 2001). One of the critical differentiating characteristics of NEU1 is that its active form exists only in a multienzyme complex along with other hydrolases: the glycosidase β-galactosidase (β-GAL) and the PPCA (Vinogradova et al., 1998). This association is essential for the stability and activity of all three enzymes, particularly NEU1, as it is critical for its catalytic activity (de Geest et al., 2002; Bonten et al., 2009). Here, it is essential to highlight that the PPCA acts as a chaperone/transport protein for NEU1. In fact, for many of its crucial activities, such as lysosomal compartmentalization, catalytic activation, and stability in lysosomes, NEU1 heavily depends on its association with PPCA (d'Azzo et al., 2015; Khan and Sergi, 2018). The interaction of NEU1 and PPCA takes place at an earlier biosynthetic stage. PPCA's C-terminal portion is critical for its interaction with NEU1 and contains a binding site for NEU1 (de Geest et al., 2002; d'Azzo et al., 2015).

Interestingly, studies suggest that the binding domain in NEU1 for PPCA has an affinity for PPCA and NEU1. Hence, in the absence of PPCA, NEU1 tends to self-associate into chain-like oligomers. However, the binding of PPCA can reverse the self-association of NEU1 by causing the disassembly of NEU1-oligomers, with the inception of a PPCA-NEU1 heterodimeric

complex (Bonten et al., 2009). Thus, it is plausible that the binding site of PPCA and NEU1 is critical. NEU1 mutations that affect its interaction with PPCA may cause disease, despite the active site of the enzyme remaining intact (de Geest et al., 2002). The absence of functional PPCA leads to another condition called Galactosialidosis (GS). It is a disease that occurs due to a combined deficiency of lysosomal neuraminidase and β-galactosidase. Patients with GS have clinical and biochemical features similar to those of sialidosis (de Geest et al., 2002). They are typically attributed to the absence of neuraminidase function (de Geest et al., 2002). Both sialidosis and GS are characterized by progressive vision impairment, bilateral macular cherry-red spots, skeletal and gait abnormalities, ataxia, seizures, and myoclonic syndrome. Knockout mouse models of sialidosis (NEU1-KO), as well as GS (CathA KO), lead to the development of systemic diseases closely resembling similar human conditions (Pshezhetsky and Ashmarina, 2013; d'Azzo et al., 2015; Khan and Sergi, 2018).

2.1 Various Mechanisms of Pathogenesis Attributed to NEU1

As noted above, In addition to the catabolic role of NEU1, recent animal studies have elucidated its role in diverse cellular regulatory mechanisms. The unique and essential role of NEU1 has been discovered in regulating exocytosis, modulation of the immune response, generation of cellular matric, and carcinogenesis through desialylation of specific protein targets (Pshezhetsky and Ashmarina, 2001; Pshezhetsky and Ashmarina, 2013; Smutova et al., 2014). In order to find a therapeutic role of NEU1 in various diseases, it is essential to examine the mechanisms of pathogenesis that have been attributed to NEU1, with the subsequent relevance in a more common condition. The following paragraphs are some of the notable roles of NEU1 discovered in the most recent studies.

3 NEU1 AS A NEGATIVE REGULATOR OF LYSOSOMAL EXOCYTOSIS

The process of lysosomal exocytosis occurs under both physiological and pathological conditions (Pshezhetsky and Ashmarina, 2013). Also, this process takes place in a variety of numerous types of tissues. Thus, any alteration in this process ultimately results in an overall loss of tissue homeostasis (Andrejewski et al., 1999; Yogalingam et al., 2008; Pshezhetsky and Ashmarina, 2013). Initially, this calcium-dependent process was associated with secretory cells such as platelets, melanocytes, mast cells, neutrophils, and macrophages. However, there is evidence that lysosomal exocytosis occurs in almost all cell types, including neurons (Rodriguez et al., 1997; Kima et al., 2000).

Several studies have established that NEU1 is a negative regulator of lysosomal exocytosis (Yogalingam et al., 2008; Pshezhetsky and Hinek, 2011). It has been demonstrated that by affecting the levels of lysosomal associated membrane protein 1 (LAMP1), NEU1 negatively regulates lysosomal exocytosis (Yogalingam et al., 2008). LAMP1 has been known to be a crucial structural constituent of lysosomes. It is localized enormously in the limiting membrane of the organelle. It is scarce at the plasma membrane unless cells undergo exocytosis (Yogalingam et al., 2008; Pshezhetsky and Hinek, 2011), during which LAMP1 plays a critical role in the docking of lysosomes at the plasma membrane (Yogalingam et al., 2008). Studies have shown that NEU1-dependent cleavage of sialic acid by LAMP1 is vital in its intracellular trafficking. NEU1 controls the sialic acid content of the luminal domain of LAMP-1, its turnover rate, and subcellular distribution, which consequently determines the lysosomal exocytosis carried out by LAMP1. Animal studies have clearly shown that in *neu1*$^{-/-}$ bone marrow (BM)-derived macrophages, the lack of NEU1 results in hypersialylated LAMP-1, with a longer half-life and a tendency to accumulate in the plasmatic membrane. While silencing LAMP1 in NEU1-deficient cells leads to normalization of several lysosomes docked at the plasmatic membrane and a decline in the extent of lysosomal exocytosis (Rodriguez et al., 1997; Kima et al., 2000; d'Azzo et al., 2015).

3.1 NEU1's Deficiency-Related Lysosomal Exocytosis and Pathological Manifestations of Sialidosis

It has been established that NEU1's loss of function results in excessive extracellular release of lysosomal luminal contents from deficient cells of numerous tissues and organs (Rodriguez et al., 1997; Andrejewski et al., 1999; Kima et al., 2000; Yogalingam et al., 2008). Studies have elucidated the role of excessive lysosomal exocytosis in several pathological manifestations characteristic of sialidosis, such as splenomegaly (de Geest et al., 2002), extramedullary hematopoiesis (de Geest et al., 2002), muscle atrophy (d'Azzo et al., 2009), and hearing loss (Wu et al., 2010).

3.2 NEU1's Deficiency-Related Lysosomal Exocytosis and Neuropsychiatric Changes

Importantly, this process has been implicated in pathologies related to the central nervous system, such as neurodegeneration (d'Azzo et al., 2015; Khan and Sergi, 2018) and changes in the emotional behavior of an animal model (Ikeda et al., 2021). It is intriguing that the role of NEU1 in AD may be supported by very recent studies performed on the Neu1-KO zebrafish model. Ikeda et al. suggested the link of Neu1 with altered emotional activity, pointing to a deregulated lysosomal exocytosis, probably as suggested 8 years earlier (Annunziata et al., 2013; Ikeda et al., 2021).

3.3 NEU1's Deficiency-Related Lysosomal Exocytosis and Altered Emotional Activity

Studies investigating the effect of NEU1 deficiency on emotional activity remain limited. However, in one exciting study, behavioral analysis was performed on Neu1-knockout zebrafish (*Neu1*-KO) (Ikeda et al., 2021). It was noticed that

although Neu1-KO zebrafish exhibited normal swimming patterns similar to wild-type (WT) zebrafish, there was a decline in shoals, as well as altered patterns of interaction with different fish species. Moreover, the aggression test also demonstrated a notable reduction in aggressive behavior in Neu1-KO zebrafish. Also, in Neu1-KO zebrafish, a downregulation of the anxiety-related genes of the hypothalamic-pituitary-adrenal axis was noticed. The authors reported the underlying mechanism to be the upregulation of *lamp1a*, an activator of lysosomal exocytosis, resulting in the accumulation of several sphingoglycolipids in the Neu1-KO Zebrafish brain. Interestingly, studies have also reported that induction of anxiety may cause an upregulation of *Neu1* in the zebrafish brain along with a simultaneous reduction in Lamp1 levels. It suggests that the significance of enhanced Neu1 and reduced lysosomal exocytosis might be crucial to suppressing boldness/exploratory activity under circumstances that require caution (Ikeda et al., 2021). Overall, it can be suggested that NEU1 deficiency may also lead to abnormal emotional behavior. It can be attributed to neuronal dysfunction induced by lysosomal exocytosis.

3.4 NEU1's Deficiency-Related Lysosomal Exocytosis and Neurodegeneration and Links to Alzheimer's Disease

Several studies have suggested a link between NEU1 and neurodegeneration (Grimm et al., 2012; Annunziata et al., 2013; Boutry et al., 2018; Khan and Sergi, 2018). In one study, $Neu1^{-/-}$ mice showed a brain phenotype with signs of early aging, with the presence of amyloid deposits similar to the plaque that is characteristic of AD, which is the most common cause of dementia among older adults (Javaid et al., 2021). The histopathological examination of the $Neu1^{-/-}$ brain revealed several multifocal, eosinophilic deposits of varying size and shape, particularly in the CA3 region of the hippocampus and the fimbria with enhanced lysosomal exocytosis (Annunziata et al., 2013). These deposits were noted to have proteinaceous material stained positive with the Congo red/Chrysamine-G derivative Methoxy-X04, a compound with a high affinity for amyloid. It is to be noted that studies performed on the zebrafish model have also reported similar results (Annunziata et al., 2013). Several observations in the study asserted that the NEU1 loss might contribute to the phenotypes of AD. For instance, it was noticed that lack of NEU1 was associated with over-sialyation of amyloid precursor protein APP, demonstrating APP to be a substrate for NEU1. Also, in $Neu1^{-/-}$ hippocampal neurons, the accumulation of amyloid precursor protein (APP) was noticed to take place at a very early age. Moreover, the levels of secreted Aβ42 appeared higher in $Neu1^{-/-}$ cerebrospinal fluid and in the medium of $Neu1^{-/-}$ hippocampal cultures compared to the corresponding control samples. Finally, cerebral injection of NEU1 in an established AD mouse model showed a considerable amount of reduction in β-amyloid plaques (Annunziata et al., 2013). In addition, in a study carried out on Neu1-KO zebrafish, in the brain of Neu1-KO zebrafish, an abnormal accumulation of GM1 ganglioside was reported (Ikeda et al., 2021). This finding is crucial since it demonstrates another correlation between NEU1 and AD. Gangliosides (a family of sialic acids with glycosphingolipids) are known to be present in high concentrations in neuronal and glial membranes and are involved in the development and maintenance of neuronal cells and tissues (Yanagisawa, 2007; Grimm et al., 2012). The involvement of these gangliosides in AD pathology is a well-established fact. Various studies have demonstrated that the concentration and composition of gangliosides are different in the AD brain, both in patients and in animal models. These gangliosides appear to accumulate in the neuronal membranes and contribute to the formation of amyloid fibrils. Notably, GM1 ganglioside (GM1), has been shown to cause upregulation in AB production and is associated with early pathological changes of AD, playing a key role in Aβ assembly in the AD brain (Yanagisawa, 2007; Grimm et al., 2012). As mentioned earlier, in NEU1-deficient-brain, an abnormal amount of GM1 ganglioside was noted to be accumulated in the brain. Hence, it is plausible that another pathway in which NEU1 deficiency may lead to AD pathology is GM1 accumulation (Ikeda et al., 2021). However, the overall data regarding the storage of gangliosides in human sialidosis patients remains inconclusive. Yet some studies have elucidated the role of NEU1 in ganglioside degradation (Boutry et al., 2018). More research in this area may provide additional crucial details. In light of the abovementioned findings, it can be said that NEU1 loss of function may result in an AD-like phenotype in the sialidosis mice, thus establishing loss of NEU1 enzyme activity as a risk factor for the development of this disease (Annunziata et al., 2013; Bonten et al., 2014).

4 NEU1 AND IMMUNE SYSTEM MODULATION

NEU1 has been reported to play a critical role in immune response modulation [11,35] (Pshezhetsky and Hinek, 2011; Pshezhetsky and Ashmarina, 2018). Various studies have reported more than one type of immune receptor that is influenced by NEU1 and thus depends on it for its functioning (Pshezhetsky and Hinek, 2011). One such receptor is FcγR, through which NEU1 appears to activate phagocytosis in macrophages [36] (Seyrantepe et al., 2010). Experimental studies have shown that NEU1 expression increases 12 folds when circulating blood monocytes and monocytic cell lines differentiate into macrophages [37] (Liang et al., 2006). Animal studies showed that in a mouse model of 10% NEU1 deficient mice, macrophages and immatures exhibited more sialyation of the cell surface and a simultaneous reduction in the ability of phagocytosis of all types. Importantly, NEU1 deficiency caused this effect *via* a decline in the transduction of signals from the Fc receptors for immunoglobulin G (FcγR) as more sialylation and impaired phosphorylation of FcγR in NEU1 deficient macrophages were

noted (Liang et al., 2006; Seyrantepe et al., 2010). Moreover, there is evidence showing sialidase to be overexpressed during the activation of T cells, B cells, macrophages, and neutrophils on the surface of activated T cells, which consequently influences immune function (Amith et al., 2009). Also, it has been demonstrated that endogenous sialidase activity increases considerably during the activation of various immune cells, including T cells, B cells, and monocytes, whereas sialylation of some surface molecules decreases (Landolfi et al., 1985; Landolfi and Cook, 1986). Another receptor important in immunomodulation that has been influenced by NEU1 is the activation of cell surface Toll-like receptors (TLR), which are critical in activating immune responses during infection (Amith et al., 2009). Studies report that ligand-induced activation of TLR-2, -3, and -4 is controlled by NEU1 sialidase activation. Additionally, the interaction of activated NEU1 with TLRs has been reported to promote intracellular signaling as studies show that TLR-4-derived signaling is impaired in the cells of NEU1-deficient mice. Also, the presence of NEU1 is critical for the lipopolysaccharide (LPS)-induced interaction of TLR-4 with the signal transducer protein, MyD88, and activation of the NFkappaB signaling pathway in macrophage and dendritic cell lines (Abdulkhalek et al., 2012; Karmakar et al., 2019). Furthermore, the hyaluronic acid (HA) receptor, CD44, is involved in multiple cell-cell and cell-matrix interactions. Another immune receptor that has been suggested to be influenced by NEU1-mediated desialylation is supported by direct and indirect evidence (Pshezhetsky and Hinek, 2011).

4.1 NEU1's Deficiency Related Immune System Changes and Pathological Menefistaions of Sialidosis

Various studies report a history of recurrent infections in sialidosis patients, attributed to the impact of NEU1 deficiency on the immune system (Monti et al., 2010; Hanamsagar et al., 2012; Li et al., 2021).

4.2 NEU1's Deficiency Related Immune System Changes and Neurodegeneration

As noted earlier, NEU1 plays a critical role in activating cell surface Toll-like receptors (TLR), which are essential in triggering immune responses during infection (Landolfi and Cook, 1986). These TLRs are also present in the central nervous system cells, such as microglia and astrocytes, which are the primary cells responsible for innate immunity in the CNS (Hanamsagar et al., 2012; Li et al., 2021). The expression of TLRs in CNS cells is up-regulated by infection, inflammation, or TLR stimulation, which accelerates the innate immune response. Significantly enough, these TLRs are also known to play a role in various neurogenerative diseases, including AD pathology (Okun et al., 2009; Hanamsagar et al., 2012). Numerous mechanisms have been suggested through which TLR plays a role in AD pathology.

Results of *in vivo* studies in a double transgenic (APPswe/PSEN1dE9) mouse model of AD demonstrated a lack of TLR4 resulted in an increased cortical and hippocampal Aβ load, suggestive of a decisive role of TLR4 in the Aβ clearance by microglial cells (Arroyo et al., 2011).

Another animal study showed TLR2 deficiency was associated with an acceleration of spatial and contextual memory impairment, which was associated with an increase in Aβ42 and transforming growth factor beta1 (TGFβ1) in the brain (Schmidt et al., 1997). Moreover, an accumulating amount of data establishes the link between impaired TLR activation and a subsequent increase in amyloid burden. As noted earlier, as NEU1 is one of the crucial factors in activating the TLR, it is conceivable that NEU1 deficiency may lead to impaired TLR activation (Karmakar et al., 2019), which in turn contributes to AD pathology (Schmidt et al., 1997; Arroyo et al., 2011; Song et al., 2011). In addition, the role of NEU1 in activating macrophages is yet another potential route through which it can be linked to AD pathology (Zhang and Jiang, 2015). Finally, there is convincing evidence that NEU1 is essential for regulating numerous immune activities in the central nervous system (Khan et al., 2021).

Researchers have demonstrated that macrophages isolated from Neu1-deficient mice exhibited a reduction in phagocytosis. Also, the macrophages taken from the Neu1-deficient mice exhibited increased sialylation and impaired phosphorylation of FcR (FcRgamma 1/CD64) and considerably reduced phosphorylation of Syk kinase when treated with IgG-opsonized beads. It is evident that Neu1 activates phagocytosis in macrophages and dendritic cells through desialylation of surface receptors, mainly *via* CD64. Therefore, it can be said that Neu1 is vital for their functional integrity (Liang et al., 2006; Seyrantepe et al., 2010). Moreover, as cells were treated with exogenous Neu1, the phagocytic capability of macrophages appeared to be restored. Hence, it is plausible that FcRg1/CD64 receptors are a substrate of NEU1, and NEU1 activation phagocytosis *via* CD64 receptors may result in an anti-inflammatory environment since this brings microglia/macrophages to the M2 state, which has been reported to be essential in reducing the pathogenesis of neurodegeneration (Sackmann et al., 2017). It is a well-established fact that one of the key issues in AD pathology is the loss of balance of Aβ production and its removal (Selkoe, 1989; Selkoe and Hardy, 2016). Also, there is an elevation in soluble Aβ at an earlier stage, leading to neuronal loss and cognitive impairment and causing abnormal tau phosphorylation, thus perpetrating tauopathy and consequently causing plaque formation (Wisniewski et al., 1990; Fiala et al., 2007). Hence, it is crucial to control the trafficking of soluble oligomers to reduce pathogenesis (Ledo et al., 2013). Studies also show that microglia, instead of performing phagocytic activity, may contribute to pathology (Eikelenboom and Veerhuis, 1996; Eikelenboom et al., 2000; Bennasroune et al., 2019). But stimulating microglia to the M2 phenotype has been shown to increase their anti-inflammatory action. These microglia possess specific markers, notably CD64 (Schmidt et al., 1997; Song et al., 2011). Since NEU1 can potentially activate macrophages into the M2 state, the notion that NEU1 may play a therapeutic role in AD *via* immune activation and immunomodulation seems plausible (Khan et al., 2021).

5 NEU1'S ROLE IN ELASTIN METABOLISM

Another critical yet relatively less highlighted role of NEU1 is constituted by the integration of elastin fibers, which is crucial for the integrity of the cardiovascular and respiratory systems and central nervous systems (Bennasroune et al., 2019). NEU1 and its activating partner CathA have been demonstrated to be part of the elastin receptor. Recent studies have highlighted the crucial role in regulating elastic fiber synthesis at various stages. NEU1 plays a critical role in their modulation (Starcher et al., 2008; Antonicelli et al., 2009; Bennasroune et al., 2019). Elastin fibers constitute the major components of the extracellular matrix. They are present abundantly in tissues such as skin, the lungs, and arteries that deal with a high degree of mechanical constraints. In such tissues, elastin is the core component surrounded by microfibril mantles (Antonicelli et al., 2009). The synthesis process of elastic fibers or elastogenesis involves the activity of NEU1, which has been demonstrated by multiple studies (Starcher et al., 2008; Bennasroune et al., 2019). Elastin metabolism is enormously disrupted due to neuraminidase-1 deficiency. In one study of the murine knockout of the Neu-1 gene, an abnormal organization of elastic fibers in the aorta with a reduced level of elastin was noticed. Also, experimental studies on cultured dermal fibroblasts from patients with lysosomal β-galactosidase, PPCA, and Neu-1 deficiencies (such as congenital sialidosis and galactosialidosis (Dickson et al., 1993).

5.1 NEU1's Deficiency-Related Impact on Elastin Metabolism and Pathological Manifestations in Sialidosis

In sialidosis, NEU1 deficiency and its related errors in elastin metabolism manifest typically with abnormalities that are characteristic of the early onset of sialidosis in children (such as failure to thrive, kyphosis, and facial dysmorphism) (Annunziata et al., 2013; Sergi, 2020). This was demonstrated in experiments in which it was noted that elastogenesis in cultured dermal fibroblasts extracted from patients with deficiencies in lysosomal β-galactosidase, PPCA, and Neu-1 deficiencies (including congenital sialidosis and GS) could be reversed by transformation with Neu-1 cDNA, treatment with bacterial sialidase (Wu et al., 2010) or substitutions in the *Neu1*gene (Bonten et al., 2014). These findings suggest a critical role of NEU1 activity in the process of correct deposition and assembly of elastic fibers (Antonicelli et al., 2009; Bennasroune et al., 2019).

5.2 NEU1's Deficiency-Related Impact on Elastin Metabolism and Neurodegeneration

Another important consideration is the role of NEU1 in elastin degradation. Elastin undergoes proteolytic degradation in some physiological and pathophysiological conditions because of a profoundly low turnover rate. Thus, its degradation becomes irrevocable and lasting. This phenomenon leads to the formation of elastin-derived peptides (EDPs) (Ma et al., 2019). A recent growing body of evidence shows that EDP is crucial in the development of numerous age-related vascular diseases. It is known that EDPs can be found in the cerebrospinal fluid of healthy individuals. However, they have been associated with various central nervous system pathologies. For example, their amount has been reported to increase in patients after ischemic stroke (Ma et al., 2019; Ma et al., 2020). Moreover, there is evidence of EDP interfering in the inflammatory process of normal astrocytes. Also, they have been known to cause an increase in the proliferation and invasiveness of astrocytoma and gliomas, which may result in a poor prognosis of central nervous system-related neoplasms. Interestingly, NEU1 has been found to play a vital role in signal processes and biological activities controlled by EDPS. Signaling events typically consist of the phosphoinositide-3-kinase γ (PI3Kγ) pathway and converge to ERK1/2 and Akt activation. This role of EDPs has been linked with cardiovascular disease, respiratory disease, cancer progression, and neurodegeneration. It is to be noted that EDPS has been demonstrated to be involved in the overproduction of beta-amyloid in a model of AD (Ma et al., 2019; Ma et al., 2020; Szychowski et al., 2021), although the precise underlying pathological mechanisms remain unknown.

6 NEU1 AND OTHER CELLULAR MECHANISMS

There are various other cellular mechanisms in which NEU1 has been demonstrated to have a critical role. For instance, it is involved in insulin signaling regulation. Multiple studies have elucidated that as insulin attaches to its receptor, the receptor, in turn, rapidly interacts with NEU1 (Dridi et al., 2013). This leads to hydrolyzation of sialic acid residues present in the glycan chains of the receptor with its subsequent activation. Moreover, studies with animal models have shown a decisive role of NEU1 in glucose metabolism and energy signaling. Furthermore, studies of sialidosis patients have shown that the genetic deficiency of NEU1 results in impaired insulin-induced phosphorylation of downstream protein kinase AKT. Notably, treatment with purified NEU1 appeared to restore this impaired signaling. Thus, it is conceivable that NEU1 is important for energy metabolism and the insulin signaling pathway (Dridi et al., 2013; Alghamdi et al., 2014; Fougerat et al., 2018).

Furthermore, various studies indicate the role of NEU1 in acting as a negative regulator of malignant properties of different types of cancer cells (Pshezhetsky and Hinek, 2011). Also, some studies have elaborated on NEU1's role in regulating the cellular mitogenic response to growth factors. Experiments performed on fibroblasts taken from sialidosis patients exhibited a fairly mitogenic solid response to the same doses of PDGF-BB and IGF-II as compared to fibroblasts of normal skin, indicative of the fact that NEU1 deficiency is associated with a greater number of cell surface receptors remaining sialylated and, consequently, more responsiveness to their respective growth factors (Pshezhetsky and Hinek, 2011).

7 NEU1 AND SIALIDOSIS

As mentioned before, NEU1 deficiency is most commonly associated with sialidosis (Bonten et al., 1996; Sergi et al., 2001; Sergi, 2020). More than 40 *NEU1* disease-causing mutations have been reported thus far, resulting in sialidosis with varying severity of symptoms (d'Azzo et al., 2015; Khan and Sergi, 2018). The most common mutation to be reported is a missense mutation (Khan and Sergi, 2018). Moreover, since sialidosis is a disease with a diversified range of symptoms with varying degrees of severity, it has been noted that this diversity is essentially due to the degree of activity in the mutant enzyme. This has been attributed to the degree of activity of the mutant enzyme, giving rise to different kinds of NEU1 variants. NEU1 variants have been divided into three categories based on biochemical properties, resulting in different subtypes of sialidosis. The mutant enzyme remains catalytically inactive in the first category and fails to localize to lysosomes. The second category is the one when the mutant enzyme remains inactive; however, it is localized to lysosomes. Finally, the third category is when the mutant enzyme shows residual activity and localizes to lysosomes (Bonten et al., 2000; Khan and Sergi, 2018). Sialidosis is generally divided into two types (Sergi, 2020). Also known as "cherry-red spot myoclonus," type I sialidosis has been known to be an attenuated and non-neuropathic form of the disease. Late-onset symptoms characterize this type, generally having decreased visual acuity, progressive visual loss, bilateral macular cherry-red spots, gait abnormalities, and myoclonus (Sobral et al., 2014). There are no physical deformities, nor is there any impairment in intelligence. However, myoclonus is often present in type I sialidosis and is the hallmark of this disease (Thomas et al., 1979; d'Azzo et al., 2015). It may initially cause difficulties in fine motor movements and intention tremors but may progress to generalized seizures, which become debilitating with the course of the disease. Thus, despite having normal muscle strength and having average intelligence, patients may become wheelchair users (Caciotti et al., 2020). The degree of severity of the symptoms in patients directly correlates with the type of NEU1 mutations and the amount of residual enzyme activity (d'Azzo et al., 2015). Recent studies have reported that atypical cases of type I sialidosis exhibited myoclonus without visual symptoms and no measurable NEU1 activity. This finding is crucial as it indicates that NEU1 mutations affecting its activity may exist in the absence of characteristic features of sialidosis (Chen et al., 2006; Canafoglia et al., 2014; d'Azzo et al., 2015; Muona et al., 2015; Mohammad et al., 2018; Bou Ghannam et al., 2019). Thus, it is imperative to gather more data regarding the symptoms of atypical cases of sialidosis. Also, it would be worth inquiring about the changes in behavior or other psychological changes in such patients. As mentioned above, decreased activity of NEU1 can cause emotional and behavioral changes in animal models (Ikeda et al., 2021). On the other hand, type II sialidosis is generally regarded as a severe type of disease. Type II sialidosis has been divided into three subtypes: congenital, hydropic, and post-congenital which are characterized by onset *in utero*. This is the most severe kind of disease that may present as hydrops fetalis, neonatal ascites, or both; patients can be stillborn or die shortly after birth following a systemic and fulminant course. The clinical presentation may include facial edema, hepatosplenomegaly, and inguinal hernias at birth. Sialidosis II is an infantile type characterized by the onset between birth and 12 months. Finally, juvenile type has been described by the onset past 2 years of age (Winter et al., 1980; Caciotti et al., 2009; Mitsiakos et al., 2019). The other clinical characteristics of type II include a coarse face, hepatosplenomegaly, dysostosis multiplex, vertebral deformities, and severe mental retardation. The appearance of macular cherry-red spots, myoclonus, hearing loss, and angiokeratoma can be observed in patients who survive for longer. Life expectancy is generally short, although it may vary according to the associated mutations and the intensity of symptoms (Donati et al., 2003; d'Azzo et al., 2015; Caciotti et al., 2020).

7.1 NEU1 Deficiency in Sialidosis and Brain Changes

The involvement of the central nervous system in sialidosis is a well-established fact. However, due to the rarity of the disease, most of our understanding of CNS involvement in sialidosis comes from animal model studies (Pshezhetsky and Ashmarina, 2018). Nevertheless, with the help of neuroimaging studies, various changes in sialidosis patients are being documented now (Pshezhetsky and Ashmarina, 2018). Sialidosis II takes a fulminant course, and early demise is the typical fate (Winter et al., 1980; Caciotti et al., 2009). Along with an early-age onset of facial dysmorphism dysplasia, there are neurodegenerative changes in the brain. Neuroimaging studies in sialidosis II patients are limited. However, cerebral ultrasound studies demonstrated pachygyria in the type II sialidosis brain. At the same time, magnetic resonance imaging (MRI) showed corpus callosum hypoplasia with the continual growth of cerebral parenchyma and the dilatation of the occipital horns of the lateral ventricles (Mitsiakos et al., 2019). Hydrocephalus has also been reported in type II sialidosis patients (Donati et al., 2003).

On the other hand, type I sialidosis has a late-onset with central nervous system involvement, typically manifesting as seizures, ataxia, and visual impairment. Therefore, most neuroimaging studies are performed on sialidosis I patients (Pshezhetsky and Ashmarina, 2018). At the onset of the disease, brain MRI may appear normal. However, diffuse atrophy is commonly reported in patients with advanced type I sialidosis. Recent MRI studies of many sialidosis patients have repeatedly reported brain atrophy of varying degrees (Palmeri et al., 2000; Sekijima et al., 2013). MRI studies also show the diffused cortical atrophy compromised white matter integrity, more pronounced in the occipital lobe. Additionally, decreased connectivity from the temporal and

occipital lobes to the hippocampus and para-hippocampus has also been noted. Moreover, a compromised posterior visual pathway, with extensive involvement of the brain's posterior part, has been related to cortical blindness in sialidosis I patients (Lai et al., 2009; Sobral et al., 2014; Lu et al., 2017; Gultekin et al., 2018; Hu et al., 2018; Coppola et al., 2020).

8 NEU1 AS A THERAPEUTIC TARGET, THERAPEUTIC INTERVENTIONS FOR SIALIDOSIS: THE OBSTACLES AND THE PROGRESS SO FAR

The rarity of sialidosis and the unique biochemical nature of NEU1 are the main hindrances to developing an efficacious sialidosis treatment. However, enzyme replacement therapy (ERT) with recombinant lysosomal hydrolases has been successfully used for various non-neuropathic LSDs (Wang et al., 2005). However, it has not been effective in sialidosis, attributable to the unique properties of NEU1. Firstly, due to the absence of a functional mannose-6-phosphate recognition marker, NEU1 is not endocytosed by mammalian cells. Therefore, researchers used a recombinant NEU1 enzyme in one study, which was purified from overexpressing insect cells, and attempted ERT in $Neu1^{-/-}$ mice. There was a considerable improvement in symptoms in systemic organs after an increased initial level of NEU1 enzyme activity with a subsequent considerable reduction of lysosomal storage. Unfortunately, after 2 weeks of treatment, a severe immune response was observed in the mice towards the exogenous NEU1 enzyme. This immunogenicity of NEU1 makes it challenging to provide enzymatic replacement therapy (Wang et al., 2005). Another feature of NEU1 that makes it challenging to use as therapy is that it tends to aggregate, and its activity depends strictly on its binding with PPCA (d'Azzo et al., 2015). However, it has been suggested that NEU1's strict dependence of the enzyme on PPCA for catalytic activation may provide its therapeutic benefits (Sobral et al., 2014). Hence, chaperone-mediated therapy has been proposed and tested in mouse models (Bonten et al., 2013). Initially, a new mouse model of the non-neuropathic attenuated type I form of sialidosis was developed, carrying a V54M amino acid substitution, which has been identified in type I sialidosis patients. In these mice, a scAAV-based PPCA-mediated chaperone gene therapy study was conducted. In one-year-old $Neu1^{-/-}$; $NEU1^{V54M}$ mice with signs of type I sialidosis pathology, a single dose of the recombinant AAV vector was injected, and then these mice were sacrificed a month later. It was observed that such therapy resulted in an overall improvement of tissue pathology. Furthermore, with an increased expression of the PPCA enzyme, in the liver of the injected mice, a 3-fold increase of the $NEU1^{V54M}$ basal activity in all the tested tissues was reported. This pharmacologic, chaperone-mediated therapy has been regarded as a promising approach for other *NEU1* mutations found in patients with type I sialidosis (Bonten et al., 2013). In addition, the possibility of environmental factors affecting the residual enzymatic activity was suggested previously and has been confirmed by more recent studies (d'Azzo and Annunziata, 2020). Researchers performed experiments to find the role of the epigenetic component in the regulation of *NEU1* gene expression. It was observed that inhibiting histone deacetylases (HDACi) leads to an upregulation of NEU1 transcription as well as enzyme levels, consequently increasing its activity. HDACs are known to be involved in the regulation of cellular pathways by causing repression of metabolic gene transcription (d'Azzo and Annunziata, 2020). Thus, the treatment of *NEU1* mRNA expression with HDACi caused an upregulation of the levels of mutant *NEU1* mRNA as well as an increase in the residual activity in fibroblasts extracted from patients with Sialidosis. It is noteworthy here that inhibition of HDACi also led to an increase in the transcription of PPCA, NEU1, and β-galactosidase in the complex. Hence, it is conceivable that epigenetic factors are another way to increase NEU1 activity. Further research in this area is imperative to understand how to target NEU1 to alleviate the symptoms (d'Azzo and Annunziata, 2020). Furthermore, another recent discovery in this vein is the potential role of dietary modification in enhancing the residual NEU1 activity. In a recent study, the effect of recombinant protective protein/cathepsin A (PPCA), along with pharmacological agents and dietary compounds, was examined on the residual activity of mutant NEU1on the primary fibroblasts of a small cohort of patients with sialidosis I (Mosca et al., 2020). The study reported a small yet consistent increment in NEU1 activity in most of the tested fibroblasts. Interestingly, this study reported the beneficial effects of betaine, a natural amino acid derivative, in type I sialidosis, the less attenuated form of the disease. It was observed that betaine was administered in mouse models with residual NEU1 activity, thus mimicking type I sialidosis. An increase was noticed in levels of mutant NEU1, but oligosaccharidurie was also observed to be resolved. The notion of dietary supplements providing beneficial results for sialidosis is hopeful. More studies are warranted to confirm these results and see if such dietary modification also brings any improvement in the symptomatology of sialidosis (Mosca et al., 2020). It is worth mentioning here that dietary supplementation of betaine has also been beneficial in other neurodegenerative diseases (Sun et al., 2017; Zhao et al., 2018). All in all, the advancement in the understanding of NEU1 activity being enhanced by environmental factors can be profoundly helpful in establishing a broader range of therapeutic interventions for sialidosis patients. Lastly, there is also evidence of testing the treatment of bone marrow transplant (BMT) in type I sialidosis patients. After BMT, despite some preservation in some neurological areas, an overall decline in motor performance was noticed. Also, hematopoietic cell transplantation has been tried in a patient with type II sialidosis, but the results were inconclusive (Gupta et al., 2022).

9 NEU1 AND ALZHEIMER'S DISEASE. INVOLVEMENT OF MORE THAN ONE CELLULAR MECHANISMS

In our previous study, we elaborated on the role of NEU1 in sialidosis and its role in AD via the immune system. Since NEU1 deficiency causes impaired phagocytosis, we hypothesized that

NEU1 could be a potential therapeutic target for AD as it may enhance effective phagocytosis in the AD brain (Khan et al., 2021). In the current studies, we aimed to highlight and summarize various other cellular mechanisms in which NEU1 has been reported to be involved in recent years. For example, impaired TLR activation is another mechanism that causes an increase in amyloid burden and, thus, causes AD pathology. NEU1 deficiency has been linked with impaired TLR activation. Thus, making the notion plausible that NEU1 is linked with AD pathology *via* an impaired TLR activation [41–44]. However, underlying pathological mechanisms need to be explored further. Additionally, NEU1 being the negative regulator of lysosomal exocytosis has been extensively discussed in the previous literature. The changes noticed in the brains of *Neu1*$^{-/-}$ mice are similar to those of AD. The over-sialyation of amyloid precursor protein APP has been attributed to a lack of NEU1 deficiency. Moreover, the aggregation of these over-sialylated APP in the lysosomes, with the extracellular release of Aβ peptides *via* excessive lysosomal exocytosis, is attributed to NEU1 deficiency. As the cerebral injection of NEU1 caused a decline in β-amyloid plaques, it is possible that NEU1 could be a potential therapeutic target for the AD brain.

Importantly, similar changes were also noticed in the Zebrafish model as well. Furthermore, in the brain of Neu1-KO zebrafish, an altered pattern of aggregation of GM1 ganglioside was noted (Ikeda et al., 2021). This finding establishes yet another link between NEU1 and AD pathology. As mentioned before, GM1 ganglioside has been demonstrated to play a critical role in AB pathology by causing an increase in AB production. Hence, the accumulation of GM1 in a NEU1 deficient brain, which has exhibited changes similar to AD, further strengthens the notion that NEU1 deficiency may contribute to AD pathology. Hence, it is plausible that NEU1 scarcity may lead to ganglioside accumulation which contributes to pathological changes related to AD (Ikeda et al., 2021). The role of elastin derived peptides (EDP) and AD pathology hints toward yet another link between AD pathology and NEU1. As noted earlier, EDPs are the products of elastin degradation and have been associated with numerous central nervous system pathologies. Notably, it seems that EDPs are also involved in the overproduction of beta-amyloid, although the underlying mechanisms remain unclear. Interestingly, some research has elucidated that NEU1 plays an essential role in numerous biological processes controlled by EDP. Moreover, NEU1 is also involved in the signaling process related to EDPs. Signaling events involving NEU1 consist of a phosphoinositide-3-kinase γ (PI3Kγ) pathway, with convergence to ERK1/2 and Akt activation. Further research in this area may provide more details on this crucial link.

Another mechanism that potentially links NEU1 to AD is *via* G protein-coupled receptor (GPCR) kinases (GRKs) (Tembely et al., 2022). G protein-coupled receptor (GPCR) kinases (GRKs) are essentially a family involving seven serine/threonine kinases (GRKs 1–7) that are involved in the phosphorylation and desensitization of GPCRs. However, evidence shows that GRKs are also associated with phosphorylation of non-GPCR proteins to manipulate various other cellular responses besides GPCR-dependent mechanisms. GRKs have also been reported to be involved in the pathological phosphorylation and accumulation of tau and amyloid pathology in AD brains (Guimaraes et al., 2021). Studies have suggested their unique role in the pathological processes involved in AD, and thus, they can be a potential therapeutic target. Studies have also indicated that the pattern of expression of the GRKs in neurons is cell type-specific in the human brain in AD subjects. Additionally, an overall positive correlation has been established between GRKs 2, 3, and 6 and soluble tau found in the AD brain (Guimaraes et al., 2021). Furthermore, it has been suggested that these kinases may have direct or indirect involvement in the altered tau solubility, tau phosphorylation, as well as tau aggregation. Interestingly, there is a line of evidence that elaborates cross-talk between GPCR and the matrix metalloproteinase 9 (MMP-9) and Tyrosine kinase receptors (RTK) or TLRs signaling pathways where NEU1 plays a critical role (Cattaneo et al., 2014; Tembely et al., 2022). This provides a unique role for NEU1 in receptor transactivation processes. Researchers have found that as GPCR agonists bind to their respective cognate receptors, induction of GPCR-signaling processes using the $G\alpha_i$ proteins, as well as MMP-9 activation, takes place, which results in an elevation of NEU1 sialidase activity. As a result of this, the increased sialidase activity of NEU1, which is bound to the RTK or TLR, leads to hydrolyzation of α-2,3-sialyl residues of the receptor, ultimately causing an RTK or TLR activation. Thus, another cellular mechanism can be noted, connecting NEU1 to AD pathology, making it a potential therapeutic target.

10 FURTHER PERSPECTIVE AND CONCLUSION

An enormous amount of research has been done in recent years exploring the role of *Neu1* in numerous cellular mechanisms, and more substrates of NEU1 are being reported over time. Interestingly, some researchers have also found a role for NEU1 in the infection caused by the SARS-CoV-2 virus (Bongiovanni et al., 2021). From the discussion in this paper, it is clear that NEU1 plays a key role in a variety of cellular mechanisms, many of which are directly or indirectly associated with neurogenerative pathologies in rare diseases like sialidosis and also have been linked to highly prevalent neurodegenerative diseases like AD. We hypothesize that in the near future, there will be some evidence of a potential contributory role of NEU1 in various non-neurologic degenerative diseases. Some studies have suggested that inhibiting Neu1 activity may positively affect drug-induced liver injury (Chen et al., 2020). Down-regulation of NEU1-regulated pathways seems to reduce the progression of various types of cancer (O'Shea et al., 2014; Machado et al., 2015). Importantly, a few studies report that inhibition of surface or secreted neuraminidase may benefit chronic neuroinflammation and subsequent microglia-mediated neurodegeneration (Allendorf, 2021). On the other hand, studies report that elevating the NEU1 levels seems to have a positive, beneficial

impact on sialidosis-related CNS neurodegeneration (d'Azzo et al., 2015; Khan and Sergi, 2018). Substantially, all these investigations point to the profoundly crucial role of NEU1 in cytologic degeneration, making it a unique and important therapeutic target for neurodegeneration. We hope that these and other studies may trigger more robust investigations to pinpoint the role of NEU1 in cellular mechanisms associated with neurobiology and neurophysiology. It is our intention to help identify therapeutic strategies for diseases like AD, which continue to indelibly associate the elderly in the 21st century.

AUTHOR CONTRIBUTIONS

AK and CMS have both contributed to the manuscript in drafting and reviewing it.

REFERENCES

Abdulkhalek, S., Guo, M., Amith, S. R., Jayanth, P., and Szewczuk, M. R. (2012). G-protein Coupled Receptor Agonists Mediate Neu1 Sialidase and Matrix Metalloproteinase-9 Cross-Talk to Induce Transactivation of TOLL-like Receptors and Cellular Signaling. *Cell Signal* 24 (11), 2035–2042. doi:10.1016/j.cellsig.2012.06.016

Alghamdi, F., Guo, M., Abdulkhalek, S., Crawford, N., Amith, S. R., and Szewczuk, M. R. (2014). A Novel Insulin Receptor-Signaling Platform and its Link to Insulin Resistance and Type 2 Diabetes. *Cell Signal* 26 (6), 1355–1368. doi:10.1016/j.cellsig.2014.02.015

Allendorf, D. (2021). Role of Neuraminidase-Mediated Desialylation in Microglial Activation. Doctoral Thesis. Doctor of Philosophy (PhD). Cambridge, UK: University of Cambridge.

Amith, S. R., Jayanth, P., Franchuk, S., Siddiqui, S., Seyrantepe, V., Gee, K., et al. (2009). Dependence of Pathogen Molecule-Induced Toll-like Receptor Activation and Cell Function on Neu1 Sialidase. *Glycoconj J.* 26 (9), 1197–1212. doi:10.1007/s10719-009-9239-8

Andrejewski, N., Punnonen, E. L., Guhde, G., Tanaka, Y., Lüllmann-Rauch, R., Hartmann, D., et al. (1999). Normal Lysosomal Morphology and Function in LAMP-1-Deficient Mice. *J. Biol. Chem.* 274 (18), 12692–12701. doi:10.1074/jbc.274.18.12692

Annunziata, I., Patterson, A., Helton, D., Hu, H., Moshiach, S., Gomero, E., et al. (2013). Lysosomal NEU1 Deficiency Affects Amyloid Precursor Protein Levels and Amyloid-β Secretion via Deregulated Lysosomal Exocytosis. *Nat. Commun.* 4, 2734. doi:10.1038/ncomms3734

Antonicelli, F., Bellon, G., Lorimier, S., and Hornebeck, W. (2009). Role of the Elastin Receptor Complex (S-Gal/Cath-A/Neu-1) in Skin Repair and Regeneration. *Wound Repair Regen.* 17 (5), 631–638. doi:10.1111/j.1524-475X.2009.00525.x

Arroyo, D. S., Soria, J. A., Gaviglio, E. A., Rodriguez-Galan, M. C., and Iribarren, P. (2011). Toll-like Receptors Are Key Players in Neurodegeneration. *Int. Immunopharmacol.* 11 (10), 1415–1421. doi:10.1016/j.intimp.2011.05.006

Bennasroune, A., Romier-Crouzet, B., Blaise, S., Laffargue, M., Efremov, R. G., Martiny, L., et al. (2019). Elastic Fibers and Elastin Receptor Complex: Neuraminidase-1 Takes the Center Stage. *Matrix Biol.* 84, 57–67. doi:10.1016/j.matbio.2019.06.007

Bongiovanni, A., Cusimano, A., Annunziata, I., and d'Azzo, A. (2021). Sialylation of Host Proteins as Targetable Risk Factor for COVID-19 Susceptibility and Spreading: A Hypothesis. *FASEB Bioadv* 3 (3), 192–197. doi:10.1096/fba.2020-00073

Bonten, E., van der Spoel, A., Fornerod, M., Grosveld, G., and d'Azzo, A. (1996). Characterization of Human Lysosomal Neuraminidase Defines the Molecular Basis of the Metabolic Storage Disorder Sialidosis. *Genes. Dev.* 10 (24), 3156–3169. doi:10.1101/gad.10.24.3156

Bonten, E. J., Annunziata, I., and d'Azzo, A. (2014). Lysosomal Multienzyme Complex: Pros and Cons of Working Together. *Cell Mol. Life Sci.* 71 (11), 2017–2032. doi:10.1007/s00018-013-1538-3

Bonten, E. J., Arts, W. F., Beck, M., Covanis, A., Donati, M. A., Parini, R., et al. (2000). Novel Mutations in Lysosomal Neuraminidase Identify Functional Domains and Determine Clinical Severity in Sialidosis. *Hum. Mol. Genet.* 9 (18), 2715–2725. doi:10.1093/hmg/9.18.2715

Bonten, E. J., Campos, Y., Zaitsev, V., Nourse, A., Waddell, B., Lewis, W., et al. (2009). Heterodimerization of the Sialidase NEU1 with the Chaperone Protective Protein/cathepsin A Prevents its Premature Oligomerization. *J. Biol. Chem.* 284 (41), 28430–28441. doi:10.1074/jbc.M109.031419

Bonten, E. J., Yogalingam, G., Hu, H., Gomero, E., van de Vlekkert, D., and d'Azzo, A. (2013). Chaperone-mediated Gene Therapy with Recombinant AAV-PPCA in a New Mouse Model of Type I Sialidosis. *Biochim. Biophys. Acta* 1832 (10), 1784–1792. doi:10.1016/j.bbadis.2013.06.002

Bou Ghannam, A. S., Mehner, L. C., and Pelak, V. S. (2019). Sialidosis Type 1 without Cherry-Red Spot. *J. Neuroophthalmol.* 39 (3), 388–390. doi:10.1097/WNO.0000000000000773

Boutry, M., Branchu, J., Lustremant, C., Pujol, C., Pernelle, J., Matusiak, R., et al. (2018). Inhibition of Lysosome Membrane Recycling Causes Accumulation of Gangliosides that Contribute to Neurodegeneration. *Cell Rep.* 23 (13), 3813–3826. doi:10.1016/j.celrep.2018.05.098

Caciotti, A., Di Rocco, M., Filocamo, M., Grossi, S., Traverso, F., d'Azzo, A., et al. (2009). Type II Sialidosis: Review of the Clinical Spectrum and Identification of a New Splicing Defect with Chitotriosidase Assessment in Two Patients. *J. Neurol.* 256 (11), 1911–1915. doi:10.1007/s00415-009-5213-4

Caciotti, A., Melani, F., Tonin, R., Cellai, L., Catarzi, S., Procopio, E., et al. (2020). Type I Sialidosis, a Normosomatic Lysosomal Disease, in the Differential Diagnosis of Late-Onset Ataxia and Myoclonus: An Overview. *Mol. Genet. Metab.* 129 (2), 47–58. doi:10.1016/j.ymgme.2019.09.005

Canafoglia, L., Robbiano, A., Pareyson, D., Panzica, F., Nanetti, L., Giovagnoli, A. R., et al. (2014). Expanding Sialidosis Spectrum by Genome-wide Screening: NEU1 Mutations in Adult-Onset Myoclonus. *Neurology* 82 (22), 2003–2006. doi:10.1212/WNL.0000000000000482

Cattaneo, F., Guerra, G., Parisi, M., De Marinis, M., Tafuri, D., Cinelli, M., et al. (2014). Cell-surface Receptors Transactivation Mediated by G Protein-Coupled Receptors. *Int. J. Mol. Sci.* 15 (11), 19700–19728. doi:10.3390/ijms151119700

Chaudhary, A., Maurya, P. K., Yadav, B. S., Singh, S., and Mani, A. (2018). Current Therapeutic Targets for Alzheimer's Disease. *J. Biomed.* 3 (3), 74–84. doi:10.7150/jbm.26783

Chen, C. M., Lai, S. C., Chen, I. C., Hsu, K. C., Lyu, R. K., Ro, L. S., et al. (2006). First Report of Two Taiwanese Siblings with Sialidosis Type I: a 10-year Follow-Up Study. *J. Neurol. Sci.* 247 (1), 65–69. doi:10.1016/j.jns.2006.03.013

Chen, S., Li, M., Jiang, W., Zheng, H., Qi, L. W., and Jiang, S. (2020). The Role of Neu1 in the Protective Effect of Dipsacoside B on Acetaminophen-Induced Liver Injury. *Ann. Transl. Med.* 8 (13), 823. doi:10.21037/atm-19-3850

Coppola, A., Iannicciello, M., Vanli-Yavuz, E. N., Rossi, S., Simonelli, F., Castellotti, B., et al. (2020). Diagnosis and Management of Type 1 Sialidosis: Clinical Insights from Long-Term Care of Four Unrelated Patients. *Brain Sci.* 10 (8), 506. doi:10.3390/brainsci10080506

d'Azzo, A., and Annunziata, I. (2020). Transcription Factor Competition Regulates Lysosomal Biogenesis and Autophagy. *Mol. Cell Oncol.* 7 (2), 1685840. doi:10.1080/23723556.2019.1685840

d'Azzo, A., Machado, E., and Annunziata, I. (2015). Pathogenesis, Emerging Therapeutic Targets and Treatment in Sialidosis. *Expert Opin. Orphan Drugs* 3 (5), 491–504. doi:10.1517/21678707.2015.1025746

d'Azzo, A., Kolodny, E. H., Bonten, E., and Annunziata, I. (2009). *Storage Disease of the Reticuloendothelial System*. New York: Nathan and Oski's.

de Geest, N., Bonten, E., Mann, L., de Sousa-Hitzler, J., Hahn, C., and d'Azzo, A. (2002). Systemic and Neurologic Abnormalities Distinguish the Lysosomal Disorders Sialidosis and Galactosialidosis in Mice. *Hum. Mol. Genet.* 11 (12), 1455–1464. doi:10.1093/hmg/11.12.1455

Dickson, D. W., Lee, S. C., Mattiace, L. A., Yen, S. H., and Brosnan, C. (1993). Microglia and Cytokines in Neurological Disease, with Special Reference to AIDS and Alzheimer's Disease. *Glia* 7 (1), 75–83. doi:10.1002/glia.440070113

Donati, M. A., Caciotti, A., Bardelli, T., Dani, C., d'Azzo, A., Morrone, A., et al. (2003). Congenital Sialidosis - from Hydrops Fetalis to Hydrocephalus. *Italian J. Pediatr.* 29, 404–410.

Dridi, L., Seyrantepe, V., Fougerat, A., Pan, X., Bonneil, E., Thibault, P., et al. (2013). Positive Regulation of Insulin Signaling by Neuraminidase 1. *Diabetes* 62 (7), 2338–2346. doi:10.2337/db12-1825

Eikelenboom, P., Rozemuller, A. J., Hoozemans, J. J., Veerhuis, R., and van Gool, W. A. (2000). Neuroinflammation and Alzheimer Disease: Clinical and Therapeutic Implications. *Alzheimer Dis. Assoc. Disord.* 14 (Suppl. 1), S54–S61. doi:10.1097/00002093-200000001-00009

Eikelenboom, P., and Veerhuis, R. (1996). The Role of Complement and Activated Microglia in the Pathogenesis of Alzheimer's Disease. *Neurobiol. Aging* 17 (5), 673–680. doi:10.1016/0197-4580(96)00108-x

Fiala, M., Cribbs, D. H., Rosenthal, M., and Bernard, G. (2007). Phagocytosis of Amyloid-Beta and Inflammation: Two Faces of Innate Immunity in Alzheimer's Disease. *J. Alzheimers Dis.* 11 (4), 457–463. doi:10.3233/jad-2007-11406

Fougerat, A., Pan, X., Smutova, V., Heveker, N., Cairo, C. W., Issad, T., et al. (2018). Neuraminidase 1 Activates Insulin Receptor and Reverses Insulin Resistance in Obese Mice. *Mol. Metab.* 12, 76–88. doi:10.1016/j.molmet.2018.03.017

Glanz, V. Y., Myasoedova, V. A., Grechko, A. V., and Orekhov, A. N. (2019). Sialidase Activity in Human Pathologies. *Eur. J. Pharmacol.* 842, 345–350. doi:10.1016/j.ejphar.2018.11.014

Grimm, M. O., Zinser, E. G., Grösgen, S., Hundsdörfer, B., Rothhaar, T. L., Burg, V. K., et al. (2012). Amyloid Precursor Protein (APP) Mediated Regulation of Ganglioside Homeostasis Linking Alzheimer's Disease Pathology with Ganglioside Metabolism. *PLoS One* 7 (3), e34095. doi:10.1371/journal.pone.0034095

Guimarães, T. R., Swanson, E., Kofler, J., and Thathiah, A. (2021). G Protein-Coupled Receptor Kinases Are Associated with Alzheimer's Disease Pathology. *Neuropathol. Appl. Neurobiol.* 47 (7), 942–957. doi:10.1111/nan.12742

Gultekin, M., Bayramov, R., Karaca, C., and Acer, N. (2018). Sialidosis Type I Presenting with a Novel Mutation and Advanced Neuroimaging Features. *Neurosci. (Riyadh)* 23 (1), 57–61. doi:10.17712/nsj.2018.1.20170328

Gupta, A. O., Patterson, M. C., Wood, T., Eisengart, J. B., Orchard, P. J., and Lund, T. C. (2022). Hematopoietic Cell Transplantation for Sialidosis Type I. *Mol. Genet. Metab. Rep.* 30, 100832. doi:10.1016/j.ymgmr.2021.100832

Hanamsagar, R., Hanke, M. L., and Kielian, T. (2012). Toll-like Receptor (TLR) and Inflammasome Actions in the Central Nervous System. *Trends Immunol.* 33 (7), 333–342. doi:10.1016/j.it.2012.03.001

Hu, S. C., Hung, K. L., Chen, H. J., and Lee, W. T. (2018). Seizure Remission and Improvement of Neurological Function in Sialidosis with Perampanel Therapy. *Epilepsy Behav. Case Rep.* 10, 32–34. doi:10.1016/j.ebcr.2018.02.005

Ikeda, A., Komamizu, M., Hayashi, A., Yamasaki, C., Okada, K., Kawabe, M., et al. (2021). Neu1 Deficiency Induces Abnormal Emotional Behavior in Zebrafish. *Sci. Rep.* 11 (1), 13477. doi:10.1038/s41598-021-92778-9

Javaid, S. F., Giebel, C., Khan, M. A., and Hashim, M. J. (2021). Epidemiology of Alzheimer's Disease and Other Dementias: Rising Global Burden and Forecasted Trends. *F1000Res* 10, 425. doi:10.12688/f1000research.50786.1

Karmakar, J., Roy, S., and Mandal, C. (2019). Modulation of TLR4 Sialylation Mediated by a Sialidase Neu1 and Impairment of its Signaling in Leishmania Donovani Infected Macrophages. *Front. Immunol.* 10, 2360. doi:10.3389/fimmu.2019.02360

Khan, A., Das, S., and Sergi, C. (2021). Therapeutic Potential of Neu1 in Alzheimer's Disease via the Immune System. *Am. J. Alzheimers Dis. Other Demen* 36, 1533317521996147. doi:10.1177/1533317521996147

Khan, A., and Sergi, C. (2018). Sialidosis: A Review of Morphology and Molecular Biology of a Rare Pediatric Disorder. *Diagn. (Basel)* 8 (2), 29. doi:10.3390/diagnostics8020029

Kima, P. E., Burleigh, B., and Andrews, N. W. (2000). Surface-targeted Lysosomal Membrane Glycoprotein-1 (Lamp-1) Enhances Lysosome Exocytosis and Cell Invasion by Trypanosoma Cruzi. *Cell Microbiol.* 2 (6), 477–486. doi:10.1046/j.1462-5822.2000.00071.x

Lai, S. C., Chen, R. S., Wu Chou, Y. H., Chang, H. C., Kao, L. Y., Huang, Y. Z., et al. (2009). A Longitudinal Study of Taiwanese Sialidosis Type 1: an Insight into the Concept of Cherry-Red Spot Myoclonus Syndrome. *Eur. J. Neurol.* 16 (8), 912–919. doi:10.1111/j.1468-1331.2009.02622.x

Landolfi, N. F., and Cook, R. G. (1986). Activated T-Lymphocytes Express Class I Molecules Which Are Hyposialylated Compared to Other Lymphocyte Populations. *Mol. Immunol.* 23 (3), 297–309. doi:10.1016/0161-5890(86)90057-x

Landolfi, N. F., Leone, J., Womack, J. E., and Cook, R. G. (1985). Activation of T Lymphocytes Results in an Increase in H-2-Encoded Neuraminidase. *Immunogenetics* 22 (2), 159–167. doi:10.1007/BF00563513

Ledo, J. H., Azevedo, E. P., Clarke, J. R., Ribeiro, F. C., Figueiredo, C. P., Foguel, D., et al. (2013). Amyloid-β Oligomers Link Depressive-like Behavior and Cognitive Deficits in Mice. *Mol. Psychiatry* 18 (10), 1053–1054. doi:10.1038/mp.2012.168

Li, L., Acioglu, C., Heary, R. F., and Elkabes, S. (2021). Role of Astroglial Toll-like Receptors (TLRs) in Central Nervous System Infections, Injury and Neurodegenerative Diseases. *Brain Behav. Immun.* 91, 740–755. doi:10.1016/j.bbi.2020.10.007

Liang, F., Seyrantepe, V., Landry, K., Ahmad, R., Ahmad, A., Stamatos, N. M., et al. (2006). Monocyte Differentiation Up-Regulates the Expression of the Lysosomal Sialidase, Neu1, and Triggers its Targeting to the Plasma Membrane via Major Histocompatibility Complex Class II-Positive Compartments. *J. Biol. Chem.* 281 (37), 27526–27538. doi:10.1074/jbc.M605633200

Lowden, J. A., and O'Brien, J. S. (1979). Sialidosis: a Review of Human Neuraminidase Deficiency. *Am. J. Hum. Genet.* 31 (1), 1–18.

Lu, C. S., Ng, S. H., Lai, S. C., Kao, L. Y., Liu, L., Lin, W. Y., et al. (2017). Cortical Damage in the Posterior Visual Pathway in Patients with Sialidosis Type 1. *Brain Imaging Behav.* 11 (1), 214–223. doi:10.1007/s11682-016-9517-6

Ma, C., Su, J., Sun, Y., Feng, Y., Shen, N., Li, B., et al. (2019). Significant Upregulation of Alzheimer's β-Amyloid Levels in a Living System Induced by Extracellular Elastin Polypeptides. *Angew. Chem. Int. Ed. Engl.* 58 (51), 18703–18709. doi:10.1002/anie.201912399

Ma, J., Ma, C., Li, J., Sun, Y., Ye, F., Liu, K., et al. (2020). Extracellular Matrix Proteins Involved in Alzheimer's Disease. *Chemistry* 26 (53), 12101–12110. doi:10.1002/chem.202000782

Machado, E., White-Gilbertson, S., van de Vlekkert, D., Janke, L., Moshiach, S., Campos, Y., et al. (2015). Regulated Lysosomal Exocytosis Mediates Cancer Progression. *Sci. Adv.* 1 (11), e1500603. doi:10.1126/sciadv.1500603

Mitsiakos, G., Gialamprinou, D., Chouchou, P., Chatziioannidis, I., and Karagianni, P. (2019). Identification of a Homozygous Deletion of the NEU1 Gene in a Patient with Type II Sialidosis Presenting Isolated Fetal Ascites and Central Nervous System Hypoplasia. *Hippokratia* 23 (4), 169–171.

Miyagi, T., and Yamaguchi, K. (2012). Mammalian Sialidases: Physiological and Pathological Roles in Cellular Functions. *Glycobiology* 22 (7), 880–896. doi:10.1093/glycob/cws057

Mohammad, A. N., Bruno, K. A., Hines, S., and Atwal, P. S. (2018). Type 1 Sialidosis Presenting with Ataxia, Seizures and Myoclonus with No Visual Involvement. *Mol. Genet. Metab. Rep.* 15, 11–14. doi:10.1016/j.ymgmr.2017.12.005

Monti, E., Bonten, E., D'Azzo, A., Bresciani, R., Venerando, B., Borsani, G., et al. (2010). Sialidases in Vertebrates: a Family of Enzymes Tailored for Several Cell Functions. *Adv. Carbohydr. Chem. Biochem.* 64, 403–479. doi:10.1016/S0065-2318(10)64007-3

Mosca, R., van de Vlekkert, D., Campos, Y., Fremuth, L. E., Cadaoas, J., Koppaka, V., et al. (2020). Conventional and Unconventional Therapeutic Strategies for Sialidosis Type I. *J. Clin. Med.* 9 (3), 695. doi:10.3390/jcm9030695

Muona, M., Berkovic, S. F., Dibbens, L. M., Oliver, K. L., Maljevic, S., Bayly, M. A., et al. (2015). A Recurrent De Novo Mutation in KCNC1 Causes Progressive Myoclonus Epilepsy. *Nat. Genet.* 47 (1), 39–46. doi:10.1038/ng.3144

O'Shea, L. K., Abdulkhalek, S., Allison, S., Neufeld, R. J., and Szewczuk, M. R. (2014). Therapeutic Targeting of Neu1 Sialidase with Oseltamivir Phosphate (Tamiflu(R)) Disables Cancer Cell Survival in Human Pancreatic Cancer with Acquired Chemoresistance. *Onco Targets Ther.* 7, 117–134. doi:10.2147/OTT.S55344

Okun, E., Griffioen, K. J., Lathia, J. D., Tang, S. C., Mattson, M. P., and Arumugam, T. V. (2009). Toll-like Receptors in Neurodegeneration. *Brain Res. Rev.* 59 (2), 278–292. doi:10.1016/j.brainresrev.2008.09.001

Palmeri, S., Villanova, M., Malandrini, A., van Diggelen, O. P., Huijmans, J. G., Ceuterick, C., et al. (2000). Type I Sialidosis: a Clinical, Biochemical and Neuroradiological Study. *Eur. Neurol.* 43 (2), 88–94. doi:10.1159/000008141

Pshezhetsky, A. V., and Ashmarina, L. I. (2013). Desialylation of Surface Receptors as a New Dimension in Cell Signaling. *Biochem. (Mosc)* 78 (7), 736–745. doi:10.1134/S0006297913070067

Pshezhetsky, A. V., and Ashmarina, M. (2018). Keeping it Trim: Roles of Neuraminidases in CNS Function. *Glycoconj J.* 35 (4), 375–386. doi:10.1007/s10719-018-9837-4

Pshezhetsky, A. V., and Ashmarina, M. (2001). Lysosomal Multienzyme Complex: Biochemistry, Genetics, and Molecular Pathophysiology. *Prog. Nucleic Acid. Res. Mol. Biol.* 69, 81–114. doi:10.1016/s0079-6603(01)69045-7

Pshezhetsky, A. V., and Hinek, A. (2011). Where Catabolism Meets Signalling: Neuraminidase 1 as a Modulator of Cell Receptors. *Glycoconj J.* 28 (7), 441–452. doi:10.1007/s10719-011-9350-5

Pshezhetsky, A. V., Richard, C., Michaud, L., Igdoura, S., Wang, S., Elsliger, M. A., et al. (1997). Cloning, Expression and Chromosomal Mapping of Human Lysosomal Sialidase and Characterization of Mutations in Sialidosis. *Nat. Genet.* 15 (3), 316–320. doi:10.1038/ng0397-316

Rodríguez, A., Webster, P., Ortego, J., and Andrews, N. W. (1997). Lysosomes Behave as Ca2+-Regulated Exocytic Vesicles in Fibroblasts and Epithelial Cells. *J. Cell Biol.* 137 (1), 93–104. doi:10.1083/jcb.137.1.93

Sackmann, V., Ansell, A., Sackmann, C., Lund, H., Harris, R. A., Hallbeck, M., et al. (2017). Anti-inflammatory (M2) Macrophage Media Reduce Transmission of Oligomeric Amyloid Beta in Differentiated SH-Sy5y Cells. *Neurobiol. Aging* 60, 173–182. doi:10.1016/j.neurobiolaging.2017.08.022

Schmidt, M., Fahnenstich, H., Haverkamp, F., Platz, H., Hansmann, M., and Bartmann, P. (1997). Sialidosis and Galactosialidosis as the Cause of Non-immunologic Hydrops Fetalis. *Z Geburtshilfe Neonatol.* 201 (5), 177–180.

Sekijima, Y., Nakamura, K., Kishida, D., Narita, A., Adachi, K., Ohno, K., et al. (2013). Clinical and Serial MRI Findings of a Sialidosis Type I Patient with a Novel Missense Mutation in the NEU1 Gene. *Intern Med.* 52 (1), 119–124. doi:10.2169/internalmedicine.52.8901

Selkoe, D. J. (1989). Amyloid Beta Protein Precursor and the Pathogenesis of Alzheimer's Disease. *Cell* 58 (4), 611–612. doi:10.1016/0092-8674(89)90093-7

Selkoe, D. J., and Hardy, J. (2016). The Amyloid Hypothesis of Alzheimer's Disease at 25 Years. *EMBO Mol. Med.* 8 (6), 595–608. doi:10.15252/emmm.201606210

Sergi, C., Beedgen, B., Kopitz, J., Zilow, E., Zoubaa, S., Otto, H. F., et al. (1999). Refractory Congenital Ascites as a Manifestation of Neonatal Sialidosis: Clinical, Biochemical and Morphological Studies in a Newborn Syrian Male Infant. *Am. J. Perinatol.* 16 (3), 133–141. doi:10.1055/s-2007-993847

Sergi, C., Penzel, R., Uhl, J., Zoubaa, S., Dietrich, H., Decker, N., et al. (2001). Prenatal Diagnosis and Fetal Pathology in a Turkish Family Harboring a Novel Nonsense Mutation in the Lysosomal Alpha-N-Acetyl-Neuraminidase (Sialidase) Gene. *Hum. Genet.* 109 (4), 421–428. doi:10.1007/s004390100592

Sergi, C. M. (2020). "Sialidosis and Galactosialidosis: Molecular Mechanism and Therapeutic Effect," in *Neurochemistry of Metabolic Diseases: Lysosomal Storage Diseases, Phenylketonuria, and Canavan Disease*. Editor S. Surendran. 3rd ed (Hauppauge, NY: Nova Science Publishers Inc).

Serrano-Pozo, A., Frosch, M. P., Masliah, E., and Hyman, B. T. (2011). Neuropathological Alterations in Alzheimer Disease. *Cold Spring Harb. Perspect. Med.* 1 (1), a006189. doi:10.1101/cshperspect.a006189

Seyrantepe, V., Iannello, A., Liang, F., Kanshin, E., Jayanth, P., Samarani, S., et al. (2010). Regulation of Phagocytosis in Macrophages by Neuraminidase 1. *J. Biol. Chem.* 285 (1), 206–215. doi:10.1074/jbc.M109.055475

Smutova, V., Albohy, A., Pan, X., Korchagina, E., Miyagi, T., Bovin, N., et al. (2014). Structural Basis for Substrate Specificity of Mammalian Neuraminidases. *PLoS One* 9 (9), e106320. doi:10.1371/journal.pone.0106320

Sobral, I., Cachulo, M. d. L., Figueira, J., and Silva, R. (2014). Sialidosis Type I: Ophthalmological Findings. *Case Rep.* 2014, bcr2014205871. doi:10.1136/bcr-2014-205871

Song, M., Jin, J., Lim, J. E., Kou, J., Pattanayak, A., Rehman, J. A., et al. (2011). TLR4 Mutation Reduces Microglial Activation, Increases Aβ Deposits and Exacerbates Cognitive Deficits in a Mouse Model of Alzheimer's Disease. *J. Neuroinflammation* 8, 92. doi:10.1186/1742-2094-8-92

Starcher, B., d'Azzo, A., Keller, P. W., Rao, G. K., Nadarajah, D., and Hinek, A. (2008). Neuraminidase-1 Is Required for the Normal Assembly of Elastic Fibers. *Am. J. Physiol. Lung Cell Mol. Physiol.* 295 (4), L637–L647. doi:10.1152/ajplung.90346.2008

Sun, J., Wen, S., Zhou, J., and Ding, S. (2017). Association between Malnutrition and Hyperhomocysteine in Alzheimer's Disease Patients and Diet Intervention of Betaine. *J. Clin. Lab. Anal.* 31 (5), e22090. doi:10.1002/jcla.22090

Szychowski, K. A., Skóra, B., and Wójtowicz, A. K. (2021). Elastin-Derived Peptides in the Central Nervous System: Friend or Foe *Cell Mol. Neurobiol*. doi:10.1007/s10571-021-01140-0

Tembely, D., Henry, A., Vanalderwiert, L., Toussaint, K., Bennasroune, A., Blaise, S., et al. (2022). The Elastin Receptor Complex: An Emerging Therapeutic Target against Age-Related Vascular Diseases. *Front. Endocrinol. (Lausanne)* 13, 815356. doi:10.3389/fendo.2022.815356

Thomas, P. K., Abrams, J. D., Swallow, D., and Stewart, G. (1979). Sialidosis Type 1: Cherry Red Spot-Myoclonus Syndrome with Sialidase Deficiency and Altered Electrophoretic Mobilities of Some Enzymes Known to Be Glycoproteins. 1. Clinical Findings. *J. Neurol. Neurosurg. Psychiatry* 42 (10), 873–880. doi:10.1136/jnnp.42.10.873

Uhl, J., Penzel, R., Sergi, C., Kopitz, J., Otto, H. F., and Cantz, M. (2002). Identification of a CTL4/Neu1 Fusion Transcript in a Sialidosis Patient. *FEBS Lett.* 521 (1-3), 19–23. doi:10.1016/s0014-5793(02)02748-5

Vinogradova, M. V., Michaud, L., Mezentsev, A. V., Lukong, K. E., El-Alfy, M., Morales, C. R., et al. (1998). Molecular Mechanism of Lysosomal Sialidase Deficiency in Galactosialidosis Involves its Rapid Degradation. *Biochem. J.* 330 (Pt 2), 641–650. doi:10.1042/bj3300641

Wang, D., Bonten, E. J., Yogalingam, G., Mann, L., and d'Azzo, A. (2005). Short-term, High Dose Enzyme Replacement Therapy in Sialidosis Mice. *Mol. Genet. Metab.* 85 (3), 181–189. doi:10.1016/j.ymgme.2005.03.007

Winter, R. M., Swallow, D. M., Baraitser, M., and Purkiss, P. (1980). Sialidosis Type 2 (Acid Neuraminidase Deficiency): Clinical and Biochemical Features of a Further Case. *Clin. Genet.* 18 (3), 203–210. doi:10.1111/j.1399-0004.1980.tb00873.x

Wisniewski, H. M., Vorbrodt, A. W., Wegiel, J., Morys, J., and Lossinsky, A. S. (1990). Ultrastructure of the Cells Forming Amyloid Fibers in Alzheimer Disease and Scrapie. *Am. J. Med. Genet. Suppl.* 7, 287–297. doi:10.1002/ajmg.1320370757

Wu, X., Steigelman, K. A., Bonten, E., Hu, H., He, W., Ren, T., et al. (2010). Vacuolization and Alterations of Lysosomal Membrane Proteins in Cochlear Marginal Cells Contribute to Hearing Loss in Neuraminidase 1-deficient Mice. *Biochim. Biophys. Acta* 1802 (2), 259–268. doi:10.1016/j.bbadis.2009.10.008

Yamaguchi, K., Hata, K., Koseki, K., Shiozaki, K., Akita, H., Wada, T., et al. (2005). Evidence for Mitochondrial Localization of a Novel Human Sialidase (NEU4). *Biochem. J.* 390 (Pt 1), 85–93. doi:10.1042/BJ20050017

Yanagisawa, K. (2007). Role of Gangliosides in Alzheimer's Disease. *Biochim. Biophys. Acta* 1768 (8), 1943–1951. doi:10.1016/j.bbamem.2007.01.018

Yogalingam, G., Bonten, E. J., van de Vlekkert, D., Hu, H., Moshiach, S., Connell, S. A., et al. (2008). Neuraminidase 1 Is a Negative Regulator of Lysosomal Exocytosis. *Dev. Cell* 15 (1), 74–86. doi:10.1016/j.devcel.2008.05.005

Zhang, F., and Jiang, L. (2015). Neuroinflammation in Alzheimer's Disease. *Neuropsychiatr. Dis. Treat.* 11, 243–256. doi:10.2147/NDT.S75546

Zhao, G., He, F., Wu, C., Li, P., Li, N., Deng, J., et al. (2018). Betaine in Inflammation: Mechanistic Aspects and Applications. *Front. Immunol.* 9, 1070. doi:10.3389/fimmu.2018.01070

Conflict of Interest: The authors declare that the research was conducted in the absence of any commercial or financial relationships that could be construed as a potential conflict of interest.

frontiers | Frontiers in Pharmacology

ORIGINAL RESEARCH
published: 08 July 2022
doi: 10.3389/fphar.2022.925828

Shumian Capsule Improves the Sleep Disorder and Mental Symptoms Through Melatonin Receptors in Sleep-Deprived Mice

Wenhua Li[1†], *Yinlong Cheng*[1†], *Yi Zhang*[2], *Yazhi Qian*[1], *Mo Wu*[1], *Wei Huang*[1], *Nan Yang*[1*] *and Yanyong Liu*[1,2*]

[1]Department of Pharmacology, Institute of Basic Medical Sciences, Chinese Academy of Medical Sciences and School of Basic Medicine, Peking Union Medical College, Beijing, China, [2]Medical College, Tibet University, Lhasa, China

Healthy sleep is vital to maintaining the body's homeostasis. With the development of modern society, sleep disorder has gradually become one of the most epidemic health problems worldwide. Shumian capsule (SMC), a kind of traditional Chinese medicine (TCM) commonly used for insomnia, exhibits antidepressant and sedative effects in clinical practice. However, the underlying mechanisms have not been fully clarified. With the aid of a network pharmacology approach and function enrichment analysis, we identified the involvement of melatonin receptors in the antidepressant and sedative effects of SMC. In sleep-deprived mice, SMC treatment significantly alleviated insomnia and relevant mental alterations by improving both sleep latency and sleep duration. However, ramelteon, a selective melatonin receptor agonist that has been approved for the treatment of insomnia, only improved sleep latency. Additionally, SMC exhibited comparable effects on mental alterations with ramelteon as determined by an open-field test (OFT) and forced swimming test (FST). Mechanistically, we revealed that the melatonin receptor MT1 and MT2 signaling pathways involved the therapeutic effects of SMC. In addition to the single effect of traditional melatonin receptor agonists on treating sleep onset insomnia, SMC had therapeutic potential for various sleep disorders, such as sleep onset insomnia and sleep maintenance insomnia. Convergingly, our findings provide theoretical support for the clinical application of SMC.

Keywords: sleep disorder, sleep deprivation, Shumian capsule, traditional Chinese medicine, melatonin receptor

OPEN ACCESS

Edited by:
George Barreto,
University of Limerick, Ireland

Reviewed by:
Gangling Chen,
China Pharmaceutical University, China
Xiangying Kong,
China Academy of Chinese Medical Sciences, China

***Correspondence:**
Nan Yang
yangnan@ibms.pumc.edu.cn
Yanyong Liu
yanyongliu@ibms.pumc.edu.cn

[†]These authors have contributed equally to this work and share first authorship

Specialty section:
This article was submitted to Neuropharmacology, a section of the journal Frontiers in Pharmacology

Received: *21 April 2022*
Accepted: *23 May 2022*
Published: *08 July 2022*

Citation:
Li W, Cheng Y, Zhang Y, Qian Y, Wu M, Huang W, Yang N and Liu Y (2022) Shumian Capsule Improves the Sleep Disorder and Mental Symptoms Through Melatonin Receptors in Sleep-Deprived Mice. Front. Pharmacol. 13:925828. doi: 10.3389/fphar.2022.925828

1 INTRODUCTION

As one of the most fundamental physiological activities, sleep is essential for many physiological functions, such as energy conservation, modulation of the immune system, brain waste clearance, cognition, and memory (Zielinski et al., 2016). With increasing social competition, people spend more time on studies and work, which always causes chronic sleep deprivation and subsequent health crises. At present, almost a quarter of the population in the world has been plagued by sleep disorders (Fang et al., 2019). Sleep disorders involve various aspects and patterns of sleep difficulties, which are often complicated by mental disorders, including post-traumatic stress disorder, major depression disorder, generalized anxiety disorder, and bipolar disorder (Smith et al., 2005).

Hypnotics are the main strategy of pharmacological intervention to treat sleep disorders. So far, commonly used hypnotics include benzodiazepines and non-benzodiazepines, as well as other medications such as melatonin receptor agonists, orexin receptor antagonists, antidepressants, and antihistamines (Feng et al., 2018; Pavlova and Latreille, 2019). However, benzodiazepines and non-benzodiazepines, antidepressants, and antihistamines have shown various side effects, such as headache, drowsiness, dizziness, grogginess, and withdrawal symptoms (Sateia et al., 2017; Feng et al., 2018). Melatonin receptor agonists (e.g., ramelteon) and orexin receptor antagonists (e.g., suvorexant) represent a new class of medications for the treatment of insomnia by acting on their respective receptor sites, but they were reported to be only applicable to treat specific types of sleep disorder (Sateia et al., 2017).

Traditional Chinese medicine (TCM) is usually processed with several combined herbs, whose therapeutic efficacy has been well recognized worldwide. In contrast to chemical drugs, multi-drug combinations and multi-target interaction endow TCM with a complex system of medical theory and practice, which is supposed to maximize their therapeutic efficacy by inducing synergic effects and simultaneously reducing possible side effects (Zhang Y et al., 2020). Shumian capsule (SMC) is a kind of TCM capsule, mainly composed of eight herbs: Ziziphi Spinosae Semen, Bupleuri Radix, Paeoniae Radix Alba, Albiziae Flos, Albiziae Cortex, *Bombyx batryticatus*, Cicadae Periostracum, and Junci Medulla. According to the theory of Traditional Chinese Medicine, Ziziphi Spinosae Semen is the sovereign medicinal, which nourishes the heart and emolliates the liver to tranquilize. Bupleuri Radix soothes the liver and removes qi stagnation, while Paeoniae Radix Alba nourishes the blood and emolliates the liver; both are the minister medicines. Albiziae Flos and Albiziae Cortex remove the depression to tranquilize; Cicadae Periostracum dispels wind, arrests convulsions, and removes phlegm to tranquilize; *B. batryticatus* disperses wind and heat to tranquilize; those four ingredients are the assistant medicines. In addition, Junci Medulla clears heart fire serving as the assistant and courier medicinal. All the ingredients in the formula combined possess the actions of soothing the liver, removing depression, and nourishing the heart to tranquilize. Several clinical studies have reported that SMC safely improves sleep quality in insomnia patients with depression and anxiety, and significantly alleviates the symptoms of insomnia, anxiety, and depression in convalescent patients of COVID-19 infection (Li et al., 2021; Wang et al., 2021; Chen et al., 2022). A systematic review and meta-analysis also confirmed the safety of SMC in the clinical application (Wang et al., 2021). However, its underlying molecular mechanisms remain unclear.

Currently, network pharmacology has become a novel and powerful solution for TCM drug evaluation and mechanism research (Zhang et al., 2019). In this study, we performed a protein-protein interaction (PPI) analysis on the intersection targets of SMC and insomnia predicted by the STRING database and constructed the drug component target disease network diagram. The function enrichment analyses were also adopted to explore the neuroregulatory activities of SMC. Our findings demonstrated that SMC improved sleep disorder through melatonin receptors (MT) MT1 and MT2 in sleep-deprived mice.

2 MATERIALS AND METHODS

2.1 Network Pharmacology Analysis

2.1.1 Identifying Targets From Active Ingredients of SMC

The active ingredients and targets of SMC were obtained using the traditional Chinese medicine systems pharmacology database and analysis platform (TCMSP) (https://tcmsp-e.com/) (screening conditions: the bioavailability (OB) ≥ 30% and drug-like properties (DL) ≥ 0.18). The data of Ziziphi Spinosae Semen, Bupleuri Radix, Paeoniae Radix Alba, and Junci Medulla were obtained from TCMSP. Partial active ingredients and targets of Albiziae Flos and Albiziae Cortex were got from the ETCM database (https://tcmip.cn/). The active ingredients of Albiziae Flos, Albiziae Cortex, *B. batryticatus*, and Cicadae Periostracum were supplemented by the Chemistry Professional Database of Chinese Academy of Sciences (http://www.organchem.csdb.cn [1978-2016]), traditional Chinese medicine database YATCM (http://cadd.pharmacy.nankai.edu.cn/yatcm/) and related article report, while the potential targets were predicted by SwissTargetPrediction website (http://swisstargetprediction.ch/). The file "drug" was generated by screening out the unqualified active ingredients (screening conditions: the bioavailability (OB) ≥ 30% and drug-like properties (DL) ≥ 0.18) and converting the target information into gene symbols in R software.

2.1.2 Searching Targets of Insomnia

The insomnia-related protein targets were screened through the Uniprot database (https://www.uniprot.org/) using the keyword "insomnia" and setting the species as "human". The file "disease" was generated by downloading the screened genes.

2.1.3 Predicting the Potential Targets of SMC for Insomnia Therapy

The target gene data of diseases and drugs were imported into the software "R for Windows." The overlapping targets among compound and insomnia targets were used to draw a Venn diagram and generate the file "drug-disease."

2.1.4 Protein–Protein Interaction Network Construction

The protein interaction relationship file was obtained by importing the intersection targets into the STRING (https://string-db.org/) database. Then, the PPI network diagram of drugs for the treatment of insomnia was obtained by importing the protein interaction relationship file into Cytoscape V3.8.0. The top 30 genes were plotted with the software "R for Windows" based on the degree.

2.1.5 Gene Ontology and Kyoto Encyclopedia of Genes and Genomes (KEGG) Pathway Enrichment Functional Analysis

We installed the "Bioconductor" packages in R software, set the p value <0.05 as the threshold, and ran the program to draw a bubble chart. The top 20 pathways of GO and KEGG enrichment analyses were sorted based on the p value.

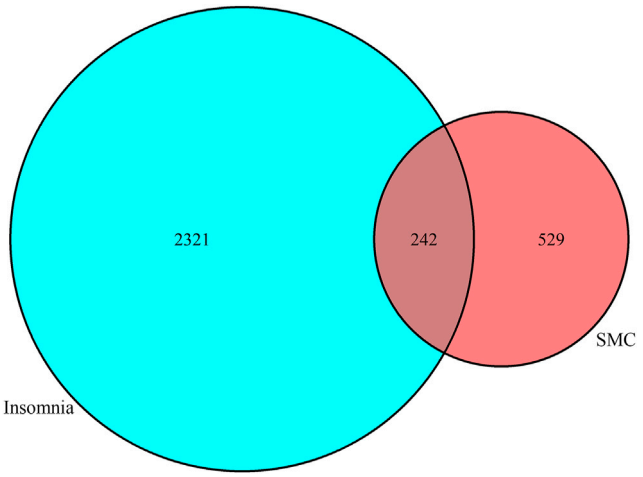

FIGURE 1 | Venn diagram revealing 242 common potential therapeutic targets between SMC and insomnia.

2.2 Experiment Verification

2.2.1 Animals

Male C57BL/6 mice of SPF grade, 8 weeks old (week, W), were purchased from SPF Biotechnology Co., Ltd. (Beijing). The mice were housed in the environment with a normal light-dark cycle (12 h of light and 12 h of dark every day), with a controlled temperature at 24 ± 2°C and 50% constant humidity. This study was conducted in accordance with procedures approved by the Institutional Animal Care and Use Committee at Peking Union Medical College (Beijing, China) (Ethics No. ACUC-A02-2022-073).

2.2.2 Establishment of a Mouse Model of Sleep Deprivation and Drug Treatment

Mice were maintained in the sleep deprivation box with 24 platforms which were 5 cm high, 3 cm in diameter, and remained 5 cm apart from others. Food and water were placed in the food trough on the lid, allowing the mice to move and eat freely. The water temperature around the platform was about 22°C, with platforms 1 cm above the water surface. Then, the mouse was individually placed on each platform. Drug treatment was performed everyday at 9 a.m. After 4-h rest, the mice were then subjected to chronic sleep deprivation for 20 h. The sleep deprivation procedure lasted for 4 weeks, and then the behavioral experiments were performed.

In the experiment of pharmacotherapeutic verification, mice were divided into six groups with 15 mice each: control, model, Ra, SMC-L, SMC-M, and SMC-H. Except for the control group, other groups were subjected to the sleep deprivation procedure. The Ra group was given 1 mg/kg (i.g.) ramelteon, while the SMC-L, SMC-M, and SMC-H groups were given 0.25 g/kg, 0.5 g/kg, and 1 g/kg (i.g.) powder of SMC respectively.

In the experiment of target verification, mice were divided into six groups of 15 mice each: control, model, Ra, SMC, SMC + LU, and SMC+4-P. Except for the group control, other groups were accepted for the sleep deprivation. The Ra group was given 1 mg/kg ramelteon every day, while the SMC, SMC + LU, and SMC+ 4-P groups were given 1 g/kg (i.g.) powder of SMC every day. Meanwhile, SMC + LU group and SMC+ 4-P group were also simultaneously given 5 mg/kg (i.p.) luzindole or 3 mg/kg (i.p.) 4-P-PDOT respectively every day, where luzindole is non-selective MT and 4-P-PDOT a selective MT2 antagonist (Boutin et al., 2020).

2.2.3 Pentobarbital Sodium Righting Reflex Test

Mice were placed on their backs following an injection of 1% pentobarbital sodium (42 mg/kg, i.p.) selected as the dose to induce complete sleep and then monitored the mice for signs of sleeping. Our standard for sleep was that the mice lost their righting reflex for more than 1 min. Sleep latency was defined as the time between the injection of pentobarbital sodium and the beginning of losing righting reflex loss. Sleep duration was defined as the time from the beginning to the recovery of righting reflex loss (Bian et al., 2021).

2.2.4 Open-Field Test

OFT was employed to assess the mental state of mice as we previously described (Wei et al., 2020; Cao et al., 2021). The open-field apparatus consisted of a square arena (40 × 40 × 38 cm), divided into 16 same small squares with lines. The 4 squares in the center of the testing area were defined as a center field, while the other 12 squares were defined as a periphery field. After adapting to the experimental environment for 2 h, each mouse was placed in the periphery field of the area and monitored for 5 min with an overhead video tracking system (Ethovision XT 10, Noldus Information Technology BV, Wageningen, the Netherlands). The time and distance traveled in the center area were measured. The box was cleaned with ethanol after each mouse.

2.2.5 Forced Swimming Test

FST was performed as previously described (Wei et al., 2020), mice were placed individually into a glass cylinder (30 cm in height and 18 cm in diameter) filled with 15 cm deep water and videotaped for 6 min. The immobility time was defined when the mice floated in a motionless position for the last 4 min without additional activity other than the necessary movements for the mice to keep their heads above the water.

2.2.6 Western Blotting Analysis

Protein was extracted from hypothalamus tissues after behavioral experiments, followed by the determination of a total protein and western blotting as reported in our previous research (Cao et al., 2021). The relative protein levels were determined by the intensity of bands using ImageJ software (National Institutes of Health) and normalized against the internal control β-actin. Antibodies against β-actin (Cat. No. 4970), clock (Cat. No. 5157), CaMKII (Cat. No. 3362), and p-CREB (Ser133) (Cat. No. 9198) were purchased from Cell Signaling Technology (Danvers, MA, United States). Antibodies against MT1 (Cat. No. SC-390328) were purchased from Santa Cruz Biotechnology (Santa Cruz, CA, United States). Antibodies against MT2 (Cat. No. ab203346) were purchased from Abcam (Cambridge, United Kingdom). Antibodies against OX1R (Cat. No. AOR-001) and OX2R

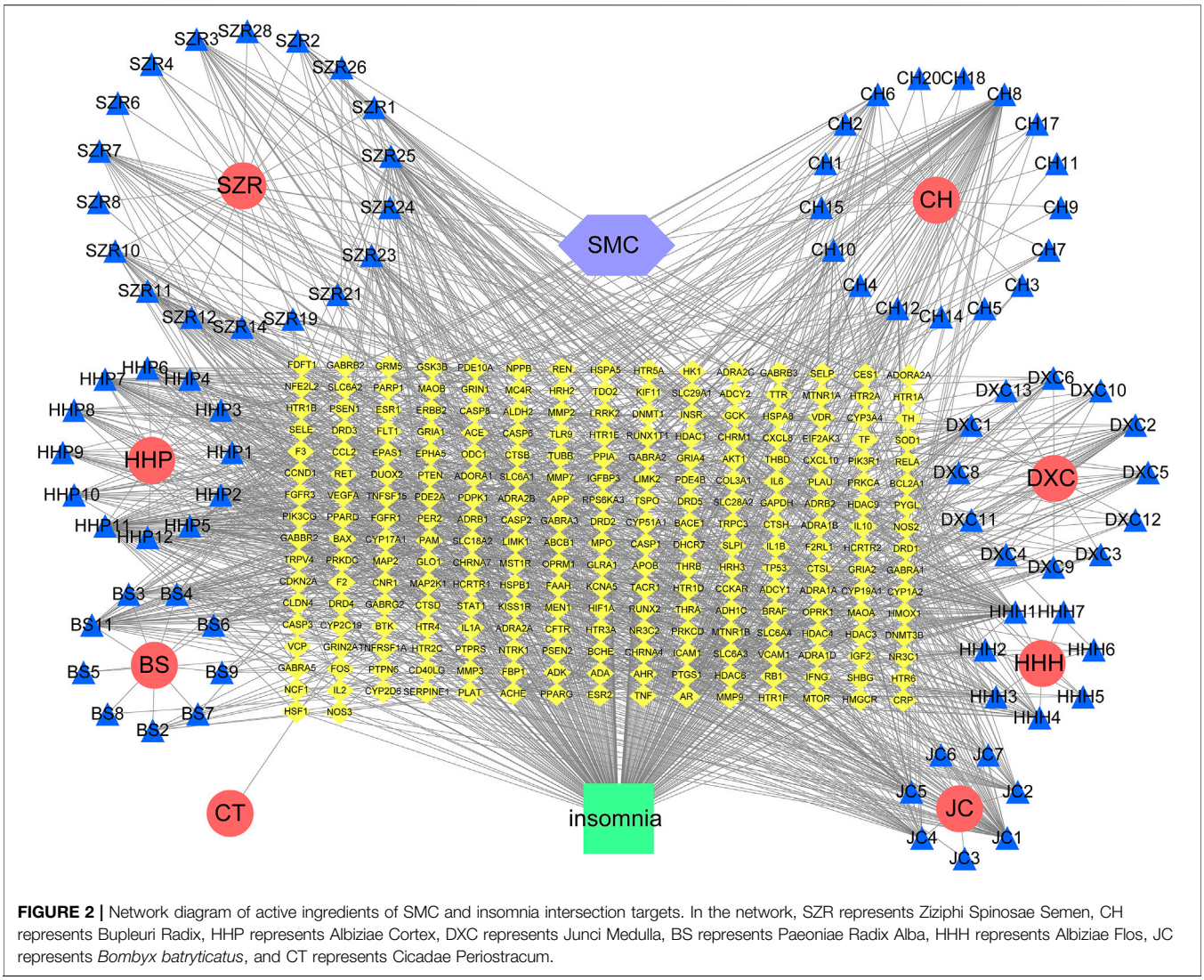

FIGURE 2 | Network diagram of active ingredients of SMC and insomnia intersection targets. In the network, SZR represents Ziziphi Spinosae Semen, CH represents Bupleuri Radix, HHP represents Albiziae Cortex, DXC represents Junci Medulla, BS represents Paeoniae Radix Alba, HHH represents Albiziae Flos, JC represents *Bombyx batryticatus*, and CT represents Cicadae Periostracum.

(Cat. No. AOR-002) were obtained from Alomone Labs (Jerusalem, Israel).

2.2.7 Statistical Analysis

All the data in our results were presented as mean ± SD. For the multi-group comparisons, the data were analyzed by one-way analysis of variance. $p < 0.05$ was considered statistically significant.

3 RESULTS

3.1 The Predictive Targets of SMC Components for Insomnia Therapy

The predictive targets activated by components of SMC were searched from the database of TCMSP and ETCM. For the components without any annotated targets, we drew their chemical formulas using the software ChemDraw, obtaining their predictive targets on the SwissTargetPrediction website. Meanwhile, the insomnia targets were searched from the Uniprot database. The obtained predictive targets were shown in the Venn diagram (**Figure 1**), in which the intersection of drug targets and insomnia targets revealed 242 potential targets in total.

3.2 Construction of Network Pharmacology

The intersection network graph between disease and drug-active ingredients targets was constructed based on the relationship between each node and drug data (**Figure 2**). The graph showed 334 nodes and 1611 connections, while the relationship between nodes was represented by connections. The herbs were represented by their pinyin abbreviation, whose components' abbreviation unified use of the abbreviation shown in **Supplementary Table S1**. The targets are marked with the abbreviation gene names in the Uniprot database.

Then, we imported the obtained 242 targets into the STRING website, setting "CONFIDENCE = 0.7", the result revealed a total of 242 nodes and 1062 edges (**Figure 3A**). The histogram counted the detailed data in the result of the STRING website, in which

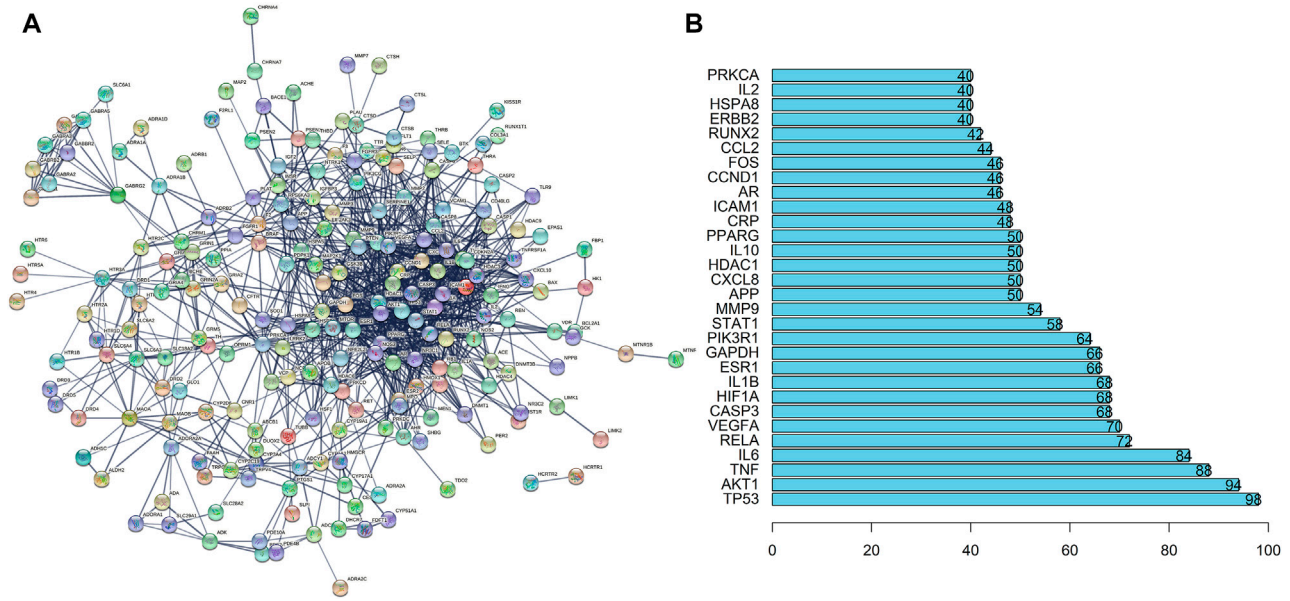

FIGURE 3 | PPI Network Analysis of intersection targets. **(A)** PPI network of potential sleep disorder targets acted by major active components of SMC. There were 242 nodes and 1062 edges in the PPI network. **(B)** The top 30 genes in the PPI network.

each bar represented the number of edges corresponding to each node (**Figure 3B**).

3.3 GO and KEGG Pathway Enrichment Functional Analysis

GO enrichment functional analysis was performed as the bubble diagram using R software and the Bioconductor data package (**Figure 4A**). In the targets of GO enrichments, the top three biological processes were neurotransmitter receptor activity, G protein-coupled amine receptor activity, and postsynaptic neurotransmitter receptor activity, which indicated that neurotransmitters and receptors in the brain are the key factors in the regulatory process from drug to sleep disorder, reminding the potent neuroregulatory activities of SMC. The obtained genes were imported into KEGG pathway enrichment functional analysis using R software and the Bioconductor data package to obtain enriched pathways. The KEGG bubble diagram was performed by the enriched pathways (**Figure 4B**). Most of the enrichments were not related to sleep disorders according to other research reports, for example, lipid and atherosclerosis, fluid shear stress and atherosclerosis, as well as chemical carcinogenesis-receptor activation. In the top 20 enrichment pathways, neuroactive ligand–receptor interaction and serotonergic synapse indicated that intercellular crosstalk between neurons through ligand–receptor combination is an important process from drug to sleep disorder.

Neuroactive ligand–receptor interaction had shown a significant correlation between SMC and sleep disorder. Thus, we further searched for the signal pathways in this enrichment based on the KEGG functional analysis to explore the key targets between SMC and sleep disorder (**Figure 4C**). Many sleep-related receptors were included in these pathways, such as GABA receptors, 5-hydroxytryptophan receptors, histamine receptors, acetyl cholinergic receptors, orexin receptors, and melatonin receptors. Among these receptors, the melatonin receptor is closely related to biological rhythms and sleep homeostasis, becoming the focus of sleep research in recent years. Meanwhile, our previous KEGG pathway analysis results highlighted the enrichment of serotonergic synapse. Melatonin and orexin are important ligands highly associated with sleep and serotonergic synapse. Melatonin synthesis relies on serotonin as a precursor and is modulated by serotonin (Lee et al., 2021), while orexin was also reported to activate the OX1R and OX2R on serotonergic neurons (Xiao et al., 2021). Based on our network pharmacology analysis results and the published research reports, we designate the melatonin receptor and orexin receptor as the potential targets between SMC and sleep disorder.

3.4 SMC Improved Sleep and Depressive Symptoms in Sleep-Deprived Mice

To investigate the efficacies of SMC in treating the sleep disorder and depressive symptoms of sleep-deprived mice, mice were randomly arranged into control groups (control), sleep deprivation group (model), ramelteon (positive drug) treatment group (Ra), and three SMC treatment groups (SMC-L, SMC-M, and SMC-H) receiving 0.25 g/kg, 0.5 g/kg, and 1 g/kg of SMC, respectively. The pentobarbital-induced sleep experiment was performed to evaluate the hypnotic effects of SMC in sleep-deprived mice. As shown in **Figure 5A**, both SMC and Ra treatments significantly recovered the prolonged sleep latency induced by sleep deprivation (**Figure 5A**). No remarkable improvement in sleep duration was observed in Ra-treated mice;

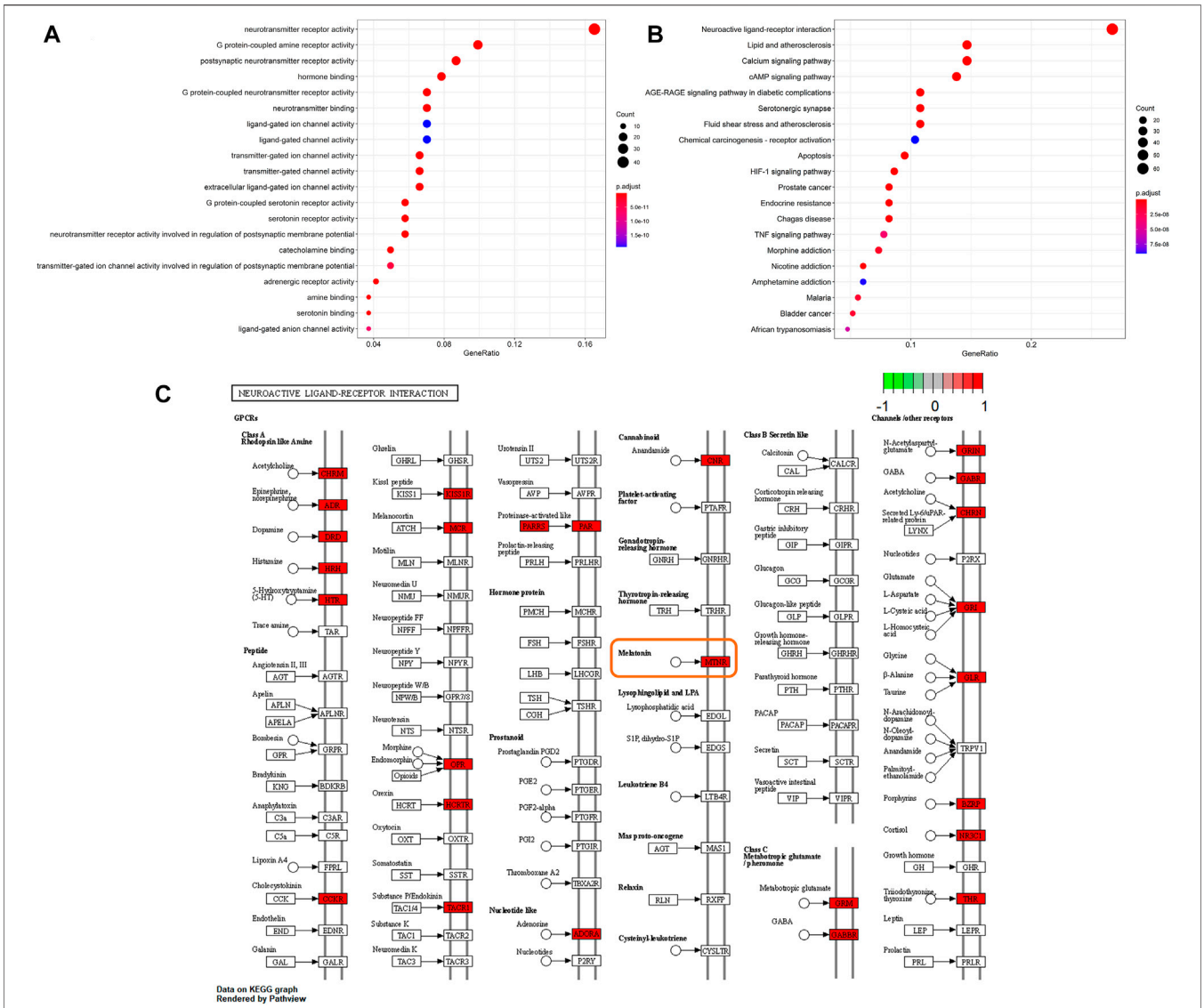

FIGURE 4 | Statistics of functional and pathway enrichment. The x-axis represents the ratio number of genes, and the y-axis shows the pathway terms. The size of the circle represents gene count. Different color of circles represents different adjusted *p*-value. **(A)** Scatter plot of top 20 enriched GO functional analysis. **(B)** Scatter plot of top 20 enriched KEGG pathways. **(C)** Signal pathways in neuroactive ligand-receptor interaction based on the KEGG functional analysis.

however, the high dose of SMC significantly improved the symptoms of sleep deprivation (**Figure 5B**).

Considering the interrelation between sleep deprivation and depression, we performed OFT to investigate if SMC improves mental behavior as previously described (Jin et al., 2019; Zhang N et al., 2020). As evident from **Figures 5C,D**, sleep-deprived mice showed less open-field distance and less stay in the center field than the control group ($p < 0.05$). Ra and the low dose of SMC significantly improved the two types of behavioral changes, and the middle dose of SMC enhanced open-field distance ($p < 0.05$). To verify the aforementioned findings, FST was also conducted to evaluate depressive-like behavior in rodents as previously described (Petit-Demouliere et al., 2005; Fan et al., 2021). Sleep-deprived mice exhibited longer forced swimming immobility time than the control group ($p < 0.05$), while treatment with ramelteon and three different doses of SMC exhibited significant improvement in the depressive-like behavior of mice ($p < 0.05$) (**Figure 5E**).

3.5 SMC Restores Melatonin Receptors and Orexin Receptor-Mediated Pathways in Sleep-Deprived Mice

To verify the roles of melatonin receptors and orexin receptors in the hypnotic effect of SMC, we determined the expression levels of melatonin receptors (MT1 and MT2) and orexin receptors (OX1R and OX2R) in the hypothalamus of mice. Sleep deprivation decreased the expression levels of MT1 and MT2 and increased the expression levels of OX1R and OX2R

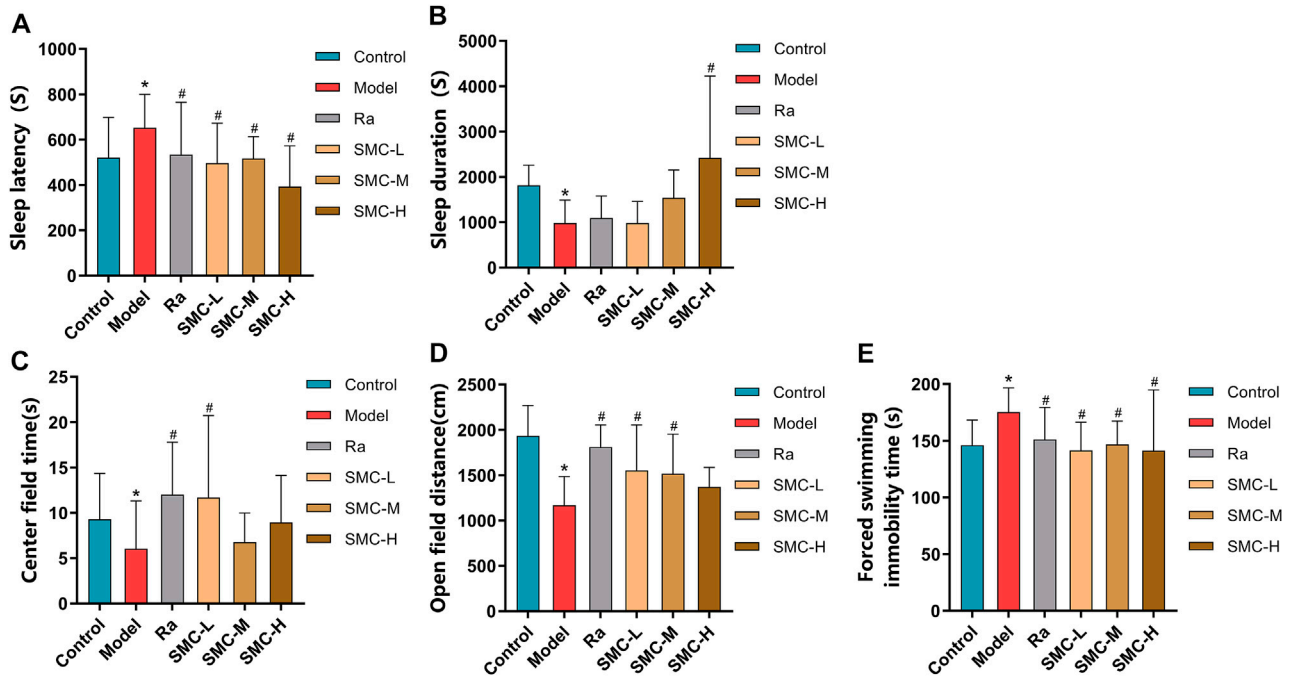

FIGURE 5 | Behavioral experimental indexes of sleep-deprived mice after being treated with ramelteon and SMC (n = 11–14). **(A)** Sleep latency. **(B)** Sleep duration. **(C)** Center field time of OFT. **(D)** Open-field distance of OFT. **(E)** Immobility time of FST. *p < 0.05 *vs*. control group; #p < 0.05 *vs*. model group. All the data were represented as the mean ± SD.

(**Figure 6A**), while ramelteon and SMC treatments restored all the alterations (**Figures 6B–E**). We further determined the expression changes of MT-mediated downstream targets. clock genes Per1 (period circadian protein homolog 1) and clock (circadian locomotor output cycles protein kaput) are positively regarded as being regulated by MT1 (Jilg et al., 2005; Von Gall et al., 2005), while the activation of MT2 will lead to the upregulation of CaMKII (Ca2+/calmodulin-dependent protein kinase II) and p-CREB (phosphor-cyclic AMP-responsive element-binding protein) (Wang et al., 2020). In our results, the levels of Per1, clock, CaMKII, and p-CREB were significantly down-regulated by sleep deprivation and restored after the treatments with ramelteon or SMC (**Figures 6A, F–I**). These data demonstrated that SMC treatment abrogated the changes in MT1 and MT2 signaling pathways induced by sleep deprivation.

3.6 MT1 and MT2 Mediate the Hypnotic Effect of SMC Treatment

To distinguish the roles of MT1 and MT2 in the hypnotic effect of SMC, sleep-deprived mice were randomly assigned to MT or MT2 antagonism prior to SMC treatment. In the pentobarbital-induced sleep experiment, non-selective MT antagonist luzindole and selective MT2 antagonist 4-P-PDOT significantly blocked the effects of SMC on sleep duration and sleep latency, while the antagonistic effect of 4-P-PDOT on sleep latency was more potent than luzindole (p < 0.05) (**Figures 7A,B**). For mental behaviors, MT2 antagonism by 4-P-PDOT attenuated the improvement of SMC on the time spent in the center field (p < 0.05), but no significant effect on open-field distance was observed for MT1 or MT2 antagonism (**Figures 7C,D**). FST also confirmed the involvement of MT2 in the therapeutic effect of SMC (**Figure 7E**).

To verify the aforementioned findings, we then examined the protein expression levels of melatonin receptors and orexin receptors. Compared with the SMC group, non-selective MT antagonist luzindole abrogated the enhancement of MT1 and MT2, while selective MT2 antagonist 4-P-PDOT only blocked the effect of SMC on MT2 (**Figures 8A–C**). Additionally, 4-P-PDOT suppressed the inhibition of SMC on OX1R but not OX2R (**Figures 8D,E**). For downstream signals of MT1 and MT2, luzindole significantly inhibited the changes of both MT1 and MT2 downstream targets, while 4-P-PDOT only significantly regulated Per1, CaMKII, and p-CREB but not clock (**Figures 8F–I**), which might be attributed to the limited inhibitory effect of 4-P-PDOT to MT1.

4 DISCUSSION

Long-term insufficient sleep brings about physiological, subjective experience, and consequent behavioral influences (Krause et al., 2017; Palmer and Alfano, 2017; Ben Simon et al., 2020). In regard to subjective experience, heightened emotional volatility and irritability, as well as reduced positive mood have been particularly associated with sleep deprivation (Ben Simon et al., 2020). Moreover, sleep disruption contributes to a higher probability of depression, anxiety, and suicide (Harvey et al., 2011; Bernert et al., 2015; Riemann et al., 2020). With regard to pathogenesis, insomnia and depression are

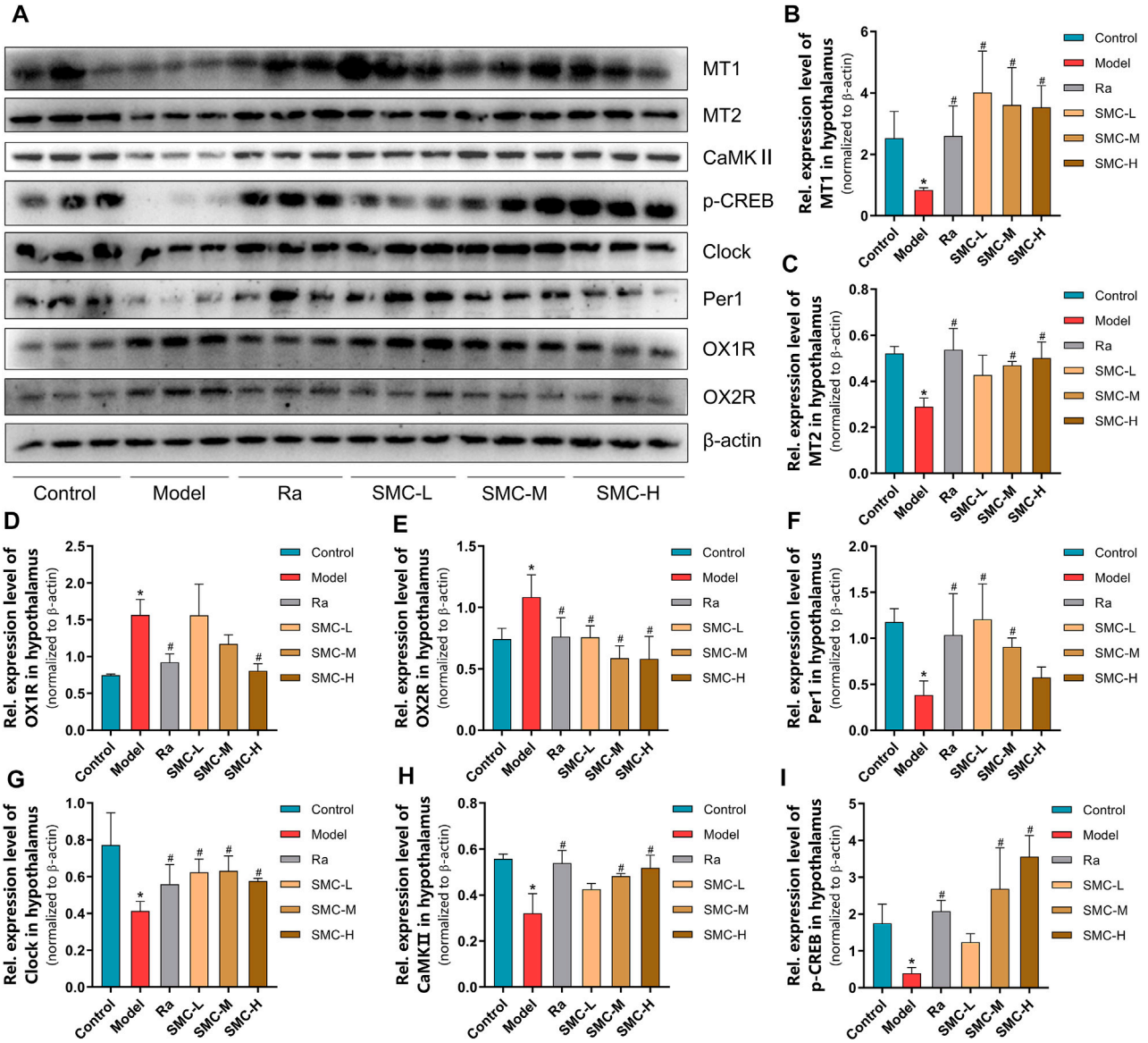

FIGURE 6 | The changes of melatonin receptors and their related proteins in sleep-deprived mice after being treated with ramelteon and different doses of SMC (n = 3). **(A)** Western blotting results. Statistical data of the MT1 levels **(B)**, the MT2 levels **(C)**, the OX1R levels **(D)**, the OX2R levels **(E)**, the Per1 levels **(F)**, the clock levels **(G)**, the CaMKII levels **(H),** and the p-CREB levels **(I)**. *p < 0.05 *vs*. control group; #p < 0.05 *vs*. model group. All the data were represented as the mean ± SD.

also partly overlapped in multiple signal pathways, such as GABAergic and orexin (Michelson et al., 2014; Riemann and Spiegelhalder, 2014; Riemann et al., 2020).

SMC is commonly used for insomnia to improve anxiety, depression, and other symptoms. However, the mechanisms behind the therapeutic functions have not been fully elucidated. Network pharmacology is a promising method that combines multiple techniques and attempts to reveal potential mechanisms and relationships by constructing biological network models. At present, network pharmacology has been broadly applied to explore the molecular mechanism of TCM.

In the present study, a total of 242 target genes between SMC and insomnia were obtained after collecting and screening from multiple databases. To annotate the functions of these targets and related pathways, the GO enrichment and KEGG pathway enrichment analysis were further conducted. GO results showed that the top three biological processes were relevant to neurotransmitter receptor, G protein-coupled amine receptor, and postsynaptic neurotransmitter receptor pathways. We further searched the signal pathway to explore the critical targets of SMC for sleep disorder therapy and multiple receptors were included, such as GABA receptors, 5-HT receptors, histamine receptors, acetyl cholinergic receptors, orexin receptors, and MT receptors. Among these receptors, the MT receptors are closely related to biological rhythms and sleep homeostasis, making them the focus of sleep research in

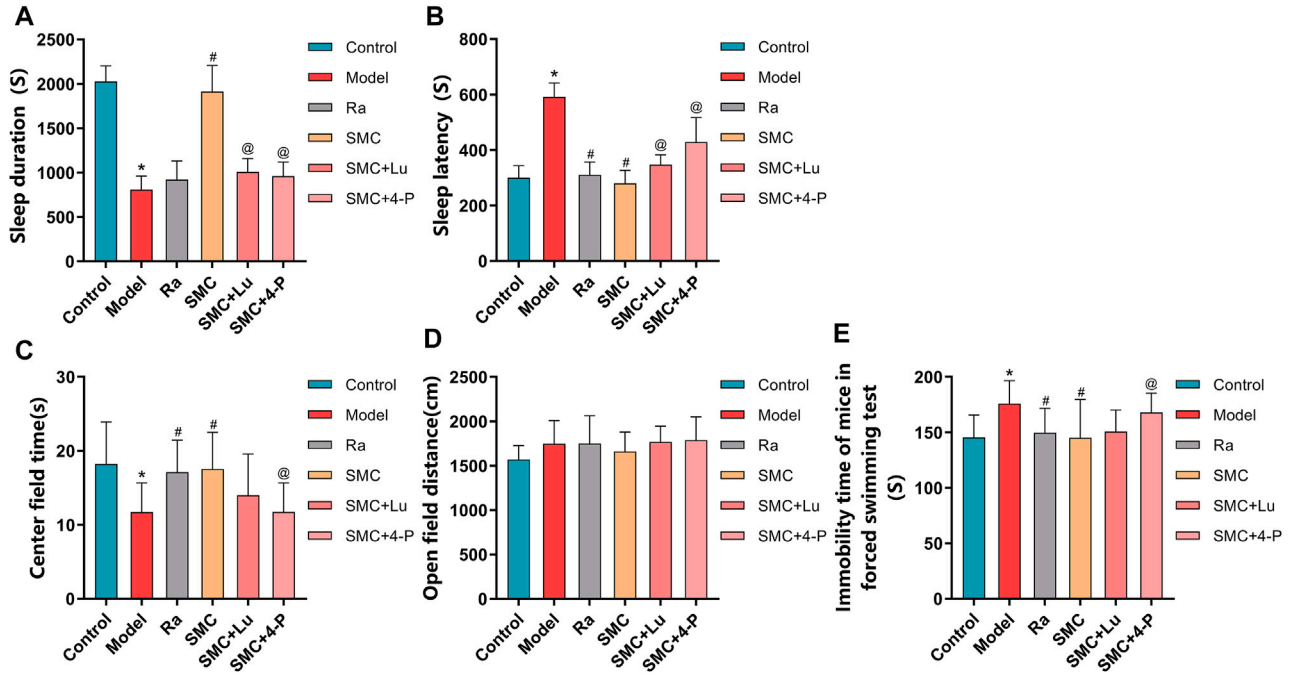

FIGURE 7 | Behavioral experimental indexes of sleep-deprived mice after being treated with ramelteon, SMC, luzindole, and 4-P-PDOT (n = 12–14). **(A)** Sleep duration. **(B)** Sleep latency. **(C)** Center field time of OFT. **(D)** Open-field distance of OFT. **(E)** Immobility time of FST. *p < 0.05 vs. Control group; #p < 0.05 *vs*. Model group; @p < 0.05 *vs*. SMC group. All the data were represented as the mean ± SD.

recent years. Based on our network pharmacology analysis results and the published research, we presumed that MT receptors as the potential targets of SMC.

Based on the findings of network pharmacology, *in vivo* experiments were performed to further validate the predictions. A mouse sleep-deprived model was adopted to generate sleep disorder and partly mental abnormality. Treatments with the MT receptor agonist ramelteon and SMC showed therapeutic efficacies. Activities of ramelteon have been well demonstrated, which is mainly related to the regulation of sleep latency (Sateia et al., 2017). SMC can improve both sleep latency and duration, indicating a different mechanism from that of ramelteon. In mental assessment, OFT has been generally used to evaluate anxiety and spontaneous activity levels (Jin et al., 2019; Zhang N et al., 2020), while FST is commonly used for depression and antidepressants screening (Petit-Demouliere et al., 2005; Fan et al., 2021). In the present study, significant differences appeared in FST rather than OFT, indicating the antidepressant effect of SMC and ramelteon. Although ramelteon has been widely used to treat sleep disorders with limited side effects, it is only applicable for sleep onset insomnia due to its single-target effect (Sateia et al., 2017). On the contrary, TCM is usually composed of multiple components, which work in a multi-target regulatory pattern. Herein, we demonstrated that SMC improved sleep latency and sleep duration, due to its regulatory activity including but not limited to melatonin receptors. Compared with the single effect of traditional melatonin receptor agonists on treating sleep onset insomnia, SMC exhibited therapeutic potential for various sleep disorders, such as sleep onset insomnia and sleep maintenance insomnia.

Both subtypes of melatonin receptors, MT1 and MT2, play important roles in mediating sleep homeostasis. MT1 is mainly regarded as a key receptor in regulating circadian rhythms. It has been reported that the oscillatory rhythm of Per1 and clock expression was severely damaged after the knockout of MT1 (Jilg et al., 2005; Von Gall et al., 2005). In mammals, transcriptional–translational loops of clock genes/proteins build up the circadian rhythm in the whole body (Harmer et al., 2001). Per1 and clock are two of the most important clock genes/proteins that participate in the transcriptional–translational loops and control the core circadian rhythm (Ripperger and Schibler, 2006; Asher and Schibler, 2011; Panda, 2016). Our results showed significant downregulation of MT1, Per1, and clock in sleep deprivation mice and recovery after SMC treatment. MT2 is thought to mainly regulate nonrapid eye movement sleep (NREM) (Gobbi and Comai, 2019). Evidence showed that MT2 activated by melatonin promotes the increase of intracellular calcium ions as well as the expression of CaMKII, reducing the phosphorylation level of CREB. As a result, the latency of NREM is reduced by restoring the inhibition of the N-methyl-D-aspartate receptor (NMDAR) which is the downstream factor of the MT2/Ca2+/CaMKII/p-CREB pathway (Wang et al., 2020). Correspondingly, our study also revealed significant changes in the MT2/Ca2+/CaMKII/p-CREB pathway, indicating that the reduced latency of NREM might be another influencing factor underlying SMC action.

Luzindole (N-0774) is a non-selective melatonin receptor antagonist, while 4-P-PDOT a potent, selective MT2

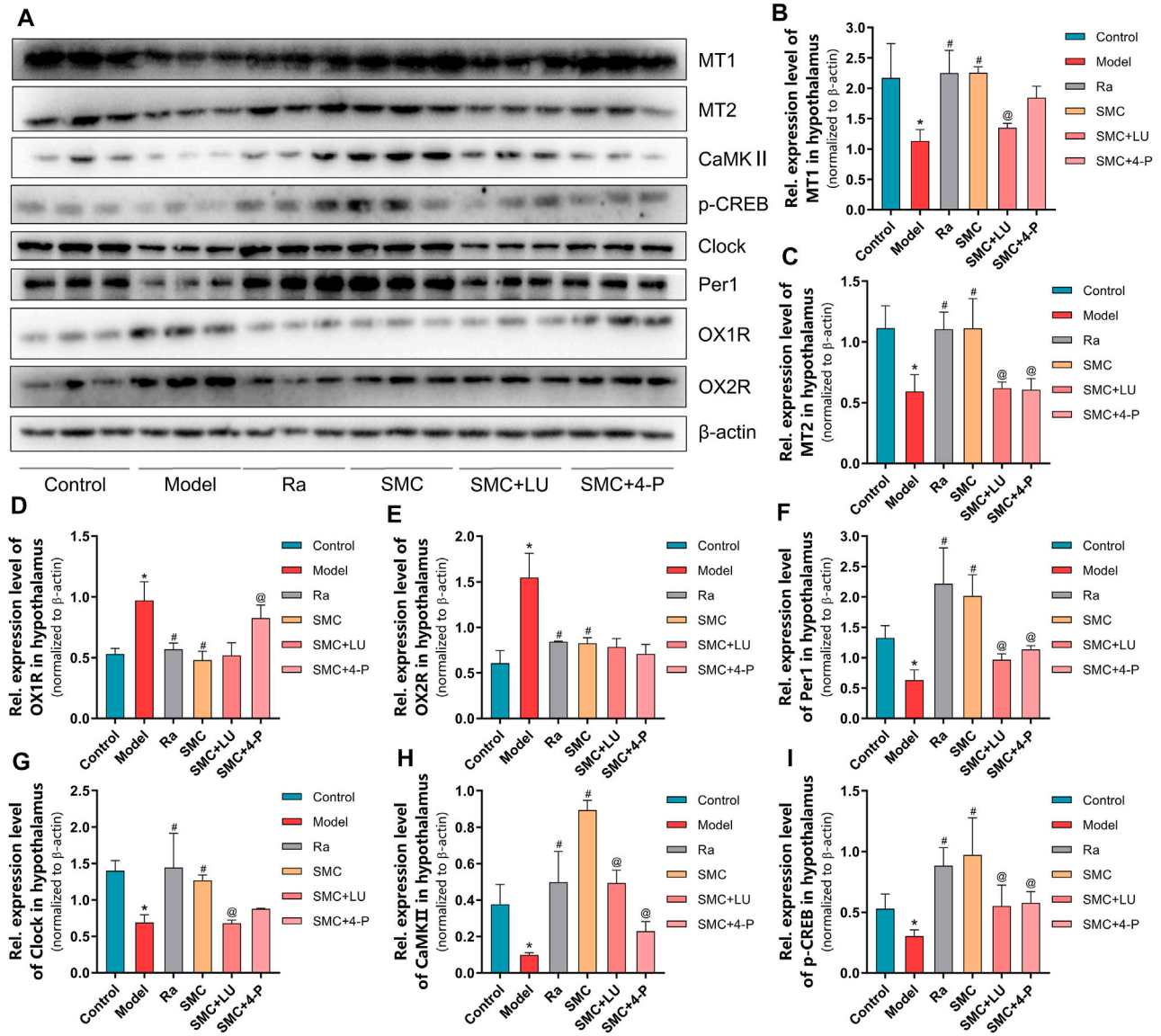

FIGURE 8 | The changes of melatonin receptors and their related proteins in sleep-deprived mice after being treated with ramelteon, SMC, as well as melatonin receptor antagonists luzindole and 4-P-PDOT ($n = 3$). **(A)** Western blotting results. Statistical data of the MT1 levels **(B)**, the MT2 levels **(C)**, the OX1R levels **(D)**, the OX2R levels **(E)**, the Per1 levels **(F)**, the clock levels **(G)**, the CaMKII levels **(H),** and the p-CREB levels **(I)**. *$p < 0.05$ *vs*. control group; #$p < 0.05$ *vs*. model group; @$p < 0.05$ *vs*. SMC group. All the data were represented as the mean ± SD.

antagonist. In this research, the disparate selectivity of luzindole and 4-P-PDOT was utilized to discriminate the contributions of MT1 and MT2. The higher blocking efficacies for luzindole and 4-P-PDOT on Per1/clock and CaMKII respectively were revealed due to the disparate selectivity in our results, which corresponds with the different signal transduction of MT1 and MT2 (Jilg et al., 2005; Von Gall et al., 2005; Wang et al., 2020). For behavioral experimental index, 4-P-PDOT showed higher blocking efficacies on sleep latency, center field time in OFT, and immobility time in FST in mice, while luzindole also revealed blocking efficacies to some extent. This phenomenon indicated that the therapeutic efficacy of SMC on sleep and mental disorder is via the combined effect of MT1 and MT2, while the MT2 showed a stronger mediational effect than MT1.

Recent research indicated that there was a regulatory relationship between MT and orexin, where MT inhibited orexin neurons in the perifornical lateral hypothalamus through the MT1 receptors and promoted sleep (Sharma et al., 2018). Our results showed that the expression levels of OX1R and OX2R increased in sleep deprivation mice, while ramelteon and SMC treatments restored the alterations. Additionally, the selective MT2 antagonist 4-P-PDOT suppressed the inhibition of SMC on OX1R but not OX2R. These results indicated that the regulation of OX1R by SMC treatment is mainly through MT receptors, while the regulation of OX2R by SMC in other different pathways.

Frankly, the present study has several limitations. First, the targets of insomnia and SMC from online databases were based on the predicted data. Thus, those unproven and undocumented targets may be omitted. Second, whether SMC treatment regulates MT receptors and their related signaling pathways directly still remains unclear. Third, the alterations of MT receptors and other related proteins were found in the hypothalamus, while other brain regions have not been determined. Consequently, additional research is required to further explore the molecular mechanisms of SMC in treating insomnia.

Taking these together, SMC improves sleep disorder and mental symptoms by regulating MT1 and MT2 and their related pathways in sleep-deprived mice and our results provide the theoretical support for the clinical application and potential expansion.

DATA AVAILABILITY STATEMENT

The original contributions presented in the study are included in the article/**Supplementary Material**; further inquiries can be directed to the corresponding authors.

ETHICS STATEMENT

The animal study was reviewed and approved by the Animal Care and Use Committee of Peking Union Medical College.

AUTHOR CONTRIBUTIONS

YL and NY were responsible for conceptualization of the study and participated in the draft writing and revising. WL and YC performed the experiments, analyzed the data, and wrote the manuscript. WH, YZ, YQ, and MW supported some experiments. All authors had read and approved this manuscript.

FUNDING

This work was primarily supported by the grants from CAMS Innovation Fund for Medical Sciences (CIFMS) (2021-I2M-1-020).

ACKNOWLEDGMENTS

We thank Guizhou Dalong Pharmaceutical Co., Ltd. for the generous gift of Shumian capsule.

SUPPLEMENTARY MATERIAL

The Supplementary Material for this article can be found online at: https://www.frontiersin.org/articles/10.3389/fphar.2022.925828/full#supplementary-material

REFERENCES

Asher, G., and Schibler, U. (2011). Crosstalk between Components of Circadian and Metabolic Cycles in Mammals. *Cell Metab.* 13 (2), 125–137. doi:10.1016/j.cmet.2011.01.006

Ben Simon, E., Vallat, R., Barnes, C. M., and Walker, M. P. (2020). Sleep Loss and the Socio-Emotional Brain. *Trends Cogn. Sci.* 24 (6), 435–450. doi:10.1016/j.tics.2020.02.003

Bernert, R. A., Kim, J. S., Iwata, N. G., and Perlis, M. L. (2015). Sleep Disturbances as an Evidence-Based Suicide Risk Factor. *Curr. Psychiatry Rep.* 17 (3), 554. doi:10.1007/s11920-015-0554-4

Bian, Z., Zhang, W., Tang, J., Fei, Q., Hu, M., Chen, X., et al. (2021). Mechanisms Underlying the Action of Ziziphi Spinosae Semen in the Treatment of Insomnia: A Study Involving Network Pharmacology and Experimental Validation. *Front. Pharmacol.* 12, 752211. doi:10.3389/fphar.2021.752211

Boutin, J. A., Witt-Enderby, P. A., Sotriffer, C., and Zlotos, D. P. (2020). Melatonin Receptor Ligands: A Pharmaco-Chemical Perspective. *J. Pineal Res.* 69 (3), e12672. doi:10.1111/jpi.12672

Cao, M., Huang, W., Chen, Y., Li, G., Liu, N., Wu, Y., et al. (2021). Chronic Restraint Stress Promotes the Mobilization and Recruitment of Myeloid-Derived Suppressor Cells through β-adrenergic-activated CXCL5-CXCR2-Erk Signaling Cascades. *Int. J. Cancer* 149 (2), 460–472. doi:10.1002/ijc.33552

Chen, S., Xu, Z., Li, Y., Wang, T., Yue, Y., Hou, Z., et al. (2022). Clinical Efficacy of the Chinese Herbal Medicine Shumian Capsule for Insomnia: A Randomized, Double-Blind, Placebo-Controlled Trial. *Neuropsychiatr. Dis. Treat.* 18, 669–679. doi:10.2147/ndt.S349427

Fan, Y., Bi, Y., and Chen, H. (2021). Salidroside Improves Chronic Stress Induced Depressive Symptoms through Microglial Activation Suppression. *Front. Pharmacol.* 12, 635762. doi:10.3389/fphar.2021.635762

Fang, H., Tu, S., Sheng, J., and Shao, A. (2019). Depression in Sleep Disturbance: A Review on a Bidirectional Relationship, Mechanisms and Treatment. *J. Cell Mol. Med.* 23 (4), 2324–2332. doi:10.1111/jcmm.14170

Feng, Z. X., Dong, H., Qu, W. M., and Zhang, W. (2018). Oral Delivered Dexmedetomidine Promotes and Consolidates Non-rapid Eye Movement Sleep via Sleep-Wake Regulation Systems in Mice. *Front. Pharmacol.* 9, 1196. doi:10.3389/fphar.2018.01196

Gobbi, G., and Comai, S. (2019). Differential Function of Melatonin MT(1) and MT(2) Receptors in REM and NREM Sleep. *Front. Endocrinol. (Lausanne)* 10, 87. doi:10.3389/fendo.2019.00087

Harmer, S. L., Panda, S., and Kay, S. A. (2001). Molecular Bases of Circadian Rhythms. *Annu. Rev. Cell Dev. Biol.* 17, 215–253. doi:10.1146/annurev.cellbio.17.1.215

Harvey, A. G., Murray, G., Chandler, R. A., and Soehner, A. (2011). Sleep Disturbance as Transdiagnostic: Consideration of Neurobiological Mechanisms. *Clin. Psychol. Rev.* 31 (2), 225–235. doi:10.1016/j.cpr.2010.04.003

Jilg, A., Moek, J., Weaver, D. R., Korf, H. W., Stehle, J. H., and Von Gall, C. (2005). Rhythms in Clock Proteins in the Mouse Pars Tuberalis Depend on MT1 Melatonin Receptor Signalling. *Eur. J. Neurosci.* 22 (11), 2845–2854. doi:10.1111/j.1460-9568.2005.04485.x

Jin, X., Liu, M. Y., Zhang, D. F., Zhong, X., Du, K., Qian, P., et al. (2019). Baicalin Mitigates Cognitive Impairment and Protects Neurons from Microglia-Mediated Neuroinflammation via Suppressing NLRP3 Inflammasomes and TLR4/NF-Kb Signaling Pathway. *CNS Neurosci. Ther.* 25 (5), 575–590. doi:10.1111/cns.13086

Krause, A. J., Simon, E. B., Mander, B. A., Greer, S. M., Saletin, J. M., Goldstein-Piekarski, A. N., et al. (2017). The Sleep-Deprived Human Brain. *Nat. Rev. Neurosci.* 18 (7), 404–418. doi:10.1038/nrn.2017.55

Lee, B. H., Hille, B., and Koh, D.-S. (2021). Serotonin Modulates Melatonin Synthesis as an Autocrine Neurotransmitter in the Pineal Gland. *Proc. Natl. Acad. Sci. U.S.A.* 118 (43), e2113852118. doi:10.1073/pnas.2113852118

Li, L., An, X. D., Zhang, Q., Tao, J. X., He, J., Chen, Y., et al. (2021). Shumian Capsule Improves Symptoms of Sleep Mood Disorder in Convalescent Patients of Corona Virus Disease 2019. *J. Tradit. Chin. Med.* 41 (6), 974–981. doi:10.19852/j.cnki.jtcm.2021.06.015

Michelson, D., Snyder, E., Paradis, E., Chengan-Liu, M., Snavely, D. B., Hutzelmann, J., et al. (2014). Safety and Efficacy of Suvorexant during 1-year Treatment of Insomnia with Subsequent Abrupt Treatment Discontinuation: a Phase 3 Randomised, Double-Blind, Placebo-Controlled Trial. *Lancet Neurol.* 13 (5), 461–471. doi:10.1016/s1474-4422(14)70053-5

Palmer, C. A., and Alfano, C. A. (2017). Sleep and Emotion Regulation: An Organizing, Integrative Review. *Sleep. Med. Rev.* 31, 6–16. doi:10.1016/j.smrv.2015.12.006

Panda, S. (2016). Circadian Physiology of Metabolism. *Science* 354 (6315), 1008–1015. doi:10.1126/science.aah4967

Pavlova, M. K., and Latreille, V. (2019). Sleep Disorders. *Am. J. Med.* 132 (3), 292–299. doi:10.1016/j.amjmed.2018.09.021

Petit-Demouliere, B., Chenu, F., and Bourin, M. (2005). Forced Swimming Test in Mice: a Review of Antidepressant Activity. *Psychopharmacol. Berl.* 177 (3), 245–255. doi:10.1007/s00213-004-2048-7

Riemann, D., Krone, L. B., Wulff, K., and Nissen, C. (2020). Sleep, Insomnia, and Depression. *Neuropsychopharmacology* 45 (1), 74–89. doi:10.1038/s41386-019-0411-y

Riemann, D., and Spiegelhalder, K. (2014). Orexin Receptor Antagonists: a New Treatment for Insomnia? *Lancet Neurol.* 13 (5), 441–443. doi:10.1016/s1474-4422(13)70311-9

Ripperger, J. A., and Schibler, U. (2006). Rhythmic CLOCK-BMAL1 Binding to Multiple E-Box Motifs Drives Circadian Dbp Transcription and Chromatin Transitions. *Nat. Genet.* 38 (3), 369–374. doi:10.1038/ng1738

Sateia, M. J., Buysse, D. J., Krystal, A. D., Neubauer, D. N., and Heald, J. L. (2017). Clinical Practice Guideline for the Pharmacologic Treatment of Chronic Insomnia in Adults: An American Academy of Sleep Medicine Clinical Practice Guideline. *J. Clin. Sleep. Med.* 13 (2), 307–349. doi:10.5664/jcsm.6470

Sharma, R., Sahota, P., and Thakkar, M. M. (2018). Melatonin Promotes Sleep in Mice by Inhibiting Orexin Neurons in the Perifornical Lateral Hypothalamus. *J. Pineal Res.* 65 (2), e12498. doi:10.1111/jpi.12498

Smith, M. T., Huang, M. I., and Manber, R. (2005). Cognitive Behavior Therapy for Chronic Insomnia Occurring within the Context of Medical and Psychiatric Disorders. *Clin. Psychol. Rev.* 25 (5), 559–592. doi:10.1016/j.cpr.2005.04.004

Von Gall, C., Weaver, D. R., Moek, J., Jilg, A., Stehle, J. H., and Korf, H. W. (2005). Melatonin Plays a Crucial Role in the Regulation of Rhythmic Clock Gene Expression in the Mouse Pars Tuberalis. *Ann. N. Y. Acad. Sci.* 1040 (1), 508–511. doi:10.1196/annals.1327.105

Wang, C., Yang, Y., Ding, X., Li, J., Zhou, X., Teng, J., et al. (2021). Efficacy and Safety of Shumian Capsules in Treating Insomnia: A Systematic Review and Meta-Analysis. *Medicine* 100 (50), e28194. doi:10.1097/md.0000000000028194

Wang, Q., Zhu, D., Ping, S., Li, C., Pang, K., Zhu, S., et al. (2020). Melatonin Recovers Sleep Phase Delayed by MK-801 through the Melatonin MT2 Receptor- Ca2+ -CaMKII-CREB Pathway in the Ventrolateral Preoptic Nucleus. *J. Pineal Res.* 69 (3), e12674. doi:10.1111/jpi.12674

Wei, Q., Zhou, W., Zheng, J., Li, D., Wang, M., Feng, L., et al. (2020). Antidepressant Effects of 3-(3,4-Methylenedioxy-5-Trifluoromethyl Phenyl)-2e-Propenoic Acid Isobutyl Amide Involve TSPO-Mediated Mitophagy Signalling Pathway. *Basic Clin. Pharmacol. Toxicol.* 127 (5), 380–388. doi:10.1111/bcpt.13452

Xiao, X., Yeghiazaryan, G., Hess, S., Klemm, P., Sieben, A., Kleinridders, A., et al. (2021). Orexin Receptors 1 and 2 in Serotonergic Neurons Differentially Regulate Peripheral Glucose Metabolism in Obesity. *Nat. Commun.* 12 (1), 5249. doi:10.1038/s41467-021-25380-2

Zhang, N., Luo, M., He, L., and Yao, L. (2020). Chemical Composition of Essential Oil from Flower of 'Shanzhizi' (Gardenia Jasminoides Ellis) and Involvement of Serotonergic System in its Anxiolytic Effect. *Molecules* 25 (20), 4702. doi:10.3390/molecules25204702

Zhang, R., Zhu, X., Bai, H., and Ning, K. (2019). Network Pharmacology Databases for Traditional Chinese Medicine: Review and Assessment. *Front. Pharmacol.* 10, 123. doi:10.3389/fphar.2019.00123

Zhang, Y., Cao, M., Wu, Y., Wang, J., Zheng, J., Liu, N., et al. (2020). Improvement in Mitochondrial Function Underlies the Effects of ANNAO Tablets on Attenuating Cerebral Ischemia-Reperfusion Injuries. *J. Ethnopharmacol.* 246, 112212. doi:10.1016/j.jep.2019.112212

Zielinski, M. R., McKenna, J. T., and McCarley, R. W. (2016). Functions and Mechanisms of Sleep. *AIMS Neurosci.* 3 (1), 67–104. doi:10.3934/Neuroscience.2016.1.67

Conflict of Interest: The authors declare that the research was conducted in the absence of any commercial or financial relationships that could be construed as a potential conflict of interest.

The reviewer XK declared a shared affiliation with the authors to the handling editor at the time of the review.

Publisher's Note: All claims expressed in this article are solely those of the authors and do not necessarily represent those of their affiliated organizations, or those of the publisher, the editors, and the reviewers. Any product that may be evaluated in this article, or claim that may be made by its manufacturer, is not guaranteed or endorsed by the publisher.

frontiers | Frontiers in Pharmacology

ORIGINAL RESEARCH
published: 14 July 2022
doi: 10.3389/fphar.2022.919269

Scorpion Venom Heat–Resistant Synthesized Peptide Increases Stress Resistance and Extends the Lifespan of *Caenorhabditis elegans via* the Insulin/IGF-1-Like Signal Pathway

Ying-Zi Wang[1,2,3†], *Song-Yu Guo*[1,2†], *Rui-Li Kong*[1,2], *Ao-Ran Sui*[1], *Zhen-Hua Wang*[1,2], *Rong-Xiao Guan*[1,2], *Kundu Supratik*[1], *Jie Zhao*[2*] and *Shao Li*[1,2*]

[1]Department of Physiology, College of Basic Medical Sciences, Liaoning Provincial Key Laboratory of Cerebral Diseases, Dalian Medical University, Dalian, China, [2]National-Local Joint Engineering Research Center for Drug-Research and Development (R&D) of Neurodegenerative Diseases, Dalian Medical University, Dalian, China, [3]The Second Affiliated Hospital of Dalian Medical University, Dalian, China

Improving healthy life expectancy by targeting aging-related pathological changes has been the spotlight of geroscience. Scorpions have been used in traditional medicine in Asia and Africa for a long time. We have isolated heat-resistant peptides from scorpion venom of Buthusmartensii Karsch (SVHRP) and found that SVHRP can attenuate microglia activation and protect *Caenorhabditis elegans* (*C. elegans*) against β-amyloid toxicity. Based on the amino acid sequence of these peptides, scorpion venom heat–resistant synthesized peptide (SVHRSP) was prepared using polypeptide synthesis technology. In the present study, we used *C. elegans* as a model organism to assess the longevity-related effects and underlying molecular mechanisms of SVHRSP *in vivo*. The results showed that SVHRSP could prolong the lifespan of worms and significantly improve the age-related physiological functions of worms. SVHRSP increases the survival rate of larvae under oxidative and heat stress and decreases the level of reactive oxygen species and fat accumulation *in vivo*. Using gene-specific mutation of *C. elegans*, we found that SVHRSP-mediated prolongation of life depends on Daf-2, Daf-16, Skn-1, and Hsf-1 genes. These results indicate that the antiaging mechanism of SVHRSP in nematodes might be mediated by the insulin/insulin-like growth factor-1 signaling pathway. Meanwhile, SVHRSP could also up-regulate the expression of stress-inducing genes Hsp-16.2, Sod-3, Gei-7, and Ctl-1 associated with aging. In general, our study may have important implications for SVHRSP to promote healthy aging and provide strategies for research and development of drugs to treat age-related diseases.

Keywords: ***Caenorhabditis elegans*, SVHRSP, stress resistance, insulin-IGF-1 like signal pathway, aging**

OPEN ACCESS

Edited by:
Yong Cheng,
Minzu University of China, China

Reviewed by:
Wenhui Huang,
Saarland University, Germany
Ling-Qiang Zhu,
Huazhong University of Science and Technology, China

***Correspondence:**
Jie Zhao
zhaoj@dmu.edu.cn
Shao Li
lishao89@dmu.edu.cn

†These authors have contributed equally to this work

Specialty section:
This article was submitted to Neuropharmacology, a section of the journal Frontiers in Pharmacology

Received: *13 April 2022*
Accepted: *31 May 2022*
Published: *14 July 2022*

Citation:
Wang Y-Z, Guo S-Y, Kong R-L, Sui A-R, Wang Z-H, Guan R-X, Supratik K, Zhao J and Li S (2022) Scorpion Venom Heat–Resistant Synthesized Peptide Increases Stress Resistance and Extends the Lifespan of Caenorhabditis elegans via the Insulin/IGF-1-Like Signal Pathway. Front. Pharmacol. 13:919269. doi: 10.3389/fphar.2022.919269

INTRODUCTION

Aging, a time-related deterioration of physiologic functions, is a global problem, occurring in all the cells, tissues, and organs (López-Otín et al., 2013). According to a report from the United Nations dated 2015, in China, the number of people over 65 years old is going to reach up to 400 million in the coming 35 years (26.9% of the total population) (Fang et al., 2015), making it one of the countries with the highest percentage of aged people in the world. Aging cannot be considered a disease, but it is one of the biggest risk factors for major age-related disorders, for instance, hypertension, diabetes, cancer, and certain neurodegenerative diseases resulting in a huge global burden (Barzilai et al., 2018). Therefore, effective components that can extend lifespan and promote healthiness have recently drawn increased attention. Hence, understanding the mechanisms responsible for lifespan extension has great potential to expose targets for drugs directed at reducing the aging process and preventing aging-associated diseases.

Caenorhabditis elegans (*C. elegans*) is considered an ideal model widely applied to investigate aging in organisms and explore new pharmacological targets (Ma L et al., 2018), due to its short lifespan, strong reproductive capacity, ease of genetic manipulation, and a proportion of homologous genes with humans. *C. elegans* also has more than 65% genes linked to human diseases, including conserved pathways for regulating lifespan (Stiernagle, 2006; Kenyon, 2010; Lapierre and Hansen, 2012).

Scorpions have been applied in traditional medicine for thousands of years in Asia and Africa for the treatment of epilepsy, rheumatoid arthritis, apoplexy, and chronic pain, along with other conditions (Zhou et al., 1989; Shao et al., 2007; Tajti et al., 2020; Tao et al., 2021). To date, more than 400 different peptides, toxins, or homologs have been extracted and purified from scorpion venom, and their functions have been identified, several of which have been found to practicably manage many worldwide medical problems and thus identified as drug candidates (Ortiz et al., 2015). Scorpion venom heat–resistant peptide (SVHRP) is used as a patented technology to extract a peptide mixture isolated from the Buthusmartensii Karsch venom in our laboratory. We have found that SVHRP exhibited significant inhibition of sodium channels in hippocampal neurons (Zhang et al., 2007), reduced susceptibility to epileptic seizures in rats (Chen et al., 2021), promoted neurogenesis in adult mice (Wang et al., 2014), protected against the neurotoxicity induced by β-amyloid in *C. elegans* (Zhang et al., 2016), protected against cerebral ischemia–reperfusion injury (Wang et al., 2020) and suppressed neuroinflammation and microglia activation (Wu et al., 2021). For now, the amino acid sequence of one major constituent of SVHRP has been determined using liquid chromatograph–mass spectrometry (LC–MS), and a synthetic peptide prepared in accordance with this sequence is called scorpion venom heat–resistant synthesized peptide (SVHRSP). In our previous study, we found that treatment with SVHRSP ameliorated 6-OHDA-induced neurotoxicity and neuroinflammation (Li et al., 2021). So, we hypothesize that SVHRSP has the potential to play an important role in antiaging. In this research, we used *C. elegans* as a model organism to assess the longevity-related effects and underlying molecular mechanisms of SVHRSP *in vivo*. We found that SVHRSP could extend lifespan, enhance oxidative and thermal stress resistance, and decrease reactive oxygen species (ROS) levels and fat accumulation by increasing the expression of genes that regulate stress responses and aging.

MATERIALS AND METHODS

The Production of Scorpion Venom Heat–Resistant Synthesized Peptide

Our research group has been engaged in the research and development of Scorpion Venom drugs for many years. We extracted the scorpion venom heat-resistant peptide (SVHRP) from the scorpion of East Asia, and then further purified SVHRP and synthesized it to obtain the scorpion venom heat-resistant synthetic peptide (SVHRSP). The amino acid sequence of SVHRSP (MW = 1524.7 d) were reported in the patent (No. ZL201610645111.7) about the chemical composition and application of SVHRSP. SVHRSP used in this study was produced by GL Biochem Ltd. (Shanghai, China) with 98% purity. ddH_2O was used as the control group in the experiment. In the previous experiments in our laboratory, we used the carbon-terminal modified peptide of SVHRSP (the same 15 amino acids as SVHRSP) for electrophysiological screening. Our results show that modified SVHRSP does not have the same effect as SVHRSP activation of sodium channels. In a similar way, modified SVHRSP did not play a role in the treatment of 6-OHDA-induced PD models of *C. elegans*. Therefore, ddH_2O was used as the control group in the experiment.

Strains and Breeding of *Caenorhabditis elegans*

C. elegans strains used in this experiment: Wild-type *C. elegans* N_2, TJ356: Daf-16 (ZLS356:GFP) IV, CF1038: Daf-16 (MU86) I, TJ375 (HSP-16.2P:GFP), CF1553: SOD-3 (pAD76:GFP), EU1 skn-1 (zu67), PS3551 hsf-1 (sy441) I, CB1370 Daf-2 (e1370) III and CF1038 Daf-16 (mu86) I. All *C. elegans* and *E. coli* OP50 were provided by the Caenorhabditis Genetics Center (CGC); *C. elegans* used in this study are both hermaphrodite nematodes. For specific nematode culture methods, see the methods used by Brenner S (Yin et al., 2014). Nematodes feed on *E. coli* OP50, a uracil deficient strain that can grow on NGM medium without excessive growth affecting nematodes' activity.

Lifespan Assay

The synchronized L4 nematodes were collected, and nematodes were selected on the NGM medium with the optimal concentration of SVHRSP. Three boards were set for each concentration, with about 50–150 nematodes on each board. In order to maintain consistency of drug concentration, fresh NGM solid medium should be replaced every 2 days, the survival status of nematodes should be observed every 2 days, and the number of alive, dead, and excluded nematodes should be

counted until the last day of the life of the last nematode (Solis and Petrascheck, 2011). The death criteria were: nematodes showed no signs of movement, and there was no reaction when the body was lightly touched with platinum wire; Exclusion criteria were: dry death on petri dish wall and cover; And nematodes burrowing into AGAR (Solis and Petrascheck, 2011). The life test should be repeated at least three times.

Food Clear Assay

In order to determine the optimal concentration of SVHRSP, so as to better and effectively evaluate whether SVHRSP has an antiaging effect and influence on *C. elegans*. The purpose of the food clear assay is to establish a method for screening the optimal concentration of SVHRSP drugs for neuronal protection and effective life extension. Experimental methods: Under the condition of 20°C, the M9 solution, 10-μl SVHRSP solution, and 80-μl *E. coli* (OP50) were adjusted to 0.5–0.8 every 10–20 μl containing 30–40 adjacent nematodes and then cultured in a 96-well plate for seven consecutive days. The OD values were measured for seven consecutive days and recorded at least three times (Voisine et al., 2007).

Lipofuscin Analysis Experiment

Lipofuscin is a highly oxidized and crosslinked protein aggregation in nematodes. It is the "marker dye" of senescence and spontaneously fluoresces blue under a fluorescence microscope (Henderson and Johnson, 2001). From 10 to 18 days, blue fluorescence could be detected in the intestinal tract of nematodes. Nematodes with different optimal drug concentrations were cultured for 5–6 days according to the feeding method in the life test. Nematodes aged from 10 to 18 days were washed with M9 at least three times and transferred to a plate containing fresh NGM. Nematodes with different SVHRSP concentrations were selected and covered with another slide in parallel to flatten the AGAR to prevent fragmentation and remove bubbles (Henderson and Johnson, 2001). Fluorescence microscopy (Leica DM4000B) (excitation wavelength 510–560 nm; emission wavelength 590–650 nm) was observed and photographed. Image J was used to analyze the spontaneous fluorescence content of lipofuscin. The lipofuscin experiment was repeated at least three times.

Body Bend Assay

Normal *C. elegans* crawl in a sinusoidal form on a solid medium, and in the aging process, the muscles of the whole body of the *elegans* degenerate, crawl slower and bend less frequently (Ruan et al., 2016). Method: use the nematodes carrying a pole with its load pick to a single *C. elegans* to exclude OP50 NGM medium when they get used to the new environment and start crawling normally. The times of sinusoidal motion body bending in 60 s were recorded (Ruan et al., 2016). Then it was picked out, and another nematode was selected to continue the experiment; 30 nematode data were recorded in each experimental group. A new NGM medium was needed when the experimental group was replaced. Repeat the bending test at least three times.

Pharyngeal Pumping Assay

The deglutition of nematodes is a regular contractile movement regulated using the neuromuscular system (Ryu et al., 2016). The pharyngeal pulsation of young adults is 250–300 times per minute on average. One of the obvious characteristics of senescence is the decrease in pharyngeal pulsation frequency. The specific method of the pharyngeal pump experiment is as follows: This experiment was carried out along with the lifespan experiment. Nematodes at the L4 stage were collected and selected to NGM medium with different optimal drug concentrations of SVHRSP. 10–20 nematodes from each group were randomly selected and transferred to the new NGM plate coated with the bacterial solution. The number of beats in the pharyngeal muscles of nematodes was observed under a microscope in 1 min. The pharyngeal pump test was repeated at least three times.

Fecundity Assay

One of the most popular theories of aging is longevity and reproduction. Using a variety of advanced animal models of aging, they found a mechanism called a "tradeoff" between longevity and fertility, in which reduced or lost fertility leads to increased longevity (Gruber et al., 2007). The synchronized L4 nematodes were collected and selected to the NGM solid medium containing different concentrations of SVHRSP. Three parallel control groups were set for each concentration, with 1–2 nematodes in each group, and cultured in the constant temperature medium at 20°C. The number of oviposition of nematodes was observed every day until the reproductive cycle of nematodes was completed. The number of oviposition of nematodes in different periods of each group was counted. The oviposition experiment was repeated at least three times.

Determination of Reactive Oxygen Specie

2, 7-dichlorodihydrofluorescein (H_2DCF-DA) was used to detect the scavenging effect of SVHRSP on active oxygen free radicals in nematodes. Its mechanism of action is that it is oxidized by intracellular ROS into DCF to detect the fluorescence intensity and determine the free radical scavenging ability of SVHRSP (Lee et al., 2009). The specific method is as follows: the synchronized L4 nematodes were collected, and nematodes were selected on an NGM medium with different optimal drug concentrations of SVHRSP. Three boards were set for each concentration, with about 20–30 nematodes on each board. The fresh medium was changed every 2 days to ensure effective drug concentration, and *C. elegans* was cultured for 5–6 days. The supernatant was homogenized slowly on ice, centrifuged at 12000 rpm, and then added to a black 96-well plate to avoid light. At the same time, the DCFDA probe reserve solution was added, and then excited at 485 nm and emitted at 530 nm wavelength. The fluorescence value was measured with a fluorescence microplate, and the ROS experiment was repeated at least three times (Lee et al., 2009).

Fat Accumulation Experiment

In N_2 wild-type worms, increased production of ROS may lead to excessive fat accumulation (Hughes et al., 2007). Methods: after

simultaneous culture, wild-type N_2 nematodes were cultured in NGM medium for 96 h. The nematodes in each group were washed with M9 buffer three times, and OP50 was cleaned. An oil red O staining kit was used for lipid staining of nematodes in each group. Control and treatment worms were placed on slides, and oil red O staining was determined using fluorescein microscope (Leica DM4000B) and quantified using ImageJ software.

Heat Shock Experiment

As nematodes age, their resistance to stress gradually decreases. The heat shock test was pretreated with 20- and 40-μM SVHRSP at 20°C for 10 days. On day 10, *C. elegans* were transferred to the new NGM petri dish and incubated at 37°C. The worms were gently touched with a platinum wire clamp every hour and marked dead if they did not respond (Strayer et al., 2003). These measurements were performed in three separate trials. Each group consisted of at least 30 animals.

Oxidative Stress Experiment

In oxidative stress tests, 20- and 40-μM SVHRSP–treated and control nematodes were transferred to a new 6-well plate containing 30% H_2O_2 (Sigma, United States). The animals were monitored hourly, and when they were immobile in the liquid medium, they were recorded as dead (Pietsch et al., 2009). These measurements were performed in three separate trials. Each group consisted of at least 30 animals.

Quantitative PCR Analysis of Gene Expression

About 800 synchronized worms were cultured with or without 20- and 40-μM SVHRSP at 20°C for 10 days. Total RNA was extracted using the RNA isolater Total RNA Extraction Reagent (Vazyme, China) and converted to cDNA. After inversion, AceQ® QPCR SYBR Green Master Mix (low Rox premixed) kit (Vazyme, China) was used for quantitative amplification. The following primers were used: Daf-16 forward primer 5′ CGGATA CCGTACTCGTGATGAT 3′ and reverse primer 5′ CCAAAC AGCCACCCAAATCA, Hsp-16.2 forward primer 5′ CTGCAG AATCTCTCCATCTGAGTC 3′ and reverse primer 5′ AGATTC GAAGCAACTGCACC 3′, SOD-3 forward primer 5′ CCACCT GTGCAAACCAGGAT 3′ and reverse primer 5′ TGCAAGTAG TAGGCGTGCTC 3′, gei-7 forward primer 5′ CTGCCATCT CCGTGGTATCC 3′ and reverse primer 5′ ACCCATGTTCCA TCGTGTCC 3′, ctl-1 forward primer 5′ TCGTTCATGCCAAGG GAGC 3′ and reverse primer 5′ GATCCCGATTCTCCAGCGAC 3′, and act-1 forward primer 5′ CCAGGAATTGCTGATCGT ATGCAGAA 3′ and reverse primer 5′ TGGAGAGGGAAGCGA GGATAGA 3′.

Daf-16 Nuclear Translocation Experiment

Under normal conditions, the insulin signaling pathway is normally activated, and a large number of phosphorylated Daf-16 is trapped in the cytoplasm, unable to enter the nucleus for transcriptional regulation. In contrast, when the insulin signaling pathway is attenuated, Daf-16 is not phosphorylated and enters the nucleus to regulate the downstream transcription factor Daf-16, thereby prolonging the lifespan. When the inactivation of the upstream kinase in the insulin signaling pathway causes it to transfer from the cytoplasm to the nucleus, three conditions occur: cytoplasm, nucleus, and intermediate position (Henderson and Johnson, 2001). The L4 TJ356 nematodes were treated with different concentrations of SVHRSP for 10 consecutive days. Each group of 20–30 TJ356 nematodes with different concentrations of SVHRSP was washed with M9 solution at least three times. The next day, the nematodes were transferred to the fresh NGM plate containing different concentrations of SVHRSP; 20–30 nematodes with different concentrations of SVHRSP were selected and covered with another slide in parallel. The AGAR was flattened to prevent breakage, and bubbles were removed. The nematodes were placed under an inverted fluorescence microscope for examination and statistical fluorescence intensity. The excitation wavelength is 488 nm, and the emission wavelength is 500–530 nm. Image J software was used to analyze the fluorescence intensity, and the nucleation experiment was repeated at least three times.

Fluorescence Measurements in the CF1553 Strain and the TJ375 Strain

The CF1553 nematodes carrying Sod-3-GFP and the TJ375 nematodes carrying Hsp-16.2-GFP were imaged using fluorescence microscope (Leica DM4000B). Two kinds of nematodes were treated with the same lifespan experiment. During imaging, the excitation wavelength was 470 nm, and GFP was recorded at 550 nm. The total fluorescence of each worm was analyzed using ImageJ software.

Experimental Statistical Analysis

GraphPad Prism 9.0 was used for experimental statistical analysis. For life tests, Kaplan–Meier survival was used, and *p*-values were calculated using log-rank tests. One-way analysis of variance (ANOVA) with Duncan's test was used multigroup comparisons of other experiments. A p-value of <0.05 was considered statistically significant.

RESULTS

Scorpion Venom Heat–Resistant Synthesized Peptide Extends the Lifespan and Reduced the Level of Lipofuscin Without Affecting the Normal Physiological Function in *Caenorhabditis elegans*

To evaluate whether SVHRSP can prolong worm lifespan and screen out the optimal drug concentration, we first treated wild-type N_2 worms with SVHRSP at a concentration of 0–200 μM on an NGM plate. The results indicate that when the concentration of SVHRSP was greater than 100 μM, the average life span of nematodes was significantly shortened, indicating that100 μM or higher concentrations of SVHRSP had significant impairment on the health status of wild-type N_2 worms (**Figure 1A**) ($p < 0.001$). In a similar way, we investigated the effects of lower doses (20-and 40-μM SVHRSP) on the worms. We discovered that the wild-type N_2

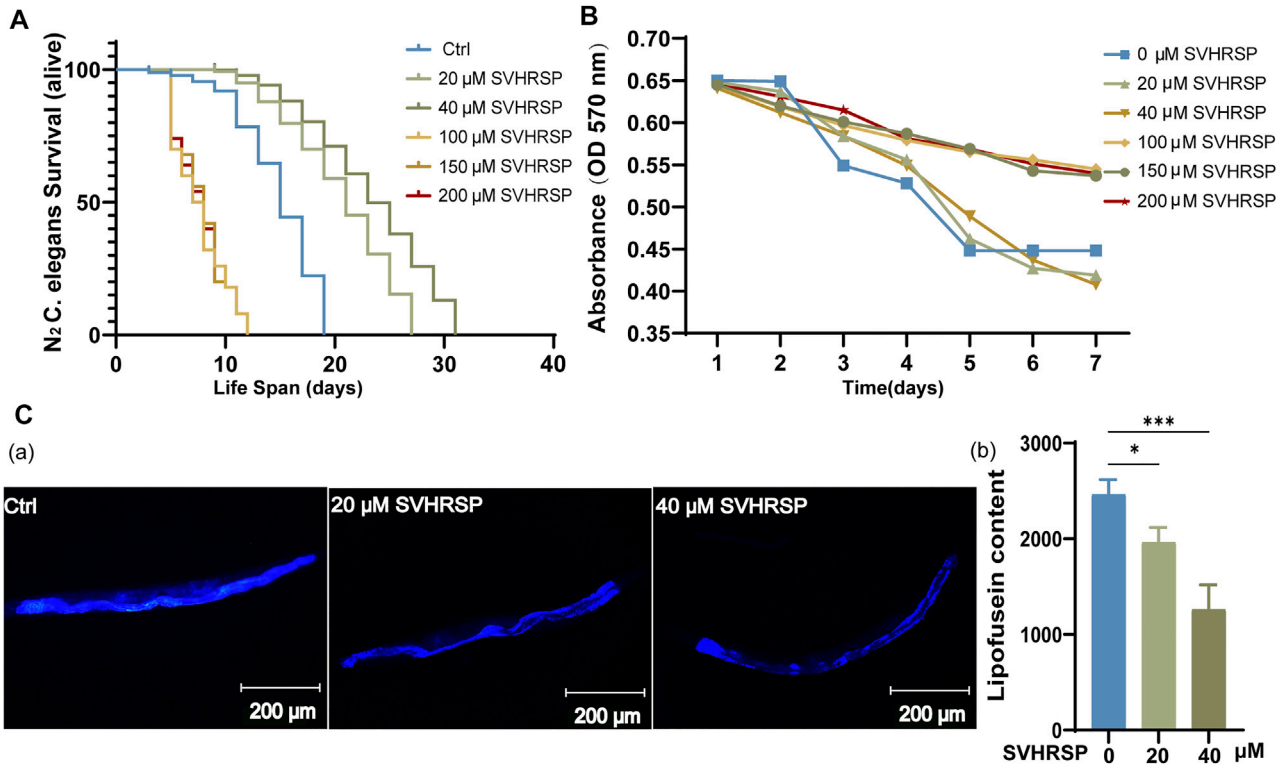

FIGURE 1 | Scorpion venom heat–resistant synthesized peptide (SVHRSP) extends the lifespan of C. *elegans*. **(A)** survival curve of *C. elegans* N_2 at 20°C treatment with 20-, 40-, 100-, 150-, or 200-μmol/L SVHRSP or with ddH_2O (control) starting from the L4 stage (day 0), the survival number of worms in each group was recorded until all worms died; 40-μMol/L SVHRSP appeared to extend the longest lifespans (***$p < 0.001$, log-rank test). **(B)** effects of SVHRSP on food intake in N_2 worms. Surplus *E. coli* OP50 was detected by OD 600. Data were analyzed by ordinary one-way analysis of variance (ANOVA) using Prism 9.0. Values are presented as mean ± SEM. *$p < 0.05$. **(C)** representative images of C. *elegans* showing the accumulation of autofluorescent lipofuscin treatment with SVHRSP or not. The scale bar was 200 μm. Total fluorescence per worm was analyzed using ImageJ software. Data were analyzed by ordinary one-way ANOVA using Prism 9.0. Values are presented as mean ± SEM; 20-μM SVHRSP: *$p < 0.05$; 40-μM SVHRSP: ***$p < 0.001$.

worms, when treated with ddH_2O (control) and doses of 20-and 40-μM SVHRSP, would survive. Posttreatment with a low dose of SVHRSP, the worm's lifespan was significantly prolonged (**Figure 1A**) ($p < 0.001$). These results indicate that SVHRSP can prolong nematode life span and has a dose–effect relationship. The results of the food intake test showed that SVHRSP at 100, 150, and 200 μM affected the feeding activity of nematodes, while SVHRSP at 20 and 40 μM had no effect on feeding activity of nematodes (**Figure 1B**) ($p < 0.05$). Therefore, 20- and 40-μM SVHRSP concentrations could be used as effective doses for subsequent experiments. As the growth of nematode age progresses, the level of lipofuscin in the nematode body keeps rising (Henderson and Johnson, 2001). This is a normal physiological phenomenon associated with the nematode body. Aging is usually accompanied by the emergence of highly oxidized and crosslinked proteins. These oxidized protein aggregates are lipofuscin. Because protease or lysosome cannot degrade lipofuscin, it is regarded as the "marker dye" of aging (Wang H et al., 2018). On the 10th day of administration, we tested the effect of 20- and 40-μM SVHRSP on lipofuscin accumulation in aged *C. elegans*. We discover that 20- and 40-μM SVHRSP can significantly reduce the level of lipofuscin in aging nematodes (**Figures 1A–C**) ($p < 0.05$, $p < 0.001$). This provides direct evidence to support the antiaging ability of SVHRSP. In conclusion, 20- and 40-μM SVHRSP can prolong the life and reduce the level of lipofuscin in nematodes. In order to know whether SVHRSP only improved lifespan or it also had positive effects on healthspan, we need to investigate further. Thus, we evaluated the effects of 20- and 40-μM SVHRSP studies on age-related physiological functions, including pharyngeal pumps, body bending, food intake, and spawning numbers. During aging, muscle cells throughout the body gradually lose their vitality, resulting in decreased activity (Ryu et al., 2016). Reduced motor capacity is the most prominent clinical feature of aging. The rhythmic beating of muscles in the pharyngeal region of *C. elegans* back of the head is called the pharyngeal pump. Aging and neuronal injury can cause the pharyngeal beating of *C. elegans* to slow down. Therefore, the pharyngeal pump rate can be selected as an indicator to evaluate the health of *C. elegans* and the efficacy of drugs (Ryu et al., 2016). We tested the changes in the pharyngeal pump and body-bending rate of nematodes treated with 20- and 40-μM SVHRSP. The results show that SVHRSP did not enhance body bending and pharyngeal pumping contraction in worms (**Supplementary Figures S1A,B**) ($p > 0.05$). The results showed that SVHRSP could not improve the locomotor capacity of nematodes caused by aging and did not

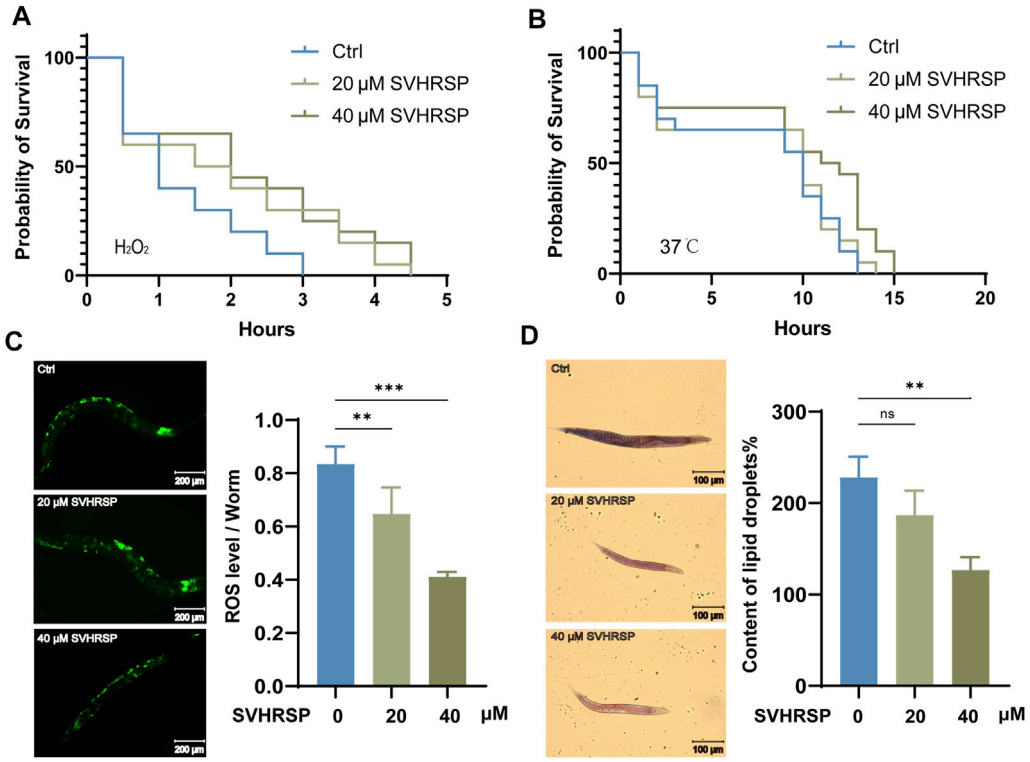

FIGURE 2 | Scorpion venom heat–resistant synthesized peptide (SVHRSP) significantly increased the resistance of nematodes to stress. **(A)** mean survival time of wild-type worms treated with 20- and 40-μM SVHRSP at 30% H_2O_2. Log-rank verifies the calculated *p*-value. **p* < 0.05 **(B)** the mean survival time of wild-type worms treated with 20- and 40-μM SVHRSP at 37°C. Log-rank verifies the calculated *p*-value. **p* < 0.05 **(C)** effects of 20- and 40-μM SVHRSP on reactive oxygen species levels in wild-type worms. **(D)** the effect of SVHRSP on fat accumulation. SVHRSP significantly inhibited the accumulation of excess fat in N_2 nematodes. Values are presented as mean ± SEM. All of these measurements were made at least three times. Log-rank and one-way analysis of variance verifies the calculated *p*-value. ns means none significant; **p* < 0.05; ***p* < 0.01; ****p* < 0.001.

improve the feeding ability of nematodes. This suggests that exercise and dietary restriction (DR) may not be one of the reasons for the antiaging mechanism of SVHRSP. One of the most popular theories of aging is longevity and reproduction. Using a variety of advanced animal models of aging, there were reports of a mechanism called a "tradeoff" between longevity and fertility, in which reduced or lost fertility leads to increased longevity (Gruber et al., 2007). However, in this study, SVHRSP did not affect the oviposition rate, suggesting that SVHRSP prolonged the lifespan of nematodes and did not lead to a reduction in nematodes' reproductive capacity. (**Supplementary Figure S1C**) ($p > 0.05$). These results indicate that SVHRSP does not affect the normal physiological functions of nematodes in the process of prolonging their lifespan.

Scorpion Venom Heat–Resistant Synthesized Peptide Increased Stress Resistance of *Caenorhabditis elegans*

As worms age, their resistance to external stimuli declines sharply, and the increase in endogenous ROS production accelerates the aging process further, thereby creating a vicious cycle. (Harman, 1956). In order to study whether SVHRSP can improve the stress resistance of nematodes, nematodes were treated with 20- and 40-μM SVHRSP. This study examined whether SVHRSP could increase the resistance of N_2 wild-type senescence *C. elegans* to acute oxidative stress and acute heat stress. On the 10th day of administration, 30% H_2O_2 was used to induce acute oxidative stress in nematodes, heat stress was induced at 37°C, and the survival time of nematodes was recorded. We discovered that SVHRSP pretreatment had a significant protective effect on these stress injuries (**Figures 2A,B**) ($p < 0.05$), suggesting that SVHRSP enhanced the resistance of nematodes to oxidative and thermal stress. Normal metabolic activity of cells produces a large accumulation of oxygen free radicals (ROS), and it has been reported that high levels of ROS can lead to aging (Harman, 1956). ROS levels in nematodes could be quantified using H_2DCF-DA fluorescent probe. In this experiment, the ROS level of N_2 wild-type senescence *C. elegans* was detected for different concentrations of SVHRSP. Our results showed that ROS accumulation was reduced in SVHRSP-pretreated worms (**Figure 2C**) (20-μM SVHRSP: $p < 0.005$, 40-μM SVHRSP: $p < 0.001$), suggesting that SVHRSP may prolong worm lifespan by reducing ROS levels in worms. It may be related to the increase in SOD activity in aged nematodes. In wild-type worms, increased ROS lead to excessive accumulation of fat (Hughes et al., 2007). Considering that SVHRSP can effectively reduce ROS levels in

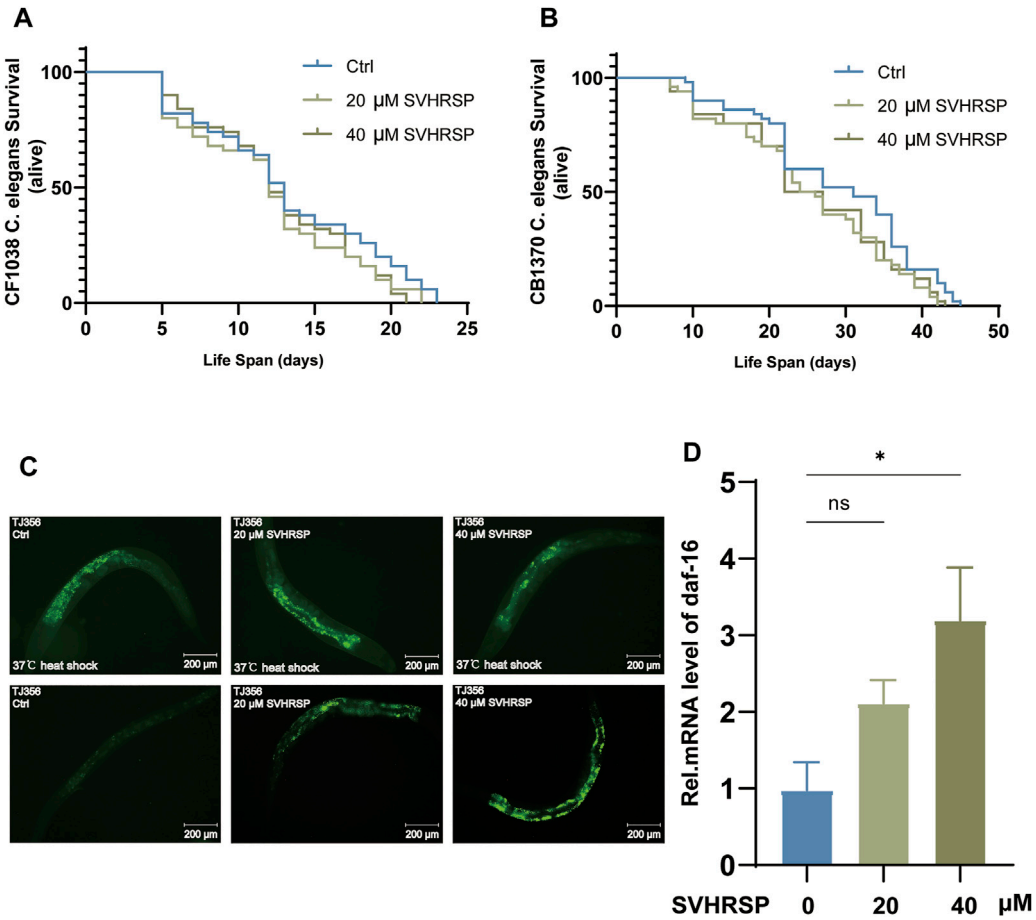

FIGURE 3 | Scorpion venom heat–resistant synthesized peptide (SVHRSP)-mediated longevity effects depended on the insulin/IGF-1-like signal (IIS) pathway. **(A)** effects of 20- and 40-μM SVHRSP untreated treatments on the lifespan of CF1038 nematodes. **(B)** effects of 20- and 40-μM SVHRSP treatments on the lifespan of CB1370 nematodes. **(C)** Fluorescence images of TJ356 nematodes treated with 20-μM and 40-μM SVHRSP, and untreated under heat stress. **(D)** Daf-16 mRNA expression levels of wild-type nematodes treated with 20- and 40-μM SVHRSP untreated. Values are presented as mean ± SEM. All of these measurements were made at least three times. Log-rank and one-way analysis of variance verifies the calculated *p*-value. ns means none significant; $^{*}p < 0.05$; $^{**}p < 0.01$; $^{***}p < 0.001$.

nematodes. SVHRSP pretreatment and untreated N_2 worms were stained with oil red O to study the effect of SVHRSP on fat deposition. The results showed that 40-μM SVHRSP significantly reduced fat accumulation in nematodes (**Figure 2D**) ($p < 0.01$). These results suggest that SVHRSP can reduce lipid accumulation caused by ROS production.

Scorpion Venom Heat–Resistant Synthesized Peptide-Mediated Longevity Extension is Associated with the Insulin/IGF-1 Signaling Pathway

According to the above experiments, SVHRSP has an excellent performance in nematodes' resistance to stress, and the insulin/insulin-like growth factor-1 signaling pathway (IIS pathway) is the most widely studied senescence-related pathway, which is related to stress, metabolism, growth, longevity, and behavior (Murphy and Hu, 2013). Daf-2 controls the activity of the conserved-phosphatidylinositol 3-kinase (PI3K)/Akt kinase cascade, which ultimately regulates the FOXO transcription factor Daf-16 (Tullet, 2015). The transcription factor controls most of the functions of this pathway and its downstream regulation of Sod-3, Hsp-16.2, Ctl-1, Gei-7, and other stress-related genes. To determine whether SVHRSP extends lifespan through the IIS pathway, we performed lifespan tests using the Daf-2 (E1370) mutant nematode CB1370 and Daf-16 (Mu86) mutant nematode CF1038 mutants *C. elegans*. The results showed that neither 20-- nor 40-μM SVHRSP could prolong the life span of CF1038 and CB1370, suggesting that Daf-2 and Daf-16 may be necessary for SVHRSP to prolong the life span of *C. elegans* (**Figures 3A,B**). ($p > 0.05$). Since Daf-16 plays an important role in the IIS pathway, the effect of SVHRSP on Daf-16 expression was further confirmed. We used transgenic nematode TJ356 ZIS356 IV to investigate whether SVHRSP could affect the expression of Daf-16. The Daf-16 gene of the nematode was labeled with GFP. An increase in culture temperature accelerates DAF-16 nuclear accumulation. When *C. elegans* was at 37°C, the amount of Daf-16 was increased by heat stress. SVHRSP can

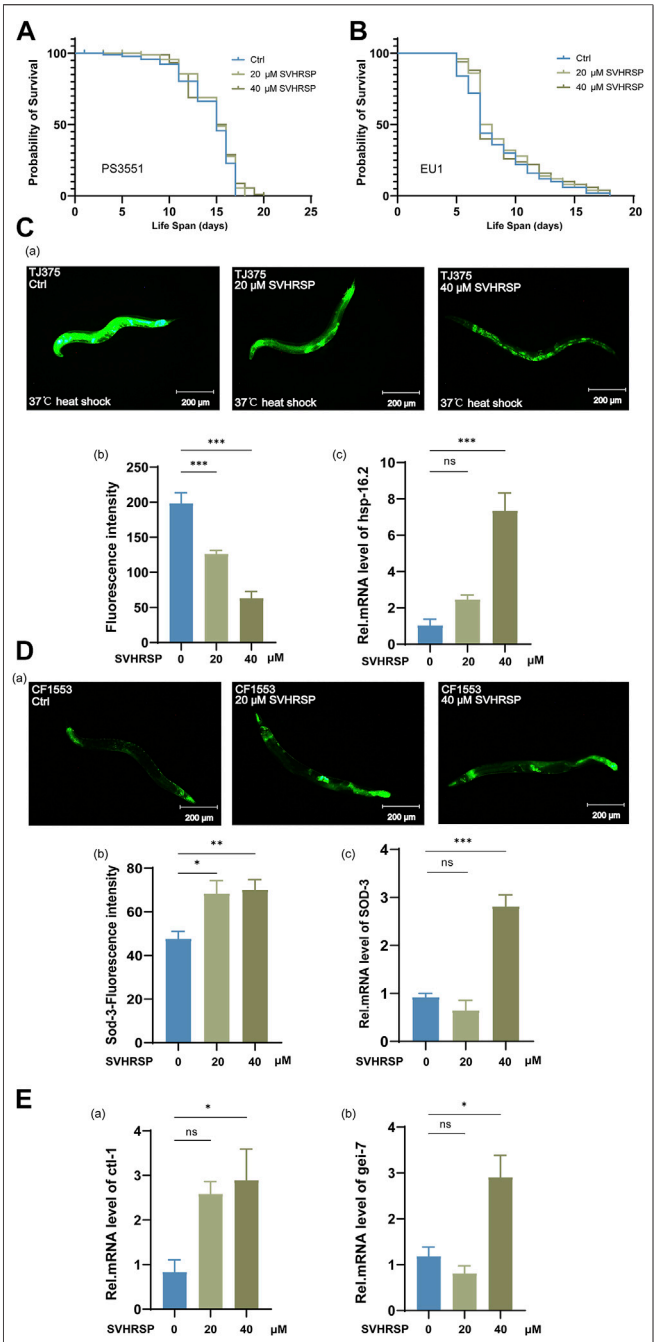

FIGURE 4 | Scorpion venom heat–resistant synthesized peptide (SVHRSP) regulates downstream gene expression of the IIS pathway. **(A)** effects of 20- and 40-μM SVHRSP untreated treatments on the lifespan of PS3551 nematodes. **(B)** -effects of 20- and 40-μM SVHRSP untreated treatments on the lifespan of EU1 nematodes. **(C) (a)** fluorescence images of TJ375 nematodes treated with 20- and 40-μM SVHRSP, and untreated under heat stress. **(b)** the GFP strength from the TJ375 strain was treated with 20- and 40-μM SVHRSP. **(c)** Hsp-16.2 mRNA levels in worms treated with 20- and 40-μM SVHRSP and controls. **(D) (a)** fluorescence images of CF1553 nematodes treated with 20- and 40-μM SVHRSP, and untreated. **(b)** the GFP intensity of CF1553(muls84) strain after 20- and 40-μM SVHRSP treatment was determined. **(c)** Sod-3mRNA levels in worms treated with 20- and 40-μM SVHRSP and controls. **(E) (a)** Ctl-1 mRNA levels in worms treated with 20- and 40-μM SVHRSP and controls. **(b)** Gei-7 mRNA levels in worms treated with 20- and 40-μM SVHRSP and controls. Values are presented as mean ± SEM. Log-rank and one-way ANOVA. ns means none significant; $^{*}p < 0.05$; $^{**}p < 0.01$; $^{***}p < 0.001$. All of these measurements were made at least three times.

reduce the damage of this stress state to *C. elegans* and reduce the amount of nuclear entry. It alleviates the stress state of the *C. elegans* itself. However, when *C. elegans* were in a normal aging state, the expression of Daf-16 was impaired, and the intake of SVHRSP improved the health status of *C. elegans* and promoted the expression of DAF-16. The results show that SVHRSP can reduce the nuclear displacement of Daf-16 at 20 and 40 μM under heat shock at 37°C, and the nuclear translocation level of TJ356 nematode was increased on day 10 of administration. (**Figure 3C**). In addition, N_2 wild-type *C. elegans* were collected on day 10 of administration, and RNA was extracted for qPCR test to detect the change in Daf-16 mRNA level, with act-1 as the steward gene. Real-time quantitative PCR results showed that 40-μM SVHRSP–treated worms had an increased mRNA level of Daf-16 compared with untreated control (**Figure 3D**). In conclusion, the effect of SVHRSP on senescence in nematodes may be mediated using the IIS pathway.

Scorpion Venom Heat–Resistant Synthesized Peptide Regulates Downstream Gene Expression of IIS Pathway

The above experiments prove that SVHRSP may be related to the IIS pathway. Moreover, SVHRSP showed excellent performance in helping *C. elegans* resist stress. Therefore, we investigated the effect of SVHRSP on downstream Daf-16 related genes. Hsf-1 is an important long-lived transcription factor that acts downstream of the IIS and is widely studied. It has been reported that downregulation of the IIS pathway, along with coactivation of Hsf-1, is necessary for the prolongation of life (Chauve et al., 2021). To investigate whether Hsf-1 is required for SVHRSP-mediated life extension, we tested the effects of 20- and 40-μM SVHRSP on Hsf-1 (SY441) mutant worms PS3551. The results showed that SVHRSP did not prolong the lifespan of Hsf-1 mutant worms PS3551 (**Figure 4A**) ($p > 0.05$), suggesting that Hsf-1 is indeed necessary for its lifespan extension.

Skn-1 is a lineal of human NRF/CNC (nuclear factor E2-related factor 2, NRF2; Capncollar, CNC) protein and plays an important role in stress response and homeostasis Skn-1 promotes longevity in otherwise WT animals (Blackwell et al., 2015). Because of SVHRSP's excellent performance in helping *C. elegans* resist stress. We used Skn-1 (ZU67) mutant *C. elegans* EU1 to conduct life span experiments. The results showed Skn-1 (ZU67) mutant's worms EU1, treated with 20- and 40-μM SVHRSP, failed to extend the lifespan when compared to ddH_2O control group (**Figure 4B**) ($p > 0.05$), suggesting that Skn-1was also required for its lifespan extension.

Our previous experiments have shown that SVHRSP enhances heat stress resistance in nematodes (**Figure 2B**). To determine

whether this is related to SVHRSP regulating specific stress response genes, we used transgenic *C. elegans* TJ375 (gpIs1) (Hsp-16.2p:GFP); the Hsp-16.2 gene of the nematode was labeled with green fluorescent protein (GFP). Inducible GFP fluorescence after >1 h heat shock at 35°C. On day 10 of administration, 20- and 40-μM SVHRSP decreased Hsp-16.2 expression in TJ375 nematodes under heat stress (**Figures 4A–C**) (20-μM SVHRSP: $p < 0.05$, 40-μM SVHRSP: $p < 0.001$). These results indicated that Hsp-16.2 could be overexpressed in *C. elegans* under heat stress, and SVHRSP could reduce the expression of Hsp-16.2. These results indicated that SVHRSP might have a protective effect on the heat stress of nematodes. In addition, N_2 wild-type *C. elegans* were collected on day 10 of administration, and RNA was extracted for qPCR test to detect the change in Hsp-16.2 mRNA level, with act-1 as the steward gene. Real-time quantitative PCR results showed that the expression of Hsp-16.2 was significantly increased after 10 days of treatment with 20- and 40-μM SVHRSP (**Figure 4C**) (40-μM SVHRSP $p < 0.01$). These results indicate that SVHRSP can increase the mRNA level of Hsp-16.2 in aging nematodes, suggesting that SVHRSP may help nematodes resist stress and delay aging by increasing the expression level of heat stress protein Hsp-16.2 in nematodes.

Considering the antioxidant effect of SVHRSP in nematodes, we studied whether the downstream gene Sod-3 of the IIS pathway has an effect on worm lifespan and stress resistance. Sod-3 has the activity of protein homodimerization and superoxide dismutase (Sod). It participates in the removal of superoxide free radicals in nematodes (Sheng et al., 2014). In order to detect the effect of SVHRSP on the expression of Sod-3 in *C. elegans*, we use the genetically-modified nematode CF1553, (muIs84) (SOD-3p:GFP + ROL-6). The Sod-3 gene of the nematode was labeled with a GFP. After 10 days of treatment with 20- and 40-μM SVHRSP, the expression level of Sod-3 in earthworms was higher than that in the control group (**Figures 4A,B,D**) (20-μM SVHRSP: $p < 0.05$; 40-μM SVHRSP: $p < 0.01$). In addition, N_2 wild-type *C. elegans* were collected on day 10 of administration, and RNA was extracted for qPCR test to detect the change in Sod-3 mRNA level, with act-1 as the steward gene. The results of real-time quantitative PCR showed that the expression of Sod-3 in nematodes treated with 20- and 40-μM SVHRSP for 10 d was significantly increased compared with the untreated group (**Figures 4C,D**). (40-μM SVHRSP: $p < 0.01$). These results suggest that SVHRSP can increase the expression of Sod-3 in nematodes, suggesting that nematodes may resist reactive oxygen generation by increasing the expression level of SOD in aging nematodes, thus maintaining homeostasis and delaying senescence.

We further investigated whether the effect of SVHRSP on lifespan was related to additional age-related genes and examined the transcriptional levels of Ctl-1 and Gei-7. Ctl-1 and Gei-7 enable catalase activity (Taub et al., 2003). It also has been predicted to enable isocitrate lyase activity and malate synthase activity, along with reports indicating significant involvement in the determination of adult lifespan (Gallo et al., 2011). Therefore, N_2 wild-type *C. elegans* were collected on day 10 of administration, and RNA was extracted for qPCR test to detect the change in Ctl-1 and Gei-7 mRNA levels, with act-1 as the steward gene. We found that the mRNA levels of Ctl-1 and Gei-7 were significantly increased after SVHRSP treatment (**Figures 4A,B,E**) (40-μM SVHRSP: $p < 0.05$). These results suggest that the effect of SVHRSP on prolonging life and improving antistress effects are partly dependent on the expression of stress-induced genes.

DISCUSSION

With increased age, the function of each component of the body decreases, and along with aging, the incidence of age-related diseases also increases. Therefore, the search for drugs that can prevent or delay aging has attracted more and more attention. More than 60% of all medicines currently on the market are related to the structure and information of natural products, so natural products are an important source of new drugs in the drug discovery process. Scorpion venom, containing a variety of toxin peptides, has diverse biological activities and is used as a medicine to strengthen human health. As an active peptide extracted from the Buthusmartensii Karsch venom, previous studies from our research group had shown that SVHRP exhibited many beneficial neuroprotective effects (Wang et al., 2007; Chen et al., 2021). SVHRSP is a synthesized peptide according to the amino acid sequence of SVHRP. In line with previous findings (Xu et al., 2021), SVHRSP alleviated neuroinflammation by downregulating microglial Nav1.6 to protect dopamine neurons (Li et al., 2021). So, we predict SVHRSP should beneficially affect lifespan.

In this study, we used *C. elegans* as a model to evaluate the effects of SVHRSP on the longevity of senescent nematodes and their related mechanisms.

In our study, we first confirmed whether SVHRSP could prolong the life span of *C. elegans*. The results showed that SVHRSP was not toxic and extended the lifespan of worms at certain concentrations (20 μM and 40 μM). As *C. elegans* age growing, *C. elegans* fat brown levels rise. This is the inevitable phenomenon of nematode growth. Lipofuscin is produced by the body's normal physiological metabolism in the aging process of highly oxidized protein aggregation because it accumulates in the body as a nematode worm signature dye (Martins et al., 2017). Our results found that supplementation with SVHRSP not only significantly extended the lifespan of *C. elegans* but also reduced the accumulation of age lipofuscin, consistent with many other natural extracts and bioactive compounds involved, such as Paullinia cupana (Boasquívis et al., 2018), Momordica charantia (Cao et al., 2018), and Polygonum multiflorum (Büchter et al., 2015), providing direct evidence to support the general antiaging capability of SVHRSP. The process of aging is usually accompanied by physiological changes, such as the gradual loss of muscle cell vitality during aging, resulting in a decrease in the motility of nematodes (Murakami et al., 2005). Pharyngeal pumping rate decreased with age, reflecting a decrease in nematode food intake and inducing DR effects (Ryu et al., 2016; Herndon et al., 2018). Many studies of natural products have demonstrated that antiaging effects improve these indicators (Fang et al., 2017; Lin et al., 2019). In addition, the relationship between longevity and fertility has been a hot topic in many theories of aging. In studies of various animal models, scientists have made an interesting discovery that reduced fertility may lead to increased longevity. (Herndon et al., 2018). Therefore, we investigated

reproductive parameters, such as oviposition volume, pharyngeal pumping rate, and body-bending ability of nematodes, to reflect the effects of oligopeptide treatment on age-related physiological indexes of nematodes (Yang et al., 2018). In this study, we found that SVHRSP did not improve the motility or pharyngeal pump rate of nematodes. These results indicated that SVHRSP could prolong the lifespan of nematodes without affecting their reproductive ability. In conclusion, the effects of exercise and DR may not be the main reasons behind SVHRSP-mediated antiaging related mechanisms, suggesting that SVHRSP extended the lifespan and reduced the level of lipofuscin without affecting the normal physiological function in *C. elegans*.

Oxidative stress is a pathological state related to aging. A large number of studies have shown that oxidative stress will cause certain damage to the body (Avanesov et al., 2014; Beckhauser et al., 2016). *C. elegans*' longevity is associated with increased resistance to external stimuli (Morley and Morimoto, 2004; Westerheide et al., 2009; Fontana et al., 2010; Schieber and Chandel, 2014). To ensure the beneficial effects of SVHRSP on nematode survival, we examined its resistance to heat and oxidative stress. The results showed that SVHRSP could enhance the resistance of nematodes to external stimuli. The free radical theory of aging is a widely accepted hypothesis that describes ROS as the key to aging and age-related diseases and that the accumulation of excessive ROS in nematodes greatly shortens the lifespan of nematodes (Avanesov et al., 2014). Nematodes normally produce large amounts of antioxidant enzymes, such as Sod, to fight ROS production and maintain balance (Wang et al., 2016). Our results suggest that SVHRSP reduces ROS accumulation in nematodes. Growing evidence has shown that enhanced ROS production can lead to excessive fat accumulation and change in fatty acid composition, at least in part depending on the Daf-16 pathway (Brunk and Terman, 2002; Hughes et al., 2007; Wang K et al., 2018). After lipid staining with oil red O, the results showed that SVHRSP could reduce fat accumulation and promote lipid metabolism in *C. elegans*. This is consistent with the results of previous ROS studies. It is implied in this study that SVHRSP enhanced tolerance to heat stress and H_2O_2-induced oxidative stress in *C. elegans* and effectively decreased ROS levels and fat accumulation levels, which are in accordance with many other antioxidants, such as flavonoids (Yang et al., 2019), Quercetin (Proshkina et al., 2016), and Naringin (Zhu et al., 2020). In conclusion, SVHRSP may play an important role in the regulation of redox balance in nematodes, which may contribute to the study of its antiaging mechanism.

The IIS pathway is an important pathway regulating aging and longevity and is related to stress, metabolism, growth, and longevity behavior (Fontana et al., 2010; Kenyon, 2010). It is highly conserved in invertebrates and mammals and is one of the most well-understood and widely studied senescence-related pathways (Panowski and Dillin, 2009). Daf-2 is a growth factor receptor of the IIS pathway, which plays a major role in nematode growth and metabolism. With the growth of nematodes, Daf-2 can downregulate the metabolic activity of nematodes. Therefore, the loss of Daf-2 can prolong the lifespan of the nematode and enhance its stress resistance, and its downregulation can promote the expression of Daf-16 downstream (Murphy et al., 2003; Rea et al., 2005; Sun et al., 2017). FOXO homolog Daf-16 of *C. elegans* is the core transcription target of the IIS pathway, which plays a positive role in regulating lifespan, stress, reproduction, lipid metabolism, and other biological processes in IIS. Its destruction reportedly speeds up the normal rate of aging, and boosting its expression can extend its lifespan (Garigan et al., 2002; Lee et al., 2003; Haithcock et al., 2005). Our results showed that SVHRSP could not prolong the life span of Daf-2 and Daf-16 mutant nematodes. These findings suggest that Daf-2 and Daf-16 may be key molecules necessary for SVHRSP to prolong the lifespan of nematodes. In another study in our lab, we used PD models of 6-OHDA-induced nematodes. The lifespan of CB1370 nematodes was significantly shortened after induction with 6-OHDA but recovered after treatment with SVHRSP (not published yet). These results suggest that the delayed life of SVHRSP may be related to Daf-2. In the following experiments, we will order daf-2 overexpressed nematodes with gene mutation for the next experiment to determine the relationship between SVHRSP and Daf-2. Considering that the IIS pathway regulates lifespan in *C. elegans* through Daf-16 nuclear localization (Narasimhan et al., 2011), we postulated that SVHRSP treatment might affect Daf-16 nuclear translocation, a necessary prerequisite for its transcriptional activation activity. Using the nematode labeled Daf-16 gene with GFP, we found SVHRSP can reduce the nuclear displacement of Daf-16 under heat shock at 37°C, and the nuclear translocation level of the TJ356 nematode was increased on day 10 of administration. And meanwhile, the expression level of Daf-16 mRNA was increased by SVHRSP in N_2 wild-type *C. elegans*.

Heat shock factor 1 (Hsf-1) regulates the expression of cellular chaperone genes to maintain the proteostasis from stresses by preventing misfolding and mistranslation (Hsu et al., 2003; Chiang et al., 2012) and regulates the expression of the IIS pathway downstream genes synergizing with Daf-16. It has been reported that overexpression of Hsf-1 results in increased longevity, whereas inhibition of Hsf-1 activity by RNAi reduces lifespan in mammals (DanQing et al., 2021). In the present research, we subsequently used worms lacking functional Hsf-1 genes, Hsf-1 (sy441), for the lifespan assays and found that SVHRSP treatment indeed failed to extend the lifespan of Hsf-1 (sy441) worms. These results implied that Hsf-1 was required for SVHRSP-mediated induced heat resistance and lifespan extension of *C. elegans*. It has been reported that baicalein mediates antioxidant effects by activating nuclear factor erythroid 2-related factor 2 (Nrf-2) in mammalian cell lines (Ma J et al., 2018). When it comes to *C. elegans*, Skn-1, homologous to mammalian Nrf-2 (An and Blackwell, 2003), is known as a major regulator of longevity and oxidative stress responses through the IIS pathway (Lee et al., 2015; Altintas et al., 2016; Tullet et al., 2017). Skn-1 has been proven to improve lifespan and ease Aβ-induced toxicity in nematodes (Edwards et al., 2014; Govindan et al., 2018). Further analysis revealed that SVHRSP failed to extend the lifespan of mutant worms for Skn-1. These results implied that Skn-1 was required for SVHRSP-mediated induced heat resistance and lifespan extension of *C. elegans*. Hsp-16.2, a downstream target gene of the IIS pathway, is known to be regulated by Hsf-1 and associated with aging and many age-related diseases (Leroux et al., 1997). Hsp-16.2 can also downregulate oxidative stress by increasing the levels of the reduced form of glutathione (Mehlen et al., 1996) and modulate longevity by interacting with nuclear hormone receptors (Morimoto,

2002). Our results also provide evidence that Hsp-16.2 could be overexpressed in *C. elegans* under heat stress, and SVHRSP could reduce the expression of Hsp-16.2. In addition, we performed a qPCR test on N_2 *C. elegans* on day 10 of administration and found that SVHRSP can increase the mRNA level of Hsp-16.2 in aging nematodes, suggesting that SVHRSP may help nematodes resist stress and delay aging by increasing the expression level of heat stress protein Hsp-16.2 in nematodes.

As a direct target of Daf-16, Sod-3 is a typical scavenger enzyme that protects the worms against ROS and declines with aging (Rangsinth et al., 2019). Its promoter contains consensus Daf-16/FOXO-binding elements (DBEs), which bind to Daf-16 and catalyze the removal of superoxide to resist oxidative stress (Oh et al., 2006). We found that SVHRSP could slow down the decline of the mRNA expression of Sod-3 with aging in worms. For further verification of the effect of SVHRSP, we analyzed the transgenic strain CF1553, carrying a Sod-3-GFP reporter gene, and found that Sod-3-GFP showed higher expression levels treated with SVHRSP, which might exert the antiaging effects of SVHRSP *via* the increasing activity of antioxidant enzymes. To this end, we detected changes in Sod-3 mRNA expression level of N_2 nematodes on day 10 of administration. We found that SVHRSP can increase the expression of Sod-3 mRNA in worms. Afterward, we also detected the expression levels of Ctl-1 and Gei-7 downstream stress-related genes of Daf-16. The results showed Ctl-1 and Gei-7, as antioxidant genes related to the IIS pathway, were also upregulated following SVHRSP treatments at the mRNA level and might be contributing to the antioxidant activity of SVHRSP. These results suggest that SVHRSP may delay aging by affecting downstream stress-related target genes through Daf-16.

CONCLUSION

Through the above experimental studies, we found that SVHRSP significantly prolonged the life span and delayed aging of nematodes through insulin/IGF-1 signal transduction and stress resistance pathways. These pathways are well conserved from worms to mammals. Our results can be the basis for developing SVHRSP-rich products with health benefits, and provide a platform for further research on the age-related or progressive diseases in mammals.

DATA AVAILABILITY STATEMENT

The raw data supporting the conclusions of this article will be made available by the authors without undue reservation.

AUTHOR CONTRIBUTIONS

Conceptualization, SL and JZ; methodology, Y-ZW, S-YG, R-LK, R-XG, and Z-HW; formal analysis, Y-ZW and S-YG; resources, R-LK and A-RS; writing—original draft preparation, Y-ZW, S-YG, and KS; writing—review and editing, SL, Y-W, and S-YG; supervision, SL and JZ; project administration, SL and JZ; these authors contributed equally to this work. All authors have read and agreed to the published version of the manuscript.

FUNDING

This research was funded by the National Natural Sciences Foundation of China (U1908208,82101275,82101661), Liaoning Provincial Key R&D Program (2019020048-JH2/103), and Liaoning Revitalization Talents Program (XLYC1902044).

SUPPLEMENTARY MATERIAL

The Supplementary Material for this article can be found online at: https://www.frontiersin.org/articles/10.3389/fphar.2022.919269/full#supplementary-material

REFERENCES

Altintas, O., Park, S., and Lee, S. J. (2016). The Role of insulin/IGF-1 Signaling in the Longevity of Model Invertebrates, *C. elegans* and *D. melanogaster*. *BMB Rep.* 49 (2), 81–92. doi:10.5483/bmbrep.2016.49.2.261

An, J. H., and Blackwell, T. K. (2003). SKN-1 Links *C. elegans* Mesendodermal Specification to a Conserved Oxidative Stress Response. *Genes Dev.* 17 (15), 1882–1893. doi:10.1101/gad.1107803

Avanesov, A. S., Ma, S., Pierce, K. A., Yim, S. H., Lee, B. C., Clish, C. B., et al. (2014). Age- and Diet-Associated Metabolome Remodeling Characterizes the Aging Process Driven by Damage Accumulation. *Elife* 3, e02077. doi:10.7554/eLife.02077

Barzilai, N., Cuervo, A. M., and Austad, S. (2018). Aging as a Biological Target for Prevention and Therapy. *JAMA* 320 (13), 1321–1322. doi:10.1001/jama.2018.9562

Beckhauser, T. F., Francis-Oliveira, J., and De Pasquale, R. (2016). Reactive Oxygen Species: Physiological and Physiopathological Effects on Synaptic Plasticity. *J. Exp. Neurosci.* 10 (Suppl. 1), 23–48. doi:10.4137/JEN.S39887

Blackwell, T. K., Steinbaugh, M. J., Hourihan, J. M., Ewald, C. Y., and Isik, M. (2015). SKN-1/Nrf, Stress Responses, and Aging in *Caenorhabditis elegans*. *Free Radic. Biol. Med.* 88, 290–301. doi:10.1016/j.freeradbiomed.2015.06.008

Boasquívis, P. F., Silva, G. M. M., Paiva, F. A., Cavalcanti, R. M., Nunez, C. V., and de Paula Oliveira, R. (2018). Guarana (Paullinia Cupana) Extract Protects *Caenorhabditis elegans* Models for Alzheimer Disease and Huntington Disease through Activation of Antioxidant and Protein Degradation Pathways. *Oxid. Med. Cell Longev.* 2018, 9241308. doi:10.1155/2018/9241308

Brunk, U. T., and Terman, A. (2002). Lipofuscin: Mechanisms of Age-Related Accumulation and Influence on Cell Function. *Free Radic. Biol. Med.* 33 (5), 611–619. doi:10.1016/s0891-5849(02)00959-0

Büchter, C., Zhao, L., Havermann, S., Honnen, S., Fritz, G., Proksch, P., et al. (2015). TSG (2,3,5,4'-Tetrahydroxystilbene-2-O- β -D-Glucoside) from the Chinese Herb Polygonum Multiflorum Increases Life Span and Stress Resistance of *Caenorhabditis elegans*. *Oxid. Med. Cell Longev.* 2015, 124357. doi:10.1155/2015/124357

Cao, X., Sun, Y., Lin, Y., Pan, Y., Farooq, U., Xiang, L., et al. (2018). Antiaging of Cucurbitane Glycosides from Fruits of Momordica Charantia L. *Oxid. Med. Cell Longev.* 2018, 1538632. doi:10.1155/2018/1538632

Chauve, L., Hodge, F., Murdoch, S., Masoudzadeh, F., Mann, H. J., Lopez-Clavijo, A., et al. (2021). Neuronal HSF-1 Coordinates the Propagation of Fat Desaturation across Tissues to Enable Adaptation to High Temperatures in *C. elegans*. *Plos Biol.* 19 (11), 33. doi:10.1371/journal.pbio.3001431

Chen, Q., Yang, P., Lin, Q., Pei, J., Jia, Y., Zhong, Z., et al. (2021). Effects of Scorpion Venom Heat-Resistant Peptide on the Hippocampal Neurons of Kainic Acid-Induced Epileptic Rats. *Braz J. Med. Biol. Res.* 54 (5), e10717. doi:10.1590/1414-431X202010717

Chiang, W. C., Ching, T. T., Lee, H. C., Mousigian, C., and Hsu, A. L. (2012). HSF-1 Regulators DDL-1/2 Link Insulin-like Signaling to Heat-Shock Responses and Modulation of Longevity. *Cell* 148 (1-2), 322–334. doi:10.1016/j.cell.2011.12.019

DanQing, L., YuJie, G., ChengPeng, Z., HongZhi, D., Yi, H., BiSheng, H., et al. (2021). N-butanol Extract of Hedyotis Diffusa Protects Transgenic *Caenorhabditis elegans* from Aβ-Induced Toxicity. *Phytother. Res.* 35 (2), 1048–1061. doi:10.1002/ptr.6871

Edwards, C., Canfield, J., Copes, N., Rehan, M., Lipps, D., and Bradshaw, P. C. (2014). D-beta-hydroxybutyrate Extends Lifespan in *C. elegans*. *Aging (Albany NY)* 6 (8), 621–644. doi:10.18632/aging.100683

Fang, E. F., Scheibye-Knudsen, M., Jahn, H. J., Li, J., Ling, L., Guo, H., et al. (2015). A Research Agenda for Aging in China in the 21st Century. *Ageing Res. Rev.* 24 (Pt B), 197–205. doi:10.1016/j.arr.2015.08.003

Fang, E. F., Waltz, T. B., Kassahun, H., Lu, Q., Kerr, J. S., Morevati, M., et al. (2017). Tomatidine Enhances Lifespan and Healthspan in *C. elegans* through Mitophagy Induction via the SKN-1/Nrf2 Pathway. *Sci. Rep.* 7, 46208. doi:10.1038/srep46208

Fontana, L., Partridge, L., and Longo, V. D. (2010). Extending Healthy Life Span-Ffrom Yeast to Humans. *Science* 328 (5976), 321–326. doi:10.1126/science.1172539

Gallo, M., Park, D., and Riddle, D. L. (2011). Increased Longevity of Some *C. elegans* Mitochondrial Mutants Explained by Activation of an Alternative Energy-Producing Pathway. *Mech. Ageing Dev.* 132 (10), 515–518. doi:10.1016/j.mad.2011.08.004

Garigan, D., Hsu, A. L., Fraser, A. G., Kamath, R. S., Ahringer, J., and Kenyon, C. (2002). Genetic Analysis of Tissue Aging in *Caenorhabditis elegans*: A Role for Heat-Shock Factor and Bacterial Proliferation. *Genetics* 161 (3), 1101–1112. doi:10.1093/genetics/161.3.1101

Govindan, S., Amirthalingam, M., Duraisamy, K., Govindhan, T., Sundararaj, N., and Palanisamy, S. (2018). Phytochemicals-induced Hormesis Protects *Caenorhabditis elegans* against α-synuclein Protein Aggregation and Stress through Modulating HSF-1 and SKN-1/Nrf2 Signaling Pathways. *Biomed. Pharmacother.* 102, 812–822. doi:10.1016/j.biopha.2018.03.128

Gruber, J., Tang, S. Y., and Halliwell, B. (2007). "Evidence for a Trade-Off between Survival and Fitness Caused by Resveratrol Treatment of *Caenorhabditis elegans*," in *Biogerontology: Mechanisms and Interventions*. Editors S. I. S. Rattan and S. Akman (Malden: Wiley-Blackwell), 530–542. doi:10.1196/annals.1395.059

Haithcock, E., Dayani, Y., Neufeld, E., Zahand, A. J., Feinstein, N., Mattout, A., et al. (2005). Age-related Changes of Nuclear Architecture in *Caenorhabditis elegans*. *Proc. Natl. Acad. Sci. U. S. A.* 102 (46), 16690–16695. doi:10.1073/pnas.0506955102

Harman, D. (1956). Aging: A Theory Based on Free Radical and Radiation Chemistry. *J. Gerontol.* 11 (3), 298–300. doi:10.1093/geronj/11.3.298

Henderson, S. T., and Johnson, T. E. (2001). daf-16 Integrates Developmental and Environmental Inputs to Mediate Aging in the Nematode *Caenorhabditis elegans*. *Curr. Biol.* 11 (24), 1975–1980. doi:10.1016/s0960-9822(01)00594-2

Herndon, L. A., Wolkow, C., and Hall, D. H. (2018). "WormAtlas Aging Handbook - Introduction to Aging in *C. elegans*," in *Wormatlas*. doi:10.3908/wormatlas.8.4

Hsu, A. L., Murphy, C. T., and Kenyon, C. (2003). Regulation of Aging and Age-Related Disease by DAF-16 and Heat-Shock Factor. *Science* 300 (5622), 1142–1145. doi:10.1126/science.1083701

Hughes, S. E., Evason, K., Xiong, C., and Kornfeld, K. (2007). Genetic and Pharmacological Factors that Influence Reproductive Aging in Nematodes. *PLoS Genet.* 3 (2), e25–265. doi:10.1371/journal.pgen.0030025

Kenyon, C. J. (2010). The Genetics of Ageing. *Nature* 464 (7288), 504–512. doi:10.1038/nature08980

Lapierre, L. R., and Hansen, M. (2012). Lessons from *C. elegans*: Signaling Pathways for Longevity. *Trends Endocrinol. Metab.* 23 (12), 637–644. doi:10.1016/j.tem.2012.07.007

Lee, S. S., Kennedy, S., Tolonen, A. C., and Ruvkun, G. (2003). DAF-16 Target Genes that Control *C. elegans* Life-Span and Metabolism. *Science* 300 (5619), 644–647. doi:10.1126/science.1083614

Lee, T. H., Mun, J. Y., Han, S. M., Yoon, G., Han, S. S., and Koo, H. S. (2009). DIC-1 Over-expression Enhances Respiratory Activity in *Caenorhabditis elegans* by Promoting Mitochondrial Cristae Formation. *Genes cells.* 14 (3), 319–327. doi:10.1111/j.1365-2443.2008.01276.x

Lee, Y., Seon, W. A. A., Artan, M., Seo, W., Hwang, A. B., Jeong, D. E., et al. (2015). "Genes and Pathways that Influence Longevity in *Caenorhabditis elegans*," in *Aging Mechanisms*, 123–169. doi:10.1007/978-4-431-55763-0_8

Leroux, M. R., Melki, R., Gordon, B., Batelier, G., and Candido, E. P. (1997). Structure-function Studies on Small Heat Shock Protein Oligomeric Assembly and Interaction with Unfolded Polypeptides. *J. Biol. Chem.* 272 (39), 24646–24656. doi:10.1074/jbc.272.39.24646

Li, X., Wu, X., Li, N., Li, D., Sui, A., Khan, K., et al. (2021). Scorpion Venom Heat-Resistant Synthesized Peptide Ameliorates 6-OHDA-Induced Neurotoxicity and Neuroinflammation: Likely Role of Nav 1.6 Inhibition in Microglia. *Br. J. Pharmacol.* 178 (17), 3553–3569. doi:10.1111/bph.15502

Lin, C., Zhang, X., Xiao, J., Zhong, Q., Kuang, Y., Cao, Y., et al. (2019). Effects on Longevity Extension and Mechanism of Action of Carnosic Acid in *Caenorhabditis elegans*. *Food Funct.* 10 (3), 1398–1410. doi:10.1039/c8fo02371a

López-Otín, C., Blasco, M. A., Partridge, L., Serrano, M., and Kroemer, G. (2013). The Hallmarks of Aging. *Cell* 153 (6), 1194–1217. doi:10.1016/j.cell.2013.05.039

Ma J, J., Li, S., Zhu, L., Guo, S., Yi, X., Cui, T., et al. (2018). Baicalein Protects Human Vitiligo Melanocytes from Oxidative Stress through Activation of NF-E2-Related Factor2 (Nrf2) Signaling Pathway. *Free Radic. Biol. Med.* 129, 492–503. doi:10.1016/j.freeradbiomed.2018.10.421

Ma L, L., Zhao, Y., Chen, Y., Cheng, B., Peng, A., and Huang, K. (2018). *Caenorhabditis elegans* as a Model System for Target Identification and Drug Screening against Neurodegenerative Diseases. *Eur. J. Pharmacol.* 819, 169–180. doi:10.1016/j.ejphar.2017.11.051

Martins, W. K., Gomide, A. B., Costa, É. T., Junqueira, H. C., Stolf, B. S., Itri, R., et al. (2017). Membrane Damage by Betulinic Acid Provides Insights into Cellular Aging. *Biochim. Biophys. Acta Gen. Subj.* 1861 (1 Pt A), 3129–3143. doi:10.1016/j.bbagen.2016.10.018

Mehlen, P., Kretz-Remy, C., Préville, X., and Arrigo, A. P. (1996). Human Hsp27, Drosophila Hsp27 and Human alphaB-Crystallin Expression-Mediated Increase in Glutathione Is Essential for the Protective Activity of These Proteins against TNFalpha-Induced Cell Death. *EMBO J.* 15 (11), 2695–2706. doi:10.1002/j.1460-2075.1996.tb00630.x

Morimoto, R. I. (2002). Dynamic Remodeling of Transcription Complexes by Molecular Chaperones. *Cell* 110 (3), 281–284. doi:10.1016/s0092-8674(02)00860-7

Morley, J. F., and Morimoto, R. I. (2004). Regulation of Longevity in *Caenorhabditis elegans* by Heat Shock Factor and Molecular Chaperones. *Mol. Biol. Cell* 15 (2), 657–664. doi:10.1091/mbc.e03-07-0532

Murakami, H., Bessinger, K., Hellmann, J., and Murakami, S. (2005). Aging-dependent and -independent Modulation of Associative Learning Behavior by Insulin/insulin-like Growth Factor-1 Signal in *Caenorhabditis elegans*. *J. Neurosci.* 25 (47), 10894–10904. doi:10.1523/JNEUROSCI.3600-04.2005

Murphy, C. T., and Hu, P. J. (2013). "Insulin/insulin-like Growth Factor Signaling in *C. elegans*," in *WormBook*, 1–43. doi:10.1895/wormbook.1.164.1

Murphy, C. T., McCarroll, S. A., Bargmann, C. I., Fraser, A., Kamath, R. S., Ahringer, J., et al. (2003). Genes that Act Downstream of DAF-16 to Influence the Lifespan of *Caenorhabditis elegans*. *Nature* 424 (6946), 277–283. doi:10.1038/nature01789

Narasimhan, S. D., Yen, K., Bansal, A., Kwon, E. S., Padmanabhan, S., and Tissenbaum, H. A. (2011). PDP-1 Links the TGF-β and IIS Pathways to Regulate Longevity, Development, and Metabolism. *PLoS Genet.* 7 (4), e1001377. doi:10.1371/journal.pgen.1001377

Oh, S. W., Mukhopadhyay, A., Dixit, B. L., Raha, T., Green, M. R., and Tissenbaum, H. A. (2006). Identification of Direct DAF-16 Targets Controlling Longevity, Metabolism and Diapause by Chromatin Immunoprecipitation. *Nat. Genet.* 38 (2), 251–257. doi:10.1038/ng1723

Ortiz, E., Gurrola, G. B., Schwartz, E. F., and Possani, L. D. (2015). Scorpion Venom Components as Potential Candidates for Drug Development. *Toxicon* 93, 125–135. doi:10.1016/j.toxicon.2014.11.233

Panowski, S. H., and Dillin, A. (2009). Signals of Youth: Endocrine Regulation of Aging in *Caenorhabditis elegans*. *Trends Endocrinol. Metab.* 20 (6), 259–264. doi:10.1016/j.tem.2009.03.006

Pietsch, K., Saul, N., Menzel, R., Stürzenbaum, S. R., and Steinberg, C. E. (2009). Quercetin Mediated Lifespan Extension in *Caenorhabditis elegans* Is Modulated by Age-1, Daf-2, Sek-1 and Unc-43. *Biogerontology* 10 (5), 565–578. doi:10.1007/s10522-008-9199-6

Proshkina, E., Lashmanova, E., Dobrovolskaya, E., Zemskaya, N., Kudryavtseva, A., Shaposhnikov, M., et al. (2016). Geroprotective and Radioprotective Activity of Quercetin, (-)-Epicatechin, and Ibuprofen in *Drosophila melanogaster*. *Front. Pharmacol.* 7, 505. doi:10.3389/fphar.2016.00505

Rangsinth, P., Prasansuklab, A., Duangjan, C., Gu, X., Meemon, K., Wink, M., et al. (2019). Leaf Extract of Caesalpinia Mimosoides Enhances Oxidative Stress Resistance and Prolongs Lifespan in *Caenorhabditis elegans*. *BMC Complement. Altern. Med.* 19 (1), 164. doi:10.1186/s12906-019-2578-5

Rea, S. L., Wu, D., Cypser, J. R., Vaupel, J. W., and Johnson, T. E. (2005). A Stress-Sensitive Reporter Predicts Longevity in Isogenic Populations of *Caenorhabditis elegans*. *Nat. Genet.* 37 (8), 894–898. doi:10.1038/ng1608

Ruan, Q., Qiao, Y., Zhao, Y., Xu, Y., Wang, M., Duan, J., et al. (2016). Beneficial Effects of Glycyrrhizae Radix Extract in Preventing Oxidative Damage and Extending the Lifespan of *Caenorhabditis elegans*. *J. Ethnopharmacol.* 177, 101–110. doi:10.1016/j.jep.2015.10.008

Ryu, D., Mouchiroud, L., Andreux, P. A., Katsyuba, E., Moullan, N., Nicolet-Dit-Félix, A. A., et al. (2016). Urolithin A Induces Mitophagy and Prolongs Lifespan in *C. elegans* and Increases Muscle Function in Rodents. *Nat. Med.* 22 (8), 879–888. doi:10.1038/nm.4132

Schieber, M., and Chandel, N. S. (2014). ROS Function in Redox Signaling and Oxidative Stress. *Curr. Biol.* 24 (10), R453–R462. doi:10.1016/j.cub.2014.03.034

Shao, J., Kang, N., Liu, Y., Song, S., Wu, C., and Zhang, J. (2007). Purification and Characterization of an Analgesic Peptide from Buthus Martensii Karsch. *Biomed. Chromatogr.* 21 (12), 1266–1271. doi:10.1002/bmc.882

Sheng, Y., Abreu, I. A., Cabelli, D. E., Maroney, M. J., Miller, A. F., Teixeira, M., et al. (2014). Superoxide Dismutases and Superoxide Reductases. *Chem. Rev.* 114 (7), 3854–3918. doi:10.1021/cr4005296

Solis, G. M., and Petrascheck, M. (2011). Measuring *Caenorhabditis elegans* Life Span in 96 Well Microtiter Plates. *J. Vis. Exp.* 49, 2496. doi:10.3791/2496

Stiernagle, T. (2006). "Maintenance of *C. elegans*," in *WormBook*, 1–11. doi:10.1895/wormbook.1.101.1

Strayer, A., Wu, Z., Christen, Y., Link, C. D., and Luo, Y. (2003). Expression of the Small Heat-Shock Protein Hsp16-2 in *Caenorhabditis elegans* Is Suppressed by Ginkgo Biloba Extract EGb 761. *FASEB J.* 17 (15), 2305–2307. doi:10.1096/fj.03-0376fje

Sun, X., Chen, W. D., and Wang, Y. D. (2017). DAF-16/FOXO Transcription Factor in Aging and Longevity. *Front. Pharmacol.* 8, 548. doi:10.3389/fphar.2017.00548

Tajti, G., Wai, D. C. C., Panyi, G., and Norton, R. S. (2020). The Voltage-Gated Potassium Channel KV1.3 as a Therapeutic Target for Venom-Derived Peptides. *Biochem. Pharmacol.* 181, 114146. doi:10.1016/j.bcp.2020.114146

Tao, J., Yin, S., Song, Y., Zeng, L., Li, S., Liu, N., et al. (2021). Novel Scorpion Venom Peptide HsTx2 Ameliorates Cerebral Ischemic Brain Injury in Rats via the MAPK Signaling Pathway. *Biochem. Biophys. Res. Commun.* 534, 442–449. doi:10.1016/j.bbrc.2020.11.062

Taub, J., Lau, J. F., Ma, C., Hahn, J. H., Hoque, R., Rothblatt, J., et al. (2003). A Cytosolic Catalase Is Needed to Extend Adult Lifespan in *C. elegans* Daf-C and Clk-1 Mutants. *Nature* 421 (6924), 764. doi:10.1038/nature01425

Tullet, J. M. A., Green, J. W., Au, C., Benedetto, A., Thompson, M. A., Clark, E., et al. (2017). The SKN-1/Nrf2 Transcription Factor Can Protect against Oxidative Stress and Increase Lifespan in *C. elegans* by Distinct Mechanisms. *Aging Cell* 16 (5), 1191–1194. doi:10.1111/acel.12627

Tullet, J. M. (2015). DAF-16 Target Identification in *C. elegans*: Past, Present and Future. *Biogerontology* 16 (2), 221–234. doi:10.1007/s10522-014-9527-y

Voisine, C., Varma, H., Walker, N., Bates, E. A., Stockwell, B. R., and Hart, A. C. (2007). Identification of Potential Therapeutic Drugs for Huntington's Disease Using *Caenorhabditis elegans*. *Plos One* 2 (6), e504. doi:10.1371/journal.pone.0000504

Wang, Y., Zhang, X. Y., Li, S., Zhang, J., Zhao, J., and Zhang, W. Q. (2007). Inhibitory Effects of Scorpion Venom Heat Resistant Protein on the Excitability of Acutely Isolated Rat Hippocampal Neurons. *Sheng Li Xue Bao* 59 (1), 87–93. doi:10.13294/j.aps.2007.01.014

Wang, T., Wang, S. W., Zhang, Y., Wu, X. F., Peng, Y., Cao, Z., et al. (2014). Scorpion Venom Heat-Resistant Peptide (SVHRP) Enhances Neurogenesis and Neurite Outgrowth of Immature Neurons in Adult Mice by Up-Regulating Brain-Derived Neurotrophic Factor (BDNF). *PLoS One* 9 (10), e109977. doi:10.1371/journal.pone.0109977

Wang, Q. Q., Huang, Y. X., Qin, C. X., Liang, M., Mao, X. L., Li, S. M., et al. (2016). Bioactive Peptides from Angelica Sinensis Protein Hydrolyzate Delay Senescence in *Caenorhabditis elegans* through Antioxidant Activities. *Oxid. Med. Cell. Longev.* 2016, 10. doi:10.1155/2016/8956981

Wang H, H., Liu, J., Li, T., and Liu, R. H. (2018). Blueberry Extract Promotes Longevity and Stress Tolerance via DAF-16 in *Caenorhabditis elegans*. *Food Funct.* 9 (10), 5273–5282. doi:10.1039/c8fo01680a

Wang K, K., Chen, S., Zhang, C., Huang, J., Wu, J., Zhou, H., et al. (2018). Enhanced ROS Production Leads to Excessive Fat Accumulation through DAF-16 in *Caenorhabditis elegans*. *Exp. Gerontol.* 112, 20–29. doi:10.1016/j.exger.2018.07.017

Wang, X. G., Zhu, D. D., Li, N., Huang, Y. L., Wang, Y. Z., Zhang, T., et al. (2020). Scorpion Venom Heat-Resistant Peptide is Neuroprotective against Cerebral Ischemia-Reperfusion Injury in Association with the NMDA-MAPK Pathway. *Neurosci. Bull.* 36 (3), 243–253. doi:10.1007/s12264-019-00425-1

Westerheide, S. D., Anckar, J., Stevens, S. M., Sistonen, L., and Morimoto, R. I. (2009). Stress-inducible Regulation of Heat Shock Factor 1 by the Deacetylase SIRT1. *Science* 323 (5917), 1063–1066. doi:10.1126/science.1165946

Wu, X.-F., Li, C., Yang, G., Wang, Y.-Z., Peng, Y., Zhu, D.-D., et al. (2021). Scorpion Venom Heat-Resistant Peptide Attenuates Microglia Activation and Neuroinflammation. *Front. Pharmacol.* 12, 704715. doi:10.3389/fphar.2021.704715

Xu, X., Xu, H., Ren, F., Huang, L., Xu, J., and Li, F. (2021). Protective Effect of Scorpion Venom Heat-Resistant Synthetic Peptide against $PM_{2.5}$-induced Microglial Polarization via TLR4-Mediated Autophagy Activating PI3K/AKT/NF-κB Signaling Pathway. *J. Neuroimmunol.* 355, 577567. doi:10.1016/j.jneuroim.2021.577567

Yang, Z. Z., Yu, Y. T., Lin, H. R., Liao, D. C., Cui, X. H., and Wang, H. B. (2018). *Lonicera japonica* Extends Lifespan and Healthspan in *Caenorhabditis elegans*. *Free Radic. Biol. Med.* 129, 310–322. doi:10.1016/j.freeradbiomed.2018.09.035

Yang, T., Fang, L., Lin, T., Li, J., Zhang, Y., Zhou, A., et al. (2019). Ultrasonicated Sour Jujube Seed Flavonoids Extract Exerts Ameliorative Antioxidant Capacity and Reduces Aβ-Induced Toxicity in *Caenorhabditis elegans*. *J. Ethnopharmacol.* 239, 111886. doi:10.1016/j.jep.2019.111886

Yin, S. M., Zhao, D., Yu, D. Q., Li, S. L., An, D., Peng, Y., et al. (2014). Neuroprotection by Scorpion Venom Heat Resistant Peptide in 6-hydroxydopamine Rat Model of Early-Stage Parkinson's Disease. *Acta Physiol. Sin.* 66 (6), 658–666. doi:10.13294/j.aps.2014.0078

Zhang, X. Y., Wang, Y., Zhang, J., Wang, J. Y., Zhao, J., Zhang, W. Q., et al. (2007). Inhibition of Sodium Channels in Acutely Isolated Hippocampal Neurons by Scorpion Venom Heat Resistant Protein. *Sheng Li Xue Bao* 59 (3), 278–284. doi:10.3321/j.issn:0371-0874.2007.03.006

Zhang, X. G., Wang, X., Zhou, T. T., Wu, X. F., Peng, Y., Zhang, W. Q., et al. (2016). Scorpion Venom Heat-Resistant Peptide Protects Transgenic *Caenorhabditis elegans* from β-Amyloid Toxicity. *Front. Pharmacol.* 7, 227. doi:10.3389/fphar.2016.00227

Zhou, X. H., Yang, D., Zhang, J. H., Liu, C. M., and Lei, K. J. (1989). Purification and N-Terminal Partial Sequence of Anti-epilepsy Peptide from Venom of the Scorpion Buthus Martensii Karsch. *Biochem. J.* 257 (2), 509–517. doi:10.1042/bj2570509

Zhu, Q., Qu, Y., Zhou, X. G., Chen, J. N., Luo, H. R., and Wu, G. S. (2020). A Dihydroflavonoid Naringin Extends the Lifespan of *C. elegans* and Delays the Progression of Aging-Related Diseases in PD/AD Models via DAF-16. *Oxid. Med. Cell Longev.* 2020, 6069354. doi:10.1155/2020/6069354

Conflict of Interest: The authors declare that the research was conducted in the absence of any commercial or financial relationships that could be construed as a potential conflict of interest.

Publisher's Note: All claims expressed in this article are solely those of the authors and do not necessarily represent those of their affiliated organizations, or those of the publisher, the editors, and the reviewers. Any product that may be evaluated in this article, or claim that may be made by its manufacturer, is not guaranteed or endorsed by the publisher.

frontiers | Frontiers in Neuroscience

REVIEW
published: 22 July 2022
doi: 10.3389/fnins.2022.922331

Microglia Pyroptosis: A Candidate Target for Neurological Diseases Treatment

Xian Wu[2†], Teng Wan[1†], Xiaoyu Gao[3†], Mingyuan Fu[3], Yunfeng Duan[2], Xiangru Shen[3‡] and Weiming Guo[1*‡]*

[1] *Huazhong University of Science and Technology Union Shenzhen Hospital, The 6th Affiliated Hospital of Shenzhen University Health Science Center, Shenzhen, China,* [2] *The First Affiliated Hospital of Hunan College of Traditional Chinese Medicine, Hunan Province Directly Affiliated TCM Hospital, Zhuzhou, China,* [3] *Hengyang Medical College, University of South China, Hengyang, China*

In addition to its profound implications in the fight against cancer, pyroptosis have important role in the regulation of neuronal injury. Microglia are not only central members of the immune regulation of the central nervous system (CNS), but are also involved in the development and homeostatic maintenance of the nervous system. Under various pathological overstimulation, microglia pyroptosis contributes to the massive release of intracellular inflammatory mediators leading to neuroinflammation and ultimately to neuronal damages. In addition, microglia pyroptosis lead to further neurological damage by decreasing the ability to cleanse harmful substances. The pathogenic roles of microglia in a variety of CNS diseases such as neurodegenerative diseases, stroke, multiple sclerosis and depression, and many other neurological disorders have been gradually unveiled. In the context of different neurological disorders, inhibition of microglia pyroptosis by targeting NOD-like receptor family pyrin domain containing (NLRP) 3, caspase-1 and gasdermins (GSDMs) by various chemical agents as well as natural products significantly improve the symptoms or outcome in animal models. This study will provide new ideas for immunomodulatory treatment of CNS diseases.

Keywords: microglia, pyroptosis, GSDMs, neuroinflammation, neurological diseases

OPEN ACCESS

Edited by:
Asma Perveen,
Glocal University, India

Reviewed by:
Xiangping Chu,
University of Missouri–Kansas City, United States
Ziyu Zhu,
Shanghai Jiao Tong University, China

***Correspondence:**
Xiangru Shen
3226618427@qq.com
Weiming Guo
253779211@qq.com

[†]These authors have contributed equally to this work and share first authorship
[‡]These authors have contributed equally to this work

Specialty section:
This article was submitted to Neuropharmacology, a section of the journal Frontiers in Neuroscience

Received: *17 April 2022*
Accepted: *23 June 2022*
Published: *22 July 2022*

Citation:
Wu X, Wan T, Gao X, Fu M, Duan Y, Shen X and Guo W (2022) Microglia Pyroptosis: A Candidate Target for Neurological Diseases Treatment. Front. Neurosci. 16:922331. doi: 10.3389/fnins.2022.922331

INTRODUCTION

The term "pyroptosis" is of ancient Greek origin, meaning fire and falling, it is characterized by early rupture of the plasma membrane and release of proinflammatory intracellular contents (Black et al., 1989). Therefore, pyroptosis is also known as inflammatory cell death in recent years (Van Opdenbosch and Lamkanfi, 2019). External stimuli such as pathogen-associated molecular patterns (PAMPs), damage-associated molecular patterns (DAMPs), dsDNA, multiple bacterial, viral antigenic components initiate cellular pyroptosis by activating different types of inflammasome receptors (Xue et al., 2019). Cell pyroptosis is mainly executed by the gasdermin family of proteins (Shi et al., 2017). The N-terminal end of the GSDM is activated by the shearing action of caspase family members. The activated GSDM-N terminus has membrane pore-forming properties and induces the formation of transmembrane pore channels and pyroptosis, along with the release of intracellularly activated inflammatory mediators (Bergsbaken et al., 2009; Shi et al., 2017). The GSDM plays an important role in the body's anti-infection and anti-cancer immunity and is expected to be a new target for anti-cancer therapy (Man et al., 2017; Loveless et al., 2021; Wu et al., 2021). However, cellular damage and inflammation caused by excessive and abnormal pyroptosis have been found to be important pathogenic factors in a variety of diseases, such as

cardiovascular diseases, motor system diseases, autoimmune diseases (McKenzie et al., 2018; Tao et al., 2020; Wang et al., 2020c). Recent studies have shown that neuronal pyroptosis is associated with neurodegenerative diseases, stroke, traumatic brain injury (TBI), infection-induced brain damage, and a variety of central nervous system (CNS) pathologies such as epilepsy (McKenzie et al., 2020a). Pyroptosis has become the focus of research on the pathogenic mechanisms of the CNS.

Microglia are the resident innate immune cells of the CNS with important immunomodulatory functions and play a critical role in the neuronal development, myelin repair, and regeneration of the nervous system (Colonna and Butovsky, 2017; Lloyd and Miron, 2019). They can regulate inflammation and oxidative stress and influence synaptic plasticity and blood-brain barrier (BBB) stability, which are essential for the regulation of CNS homeostasis (Li and Barres, 2018; Zhou et al., 2019; Ronaldson and Davis, 2020). Although the concept of microglia polarization is currently controversial, the binary classification of microglia according to their beneficial or harmful function is still widely used today (Hu et al., 2015; Ransohoff, 2016a; Wan et al., 2022b). Recent studies suggest that its function is not limited to regulating development and simply removing cellular debris in disease, but that its abundance of modifiable genes also provides a large number of targets for regulating neurological diseases (Prinz et al., 2021). Given the multifunctional regulatory properties of microglia in the CNS, their association with epilepsy, neuropathic pain, ischemic stroke, neurodegenerative diseases, and depression are also being preliminarily revealed (Orihuela et al., 2016; Nestle et al., 2020; Yao et al., 2021). The links between the physiopathological functional state of microglia and various neurological diseases have been extensively investigated.

Microglia pyroptosis is an important manifestation of neuroinflammation and is closely associated with the development of several neurological diseases, such as ischemic brain injury, stroke, and neurodegenerative diseases. Microglia pyroptosis-induced inflammatory responses are associated with neurodegeneration and cell death in the brains of Parkinson's patients (Zhang et al., 2016). IL-1β and IL-18 levels were found to be significantly higher in the cerebrospinal fluid of Parkinson's patients with microglia pyroptosis than in the healthy controls (Zhang et al., 2016; Chang et al., 2020; Hu et al., 2020; Xu et al., 2021b). In addition, it was shown that inhibition of microglia pyroptosis by reducing the levels of the NLRP3 complex with CD73 or reduced advanced oxidation protein products (AOPPs) alleviated spinal cord injury (SCI) induced by persistent neuroinflammation (Liu et al., 2020; Xu et al., 2021b). In a mouse model of intracerebral hemorrhage (ICH), inhibiting microglia pyroptosis by suppressing NLRP3 complexes could improve SCI symptoms. In the ICH mouse model, the anti-inflammatory effect of Didymin was partially associated with its anti-microglia pyroptosis effect (Gu et al., 2022). This paper reviews the recent association between microglia pyroptosis and various neurological disorders, as well as the currently available or potential agents that regulate microglia pyroptosis, thus providing new ideas for the treatment of neurological disorders.

Abbreviations: CNS, central nervous system; NLRP3, NOD-like receptor thermal protein domain associated protein 3; GSDMs, caspase-1 and gasdermins; PAMPs, pathogen-associated molecular patterns; DAMPs, damage-associated molecular patterns; TBI, traumatic brain injury; BBB, blood-brain barrier; LPS, lipopolysaccharide; IFN-γ, interferon-γ; Aβ, amyloid-beta peptides; IL-1β, interleukin-1β; AOPPs, advanced oxidation protein products; SCI, spinal cord injury; ICH, intracerebral hemorrhage; MLKL, mixed lineage kinase domain-like proteins; PRRs, pattern recognition receptors; TLRs, toll-like receptor; AIM2, absent in melanoma 2; MS, multiple sclerosis; PDE8A, phosphodiesterase 8A; cAMP, cyclic adenosine monophosphate; ADP, adenosine diphosphate; MCAO, middle cerebral artery occlusion; NOX4, NADPH oxidase 4; GPX4, glutathione peroxidase 4; AD, Alzheimer's disease; CARD/ASC, caspase activation and recruitment domain; ACEI, angiotensin-converting enzyme I; PD, Parkinson's disease; 6-OHDA, 6-hydroxydopamine; MPTP, 1-Methyl-4-phenyl-1,2,3,6-tetrahydropyridine; HD, Huntington's disease; HTT, Huntington's protein; MAPK, mitogen-activated protein kinase; HIF-1α, hypoxia inducible factor-1α; ROS, reactive oxygen species; OGD/R, oxygen-glucose deprivation and reoxygenation; OM-MSCs, olfactory mucosa mesenchymal stem cells; EAE, experimental autoimmune encephalomyelitis; CUMS, chronic unpredictable mild stress; Nrf2, nuclear factor-erythroid 2 -related factor 2; DLB, depressive-like behavior; CSDS, chronic social defeat stress; TREM, triggering receptor expressed on myeloid cells; CCR5, C-C chemokine receptor 5; SAH, subarachnoid hemorrhage; PKA, protein kinase A; CREB, cAMP response element binding; Dex, Dexmedetomidine; P2X7R, purinergic 2X7 receptor; SAFI, salvianolic acids for injection; BIRI, brain ischemia reperfusion injury; CCH, chronic cerebral hypoperfusion; DM, diabetes mellitus; DDX3X, DEAD-box helicase 3 X-linked; SITR1, sirtuin1, CaMKII, Ca2+/calcium/calmodulin-dependent protein kinase II; APP, amyloid precursor protein; PS1, presenilin-1; NF-?B, nuclear factor-kappa B; PAS-NA, Para-aminosalicylic acid; HO-1, heme oxygenase-1; DI, dimethyl itaconate; SFN, sulforaphane; MyD88, myeloid differentiation factor 88; PF, Paeoniflorin; iBMDM, immortalized bone marrow-derived macrophages; MAF, Mafenide; PI3K, phosphatidylinositol 3-kinase.

PYROPTOSIS

Pyroptosis as a Phenotype of Inflammatory Cell Death

Pyroptosis is a type of programmed cell death but is different from apoptosis and necrosis. Both pyroptosis and necrosis are part of the same lytic programmed death and eventually release contents leading to inflammation (Frank and Vince, 2019). However, the mechanisms and cell morphology are different, which may be due to the different biochemical activities of the gasdermin D (GSDMD) and mixed lineage kinase domain-like proteins (MLKL) that mediate pyroptosis (Jorgensen and Miao, 2015). Pyroptosis is one of the defense mechanisms of host cells against pathogens. Usually external pathogens promote cellular pyroptosis activation, while a few pathogens have the ability to inhibit host cell pyroptosis (Bergsbaken et al., 2009). With the rupture of the plasma membrane, exposed extracellular pathogens are further targeted and cleared by recruited immune cells. Classical microglia pyroptosis is divided into two main steps. The initiation step refers mainly to microbial and inflammatory mediator-mediated activation of inflammation-associated genes. This is followed by the activation of inflammasome and downstream pyroptosis-related pathways, culminating in cell death mediated by the pore-forming protein GSDMD (Vande Walle and Lamkanfi, 2016; Fang et al., 2020). In addition,

the non-classical pyroptosis pathway GSDMD activation is independent of caspase-1. Caspase-4/5/11 are directly stimulated by LPS and thus activate downstream GSDMD (Shi et al., 2014).

Mechanism and Regulation of Pyroptosis

Inflammasomes are multiprotein complexes containing pattern recognition receptors (PRRs) that mediate the innate immune response of the body to infectious microbes and host protein molecules. The PRR family typically contains multiple members, including Toll-like receptors (TLRs), Nod-like receptors (NLRs) (Kanneganti et al., 2007; Sahoo, 2020). PRRs in inflammasomes sense and recognize PAMPs and DAMPs of host or environmental origin (Guo et al., 2015). In mammals, in addition to the most common NLRP3, different types of inflammasome receptors such as absent in melanoma 2 (AIM2), NLRC4, NLRP1b, and NLRP6 recognize different activation signals and activate downstream caspase-1 (Xue et al., 2019; Fang et al., 2020). Upon activation, caspase-1 mediates the shear activation of IL-1β and IL-18, as well as GSDMD, leading to the formation of membrane pores, cell swelling, release of cell contents, and ultimately pyroptosis (Voet et al., 2019; Wang et al., 2019; Xue et al., 2019). Because NLRP3 inflammasomes have a wide recognition range, targeting NLRP3 to regulate pyroptosis has become one of the focal points of current research. Isoflurane general anesthesia induces pyroptosis by activating NLRP3 inflammasomes, while NLRP3 inhibitor MCC950 attenuates pyroptosis-related cognitive dysfunction (Fan et al., 2018). Additionally, isoliquiritin and kanglexin improve depression by downregulating NLRP3 levels and subsequent neuronal pyroptosis (Bian et al., 2020; Li et al., 2021a).

GSDMD is highly expressed in the epithelium and skin of the gastrointestinal tract, yet its function remains largely unknown. As the executioner of pyroptosis, GSDMD is only one member of the GSDM family, with other members including GSDMA, GSDMB, GSDMC, GSDMD, DFNA5, and DFNB59 (Shi et al., 2017). In the GSDM family, the sequence homology is about 45%, with the GSDM-N structural domain being the most conserved region. It was concluded that the GSDM-N domain of GSDMD is thought to possess extremely strong pore-forming toxicity and then induce pyroptosis (Shi et al., 2015; Ding et al., 2016). In studies in mouse models, different species of GSDM activation have similar pore-forming properties. At present, the upstream and downstream signal regulation mechanism of pyroptosis executive protein GSDMD is clearly studied (Shi et al., 2017). Recent studies have found that streptococcal pyrogenic exotoxin B shears GSDMA and thus induce pyroptosis, while the upstream regulatory mechanisms of the remaining GSDM members are still unknown (Deng et al., 2022). The GSDMD proteins are in an autoinhibited state in the normal state (Ding et al., 2016). GSDMD contains about 480 amino acids, and it is connected to two structural domains, GSDM-N terminus and GSDM-C terminus, by a long loop. Activated caspase-1 and caspase-11 efficiently cleave the GSDMD at an aspartate site within the loop. This cleavage is essential for release of pore-forming GSDM-N terminus (Shi et al., 2015). The role of pyroptosis in CNS disease has emerged in multiple animal disease models. VX-765, a small molecule inhibitor of caspase-1, reduces the expression of inflammasomes and pyroptosis-associated proteins in the CNS, thereby inhibiting axonal injury in multiple sclerosis (MS) (McKenzie et al., 2018). Caspase-1 gene ablation in mice model significantly inhibited TBI-induced pyroptosis and neurological damage (Liu et al., 2018).

Studies on the molecular regulation of its non-canonical pathway of pyroptosis, especially caspase-11-related, are currently more limited. LPS-mediated caspase-11-dependent non-classical pyroptosis pathway can be inhibited by ethyl pyruvate (Qiu et al., 2020). Regulation of caspase-11 is thought to be possibly related to phosphodiesterase 8A (PDE8A) mediated cyclic adenosine monophosphate (cAMP) metabolism (Hou et al., 2019). Adenosine diphosphate (ADP) -ribosylation of caspase-11 was found to protect cells from pyroptosis in Shigella-infected mice (Li et al., 2021b). AIM2 is also a target for regulating pyroptosis. *In vitro*, andrographolide significantly inhibited AIM2 inflammasomes and blocked caspase1/GSDMD-mediated myeloid-derived macrophage pyroptosis (Gao et al., 2019). LncRNA MEG3 induced cellular pyroptosis of middle cerebral artery occlusion (MCAO) mice in ischemic brain by sponging miR-485 targeting AIM2 (Liang et al., 2020a). Thus, non-coding RNAs are also important for regulating pyroptosis. In cellular experiments in diabetic retinopathy, overexpression of miR-590-3p was found to downregulate caspase-1-dependent pyroptosis *via* downregulation of NLRP1 and downstream NADPH oxidase 4 (NOX4) pathway (Gu et al., 2019). As the study of pyroptosis in human diseases has advanced, chemotherapeutic drugs and miRNAs have now been found to inhibit malignant progression of tumors by inducing tumor pyroptosis (Xia et al., 2019). Targeting pyroptosis has an unignorable role in the treatment of diseases.

Crosstalk Between Pyroptosis and Other Kinds of Cell Death

There is a link between apoptosis and pyroptosis. After apoptosis, the absence of macrophages to remove the apoptotic cells trigger GSDMD-mediated secondary cell death with a pathological pattern similar to pyroptosis (Kovacs and Miao, 2017; Rogers et al., 2017). When GSDMD expression is too low or in the presence of GSDMD defects, caspase-1 induces apoptosis *via* the Bid-caspase 9-caspase 3 axis or caspase-7 (Taabazuing et al., 2017; Tsuchiya et al., 2019). However, if the cleavage site of GSDMD is designed as a recognition site for caspase-3, it may convert apoptosis into pyroptosis (Wang et al., 2017). In addition, oxidation of phospholipids may also be associated with GSDMD activation-induced pyroptosis. Glutathione peroxidase 4 (GPX4) and vitamin E inhibit pyroptosis in mouse macrophages by suppressing lipid peroxidation (Imai and Nakagawa, 2003). In contrast, myeloid-specific GPX4 deficiency leads to a significant increase in caspase-1 and caspase-11-mediated GSDMD lysis (Kang et al., 2018). Meanwhile, GPX4 plays an important role in regulating ferroptosis. This suggests the potential connection between pyroptosis and ferroptosis.

MICROGLIA PYROPTOSIS AND NEUROLOGICAL DISEASES

Neurodegenerative Diseases

Neurodegenerative diseases are a series of disorders caused by progressive loss of neurons in the CNS (Yu et al., 2017). The main pathological changes include amyloid deposition and progressive neurodegenerative changes. Among them, amyloid proteins including Aβ, tau and α-synuclein exhibit similar properties to prion proteins in pathological experiments and are able to self-replicate and spread throughout the nervous system (Vaquer-Alicea and Diamond, 2019; Tian et al., 2020). Microglia play an important role in the course of neurodegenerative diseases (Wan et al., 2022a). In the development of Alzheimer's disease (AD), the caspase activation and recruitment domain (CARD/ASC)-containing bridging proteins released by microglia pyroptosis rapidly bind to Aβ and increase the formation of Aβ oligomers and aggregates (Venegas et al., 2017). The formed ASC-Aβ complex also leads to multiple responses in surrounding cells, such as increased caspase-1 activation, IL-1β maturation and GSDMD cleavage, and promotes NLRP3 inflammasome formation and pyroptosis in neighboring microglia (Heneka et al., 2018; Luciunaite et al., 2020). In addition, microglia pyroptosis lead to more ASC release, thereby exacerbating pyroptosis-induced neuroinflammatory damage (Friker et al., 2020). The ASC-Aβ complex also promotes microglia activation and secretion of inflammatory mediators and neurotoxic cytokines, while the efficiency of Aβ degradation in microglia is reduced (Sarlus and Heneka, 2017). In the early stages of AD, microglia in patients are activated by Aβ, which is removed by receptor-mediated phagocytosis and degradation, inhibiting to some extent the deposition of Aβ in the interstitial (Newcombe et al., 2018). However, as Aβ accumulates, microglia are continuously activated and produce excessive amounts of pro-inflammatory cytokines (Van Zeller et al., 2021). In addition, the autocrine secretion of membrane receptors from microglia that bind and help microglia phagocytose Aβ gradually decreases, and the activity of various degradative enzymes, such as enkephalinase, insulin-degrading enzymes, and angiotensin-converting enzyme I (ACEI) decreases, further leading to reduced clearance of Aβ and continued microglial cell stimulation (Yu and Ye, 2015; Van Zeller et al., 2021). Researchers have speculated that tau and Aβ are functionally similar. Tau protein also activates inflammasomes and induces microglia pyroptosis *via* the NLRP3-ASC axis (Stancu et al., 2019). This finding is supported by the results of several necropsy analyses (Ransohoff, 2016b; Leyns and Holtzman, 2017).

The pathological marker of Parkinson's disease (PD) differs considerably from that of AD. The pathological marker of PD is fibrillar α-synuclein, which tends to accumulate in neurons and eventually leads to the formation of Lewy bodies (Przedborski, 2017). Similar to Aβ, α-synuclein also induces the activation of microglia NLRP3 inflammasomes and thus promotes the release of ASC from microglia and the formation of extracellular ASC patches (Zhou et al., 2016; de Alba, 2019). Delayed and strong activation of NLRP3 inflammasomes and a significant increase in extracellular ASC release were observed in LPS and α-synuclein-stimulated activated mouse microglia, but microglia did not undergo pyroptosis (Gordon et al., 2018). Furthermore, activation of pyroptosis-related pathways was associated with the metabolism of α-synuclein. It was shown that the activation and aggregation of inflammasomes in neuronal cells are closely related to the cleavage of extracellular α-synuclein (Wang et al., 2016; Hu et al., 2022). In BE (2)-M17 human dopaminergic neuroblastoma cells, caspase-1 activated by inflammasomes was found to cleave α-synuclein *in vitro* and produce aggregates with neuronal toxicity (Wang et al., 2016). In a rat model of PD induced by LPS and 6-hydroxydopamine (6-OHDA), NLRP3 inflammasomes components were found to be highly expressed in microglia, and caspase-1 inhibitor (Ac-YVAD-CMK) reversed this result (Mao et al., 2017). This suggests that microglia pyroptosis may be associated with pathological cleavage of extracellular α-synuclein and the formation of Lewy bodies. However, whether α-synuclein ultimately induces microglia pyroptosis may depend on the concentration of α-synuclein, and the quantification of this concentration needs to be determined by further studies. Furthermore, in N-methyl-4-phenyl-1,2,3,6-tetrahydropyridine (MPTP)-induced PD mice, baicalein inhibited NLRP3/caspase-1/GSDMD pathway-mediated microglia pyroptosis, thereby reducing PD symptoms (Rui et al., 2020). These studies suggest that inhibition of microglia pyroptosis may alleviate the progression of PD.

Caspase-1 plays a key role in the process of pyroptosis. The activation of Caspase-1 exists in the brain of Huntington's disease (HD) patients and in HD mouse models, and the inhibition of caspase-1 in HD mouse models can slow down the progression of the disease (Ona et al., 1999; Paldino et al., 2020). Huntington's protein (HTT) is the key to the disease and activated caspase-1 hydrolyzes and cleaves HTT to produce an N-terminal mutated fragment (N-htt), leading to neuronal dysfunction and death (Kim et al., 2001; Sanchez Mejia and Friedlander, 2001). This suggests that pyroptosis may be potentially linked to the pathological generation of HTT. The current study shows that HD patients have distinct neuroinflammatory features at the site of brain lesions, while no upregulation of immune cells from the periphery, such as lymphocytes and neutrophils, was found in the brain tissue of HD patients (Bjorkqvist et al., 2008; Palpagama et al., 2019). Significant NLRP3 activation was found in microglia in a mouse model of HD, suggesting a potential link between neuroinflammation triggered by microglia pyroptosis and HD (Siew et al., 2019). However, a different result has been obtained that NLRP3 expression levels were significantly elevated in other cells of the striatum of HD mice, but no significant NLRP3 activation was found in microglia (Paldino et al., 2020). This heterogeneity of results due to the spatial location of the brain needs to be elucidated by more in-depth studies.

Ischemic Stroke

Ischemic stroke and secondary cerebral ischemia-reperfusion injury are both very serious cerebrovascular diseases (Graeser et al., 2019). Ischemia and hypoxia trigger a series of neurological damage responses such as oxidative stress and neuroinflammation (Langhauser et al., 2012; Nabavi et al., 2015).

Neuroinflammation induced by microglia pyroptosis is thought to be a key factor promoting neuronal damage after ischemia (Ceulemans et al., 2010). On the one hand, neuroinflammation promotes the clearance of dead cellular debris induced by reduced cerebral blood flow and ischemia-reperfusion (Xu et al., 2019a). On the other hand, it may lead to infarct exacerbation and low neuronal plasticity (Kriz, 2006). Microglia are one of the most important phagocytic cells for the removal of necrotic substances, but hyperactivation-induced microglia pyroptosis is an important cause of exacerbation of neuroinflammation-related damage after stroke (Iadecola and Anrather, 2011; Xu et al., 2019a). In the mouse MCAO-induced I/R model, microglia GSDMD expression is elevated in the ischemic region, which mediates microglia pyroptosis and neuroinflammation-related injury (Voet et al., 2019; Zhang et al., 2019; Wang et al., 2020b).

It has been found that NLRP3 expression is increased in microglia of ischemic stroke patients, and increased expression of NLRP3 inflammasomes component proteins and downstream products IL-1β and IL-18 was also observed in the mouse MCAO/R model (Fann et al., 2013). Many studies have revealed that the mechanism of NLRP3 inflammasome in microglia involved in the regulation of cerebral ischemic injury may be related to the NF-κB pathway, mitogen-activated protein kinase (MAPK) signaling pathway, Hypoxia Inducible Factor-1α (HIF-1α), reactive oxygen species (ROS) production (Ma et al., 2014; Fann et al., 2018; Jiang et al., 2020). In oxygen-glucose deprivation and reoxygenation (OGD/R) and MCAO/R-treated rat BV2 microglia, Salidroside (Sal) was found to inhibit microglia NLRP3 inflammasomes activation by suppressing the TLR4/NF-κB signaling pathway, thereby inhibited I/R-induced BV2 cells pyroptosis and further neuronal damage (Liu et al., 2021). A similar phenomenon was observed from the Meisoindigo-treated MCAO mouse model (Ye et al., 2019; Liu et al., 2021). These studies suggest that amelioration of ischemic stroke can be achieved by inhibiting the TLR4/NF-κB signaling pathway. In a human cell assay, ROS levels in OGD/R-treated human BV2 microglia were significantly higher than those in the untreated group, and co-culture with hypoxia-pretreated olfactory mucosa mesenchymal stem cells (OM-MSCs) showed reduced ROS levels and less pyroptosis (Huang et al., 2020). OM-MSCs have immunomodulatory and reparative functions and replace or repair damaged cells, and OM-MSCs upregulate the expression and release of HIF-1α under OGD/R conditions, suppressing the expression of NLRP3 inflammasome and pyroptosis-related proteins in co-cultured BV2 microglia and reducing the pyroptosis of BV2 microglia under OGD/R conditions (Coppin et al., 2019; Dabrowska et al., 2019; Huang et al., 2020). These studies suggest that ischemia-induced production of HIF-1α and ROS play a key role in pyroptosis regulation in BV2 microglia under OGD/R conditions. Another study found that NLRP3 inflammasomes expression levels were not altered in a mouse OGD model, and only NLRC4 inflammasome expression was upregulated and induced BV2 microglia pyroptosis. Knockdown of NLRC4 by siRNA significantly reduced pyroptosis in microglia under ischemic conditions (Poh et al., 2019). The difference in NLRP3 and NLRC4 expression under ischemic stroke conditions remains to be elucidated.

Multiple Sclerosis

MS is an incurable progressive demyelinating disease of the CNS characterized by multiple demyelinating plaques in the white matter, neurodegeneration, and axonal transection or loss (Kornek and Lassmann, 2003; Dendrou et al., 2015). The etiology of MS is not yet clear. Previous studies have shown increased expression of NLRP3 inflammasomes activation and its downstream products in CNS tissue and peripheral serum in MS patients compared to non-MS patients, leading to BBB damage and neurotoxicity (Huang et al., 2004; Burm et al., 2016; McKenzie et al., 2018). In addition, a study found a large number of GSDMD-immunopositive cell fragments in the frontal white matter of cadavers from MS patients, suggesting a potential link between GSDMD-mediated microglia pyroptosis and MS (McKenzie et al., 2018). Because MS is a human-specific disease, it can only be partially simulated in animal models, such as the animal experimental autoimmune encephalomyelitis (EAE) model, which has approximately the same neuropathological features as MS and assist in determining the factors influencing MS (Ransohoff, 2012; Kipp et al., 2017). It has been found that the expression level of NLRP3/ASC-caspase/GSDMD pathway is significantly increased in mouse EAE models, while the use of Liraglutide significantly downregulates the protein level of caspase-1 and microglia pyroptosis levels (Song et al., 2022). Another study showed that in addition to caspase-1, caspase-3 and caspase-7 also mediated microglia pyroptosis in post-mortem brain tissue from patients with progressive MS and in a mouse EAE model. This study found that caspase-1 activates caspase-3/7 in MS patients and EAE mouse models, and caspase-3/7 and its substrates, such as PARP, DFF45 and ROCK1, after cleavage activation, induce GSDMD-mediated microglial cell pyroptosis by disrupting the cellular protein hydrolysis network and promoting microglial cell nuclear cohesion glial cell pyroptosis (McKenzie et al., 2020b).

Major Depressive Disorder

Major depressive disorder (MDD) is a serious neuropsychiatric disorder that remains a medical management challenge (Malhi and Mann, 2018). The direct pathogenesis of depression remains unclear, and some studies now suggest a close relationship between MDD and neuroinflammation triggered by NLRP3 inflammasomes (Raedler, 2011; Dey and Hankey Giblin, 2018). In patients with MDD, untreated patients have increased levels of IL-1β and IL-18 in the circulation and increased expression of NLRP3 compared to patients treated with the antidepressant amitriptyline (Raedler, 2011). The expression of NLRP3 was increased. Elevated IL-1β mRNA and protein levels were also found in the prefrontal cortex in a chronic mild stress (CMS)-induced depression model in rats, while no similar phenomenon was observed in blood (Pan et al., 2014). The same phenomenon was not observed in blood. In the chronic unpredictable mild stress (CUMS)-induced depression mouse model, researchers found significantly elevated levels of IL-1β protein in serum and hippocampus, but not in NLRP3 knockout mice, probably

because NLRP3 knockout inhibited MAPK pathway and NF-κB pathway activation (Su et al., 2017). Many studies have also revealed other mechanisms involved in the regulation of MDD by NLRP3 inflammasomes in microglia, which may be related to dysregulation of miRNA-27a/SYK/NF-κB pathway, nuclear factor-erythroid 2 -related factor 2 (Nrf2) (Ajami et al., 2011; Eggen et al., 2013; Arioz et al., 2019; Li et al., 2021a). In the LPS-induced mouse Depressive-like behavior (DLB) model, Melatonin pretreatment inhibited Keap-1-mediated Nrf2 proteasomal degradation, suppressed NLRP3 inflammasomes activation, downregulated GSDMD cleavage, and ultimately protected N9 microglia from pyroptosis (Arioz et al., 2019). Similarly, in MDD patients and in LPS or chronic social defeat stress (CSDS)-induced depression models in mice, the use of Isoliquiritin upregulated miRNA-27a expression and downregulated SYK expression, thereby protecting microglia from pyroptosis and alleviating MDD symptoms in mice (Li et al., 2021a). These experiments illustrate that microglia pyroptosis is closely linked to MDD. Interestingly, in a CMS-induced mouse depression model, astrocyte NLRP3 inflammasomes and GSDMD in the hippocampus of mice were found to activate and induce cell pyroptosis, while microglia did not show significant pyroptosis (Catanese et al., 2021) (**Figure 1**).

REGULATION OF MICROGLIA PYROPTOSIS FOR TREATMENT OF NEUROLOGICAL DISEASES

Targeting the Regulation of NLRP3

Targeting NLRP-related proteins to regulate microglia pyroptosis affect the progression of multiple neurological diseases. Targeting NLRP to inhibit pyroptosis plays a neuroprotective role in stroke. The human-specific gene CHRFAM7A inhibits NLRP3 inflammasomes activation and reduces intracellular levels of NLRP3, a pyroptosis-related protein, thereby reducing OGD/R-induced neurological damage (Cao et al., 2021). The triggering receptor expressed on myeloid cells (TREM)-1 antagonist LP17 inhibited microglia pyroptosis and effectively improved neurological function in subarachnoid hemorrhage (SAH) patients (Liang et al., 2020b; Xu et al., 2021a). C-C chemokine receptor 5 (CCR5) activation promotes microglia pyroptosis and neurological deficits after ICH in mice *via* the protein kinase A (PKA)/cAMP response element binding (CREB)/NLRP1 signaling pathway. Maraviroc inhibition of CCR5 improves neurological function in ICH patients (Yan et al., 2021). Dexmedetomidine (Dex) inhibits microglia pyroptosis by blocking the purinergic 2X7 receptor (P2X7R)/NLRP3 pathway, thereby providing protection against ischemic brain injury (Sun et al., 2021). Andrographolide and Curcumin effectively reduce neurostructural damage and functional impairment caused by stroke by inhibiting NF-κB signaling and NLRP3 inflammasomes-mediated microglia pyroptosis (Li et al., 2018; Ran et al., 2021). Salvianolic acids for injection (SAFI) reduced brain ischemia reperfusion injury (BIRI) by reducing the shift in microglia phenotype from M1 to M2 and inhibiting microglia NLRP3 inflammasomes-induced pyroptosis (Ma et al., 2021). The plasma containing Melatonin has been shown to reduce BIRI. Melatonin-containing plasma exosomes inhibited ischemia-induced inflammatory responses and pyroptosis by modulating the TLR4/NF-κB signaling pathway (Wang et al., 2020a).

Targeting NLRP3 to inhibit microglia pyroptosis inhibition alleviates cognitive impairment. NLRP3 inhibitors MCC950 and the ethyl acetate fraction of Bungeanum improve cognitive function in mice by inhibiting LPS-induced caspase-1 activation and pyroptosis in microglia (Dempsey et al., 2017; Zhao et al., 2021). Curcumin treatment significantly improved diabetes mellitus (DM)/chronic cerebral hypoperfusion (CCH)-induced cognitive impairment by modulating the TREM2/TLR4/NF-κB pathway and reducing NLRP3-dependent pyroptosis (Zheng et al., 2021). Studies have shown that chronic aluminum exposure is associated with the development of AD and cognitive impairment (Klotz et al., 2017). Aluminum exposure causes microglia pyroptosis and neuroinflammation through the DEAD-box helicase 3 X-linked (DDX3X)/NLRP3 inflammasomes signaling pathway, while Resveratrol alleviates aluminum exposure-induced neurological damage by activating sirtuin1 (SIRT1) (Hao et al., 2021). Hypoxic preconditioning of the Ca2+/calcium/calmodulin-dependent protein kinase II (CaMKII)/CREB signaling pathway inhibited microglia pyroptosis and thereby improved Amyloid precursor protein (APP)/CREB signaling in presenilin-1 (PS1) mice with brain damage (Song et al., 2021).

A variety of agents effectively inhibit PD progression by targeting microglia pyroptosis. Baicalein reverses MPTP-induced neuroinflammation in mice by inhibiting the NLRP3/caspase-1/GSDMD pathway and has a role in PD treatment (Rui et al., 2020). Kaemperfol ameliorates behavioral deficits in PD rats by inhibiting p38MAPK/NF-κB pathway, inhibiting microglia activation, and downregulating pyroptosis-related proteins (Cai et al., 2022). In a mouse model of depression, Quercetin (Qu) and Isoliquiritin treatment inhibited microglia pyroptosis-mediated neurotoxicity and thus exerted antidepressant effects (Han et al., 2021; Li et al., 2021a).

Notably, nuclear factor-kappa B (NF-κB) signaling plays a key role in the formation of NLRP3 inflammasomes in the study of the whole range of pyroptosis regulation-related signals (Yuan et al., 2021). Para-aminosalicylic acid (PAS-Na) antagonizes Mn-induced activation of NLRP3 inflammasomes in the basal ganglia of rats by inhibiting activation of the NF-κB pathway and oxidative stress induced by BV2 cell pyroptosis (Peng et al., 2020). Nrf-2 activates heme oxygenase-1 (HO-1), and Dimethyl itaconate (DI) are involved in the Nrf-2/ HO-1 pathway inhibit NLRP3 inflammasomes assembly and GSDMD cleavage and induces cellular autophagy (Yang et al., 2021). Sulforaphane (SFN) and Dimethyl fumarate (DMF) activate nuclear factor erythroid 2-related factor 2 (Nrf2) and inhibit NF-κB, thereby inhibiting NLRP3 inflammasomes formation and subsequent microglial cell pyroptosis in mice (Tastan et al., 2021; Tufekci et al., 2021). In palmitic acid-treated BV2 cells, miR-124 inhibited microglia pro-inflammatory responses by suppressing the TLR4/myeloid differentiation factor 88 (MyD88)/NF-κB signaling pathway (Yang et al., 2022). Microglia

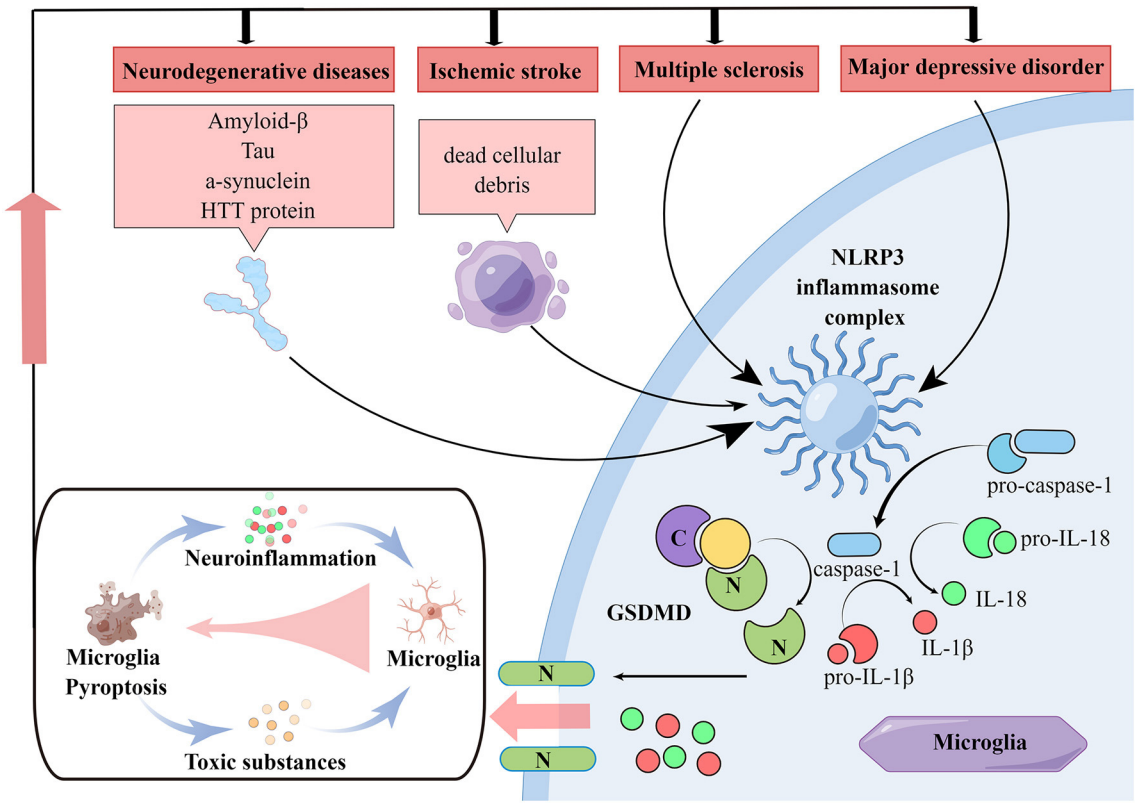

FIGURE 1 | Pathologies of neurological diseases associated with microglia pyroptosis. In various neurological diseases, NLRP3 inflammasome in microglia can be activated and then the caspase-1 is activated. Activated caspase-1 on the one hand cleaves GSDMD, which produces N-terminal structural domain and induces cell membrane perforation and subsequent pyroptosis. On the other hand, activated caspase-1 cleaves IL-1β and IL-18 precursors, rising the extracellular level of IL-1β and IL-18 and amplify neuroinflammatory responses. In neurodegenerative diseases, various misfolded aggregated proteins are taken up by microglia, leading to NLRP3 inflammasome activation and microglia pyroptosis. While in ischemia stroke, ischemic necrotic cell debris is taken up by microglia performing immune clearance functions, leading to microglia NLRP3 inflammasome activation. Microglia NLRP3 inflammasome activation is also present in MDD and MS. All these diseases lead to NLRP3-dependent microglia pyroptosis and neuroinflammation. Moreover, worsening neuroinflammation promotes the production of multiple pathological markers of neurological disease and induces microglia pyroptosis, which leads to persistent disease progression.

pyroptosis plays a crucial role in secondary injury of SCI (Xu et al., 2020). Celastrol inhibits microglia activation and NF-κB/p-p65 expression *in vivo* and *in vitro*, and attenuates the inflammatory response in SCI induction (Dai et al., 2019).

Regulation of Caspase and GSDM

Given the important role of caspases and GSDM family-related proteins in cell pyroptosis, numerous drug trials targeting them have been initiated. AC-YVAD-CMK, a selective inhibitor of caspase-1, was found to inhibit microglia pyroptosis and induce an anti-inflammatory phenotype in microglia, thereby improving ICH mice (Lin et al., 2018). The caspase-1 inhibitor VX765 has been found to reduce neurological damage after TBI by inhibiting pyroptosis and the high-mobility cassette-1/TLR4/ NF-κB pathway activity, resulting in a better therapeutic effect on TBI (Sun et al., 2020). Clinical doses of sevoflurane exacerbated AD progression *via* the NLRP3/caspase-1/GSDMD axis. VX-765 significantly inhibited the activation of microglia pyroptosis-related pathways and attenuated sevoflurane-induced release of IL-1, IL-18 and tau-related kinases and phosphatases (Xu et al., 2019b; Tian et al., 2021a). Paeoniflorin (PF) exerted antidepressant effects by inhibiting caspase-11-dependent pyroptosis signaling induced by hyperactivation of hippocampal microglia in ricin-treated mice, and attenuated neuroinflammatory responses (Tian et al., 2021b). Under neuroinflammatory conditions, caspase-3/7 activation promotes GSDMD-associated microglia pyroptosis, and inhibition of GSDMD by siRNA transduction inhibits microglia pyroptosis, providing a new therapeutic opportunity for neuroinflammatory diseases such as MS (McKenzie et al., 2018, 2020b).

Mafenide (MAF) inhibits GSDMD cleavage through direct binding to the GSDMD-Asp275 site, downregulates p30-GSDMD expression, and suppresses bone marrow-derived macrophages (iBMDM) and BV2 microglia pyroptosis (Han et al., 2020b). In contrast, Sulfa-4 and Sulfa-22 target GSDMD cleavage, inhibit pyroptosis and inflammatory factor release, and have a therapeutic effect on neuroinflammation in AD (Esmaeili-Mahani et al.,

TABLE 1 | Regulation of microglia pyroptosis by various reagents for treatment of neurological diseases.

Reagent	Objectives	Significance	Mechanism	References
OGD/R	Cerebral I/R injury patients	Attenuated cerebral I/R injury	Inhibiting microglia pyroptosis in a NLRP3/Caspase-1 pathway-dependent manner and promoting microglia polarization to M2 phenotype	Eggen et al., 2013
LP17	SAH mouse model	Ameliorated microglial pyroptosis	Diminishing levels of GSDMD-N and IL-1β production	Catanese et al., 2021
LP17	MCAO rat model	Ameliorated neuronal damage and alleviates neuro-inflammation	Reducing oxidative stress and pyroptosis	Cao et al., 2021
MVC	Adult male ICH mice	Ameliorated neuronal pyroptosis and neurological deficits	Inhibiting CCR5/PKA/CREB/NLRP1 signaling pathway	Xu et al., 2021a
Dex	p-MCAO rat model	Inhibited microglia pyroptosis	Blocking the P2X7R/NLRP3/Caspase-1 pathway	Liang et al., 2020b
Andro	Adult SBI male rats	Inhibited microglia pyroptosis and reduced neuronal cell death and degeneration	Inhibiting NF-κB signaling pathway and suppressing the assembly of NLRP3 inflammasome	Yan et al., 2021
curcumin	MCAO mice model	Attenuated microglial pyroptosis	Suppressing NF-κB/NLRP3 signaling pathway	Sun et al., 2021
SAFI	MCAO/R rat model and OGD/R co-cultured primary neurons and primary microglia model	Exert neuroprotective effect	Reducing neuronal apoptosis, switching microglial phenotype from M1 toward M2, and inhibiting NLRP3 inflammasome/ pyroptosis axis in microglia	Li et al., 2018
Basal plasma exosomes melatonin	Focal cerebral ischemia rat model	Decreased neuroinflammation and microglial pyroptosis	Regulation of the TLR4/NF-κB signaling pathway	Ran et al., 2021
MCC950	APP/PS1 mouse model	Reduced Aβ accumulation and improved cognitive function	Inhibiting caspase 1, inflammasome and microglial activation	Ma et al., 2021
Z. bungeanum	Aging mice model and LPS/ATP-induced BV-2 microglial cells	Ameliorated cognitive deficits	Ameliorating oxidative stress and suppressing the NLRP3 inflammasome pathway and GSDMD-mediated pyroptosis	Wang et al., 2020a
Curcumin	DM and CCH rat model	Improved DM/CCH-induced cognitive deficits and attenuated neuronal cell death	Suppressing neuroinflammation induced by microglial activation, regulating the TREM2/TLR4 /NF-κB pathway, alleviating apoptosis and reducing NLRP3-dependent pyroptosis	Dempsey et al., 2017
Rsv	AlCl3 mice model	Ameliorated neuroinflammation and cognitive deficits	Activating SIRT1	Zheng et al., 2021
U50488H	APP/PS1 mouse model	Inhibited microglia pyroptosis and improved the synaptic plasticity	Inhibiting the Ca 2+/CaMKII/CREB signaling pathway	Klotz et al., 2017
MPTP	PD mice model	Reversed MPTP-induced neuroinflammation	Suppressing NLRP3/caspase-1/GSDMD pathway	Hao et al., 2021
6-OHDA	PD rat model and BV2 inflammatory cells	Inhibited microglia pyroptosis and neuroinflammatory response	Inhibiting p38MAPK/NF-κB signaling pathway	Song et al., 2021
Isoliquiritin	Depressed patients and mice	Decreased microglia pyroptosis	Inhibiting miRNA-27a/SYK/NF-κB signaling pathway	Deng et al., 2022
Qu	Depression and PD mouse models	Ameliorated neuronal injury	Inhibiting mtROS-mediated NLRP3 inflammasome activation	Rui et al., 2020
Mn	BV2 microglial cell line and male rats	Inhibited NLRP3 inflammasome dependent pyroptosis	Inhibiting NF-κB pathway activation and oxidative stress	Han et al., 2021
DI	BV2 microglial cells line	Inhibited microglia pyroptosis	Regulating Nrf-2/HO-1 pathway	Yuan et al., 2021
SFN	Murine microglial cells	Suppressing NLRP3 inflammasome and microglia pyroptosis	Inhibiting NF-κB nuclear translocation and Nrf2 mediated miRNAs expression modulation	Peng et al., 2020
DMF	N9 microglial cells	Inhibiting pyroptotic cell death	Decreasing miR-146a and miR-155 and regulating Nrf-2/HO-1 pathway	Yang et al., 2021

(Continued)

TABLE 1 | Continued

Reagent	Objectives	Significance	Mechanism	References
Palmitic acid	BV2 cells	Preventing microglial proinflammatory response	Downregulating TLR4/MyD88/NF-κB p65 signaling	Tufekci et al., 2021
-	SCI BV2 cells	Enhancing microglial pyroptosis	Activating PI3K/AKT pathway and promoting the expression of lncRNA-F630028O10Rik	Tastan et al., 2021
Celastrol	SCI rat model	Attenuated inflammatory response	Inhibiting the expression of NF-κB/p-p65	Yang et al., 2022
AC-YVAD-CMK	ICH mice model	Inhibited pyroptosis	Reducing caspase-1 activation and inhibiting IL-1 β production and maturation	Xu et al., 2020
VX765	CCI mouse model	Inhibited pyroptosis and inflammatory mediator expression	Inhibiting caspase-1 activation and HMGB1/TLR4/NF-kappa B pathway	Dai et al., 2019
VX765	Septic mice model	Reversed cognitive dysfunction	Inhibiting caspase-1	Lin et al., 2018
Sevoflurane	APP/PS1 mice model	Aggravated the progression of AD	Activating NLRP3/caspase-1/GSDMD axis	Sun et al., 2020
PF	Depression mouse model	Alleviated neuroinflammation and exerted antidepressant effects	Inhibiting the enhanced expression of GSDMD and pyroptosis signaling transduction including caspase−1, NLRP3, and IL-1β	Xu et al., 2019b
VX-765	MS animal model, EAE	Reduced pyroptosis	Inhibiting the expression of caspase-1	Wang et al., 2020c
MAF	Mouse BV2 microglia	Inhibited GSDMD cleavage and reduced the levels of inflammatory factors	Directly binding to the GSDMD-Asp275 site	Tian et al., 2021a
LPS and nigericin	APP/PS1 double transgenic mouse model	Improved the memory ability and behavior	Inhibiting the release of inflammatory cytokines	Han et al., 2020b
CD73	C57BL/6J CD73 deficient mice and wild-type mice	Decreased microglia pyroptosis	Suppressing the activation of NLRP3 inflammasome complexes	Xu et al., 2021b

OGD/R, oxygen-glucose deprivation/reoxygenation; I/R, ischemia-reperfusion; SAH, subarachnoid hemorrhage; TREM-1, triggering receptor expressed on myeloid cells 1; GSDMD-N, N-terminal fragment of GSDMD; IL, interleukin; MCAO, middle cerebral artery occlusion; MVC, maraviroc; ICH, intracerebral hemorrhage; CCR5, C-C chemokine receptor 5; PKA, protein kinase A, CREB, cAMP response element binding; NLRP1, nucleotide-binding domain leucine-rich repeat pyrin domain containing 1; Dex, Dexmedetomidine; p-MCAO, permanent MCAO; P2X7R, purinergic 2X7 receptor; Andro, Andrographolide; SBI, secondary brain injury; TLR4, toll-like receptor 4; NF-κB, nuclear transcription factor-κB; SAFI, Salvianolic Acids for Injection; MCAO/R, MCAO/reperfusion; APP, amyloid precursor protein; PS1, presenilin 1; Rsv, Resveratrol; AlCl3, aluminum chloride; SIRT1, sirtuin 1; KOR, κ opioid receptor; CaMKII, calcium/calmodulin dependent protein kinase II; CREB, cyclic adenosine monophosphate response element binding protein; MPTP, N-methyl-4-phenyl-1,2,3,6-tetrahydropyridine; PD, Parkinson's disease; KAE, kaemperfol; 6-OHDA, 6-hydroxydopamine; Qu, Quercetin; Mn, manganese; PAS-Na, sodium para-aminosalicylic acid; DI, dimethyl itaconate; Nrf 2, nuclear factor erythroid 2 related factor 2; HO 1, heme oxygenase 1; SFN, sulforaphane; DMF, dimethyl fumarate; SCI, spinal cord injury; lncRNAs, long non-coding RNAs; CCI, controlled cortical impact; HMGB1, high-mobility cassette-1; AD, azheimer's disease; PF, paeoniflorin; MAF, mafenide; EAE, experimental autoimmune encephalomyelitis.

2021). MiRNA-22 was negatively correlated with the expression of inflammatory factors in AD patients (Han et al., 2020a). Adipose-derived mesenchymal stem cells miRNA-22 loaded exosomes (Exo-miRNA-22) inhibited microglia pyroptosis and decreased inflammatory factor release by targeting GSDMD, and improved neurological function in AD mice (Zhai et al., 2021). GSDMD-mediated microglia pyroptosis is involved in kainic acid-induced seizures, and DMF, as an inhibitor of GSDMD N-terminal fragments (GSDMD-N), significantly reduce microglia pyroptosis and the expression of inflammatory factors such as IL-1 and IL-18, and play a certain role in the treatment of epilepsy (Xia et al., 2021). In SCI, the immunosuppressive molecule CD73 attenuates GSDMD-mediated microglia pyroptosis by promoting the phosphatidylinositol 3-kinase (PI3K)/AKT/Foxo1 signaling pathway (Xu et al., 2021b). **Table 1** graphically covers the mechanisms in which the various drugs mentioned above modulate neurological disorders by targeting microglia pyroptosis.

SUMMARY AND FUTURE PROSPECT

Microglia pyroptosis is now a common cause of secondary neuronal injury. However, direct studies on microglia pyroptosis are still lacking. And there are still many questions related to pyroptosis that remain to be addressed. For example, it is true that some bacteria are thought to have evolved mechanisms to resist pyroptosis and thus evade immunity, such as Shigella. However, it is still widely believed that pathogen-associated PAMP and DAMP activate the pyroptosis pathway by activating GSDMD-associated proteins in the downstream pathway. The pyroptosis pathway has been more extensively studied and more activation pathways have been identified. In addition to the classical caspase-1-mediated pyroptosis pathway, the LPS-mediated caspase-4/5/11 non-classical pyroptosis pathway, and pyroptosis *via* apoptotic transformation.

Currently, inhibition of microglia pyroptosis has been affirmed in various neurological disease models for its associated therapeutic effects. Dexmedetomidine, Andrographolide,

Curcumin and Salvianolic acids for injection have shown their relevant therapeutic effects by targeting NLRP3, caspases and GSDMs. This provides new ideas for immunomodulatory therapy of the CNS. However, there are still some questions about the place of NLRP3 in pyroptosis in specific neurological diseases. For example, in a mouse model of OGD studying ischemic stroke, elevated NLRC4 is thought to contribute to microglia pyroptosis without a significant association with NLRP3. Significantly elevated levels of NLRP3 expression in other cells of the striatum of HD mice, but no significant NLRP3 activation was found in microglia. In a CMS-induced depression model in mice, astrocytes in the hippocampus showed cellular pyroptosis, while microglia did not show significant pyroptosis. In contrast, in PD, microglia pyroptosis may be related to α-synuclein concentration. Therefore, the initiation mechanism of microglia pyroptosis in different diseases and its differences in spatial and temporal aspects need to be more elucidated.

AUTHOR CONTRIBUTIONS

XW and TW designed this article. TW, XG, and MF wrote the manuscript and prepared the figures. TW, XS, and YD critically revised the manuscript for important intellectual content. All authors read and approved the final manuscript and agreed to be accountable for all aspects of this work.

ACKNOWLEDGMENTS

We thank Gang Fan for his suggestions on the design and revision of this article.

REFERENCES

Ajami, B., Bennett, J. L., Krieger, C., McNagny, K. M., and Rossi, F. M. (2011). Infiltrating monocytes trigger EAE progression, but do not contribute to the resident microglia pool. *Nat. Neurosci.* 14, 1142–1149. doi: 10.1038/nn.2887

Arioz, B. I., Tastan, B., Tarakcioglu, E., Tufekci, K. U., Olcum, M., Ersoy, N., et al. (2019). Melatonin attenuates LPS-induced acute depressive-like behaviors and microglial NLRP3 inflammasome activation through the SIRT1/Nrf2 pathway. *Front. Immunol.* 10, 1511. doi: 10.3389/fimmu.2019.01511

Bergsbaken, T., Fink, S. L., and Cookson, B. T. (2009). Pyroptosis: host cell death and inflammation. *Nat. Rev. Microbiol.* 7, 99–109. doi: 10.1038/nrmicro2070

Bian, Y., Li, X., Pang, P., Hu, X. L., Yu, S. T., Liu, Y. N., et al. (2020). Kanglexin, a novel anthraquinone compound, protects against myocardial ischemic injury in mice by suppressing NLRP3 and pyroptosis. *Acta. Pharmacol. Sinica*. 41, 319–326. doi: 10.1038/s41401-019-0307-8

Bjorkqvist, M., Wild, E. J., Thiele, J., Silvestroni, A., Andre, R., Lahiri, N., et al. (2008). A novel pathogenic pathway of immune activation detectable before clinical onset in Huntington's disease. *J. Exp. Med.* 205, 1869–1877. doi: 10.1084/jem.20080178

Black, R. A., Kronheim, S. R., Merriam, J. E., March, C. J., and Hopp, T. P. (1989). A. pre-aspartate-specific protease from human leukocytes that cleaves pro-interleukin-1 beta. *J. Biol. Chem.* 264, 5323–6. doi: 10.1016/S0021-9258(18)83546-3

Burm, S. M., Peferoen, L. A., Zuiderwijk-Sick, E. A., and Haanstra, K. G. T, Hart, B. A., van der Valk, P., et al. (2016). Expression of IL-1beta in rhesus EAE and MS lesions is mainly induced in the CNS itself. *J. Neuroinflam.* 13, 138. doi: 10.1186/s12974-016-0605-8

Cai, M., Zhuang, W., Lv, E., Liu, Z., Wang, Y., Zhang, W., et al. (2022). Kaemperfol alleviates pyroptosis and microglia-mediated neuroinflammation in Parkinson's disease *via* inhibiting p38MAPK/NF-κB signaling pathway. *Neurochem. Int.* 152, 105221. doi: 10.1016/j.neuint.2021.105221

Cao, X., Wang, Y., and Gao, L. (2021). CHRFAM7A overexpression attenuates cerebral ischemia-reperfusion injury *via* inhibiting microglia pyroptosis mediated by the NLRP3/Caspase-1 pathway. *Inflammation.* 44, 1023–1034. doi: 10.1007/s10753-020-01398-4

Catanese, S., Aringhieri, G., Vivaldi, C., Salani, F., Vitali, S., Pecora, I., et al. (2021). Role of baseline computed-tomography-evaluated body composition in predicting outcome and toxicity from first-line therapy in advanced gastric cancer patients. *J. Clin. Med.* 10, 1079. doi: 10.3390/jcm10051079

Ceulemans, A. G., Zgavc, T., Kooijman, R., Hachimi-Idrissi, S., Sarre, S., Michotte, Y., et al. (2010). The dual role of the neuroinflammatory response after ischemic stroke: modulatory effects of hypothermia. *J. Neuroinflam.* 7, 74. doi: 10.1186/1742-2094-7-74

Chang, Y., Zhu, J., Wang, D., Li, H., He, Y., Liu, K., et al. (2020). NLRP3 inflammasome-mediated microglial pyroptosis is critically involved in the development of post-cardiac arrest brain injury. *J. Neuroinflam.* 17, 219. doi: 10.1186/s12974-020-01879-1

Colonna, M., and Butovsky, O. (2017). Microglia function in the central nervous system during health and neurodegeneration. *Ann. Rev. Immunol.* 35, 441–468. doi: 10.1146/annurev-immunol-051116-052358

Coppin, L., Sokal, E., and Stephenne, X. (2019). Thrombogenic risk induced by intravascular mesenchymal stem cell therapy: current status and future perspectives. *Cells.* 8, 1160. doi: 10.3390/cells8101160

Dabrowska, S., Andrzejewska, A., Lukomska, B., and Janowski, M. (2019). Neuroinflammation as a target for treatment of stroke using mesenchymal stem cells and extracellular vesicles. *J. Neuroinflam.* 16, 178. doi: 10.1186/s12974-019-1571-8

Dai, W., Wang, X., Teng, H., Li, C., Wang, B., Wang, J., et al. (2019). Celastrol inhibits microglial pyroptosis and attenuates inflammatory reaction in acute spinal cord injury rats. *Int. Immunopharmacol.* 66, 215–223. doi: 10.1016/j.intimp.2018.11.029

de Alba, E. (2019). Structure, interactions and self-assembly of ASC-dependent inflammasomes. *Arch. Biochem. Biophys.* 670, 15–31. doi: 10.1016/j.abb.2019.05.023

Dempsey, C., Rubio Araiz, A., Bryson, K. J., Finucane, O., Larkin, C., Mills, E. L., et al. (2017). Inhibiting the NLRP3 inflammasome with MCC950 promotes non-phlogistic clearance of amyloid-β and cognitive function in APP/PS1 mice. *Brain Behav. Immun.* 61, 306–316. doi: 10.1016/j.bbi.2016.12.014

Dendrou, C. A., Fugger, L., and Friese, M. A. (2015). Immunopathology of multiple sclerosis. *Nat. Rev. Immunol.* 15, 545–558. doi: 10.1038/nri3871

Deng, W., Bai, Y., Deng, F., Pan, Y., Mei, S., Zheng, Z., et al. (2022). Streptococcal pyrogenic exotoxin B cleaves GSDMA and triggers pyroptosis. *Nature.* 602, 496–502. doi: 10.1038/s41586-021-04384-4

Dey, A., and Hankey Giblin, P. A. (2018). Insights into macrophage heterogeneity and cytokine-induced neuroinflammation in major depressive disorder. *Pharmaceuticals.* 11, 64. doi: 10.3390/ph11030064

Ding, J., Wang, K., Liu, W., She, Y., Sun, Q., Shi, J., et al. (2016). Pore-forming activity and structural autoinhibition of the gasdermin family. *Nature.* 535, 111–116. doi: 10.1038/nature18590

Eggen, B. J., Raj, D., Hanisch, U. K., and Boddeke, H. W. (2013). Microglial phenotype and adaptation. *J. Neuroimmune Pharmacol.* 8, 807–823. doi: 10.1007/s11481-013-9490-4

Esmaeili-Mahani, S., Haghparast, E., Nezhadi, A., Abbasnejad, M., and Sheibani, V. (2021). Apelin-13 prevents hippocampal synaptic plasticity impairment in Parkinsonism rats. *J. Chem. Neuroanat.* 111, 101884. doi: 10.1016/j.jchemneu.2020.101884

Fan, Y., Du, L., Fu, Q., Zhou, Z., Zhang, J., Li, G., et al. (2018). Inhibiting the NLRP3 inflammasome with MCC950 ameliorates isoflurane-induced pyroptosis and cognitive impairment in aged mice. *Front. Cell. Neurosci.* 12, 426. doi: 10.3389/fncel.2018.00426

Fang, Y., Tian, S., Pan, Y., Li, W., Wang, Q., Tang, Y., et al. (2020). Pyroptosis: a new frontier in cancer. *Biomed. Pharmacother.* 121, 109595. doi: 10.1016/j.biopha.2019.109595

Fann, D. Y., Lee, S. Y., Manzanero, S., Tang, S. C., Gelderblom, M., Chunduri, P., et al. (2013). Intravenous immunoglobulin suppresses NLRP1 and NLRP3 inflammasome-mediated neuronal death in ischemic stroke. *Cell Death Dis.* 4, e790. doi: 10.1038/cddis.2013.326

Fann, D. Y., Lim, Y. A., Cheng, Y. L., Lok, K. Z., Chunduri, P., Baik, S. H., et al. (2018). Evidence that NF-kappaB and MAPK signaling promotes NLRP inflammasome activation in neurons following ischemic stroke. *Mol. Neurobiol.* 55, 1082–1096. doi: 10.1007/s12035-017-0394-9

Frank, D., and Vince, J. E. (2019). Pyroptosis versus necroptosis: similarities, differences, and crosstalk. *Cell Death Diff.* 26, 99–114. doi: 10.1038/s41418-018-0212-6

Friker, L. L., Scheiblich, H., Hochheiser, I. V., Brinkschulte, R., Riedel, D., Latz, E., et al. (2020). Beta-amyloid clustering around ASC fibrils boosts its toxicity in microglia. *Cell Rep.* 30, 3743–54.e6. doi: 10.1016/j.celrep.2020.02.025

Gao, J., Peng, S., Shan, X., Deng, G., Shen, L., Sun, J., et al. (2019). Inhibition of AIM2 inflammasome-mediated pyroptosis by Andrographolide contributes to amelioration of radiation-induced lung inflammation and fibrosis. *Cell Death Dis.* 10, 957. doi: 10.1038/s41419-019-2195-8

Gordon, R., Albornoz, E. A., Christie, D. C., Langley, M. R., Kumar, V., Mantovani, S., et al. (2018). Inflammasome inhibition prevents alpha-synuclein pathology and dopaminergic neurodegeneration in mice. *Sci. Transl. Med.* 10, eaah4066. doi: 10.1126/scitranslmed.aah4066

Graeser, M., Thieben, F., Szwargulski, P., Werner, F., Gdaniec, N., Boberg, M., et al. (2019). Human-sized magnetic particle imaging for brain applications. *Nat. Commun.* 10, 1936. doi: 10.1038/s41467-019-09704-x

Gu, C., Draga, D., Zhou, C., Su, T., Zou, C., Gu, Q., et al. (2019). miR-590-3p inhibits pyroptosis in diabetic retinopathy by targeting NLRP1 and inactivating the NOX4 signaling pathway. *Investig. Ophthalmol. Visual Sci.* 60, 4215–4223. doi: 10.1167/iovs.19-27825

Gu, L., Sun, M., Li, R., Zhang, X., Tao, Y., Yuan, Y., et al. (2022). Didymin suppresses microglia pyroptosis and neuroinflammation through the Asc/Caspase-1/GSDMD pathway following experimental intracerebral hemorrhage. *Front. Immunol.* 13, 810582. doi: 10.3389/fimmu.2022.810582

Guo, H., Callaway, J. B., and Ting, J. P. (2015). Inflammasomes: mechanism of action, role in disease, and therapeutics. *Nat. Med.* 21, 677–687. doi: 10.1038/nm.3893

Han, C., Guo, L., Yang, Y., Guan, Q., Shen, H., Sheng, Y., et al. (2020a). Mechanism of microRNA-22 in regulating neuroinflammation in Alzheimer's disease. *Brain Behav.* 10, e01627. doi: 10.1002/brb3.1627

Han, C., Yang, Y., Yu, A., Guo, L., Guan, Q., Shen, H., et al. (2020b). Investigation on the mechanism of mafenide in inhibiting pyroptosis and the release of inflammatory factors. *Eur. J. Pharm. Sci.* 147, 105303. doi: 10.1016/j.ejps.2020.105303

Han, X., Xu, T., Fang, Q., Zhang, H., Yue, L., Hu, G., et al. (2021). Quercetin hinders microglial activation to alleviate neurotoxicity *via* the interplay between NLRP3 inflammasome and mitophagy. *Redox Biol.* 44, 102010. doi: 10.1016/j.redox.2021.102010

Hao, W., Hao, C., Wu, C., Xu, Y., Wu, S., Lu, X., et al. (2021). Aluminum impairs cognitive function by activating DDX3X-NLRP3-mediated pyroptosis signaling pathway. *Food Chem. Toxicol.* 157, 112591. doi: 10.1016/j.fct.2021.112591

Heneka, M. T., McManus, R. M., and Latz, E. (2018). Inflammasome signalling in brain function and neurodegenerative disease. *Nat. Rev. Neurosci.* 19, 610–621. doi: 10.1038/s41583-018-0055-7

Hou, C., Jiang, F., Ma, H., Zhu, Q., Wang, Z., Zhao, B., et al. (2019). Prognostic role of preoperative platelet, fibrinogen, and D-dimer levels in patients with non-small cell lung cancer: a multicenter prospective study. *Thoracic Cancer.* 10, 304–311. doi: 10.1111/1759-7714.12956

Hu, J., Zeng, C., Wei, J., Duan, F., Liu, S., Zhao, Y., et al. (2020). The combination of Panax ginseng and Angelica sinensis alleviates ischemia brain injury by suppressing NLRP3 inflammasome activation and microglial pyroptosis. *Phytomed. Int. J. Phytother. Phytopharmacol.* 76, 153251. doi: 10.1016/j.phymed.2020.153251

Hu, Q., Hong, M., Huang, M., Gong, Q., Zhang, X., Uversky, V. N., et al. (2022). Age-dependent aggregation of alpha-synuclein in the nervous system of gut-brain axis is associated with caspase-1 activation. *Metab. Brain Dis.* 37, 1669–1681. doi: 10.1007/s11011-022-00917-6

Hu, X., Leak, R. K., Shi, Y., Suenaga, J., Gao, Y., Zheng, P., et al. (2015). Microglial and macrophage polarization—new prospects for brain repair. *Nature Rev. Neurol.* 11, 56–64. doi: 10.1038/nrneurol.2014.207

Huang, W. X., Huang, P., and Hillert, J. (2004). Increased expression of caspase-1 and interleukin-18 in peripheral blood mononuclear cells in patients with multiple sclerosis. *Mult. Scler.* 10, 482–487. doi: 10.1191/1352458504ms1071oa

Huang, Y., Tan, F., Zhuo, Y., Liu, J., He, J., Duan, D., et al. (2020). Hypoxia-preconditioned olfactory mucosa mesenchymal stem cells abolish cerebral ischemia/reperfusion-induced pyroptosis and apoptotic death of microglial cells by activating HIF-1alpha. *Aging.* 12, 10931–10950. doi: 10.18632/aging.103307

Iadecola, C., and Anrather, J. (2011). The immunology of stroke: from mechanisms to translation. *Nat. Med.* 17, 796–808. doi: 10.1038/nm.2399

Imai, H., and Nakagawa, Y. (2003). Biological significance of phospholipid hydroperoxide glutathione peroxidase (PHGPx, GPx4) in mammalian cells. *Free Rad. Biol. Med.* 34, 145–169. doi: 10.1016/S0891-5849(02)01197-8

Jiang, Q., Geng, X., Warren, J., Eugene Paul Cosky, E., Kaura, S., Stone, C., et al. (2020). Hypoxia inducible factor-1alpha (HIF-1alpha) mediates NLRP3 inflammasome-dependent-pyroptotic and apoptotic cell death following ischemic stroke. *Neuroscience.* 448, 126–139. doi: 10.1016/j.neuroscience.2020.09.036

Jorgensen, I., and Miao, E. A. (2015). Pyroptotic cell death defends against intracellular pathogens. *Immunol. Rev.* 265, 130–142. doi: 10.1111/imr.12287

Kang, R., Zeng, L., Zhu, S., Xie, Y., Liu, J., Wen, Q., et al. (2018). Lipid peroxidation drives gasdermin D-mediated pyroptosis in lethal polymicrobial sepsis. *Cell Host Microbe.* 24, 97–108.e4. doi: 10.1016/j.chom.2018.05.009

Kanneganti, T. D., Lamkanfi, M., and Núñez, G. (2007). Intracellular NOD-like receptors in host defense and disease. *Immunity.* 27, 549–559. doi: 10.1016/j.immuni.2007.10.002

Kim, Y. J., Yi, Y., Sapp, E., Wang, Y., Cuiffo, B., Kegel, K. B., et al. (2001). Caspase 3-cleaved N-terminal fragments of wild-type and mutant huntingtin are present in normal and Huntington's disease brains, associate with membranes, and undergo calpain-dependent proteolysis. *Proc. Natl. Acad. Sci. U. S. A.* 98, 12784–12789. doi: 10.1073/pnas.221451398

Kipp, M., Nyamoya, S., Hochstrasser, T., and Amor, S. (2017). Multiple sclerosis animal models: a clinical and histopathological perspective. *Brain Pathol.* 27, 123–137. doi: 10.1111/bpa.12454

Klotz, K., Weistenhöfer, W., Neff, F., Hartwig, A., van Thriel, C., Drexler, H., et al. (2017). The health effects of aluminum exposure. *Deutsches Arzteblatt Int.* 114, 653–659. doi: 10.3238/arztebl.2017.0653

Kornek, B., and Lassmann, H. (2003). Neuropathology of multiple sclerosis-new concepts. *Brain Res. Bull.* 61, 321–326. doi: 10.1016/S0361-9230(03)00095-9

Kovacs, S. B., and Miao, E. A. (2017). Gasdermins: effectors of pyroptosis. *Trends Cell Biol.* 27, 673–684. doi: 10.1016/j.tcb.2017.05.005

Kriz, J. (2006). Inflammation in ischemic brain injury: timing is important. *Crit. Rev. Neurobiol.* 18, 145–157. doi: 10.1615/CritRevNeurobiol.v18.i1-2.150

Langhauser, F., Gob, E., Kraft, P., Geis, C., Schmitt, J., Brede, M., et al. (2012). Kininogen deficiency protects from ischemic neurodegeneration in mice by reducing thrombosis, blood-brain barrier damage, and inflammation. *Blood.* 120, 4082–4092. doi: 10.1182/blood-2012-06-440057

Leyns, C. E. G., and Holtzman, D. M. (2017). Glial contributions to neurodegeneration in tauopathies. *Mol. Neurodegener.* 12, 50. doi: 10.1186/s13024-017-0192-x

Li, Q., and Barres, B. A. (2018). Microglia and macrophages in brain homeostasis and disease. *Nat. Rev. Immunol.* 18, 225–242. doi: 10.1038/nri.2017.125

Li, X., Wang, T., Zhang, D., Li, H., Shen, H., Ding, X., et al. (2018). Andrographolide ameliorates intracerebral hemorrhage induced secondary brain injury by inhibiting neuroinflammation induction. *Neuropharmacology.* 141, 305–315. doi: 10.1016/j.neuropharm.2018.09.015

Li, Y., Song, W., Tong, Y., Zhang, X., Zhao, J., Gao, X., et al. (2021a). Isoliquiritin ameliorates depression by suppressing NLRP3-mediated pyroptosis *via* miRNA-27a/SYK/NF-κB axis. *J. Neuroinflam.* 18, 1. doi: 10.1186/s12974-020-02040-8

Li, Z., Liu, W., Fu, J., Cheng, S., Xu, Y., Wang, Z., et al. (2021b). Shigella evades pyroptosis by arginine ADP-riboxanation of caspase-11. *Nature.* 599, 290–295. doi: 10.1038/s41586-021-04020-1

Liang, J., Wang, Q., Li, J. Q., Guo, T., and Yu, D. (2020a). Long non-coding RNA MEG3 promotes cerebral ischemia-reperfusion injury through increasing pyroptosis by targeting miR-485/AIM2 axis. *Exp. Neurol.* 325, 113139. doi: 10.1016/j.expneurol.2019.113139

Liang, Y. B., Song, P. P., Zhu, Y. H., Xu, J. M., Zhu, P. Z., Liu, R. R., et al. (2020b). TREM-1-targeting LP17 attenuates cerebral ischemia-induced neuronal injury by inhibiting oxidative stress and pyroptosis. *Biochem. Biophys. Res. Commun.* 529, 554–561. doi: 10.1016/j.bbrc.2020.05.056

Lin, X., Ye, H., Siaw-Debrah, F., Pan, S., He, Z., Ni, H., et al. (2018). AC-YVAD-CMK inhibits pyroptosis and improves functional outcome after intracerebral hemorrhage. *Biomed. Res. Int.* 2018, 3706047. doi: 10.1155/2018/3706047

Liu, J., Ma, W., Zang, C. H., Wang, G. D., Zhang, S. J., Wu, H. J., et al. (2021). Salidroside inhibits NLRP3 inflammasome activation and apoptosis in microglia induced by cerebral ischemia/reperfusion injury by inhibiting the TLR4/NF-kappaB signaling pathway. *Ann. Transl. Med.* 9, 1694. doi: 10.21037/atm-21-5752

Liu, W., Chen, Y., Meng, J., Wu, M., Bi, F., Chang, C., et al. (2018). Ablation of caspase-1 protects against TBI-induced pyroptosis *in vitro* and *in vivo*. *J. Neuroinflam.* 15, 48. doi: 10.1186/s12974-018-1083-y

Liu, Z., Yao, X., Jiang, W., Li, W., Zhu, S., Liao, C., et al. (2020). Advanced oxidation protein products induce microglia-mediated neuroinflammation *via* MAPKs-NF-κB signaling pathway and pyroptosis after secondary spinal cord injury. *J Neuroinflam.* 17, 90. doi: 10.1186/s12974-020-01751-2

Lloyd, A. F., and Miron, V. E. (2019). The pro-remyelination properties of microglia in the central nervous system. *Nat. Rev. Neurol.* 15, 447–458. doi: 10.1038/s41582-019-0184-2

Loveless, R., Bloomquist, R., and Teng, Y. (2021). Pyroptosis at the forefront of anticancer immunity. *J. Exp. Clin. Cancer Res. CR.* 40, 264. doi: 10.1186/s13046-021-02065-8

Luciunaite, A., McManus, R. M., Jankunec, M., Racz, I., Dansokho, C., Dalgediene, I., et al. (2020). Soluble Abeta oligomers and protofibrils induce NLRP3 inflammasome activation in microglia. *J. Neurochem.* 155, 650–661. doi: 10.1111/jnc.14945

Ma, D. C., Zhang, N. N., Zhang, Y. N., and Chen, H. S. (2021). Salvianolic Acids for Injection alleviates cerebral ischemia/reperfusion injury by switching M1/M2 phenotypes and inhibiting NLRP3 inflammasome/pyroptosis axis in microglia *in vivo* and *in vitro*. *J. Ethnopharmacol.* 270, 113776. doi: 10.1016/j.jep.2021.113776

Ma, Q., Chen, S., Hu, Q., Feng, H., Zhang, J. H., Tang, J., et al. (2014). NLRP3 inflammasome contributes to inflammation after intracerebral hemorrhage. *Ann. Neurol.* 75, 209–219. doi: 10.1002/ana.24070

Malhi, G. S., and Mann, J. J. (2018). Depression. *Lancet*. 392, 2299–2312. doi: 10.1016/S0140-6736(18)31948-2

Man, S. M., Karki, R., and Kanneganti, T. D. (2017). Molecular mechanisms and functions of pyroptosis, inflammatory caspases and inflammasomes in infectious diseases. *Immunol. Rev.* 277, 61–75. doi: 10.1111/imr.12534

Mao, Z., Liu, C., Ji, S., Yang, Q., Ye, H., Han, H., et al. (2017). The NLRP3 inflammasome is involved in the pathogenesis of Parkinson's disease in rats. *Neurochem. Res.* 42, 1104–1115. doi: 10.1007/s11064-017-2185-0

McKenzie, B. A., Dixit, V. M., and Power, C. (2020a). Fiery cell death: pyroptosis in the central nervous system. *Trends Neurosci.* 43, 55–73. doi: 10.1016/j.tins.2019.11.005

McKenzie, B. A., Fernandes, J. P., Doan, M. A. L., Schmitt, L. M., Branton, W. G., Power, C., et al. (2020b). Activation of the executioner caspases-3 and−7 promotes microglial pyroptosis in models of multiple sclerosis. *J. Neuroinflam.* 17, 253. doi: 10.1186/s12974-020-01902-5

McKenzie, B. A., Mamik, M. K., Saito, L. B., Boghozian, R., Monaco, M. C., Major, E. O., et al. (2018). Caspase-1 inhibition prevents glial inflammasome activation and pyroptosis in models of multiple sclerosis. *Proc. Natl. Acad. Sci. U. S. A.* 115, E6065–e74. doi: 10.1073/pnas.1722041115

Nabavi, S. F., Sureda, A., Habtemariam, S., and Nabavi, S. M. (2015). Ginsenoside Rd and ischemic stroke; a short review of literatures. *J. Ginseng. Res.* 39, 299–303. doi: 10.1016/j.jgr.2015.02.002

Nestle, U., Adebahr, S., Kaier, K., Gkika, E., Schimek-Jasch, T., Hechtner, M., et al. (2020). Quality of life after pulmonary stereotactic fractionated radiotherapy (SBRT): Results of the phase II STRIPE trial. *Radiother. Oncol. J. Eur. Soc. Therap. Radiol. Oncol.* 148, 82–88. doi: 10.1016/j.radonc.2020.03.018

Newcombe, E. A., Camats-Perna, J., Silva, M. L., Valmas, N., Huat, T. J., Medeiros, R., et al. (2018). Inflammation: the link between comorbidities, genetics, and Alzheimer's disease. *J. Neuroinflam.* 15, 276. doi: 10.1186/s12974-018-1313-3

Ona, V. O., Li, M., Vonsattel, J. P., Andrews, L. J., Khan, S. Q., Chung, W. M., et al. (1999). Inhibition of caspase-1 slows disease progression in a mouse model of Huntington's disease. *Nature*. 399, 263–267. doi: 10.1038/20446

Orihuela, R., McPherson, C. A., and Harry, G. J. (2016). Microglial M1/M2 polarization and metabolic states. *Br. J. Pharmacol.* 173, 649–665. doi: 10.1111/bph.13139

Paldino, E., D'Angelo, V., Sancesario, G., and Fusco, F. R. (2020). Pyroptotic cell death in the R6/2 mouse model of Huntington's disease: new insight on the inflammasome. *Cell Death Discov.* 6, 69. doi: 10.1038/s41420-020-00293-z

Palpagama, T. H., Waldvogel, H. J., Faull, R. L. M., and Kwakowsky, A. (2019). The role of microglia and astrocytes in Huntington's disease. *Front. Mol. Neurosci.* 12, 258. doi: 10.3389/fnmol.2019.00258

Pan, Y., Chen, X. Y., Zhang, Q. Y., and Kong, L. D. (2014). Microglial NLRP3 inflammasome activation mediates IL-1beta-related inflammation in prefrontal cortex of depressive rats. *Brain Behav. Immun.* 41, 90–100. doi: 10.1016/j.bbi.2014.04.007

Peng, D., Li, J., Deng, Y., Zhu, X., Zhao, L., Zhang, Y., et al. (2020). Sodium para-aminosalicylic acid inhibits manganese-induced NLRP3 inflammasome-dependent pyroptosis by inhibiting NF-κB pathway activation and oxidative stress. *J. Neuroinflam.* 17, 343. doi: 10.1186/s12974-020-02018-6

Poh, L., Kang, S. W., Baik, S. H., Ng, G. Y. Q., She, D. T., Balaganapathy, P., et al. (2019). Evidence that NLRC4 inflammasome mediates apoptotic and pyroptotic microglial death following ischemic stroke. *Brain Behav. Immun.* 75, 34–47. doi: 10.1016/j.bbi.2018.09.001

Prinz, M., Masuda, T., Wheeler, M. A., and Quintana, F. J. (2021). Microglia and central nervous system-associated macrophages-from origin to disease modulation. *Ann. Rev. Immunol.* 39, 251–277. doi: 10.1146/annurev-immunol-093019-110159

Przedborski, S. (2017). The two-century journey of Parkinson disease research. *Nat. Rev. Neurosci.* 18, 251–259. doi: 10.1038/nrn.2017.25

Qiu, X., Cheng, X., Zhang, J., Yuan, C., Zhao, M., Yang, X., et al. (2020). Ethyl pyruvate confers protection against endotoxemia and sepsis by inhibiting caspase-11-dependent cell pyroptosis. *Int. Immunopharmacol.* 78, 106016. doi: 10.1016/j.intimp.2019.106016

Raedler, T. J. (2011). Inflammatory mechanisms in major depressive disorder. *Curr. Opin. Psychiatry*. 24, 519–525. doi: 10.1097/YCO.0b013e32834b9db6

Ran, Y., Su, W., Gao, F., Ding, Z., Yang, S., Ye, L., et al. (2021). Curcumin ameliorates white matter injury after ischemic stroke by inhibiting microglia/macrophage pyroptosis through NF-kappaB suppression and NLRP3 inflammasome inhibition. *Oxid. Med. Cell Longev.* 2021, 1552127. doi: 10.1155/2021/1552127

Ransohoff, R. M. (2012). Animal models of multiple sclerosis: the good, the bad and the bottom line. *Nat. Neurosci.* 15, 1074–1077. doi: 10.1038/nn.3168

Ransohoff, R. M. (2016a). A polarizing question: do M1 and M2 microglia exist? *Nat. Neurosci.* 19, 987–991. doi: 10.1038/nn.4338

Ransohoff, R. M. (2016b). How neuroinflammation contributes to neurodegeneration. *Science*. 353, 777–783. doi: 10.1126/science.aag2590

Rogers, C., Fernandes-Alnemri, T., Mayes, L., Alnemri, D., Cingolani, G., Alnemri, E. S., et al. (2017). Cleavage of DFNA5 by caspase-3 during apoptosis mediates progression to secondary necrotic/pyroptotic cell death. *Nat. Commun.* 8, 14128. doi: 10.1038/ncomms14128

Ronaldson, P. T., and Davis, T. P. (2020). Regulation of blood-brain barrier integrity by microglia in health and disease: a therapeutic opportunity. *J. Cerebral Blood Flow Metabol.* 40:S6–s24. doi: 10.1177/0271678X20951995

Rui, W., Li, S., Xiao, H., Xiao, M., and Shi, J. (2020). Baicalein attenuates neuroinflammation by inhibiting NLRP3/caspase-1/GSDMD pathway in MPTP induced mice model of Parkinson's disease. *Int. J. Neuropsychopharmacol.* 23, 762–773. doi: 10.1093/ijnp/pyaa060

Sahoo, B. R. (2020). Structure of fish Toll-like receptors (TLR) and NOD-like receptors (NLR). *Int. J. Biol. Macromol.* 161, 1602–1617. doi: 10.1016/j.ijbiomac.2020.07.293

Sanchez Mejia, R. O., and Friedlander, R. M. (2001). Caspases in Huntington's disease. *Neuroscientist*. 7, 480–489. doi: 10.1177/107385840100700604

Sarlus, H., and Heneka, M. T. (2017). Microglia in Alzheimer's disease. *J. Clin. Invest*. 127, 3240–3249. doi: 10.1172/JCI90606

Shi, J., Gao, W., and Shao, F. (2017). Pyroptosis: gasdermin-mediated programmed necrotic cell death. *Trends Biochem. Sci*. 42, 245–254. doi: 10.1016/j.tibs.2016.10.004

Shi, J., Zhao, Y., Wang, K., Shi, X., Wang, Y., Huang, H., et al. (2015). Cleavage of GSDMD by inflammatory caspases determines pyroptotic cell death. *Nature*. 526, 660–665. doi: 10.1038/nature15514

Shi, J., Zhao, Y., Wang, Y., Gao, W., Ding, J., Li, P., et al. (2014). Inflammatory caspases are innate immune receptors for intracellular LPS. *Nature*. 514, 187–192. doi: 10.1038/nature13683

Siew, J. J., Chen, H. M., Chen, H. Y., Chen, H. L., Chen, C. M., Soong, B. W., et al. (2019). Galectin-3 is required for the microglia-mediated brain inflammation in a model of Huntington's disease. *Nat. Commun*. 10, 3473. doi: 10.1038/s41467-019-11441-0

Song, S., Guo, R., Mehmood, A., Zhang, L., Yin, B., Yuan, C., et al. (2022). Liraglutide attenuate central nervous inflammation and demyelination through AMPK and pyroptosis-related NLRP3 pathway. *CNS Neurosci. Ther*. 28, 422–434. doi: 10.1111/cns.13791

Song, X., Cui, Z., He, J., Yang, T., and Sun, X. (2021). κ-opioid receptor agonist, U50488H, inhibits pyroptosis through NLRP3 *via* the Ca(2+)/CaMKII/CREB signaling pathway and improves synaptic plasticity in APP/PS1 mice. *Mol. Med. Rep*. 24, 12168. doi: 10.3892/mmr.2021.12168

Stancu, I. C., Cremers, N., Vanrusselt, H., Couturier, J., Vanoosthuyse, A., Kessels, S., et al. (2019). Aggregated Tau activates NLRP3-ASC inflammasome exacerbating exogenously seeded and non-exogenously seeded Tau pathology *in vivo*. *Acta Neuropathol*. 137, 599–617. doi: 10.1007/s00401-018-01957-y

Su, W. J., Zhang, Y., Chen, Y., Gong, H., Lian, Y. J., Peng, W., et al. (2017). NLRP3 gene knockout blocks NF-kappaB and MAPK signaling pathway in CUMS-induced depression mouse model. *Behav. Brain Res*. 322, 1–8. doi: 10.1016/j.bbr.2017.01.018

Sun, K., Zhang, J., Yang, Q., Zhu, J., Zhang, X., Wu, K., et al. (2021). Dexmedetomidine exerts a protective effect on ischemic brain injury by inhibiting the P2X7R/NLRP3/Caspase-1 signaling pathway. *Brain Res. Bull*. 174, 11–21. doi: 10.1016/j.brainresbull.2021.05.006

Sun, Z., Nyanzu, M., Yang, S., Zhu, X., Wang, K., Ru, J., et al. (2020). VX765 attenuates pyroptosis and HMGB1/TLR4/NF-κB pathways to improve functional outcomes in TBI mice. *Oxid. Med. Cell Longev*. 2020, 7879629. doi: 10.1155/2020/7879629

Taabazuing, C. Y., Okondo, M. C., and Bachovchin, D. A. (2017). Pyroptosis and apoptosis pathways engage in bidirectional crosstalk in monocytes and macrophages. *Cell Chem. Biol*. 24, 507–14.e4. doi: 10.1016/j.chembiol.2017.03.009

Tao, Z., Wang, J., Wen, K., Yao, R., Da, W., Zhou, S., et al. (2020). Pyroptosis in Osteoblasts: a novel hypothesis underlying the pathogenesis of osteoporosis. *Front. Endocrinol*. 11, 548812. doi: 10.3389/fendo.2020.548812

Tastan, B., Arioz, B. I., Tufekci, K. U., Tarakcioglu, E., Gonul, C. P., Genc, K., et al. (2021). Dimethyl fumarate alleviates NLRP3 inflammasome activation in microglia and sickness behavior in LPS-challenged mice. *Front. Immunol*. 12, 737065. doi: 10.3389/fimmu.2021.737065

Tian, D., Xing, Y., Gao, W., Zhang, H., Song, Y., Tian, Y., et al. (2021a). Sevoflurane aggravates the progress of Alzheimer's disease through NLRP3/Caspase-1/Gasdermin D pathway. *Front. Cell Dev. Biol*. 9, 801422. doi: 10.3389/fcell.2021.801422

Tian, D. D., Wang, M., Liu, A., Gao, M. R., Qiu, C., Yu, W., et al. (2021b). Antidepressant effect of paeoniflorin is through inhibiting pyroptosis CASP-11/GSDMD pathway. *Mol. Neurobiol*. 58, 761–776. doi: 10.1007/s12035-020-02144-5

Tian, Y., Meng, L., and Zhang, Z. (2020). What is strain in neurodegenerative diseases? *Cell Mol. Life Sci*. 77, 665–676. doi: 10.1007/s00018-019-03298-9

Tsuchiya, K., Nakajima, S., Hosojima, S., Thi Nguyen, D., Hattori, T., Manh Le, T., et al. (2019). Caspase-1 initiates apoptosis in the absence of gasdermin D. *Nat. Commun*. 10, 2091. doi: 10.1038/s41467-019-09753-2

Tufekci, K. U., Ercan, I., Isci, K. B., Olcum, M., Tastan, B., Gonul, C. P., et al. (2021). Sulforaphane inhibits NLRP3 inflammasome activation in microglia through Nrf2-mediated miRNA alteration. *Immunol. Lett*. 233, 20–30. doi: 10.1016/j.imlet.2021.03.004

Van Opdenbosch, N., and Lamkanfi, M. (2019). Caspases in cell death, inflammation, and disease. *Immunity*. 50, 1352–1364. doi: 10.1016/j.immuni.2019.05.020

Van Zeller, M., Dias, D., Sebastiao, A. M., and Valente, C. A. (2021). NLRP3 Inflammasome: a starring role in amyloid-beta- and tau-driven pathological events in Alzheimer's disease. *J. Alzheimers Dis*. 83, 939–961. doi: 10.3233/JAD-210268

Vande Walle, L., and Lamkanfi, M. (2016). Pyroptosis. *Curr. Biol*. 26, R568–R72. doi: 10.1016/j.cub.2016.02.019

Vaquer-Alicea, J., and Diamond, M. I. (2019). Propagation of protein aggregation in neurodegenerative diseases. *Annu. Rev. Biochem*. 88, 785–810. doi: 10.1146/annurev-biochem-061516-045049

Venegas, C., Kumar, S., Franklin, B. S., Dierkes, T., Brinkschulte, R., Tejera, D., et al. (2017). Microglia-derived ASC specks cross-seed amyloid-beta in Alzheimer's disease. *Nature*. 552, 355–361. doi: 10.1038/nature25158

Voet, S., Srinivasan, S., Lamkanfi, M., and van Loo, G. (2019). Inflammasomes in neuroinflammatory and neurodegenerative diseases. *EMBO Mol. Med*. 11, 248. doi: 10.15252/emmm.201810248

Wan, T., Fu, M., Jiang, Y., Jiang, W., Li, P., Zhou, S., et al. (2022a). Research progress on mechanism of neuroprotective roles of apelin-13 in prevention and treatment of Alzheimer's disease. *Neurochem. Res*. 47, 205–217. doi: 10.1007/s11064-021-03448-1

Wan, T., Huang, Y., Gao, X., Wu, W., and Guo, W. (2022b). Microglia polarization: a novel target of exosome for stroke treatment. *Front. Cell Dev. Biol*. 10, 842320. doi: 10.3389/fcell.2022.842320

Wang, K., Ru, J., Zhang, H., Chen, J., Lin, X., Lin, Z., et al. (2020a). Melatonin enhances the therapeutic effect of plasma exosomes against cerebral ischemia-induced pyroptosis through the TLR4/NF-κB PATHWAY. *Front Neurosci*. 14, 848. doi: 10.3389/fnins.2020.00848

Wang, K., Sun, Z., Ru, J., Wang, S., Huang, L., Ruan, L., et al. (2020b). Ablation of GSDMD improves outcome of ischemic stroke through blocking canonical and non-canonical inflammasomes dependent pyroptosis in microglia. *Front. Neurol*. 11, 577927. doi: 10.3389/fneur.2020.577927

Wang, Q., Wu, J., Zeng, Y., Chen, K., Wang, C., Yang, S., et al. (2020c). Pyroptosis: A pro-inflammatory type of cell death in cardiovascular disease. *Clin. Chim. Acta Int. J. Clin. Chem*. 510, 62–72. doi: 10.1016/j.cca.2020.06.044

Wang, S., Yuan, Y. H., Chen, N. H., and Wang, H. B. (2019). The mechanisms of NLRP3 inflammasome/pyroptosis activation and their role in Parkinson's disease. *Int. Immunopharmacol*. 67, 458–464. doi: 10.1016/j.intimp.2018.12.019

Wang, W., Nguyen, L. T., Burlak, C., Chegini, F., Guo, F., Chataway, T., et al. (2016). Caspase-1 causes truncation and aggregation of the Parkinson's disease-associated protein alpha-synuclein. *Proc. Natl. Acad. Sci. U. S. A*. 113, 9587–9592. doi: 10.1073/pnas.1610099113

Wang, Y., Gao, W., Shi, X., Ding, J., Liu, W., He, H., et al. (2017). Chemotherapy drugs induce pyroptosis through caspase-3 cleavage of a gasdermin. *Nature*. 547, 99–103. doi: 10.1038/nature22393

Wu, D., Wang, S., Yu, G., and Chen, X. (2021). Cell death mediated by the pyroptosis pathway with the aid of nanotechnology: prospects for cancer therapy. *Angewandte Chem.*. 60, 8018–8034. doi: 10.1002/anie.202010281

Xia, L., Liu, L., Cai, Y., Zhang, Y., Tong, F., Wang, Q., et al. (2021). Inhibition of gasdermin D-mediated pyroptosis attenuates the severity of seizures and astroglial damage in kainic acid-induced epileptic mice. *Front. Pharmacol*. 12, 751644. doi: 10.3389/fphar.2021.751644

Xia, X., Wang, X., Cheng, Z., Qin, W., Lei, L., Jiang, J., et al. (2019). The role of pyroptosis in cancer: pro-cancer or pro-"host"? *Cell Death Dis*. 10, 650. doi: 10.1038/s41419-019-1883-8

Xu, P., Hong, Y., Xie, Y., Yuan, K., Li, J., Sun, R., et al. (2021a). TREM-1 exacerbates neuroinflammatory injury *via* NLRP3 inflammasome-mediated pyroptosis in experimental subarachnoid hemorrhage. *Transl. Stroke Res*. 12, 643–659. doi: 10.1007/s12975-020-00840-x

Xu, P., Zhang, X., Liu, Q., Xie, Y., Shi, X., Chen, J., et al. (2019a). Microglial TREM-1 receptor mediates neuroinflammatory injury *via* interaction with SYK in experimental ischemic stroke. *Cell Death Dis*. 10, 555. doi: 10.1038/s41419-019-1777-9

Xu, S., Wang, J., Jiang, J., Song, J., Zhu, W., Zhang, F., et al. (2020). TLR4 promotes microglial pyroptosis *via* lncRNA-F630028O10Rik by activating PI3K/AKT pathway after spinal cord injury. *Cell Death Dis*. 11, 693. doi: 10.1038/s41419-020-02824-z

Xu, S., Wang, J., Zhong, J., Shao, M., Jiang, J., Song, J., et al. (2021b). CD73 alleviates GSDMD-mediated microglia pyroptosis in spinal cord injury through PI3K/AKT/Foxo1 signaling. *Clin. Transl. Med*. 11, e269. doi: 10.1002/ctm2.269

Xu, X. E., Liu, L., Wang, Y. C., Wang, C. T., Zheng, Q., Liu, Q. X., et al. (2019b). Caspase-1 inhibitor exerts brain-protective effects against sepsis-associated encephalopathy and cognitive impairments in a mouse model of sepsis. *Brain Behav. Immun*. 80, 859–870. doi: 10.1016/j.bbi.2019.05.038

Xue, Y., Enosi Tuipulotu, D., Tan, W. H., Kay, C., and Man, S. M. (2019). Emerging activators and regulators of inflammasomes and pyroptosis. *Trends Immunol*. 40, 1035–1052. doi: 10.1016/j.it.2019.09.005

Yan, J., Xu, W., Lenahan, C., Huang, L., Wen, J., Li, G., et al. (2021). CCR5 Activation promotes NLRP1-dependent neuronal pyroptosis *via* CCR5/PKA/CREB pathway after intracerebral hemorrhage. *Stroke*. 52, 4021–4032. doi: 10.1161/STROKEAHA.120.033285

Yang, C., Sui, G., Wang, L., Chen, Z., and Wang, F. (2022). MiR-124 prevents the microglial proinflammatory response by inhibiting the activities of TLR4 and downstream NLRP3 in palmitic acid-treated BV2 cells. *J. Mol. Neurosci*. 72, 496–506. doi: 10.1007/s12031-021-01921-8

Yang, S., Zhang, X., Zhang, H., Lin, X., Chen, X., Zhang, Y., et al. (2021). Dimethyl itaconate inhibits LPSinduced microglia inflammation and inflammasomemediated pyroptosis *via* inducing autophagy and regulating the Nrf2/HO1 signaling pathway. *Mol. Med. Rep*. 24, 12311. doi: 10.3892/mmr.2021.12311

Yao, Y., Li, C., Qian, F., Zhao, Y., Shi, X., Hong, D., et al. (2021). Ginsenoside Rg1 inhibits microglia pyroptosis induced by lipopolysaccharide through regulating STAT3 signaling. *J. Inflam. Res*. 14, 6619–6632. doi: 10.2147/JIR.S326888

Ye, Y., Jin, T., Zhang, X., Zeng, Z., Ye, B., Wang, J., et al. (2019). Meisoindigo protects against focal cerebral ischemia-reperfusion injury by inhibiting NLRP3 inflammasome activation and regulating microglia/macrophage polarization *via* TLR4/NF-kappaB signaling pathway. *Front. Cell Neurosci*. 13, 553. doi: 10.3389/fncel.2019.00553

Yu, M., Fu, Y., Liang, Y., Song, H., Yao, Y., Wu, P., et al. (2017). Suppression of MAPK11 or HIPK3 reduces mutant Huntingtin levels in Huntington's disease models. *Cell Res*. 27, 1441–1465. doi: 10.1038/cr.2017.113

Yu, Y., and Ye, R. D. (2015). Microglial abeta receptors in Alzheimer's disease. *Cell Mol. Neurobiol*. 35, 71–83. doi: 10.1007/s10571-014-0101-6

Yuan, L., Zhu, Y., Huang, S., Lin, L., Jiang, X., Chen, S., et al. (2021). NF-κB/ROS and ERK pathways regulate NLRP3 inflammasome activation in Listeria monocytogenes infected BV2 microglia cells. *J. Microbiol*. 59, 771–781. doi: 10.1007/s12275-021-0692-9

Zhai, L., Shen, H., Sheng, Y., and Guan, Q. A. D. M. S. C. (2021). Exo-MicroRNA-22 improve neurological function and neuroinflammation in mice with Alzheimer's disease. *J. Cell. Mol. Med*. 25, 7513–7523. doi: 10.1111/jcmm.16787

Zhang, D., Qian, J., Zhang, P., Li, H., Shen, H., Li, X., et al. (2019). Gasdermin D serves as a key executioner of pyroptosis in experimental cerebral ischemia and reperfusion model both *in vivo* and *in vitro*. *J. Neurosci. Res*. 97, 645–660. doi: 10.1002/jnr.24385

Zhang, P., Shao, X. Y., Qi, G. J., Chen, Q., Bu, L. L., Chen, L. J., et al. (2016). Cdk5-dependent activation of neuronal inflammasomes in Parkinson's disease. *Mov. Disord*. 31, 366–376. doi: 10.1002/mds.26488

Zhao, M., Dai, Y., Li, P., Wang, J., Ma, T., Xu, S., et al. (2021). Inhibition of NLRP3 inflammasome activation and pyroptosis with the ethyl acetate fraction of Bungeanum ameliorated cognitive dysfunction in aged mice. *Food Funct*. 12, 10443–10458. doi: 10.1039/D1FO00876E

Zheng, Y., Zhang, J., Zhao, Y., Zhang, Y., Zhang, X., Guan, J., et al. (2021). Curcumin protects against cognitive impairments in a rat model of chronic cerebral hypoperfusion combined with diabetes mellitus by suppressing neuroinflammation, apoptosis, and pyroptosis. *Int. Immunopharmacol*. 93, 107422. doi: 10.1016/j.intimp.2021.107422

Zhou, L. J., Peng, J., Xu, Y. N., Zeng, W. J., Zhang, J., Wei, X., et al. (2019). Microglia are indispensable for synaptic plasticity in the spinal dorsal horn and chronic pain. *Cell Rep*. 27, 3844–59.e6. doi: 10.1016/j.celrep.2019.05.087

Zhou, Y., Lu, M., Du, R. H., Qiao, C., Jiang, C. Y., Zhang, K. Z., et al. (2016). MicroRNA-7 targets Nod-like receptor protein 3 inflammasome to modulate neuroinflammation in the pathogenesis of Parkinson's disease. *Mol. Neurodegener*. 11, 28. doi: 10.1186/s13024-016-0094-3

Conflict of Interest: The authors declare that the research was conducted in the absence of any commercial or financial relationships that could be construed as a potential conflict of interest.

Publisher's Note: All claims expressed in this article are solely those of the authors and do not necessarily represent those of their affiliated organizations, or those of the publisher, the editors and the reviewers. Any product that may be evaluated in this article, or claim that may be made by its manufacturer, is not guaranteed or endorsed by the publisher.

frontiers | Frontiers in Pharmacology

SYSTEMATIC REVIEW
published: 22 July 2022
doi: 10.3389/fphar.2022.924747

The Efficacy and Safety of Ischemic Stroke Therapies: An Umbrella Review

Yongbiao Li[1], Ruyi Cui[2], Fangcheng Fan[1], Yangyang Lu[1], Yangwen Ai[1], Hua Liu[1], Shaobao Liu[1], Yang Du[1], Zhiping Qin[1], Wenjing Sun[1], Qianqian Yu[3], Qingshan Liu[1] and Yong Cheng[1,4]**

[1]Key Laboratory of Ethnomedicine of Ministry of Education, School of Pharmacy, Center on Translational Neuroscience, Minzu University of China, Beijing, China, [2]Institute of Chinese Materia Medica, China Academy of Chinese Medical Sciences, Beijing, China, [3]The People's Hospital of Xin Tai City (Nephropathy Department), Beijing, China, [4]Institute of National Security, Minzu University of China, Beijing, China

Background: Ischemic stroke is a leading cause of morbidity and mortality in neurological diseases. Numerous studies have evaluated the efficacy and safety of ischemic stroke therapies, but clinical data were largely inconsistent. Therefore, it is necessary to summarize and analyze the published clinical research data in the field.

Objective: We aimed to perform an umbrella review to evaluate the efficacy and safety of ischemic stroke therapies.

Methods: We conducted a search for meta-analyses and systematic reviews on PubMed, the Cochrane Library, and the Web of Science to address this issue. We examined neurological function deficit and cognitive function scores, quality of life, and activities of daily living as efficacy endpoints and the incidence of adverse events as safety profiles.

Results: Forty-three eligible studies including 377 studies were included in the umbrella review. The results showed that thrombolytic therapy (tPA; alteplase, tenecteplase, and desmoteplase), mechanical thrombectomy (MTE), edaravone with tPA, stem cell-based therapies, stent retrievers, acupuncture with Western medicines, autologous bone marrow stromal cells, antiplatelet agents (aspirin, clopidogrel, and tirofiban), statins, and Western medicines with blood-activating and stasis-dispelling herbs (NaoShuanTong capsule, Ginkgo biloba, Tongqiao Huoxue Decoction, Xuesaitong injection) can improve the neurological deficits and activities of daily living, and the adverse effects were mild for the treatment of ischemic stroke. Moreover, ligustrazine, safflower yellow, statins, albumin, colchicine, MLC601, salvianolic acids, and DL-3-n-butylphthalide showed serious adverse events, intracranial hemorrhage, or mortality in ischemic stroke patients.

Conclusion: Our study demonstrated that tPA, edaravone and tPA, tPA and MTE, acupuncture and Western medicines, and blood-activating and stasis-dispelling herbs with Western medicines are the optimum neurological function and activities of daily living medication for patients with ischemic stroke.

Systematic Review Registration: https://inplasy.com/, identifier [INPLASY202250145].

Keywords: ischemic stroke, clinical trial, systematic review, umbrella review, neurological functional

OPEN ACCESS

Edited by:
Ning Liu,
Tulane University, United States

Reviewed by:
Zhengbu Liao,
First Affiliated Hospital of Chongqing Medical University, China
Ifechukwude Biose,
Tulane University, United States

****Correspondence:***
Qingshan Liu
nlqsh@163.com
Yong Cheng
yongcheng@muc.edu.cn

Specialty section:
This article was submitted to Neuropharmacology, a section of the journal Frontiers in Pharmacology

Received: *20 April 2022*
Accepted: *16 June 2022*
Published: *22 July 2022*

Citation:
Li Y, Cui R, Fan F, Lu Y, Ai Y, Liu H, Liu S, Du Y, Qin Z, Sun W, Yu Q, Liu Q and Cheng Y (2022) The Efficacy and Safety of Ischemic Stroke Therapies: An Umbrella Review. Front. Pharmacol. 13:924747. doi: 10.3389/fphar.2022.924747

INTRODUCTION

Ischemic stroke is a major cause of death and disability, so prevention and effective treatment of stroke are of utmost importance in China and the West. The World Health Organization has suggested that an incidence of stroke occurs once every 5 s worldwide, approximately one-third of strokes are fatal, and another third leave survivors with permanent disability (Donkor, 2018). Moreover, surviving stroke patients impose a heavy medical burden on families and communities (Go et al., 2014). However, little is known about the efficacy and safety of treatments of ischemic stroke in the hyper-acute (0–24 h) and acute phases (1–7 days) and recovery period (>7 days) post-stroke in humans (Marzolini et al., 2019). The key challenge in the treatment of stroke is to identify the most effective way to implement the efficacious interventions currently available.

Some evidence supports national guidelines recommending the use of recombinant tissue plasminogen activator (tPA) thrombolysis for the treatment of hyperacute ischemic stroke, which can significantly improve neurological deficits (Li et al., 2017; Zhou et al., 2020). In addition, the guidelines also recommend antithrombotic (including antiplatelet and anticoagulant therapy), neuroprotection, traditional Chinese medicine, statins, and control of high-risk factors for secondary prevention of ischemic stroke (Practice, 2021). Additionally, as a bradykinin B1 and B2 receptor agonist, HUK provides functional benefits (Patel and McMullen, 2017). Furthermore, other neuroprotective drugs are supported by comprehensive clinical reports that demonstrate their efficacy and safety in improving cognitive impairment or other major domains (Practice, 2021).

Attempts to many systematic reviews and meta-analyses have been conducted to analyze the different stroke treatments. These studies, however, did not provide comprehensive appraisals of stroke therapies, and some results are still conflicting (Wu et al., 2007). A review of the latest literature, having removed repeated studies and research involving complications, followed by a meta-analysis to derive at pooled prevalence, was needed. Therefore, the present study aimed to perform an umbrella review of the systematic reviews and meta-analyses of stroke therapies through a comprehensive and updated literature search and to reach a definitive conclusion by integrating all available meta-analyses to identify which of the commercially available treatments for ischemic stroke patients are efficacious and safe.

MATERIALS AND METHODS

Our study was performed in accordance with the standard guidelines of Preferred Reporting Items for Systematic reviews and Meta-analysis (PRISMA) (Moher et al., 2009). The protocol for this review was prospectively registered at INPLASY PROTOCOL (INPLASY202250145).

Search Strategy and Quality Assessment

A systematic search of published peer-reviewed English language literature was conducted using PubMed, Web of Science, and the Cochrane Library until March 2022. The database search terms were as follows: (Ischemic stroke) and (systematic review or meta-analysis) and clinical trial. We included meta-analyses and systematic reviews that determined the efficacy and safety of treatments in patients with stroke. Inclusion criteria were: 1) written in English; 2) published systematic review or meta-analyses; 3) including any evaluation of clinical assessment scales for stroke; 4) published in peer-reviewed journals. Studies were excluded if 1) unpublished studies; 2) no necessary sample data; 3) patients were diagnosed with other strokes; 4) the study reported insufficient details and other outcomes; and 5) the study presented the risk of bias/study limitations.

The AMSTAR2 tool was used to evaluate systematic reviews and meta-analyses (Shea et al., 2007; De Santis et al., 2021). The methodological quality of the studies was determined by the percentage of AMSTAR2 score. The percentage of AMSTAR2 score was classified into 0–33%, 34–66%, and 67%–100% indicating low quality, medium quality, and high quality, respectively.

We searched for related articles using keywords and filtering titles, and two investigators screened the literature independently. Articles were downloaded and the abstracts screened using inclusion criteria, deleting any irrelevant or repetitive articles. Thereafter, we manually searched the reference lists of the chosen studies for any other relevant studies not found in our initial search. Finally, a full-text search was performed to extract and then analyze the data from articles.

Data Extraction

According to the following criteria, three investigators (Yongbiao Li, Ruyi Cui, and Fangcheng Fan.) independently selected those trials that met the inclusion criteria. The main characteristics of the selected study were extracted in a table including the year of publication, study design, number of studies, and regimens for the treatment. We included results evaluating the efficacy of drugs in patients with at least one of the clinical assessment scales: 1) the incidence of intracranial hemorrhage (sICH); 2) the primary outcomes included: global neurological deficit scores such as the National Institutes of Health Stroke Scale (NIHSS) score ≤1 and the Neurological Function Deficit Scores (NFDS); 3) all-cause mortality; 4) dependence assessed by Barthel Index (BI) scores ≥95; 5) modified Rankin Scale score of 0–1 or return to baseline (mRS); 6) clinical effect, defined according to the nationally approved criteria, is divided into essentially recovered, significant improvement, improvement, no change, deterioration, and death (the first three categories are judged to be effective); 7) the secondary outcomes included the following: cognitive function scoring; related hemorheology and lipid metabolism outcomes; quality of life; and 8) incidence of adverse events (AE). The selection of assessments was extracted on study size, sample size, mean difference (Fixed, 95% CI) or odds ratio (Fixed, 95% CI), and heterogeneity (I^2). A percentage of 0–25% was classified as mild, 26–50%, as moderate, and 51–75%, as significant between-study heterogeneity. If I^2 > 50%, a random-effects model was used for the analysis, or the data were analyzed on the fixed-effects model (Wang et al., 2016).

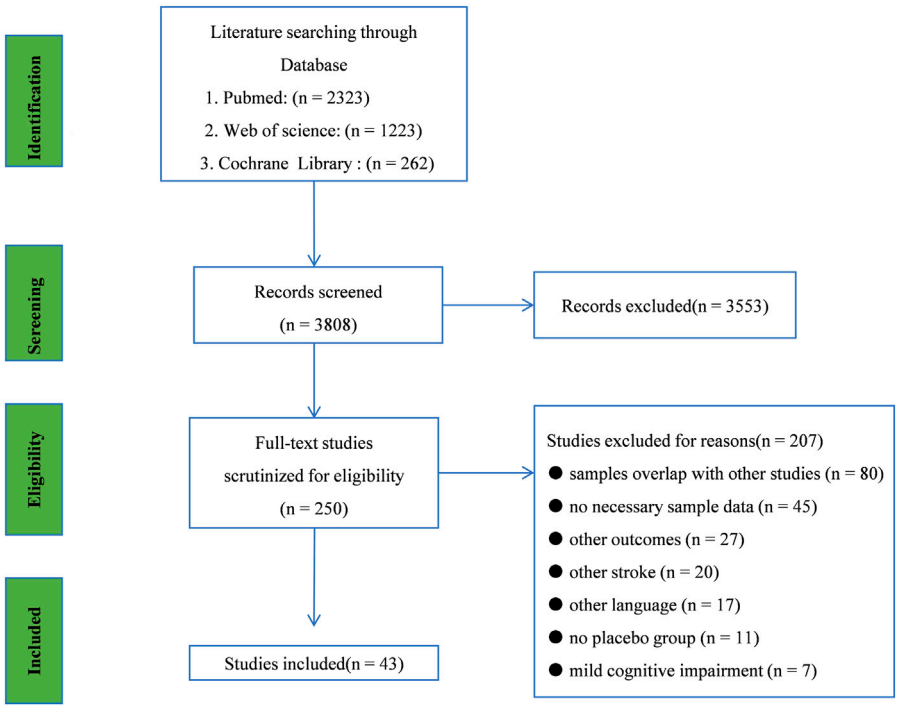

FIGURE 1 | Searching and screening process: literature search and study selection Through the initial search, we retrieved a total of 3,808 records from PubMed, Web of Science, and Cochrane Library. After examining the titles and abstracts, 250 studies were selected for further full-text scrutiny. In all, 207 studies were excluded due to the following reasons: sample overlap with other studies ($n = 80$), no necessary sample data ($n = 45$), other outcomes ($n = 27$), other stroke ($n = 20$), other language ($n = 17$), no placebo group ($n = 11$), and mild cognitive impairment ($n = 7$).

Statistical Analysis

The sample size and mean difference were used to calculate the four clinical assessment scales. NIHSS/mRS/BI scores were used to evaluate neurological status, and behavioral symptoms in patients were calculated by NFDS. We focused on the clinical effect is divided into essentially recovered, significant improvement, no change, deterioration; cognitive function scoring; quality of life as activities of daily living. All data analyses were performed by GraphPad Prism 5.0 software. The results were expressed as OR ± SD (standard deviation). The adverse events have assessed the incidence of adverse events, and the OR was calculated. Therefore, mean difference or odds ratio with 95% CI and p values were used to assess the efficacy and safety of the study medications.

RESULTS

Literature search and study selection through the initial search, we retrieved a total of 3,808 records from PubMed, Web of Science, and Cochrane Library. After examining the titles and abstracts, 250 studies were selected for further full-text scrutiny. In all, 207 studies were excluded due to the following reasons: samples overlap with other studies ($n = 80$), no necessary sample data ($n = 45$), other outcomes ($n = 27$), other stroke ($n = 20$), other language ($n = 17$), no placebo group ($n = 11$), mild cognitive impairment ($n = 7$), (**Figure 1**). Thus, 43 studies were included in the umbrella review: Pan et al., 2020; Pan et al., 2020); Liu et al., 2021); (Liu et al., 2011); Blann et al., 2015); (Blann et al., 2015); Emberson et al., 2014) (Emberson et al., 2014); Peng et al., 2014); (Peng et al., 2014); Zhang et al., 2019); Shang et al., 2019); Puñal-Riobóo et al., 2015; Yuan et al., 2008; (Fu et al., 2013), Fan et al., 2014), Lin et al., 2014); Xu et al., 2015); Cao and Li, (2015); Marmagkiolis et al., 2015); Zheng et al., 2017), Li et al., 2017), Zhang et al., 2017), Chong et al., 2020); (Zhao et al., 2021), Li et al. (2020); (Li et al., 2020), Gao et al., 2021); Huang et al., 2020); (Huang and Xiao, 2021), Liu et al., 2022), Feng et al., 2021), Lee et al. (2010); Zhou et al., 2022); Hu et al., 2021); Hong and Lee, 2015, Liu et al., 2021); (Liu et al., 2021), Xin et al., 2020); Katsanos et al., 2020), Wang et al., 2021), Liu et al., 2019; (Liu et al., 2019), Xu et al., 2019); (Zhang et al., 2019), (Huang et al., 2020), Yang et al., 2015), Yang et al., 2015), (Ni et al., 2020); (Thelengana et al., 2019), Shi et al., 2014) and (Siddiqui et al., 2013), (Liu et al., 2016), Kaesmacher et al., 2019); (Kaesmacher et al., 2019), Li et al., 2014). The main characteristics, bias analysis, and the quality scores of the included studies are shown in **Table 1** and **Supplementary material**.

As shown in **Table 1**, a total of 377 clinical trials were included, with 43 drug therapies in the treatment groups. All studies were randomized controlled clinical trials, and the treatment duration ranged from 1 to 72 weeks. In total, 24 meta-analyses included were of high quality according to AMSTAR2 score, 12 meta-analyses included were of middle quality according to AMSTAR2 score, and seven meta-analyses included were of

TABLE 1 | Description and AMSTAR2 scores of included studies.

Study	Condition	Studies included	Study duration (median, range)	Daily dose (median, range)	Outcome	AMSTAR2 score	Study quality
Ni et al. (2013)	Ligustrazine versus placebo	3	14w (2w–48w)	240 mg/day	1. Effect and 2. sICH	5/11	low
Xin et al. (2020)	Heparin versus Placebo	9	12w	<40 mg/day	1. mRS, 2. NIHSS, 3. sICH, 4. DOS, and 5. AE	7/11	middle
Shang et al. (2019)	MTE versus placebo	7	12w	NA	1. mRS and 2. sICH	8/11	high
Kaesmacher et al. (2019)	tPA plus MTE versus placebo	12	12w	NA	1. mRS and 2. sICH	9/11	high
Li et al. (2014)	Acupuncture plus XM versus placebo	17	12W	NA	1. Effect	8/11	high
Liu et al. (2021)	Nimodipine versus placebo	8	18w (12w–24w)	NA	1. Effect, and 2. NFDs	10/11	high
Blann et al. (2015)	Aspirin plus clopidogrel versus placebo	24	12w	60 mg/day	1. Effect and2. sICH	9/11	high
Emberson et al. (2014)	tPA versus placebo	12	3 h (0–6 h)	<0.85 mg/kg/day	1. Effect, 2. sICH, and 3. NIHSS	10/11	high
Peng et al. (2014)	XNJ versus placebo	13	4w	45 ml (30–60 ml/day)	1. Effect, 2. NFDs, and 3. AE	6/11	middle
Zhang et al. (2019)	NST versus placebo	13	12w	50 mg/day	1. Effect, 2. NFDs, 3 .BI, and 4. mRS	10/11	high
Yuan et al. (2008)	Chuanxiong versus Placebo	3	24w (1w–48w)	120 mg (80–160 mg/day)	1. NFDs and 2. AE	10/11	high
Fu et al. (2013)	XXMT versus placebo	8	12w (4w–24w)	NA	1. NIHSS, 2. mRS, and 3. Effect	5/11	low
Fan et al. (2014)	Safflower yellow versus placebo	7	2w	50 mg/day	1. Effect, 2. NFDs, and 3. AE	5/11	low
Lu et al. (2014)	Rhubarb versus placebo	12	2w (1w–4w)	NA	1. Effect, 2. NFDs, 3. BI, 4. NIHSS, and 5. AE	6/11	middle
Xu et al. (2015)	WD versus placebo	13	2w (2w–4w)	NA	1. Effect, 2. sICH, and 3. NFDS	4/11	low
Cao and Li. (2015)	MSCs versus placebo	5	3w (1w–6w)	5×10^7-2.6×10^8 cell	1. NIHSS, 2. mRS, 3. BI, and 4. AE	6/11	middle
Marmagkiolis et al. (2015)	stent retrievers versus placebo	5	12w	NA	1. mRS, 2. sICH, and 3. AE	8/11	high
Zheng et al. (2017)	Puerarin versus placebo	16	1w (1w–2w)	300 mg (100–500 mg/day)	1. Effect and 2. NFDs	6/11	middle
Li et al. (2017)	Alpha1 versus placebo	6	6 h (3–9 h)	90 mg/kg/day	1. Effect, 2. sICH, and 3. AE	8/11	high
Zhang et al. (2017)	Cerebrolysin versus placebo	7	12w (1w–12w)	50 ml/day	1. mRS, 2. BI, and 3. AE	9/11	high
Chong et al. (2020)	Ginkgo biloba versus placebo	12	12w (1w–12w)	100 mg (40–160 mg)/day	1. NIHSS, 2. NFDs, 3. sICH, and 4. AE	9/11	high
Li et al. (2020)	Stem cell-based versus placebo	9	12w (1w–12w)	5×10^6-2.97×10^9 cell	1. NIHSS, 2. mRS, 3. BI, and 4. AE	9/11	high
Zhou et al. (2020)	tirofiban versus placebo	6	18w (12w–24w)	(0.1-0.4 ug/kg/day)	1. Effect, 2. sICH, and 3. AE	5/11	low
Gao et al. (2021)	BHD versus placebo	11	16w (8w–24w)	NA	1. Effect, 2. NIHSS, and 3. AE	9/11	high
Huang and Xiao. (2021)	Albumin versus placebo	4	15w (2w–48w)	1.3 mg (0.6–2 mg/kg/day)	1. Effect	9/11	high
Liu et al. (2022)	DZSM versus placebo	28	7w (1w–13w)	NA	1. mRS, 2. NFDs, 3. BI, and 4. NIHSS	10/11	high
Feng et al. (2021)	XST plus XM versus placebo	12	2w (2w–4w)	NA	1.Effect and 2. NIHSS	5/11	middle
Lee et al. (2010)	Intra-A versus placebo	5	12w	NA	1. mRS, 2. BI, and 3. NIHSS	5/11	middle
Zhou et al. (2022)	TQHX plus XM versus placebo	12	4w	NA	1. Effect and 2. NFDs	9/11	high
Hu et al. (2021)	Edaravone plus rt-PA versus placebo	17	2w (1w–4w)	60 mg/day	1. sICH and 2. NIHSS	5/11	middle
Hong and Lee. (2015)	Statins versus placebo	18	6w (1w–12w)	8 mg/kg/day	1. Effect and 2. NFDs	9/11	high

(Continued on following page)

TABLE 1 | (*Continued*) Description and AMSTAR2 scores of included studies.

Study	Condition	Studies included	Study duration (median, range)	Daily dose (median, range)	Outcome	AMSTAR2 score	Study quality
Liu et al. (2021)	ZL versus placebo	7	2w	1.4 mg (1.2–1.6 g/day)	1. mRS, 2. BI, and 3. NIHSS	7/11	middle
Xin et al. (2020)	salvianolic acids versus placebo	12	2w (1w–4w)	200 mg (100–300 mg/day)	1. Effect, 2. NIHSS, 3. mRS, and 4. BI	4/11	low
Katsanos et al. (2020)	Colchicine versus placebo	4	74w (4w–144w)	0.5 mg/day	1. AE	3/11	low
Liu et al. (2019)	ANP versus placebo	18	2w	3 g/day	1. Effect, 2. NIHSS, and 3. NFDs	9/11	high
Xu et al. (2015)	NBP versus placebo	12	6w (1w–12w)	100 mg/day	1. BI, 2. NIHSS, and 3. AE	9/11	high
Wang et al. (2021)	Pntsp versus placebo	20	6w (2w–10w)	470 mg (140–800 mg/day)	1. NIHSS, 2. mRS, 3. BI, and 4. AE	10/11	high
Huang et al. (2020)	HUK versus placebo	16	3 h (0–6 h)	0.15 PNA	1. NIHSS, 2. NFDs, and 3. AE	7/11	middle
Yang et al. (2015)	Mailuoning versus Placebo	21	12w	204 mg (8–400 mg/day)	1. Effect, 2. NFDs, 3. BI, 4. NIHSS, and 5. AE	9/11	high
Ni et al. (2020)	Cinepazide maleate versus placebo	4	7w (2w-12w)	320 mg/day	1. mRS, 2. BI, and 3. AE	7/11	middle
Thelengana et al. (2019)	TNK versus placebo	4	3 h (0–6 h)	0.15 mg (0.1–0.2 mg/kg/day)	1. Effect, 2. NFDs, 3. BI, 4. NIHSS, and 5. AE	9/12	high
Shi et al. (2014)	Cilostazol versus placebo	6	30w (1w-60w)	690 mg (80–1300 mg/day)	1. sICH and 2. AE	10/11	high
Siddiqui et al. (2013)	MLC601 versus placebo	2	13w (2w-24w)	405 mg (10–800 mg/day)	1. NFDs and 2. BI	5/11	low

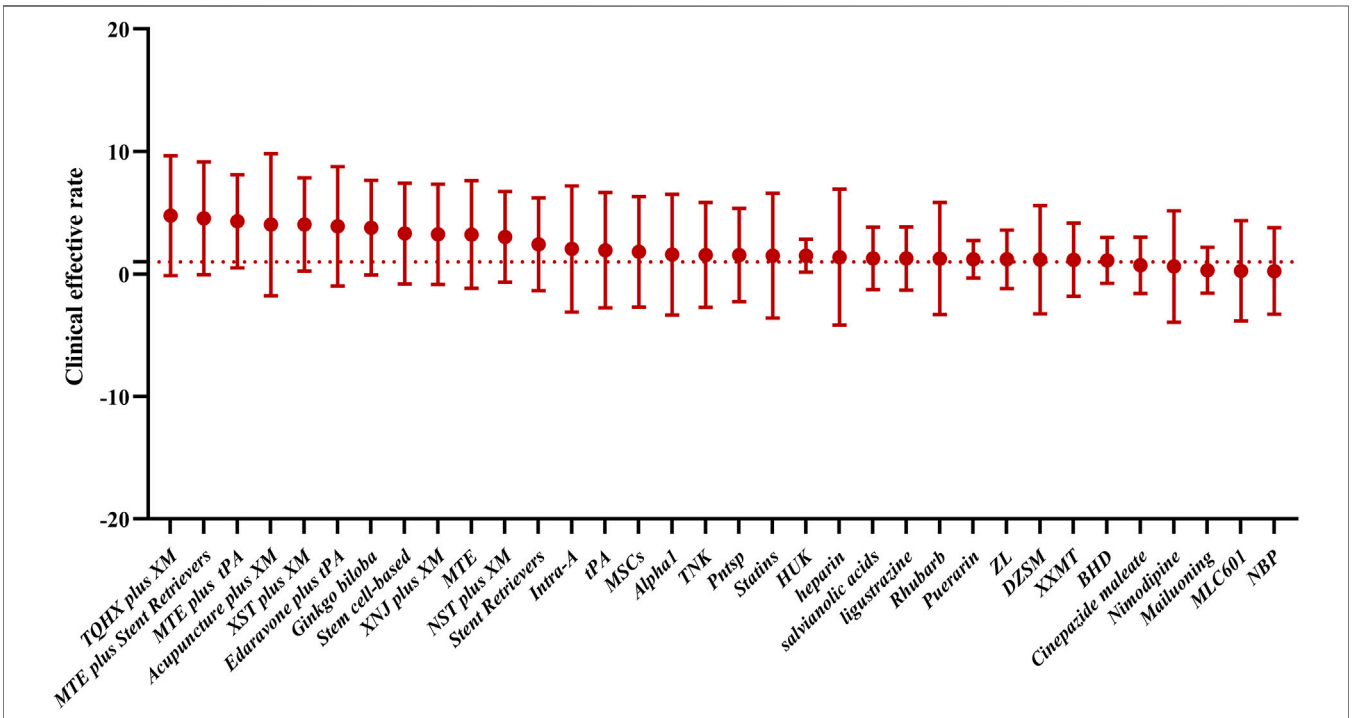

FIGURE 2 | Total clinical efficacy was used to evaluate the effect of drug therapy on ischemic stroke. In this study, the possible order of efficacy of the drugs was TQHX plus XM, MTE plus stent retrievers, MTE plus tPA, acupuncture plus XM, XST plus XM, edaravone plus tPA, Ginkgo biloba, stem cell-based therapy, XNJ plus XM, MTE, NST plus XM, stent retrievers, intra-A, tPA, MSCs, Alpha1, TNK, Pntsp, statins, HUK, heparin, salvianolic acids, ligustrazine, rhubarb, puerarin, ZL, DZSM, XXMT, BHD, cinepazide maleate, nimodipine, Mailuoning, MLC601, and NBP.

TABLE 2 | Results of pairwise meta-analyses for the clinical effect.

Comparative medication	Reference medication	Number of studies	Pairwise meta-analyses					
			Number of control	Number of patients	MD/OR/RR	95% CI	I^2	*P*
Ligustrazine	Placebo	3	321	322	1.28	[1.10, 1.50]	NA	0.05
Acupuncture	Placebo	14	643	536	4.04	[2.93, 5.57]	0	0.00001
tPA	Placebo	4	814	804	1.95	[1.10, 2.56]	NA	0.002
Nimodipine	Placebo	8	677	806	0.62	[0.50, 0.78]	NA	0.0001
Aspirin plus clopidogrel	Placebo	12	100	100	1.82	[1.08, 2.57]	NA	0.001
XNJ	Placebo	13	431	408	3.25	[2.30, 4.59]	0	0.00001
NST	Placebo	13	246	243	3.04	[1.76, 5.26]	0	0.00001
Stem cell-based therapy	Placebo	20	950	844	3.31	[2.54, 4.31]	0	0.0001
Edaravone plus rt-PA	Placebo	15	591	591	3.90	[3.02, 5.02]	0	0.0001
XXMT	Placebo	8	242	289	1.17	[1.09, 1.26]	0	0.0001
Rhubarb	Placebo	12	350	438	1.27	[1.18, 1.37]	18	0.00001
WD	Placebo	13	3,773	3,341	1.60	[1.43, 1.79]	46	0.0001
Puerarin	Placebo	16	1,427	1,540	1.22	[1.17, 1.28]	47	0.00001
Alpha1	Placebo	6	217	222	1.59	[1.08, 2.35]	0	0.019
BHD	Placebo	11	350	334	1.12	[0.99, 1.27]	69	0.002
XST plus XM	Placebo	12	879	890	4.04	[2.86, 5.73]	NA	0.001
Ginkgo biloba	Placebo	9	417	416	3.79	[2.49, 5.78]	NA	0.0001
TQHX plus XM	Placebo	12	733	755	5.43	[3.77, 7.82]	NA	0.0001
ZL	Placebo	7	293	278	1.2	[1.12, 2.29]	0	0.0001
HUK	Placebo	9	338	338	1.30	[1.21, 1.41]	0	0.00001
Statins	Placebo	18	3,013	2,988	1.5	[1.29, 1.75]	0	0.01
Salvianolic acids	Placebo	12	1884	1893	1.29	[1.25, 1.33]	14	0.00001
Pntsp	Placebo	20	48	48	1.55	[1.37, 2.55]	0	0.0001
DZSM	Placebo	5	341	340	1.18	[1.12, 1.24]	85.7	0.0001

CI, confidence interval; MD, mean difference; OR, risk ratio; I^2, heterogeneity, NST, NaoShuanTong capsule; XNJ, Xingnaojing capsule; XXMT, Xiaoxuming decoction; Pntsp, Panax notoginseng *Saponin; XST, plus XM: Xuesaitong injection plus Western medicines; TQHX, Tongqiao Huoxue decoction; ZL, Zhilong Huoxue Tongyu capsule; BHD, Buyang Huanwu decoction; Alpaga1: Desmoteplase; WD, Wen Dan Decoction. Western medicines (XM) (tPA, antiplatelet agents, statins, and edaravone).*

low quality according to AMSTAR2 score. The total clinical efficacy was used to evaluate the effect of drug therapy on ischemic stroke (**Figure 2**).

Clinical Effect

Clinical effective rate was observed in 18 studies. Detailed characteristics of included studies are listed in **Table 2**. The clinical effect of ligustrazine (OR: 1.28, 95% CI: 1.10–1.50), nimodipine (OR: 0.62, 95% CI: 0.50–0.78), aspirin plus clopidogrel (OR: 1.82, 95% CI: 1.08–2.57), tissue plasminogen (tPA) (RR: 1.95, 95% CI: 1.10–2.56), Wen Dan Decoction (WD) (OR: 1.60, 95% CI: 1.43–1.79), Xingnaojing capsule and Western medicines (XNJ) (OR: 3.25, 95% CI: 2.30–4.59), NaoShuanTong capsule plus Western medicines (NST plus XM) (OR: 3.04, 95% CI: 1.76–5.26), Xiaoxuming decoction (XXMT) (OR: 1.17, 95% CI: 1.09–1.26), Rhubarb (OR: 1.27, 95% CI: 1.18–1.37), stem cell-based (OR: 3.31, 95% CI: 2.54–4.31), puerarin (RR: 1.22, 95% CI: 1.17–1.28), Buyang Huanwu decoction (BHD) (OR: 1.12, 95% CI: 0.99–1.27), statins (OR: 1.5, 95% CI: 1.29–1.75), salvianolic acids (OR: 1.29, 95% CI: 1.25–1.33), *Panax notoginseng* saponin (Pntsp) (RR: 1.55, 95% CI: 1.37–2.55), Xuesaitong injection plus western medicines (XST plus XM) (OR: 4.04, 95% CI: 2.86–5.73), Tongqiao Huoxue Decoction plus Western medicines (TQHX plus XM) (OR: 5.43, 95% CI: 3.77–7.82), Ginkgo biloba (RR: 3.79, 95% CI: 2.49–5.78), edaravone plus rt-PA (OR: 3.90, 95% CI: 3.02–5.02) Zhilong Huoxue Tongyu capsule (ZL) (RR: 1.2, 95% CI: 1.12–2.29), desmoteplase (alpha1) (OR: 1.59, 95% CI: 1.08–2.35), acupuncture plus XM (OR: 4.04, 95% CI: 2.93–5.57), and DZSM (Dengzhan Shengmai capsule) (OR: 1.18, 95% CI: 1.12 to 1.24) was significantly better compared with placebo. Moreover, ANP, ZL, and edaravone combined with western medicines significantly improve the total clinical effective rate compared to placebo.

NIHSS Score

The effects of the medications on clinical change were assessed by National Institutes of Health Stroke Scale (**Table 3**). Eight studies (20.0%) showed that XXMT (MD: −1.86, 95% CI: −3.25–−0.48), safflower yellow (MD: −3.42, 95% CI: −5.38–−2.98), MSCs (MD: −1.85, 95% CI: −2.77–−0.93), ZL (MD: −2.6, 95% CI: −3.41–−1.79), salvianolic acids (MD: −1.44, 95% CI: −1.97–−0.91), heparin (OR: 1.95, 95% CI: 0.74–5.11), XST (MD: −3.17, 95% CI: −4.14 to −2.20), intra-arterial fibrinolysis (Intra-A) (OR: 2.24, 95% CI: 1.27–3.95), edaravone plus rt-PA (MD: 3.95, 95% CI: 2.92–4.99), and human urinary kallidinogenase (HUK) (MD: −1.65, 95% CI, −2.12–−1.71) were significantly different compared with placebo. In contrast, DL-3-n-butylphthalide (NBP) (OR: 0.73, 95% CI: −0.14 to 1.59, $p = 0.1$), BHD (MD: 1.66, 95% CI: −1.08 to 4.40, $p = 0.1$), and DZSM (MD: 0.57, 95% CI: 0.44.0.73, $p = 0.11$) showed no change or a deterioration.

Rankin Scale (mRS) Score

From our search, the effects of the medications on clinical change were assessed by Rankin Score (mRS) (**Table 4**). In total, 18 studies (42.5%) including tPA (OR: 1.31, 95% CI: 1.07–3.59), tPA plus mechanical thrombectomy (MTE) (OR: 4.32, 95% CI: 2.16–7.46),

TABLE 3 | Results of pairwise meta-analyses for the NIHSS score.

Comparative medication	Reference medication	Number of studies	Pairwise meta-analyses					
			Number of control	Number of patients	MD/OR/RR	95% CI	I^2	*P*
Heparin	Placebo	9	260	317	1.95	[0.74, 5.11]	80	0.03
XXMT	Placebo	8	91	95	−1.86	[−3.25, −0.48]	10	0.008
Safflower yellow	Placebo	7	368	394	−3.42	[−5.38, −2.98]	82	0.004
MSCs	Placebo	5	52	57	−1.85	[−2.77, −0.93]	24	0.0001
BHD	Placebo	11	96	96	1.66	[−1.08, 4.40]	64	0.1
XST	Placebo	12	879	890	−3.17	[−4.14, −2.20]	NA	0.001
Intra-A	Placebo	5	130	204	2.24	[1.27, 3.95]	0	0.005
Edaravone plus rt-PA	Placebo	17	860	859	3.95	[2.92, 4.99]	92	0.0001
ZL	Placebo	7	115	330	−2.6	[−3.41, −1.79]	50	0.0001
Salvianolic acids	Placebo	12	435	462	−1.44	[−1.97, −0.91]	57	0.001
NBP	Placebo	12	108	108	0.73	[−0.14, 1.59]	89	0.1
HUK	Placebo	16	667	659	−1.65	[−2.12, −1.71]	84	0.00001
DZSM	Placebo	5	341	340	0.57	[0.44, 0.73]	44.2	0.11

CI, confidence interval; MD, mean difference; OR, risk ratio; I^2, heterogeneity; rt-PA, alteplase; MSCs, autologous bone marrow stromal cells; XXMT, Xiaoxuming decoction; XST, Xuesaitong injection; NBP, DL-3-n-butylphthalide; BHD, Buyang Huanwu decoction; Intra-A, intra-arterial Fibrinolysis; HUK, human urinary kallidinogenase.

TABLE 4 | Results of pairwise meta-analyses for the mRS score.

Comparative medication	Reference medication	Number of studies	Pairwise meta-analyses					
			Number of control	Number of patients	MD/OR/RR	95% CI	I^2	*P*
Heparin	Placebo	12	2,145	550	1.38	[0.61, 3.56]	83	0.01
Safflower yellow	Placebo	13	368	394	−4.18	[−5.38,−2.98]	52	0.1
Rhubarb	Placebo	13	350	438	3.11	[2.06, 4.68]	18	< 0.05
MSCs	Placebo	7	86	86	1.81	[0.37, 8.95]	57	0.47
tPA	Placebo	4	814	804	1.31	[1.07, 3.59]	NA	0.01
MTE	Placebo	5	414	404	3.23	[1.75, 7.33]	NA	0.008
MTE plus stent retrievers	Placebo	5	142	143	4.56	[2.63, 7.9]	0	0.0001
tPA plus MTE	Placebo	17	2639	2640	4.32	[2.16, 7.46]	51	0.01
Stent retrievers	Placebo	5	653	634	2.43	[1.91, 3.09]	0	0.00001
Cerebrolysin	Placebo	5	971	808	−0.49	[−1.21, 0.24]	73.6	0.052
Intra-A	Placebo	12	171	224	2.05	[1.33, 3.14]	0	0.001
ZL	Placebo	9	45	60	−0.57	[−0.84, −0.30]	37	0.0001
Salvianolic acids	Placebo	7	210	242	−0.88	[−1.11, −0.64]	0	0.001
DZSM	Placebo	28	341	340	−0.75	[−1.02, −0.48]	85.9	0.0001
Cinepazide maleate	Placebo	4	236	234	0.607	[0.46, 0.801]	NA	0.0004

CI, confidence interval; MD, mean difference; OR, risk ratio; I^2, heterogeneity; MSCs, autologous bone marrow stromal cells; NST, NaoShuanTong capsule; tPA: tissue plasminogen XNJ, Xingnaojing capsule; MTE: mechanical thrombectomy, ZL, Zhilong Huoxue Tongyu capsule; Intra-A, intra-arterial fibrinolysis.

MTE (OR: 3.23, 95% CI: 1.75–7.33), stent retrievers (OR: 2.43, 95% CI: 1.91–3.09), cerebrolysin (RR: −049, 95% CI: −1.21 to 0.24), ZL (MD: −0.57, 95% CI: −0.84 to −0.30), salvianolic acids (MD: −0.88, 95% CI: −1.11–−0.64), heparin (OR: 1.38, 95% CI: 0.61–3.56) and Rhubarb (OR: 3.11, 95% CI: 2.06–4.68), Intra-A (RR: 2.05, 95% CI: 1.33–3.14), DZSM (MD: −0.75, 95% CI: −1.02–−0.48), and cinepazide maleate (MD: 0.607, 95% CI: 0.46–0.801) showed better outcomes for mRS score than placebo. The other treatments "Safflower yellow (MD: −4.18, 95% CI: −5.38–−2.98, $p = 0.1$) and MSCs (RR: 1.81, 95% CI: 0.37–8.95, $p = 0.47$)" indicated no significant difference in effectiveness as compared to placebo.

Barthel Index Score

The effects of the medications on clinical change were assessed by Barthel Index (BI) Score (**Table 5**). Ten studies (25%) showed that autologous bone marrow stromal cells (MSCs) (MD: 2.50, 95% CI: −4.69–9.68), TQHX plus XM (MD: 2.45, 95% CI: 1.16–3.73), ZL (MD: 9.75, 95% CI: 7.15–12.36), NST (MD: 8.15, 95% CI: 3.79–12.52), Intra-A (MD: 1.6, 95% CI: 1.01–2.51), DZSM (MD: 8.97, 95% CI: 5.88,12.05) and cinepazide maleate (MD: 0.719, 95% CI: 0.542, 0.956), and MLC601 (MD: 2.35, 95% CI: 1.31, 4.23) were significantly different compared with placebo. In contrast, NBP (MD: 1.65, 95% CI: 1.25–2.04), $p = 0.08$) showed no difference compared to placebo.

Neurological Function Deficit Score

Table 6 presents the results of the comparisons of behavioral symptoms; a total of seven studies were assessed by NFD scores. Patients treated with XNJ (MD: −3.78, 95% CI:

TABLE 5 | Results of pairwise meta-analyses for the BI score.

Comparative medication	Reference medication	Number of studies	Pairwise meta-analyses					
			Number of control	Number of patients	MD/OR/RR	95% CI	I^2	*P*
NST	Placebo	13	304	289	8.15	[3.79, 12.52]	75	0.0005
MSCs	Placebo	5	88	88	2.50	[−4.69,9.68]	74	< 0.05
Intra-A	Placebo	5	139	204	1.6	[1.01, 2.51]	0	0.04
TQHX plus XM	Placebo	12	225	226	2.45	[1.16, 3.73]	89	0.0001
ZL	Placebo	7	115	130	9.75	[7.15, 12.36]	0	0.001
NBP	Placebo	12	165	160	1.65	[1.25, 2.04]	67	0.08
DZSM	Placebo	5	341	340	8.97	[5.88, 12.05]	85.9	0.0001
Cinepazide maleate	Placebo	4	236	236	0.719	[0.542, 0.956]	0	0.012
MLC601	Placebo	2	237	436	2.35	[1.31, 4.23]	0	0.004

CI, confidence interval; MD, mean difference; OR, risk ratio; I^2, heterogeneity; MSCs, autologous bone marrow stromal cells; NST, NaoShuanTong capsule; TQHX, Tongqiao Huoxue Decoction; ZL, Zhilong Huoxue Tongyu capsule; NBP, DL-3-n-butylphthalide; BHD, Buyang Huanwu decoction; Intra-A, intra-arterial fibrinolysis.

TABLE 6 | Results of pairwise meta-analyses for NFDs.

Comparative medication	Reference medication	Number of studies	Pairwise meta-analyses					
			Number of control	Number of patients	MD/OR/RR	95% CI	I^2	*P*
XNJ	Placebo	13	356	347	−3.78	[−4.75, −2.81]	54	0.00001
NST	Placebo	13	100	100	8.15	[10.11, 49.10]	95	0.0005
Chuanxiong	Placebo	3	80	81	−3.11	[−5.22, −1.00]	0	0.0039
Safflower yellow	Placebo	7	368	394	3.11	[2.06, 4.68]	0	0.00001
Rhubarb	Placebo	12	210	210	−3.36	[−6.10, −0.62]	89	0.00001
Puerarin	Placebo	16	659	699	−3.69	[−4.67, −2.71]	70	0.00001
Albumin	Placebo	4	804	807	1.04	[0.85, 1.27]	0	0.65
Salvianolic acids	Placebo	12	235	235	−8.65	[−11.10, −6.20]	31	0.001
Pntsp	Placebo	20	1464	1435	−3.36	[−4.20, −2.53]	74	0.0001
Nimodipine	Placebo	8	677	806	0.54	[0.50, 0.78]	NA	0.0001
HUK	Placebo	9	338	338	1.30	[1.21, 1.41]	0	0.00001
DZSM	Placebo	5	341	340	−2.81	[−4.17, −1.44]	85.9	0.1
Mailuoning	Placebo	15	736	755	0.31	[0.23, 0.42]	0	0.001
TNK	Placebo	4	656	671	1.56	[1.0, 2.43]	0	0.05
MLC601	Placebo	2	275	520	0.27	[−0.02, 0.55]	66	0.06

CI, confidence interval; MD, mean difference; OR, risk ratio; I^2, heterogeneity, NST, NaoShuanTong capsule; XNJ, Xingnaojing capsule; Pntsp, Panax notoginseng *Saponin; TQHX, Tongqiao Huoxue decoction; TNK, tenecteplase.*

−4.75 to −2.81), NST (MD: 8.15, 95% CI: 10.11–49.10), Chuanxiong (MD: −3.11, 95% CI: −5.22–−1.00), Safflower yellow (MD: 3.11, 95% CI: 2.06–4.68), Rhubarb (MD: −3.36, 95% CI: −6.10–−0.62), Puerarin (MD: −3.69, 95% CI: −4.67–−2.71), Pntsp (MD: −3.36, 95% CI: −4.20–−2.53), HUK (MD, 1.30, 95% CI, 1.21 to 1.41), and Mailuoning (OR: 0.31, 95% CI: 0.23–0.42) showed better behavioral symptoms than those administered ($p < 0.05$). Moreover, Ginkgo biloba use was also associated with an improvement in activities of daily living and functional outcomes (MD: 9.52; 4.66 to 14.33, $p < 0.001$). Subgroup analysis suggests that the impact was larger when using an injectable formulation of Ginkgo biloba compared to the oral formulation. The other treatments indicated no significant difference in effectiveness as compared to placebo ($p > 0.05$) (Albumin (MD: 1.04, 95% CI: 0.85–1.27). TNK (MD: 1.56, 95% CI: 1.0–2.43), DZSM (MD: −2.81, 95% CI: 4.17–−1.44), and MLC601 (MD: 0.27, 95% CI: −0.02–0.55).

Extracranial Hemorrhage (sICH)

The sICH events resulting from administration of other treatments were mild, and Safflower yellow ($p = 0.93$), stent retrievers (OR: 1.08, 95% CI: 0.64–2.30), Alpha1 (OR: 1.25, 95% CI: 0.97–1.62), Ginkgo biloba (OR: 0.82, 95% CI: 0.43–1.57), tirofiban (OR: 1.14, 95% CI: 0.72–1.82), heparin (OR: 0.71, 95% CI: 0.25–2.05), edaravone plus rt-PA (OR: 0.44, 95% CI: 0.29–0.66), MTE plus stent retrievers (OR: 0.59, 95% CI: 0.35–0.97), MTE (OR: 3.05, 95% CI: 0.44–21.23), MTE plus tPA (OR: 0.93, 95% CI: 0.72–1.19), TNK (OR: 1.07, 95% CI: 0.6–1.93), and cilostazol (OR: 0.29, 95% CI: 0.15–0.56) had no significant difference on sICH events between these groups and placebo groups (**Table 7**).

TABLE 7 | Results of pairwise meta-analyses for extracranial hemorrhage.

Comparative medication	Reference medication	Number of studies	Pairwise meta-analyses					
			Number of control	Number of patients	MD/OR/RR	95% CI	I^2	*P*
Heparin	Placebo	9	288	330	0.71	[0.25, 2.05]	32	0.22
Safflower yellow	Placebo	7	368	394	NA	NA	0	0.93
Stent retrievers	Placebo	5	652	634	1.08	[0.64, 2.30]	0	0.63
Ginkgo biloba	Placebo	12	266	281	0.82	[0.43, 1.57]	0	0.443
Tirofiban	Placebo	6	216	213	1.14	[0.72, 1.82]	0	0.57
Edaravone plus rt-PA	Placebo	8	221	221	0.44	[0.29, 0.66]	0	0.93
Alpha 1	Placebo	6	467	595	1.25	[0.97, 1.62]	9	0.09
TNK	Placebo	4	658	676	1.07	[0.6, 1.93]	0	0.81
MTE plus stent retrievers	Placebo	5	146	144	0.59	[0.35,0.97]	0	0.83
MTE	Placebo	5	141	140	3.05	[0.44, 21.23]	0	0.25
tPA plus MTE	Placebo	7	2639	2640	0.93	[0.72, 1.19]	29	0.13
Cilostazol	Placebo	6	1728	1731	0.29	[0.15, 0.56]	0	0.77

CI, confidence interval; MD, mean difference; OR, risk ratio; I^2, heterogeneity, TNK, tenecteplase.

TABLE 8 | Results of pairwise meta-analyses for mortality.

Comparative medication	Reference medication	Number of studies	Pairwise meta-analyses					
			Number of control	Number of patients	MD/OR/RR	95% CI	I^2	*P*
Ligustrazine	Placebo	3	321	322	1.67	[1.02, 2.67]	95	< 0.05
Heparin	Placebo	9	2703	1145	0.9	[0.74, 1.09]	1	0.42
tPA	Placebo	4	814	804	1.04	[0.75, 1.43]	NA	0.83
Stent retrievers	Placebo	5	653	634	0.81	[0.58, 1.12]	29	0.19
Alpha 1	Placebo	6	467	595	1.05	[0.7, 1.59]	0	0.8
Cerebrolysin	Placebo	7	971	808	0.82	[0.55, 1.22]	0	0.81
Ginkgo biloba	Placebo	12	213	228	1.21	[0.29, 5.09]	43	1.8
Stem cell-based therapy	Placebo	9	218	217	0.6	[0.35, 1.03]	4	0.4
Tirofiban	Placebo	6	218	223	0.53	[0.13, 2.07]	63	0.1
Albumin	Placebo	4	1928	1938	1.1	[0.9, 1.34]	0	0.51
Intra-A	Placebo	5	171	224	0.83	[0.48, 1.39]	0	0.46
Edaravone plus rt-PA	Placebo	4	474	472	0.43	[0.13, 1.42]	0	0.87
Statins	Placebo	18	3034	3021	0.85	[0.77, 0.93]	0	0.003
DZSM	Placebo	5	341	340	0.54	[0.31, 0.95]	85.9	0.23
TNK	Placebo	4	658	676	1.03	[0.69, 1.52]	0	0.9
Cilostazol	Placebo	6	1728	1731	0.80	[0.42, 1.53]	0	0.52

CI, confidence interval; MD, mean difference; OR, risk ratio; I^2, heterogeneity; Intra-A, intra-arterial fibrinolysis; rt-PA, alteplase; TNK, tenecteplase.

Mortality

Fifteen studies reported all-cause mortality at the end of follow-up. Ligustrazine (OR: 1.67, 95% CI: 1.02–2.67), statins (OR: 0.85, 95% CI: 0.77–0.93) were significant different compared with placebo. In contrast, stent retrievers (OR: 0.81, 95% CI: 0.58–1.12), cerebrolysin (OR: 0.82, 95% CI: 0.55–1.22), Ginkgo biloba (OR: 1.21, 95% CI: 0.29–5.09), stem cell-based (MD: 0.6, 95% CI: 0.35–1.03), tirofiban (OR: 0.53, 95% CI: 0.13–2.07), albumin (OR: 1.1, 95% CI: 0.9–1.34), Alpha1 (OR: 1.05, 95% CI: 0.7–1.59), heparin (OR: 0.9, 95% CI: 0.74–1.09), Intra-A (OR: 0.83, 95% CI: 0.48–1.39), edaravone plus rt-PA (MD: 0.43, 95% CI: 0.13–1.42), tPA (OR: 1.04, 95% CI: 0.75–1.43), DZSM (MD: 0.54, 95% CI: 0.31–0.95), TNK (MD: 1.03, 95% CI: 0.69–1.52), and cilostazol (MD: 0.80, 95% CI: 0.42 to 1.53, $p = 0.52$) had no significant differences of mortality events between these groups and placebo groups ($p > 0.05$) (**Table 8**).

Adverse Events

Adverse events of the meta-analysis of participants with at least one adverse event indicated a beneficial effect in favor of placebo treatment compared with salvianolic acids (OR: 1.45, 95% CI: 1.11–1.91, $p = 0.007$), Pntsp (*RR*: 0.62, 95% CI: 0.39–0.97, $p = 0.04$), colchicine (OR: 0.31, 95% CI: 0.13–0.71, $p = 0.006$), and NBP (RR: 3.55, 95% CI, 1.19 –10.56; $p < 0:05$). The adverse events resulting from administration of other treatments were mild, and Chuanxiong (OR: 1.02, 95% CI: 0.35–2.96), MSCs (RR: 0.43, 95% CI: 0.18–1.05), Cerebrolysin (OR: 1.18, 95% CI: 0.86–1.64), Ginkgo biloba (OR: 1.48, 95% CI: 0.51–2.71), Stem cell-based (MD: 2.59, 95% CI: 0.11–5.93), TQHX (OR: 1.78, 95% CI: 0.51–6.2), HUK (RR: 0.01, 95% CI: 0.02–0.04), Mailuoning (OR: 1.39, 95% CI: 0.28–6.76), and cinepazide maleate had no significant differences in adverse events between these groups and placebo groups ($p > 0.05$) (**Table 9**). Among all of the trials, in the

TABLE 9 | Results of pairwise meta-analyses for AE.

Comparative medication	Reference medication	Number of studies	Pairwise meta-analyses					
			Number of control	Number of patients	MD/OR/RR	95% CI	I^2	*P*
Chuanxiong	Placebo	3	50	49	1.02	[0.35, 2.96]	NA	0.09
MSCs	Placebo	5	64	44	0.43	[0.18, 1.05]	0	0.06
Cerebrolysin	Placebo	7	971	808	1.18	[0.86, 1.64]	23	0.27
Ginkgo biloba	Placebo	12	388	406	1.48	[0.51, 2.71]	54	0.07
Stem cell-based therapy	Placebo	9	136	139	2.59	[0.11, 5.93]	0	0.87
TQHX plus XM	Placebo	12	180	180	1.78	[0.51, 6.2]	0	0.36
Salvianolic acids	Placebo	12	1496	1498	1.45	[1.11, 1.91]	0	0.007
Colchicine	Placebo	4	2764	2788	0.31	[0.13, 0.71]	0	0.006
NBP	Placebo	4	108	108	3.55	[1.19, 10.56]	0	< 0.05
Pntsp	Placebo	20	361	354	0.62	[0.39, 0.97]	0	0.04
HUK	Placebo	9	387	387	0.01	[0.02, 0.04]	0	0.50
Mailuoning	Placebo	2	64	65	1.39	[0.28, 6.76]	0	0.57
cinepazide maleate	Placebo	NA	648	643	NA	NA	NA	0.82

CI, confidence interval; MD, mean difference; OR, risk ratio; I^2, heterogeneity; MSCs, Pntsp, Panax notoginseng *Saponin; autologous bone marrow stromal cells; TQHX, Tongqiao Huoxue Decoction.*

HUK groups, six cases of hypotension, four cases of fever, two cases of flushing, two cases of vomiting, one case of headache, one case of arrhythmia, and one case of pruritus were reported. In addition, no deaths and four serious adverse events were reported in the MLC601 group.

DISCUSSION

Our umbrella review was conducted on the data derived from treatments for ischemic stroke patients, which was used to appraise the relative effectiveness and safety of therapies. We attempted to summarize data from published systematic reviews and meta-analyses to find if there are significant beneficial treatments for ischemic stroke patients. Our study showed that thrombolytic therapy (rt-PA, TNK, and alpha1), MTE, stem cell-based therapies, stent retrievers, acupuncture plus XM, MSCs, antiplatelet agents (aspirin, clopidogrel, and tirofiban), statins, and blood-activating and stasis-dispelling herbs can improve the neurological deficits and activities of daily living in patients with ischemic stroke. MTE plus Stent Retrievers or tPA, TQHX plus XM, XST plus XM, and NST plus XM show better clinical efficacy and safety. Ligustrazine, safflower yellow, statins, Pntsp, albumin, HUK, colchicine, MLC601, salvianolic acids, and NBP have no important impact on neurological deficits or activities of daily living. In addition, tPA, MTE, stem cell-based therapies, Stent Retrievers, Acupuncture, NST, Ginkgo biloba, TQHX, XST, and XNJ show no serious adverse events in ischemic stroke patients. Our results need to be interpreted with caution to determine the optimal treatment strategy for ischemic stroke patients.

The effects of tPA may be considerable for ischemic stroke which is incurable with current treatment paradigms, and other medications that may slow down the progression of ischemic stroke patients are worth exploring. Previous studies have showed that tPA or MTE has beneficial effects on hyperacute period ischemic stroke (Thelengana et al., 2019) (Liu et al., 2016), while one study demonstrated that tPA plus MTE performed best (Kaesmacher et al., 2019). Our results indicated that all tPA, MTE, MTE plus tPA, MTE plus Stent Retrievers, TQHX plus XM, XST plus XM, and NST plus XM were more effective for neurological function or activities of daily living compared with placebo. Researches have demonstrated that there was a higher effect of Stent Retrievers and MTE observed for acute ischemic stroke than that observed for the mild ischemic stroke patients (Punal-Rioboo et al., 2015). Similar to these studies, Stent Retrievers and MTE treatment showed statistically significant improvement in clinical effect compared to placebo in our study. Research studies have demonstrated that Human serum albumin has shown remarkable efficacy in rodent models of ischemic stroke (Huang and Xiao, 2021). Unfortunately, our study has demonstrated that showing no statistically significant difference between the albumin and control groups ($p > 0.05$). Considering pulmonary edema and other complications are more likely to occur in such patients after albumin infusion, the administration of albumin therapy for acute ischemic stroke should be carried out with utmost caution.

The behavioral symptoms of patients with ischemic stroke are often evaluated by NFDS/NIHSS/BI/mRS, which assesses the severity and frequency of neuropsychiatric symptoms. As a result, previous meta-analyses have reported that the efficacy of blood-activating and stasis-dispelling herbs may be related to the severity of ischemic stroke. In addition, tPA, MTE plus tPA, MTE plus Stent Retrievers, blood-activating and stasis-dispelling herbs plus XM was reported as only a modest but significant effect found on behavior in ischemic stroke patients (Peng et al., 2014; Punal-Rioboo et al., 2015; Kaesmacher et al., 2019; Shang et al., 2019; Zhang et al., 2019). In our study, Alpha1 was more effective for neurological improvement rate compared with placebo. Unfortunately, the lack of placebo controls in NFDS/NIHSS/BI/mRS score studies may limit their validity. Interestingly, MSCs are not significant in mRS score but significant in NIHSS/BI score. Moreover, nimodipine can significantly improve clinical outcomes compared with

placebo, although it does not significantly reduce the incidence rate of recurrent hemorrhage and adverse reactions. In addition, tPA and MTE affected mRS scores and was recommended by the FDA. We considered treatment with ligustrazine, Safflower yellow albumin, MLC601, ANP, rhubarb, and NBP to not affect neurological deficits and activities of daily living because of the lack of statistical significance of results. Patients with ischemic stroke deteriorate progressively with varying degrees of severity of disease, which may affect the results obtained from pooling data. Moreover, measurement time after dosing can affect NFDS/NIHSS/BI/mRS scoring results and cause them to be biased.

Previous meta-analyses have demonstrated that patients treated with intra-arterial fibrinolysis provided a modest and better improvement in clinical effect change (Roaldsen et al., 2022). In addition, drug combination shows a statistically significant advantage compared to placebo the short-term and long-term analysis. Although the effect of single blood-activating and stasis-dispelling herbs (TQHX, NST, XST, etc.) use is not ideal (Erratum, 2017), they show a modest and better effect in combination with XM (Wu et al., 2007). Furthermore, ischemic stroke agents are likely to have an important effect on increasing neurological function or activities of daily living in mild to moderate ischemic stroke patients. In this study, the quality evaluated by AMSTAR2 scores of systematic reviews of ligustrazine, safflower yellow, cerebrolysin, BHD, salvianolic acids, and ZL was low, and these may not have an important impact on neurological function or activities of daily living. First, ischemic stroke is a sudden disease, our review mainly selected clinical studies to demonstrate short-term efficacy on neurological function. Although long-term clinical trials are ethically questionable, those that are high-quality are essential to uncover comparative differences between treatments of ischemic stroke. Second, we believe that further analyses are needed to clarify the factors associated with the increased placebo effect over time in global clinical trials. In the treatment of ischemic stroke, the safety of the treatments is critical since they should be taken on a long-term basis. The number of participants with at least one serious adverse event such as nausea, diarrhea, cardiovascular, gastrointestinal, and other disorders was extracted. Previous meta-analyses have demonstrated that acute and convalescent stroke patients treated with antiplatelet agents showed a modest improvement, although there is a risk of intracranial hemorrhage (Zhou et al., 2020). In this review, edoxaban was likely to provide more protection from stroke and sICH than placebo, aspirin alone, or aspirin plus clopidogrel in both clinical trials and unselected community populations. Moreover, statins were found to be effective for primary and secondary prevention of ischemic stroke in the study through the aggressive reduction of cholesterol. Some studies have found that using statins before an ischemic stroke can increase collateral circulation and improve prognosis. Despite an increased risk of bleeding conversion, thrombolytic use of statins resulted in overall improvement. Recent studies have also found statins to be associated with atrial fibrillation. In addition, the promotion of collateral circulation by neuroprotective drugs may be related to the induction of NO synthesis and angiogenesis in vascular endothelium (Hu et al., 2021). In addition, the incidence of withdrawals due to adverse events tended to be higher in the salvianolic acids albumin, MLC601, and NBP treatment than in placebo groups. Moreover, our study summarized that MTE, stem cell-based therapies, stent retrievers, acupuncture plus XM, NST, Ginkgo biloba, TQHX, XST, and XNJ show no serious adverse events in ischemic stroke patients.

In recent years, stem cell-based therapies (MSCs, stem cell-based) as a treatment to investigate ischemic stroke patients has been a potential therapy (Cao and Li, 2015; Li et al., 2020). A previous study has shown that Intra-A results in a better beneficial effect for cognition and activities of daily living (Lee et al., 2010). Similar to these studies, stem cell-based therapies may show effectiveness for neurological deficits and activities of daily living in this study. However, clinical trials of stem cell-based therapies for ischemic stroke are still in the early stage. Many factors such as cell types, cell numbers, delivery routes, time windows, and medical and rehabilitation therapies affect the efficacy of stem cells. Well-designed RCTs are necessary to explore the benefit of stem cell-based therapies as treatment in patients with ischemic stroke, and further research effects should be carefully explored.

In general, the treatment for patients with ischemic stroke is aimed at promoting independence, clear embolism, maintaining function, and treating symptoms. Previous meta-analyses and reviews have focused on the possible effectiveness and safety of stem cell-based therapies, stent retrievers, acupuncture, MSCs, antiplatelet agents, statins, and blood-activating and stasis-dispelling herbs (Li et al., 2014; Cao and Li, 2015; Punal-Rioboo et al., 2015; Shang et al., 2019; Zhang et al., 2019; Li et al., 2020; Zhao et al., 2021; Zhou et al., 2022), even though patients experience modest efficacy and many adverse events with the treatment. As a result, we need to identify an efficacious and safe treatment paradigm for ischemic stroke patients. Studies have shown that MTE plus tPA, MTE plus Stent Retrievers, TQHX plus XM, XST plus XM, NST plus XM, and acupuncture plus XM improved neurological deficits and activities of daily living, and the adverse effects were mild for the treatment of ischemic stroke (Li et al., 2014; Kaesmacher et al., 2019; Shang et al., 2019; Li et al., 2020; Shen et al., 2020). However, a larger sample size and long-term follow-up studies are needed to find the reliability of this medication. Due to tPA, MTE, tPA plus edaravone, blood-activating, and stasis-dispelling herbs plus XM efficacy in improving neurological deficits and activities of daily living, we believe that tPA or tPA plus other drugs can be employed as first-line treatment.

Limitations

The limitations to this study should be acknowledged. First, direct comparative evidence of treatments for ischemic stroke patients in our included studies was limited. Second, other factors may have led to the umbrella review inconsistencies, such as the duration and

quality of studies. Furthermore, a considerable number of studies could not be included as they did not have the abovementioned data.

CONCLUSION

In conclusion, our study suggested that tPA, tPA plus MTE, acupuncture plus XM, tPA plus edaravone, and blood-activating and stasis-dispelling herbs plus XM are the optimum cognitive and activities of daily living medication for patients with ischemic stroke. In the future, the combination of well-tolerated agents and other significant beneficial treatments should be used for patients with ischemic stroke, which will contribute to the successful construction of a similar study.

DATA AVAILABILITY STATEMENT

The original contributions presented in the study are included in the article/**Supplementary Material**; further inquiries can be directed to the corresponding author.

AUTHOR CONTRIBUTIONS

QL and YC conceived and designed the review. YOL, RC, FF, YL, YA, HL, SL, YD, QY, ZQ, and WS looked up the literature. YOL wrote the manuscript. QL and YC revised the manuscript. All authors read and approved the final manuscript.

FUNDING

This study was supported by the National Natural Science Foundation of China (82174085).

SUPPLEMENTARY MATERIAL

The Supplementary Material for this article can be found online at: https://www.frontiersin.org/articles/10.3389/fphar.2022.924747/full#supplementary-material

REFERENCES

Blann, A. D., Skjøth, F., Rasmussen, L. H., Larsen, T. B., and Lip, G. Y. (2015). Edoxaban versus placebo, aspirin, or aspirin plus clopidogrel for stroke prevention in atrial fibrillation. An indirect comparison analysis. *Thromb. Haemost.* 114 (2), 403–409. doi:10.1160/TH15-05-0383

Cao, W., and Li, P. (2015). Effectiveness and Safety of Autologous Bone Marrow Stromal Cells Transplantation After Ischemic Stroke: A Meta-Analysis. *Med. Sci. Monit.* 21, 2190–2195. doi:10.12659/MSM.895081

Chong, P. Z., Ng, H. Y., Tai, J. T., and Lee, S. W. H. (2020). Efficacy and Safety of Ginkgo biloba in Patients with Acute Ischemic Stroke: A Systematic Review and Meta-Analysis. *Am. J. Chin. Med.* 48 (3), 513–534. doi:10.1142/S0192415X20500263

De Santis, K. K., Lorenz, R. C., Lakeberg, M., and Matthias, K. (2021). The application of AMSTAR2 in 32 overviews of systematic reviews of interventions for mental and behavioural disorders: A cross-sectional study. *Res. Syn. Meth.* doi:10.1002/jrsm.1532

Donkor, E. S. (2018). Stroke in the21stCentury: A Snapshot of the Burden, Epidemiology, and Quality of Life. *Stroke Res. Treat.* 2018, 1–10. doi:10.1155/2018/3238165

Emberson, J., Lees, K. R., Lyden, P., Blackwell, L., Albers, G., Bluhmki, E., et al. (2014). Stroke Thrombolysis Trialists' Collaborative, GEffect of treatment delay, age, and stroke severity on the effects of intravenous thrombolysis with alteplase for acute ischaemic stroke: a meta-analysis of individual patient data from randomised trials. *Lancet* 384 (9958), 1929–1935. doi:10.1016/S0140-6736(14)60584-5

Erratum (2017). Erratum: Traditional chinese patent medicine for acute ischemic stroke: an overview of systematic reviews based on the GRADE approach: Erratum. *Med. Baltim.* 96 (32), e7810. doi:10.1097/MD.0000000000007810

Fan, S., Lin, N., Shan, G., Zuo, P., and Cui, L. (2014). Safflower yellow for acute ischemic stroke: A systematic review of randomized controlled trials. *Complement. Ther. Med.* 22 (2), 354–361. doi:10.1016/j.ctim.2014.01.001

Feng, L., Wu, X. J., Cao, T., and Wu, B. (2021). The efficacy and safety of Xuesaitong injection combined with western medicines in the treatment of ischemic stroke: an updated systematic review and meta-analysis. *Ann. Palliat. Med.* 10 (9), 9523–9534. doi:10.21037/apm-21-1828

Fu, D. L., Lu, L., Zhu, W., Li, J. H., Li, H. Q., Liu, A. J., et al. (2013). Xiaoxuming decoction for acute ischemic stroke: a systematic review and meta-analysis. *J. Ethnopharmacol.* 148 (1), 1–13. doi:10.1016/j.jep.2013.04.002

Gao, L., Xiao, Z., Jia, C., and Wang, W. (2021). Effect of Buyang Huanwu decoction for the rehabilitation of ischemic stroke patients: a meta-analysis of randomized controlled trials. *Health Qual. Life Outcomes* 19 (1), 79. doi:10.1186/s12955-021-01728-6

Go, A. S., Mozaffarian, D., Roger, V. L., Benjamin, E. J., Berry, J. D., and Blaha, M. J. (2014). Stroke Statistics, SExecutive summary: heart disease and stroke statistics--2014 update: a report from the American Heart Association. *Circulation* 129 (3), 399–410. doi:10.1161/01.cir.0000442015.53336.12

Hong, K. S., and Lee, J. S. (2015). Statins in Acute Ischemic Stroke: A Systematic Review. *J. Stroke* 17 (3), 282–301. doi:10.5853/jos.2015.17.3.282

Hu, R., Guo, Y., Lin, Y., Tang, Y., Tang, Q., Wang, X., et al. (2021). Safety and efficacy of edaravone combined with alteplase for patients with acute ischemic stroke: A systematic review and meta-analysis. *Pharmazie* 76 (2), 109–113. doi:10.1691/ph.2021.0949

Huang, Y., Wang, B., Zhang, Y., Wang, P., and Zhang, X. (2020). Efficacy and safety of human urinary kallidinogenase for acute ischemic stroke: a meta-analysis. *J. Int. Med. Res.* 48 (9), 300060520943452. doi:10.1177/0300060520943452

Huang, Y., and Xiao, Z. (2021). Albumin therapy for acute ischemic stroke: a meta-analysis. *Neurol. Sci.* 42 (7), 2713–2719. doi:10.1007/s10072-021-05244-9

Kaesmacher, J., Mordasini, P., Arnold, M., López-Cancio, E., Cerdá, N., Boeckh-Behrens, T., et al. (2019). Direct mechanical thrombectomy in tPA-ineligible and -eligible patients versus the bridging approach: a meta-analysis. *J. Neurointerv Surg.* 11 (1), 20–27. doi:10.1136/neurintsurg-2018-013834

Katsanos, A. H., Palaiodimou, L., Price, C., Giannopoulos, S., Lemmens, R., Kosmidou, M., et al. (2020). Colchicine for stroke prevention in patients with coronary artery disease: a systematic review and meta-analysis. *Eur. J. Neurol.* 27 (6), 1035–1038. doi:10.1111/ene.14198

Lee, M., Hong, K. S., and Saver, J. L. (2010). Efficacy of intra-arterial fibrinolysis for acute ischemic stroke: meta-analysis of randomized controlled trials. *Stroke* 41 (5), 932–937. doi:10.1161/STROKEAHA.109.574335

Li, L., Zhang, H., Meng, S. Q., and Qian, H. Z. (2014). An updated meta-analysis of the efficacy and safety of acupuncture treatment for cerebral infarction. *PLoS One* 9 (12), e114057. doi:10.1371/journal.pone.0114057

Li, X., Ling, L., Li, C., and Ma, Q. (2017). Efficacy and safety of desmoteplase in acute ischemic stroke patients: A systematic review and meta-analysis. *Med. Baltim.* 96 (18), e6667. doi:10.1097/MD.0000000000006667

Li, Z., Dong, X., Tian, M., Liu, C., Wang, K., Li, L., et al. (2020). Stem cell-based therapies for ischemic stroke: a systematic review and meta-analysis of clinical trials. *Stem Cell Res. Ther.* 11 (1), 252. doi:10.1186/s13287-020-01762-z

Lisboa, R. C., Jovanovic, B. D., and Alberts, M. J. (2002). Analysis of the safety and efficacy of intra-arterial thrombolytic therapy in ischemic stroke. *Stroke* 33 (12), 2866–2871. doi:10.1161/01.str.0000038987.62325.14

Liu, G. J., Luo, J., Zhang, L. P., Wang, Z. J., Xu, L. L., He, G. H., et al. (2011). Meta-analysis of the effectiveness and safety of prophylactic use of nimodipine in patients with an aneurysmal subarachnoid haemorrhage. *CNS Neurol. Disord. Drug Targets* 10 (7), 834–844. doi:10.2174/187152711798072383

Liu, H., Yan, Y., Pang, P., Mao, J., Hu, X., Li, D., et al. (2019). Angong Niuhuang Pill as adjuvant therapy for treating acute cerebral infarction and intracerebral hemorrhage: A meta-analysis of randomized controlled trials. *J. Ethnopharmacol.* 237, 307–313. doi:10.1016/j.jep.2019.03.043

Liu, M., Pu, Y., Gu, J., He, Q., Liu, Y., Zeng, Y., et al. (2021). Evaluation of Zhilong Huoxue Tongyu capsule in the treatment of acute cerebral infarction: A systematic review and meta-analysis of randomized controlled trials. *Phytomedicine* 86, 153566. doi:10.1016/j.phymed.2021.153566

Liu, X., Li, Y., Bai, N., Yu, C., Xiao, Y., Li, C., et al. (2022). Updated evidence of Dengzhan Shengmai capsule against ischemic stroke: A systematic review and meta-analysis. *J. Ethnopharmacol.* 283, 114675. doi:10.1016/j.jep.2021.114675

Liu, Y., Zhang, L., and Hong, P. (2016). Efficacy and Safety of Mechanical Thrombectomy in Treating Acute Ischemic Stroke: A Meta Analysis. *J. Invest Surg.* 29 (2), 106–111. doi:10.3109/08941939.2015.1067738

Lu, L., Li, H. Q., Fu, D. L., Zheng, G. Q., and Fan, J. P. (2014). Rhubarb root and rhizome-based Chinese herbal prescriptions for acute ischemic stroke: a systematic review and meta-analysis. *Complement. Ther. Med.* 22 (6), 1060–1070. doi:10.1016/j.ctim.2014.10.002

Marmagkiolis, K., Hakeem, A., Cilingiroglu, M., Gundogdu, B., Iliescu, C., Tsitlakidou, D., et al. (2015). Safety and Efficacy of Stent Retrievers for the Management of Acute Ischemic Stroke: Comprehensive Review and Meta-Analysis. *JACC Cardiovasc Interv.* 8 (13), 1758–1765. doi:10.1016/j.jcin.2015.07.021

Marzolini, S., Robertson, A. D., Oh, P., Goodman, J. M., Corbett, D., Du, X., et al. (2019). Aerobic Training and Mobilization Early Post-stroke: Cautions and Considerations. *Front. Neurol.* 10, 1187. doi:10.3389/fneur.2019.01187

Moher, D., Liberati, A., Tetzlaff, J., Altman, D. G., and Group, P. (2009). Preferred reporting items for systematic reviews and meta-analyses: the PRISMA statement. *BMJ* 339 (7), b2535. doi:10.1371/journal.pmed.100009710.1136/bmj.b2535

Ni, J., Chen, H., Chen, G., Ji, Y., Yi, F., Zhang, Z., et al. (2020). Efficacy and safety of cinepazide maleate injection in patients with acute ischemic stroke: a multicenter, randomized, double-blind, placebo-controlled trial. *BMC Neurol.* 20 (1), 282. doi:10.1186/s12883-020-01844-8

Ni, X., Ni, X., Liu, S., and Guo, X. (2013). Medium- and long-term efficacy of ligustrazine plus conventional medication on ischemic stroke: a systematic review and meta-analysis. *J. Tradit. Chin. Med.* 33 (6), 715–720. doi:10.1016/s0254-6272(14)60002-9

Pan, X., Li, J., Xu, L., Deng, S., and Wang, Z. (2020). Safety of Prophylactic Heparin in the Prevention of Venous Thromboembolism After Spontaneous Intracerebral Hemorrhage: A Meta-analysis. *J. Neurol. Surg. A Cent. Eur. Neurosurg.* 81 (3), 253–260. doi:10.1055/s-0039-3400497

Patel, R. A. G., and McMullen, P. W. (2017). Neuroprotection in the Treatment of Acute Ischemic Stroke. *Prog. Cardiovasc Dis.* 59 (6), 542–548. doi:10.1016/j.pcad.2017.04.005

Peng, W., Yang, J., Wang, Y., Wang, W., Xu, J., Wang, L., et al. (2014). Systematic review and meta-analysis of randomized controlled trials of xingnaojing treatment for stroke. *Evidence-Based Complementary Altern. Med.* 2014, 1–9. doi:10.1155/2014/210851

Practice, C. M. (2021). Guideline for primary care of ischemic stroke (2021). *Chin. J. General Pract.* 20 (9). doi:10.3760/cma.j.cn114798-20210804-00590

Puñal-Riobóo, J., Atienza, G., and Blanco, M. (2015). Safety and Efficacy of Mechanical Thrombectomy Using Stent Retrievers in the Endovascular Treatment of Acute Ischaemic Stroke: A Systematic Review. *Interv. Neurol.* 3 (3-4), 149–164. doi:10.1159/000430474

Roaldsen, M. B., Jusufovic, M., and Lindekleiv, H. (2022). Cochrane Review on Endovascular Thrombectomy and Intra-Arterial Interventions for Acute Ischemic Stroke. *Stroke* 53 (5), e193–e194. doi:10.1161/STROKEAHA.121.036285

Shang, X. J., Shi, Z. H., He, C. F., Zhang, S., Bai, Y. J., Guo, Y. T., et al. (2019). Efficacy and safety of endovascular thrombectomy in mild ischemic stroke: results from a retrospective study and meta-analysis of previous trials. *BMC Neurol.* 19 (1), 150. doi:10.1186/s12883-019-1372-9

Shea, B. J., Grimshaw, J. M., Wells, G. A., Boers, M., Andersson, N., Hamel, C., et al. (2007). Development of AMSTAR: a measurement tool to assess the methodological quality of systematic reviews. *BMC Med. Res. Methodol.* 7, 10. doi:10.1186/1471-2288-7-10

Shen, T., Zhou, J., and Zhao, Y. (2020). Efficacy and safety of different doses of tenecteplase for the treatment of acute ischemic stroke: A protocol for a systematic review and network meta-analysis. *Med. Baltim.* 99 (49), e23379. doi:10.1097/MD.0000000000023379

Shi, L., Pu, J., Xu, L., Malaguit, J., Zhang, J., and Chen, S. (2014). The efficacy and safety of cilostazol for the secondary prevention of ischemic stroke in acute and chronic phases in Asian population--an updated meta-analysis. *BMC Neurol.* 14, 251. doi:10.1186/s12883-014-0251-7

Siddiqui, F. J., Venketasubramanian, N., Chan, E. S., and Chen, C. (2013). Efficacy and safety of MLC601 (NeuroAiD®), a traditional Chinese medicine, in poststroke recovery: a systematic review. *Cerebrovasc. Dis.* 35 (Suppl. 1), 8–17. doi:10.1159/000346231

Thelengana, A., Radhakrishnan, D. M., Prasad, M., Kumar, A., and Prasad, K. (2019). Tenecteplase versus alteplase in acute ischemic stroke: systematic review and meta-analysis. *Acta Neurol. Belg* 119 (3), 359–367. doi:10.1007/s13760-018-0933-9

Wang, L. D., Xu, Z. M., Liang, X., Qiu, W. R., Liu, S. J., Dai, L. L., et al. (2021). Systematic Review and Meta-Analysis on Randomized Controlled Trials on Efficacy and Safety of Panax Notoginseng Saponins in Treatment of Acute Ischemic Stroke. *Evid. Based Complement. Altern. Med.* 2021, 4694076. doi:10.1155/2021/4694076

Wang, Z., Wei, X., Yang, J., Suo, J., Chen, J., Liu, X., et al. (2016). Chronic exposure to aluminum and risk of Alzheimer's disease: A meta-analysis. *Neurosci. Lett.* 610, 200–206. doi:10.1016/j.neulet.2015.11.014

Wu, B., Liu, M., Liu, H., Li, W., Tan, S., Zhang, S., et al. (2007). Meta-analysis of traditional Chinese patent medicine for ischemic stroke. *Stroke* 38 (6), 1973–1979. doi:10.1161/STROKEAHA.106.473165

Xin, M., Hao, Y., Huang, G., Wang, X., Liang, Z., Miao, J., et al. (2020). The efficacy and safety of salvianolic acids on acute cerebral infarction treatment: A protocol for systematic review and meta analysis. *Med. Baltim.* 99 (23), e20059. doi:10.1097/MD.0000000000020059

Xu, J. H., Huang, Y. M., Ling, W., Li, Y., Wang, M., Chen, X. Y., et al. (2015). Wen Dan Decoction for hemorrhagic stroke and ischemic stroke. *Complement. Ther. Med.* 23 (2), 298–308. doi:10.1016/j.ctim.2015.01.00110.1155/2021/4265219

Xu, Z. Q., Zhou, Y., Shao, B. Z., Zhang, J. J., and Liu, C. (2019). A Systematic Review of Neuroprotective Efficacy and Safety of DL-3-N-Butylphthalide in Ischemic Stroke. *Am. J. Chin. Med.* 47 (3), 507–525. doi:10.1142/S0192415X19500265

Yang, W., Shi, Z., Yang, H. Q., Teng, J., Zhao, J., and Xiang, G. (2015). Mailuoning for acute ischaemic stroke. *Cochrane Database Syst. Rev.* 1, CD007028. doi:10.1002/14651858.CD007028.pub3

Yuan, Y., Zeng, X., Luo, Y., Li, Z., and Wu, T. (2008). Chuanxiong-type preparations for acute ischemic stroke. *Cochrane Database Syst. Rev.* 4, CD005569. doi:10.1002/14651858.CD005569.pub2

Zhang, D., Dong, Y., Li, Y., Chen, J., Wang, J., and Hou, L. (2017). Efficacy and Safety of Cerebrolysin for Acute Ischemic Stroke: A Meta-Analysis of Randomized Controlled Trials. *Biomed. Res. Int.* 2017, 4191670. doi:10.1155/2017/4191670

Zhang, H., Xing, Y., Chang, J., Wang, L., An, N., Tian, C., et al. (2019). Efficacy and Safety of NaoShuanTong Capsule in the Treatment of Ischemic Stroke: A Meta-Analysis. *Front. Pharmacol.* 10, 1133. doi:10.3389/fphar.2019.01133

Zhao, S., Zheng, H., Du, Y., Zhang, R., Chen, P., Ren, R., et al. (2021). The Clinical Efficacy of Ginkgo biloba Leaf Preparation on Ischemic Stroke: A Systematic Review and Meta-Analysis. *Evid. Based Complement. Altern. Med.* 2021, 4265219. doi:10.1155/2021/4265219

Zheng, Q. H., Li, X. L., Mei, Z. G., Xiong, L., Mei, Q. X., Wang, J. F., et al. (2017). Efficacy and safety of puerarin injection in curing acute ischemic stroke: A

meta-analysis of randomized controlled trials. *Med. Baltim.* 96 (1), e5803. doi:10.1097/MD.0000000000005803

Zhou, J., Gao, Y., and Ma, Q. L. (2020). Safety and efficacy of tirofiban in acute ischemic stroke patients Not receiving endovascular treatment: a systematic review and meta-analysis. *Eur. Rev. Med. Pharmacol. Sci.* 24 (3), 1492–1503. doi:10.26355/eurrev_202002_20208

Zhou, X., Shao, T., Xie, X., Ding, M., Jiang, X., Su, P., et al. (2022). Tongqiao Huoxue Decoction for the treatment of acute ischemic stroke: A Systematic Review and meta-analysis. *J. Ethnopharmacol.* 283, 114693. doi:10.1016/j.jep.2021.114693

Conflict of Interest: The authors declare that the research was conducted in the absence of any commercial or financial relationships that could be construed as a potential conflict of interest.

Publisher's Note: All claims expressed in this article are solely those of the authors and do not necessarily represent those of their affiliated organizations, or those of the publisher, the editors, and the reviewers. Any product that may be evaluated in this article, or claim that may be made by its manufacturer, is not guaranteed or endorsed by the publisher.

frontiers | Frontiers in Pharmacology

TYPE Review
PUBLISHED 04 August 2022
DOI 10.3389/fphar.2022.925514

OPEN ACCESS

EDITED BY
Rui Liu,
Chinese Academy of Medical Sciences, China

REVIEWED BY
Claudia Bregonzio,
CCT CONICET Córdoba, Argentina
Bechan Sharma,
Allahabad University, India

*CORRESPONDENCE
Jiaxu Chen,
chenjiaxu@hotmail.com

†These authors have contributed equally to this work and share first authorship

SPECIALTY SECTION
This article was submitted to Neuropharmacology, a section of the journal Frontiers in Pharmacology

RECEIVED 21 April 2022
ACCEPTED 27 June 2022
PUBLISHED 04 August 2022

CITATION
Chen J, Lei C, Li X, Wu Q, Liu C, Ma Q and Chen J (2022), Research progress on classical traditional chinese medicine formula xiaoyaosan in the treatment of depression.
Front. Pharmacol. 13:925514.
doi: 10.3389/fphar.2022.925514

Research progress on classical traditional chinese medicine formula xiaoyaosan in the treatment of depression

Jianbei Chen[1†], Chaofang Lei[1†], Xiaojuan Li[2], Qian Wu[1], Chenyue Liu[3], Qingyu Ma[2] and Jiaxu Chen[1,2*]

[1]School of Traditional Chinese Medicine, Beijing University of Chinese Medicine, Beijing, China, [2]Formula-pattern Research Center, School of Traditional Chinese Medicine, Jinan University, Guangzhou, China, [3]Institute of Chinese Materia Medica, China Academy of Chinese Medical Sciences, Beijing, China

Depression is an emotional disorder that is problematic in psychiatry owing to its unclear etiology and unknown pathogenesis. Traditional Chinese medicine formulations such as Xiaoyaosan have been widely used throughout history to treat depression. In this review, we have focused on recent evidences elucidating the links between Xiaoyaosan and the treatment of depression. Data from animal and clinical studies, focusing on the pharmacological mechanisms, clinical applications, and effective materials that form the basis for the treatment of depression are presented and discussed. We found that the antidepressant effects of Xiaoyaosan are related to the effects of monoamine neurotransmitters, regulation of the hypothalamic-pituitary-adrenal axis, neuroplasticity, synaptic plasticity, inflammatory response, neuroprotection, brain-gut axis, regulation of intestinal microbiota, oxidative stress, and autophagy for reducing neuronal apoptosis. This review highlights the current evidence supporting the use of Xiaoyaosan as an antidepressant and provides an overview of the potential mechanisms involved.

KEYWORDS

xiaoyaosan, TCM, depression, clinical application, pharmacological mechanism, research progress, review

1 Introduction

Depression is a common emotion-related psychiatric disease encountered in clinical practice, with a global prevalence of 4.4–5%. Its primary clinical characteristics include lasting depression, impaired thinking and cognitive function, and decreased activity, in addition self-mutilation, suicide, and other associated behaviors can also occur in more severe cases (Ferrari et al., 2013; Smith 2014). According to the Global Burden of Disease Study 2013, major depressive disorder (MDD) is the second leading cause of years lived with disability (Vos et al., 2015). The population-attributable risk for depression and all causes of death is 12.7% and for depression and suicide it reaches 11.2% (Walker et al., 2015). According to the World Health Organization (WHO), depression has become one

of the main global causes of disability, and it is expected to become a main disease burden and a major cause for increased medical expenses by 2030 (Mathers 2008; Yao et al., 2015). Due to the complex and diversified clinical manifestations of depression, it is difficult to predict the course and prognosis of this disease. Furthermore, patient responses to treatment are also variable, making diagnosis and treatment even more complex. Modern medical research has demonstrated that genetic factors can determine the susceptibility to depression, while environmental factors can be triggers. The occurrence and development of depression is thus closely related to physiological state, psychological state, and social environment of an individual (Figueiredo et al., 2015; Raič 2017). Although the pathogenesis of depression remains unknown, current medical theories consider the effects of monoamine neurotransmitters, immunodeficiency, hypothalamus-pituitary-adrenal (HPA) axis system activation, the neuroplasticity/synaptoplasticity hypothesis, and the intestinal microbiota hypotheses. In diagnosed patients, the concentration of monoamine neurotransmitters such as 5-hydroxytryptamine (5-HT), norepinephrine (NE), and dopamine (DA) are decreased, disrupting normal neuronal activities. Furthermore, an increase of interleukin-6 (IL-6), IL-1β, and tumor necrosis factor-alpha (TNF-α) results in immune system imbalance, and the over-activation of the HPA axis leads to neuroendocrine system dysfunction. Nerve cell plasticity is changed by neuronal injury and decreased brain-derived neurotrophic factor (BDNF) content, and dysregulation of the intestinal flora composition and function may result in metabolic abnormalities that lead to depression (Felger, 2016; Grace, 2016). These theories have been crucial for guiding the clinical treatment of depression. However, depression is currently treated in western medicine by using oral antidepressants, with limited response rate and delayed onset of efficacy due to their long therapeutic cycles, notable side effects, high price, and poor compliance (Health Quality, 2017). These drugs all act on specific parts of the brain and modulate brain function accordingly. However, most of these drugs can be severely toxic to patients, and chronic treatment of depression can also lead to structural changes in certain parts of the brain (Siddiqi et al., 2022). An increasing number of studies has demonstrated the outstanding efficacy of traditional Chinese medicine (TCM) and its compound preparations in the treatment of depression, with benefits such as high remission rates, long-lasting antidepressant effects, and fewer adverse reactions (Liu et al., 2015; Wu et al., 2015). TCM could thus be used to source a prospective alternative therapy for the treatment of depression. Phytochemicals are a safe, cost-effective, and highly effective antidepressant. A growing number of preclinical and clinical studies have revealed a complex array of psychoactive substances in herbal medicines that are beneficial in the treatment of depression (Sarris et al., 2011). Plant molecules isolated from medicinal plants produce antidepressant effects by modulating the levels of neurotransmitters such as dopamine, serotonin, and norepinephrine in different parts of the brain. The antidepressant mechanism of action of phytochemicals also includes negative regulation of monoamine oxidase and acetylcholinesterase activity and prevention of hyperactivity of the HPA axis. It also has strong antioxidant and anti-inflammatory potential, which provide synergistic effects for its antidepressant function (Kumar and Sharma 2022). Some herbal remedies have been approved by regulatory agencies to treat mental illness. For example, the Brazilian Health Regulatory Agency (Anvisa) has approved certain products derived from passionflower, valerian, cohosh, and Piper methysticum for the treatment of anxiety or depression. The European Medicines Agency has listed *Hypericum perforatum* (St. John's Wort), *Melissa officinalis* L. (Melissa leaf), and *V. officinalis* L. (Valerian root) as plants approved for the treatment of stress and mood disorders (Fathinezhad et al., 2019). The State Drug Administration of China approved the traditional Chinese medicines Jieyuchufan Capsule, Morinda Oligosaccharide Capsule, and Shuganjieyu Capsule to treat mild to moderate depression. In addition, Xiaoyaosan is another popular Chinese herbal formula and one of the most widely used Chinese herbal formulas for the treatment of depression in China. This means that, with the continuous development of traditional Chinese medicine, the treatment of depression using plants has gradually been more widely recognized in the world, and the use of effective natural medicines instead of chemicals has become a new trend in the development of international medicine.

In TCM, depression is categorized as an "emotional disease" and it is described as "insomnia," "lily disease," and "depression syndrome". Research on the formulations of TCMs is ongoing. Studies have found that some TCM formulations used to treat depression have multiple targets, low toxicity, and strong efficacy but their molecular mechanisms have not yet been fully clarified (Gao et al., 2013). Xiaoyaosan (XYS) which was first recorded in the *Taiping Huimin Heji Jufang* (Pharmacopeia of the Welfare Dispensary Bureau) by the Song Dynasty (960–1127 AD) is a classic Chinese medicinal compound. Its functions include reconciling the liver and spleen, soothing the liver, invigorating the spleen, nourishing the blood, and relieving depression. It is mainly used to treat liver stagnation, blood deficiency, and spleen weakness (Zhang et al., 2012; Du et al., 2014). XYS has been utilized in clinical practice in China for over 1,000 years, and it has often been used to treat a variety of conditions including depression, functional dyspepsia, chronic gastritis, and perimenopausal syndrome. Statistics on the frequency of symptoms treated using TCM show that the most common conditions related to depression were liver Qi stagnation and spleen deficiency. XYS is prepared using a traditional recipe that requires eight commonly used Chinese herbs [Chaihu (*Radix Bupleuri*), Danggui (*Radix Angelicae Sinensis*), Baishao (*Radix Paeoniae Alba*), Baizhu (*Rhizoma Atractylodis Macrocephalae*), Fuling (*Poria*), Bohe (*Herba Menthae Haplocalyx*), Shengjiang

(*Rhizoma Zingiberis*), and Gancao (*Radix Glycyrrhizae*)], which have been used for centuries to treat mental illnesses, including depression (see Table 1). In the treatment of depression, XYS has unique theoretical advantage and rich scientific connotation, as it is consistent with the overall concept and characteristics of TCM based on syndrome differentiation. Clinically, XYS is the most common TCM prescribed for the treatment of anxiety and depression caused by liver Qi stagnation, blood deficiency, and spleen deficiency (Zhou et al., 2011). XYS is often used as a single treatment or in combination with other western drugs in the treatment of depression. Clinical studies have shown that XYS has significant antidepressant effects without evident adverse reactions (Qin et al., 2010). This article provides an overview of existing clinical and experimental research, describing the pathogenesis of depression and potential therapeutic targets, while systematically reviewing the research progress of treating depression using XYS.

2 Clinical applications of XYS for the treatment of depression

The use of XYS alone or in combination with western medicines has been found to relieve symptoms of depression with fewer side effects than traditional antidepressants, and it is thus considered a promising antidepressant for future use. A systematic review has shown that XYS and antidepressants have a significant comprehensive effect on the treatment of depression. The Hamilton depression scale (HAMD) and self-rating depression scale (SDS) scores of XYS were superior to those of antidepressants alone without significant side effects (Kou and Chen 2012; Zhang et al., 2012). Based on gas chromatography—mass spectrometry (GC-MS) metabolomics, Liu et al. found that the plasma metabolic profile of patients with depression was different when compared with a healthy control group, and that XYS significantly regulated depression symptoms by reversing metabolite and pathway levels to that of the control group (Liu X. et al., 2020). By recruiting 25 patients with depression and 33 healthy volunteers and using GC-MS urinary quantitative metabolomics, XYS was found to have a better priority for the treatment of depression (Tian et al., 2016). Chen et al. found that the Xiao Yao Pill containing Chaihu had a regulatory effect on the nervous and endocrine systems of patients with liver Qi stagnation and spleen deficiency syndrome (LSSDS), and helped to improve their clinical performance (Chen et al., 2005). A meta-analysis of ten randomized controlled trials involving 735 patients showed that when compared with antidepressants alone, XYS as an adjuvant therapy was beneficial in relieving depression symptoms. Furthermore, XYS in combination with antidepressants could improve the efficacy of the latter and reduce their HAMD scores and adverse reactions such as insomnia and constipation (Man et al., 2014). Another meta-analysis conducted for 607 patients with post-stroke depression (PSD) identified from seven trials revealed that using XYS as an adjuvant therapy was beneficial without adverse effects, reducing both the HAMD and Scandinavian stroke scale scores evidenced when using the antidepressants alone (Jin et al., 2018). A clinical study of 180 patients with functional dyspepsia (FD) associated with perimenopausal depression, found that Xiaoyao Pill (XYS) had positive therapeutic effects on the Hamilton depression rating scale (HRSD), gastrin, motilin levels, and gastric emptied rate of perimenopausal FD patients, and it could effectively improve related symptoms (Du et al., 2014). The TCM derived from Jiawei Xiaoyao (JWXY) also had positive effects when used as a main prescription (Su et al., 2019). For mild to moderate depression with anxiety symptoms, JWXY was as effective as sertraline in reducing depressive symptoms and it showed a faster onset and longer lasting effect than sertraline in the reduction of anxiety symptoms; it also improved sleep quality and physical anxiety symptoms. As JWXY is safe and cheaper than traditional antidepressants, it may be the preferred choice for treating depression with anxiety symptoms. Xiaoyaosan can effectively improve blood sugar level and depressive symptoms, regulate the body's cortisol (Cor) and adrenocorticotropic hormone (ACTH) levels, and reduce the adverse reactions caused by antidepressant drugs in the treatment of the depressive disorder of type 2 diabetes with liver stagnation and spleen deficiency (Zhang J. et al., 2021). The clinical efficacy of Jiawei Xiaoyaosan combined with fluoxetine in the treatment of depression is good, and it can significantly improve the depression state of patients (Liu J. et al., 2020). The clinical efficacy of Danzhi Xiaoyaosan in the treatment of mild to moderate depression is significant, and its side effects are small. Part of its antidepressant mechanism may be achieved by regulating serum 5-HT, CORT, and BDNF (He 2019). With the progress of treatment, Xiaoyao Powder can restore the functions of the hypothalamic-pituitary-gonadal axis and the HPA (Jiang et al., 2015). Sixty patients with mild to moderate depression were randomly divided into two groups to observe the clinical efficacy of Xiaoyaosan. The results showed that Xiaoyaosan can significantly improve the clinical symptoms of mild to moderate depression without adverse reactions (Yang and Lin, 2015). Xiaoyaosan combined with sertraline can quickly and effectively enhance the clinical efficacy of sertraline and improve clinical symptoms, which is worthy of clinical promotion (Zhang, 2015). Some researchers have found that Xiaoyaosan has a definite effect in the treatment of depression and that the effect is fast: most patients return to normal after 6 weeks of treatment (Feng et al., 2014). Overall, these clinical studies have shown that XYS is effective for depression treatment and generally well-tolerated without

obvious adverse reactions (see Table 2). It can be used safely when based on reasonable syndrome differentiation.

3 Pharmacological mechanisms of XYS for the treatment of depression

3.1 Neurotransmitters and their receptors

Figure 1 one of the current hypotheses for the pathogenesis of depression is the monoamine neurotransmitter hypothesis. Monoamine neurotransmitters, also known as biological amine neurotransmitters, have a wide range of biological activities, and are important for functions such as the regulation of body temperature, emotional responses, behavioral state, and mental activities. The monoamine neurotransmitter hypothesis suggests that the loss or decrease of NE, 5-HT, or other monoamine neurotransmitters in the central and peripheral regions may induce depression (Carpenter et al., 2004; Castrén 2005). Zhang et al. (Zhang et al., 2018) found that a Jiawei Xiaoyao (XYS) capsule promoted the increase of cortisol levels and expression of tyrosine hydroxylase, and improved the expression of monoamine neurotransmitters (including 5-HT and NE). The modified Xiaoyao capsule could also save the depressive phenotype and cognitive behavior of zebrafish by changing the levels of endogenous cortisol and monoamine neurotransmitters. Dysregulation of monoamine neurotransmitters and their receptors, especially 5-HT, may thus be the basic cause of depression. Studies have found that XYS up-regulated the 5-HT content in the cerebral cortex of the rat depression model induced by chronic restraint stress (CRS) (Bao et al., 2008), and increased the 5-HT content in the hippocampus of rat with postpartum depression (Wang and Qin 2010). Activation of the 5-HT1A receptor has been shown to increase the release of DA. Yin et al. found that XYS/room temperature super-extraction systems (RTSES) could significantly increase the shuttle activity of C57BL/6J mouse and reduce the resting time on the forced swimming test (FST) and tail suspension test (TST), as well as increase insulin sensitivity in mice with anxiety and depression caused by reserpine. The insulin sensitivity of mice also confirmed that the activation of the brain 5-HT1A receptor led to the anxiolytic and antidepressant effects of the XYS/RTSES treatment (Yin et al., 2012). XYS may thus be a modulator of monoamine neurotransmitters (Kong et al., 2010). 5-HT comes from tryptophan, tryptophan generates 5-hydroxytryptophan (5-HTP) under the action of tryptophan hydroxylase, and then decarboxylates under the catalysis of 5-hydroxytryptophan decarboxylase to generate 5-HT. Therefore, the level of tryptophan affects the amount of 5-HT in the brain. In order to further clarify the mechanism of the decline of monoamine neurotransmitters, some studies have found that the activity of indoleamine 2,3-dioxygenase (IDO) in the serum of patients with depression is significantly increased, and the rate of tryptophan decomposition is accelerated. This inhibits the metabolism of tryptophan to the 5-HT pathway and reduces the concentration of the neurotransmitter 5-HT in the synaptic cleft, thereby accelerating the occurrence of depression. Stress-induced stimulation of indoleamine 2, 3-dioxygenase 1 (IDO1) can affect the metabolic conversion of tryptophan to kynurenine and thus reduce the ability of tryptophan hydroxylase (TPH) to synthesize 5-HT. XYS can reduce the number of microglial cells and the expression of IDO1 in the dorsal fissure nucleus of depressed mice, and inhibit 5-HT synthesis (Wang M. et al., 2018). As tryptophan is the precursor of 5-HT, microorganisms can activate IDO1 to deplete tryptophan through the kynurenine pathway, resulting in the decrease of 5-HT, which leads to depression. Jiao et al. found that XYS could improve the metabolism of tryptophan by adjusting the expression levels of TPH2 and IDO1 in a rat depression model established using the chronic fixed stress (CFS) method, thereby exerting an antidepressant effect (Jiao et al., 2019). Ding et al. (Ding et al., 2014) found that after exposure to continuous chronic stress, the activated locus coeruleus (LC)-NE system had a significant impact on the occurrence and development of depression in rat. After XYS treatment, the expression of NE, thyroid hormone (TH), and adrenocorticotropin-releasing factor (CRF) in rat was significantly reduced when compared with the control group. Zhang et al. found that XYS treatment affected the levels of DA, 3,4-dihydroxyphenylacetic acid (DOPAC), and homovanillic acid (HVA) in the various brain regions of chronic unpredictable mild stress (CUMS) rat model; levels were significantly reduced in the prefrontal cortex and the nucleus accumbens, along with DA receptor 1 (D1R) mRNA and protein expression. The specific mechanism of XYS may be related to the free and unrestricted dopamine (DA) scattered in the central nervous system and to the increased expression of its receptors and transporters (Zhang H. et al., 2021). Guo et al. found that XYS may play an anti-depressive role by increasing progesterone and allopregnanolone and decreasing pregnenolone (PREG) in the hippocampus and amygdala of the CUMS-stimulated rat model, thereby enhancing the release of γ-aminobutyric acid (GABA) and N-methyl-D-aspartate (NMDA) receptors, inhibiting the release of glutamate receptors, and reducing the inhibitory effects of GABA (Guo et al., 2017). These results indicate that XYS can effectively improve the depression-like behavior of rat by inhibiting the activity of LC-NE neurons. In summary, the antidepressant mechanism of XYS has been shown to be related to monoamine neurotransmitters (see Figure 2).

3.2 Neuroendocrine (HPA) axis

Depression is categorized as a mental disorder, and neuroendocrine experiments have found that endocrine

hormones are closely related to behavior and mood. From the perspective of neurobiology, the occurrence of depression is closely related to the dysfunction of the HPA axis (Cai et al., 2015). When the human brain is stimulated by stress, the cerebral cortex is affected, the hypothalamus sends out signals, HPA axis participates in neuroendocrine regulation, and secretion of corticotropin releasing factor (CRF) increases. Excessive CRF is transferred from the portal system to the pituitary gland to synthesize adrenocorticotropic hormone (ACTH), which circulates throughout the body stimulating the adrenal cortex to produce cortisol (Olloquequi et al., 2018). The mechanism of the hyperactivity of the HPA axis is the excessive secretion of CRF. CRF is a key factor in regulating the stress response of the body and is related to various mental diseases such as depression. In addition, cortisol content in depression patients is closely related to the clinical manifestations of disease and cortisol has a key role in the pathogenesis of depression. XYS has been shown to regulate HPA axis disorders in the depression rat model at multiple targets and levels and to increase the expression and accelerate the transport of central glucocorticoid receptors in depressed rat (Chen et al., 2008b). Lu et al. found that XYS could promote the expression of glucocorticoid receptors and restore the negative feedback regulation of the HPA axis, thereby relieving depression (Lu et al., 2018). Wu et al. found that Danzhi XYS could inhibit overactivity of the HPA axis, regulate monoamines and amino acid neurotransmitters in the hippocampus, and improve the depression-like behavior of rat under chronic stress (Wu et al., 2016). Zhu et al. found that XYS could improve depression-like behavior by down-regulating the level of corticotropin-releasing hormone (CRH) receptor 2 in social isolation and CUMS models, and improve HPA axis overactivation (Zhu et al., 2014). The apelin/APJ system is considered to play an important role in the function of the HPA axis. Yan et al. found that XYS could improve depressive behavior by up-regulating hypothalamic apelin levels and down-regulating hypothalamic APJ levels in a CUMS rat model. Thus, changes in the hypothalamic apelin/APJ system may be a depression target, and XYS may have a regulatory effect on it (Yan et al., 2018). Chronic stress can destroy the permeability of the blood-brain barrier (BBB) (Duffy et al., 2014). Glucocorticoids (GCs) are important hormones in the human body, and their secretion is mainly regulated by the HPA axis. Yu et al. found that XYS can partially reverse the inhibition of GCs-induced cell proliferation and invasion promoting the expression of tight junction-related genes; this allows reversing the damage to the BBB permeability induced by chronic stress (Yu et al., 2020). Despite these breakthroughs, the exact mechanism by which XYS restores the HPA axis still needs to be clarified (see Figure 3).

3.3 Neuroplasticity and synaptic plasticity

Synaptic plasticity is an important part of learning and memory from the perspective of neurobiology. It indicates that the structure and function of synapses can change under the influence of the continuous activity of neurons, with adjustable characteristics. Synapses are thus crucial for neuronal networks and information transmission (Kim et al., 2006). Furthermore, when synaptic plasticity is reduced and neurons are functionally impaired, learning and memory are also impaired (Coleman et al., 2004), which is associated with a variety of neuropsychiatric diseases (Südhof, 2008; Gilman et al., 2011). In recent years, an increasing number of studies has shown there is a close relationship between synaptic plasticity and depression, and improving synaptic plasticity can help reversing depressive symptoms and the associated cognitive decline (Sullivan et al., 2000). Synapses are crucial for the transmission and processing of information between neurons, and reductions in the number of synapses or structural damage to neurons will affect the release of neurotransmitters, resulting in information transmission disorders in the central nervous system. Using electron microscopy, Liang et al. found that the pyramidal cells in the hippocampal CA1 region of the chronic stress rat model had several ultrastructural damages to the nucleus, mitochondria, and other important organelles and synapses, while the XYS group had no evident abnormalities in the CA1 region (Liang et al., 2009). Ao et al. found that polyphasic stress could damage synaptic structures and affect their connections in rat, whereas XYS could reduce the stress damage to the original synapses and synaptic connections, promote the formation of new synapses and synaptic connections, and reduce learning and memory impairment (Ao et al., 2006).

3.3.1 α-Amino-3-hydroxy-5-methyl-4-isoxazolepropionic acid (AMPA) receptors

Numerous studies have shown that the pathogenesis of depression may be closely related to a disorder in the glutamatergic system (Henter et al., 2018; Moriguchi et al., 2019). Glutamate is the main excitatory neurotransmitter of the central nervous system, and it plays an important role in the differentiation, development, and growth of neurons. Glutamate is also involved in synaptic signal transmission and learning and memory processes, and it plays a key role in the maintenance of synaptic stability and plasticity (McDonald and Johnston 1990). Studies have shown that AMPA receptors, as ionotropic glutamate receptors, are important in both synaptic plasticity and cell death caused by neurological disease and dysfunction (Whitehead et al., 2017). AMPA receptors can participate in the pathogenesis of depression by changing synaptic plasticity, and directly or indirectly participate in the mechanism of depression as antidepressants (Aleksandrova et al., 2017; Zhou et al., 2019). Liang et al. found that chronic immobilization stress (CIS) induced a decrease in GluR2 mRNA and an increase in GluR1 mRNA in the hippocampal CA1 area of rats; ultrastructural damage was also observed in this region. However, XYS could reverse this

trend, indicating it can produce a certain antidepressant effect, and suggesting it is related to the hippocampal synaptic plasticity of AMPA receptors (Liang et al., 2013). The PDZ domain of 95 kDa postsynaptic density protein (PSD-95) regulates the function of AMPA receptors through protein-protein interactions. PSD-95 can combine with molecules in the NMDA receptor signaling pathway to form a signaling complex. Meng et al. found that XYS can reverse the slow weight gain and related symptoms of LSSDS in rat exposed to chronic immobilization stress (CIS), and up-regulate the levels of the hippocampal PSD-95 and synaptophysin, thereby improving learning and memory impairment and synaptic plasticity (Meng et al., 2013). Xi et al. found that XYS (FWP) could reverse the decrease of GluR1 and GluR2/3 in hippocampal region CA3, p-GluR1 in hippocampal region CA3, and p-GluR2 in hippocampal regions CA1 and CA3 induced by CRS in rat models and inhibit the increase of GluR1 in hippocampal region CA1 and DG, p-GluR1 in hippocampal region CA1, and p-GluR2 and GluR3 in amygdala BLA. It is suggested that FWP may play an antidepressant role by regulating AMPA-type glutamate receptor homeostasis in the amygdala and hippocampus to relieve the symptoms of liver depression and Malcan deficiency syndrome (Xi et al., 2020).

Glutamate concentration and action time beyond the physiological range will lead to the production of excitatory neurotoxicity damage to neurons. This is one of the pathological mechanisms of social stress disorders, such as affective disorder. This mechanism is associated with damage to astrocytes (AS) and excitatory amino acid transporters (EAATs) due to long-term stress. Zhou et al. found that XYS exerted antidepressant effects through the NR2B and PI3K/Akt signaling pathways to alleviate hippocampal neuronal damage induced by glutamate-mediated excitotoxicity in rat (Zhou et al., 2021). Liu et al. found that XYS could reverse the expression of glial fibrillary acidic protein (GFAP), EAAT1, EAAT2, and Neuronal nuclei antigen (NeuN) in the prefrontal cortex of CUMS mice, and increase the content of glutamate, thereby exerting antidepressant effects (Liu et al., 2019). Ding et al. found that XYS could regulate the depression-like behavior of mice induced by CUMS, which might be related to changes in the hippocampal glutamate/glutamine cycle and glutamate transporter (GLT) 1, suggesting that the antidepressant effect of XYS is related to the glutamate energy system (Ding et al., 2017a). Chen et al. found that XYS may regulate glutamine and glutamate metabolism in rat to maintain the ammonia nitrogen balance and promote energy metabolism, thereby improving depression-like behavior and liver injury symptoms induced by CUMS (Chen et al., 2020a). Ding et al. found that chronic administration of XYS may normalize the expression of the glial fibrillary acidic protein (GFAP) in the hippocampus of mice with CUMS, thereby exerting an antidepressant effect (Ding et al., 2017b).

3.3.2 NMDA receptors

The dysfunction of N-methyl-D-aspartic acid receptor (NMDA) receptors is related to certain neuropsychiatric disorders (Zoicas and Kornhuber 2019), and there is substantial evidence supporting NMDA receptor dysfunction in patients with depression (Balu 2016). Song et al. found that XYS could improve the body weight and food intake of rat exposed to CUMS, affect the activity of AS, reverse the changes of corticosterone in the HPA axis, and downregulate the level of NMDA receptors in the hippocampus (Song et al., 2020).

3.3.3 BDNF

The expression of neurotrophic factors in the serum and brain regions of patients with depression are significantly different from those of healthy people, suggesting that neurotrophic factors may become new markers for depression. BDNF is the most abundant neurotrophic protein in the brain tissue, and it is crucial for the growth, proliferation, survival, and synaptic activity of neurons (Machaalani and Chen 2018). BDNF protein and mRNA expression can be detected in various parts of the cerebral cortex, hippocampus, olfactory bulb, basal forebrain, midbrain, and hypothalamus (Bathina and Das 2015). Due to its role in regulating the synaptic structure and neuroplasticity, BDNF has attracted extensive attention in the pathogenesis of stress disorders. As a key molecule in central nervous system cascade signaling, BDNF is closely related to the occurrence of depression, and it is an important target of antidepressant therapies. Evidence from clinical studies has shown that part of the pathophysiology of depression is the down-regulation of BDNF and its tyrosine receptor kinase B (TrkB), which in turn leads to neuron atrophy and loss in different brain regions, including the hippocampus. Studies have found that XYS (Ding et al., 2017b) could prevent depression-like behaviors by increasing the expression of BDNF. After treatment with XYS for 28 days, BDNF gene expression in the depressed rat model was up-regulated while the expression of BDNF and cyclic AMP response element binding (CREB) proteins was significantly increased (Wang J. et al., 2018). Xiaoyao Jieyu Powder (XYS) was found to improve post-stroke depression in rat by regulating BDNF, the cannabinoid receptor, and CRF in the ventral tegmental area of the midbrain (Wang C. et al., 2019). Studies have also confirmed that XYS has anti-anxiety and anti-depressive effects (Zhi-wei et al., 2004; Chen et al., 2008a), as well as a beneficial effects on stressed rat. The BDNF of the frontal cortex and hippocampal CA1 area of rat exposed to CIS decreased, while the levels of TrkB and neurotrophin 3 (NT3) increased, but XYS could reverse this trend to a large extent. Curcumin is one of the main components of XYS. Studies have found that it can increase hippocampal neurogenesis in chronically stressed rat and prevent the stress-induced reduction of 5-HT1A mRNA and BDNF protein levels in hippocampal subregions. These two molecules are involved in hippocampal neurogenesis. Moreover, curcumin can reverse or protect hippocampal neurons from chronic stress induced damage by up-regulating the 5-HT1A receptor and

BDNF, which may be the basis of antidepressant effect of curcumin (Xu et al., 2007). In addition, XYS promoted lipopolysaccharide-induced hippocampal neurogenesis by increasing BDNF, nerve growth factor (NGF), TrkB, TrkA, and CREB (Fang et al., 2020). Modified XYS (MXYS) significantly improved body weight and depression-like behavior, up-regulated BDNF level, and restored hippocampal neurogenesis in CUMS exposed mice (Gao et al., 2018). The neurotrophic theory, as the central theory for depression, provides a good explanation for the pathogenesis of depression with some shortcomings. BDNF and TrkB, as the most important members of the neurotrophic factor family, are thought to be closely related to depression, and often work together. Therefore, the antidepressant effects of XYS may be carried out via the BDNF/TrkB signaling pathway (see Figure 4).

3.4 Neuroinflammation

Recent studies have found that neuroinflammation is associated with the occurrence of depression, and that NLRP3 inflammasomes, cytokines, astrocytes, and microglia are all involved. NLRP3 is a regulator of the inflammatory response and can regulate the expression of IL-1β. Microglia are activated during infection or stress, leading to elevated levels of inflammatory factors in the brain that disrupt neuronal structure and function. Astrocytes sense the inflammatory signals activated by microglia. Activated astrocytes are divided into M1 type and M2 type. Those of the M1 type release a variety of pro-inflammatory factors and have neurotoxic effects. Those of the M2 type can up-regulate neurotrophic factors, promote the release of anti-inflammatory factors, and have neuroprotective effects. The secretion of pro-inflammatory cytokines such as IL-1β, IL-6, and TNF-α is increased in patients with depression, while the secretion of anti-inflammatory cytokines such as IL-4 and IL-10, among others, is decreased (Howren et al., 2009; Dowlati et al., 2010). Animal experiments have shown that the lateral ventricular injection of lipopolysaccharides (LPSs) can induce a neuroinflammatory state in the hippocampus and increase the mRNA expression of pro-inflammatory cytokines IL-6 and TNF-α (Tang et al., 2016), which leads to depression-like behavior. Consequently, the occurrence of depression is associated with inflammation. Chen et al. found that XYS could improve depression-like behaviors by regulating the NLRP3 inflammasome in the cerebral cortex of rat exposed to CIS (Chen et al., 2020b). The mitogen-activated protein kinase (MAPK) signaling pathway is involved in a variety of pathological processes. The c-Jun N-terminal kinase (JNK) is part of this pathway, and it plays an important role in apoptosis and neurological diseases. Li et al. suggested that XYS could alleviate hippocampal neuronal injury and reverse the effects measured in the hypertension labyrinth test, through the activation of the TNF-α/Janus kinase 2 (JAK2)/Signal transducer and activator of transcription 3 (STAT3) pathway in a rat model of CIS-induced anxiety (Li et al., 2017). Fang et al. found that Xiaoyao Pills (XYS) could improve the inflammatory response and nerve damage of hippocampal neurons induced by LPSs, as well as down-regulate the levels of inflammation-related cytokines and mediators, thereby exerting neuroprotective effects (Fang et al., 2020). After treatment with XYS, mouse body weight, behavior (as measured in novel, inhibition of feeding, open field, and maze tests), and hippocampal JNK, phosphorylated JNK (pJNK) and phosphorylated c-Jun (pcJun) levels changed, indicating XYS may act in the JNK signaling pathway for chronic stress in a mice depression model (Zhao et al., 2017; Zhao et al., 2020) (see Figure 5).

3.5 Neuroprotection

Yuan et al. found the antidepressant XYS mechanisms were related to neuroprotection using system-network pharmacological analysis (Yuan et al., 2020). Yin et al. found that in reserpine-induced anxiety and depression models, XYS/RTSE improved blood glucose regulation, increased insulin sensitivity, and had a neuroprotective effect on the glial cell injury system (Yin et al., 2012). Li et al. found that XYS reversed the damage observed in the hippocampal structure and function of rat exposed to CIS for 21 days, and had the ability to enhance immunity and stress resistance, promoting the regeneration of nerve cells (Li et al., 2019). Meng et al. found that the XYS decoction may help reducing hippocampal neuron apoptosis induced by oxidative stress, suggesting that the antidepressant effects of XYS may be caused by its protective effects on hippocampal neurons (Meng et al., 2012). Liu et al. found that XYS could protect the hippocampal neurons of ovariectomized rat and restore hippocampal E2 levels, thereby improving cognitive ability (Liu L. et al., 2020).

3.6 Brain-gut axis

The brain-gut axis is a two-way information communication system that integrates the neural, immune, endocrine, and metabolic pathways between the brain and the gastrointestinal tract (GI) (Appleton 2018). The information acquired by exogenous factors such as vision and hearing and endogenous factors such as thinking and emotion is transmitted from the brain to the GI, which then regulates its movements and secretions. Stimulation of the GI can also affect the activity of the central nervous system through the brain-gut axis. Recent studies have shown that functional disorders in the brain-gut microbiota axis plays an important role in the pathogenesis and progression of depression (Chen et al., 2018). Patients with depression have intestinal microbiota disorders, which are manifested as declines in the diversity and richness of the gut microbiota (Aizawa et al., 2016). In fact, regulating of the intestinal microbiota has become a hot topic in neuroscience and psychology, particularly how this affects psychological diseases such as depression and anxiety. Therefore, maintaining the balance of intestinal microbiota to adjust and affect the brain function may be an intervention method of great significance for the prevention and treatment of depression.

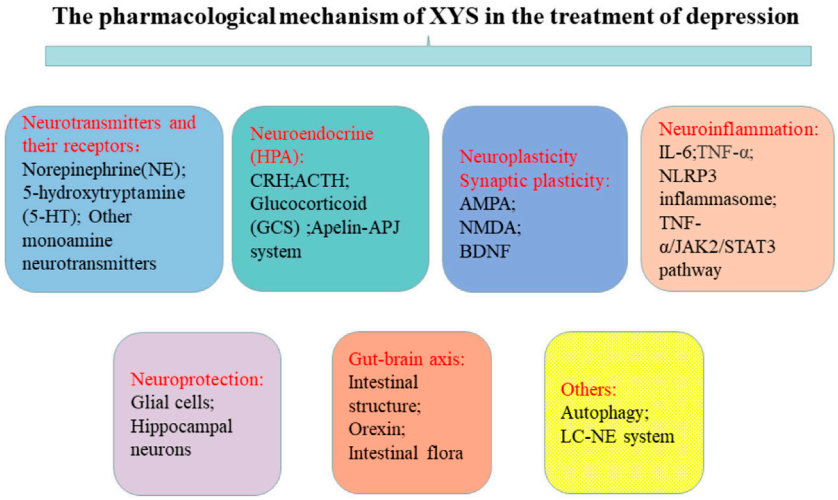

FIGURE 1
Potential therapeutic targets based on the pathogenesis of depression. The treatment goals of depression include neurotransmitters and their receptors, neuroendocrine (HPA), neuroplasticity synaptic plasticity, neuroinflammation, neuroprotection, and the gut-brain axis.

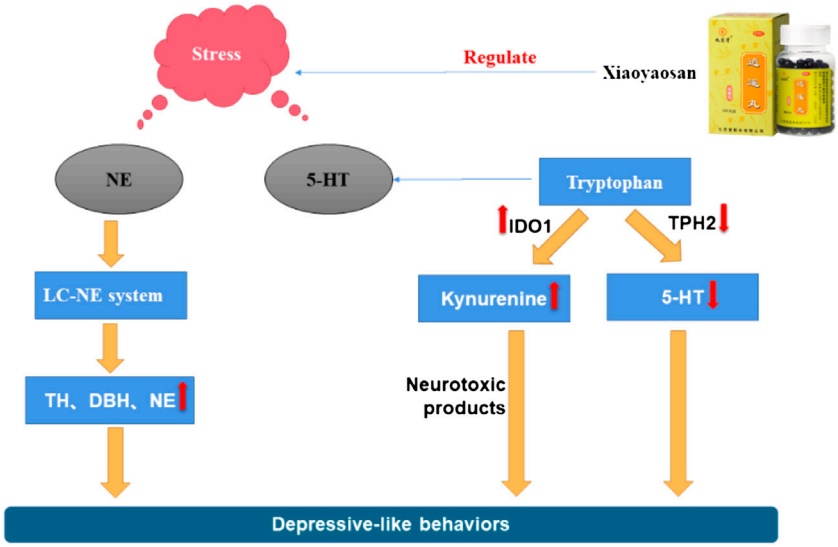

FIGURE 2
Mechanism of the stress-induced changes in NE and 5-HT and the regulating effect of Xiaoyaosan.

3.6.1 Intestinal structure

In rodent models, psychological stimuli and stress increase gut permeability and promote bacteria to the systemic circulation and brain, thereby increasing the underlying incidence of depression. The expression of C-type natriuretic peptide (CNP) and natriuretic peptide receptor (NPR)-B in depressed rat decreased after XYS treatment, suggesting XYS may improve the symptoms of depressive gastrointestinal dysfunction by down-regulating the CNP signaling pathway (Li et al., 2015). Ding et al. found that XYS alleviated depression-like behaviors in rat with CUMS, effectively reversed the pathological and ultrastructural changes in the rat's colon, thereby restoring intestinal permeability, and increased the level of serotonin in the hypothalamus and colonic mucosa (Ding et al., 2020). These results suggested XYS may improve the intestinal barrier function through the brain-gut axis and thus exert an antidepressant effect.

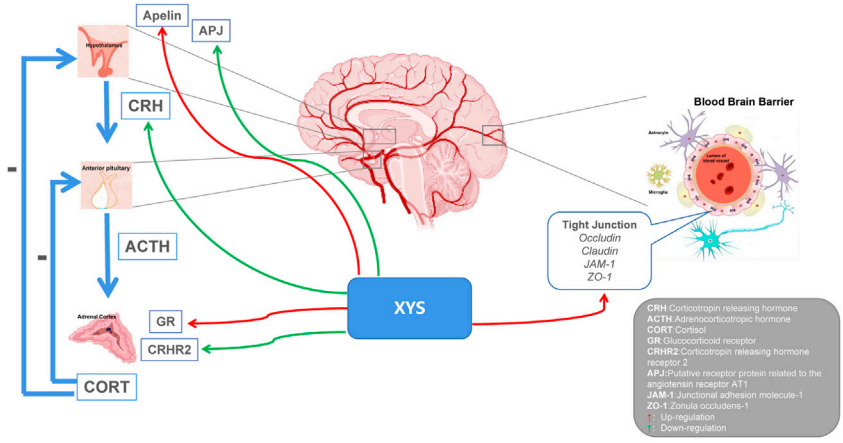

FIGURE 3
Potential relationship between Xiaoyaosan, depression and HPA axis. Xiaoyaosan can up-regulate the level of apelin in the hypothalamus and down-regulate the level of APJ in the hypothalamus. Down-regulation of CRH and CRHR2 levels, up-regulation of GR expression, and regulation of HPA axis hyperactivity. Elevate the expression of tight junction-related genes and reverse the damage of glucocorticoids to the permeability of the blood-brain barrier. Red arrows indicate upregulation. Green arrows indicate downregulation.

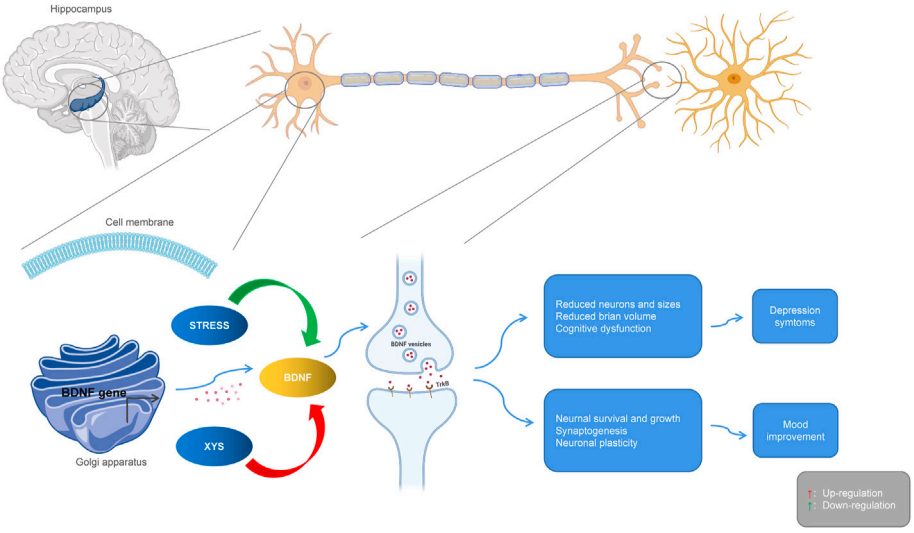

FIGURE 4
Interactions between Xiaoyaosan, depression and BDNF. Stress downregulates BDNF, leading to atrophy and loss of hippocampal neurons, producing depressive symptoms. Xiaoyaosan up-regulates BDNF, promotes neuron survival and synaptogenesis, and improves depressive mood. Red arrows indicate upregulation. Green arrows indicate downregulation.

3.6.2 Orexin, neuropeptide Y (NPY), and proopiomelanocortin (POMC)

Increasing evidence has shown that the orexin system is related to the pathogenesis of depression, and that its regulation is closely related to the occurrence and development of mental diseases. Hou et al. found XYS could increase the expression of orexin A/Oxidation resistance 1 (OXR1) in the lateral hypothalamus of CIS-induced depression rat model, indicating XYS could improve depression symptoms by regulating orexin A/OXR1 (Hou et al., 2020). Ma et al. found that XYS improved anorexia symptoms and depression-like behaviors in rat under CUMS by regulating the hypothalamic nesfatin 1 (NES1)-

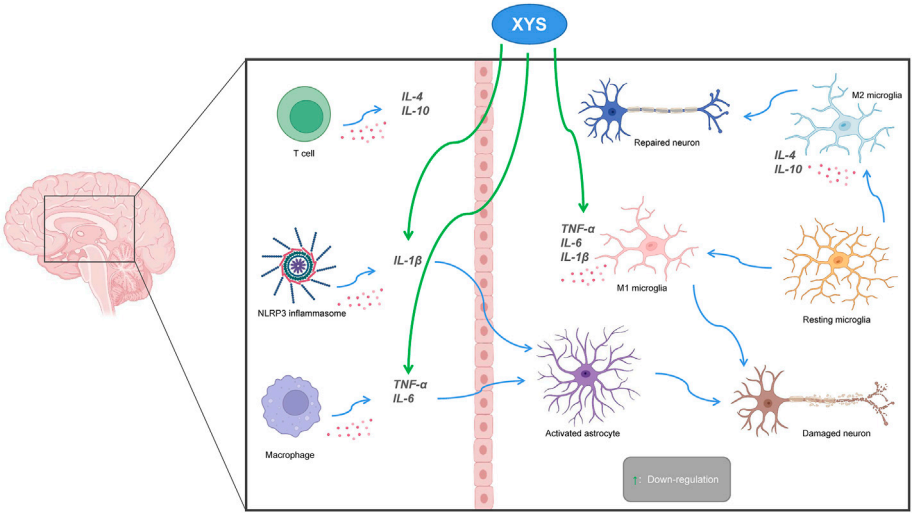

FIGURE 5
The relationship between Xiaoyaosan, depression and neuroinflammation. Pro-inflammatory cytokines (IL 1β, IL6, TNF-α) activate astrocytes, leading to neuronal destruction. Down-regulation of pro-inflammatory cytokines by Xiaoyaosan inhibits activation of astrocytes and avoids neuronal damage. M2 microglia produce anti-inflammatory cytokines (IL4, IL10) that promote neuronal repair. Green arrows indicate downregulation.

TABLE 1 Composition of XYS and Eight ingredients in XYS sample (XYS is derived from "Taiping Huimin Heji Jufang" and is composed of these eight Chinese medicines) (Ding et al., 2017a).

Medicinal plant	Amount(g)
Radix Angelicae Sinensis	15
Radix Paeoniae	15
Radix Bupleuri	15
Radix Glycyrrhizae	6
Poria ((Poria cocos	15
Rhizoma Atractylodis Macrocephalae	15
Herba Menthae	6
Rhizoma Zingiberis Recens	15

Eight ingredients in XYS sample

Ingredient	PubChem CID	Molecular Formula	Molecular Weight	Molecular structure	Separationtechnology	Characterization techniques	References
Palmitic acid	985	C16H32O2	256.42 g/mol	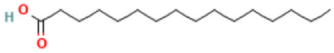	freeze drying, extraction separation	chromatography, spectrometry	Piovesana, Aita et al. (2021)
Curcumin	969516	C21H20O6	368.4 g/mol	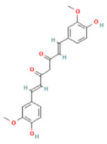	ultrasonic, pressurized liquid extraction, microwave, reflux	chromatography, spectrometry, Fourier transform infrared (FT-IR), Near-infrared (NIR), Raman, and ultraviolet/visible (UV-Vis)	Kotha and Luthria (2019)

(Continued on following page)

TABLE 1 (*Continued*) Composition of XYS and Eight ingredients in XYS sample (XYS is derived from "Taiping Huimin Heji Jufang" and is composed of these eight Chinese medicines) (Ding et al., 2017a).

Medicinal plant	Amount(g)						
Liquiritin	503737	C21H22O9	418.4 g/mol	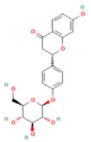	extraction, drying, centrifugal separation	Chromatography, Fourier transform infrared (FTIR), Electrospray ionization mass spectrometry (ESI-MS), 1H Nuclear Magnetic Resonance (NMR) and 13C NMR spectra	Wang, Shan et al. (2020)
Saikosaponin D	107793	C42H68O13	781 g/mol	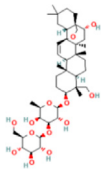	accelerated solvent extraction (ASE), centrifugal separation, drying, heat-reflux extraction, ultrasonic-assisted extraction, solvent-partitioning extraction	High performance liquid chromatography coupled with mass spectrometer (HPLC-MS), Liquid chromatography coupled with tandem mass spectrometry (LC-MS/MS)	Li, Li et al. (2018)
Paeoniflorin	442534	C23H28O11	480.5 g/mol	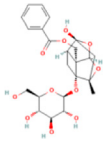	drying, extraction, chromatographic separation	NMR	Papandreou, Magiatis et al. (2002)
Saikosaponin B1	9,875,547	C42H68O13	781 g/mol	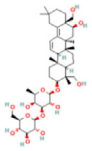	drying, filter separation	High Performance Liquid Chromatography (HPLC)	Ohtake, Nakai et al. (2004)
Atractylenolide II	14,448,070	C15H20O2	232.32 g/mol	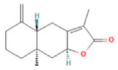	chromatographic separation, drying, extraction	HPLC	Zhang, Liu et al. (2017)
Pachymic acid	5,484,385	C33H52O5	528.8 g/mol	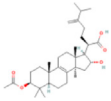	chromatographic separation, extraction	NMR, IR spectra	Zhou, Zhang et al. (2008)

oxytocin (OT)-POMC neural pathway (Ma et al., 2019). Wang et al. found that a XYS decoction could regulate the expression of the leptin receptor (OB-R) and NPY in the hypothalamus of rat under CIS, while relieving discomfort symptoms such as loss of appetite and weight (Wang et al., 2012).

3.6.3 Intestinal microbiota

Patients with depression show symptoms of psychological disorders which are often accompanied by symptoms of gastrointestinal dysfunction, such as functional dyspepsia and irritable bowel syndrome (Xie et al., 2013). They can also have lack of appetite, and variations in body weight are likely to be closely related to maladjustments in the intestinal microbiota. Recent studies indicate that botanicals and active ingredients, including XYS, improve depression-like behaviors by modulating GI microbiota. Furthermore, XYS may have an antidepressant role by regulating intestinal microbiota and its metabolites such as short-chain fatty acids (Zhu et al., 2019). Qiu et al. found XYS could regulate intestinal microbiota dysbiosis in rat with functional dyspepsia and LSSD exposed to CUMS (Qiu et al., 2017). Hao et al. found XYS improved the depressive and anxious behaviors of antibiotic-induced microbiome-depleted (AIMD) mice; the anti-depressant and anti-anxiety effects of XYS may be exerted via intestinal microbiota regulation and inhibition of the

TABLE 2 The clinical application of XYS in the treatment of depression.

Characteristics of study

Study ID	Population	Study design	Sample	Experiment group	Control group	Course (week)	Outcomes	administration pathway	Followup (month)	adverse reaction	relapses
Du, Ming et al. (2014)	functional dyspepsia (FD) associated with perimenopausal depression	RCT	Exp: 90								
			Con: 90	Xiaoyao pill	Placebo	8	HRSD, gastric emptying rate	Exp: 3g, bid	6	none	Exp: 0
								Con: 3g, bid			Con: 5
Chen, Ji et al. (2005)	Liver stagnation and spleen deficiency syndrome (LSSDS)	RCT	Exp: 41								
			Con: 17	Xiao Yao Wan	Zhi Bai Di Huang Wan	4	Self-rating anxiety scale and self-rating depression scale, β-endorphin, Epinephrine and Dopamine	Exp: 8 pills, tid	0	none	Exp: 0
								Con: 8 pills, tid			Con: 0
Su, Fan et al. (2019)	mild to moderate depression with anxiety symptoms	RCT	Exp: 105								
			Con: 105	Jiawei Xiaoyao (JWXY) capsule + sertraline placebo	Sertraline + JWXY placebo	8	HAMD, HAMA and the Clinical Global Impression Scale	Exp: Jiawei Xiaoyao capsule 10 g* 2/d + sertraline placebo	1	Exp: dry mouth, headache, sweating, nausea, dizziness	Exp: 14
										Con: sertraline 50 mg/d + Jiawei Xiaoyao placebo	Con: 21
Zhang et al. (2021b)	type 2 diabetes with comorbid depression of liver spleen deficiency type	RCT	Exp: 46								
			Con: 46	Xiaoyaosan + escitalopram oxalate tablets	escitalopram oxalate tablets	6	HAMD, SDS, FPG, 2 hPG, HbA1c, COR, ACTH	Exp: Xiaoyaosan (Granule, 1 dose/d) + Con			
								Con: 5–10mg, qd	0	none	Exp: 0
											Con: 0

(Continued on following page)

10.3389/fphar.2022.925514

TABLE 2 (*Continued*) The clinical application of XYS in the treatment of depression.

Characteristics of study

Study ID	Population	Study design	Sample	Experiment group	Control group	Course (week)	Outcomes	administration pathway	Followup (month)	adverse reaction	relapses
Liu et al. (2020a)	depression	RCT	Exp: 40								
			Con: 40	Xiaoyaosan + fluoxetine	fluoxetine	8	HAMD, SDS	Exp: Xiaoyaosan (Decoction, 1 dose/d) + Con			
								Con: 20mg, bid	0	Exp: leukopenia, gastrointestinal reactions, dizziness, edema	Exp: 0
										Con: leukopenia, gastrointestinal reactions, dizziness, edema	Con: 0
He. (2019)	mild to moderate depression	RCT	Exp: 46								
			Con: 46	Danzhi Xiaoyaosan	Sertraline	8	HAMD, SDS, 5-HT, CORT, ACTH	Exp: Danzhi Xiaoyaosan (Decoction, 1 dose/d)			
								Con: 50mg, qd	0	Exp: gastrointestinal reactions	
										Con: gastrointestinal reactions	Exp: 0
											Con: 0
Jiang, Zhou et al. (2015)	depression	RCT	Exp: 44								
			Con: 44	Xiaoyaosan + citalopram	citalopram	6	HAMD, CORT, ACTH, T3, T4, TSH, E2	Exp: Xiaoyaosan (Decoction, 1 dose/d) + Con			
								Con: 20mg, qd	0	Exp: nausea, vomiting, tachycardia	
										Con: nausea, vomiting, tachycardia	Exp: 0
											Con: 0

(Continued on following page)

10.3389/fphar.2022.925514

TABLE 2 (*Continued*) The clinical application of XYS in the treatment of depression.

Characteristics of study

Study ID	Population	Study design	Sample	Experiment group	Control group	Course (week)	Outcomes	administration pathway	Followup (month)	adverse reaction	relapses
Yang and Lin, (2015)	mild to moderate depression	RCT	Exp: 30								
			Con: 30	Xiaoyaosan	Flupentixol and Melitracen Tablets	4	HAMD	Exp: Xiaoyaosan (Decoction, 1 dose/d)			
								Con: 10mg, qd	0	none	Exp: 0
											Con: 0
Zhang. 2015	depression	RCT	Exp: 56								
			Con: 56	Xiaoyao pill + sertraline	sertraline	6	HAMD	Exp: Xiaoyao pill (8 pills, tid) + Con			
								Con: 50–100mg, qd/bid	0	none	Exp: 0
											Con: 0
Feng, Tian et al. (2014)	depression	single-arm clinical trials	Exp: 62	Xiaoyaosan	-	8	HAMD, CGI, TCM syndrome scale	Exp: Xiaoyaosan (Decoction, 1 dose/d)	0	Exp: dry mouth, thirst, nausea	Exp: 0
											Con: 0

10.3389/fphar.2022.925514

moderate activation of NLRP3 inflammasomes in the colon (Hao et al., 2021). Zhang et al. found that XYS could effectively improve the progression of colorectal cancer in mice exposed to a Chronic restraint stress (CRS) model, while protecting the integrity of the intestinal barrier, with some regulatory effects of the intestinal microbiota (Zhang et al., 2020).

3.7 Others

Autophagy is a lysosomal-dependent protein degradation pathway, which maintains the homeostasis of the intracellular environment through the degradation and recycling of damaged organelles and long-lived proteins; however, excessive autophagy is damaging (Klionsky et al., 2016). Previous studies have shown that in the process of depression, there is obvious autophagy activation, which leads to decreased survival rates for neurons and glial cells and to neuronal apoptosis (Zschocke et al., 2011). Wang et al. found that mice under CUMS and isolation exhibited depression-like behaviors *in vivo* and exhibited mixed apoptotic/autophagy phenotypes in the hippocampus; modified XYS alleviated neuronal apoptosis by regulating autophagy (Wang M. et al., 2019). Chronic stress induces an increase of NE transporter (NET) in the locus coeruleus, and disorders in the NE system may be one of the most important causes of depression (Chen et al., 2012). Ding et al. found that after exposure to persistent chronic stress, the activated LC-NE system had a significant effect on the occurrence and development of depression in rat (Ding et al., 2014). After Xiaoyao powder (XYS) treatment, the expression of NE, thyroid hormone (TH), and CRF decreased significantly in the experimental group when compared with the control group. These results indicated XYS can effectively improve depression-like behaviors in rat by inhibiting the activity of LC-NE neurons.

4 Conclusion and future directions

Depression presents an ongoing challenge for modern medicine as the pathogenesis of this disease is not fully understood, and there is no definite treatment method that can successfully stop or reverse depression. XYS is an important and valuable traditional Chinese medicine with a high level of safety and efficacy, and it could be used more widely for the treatment of depression in the future. Previous research into the mechanisms of the effects of XYS have been too broad. In the future, rather than only measuring the observed effects of XYS treatment using commercial products, in-depth research on specific genes or pathways with solid experimental basis should be conducted. It is also necessary to examine the existing hypotheses of depression using gene chip technology to detect whole genome changes and clarify the expression trends of each depression-related gene. Furthermore, there is also a lack of high quality standardized clinical studies that include a large number of patients and multiple centers and are performed as high-quality, randomized, double-blind controlled trials to verify the clinical efficacy of XYS for the treatment of depression. The occurrence of disease involves many aspects of body function, and the study of a single pathogenic factor cannot fundamentally clarify the nature of depression. The metabolic transformation of XYS components after entering the human body must also be considered in future investigations. In future studies, we must comprehensively apply various research techniques and methods to clarify the mechanisms of the action of the XYS antidepressant, and further explain these mechanisms using bioinformatics, network pharmacology, and metabolomics, to provide a basis for the research and development of TCM antidepressant drugs.

Author contributions

JC and CL designed the research protocol and write the essay, they contributed equally to this work and share first authorship, QW extracted useful information from included studies, CL downloaded and screened literatures, XL and QM helped check the writing of the essay, JC as main reviewers screened titles and abstracts for eligibility.

Funding

This research work and publication were financially supported by Key Program of National Natural Science Foundation of China (Grant no. 81630104), and National Natural Science Foundation of China (Grant no. 81973748 and Grant no. 82174278).

Acknowledgments

JC and CL designed the research protocol and write the essay, QW extracted useful information from included studies, CL downloaded and screened literatures, XL and QM helped check the writing of the essay, JC as main reviewers screened titles and abstracts for eligibility.

Conflict of interest

The authors declare that the research was conducted in the absence of any commercial or financial relationships that could be construed as a potential conflict of interest.

Publisher's note

All claims expressed in this article are solely those of the authors and do not necessarily represent those of their affiliated

organizations, or those of the publisher, the editors and the reviewers. Any product that may be evaluated in this article, or claim that may be made by its manufacturer, is not guaranteed or endorsed by the publisher.

References

Aizawa, E., Tsuji, H., Asahara, T., Takahashi, T., Teraishi, T., Yoshida, S., et al. (2016). Possible association of Bifidobacterium and Lactobacillus in the gut microbiota of patients with major depressive disorder. *J. Affect. Disord.* 202, 254–257. doi:10.1016/j.jad.2016.05.038

Aleksandrova, L. R., Phillips, A. G., and Wang, Y. T. (2017). Antidepressant effects of ketamine and the roles of AMPA glutamate receptors and other mechanisms beyond NMDA receptor antagonism. *J. Psychiatry Neurosci.* 42 (4), 222–229. doi:10.1503/jpn.160175

Ao, H., Xu, Z., Yan, C., Wu, L., and Wang, W. (2006). The effect of Xiaoxiao Powder on the structural plasticity of hippocampal synaptosomes in chronic stress rats. *Propr. Chin. Med.* 28 (5), 697–700. doi:10.3969/j.issn.1001-1528.2006.05.0

Appleton, J. (2018). The gut-brain axis: Influence of microbiota on mood and mental health. *Integr. Med.* 17 (4), 28–32.

Balu, D. T. (2016). The NMDA receptor and schizophrenia: From pathophysiology to treatment. *Adv. Pharmacol.* 76, 351–382. doi:10.1016/bs.apha.2016.01.006

Bao, L., Chen, J., Huang, L., Chen, W., Lin, Q., Yao, X.-S., et al. (2008). Effects of Xiaoyao Wan on the behavioral despair and stress depression mice. *Zhong Yao Cai* 31 (9), 1360–1364. doi:10.13863/j.issn1001-4454.2008.09.027

Bathina, S., and Das, U. N. (2015). Brain-derived neurotrophic factor and its clinical implications. *Arch. Med. Sci.* 11 (6), 1164–1178. doi:10.5114/aoms.2015.56342

Cai, L., Li, R., Tang, W.-j., Meng, G., Hu, X.-y., Wu, T.-n., et al. (2015). Antidepressant-like effect of geniposide on chronic unpredictable mild stress-induced depressive rats by regulating the hypothalamus–pituitary–adrenal axis. *Eur. Neuropsychopharmacol.* 25 (8), 1332–1341. doi:10.1016/j.euroneuro.2015.04.009

Carpenter, L. L., Moreno, F. A., Kling, M. A., Anderson, G. M., Regenold, W. T., Labiner, D. M., et al. (2004). Effect of vagus nerve stimulation on cerebrospinal fluid monoamine metabolites, norepinephrine, and gamma-aminobutyric acid concentrations in depressed patients. *Biol. Psychiatry* 56 (6), 418–426. doi:10.1016/j.biopsych.2004.06.025

Castrén, E. (2005). Is mood chemistry? *Nat. Rev. Neurosci.* 6 (3), 241–246. doi:10.1038/nrn1629

Chen, C., Yin, Q., Tian, J., Gao, X., Qin, X., Du, G., et al. (2020a). Studies on the potential link between antidepressant effect of Xiaoyao San and its pharmacological activity of hepatoprotection based on multi-platform metabolomics. *J. Ethnopharmacol.* 249, 112432. doi:10.1016/j.jep.2019.112432

Chen, C., Yu, R., Xue, Z., Yan, Z., Bian, Q., Hou, Y., et al. (2020b). Xiaoyaosan improves depressive-like behaviors by regulating the NLRP3 signaling pathway in the rat cerebral cortex. *J. Traditional Chin. Med. Sci.* 7 (3), 265–273. doi:10.1016/j.jtcms.2020.08.001

Chen, J.-j., Zheng, P., Liu, Y.-y., Zhong, X.-g., Wang, H.-y., Guo, Y.-j., et al. (2018). Sex differences in gut microbiota in patients with major depressive disorder. *Neuropsychiatr. Dis. Treat.* 14, 647–655. doi:10.2147/NDT.S159322

Chen, J.-X., Ji, B., Lu, Z.-L., and Hu, L.-S. (2005). Effects of chai hu (radix burpleuri) containing formulation on plasma beta-endorphin, epinephrine and dopamine on patients. *Am. J. Chin. Med.* 33 (05), 737–745. doi:10.1142/S0192415X05003296

Chen, J.-X., Li, W., Zhao, X., and Yang, J.-X. (2008a). Effects of the Chinese traditional prescription Xiaoyaosan decoction on chronic immobilization stress-induced changes in behavior and brain BDNF, TrkB, and NT-3 in rats. *Cell. Mol. Neurobiol.* 28 (5), 745–755. doi:10.1007/s10571-007-9169-6

Chen, J.-X., Tang, Y.-T., and Yang, J.-X. (2008b). Changes of glucocorticoid receptor and levels of CRF mRNA, POMC mRNA in brain of chronic immobilization stress rats. *Cell. Mol. Neurobiol.* 28 (2), 237–244. doi:10.1007/s10571-007-9170-0

Chen, P., Fan, Y., Li, Y., Sun, Z., Bissette, G., Zhu, M.-Y., et al. (2012). Chronic social defeat up-regulates expression of norepinephrine transporter in rat brains. *Neurochem. Int.* 60 (1), 9–20. doi:10.1016/j.neuint.2011.11.003

Coleman, P., Federoff, H., and Kurlan, R. (2004). A focus on the synapse for neuroprotection in Alzheimer disease and other dementias. *Neurology* 63 (7), 1155–1162. doi:10.1212/01.wnl.0000140626.48118.0a

Ding, F., Wu, J., Liu, C., Bian, Q., Qiu, W., Ma, Q., et al. (2020). Effect of Xiaoyaosan on colon morphology and intestinal permeability in rats with chronic unpredictable mild stress. *Front. Pharmacol.* 11, 1069. doi:10.3389/fphar.2020.01069

Ding, X.-F., Li, Y.-H., Chen, J.-X., Sun, L.-J., Jiao, H.-Y., Wang, X.-X., et al. (2017a). Involvement of the glutamate/glutamine cycle and glutamate transporter GLT-1 in antidepressant-like effects of Xiao Yao san on chronically stressed mice. *BMC Complement. Altern. Med.* 17 (1), 326. doi:10.1186/s12906-017-1830-0

Ding, X.-F., Liu, Y., Yan, Z.-Y., Li, X.-J., Ma, Q.-Y., Jin, Z.-Y., et al. (2017b). Involvement of normalized glial fibrillary acidic protein expression in the hippocampi in antidepressant-like effects of xiaoyaosan on chronically stressed mice. *Evidence-Based Complementary Altern. Med.* 2017, 1–13. doi:10.1155/2017/1960584

Ding, X.-F., Zhao, X.-H., Tao, Y., Zhong, W.-C., Fan, Q., Diao, J.-X., et al. (2014). Xiao yao san improves depressive-like behaviors in rats with chronic immobilization stress through modulation of locus coeruleus-norepinephrine system. *Evid. Based. Complement. Altern. Med.* 2014, 605914. doi:10.1155/2014/605914

Dowlati, Y., Herrmann, N., Swardfager, W., Liu, H., Sham, L., Reim, E. K., et al. (2010). A meta-analysis of cytokines in major depression. *Biol. Psychiatry* 67 (5), 446–457. doi:10.1016/j.biopsych.2009.09.033

Du, H.-G., Ming, L., Chen, S.-J., and Li, C.-D. (2014). Xiaoyao pill for treatment of functional dyspepsia in perimenopausal women with depression. *World J. Gastroenterol.* 20 (44), 16739–16744. doi:10.3748/wjg.v20.i44.16739

Duffy, B., Chun, K., Ma, D., Lythgoe, M., and Scott, R. (2014). Dexamethasone exacerbates cerebral edema and brain injury following lithium-pilocarpine induced status epilepticus. *Neurobiol. Dis.* 63, 229–236. doi:10.1016/j.nbd.2013.12.001

Fang, Y., Shi, B., Liu, X., Luo, J., Rao, Z., Liu, R., et al. (2020). Xiaoyao Pills attenuate inflammation and nerve injury induced by lipopolysaccharide in hippocampal neurons *in vitro*. *Neural Plast.* 2020, 8841332. doi:10.1155/2020/8841332

Fathinezhad, Z., Sewell, R. D., Lorigooini, Z., and Rafieian-Kopaei, M. (2019). Depression and treatment with effective herbs. *Curr. Pharm. Des.* 25 (6), 738–745. doi:10.2174/1381612825666190402105803

Felger, C. J. (2016). The role of dopamine in inflammation-associated depression: Mechanisms and therapeutic implications. *Curr. Top. Behav. Neurosci.* 31, 199–219. (Chapter 13). doi:10.1007/7854_2016_13

Feng, G., Tian, J., Wu, Y., Zhao, S., Zhang, L., and Qin, X. (2014). Xiaoyao powder treating depression clinical research [J]. *J. liaoning traditional Chin. Med. J.* 9 (3), 512–516. doi:10.13192/j.issn.1000-1719.2014.03.055

Ferrari, A., Somerville, A., Baxter, A., Norman, R., Patten, S., Vos, T., et al. (2013). Global variation in the prevalence and incidence of major depressive disorder: A systematic review of the epidemiological literature. *Psychol. Med.* 43 (3), 471–481. doi:10.1017/S0033291712001511

Figueiredo, F. P., Parada, A. P., Araujo, L., Jr, W. S., and Del-Ben, C. M. (2015). The influence of genetic factors on peripartum depression: A systematic review. *J. Affect. Disord.* 172, 265–273. doi:10.1016/j.jad.2014.10.016

Gao, J., Inagaki, Y., Li, X., Kokudo, N., and Tang, W. (2013). Research progress on natural products from traditional Chinese medicine in treatment of Alzheimer's disease. *Drug Discov. Ther.* 7 (2), 46–57. doi:10.5582/ddt.2013.v7.2.46

Gao, L., Huang, P., Dong, Z., Gao, T., Huang, S., Zhou, C., et al. (2018). Modified xiaoyaosan (MXYS) exerts anti-depressive effects by rectifying the brain blood oxygen level-dependent fMRI signals and improving hippocampal neurogenesis in mice. *Front. Pharmacol.* 9, 1098. doi:10.3389/fphar.2018.01098

Gilman, S. R., Iossifov, I., Dan, L., Ronemus, M., Wigler, M., Vitkup, D., et al. (2011). Rare de novo variants associated with autism implicate a large functional network of genes involved in formation and function of synapses. *Neuron* 70 (5), 898–907. doi:10.1016/j.neuron.2011.05.021

Grace, A. (2016). Dysregulation of the dopamine system in the pathophysiology of schizophrenia and depression. *Nat. Rev. Neurosci.* 17, 524–532. doi:10.1038/nrn.2016.57

Guo, X., Qiu, W., Liu, Y., Zhang, Y., Zhao, H., Chen, J., et al. (2017). Effects of refined xiaoyaosan on depressive-like behaviors in rats with chronic unpredictable

mild stress through neurosteroids, their synthesis and metabolic enzymes. *Molecules* 22 (8), E1386. doi:10.3390/molecules22081386

Hao, W., Wu, J., Yuan, N., Gong, L., Huang, J., Ma, Q., et al. (2021). Xiaoyaosan improves antibiotic-induced depressive-like and anxiety-like behavior in mice through modulating the gut microbiota and regulating the NLRP3 inflammasome in the colon. *Front. Pharmacol.* 12, 619103. doi:10.3389/fphar.2021.619103

He, X. (2019). Clinical observation and mechanism study of Danzhi Xiaoyao Powder in the treatment of mild and moderate depression [J]. *famous Dr.* 26 (02).

Health Quality, O. (2017). Psychotherapy for major depressive disorder and generalized anxiety disorder: A health technology assessment. *Ont. Health Technol. Assess. Ser.* 17 (15), 1–167.

Henter, I. D., de Sousa, R. T., and Zarate, C. A., Jr (2018). Glutamatergic modulators in depression. *Harv. Rev. Psychiatry* 26 (6), 307–319. doi:10.1097/HRP.0000000000000183

Hou, Y., Liu, Y., Liu, C., Yan, Z., Ma, Q., Chen, J., et al. (2020). Xiaoyaosan regulates depression-related behaviors with physical symptoms by modulating Orexin A/OxR1 in the hypothalamus. *Anat. Rec.* 303 (8), 2144–2153. doi:10.1002/ar.24386

Howren, M. B., Lamkin, D. M., and Suls, J. (2009). Associations of depression with C-reactive protein, IL-1, and IL-6: A meta-analysis. *Psychosom. Med.* 71 (2), 171–186. doi:10.1097/PSY.0b013e3181907c1b

Jiang, J., Zhou, Y., Yang, Y., and Liang, L. (2015). Effect of xiaoxiao Powder plus citalopram on HPA, HPT and HPG axis of depression [J]. *J. Mod. Integr. Chin. West. Med.* 24 (33), 3715–3717. doi:10.3969/j.issn.1008-8849.2015.33.026

Jiao, H., Yan, Z., Ma, Q., Li, X., Jiang, Y., Liu, Y., et al. (2019). Influence of Xiaoyaosan on depressive-like behaviors in chronic stress-depressed rats through regulating tryptophan metabolism in hippocampus. *Neuropsychiatr. Dis. Treat.* 15, 21–31. doi:10.2147/NDT.S185295

Jin, X., Jiang, M., Gong, D., Chen, Y., and Fan, Y. (2018). Efficacy and safety of xiaoyao formula as an adjuvant treatment for post-stroke depression: A meta-analysis. *Explore* 14 (3), 224–229. doi:10.1016/j.explore.2017.12.007

Kim, J. H., Park, Y. K., Kim, J. H., Kwon, T. H., and Chung, H. S. (2006). Transient recovery of synaptic transmission is related to rapid energy depletion during hypoxia. *Neurosci. Lett.* 400 (1-2), 1–6. doi:10.1016/j.neulet.2006.01.035

Klionsky, D. J., Abdelmohsen, K., Abe, A., Abedin, M. J., Abeliovich, H., Acevedo Arozena, A., et al. (2016). Guidelines for the use and interpretation of assays for monitoring autophagy (3rd edition). *autophagy* 12 (1), 1–222. doi:10.1080/15548627.2015.1100356

Kong, M., Xing, C.-Y., and Shu, X.-C. (2010). Influence of ease powder decoction on expression of Hippocampus 5-HT_ (1A) receptor and 5-HT_ (2A) receptor in rat model of sleep deprivation depression [J]. *Chin. J. Exp. Traditional Med. Formulae* 14. doi:10.13422/j.cnki.syfjx.2010.14.063

Kotha, R. R., and Luthria, D. L. (2019). Curcumin: Biological, pharmaceutical, nutraceutical, and analytical aspects. *Molecules* 24 (16), 2930. doi:10.3390/molecules24162930

Kou, M.-J., and Chen, J.-X. (2012). Integrated traditional and western medicine for treatment of depression based on syndrome differentiation: A meta-analysis of randomized controlled trials based on the Hamilton depression scale. *J. Traditional Chin. Med.* 32 (1), 1–5. doi:10.1016/s0254-6272(12)60023-5

Kumar, A., and Sharma, B. (2022). Biomedical implications of plant-based principles as antidepressants: Prospects for novel drug development. *Mini Rev. Med. Chem.* 22 (6), 904–926. doi:10.2174/1389557521666210415112601

Li, P., Tang, X.-D., Cai, Z.-X., Qiu, J.-J., Lin, X.-L., Zhu, T., et al. (2015). CNP signal pathway up-regulated in rectum of depressed rats and the interventional effect of Xiaoyaosan. *World J. Gastroenterol.* 21 (5), 1518–1530. doi:10.3748/wjg.v21.i5.1518

Li, X.-H., Zhou, X.-M., Li, X.-J., Liu, Y.-Y., Liu, Q., Guo, X.-L., et al. (2019). Effects of Xiaoyaosan on the hippocampal gene expression profile in rats subjected to chronic immobilization stress. *Front. Psychiatry* 10, 178. doi:10.3389/fpsyt.2019.00178

Li, X.-J., Ma, Q.-Y., Jiang, Y.-M., Bai, X.-H., Yan, Z.-Y., Liu, Q., et al. (2017). Xiaoyaosan exerts anxiolytic-like effects by down-regulating the TNF-α/JAK2-STAT3 pathway in the rat hippocampus. *Sci. Rep.* 7 (1), 353. doi:10.1038/s41598-017-00496-y

Li, X., Li, X., Huang, N., Liu, R., and Sun, R. (2018). A comprehensive review and perspectives on pharmacology and toxicology of saikosaponins. *Phytomedicine* 50, 73–87. doi:10.1016/j.phymed.2018.09.174

Liang, Y., Chen, J., Guo, X., Yue, G., Yang, M., and Ge, G. (2009). Effect of xiaoyao powder on neuron ultrastructure of limbic system in rats with liver depression and spleen deficiency. *China J. traditional Chin. Med.* 24 (05), 577–581.

Liang, Y., Guo, X.-L., Chen, J.-X., and Yue, G.-X. (2013). Effects of the Chinese traditional prescription Xiaoyaosan decoction on chronic immobilization stress-induced changes in behavior and ultrastructure in rat hippocampus. *Evidence-Based Complementary Altern. Med.* 2013, 1–8. doi:10.1155/2013/984797

Liu, J., Fang, Y., Yang, L., Qin, X., Du, G., Gao, X., et al. (2015). A qualitative, and quantitative determination and pharmacokinetic study of four polyacetylenes from Radix Bupleuri by UPLC-PDA–MS. *J. Pharm. Biomed. Anal.* 111, 257–265. doi:10.1016/j.jpba.2015.04.002

Liu, J., Lin, J., Liu, Z., and Pan, Z. (2020a). Clinical observation of modified xiaoyao SAN combined with fluoxetine hydrochloride in the treatment of depression [J]. *Chin. Folk. Ther.* 28 (06), 58–60. doi:10.19621/j.cnki.11-3555/r.2020.0628

Liu, L., Ge, F., Yang, H., Shi, H., Lu, W., Sun, Z., et al. (2020b). Xiao-Yao-San formula improves cognitive ability by protecting the hippocampal neurons in ovariectomized rats. *Evid. Based. Complement. Altern. Med.* 2020, 4156145. doi:10.1155/2020/4156145

Liu, X., Liu, C., Tian, J., Gao, X., Li, K., Du, G., et al. (2020c). Plasma metabolomics of depressed patients and treatment with Xiaoyaosan based on mass spectrometry technique. *J. Ethnopharmacol.* 246, 112219. doi:10.1016/j.jep.2019.112219

Liu, Y., Ding, X.-f., Wang, X.-x., Zou, X.-j., Li, X.-j., Liu, Y.-y., et al. (2019). Xiaoyaosan exerts antidepressant-like effects by regulating the functions of astrocytes and EAATs in the prefrontal cortex of mice. *BMC Complement. Altern. Med.* 19 (1), 215. doi:10.1186/s12906-019-2613-6

Lu, J., Fu, L., Qin, G., Shi, P., and Fu, W. (2018). The regulatory effect of Xiaoyao San on glucocorticoid receptors under the condition of chronic stress. *Cell. Mol. Biol.* 64 (6), 103–109. doi:10.14715/cmb/2018.64.6.17

Ma, Q., Li, X., Yan, Z., Jiao, H., Wang, T., Hou, Y., et al. (2019). Xiaoyaosan ameliorates chronic immobilization stress-induced depression-like behaviors and anorexia in rats: The role of the nesfatin-1–oxytocin–proopiomelanocortin neural pathway in the hypothalamus. *Front. Psychiatry* 10, 910. doi:10.3389/fpsyt.2019.00910

Machaalani, R., and Chen, H. (2018). Brain derived neurotrophic factor (BDNF), its tyrosine kinase receptor B (TrkB) and nicotine. *Neurotoxicology* 65, 186–195. doi:10.1016/j.neuro.2018.02.014

Man, C., Li, C., Gong, D., Xu, J., and Fan, Y. (2014). Meta-analysis of Chinese herbal Xiaoyao formula as an adjuvant treatment in relieving depression in Chinese patients. *Complement. Ther. Med.* 22 (2), 362–370. doi:10.1016/j.ctim.2014.02.001

Mathers, C. (2008). *The global burden of disease: 2004 update*. Geneva: World Health Organization.

McDonald, J. W., and Johnston, M. V. (1990). Physiological and pathophysiological roles of excitatory amino acids during central nervous system development. *Brain Res. Brain Res. Rev.* 15 (1), 41–70. doi:10.1016/0165-0173(90)90011-c

Meng, Z.-Z., Chen, J.-X., Jiang, Y.-M., and Zhang, H.-T. (2013). Effect of xiaoyaosan decoction on learning and memory deficit in rats induced by chronic immobilization stress. *Evidence-Based Complementary Altern. Med.* 2013, 1–8. doi:10.1155/2013/297154

Meng, Z.-z., Hu, J.-h., Chen, J.-x., and Yue, G.-x. (2012). Xiaoyaosan decoction, a traditional Chinese medicine, inhibits oxidative-stress-induced hippocampus neuron apoptosis *in vitro*. *Evid. Based. Complement. Altern. Med.* 2012, 489254. doi:10.1155/2012/489254

Moriguchi, S., Takamiya, A., Noda, Y., Horita, N., Wada, M., Tsugawa, S., et al. (2019). Glutamatergic neurometabolite levels in major depressive disorder: A systematic review and meta-analysis of proton magnetic resonance spectroscopy studies. *Mol. Psychiatry* 24 (7), 952–964. doi:10.1038/s41380-018-0252-9

Ohtake, N., Nakai, Y., Yamamoto, M., Sakakibara, I., Takeda, S., Amagaya, S., et al. (2004). Separation and isolation methods for analysis of the active principles of Sho-saiko-to (SST) oriental medicine. *J. Chromatogr. B Anal. Technol. Biomed. Life Sci.* 812 (1-2), 135–148. doi:10.1016/j.jchromb.2004.06.051

Olloquequi, J., Cornejo-Córdova, E., Verdaguer, E., Soriano, F. X., Binvignat, O., Auladell, C., et al. (2018). Excitotoxicity in the pathogenesis of neurological and psychiatric disorders: Therapeutic implications. *J. Psychopharmacol.* 32, 265–275. doi:10.1177/0269881118754680

Papandreou, V., Magiatis, P., Kalpoutzakis, E., Skaltsounis, A.-L., and Harvala, C. (2002). Paeonicluside, a new salicylic glycoside from the Greek endemic species Paeonia clusii. *Z. Naturforsch. C J. Biosci.* 57 (3-4), 235–238. doi:10.1515/znc-2002-3-406

Piovesana, S., Aita, S. E., Cannazza, G., Capriotti, A. L., Cavaliere, C., Cerrato, A., et al. (2021). In-depth cannabis fatty acid profiling by ultra-high performance liquid chromatography coupled to high resolution mass spectrometry. *Talanta* 228, 122249. doi:10.1016/j.talanta.2021.122249

Qin, X., Li, P., Han, M., Liu, Z., and Liu, J. (2010). Systematic review of randomize controlled trials of Xiaoyao powder in treatment of depression. *J. Traditional Chin. Med.* (06), 500–505. doi:10.13288/j.11-2166/r.2010.06.007

Qiu, J.-J., Liu, Z., Zhao, P., Wang, X.-J., Li, Y.-C., Sui, H., et al. (2017). Gut microbial diversity analysis using Illumina sequencing for functional dyspepsia with liver depression-spleen deficiency syndrome and the interventional Xiaoyaosan in a rat model. *World J. Gastroenterol.* 23 (5), 810–816. doi:10.3748/wjg.v23.i5.810

Raič, M. (2017). Depression and heart diseases: Leading health problems. *Psychiatr. Danub.* 29 (Suppl. 4), 770–777.

Sarris, J., Panossian, A., Schweitzer, I., Stough, C., and Scholey, A. (2011). Herbal medicine for depression, anxiety and insomnia: A review of psychopharmacology and clinical evidence. *Eur. Neuropsychopharmacol.* 21 (12), 841–860. doi:10.1016/j.euroneuro.2011.04.002

Siddiqi, N. J., de Lourdes Pereira, M., and Sharma, B. (2022). Neuroanatomical, biochemical, and functional modifications in brain induced by treatment with antidepressants. *Mol. Neurobiol.* 59 (6), 3564–3584. doi:10.1007/s12035-022-02780-z

Smith, K. (2014). Mental health: A world of depression. *Nature* 515 (7526), 181. doi:10.1038/515180a

Song, M., Zhang, J., Li, X., Liu, Y., Wang, T., Yan, Z., et al. (2020). Effects of xiaoyaosan on depressive-like behaviors in rats with chronic unpredictable mild stress through HPA Axis induced astrocytic activities. *Front. Psychiatry* 11, 545823. doi:10.3389/fpsyt.2020.545823

Su, R., Fan, J., Li, T., Cao, X., Zhou, J., Han, Z., et al. (2019). Jiawei xiaoyao capsule treatment for mild to moderate major depression with anxiety symptoms: A randomized, double-blind, double-dummy, controlled, multicenter, parallel-treatment trial. *J. Tradit. Chin. Med.* 39 (3), 410–417. doi:10.19852/j.cnki.jtcm.2019.03.014

Südhof, T. C. (2008). Neuroligins and neurexins link synaptic function to cognitive disease. *Nature* 455 (7215), 903–911. doi:10.1038/nature07456

Sullivan, P. F., Neale, M. C., and Kendler, K. S. (2000). Genetic epidemiology of major depression: review and meta-analysis. *Am. J. Psychiatry* 157 (10), 1552–1562. doi:10.1176/appi.ajp.157.10.1552

Tang, M.-m., Lin, W.-j., Pan, Y.-q., Guan, X.-t., and Li, Y.-c. (2016). Hippocampal neurogenesis dysfunction linked to depressive-like behaviors in a neuroinflammation induced model of depression. *Physiol. Behav.* 161, 166–173. doi:10.1016/j.physbeh.2016.04.034

Tian, J.-S., Peng, G.-J., Wu, Y.-F., Zhou, J.-J., Xiang, H., Gao, X.-X., et al. (2016). A GC–MS urinary quantitative metabolomics analysis in depressed patients treated with TCM formula of Xiaoyaosan. *J. Chromatogr. B Anal. Technol. Biomed. Life Sci.* 1026, 227–235. doi:10.1016/j.jchromb.2015.12.026

Vos, T., Barber, R. M., Bell, B., Bertozzi-Villa, A., Biryukov, S., Bolliger, I., et al. (2015). Global, regional, and national incidence, prevalence, and years lived with disability for 301 acute and chronic diseases and injuries in 188 countries, 1990–2013: A systematic analysis for the global burden of disease study 2013. *Lancet* 386 (9995), 743–800. doi:10.1016/S0140-6736(15)60692-4

Walker, E. R., McGee, R. E., and Druss, B. G. (2015). Mortality in mental disorders and global disease burden implications: A systematic review and meta-analysis. *JAMA psychiatry* 72 (4), 334–341. doi:10.1001/jamapsychiatry.2014.2502

Wang, C., Wu, C., Yan, Z., and Cheng, X. (2019a). Ameliorative effect of Xiaoyao-jieyu-san on post-stroke depression and its potential mechanisms. *J. Nat. Med.* 73 (1), 76–84. doi:10.1007/s11418-018-1243-5

Wang, H., Shan, H., and Lü, H. (2020). Preparative separation and purification of liquiritin and glycyrrhizic acid from Glycyrrhiza uralensis fisch by high-speed countercurrent chromatography. *J. Chromatogr. Sci.* 58 (9), 823–830. doi:10.1093/chromsci/bmaa050

Wang, J., Li, X., He, S., Hu, L., Guo, J., Huang, X., et al. (2018a). Regulation of the kynurenine metabolism pathway by Xiaoyao San and the underlying effect in the hippocampus of the depressed rat. *J. Ethnopharmacol.* 214, 13–21. doi:10.1016/j.jep.2017.11.037

Wang, M., Bi, Y., Zeng, S., Liu, Y., Shao, M., Liu, K., et al. (2019b). Modified Xiaoyao San ameliorates depressive-like behaviors by triggering autophagosome formation to alleviate neuronal apoptosis. *Biomed. Pharmacother.* 111, 1057–1065. doi:10.1016/j.biopha.2018.12.141

Wang, M., Huang, W., Gao, T., Zhao, X., and Lv, Z. (2018b). Effects of Xiao yao san on interferon-α-induced depression in mice. *Brain Res. Bull.* 139, 197–202. doi:10.1016/j.brainresbull.2017.12.001

Wang, S.-X., Chen, J.-X., Yue, G.-X., Bai, M.-H., Kou, M.-J., Jin, Z.-Y., et al. (2012). Xiaoyaosan decoction regulates changes in neuropeptide y and leptin receptor in the rat arcuate nucleus after chronic immobilization stress. *Evidence-Based Complementary Altern. Med.* 2012, 1–16. doi:10.1155/2012/381278

Wang, T., and Qin, F. (2010). Effects of Chinese herbal medicine Xiaoyao Powder on monoamine neurotransmitters in hippocampus of rats with postpartum depression. *Zhong xi yi jie he xue bao= J. Chin. Integr. Med.* 8 (11), 1075–1079. doi:10.3736/jcim20101112

Whitehead, G., Regan, P., Whitcomb, D. J., and Cho, K. (2017). Ca2+-permeable AMPA receptor: A new perspective on amyloid-beta mediated pathophysiology of alzheimer's disease. *Neuropharmacology* 112, 221–227. doi:10.1016/j.neuropharm.2016.08.022

Wu, L.-L., Liu, Y., Yan, C., Pan, Y., Su, J.-F., Wu, W.-K., et al. (2016). Antidepressant-like effects of fractions prepared from danzhi-xiaoyao-san decoction in rats with chronic unpredictable mild stress: Effects on hypothalamic-pituitary-adrenal axis, arginine vasopressin, and neurotransmitters. *Evid. Based. Complement. Altern. Med.* 2016, 6784689. doi:10.1155/2016/6784689

Wu, R., Zhu, D., Xia, Y., Wang, H., Tao, W., Xue, W., et al. (2015). A role of yueju in fast-onset antidepressant action on major depressive disorder and serum BDNF expression: A randomly double-blind, fluoxetine-adjunct, placebo-controlled, pilot clinical study. *Neuropsychiatr. Dis. Treat.* 11, 2013–2021. doi:10.2147/NDT.S86585

Xi, S., Yue, G., Liu, Y., Wang, Y., Qiu, Y., Li, Z., et al. (2020). Free Wanderer Powder regulates AMPA receptor homeostasis in chronic restraint stress-induced rat model of depression with liver-depression and spleen-deficiency syndrome. *Aging (Albany NY)* 12 (19), 19563–19584. doi:10.18632/aging.103912

Xie, Y., Huang, X., Hu, S.-y., Qiu, X.-j., Zhang, Y.-j., Ren, P., et al. (2013). Meranzin hydrate exhibits anti-depressive and prokinetic-like effects through regulation of the shared alpha 2-adrenoceptor in the brain–gut axis of rats in the forced swimming test. *Neuropharmacology* 67, 318–325. doi:10.1016/j.neuropharm.2012.10.003

Xu, Y., Ku, B., Cui, L., Li, X., Barish, P. A., Foster, T. C., et al. (2007). Curcumin reverses impaired hippocampal neurogenesis and increases serotonin receptor 1A mRNA and brain-derived neurotrophic factor expression in chronically stressed rats. *Brain Res.* 1162, 9–18. doi:10.1016/j.brainres.2007.05.071

Yan, Z., Jiao, H., Ding, X., Ma, Q., Li, X., Pan, Q., et al. (2018). Xiaoyaosan improves depressive-like behaviors in mice through regulating apelin-APJ system in hypothalamus. *Molecules* 23 (5), 1073. doi:10.3390/molecules23051073

Yang, C., and Lin, H. (2015). Observation of xiaoyao powder in treatment of 30 cases of mild and moderate depression [J]. *J. Pract. traditional Chin. Med.* 31 (05), 381. doi:10.3969/j.issn.1004-2814.2015.05.010

Yao, Y., Huang, H.-Y., Yang, Y.-X., and Guo, J.-Y. (2015). Cinnamic aldehyde treatment alleviates chronic unexpected stress-induced depressive-like behaviors via targeting cyclooxygenase-2 in mid-aged rats. *J. Ethnopharmacol.* 162, 97–103. doi:10.1016/j.jep.2014.12.047

Yin, S.-H., Wang, C.-C., Cheng, T.-J., Chang, C.-Y., Lin, K.-C., Kan, W.-C., et al. (2012). Room-temperature super-extraction system (RTSES) optimizes the anxiolytic-and antidepressant-like behavioural effects of traditional Xiao-Yao-San in mice. *Chin. Med.* 7 (1), 24. doi:10.1186/1749-8546-7-24

Yu, S., Fu, L., Lu, J., Wang, Z., and Fu, W. (2020). Xiao-Yao-San reduces blood-brain barrier injury induced by chronic stress *in vitro* and vivo via glucocorticoid receptor-mediated upregulation of Occludin. *J. Ethnopharmacol.* 246, 112165. doi:10.1016/j.jep.2019.112165

Yuan, N., Gong, L., Tang, K., He, L., Hao, W., Li, X., et al. (2020). An integrated pharmacology-based analysis for antidepressant mechanism of Chinese herbal formula Xiao-Yao-San. *Front. Pharmacol.* 11, 284. doi:10.3389/fphar.2020.00284

Zhang, H., Yue, G., Liang, Y., Yang, J., Li, Y., Wu, W., et al. (2021a). Effect of Xiaoyaosan on central dopamine and its receptors in chronic mild unpredictable stress depression rats. *Chin. J. Basic Med.* 27 (11), 1725–1730. doi:10.19945/j.cnki.issn.1006-3250.2021.11.012

Zhang, J. (2015). Clinical observation of xiaoyao pill combined with sertraline in the treatment of depression [J]. *Chin. Med. Sci.* 5 (05), 75–79.

Zhang, J., Lin, J., and Ji, B. (2021b). Clinical observation of Xiaoyao Powder in treatment of type 2 diabetes comorbidities depression disorder [J]. *Hebei Tradit. Chin. Med.* 43 (12), 1979–1983. doi:10.3969/j.issn.1002-2619.2021.12.010

Zhang, N., Liu, C., Sun, T.-M., Ran, X.-K., Kang, T.-G., Dou, D.-Q., et al. (2017). Two new compounds from Atractylodes macrocephala with neuroprotective activity. *J. Asian Nat. Prod. Res.* 19 (1), 35–41. doi:10.1080/10286020.2016.1247351

Zhang, S., Liu, X., Sun, M., Zhang, Q., Li, T., Li, X., et al. (2018). Reversal of reserpine-induced depression and cognitive disorder in zebrafish by sertraline and Traditional Chinese Medicine (TCM). *Behav. Brain Funct.* 14 (1), 13. doi:10.1186/s12993-018-0145-8

Zhang, Y., Han, M., Liu, Z., Wang, J., He, Q., and Liu, J. (2012). Chinese herbal formula xiao yao san for treatment of depression: A systematic review of randomized controlled trials. *Evidence-Based Complementary Altern. Med.* 2012. doi:10.1155/2012/931636

Zhang, Z., Shao, S., Zhang, Y., Jia, R., Hu, X., Liu, H., et al. (2020). Xiaoyaosan slows cancer progression and ameliorates gut dysbiosis in mice with chronic restraint stress and colorectal cancer xenografts. *Biomed. Pharmacother.* 132, 110916. doi:10.1016/j.biopha.2020.110916

Zhao, H.-B., Jiang, Y.-M., Hou, Y.-J., Yan, Z.-Y., Liu, Y.-Y., Li, X.-J., et al. (2020). Xiaoyaosan produces antidepressant effects in rats via the JNK signaling pathway. *Complement. Med. Res.* 27 (1), 47–54. doi:10.1159/000501995

Zhao, H.-B., Jiang, Y.-M., Li, X.-J., Liu, Y.-Y., Bai, X.-H., Li, N., et al. (2017). Xiao yao san improves the anxiety-like behaviors of rats induced by chronic immobilization stress: The involvement of the jnk signaling pathway in the hippocampus. *Biol. Pharm. Bull.* 40 (2), 187–194. doi:10.1248/bpb.b16-00694

Zhi-wei, X., Hai-qing, A., and Can, Y. (2004). Effect of Xiao Yao San on capability of learn and remember of space about rats under chronic psychological stress model. *Chin. J. Behav. Med. Sci.* 13 (5), 484–485. doi:10.3760/cma.j.issn.1674-6554.2004.05.002

Zhou, H.-Y., He, J.-G., Hu, Z.-L., Xue, S.-G., Xu, J.-F., Cui, Q.-Q., et al. (2019). A-kinase anchoring protein 150 and protein kinase A complex in the basolateral amygdala contributes to depressive-like behaviors induced by chronic restraint stress. *Biol. Psychiatry* 86 (2), 131–142. doi:10.1016/j.biopsych.2019.03.967

Zhou, L., Zhang, Y., Gapter, L. A., Ling, H., Agarwal, R., Ng, K.-y., et al. (2008). Cytotoxic and anti-oxidant activities of lanostane-type triterpenes isolated from Poria cocos. *Chem. Pharm. Bull.* 56 (10), 1459–1462. doi:10.1248/cpb.56.1459

Zhou, X. M., Liu, C. Y., Liu, Y. Y., Ma, Q. Y., Chen, J. X., Jiang, Y. M., et al. (2021). Xiaoyaosan alleviates hippocampal glutamate-induced toxicity in the CUMS rats via NR2B and PI3K/akt signaling pathway. *Front. Pharmacol.* 12, 586788. doi:10.3389/fphar.2021.586788

Zhou, Y., Lu, L., Li, Z., Gao, X., Tian, J., Zhang, L., et al. (2011). Antidepressant-like effects of the fractions of Xiaoyaosan on rat model of chronic unpredictable mild stress. *J. Ethnopharmacol.* 137 (1), 236–244. doi:10.1016/j.jep.2011.05.016

Zhu, H.-Z., Liang, Y.-D., Ma, Q.-Y., Hao, W.-Z., Li, X.-J., Wu, M.-S., et al. (2019). Xiaoyaosan improves depressive-like behavior in rats with chronic immobilization stress through modulation of the gut microbiota. *Biomed. Pharmacother.* 112, 108621. doi:10.1016/j.biopha.2019.108621

Zhu, X., Xia, O., Han, W., Shao, M., Jing, L., Fan, Q., et al. (2014). Xiao Yao San improves depressive-like behavior in rats through modulation of β-arrestin 2-mediated pathways in hippocampus. *Evidence-based Complementary Altern. Med.* 2014, 902516. doi:10.1155/2014/902516

Zoicas, I., and Kornhuber, J. (2019). The role of the N-methyl-D-aspartate receptors in social behavior in rodents. *Int. J. Mol. Sci.* 20 (22), 5599. doi:10.3390/ijms20225599

Zschocke, J., Zimmermann, N., Berning, B., Ganal, V., Holsboer, F., Rein, T., et al. (2011). Antidepressant drugs diversely affect autophagy pathways in astrocytes and neurons—Dissociation from cholesterol homeostasis. *Neuropsychopharmacology* 36 (8), 1754–1768. doi:10.1038/npp.2011.57

frontiers | Frontiers in Pharmacology

ORIGINAL RESEARCH
published: 15 August 2022
doi: 10.3389/fphar.2022.907437

Cryo-EM Structure and Activator Screening of Human Tryptophan Hydroxylase 2

Kongfu Zhu[1†], Chao Liu[1†], Yuanzhu Gao[2], Jianping Lu[3], Daping Wang[1,4] and Huawei Zhang[1,5*]*

[1]Department of Biomedical Engineering, Southern University of Science and Technology, Shenzhen, China, [2]Cryo-EM Facility Center, Southern University of Science and Technology, Shenzhen, China, [3]Department of Child and Adolescent Psychiatry, Shenzhen Kangning Hospital, Shenzhen Mental Health Center, Shenzhen, China, [4]Department of Orthopedics, Shenzhen Intelligent Orthopaedics and Biomedical Innovation Platform, Guangdong Provincial Research Center for Artificial Intelligence and Digital Orthopedic Technology, Shenzhen Second People's Hospital, The First Affiliated Hospital of Shenzhen University, Shenzhen, China, [5]Guangdong Provincial Key Laboratory of Advanced Biomaterials, Southern University of Science and Technology, Shenzhen, China

OPEN ACCESS

Edited by:
Asma Perveen,
Glocal University, India

Reviewed by:
Jennifer Cash,
University of California, Davis, United States
Sagar Chittori,
St. Jude Children's Research Hospital, United States

***Correspondence:**
Daping Wang
wangdp@mail.sustech.edu.cn
Huawei Zhang
zhanghw@sustech.edu.cn

[†]These authors have contributed equally to this work and share first authorship

Specialty section:
This article was submitted to Neuropharmacology, a section of the journal Frontiers in Pharmacology

Received: 29 March 2022
Accepted: 23 June 2022
Published: 15 August 2022

Citation:
Zhu K, Liu C, Gao Y, Lu J, Wang D and Zhang H (2022) Cryo-EM Structure and Activator Screening of Human Tryptophan Hydroxylase 2. Front. Pharmacol. 13:907437. doi: 10.3389/fphar.2022.907437

Human tryptophan hydroxylase 2 (TPH2) is the rate-limiting enzyme in the synthesis of serotonin. Its dysfunction has been implicated in various psychiatric disorders such as depression, autism, and bipolar disorder. TPH2 is typically decreased in stability and catalytic activity in patients; thus, screening of molecules capable of binding and stabilizing the structure of TPH2 in activated conformation is desired for drug development in mental disorder treatment. Here, we solved the 3.0 Å cryo-EM structure of the TPH2 tetramer. Then, based on the structure, we conducted allosteric site prediction and small-molecule activator screening to the obtained cavity. ZINC000068568685 was successfully selected as the best candidate with highest binding affinity. To better understand the driving forces and binding stability of the complex, we performed molecular dynamics simulation, which indicates that ZINC000068568685 has great potential to stabilize the folding of the TPH2 tetramer to facilitate its activity. The research might shed light on the development of novel drugs targeting TPH2 for the treatment of psychological disorders.

Keywords: serotonin, psychological disorders, TPH2, virtual screening, MD simulation

INTRODUCTION

The biogenic monoamine serotonin (5-hydroxytrptamine, 5-HT), defined as a neurotransmitter or a hormone, has been implicated in various physiological functions ranging from cell growth and development to metabolic processes (Weaver et al., 2016; Okaty et al., 2019; Bacqué-Cazenave et al., 2020). Many psychiatric disorders such as depression, autism, and bipolar disorder, as well as Alzheimer's disease, are closely associated with the dysregulation of the serotonin secretion (Mansour et al., 2005; DeFilippis and Wagner, 2014; Kraus et al., 2017; Chakraborty et al., 2019; Takumi et al., 2020). Serotonin is also reported to play important roles in inflammatory, osteoporosis, gastrointestinal, and cardiovascular diseases (Ayme-Dietrich et al., 2017; D'Amelio and Sassi, 2018; Balakrishna et al., 2021). The regulation of the serotonin signaling, recycling, and degradation has emerged to be potential targets for the therapy of related diseases (Bader, 2020).

Serotonin is synthesized from tryptophan by tryptophan hydroxylase (TPH) and subsequent aromatic amino acid decarboxylase (AADC) (González-Castro et al., 2014; Zhang, 2016). AADC also catalyzes the formation of other monoamines and thus is not specific for serotonin synthesis

(Montioli et al., 2020; Montioli and Borri Voltattorni, 2021). By contrast, TPH is specific and acts as the rate-limiting enzyme for serotonin synthesis and is considered as a crucial target for the regulation of the serotonergic system (Swami and Weber, 2018). There are two distinct TPH homologies in humans, TPH1 and TPH2, which are separately located on chromosomes 11 and 12, respectively, sharing 71% sequence identity in amino acids (McKinney et al., 2005). TPH1 and TPH2, together with phenylalanine hydroxylase (PAH) and tyrosine hydroxylase (TH), form the family of pterin-dependent aromatic amino acid hydroxylases (AAAHs) that catalyze the hydroxylation of their respective aromatic amino acid substrates in a conserved mechanism, with molecular oxygen, tetrahydrobiopterin (BH4), and Fe^{2+} as cofactors (Patel et al., 2016; Waløen et al., 2017). The members of AAAHs are all similarly composed of three domains in structures: an N-terminal regulatory domain for robustly modulating its activity, a catalytic domain for substrate binding, and a C-terminal domain for maintaining the oligomerization states (Cao et al., 2010).

The oligomerization state is critical for the activities of AAAH families. The C-terminal domain is important for their oligomerization. Previous studies have shown that the deletion of C-terminal residues will decrease and nearly abolish the activities of TPH2 (Tenner et al., 2007). The addition of phenylalanine will shift the state of the TPH2 variant from monomer to dimer and change its activity by threefold (Tidemand et al., 2016). In pathological conditions such as Parkinson's disease, TPH2 may form disulfide-bonded aggregates upon oxidation and eventually affect its activity (Kuhn et al., 2011). Studies on PAH have also shown that PAH exists in the solution as a dimer and two architecturally distinct tetramers, while its substrate phenylalanine is involved in the regulation of PAH states and affect its activity (Arturo et al., 2016; Flydal et al., 2019). Patel et al. (2016) also reported that phenylalanine can bind to the dimerization interface and regulatory domain of PAH and regulate its activity (Patel et al., 2016). A previous report on human TH showed that it exists as enzymatically stable tetramers and octamers in the solution, and missense mutations on the interface will disrupt its oligomeric states, decrease its activity, and eventually cause disease such as DOPA-responsive dystonia (Szigetvari et al., 2019).

Although TPH1 and TPH2 are highly conserved in both structural and catalytic mechanisms, there are many differences in their phosphorylation sites, expression patterns, and physiological processes (McKinney et al., 2005). TPH1 is dominantly expressed in the enterochromaffin cells of the gut epithelium, where serotonin is synthesized and taken up by platelets via serotonin transporters (Schoenichen et al., 2019). TPH1 also functions in other tissues such as the lung, pancreas, and kidney as well as the pineal gland, where serotonin is synthesized as a precursor for melatonin, a hormone that functions in sleep and pain (Coon et al., 1996; Côté et al., 2003; Walther and Bader, 2003). Most of the circulating serotonin is deviated from TPH1 but not TPH2 (Gershon, 2013). TPH2 is dominantly expressed in the central nervous system, where TPH1 is not expressed (Walther et al., 2003; Patel et al., 2004). TPH2 was found in the Raphe nuclei of the brain stem and plays multiple roles in neurometabolic and neuropsychiatric disorders (Liu et al., 2021). A small amount of TPH2 is expressed in the enteric nervous system, where it functions similarly as TPH1 (Neal et al., 2009; Li et al., 2011).

The serotonin level is decreased in the brain; meanwhile, its level is increased in peripheral blood in most psychiatric disorders (Gabriele et al., 2014; David and Gardier, 2016), indicating that the activity of THP2 is decreased and the activity of TPH1 is increased. Thus, an activation on TPH2 and inhibition on TPH1 are desired. Inhibitors targeting TPH1 have been designed and developed for a long time (Engelman et al., 1967; Stokes et al., 2000; Zimmer et al., 2002). However, owing to the extremely low stability of TPH2, the structural and biochemical characterization of TPH2 has not been revealed for a long time (D'Sa et al., 1996; McKinney et al., 2004). In our report, we determined the cryo-EM structure of human TPH2 in tetrameric conformation at 3.0 Å resolution. After that, we carried out allosteric site prediction and small-molecule screening using the virtual screening technology. ZINC000068568685 (Cmpd 1) was successfully selected as the best candidate with highest score of −10.8 kcal/mol. To get more insight into the driving forces and binding stability of the complex, we performed molecular dynamics (MD) simulation, which indicates that Cmpd 1 has great potential to stabilize the formation of the TPH2 tetramer to facilitate its activity. Our research might shed light on the development of novel drugs targeting TPH2 for the treatment of mental disorders.

MATERIALS AND METHODS

Gene Cloning, Protein Expression, and Purification

The full-length human TPH2 gene was purchased from Sino Biological Co., Ltd, and reconstructed to pCAG with an N-terminal Twin-Strep-tag and a 3×Flag-tag. The construct was then transfected into Expi293F (Thermo Scientific) with PEI reagent and cultured for 72 h at 37°C under 8% CO_2. After that, cells were harvested, resuspended, and lysed by sonication in buffer A (50 mM HEPES pH 7.5, 150 mM NaCl, 0.1 mM FeSO4, 0.1 mM tryptophan, 0.1 mM EDTA, 10% v/v glycerol, 2% Tween-20, and 1 mM PMSF). Insoluble material was removed by centrifugation at 15,000 g and the supernatant was loaded on a 2 ml Strep-Tactin®XT column equilibrated with lysis buffer. The column was washed successively with 2 mM ATP in buffer A to remove the endogenously expressed HSP70 protein before TPH2 was eluted in steps with three times of buffer A containing 5, 25, and 50 mM biotin. Fractions containing pure TPH2 protein were identified using SDS-PAGE and further purified using size exclusion chromatography. TPH2 was loaded on a Superose™ 6 Increase 10/300 GL column attached to an AKTA pure system (Cytiva) equilibrated in buffer B (50 mM HEPES pH 7.5, 150 mM NaCl, 0.02% w/v glyco-diosgenin). Fractions were assessed using SDS-PAGE and concentrated for cryo-EM analysis. Approximately 0.25 mg of full-length TPH2 can be obtained from 500 ml of cells.

Cryo-Electron Microscopy

The freshly purified TPH2 was used to prepare cryo-EM grids. A drop of 4 μl TPH2 solution at the concentration of about 2.5 mg/ml was loaded to the holey film grid (Ni-Ti R2/2, 300 mesh). The grid was glow-discharged prior to sample loading and then blotted for 2.5 s under 100% humidity at 4°C using Vitrobot Mark IV (Thermo Scientific). After that, the grid was plunged into liquid ethane, which was precooled by liquid nitrogen. The grid was then observed using a Titan Krios microscope (Thermo Scientific) operated at 300 kV and equipped with a K2 Summit camera (Gatan). All images were recorded automatically using SerialEM under a nominal defocus value ranging from −1.5 to −2.5 μm and a nominal magnification of ×165 k, corresponding to a pixel size of 0.842 Å. Each micrograph was dose-fractionated to 32 frames with 0.1125 s exposure time in each frame. The dose rate was 1.1 counts per physical pixel per second, corresponding to 1.5625 electrons per square angstrom per second.

Cryo-EM Image Processing

For all micrographs, motion correction was carried out immediately after data collection using the MotionCor2 program (Zheng et al., 2017). After that, 5,559 micrographs were imported to RELION 3.1.2 (Scheres, 2016) for further processing. CTFFIND 4.1 was applied to evaluate the defocus parameters (Rohou and Grigorieff, 2015). A total of 1,416,664 particles were picked using Gautomatch with the template of the crystal structure of PAH (PDB entry: 5DEN). Particles were imported into cryoSPARC for further analysis. After several rounds of 2D classification, 486,660 particles remained for 3D classification. One of the best 3D classes with the highest quality in resolution was selected and performed for refinement and postprocessing, which resulted in a final map at 3.0 Å overall resolution with D2 symmetry. The resolution was estimated using the gold-standard Fourier shell correlation at the cutoff value of 0.143. All 3D reconstruction structures were visualized using Chimera 1.15 (Pettersen et al., 2004).

Model Building, Refinement, and Validation

The cryo-EM model of TPH2 was primarily generated in PHNIX (Adams et al., 2010) by docking the crystal structure of human TPH2 (PDB ID 4V06) into our map and then manually revised in Coot (Emsley and Cowtan, 2004). After that, the model was refined using the real-space refinement module in the Phenix program and subsequently fixed manually in Coot. At last, the model was validated using the MolProbity tool in Phenix. The figures of the model were visualized and prepared in PyMOL (Barber, 2021) and Chimera. Structural analysis was performed using LigPlot+ (Laskowski and Swindells, 2011).

Allosteric Site Prediction

The allosteric site prediction was performed using the CavityPlus web server (Xu et al., 2018). First, we input the structure of the TPH2 tetramer and applied the cavity program to detect the potential cavity and ranked them using druggability scores. Based on the detected cavities, the submodule CorrSite 2.0 program was used to identify potential allosteric ligand binding sites. Allosteric site prediction was performed using default parameters.

AutoDock Dataset Acquisition

The ZINC15 database (Istifli, 2020) provides a large quantity of small molecules. We downloaded approximately 180,000 drug compounds as the data list based on their log P and pH values. All these compounds are standard, in-stock, neutral lead-like small molecules, based on which we can use relevant software to decide their protonation states and add hydrogen atoms and charges so as to do subsequent procedures for molecular docking.

Molecular Docking

After the three-dimensional structure of TPH2 was determined using cryo-EM, its protonation state was obtained, H atoms were added, and atomic radius was assigned using AutoDock prior to molecular docking. Then, following the AutoDock algorithm, we added nonpolar hydrogen atoms to heavy atoms and docked small molecules into the target protein using the AutoDock Vina v1.2.0 program (Koebel et al., 2016; Vieira and Sousa, 2019). The Gasteiger partial charge (Bikadi and Hazai, 2009; Mittal et al., 2009) was used, and the active pocket was chosen to just cover the vital amino acid identified in the allosteric site prediction step (Jain, 2006). The grid spacing was hereby set to 0.508 Å with a box size of 50 × 48 × 47 to be the active pocket. In total, 10 docking modes were set for each molecule, and the best one was kept for MM/PBSA calculations. The chosen mode had the expected lowest binding affinity. We used an MPI-based parallel implementation of the AutoDock Vina program VinaLC (Zhang et al., 2013) for a large quantity of docking computations.

Energy Minimization Step

Energy minimization, which requires the location of the simulation system's energy minimum, is a key determining step before MD. It tries to decide the most stable molecular 3D structure under the specified potential to ensure that steric hindrance or the geometric structure is excluded. Afterward, the solvent and charge are added. Then, the steepest descent method is chosen as the algorithm (Donnelly et al., 2021).

Equilibration Procedure

Before MD simulation begins, we should do two equilibration procedures: NVT equilibration and NPT equilibration. Under an NVT ensemble, temperature is supposed to reach maximum toward the desired value. Velocity-rescale is chosen as the heat-bath algorithm. NPT equilibration is implemented under an NPT ensemble, and Parrinello–Rahman is selected as the pressure-bath algorithm. Periodic boundary conditions are applied to both equilibrations. The simulation durations are both 100 ps.

Molecular Dynamics Simulation

The 3D coordinates were obtained from the TPH2 cryo-EM structure at 3.0 Å resolution. Then, the MD simulation was

implemented using the Gromacs 2019.6 software package (Faccioli et al., 2012; van der Spoel et al., 2012; Zhang et al., 2019) with the AMBER99SB-ILDN force field (Somavarapu and Kepp, 2015; Ouyang et al., 2018) for the protein and the TIP3P force field (Ong and Liow, 2019) for the water solvent. The appropriate number of sodium counter ions were added to neutralize the system. VMD (Humphrey et al., 1996; Fernandes et al., 2019) and XMGRACE software programs (Machné et al., 2006; Saranya Ganesh et al., 2020; Yalameha et al., 2022) were employed to visualize the molecules.

Here, we introduce the root-mean-square deviation (RMSD) indicator, which quantitatively assesses the difference between the target structure and the reference structure. This value can recognize large protein structure changes from the beginning point. A levering off of this curve usually reveals protein stabilization.

$$RMSD = \sqrt{\frac{\sum_{j=0}^{N}\left[m_j*\left(X_j - Y_j\right)^2\right]}{M}}$$

Another numerical value similar to RMSD that usually measures the spatial changes of biomolecules is root-mean-square fluctuation (RMSF). RMSF is a per-residue or per-atom quantity that describes each residue's or atom's change over the whole trajectory. It measures each individual residue or atom flexibility, or how much a specific residue or atom vibrates over the simulation course.

$$RMSF = \sqrt{\frac{1}{T}\sum_{t=1}^{T}\sum_{j=1}^{N}\left(x_j(t) - \overline{x_j}\right)^2}$$

The radius of gyration (Rg) is commonly described as the imaginary distance from the centroid. It describes the compactness of a protein, which can be formulated as follows:

$$k = \sqrt{\frac{I}{m}}$$

Prior to computing the above three parameters, we treat the MD trajectories and make sure no periodic boundary condition is applied.

MM/PBSA Energy Decomposition

The free energy of binding (ΔG_{bind}) is used to judge how a ligand changes from the solvated mode to the protein-bound mode, and it is supposed to be a large negative free energy. In thermodynamics, this term consists of the enthalpic change (ΔH) and the entropic change (ΔS).

$$\Delta G_{bind} = \Delta H - T\Delta S$$

The values for ΔH on the right-hand side can be decomposed into three terms:

$$\Delta H = \Delta E_{MM} + \Delta G_{PB} + \Delta G_{np}$$

Therefore, ΔG_{bind} can be rewritten as

$$\Delta G_{bind} = \left(\Delta E_{MM} + \Delta G_{PB} + \Delta G_{np}\right) - T\Delta S$$

In this equation, ΔG_{np}, ΔG_{PB}, and ΔE_{MM} denote the nonpolar solvation energy, the Poisson–Boltzmann energy, and the molecular mechanics energy, respectively. $\Delta G_{np} + \Delta G_{PB}$ are combined as ΔG_{PBSA}. ΔE_{MM} consists of internal, van der Waals, and Coulombic energies.

For the MM/PBSA computation, the chief aim is to identify important residues that bind most closely to the corresponding protein. The nonpolar solvation free energy follows a linear relationship with the solvent-accessible surface area (SASA):

$$\Delta G_{np} = \gamma SASA + \beta$$

In this calculation, we set the force field for the protein as amber99sb-ildn and the ligand force field as generalized AMBER force field (GAFF) (Ozpinar et al., 2010) to make energy decomposition.

RESULTS AND DISCUSSION

Purification and Structure Determination of Tryptophan Hydroxylase 2 Tetramer

Determining the oligomeric states and atomic models of TPH2 is critical to understand its physiological roles and to develop novel interventions. The crystal structure of the TPH2 catalytic domain has been deposited in the Protein Data Bank previously (PDB: 4V06). However, there is no associated publication available, and thus, detailed description is lacking. In the crystal structure, TPH2 is deposited as a dimer form in the asymmetric unit. However, when symmetry and crystal packing were considered, a possible tetramer form can be found in the unit cell, but it is still hard to tell its oligomeric states in the solution. Thus, we set out to determine the solution structures of human TPH2 using the cryo-EM method using its full-length form.

Using the optimized expression and purification methods, we successfully obtained the full-length human TPH2 in given conditions. The size exclusion chromatography profile and the SDS-PAGE result displayed in **Figure 1A** indicate that the obtained protein is at high purity and in the monodisperse oligomerization state. After several rounds of cryo-EM sample preparation, image collection, and data processing, we finally determined the structure of TPH2 in its tetrameric conformation at 3.0 Å resolution (**Supplementary Figure S1**, **Table 1**, EMDB-32540, PDB: 7WIY). The representative 2D classes in **Figure 1B** show that the symmetric tetramer is the predominant form, while there are also a small population of tetrameric particles without symmetry, and the four monomers are not precisely the same (with red box), which might indicate several potential transition states between different assemble states. However, we failed to determine the three-dimensional structures in high resolution for those special states because of its small population and insufficient projections in 2D classes. To boost the quality

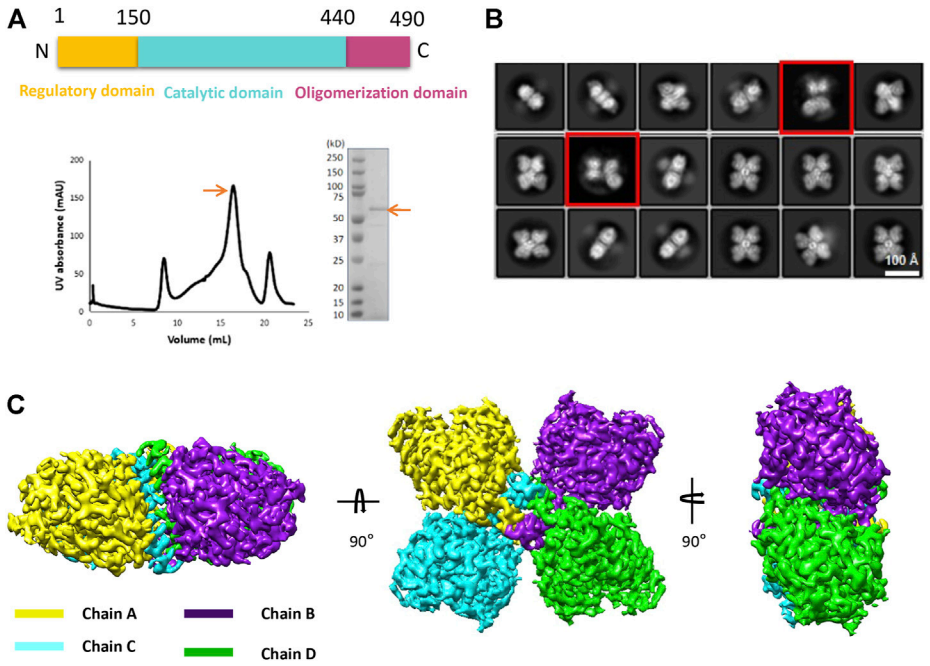

FIGURE 1 | Purification and structure determination of human tryptophan hydroxylase 2 (TPH2). **(A)** domain organization, size exclusion chromatography profile, and SDS-PAGE analysis of TPH2 in peak fraction. The target items are indicated with arrows. **(B)** 2D class average of cryo-EM micrographs of TPH2. The red box indicates the TPH2 asymmetric tetramer in a dynamic state. **(C)** cryo-EM 3D map of TPH2 tetramer in different views and colored by chain.

TABLE 1 | Summary of data collection, processing, and atom model statistics.

Data collection	
EM equipment	Titan Krios (Thermo Fisher)
Voltage (kV)	300
Detector	Gatan K2 Summit
Energy filter	Gatan GIF, 20 eV slit
Pixel size (Å)	0.842
Total Electron dose (e-/Å2)	50
Defocus range (μm)	−1.5 to −2.5
3D Reconstruction	
Software	Relion/CryoSPARC
Number of micrographs	5559
Final particles	110,963
Symmetry	D2
Final resolution (Å)	3.0
Map sharpening B-factor (Å^2)	172.5
Refinement	
Software	Phenix
Model composition	
Protein residues	240 × 4
ligand	4 Fe^{2+}; 4 IMD
R.M.S. deviations	
Bonds length (Å)	0.009
Bonds Angle (°)	0.707
Ramachandran plot statistics (%)	
Preferred	90.61
Allowed	9.39
Outliers	0

of the map, only the particles with clear symmetry were selected during the data processing. The final postprocessed 3D map is shown in **Figure 1C**. TPH2 is assembled by four protomers in a D2 symmetry, which is different from the previously deposited crystal structure in dimer form.

Overall Structure Analysis of Tryptophan Hydroxylase 2

The structure of TPH2 is dominantly formed with helices. As shown in **Figure 2A**, there are 17 helices (labeled as H1–H17) and 4 β sheets in the TPH2 monomer, together with Fe^{2+} and imidazole as cofactors. The TPH2 monomer contains the catalytic domain and oligomeric domain but lacks the N-terminal regulatory domain, although full-length TPH2 was used for sample preparation. Since the affinity tag used for purification was located in the N-terminus and the protein can be successfully purified, we speculate that TPH2 exists as a full-length version in the sample solution and the N-terminus is not degraded. Besides, the outcomes of SDS-PAGE also indicate that the molecular mass of the sample is in agreement with the full-length ones. Thus, it is most likely that its N-terminal regulatory domain is too flexible to align the signal during 3D construction and thus is not seen in the final map. The crystal structure (PDB:4V06) also misses the N-terminal domain, resembling the cryo-EM structure with the RMSD value at 0.789 Å when chain A of each model was aligned, although the crystal structure is in dimer form in the asymmetric unit as deposited and the cryo-EM structure is in

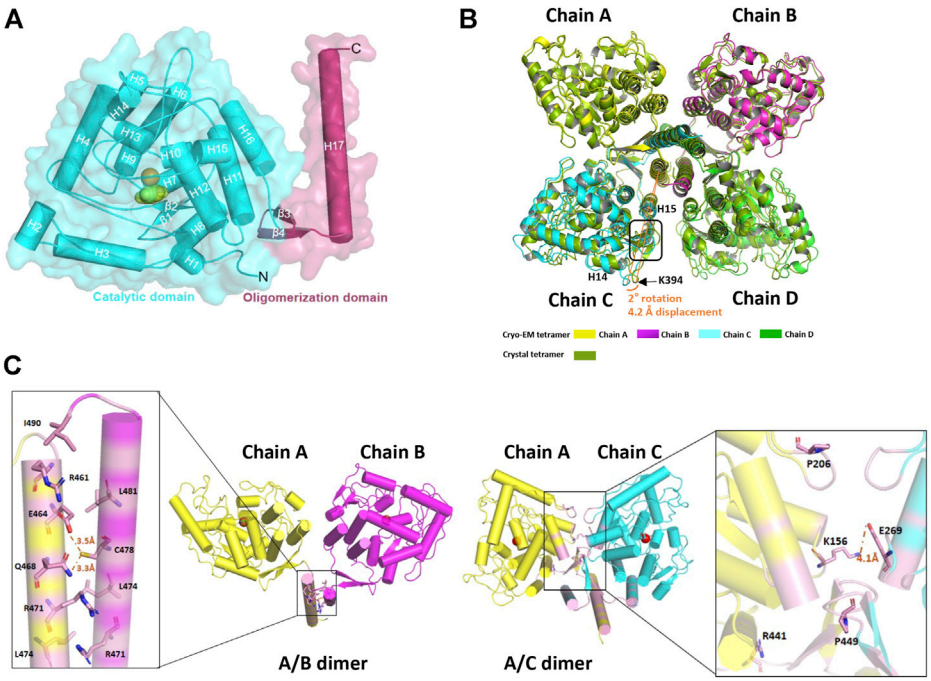

FIGURE 2 | Structure analysis of human tryptophan hydroxylase 2 (TPH2). **(A)** cartoon display of TPH2 monomer. The catalytic domain is colored cyan, while the oligomerization domain is colored warm pink. **(B)** superposition of the cryo-EM structure with the crystal structure of TPH2 (PDB entry: 4V06). The cryo-EM structure of TPH2 in tetramer is colored by chain, while the crystal structure is colored split pea. The tetramer of the crystal structure is obtained by dimer using the symmetry option. The arrow and curve indicate the different secondary structures and the rotation they adapted. **(C)** interfaces analysis of TPH2 dimers. The left shows the interface of chain A and chain B, and the right shows the interface of chain A and chain C. The interface is shown in light magenta. Key residues across interfaces of chain A/B and chain A/C are shown as sticks.

tetramer form. Using the symmetry option, we prepared the tetramer form of TPH2 based on the crystal structure and superimposed it with the cryo-EM tetramer structure with chain A as the reference. We found that the chain C–D of the crystal structure and cryo-EM structure shows about 2° rotation (with reference to the central oligomerization helix domain) and about 4.2 Å displacement (with reference to Cα from K394) (**Figure 2B**). This observation is similar to that in a previous report that different conformational oligomers of human phenylalanine hydroxylase show a rotation of ~3° and displacements up to 3 Å (Flydal et al., 2019). Besides, the secondary structure of the loops between H14 and H15 was transformed to three pairs of β sheets in the crystal structure (inside the rectangle box in **Figure 2B**). The cryo-EM model seems to fold less tightly than the crystal structure and shows more flexible and dynamic properties. A previous report showed that the binding of the N-terminal regulatory domain to the catalytic domain will inhibit TPH2 activity and thus acts as a negative regulator (Tenner et al., 2007). The deletion of the N-terminal domain has also been demonstrated to abolish its inhibitory effect (Tenner et al., 2007). Therefore, both the crystal structure and the cryo-EM structure might represent the activated state of TPH2, because their N-terminal is not bound closely to the catalytic domain whether it resulted from truncation or flexibility.

Interface Analysis of the Tryptophan Hydroxylase 2

The oligomeric state of the AAAH protein family has been reported to be essential for their function (Flydal and Martinez, 2013). For example, the deletion of the C-terminal 19 amino acids of TH leads to 70% reduction of enzyme activity (Walker et al., 1994). Likewise, the removal of the last 51 amino acids of TPH2 also dramatically interferes with the tetrameric conformation and nearly abolishes the activity of TPH2 (Tenner et al., 2007). To better understand the assembly mechanisms of TPH2 oligomerization, we performed the interface analysis of the TPH2 tetramer. Two types of interfaces were identified and shown in **Figure 2C**. For the A/B interface, the C-terminal helix 17 of each chain forms a leucine zipper–like motif to maintain their interaction. The interface area is calculated to be 882 $Å^2$, involving 13 amino acids of each chain such as R461, R471, L474, L481, and I490. However, it gets complicated for the A/C interface, which forms a much tighter and consolidated interface. The interface area expands to be approximately 1,838 $Å^2$, and there are 27 amino acids participating in the interaction, located at not only helix 17 but also helix 11/15/16, as well as the antiparalleled β3/β4 sheets and some nearby loops. Nonbonded contact including the hydrophobic effect and van der Waals forces plays the most essential roles. The mutants of those represented residues such as R441H and P449R are the

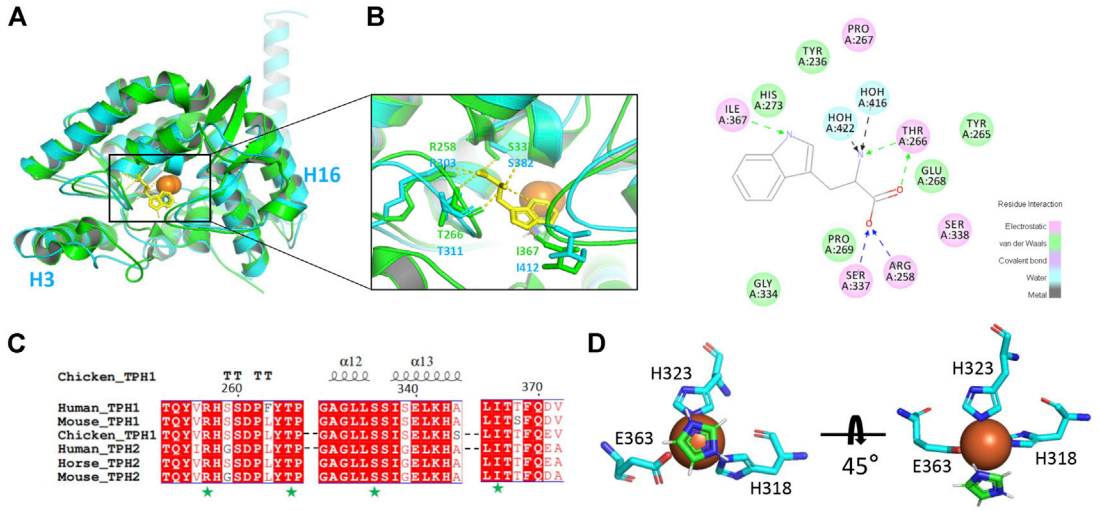

FIGURE 3 | Cofactor and substrate binding site analysis. **(A)** superimposition of human tryptophan hydroxylase 2 (TPH2) with chicken TPH1 and substrate binding environment analysis. The human TPH2 is in cyan, and the chicken TPH1 is in chartreuse. The substrate tryptophan is depicted as sticks in yellow. The residues participating in binding are shown as sticks in corresponding colors. **(B)** schematic graph of all the residues interacting with tryptophan of chicken TPH1 is displayed. Electrostatic interaction is shown in pink, van der Waals interaction is shown in green, and water–ligand interaction is shown in cyan. **(C)** primary sequence alignment of human TPH2 and chicken TPH1 produced by MULTALIN and Esprit, in which amino acids with red background represent identity. The secondary structure of chicken TPH1 is depicted on the top, and the substrate binding sites are pointed below with a green pentagram. **(D)** display of Fe^{2+} and imidazole binding environment.

most deleterious factors impairing the stability of TPH2 and are prevalent in depression, bipolar disorder, and autism patients. P206 is also directly involved in the hydrophobic environment and affects the stability of the A/C interface, which explains the catastrophic effect of the P206S mutant in a previous report (Cichon et al., 2008). Besides, we also identified three hydrogen bonds mediated by E464, E468, and C478 in the A/B interface and a stable salt bridge between K157 and E269 in the A/C interface, which certainly contribute to the oligomeric assembly. Therefore, understanding the assembly mechanism of TPH2 may be beneficial to reveal the catalytic processes, explaining and predicting the deleterious mutants in patients.

Decoding of Tryptophan Hydroxylase 2 Catalytic Mechanism

To get insight into the catalytic mechanism of TPH2, we superimposed and compared the obtained cryo-EM structure of human TPH2 with that of chicken TPH1, which is the only reported structure of TPH with substrate binding (PDB: 3E2T) (Windahl et al., 2008). As shown in **Figure 3A**, they highly resemble each other in whole although there are movements of H3 and H16 for TPH2. **Figure 3B** shows that R258, T266, S337, and I367 of chicken TPH1 determine the tryptophan binding specificity, and two water molecules around also contribute to the correct orientation of the substrate. The four residues also match well with the counterpart positions R303, T311, S382, and I412 in TPH2. Further analysis of the four residues also explains the disastrous effects of variants R303W and S383F of TPH2 in patients as in a previous report (Pereira et al., 2020). R303W could immediately reduce the substrate binding affinity and specificity. In contrast, S383F may impair the stability and mobility of the catalytic domain and thus destroy the substrate binding by changing the configuration of S382, according to a previous MD study (Pereira et al., 2020). To further investigate the potential substrate binding sites of human TPH2, we performed sequence alignment of the substrate binding regions using TPHs from different species including human, chicken, mouse, and horse, with reference to the binding site analysis of tryptophan in chicken TPH1. The results shown in **Figure 3C** indicate that the four functional residues are quite conserved across different species. It is possible that residues R303, T311, S382, and I412 are involved in the substrate binding in human TPH2. Furthermore, we performed interaction analysis of the Fe^{2+} cofactor with the active site of the TPH2 cryo-EM structure. **Figure 3D** shows that catalytic iron binds to conserved H318, H323, and E363, which form a 2-His-1-carboxylate facial triad, in a similar manner to that observed in other AAAHs enzymes. The nearby density can fit well with imidazole, and this is in agreement with the crystal structure, although the orientation of imidazole is slightly different. Further studies on decoding the catalytic mechanism are essential and may facilitate the design and development of molecules to stabilize and increase the activity of TPH2.

Small-Molecule Screening

As discussed before, the oligomerization of TPH2 affects its activity dramatically, so we conducted computer-aided drug design based on the cryo-EM structure of the TPH2 tetramer. Prior to that, we carried out the allosteric site prediction of TPH2 using the CavityPlus web server, which lists the potential cavities according to the scores of druggability. Those

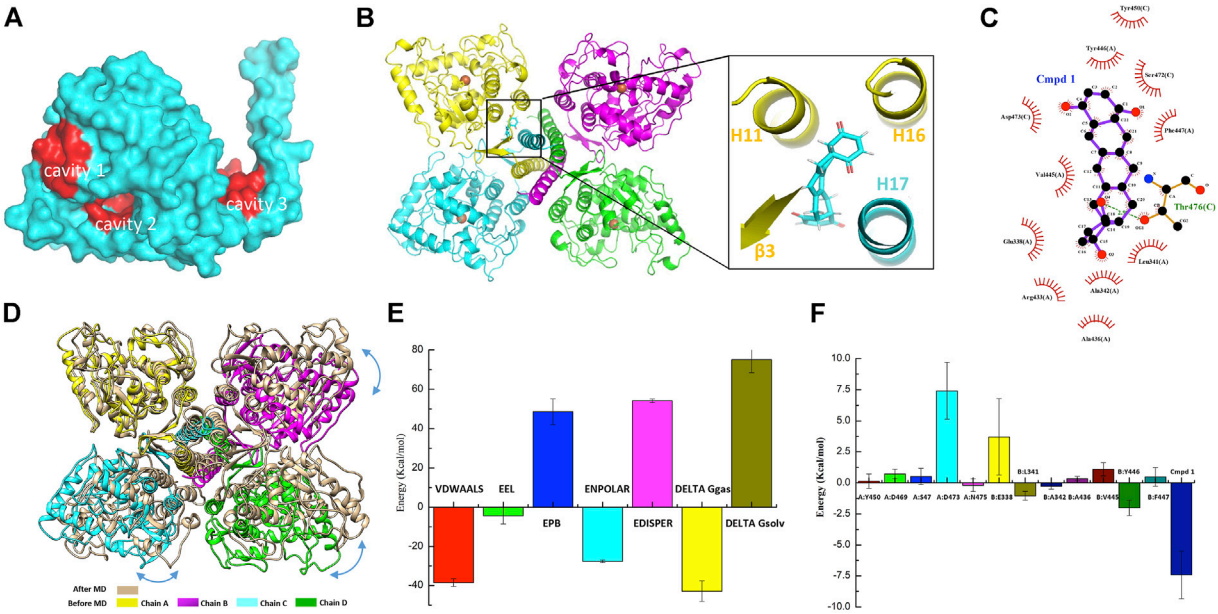

FIGURE 4 | Small-molecule screening based on the cryo-EM structure of tryptophan hydroxylase 2 (TPH2). **(A)** representative cavities of TPH2 predicted using the CavityPlus web server. The cavity zones with high scores for allosteric sites are colored red. **(B)** cartoon display of TPH2 tetramer binding with the small-molecule Cmpd 1. Structure of Cmpd 1 was shown as sticks in the insert. **(C)** key residues are shown in the interaction analysis of Cmpd 1 and TPH2. **(D)** Structural alignment and conformational changes of Cmpd 1–bound TPH2 structures before and after simulation. Double arrow curves in blue color indicate the rotation of chains B–D with chain A as reference. **(E)** illustration of energy difference for the receptor–ligand complex. VDWAALS denotes the van der Waals energy, EEL denotes the electrostatic energy, ENPOLAR denotes the nonpolar solvation energy, and EPB denotes the Poisson–Boltzmann energy. **(F)** per-residue decomposition energies for the TPH2 with Cmpd 1 bound after simulation using MM/PBSA.

top candidates are typically distributed to three zones as indicated in **Figure 4A**. Cavity 1 and cavity 2 zones are involved in substrate and cofactor binding, where binding of small molecules would inhibit its activity in theory. Cavity 3 shows the highest score of druggability, and the binding of a ligand might promote and stabilize the formation of the tetramer state, indicating it is more suitable for drug screening. Therefore, we used virtual screening technology based on cavity 3 with the ZINC15 database where we selected approximately 180,000 small molecules to screen the most desired candidate to bind and stabilize the tetramer conformation of TPH2. **Supplementary Table S1** shows the top 20 ZINC IDs and their binding affinity to TPH2. The binding affinity defines the favor of a ligand to the receptor. The larger the negative value is, the stronger binding force it illustrates. As shown in **Figure 4B**, Cmpd 1 possesses the most negative binding affinity at −10.8 kcal/mol and is conceived as the best ligand. The predicted complex of the Cmpd 1 with the TPH2 tetramer after docking is shown in **Figure 4B**, where the protein is shown as a cartoon and the ligand is displayed in sticks. The capture suggests that the small-molecule Cmpd 1 fits well with the given cavity. Cmpd 1 was coordinated by helices H11, H16, and H17 and sheet β3. Further analysis using LigPlot + reveals that residues E338, L341, A342, A436, R433, V445, Y446, and F447 from chain A, together with residues Y450, S472, D473 and T476 from chain C, may be involved in the binding of Cmpd 1 to TPH2 (**Figure 4C**).

Energy Minimization, Equilibration, and Unrestrained Molecular Dynamics Simulation

Energy minimization and equilibration are performed before conducting MD simulation. The topology file was produced by AMBER99SB-ILDN for the TPH2 tetramer and TIP3P for water. As illustrated in **Supplementary Figure S2A**, the initial potential energy is -5.17×10^5 kJ/mol, which descends steeply and stabilizes at 5.16×10^6 kJ/mol after 2,500 steps of minimization. **Supplementary Figure S2B** shows that the system was heated gradually in the NVT ensemble to 300 K in 100 ps followed by EM. The original velocities corresponding to the starting temperature were assigned from a Maxwellian distribution. Afterward, we performed the pressure equilibration, as shown in **Supplementary Figure S2C**. The input file is generally similar to the parameter file of NVT equilibration. The Parrinello–Rahman barostat is exerted to the pressure coupling section. In the process of NPT equilibration, the mean value of pressure was 0.8 ± 59.3 bar, and the reference pressure was set to 1 bar. The minor difference in the mean value indicates the success of the simulation, and the deviation is due to the large size of the protein. The pressure value changes widely during the process of MD simulation, as indicated by the large RMSF. Taking the pressure into consideration, the running average of the density is calculated and demonstrated in **Supplementary Figure S2D**; the expected density of the SPC/E

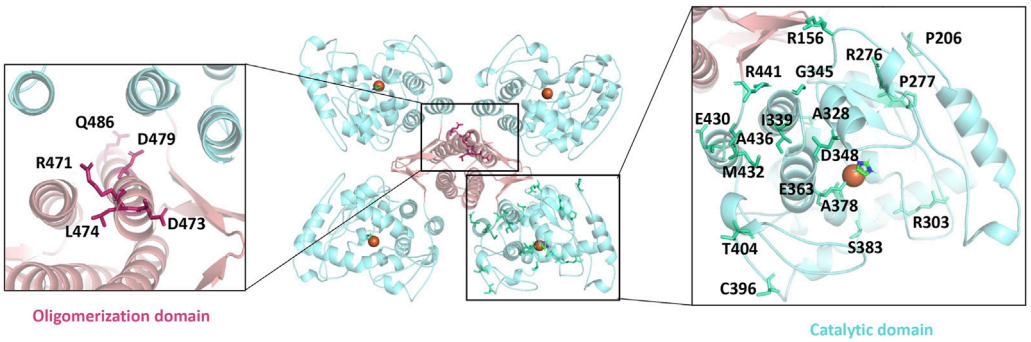

FIGURE 5 | Mapping the disease-causing mutations on tryptophan hydroxylase 2 structures. The left panel shows the mutants of the oligomerization domain, and the right panel shows the catalytic domain. All mutants are shown as sticks.

mode is 1,008 kg/m^3, and the experimental value is 1,000 kg/m^3. The obtained average over the entire period is 1,008 ± 2 kg/m^3, which is close to the two mentioned values and validates the success of the simulation process. The density values are stable over the entire course, indicating that the system is equilibrated well for both pressure and density.

MD simulation was performed to investigate the binding process of Cmpd 1 to TPH2. **Supplementary Figure S3A** demonstrates the RMSD value relative to the minimized and equilibrated models (black line) as well as to the cryo-EM structure of the TPH2 tetramer (red line) after docking. The RMSD levels off to ~0.45 nm (4.5 Å) of both time series in the plot, manifesting the stability of the TPH2 complex, although slight differences exist between the two lines when t = 0, which makes sense for the impact of EM. After that, we analyzed the radius of gyration (Rg) of the complex, which is a measurement of compactness and might provide further information about its stability. The Rg value is theoretically steady for a stably folded protein, and it changes over time once the protein unfolds. From the results of the MD simulation, which is shown in **Supplementary Figure S3B**, the TPH2 tetramer complex is quite stable since the Rg value is basically unchanged over the course of 100 ns at 300 K. RMSF is another useful measurement to describe the stability of biomacromolecules, which instructs how much an individual residue or atom moves over the MD simulation process; a higher value usually indicates greater flexibility. The results are shown in **Supplementary Figure S3C**; the greatest score comes from atoms 21818 and 10908 from residue I490 (**Figure 2C**), as well as from atom 21803 from residue L488 in the chain A/B interface, which implies the important roles of these interface residues in maintaining the stability of the TPH2 complex. After MD simulation, we compared the conformational changes with Cmpd 1 during the simulation. The structural alignment shown in **Figure 4D** indicates that the C-terminal oligomerization domain has relatively larger conformational changes. When superimposed with chain A, chains B–D have a relative rotation, similar to that observed in the TPH2 crystal structure (**Figure 2B**). Analysis on the chain A/C major interface shows that the number of salt bridges increase from 3 to 9 for TPH2 with Cmpd 1 bound, while as control there is only five salt bridges after simulation for the TPH2 without a ligand bound. This indicates that binding of Cmpd 1 will stabilize TPH2 and serve as the activator of TPH2. We also compared Cmpd 1 with other top hits and found that binding of Cmpd 1 to TPH2 will give the largest RMSD with 3.567 Å compared with the structure before simulation (RMSD: 2.546 for the unbound form and 3.567, 2.667, 2.893, 3.437, 3.155, 2.396, 2.805, 2.585, 2.794, and 2.270 for top 1–10 hits, respectively).

MM/PBSA Free Energy Calculation

The free energy of binding shows the suitability of the ligand transited from the solvated mode to the protein-bound mode. Models with lower free energies are convinced to be more stable and rigid than those with higher ones. In our study, we conducted free energy estimation using the approach of MM/PBSA to characterize the stability of the TPH2 complex in a semiquantitative method (Thompson et al., 2008; Cavalheiro et al., 2017; Poli et al., 2020). The binding free energies of the TPH2 tetramer are summarized in **Supplementary Table S2**, which basically includes the electrostatic energy (EEL), van der Waals energy (VDWAALS), and nonpolar solvation energy (ENPOLAR). The graphical result is also shown in **Figure 4E**, which clearly illustrates that van der Waals energy contributes most to favor the binding and interacting of Cmpd 1 to the TPH2 tetramer. To better understand the interaction of the TPH2 complex, we performed MM/PBSA decomposition analysis, demonstrated in **Figure 4F**, and we can see that Y446, L341, and A342 (**Figure 4C**) are most critical in mediating the formation of the complex owing to their highest energy contributions, which have also been deciphered to participate in the confinement of dimeric interfaces.

CONCLUSION

Serotonin participates in various metabolic processes, and its dysregulation of expression or activation results in several types of mental illnesses including depression, autism, and bipolar disorder as well as Alzheimer's disease, placing a huge burden on the patients and the families (Chakraborty et al., 2019; Bacqué-Cazenave et al., 2020; Takumi et al., 2020). TPH is the rate-limiting enzyme during the whole process of serotonin secretion and therefore considered as a target for the regulation of serotonin concentration (Waløen et al., 2017). In general, a decrease of serotonin in the brain and an increase in the periphery of the

patients occurs simultaneously. Thus, the two main sources of serotonin are TPH2 in the brain and TPH1 in the periphery, and an activation in TPH2 and an inhibition in TPH1 are desired (Bader, 2020). Although several TPH1 inhibitors have been developed for elevating serotonin levels in peripheral tissues, the severe side effects such as impairing the activity of TPH2 hampered their clinical applications (Crane et al., 2015). In particular, there are as many as 46 disease-causing mutations of TPH2 identified to affect its folding and finally its catalytic activity (Pereira et al., 2020). The oligomerization domain and catalytic domain are two hot spots for those mutations. Some of those residues are mapped in **Figure 5**, including R471, D473, L474, D479, and Q486 from the oligomerization domain, as well as R156, P206, R276, P277, R303, A328, I339, G345, D348, E363, A378, S383, C396, T404, E430, M432, A436, and R441 from the catalytic domain. Besides, the redox state also impairs the function of TPH2, and the oxidation-facilitated disulfide cross-linking of C357 and C406 promotes the misfolding and aggregating that lead to the formation of high-molecular-weight aggregates with the tendency to be degraded and inhibit the enzyme activity as demonstrated *in vitro* and in the cellular level (Yohrling et al., 2000; Kuhn et al., 2011). The oxidation also obstructs the obtaining of protein *in vitro*. TPH2 activation and stabilization are hence regarded as two most meaningful and valuable directions for the treatment of psychological disorders.

In this research, we reported the cryo-EM structure of human TPH2 at 3.0 Å in the tetramer state, which explains the pathogenesis of TPH2 mutants such as P206S, R441H, and P449R and provides the fundamental information for drug design. To obtain the stabilizers and activators of TPH2, we conducted virtual screening accompanied with MD simulations, which is now a rapidly growing method for faster and cost-efficient drug discovery. The outcomes indicate that Cmpd 1 in the ZINC15 database has the greatest potential to work on it, shedding light on the development of novel drugs for the treatment of psychology disorders. Although it could represent challenges to chemically synthesize Cmpd 1, experimental investigation will be the next direction to develop novel therapies based on our study. For example, it will provide more details to investigate how Cmpd 1 could affect the dimer–tetramer equilibrium using solution measurements such as dynamic light scattering or photometry and to analyze the complex structure of TPH2 bound with Cmpd 1 by cryo-EM. The investigation on the phosphorylation and interaction of TPH2 N-terminal to 14-3-3 proteins is another route worth trying, although we still face a wide range of challenges to nail it (Winge et al., 2008; Broadbelt et al., 2012; Skjevik et al., 2014). More efforts on understanding the mechanism of the TPH2 regulatory process must be taken to foster the drug design and discovery.

DATA AVAILABILITY STATEMENT

The original contributions presented in the study are included in the article/**Supplementary Materials**, and further inquiries can be directed to the corresponding authors.

AUTHOR CONTRIBUTIONS

DW, HZ, and JL designed and supervised the whole project. KZ and HZ prepared the samples, built the model, and performed data analysis. HZ and YG processed the cryo-EM data. CL performed docking and molecular dynamics. KZ, HZ, and CL prepared the manuscript.

FUNDING

This work was funded by the National Natural Science Foundation of China (No. 31900046, No.81972085, and No. 82172465), the Science and Technology Innovation Committee of Shenzhen (No. JCYJ20200109150700942), the Key-Area Research and Development Program of Guangdong Province (2019B030335001), the Shenzhen Fund for Guangdong Provincial High Level Clinical Key Specialties (No. SZGSP013), the Shenzhen Key Medical Discipline Construction Fund (No. SZXK042), and the Guangdong Provincial Key Laboratory of Advanced Biomaterials (2022B1212010003).

ACKNOWLEDGMENTS

We thank the Cryo-EM Center of Southern University of Science and Technology for data collection and HPC-Service Station. We are grateful for the assistance of the SUSTech Core Research Facilities. The docking and molecular dynamics simulation were performed at the Center for Computational Science and Engineering at the Southern University of Science and Technology.

SUPPLEMENTARY MATERIAL

The Supplementary Material for this article can be found online at: https://www.frontiersin.org/articles/10.3389/fphar.2022.907437/full#supplementary-material

Supplementary Figure S1 | Data processing of human tryptophan hydroxylase 2. Procedure of data processing was illustrated. The collected micrographs were display after motion correction. The resolution of the final map was estimated based on the golden standard FSC curves at 0.143 criteria.

Supplementary Figure S2 | Energy minimization and equilibration. **(A)** variation of potential energy with energy minimization step. **(B)** variation of temperature within 100 ps. **(C)** variation of pressure within 100 ps. **(D)** variation of density within 100 ps.

Supplementary Figure S3 | Molecular dynamics simulations of tryptophan hydroxylase 2 (TPH2) binding to the ligand. **(A)** root-mean-square deviation (RMSD) relative to the equilibrated system and the TPH2 complex. The black line represents the equilibrated system while the red one corresponds to the TPH2 complex. **(B)** variation of radius of gyration. **(C)** RMS fluctuation for all atoms.

Supplementary Table S1 | Docking results of VinaLC between protein and ligands.

Supplementary Table S2 | Energy difference for the receptor–ligand complex.

REFERENCES

Adams, P. D., Afonine, P. V., Bunkóczi, G., Chen, V. B., Davis, I. W., Echols, N., et al. (2010). PHENIX: a Comprehensive Python-Based System for Macromolecular Structure Solution. *Acta Crystallogr. D. Biol. Crystallogr.* 66 (Pt 2), 213–221. doi:10.1107/S0907444909052925

Arturo, E. C., Gupta, K., Héroux, A., Stith, L., Cross, P. J., Parker, E. J., et al. (2016). First Structure of Full-Length Mammalian Phenylalanine Hydroxylase Reveals the Architecture of an Autoinhibited Tetramer. *Proc. Natl. Acad. Sci. U. S. A.* 113 (9), 2394–2399. doi:10.1073/pnas.1516967113

Ayme-Dietrich, E., Aubertin-Kirch, G., Maroteaux, L., and Monassier, L. (2017). Cardiovascular Remodeling and the Peripheral Serotonergic System. *Arch. Cardiovasc Dis.* 110 (1), 51–59. doi:10.1016/j.acvd.2016.08.002

Bacqué-Cazenave, J., Bharatiya, R., Barrière, G., Delbecque, J.-P., Bouguiyoud, N., Di Giovanni, G., et al. (2020). Serotonin in Animal Cognition and Behavior. *Int. J. Mol. Sci.* 21 (5), 1649. doi:10.3390/ijms21051649

Bader, M. (2020). Inhibition of Serotonin Synthesis: A Novel Therapeutic Paradigm. *Pharmacol. Ther.* 205, 107423. doi:10.1016/j.pharmthera.2019.107423

Balakrishna, P., George, S., Hatoum, H., and Mukherjee, S. (2021). Serotonin Pathway in Cancer. *Int. J. Mol. Sci.* 22 (3), 1268. doi:10.3390/ijms22031268

Barber, R. D. (2021). Software to Visualize Proteins and Perform Structural Alignments. *Curr. Protoc.* 1 (11), e292. doi:10.1002/cpz1.292

Bikadi, Z., and Hazai, E. (2009). Application of the PM6 Semi-empirical Method to Modeling Proteins Enhances Docking Accuracy of AutoDock. *J. Cheminform* 1, 15. doi:10.1186/1758-2946-1-15

Broadbelt, K. G., Rivera, K. D., Paterson, D. S., Duncan, J. R., Trachtenberg, F. L., Paulo, J. A., et al. (2012). Brainstem Deficiency of the 14-3-3 Regulator of Serotonin Synthesis: a Proteomics Analysis in the Sudden Infant Death Syndrome. *Mol. Cell Proteomics* 11 (1), M111.009530. doi:10.1074/mcp.M111.009530

Cao, J., Shi, F., Liu, X., Huang, G., and Zhou, M. (2010). Phylogenetic Analysis and Evolution of Aromatic Amino Acid Hydroxylase. *FEBS Lett.* 584 (23), 4775–4782. doi:10.1016/j.febslet.2010.11.005

Cavalheiro, J. P. d. V. H., Pires, N. M. M., and Dong, T. (2017). "MM-PBSA: Challenges and Opportunities," in *2017 10th International Congress on Image and Signal Processing*, (Shanghai, China: BioMedical Engineering and Informatics CISP-BMEI), 1–6.

Chakraborty, S., Lennon, J. C., Malkaram, S. A., Zeng, Y., Fisher, D. W., and Dong, H. (2019). Serotonergic System, Cognition, and BPSD in Alzheimer's Disease. *Neurosci. Lett.* 704, 36–44. doi:10.1016/j.neulet.2019.03.050

Cichon, S., Winge, I., Mattheisen, M., Georgi, A., Karpushova, A., Freudenberg, J., et al. (2008). Brain-specific Tryptophan Hydroxylase 2 (TPH2): a Functional Pro206Ser Substitution and Variation in the 5'-region Are Associated with Bipolar Affective Disorder. *Hum. Mol. Genet.* 17 (1), 87–97. doi:10.1093/hmg/ddm286

Coon, S. L., Mazuruk, K., Bernard, M., Roseboom, P. H., Klein, D. C., and Rodriguez, I. R. (1996). The Human Serotonin N-Acetyltransferase (EC 2.3.1.87) Gene (AANAT): Structure, Chromosomal Localization, and Tissue Expression. *Genomics* 34 (1), 76–84. doi:10.1006/geno.1996.0243

Côté, F., Thévenot, E., Fligny, C., Fromes, Y., Darmon, M., Ripoche, M.-A., et al. (2003). Disruption of the Nonneuronal Tph1 Gene Demonstrates the Importance of Peripheral Serotonin in Cardiac Function. *Proc. Natl. Acad. Sci. U.S.A.* 100 (23), 13525–13530. doi:10.1073/pnas.2233056100

Crane, J. D., Palanivel, R., Mottillo, E. P., Bujak, A. L., Wang, H., Ford, R. J., et al. (2015). Inhibiting Peripheral Serotonin Synthesis Reduces Obesity and Metabolic Dysfunction by Promoting Brown Adipose Tissue Thermogenesis. *Nat. Med.* 21 (2), 166–172. doi:10.1038/nm.3766

D'Sa, C. M., Arthur, R. E., Jr., States, J. C., and Kuhn, D. M. (1996). Tryptophan Hydroxylase: Cloning and Expression of the Rat Brain Enzyme in Mammalian Cells. *J. Neurochem.* 67 (3), 900–906. doi:10.1046/j.1471-4159.1996.67030900.x

D'Amelio, P., and Sassi, F. (2018). Gut Microbiota, Immune System, and Bone. *Calcif. Tissue Int.* 102 (4), 415–425. doi:10.1007/s00223-017-0331-y

David, D. J., and Gardier, A. M. (2016). Les bases de pharmacologie fondamentale du système sérotoninergique : application à la réponse antidépressive. *L'Encéphale* 42 (3), 255–263. doi:10.1016/j.encep.2016.03.012

DeFilippis, M., and Wagner, K. D. (2014). Management of Treatment-Resistant Depression in Children and Adolescents. *Paediatr. Drugs* 16 (5), 353–361. doi:10.1007/s40272-014-0088-y

Donnelly, S. M., Lopez, N. A., and Dodin, I. Y. (2021). Steepest-descent Algorithm for Simulating Plasma-Wave Caustics via Metaplectic Geometrical Optics. *Phys. Rev. E* 104 (2-2), 025304. doi:10.1103/PhysRevE.104.025304

Emsley, P., and Cowtan, K. (2004). Coot: Model-Building Tools for Molecular Graphics. *Acta Crystallogr. D. Biol. Crystallogr.* 60 (Pt 12 Pt 1), 2126–2132. doi:10.1107/s0907444904019158

Engelman, K., Lovenberg, W., and Sjoerdsma, A. (1967). Inhibition of Serotonin Synthesis by Para-Chlorophenylalanine in Patients with the Carcinoid Syndrome. *N. Engl. J. Med.* 277 (21), 1103–1108. doi:10.1056/nejm196711232772101

Faccioli, R. A., Da Silva, I. N., Delbem, A. C. B., Brancini, G. T. P., and Caliri, A. (2012). *PROTPRED-GROMACS: EVOLUTIONAY ALGORITHM WITH GROMACS FOR PROTEIN STRUCTURE PREDICTION*, 120–130. doi:10.1142/9789814397711_0009

Fernandes, H. S., Sousa, S. F., and Cerqueira, N. M. F. S. A. (2019). VMD Store-A VMD Plugin to Browse, Discover, and Install VMD Extensions. *J. Chem. Inf. Model* 59 (11), 4519–4523. doi:10.1021/acs.jcim.9b00739

Flydal, M. I., Alcorlo-Pagés, M., Johannessen, F. G., Martínez-Caballero, S., Skjærven, L., Fernandez-Leiro, R., et al. (2019). Structure of Full-Length Human Phenylalanine Hydroxylase in Complex with Tetrahydrobiopterin. *Proc. Natl. Acad. Sci. U. S. A.* 116 (23), 11229–11234. doi:10.1073/pnas.1902639116

Flydal, M. I., and Martinez, A. (2013). Phenylalanine Hydroxylase: Function, Structure, and Regulation. *IUBMB Life* 65 (4), 341–349. doi:10.1002/iub.1150

Gabriele, S., Sacco, R., and Persico, A. M. (2014). Blood Serotonin Levels in Autism Spectrum Disorder: A Systematic Review and Meta-Analysis. *Eur. Neuropsychopharmacol.* 24 (6), 919–929. doi:10.1016/j.euroneuro.2014.02.004

Gershon, M. D. (2013). 5-Hydroxytryptamine (Serotonin) in the Gastrointestinal Tract. *Curr. Opin. Endocrinol. Diabetes Obes.* 20 (1), 14–21. doi:10.1097/MED.0b013e32835bc703

González-Castro, T. B., Juárez-Rojop, I., López-Narváez, M. L., and Tovilla-Zárate, C. A. (2014). Association of TPH-1 and TPH-2 Gene Polymorphisms with Suicidal Behavior: a Systematic Review and Meta-Analysis. *BMC psychiatry* 14, 196. doi:10.1186/1471-244X-14-196

Humphrey, W., Dalke, A., and Schulten, K. (1996). VMD: Visual Molecular Dynamics. *J. Mol. Graph* 14 (1), 33-8–27-38. doi:10.1016/0263-7855(96)00018-5

Istifli, E. (2021). Virtual Screening and Molecular Docking Studies of Certain Lead-like Compounds from ZINC15 Database against COVID-19 Mpro Enzyme. *Ann. Clin. Anal. Med.* 12. doi:10.4328/ACAM.20389

Jain, A. N. (2006). Scoring Functions for Protein-Ligand Docking. *Curr. Protein Pept. Sci.* 7 (5), 407–420. doi:10.2174/138920306778559395

Koebel, M. R., Schmadeke, G., Posner, R. G., and Sirimulla, S. (2016). AutoDock VinaXB: Implementation of XBSF, New Empirical Halogen Bond Scoring Function, into AutoDock Vina. *J. Cheminform* 8, 27. doi:10.1186/s13321-016-0139-1

Kraus, C., Castrén, E., Kasper, S., and Lanzenberger, R. (2017). Serotonin and Neuroplasticity - Links between Molecular, Functional and Structural Pathophysiology in Depression. *Neurosci. Biobehav Rev.* 77, 317–326. doi:10.1016/j.neubiorev.2017.03.007

Kuhn, D. M., Sykes, C. E., Geddes, T. J., Jaunarajs, K. L., and Bishop, C. (2011). Tryptophan Hydroxylase 2 Aggregates through Disulfide Cross-Linking upon Oxidation: Possible Link to Serotonin Deficits and Non-motor Symptoms in Parkinson's Disease. *J. Neurochem.* 116 (3), 426–437. doi:10.1111/j.1471-4159.2010.07123.x

Laskowski, R. A., and Swindells, M. B. (2011). LigPlot+: Multiple Ligand-Protein Interaction Diagrams for Drug Discovery. *J. Chem. Inf. Model* 51 (10), 2778–2786. doi:10.1021/ci200227u

Li, Z., Chalazonitis, A., Huang, Y. Y., Mann, J. J., Margolis, K. G., Yang, Q. M., et al. (2011). Essential Roles of Enteric Neuronal Serotonin in Gastrointestinal Motility and the Development/survival of Enteric Dopaminergic Neurons. *J. Neurosci.* 31 (24), 8998–9009. doi:10.1523/JNEUROSCI.6684-10.2011

Liu, H., Wang, C., Yu, M., Yang, Y., He, Y., Liu, H., et al. (2021). TPH2 in the Dorsal Raphe Nuclei Regulates Energy Balance in a Sex-dependent Manner. *Endocrinology* 162 (1), bqaa183. doi:10.1210/endocr/bqaa183

Machne, R., Finney, A., Muller, S., Lu, J., Widder, S., and Flamm, C. (2006). The SBML ODE Solver Library: a Native API for Symbolic and Fast Numerical Analysis of Reaction Networks. *Bioinformatics* 22 (11), 1406–1407. doi:10.1093/bioinformatics/btl086

Mansour, H. A., Talkowski, M. E., Wood, J., Pless, L., Bamne, M., Chowdari, K. V., et al. (2005). Serotonin Gene Polymorphisms and Bipolar I Disorder: Focus on the Serotonin Transporter. *Ann. Med.* 37 (8), 590–602. doi:10.1080/07853890500357428

McKinney, J., Knappskog, P. M., and Haavik, J. (2005). Different Properties of the Central and Peripheral Forms of Human Tryptophan Hydroxylase. *J. Neurochem.* 92 (2), 311–320. doi:10.1111/j.1471-4159.2004.02850.x

McKinney, J., Knappskog, P. M., Pereira, J., Ekern, T., Toska, K., Kuitert, B. B., et al. (2004). Expression and Purification of Human Tryptophan Hydroxylase from *Escherichia coli* and Pichia pastoris. *Protein Expr. Purif.* 33 (2), 185–194. doi:10.1016/j.pep.2003.09.014

Mittal, R. R., Harris, L., McKinnon, R. A., and Sorich, M. J. (2009). Partial Charge Calculation Method Affects CoMFA QSAR Prediction Accuracy. *J. Chem. Inf. Model* 49 (3), 704–709. doi:10.1021/ci800390m

Montioli, R., Bisello, G., Dindo, M., Rossignoli, G., Voltattorni, C. B., and Bertoldi, M. (2020). New Variants of AADC Deficiency Expand the Knowledge of Enzymatic Phenotypes. *Arch. Biochem. Biophys.* 682, 108263. doi:10.1016/j.abb.2020.108263

Montioli, R., and Borri Voltattorni, C. (2021). Aromatic Amino Acid Decarboxylase Deficiency: The Added Value of Biochemistry. *Int. J. Mol. Sci.* 22 (6), 3146. doi:10.3390/ijms22063146

Neal, K. B., Parry, L. J., and Bornstein, J. C. (2009). Strain-specific Genetics, Anatomy and Function of Enteric Neural Serotonergic Pathways in Inbred Mice. *J. Physiol.* 587 (3), 567–586. doi:10.1113/jphysiol.2008.160416

Okaty, B. W., Commons, K. G., and Dymecki, S. M. (2019). Embracing Diversity in the 5-HT Neuronal System. *Nat. Rev. Neurosci.* 20 (7), 397–424. doi:10.1038/s41583-019-0151-3

Ong, E. E. S., and Liow, J.-L. (2019). The Temperature-dependent Structure, Hydrogen Bonding and Other Related Dynamic Properties of the Standard TIP3P and CHARMM-Modified TIP3P Water Models. *Fluid Phase Equilibria* 481, 55–65. doi:10.1016/j.fluid.2018.10.016

Ouyang, Y., Zhao, L., and Zhang, Z. (2018). Characterization of the Structural Ensembles of P53 TAD2 by Molecular Dynamics Simulations with Different Force Fields. *Phys. Chem. Chem. Phys.* 20 (13), 8676–8684. doi:10.1039/c8cp00067k

Ozpinar, G. A., Peukert, W., and Clark, T. (2010). An Improved Generalized AMBER Force Field (GAFF) for Urea. *J. Mol. Model* 16 (9), 1427–1440. doi:10.1007/s00894-010-0650-7

Patel, D., Kopec, J., Fitzpatrick, F., McCorvie, T. J., and Yue, W. W. (2016). Structural Basis for Ligand-dependent Dimerization of Phenylalanine Hydroxylase Regulatory Domain. *Sci. Rep.* 6, 23748. doi:10.1038/srep23748

Patel, P. D., Pontrello, C., and Burke, S. (2004). Robust and Tissue-specific Expression of TPH2 versus TPH1 in Rat Raphe and Pineal Gland. *Biol. Psychiatry* 55 (4), 428–433. doi:10.1016/j.biopsych.2003.09.002

Pereira, G. R. C., Tavares, G. D. B., de Freitas, M. C., and De Mesquita, J. F. (2020). In Silico analysis of the Tryptophan Hydroxylase 2 (TPH2) Protein Variants Related to Psychiatric Disorders. *PLoS One* 15 (3), e0229730. doi:10.1371/journal.pone.0229730

Pettersen, E. F., Goddard, T. D., Huang, C. C., Couch, G. S., Greenblatt, D. M., Meng, E. C., et al. (2004). UCSF Chimera-Aa Visualization System for Exploratory Research and Analysis. *J. Comput. Chem.* 25 (13), 1605–1612. doi:10.1002/jcc.20084

Poli, G., Granchi, C., Rizzolio, F., and Tuccinardi, T. (2020). Application of MM-PBSA Methods in Virtual Screening. *Molecules* 25 (8). doi:10.3390/molecules25081971

Rohou, A., and Grigorieff, N. (2015). CTFFIND4: Fast and Accurate Defocus Estimation from Electron Micrographs. *J. Struct. Biol.* 192 (2), 216–221. doi:10.1016/j.jsb.2015.08.008

Saranya Ganesh, S., Sahai, A. K., Abhilash, S., Joseph, S., Kaur, M., and Phani, R. (2020). An Improved Cyclogenesis Potential and Storm Evolution Parameter for North Indian Ocean. *Earth Space Sci.* 7 (10), e2020EA001209. doi:10.1029/2020EA001209

Scheres, S. H. (2016). Processing of Structurally Heterogeneous Cryo-EM Data in RELION. *Methods Enzymol.* 579, 125–157. doi:10.1016/bs.mie.2016.04.012

Schoenichen, C., Bode, C., and Duerschmied, D. (2019). Role of Platelet Serotonin in Innate Immune Cell Recruitment. *Front. Biosci. (Landmark Ed.* 24 (3), 514–526. doi:10.2741/4732

Skjevik, A. A., Mileni, M., Baumann, A., Halskau, O., Teigen, K., Stevens, R. C., et al. (2014). The N-Terminal Sequence of Tyrosine Hydroxylase Is a Conformationally Versatile Motif that Binds 14-3-3 Proteins and Membranes. *J. Mol. Biol.* 426 (1), 150–168. doi:10.1016/j.jmb.2013.09.012

Somavarapu, A. K., and Kepp, K. P. (2015). The Dependence of Amyloid-β Dynamics on Protein Force Fields and Water Models. *Chemphyschem* 16 (15), 3278–3289. doi:10.1002/cphc.201500415

Stokes, A. H., Xu, Y., Daunais, J. A., Tamir, H., Gershon, M. D., Butkerait, P., et al. (2000). p-Ethynylphenylalanine: a Potent Inhibitor of Tryptophan Hydroxylase. *J. Neurochem.* 74 (5), 2067–2073. doi:10.1046/j.1471-4159.2000.0742067.x

Swami, T., and Weber, H. C. (2018). Updates on the Biology of Serotonin and Tryptophan Hydroxylase. *Curr. Opin. Endocrinol. Diabetes Obes.* 25 (1), 12–21. doi:10.1097/MED.0000000000000383

Szigetvari, P. D., Muruganandam, G., Kallio, J. P., Hallin, E. I., Fossbakk, A., Loris, R., et al. (2019). The Quaternary Structure of Human Tyrosine Hydroxylase: Effects of Dystonia-Associated Missense Variants on Oligomeric State and Enzyme Activity. *J. Neurochem.* 148 (2), 291–306. doi:10.1111/jnc.14624

Takumi, T., Tamada, K., Hatanaka, F., Nakai, N., and Bolton, P. F. (2020). Behavioral Neuroscience of Autism. *Neurosci. Biobehav Rev.* 110, 60–76. doi:10.1016/j.neubiorev.2019.04.012

Tenner, K., Walther, D., and Bader, M. (2007). Influence of Human Tryptophan Hydroxylase 2 N- and C-Terminus on Enzymatic Activity and Oligomerization. *J. Neurochem.* 102 (6), 1887–1894. doi:10.1111/j.1471-4159.2007.04664.x

Thompson, D. C., Humblet, C., and Joseph-McCarthy, D. (2008). Investigation of MM-PBSA Rescoring of Docking Poses. *J. Chem. Inf. Model* 48 (5), 1081–1091. doi:10.1021/ci700470c

Tidemand, K. D., Christensen, H. E., Hoeck, N., Harris, P., Boesen, J., and Peters, G. H. (2016). Stabilization of Tryptophan Hydroxylase 2 by L-Phenylalanine-Induced Dimerization. *FEBS Open Bio* 6 (10), 987–999. doi:10.1002/2211-5463.12100

van der Spoel, D., van Maaren, P. J., and Caleman, C. (2012). GROMACS Molecule & Liquid Database. *Bioinformatics* 28 (5), 752–753. doi:10.1093/bioinformatics/bts020

Vieira, T. F., and Sousa, S. F. (2019). Comparing AutoDock and Vina in Ligand/Decoy Discrimination for Virtual Screening. *Appl. Sci.* 9 (21), 4538. doi:10.3390/app9214538

Walker, S. J., Liu, X., Roskoski, R., and Vrana, K. E. (1994). Catalytic Core of Rat Tyrosine Hydroxylase: Terminal Deletion Analysis of Bacterially Expressed Enzyme. *Biochim. Biophys. Acta* 1206 (1), 113–119. doi:10.1016/0167-4838(94)90079-5

Waløen, K., Kleppe, R., Martinez, A., and Haavik, J. (2017). Tyrosine and Tryptophan Hydroxylases as Therapeutic Targets in Human Disease. *Expert Opin. Ther. Targets* 21 (2), 167–180. doi:10.1080/14728222.2017.1272581

Walther, D. J., and Bader, M. (2003). A Unique Central Tryptophan Hydroxylase Isoform. *Biochem. Pharmacol.* 66 (9), 1673–1680. doi:10.1016/S0006-2952(03)00556-2

Walther, D. J., Peter, J. U., Bashammakh, S., Hörtnagl, H., Voits, M., Fink, H., et al. (2003). Synthesis of Serotonin by a Second Tryptophan Hydroxylase Isoform. *Science* 299 (5603), 76–76. doi:10.1126/science.1078197

Weaver, S. R., Laporta, J., Moore, S. A., and Hernandez, L. L. (2016). Serotonin and Calcium Homeostasis during the Transition Period. *Domest. Anim. Endocrinol.* 56 Suppl, S147–S154. doi:10.1016/j.domaniend.2015.11.004

Windahl, M. S., Petersen, C. R., Christensen, H. E., and Harris, P. (2008). Crystal Structure of Tryptophan Hydroxylase with Bound Amino Acid Substrate. *Biochemistry* 47 (46), 12087–12094. doi:10.1021/bi8015263

Winge, I., McKinney, J. A., Ying, M., D'Santos, C. S., Kleppe, R., Knappskog, P. M., et al. (2008). Activation and Stabilization of Human Tryptophan Hydroxylase 2 by Phosphorylation and 14-3-3 Binding. *Biochem. J.* 410 (1), 195–204. doi:10.1042/bj20071033

Xu, Y., Wang, S., Hu, Q., Gao, S., Ma, X., Zhang, W., et al. (2018). CavityPlus: a Web Server for Protein Cavity Detection with Pharmacophore Modelling, Allosteric Site Identification and Covalent Ligand Binding Ability Prediction. *Nucleic Acids Res.* 46 (W1), W374–w379. doi:10.1093/nar/gky380

Yalameha, S., Nourbakhsh, Z., and Vashaee, D. (2022). ElTools: A Tool for Analyzing Anisotropic Elastic Properties of the 2D and 3D Materials. *Comput. Phys. Commun.* 271, 108195. doi:10.1016/j.cpc.2021.108195

Yohrling, G. J., Jiang, G. C., Mockus, S. M., and Vrana, K. E. (2000). Intersubunit Binding Domains within Tyrosine Hydroxylase and Tryptophan Hydroxylase. *J. Neurosci. Res.* 61 (3), 313–320. doi:10.1002/1097-4547(20000801)61:3<313::AID-JNR9>3.0.CO;2-9

Zhang, M. (2016). Two-step Production of Monoamines in Monoenzymatic Cells in the Spinal Cord: a Different Control Strategy of Neurotransmitter Supply? *Neural Regen. Res.* 11 (12), 1904–1909. doi:10.4103/1673-5374.197124

Zhang, T., Li, Y., Gao, P., Shao, Q., Shao, M., Zhang, M., et al. (2019). "SW_GROMACS: Accelerate GROMACS on Sunway TaihuLight," in *Proceedings of the International Conference for High Performance Computing, Networking, Storage and Analysis* (Denver, Colorado: Association for Computing Machinery).

Zhang, X., Wong, S. E., and Lightstone, F. C. (2013). Message Passing Interface and Multithreading Hybrid for Parallel Molecular Docking of Large Databases on Petascale High Performance Computing Machines. *J. Comput. Chem.* 34 (11), 915–927. doi:10.1002/jcc.23214

Zheng, S. Q., Palovcak, E., Armache, J. P., Verba, K. A., Cheng, Y., and Agard, D. A. (2017). MotionCor2: Anisotropic Correction of Beam-Induced Motion for Improved Cryo-Electron Microscopy. *Nat. Methods* 14 (4), 331–332. doi:10.1038/nmeth.4193

Zimmer, L., Luxen, A., Giacomelli, F., and Pujol, J. F. (2002). Short- and Long-Term Effects of P-Ethynylphenylalanine on Brain Serotonin Levels. *Neurochem. Res.* 27 (4), 269–275. doi:10.1023/a:1014998926763

Conflict of Interest: The authors declare that the research was conducted in the absence of any commercial or financial relationships that could be construed as a potential conflict of interest.

Publisher's Note: All claims expressed in this article are solely those of the authors and do not necessarily represent those of their affiliated organizations, or those of the publisher, the editors, and the reviewers. Any product that may be evaluated in this article, or claim that may be made by its manufacturer, is not guaranteed or endorsed by the publisher.

frontiers | Frontiers in Pharmacology

TYPE Review
PUBLISHED 29 August 2022
DOI 10.3389/fphar.2022.903099

OPEN ACCESS

EDITED BY
Liu Qing-Shan,
Minzu University of China, China

REVIEWED BY
Ian James Martins,
University of Western Australia, Australia
Li Zeng,
Chinese Academy of Medical Sciences and Peking Union Medical College, China

*CORRESPONDENCE
Ghulam Md Ashraf,
ashraf.gm@gmail.com
Abubakr M. Idris,
abubakridris@hotmail.com
Talha Bin Emran,
talhabmb@bgctub.ac.bd
Simona Cavalu,
simona.cavalu@gmail.com

†These authors have contributed equally to this work

SPECIALTY SECTION
This article was submitted to Neuropharmacology, a section of the journal Frontiers in Pharmacology

RECEIVED 23 March 2022
ACCEPTED 14 July 2022
PUBLISHED 29 August 2022

CITATION
Islam F, Shohag S, Akhter S, Islam MR, Sultana S, Mitra S, Chandran D, Khandaker MU, Ashraf GM, Idris AM, Emran TB and Cavalu S (2022), Exposure of metal toxicity in Alzheimer's disease: An extensive review.
Front. Pharmacol. 13:903099.
doi: 10.3389/fphar.2022.903099

Exposure of metal toxicity in Alzheimer's disease: An extensive review

Fahadul Islam[1†], Sheikh Shohag[2†], Shomaya Akhter[2], Md. Rezaul Islam[1], Sharifa Sultana[1], Saikat Mitra[3], Deepak Chandran[4], Mayeen Uddin Khandaker[5], Ghulam Md Ashraf[6,7]*, Abubakr M. Idris[8,9]*, Talha Bin Emran[10]* and Simona Cavalu[11]*

[1]Department of Pharmacy, Faculty of Allied Health Sciences, Daffodil International University, Dhaka, Bangladesh, [2]Department of Genetic Engineering and Biotechnology, Faculty of Earth and Ocean Science, Bangabandhu Sheikh Mujibur Rahman Maritime University, Dhaka, Bangladesh, [3]Department of Pharmacy, Faculty of Pharmacy, University of Dhaka, Dhaka, Bangladesh, [4]Department of Veterinary Sciences and Animal Husbandry, Amrita School of Agricultural Sciences, Amrita Vishwa Vidyapeetham University, Coimbatore, India, [5]Centre for Applied Physics and Radiation Technologies, School of Engineering and Technology, Sunway University, Subang Jaya, Malaysia, [6]Pre-Clinical Research Unit, King Fahd Medical Research Center, King Abdulaziz University, Jeddah, Saudi Arabia, [7]Department of Medical Laboratory Technology, Faculty of Applied Medical Sciences, King Abdulaziz University, Jeddah, Saudi Arabia, [8]Department of Chemistry, College of Science, King Khalid University, Abha, Saudi Arabia, [9]Research Center for Advanced Materials Science (RCAMS), King Khalid University, Abha, Saudi Arabia, [10]Department of Pharmacy, BGC Trust University Bangladesh, Chittagong, Bangladesh, [11]Faculty of Medicine and Pharmacy, University of Oradea, Oradea, Romania

Metals serve important roles in the human body, including the maintenance of cell structure and the regulation of gene expression, the antioxidant response, and neurotransmission. High metal uptake in the nervous system is harmful because it can cause oxidative stress, disrupt mitochondrial function, and impair the activity of various enzymes. Metal accumulation can cause lifelong deterioration, including severe neurological problems. There is a strong association between accidental metal exposure and various neurodegenerative disorders, including Alzheimer's disease (AD), the most common form of dementia that causes degeneration in the aged. Chronic exposure to various metals is a well-known environmental risk factor that has become more widespread due to the rapid pace at which human activities are releasing large amounts of metals into the environment. Consequently, humans are exposed to both biometals and heavy metals, affecting metal homeostasis at molecular and biological levels. This review highlights how these metals affect brain physiology and immunity and their roles in creating harmful proteins such as β-amyloid and tau in AD. In addition, we address findings that confirm the disruption of immune-related pathways as a significant toxicity mechanism through which metals may contribute to AD.

KEYWORDS

alzheimer's disease, metal-induced toxicity, amyloid-beta, biometals, heavy metals, neurotoxicity

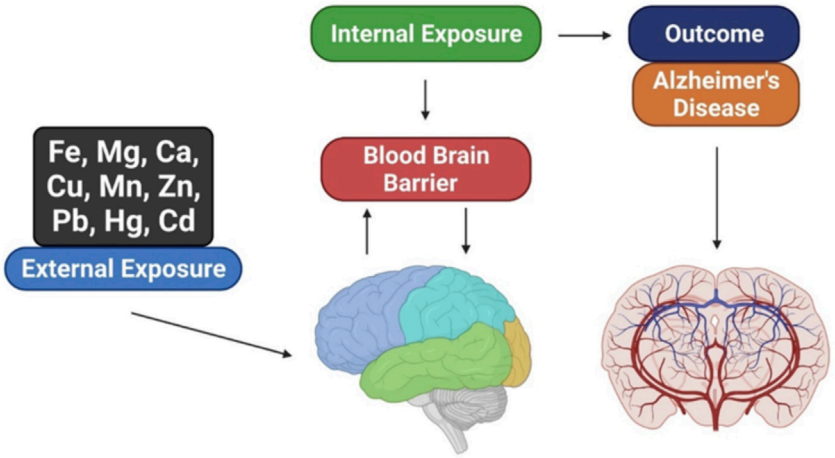

GRAPHICAL ABSTRACT

Introduction

Alzheimer's disease (AD) is a neurodegenerative disorder (NDD) that causes dementia in the elderly and has diverse implications (Islam et al., 2022b; 2022a). Neuropathological changes in the AD brain are linked to the aggregation of amyloid-β (Aβ) and the microtubule-associated tau protein in neurofibrillary tangles (NFTs), leading to cognitive impairment of neuronal connectivity and neuron loss (Kolarova et al., 2012). Aβ′s structure and harmful effects in causing oxidative stress (OS), autophagy, and neuroinflammation have been widely studied (Jomova et al., 2010; Uddin et al., 2020b). Several pharmacological candidates that remove or reduce Aβ production in AD treatment have been identified (Uddin et al., 2020a). In recent years, it has been determined that Aβ aggregation is not the initial event in AD pathogenesis but rather a later event (Kepp, 2017).

New research methodologies are required to develop successful AD treatments. According to various studies, homeostasis of key biometals such as calcium, magnesium, manganese, copper, zinc, and iron is disrupted in AD. Moreover, these metals play an important role in tau and Aβ metabolism and aggregation. It has been hypothesized that targeting metal interactions with Aβ may be effective in preventing AD (Li et al., 2017; Huat et al., 2019). The pathophysiological effects of metal imbalance in the brain have been established by several studies (Zhang Z. et al., 2016). Akhtar et al. found that intervention with chromium picolinate reduced streptozotocin-induced cognitive impairment (Akhtar et al., 2020). Furthermore, chromium picolinate treatment improved cognition and reduced oxidative damage, mitochondrial dysfunction and neuroinflammation, and increased insulin signaling, reversing AD pathophysiology. Nonetheless, some argue that impaired biometal activity is the cause of AD. The blood-brain barrier (BBB) makes treating brain disorders challenging. Because biometals cannot passively permeate the BBB, the metal imbalance in the AD brain cannot be attributed solely to decreased or increased exposure to metals but rather to a more complex initial intracellular ion distribution. Metal exporting, importing, and sequestering proteins maintain metal homeostasis in the brain (Harilal et al., 2020). Heavy metal accumulation in the human body harms various organs, particularly the brain. Several studies have focused on the neurological functions of cadmium, mercury, and lead in the brain (Kabir et al., 2021).

This review highlights the effects of biometals and heavy metals on the brain, including how they contribute to AD and immune system dysregulation. It also identifies treatment options for metal-induced neurotoxicity and important directions for future research.

Pathogenic mechanisms of biometal–induced AD pathology

Iron (Fe)

Iron (Fe) is an essential trace metal that causes oxidative damage and may contribute to NDD development. Several studies have shown a correlation between AD and oxidative damage (Levine, 1997). The putamen and globus pallidus have been found to contain higher iron levels in the brains of AD patients (Levine, 1997; Moon et al., 2016). However, serum iron levels in these AD patients were lower or unchanged compared to healthy individuals. The iron levels in the cerebrospinal fluid (CSF) were not affected by AD (Ficiarà et al., 2021). However,

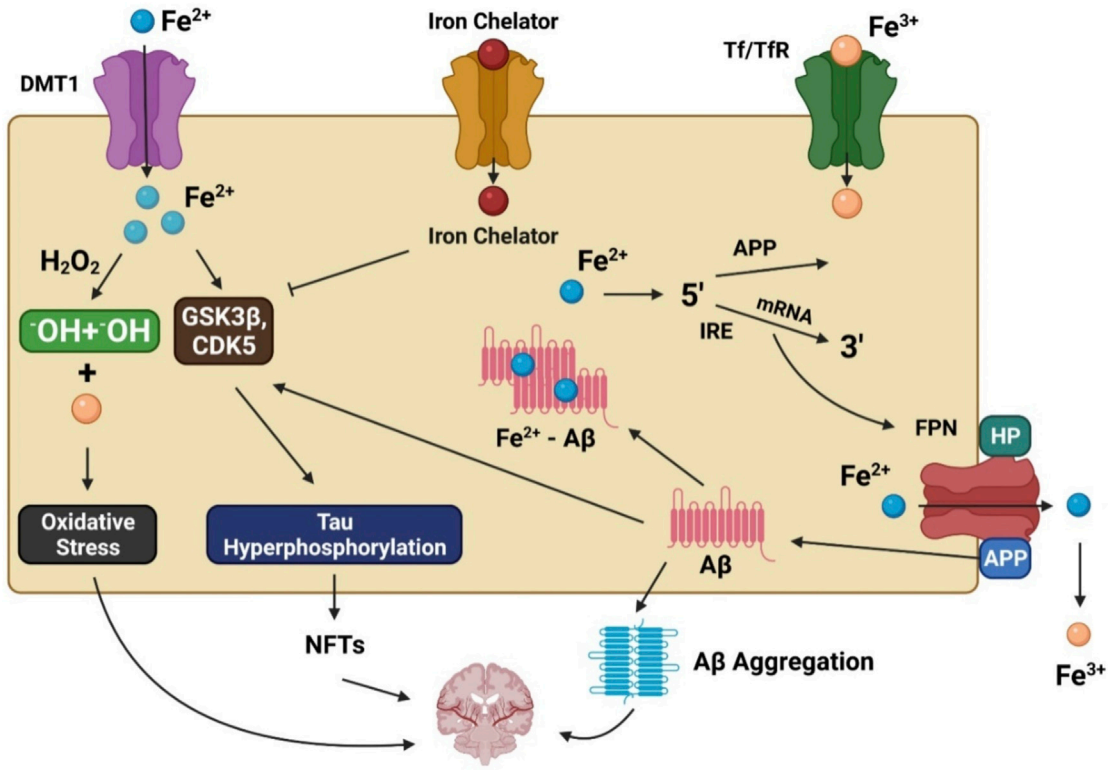

FIGURE 1
The involvement of iron in Alzheimer's disease pathogenesis. DMT1 allows ferrous iron (Fe^{2+}) to pass through the cell directly, while transferrin (Tf)-ferric iron (Fe^{3+}) penetrates via endocytosis mediated by the transferrin receptor (TfR). Increased Fe^{2+} levels trigger the Fenton reaction, which produces the hydroxyl radical (•OH), resulting in oxidative stress and neurotoxicity. Moreover, Fe^{2+} can increase tau phosphorylation by activating glycogen synthase kinase 3β (GSK3β) and cyclin-dependent kinase 5 (CDK5), resulting in neurofibrillary tangle development (NFTs). GSK3 and CDK5 are inhibited by iron chelators, which diminish tau phosphorylation. Fe2+ interacts to the iron responsive element (IRE) in the 5′ UTR area of amyloid precursor protein (APP) mRNA in the biological environment, resulting in the stimulation of APP translation and the production of amyloid beta (Aβ).

further research is required to confirm this observation due to the limited sample size of this CSF study.

Ferritin is an iron storage protein present at high levels in AD brain tissue (Quintana et al., 2006). Therefore, CSF ferritin may be a suitable measure of the amount of iron in the brain. Ferritin production (Thirupathi and Chang, 2019) and secretion (Zhang et al., 2006) by glial cells is dependent on cellular iron levels in cultured systems. CSF ferritin levels are thought to be representative of iron levels in the brain and can be useful in clinical settings. CSF ferritin levels are reduced in restless legs syndrome, a condition caused by low brain iron levels that are treated with iron supplements (Chawla et al., 2019). CSF ferritin levels were reportedly higher in AD patients (Kuiper et al., 1994). However, this observation was not confirmed in later studies with larger clinical cohorts (Paterson et al., 2014). Meta-analysis and cross-referenced statistical methods have been used to assess the iron content of twelve different regions of the brain. They found iron levels were higher in eight brain regions that were statistically linked to clinical AD diagnosis, and yellow blood iron levels and iron overload symptoms in the brain were present in AD patients whose iron homeostasis was unbalanced (Tao et al., 2014). However, a meta-regression analysis found that disparities in serum iron levels might result from differences in average participant age between trials (Wang et al., 2015).

Unfortunately, there is no well-supported explanation for these anomalies that lead to increased oxidative stress in AD patients because of their higher iron levels. For iron homeostasis to be maintained, there must be a dynamic interaction between iron efflux and influx in which many transporter proteins play a significant role. Iron accumulation in affected regions of the brain may be partially caused by dysfunction of the iron exporter ferroportin (FPN) and iron importers such as lactoferrin (Lf), melanotransferrin (MTf), divalent metal transporter 1 (DMT1), and transferrin (Tf) in AD patients (Figure 1). DMT1 and FPN are iron metabolism-related proteins involved in AD progression (Raha et al., 2014). *DMT1* is not expressed in oligodendrocytes or astrocytes. The Fe^{2+} influx process is associated with DMT1 (Song et al., 2007), which has two isoforms, DMT1+IRE and

DMT1-IRE, that colocalize with Aβ in AD brain plaques. Additionally, levels of both isoforms were found to be increased in the hippocampus and frontal cortex of amyloid precursor protein (APP)/presenilin-1 (PSEN1) transgenic mice and associated with decreased *FPN* expression (Xian-Hui et al., 2015). The colocalization of FPN and hepcidin in astrocytes was associated with decreased *FPN* expression in the brains of AD patients. When hepcidin is repressed, the iron export process is inhibited, causing an iron buildup within cells (Raha et al., 2014). Studies have found that inhibition of APP-induced iron export reduces soluble tau levels leading to increased iron retention, which can be achieved using lithium (Lei et al., 2012, 2017) or an iron chelator (Lei et al., 2015). Moreover, sirtuin two regulates cellular iron homeostasis by deacetylating nuclear factor erythroid-derived 2-related factor 2, a transcription factor involved in the FPN synthesis regulation (Yang et al., 2017).

DMT1 and *FPN* expression is reduced by chemicals present in Chinese herbs that may represent a novel approach for reducing iron overload-related impairment in AD patients (Xian-Hui et al., 2015). The Tf-transferrin receptor (TfR) complex facilitates iron uptake in BBB endothelial cells. Endocytosis of Tf-bound iron across the BBB can be facilitated by receptors, enabling iron transport. Significantly different CSF Tf levels were found in individuals carrying mutations than in relatives who did not have these mutations (Moos and Morgan, 2000; Ringman et al., 2012). Tf and Lf consist of two lobes, each with a Fe^{3+} binding site (Baker et al., 1994). *Lf* expression is elevated in macrophages and monocytes and fibrillar-type side population cells (SPs) in the cerebral cortex of AD patients. In addition, the aging process is mediated by SP creation. The endocytic process that eliminates Aβ is associated with the cell surface receptor lipoprotein receptor-related protein (LRP). Another beneficial function of Lf is its binding to LRP, dramatically improving the soluble amyloid removal instead of production (An et al., 2009; Wang et al., 2010). An Lf-based liposomal delivery method for neuron growth factors has been developed and used clinically, helping to prevent or reduce the spread of AD (Meng et al., 2015).

Magnesium (Mg)

Magnesium helps keep intracellular calcium concentrations high under normal conditions by preventing calcium-induced excitatory responses (Levitsky and Takahashi, 2013). However, calcium and magnesium imbalances affect multiple processes that contribute to various health problems, including dementia (Volpe, 2013). Several studies have explored the effect of magnesium in AD pathogenesis. Hyperphosphorylated tau aggregation *in vitro* has been associated with magnesium deficiency (Yang and Ksiezak-Reding, 1999). Moreover, magnesium-L-threonate supplements reduce the enzyme β-secretase (BACE1), reducing levels of APP C-terminal fragments and free APP, reducing AD-associated cognitive impairment and synaptic loss (Li et al., 2014). Magnesium sulfate therapy reduces hyperphosphorylated tau levels by lowering glycogen synthase kinase 3 (GSK3) levels and blocking its phosphorylation, and enhancing phosphatidylinositol three kinase (PI3K) and protein kinase B (PKB) activity (Gomez-Ramos et al., 2006; Xu et al., 2014). Therefore, a neuroprotective magnesium effect may contribute to AD development.

Magnesium has been shown to alleviate chronic neuroinflammation by decreasing the calcium influx through N-methyl-D-aspartate receptors (NMDARs), a type of calcium-permeable cationic channel that contributes to the formation of long-term memories and learning activated by glutamate. Aggregation-induced NMDAR overactivation is observed in early-stage AD (Parameshwaran et al., 2008). There are two NMDAR subtypes identified in brain regions affected by AD with which magnesium interacts as an endogenous inhibitor (Kotermanski and Johnson, 2009).

Calcium influx into post-synaptic neurons was reduced by adding magnesium to block channels, reducing excitotoxic cell death in dementia. The activation of adenosine triphosphate (ATP)-gated P2X purinergic receptors (P2XRs) has also been associated with the onset of NDDs (Witting et al., 2004). Calcium enters and leaves cells through membrane pores formed by microglia using P2X7R oligomers (North, 2002). P2X7R and purinergic receptor-mediated neuroinflammation has been alleviated by magnesium in tissue culture, suggesting that increased magnesium levels may be an effective inhibitor of calcium entry via cell surface channels (Lee et al., 2011).

Transporters, exchangers, channels, and various buffering proteins maintain cellular calcium and magnesium levels. Magnesium transporter 1 (MagT1), cyclin M (CNNM) transporter, and transient receptor potential melastatin six and 7 (TRP-M6) enhance magnesium entry into cells. Magnesium release is through solute carrier family 41 member 1 (SLC41A1) and a sodium-independent magnesium exchanger (Romani, 2011; de Baaij et al., 2015). Several transporters, including calcium channels, are involved in maintaining intracellular calcium equilibrium. Calcium levels in the brain are increased by NMDAR, voltage-gated calcium channels, and store-operated channels. Buffer proteins such as calbindin can store calcium in the endoplasmic reticulum (ER), while the calcium-ATPase pump and sodium-calcium exchanger promote cellular calcium release. The AD brain's ER-Ca dynamics are significantly affected by the activation of two types of calcium receptors and plasma membrane calcium-permeable channels (Tu et al., 2006; Cheung et al., 2008). However, the role of magnesium transporters in AD pathogenesis remains unknown. It was found that the physiological function of transient receptor potential cation channel subfamily M member 7 (TRPM7) is coordinated by presenilins, leading to familial AD (Oh et al., 2012). TRPM2 was

removed from APP/PS1 mouse models to reduce ER stress and age-dependent memory impairments. In addition, *in vitro* studies showed that TRPM2 knockdown prevented an increase in the magnitude of the whole-cell current induced by Aβ, highlighting the importance of TRPM2 in the neuronal toxicity caused by Aβ. TRPM2 alterations have also been connected to calcium imbalance, despite their role in controlling magnesium associated with AD (Ostapchenko et al., 2015).

Calcium (Ca)

Calcium has been identified as a widespread second messenger and regulator of cell functions (Komuro and Kumada, 2005). An *in vitro* study found it to contribute to the aggregation of hyperphosphorylated tau (Yang and Ksiezak-Reding, 1999). Calcium ion concentrations in the nervous system are tightly regulated by several mechanisms, including calcium channels, pumps, and binding proteins, and other metal ions such as magnesium. Magnesium has been found to be a calcium antagonist (Levitsky and Takahashi, 2013). There are a number of processes altered by calcium disturbances, including in NDDs such as AD (Volpe, 2013). Calcium-mediated neuroinflammation associated with NMDAR stimulation is reduced by magnesium through this pathway, preventing the long-term activation of the NMDAR-induced calcium influx. Because of their role in synaptic activities such as memory and learning, NMDARs are crucial calcium-permeable cationic channels. Overactivation of NMDARs by Aβ aggregation can occur in the early stages of AD (Parameshwaran et al., 2008). Continuous calcium influx can increase intracellular calcium concentrations, activating various enzymatic activities resulting in neuronal death, protein degradation, and oxidative stress (Mota et al., 2014). Several calcium transporters maintain intracellular calcium equilibrium. NMDARs and voltage-gated calcium channels are some of the receptors responsible for elevated calcium concentrations in the body. Calcium-ATPase pump and sodium-calcium transporter drive calcium release from cells, while buffer proteins such as calbindin store it in the ER. ER-Ca dynamics in the AD brain are significantly influenced by mutated presenilins, which activate two types of calcium receptors and plasma membrane calcium-permeable channels (Tu et al., 2006; Cheung et al., 2008). It has also been shown that Aβ oligomers can either activate calcium-permeable channels or bind to NMDARs, facilitating calcium influx into cells (Diaz et al., 2009; Arbel-Ornath et al., 2017).

Aluminum (Al)

Aluminum is the third most abundant element in the earth's crust and the most abundant metal. It is used in many applications, including food preservation, cans, cookware, automobiles, and vaccine adjuvants (Shaw and Tomljenovic, 2013). In mammals, specific functions of aluminum are obscure because of its toxicity to living organisms due to its strong reactivity with carbon and oxygen. The kidney quickly eliminates aluminum from food and environmental sources in humans. However, aluminum salts in vaccine adjuvants are biologically active and accumulate in the nervous system. Aluminum has been associated with AD and other NDDs (Aoun Sebaiti et al., 2018). It was found to accumulate with Aβ peptide in the brains of individuals with dialysis-associated encephalopathy (Ogunlade et al., 2022). Surprisingly, their symptoms disappeared soon after its removal from the dialysis solution (Exley and Mold, 2019). A recent meta-analysis found that chronic aluminum exposure increased the incidence of AD by almost 70% (Wang et al., 2016). Furthermore, an association between numbers of AD patients and their exposure to aluminum-adjuvanted vaccines was identified (Shaw and Tomljenovic, 2013), with increased levels of aluminum found in their hair, blood, and urine (Dórea, 2020). Aluminum hydroxide injections cause long-term memory loss, anxiety, and neurodegeneration in the spinal cord and motor cortex in mice (Shaw and Tomljenovic, 2013). Oxidative stress and mitochondrial dysfunction may also be responsible for neurological damage. However, several studies do not account for confounding factors such as genetic backgrounds that may predispose an individual to aluminum-induced neurological dysfunction. Aluminum-induced neurotoxicity is likely due to a combination of genetic and environmental factors (Wong-Guerra et al., 2021).

Pathogenic mechanisms of heavy metal-induced AD pathology

Copper (Cu)

The neurological system is very sensitive to heavy metals. Copper is an important transition metal involved in numerous biological processes, including energy metabolism and antioxidant defense. In addition, copper is involved in protecting against free radicals, cell respiration, and neurotransmitter synthesis (Zatta and Frank, 2007; Scheiber and Dringen, 2013). Copper deficiency may affect the production and maintenance of myelin causing neuronal degeneration (Table 1). In NDDs such as AD, copper levels are altered. However, the role of copper in AD remains enigmatic. Copper levels in senile plaques are abnormally high (Lovell et al., 1998). A deficiency in total copper in AD brain tissue has been observed in various studies (Deibel et al., 1996) and a recent meta-analysis that also found elevated plasma and

TABLE 1 Some heavy metal-induced Alzheimer's disease-associated molecular objects.

Physical/ chemical/ clinical properties	Arsenic (As)	Lead (Pb)	Cadmium (Cd)	Mercury (Hg)
Absorption	Organic: also binds as trivalent and pentavalent>90%; inhalation: absorption is dependent on particle size; GI inorganic: trivalent and pentavalent salts >90%	Skin: alkyl lead compounds (methyl and tetraethyl lead) because of their lipid solubility; inhalation: up to 90% depending on particle size; GI: Adults have a GI of 5–10%, whereas children have a GI of 40%	Inhalation 10–40%; GI 1.5–5%	GI: inorganic salts can be absorbed and transformed to organic mercury by bacteria in the stomach; inhalation: elemental mercury is entirely absorbed
Distribution	Concentrates in the skin, nails, and hair; accumulates in the lungs, heart, kidney, liver, muscle, and brain tissue	Initially carried in red blood cells and dispersed to soft tissues (kidney and liver); primarily as a phosphate salt in bone, teeth, and hair	Binds to albumin and blood cells at first, then to metallothionene in the liver and kidney	Hg (vapor) penetrates membranes easily and quickly from the lungs to the CNS. Organic salts (lipid soluble) are equally distributed and eliminated by intestinal (intracellular) feces. Salts that are inorganic concentrate in the blood, plasma, and kidneys (renal elimination)
Half-life	7–10 h	Blood: 30–60 days; bone: 20–30 years	10–20 years	60–70 days
Sources of exposure	GI: food and well water Environmental: smelting ore waste, such as Ga in semiconductors, herbicides, and insecticides; inhalation: smelting fumes and dust	GI: paint, pottery, moonshine; inhalation: metal fumes skin: tetraethyl lead in gasoline	Inhalation: industrial, metal fumes, tobacco; environmental: electroplating, galvanization, plastics, batteries; GI: pigments, polishes, antique toys	Environmental: electronics and plastic industry; seed fungicide treatment; dentistry
Mechanism of toxicity	Membranes: Capillary endothelium protein damage increased vascular permeability, resulting in vasodilation and vascular collapse; inhibition of sulfhydryl group containing enzymes; suppression of anaerobic and oxidative phosphorylation (substitutes for inorganic phosphate in synthesis of high-energy phosphates)	Heme production is inhibited; heme is a key structural component of hemoglobin, myoglobin, and cytochromes		
Binds to proteins' sulfhydryl groups (-SH groups)	Inhalation: emphysema, local irritation, and suppression of alpha1-antitrypsin; oral: kidney: proximal tubular damage (proteinuria) linked to beta2-acroglobulin	Protein precipitation and destruction of mucosal membranes due to salt dissociation; necrosis of the proximal tubular epithelium; inhibition of sulfhydryl (-SH) group containing enzymes		
Treatments	Exclusion from exposureAcute: supportive therapy: fluid, electrolyte replacement, blood pressure support (dopamine); chronic: penicillamine w/o dialysisrsine gas (AsH_3) acts as a hemolytic agent with secondary to renal failure. Supportive therapy: transfusion; chelators have not been proved to be effective	Treatment with chelators such as CaNa2EDTA, BAL, dimercaprol, and D-penicillamine after removal from exposure	Removal from exposure, chelation therapy using CaNa2EDTA, and BAL, although the BAL-Cd combination is exceedingly toxic and is not utilized	Removal from exposure; Hg and Hg salts >4 μg/dl: 2,3-dimercaptopropanol (BAL), β, β-dimethyl cysteine (penicillamine), most effective is N-acetyl-β, β-dimethyl cysteine (N-acetyl-penicillamine); methyl Hg-supportive treatment (nonabsorbablethiol resins can be given orally to reduce methyl Hg level in gut)
Humans' maximum allowable dosage	10–50 μ gkg $^{-1}$ (EPA References)	5 μ gkg $^{-1}$day $^{-1}$ (EPA References)	0.5–1 μ gkg $^{-1}$day $^{-1}$ (EPA References)	0.1–2 μ gkg $^{-1}$day $^{-1}$ (EPA References)
References	(Yadav et al., 2010; Sharma et al., 2014)	(Sharma et al., 2014; Kumar Singh et al., 2018)	(Sharma et al., 2014; Batool et al., 2019)	(Sharma et al., 2014; Patel and Rao, 2015)

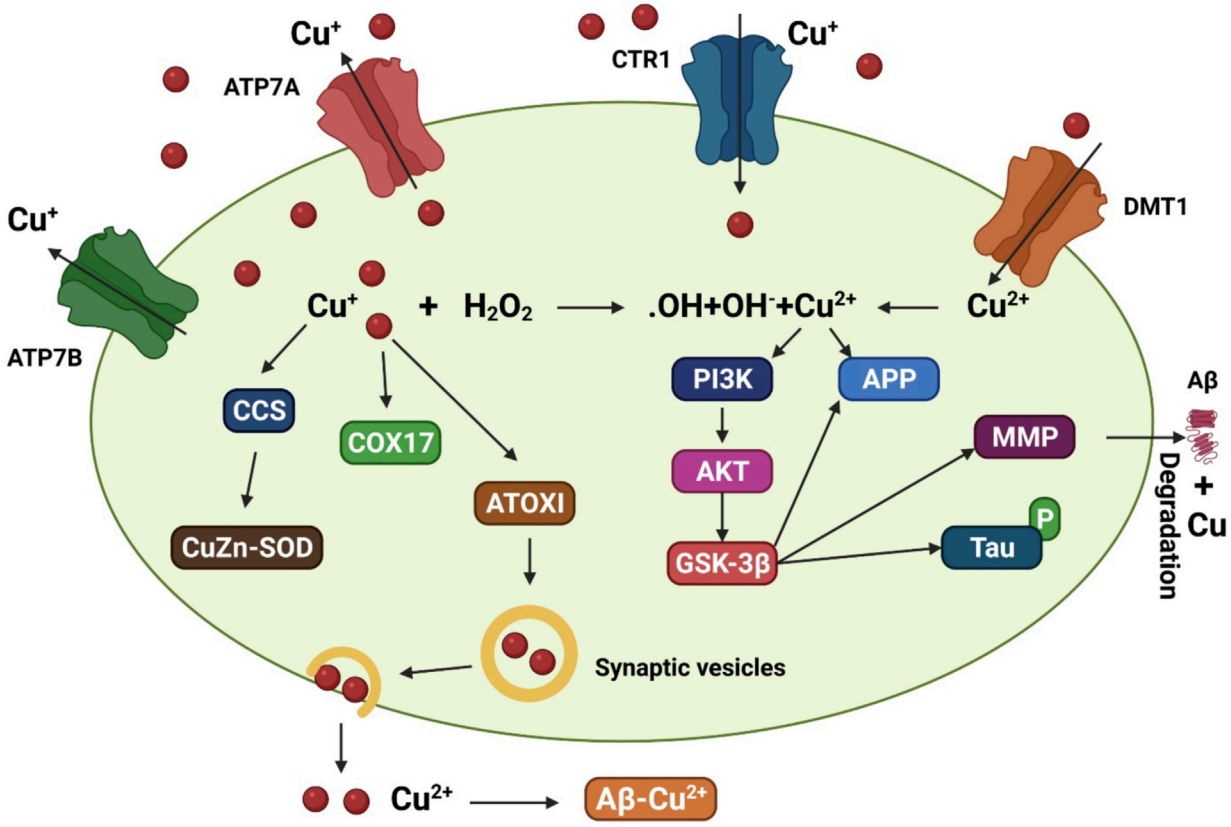

FIGURE 2
A model that depicts the copper transit system and its link to AD. Copper transporter 1 (CTR1) transports Cu^{+} into brain cells. Cu^{2+} uptake is aided by DMT1. Various Cu chaperones, including such copper chaperone for superoxide dismutase (CCS), cytochrome oxidase enzyme complex (COX17), and antioxidant protein (ATOX1), sequester accumulated Cu into particular cellular sites. ATOX1 is thought to transfer Cu^{+} to ATP7A (copper-transporting P-type ATPase) and ATP7B, which aid in the import of Cu^{+} into synaptic vesicles for release and/or facilitate Cu export straightforwardly. Increased oxidative stress may be caused by excessive intracellular Cu^{+} activating the Fenton reaction. Cu^{2+} also leads to tau hyperphosphorylation by stimulating the glycogen synthase kinase 3β (GSK3β) pathway, which is implicated in the production of the matrix metalloproteinases (MMP) important for Aβ breakdown. Copper interacts to Aβ in the synaptic cleft, facilitating the production of senile plaques.

serum copper levels in AD patients (Klevay, 2008). However, no significant difference in copper levels was observed in the CSF of healthy individuals and AD patients (Ventriglia et al., 2012; Vaz et al., 2018).

Copper precipitates in large amounts in senile plaques, causing copper insufficiency elsewhere in the body. Copper has been shown to negatively influence the pathological mechanisms of Aβ and tau (Sparks and Schreurs, 2003; Kitazawa et al., 2009), potentially explaining this heterogeneity. Copper has a strong affinity for Aβ and stimulates the production of its oligomers (Tõugu et al., 2008; Jin et al., 2011). Because copper and Aβ can catalytically produce hydrogen peroxide *in vitro*, oxidative stress may be a factor in copper-mediated Aβ oligomer cytotoxicity. Copper chelators such as clioquinol can counteract Cu-Aβ toxicity (Adlard et al., 2008; Matlack et al., 2014). Copper is also present in A precursor-like protein 2 (APLP2) and APP (Barnham et al., 2003). Indeed, higher copper levels in the cerebral cortex of mice missing APP or APLP2 indicate that the copper transporter APP may also function as a chelator (White et al., 1999b). However, another study by the same authors found that APP deletion in cortical neurons had no impact on copper uptake (White et al., 1999a), suggesting that they may not be a copper carrier but instead reflect improper copper interactions.

Copper increases exocytosis and decreases endocytosis, facilitating the redistribution of APP to the cell membrane (Acevedo et al., 2011). Copper has also been shown to enhance the GSK3-mediated dephosphorylation of endogenous APP and facilitate its proteolytic degradation into Aβ (Acevedo et al., 2014). In addition, the binding of copper to the microtubule-binding domain of tau causes its aggregation *in vitro* (Su et al., 2007). Hydrogen peroxide production was induced by copper exposure in a mouse AD

model (Kitazawa et al., 2009). The activation of cyclin-dependent kinase 5 (CDK5) and GSK3 pathways is believed to be how copper mediates tau phosphorylation (Crouch et al., 2009).

Copper trafficking mechanisms in the AD brain are well understood. P-type ATPases, particularly ATP7A and ATP7B, play a crucial role in controlling monovalent copper in cells together with the transporters, high-affinity copper uptake proteins 1 (CTR1) and 2 (CTR2) (Kuo et al., 2006; Yu et al., 2017). Copper-containing enzymes are synthesized by DMT1 in cells that receive divalent copper from DMT1 (Zheng and Monnot, 2012). However, ATP hydrolysis can reduce copper overload in cells, and this process is used by both ATP7A and ATP7B to export copper from cells.

In addition to transporters, many molecular chaperones such as antioxidant protein 1, the enzyme complex cytochrome oxidase, and copper chaperone for superoxide dismutase (SOD) contribute to copper delivery (Harris, 2001). Studies found that genetically deleting the copper transporter 1C (CTR1C) gene, a member of the CTR1 family with high homology to its human ortholog, in a *Drosophila* AD model drastically decreased levels of copper accumulation in the brain (Lang et al., 2013). In addition, when another copper importer, copper transporter 1B (CTR1B), was suppressed or when the copper exporter ATPase copper transporting 7 (ATP7) gene was overexpressed in this AD model, the same outcome was observed (Figure 2). Flies with CTR1 knocked down had higher levels of Aβ production but lower levels of oxidative stress, suggesting that increased Aβ oligomers or Aβ aggregates are less harmful with reduced copper influx (Lang et al., 2013). When amyloid plaques are present, ATP7-alpha (ATP7A) levels are increased in nearby activated microglial cells, leading to a dramatic shift in copper trafficking. AD can be associated with inflammation-induced copper dyshomeostasis in microglia based on this neuromechanism (Zheng et al., 2010). An accumulation of single nucleotide polymorphisms in the ATP7-beta (*ATP7B*) gene is associated with an increased risk of AD development, indicating that changes in copper homeostasis may accelerate AD-associated neurodegeneration (Bucossi et al., 2011; Squitti et al., 2013).

Manganese (Mn)

Manganese is an essential trace element contributing to the growth of human tissues and the regulation of intracellular homeostasis (Prakash et al., 2017). SOD and glutamine synthetase are two important manganese-dependent enzyme cofactors. There is increasing evidence that manganese overload is associated with NDDs and that even a slight manganese excess can cause symptoms that are comparable with manganese (Park et al., 2014). This cell toxicity is caused by various mechanisms, including oxidative stress and mitochondrial dysfunction, abnormal energy metabolism, toxic chemical accumulation, cellular depletion of antioxidant defenses, and autophagy (Guilarte, 2013; Martinez-Finley et al., 2013). Manganese levels in the brains of AD patients with dementia were found to be significantly higher than in healthy individuals, with the highest concentrations in the parietal cortex (Srivastava and Jain, 2002; Tong et al., 2014). Plaques were disseminated in monkeys exposed to chronic manganese levels. The p53 pathway targets the most affected gene in the frontal cortex, amyloid-beta precursor-like protein 1 (APLP1) (Guilarte, 2010). The frontal cortex appears to be a primary target of manganese exposure, contributing to early dementia (Schneider et al., 2013). The mechanism by which manganese treatment elevates Aβ peptide levels is likely related to the disruption of Aβ degradation (Tong et al., 2014). A recent study found, similar to other biometals, manganese can weakly bind to a specific region of Aβ (Wallin et al., 2016). Additional research is required to fully understand these initial findings and determine how manganese binding to Aβ affects Aβ aggregation.

The antioxidant enzyme Mn-SOD contains manganese and is crucial for maintaining mitochondrial health. Oxidative respiration is inhibited by increased manganese, increasing reactive oxygen species (ROS) generation and mitochondrial dysfunction (Gunter et al., 2006). Aβ plaque deposition and tau phosphorylation in a transgenic AD mouse model were elevated when Mn-SOD was partially inhibited (Li et al., 2004; Melov et al., 2007). However, the overexpression of Mn-SOD reduced the load of cortical plaques associated with AD pathology (Dumont et al., 2009), associating AD pathogenesis with mitochondrial oxidative stress. Because manganese and iron compete to some extent for binding sites and transport channels in the Golgi apparatus, it has been hypothesized that excessive manganese absorption causes Golgi iron deficiency (Carmona et al., 2010).

Manganese transport is mediated by numerous importers, such as the dopamine transporter (DAT), DMT1, Tf/TfR, zinc transporters 4 (ZIP4) and 8 (ZIP8), secretory route Ca^{2+}-ATPase 1 (SPCA1), ATPase cation transporting 13A2 (ATP13A2/PARK9), solute carrier family 30 member 10 (SLC30A10), and FPN (Figure 3) DMT1 was the first mammalian transporter for cellular manganese absorption and an iron influx transporter. When iron is scarce, DMT1 facilitates the efficient transfer of manganese across the BBB (Garrick et al., 2006). Trivalent manganese enters cells by ligand-receptor endocytosis, while divalent manganese enters cells via DMT1 (Subramaniam et al., 2002). Zinc-binding ZIP8 and zinc transporters 14 (ZIP14) have been found by multiple studies to contribute to manganese absorption in the liver and lungs (Aydemir et al., 2017; Lin et al., 2017).

Recent studies have focused on the role of exporter proteins in maintaining manganese levels. The cell surface-located efflux exporter SLC30A10 was identified in genome research to be a

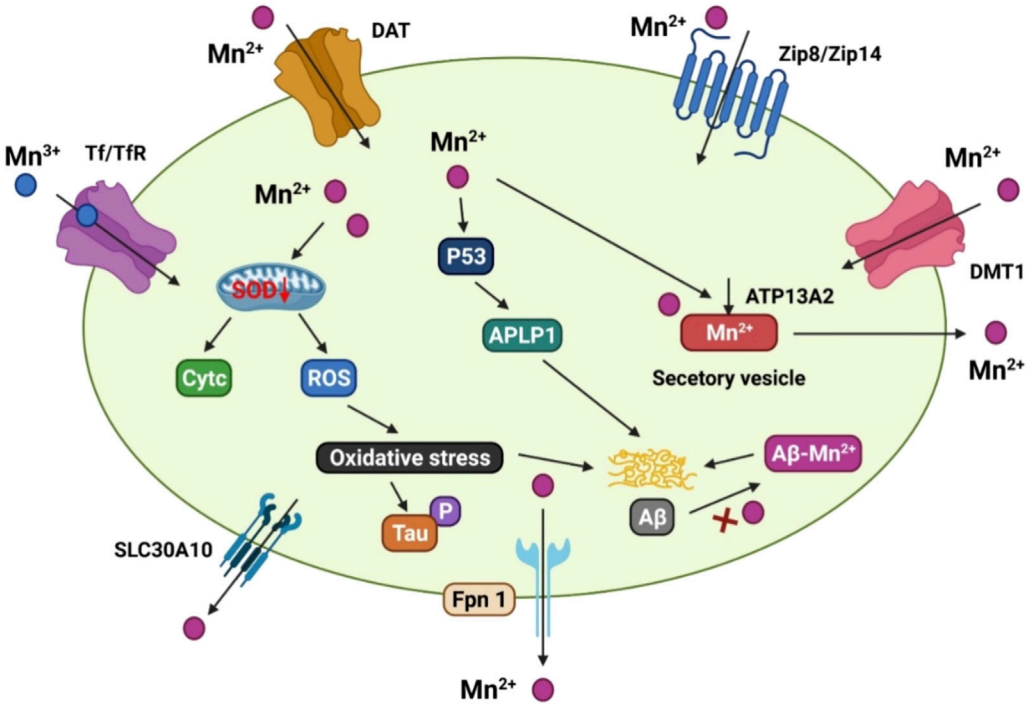

FIGURE 3
The manganese transport mechanism, and its association with Alzheimer's disease. DMT1, ZIP8/ZIP14, and dopamine transporter (DAT) are involved for Mn^{2+} inflow on the cell membrane, whereas Tf/TfR mediates Mn^{3+} entrance into the endosome via endocytosis and is then released into the cytoplasm by DMT1. SLC30A10 and Fpn, on the other hand, transport Mn^{2+} out of cells. ATP13A2 and SPCA1 also transport Mn^{2+} into the lysosomes and Golgi for bioavailability, or produce secretory vesicles that aid Mn^{2+} efflux. Mn^{2+} conditions can cause mitochondrial oxidative stress in the AD brain, which accelerates tau phosphorylation. In addition, elevated Mn^{2+} levels boost the production of p53 and its transcriptional target gene, amyloid-b precursor-like protein 1 (APLP1), which encodes amyloid precursor protein (APP). The production of Aβ peptides is aided by enhanced APLP1 expression. Mn^{2+} could potentially attach to Aβ and help its aggregation.

potential zinc and manganese transporter. There is an increased accumulation of manganese in the brain of Parkinson's disease patients who carry SLC30A10 mutations (Tuschl et al., 2016). In the frontal cortex of AD patients and APP/PS1 transgenic mice, SLC30A10 levels are consistently lower, indicating that its dysregulation may be a contributing factor to the AD onset and progression (Bosomworth et al., 2013).

Several studies have shown that the iron exporter FPN operates as a cellular manganese exporter in a pH-dependent manner to reduce manganese buildup and cytotoxicity in the body (Madejczyk and Ballatori, 2012). The ATP13A2 cation transporter transports manganese and zinc, among others. Overexpression of ATP13A2 has been shown to lower intracellular manganese concentrations, lowering manganese-induced mortality. ATP13A2 loss-of-function mutations are associated with increased α-synuclein and Aβ plaques in Lewy body dementia (Murphy et al., 2014).

SPCA1 homolog calcium-transporting ATPase 1 (PMR1) has been shown to mediate calcium and manganese transport, and the ectopic expression of SPCA1 in yeast increases their susceptibility to manganese poisoning (Ton et al., 2002). While SPCA1 has been proposed as a secondary regulator of cellular manganese homeostasis, the affinity between SPCA1 and manganese and the roles of SPCA1 in AD pathogenesis requires further research.

Zinc (Zn)

The brain is the organ with the highest concentration of zinc in the body. Zinc-dependent transcription factors and enzymes represent more than 2,000 proteins in the brain, and zinc is found in 70% of all brain proteins studied so far (Takeda, 2000). Zinc is transported into the brain parenchyma across the BBB and CSF barriers. For example, zinc can be transported across the BBB through its interaction with L-histidine in both plasma and CSF (Takeda, 2001). In the CSF and extracellular fluid compartments, zinc can be readily exchanged following its uptake by the body (Takeda, 2001). One of the three families of proteins that regulates zinc homeostasis in the brain is the zinc-binding proteins (ZBPs), which are primarily responsible for regulating intracellular zinc levels (Mocchegiani et al., 2001;

Vanea et al., 2014; Islam et al., 2022c, 2022c, 2022c). Zinc uptake from extracellular fluids into neurons and glia is regulated by zinc and iron-like regulatory proteins, while zinc outflow from cells is regulated by zinc transporters (Liuzzi and Cousins, 2004; Kambe et al., 2015). Interestingly, many zinc regulatory proteins also regulate other metal anions.

Glutamatergic nerve terminals in the brain are particularly rich in zinc ions, which can be released into the environment during neuronal activity (Paoletti et al., 2009; Sensi et al., 2011). Synaptic zinc release influences the development and function of glutamatergic receptors such as NMDA and receptors for glycine ionotropic and gamma-aminobutyric acid (GABA) and other neurotransmitters (Smart et al., 2004). Therefore, zinc is crucial for memory and behavior since it is associated with the balance between excitation and inhibition in the brain (Frederickson and Danscher, 1990).

There is a broad spectrum of neurological disorders caused by the disruption of zinc homeostasis (Doraiswamy and Finefrock, 2004; Mocchegiani et al., 2005). While zinc lacks redox activity, high zinc levels in the extracellular fluid have been shown to cause neurotoxicity and alter protein aggregation (Cuajungco and Lees, 1997; Frederickson et al., 2005). The discovery that zinc can precipitate Aβ into plaques at concentrations >300 nM generated interest in its function in AD (Bush et al., 1994). Synaptic transmission boosts the concentration of zine in the extracellular fluid, potentially explaining why Aβ deposition occurs in the brains of AD patients (Deshpande et al., 2009). Plaques and the cerebral amyloid angiopathy around affected blood vessels contain zinc-rich metalloprotein Aβ, itself a metalloprotein containing zinc binding sites (Bush et al., 1993; Suh et al., 2000; Maynard et al., 2005). The increase of Zn^{2+} in presynaptic vesicles in Tg2576 transgenic mice crossed with zinc transporter three knockout mice have been shown to reduce plaque load, demonstrating that synaptic zinc contributes to Aβ deposition (Lee et al., 2002). When zinc is sequestered by Aβ, it inhibits APP ferroxidase function, resulting in increased iron and ROS levels (Mucke et al., 2000; Duce et al., 2010).

Extrinsic zinc-chelator CEDAA combined with cadmium can reverse the attenuation of long-term potentiation (LTP) in dentate granule cells produced by Aβ and zinc treatment in dentate granule cells *in vivo* (Takeda et al., 2017). Consequently, zinc chelators or ionophores can restore the physiological metal ions sequestered inside extracellular Aβ aggregates, resulting in biochemical and anatomical alterations that contribute to improved cognition (Adlard et al., 2008, 2011, 2015). Despite the overwhelming evidence that zinc and copper chelators minimize Aβ accumulation, it has recently been shown that this may have unintended negative consequences for brains in good health (Adlard et al., 2008). The zinc/copper chelator clioquinol decreased memory function in young mice (2.5 months old) by depleting zinc levels in their brains. The brain-derived neurotrophic factor (BDNF) associated with synaptic plasticity and dendritic spine density has been shown to increase *in vivo* (Frazzini et al., 2018). The hippocampus, cortex, and striatum were all affected, but the cerebellum, which is devoid of zinc reservoirs, was unaffected (Wall, 2005; Frazzini et al., 2018). The role of zinc in promoting its effects, particularly at the cellular and molecular levels of the brain, remains to be studied in greater detail.

Lead (Pb)

One of the most common names for the heavy metal plumbum (Pb) is lead. While the dangers of lead poisoning had been understood for many years, the association between white lead paint on porches and railings in Brisbane, Australia, and severe neurological abnormalities in children was not recognized until 1892 (Needleman, 2009). The half-life of environmental lead in the bloodstream is 30 days. Lead attaches to blood cells and travels throughout the body, eventually accumulating in the bones. Bone-deposited lead has a half-life of 20–30 years. Bone demineralization during pregnancy, menopause, lactation, and aging induces the release of accumulated lead into the bloodstream (Nash et al., 2004; Rastogi et al., 2007).

Many systems in the body are affected by lead in the blood, but the central nervous system is by far the most vulnerable. The effects of lead on the brain can be divided into two categories: morphological and pharmacological. Neuronal differentiation, myelination, and synaptogenesis are examples of morphological effects (Brubaker et al., 2009; Hu et al., 2014; Senut et al., 2014). Biometal-dependent systems can be disrupted due to binding site competition between lead and other biometals, particularly calcium and zinc. Lead rapidly crosses the BBB and severely damages the brain due to its capacity to substitute for calcium ions (Sanders et al., 2009). The GABAergic, dopaminergic, and cholinergic systems and NMDA receptors are inhibited by lead, interfering with neurotransmitter release. Additionally, lead binds to sulfhydryl groups in glutathione, a crucial antioxidant present in cells, removing its antioxidant properties (Bijoor et al., 2012; Flora et al., 2012).

Lead exposure during childhood has been shown to cause cognitive and behavioral problems (Mazumdar et al., 2011; Reuben et al., 2017). Neuronal alterations in hippocampal CA1 pyramidal neurons associated with memory loss and learning impairments are associated with juvenile lead exposure. Animals exposed to lead while pregnant or after birth suffer from memory loss and cognitive decline in old age (Hu et al., 2008; Bihaqi et al., 2014). Low-level gestational lead exposure has been shown to change the hippocampus dendritic spines by decreasing neuroligin-1 protein levels, resulting in memory and learning problems (Zhao et al., 2018). A probable link between AD development and the long-term effects of lead exposure in childhood has been

suggested. According to a long-term study of former organolead production workers, lead exposure causes cognitive impairment over time and leaves permanent brain damage (Schwartz et al., 2000; Stewart et al., 2006).

Lead has been associated with a number of AD hallmarks, including Aβ buildup, tau pathology, and inflammation. Moreover, early lead exposure caused an addiction-like disease in young rats, resulting in increased *APP* and *BACE1* expression, and inducing Aβ buildup and plaque development in the hippocampus and cortex, respectively (Zhou et al., 2018). *APP* and *BACE1* expression were found to be upregulated in aged rat brains following prenatal exposure to lead (Basha et al., 2005). Lead exposure in childhood boosted the expression of *APP*, *BACE1*, and transcription factor-specific protein 1 (*Sp1*) to a similar extent and facilitated Aβ deposition in elderly monkeys (Wu et al., 2008). Lead, cadmium, and arsenic exposure synergistically increased *APP* and *BACE1* expression, strongly inducing Aβ production (Ashok et al., 2015). Exposure to lead during development activates the sterol regulatory element-binding protein 2 (SREBP2)-BACE1 pathway, affecting normal cholesterin metabolism in the early brain (Wu et al., 2008).

It has been well established that dysregulation of cholesterol homeostasis in the brain plays a significant role in the genesis of AD and Aβ production (Maria Giudetti et al., 2015). Acute lead exposure has been shown to enhance Aβ accumulation in the brain tissue and CSF by disrupting low-density lipoprotein receptor-related protein 1 (LRP-1)-mediated clearance of the peptide (Gu et al., 2011). Notably, lead exposure also increases levels of total and hyperphosphorylated tau. It has been shown that lead exposure increases the protein levels of tau and phosphorylated tau in SH-SY5Y neuroblastoma cells (Bihaqi et al., 2017). Tau expression and serine/threonine phosphatase and CDK5 activities in the brain are all up-regulated following lead exposure early in life (Bihaqi and Zawia, 2013). GSK3 and caspase-3-mediated tauopathy have recently been associated with lead exposure (Bihaqi et al., 2018).

Neuronal death occurs as a result of an inflammatory response to lead exposure. Tumor necrosis factor-alpha (TNF-α) and granulocyte-colony stimulating factor levels are higher in individuals exposed to lead than in those who were not (Di Lorenzo et al., 2007). The persistent stimulation of glial cells in a rat model was accompanied by inflammation and neurodegeneration. Microglia are activated and pro-inflammatory proteins such as inducible nitric oxide synthase (iNOS), interleukin one β (IL-1β), and TNF-α. AD-related brain neurotoxicity is thought to be caused in part by the substances listed above. Lead exposure leads to increased microglial activation and poorer LTP (Liu et al., 2012). The activation of the transcription factor nuclear factor kappa B (NF-κB) and the overexpression of cyclooxygenase-2 is the cause of lead-induced activation of microglia. Other microglial pathways associated with lead exposure include extracellular signal-regulated kinase (ERK) and PKB activation (Kumawat et al., 2014). Additionally, lead exposure was found to stimulate TLR4-MyD88-NF-κB signaling, affecting hippocampal neurogenesis and plasticity (Liu et al., 2015). Lead activation results in increased synthesis of proinflammatory cytokines and generation of reactive nitrogen species (RNS) and ROS (Altmann et al., 1999). These findings conclusively show that long-term lead exposure raises AD risk. However, in the absence of medications to counter lead poisoning, exposure should be avoided.

Mercury (Hg)

AD has been associated with mercury exposure. Numerous studies have found elevated mercury levels in the blood and brain tissue of AD patients (Ehmann et al., 1986; Thompson et al., 1988; Hock et al., 1998). Consequently, mercury levels have been found to be higher in hair samples. In a comparison of patients with and without degenerative brain diseases, mercury levels in patients with degenerative brain diseases were higher than in patients without (Mano et al., 1989). Indeed, mercury in the neurological system has been found to cause memory loss, attention problems, and even dementia, a common indicator of AD (Zahir et al., 2005; Mutter et al., 2010).

Cadmium (Cd)

Cadmium is an abundant heavy metal in the environment and a naturally occurring carcinogen that causes cancer in humans. Unlike other heavy metals, cadmium is water-soluble, allowing it to be transmitted from the soil to plants and accumulate in the food chain (Qadir et al., 2014; Laslo et al., 2022, 2022). For example, tobacco can tolerate high levels of cadmium despite its potentially harmful effects on other plants (Huang and Goldsbrough, 1988; Zhang M. et al., 2016). Consequently, the general public's risk for cadmium-related morbidities is increased by their use of tobacco products or inhalation of tobacco smoke (Richter et al., 2017).

Cadmium has a half-life of 20–40 years in the kidneys and liver after entering the body (Suwazono et al., 2009; Fransson et al., 2014). Cadmium has been shown to pass through the BBB and accumulate in the brain, causing neurotoxicity (Wang and Du, 2013). Older individuals with high blood cadmium levels were found more likely to die from AD-related causes (Wang and Du, 2013; Min and Min, 2016). A growing body of evidence suggests that cadmium may contribute to the aggregation of Aβ plaques in AD patients (Li et al., 2012). Cadmium administration to APP/PS1 mice caused an increase in plaque size and quantity *in vivo* (Li et al., 2012). Cadmium ions can promote plaque development through their interaction with Aβ (Notarachille et al., 2014). Cadmium therapy has also been proposed to

suppress the expression of β-secretase and neutral endopeptidase, which are both important for decreasing Aβ levels in the brain (Li et al., 2012). The synergistic effect of cadmium, lead, and arsenic greatly improves amyloidogenesis by increasing *APP*, *BACE1*, and *PSEN1* expression, suggesting that cadmium interacts with other metals in AD (Ashok et al., 2015).

In addition to its effects on Aβ, cadmium has been implicated in tau conformation and self-aggregation in the AD brain (del Pino et al., 2016). The third repeat (R3) of the microtubule-binding domain of tau has been shown to bind to cadmium. Tau self-aggregation is facilitated by the loss of the random coil conformation and gain of a helix shape of the R3 domain. Cadmium therapy suppresses muscarinic M1 receptors, known to adversely regulate GSK3 and increase levels of total and phosphorylated tau (Medeiros et al., 2011; del Pino et al., 2016). These findings are consistent with the view that cadmium may play a role in AD development.

Nontoxic cadmium exposure has been shown to activate the MAPK and NF-κB signaling pathways, leading to neuroinflammation and neuronal death in humans (Phuagkhaopong et al., 2017). Increased expression of interleukins 6 (IL-6) and 8 (IL-8) has been associated with AD development. The MAPK and PI3K/AKT signaling pathways have also been found to contribute to cadmium cytotoxicity in astrocytes (Jiang et al., 2015). Therefore, central nervous system (CNS) illnesses such as AD and Parkinson's disease may be prevented by controlling cadmium-induced Ca^{2+} homeostasis. However, adverse neuroinflammation has yet to be associated with cadmium exposure in animal AD models.

Neurotoxicity induced by metal mixtures

Most studies of metal neurotoxicity have focused on one specific metal. However, the reality is that we live in a world where metals coexist, making research more complex. Since numerous metals such as iron, manganese, copper, cadmium, and zinc are transported or controlled by overlapping signaling pathways, fluctuations in the levels of one metal can significantly impact the homeostasis of another. The combined effects of exposure to multiple metals have been rarely studied. However, cadmium, mercury, and manganese have been studied in the context of lead neurotoxicity (Sanders et al., 2015).

Prenatal exposure to lead is more harmful to brain development than prenatal exposure to just one metal. Children exposed to high levels of cadmium during pregnancy may experience problems with their mental and motor development if their lead levels are also high (McDermott et al., 2011; Kim et al., 2013; Sanders et al., 2015). In addition, prenatal exposure to high levels of both lead and manganese led to a greater number of cognitive and language impairments in infants by the age of two compared to exposure to each alone (Lin et al., 2013). Furthermore, lead exposure was associated with poorer IQ scores in children with high blood manganese levels, but only if they also had high blood manganese levels. Rather than functioning cooperatively, lead and arsenic exposure appears to function noncooperatively since their combined effects on cognitive deficiency were not additive, contrary to the findings with lead and cadmium, manganese, or mercury exposure (Kim et al., 2009; Yorifuji et al., 2011).

The retention and redistribution of individual metals in rodents can be improved by the co-administration of two metals (Kalia et al., 1984). Chandra et al. gave rats lead intraperitoneally along with manganese orally and found they experienced more severe changes in motor activity, learning ability, biogenic amine, and brain lead levels than rats given manganese or lead alone (Chandra et al., 1983). The central monoaminergic systems of mice have been found to be affected by an interaction of arsenic/lead. While single metal treatments lowered norepinephrine in the hippocampus, combined treatments of arsenic and lead increased serotonin levels in the midbrain and frontal cortex and lead accumulation in the brain (Mejía et al., 1997). When rats were fed mining waste containing arsenic, cadmium, manganese, and lead orally, arsenic and manganese were shown to accumulate in the brain, and dopamine release was reduced over time with LTP.

Manganese has been shown to exacerbate the well-documented neurotoxic effects of lead in children at younger ages (Rodríguez et al., 1998; Sanders et al., 2015). Rat motor parameters were significantly reduced after exposure to a mixture of arsenic, manganese, and lead rather than a single metal alone. Because humans are frequently simultaneously exposed to multiple metals in the real world and metal overexposure is frequently associated with neurotoxicity, additional research into the health effects of mixed metal exposure is urgently needed in the near future.

Treatment for metal-induced neurotoxicity

The initial steps in treating individuals poisoned by metals are to remove them from the hazardous area and then perform gastrointestinal decontamination. For example, a fast fall in blood plasma manganese levels was observed after manganese supplementation was discontinued in children with cholestasis receiving total parenteral nourishment (Hambidge et al., 1989). Plasma-based therapy may be ineffective in individuals with chronic metal exposure because the metals will already have accumulated in the bones, brain, and other tissues. Chelation therapy, in which multiple metals are removed from the body, is a common treatment for chronic and acute metal poisoning. Chelators include D-penicillamine, calcium disodium edetate ($CaNa_2$ EDTA), British antilewisite (BAL), and Cuprimine

(Jang and Hoffman, 2011; Cavalu et al., 2020). However, chelators can cause side effects such as headaches, weariness, renal failure, nasal congestion, and life-threatening hypocalcemia (Jang and Hoffman, 2011). The most important considerations when performing chelation therapy are the specificity and dosage of the chelators.

The identification of individual metal exporters has led to the development of innovative therapies for metal-induced neurotoxicity. Mutations in the newly discovered manganese transporter *SLC30A10* cause dystonia, hypermanganesemia, parkinsonism, and manganism, a condition characterized by the release of too much intracellular manganese (Choi et al., 2007; Quadri et al., 2012; Leyva-Illades et al., 2014; Chen et al., 2015b). While a comprehensive investigation of its substrates has not yet been completed, it appears to only transport manganese (Leyva-Illades et al., 2014; Chen et al., 2015a). Pharmaceuticals containing compounds that enhance SLC30A10 export stimulated manganese efflux but have little effect on other metals. The risks of chelation can be greatly reduced using this technique. However, the specific transporters for different metals, such as SLC30A10 for manganese, remain largely unknown and must be exhaustively studied in the future to enable the development of new therapies for metal-induced toxicity.

Metal exposure on public health: Low and middle-income countries

The most significant natural resource is water. Surface water samples from the Rupsariver in Bangladesh were taken in the summer and winter seasons, and pH, electrical conductivity (EC), chromium, nickel, copper, arsenic, cadmium, and lead levels were determined to assess the risk of metal toxicity, identify its potential sources, and predict health risk from metals in water. Their average concentrations and standard deviations in the summer season were determined to be: chromium (7.20 ± 0.613 g/L), lead (7.09 ± 0.904 g/L), arsenic (5.45 ± 0.441 g/L), copper (5.36 ± 0.471 g/L), nickel (3.85 ± 0.694 g/L), and cadmium (0.975 ± 0.106 g/L). Similarly, in the winter season, they were determined to be: chromium (8.87 ± 0.756 g/L), lead (7.32 ± 0.93 g/L), arsenic (6.05 ± 0.490 g/L), copper (6.02 ± 0.529 g/L), nickel (5.48 ± 0.986 g/L), and cadmium (1.38 ± 0.151 g/L). Methods such as correlation analysis, principal component analysis (PCA), and cluster analysis (CA) were used to identify the source of harmful metals in the water [1]. Except for copper, total heavy metal toxicity load and heavy metal evaluation index values exceeded permitted levels. During both seasons, 85% of the total samples were determined to pose moderate ecological risks, while the remaining 15% posed low ecological risks, based on the ecological risk index classification. Oral exposure revealed a high non-carcinogenic risk for a single element (Proshad et al., 2021). The oral exposure hazard index values were 4.17 for adult males, 3.67 for adult females, and 8.64 for children, indicating that non-carcinogenic effects are likely. The carcinogenic risks of nickel and arsenic from regular oral and dermal contact were higher than the standard value ($>1.0 \times 10^{-4}$), indicating potential cancer risks to adult males and females and children in the studied area (Proshad et al., 2021).

Around 25% of global fatalities and disorders are caused by harmful environmental exposures (Heng et al., 2022). Metals are a common source of dangerous environmental exposure, with levels regularly exceeding the recommended limits. Currently, 632 million children in lower-middle-income countries (LMICs) have blood lead levels above both the US Centers for Disease Control's former public health action standard of 5 μg/dl (Ericson et al., 2021) and the updated 2021 standard of 3.5 μg/dl (Sink, 2022). Manganese levels in drinking water surpass 400 μg/L in over 50 nations, including Bangladesh, Cambodia, Egypt, and Ghana. While the World Health Organization (WHO) no longer provides manganese guidelines (Frisbie et al., 2012), studies have indicated that excessive levels are associated with a variety of adverse effects, including impaired intellectual performance in children (Ericson et al., 2007). More than 4.5 million people in Latin America are chronically exposed to arsenic in their drinking water, in some cases more than 200 times higher than the limit of 10 μg/L set by WHO (McClintock et al., 2012).

Many heavy metals pollute the air, water, and soil environment due to their unregulated use in agriculture, mining, smelting, illegal refining, and industrial production. Because they are non-biodegradable, their environmental concentrations may gradually increase over time. Consequently, cumulative human population exposures can have long-term consequences (Tchounwou et al., 2012). Children are more vulnerable to the negative health impacts of environmental exposures because of their rapid neurodevelopment. The brain is most plastic during the first 1,000 days of life, during which it undergoes a series of complex processes such as neurogenesis, myelination, and synaptic pruning (Grantham-McGregor et al., 2007). These processes build over time, leading to important cognitive functions such as language and speech, attention, conduct, and reasoning (Villar et al., 2019). Therefore, perturbations in their biological environment, such as toxicant exposure, can disrupt the precise orchestration of events, resulting in irreversible downstream effects such as neurodevelopmental delays, behavioral issues, and learning difficulties (Davis et al., 2019). In addition to this stage of fast brain plasticity, children are more vulnerable to adverse environmental exposures than adults due to additional biological and social reasons. Children consume more food and water in proportion to their body weight, spend more time on the ground and the floor, and eat more non-food things (Mamtani et al., 2011).

The negative impacts of heavy metals on child neurodevelopment have been extensively studied in high-

income countries (HICs). Lead is the heavy metal with the greatest evidence of neurodevelopmental harm, with a dose-dependent drop in IQ scores (Searle et al., 2014). Even with blood lead levels below five ug/dL, the National Toxicology Program found the data sufficient to detect the detrimental effects of lead on cognition and heightened attention-related and other problematic behaviors (Budtz-Jørgensen et al., 2013). Other metals, such as arsenic, cadmium, manganese, and mercury, have also been found to negatively impact several aspects of neurodevelopment, including cognition and behavior (Ericson et al., 2007; Jett et al., 2020). There is inconclusive evidence about the impact of prenatal arsenic exposure on neurodevelopment (Freire et al., 2018; Jiang et al., 2018). However, the majority of studies evaluating the association between heavy metals and infant neurodevelopment take place in HICs rather than LMICS, which account for 90% of children worldwide (Husain et al., 2021). An estimated 43% of children in LMICs do not reach their full neurodevelopmental potential due to various factors, including environmental exposures (Lu et al., 2016). This inability to realize their full potential influences their quality of life and economic potential, highlighting the importance of understanding the effects of metals on neurodevelopment in LMICs environments (Grantham-McGregor et al., 2007).

Conclusion and future prospects

An imbalance of metal ions is initiated or mediated by a cascade of processes that inevitably leads to neural network dysfunction in many NDDs, including oxidative stress, protein misfolding and aggregation, mitochondrial dysfunction, and energy depletion. The fundamental mechanisms underlying some of these activities remain unknown, and how ion homeostasis is maintained and disrupted in the brain is becoming a contentious issue. The importance of inadequately liganded metals has been overlooked in the past. A better understanding of the multiple factors implicated in these processes is crucial for determining the pathophysiological mechanisms underlying the abundance of metal ions and developing therapeutic approaches that can disrupt the chain of pathological events that occur in many NDDs, including AD, the etiology of which remains unknown for many. It remains unclear whether different metals, such as iron, zinc, copper, and aluminum, have similar or dissimilar modes of action. Understanding these mechanisms requires a multisystem integrative approach, leading to future advancements in neurodegenerative research.

The intricate association between biometal metabolism, genetic and environmental exposures, and the pathophysiology of NDDs merits additional exploration, particularly in light of recent developments in metal neurobiology. While the corroboration from experimental and transgenic animal studies is compelling, when combined with findings for the human brain, they suggest that metal ions play a significant role in neurodegeneration but do not provide conclusive answers on the causality of metal-related processes or efficacious preventive and therapeutic approaches in humans. Metalloproteomics developments have contributed to improved knowledge of the mechanics and exact involvement of metalloenzymes and proteins in the brain (Lothian et al., 2013).

There is little that can be done to slow the progression of neurodegeneration at present. Its multifaceted presentation requires a fundamental change toward developing multidrug treatments. Metal ions are implicated in the majority of these degenerative disorders, making them a promising target for future therapeutic approaches. One strategy is to chelate and sequester the ions, limiting their ability to interfere with protein folding or prevent them from undergoing oxidative processes (Fasae et al., 2021). Redistributing metal ions with newer approaches has therapeutic effects. Recent research suggests that treating cellular copper shortage may help to prevent neurodegeneration (Gromadzka et al., 2020). Similarly, iron-chelating drugs such as hydroxypyridones may facilitate the redistribution of iron through mobilization with transferrin to treat several NDDs, including AD (Singh et al., 2019). Many drugs have recently been developed to reduce metal ions associated with both metal-induced Aβ aggregation and ROS generated by this and other aggregates through chelation. Developing drugs with a multitargeted action may be the next step in treating NDDs such as AD (Sales et al., 2019), but they will need to be validated and evaluated further.

Author contributions

FI, SSh, SA, and TE conceptualized and designed the manuscript, participating in drafting the article and/or acquisition of data, and/or analysis and interpretation of data; FI, MI, SSu, SM, and DC prepared the figures and tables. FI, MK, GMA, AI, TE, and SC wrote, edited and revised the manuscript critically. TE and GA revised the final written. All authors critically revised the manuscript concerning intellectual content and approved the final manuscript.

Acknowledgments

The authors would like to express their gratitude to King Khalid University, Saudi Arabia, for providing administrative and technical support.

Conflict of interest

The authors declare that the research was conducted in the absence of any commercial or financial relationships that could be construed as a potential conflict of interest.

Publisher's note

References

Acevedo, K. M., Hung, Y. H., Dalziel, A. H., Li, Q. X., Laughton, K., Wikhe, K., et al. (2011). Copper promotes the trafficking of the amyloid precursor protein. *J. Biol. Chem.* 286, 8252–8262. doi:10.1074/jbc.M110.128512

Acevedo, K. M., Opazo, C. M., Norrish, D., Challis, L. M., Li, Q. X., White, A. R., et al. (2014). Phosphorylation of amyloid precursor protein at threonine 668 is essential for its copper-responsive trafficking in SH-SY5Y neuroblastoma cells. *J. Biol. Chem.* 289, 11007–11019. doi:10.1074/jbc.M113.538710

Adlard, P. A., Bica, L., White, A. R., Nurjono, M., Filiz, G., Crouch, P. J., et al. (2011). Metal ionophore treatment restores dendritic spine density and synaptic protein levels in a mouse model of Alzheimer's disease. *PLoS One* 6, e17669. doi:10.1371/journal.pone.0017669

Adlard, P. A., Cherny, R. A., Finkelstein, D. I., Gautier, E., Robb, E., Cortes, M., et al. (2008). Rapid restoration of cognition in Alzheimer's transgenic mice with 8-hydroxy quinoline analogs is associated with decreased interstitial Abeta. *Neuron* 59, 43–55. doi:10.1016/j.neuron.2008.06.018

Adlard, P. A., Parncutt, J., Lal, V., James, S., Hare, D., Doble, P., et al. (2015). Metal chaperones prevent zinc-mediated cognitive decline. *Neurobiol. Dis.* 81, 196–202. doi:10.1016/j.nbd.2014.12.012

Akhtar, A., Dhaliwal, J., Saroj, P., Uniyal, A., Bishnoi, M., Sah, S. P., et al. (2020). Chromium picolinate attenuates cognitive deficit in ICV-STZ rat paradigm of sporadic Alzheimer's-like dementia via targeting neuroinflammatory and IRS-1/PI3K/AKT/GSK-3β pathway. *Inflammopharmacology* 28, 385–400. doi:10.1007/s10787-019-00681-7

Altmann, P., Cunningham, J., Dhanesha, U., Ballard, M., Thompson, J., and Marsh, F. (1999). Disturbance of cerebral function in people exposed to drinking water contaminated with aluminium sulphate: Retrospective study of the Camelford water incident. *Br. Med. J.* 319, 807–811. doi:10.1136/bmj.319.7213.807

An, L., Sato, H., Konishi, Y., Walker, D. G., Beach, T. G., Rogers, J., et al. (2009). Expression and localization of lactotransferrin messenger RNA in the cortex of Alzheimer's disease. *Neurosci. Lett.* 452, 277–280. doi:10.1016/j.neulet.2009.01.071

Aoun Sebaiti, M., Abrivard, M., Blanc-Durand, P., Van Der Gucht, A., Souvannanorath, S., Kauv, P., et al. (2018). Macrophagic myofasciitis-associated dysfunctioning: An update of neuropsychological and neuroimaging features. *Best. Pract. Res. Clin. Rheumatol.* 32, 640–650. doi:10.1016/j.berh.2019.04.003

Arbel-Ornath, M., Hudry, E., Boivin, J. R., Hashimoto, T., Takeda, S., Kuchibhotla, K. V., et al. (2017). Soluble oligomeric amyloid-β induces calcium dyshomeostasis that precedes synapse loss in the living mouse brain. *Mol. Neurodegener.* 12, 27. doi:10.1186/s13024-017-0169-9

Ashok, A., Rai, N. K., Tripathi, S., and Bandyopadhyay, S. (2015). Exposure to As-Cd-and Pb-mixture induces Aβ, amyloidogenic APP processing and cognitive impairments via oxidative stress-dependent neuroinflammation in young rats. *Toxicol. Sci.* 143, 64–80. doi:10.1093/toxsci/kfu208

Aydemir, T. B., Kim, M. H., Kim, J., Colon-Perez, L. M., Banan, G., Mareci, T. H., et al. (2017). Metal transporter Zip14 (Slc39a14) deletion in mice increases manganese deposition and produces neurotoxic signatures and diminished motor activity. *J. Neurosci.* 37, 5996–6006. doi:10.1523/JNEUROSCI.0285-17.2017

Baker, E. N., Anderson, B. F., Baker, H. M., Day, C. L., Haridas, M., Norris, G. E., et al. (1994). Three-dimensional structure of lactoferrin in various functional states. *Adv. Exp. Med. Biol.* 357, 1–12. doi:10.1007/978-1-4615-2548-6_1

Barnham, K. J., McKinstry, W. J., Multhaup, G., Galatis, D., Morton, C. J., Curtain, C. C., et al. (2003). Structure of the Alzheimer's disease amyloid precursor protein copper binding domain. A regulator of neuronal copper homeostasis. *J. Biol. Chem.* 278, 17401–17407. doi:10.1074/jbc.M300629200

Basha, M. R., Murali, M., Siddiqi, H. K., Ghosal, K., Siddiqi, O. K., Lashuel, H. A., et al. (2005). Lead (Pb) exposure and its effect on APP proteolysis and Abeta aggregation. *FASEB J.* 19, 2083–2084. doi:10.1096/fj.05-4375fje

Batool, Z., Agha, F., Tabassum, S., Batool, T. S., Siddiqui, R. A., Haider, S., et al. (2019). Prevention of cadmium-induced neurotoxicity in rats by essential nutrients present in nuts. *Acta Neurobiol. Exp. (Wars).* 79, 169–183. doi:10.21307/ane-2019-015

Bihaqi, S. W., Alansi, B., Masoud, A. M., Mushtaq, F., Subaiea, G. M., Zawia, N. H., et al. (2018). Influence of early life lead (Pb) exposure on α-synuclein, GSK-3β and caspase-3 mediated tauopathy: Implications on alzheimer's disease. *Curr. Alzheimer Res.* 15, 1114–1122. doi:10.2174/1567205015666180801095925

Bihaqi, S. W., Bahmani, A., Adem, A., and Zawia, N. H. (2014). Infantile postnatal exposure to lead (Pb) enhances tau expression in the cerebral cortex of aged mice: Relevance to AD. *Neurotoxicology* 44, 114–120. doi:10.1016/j.neuro.2014.06.008

Bihaqi, S. W., Eid, A., and Zawia, N. H. (2017). Lead exposure and tau hyperphosphorylation: An *in-vitro* study. *Neurotoxicology* 62, 218–223. doi:10.1016/j.neuro.2017.07.029

Bihaqi, S. W., and Zawia, N. H. (2013). Enhanced taupathy and AD-like pathology in aged primate brains decades after infantile exposure to lead (Pb). *Neurotoxicology* 39, 95–101. doi:10.1016/j.neuro.2013.07.010

Bijoor, A. R., Sudha, S., and Venkatesh, T. (2012). Neurochemical and neurobehavioral effects of low lead exposure on the developing brain. *Indian J. Clin. biochem.* 27, 147–151. doi:10.1007/s12291-012-0190-2

Bosomworth, H. J., Adlard, P. A., Ford, D., and Valentine, R. A. (2013). Altered expression of ZnT10 in alzheimer's disease brain. *PLoS One* 8, e65475. doi:10.1371/journal.pone.0065475

Brubaker, C. J., Schmithorst, V. J., Haynes, E. N., Dietrich, K. N., Egelhoff, J. C., Lindquist, D. M., et al. (2009). Altered myelination and axonal integrity in adults with childhood lead exposure: A diffusion tensor imaging study. *Neurotoxicology* 30, 867–875. doi:10.1016/j.neuro.2009.07.007

Bucossi, S., Mariani, S., Ventriglia, M., Polimanti, R., Gennarelli, M., Bonvicini, C., et al. (2011). Association between the c. 2495 A>G ATP7B polymorphism and sporadic Alzheimer's disease. *Int. J. Alzheimers Dis.*, 973692. doi:10.4061/2011/973692

Budtz-Jørgensen, E., Bellinger, D. C., Lanphear, B. P., Grandjean, P., Hornung, R., Khoury, J., et al. (2013). An international pooled analysis for obtaining a benchmark dose for environmental lead exposure in children. *Risk Anal.* 33, 450–461. doi:10.1111/j.1539-6924.2012.01882.x

Bush, A. I., Multhaup, G., Moir, R. D., Williamson, T. G., Small, D. H., Rumble, B., et al. (1993). A novel zinc(II) binding site modulates the function of the βA4 amyloid protein precursor of Alzheimer's disease. *J. Biol. Chem.* 268, 16109–16112. doi:10.1016/s0021-9258(19)85394-2

Bush, A. I., Pettingell, W. H., Multhaup, G., Paradis, M. D., Vonsattel, J. P., Gusella, J. F., et al. (1994). Rapid induction of Alzheimer Aβ amyloid formation by zinc. *Science* 265, 1464–1467. doi:10.1126/science.8073293

Carmona, A., Devès, G., Roudeau, S., Cloetens, P., Bohic, S., Ortega, R., et al. (2010). Manganese accumulates within golgi apparatus in dopaminergic cells as revealed by synchrotron X-ray fluorescence nanoimaging. *ACS Chem. Neurosci.* 1, 194–203. doi:10.1021/cn900021z

Cavalu, S., Fritea, L., Brocks, M., Barbaro, K., Murvai, G., Costea, T. O., et al. (2020). *Novel Hybrid Composites Based on PVA/SeTiO 2 Nanoparticles and Natural Hydroxyapatite for Orthopedic Applications: Correlations between Structural, Morphological and Biocompatibility Properties*, 13. doi:10.3390/MA13092077*Mater, Basel, Switz.*

Chandra, S. V., Murthy, R. C., Saxena, D. K., and Lal, B. (1983). Effects of pre- and postnatal combined exposure to Pb and Mn on brain development in rats. *Ind. Health* 21, 273–279. doi:10.2486/indhealth.21.273

Chawla, S., Gulyani, S., Allen, R. P., Earley, C. J., Li, X., Van Zijl, P., et al. (2019). Extracellular vesicles reveal abnormalities in neuronal iron metabolism in restless legs syndrome. *Sleep* 42, zsz079. doi:10.1093/sleep/zsz079

Chen, P., Bowman, A. B., Mukhopadhyay, S., and Aschner, M. (2015a). SLC30A10: A novel manganese transporter. *Worm* 4, e1042648. doi:10.1080/21624054.2015.1042648

Chen, P., Chakraborty, S., Mukhopadhyay, S., Lee, E., Paoliello, M. M. B., Bowman, A. B., et al. (2015b). Manganese homeostasis in the nervous system. *J. Neurochem.* 134, 601–610. doi:10.1111/jnc.13170

Cheung, K. H., Shineman, D., Müller, M., Cárdenas, C., Mei, L., Yang, J., et al. (2008). Mechanism of Ca2+ disruption in alzheimer's disease by presenilin

regulation of InsP3 receptor channel gating. *Neuron* 58, 871–883. doi:10.1016/j.neuron.2008.04.015

Choi, C. J., Anantharam, V., Saetveit, N. J., Houk, R. S., Kanthasamy, A., Kanthasamy, A. G., et al. (2007). Normal cellular prion protein protects against manganese-induced oxidative stress and apoptotic cell death. *Toxicol. Sci.* 98, 495–509. doi:10.1093/toxsci/kfm099

Crouch, P. J., Lin, W. H., Adlard, P. A., Cortes, M., Lal, V., Filiz, G., et al. (2009). Increasing Cu bioavailability inhibits Aβ oligomers and tau phosphorylation. *Proc. Natl. Acad. Sci. U. S. A.* 106, 381–386. doi:10.1073/pnas.0809057106

Cuajungco, M. P., and Lees, G. J. (1997). Zinc metabolism in the brain: Relevance to human neurodegenerative disorders. *Neurobiol. Dis.* 4, 137–169. doi:10.1006/nbdi.1997.0163

Davis, A. N., Carlo, G., Gulseven, Z., Palermo, F., Lin, C. H., Nagel, S. C., et al. (2019). Exposure to environmental toxicants and young children's cognitive and social development. *Rev. Environ. Health* 34, 35–56. doi:10.1515/reveh-2018-0045

de Baaij, J. H. F., Hoenderop, J. G. J., and Bindels, R. J. M. (2015). Magnesium in man: Implications for health and disease. *Physiol. Rev.* 95, 1–46. doi:10.1152/physrev.00012.2014

Deibel, M. A., Ehmann, W. D., and Markesbery, W. R. (1996). Copper, iron, and zinc imbalances in severely degenerated brain regions in Alzheimer's disease: Possible relation to oxidative stress. *J. Neurol. Sci.* 143, 137–142. doi:10.1016/S0022-510X(96)00203-1

del Pino, J., Zeballos, G., Anadón, M. J., Moyano, P., Díaz, M. J., García, J. M., et al. (2016). Cadmium-induced cell death of basal forebrain cholinergic neurons mediated by muscarinic M1 receptor blockade, increase in GSK-3β enzyme, β-amyloid and tau protein levels. *Arch. Toxicol.* 90, 1081–1092. doi:10.1007/s00204-015-1540-7

Deshpande, A., Kawai, H., Metherate, R., Glabe, C. G., and Busciglio, J. (2009). A role for synaptic zinc in activity-dependent Abeta oligomer formation and accumulation at excitatory synapses. *J. Neurosci.* 29, 4004–4015. doi:10.1523/JNEUROSCI.5980-08.2009

Di Lorenzo, L., Vacca, A., Corfiati, M., Lovreglio, P., and Soleo, L. (2007). Evaluation of tumor necrosis factor-alpha and granulocyte colony-stimulating factor serum levels in lead-exposed smoker workers. *Int. J. Immunopathol. Pharmacol.* 20, 239–247. doi:10.1177/039463200702000204

Diaz, J. C., Simakova, O., Jacobson, K. A., Arispe, N., and Pollard, H. B. (2009). Small molecule blockers of the Alzheimer Abeta calcium channel potently protect neurons from Abeta cytotoxicity. *Proc. Natl. Acad. Sci. U. S. A.* 106, 3348–3353. doi:10.1073/pnas.0813355106

Doraiswamy, P. M., and Finefrock, A. E. (2004). Metals in our minds: Therapeutic implications for neurodegenerative disorders. *Lancet. Neurol.* 3, 431–434. doi:10.1016/S1474-4422(04)00809-9

Dórea, J. G. (2020). Neurotoxic effects of combined exposures to aluminum and mercury in early life (infancy). *Environ. Res.* 188, 109734. doi:10.1016/j.envres.2020.109734

Duce, J. A., Tsatsanis, A., Cater, M. A., James, S. A., Robb, E., Wikhe, K., et al. (2010). Iron-export ferroxidase activity of β-amyloid precursor protein is inhibited by zinc in alzheimer's disease. *Cell* 142, 857–867. doi:10.1016/j.cell.2010.08.014

Dumont, M., Wille, E., Stack, C., Calingasan, N. Y., Beal, M. F., Lin, M. T., et al. (2009). Reduction of oxidative stress, amyloid deposition, and memory deficit by manganese superoxide dismutase overexpression in a transgenic mouse model of Alzheimer's disease. *FASEB J.* 23, 2459–2466. doi:10.1096/fj.09-132928

Ehmann, W. D., Markesbery, W. R., Alauddin, M., Hossain, T. I., and Brubaker, E. H. (1986). Brain trace elements in Alzheimer's disease. *Neurotoxicology* 7, 195–206.

Ericson, B., Hu, H., Nash, E., Ferraro, G., Sinitsky, J., Taylor, M. P., et al. (2021). Blood lead levels in low-income and middle-income countries: A systematic review. *Lancet. Planet. Health* 5, e145–e153. doi:10.1016/S2542-5196(20)30278-3

Ericson, J. E., Crinella, F. M., Clarke-Stewart, K. A., Allhusen, V. D., Chan, T., Robertson, R. T., et al. (2007). Prenatal manganese levels linked to childhood behavioral disinhibition. *Neurotoxicol. Teratol.* 29, 181–187. doi:10.1016/j.ntt.2006.09.020

Exley, C., and Mold, M. J. (2019). Aluminium in human brain tissue: How much is too much? *J. Biol. Inorg. Chem.* 24, 1279–1282. doi:10.1007/s00775-019-01710-0

Fasae, K. D., Abolaji, A. O., Faloye, T. R., Odunsi, A. Y., Oyetayo, B. O., Enya, J. I., et al. (2021). Metallobiology and therapeutic chelation of biometals (copper, zinc and iron) in Alzheimer's disease: Limitations, and current and future perspectives. *J. Trace Elem. Med. Biol.* 67, 126779. doi:10.1016/j.jtemb.2021.126779

Ficiarà, E., Boschi, S., Ansari, S., D'Agata, F., Abollino, O., Caroppo, P., et al. (2021). Machine learning profiling of alzheimer's disease patients based on current cerebrospinal fluid markers and iron content in biofluids. *Front. Aging Neurosci.* 13, 607858. doi:10.3389/fnagi.2021.607858

Flora, G., Gupta, D., and Tiwari, A. (2012). Toxicity of lead: A review with recent updates. *Interdiscip. Toxicol.* 5, 47–58. doi:10.2478/v10102-012-0009-2

Fransson, M. N., Barregard, L., Sallsten, G., Akerstrom, M., and Johanson, G. (2014). Physiologically-based toxicokinetic model for cadmium using markov-chain Monte Carlo analysis of concentrations in blood, urine, and kidney cortex from living kidney donors. *Toxicol. Sci.* 141, 365–376. doi:10.1093/toxsci/kfu129

Frazzini, V., Granzotto, A., Bomba, M., Massetti, N., Castelli, V., D'Aurora, M., et al. (2018). The pharmacological perturbation of brain zinc impairs BDNF-related signaling and the cognitive performances of young mice. *Sci. Rep.* 8, 9768. doi:10.1038/s41598-018-28083-9

Frederickson, C. J., and Danscher, G. (1990). Zinc-containing neurons in hippocampus and related CNS structures. *Prog. Brain Res.* 83, 71–84. doi:10.1016/S0079-6123(08)61242-X

Frederickson, C. J., Koh, J. Y., and Bush, A. I. (2005). The neurobiology of zinc in health and disease. *Nat. Rev. Neurosci.* 6, 449–462. doi:10.1038/nrn1671

Freire, C., Amaya, E., Gil, F., Fernández, M. F., Murcia, M., Llop, S., et al. (2018). Prenatal co-exposure to neurotoxic metals and neurodevelopment in preschool children: The Environment and Childhood (INMA) Project. *Sci. Total Environ.* 621, 340–351. doi:10.1016/j.scitotenv.2017.11.273

Frisbie, S. H., Mitchell, E. J., Dustin, H., Maynard, D. M., and Sarkar, B. (2012). World health organization discontinues its drinking-water guideline for manganese. *Environ. Health Perspect.* 120, 775–778. doi:10.1289/ehp.1104693

Garrick, M. D., Singleton, S. T., Vargas, F., Kuo, H. C., Zhao, L., Knöpfel, M., et al. (2006). DMT1: Which metals does it transport? *Biol. Res.* 39, 79–85. doi:10.4067/S0716-97602006000100009

Gomez-Ramos, A., Dominguez, J., Zafra, D., Corominola, H., Gomis, R., Guinovart, J., et al. (2006). Inhibition of GSK3 dependent tau phosphorylation by metals. *Curr. Alzheimer Res.* 3, 123–127. doi:10.2174/156720506776383059

Grantham-McGregor, S., Cheung, Y. B., Cueto, S., Glewwe, P., Richter, L., and Strupp, B. (2007). Developmental potential in the first 5 years for children in developing countries. *Lancet* 369, 60–70. doi:10.1016/S0140-6736(07)60032-4

Gromadzka, G., Tarnacka, B., Flaga, A., and Adamczyk, A. (2020). Copper dyshomeostasis in neurodegenerative diseases—Therapeutic implications. *Int. J. Mol. Sci.* 21, E9259. doi:10.3390/ijms21239259

Gu, H., Wei, X., Monnot, A. D., Fontanilla, C. V., Behl, M., Farlow, M. R., et al. (2011). Lead exposure increases levels of β-amyloid in the brain and CSF and inhibits LRP1 expression in APP transgenic mice. *Neurosci. Lett.* 490, 16–20. doi:10.1016/j.neulet.2010.12.017

Guilarte, T. R. (2010). APLP1, Alzheimer's-like pathology and neurodegeneration in the frontal cortex of manganese-exposed non-human primates. *Neurotoxicology* 31, 572–574. doi:10.1016/j.neuro.2010.02.004

Guilarte, T. R. (2013). Manganese neurotoxicity: New perspectives from behavioral, neuroimaging, and neuropathological studies in humans and non-human primates. *Front. Aging Neurosci.* 5, 23. doi:10.3389/fnagi.2013.00023

Gunter, T. E., Gavin, C. E., Aschner, M., and Gunter, K. K. (2006). Speciation of manganese in cells and mitochondria: A search for the proximal cause of manganese neurotoxicity. *Neurotoxicology* 27, 765–776. doi:10.1016/j.neuro.2006.05.002

Hambidge, K. M., Sokol, R. J., Fidanza, S. J., and Goodall, M. A. (1989). Plasma manganese concentrations in infants and children receiving parenteral nutrition. *JPEN. J. Parenter. Enter. Nutr.* 13, 168–171. doi:10.1177/014860718901300216

Harilal, S., Jose, J., Parambi, D. G. T., Kumar, R., Unnikrishnan, M. K., Uddin, M. S., et al. (2020). Revisiting the blood-brain barrier: A hard nut to crack in the transportation of drug molecules. *Brain Res. Bull.* 160, 121–140. doi:10.1016/j.brainresbull.2020.03.018

Harris, E. D. (2001). Copper homeostasis: The role of cellular transporters. *Nutr. Rev.* 59, 281–285. doi:10.1111/j.1753-4887.2001.tb07017.x

Heng, Y. Y., Asad, I., Coleman, B., Menard, L., Benki-Nugent, S., Were, F. H., et al. (2022). Heavy metals and neurodevelopment of children in low and middle-income countries: A systematic review. *PLoS One* 17, e0265536. doi:10.1371/journal.pone.0265536

Hock, C., Drasch, G., Golombowski, S., Müller-Spahn, F., Willershausen-Zönnchen, B., Schwarz, P., et al. (1998). Increased blood mercury levels in patients with Alzheimer's disease. *J. Neural Transm.* 105, 59–68. doi:10.1007/s007020050038

Hu, F., Xu, L., Liu, Z. H., Ge, M. M., Ruan, D. Y., Wang, H. L., et al. (2014). Developmental lead exposure alters synaptogenesis through inhibiting canonical wnt pathway *in vivo* and *in vitro*. *PLoS One* 9, e101894. doi:10.1371/journal.pone.0101894

Hu, Q., Fu, H., Ren, T., Wang, S., Zhou, W., Song, H., et al. (2008). Maternal low-level lead exposure reduces the expression of PSA-NCAM and the activity of

sialyltransferase in the hippocampi of neonatal rat pups. *Neurotoxicology* 29, 675–681. doi:10.1016/j.neuro.2008.04.002

Huang, B., and Goldsbrough, P. B. (1988). Cadmium tolerance in tobacco cell culture and its relevance to temperature stress. *Plant Cell Rep.* 7, 119–122. doi:10.1007/BF00270119

Huat, T. J., Camats-Perna, J., Newcombe, E. A., Valmas, N., Kitazawa, M., Medeiros, R., et al. (2019). Metal toxicity links to alzheimer's disease and neuroinflammation. *J. Mol. Biol.* 431, 1843–1868. doi:10.1016/j.jmb.2019.01.018

Husain, M. J., Datta, B. K., and Kostova, D. (2021). Disease and demography: A systems-dynamic cohort-component population model to assess the implications of disease-specific mortality targets. *BMJ Open* 11, e043313. doi:10.1136/bmjopen-2020-043313

Islam, F., Khadija, J. F., Harun-Or-Rashid, M., Rahaman, M. S., Nafady, M. H., Islam, M. R., et al. (2022a). Bioactive compounds and their derivatives: An insight into prospective phytotherapeutic approach against alzheimer's disease. *Oxid. Med. Cell. Longev.* 2022, 5100904. doi:10.1155/2022/5100904

Islam, F., Nafady, M. H., Islam, M. R., Saha, S., Rashid, S., Akter, A., et al. (2022b2022). Resveratrol and neuroprotection: An insight into prospective therapeutic approaches against alzheimer's disease from bench to bedside. *Mol. Neurobiol.* 59, 4384–4404. doi:10.1007/S12035-022-02859-7

Islam, F., Shohag, S., Uddin, M. J., Islam, M. R., Nafady, M. H., Akter, A., et al. (2022c)., 15. Basel, Switzerland, 2160. doi:10.3390/MA15062160Exploring the journey of zinc oxide nanoparticles (ZnO-NPs) toward biomedical applications*Materials*

Jang, D. H., and Hoffman, R. S. (2011). Heavy metal chelation in neurotoxic exposures. *Neurol. Clin.* 29, 607–622. doi:10.1016/j.ncl.2011.05.002

Jett, D. A., Sibrizzi, C. A., Blain, R. B., Hartman, P. A., Lein, P. J., Taylor, K. W., et al. (2020). A national toxicology program systematic review of the evidence for long-term effects after acute exposure to sarin nerve agent. *Crit. Rev. Toxicol.* 50, 474–490. doi:10.1080/10408444.2020.1787330

Jiang, C. Bin, Hsueh, Y. M., Kuo, G. L., Hsu, C. H., Chang, J. H., Chien, L. C., et al. (2018). Preliminary study of urinary arsenic concentration and arsenic methylation capacity effects on neurodevelopment in very low birth weight preterm children under 24 months of corrected age. *Medicine* 97, e12800. doi:10.1097/MD.0000000000012800

Jiang, J. H., Ge, G., Gao, K., Pang, Y., Chai, R. C., Jia, X. H., et al. (2015). Calcium signaling involvement in cadmium-induced astrocyte cytotoxicity and cell death through activation of MAPK and PI3K/akt signaling pathways. *Neurochem. Res.* 40, 1929–1944. doi:10.1007/s11064-015-1686-y

Jin, L., Wu, W. H., Li, Q. Y., Zhao, Y. F., and Li, Y. M. (2011). Copper inducing Aβ42 rather than Aβ40 nanoscale oligomer formation is the key process for Aβ neurotoxicity. *Nanoscale* 3, 4746–4751. doi:10.1039/c1nr11029b

Jomova, K., Vondrakova, D., Lawson, M., and Valko, M. (2010). Metals, oxidative stress and neurodegenerative disorders. *Mol. Cell. Biochem.* 345, 91–104. doi:10.1007/s11010-010-0563-x

Kabir, M. T., Uddin, M. S., Zaman, S., Begum, Y., Ashraf, G. M., Bin-Jumah, M. N., et al. (2021). Molecular mechanisms of metal toxicity in the pathogenesis of alzheimer's disease. *Mol. Neurobiol.* 58, 1–20. doi:10.1007/s12035-020-02096-w

Kalia, K., Murthy., R. C., and Chandra, S. V. (1984). Tissue disposition of 54Mn in lead pretreated rats. *Ind. Health* 22, 49–52. doi:10.2486/indhealth.22.49

Kambe, T., Tsuji, T., Hashimoto, A., and Itsumura, N. (2015). The physiological, biochemical, and molecular roles of zinc transporters in zinc homeostasis and metabolism. *Physiol. Rev.* 95, 749–784. doi:10.1152/physrev.00035.2014

Kepp, K. P. (2017). Ten challenges of the amyloid hypothesis of alzheimer's disease. *J. Alzheimer's Dis.* 55, 447–457. doi:10.3233/JAD-160550

Kim, Y., Ha, E. H., Park, H., Ha, M., Kim, Y., Hong, Y. C., et al. (2013). Prenatal lead and cadmium co-exposure and infant neurodevelopment at 6 months of age: The Mothers and Children's Environmental Health (MOCEH) study. *Neurotoxicology* 35, 15–22. doi:10.1016/j.neuro.2012.11.006

Kim, Y., Kim, B. N., Hong, Y. C., Shin, M. S., Yoo, H. J., Kim, J. W., et al. (2009). Co-exposure to environmental lead and manganese affects the intelligence of school-aged children. *Neurotoxicology* 30, 564–571. doi:10.1016/j.neuro.2009.03.012

Kitazawa, M., Cheng, D., and Laferla, F. M. (2009). Chronic copper exposure exacerbates both amyloid and tau pathology and selectively dysregulates cdk5 in a mouse model of AD. *J. Neurochem.* 108, 1550–1560. doi:10.1111/j.1471-4159.2009.05901.x

Klevay, L. M. (2008). Alzheimer's disease as copper deficiency. *Med. Hypotheses* 70, 802–807. doi:10.1016/j.mehy.2007.04.051

Kolarova, M., García-Sierra, F., Bartos, A., Ricny, J., and Ripova, D. (2012). Structure and pathology of tau protein in Alzheimer disease. *Int. J. Alzheimers Dis.*, 731526. doi:10.1155/2012/731526

Komuro, H., and Kumada, T. (2005). Ca2+ transients control CNS neuronal migration. *Cell Calcium* 37, 387–393. doi:10.1016/j.ceca.2005.01.006

Kotermanski, S. E., and Johnson, J. W. (2009). Mg 2+ imparts NMDA receptor subtype selectivity to the Alzheimer's drug memantine. *J. Neurosci.* 29, 2774–2779. doi:10.1523/JNEUROSCI.3703-08.2009

Kuiper, M. A., Mulder, C., van Kamp, G. J., Scheltens, P., and Wolters, E. C. (1994). Cerebrospinal fluid ferritin levels of patients with Parkinson's disease, Alzheimer's disease, and multiple system atrophy. *J. Neural Transm. Park. Dis. Dement. Sect.* 7, 109–114. doi:10.1007/BF02260965

Kumar Singh, P., Kumar Singh, M., Singh Yadav, R., Kumar Dixit, R., Mehrotra, A., Nath, R., et al. (2018). Attenuation of lead-induced neurotoxicity by omega-3 fatty acid in rats. *Ann. Neurosci.* 24, 221–232. doi:10.1159/000481808

Kumawat, K. L., Kaushik, D. K., Goswami, P., and Basu, A. (2014). Acute exposure to lead acetate activates microglia and induces subsequent bystander neuronal death via caspase-3 activation. *Neurotoxicology* 41, 143–153. doi:10.1016/j.neuro.2014.02.002

Kuo, Y. M., Gybina, A. A., Pyatskowit, J. W., Gitschier, J., and Prohaska, J. R. (2006). Copper transport protein (Ctr1) levels in mice are tissue specific and dependent on copper status. *J. Nutr.* 136, 21–26. doi:10.1093/jn/136.1.21

Lang, M., Fan, Q., Wang, L., Zheng, Y., Xiao, G., Wang, X., et al. (2013). Inhibition of human high-affinity copper importer Ctr1 orthologous in the nervous system of Drosophila ameliorates Aβ42-induced Alzheimer's disease-like symptoms. *Neurobiol. Aging* 34, 2604–2612. doi:10.1016/j.neurobiolaging.2013.05.029

Laslo, V., Pinzaru, S. C., Zaguła, G., Kluz, M., Vicas, S. I., Cavalu, S., et al. (2022). Synergic effect of selenium nanoparticles and lactic acid bacteria in reduction cadmium toxicity. *J. Mol. Struct.* 1247, 131325. doi:10.1016/J.MOLSTRUC.2021.131325

Lee, J. Y., Cole, T. B., Palmiter, R. D., Suh, S. W., and Koh, J. Y. (2002). Contribution by synaptic zinc to the gender-disparate plaque formation in human Swedish mutant APP transgenic mice. *Proc. Natl. Acad. Sci. U. S. A.* 99, 7705–7710. doi:10.1073/pnas.092034699

Lee, M., Jantaratnotai, N., McGeer, E., McLarnon, J. G., and McGeer, P. L. (2011). Mg2+ ions reduce microglial and THP-1 cell neurotoxicity by inhibiting Ca2+ entry through purinergic channels. *Brain Res.* 1369, 21–35. doi:10.1016/j.brainres.2010.10.084

Lei, P., Ayton, S., Appukuttan, A. T., Moon, S., Duce, J. A., Volitakis, I., et al. (2017). Lithium suppression of tau induces brain iron accumulation and neurodegeneration. *Mol. Psychiatry* 22, 396–406. doi:10.1038/mp.2016.96

Lei, P., Ayton, S., Appukuttan, A. T., Volitakis, I., Adlard, P. A., Finkelstein, D. I., et al. (2015). Clioquinol rescues Parkinsonism and dementia phenotypes of the tau knockout mouse. *Neurobiol. Dis.* 81, 168–175. doi:10.1016/j.nbd.2015.03.015

Lei, P., Ayton, S., Finkelstein, D. I., Spoerri, L., Ciccotosto, G. D., Wright, D. K., et al. (2012). Tau deficiency induces parkinsonism with dementia by impairing APP-mediated iron export. *Nat. Med.* 18, 291–295. doi:10.1038/nm.2613

Levine, S. M. (1997). Iron deposits in multiple sclerosis and Alzheimer's disease brains. *Brain Res.* 760, 298–303. doi:10.1016/S0006-8993(97)00470-8

Levitsky, D. O., and Takahashi, M. (2013). Interplay of Ca2+ and Mg2+ in Sodium-Calcium exchanger and in other Ca2+-binding proteins: Magnesium, watchdog that blocks each turn if able. *Adv. Exp. Med. Biol.* 961, 65–78. doi:10.1007/978-1-4614-4756-6_7

Leyva-Illades, D., Chen, P., Zogzas, C. E., Hutchens, S., Mercado, J. M., Swaim, C. D., et al. (2014). SLC30A10 is a cell surface-localized manganese efflux transporter, and parkinsonism-causing mutations block its intracellular trafficking and efflux activity. *J. Neurosci.* 34, 14079–14095. doi:10.1523/JNEUROSCI.2329-14.2014

Li, F., Calingasan, N. Y., Yu, F., Mauck, W. M., Toidze, M., Almeida, C. G., et al. (2004). Increased plaque burden in brains of APP mutant MnSOD heterozygous knockout mice. *J. Neurochem.* 89, 1308–1312. doi:10.1111/j.1471-4159.2004.02455.x

Li, W., Yu, J., Liu, Y., Huang, X., Abumaria, N., Zhu, Y., et al. (2014). Elevation of brain magnesium prevents synaptic loss and reverses cognitive deficits in Alzheimer's disease mouse model. *Mol. Brain* 7, 65. doi:10.1186/s13041-014-0065-y

Li, X., Lv, Y., Yu, S., Zhao, H., and Yao, L. (2012). The effect of cadmium on Aβ levels in APP/PS1 transgenic mice. *Exp. Ther. Med.* 4, 125–130. doi:10.3892/etm.2012.562

Li, Y., Jiao, Q., Xu, H., Du, X., Shi, L., Jia, F., et al. (2017). Biometal dyshomeostasis and toxic metal accumulations in the development of alzheimer's disease. *Front. Mol. Neurosci.* 10, 339. doi:10.3389/fnmol.2017.00339

Lin, C. C., Chen, Y. C., Su, F. C., Lin, C. M., Liao, H. F., Hwang, Y. H., et al. (2013). *In utero* exposure to environmental lead and manganese and neurodevelopment at 2 years of age. *Environ. Res.* 123, 52–57. doi:10.1016/j.envres.2013.03.003

Lin, W., Vann, D. R., Doulias, P. T., Wang, T., Landesberg, G., Li, X., et al. (2017). Hepatic metal ion transporter ZIP8 regulates manganese homeostasis and manganese-dependent enzyme activity. *J. Clin. Invest.* 127, 2407–2417. doi:10.1172/JCI90896

Liu, J. T., Chen, B. Y., Zhang, J. Q., Kuang, F., and Chen, L. W. (2015). Lead exposure induced microgliosis and astrogliosis in hippocampus of young mice potentially by triggering TLR4-MyD88-NFκB signaling cascades. *Toxicol. Lett.* 239, 97–107. doi:10.1016/j.toxlet.2015.09.015

Liu, M. C., Liu, X. Q., Wang, W., Shen, X. F., Che, H. L., Guo, Y. Y., et al. (2012). Involvement of microglia activation in the lead induced long-term potentiation impairment. *PLoS One* 7, e43924. doi:10.1371/journal.pone.0043924

Liuzzi, J. P., and Cousins, R. J. (2004). Mammalian zinc transporters. *Annu. Rev. Nutr.* 24, 151–172. doi:10.1146/annurev.nutr.24.012003.132402

Lothian, A., Hare, D. J., Grimm, R., Ryan, T. M., Masters, C. L., Roberts, B. R., et al. (2013). Metalloproteomics: Principles, challenges, and applications to neurodegeneration. *Front. Aging Neurosci.* 5, 35. doi:10.3389/fnagi.2013.00035

Lovell, M. A., Robertson, J. D., Teesdale, W. J., Campbell, J. L., and Markesbery, W. R. (1998). Copper, iron and zinc in Alzheimer's disease senile plaques. *J. Neurol. Sci.* 158, 47–52. doi:10.1016/S0022-510X(98)00092-6

Lu, C., Black, M. M., and Richter, L. M. (2016). Risk of poor development in young children in low-income and middle-income countries: An estimation and analysis at the global, regional, and country level. *Lancet. Glob. Health* 4, e916–e922. doi:10.1016/S2214-109X(16)30266-2

Madejczyk, M. S., and Ballatori, N. (2012). The iron transporter ferroportin can also function as a manganese exporter. *Biochim. Biophys. Acta* 1818, 651–657. doi:10.1016/j.bbamem.2011.12.002

Mamtani, R., Stern, P., Dawood, I., and Cheema, S. (2011). Metals and disease: A global primary health care perspective. *J. Toxicol.*, 319136. doi:10.1155/2011/319136

Mano, Y., Takayanagi, T., Ishitani, A., and Hirota, T. (1989). Mercury in hair of patients with ALS. *Clin. Neurol.* 29, 844–848.

Maria Giudetti, A., Romano, A., Michele Lavecchia, A., and Gaetani, S. (2015). The role of brain cholesterol and its oxidized products in alzheimer's disease. *Curr. Alzheimer Res.* 13, 198–205. doi:10.2174/1567205012666150921103426

Martinez-Finley, E. J., Gavin, C. E., Aschner, M., and Gunter, T. E. (2013). Manganese neurotoxicity and the role of reactive oxygen species. *Free Radic. Biol. Med.* 62, 65–75. doi:10.1016/j.freeradbiomed.2013.01.032

Matlack, K. E. S., Tardiff, D. F., Narayan, P., Hamamichi, S., Caldwell, K. A., Caldwell, G. A., et al. (2014). Clioquinol promotes the degradation of metal-dependent amyloid-β (Aβ) oligomers to restore endocytosis and ameliorate Aβ toxicity. *Proc. Natl. Acad. Sci. U. S. A.* 111, 4013–4018. doi:10.1073/pnas.1402228111

Maynard, C. J., Bush, A. I., Masters, C. L., Cappai, R., and Li, Q. X. (2005). Metals and amyloid-β in Alzheimer's disease. *Int. J. Exp. Pathol.* 86, 147–159. doi:10.1111/j.0959-9673.2005.00434.x

Mazumdar, M., Bellinger, D. C., Gregas, M., Abanilla, K., Bacic, J., Needleman, H. L., et al. (2011). Low-level environmental lead exposure in childhood and adult intellectual function: A follow-up study. *Environ. Health* 10, 24. doi:10.1186/1476-069X-10-24

McClintock, T. R., Chen, Y., Bundschuh, J., Oliver, J. T., Navoni, J., Olmos, V., et al. (2012). Arsenic exposure in Latin America: Biomarkers, risk assessments and related health effects. *Sci. Total Environ.* 429, 76–91. doi:10.1016/j.scitotenv.2011.08.051

McDermott, S., Wu, J., Cai, B., Lawson, A., and Marjorie Aelion, C. (2011). Probability of intellectual disability is associated with soil concentrations of arsenic and lead. *Chemosphere* 84, 31–38. doi:10.1016/j.chemosphere.2011.02.088

Medeiros, R., Kitazawa, M., Caccamo, A., Baglietto-Vargas, D., Estrada-Hernandez, T., Cribbs, D. H., et al. (2011). Loss of muscarinic M1 receptor exacerbates Alzheimer's disease-like pathology and cognitive decline. *Am. J. Pathol.* 179, 980–991. doi:10.1016/j.ajpath.2011.04.041

Mejía, J. J., Díaz-Barriga, F., Calderón, J., Ríos, C., and Jiménez-Capdeville, M. E. (1997). Effects of lead-arsenic combined exposure on central monoaminergic systems. *Neurotoxicol. Teratol.* 19, 489–497. doi:10.1016/S0892-0362(97)00066-4

Melov, S., Adlard, P. A., Morten, K., Johnson, F., Golden, T. R., Hinerfeld, D., et al. (2007). Mitochondrial oxidative stress causes hyperphosphorylation of tau. *PLoS One* 2, e536. doi:10.1371/journal.pone.0000536

Meng, F., Asghar, S., Gao, S., Su, Z., Song, J., Huo, M., et al. (2015). A novel LDL-mimic nanocarrier for the targeted delivery of curcumin into the brain to treat Alzheimer's disease. *Colloids Surf. B Biointerfaces* 134, 88–97. doi:10.1016/j.colsurfb.2015.06.025

Min, J. Y., and Min, K. B. (2016). Blood cadmium levels and Alzheimer's disease mortality risk in older US adults. *Environ. Health* 15, 69. doi:10.1186/s12940-016-0155-7

Mocchegiani, E., Bertoni-Freddari, C., Marcellini, F., and Malavolta, M. (2005). Brain, aging and neurodegeneration: Role of zinc ion availability. *Prog. Neurobiol.* 75, 367–390. doi:10.1016/j.pneurobio.2005.04.005

Mocchegiani, E., Giacconi, R., Cipriano, C., Muzzioli, M., Fattoretti, P., Bertoni-Freddari, C., et al. (2001). Zinc-bound metallothioneins as potential biological markers of ageing. *Brain Res. Bull.* 55, 147–153. doi:10.1016/S0361-9230(01)00468-3

Moon, Y., Han, S. H., and Moon, W. J. (2016). Patterns of brain iron accumulation in vascular dementia and alzheimer's dementia using quantitative susceptibility mapping imaging. *J. Alzheimer's Dis.* 51, 737–745. doi:10.3233/JAD-151037

Moos, T., and Morgan, E. H. (2000). Transferrin and transferrin receptor function in brain barrier systems. *Cell. Mol. Neurobiol.* 20, 77–95. doi:10.1023/A:1006948027674

Mota, S. I., Ferreira, I. L., and Rego, A. C. (2014). Dysfunctional synapse in Alzheimer's disease - a focus on NMDA receptors. *Neuropharmacology* 76, 16–26. doi:10.1016/j.neuropharm.2013.08.013

Mucke, L., Masliah, E., Yu, G. Q., Mallory, M., Rockenstein, E. M., Tatsuno, G., et al. (2000). High-level neuronal expression of aβ_{1-42}in wild-type human amyloid protein precursor transgenic mice: Synaptotoxicity without plaque formation. *J. Neurosci.* 20, 4050–4058. doi:10.1523/jneurosci.20-11-04050.2000

Murphy, K. E., Cottle, L., Gysbers, A. M., Cooper, A. A., and Halliday, G. M. (2014). ATP13A2 (PARK9) protein levels are reduced in brain tissue of cases with Lewy bodies. *Acta Neuropathol. Commun.* 2, 11. doi:10.1186/2051-5960-1-11

Mutter, J., Curth, A., Naumann, J., Deth, R., and Walach, H. (2010). Does inorganic mercury play a role in alzheimer's disease? A systematic review and an integrated molecular mechanism. *J. Alzheimer's Dis.* 22, 357–374. doi:10.3233/JAD-2010-100705

Nash, D., Magder, L. S., Sherwin, R., Rubin, R. J., and Silbergeld, E. K. (2004). Bone density-related predictors of blood lead level among peri- and postmenopausal women in the United States: The third national health and nutrition examination survey, 1988-1994. *Am. J. Epidemiol.* 160, 901–911. doi:10.1093/aje/kwh296

Needleman, H. (2009). Low level lead exposure: History and discovery. *Ann. Epidemiol.* 19, 235–238. doi:10.1016/j.annepidem.2009.01.022

North, R. A. (2002). Molecular physiology of P2X receptors. *Physiol. Rev.* 82, 1013–1067. doi:10.1152/physrev.00015.2002

Notarachille, G., Arnesano, F., Calò, V., and Meleleo, D. (2014). Heavy metals toxicity: Effect of cadmium ions on amyloid beta protein 1-42. Possible implications for Alzheimer's disease. *BioMetals* 27, 371–388. doi:10.1007/s10534-014-9719-6

Ogunlade, B., Adelakun, S. A., and Agie, J. A. (2022). Nutritional supplementation of gallic acid ameliorates Alzheimer-type hippocampal neurodegeneration and cognitive impairment induced by aluminum chloride exposure in adult Wistar rats. *Drug Chem. Toxicol.* 45, 651–662. doi:10.1080/01480545.2020.1754849

Oh, H. G., Chun, Y. S., Kim, Y., Youn, S. H., Shin, S., Park, M. K., et al. (2012). Modulation of transient receptor potential melastatin related 7 channel by presenilins. *Dev. Neurobiol.* 72, 865–877. doi:10.1002/dneu.22001

Ostapchenko, V. G., Chen, M., Guzman, M. S., Xie, Y. F., Lavine, N., Fan, J., et al. (2015). The transient receptor potential melastatin 2 (TRPM2) channel contributes to β-amyloid oligomer-related neurotoxicity and memory impairment. *J. Neurosci.* 35, 15157–15169. doi:10.1523/JNEUROSCI.4081-14.2015

Paoletti, P., Vergnano, A. M., Barbour, B., and Casado, M. (2009). Zinc at glutamatergic synapses. *Neuroscience* 158, 126–136. doi:10.1016/j.neuroscience.2008.01.061

Parameshwaran, K., Dhanasekaran, M., and Suppiramaniam, V. (2008). Amyloid beta peptides and glutamatergic synaptic dysregulation. *Exp. Neurol.* 210, 7–13. doi:10.1016/j.expneurol.2007.10.008

Park, J. H., Lee, D. W., Park, K. S., and Joung, H. (2014). Serum trace metal levels in Alzheimer's disease and normal control groups. *Am. J. Alzheimers Dis. Other Demen.* 29, 76–83. doi:10.1177/1533317513506778

Patel, T. A., and Rao, M. V. (2015). Ameliorative effect of certain antioxidants against mercury induced genotoxicity in peripheral blood lymphocytes. *Drug Chem. Toxicol.* 38, 408–414. doi:10.3109/01480545.2014.975354

Paterson, R. W., Bartlett, J. W., Blennow, K., Fox, N. C., Shaw, L. M., Trojanowski, J. Q., et al. (2014). Cerebrospinal fluid markers including trefoil factor 3 are associated with neurodegeneration in amyloid-positive individuals. *Transl. Psychiatry* 4, e419. doi:10.1038/tp.2014.58

Phuagkhaopong, S., Ospondpant, D., Kasemsuk, T., Sibmooh, N., Soodvilai, S., Power, C., et al. (2017). Cadmium-induced IL-6 and IL-8 expression and release from astrocytes are mediated by MAPK and NF-κB pathways. *Neurotoxicology* 60, 82–91. doi:10.1016/j.neuro.2017.03.001

Prakash, A., Dhaliwal, G. K., Kumar, P., and Majeed, A. B. A. (2017). Brain biometals and Alzheimer's disease–boon or bane? *Int. J. Neurosci.* 127, 99–108. doi:10.3109/00207454.2016.1174118

Proshad, R., Islam, S., Tusher, T. R., Zhang, D., Khadka, S., Gao, J., et al. (2021). Appraisal of heavy metal toxicity in surface water with human health risk by a novel approach: A study on an urban river in vicinity to industrial areas of Bangladesh. *Toxin Rev.* 40, 803–819. doi:10.1080/15569543.2020.1780615

Qadir, S., Jamshieed, S., Rasool, S., Ashraf, M., Akram, N. A., Ahmad, P., et al. (2014). Modulation of plant growth and metabolism in cadmium-enriched environments. *Rev. Environ. Contam. Toxicol.* 229, 51–88. doi:10.1007/978-3-319-03777-6_4

Quadri, M., Federico, A., Zhao, T., Breedveld, G. J., Battisti, C., Delnooz, C., et al. (2012). Mutations in SLC30A10 cause parkinsonism and dystonia with hypermanganesemia, polycythemia, and chronic liver disease. *Am. J. Hum. Genet.* 90, 467–477. doi:10.1016/j.ajhg.2012.01.017

Quintana, C., Bellefqih, S., Laval, J. Y., Guerquin-Kern, J. L., Wu, T. D., Avila, J., et al. (2006). Study of the localization of iron, ferritin, and hemosiderin in Alzheimer's disease hippocampus by analytical microscopy at the subcellular level. *J. Struct. Biol.* 153, 42–54. doi:10.1016/j.jsb.2005.11.001

Raha, A. A., Vaishnav, R. A., Friedland, R. P., Bomford, A., and Raha-Chowdhury, R. (2014). The systemic iron-regulatory proteins hepcidin and ferroportin are reduced in the brain in Alzheimer's disease. *Acta Neuropathol. Commun.* 2, 55. doi:10.1186/2051-5960-1-55

Rastogi, S., Nandlike, K., and Fenster, W. (2007). Elevated blood lead levels in pregnant women: Identification of a high-risk population and interventions. *J. Perinat. Med.* 35, 492–496. doi:10.1515/JPM.2007.131

Reuben, A., Caspi, A., Belsky, D. W., Broadbent, J., Harrington, H., Sugden, K., et al. (2017). Association of childhood blood lead levels with cognitive function and socioeconomic status at age 38 years and with IQ change and socioeconomic mobility between childhood and adulthood. *JAMA - J. Am. Med. Assoc.* 317, 1244–1251. doi:10.1001/jama.2017.1712

Richter, P., Faroon, O., and Pappas, R. S. (2017). Cadmium and cadmium/zinc ratios and tobacco-related morbidities. *Int. J. Environ. Res. Public Health* 14, E1154. doi:10.3390/ijerph14101154

Ringman, J. M., Schulman, H., Becker, C., Jones, T., Bai, Y., Immermann, F., et al. (2012). Proteomic changes in cerebrospinal fluid of presymptomatic and affected persons carrying familial Alzheimer disease mutations. *Arch. Neurol.* 69, 96–104. doi:10.1001/archneurol.2011.642

Rodríguez, V. M., Dufour, L., Carrizales, L., Díaz-Barriga, F., and Jiménez-Capdeville, M. E. (1998). Effects of oral exposure to mining waste on *in vivo* dopamine release from rat striatum. *Environ. Health Perspect.* 106, 487–491. doi:10.1289/ehp.106-1533203

Romani, A. M. P. (2011). Cellular magnesium homeostasis. *Arch. Biochem. Biophys.* 512, 1–23. doi:10.1016/j.abb.2011.05.010

Sales, T. A., Prandi, I. G., de Castro, A. A., Leal, D. H. S., da Cunha, E. F. F., Kuca, K., et al. (2019). Recent developments in metal-based drugs and chelating agents for neurodegenerative diseases treatments. *Int. J. Mol. Sci.* 20, E1829. doi:10.3390/ijms20081829

Sanders, A. P., Claus Henn, B., and Wright, R. O. (2015). Perinatal and childhood exposure to cadmium, manganese, and metal mixtures and effects on cognition and behavior: A review of recent literature. *Curr. Environ. Health Rep.* 2, 284–294. doi:10.1007/s40572-015-0058-8

Sanders, T., Liu, Y., Buchner, V., and Tchounwou, P. B. (2009). Neurotoxic effects and biomarkers of lead exposure: A review. *Rev. Environ. Health* 24, 15–45. doi:10.1515/REVEH.2009.24.1.15

Scheiber, I. F., and Dringen, R. (2013). Astrocyte functions in the copper homeostasis of the brain. *Neurochem. Int.* 62, 556–565. doi:10.1016/j.neuint.2012.08.017

Schneider, J. S., Williams, C., Ault, M., and Guilarte, T. R. (2013). Chronic manganese exposure impairs visuospatial associative learning in non-human primates. *Toxicol. Lett.* 221, 146–151. doi:10.1016/j.toxlet.2013.06.211

Schwartz, B. S., Stewart, W. F., Bolla, K. I., Simon, D., Bandeen-Roche, K., Gordon, B., et al. (2000). Past adult lead exposure is associated with longitudinal decline in cognitive function. *Neurology* 55, 1144–1150. doi:10.1212/WNL.55.8.1144

Searle, A. K., Baghurst, P. A., van Hooff, M., Sawyer, M. G., Sim, M. R., Galletly, C., et al. (2014). Tracing the long-term legacy of childhood lead exposure: A review of three decades of the port pirie cohort study. *Neurotoxicology* 43, 46–56. doi:10.1016/j.neuro.2014.04.004

Sensi, S. L., Paoletti, P., Koh, J. Y., Aizenman, E., Bush, A. I., Hershfinkel, M., et al. (2011). The neurophysiology and pathology of brain zinc. *J. Neurosci.* 31, 16076–16085. doi:10.1523/JNEUROSCI.3454-11.2011

Senut, M. C., Sen, A., Cingolani, P., Shaik, A., Land, S. J., Ruden, D. M., et al. (2014). Lead exposure disrupts global DNA methylation in human embryonic stem cells and alters their neuronal differentiation. *Toxicol. Sci.* 139, 142–161. doi:10.1093/toxsci/kfu028

Sharma, B., Singh, S., and Siddiqi, N. J. (2014). Biomedical implications of heavy metals induced imbalances in redox systems. *Biomed. Res. Int.*, 640754. doi:10.1155/2014/640754

Shaw, C. A., and Tomljenovic, L. (2013). Aluminum in the central nervous system (CNS): Toxicity in humans and animals, vaccine adjuvants, and autoimmunity. *Immunol. Res.* 56, 304–316. doi:10.1007/s12026-013-8403-1

Singh, Y. P., Pandey, A., Vishwakarma, S., and Modi, G. (2019). A review on iron chelators as potential therapeutic agents for the treatment of Alzheimer's and Parkinson's diseases. *Mol. Divers.* 23, 509–526. doi:10.1007/s11030-018-9878-4

Sink, M. (2022). Elevated blood lead levels as eligibility criteria for early elevated blood lead levels as eligibility criteria for early intervention programs intervention programs elevated blood lead levels as eligibility criteria for early intervention programs. *Heal. Matrix J. Law-Health Matrix J. Law-Medicine Med.* 32, 531. Available at: https://scholarlycommons.law.case.edu/healthmatrix/vol32/iss1/11 (Accessed May 23, 2022).

Smart, T. G., Hosie, A. M., and Miller, P. S. (2004). Zn2+ ions: Modulators of excitatory and inhibitory synaptic activity. *Neuroscientist* 10, 432–442. doi:10.1177/1073858404263463

Song, N., Jiang, H., Wang, J., and Xie, J. X. (2007). Divalent metal transporter 1 up-regulation is involved in the 6-hydroxydopamine-induced ferrous iron influx. *J. Neurosci. Res.* 85, 3118–3126. doi:10.1002/jnr.21430

Sparks, D. L., and Schreurs, B. G. (2003). Trace amounts of copper in water induce β-amyloid plaques and learning deficits in a rabbit model of Alzheimer's disease. *Proc. Natl. Acad. Sci. U. S. A.* 100, 11065–11069. doi:10.1073/pnas.1832769100

Squitti, R., Polimanti, R., Bucossi, S., Ventriglia, M., Mariani, S., Manfellotto, D., et al. (2013). Linkage disequilibrium and haplotype analysis of the ATP7B gene in alzheimer's disease. *Rejuvenation Res.* 16, 3–10. doi:10.1089/rej.2012.1357

Srivastava, R. A. K., and Jain, J. C. (2002). Scavenger receptor class B type I expression and elemental analysis in cerebellum and parietal cortex regions of the Alzheimer's disease brain. *J. Neurol. Sci.* 196, 45–52. doi:10.1016/S0022-510X(02)00026-6

Stewart, W. F., Schwartz, B. S., Davatzikos, C., Shen, D., Liu, D., Wu, X., et al. (2006). Past adult lead exposure is linked to neurodegeneration measured by brain MRI. *Neurology* 66, 1476–1484. doi:10.1212/01.wnl.0000216138.69777.15

Su, X. Y., Wu, W. H., Huang, Z. P., Hu, J., Lei, P., Yu, C. H., et al. (2007). Hydrogen peroxide can be generated by tau in the presence of Cu(II). *Biochem. Biophys. Res. Commun.* 358, 661–665. doi:10.1016/j.bbrc.2007.04.191

Subramaniam, V. N., Summerville, L., and Wallace, D. F. (2002). Molecular and cellular characterization of transferrin receptor 2. *Cell biochem. Biophys.* 36, 235–239. doi:10.1385/CBB:36:2-3:235

Suh, S. W., Jensen, K. B., Jensen, M. S., Silva, D. S., Kesslak, P. J., Danscher, G., et al. (2000). Histochemically-reactive zinc in amyloid plaques, angiopathy, and degenerating neurons of Alzheimer's diseased brains. *Brain Res.* 852, 274–278. doi:10.1016/S0006-8993(99)02096-X

Suwazono, Y., Kido, T., Nakagawa, H., Nishijo, M., Honda, R., Kobayashi, E., et al. (2009). Biological half-life of cadmium in the urine of inhabitants after cessation of cadmium exposure. *Biomarkers* 14, 77–81. doi:10.1080/13547500902730698

Takeda, A. (2000). Movement of zinc and its functional significance in the brain. *Brain Res. Brain Res. Rev.* 34, 137–148. doi:10.1016/S0165-0173(00)00044-8

Takeda, A., Tamano, H., Tempaku, M., Sasaki, M., Uematsu, C., Sato, S., et al. (2017). Extracellular Zn2+ is essential for amyloid β1-42-induced cognitive decline in the normal brain and its rescue. *J. Neurosci.* 37, 7253–7262. doi:10.1523/JNEUROSCI.0954-17.2017

Takeda, A. (2001). Zinc homeostasis and functions of zinc in the brain. *Biometals.* 14, 343–351. doi:10.1023/A:1012982123386

Tao, Y., Wang, Y., Rogers, J. T., and Wang, F. (2014). Perturbed iron distribution in alzheimer's disease serum, cerebrospinal fluid, and selected brain regions: A systematic review and meta-analysis. *J. Alzheimer's Dis.* 42, 679–690. doi:10.3233/JAD-140396

Tchounwou, P. B., Yedjou, C. G., Patlolla, A. K., and Sutton, D. J. (2012). Heavy metal toxicity and the environment. *Exp. Suppl.* 101, 133–164. doi:10.1007/978-3-7643-8340-4_6

Thirupathi, A., and Chang, Y. Z. (2019). Brain iron metabolism and CNS diseases. *Adv. Exp. Med. Biol.* 1173, 1–19. doi:10.1007/978-981-13-9589-5_1

Thompson, C. M., Markesbery, W. R., Ehmann, W. D., Mao, Y. X., and Vance, D. E. (1988). Regional brain trace-element studies in Alzheimer's disease. *Neurotoxicology* 9, 1–7.

Ton, V. K., Mandal, D., Vahadji, C., and Rao, R. (2002). Functional expression in yeast of the human secretory pathway Ca2+, Mn2+-ATPase defective in Hailey-Hailey disease. *J. Biol. Chem.* 277, 6422–6427. doi:10.1074/jbc.M110612200

Tong, Y., Yang, H., Tian, X., Wang, H., Zhou, T., Zhang, S., et al. (2014). High manganese, a risk for Alzheimer's disease: High manganese induces amyloid-β related cognitive impairment. *J. Alzheimer's Dis.* 42, 865–878. doi:10.3233/JAD-140534

Tõugu, V., Karafin, A., and Palumaa, P. (2008). Binding of zinc(II) and copper(II) to the full-length Alzheimer's amyloid-β peptide. *J. Neurochem.* 104, 1249–1259. doi:10.1111/j.1471-4159.2007.05061.x

Tu, H., Nelson, O., Bezprozvanny, A., Wang, Z., Lee, S. F., Hao, Y. H., et al. (2006). Presenilins form ER Ca2+ leak channels, a function disrupted by familial alzheimer's disease-linked mutations. *Cell* 126, 981–993. doi:10.1016/j.cell.2006.06.059

Tuschl, K., Clayton, P. T., Gospe, S. M., Gulab, S., Ibrahim, S., Singhi, P., et al. (2016). Erratum: Syndrome of hepatic cirrhosis, dystonia, polycythemia, and hypermanganesemia caused by mutations in SLC30A10, a manganese transporter in man. *Am. J. Hum. Genet. J. Hum. Genet.* 201299 (457–466), 90521. doi:10.1016/j.ajhg.2012.01.01810.1016/j.ajhg.2016.07.015

Uddin, M. S., Kabir, M. T., Jeandet, P., Mathew, B., Ashraf, G. M., Perveen, A., et al. (2020a2020). Novel anti-Alzheimer's therapeutic molecules targeting amyloid precursor protein processing. *Oxid. Med. Cell. Longev.*, 7039138. doi:10.1155/2020/7039138

Uddin, M. S., Kabir, M. T., Mamun, A. Al, Barreto, G. E., Rashid, M., Perveen, A., et al. (2020b). Pharmacological approaches to mitigate neuroinflammation in Alzheimer's disease. *Int. Immunopharmacol.* 84, 106479. doi:10.1016/j.intimp.2020.106479

Vanea, E., Moraru, C., Vulpoi, A., Cavalu, S., and Simon, V. (2014). Freeze-dried and spray-dried zinc-containing silica microparticles entrapping insulin. *J. Biomater. Appl.* 28, 1190–1199. doi:10.1177/0885328213501216

Vaz, F. N. C., Fermino, B. L., Haskel, M. V. L., Wouk, J., de Freitas, G. B. L., Fabbri, R., et al. (2018). The relationship between copper, iron, and selenium levels and alzheimer disease. *Biol. Trace Elem. Res.* 181, 185–191. doi:10.1007/s12011-017-1042-y

Ventriglia, M., Bucossi, S., Panetta, V., and Squitti, R. (2012). Copper in Alzheimer's disease: A meta-analysis of serum, plasma, and cerebrospinal fluid studies. *J. Alzheimer's Dis.* 30 (9981-984), 30981–30984. doi:10.3233/JAD-2012-120244

Villar, J., Fernandes, M., Purwar, M., Staines-Urias, E., Di Nicola, P., Cheikh Ismail, L., et al. (2019). Neurodevelopmental milestones and associated behaviours are similar among healthy children across diverse geographical locations. *Nat. Commun.* 10, 511. doi:10.1038/s41467-018-07983-4

Volpe, S. L. (2013). Magnesium in disease prevention and overall health. *Adv. Nutr.* 4, 378S–83S. doi:10.3945/an.112.003483

Wall, M. J. (2005). A role for zinc in cerebellar synaptic transmission? *Cerebellum* 4, 224–229. doi:10.1080/14734220500242084

Wallin, C., Kulkarni, Y. S., Abelein, A., Jarvet, J., Liao, Q., Strodel, B., et al. (2016). Characterization of Mn(II) ion binding to the amyloid-β peptide in Alzheimer's disease. *J. Trace Elem. Med. Biol.* 38, 183–193. doi:10.1016/j.jtemb.2016.03.009

Wang, B., and Du, Y. (2013). Cadmium and its neurotoxic effects. *Oxid. Med. Cell. Longev.*, 898034. doi:10.1155/2013/898034

Wang, L., Sato, H., Zhao, S., and Tooyama, I. (2010). Deposition of lactoferrin in fibrillar-type senile plaques in the brains of transgenic mouse models of Alzheimer's disease. *Neurosci. Lett.* 481, 164–167. doi:10.1016/j.neulet.2010.06.079

Wang, Z., Wei, X., Yang, J., Suo, J., Chen, J., Liu, X., et al. (2016). Chronic exposure to aluminum and risk of alzheimer's disease: A meta-analysis. *Neurosci. Lett.* 610, 200–206. doi:10.1016/j.neulet.2015.11.014

Wang, Z. X., Tan, L., Wang, H. F., Ma, J., Liu, J., Tan, M. S., et al. (2015). Serum iron, zinc, and copper levels in patients with alzheimer's disease: A replication study and meta-analyses. *J. Alzheimer's Dis.* 47, 565–581. doi:10.3233/JAD-143108

White, A. R., Multhaup, G., Maher, F., Bellingham, S., Camakaris, J., Zheng, H., et al. (1999a). The Alzheimer's disease amyloid precursor protein modulates copper- induced toxicity and oxidative stress in primary neuronal cultures. *J. Neurosci.* 19, 9170–9179. doi:10.1523/jneurosci.19-21-09170.1999

White, A. R., Reyes, R., Mercer, J. F. B., Camakaris, J., Zheng, H., Bush, A. I., et al. (1999b). Copper levels are increased in the cerebral cortex and liver of APP and APLP2 knockout mice. *Brain Res.* 842, 439–444. doi:10.1016/S0006-8993(99)01861-2

Witting, A., Walter, L., Wacker, J., Möller, T., and Stella, N. (2004). P2X7 receptors control 2-arachidonoylglycerol production by microglial cells. *Proc. Natl. Acad. Sci. U. S. A.* 101, 3214–3219. doi:10.1073/pnas.0306707101

Wong-Guerra, M., Montano-Peguero, Y., Ramírez-Sánchez, J., Jiménez-Martin, J., Fonseca-Fonseca, L. A., Hernández-Enseñat, D., et al. (2021). JM-20 treatment prevents neuronal damage and memory impairment induced by aluminum chloride in rats. *Neurotoxicology* 87, 70–85. doi:10.1016/j.neuro.2021.08.017

Wu, J., Basha, M. R., Brock, B., Cox, D. P., Cardozo-Pelaez, F., McPherson, C. A., et al. (2008). Alzheimer's Disease (AD)-like pathology in aged monkeys after infantile exposure to environmental metal lead (Pb): Evidence for a developmental origin and environmental link for AD. *J. Neurosci.* 28, 3–9. doi:10.1523/JNEUROSCI.4405-07.2008

Xian-Hui, D., Wei-Juan, G., Tie-Mei, S., Hong-Lin, X., Jiang-Tao, B., Jing-Yi, Z., et al. (2015). Age-related changes of brain iron load changes in the frontal cortex in APPswe/PS1δE9 transgenic mouse model of Alzheimer's disease. *J. Trace Elem. Med. Biol.* 30, 118–123. doi:10.1016/j.jtemb.2014.11.009

Xu, Z. P., Li, L., Bao, J., Wang, Z. H., Zeng, J., Liu, E. J., et al. (2014). Magnesium protects cognitive functions and synaptic plasticity in streptozotocin-induced sporadic Alzheimer's model. *PLoS One* 9, e108645. doi:10.1371/journal.pone.0108645

Yadav, R. S., Shukla, R. K., Sankhwar, M. L., Patel, D. K., Ansari, R. W., Pant, A. B., et al. (2010). Neuroprotective effect of curcumin in arsenic-induced neurotoxicity in rats. *Neurotoxicology* 31, 533–539. doi:10.1016/j.neuro.2010.05.001

Yang, L. S., and Ksiezak-Reding, H. (1999). Ca2+ and Mg2+ selectively induce aggregates of PHF-Tau but not normal human Tau. *J. Neurosci. Res.* 55, 36–43. doi:10.1002/(SICI)1097-4547(19990101)55:1<36:AID-JNR5>3.0.CO;2-E

Yang, X., Park, S. H., Chang, H. C., Shapiro, J. S., Vassilopoulos, A., Sawicki, K. T., et al. (2017). Sirtuin 2 regulates cellular iron homeostasis via deacetylation of transcription factor NRF2. *J. Clin. Invest.* 127, 1505–1516. doi:10.1172/JCI88574

Yorifuji, T., Debes, F., Weihe, P., and Grandjean, P. (2011). Prenatal exposure to lead and cognitive deficit in 7- and 14-year-old children in the presence of concomitant exposure to similar molar concentration of methylmercury. *Neurotoxicol. Teratol.* 33, 205–211. doi:10.1016/j.ntt.2010.09.004

Yu, C. H., Dolgova, N. V., and Dmitriev, O. Y. (2017). Dynamics of the metal binding domains and regulation of the human copper transporters ATP7B and ATP7A. *IUBMB Life* 69, 226–235. doi:10.1002/iub.1611

Zahir, F., Rizwi, S. J., Haq, S. K., and Khan, R. H. (2005). Low dose mercury toxicity and human health. *Environ. Toxicol. Pharmacol.* 20, 351–360. doi:10.1016/j.etap.2005.03.007

Zatta, P., and Frank, A. (2007). Copper deficiency and neurological disorders in man and animals. *Brain Res. Rev.* 54, 19–33. doi:10.1016/j.brainresrev.2006.10.001

Zhang, M., Mo, H., Sun, W., Guo, Y., and Li, J. (2016a). Systematic isolation and characterization of cadmium tolerant genes in tobacco: A cDNA library construction and screening approach. *PLoS One* 11, e0161147. doi:10.1371/journal.pone.0161147

Zhang, X., Surguladze, N., Slagle-Webb, B., Cozzi, A., and Connor, J. R. (2006). Cellular iron status influences the functional relationship between microglia and oligodendrocytes. *Glia* 54, 795–804. doi:10.1002/glia.20416

Zhang, Z., Miah, M., Culbreth, M., and Aschner, M. (2016b). Autophagy in neurodegenerative diseases and metal neurotoxicity. *Neurochem. Res.* 41, 409–422. doi:10.1007/s11064-016-1844-x

Zhao, Z. H., Zheng, G., Wang, T., Du, K. J., Han, X., Luo, W. J., et al. (2018). Low-level gestational lead exposure alters dendritic spine plasticity in the Hippocampus and reduces learning and memory in rats. *Sci. Rep.* 8, 3533. doi:10.1038/s41598-018-21521-8

Zheng, W., and Monnot, A. D. (2012). Regulation of brain iron and copper homeostasis by brain barrier systems: Implication in neurodegenerative diseases. *Pharmacol. Ther.* 133, 177–188. doi:10.1016/j.pharmthera.2011.10.006

Zheng, Z., White, C., Lee, J., Peterson, T. S., Bush, A. I., Sun, G. Y., et al. (2010). Altered microglial copper homeostasis in a mouse model of Alzheimer's disease. *J. Neurochem.* 114, 1630–1638. doi:10.1111/j.1471-4159.2010.06888.x

Zhou, C. C., Gao, Z. Y., Wang, J., Wu, M. Q., Hu, S., Chen, F., et al. (2018). Lead exposure induces Alzheimers's disease (AD)-like pathology and disturbes cholesterol metabolism in the young rat brain. *Toxicol. Lett.* 296, 173–183. doi:10.1016/j.toxlet.2018.06.1065

frontiers | Frontiers in Neuroscience

TYPE Original Research
PUBLISHED 20 September 2022
DOI 10.3389/fnins.2022.917489

OPEN ACCESS

EDITED BY
Ying Xu,
University at Buffalo, United States

REVIEWED BY
Saivageethi Nuthikattu,
University of California, Davis, United States
Murali Vijayan,
Texas Tech University Health Sciences Center, United States
Junchao Shi,
University of California, Riverside, United States

*CORRESPONDENCE
Zhuorong Li
lizhuorong@imb.pumc.edu.cn
Rui Liu
liurui@imb.pumc.edu.cn

†These authors have contributed equally to this work

SPECIALTY SECTION
This article was submitted to Neuropharmacology, a section of the journal Frontiers in Neuroscience

RECEIVED 22 April 2022
ACCEPTED 22 August 2022
PUBLISHED 20 September 2022

CITATION
Zhao K, Zeng L, Cai Z, Liu M, Sun T, Li Z and Liu R (2022) RNA sequencing-based identification of the regulatory mechanism of microRNAs, transcription factors, and corresponding target genes involved in vascular dementia. *Front. Neurosci.* 16:917489. doi: 10.3389/fnins.2022.917489

RNA sequencing-based identification of the regulatory mechanism of microRNAs, transcription factors, and corresponding target genes involved in vascular dementia

Kaiyue Zhao†, Li Zeng†, Zhongdi Cai, Mimin Liu, Ting Sun, Zhuorong Li* and Rui Liu*

Institute of Medicinal Biotechnology, Chinese Academy of Medical Sciences and Peking Union Medical College, Beijing, China

Vascular dementia (VaD) is the second most common form of dementia with uncertain mechanisms and no effective treatments. microRNAs (miRNAs) and transcription factors (TFs) are considered regulatory factors of genes involved in many diseases. Therefore, this work investigated the aberrantly expressed miRNAs, TFs, corresponding target genes, and their co-regulatory networks in the cortex of rats with bilateral common carotid artery occlusion (2VO) to uncover the potential mechanism and biomarkers of VaD. Differentially expressed genes (DEGs), miRNAs (DEMs), and TFs (DETFs) were identified using RNA sequencing, and their interaction networks were constructed using Cytoscape. The results showed that rats with 2VO had declined cognitive abilities and neuronal loss in the cortex than sham rats. DEGs, DEMs, and DETFs were discriminated between rats with 2VO and sham rats in the cortex, as shown by the 13 aberrantly expressed miRNAs, 805 mRNAs, and 63 TFs. The miRNA-TF-target gene network was constructed, showing 523 nodes and 7237 edges. Five miRNAs (miR-5132-5p, miR-764-3p, miR-223-3p, miR-145-5p, and miR-122-5p), ten TFs (*Mxi1*, *Nfatc4*, *Rxrg*, *Zfp523*, *Foxj2*, *Nkx6-1*, *Klf4*, *Klf5*, *Csrnp1*, and *Prdm6*), and seven target genes (*Serpine1*, *Nedd4l*, *Pxn*, *Col1a1*, *Plec*, *Trip12*, and *Tpm1*) were chosen as the significant nodes to construct feed-forward loops (FFLs). Gene Ontology and pathway enrichment analysis revealed that these miRNA and TF-associated genes are mostly involved in the PI3K/Akt, neuroactive ligand–receptor interaction, calcium signaling, and Wnt signaling pathways, along with central locations around the cell membrane. They exert functions such as growth factor binding, integrin binding, and extracellular matrix structural constituent, with representative biological processes like vasculature development, cell–substrate adhesion, cellular response to growth factor stimulus, and synaptic

transmission. Furthermore, the expression of three miRNAs (miR-145-5p, miR-122-5p, and miR-5132-5p), six TFs (*Csrnp1*, *Klf4*, *Nfatc4*, *Rxrg*, *Foxj2*, and *Klf5*), and five mRNAs (*Serpine1*, *Plec*, *Nedd4l*, *Trip12*, and *Tpm1*) were significantly changed in rats with VaD, in line with the outcome of RNA sequencing. In the potential FFL, miR-145-5p directly bound *Csrnp1* and decreased its mRNA expression. These results might help the understanding of the underlying regulatory mechanisms of miRNA-TF-genes, providing potential therapeutic targets in VaD.

KEYWORDS

microRNA, RNA sequencing, regulatory network, transcription factor, vascular dementia

Introduction

Vascular dementia (VaD) is the second cause of dementia after Alzheimer's disease (AD), characterized by brain impairments due to inadequate blood perfusion. The patients suffering from VaD undergo cognitive decline and executive dysfunction. Stroke and infarct of cerebral vessels are associated with VaD, and hypertension, atherosclerosis, cardiac disease, and diabetes are additional risks for developing VaD (Venkat et al., 2015). The acute or chronic deterioration of cerebral vessels causes oxygen deprivation following the energy strike of neurons, leading to oxygen stress reaction, microglial and astroglia activation, mitochondrial injuries, loss of synaptic function, neuron apoptosis, or necrosis (Sun, 2018). The pathology of VaD is complex and unclear due to the heterogeneity of vascular diseases. Neuroimaging assessment and cognitive evaluation are the current methods in the diagnosis of VaD, but both have shortcomings, thus weakening the accuracy of the diagnosis (van der Flier et al., 2018). Besides, no officially therapeutic drugs are approved for VaD management, and drugs used for improving cognitive impairments mainly for AD are tentatively used in VaD, such as cholinesterase inhibitors and memantine (O'Brien and Thomas, 2015). Thus, the investigation of the VaD mechanism of action is urgently needed to facilitate the diagnosis or intervention of this disease.

MicroRNAs (miRNAs) are short non-coding RNAs repressing mRNA expression post-transcriptionally through the induction of degradation or translational repression of the target gene. Dysregulated miRNAs act as potential biomarkers in the diagnosis and prognosis of several diseases (Ragusa et al., 2016; Jiang et al., 2022). They also serve as targets for the intervention on the symptoms of the disease (Chen et al., 2017; Yao et al., 2017; Zeng et al., 2021a; Sun et al., 2022). Multiple miRNAs such as miR-145, novel miRNA PC-5P-12969, and miR-134-5p are reported as dysregulated in the process of neurological injuries induced by ischemia and are involved in the cognitive impairment of VaD (Dharap et al., 2009; Liu et al., 2019; Vijayan et al., 2019).

Aberrantly expressed miRNAs are closely associated with transcription factors (TFs). In turn, TFs are involved in the control of signaling pathways with miRNAs through the activation or suppression of the transcription of target genes by binding to the promoter and enhancer sequences (Spitz and Furlong, 2012; Inukai et al., 2017; Zhang et al., 2018). Furthermore, TFs and miRNAs interact with each other through complex molecular regulatory mechanisms (Zhang et al., 2015), which play a crucial part in the pathogenesis of VaD (Saggu et al., 2016; Han et al., 2020; Yang and Zhang, 2021). For example, the nuclear factor erythroid 2-related factor 2 (*Nrf2*), considered as the essential transcription factor for antioxidant responses, controls the transcription of a series of anti-oxidative and anti-inflammatory genes (Li et al., 2020a; Saha et al., 2020); as the functional target of miR-153 and miR-144, *Nrf2* ameliorates oxidative stress and inhibits the apoptotic signaling pathways (Chu et al., 2019; Zhu et al., 2019). Forkhead box P2 (*Foxp2*) is another transcription factor involved in early VaD and improves cognitive impairment in rats with VaD through the upregulation of synaptic proteins through the miR-134-5p/*Foxp2*/*Syn1* axis (Liu et al., 2019). The protective effect of acupuncture treatment in a rodent model of VaD may be related to the suppression of the miR-93-induced TLR4/MyD88/NF-κB pathway (Wang et al., 2020). However, the interrelationship of miRNAs, TFs, and target genes in VaD has not been fully elucidated.

In the present study, rats subjected to bilateral vessel occlusion (2VO), a widely accepted model induced by chronic blood hypoperfusion (Weinstock and Shoham, 2004), were used to mimic the pathology of VaD. Dysregulated miRNAs and mRNAs were obtained from the transcriptome sequencing of rats with VaD and sham rats. The regulation of differentially expressed miRNAs (DEMs), TFs (DETFs), and target genes (DEGs) was analyzed, followed by the construction of an integrative co-regulatory gene expression network. The expression of key DEMs, DETFs, and DEGs and their potential

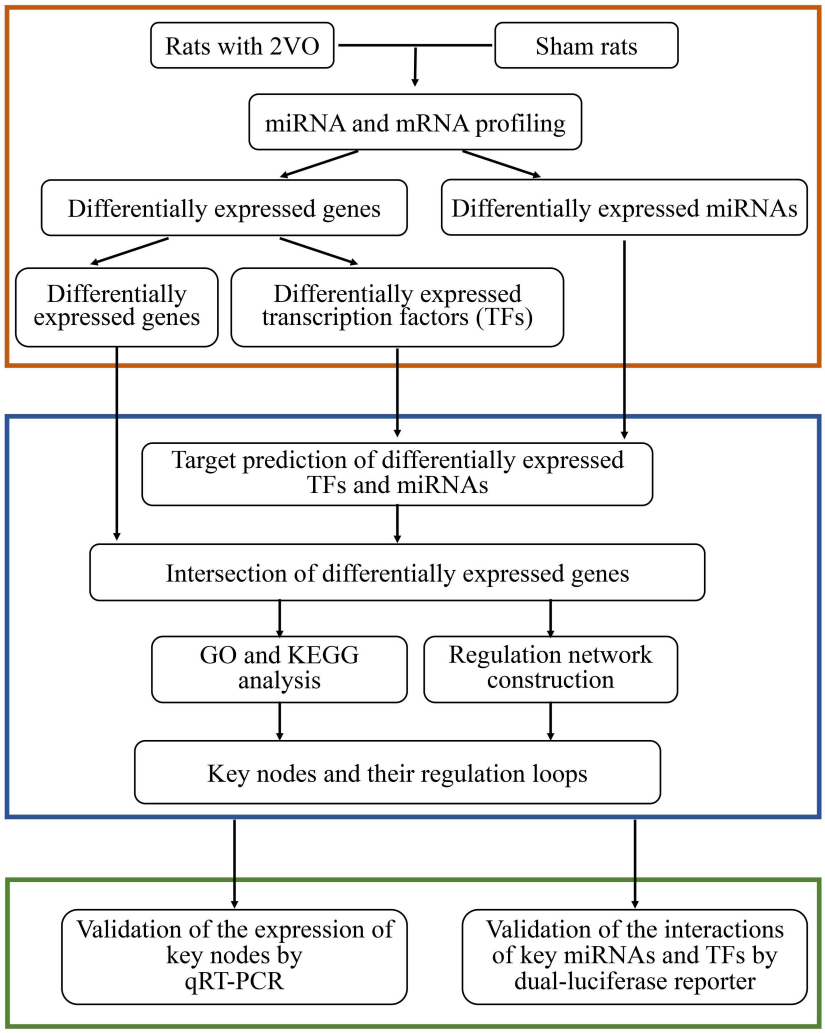

FIGURE 1
Workflow of the present study.

interaction were further verified to provide new insights into the mechanism of VaD. The workflow of the present study is presented in **Figure 1**.

Materials and methods

Animals

Male Sprague–Dawley (SD) rats (270 ± 10 g in weight, 7-week-old) were purchased from the Zhishan Healthcare Research Institute (Beijing, China) and maintained under the specified pathogen-free conditions with regular rat chow and water *ad libitum*. After 1 week of adaptively feeding, they were used for the construction of the *in vivo* VaD model as previously reported (Niu et al., 2019; Guo et al., 2020; Mao et al., 2020). All the experimental procedures were approved by the Committee of the Institute of Medicinal Biotechnology, China (No. IMB-201807-D8-03). Eighteen rats were randomly assigned to two groups and subjected to surgery. Nine rats in each group were subjected to the Morris water maze (MWM) test and then randomly divided into three equal parts to collect the cerebral cortex for the RNA sequencing analysis, histological examination by Nissl staining, and gene validation analysis. The overall experimental protocol is shown in **Figure 2A**.

Surgical procedure for bilateral vessel occlusion in rats

The VaD model was induced in rats by the permanent occlusion of the bilateral common carotid artery, as described

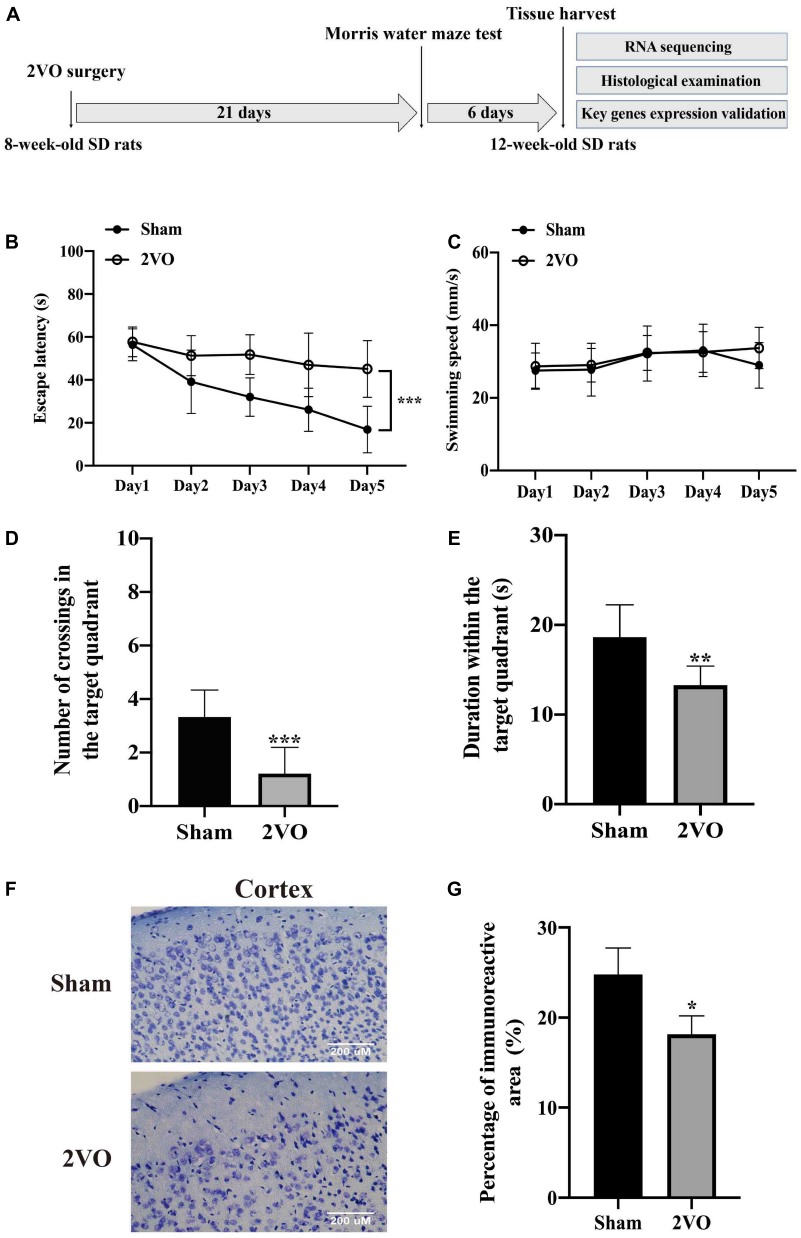

FIGURE 2
Cognitive decline and neuronal injury in rats with 2VO compared with sham rats. **(A)** Timeline of the *in vivo* experiment. 8-week-old SD rats were subjected to the bilateral common carotid artery occlusion, followed by the cognitive impairment test after 3 weeks. The cerebral cortices were finally collected from the 12-week-old SD rats. 2VO: bilateral common carotid artery occlusion. **(B)** Escape latency of rats in the navigation test for five consecutive days (n = 9). **(C)** Swimming speed of rats during the navigation test (n = 9). **(D)** Number of crossings of rats to find platforms previously located in the probe test (n = 9). **(E)** Duration time in the target quadrant in the probe test (n = 9). **(F)** Representative images of Nissl staining in the cortex of 2VO and sham rats. **(G)** Quantification of Nissl staining (n = 3). Results are presented as mean ± SD. *$P < 0.05$, **$P < 0.01$, ***$P < 0.001$ *vs*. sham.

in our previous work (Jiang et al., 2021). Briefly, rats were anesthetized with an intraperitoneal injection of 2% sodium pentobarbital (30 mg/kg). The bilateral common carotid arteries were gently separated and permanently ligated with a 5–0 silk thread. Rats in the sham group underwent the same procedure except for the arterial ligation.

Spatial cognitive evaluation

The MWM test was performed for the spatial cognitive evaluation on the 21st day after the occlusion surgery, as previously described (Liu et al., 2018; Jiang et al., 2021). The test was represented by the navigation trial and the probe test.

The navigation test lasted for five consecutive days. The rats experienced four pieces of training for the ability to search the underwater platform each day. The time the rats spent searching the platform was recorded as the escape latency. The probe test was performed 24 h after the navigation test, in which the hidden platform was removed, and the time the rats spent in the target quadrant and the frequency crossing the platform were recorded.

Histological examination

After the MWM test, routine Nissl staining was performed to evaluate the neuronal injury induced by 2VO. Briefly, rats were anesthetized with sodium pentobarbital and transcardially perfused with saline and 4% paraformaldehyde (PFA). The isolated whole brains were fixed in 4% PFA for 24 h at 4°C and then cryoprotected in ascending sucrose series gradient in phosphate-buffered saline. The slide-mounted brain sections (4 μm thick) were differentiated in 95% ethyl alcohol, rinsed in 75% ethyl alcohol and distilled water, and stained with 0.1% cresyl violet solution (Sigma, St. Louis, MI, United States). After a rinse in distilled water and dehydration in 95 and 100% ethyl alcohol, the sections were finally cleared in xylene for 2–3 min and mounted with Permount (Sigma, St. Louis, MI, United States). Images were acquired using a fluorescence microscope (Olympus, Tokyo, Japan).

RNA isolation, library preparation, sequencing, and data processing

The protocols of total RNA isolation and sequencing of miRNA or mRNA were the same as described in our previous work (Zeng et al., 2021b). Briefly, total RNA was extracted using the Total RNA Extractor (Trizol) kit (B511311, Sangon, China) according to the manufacturer's protocol, and the sample quality was evaluated using a 1.0% agarose gel for RNA integrity and genomic pollution. An amount of 2 μg RNA per sample was used as input material for the RNA sample preparation. Next, six mRNA sequencing libraries were constructed from six total RNA samples using VAHTSTM mRNA-seq V2 Library Prep Kit for Illumina® (NR601-02, Vazyme, China). Moreover, six sequencing libraries of miRNA were prepared from the same six total RNA samples using TruSeq Small RNA Sample Prep Kits (RS-200-0024, Illumina, United States), following the manufacturer's recommendations. The library quality was assessed on the Agilent Bioanalyzer 2100 system. Then, paired-end sequencing of the mRNA library was performed on the HiSeq XTen sequencers (Illumina, San Diego, CA, United States). Single-end sequencing of the miRNA library was conducted on the Illumina HiSeq 2500 (LC-BIO, Hangzhou, China).

The quality control of the original sequencing data (raw reads) was evaluated by FastQC V0.11.5, and then Cutadapt V1.14 was used to remove adaptors (cutoff value Q lower than 20). The clean reads were obtained using Trimmomatic V0.36 after removing low-quality bases at both ends. Thus, a mean of 57,348,784 reads with a Q30 ratio higher than 96.41% for mRNA was obtained. A standard of 25708013 reads with a Q30 ratio greater than 95.94% for miRNA was achieved (**Supplementary Tables 1**, **2**). Next, the clean reads were compared with the reference genome through miRbase for miRNA and HISAT2 V2.1.0 for mRNA. Hence, the unique value of mapping for mRNA is listed in **Supplementary Table 3**. Additionally, the gene expression was expressed as counts for miRNA or transcripts per million (TPM) for mRNA. TPM is the normalized count of mRNA, which considers sequencing depth and gene length simultaneously.

Our RNA sequencing data were submitted to Gene Expression Omnibus (GEO), with the accession number GSE199508.

mRNA and microRNAs profiling

The differential expression of mRNA and miRNA in the rats with 2VO and sham rats was separately evaluated by the DESeq2 V1.12.4 and by the edgeR V3.18.1. The read counts were normalized to TPM for mRNA and to reads per million (RPM) for miRNA before the analysis. A threshold was set for filtering out low-expressed miRNAs with the RPM value less than 0.05 and TPM less than 1. The DEMs and mRNAs (DEGs) were statistically analyzed by setting a *P*-value as 0.05 and the Log_2 (foldchange) absolute value of more than 1. Then, the results of the DEGs and DEMs were visualized as volcano diagrams and heatmap with hierarchical clustering using the pheatmap program. In addition, the sequence homology of the known DEMs with significant dysregulation was evaluated using the miRBase[1] database supported by RNACentral.

Identification of differentially expressed transcription factors and regulatory pairs among differentially expressed microRNAs, differentially expressed transcription factors, and differentially expressed genes

The transcription factors of *Rattus norvegicus* were collected from the AnimalTFDB3.0 database[2] to identify DETFs from the DEGs of the present transcriptome. The intersection of DEGs

1 http://www.mirbase.org/

2 http://bioinfo.life.hust.edu.cn/AnimalTFDB/

and transcription factors from AnimalTFDB3.0 was obtained, followed by a visualization *via* Bioinformatics[3], an online data processing platform.

As regards the DEMs, target prediction of DEMs was first performed with the help of three databases: miRanda[4], miRWalk2.0[5], and TargetScanHumanV7.2[6]. The miRNA-gene regulatory pairs were subsequently generated through the overlap of those predictions, targets, and DEGs. Based on the miRNA-gene regulatory pairs, miRNA-TF regulatory pairs were developed through the extraction of the DETFs from the DEGs regulated by DEMs. As regards the DETFs, the target prediction of TFs was performed using CistromeDB[7] and hTFtarget[8], developed based on the data of the ChIP-seq experiments (chromatin immunoprecipitation followed by sequencing), and targets with scores less than 4.0 were excluded. Likewise, the targets of DETFs were overlapped with those of DEGs, generating the TF-gene regulatory pairs. Furthermore, backward prediction based on DEMs for corresponding DETFs was developed to acquire the TF-miRNA regulatory pairs. Briefly, sequences covering the upstream of the transcription start sites (TSSs) for 5 kb and downstream for 1 kb were considered as the putative promoter region of DEMs and then were downloaded from NCBI[9]. Subsequently, those sequences were uploaded into PROMO V3.0.2[10] for the target-TF prediction of DEMs. Finally, four types of regulatory pairs among DEMs, DETFs, and DEGs were obtained, including miRNA-gene, miRNA-TF, TF-gene, and TF-miRNA regulatory pairs. The acquisition of the regulatory pairs was displayed as a Venn diagram using the online platform Bioinformatics.

Gene ontology and Kyoto Encyclopedia of Genes and Genomes pathway analyses

The miRNA/TF-associated genes were the focus of gene ontology (GO) and Kyoto Encyclopedia of Genes and Genomes (KEGG) enrichment analyses to discover genes highly associated with VaD and deeply involved in the miRNA/TF regulated network. In detail, miRNA/TF-associated genes were the DEGs jointly regulated by DEMs and DETFs, generated from the three sets, including sets of DEMs prediction targets, sets of DETFs prediction targets, and sets of DEGs. Then, Metascape online platform[11] was performed to enrich the molecular function, cellular component, biological process, and the KEGG pathways of miRNA/TF-associated genes in *Rattus norvegicus* with a *P*-value less than 0.01 as the cutoff value. The top 20 GO terms and top 10 signaling pathways by KEGG analysis are shown as bar charts and Chordal graph, respectively.

Construction of the microRNA-transcription factor-gene and protein-protein interaction network

An miRNA-TF-gene (M-T-G) network was constructed based on the aforementioned regulatory pairs among DEMs, DETFs, and miRNA/TF-associated genes, followed by a visualization using Cytoscape V3.8.2[12] to investigate the gene regulation network associated with miRNAs and TFs in VaD. Since the key nodes exert critical effects on the network, key miRNAs, TFs, and genes were obtained for further analysis. First, key miRNAs and TFs were analyzed by two plug-ins of Cytoscape and scored with several parameters, including closeness centrality (CC), betweenness centrality (BC), average shortest path length, outdegree, and neighborhood connectivity retrieved from CytoHubba, as well as the occurrence provided by Motif-Discover. Second, key genes were selected from the miRNA/TF-associated gene set by integrating the protein-protein interaction (PPI) and CytoHubba analytic methods. The STRING V11.5 software[13] was used to describe the interactive network within miRNA/TF-associated genes through the setting of the confidence score as 0.7. Then, the PPI network of miRNA/TF-associated genes was assessed by the CytoHubba plug-in. Key genes were selected using several topological parameters, including maximum neighborhood component (MNC), maximal clique centrality (MCC), degree, betweenness, and closeness. Additionally, regulatory loops among key miRNAs, TFs, and genes were displayed after visualization in Cytoscape V3.8.2 (see text footnote 12).

Quantitative real-time polymerase chain reaction analysis

Total RNA was extracted from the cortex of rats and HEK293 cells using the Ultrapure RNA Kit (CWBIO, Beijing, China). miRNA 1st Strand cDNA Synthesis Kit and miRNA Universal SYBR qPCR Master Mix (Vazyme, Nanjing, China) were used to measure the expression of DEMs in the 2VO

3 http://www.bioinformatics.com.cn

4 https://www.bioinformatics.com.cn/local_miranda_miRNA_target_prediction_120

5 http://mirwalk.umm.uni-heidelberg.de/

6 http://www.targetscan.org/vert_72/

7 http://www.cistrome.org/db

8 http://bioinfo.life.hust.edu.cn/hTFtarget#!/

9 www.ncbi.nlm.nih.gov/

10 alggen.lsi.upc.es/cgi-bin/promo_v3/promo/promoinit.cgi?dirDB=TF_8.3

11 https://metascape.org/gp/index.html#/main/step1

12 https://www.cytoscape.org/

13 https://www.string-db.org/

TABLE 1 Primers for qRT-PCR and nucleotide sequences for transfection.

Name	Sequence
miR-145-5p RT	5′-GTCGTATCCAGTGCAGGGTCCGAGG TATTCGCACTGGATACGACAGGGAT-3′
miR-122-5p-RT	5′-GTCGTATCCAGTGCAGGGTCCGAGG TATTCGCACTGGATACGACCAAACA-3′
miR-21-5p-RT	5′-GTCGTATCCAGTGCAGGGTCCGAGG TATTCGCACTGGATACGACTCAACA-3′
miR-5132-5p RT	5′-GTCGTATCCAGTGCAGGGTCCGAGGT ATTCGCACTGGATACGACAGCCTG
U6 RT	GTCGTATCCAGTGCAGGGTCCGAGGTA-3′ TTCGCACTGGATACGACAAAATA
miR-145-5p-F	5′-CGGTCCAGTTTTCCCAGGA-3′
miR-145-5p-R	5′-AGTGCAGGGTCCGAGGTATT-3′
miR-122-5p-F	5′-CGCGTGGAGTGTGACAATGG-3′
miR-122-5p-R	5′-AGTGCAGGGTCCGAGGTATT-3′
miR-5132-5p-F	5′-GATATCGTGGGGCGGTGGA-3′
miR-5132-5p-R	5′-CAGTGCAGGGTCCGAGGT-3′
miR-764-3p-F	5′-AACAAGGAGGAGGCCATAGTG-3′
miR-764-3p R	5′-CAGTGCAGGGTCCGAGGT-3′
U6-F	5′-CAAATTCGTGAAGCGTTCCA-3′
U6-R	5′-AGTGCAGGGTCCGAGGTATT-3′
Serpine1-F	5′-GCGTCTTCCTCCACAGCCATTC-3′
Serpine1-R	5′-TGTCTCTGTTGGATTGTGCCGAAC-3′
Nedd4l-F	5′-CGCCGTGCTGTGAAAGATACCC-3′
Nedd4l-R	5′-GTGTGACTTTGTGTTGTGGTTTGGG-3′
Tpm1-F	5′-GTAGCATCTCTGAACAGACGCATCC-3′
Tpm1-R	5′-CAGCCTTCTCAGCCTCCTCCAG-3′
Pxn-F	5′-CAGCCAGCAGCAGACCAGAATC-3′
Pxn-R	5′-ACTGCCGCTCTACATCCACTCTC-3′
Plec-F	5′-CACCGCACTGAACTCGCTACAC-3′
Plec-R	5′-GCTCGGCATCTTGGTCACTCTG-3′
Trip12-F	5′-CCGAATCAACTGGTGCCGAAGAG-3′
Trip12-R	5′-AGGAGGAAGTAGAGGCAGCAGAAG-3′
Col1a1-F	5′-TGTTGGTCCTGCTGGCAAGAATG-3′
Col1a1-R	5′-GTCACCTTGTTCGCCTGTCTCAC-3′
Klf5-F	5′-AGACGAGACAGTGCCTCAGTGG-3′
Klf5-R	5′-GCCAGTTCTCAGGTGCGTGATG-3′
Csrnp1-F	5′-ACGCTTCTGTAGAGGAGGACTTGG-3′
Csrnp1-R	5′-CCGAGGTGGATAGGGCTGTAGG-3′
Rxrg-F	5′-CGAATCCTACGGCGACATGAGTG-3′
Rxrg-R	5′-AACAAGGGTGAAGAGCTGCTTATCC-3′
Klf4-F-F	5′-GGACGGCTGTGGGTGGAAATTC-3′
Klf4-R	5′-TGTCGCACTTCTGGCACTGAAAG-3′
Nfatc4-F	5′-GCGGTCGTGTTCTTGAGTGTCC-3′
Nfatc4-R	5′-CAAAGCCTTCTGGTGGAGGGTAATC-3′
Foxj2-F	5′-ACCCGCAAGCCTCTCATCTCTAC-3′
Foxj2-R	5′-GTGGTGTGTTGGGCGACTGTATC-3′
Nkx6-1-F	5′-AGAGTCAGGTCAAGGTCTGGTTCC-3′
Nkx6-1-R	5′-ATCGTCGTCGTCCTCCTCGTTC-3′
Prdm6-F	5′-CCACCACCCTCAACAACCACATC-3′
Prdm6-R	5′-GTCTTCCAAACGCTTCAGCAAACAG-3′
Mxi1-F	5′-GCGAGAGGAGATTGAAGTGGATGTG-3′
Mxi1-R	5′-TGATGCTGGTGGTACTGATGTTGTC-3′
Zfp523-F	5′-CAATGGCAAAGGGCAGCAAGTTG-3′
Zfp523-R	5′-AGTGATGGGCAGTGGTGTAGAGG-3′
Gapdh-F	5′-CAAGGTCATCCATGACAACTTTG-3′
Gapdh-R	5′-GGGCCATCCACAGTCTCCT-3′
KLF5-F	5′-AGTGCCTCAGTCGTAGACCAGTTC-3′
KLF5-R	5′-GCCAGTTCTCAGGTGAGTGATGTC-3′
CSRNP1-F	5′-ATGCCATTGATGACGCCTCTGTG-3′
CSRNP1-R	5′-GGCTGGGTAGGGCTGTAGGAAG-3′
ACTB-R	5′-ATACTCCTGCTTGCTGATCC-3′ ATACTCCTGCTTGCTGATCC ATACTCCTGCTTGCTGATCC
ACTB-F	5′-CCTGTACGCCAACACAGTGC-3′ CCTGTACGCCAACACAGTGC CCTGTACGCCAACACAGTGC
miR-145-5p mimics	sense 5′-GUCCAGUUUUCCCAGGAAUCCCU-3′
	antisense 5′-GGAUUCCUGGGAAAACUGGACUU-3′
miR-122-5p mimics	sense 5′-UGGAGUGUGACAAUGGUGUUUG-3′
	antisense 5′-AACACCAUUGUCACACUCCAUU-3′
Negative control (NC)	sense 5′-UUCUCCGAACGUGUCACGUTT-3′
	antisense 5′-ACGUGACACGUUCGGAGAATT-3′

rat model. Likewise, the DEGs in the rats with 2VO were also measured using Hiscript®III RT SuperMix for qPCR and ChamQ Universal SYBR qPCR Master Mix (Vazyme, Nanjing, China). Quantitative real-time polymerase chain reaction (qRT-PCR) analyses for miRNA and mRNA were performed following the manufacturer's recommendations. The expression of miRNA and mRNA was calculated by the $2^{-\Delta\Delta CT}$ method (Yi et al., 2021). The primes in this study were synthesized from Sangon Biotech (Shanghai, China) and are listed in **Table 1**. U6 small RNA was used as the internal reference for miRNA. *Gapdh* and *ACTB* were used as the reference genes for mRNA.

Cell culture and transfection

Human embryonic kidney (HEK293) cells were cultured in DMEM supplemented with 10% FBS (Gibco/Invitrogen, Grand Island, NY, United States) and were incubated following the instructions of the American Tissue Culture Collection. HEK293 cells were seeded into 24-well plates and 6-well plates for transfection after reaching 70% growth confluence using Lipofectamine 2000 (Invitrogen, Carlsbad, CA, United States). Mimics were purchased from Genepharma (Suzhou, China) and were transfected into HEK293 cells to evaluate the regulatory

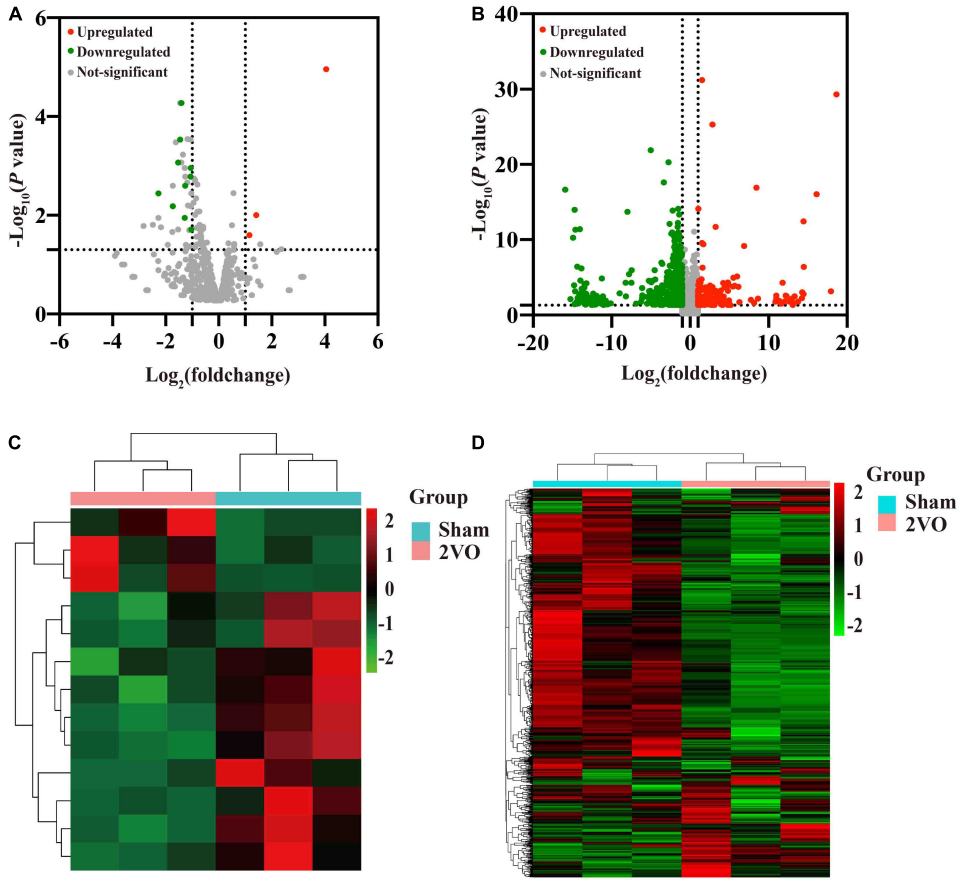

FIGURE 3
Volcano plots of the transcriptome and hierarchical cluster analysis of the DEMs and DEGs in the cortex of 2VO and sham rats. **(A)** Volcano plots of the differentially expressed miRNAs (DEMs) in the cortex of rats with 2VO compared with sham rats. **(B)** Differentially expressed mRNAs (DEGs) in the cortex of rats with 2VO compared with sham rats. Red dots indicate the upregulated DEMs and DEGs in the brains of rats with 2VO, while green dots indicate downregulated DEMs and DEGs. The molecules with no statistically different changes in rats with 2VO are shown as gray dots. **(C)** Hierarchical clustering analysis of DEMs. **(D)** Hierarchical clustering analysis of DEGs. The *X*-axis shows the cluster analysis of samples, the top blue bar indicates the sham group, and the top red bar indicates the group of rats with 2VO. The *Y*-axis shows the cluster analysis of miRNAs or mRNAs. Upregulated DEMs and DEGs are shown in red, and downregulated DEMs and DEGs are shown in green.

relationship of miR-145-5p over *Csrnp1* and miR-122-5p over *Klf5*; the sequences of mimics and negative control (NC) are listed in Table 1.

Dual-luciferase reporter assay

Dual-luciferase reporter experiment was used to verify the direct action between miR-145-5p and miR-122-5p over *Csrnp1* and *Klf5*. The binding sequences in the 3′UTR of *Csrnp1* and *Klf5* were provided by miRWalk (see text footnote 5) and cloned into the pmirGLO plasmid vector (Sangon Biotech, Shanghai, China) after amplification. Subsequently, plasmids containing wild-type (WT) binding sequences were transfected into HEK293 cells along with miR-145-5p mimics or miR-122-5p mimics, using NC as the control group. The plasmids with the mutant-type (MUT) binding sequences were also synthesized and transfected into HEK293 cells along with miR-145-5p mimics, miR-122-5p mimics, or NC. The cells were collected at 48 h after transfection and analyzed using the Dual-Luciferase Reporter Assay Kit (Vanzyme, Nanjing, China) under the manufacturer's recommendations. The activity of renilla luciferase was considered as the endogenous control of firefly luciferase.

Dataset acquisition and data processing

Gene expression datasets of miRNA and mRNA related to VaD were selected from the GEO[14], with the species limitation (human, mouse, and rat) and the biological

14 https://www.ncbi.nlm.nih.gov/gds/

sample type (blood and different brain regions). Ten GEO datasets containing the expression level of miRNA associated with VaD were selected, including GSE193012, GSE178500, GSE86291, GSE100488, GSE111794, GSE48028, GSE184975, GSE29287, GSE46266, and GSE46269. Meanwhile, 22 GEO datasets of mRNA expression status involved in VaD were collected, including GSE104381, GSE201482, GSE186798, GSE80681, GSE60820, GSE97537, GSE202659, GSE173544, GSE173714, GSE131193, GSE45703, GSE163614, GSE106680, GSE21136, GSE157628, GSE111782, GSE134257, GSE107983, GSE37777, GSE17929, GSE162072, and GSE148841. The significantly dysregulated genes were obtained by setting the absolute value of Log_2 (foldchange) greater than 1 and the *P*-value less than 0.05.

Statistical analysis

IBM SPSS Statistics (version 25.0, IBM, NY, United States) was used for analyzing the escape latency and the swimming speed in the MWM test with ANOVA, followed by Tukey's *post hoc* analyses among groups. The unpaired *t*-test was used for the remaining statistical analyses using the GraphPad Prism version 8.0 software (GraphPad Inc., CA, United States). Results are expressed as mean ± standard deviation (SD). Besides, unpaired *t*-test and fold change analyses were applied to distinguish DEMs and DEGs among rats with 2VO and sham rats with a threshold set as $P < 0.05$ and Log_2 (foldchange) absolute value greater than 1.

Results

Spatial cognition and neuronal survival are declined in rats with vascular dementia

Rats with 2VO showed a longer escape latency in the MWM test than the sham rats (**Figure 2B**, $P < 0.001$), while the swimming speed was not different between these two groups (**Figure 2C**), indicating that the decline in the learning ability in rats with 2VO was not due to the influence of motor ability. Moreover, rats with 2VO showed less crossings of the target platform (**Figure 2D**, $P < 0.001$) and shorter duration in the target quadrant than sham rats (**Figure 2E**, $P < 0.01$), suggesting the occurrence of the loss of memory in rats with 2VO. Furthermore, fewer Nissl bodies were found in the cortex of rats with 2VO (**Figures 2F,G**, $P < 0.05$ *vs.* sham rats). Together, these results supported the cognitive deficits and neuronal damage in the VaD model.

Identification of differentially expressed microRNAs and differentially expressed genes related to vascular dementia

Thirteen known DEMs and 805 DEGs were identified between rats with 2VO and sham rats, including ten downregulated and three upregulated DEMs and 602 downregulated and 203 upregulated DEGs. The volcano diagram illustrated the distribution of DEMs and DEGs acquired from the cortex of the rats with 2VO compared to the sham ones (**Figures 3A,B**). Further hieratical clustering analysis revealed a differential sequencing expression profiling of these DEMs and DEGs among samples, as shown in **Figures 3C,D**. Moreover, among the DEMs, ten miRNAs were conserved among humans, mice, and rats according to miRBase (see text footnote 1), while miR-5132-5p, miR-764-3p, and miR-802-5p were not conserved (**Table 2**).

Identification of transcription factors and microRNA-transcription factor regulatory pairs associated with vascular dementia

A total of 63 VaD-associated DETFs, divided into 18 upregulated and 45 downregulated TFs, were identified among the intersection of 805 DEGs in the cortex of rats with 2VO from RNA sequencing data and 1478 TFs of *Rattus norvegicus* from the AnimalTFDB database, which were useful to investigate the abnormally changed TFs involved in VaD (**Figure 4A**). The regulatory interactions, the expression fold change, and the *P*-value of 63 disease-related DETFs are listed in **Supplementary Table 4**.

A total of 3332 putative target genes of 13 DEMs and 30,002 presumptive target genes of 63 DETFs were obtained to investigate the involvement of miRNAs and TFs in the regulation of disease-related genes through a combination of the predicted results from multiple sources, including miRanda, miRWalk2.0, and TargetScanHumanV7.2 for DEMs, and CistromeDB and hTFtarget for DETFs, as described in paragraph 3.7 of the Materials and Methods (**Figure 4B**). Finally, a total of 460 common miRNA/TF-associated target genes were generated from the intersection among three defined sets of all predicted genes from DEMs, DETFs, and DEGs (**Figure 4B**).

In addition, the regulatory relationship between miRNAs and TFs related to VaD was also identified. As for miRNA-TF regulatory pairs (the action of miRNA on TF), thirteen DEMs targeted 49 TFs by overlapping 3332 targets of DEMs and 63 DETFs (**Figure 4C**). Regarding the TF-miRNA regulatory pairs (the action of TF on miRNA), 37 DETFs were identified as having the regulatory effect on 13 DEMs after overlapping 63

TABLE 2 Sequence and sequence homology of DEMs.

Name	Mature sequence	Log_2 (foldchange)	*P*-value	Sequence homology
miR-21-5p	5′-UAGCUUAUCAGACUGAUGUUGA-3′	−2.2700	0.017800	rat, mouse, human
miR-511-3p	5′-AAUGUGUAGCAAAAGACAGGA-3′	−1.7300	0.003990	rat, mouse, human
miR-145-5p	5′-GUCCAGUUUUCCCAGGAAUCCCU-3′	−1.5300	0.030800	rat, mouse, human
miR-10b-5p	5′-CCCUGUAGAACCGAAUUUGUGU-3′	−1.4600	0.056800	rat, mouse, human
miR-143-3p	5′-UGAGAUGAAGCACUGUAGCUCA-3′	−1.4100	0.001360	rat, mouse, human
miR-214-3p	5′-ACAGCAGGCACAGACAGGCAG-3′	−1.2800	0.001750	rat, mouse, human
miR-764-3p	5′-GAGGAGGCCAUAGUGGCAACUGU-3′	−1.2700	0.002600	rat, mouse
miR-10a-5p	5′-UACCCUGUAGAUCCGAAUUUGUG-3′	−1.0600	0.000464	rat, mouse, human
miR-223-3p	5′-UGUCAGUUUGUCAAAUACCCC-3′	−1.0500	0.010400	rat, mouse, human
miR-155-5p	5′-UUAAUGCUAAUUGUGAUAGGGGU-3′	−1.0400	0.005740	rat, mouse, human
miR-122-5p	5′-UGGAGUGUGACAAUGGUGUUUG-3′	4.0500	0.011800	rat, mouse, human
miR-5132-5p	5′-CGUGGGGCGGUGGACCCAGGCU-3′	1.4200	0.015700	rat, mouse
miR-802-5p	5′-UCAGUAACAAAGAUUCAUCCU-3′	1.1500	0.039800	rat, mouse

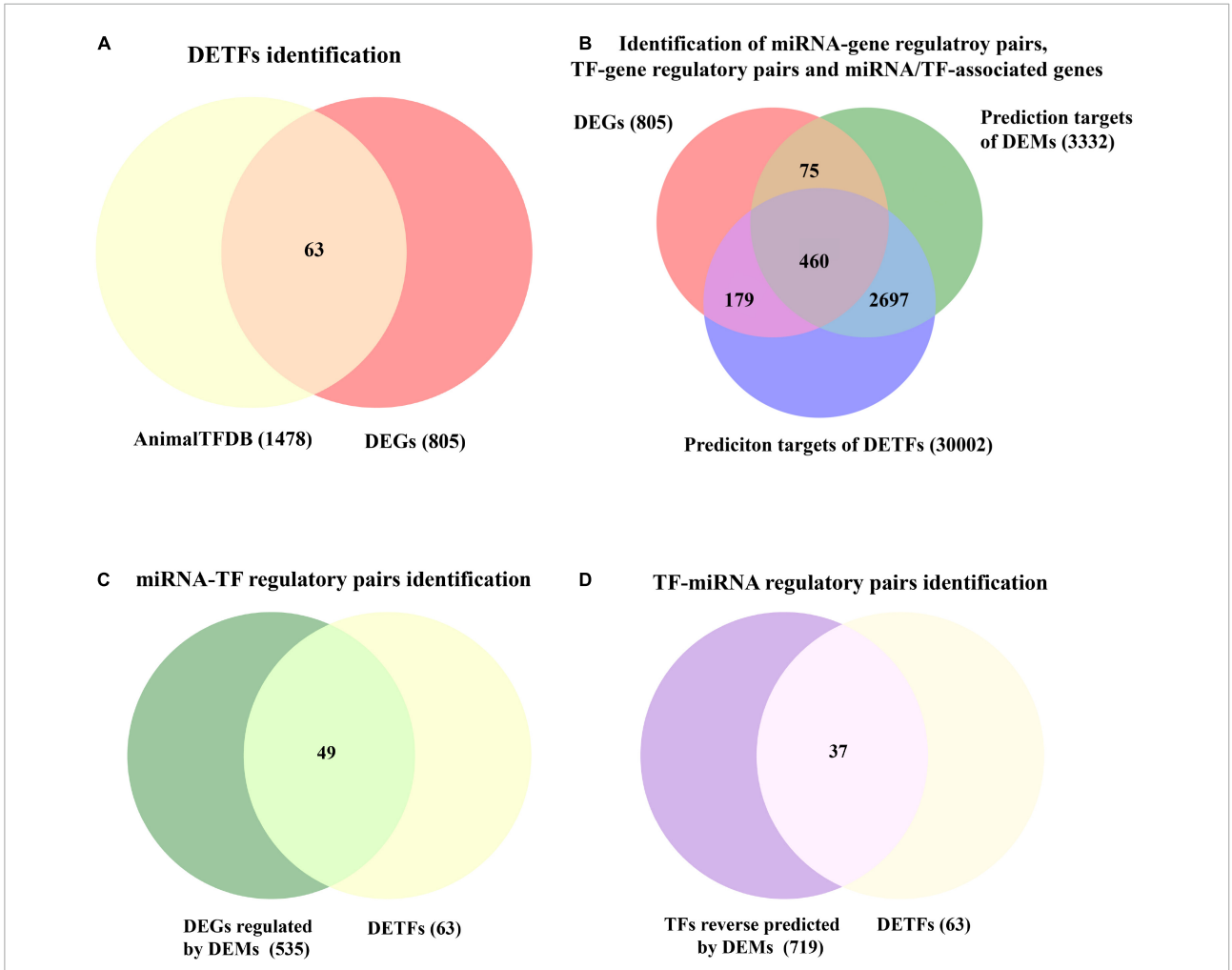

FIGURE 4
Identification of DETFs and DEGs jointly regulated by DEMs and DETFs. **(A)** Identification of 63 DETFs from DEGs using the Venn diagram. **(B)** Target prediction of DEMs and DETFs. A total of 535 miRNA-gene regulatory pairs, 639 TF-gene regulatory pairs, and 460 miRNA/TF-associated DEGs are identified. **(C)** Identification of 49 miRNA-TF regulatory pairs in total. **(D)** Identification of 37 TF-miRNA regulatory pairs.

DETFs and 719 TFs through reverse prediction of DEMs using the PROMO database (Figure 4D).

Gene ontology and pathway enrichment analyses

The enrichment analysis of 460 target genes, including aspects of biological process (BP), cell composition (CC), and molecular function (MF), was performed to evaluate the biological function of these common miRNA/TF-associated target genes. Vasculature development, cell-substrate adhesion, wound healing, cellular response to growth factor stimulus, regulation of ERK1, ERK2 cascade, and cholinergic synaptic transmission were included in the top 20 items of BP category, as shown in Figure 5A. The most enriched results of CC were oriented to the cell membrane and cell organelles, such as myofibril, cell cortex, plasma membrane protein complex, early endosome, and dopaminergic synapse (Figure 5B). The main enrichment processes of MF were related to growth factor binding, integrin binding, extracellular matrix structural constituent, collagen binding, actin binding, anion transmembrane transporter activity, and calcium ion binding (Figure 5C).

A total of 37 KEGG pathways were discovered, and the top 10 pathways were obtained after removing uncorrelated pathways such as "cancer" according to a P-value < 0.01. The results indicated that these common targets were mostly closely related to the PI3K-Akt signaling pathway, neuroactive ligand-receptor interaction, calcium signaling pathway, and Wnt signaling pathway, which were mainly associated with apoptosis, hypoxia, inflammation, angiogenesis, and neurodegeneration involved in VaD (Figure 5D).

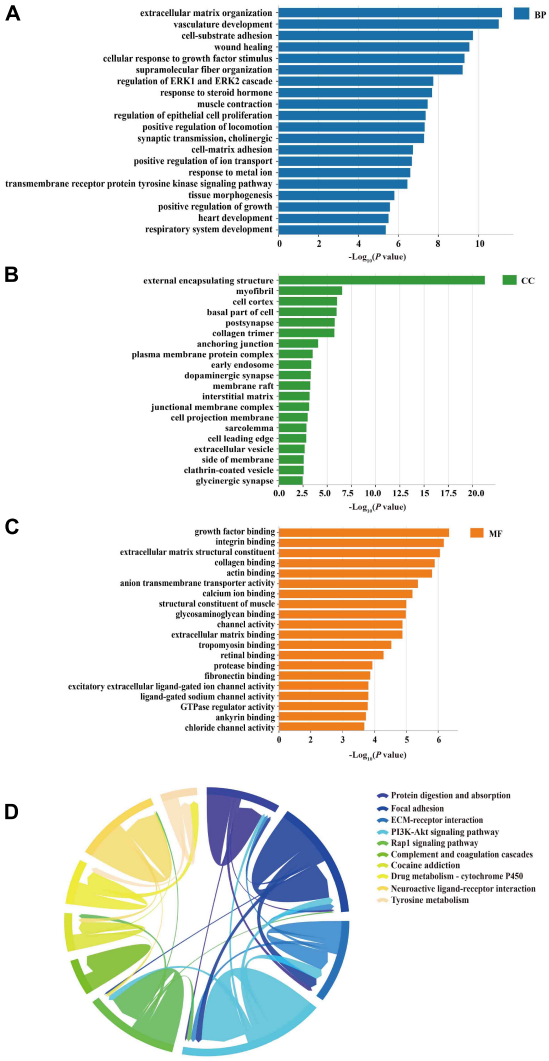

FIGURE 5
Gene ontology (GO) and KEGG enrichment analyses. **(A)** Top 20 GO terms of biological process (BP) as enrichment of 460 miRNA/TF-associated genes, including vasculature development and regulation of ERK1 and ERK2 cascade. **(B)** Top 20 GO terms of cellular components (CC) from the enrichment analysis of the 460 genes, including myofibril and cell cortex. **(C)** Bar charts of molecular function (MF) enrichment of the 460 genes, including growth factor binding and integrin binding. **(D)** Top 10 signaling pathways of KEGG enrichment analysis presented in the form of a Chordal graph, such as the PI3K-Akt signaling pathway and Wnt signaling pathway. Pathways are distinguished by different colors. The top 10 pathways are listed on the right side according to the P-value (from top to bottom in ascending order). Each line represents the association between two pathways. The thicker the line, the more common enriched genes between the two pathways and the stronger the association.

Construction of the microRNA-transcription factor-gene regulatory network and protein-protein interaction network

Transcription factors and genes associated with VaD, 13 DEMs, 460 miRNA/TF-associated target genes, and 49 VaD-associated DETFs were involved in the M-T-G network to elucidate the regulatory relationship among these miRNAs. The other 14 VaD-associated TFs were excluded from the network due to their poor association with these acquired miRNA/TF-associated target genes. Finally, the M-T-G network was constructed, resulting composed of 522 nodes, 7537 edges, and four types of regulatory relationships, including the miRNA-gene, TF-gene, miRNA-TF, and TF-miRNA actions (Figure 6A). Additionally, edges projected from DEMs were colored red, while DETFs were blue. Next, 460 miRNA/TF-associated target genes were uploaded into the STRTING software, and the interactions scored under 0.7 were removed, generating a functional protein association network with 205 nodes and 304 edges (Figure 6B). Furthermore, dysregulated key genes were identified by integrating the results from STRING and

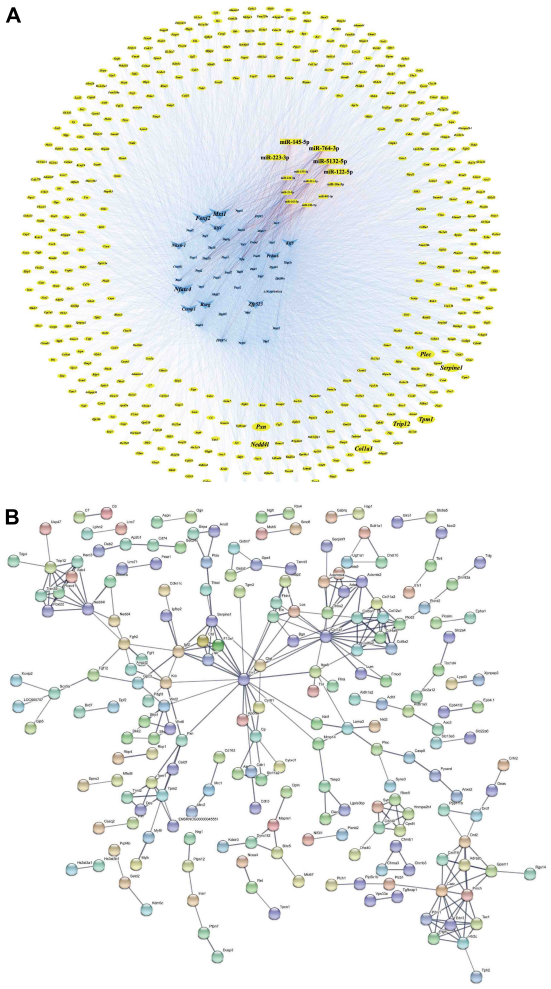

FIGURE 6
M-T-G and PPI networks. **(A)** Establishment of the M-T-G network of 13 DEMs, 49 DETFs, and 460 DEGs. The genes, miRNAs, and TFs are represented by yellow circles, red rectangles, and blue triangles, respectively. The key nodes are highlighted with larger sizes. **(B)** Establishment of the PPI network based on the 460 joint targets of DEMs and DETFs.

cytohubba plug-in, including *Serpine1*, *Pxn*, *Nedd4l*, *Col1a1*, *Plec*, *Trip12*, and *Tpm1* (Table 3).

Identification of the involved feed-forward loop and key nodes

miRNAs and TFs are important regulatory elements for gene expression. One of the most common regulatory patterns among miRNAs, TFs, and genes is the three-node regulatory motif composed of the feed-forward loop (FFL) and composite loop (Lin et al., 2015). Specifically, miRNA and TF simultaneously regulate one target with a single direction action within the three-node FFL motif, while their regulation on the common target is bilateral in the three-node composite motif (Zhang et al., 2015).

TABLE 3 Summary of key genes.

Name	Type	Log_2 (foldchange)	*P*-value	*Z*-score
Plec	gene	−3.5300	0.006660	0.775000
Col1a1	gene	−2.0100	0.000001	1.680000
Pxn	gene	−1.9300	0.001040	1.280000
Serpine1	gene	−1.4300	0.034000	0.732000
Tpm1	gene	4.8400	0.041300	0.756000
Nedd4l	gene	3.8700	0.002240	0.940000
Trip12	gene	2.5500	0.000124	0.578000

TABLE 4 Summary of key TFs and miRNAs.

Name	Type	Occurrences	*Z*-score
Mxi1	transcription factor	47100	1.4600
Nfatc4	transcription factor	150000	1.4000
Rxrg	transcription factor	162000	1.3700
Zfp523	transcription factor	64700	1.3600
Foxj2	transcription factor	28700	1.3600
Nkx6-1	transcription factor	35200	0.7900
Klf4	transcription factor	51000	0.6140
Klf5	transcription factor	104000	0.4840
Csrnp1	transcription factor	53600	0.3760
Prdm6	transcription factor	39300	0.3620
miR-5132-5p	miRNA	2.2200	1.4200
miR-764-3p	miRNA	1.6300	1.0700
miR-223-3p	miRNA	0.9200	0.9090
miR-145-5p	miRNA	0.5090	0.8110
miR-122-5p	miRNA	0.7340	0.5950

Differentially expressed transcription factors, DEGs, key miRNAs, and TFs were analyzed based on the aforementioned M-T-G network using CytoHubba and Motif-Discovery plugins to further investigate the regulatory motifs of DEMs in VaD. In the present analysis, those key nodes were selected according to the scores measured by the topological properties described in the Materials and Methods and explained in detail in Tables 3, 4. The top 10 of the 63 DETFs were selected, such as *Mxi1*, *Nfatc4*, *Rxrg*, *Zfp523*, *Foxj2*, *Nkx6*-1, *Klf4*, *Klf5*, *Csrnp1*, and *Prdm6*. Top 5 miRNAs of the 13 DEMs were selected, such as miR-5132-5p, miR-764-3p, miR-223-3p, miR-145-5p, and miR-122-5p. Then, an M-T-G subgraph was established based on the key nodes and included 7 DEGs, 10 DETFs, and 5 DEMs (Figure 7A). Subsequently, three-node FFLs were constructed based on the regulatory relationships among these key nodes. The composite loop with key nodes is shown in Figure 7B. Three-node FFLs, including miRNA-dominating and TF-dominating FFLs, are shown in Figures 7C,D. Finally, eleven FFLs mediated by key TFs or key miRNAs and eleven composite loops were constructed (Figures 8, 9). These loops

composed of key nodes represented a highly mutual interaction, demonstrating a complex regulatory network in the pathology of VaD.

Verification of key nodes and regulatory relationship

Before the experimental verification of the expression or interaction among key nodes in the M-T-G network, the expression pattern of these key nodes (key miRNAs, key TFs, and key genes) was assessed using several published GEO datasets associated with VaD from different types of biological samples of several organisms such as human, rat, and mouse. **Supplementary Table 5** shows that four key miRNAs, such as miR-145-5p, miR-122-5p, miR-223-3p, and miR-764-3p, were dysregulated in several brain regions of rodent models related to VaD, including the hippocampus, cerebral cortex, striatum, and subventricular zone. Among them, miR-145-5p, miR-122-5p, and miR-223-3p in the hippocampus of mice suffering from VaD-related disease displayed similar expression patterns to our sequencing analysis. Additionally, two key TFs, *Klf4* and *Foxj2*, were significantly downregulated in the hippocampus of the mouse models of cerebral ischemia, as consistent with our analysis. Moreover, five key TFs, such as *Klf5*, *Csrnp1*, *Mxi1*, *Rxrg*, and *Zfp523*, were significantly dysregulated in the blood or cortical tissues of rodent models related to VaD, as shown in **Supplementary Table 6**. *Serpine1* was significantly downregulated in the hippocampus under the VaD-related pathological conditions. The other five key genes, *Tpm1*, *Col1a1*, *Pxn*, *Nedd4l*, and *Plec*, were significantly dysregulated in the rodent model related to VaD, aligned with our RNA sequencing analysis (**Supplementary Table 7**).

Quantitative real-time polymerase chain reaction analysis of the genes in the cortical tissues of rats with 2VO and sham rats was performed to confirm the changes in the expression of these key nodes in the predicted FFLs. In these detected nodes, the differential expression of key miRNAs, including miR-145-5p, miR-122-5p, and miR-5132-5p, TFs including *Csrnp1*, *Klf4*, *Nfatc4*, *Rxrg*, *Foxj2*, and *Klf5*, and target genes including *Serpine1*, *Plec*, *Nedd4l*, *Trip12*, and *Tpm1* between rats with 2VO and sham rats were in line with the results analyzed by RNA sequencing (**Figures 10A–C**, $P < 0.05$-0.01 *vs.* sham). Although the expression of several key nodes, including *Nkx6-1*, *Prdm6*, and *Zfp523*, were in line with the sequencing results, the statistical difference in rats with 2VO was not significant as compared with sham rats. In addition, some of the predicted key nodes completely deviated from the sequencing results, including miR-764-3p, miR-223-3p, *Mxi1*, *Pxn*, and *Col1a1* (all $P < 0.05$ *vs.* sham). Since the changing trend of most predicted key nodes was similar to that in the sequencing analysis, our speculation was that the abnormal expression of these key miRNAs and genes in VaD within the FFLs was reliable.

As for the validation of the analyzed regulatory relationship, two key DEMs (miR-145-5p and miR-122-5p) were chosen to verify the miRNA-TF regulatory pairs thanks to their excellent sequence conservation, consistency of the expression pattern, and associations with the brain injury caused by hypoxia (Li et al., 2020b; Yang et al., 2021). *Csrnp1* and *Klf5* were then selected, since they are the targets of miR-145-5p and miR-122-5p due to their most significant different expression according to the value of Log_2 (foldchange). The construction of recombinant plasmids containing MUT binding sites or WT binding sites for luciferase assessment is shown in **Figures 10D,E**. The dual-luciferase reporter assay revealed that miR-145-5p directly targeted *Csrnp1*, which was in line with the bioinformatic analysis of their potential relationship within the FFL (**Figures 10F,G**, $P < 0.001$ *vs.* NC). However, the connection between miR-122-5p and *Klf5* was not found in the dual-luciferase reporter experiment. Furthermore, the expression of *Csrnp1* in HEK293 cells was significantly downregulated in the presence of miR-145-5p mimics (**Figures 10H,I**, $P < 0.05$ *vs.* NC), while no statistical difference was found in the expression of *Klf5* when transfected with miR-122-5p mimics compared to the NC. Thus, miR-145-5p-*Csrnp1*, the key miRNA-TF regulatory pair in the predicted FFL involved in VaD, was obtained through qRT-PCR analysis and target verification.

Discussion

Vascular dementia is a severe progressively cognitive dysfunction troubling a growing population of the elderly and without curative treatment or definite criteria for diagnosis. Thus, an early intervention on the disease and the control of risk factors are crucial steps in reducing the incidence of dementia (Morovic et al., 2019). The pathology of VaD refers to multiple processes, such as endothelial dysfunction, blood-brain barrier (BBB) destruction, and neuroinflammation, suggesting that an approach focusing on a single target is inappropriate (Cipollini et al., 2019). Therefore, a deep understanding of the aberrant genetic changes and their associated molecular mechanisms involved in the VaD pathophysiology may provide new therapeutic methods.

In the present study, rats with 2VO were used as a model of VaD, which exhibited cognitive impairments and neuropathological changes that spread in the brain, such as neuronal apoptosis, synaptic loss, and failure of neuronal signaling (Farkas et al., 2007). There is evidence supporting that the cerebral cortex participates in learning and memory, coupling with the hippocampus to mediate memory consolidation (Maingret et al., 2016; Wais et al., 2018). The cortex may be more vulnerable to BBB leak induced by biochemical mediators of cerebral hypoperfusion than other brain regions (Tayler et al., 2021). Furthermore, the risk of VaD may be higher for men than for women with the increase

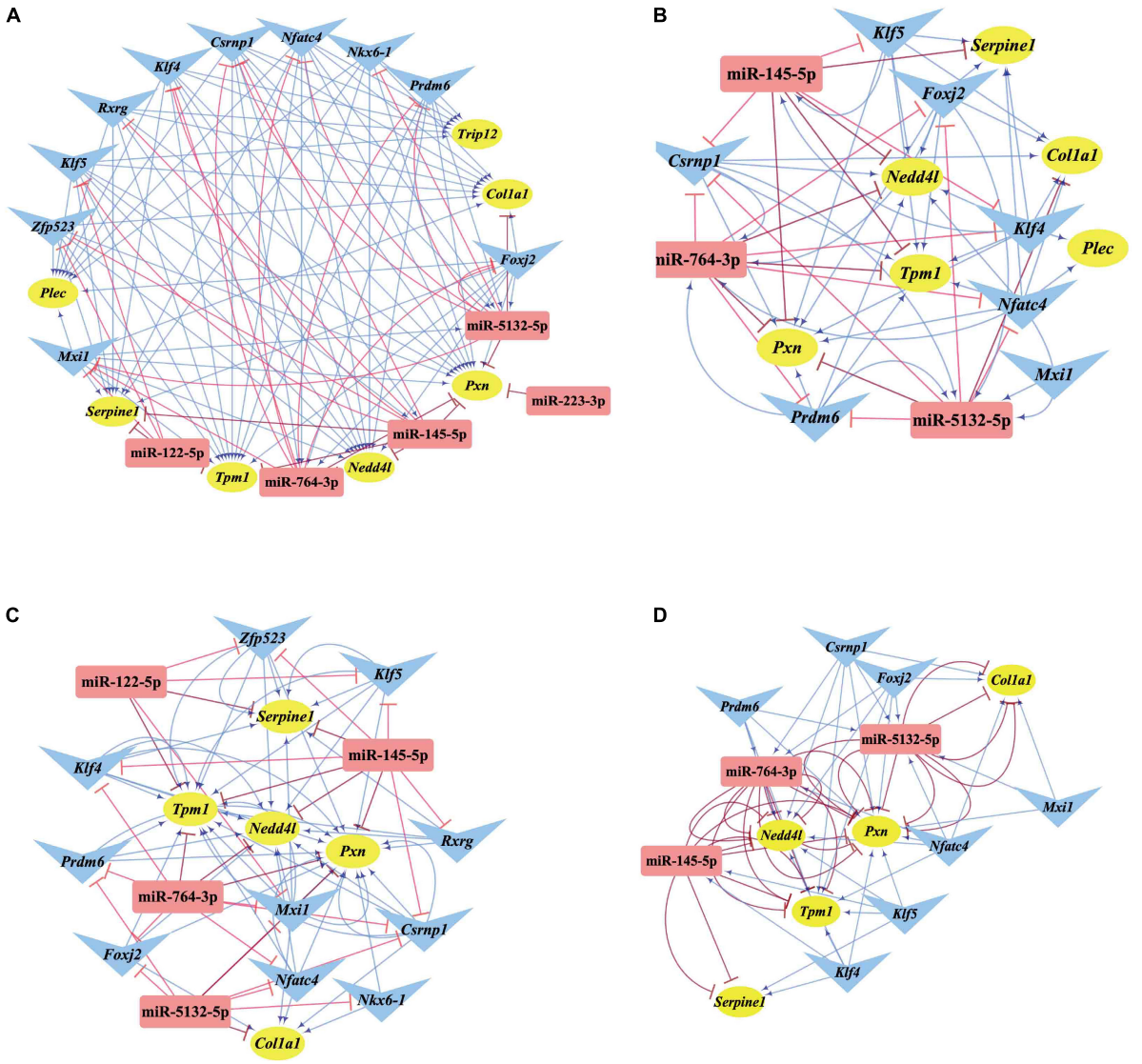

FIGURE 7
Regulatory relationships of the M-T-G subgraph network, composite loops, and FFLs. **(A)** Establishment of the M-T-G subgraph network of the key nodes based on 7 DEGs, 10 DETFs, and 5 DEMs. **(B)** Summary of all the composite loops based on the M-T-G subgraph network. **(C)** Collection of the miRNA-mediated FFLs extracted from the M-T-G subgraph network. **(D)** Gathering of TF-mediated FFLs of key DETFs. The target genes, miRNAs, and TFs are represented with yellow circles, red rectangles, and blue triangles, respectively. The edges radiated from miRNAs are marked in red and T-shaped blunt arrow ends, while the edges projecting from TFs are marked in blue and sharp arrow ends.

in age (Ruitenberg et al., 2001). Considering the possible interference of gender on the heterogeneity of results, our study detected the learning and memory-behavioral decline and cortical histopathological changes in the neurons of male rats suffering from 2VO; subsequently, DEMs, DETFs, and DEGs in the etiology of VaD were discovered using RNA sequencing in these rats combined with bioinformatics and experimental analyses to identify novel potential targets and understand their molecular mechanisms in VaD.

Among these differentially expressed genes, 805 DEGs were obtained based on the transcriptome sequencing and included 602 downregulated and 203 upregulated mRNAs. Seven genes were defined as key genes according to the M-T-G network and PPI network for their tight associations with the regulation of miRNAs and TFs in VaD. Among these seven key genes, the involvement of *Col1a1*, *Plec*, and *Trip12* in VaD was reported for the first time. As regards other key genes, *Serpine1* was significantly downregulated in VaD according to the present study and was also downregulated in small vessel brain injury as previously reported, which is a significant vascular factor for cognitive impairment (Knottnerus et al., 2010; Pantoni, 2010). Moreover, *Serpine1* was downregulated not only in the cortical

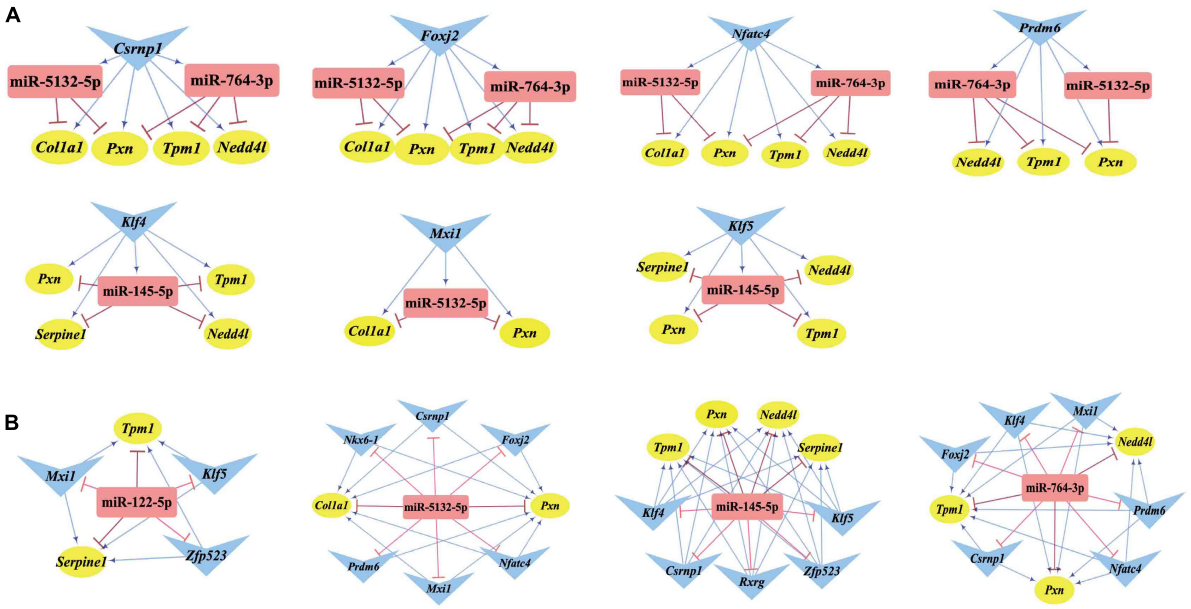

FIGURE 8
Three-node FFLs formed by key nodes. **(A)** TFs-mediated three-node FFLs of individual key DETFs. **(B)** A total of four miRNA-mediated three-node FFLs of key DEMs of the present study. The gene, miRNA, and TF are represented with yellow circles, red rectangles, and blue triangles, respectively. The terminal of the edges radiating from the miRNA is marked in red and T-type blunt arrow, while the one that changed to sharp arrow for the edges that radiate from TF is in blue color.

brain of rats with 2VO but also in the hippocampus of the mice under chronic cerebral hypoperfusion based on the analysis of GEO datasets. *Serpine1* exerts neuroprotective effects through the inhibition of the endogenous mitochondrial apoptosis pathway and the stabilization of the neuronal networks depending on the MAPK/ERK pathway (Soeda et al., 2008; Iwaki et al., 2012). Furthermore, *Seprine1* is regulated by miR-301a and HIF-1α in response to hypoxia (Gonsalves et al., 2015). In our study, the expression of novel regulators of *Seprine1* in VaD was found based on sequencing and bioinformatic analysis, such as miR-145-5p, miR-122-5p, *Klf5*, and *Klf4*. Another upregulated key gene, such as *Nedd4l*, was also involved in several FFLs of our study dominated by key miRNAs or TFs, such as miR-145-5p, miR-764-3p, *Csrnp1*, *Klf5*, and *Klf4*. It was also confirmed that *Nedd4l* was significantly upregulated in the brain of rats with acute cerebral ischemia (Kim et al., 2021) and might function in exacerbating the toxicity of accumulated excitatory transmitters out of the cells in ischemia through the regulation of the degradation of glutamate transporters (Sopjani et al., 2010; Vina-Vilaseca and Sorkin, 2010). Moreover, *Nedd4l* was reported as regulated by miR-454 to induce a cardioprotective effect (Wang Y. et al., 2021). Besides, Tpm1 has a potential association with cognitive impairments as it was reported as a potential biomarker of AD for its upregulation in the platelets of AD and MCI patients (Reumiller et al., 2018). Tpm1 was regulated by almost all key miRNAs and TFs in our M-T-G network, indicating that it might play an important role in VaD.

Gene ontology and KEGG pathway analyses were performed to better understand the biological functions and potential mechanisms of the common miRNA/TF-associated targets in the pathogenesis of VaD. GO enrichment analysis indicated that these targets were mainly involved in cell membrane and organelles, including cell cortex, postsynapse, dopaminergic synapse, basal part of cell, plasma membrane protein complex, and early endosome. Functional enrichment analysis revealed important roles of these common targets involved in the biological processes related to synaptic transmission, cell proliferation, migration, and vasculature development. These results partly explained the target functions associated with the pathogenesis of VaD. The KEGG enrichment analysis summarized 37 pathways closely related to VaD, including PI3K-AKT signaling pathway, neuroactive ligand–receptor interaction, calcium signaling pathway, and WNT signaling pathway. It has been reported that the upregulation of the PI3K-AKT signaling pathway exerts a protective function in VaD through the promotion of the expression of BCL-2 (Chen et al., 2018). The activation of the Wnt signaling pathway may improve the cognitive ability of rats with 2VO (Jin et al., 2017). Therefore, these results suggest that these common miRNA/TF-associated targets potentially mediated VaD pathogenesis through multiple signaling pathways. These potential mechanisms of targets in the pathogenesis of VaD require further investigation.

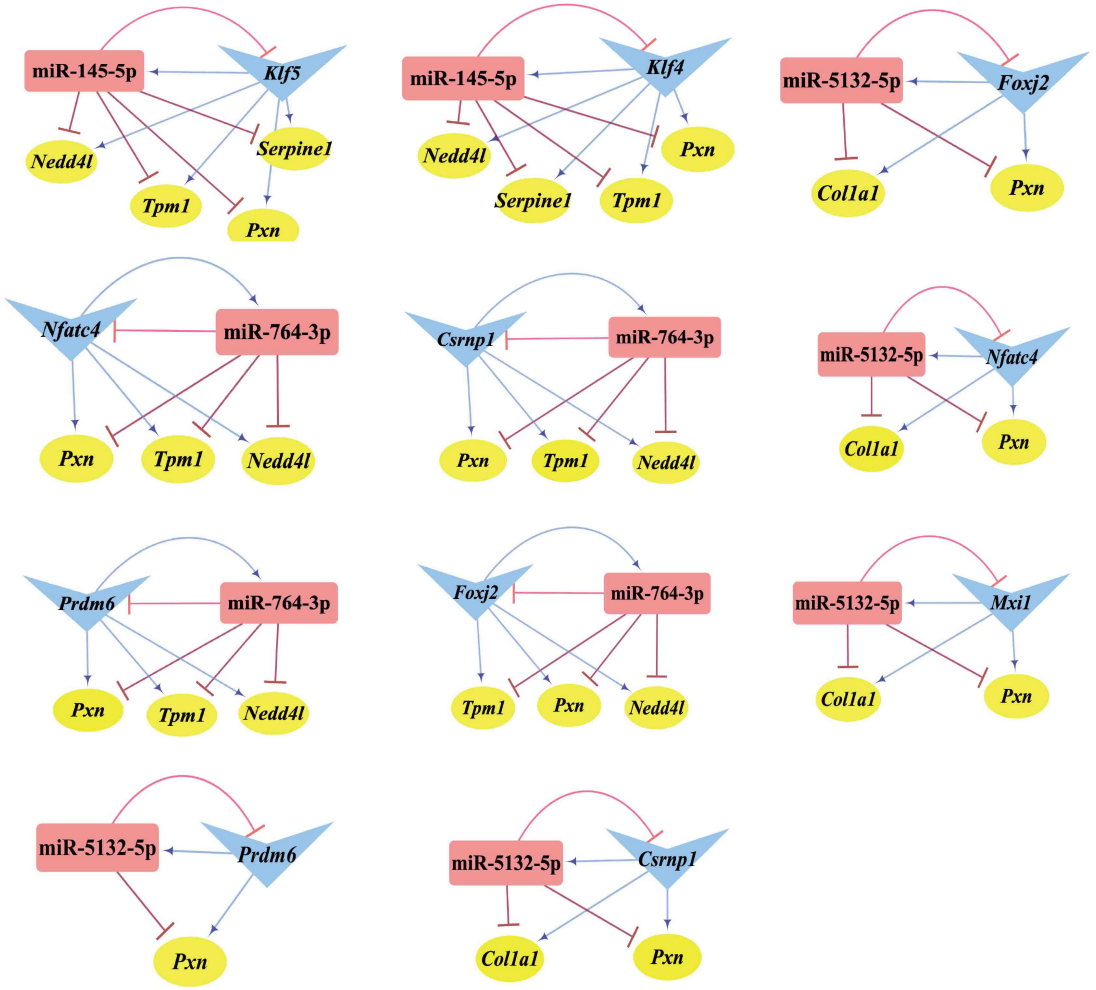

FIGURE 9
Composite loops among key miRNAs, TFs, and genes. Collection of composite loops of key nodes based on mutual regulatory miRNA-TF pairs. The gene, miRNA, and TF are represented with yellow circles, red rectangles, and blue triangles, respectively. The terminal of the edges radiating from the miRNA is marked in red and T-type blunt arrow, while the one that changed to sharp arrow for the edges radiated from TF is in blue color.

Regarding the miRNAs, thirteen DEMs in the cortices of 2VO rats were identified by the RNA sequencing analyses, indicating their potential function in VaD. Among these DEMs, ten out of thirteen were conserved among different species based on miRBase. Next, five key DEMs were selected from the M-T-G network of VaD, such as miR-122-5p, miR-223-3p, miR-145-5p, miR-5132-5p, and miR-764-3p, which were identified for the first time in VaD. Among these five key DEMs, miR-122-5p, miR-223-3p, and miR-145-5p attracted more attention as they have excellent sequence homology, which has been reported as dysregulated in the blood of patients who have cancer, cardiovascular diseases, and neurodegenerative diseases (Maruyama et al., 2018; Mancuso et al., 2019; Ashirbekov et al., 2020; Pinho et al., 2020; Singh et al., 2020). However, after the experimental verification using qRT-PCR, the expression changes of miR-223-3p and miR-764-3p were inconsistent with the RNA sequencing outcome. Among the key miRNAs with consistent changes with RNA sequencing, miR-5132-5p is reported for the first time as associated with 2VO and upregulated in rats with this disease. Moreover, the level of miR-145-5p and miR-122-5p was dysregulated in the cerebrospinal fluid or plasma of patients with cerebral vascular disease as suggested by the other GEO datasets. miR-145-5p is closely related to various cardiovascular diseases. For example, miR-145-5p suppresses the activation of activated microglia cells in cerebral infarction by targeting the 3′UTR of *PLA2G4A* (Qi et al., 2017). miR-145-5p also protects cardiac microvascular endothelial cells against hypoxia/reoxygenation injury by suppressing *Smad4* expression (Li et al., 2020b). miR-122-5p is involved in the

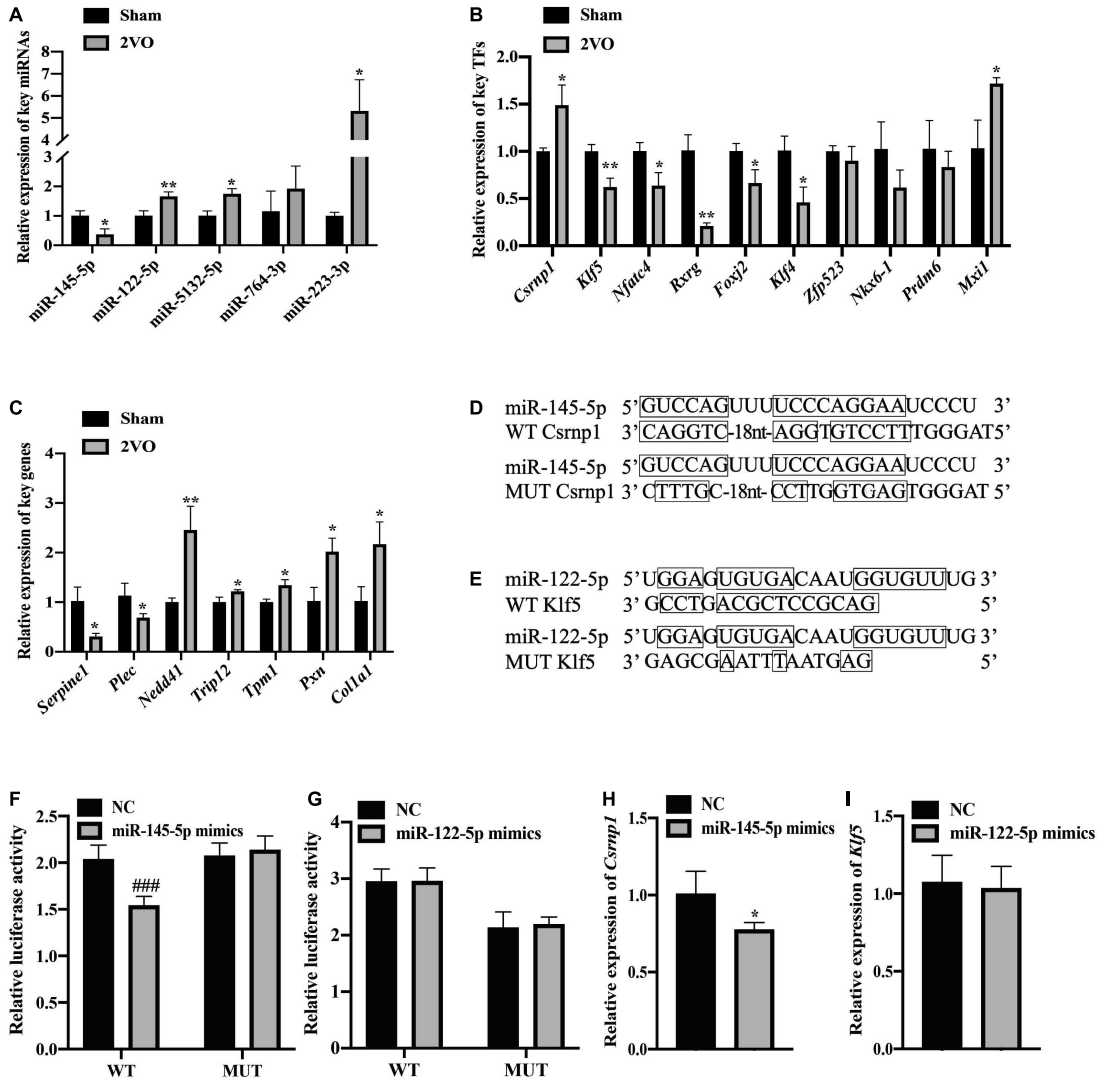

FIGURE 10
Validation of the expression and regulatory relationship. **(A)** Verification of the differential expression of the key miRNAs using qRT-PCR (n = 3). **(B)** Relative expression of the key TFs in the cortex of the rats with 2VO compared with the sham rats using qRT-PCR analysis (n = 3). **(C)** Relative expression of the key genes using qRT-PCR analysis (n = 3). **(D)** Wild-type (WT) or mutant-type (MUT) binding sites for the combination of miR-145-5p and *Csrnp1* in the dual-luciferase reporter assay. **(E)** Binding sites of the wild or mutant type of miR-122-5p and *Klf5*. **(F)** Direct interaction of miR-145-5p/*Csrnp1* by dual-luciferase reporter assay (n = 6). **(G)** No direct interaction of miR-122-5p/*Klf5* by dual-luciferase reporter assay (n = 6). **(H)** Significant decrease of the *Csrnp1* expression in the presence of miR-145-5p mimics. **(I)** No difference in the *Klf5* expression in the presence of miR-122-5p. Results are presented as mean ± SD. $^{*}P < 0.05$, $^{**}P < 0.01$ *vs.* Sham. $^{\#\#\#}P < 0.001$ *vs.* NC.

inhibition of cardiac fibroblast differentiation induced by apigenin through targeting the transcription factor HIF-1α (Feng et al., 2021); it is regulated by another transcription factor HNF4α in type 2 diabetic mice (Xu et al., 2020), indicating a regulation between miRNA and TF in different diseases.

As regards the TFs, a total of 63 TFs were differentially expressed in rats with 2VO. Ten DETFs were selected from the M-T-G network as the key TFs, divided into nine downregulated TFs and one upregulated TFs. These ten dysregulated TFs were found in VaD for the first time. *Klf5*, the most downregulated TF, is an active factor associated with miRNAs in cancer and cardiovascular disease (Drosatos et al., 2016; Yang et al., 2018; Nan et al., 2021; Wang Y. et al., 2021). *Klf5* was significantly downregulated in the blood of rats with ischemic stroke obtained from the GSE21136. Additionally, a previous study revealed the negative role of *Klf5* in neuronal apoptosis of ischemic stroke through the JNK pathway (Chang et al., 2020). As the most upregulated key TF, *Csrnp1* is reported as a tumor suppressor factor and mediates cardiomyocyte apoptosis induced by restraint stress through the WNT/β-catenin signaling (Ye et al., 2017). Besides, other

RNA-sequencing datasets confirmed the upregulation of *Csrnp1* in VaD in humans, rats, and mice, which was consistent with our analysis. Furthermore, *Csrnp1* is highly associated with hypoxic-ischemic encephalopathy, according to RNA sequencing (Xiong et al., 2020). *Nfatc4* was identified as involved in hippocampal plasticity, axonal growth, neuronal survival, and apoptosis (Bradley et al., 2005). A previous study revealed that *Nfatc4* is essential for BDNF-dependent neuron survival and the spatial memory of hippocamp in adult-born neurons (Quadrato et al., 2012).

As regards the regulatory loops, the M-T-G network was constructed based on 13 DEMs, 49 DETFs, and 460 DEGs. Then, key nodes were identified from the M-T-G network. The regulatory relationships among key nodes were manifested as 11 FFLs and 11 composite loops, illustrating that these identified miRNAs, TFs, and target genes possessed significant predictive values in the involvement in VaD. miR-145-5p and miR-122-5p were significantly dysregulated, as supported by the sequencing, qRT-PCR analysis, and the comprehensive comparison of expression patterns among public datasets associated with VaD. miR-122-5p and miR-145-5p are involved in the pathological process of ischemic stroke through the targeting of *Nurr1* and *SEMA3A*, as previously reported (Xie et al., 2017; Yang et al., 2021). Additionally, miR-145-5p directly regulates the expression of *Samd4* in cardiac microvascular endothelial cell injury induced by hypoxia (Li et al., 2020b). Based on the potential interactions of the constructed FFLs and composite loops, the regulatory relationship of miR-145-5p over *Csrnp1* was further validated by dual-luciferase reporter assay and gene expression using a gain-of-function experiment, in line with the bioinformatic prediction. As the most dysregulated transcription factor, *Csrnp1* was reported to mainly function in tumors or cardiac diseases, but little is known on the role of this gene in VaD. Interestingly, *Klf5* was the most downregulated key transcription factor and targeted by miR-145-5p and miR-122-5p simultaneously, according to miRNA-mediated FFLs. Although the direct interaction of *Klf5* and miR-145-5p was previously established (Liang et al., 2018; Zhou et al., 2019), the correlation of miR-122-5p and *Klf5* was found neither by dual-luciferase reporter assay nor by expression analysis based on miRNA gain-of-function.

Our study is just the beginning of this complex study, since still many challenges and problems should be solved in the future. First, larger sample sizes and more profound mechanistic research are needed to confirm our findings on these identified key miRNAs and TFs. Second, gender factors and more vulnerable brain regions of cerebral hypoperfusion should be the focus of our subsequent work to obtain a comprehensive elucidation of the transcriptome changes for new perspectives to understand the complex pathology of VaD. Third, profiling the transcript features of non-canonical small non-coding RNAs, including rsRNA, tsRNA, and snosRNA, that were obtained in the present sequencing is necessary, referring to the previous report (Shi et al., 2021), since they gained increasing attention as regulators of gene expression and biomarkers of diseases, such as transfer-RNA-derived small RNA (Li et al., 2020c; Zhang et al., 2020; Shi et al., 2022). Finally, more key genes and their interactions should be explored from the constructed FFLs and composite loops with potential functions in the pathogenesis of VaD.

In conclusion, the aberrantly expressed miRNAs, TFs, and target genes related to VaD were identified using RNA sequencing analyses in the cortex of rats with 2VO. The biological functions and potential mechanisms of these identified miRNAs and TFs were analyzed. In line with the bioinformatics analyses, three miRNAs, six TFs, and five mRNAs were confirmed as significantly differentially expressed in rats with VaD, and the interaction of miR-145-5p and *Csrnp1* was verified. Our findings might provide new insights into the molecular mechanism of VaD.

Data availability statement

Publicly available datasets were analyzed in this study. This data can be found here: the RNA sequencing data used in the present study were submitted to Gene Expression Omnibus and the accession number GSE199508 was obtained.

Ethics statement

The animal study was reviewed and approved by the Ethics Committee of the Institute of Medicinal Biotechnology, Chinese Academy of Medical Sciences (Beijing, China).

Author contributions

RL and ZL contributed to the conception and designation of the research, interpreted results, and revised the manuscript. KZ and LZ conducted the miRNA and mRNA profiling analysis and key nodes assays, performed the qRT-PCR and the dual-luciferase reporter experiments, and drafted the manuscript. ZC, ML, and TS performed the M-T-G network analysis and prepared the figures. All authors contributed to manuscript revision, read, and approved the submitted version.

Funding

This study was supported by the National Natural Science Foundation of China (U1803281 and 82173806) and Chinese Academy of Medical Sciences (CAMS) Innovation Fund for Medical Science (2022-I2M-2-002 and 2021-1-I2M-030).

Conflict of interest

The authors declare that the research was conducted in the absence of any commercial or financial relationships that could be construed as a potential conflict of interest.

Publisher's note

All claims expressed in this article are solely those of the authors and do not necessarily represent those of their affiliated organizations, or those of the publisher, the editors and the reviewers. Any product that may be evaluated in this article, or claim that may be made by its manufacturer, is not guaranteed or endorsed by the publisher.

Supplementary material

The Supplementary Material for this article can be found online at: https://www.frontiersin.org/articles/10.3389/fnins.2022.917489/full#supplementary-material

References

Ashirbekov, Y., Abaildayev, A., Omarbayeva, N., Botbayev, D., Belkozhayev, A., Askandirova, A., et al. (2020). Combination of circulating miR-145-5p/miR-191-5p as biomarker for breast cancer detection. *PeerJ* 8:e10494. doi: 10.7717/peerj.10494

Bradley, K. C., Groth, R. D., and Mermelstein, P. G. (2005). Immunolocalization of NFATc4 in the adult mouse brain. *J. Neurosci. Res.* 82, 762–770. doi: 10.1002/jnr.20695

Chang, L., Zhang, W., Shi, S., Peng, Y., Wang, D., Zhang, L., et al. (2020). microRNA-195 attenuates neuronal apoptosis in rats with ischemic stroke through inhibiting KLF5-mediated activation of the JNK signaling pathway. *Mol. Med.* 26:31. doi: 10.1186/s10020-020-00150-w

Chen, D. P., Hou, S. H., Chen, Y. G., Chen, M. S., Hu, Z. Z., and Zhang, Z. J. (2018). L-butyl phthalein improves neural function of vascular dementia mice by regulating the PI3K/AKT signaling pathway. *Med. Pharmacol. Sci.* 22, 5377–5384. doi: 10.26355/eurrev_201808_15740

Chen, X., Jiang, X. M., Zhao, L. J., Sun, L. L., Yan, M. L., Tian, Y., et al. (2017). MicroRNA-195 prevents dendritic degeneration and neuron death in rats following chronic brain hypoperfusion. *Cell Death Dis.* 8:e2850. doi: 10.1038/cddis.2017.243

Chu, S. F., Zhang, Z., Zhou, X., He, W. B., Chen, C., Luo, P., et al. (2019). Ginsenoside Rg1 protects against ischemic/reperfusion-induced neuronal injury through miR-144/Nrf2/ARE pathway. *Acta Pharmacol. Sin.* 40, 13–25. doi: 10.1038/s41401-018-0154-z

Cipollini, V., Troili, F., and Giubilei, F. (2019). Emerging Biomarkers in Vascular Cognitive Impairment and Dementia: From Pathophysiological Pathways to Clinical Application. *Int. J. Mol. Sci.* 20:2812. doi: 10.3390/ijms20112812

Dharap, A., Bowen, K., Place, R., Li, L. C., and Vemuganti, R. (2009). Transient focal ischemia induces extensive temporal changes in rat cerebral microRNAome. *J. Cereb. Blood Flow Metab.* 29, 675–687. doi: 10.1038/jcbfm.2008.157

Drosatos, K., Pollak, N. M., Pol, C. J., Ntziachristos, P., Willecke, F., Valenti, M. C., et al. (2016). Cardiac Myocyte KLF5 Regulates Ppara Expression and Cardiac Function. *Circ. Res.* 118, 241–253.

Farkas, E., Luiten, P. G., and Bari, F. (2007). Permanent, bilateral common carotid artery occlusion in the rat: A model for chronic cerebral hypoperfusion-related neurodegenerative diseases. *Brain Res. Rev.* 54, 162–180. doi: 10.1016/j.brainresrev.2007.01.003

Feng, W., Ying, Z., Ke, F., and Mei-Lin, X. (2021). Apigenin suppresses TGF-β1-induced cardiac fibroblast differentiation and collagen synthesis through the downregulation of HIF-1α expression by miR-122-5p. *Phytomedicine* 83:153481. doi: 10.1016/j.phymed.2021.153481

Gonsalves, C. S., Li, C., Malik, P., Tahara, S. M., and Kalra, V. K. (2015). Peroxisome proliferator-activated receptor-α-mediated transcription of miR-301a and miR-454 and their host gene SKA2 regulates endothelin-1 and PAI-1 expression in sickle cell disease. *Biosci. Rep.* 35:e00275. doi: 10.1042/BSR20150190

Guo, T., Fang, J., Tong, Z. Y., He, S., and Luo, Y. (2020). Transcranial Direct Current Stimulation Ameliorates Cognitive Impairment via Modulating Oxidative Stress, Inflammation, and Autophagy in a Rat Model of Vascular Dementia. *Front. Neurosci.* 14:28. doi: 10.3389/fnins.2020.00028

Han, B., Jiang, W., Liu, H., Wang, J., Zheng, K., Cui, P., et al. (2020). Upregulation of neuronal PGC-1α ameliorates cognitive impairment induced by chronic cerebral hypoperfusion. *Theranostics* 10, 2832–2848. doi: 10.7150/thno.37119

Inukai, S., Kock, K. H., and Bulyk, M. L. (2017). Transcription factor-DNA binding: Beyond binding site motifs. *Curr. Opin. Genet. Dev.* 43, 110–119. doi: 10.1016/j.gde.2017.02.007

Iwaki, T., Urano, T., and Umemura, K. (2012). PAI-1, progress in understanding the clinical problem and its aetiology. *Br. J. Haematol.* 157, 291–298. doi: 10.1111/j.1365-2141.2012.09074.x

Jiang, H., Ashraf, G. M., Liu, M., Zhao, K., Wang, Y., Wang, L., et al. (2021). Tilianin Ameliorates Cognitive Dysfunction and Neuronal Damage in Rats with Vascular Dementia via p-CaMKII/ERK/CREB and ox-CaMKII-Dependent MAPK/NF-κB Pathways. *Oxid. Med. Cell. Longev.* 2021:6673967. doi: 10.1155/2021/6673967

Jiang, H., Liu, J., Guo, S., Zeng, L., Cai, Z., Zhang, J., et al. (2022). miR-23b-3p rescues cognition in Alzheimer's disease by reducing tau phosphorylation and apoptosis via GSK-3β signaling pathways. *Mol. Ther. Nucl. Acids* 28, 539–557. doi: 10.1016/j.omtn.2022.04.008

Jin, X., Li, T., Zhang, L., Ma, J., Yu, L., Li, C., et al. (2017). Environmental Enrichment Improves Spatial Learning and Memory in Vascular Dementia Rats with Activation of Wnt/β-Catenin Signal Pathway. *Med. Sci. Monit.* 23, 207–215. doi: 10.12659/msm.902728

Kim, T., Chokkalla, A. K., and Vemuganti, R. (2021). Deletion of ubiquitin ligase Nedd4l exacerbates ischemic brain damage. *J. Cereb. Blood Flow Metab.* 41, 1058–1066. doi: 10.1177/0271678X20943804

Knottnerus, I. L., Govers-Riemslag, J. W., Hamulyak, K., Rouhl, R. P., Staals, J., Spronk, H. M., et al. (2010). Endothelial activation in lacunar stroke subtypes. *Stroke* 41, 1617–1622. doi: 10.1161/STROKEAHA.109.576223

Li, H. L., Lan, T. J., Yun, C. X., Yang, K. D., Du, Z. C., Luo, X. F., et al. (2020a). Mangiferin exerts neuroprotective activity against lead-induced toxicity and oxidative stress via Nrf2 pathway. *Chin. Herb. Med.* 12, 36–46. doi: 10.1016/j.chmed.2019.12.002

Li, L. L., Mao, C. D., Wang, G. P., Wang, N., and Xue, A. G. (2020b). MiR-145-5p alleviates hypoxia/reoxygenation- induced cardiac microvascular endothelial cell injury in coronary heart disease by inhibiting Smad4 expression. *Eur. Rev. Med. Pharmacol. Sci.* 24, 5008–5017. doi: 10.26355/eurrev_202005_21192

Li, P. F., Guo, S. C., Liu, T., Cui, H., Feng, D., Yang, A., et al. (2020c). Integrative analysis of transcriptomes highlights potential functions of transfer-RNA-derived small RNAs in experimental intracerebral hemorrhage. *Aging* 12, 22794–22813. doi: 10.18632/aging.103938

Liang, H., Sun, H., Yang, J., and Yi, C. (2018). miR-145-5p reduces proliferation and migration of hepatocellular carcinoma by targeting KLF5. *Mol. Med. Rep.* 17, 8332–8338. doi: 10.3892/mmr.2018.8880

Lin, Y., Zhang, Q., Zhang, H. M., Liu, W., Liu, C. J., Li, Q., et al. (2015). Transcription factor and miRNA co-regulatory network reveals shared and specific regulators in the development of B cell and T cell. *Sci. Rep.* 5:15215. doi: 10.1038/srep15215

Liu, Q. S., Jiang, H. L., Wang, Y., Wang, L. L., Zhang, J. X., He, C. H., et al. (2018). Total flavonoid extract from Dracoephalum moldavica L. attenuates β-amyloid-induced toxicity through anti-amyloidogenesis and neurotrophic pathways. *Life Sci.* 193, 214–225. doi: 10.1016/j.lfs.2017.10.041

Liu, X., Zhang, R., Wu, Z., Si, W., Ren, Z., Zhang, S., et al. (2019). miR-134-5p/Foxp2/Syn1 is involved in cognitive impairment in an early vascular dementia rat model. *Int. J. Mol. Med*. 44, 1729–1740. doi: 10.3892/ijmm.2019.4331

Maingret, N., Girardeau, G., Todorova, R., Goutierre, M., and Zugaro, M. (2016). Hippocampo-cortical coupling mediates memory consolidation during sleep. *Nat. Neurosci*. 19, 959–964. doi: 10.1038/nn.4304

Mancuso, R., Agostini, S., Hernis, A., Zanzottera, M., Bianchi, A., and Clerici, M. (2019). Circulatory miR-223-3p Discriminates Between Parkinson's and Alzheimer's Patients. *Sci. Rep*. 9:9393. doi: 10.1038/s41598-019-45687-x

Mao, M., Xu, Y., Zhang, X. Y., Yang, L., An, X. B., Qu, Y., et al. (2020). MicroRNA-195 prevents hippocampal microglial/macrophage polarization towards the M1 phenotype induced by chronic brain hypoperfusion through regulating CX3CL1/CX3CR1 signaling. *J. Neuroinflamm.* 17:244. doi: 10.1186/s12974-020-01919-w

Maruyama, S., Furuya, S., Shiraishi, K., Shimizu, H., Akaike, H., Hosomura, N., et al. (2018). miR-122-5p as a novel biomarker for alpha-fetoprotein-producing gastric cancer. *World J. Gastrointest. Oncol*. 10, 344–350. doi: 10.4251/wjgo.v10.i10.344

Morovic, S., Budincevic, H., Govori, V., and Demarin, V. (2019). Possibilities of Dementia Prevention - It is Never Too Early to Start. *J. Med. Life* 12, 332–337. doi: 10.25122/jml-2019-0088

Nan, S., Wang, Y., Xu, C., and Wang, H. (2021). Interfering microRNA-410 attenuates atherosclerosis via the HDAC1/KLF5/IKBα/NF-κB axis. *Mol. Ther. Nucl. Acids* 24, 646–657. doi: 10.1016/j.omtn.2021.03.009

Niu, X. L., Jiang, X., Xu, G. D., Zheng, G. M., Tang, Z. P., Yin, N., et al. (2019). DL-3-n-butylphthalide alleviates vascular cognitive impairment by regulating endoplasmic reticulum stress and the Shh/Ptch1 signaling-pathway in rats. *J. Cell. Physiol.* 234, 12604–12614. doi: 10.1002/jcp.27332

O'Brien, J. T., and Thomas, A. (2015). Vascular dementia. *Lancet* 386, 1698–1706. doi: 10.1016/S0140-6736(15)00463-8

Pantoni, L. (2010). Cerebral small vessel disease: From pathogenesis and clinical characteristics to therapeutic challenges. *Lancet Neurol*. 9, 689–701. doi: 10.1016/S1474-4422(10)70104-6

Pinho, J. D., Silva, G., Teixeira Júnior, A., Belfort, M., Mendes, J. M., Cunha, I., et al. (2020). MIR-107, MIR-223-3P and MIR-21-5P Reveals Potential Biomarkers in Penile Cancer. *Asian Pac. J. Cancer Prev*. 21, 391–397. doi: 10.31557/APJCP.2020.21.2.391

Qi, X., Shao, M., Sun, H., Shen, Y., Meng, D., and Huo, W. (2017). Long non-coding RNA SNHG14 promotes microglia activation by regulating miR-145-5p/PLA2G4A in cerebral infarction. *Neuroscience* 348, 98–106. doi: 10.1016/j.neuroscience.2017.02.002

Quadrato, G., Benevento, M., Alber, S., Jacob, C., Floriddia, E. M., Nguyen, T., et al. (2012). Nuclear factor of activated T cells (NFATc4) is required for BDNF-dependent survival of adult-born neurons and spatial memory formation in the hippocampus. *Proc. Natl. Acad. Sci. U.S.A*. 109:E1499–E1508. doi: 10.1073/pnas.1202068109

Ragusa, M., Bosco, P., Tamburello, L., Barbagallo, C., Condorelli, A. G., Tornitore, M., et al. (2016). miRNAs Plasma Profiles in Vascular Dementia: Biomolecular Data and Biomedical Implications. *Front. Cell. Neurosci*. 10:51. doi: 10.3389/fncel.2016.00051

Reumiller, C. M., Schmidt, G. J., Dhrami, I., Umlauf, E., Rappold, E., and Zellner, M. (2018). Gender-related increase of tropomyosin-1 abundance in platelets of Alzheimer's disease and mild cognitive impairment patients. *J. Proteom*. 178, 73–81. doi: 10.1016/j.jprot.2017.12.018

Ruitenberg, A., Ott, A., van Swieten, J. C., Hofman, A., and Breteler, M. M. (2001). Incidence of dementia: Does gender make a difference? *Neurobiol. Aging* 22, 575–580. doi: 10.1016/s0197-4580(01)00231-7

Saggu, R., Schumacher, T., Gerich, F., Rakers, C., Tai, K., Delekate, A., et al. (2016). Astroglial NF-kB contributes to white matter damage and cognitive impairment in a mouse model of vascular dementia. *Acta Neuropathol. Commun*. 4:76. doi: 10.1186/s40478-016-0350-3

Saha, S., Buttari, B., Panieri, E., Profumo, E., and Saso, L. (2020). An Overview of Nrf2 Signaling Pathway and Its Role in Inflammation. *Molecules* 25:5474. doi: 10.3390/molecules25225474

Shi, J., Zhang, Y., Tan, D., Zhang, X., Yan, M., Zhang, Y., et al. (2021). PANDORA-seq expands the repertoire of regulatory small RNAs by overcoming RNA modifications. *Nat. Cell Biol.* 23, 424–436. doi: 10.1038/s41556-021-00652-7

Shi, J., Zhou, T., and Chen, Q. (2022). Exploring the expanding universe of small RNAs. *Nat. Cell Biol.* 24, 415–423. doi: 10.1038/s41556-022-00880-5

Singh, S., de Ronde, M., Kok, M., Beijk, M. A., De Winter, R. J., van der Wal, A. C., et al. (2020). MiR-223-3p and miR-122-5p as circulating biomarkers for plaque instability. *Open Heart* 7:e001223. doi: 10.1136/openhrt-2019-001223

Soeda, S., Koyanagi, S., Kuramoto, Y., Kimura, M., Oda, M., Kozako, T., et al. (2008). Anti-apoptotic roles of plasminogen activator inhibitor-1 as a neurotrophic factor in the central nervous system. *Thromb. Haemost*. 100, 1014–1020. doi: 10.1160/th08-04-0259

Sopjani, M., Alesutan, I., Dërmaku-Sopjani, M., Fraser, S., Kemp, B. E., Föller, M., et al. (2010). Down-regulation of Na+-coupled glutamate transporter EAAT3 and EAAT4 by AMP-activated protein kinase. *J. Neurochem*. 113, 1426–1435. doi: 10.1111/j.1471-4159.2010.06678.x

Spitz, F., and Furlong, E. E. (2012). Transcription factors: From enhancer binding to developmental control. *Nat. Rev. Genet*. 13, 613–626. doi: 10.1038/nrg3207

Sun, M. K. (2018). Potential Therapeutics for Vascular Cognitive Impairment and Dementia. *Curr. Neuropharmacol.* 16, 1036–1044. doi: 10.2174/1570159X15666171016164734

Sun, T., Zhao, K., Liu, M., Cai, Z., Zeng, L., Zhang, J., et al. (2022). miR-30a-5p induces Aβ production via inhibiting the nonamyloidogenic pathway in Alzheimer's disease. *Pharmacol. Res.* 178:106153. doi: 10.1016/j.phrs.2022.106153

Tayler, H., Miners, J. S., Güzel, Ö, MacLachlan, R., and Love, S. (2021). Mediators of cerebral hypoperfusion and blood-brain barrier leakiness in Alzheimer's disease, vascular dementia and mixed dementia. *Brain Pathol.* 31:e12935.

van der Flier, W. M., Skoog, I., Schneider, J. A., Pantoni, L., Mok, V., Chen, C., et al. (2018). Vascular cognitive impairment. *Nat. Rev. Dis. Primers* 4:18003. doi: 10.1038/nrdp.2018.3

Venkat, P., Chopp, M., and Chen, J. (2015). Models and mechanisms of vascular dementia. *Exp. Neurol.* 272, 97–108. doi: 10.1016/j.expneurol.2015.05.006

Vijayan, M., Alamri, F. F., Al Shoyaib, A., Karamyan, V. T., and Reddy, P. H. (2019). Novel miRNA PC-5P-12969 in IschemiczStroke. *Mol. Neurobiol*. 56, 6976–6985. doi: 10.1007/s12035-019-1562-x

Vina-Vilaseca, A., and Sorkin, A. (2010). Lysine 63-linked polyubiquitination of the dopamine transporter requires WW3 and WW4 domains of Nedd4-2 and UBE2D ubiquitin-conjugating enzymes. *J. Biol. Chem*. 285, 7645–7656. doi: 10.1074/jbc.M109.058990

Wais, P. E., Montgomery, O., Stark, C., and Gazzaley, A. (2018). Evidence of a Causal Role for mid-Ventrolateral Prefrontal Cortex Based Functional Networks in Retrieving High-Fidelity Memory. *Sci. Rep*. 8:14877. doi: 10.1038/s41598-018-33164-w

Wang, L., Yang, J. W., Lin, L. T., Huang, J., Wang, X. R., Su, X. T., et al. (2020). Acupuncture Attenuates Inflammation in Microglia of Vascular Dementia Rats by Inhibiting miR-93-Mediated TLR4/MyD88/NF-κB Signaling Pathway. *Oxid. Med. Cell. Longev*. 2020:8253904. doi: 10.1155/2020/8253904

Wang, Y., Pan, W., Bai, X., Wang, X., Wang, Y., and Yin, Y. (2021). microRNA-454-mediated NEDD4-2/TrkA/cAMP axis in heart failure: Mechanisms and cardioprotective implications. *J. Cell. Mol. Med*. 25, 5082–5098. doi: 10.1111/jcmm.16491

Wang, F., Ge, J., Huang, S., Zhou, C., Sun, Z., Song, Y., et al. (2021). KLF5/LINC00346/miR-148a-3p axis regulates inflammation and endothelial cell injury in atherosclerosis. *Int. J. Mol. Med*. 48:152. doi: 10.3892/ijmm.2021.4985

Weinstock, M., and Shoham, S. (2004). Rat models of dementia based on reductions in regional glucose metabolism, cerebral blood flow and cytochrome oxidase activity. *J. Neural Transm.* 111, 347–366. doi: 10.1007/s00702-003-0058-y

Xie, X., Peng, L., Zhu, J., Zhou, Y., Li, L., Chen, Y., et al. (2017). miR-145-5p/Nurr1/TNF-α Signaling-Induced Microglia Activation Regulates Neuron Injury of Acute Cerebral Ischemic/Reperfusion in Rats. *Front. Mol. Neurosci*. 10:383. doi: 10.3389/fnmol.2017.00383

Xiong, L. L., Xue, L. L., Al-Hawwas, M., Huang, J., Niu, R. Z., Tan, Y. X., et al. (2020). Single-nucleotide polymorphism screening and RNA sequencing of key messenger RNAs associated with neonatal hypoxic-ischemia brain damage. *Neural Regen. Res*. 15, 86–95. doi: 10.4103/1673-5374.264469

Xu, X., Chen, Y., Zhu, D., Zhao, T., Xu, R., Wang, J., et al. (2020). FX5 as a non-steroidal GR antagonist improved glucose homeostasis in type 2 diabetic mice via GR/HNF4α/miR-122-5p pathway. *Aging* 13, 2436–2458. doi: 10.18632/aging.202275

Yang, C., Zheng, J., Xue, Y., Yu, H., Liu, X., Ma, J., et al. (2018). The Effect of MCM3AP-AS1/miR-211/KLF5/AGGF1 Axis Regulating Glioblastoma Angiogenesis. *Front. Mol. Neurosci*. 10:437. doi: 10.3389/fnmol.2017.00437

Yang, L., Wang, L., Wang, J., and Liu, P. (2021). Long non-coding RNA Gm11974 aggravates oxygen-glucose deprivation-induced injury via miR-122-5p/SEMA3A axis in ischaemic stroke. *Metab. Brain Dis*. 36, 2059–2069. doi: 10.1007/s11011-021-00792-7

Yang, T., and Zhang, F. (2021). Targeting Transcription Factor Nrf2 (Nuclear Factor Erythroid 2-Related Factor 2) for the Intervention of Vascular Cognitive

Impairment and Dementia. *Arterioscler. Thromb. Vasc. Biol.* 41, 97–116. doi: 10.1161/ATVBAHA.120.314804

Yao, Z. H., Yao, X. L., Zhang, Y., Zhang, S. F., and Hu, J. (2017). miR-132 Down-regulates Methyl CpG Binding Protein 2 (MeCP2) During Cognitive Dysfunction Following Chronic Cerebral Hypoperfusion. *Curr. Neurovasc. Res.* 14, 385–396. doi: 10.2174/1567202614666171101115308

Ye, X., Lin, J., Lin, Z., Xue, A., Li, L., Zhao, Z., et al. (2017). Axin1 up-regulated 1 accelerates stress-induced cardiomyocytes apoptosis through activating Wnt/β-catenin signaling. *Exp. Cell Res.* 359, 441–448. doi: 10.1016/j.yexcr.2017.08.027

Yi, L. T., Zhu, J. X., Dong, S. Q., Chen, M., and Li, C. F. (2021). Berberine exerts antidepressant-like effects via regulating miR-34a-synaptotagmin1/Bcl-2 axis. *Chin. Her. Med.* 13, 116–123. doi: 10.1016/j.chmed.2020.11.001

Zeng, L., Jiang, H., Ashraf, G. M., Liu, J., Wang, L., Zhao, K., et al. (2021a). Implications of miR-148a-3p/p35/PTEN signaling in tau hyperphosphorylation and autoregulatory feedforward of Akt/CREB in Alzheimer's disease. *Mol. Ther. Nucl. Acids* 27, 256–275. doi: 10.1016/j.omtn.2021.11.019

Zeng, L., Jiang, H. L., Ashraf, G. M., Li, Z. R., and Liu, R. (2021b). MicroRNA and mRNA profiling of cerebral cortex in a transgenic mouse model of Alzheimer's disease by RNA sequencing. *Neural Regen. Res.* 16, 2099–2108. doi: 10.4103/1673-5374.308104

Zhang, F., Chen, K., Tao, H., Kang, T., Xiong, Q., Zeng, Q., et al. (2018). miR-25-3p, Positively Regulated by Transcription Factor AP-2α, Regulates the Metabolism of C2C12 Cells by Targeting Akt1. *Int. J. Mol. Sci.* 19:773. doi: 10.3390/ijms19030773

Zhang, H. M., Kuang, S., Xiong, X., Gao, T., Liu, C., and Guo, A. Y. (2015). Transcription factor and microRNA co-regulatory loops: Important regulatory motifs in biological processes and diseases. *Brief. Bioinform.* 16, 45–58. doi: 10.1093/bib/bbt085

Zhang, X., Trebak, F., Souza, L., Shi, J., Zhou, T., Kehoe, P. G., et al. (2020). Small RNA modifications in Alzheimer's disease. *Neurobiol. Dis.* 145:105058. doi: 10.1016/j.nbd.2020.105058

Zhou, T., Chen, S., and Mao, X. (2019). miR-145-5p affects the differentiation of gastric cancer by targeting KLF5 directly. *J. Cell. Physiol.* 234, 7634–7644. doi: 10.1002/jcp.27525

Zhu, X., Zhao, Y., Hou, W., and Guo, L. (2019). MiR-153 regulates cardiomyocyte apoptosis by targeting Nrf2/HO-1 signaling. *Chromosom. Res.* 27, 167–178. doi: 10.1007/s10577-019-09608-y

Advantages of publishing in Frontiers

OPEN ACCESS
Articles are free to read for greatest visibility and readership

FAST PUBLICATION
Around 90 days from submission to decision

HIGH QUALITY PEER-REVIEW
Rigorous, collaborative, and constructive peer-review

TRANSPARENT PEER-REVIEW
Editors and reviewers acknowledged by name on published articles

Frontiers
Avenue du Tribunal-Fédéral 34
1005 Lausanne | Switzerland

Visit us: www.frontiersin.org
Contact us: frontiersin.org/about/contact

REPRODUCIBILITY OF RESEARCH
Support open data and methods to enhance research reproducibility

DIGITAL PUBLISHING
Articles designed for optimal readership across devices

FOLLOW US
@frontiersin

IMPACT METRICS
Advanced article metrics track visibility across digital media

EXTENSIVE PROMOTION
Marketing and promotion of impactful research

LOOP RESEARCH NETWORK
Our network increases your article's readership